

Volume 10 Issue 3

March 2019



ISSN 2156-5570(Online)

ISSN 2158-107X(Print)



www.ijacsa.thesai.org

Editorial Preface

From the Desk of Managing Editor...

It may be difficult to imagine that almost half a century ago we used computers far less sophisticated than current home desktop computers to put a man on the moon. In that 50 year span, the field of computer science has exploded.

Computer science has opened new avenues for thought and experimentation. What began as a way to simplify the calculation process has given birth to technology once only imagined by the human mind. The ability to communicate and share ideas even though collaborators are half a world away and exploration of not just the stars above but the internal workings of the human genome are some of the ways that this field has moved at an exponential pace.

At the International Journal of Advanced Computer Science and Applications it is our mission to provide an outlet for quality research. We want to promote universal access and opportunities for the international scientific community to share and disseminate scientific and technical information.

We believe in spreading knowledge of computer science and its applications to all classes of audiences. That is why we deliver up-to-date, authoritative coverage and offer open access of all our articles. Our archives have served as a place to provoke philosophical, theoretical, and empirical ideas from some of the finest minds in the field.

We utilize the talents and experience of editor and reviewers working at Universities and Institutions from around the world. We would like to express our gratitude to all authors, whose research results have been published in our journal, as well as our referees for their in-depth evaluations. Our high standards are maintained through a double blind review process.

We hope that this edition of IJACSA inspires and entices you to submit your own contributions in upcoming issues. Thank you for sharing wisdom.

Thank you for Sharing Wisdom!

Managing Editor

IJACSA

Volume 10 Issue 3 March 2019

ISSN 2156-5570 (Online)

ISSN 2158-107X (Print)

©2013 The Science and Information (SAI) Organization

Editorial Board

Editor-in-Chief

Dr. Kohei Arai - Saga University

Domains of Research: Technology Trends, Computer Vision, Decision Making, Information Retrieval, Networking, Simulation

Associate Editors

Chao-Tung Yang

Department of Computer Science, Tunghai University, Taiwan

Domain of Research: Software Engineering and Quality, High Performance Computing, Parallel and Distributed Computing, Parallel Computing

Elena SCUTELNICU

"Dunarea de Jos" University of Galati, Romania

Domain of Research: e-Learning, e-Learning Tools, Simulation

Krassen Stefanov

Professor at Sofia University St. Kliment Ohridski, Bulgaria

Domains of Research: e-Learning, Agents and Multi-agent Systems, Artificial Intelligence, Big Data, Cloud Computing, Data Retrieval and Data Mining, Distributed Systems, e-Learning Organisational Issues, e-Learning Tools, Educational Systems Design, Human Computer Interaction, Internet Security, Knowledge Engineering and Mining, Knowledge Representation, Ontology Engineering, Social Computing, Web-based Learning Communities, Wireless/ Mobile Applications

Maria-Angeles Grado-Caffaro

Scientific Consultant, Italy

Domain of Research: Electronics, Sensing and Sensor Networks

Mohd Helmy Abd Wahab

Universiti Tun Hussein Onn Malaysia

Domain of Research: Intelligent Systems, Data Mining, Databases

T. V. Prasad

Lingaya's University, India

Domain of Research: Intelligent Systems, Bioinformatics, Image Processing, Knowledge Representation, Natural Language Processing, Robotics

CONTENTS

Paper 1: LSB based Image Steganography by using the Fast Marching Method

Authors: Xiaoli Huan, Hong Zhou, Jiling Zhong

PAGE 1 – 5

Paper 2: Developing Deep Learning Models to Simulate Human Declarative Episodic Memory Storage

Authors: Abu Kamruzzaman, Charles C. Tappert

PAGE 6 – 15

Paper 3: Automatic Control of Colonoscope Movement for Modern Colonoscopy

Authors: Helga Silaghi, Viorica Spoiala, Alexandru Marius Silaghi, Tiberia Ioana Ilias, Cornelia Győrödi, Claudiu Costea, Sanda Dale, Ovidiu Cristian Fratila

PAGE 16 – 19

Paper 4: Performance Analysis of Open Source Solution "ntop" for Active and Passive Packet Analysis Relating to Application and Transport Layer

Authors: Sirajuddin Qureshi, Dr Gordhan Das, Saima Tunio, Faheem Ullah, Ahsan Nazir, Ahsan Wajahat

PAGE 20 – 27

Paper 5: Achieving Flatness: Honeywords Generation Method for Passwords based on user behaviours

Authors: Omar Z. Akif, Ann F. Sabeeh, G. J. Rodgers, H. S. Al-Raweshidy

PAGE 28 – 37

Paper 6: Robust Recurrent Cerebellar Model Articulation Controller for Non-Linear MIMO Systems

Authors: Xuan-Kien Dang, Van-Phuong Ta

PAGE 38 – 47

Paper 7: Empirical Assessment of Ensemble based Approaches to Classify Imbalanced Data in Binary Classification

Authors: Prabhjot Kaur, Anjana Gosain

PAGE 48 – 58

Paper 8: Applying Diffie-Hellman Algorithm to Solve the Key Agreement Problem in Mobile Blockchain-based Sensing Applications

Authors: Nsikak Pius Owoh, Manmeet Mahinderjit Singh

PAGE 59 – 68

Paper 9: Optimizing the Hyperparameter of Feature Extraction and Machine Learning Classification Algorithms

Authors: Sani Muhammad Isa, Rizaldi Suwandi, Yosefina Pricilia Andrean

PAGE 69 – 76

Paper 10: Stabilizing Average Queue Length in Active Queue Management Method

Authors: Mahmoud Baklizi

PAGE 77 – 83

Paper 11: Survey on Human Activity Recognition based on Acceleration Data

Authors: Salwa O. Slim, Ayman Atia, Marwa M.A. Elfattah, Mostafa-Sami M. Mostafa

PAGE 84 – 98

- Paper 12: A Systematic Review of Domains, Techniques, Delivery Modes and Validation Methods for Intelligent Tutoring Systems
Authors: Aized Amin Soofi, Moiz Uddin Ahmed
PAGE 99 – 107
- Paper 13: Personalized Recommender by Exploiting Domain based Expert for Enhancing Collaborative Filtering Algorithm :PReC
Authors: Mrs. M. Sridevi, Dr. R. Rajeswara Rao
PAGE 108 – 115
- Paper 14: Model Reference Adaptive Control Design for Nonlinear Plants
Authors: Wafa Ghozlane, Jilani Knani
PAGE 116 – 124
- Paper 15: Diagnosis of Parkinson's Disease based on Wavelet Transform and Mel Frequency Cepstral Coefficients
Authors: Taoufiq BELHOUSINE DRISSI, Soumaya ZAYRIT, Benayad NSIRI, Abdelkrim AMMOUMMOU
PAGE 125 – 132
- Paper 16: Risk Factors for Software Requirements Change Implementation
Authors: Marfizah A.Rahman, Rozilawati Razali, Fatim Filzahti Ismail
PAGE 133 – 139
- Paper 17: Managing and Reducing Handoffs Latency in Wireless Local Area Networks using Multi-Channel Virtual Access Points
Authors: Kamran Javed, Fowad Talib, Mubeen Iqbal, Asif Hussain Khan
PAGE 140 – 145
- Paper 18: An Enhancement on Mobile Social Network using Social Link Prediction with Improved Human Trajectory Internet Data Mining
Authors: B. Suryakumar, Dr. E. Ramadevi
PAGE 146 – 150
- Paper 19: Using FDD for Small Project: An Empirical Case Study
Authors: Shabib Aftab, Zahid Nawaz, Faiza Anwer, Munir Ahmad, Ahmed Iqbal, Ashfaq Ahmad Jan, Muhammad Salman Bashir
PAGE 151 – 158
- Paper 20: Opinion Mining: An Approach to Feature Engineering
Authors: Shafaq Siddiqui, M. Abdul Rehman, Sher M. Daudpota, Ahmad Waqas
PAGE 159 – 165
- Paper 21: Cloud Server Security using Bio-Cryptography
Authors: Zarnab Khalid, Muhammad Rizwan, Aysha Shabbir, Maryam Shabbir, Fahad Ahmad, Jaweria Manzoor
PAGE 166 – 172
- Paper 22: Enhanced Physical Document Management using NFC with Verification for Security and Privacy
Authors: Z. Zainal Abidin, N.A. Zakaria, Z. Abal Abas, A.A. Anuar, N. Harum, M.R. Baharon, Z. Ayop
PAGE 173 – 178

Paper 23: A Machine Learning Approach for Predicting Nicotine Dependence

Authors: Mohammad Kharabsheh, Omar Meqdadi, Mohammad Alabed, Sreenivas Veeranki, Ahmad Abbadi, Sukaina Alzyoud

PAGE 179 – 184

Paper 24: The Opportunities and the Limitations of Using the Independent Post-Editor Technology in Translation Education

Authors: Burcu TÜRKMEN, Muhammed Zahit CAN

PAGE 185 – 192

Paper 25: On Telemedicine Implementations in Ghana

Authors: E. T. Tchao, Isaac Acquah, S. D. Kotey, C. S. Aggor, J. J. Kponyo

PAGE 193 – 201

Paper 26: V-ITS: Video-based Intelligent Transportation System for Monitoring Vehicle Illegal Activities

Authors: Qaisar Abbas

PAGE 202 – 208

Paper 27: Analysis of Doppler Effects in Underwater Acoustic Channels using Parabolic Expansion Modeling

Authors: Ranjani G, Sadashivappa G

PAGE 209 – 214

Paper 28: Automated Grading Systems for Programming Assignments: A Literature Review

Authors: Hussam Aldriye, Asma Alkhalaf, Muath Alkhalaf

PAGE 215 – 222

Paper 29: Supply Chain Modeling and Simulation using SIMAN ARENA® a Case Study

Authors: Azougagh Yassine, Benhida Khalid, Elfezazi Said

PAGE 223 – 230

Paper 30: An Agglomerative Hierarchical Clustering with Association Rules for Discovering Climate Change Patterns

Authors: Mahmoud Sammour, Zulaiha Ali Othman, Zurina Muda, Roliana Ibrahim

PAGE 231 – 239

Paper 31: Regularization Activation Function for Extreme Learning Machine

Authors: Noraini Ismail, Zulaiha Ali Othman, Noor Azah Samsudin

PAGE 240 – 247

Paper 32: Energy-Aware Routing Hole Detection Algorithm in the Hierarchical Wireless Sensor Network

Authors: Najm Us Sama, Kartinah Bt Zen, Atiq Ur Rahman, Aziz Ud Din

PAGE 248 – 253

Paper 33: Microsatellite's Detection using the S-Transform Analysis based on the Synthetic and Experimental Coding

Authors: Soumaya Zribi, Imen Messaoudi, Afef Elloumi Oueslati, Zied Lachiri

PAGE 254 – 263

Paper 34: Location Prediction in a Smart Environment

Authors: Wael Ali Alosaimi, Ahmed Binmahfoudh, Roobaea Alroobaea, Atef Zaguia

PAGE 264 – 269

Paper 35: Low-fidelity Prototype Design for Serious Game for Slow-reading Students

Authors: Saffa Raihan Zainal Abidin, Siti Fadzilah Mat Noor, Noraidah Sahari Ashaari

PAGE 270 – 276

Paper 36: Experimentation for Modular Robot Simulation by Python Coding to Establish Multiple Configurations

Authors: Muhammad Haziq Hasbulah, Fairul Azni Jafar, Mohd. Hisham Nordin, Kazutaka Yokota

PAGE 277 – 282

Paper 37: A Novel Assessment to Achieve Maximum Efficiency in Optimizing Software Failures

Authors: Jagadeesh Medapati, Prof Anand Chandulal J, Prof Rajinikanth T V

PAGE 283 – 291

Paper 38: Process Capability Indices under Non-Normality Conditions using Johnson Systems

Authors: Suboohi Safdar, Dr. Ejaz Ahmed, Dr. Tahseen Ahmed Jilani, Dr. Arfa Maqsood

PAGE 292 – 299

Paper 39: Application of Artificial Neural Network and Information Gain in Building Case-Based Reasoning for Telemarketing Prediction

Authors: S.M.F.D Syed Mustapha, Abdulmajeed Alsufyani

PAGE 300 – 306

Paper 40: A Survey on Opportunistic Routing

Authors: Saleh A. Khawatreh, Mustafa Abdullah, Enas N. Alzubi

PAGE 307 – 313

Paper 41: Optimal Design of a Variable Coefficient Fractional Order PID Controller by using Heuristic Optimization Algorithms

Authors: Omer Aydogdu, Mehmet Korkmaz

PAGE 314 – 321

Paper 42: Speaker Identification based on Hybrid Feature Extraction Techniques

Authors: Feras E. Abualadas, Akram M. Zeki, Muzhir Shaban Al-Ani, Az-Eddine Messikh

PAGE 322 – 327

Paper 43: ATAM: Arabic Traffic Analysis Model for Twitter

Authors: Amani AlFarasani, Tahani AlHarthi, Sarah AlHumoud

PAGE 328 – 336

Paper 44: An Effective Approach to Analyze Algorithms with Linear $O(n)$ Worst-Case Asymptotic Complexity

Authors: Qazi Haseeb Yousaf, Muhammad Arif Shah, Rashid Naseem, Karzan Wakil, Ghufraan Ullah

PAGE 337 – 342

Paper 45: Implementation of Multi-Agent based Digital Rights Management System for Distance Education (DRMSDE) using JADE

Authors: Ajit Kumar Singh, Akash Nag, Sunil Karforma, Sripati Mukhopadhyay

PAGE 343 – 352

Paper 46: A Review on Security Issues and their Impact on Hybrid Cloud Computing Environment

Authors: Mohsin Raza, Ayesha Imtiaz, Umar Shoaib

PAGE 353 – 357

Paper 47: Enhanced Random Early Detection using Responsive Congestion Indicators

Authors: Ahmad Adel Abu-Shareha

PAGE 358 – 367

Paper 48: Recognition and Classification of Power Quality Disturbances by DWT-MRA and SVM Classifier

Authors: Fayyaz Jandan, Suhail Khokhar, Syed Abid Ali Shaha, Farhan Abbasi

PAGE 368 – 377

Paper 49: Smart Parking Architecture based on Multi Agent System

Authors: Sofia Belkhala, Siham Benhadou, Khalid Boukhdar, Hicham Medromi

PAGE 378 – 382

Paper 50: Towards Implementing Framework to Generate Myopathic Signals

Authors: Amira Dridi, Jassem Mtimef, Slim Yacoub

PAGE 383 – 389

Paper 51: Towards the Performance Investigation of Automatic Melanoma Diagnosis Applications

Authors: Amna Asif, Iram Fatima, Adeel Anjum, Saif U. R. Malik

PAGE 390 – 399

Paper 52: Multi-Objective Ant Colony Optimization for Automatic Social Media Comments Summarization

Authors: Lucky, Abba Suganda Girsang

PAGE 400 – 408

Paper 53: Classification of Melanoma Skin Cancer using Convolutional Neural Network

Authors: Rina Refianti, Achmad Benny Mutiara, Rachmadinna Poetri Priyandini

PAGE 409 – 417

Paper 54: Leveraging A Multi-Objective Approach to Data Replication in Cloud Computing Environment to Support Big Data Applications

Authors: Mohammad Shorfuzzaman, Mehedi Masud

PAGE 418 – 429

Paper 55: A Categorical Model of Process Co-Simulation

Authors: Daniel-Cristian Crăciunean, Dimitris Karagiannis

PAGE 430 – 438

Paper 56: An Enhanced Concept based Approach for user Centered Health Information Retrieval to Address Readability Issues

Authors: Ibrahim Umar Kontagora, Isredza Rahmi A. Hamid, Nurul Aswa Omar

PAGE 439 – 446

Paper 57: Microcontroller-based RFID, GSM and GPS for Motorcycle Security System

Authors: Kunnu Purwanto, Iswanto, Tony Khristanto Hariadi, Muhammad Yusvin Muhtar

PAGE 447 – 451

Paper 58: Efficient Arnold and Singular Value Decomposition based Chaotic Image Encryption

Authors: Ashraf Afifi

PAGE 452 – 457

Paper 59: Finding Attractive Research Areas for Young Scientists

Authors: Nouman Malik, Hikmat Ullah Khan, Muhammad Ramzan, Muhammad Shahzad Faisal, Ahsan Mahmood

PAGE 458 – 462

Paper 60: Improvement in Classification Algorithms through Model Stacking with the Consideration of their Correlation
Authors: Muhammad Azam, Dr. Tanvir Ahmed, Dr. M. Usman Hashmi, Rehan Ahmad, Abdul Manan, Muhammad Adrees, Fahad Sabah

PAGE 463 – 475

Paper 61: Image Retrieval using Visual Phrases

Authors: Benish Anwar, Junaid Baber, Atiq Ahmed, Maheen Bakhtyar, Sher Muhammad Daudpota, Anwar Ali Sanjrani, Ihsan Ullah

PAGE 476 – 480

Paper 62: An Improved Particle Swarm Optimization Algorithm with Chi-Square Mutation Strategy

Authors: Waqas Haider Bangyal, Hafiz Tayyab Rauf, Hafsa Batool, Saad Abdullah Bangyal, Jamil Ahmed, Sobia Pervaiz

PAGE 481 – 491

Paper 63: Real Time Analysis of Crowd Behaviour for Automatic and Accurate Surveillance

Authors: E Padmalatha, Karedla Anantha Sashi Sekhar, Dasarada Ram Reddy Mudiam

PAGE 492 – 496

Paper 64: Impacts of Unbalanced Test Data on the Evaluation of Classification Methods

Authors: Manh Hung Nguyen

PAGE 497 – 502

Paper 65: A Hybrid Exam Scheduling Technique based on Graph Coloring and Genetic Algorithms Targeted towards Student Comfort

Authors: Osama Al-Haj Hassan, Osama Qtaish, Maher Abuhamdeh, Mohammad Al-Haj Hassan

PAGE 503 – 512

Paper 66: Developing a Framework for Analyzing Heterogeneous Data from Social Networks

Authors: Aritra Paul, Mohammad Shamsul Arefin, Rezaul Karim

PAGE 513 – 521

Paper 67: Energy Efficient Camera Solution for Video Surveillance

Authors: Misbah Ahmad, Imran Ahmed, Kaleem Ullah, Iqbal Khan, Ayesha Khattak, Awais Adnan

PAGE 522 – 529

Paper 68: A Gender-Neutral Approach to Detect Early Alzheimer's Disease Applying a Three-layer NN

Authors: Shithi Maitra, Tonmoy Hossain, Abdullah Al-Sakin, Sheikh Inzamamuzzaman, Md. Mamun Or Rashid, Syeda Shabnam Hasan

PAGE 530 – 538

Paper 69: Optimal Pragmatic Clustering for Wireless Networks

Authors: Suzan Basloom, Nadine Akkari, Ghadah Aldabbagh

PAGE 539 – 544

Paper 70: Analysis of ECG Signal Processing and Filtering Algorithms

Authors: Zia-ul-Haque, Rizwan Qureshi, Mehmood Nawaz, Faheem Yar Khuhawar, Nazish Tunio, Muhammad Uzair

PAGE 545 – 550

Paper 71: Non-Linear EH Relaying in Delay-Transmission Mode over η - μ Fading Channels

Authors: Ayaz Hussain, Inayat Ali, Ramesh Kumar, Zahoor Ahmed

PAGE 551 – 555

Paper 72: Exploring Mechanisms for Pattern Formation through Coupled Bulk-Surface PDEs in Case of Non-linear Reactions

Authors: Muflih Alhazmi

PAGE 556 – 568

Paper 73: Efficient Load Balancing in Cloud Computing using Multi-Layered Mamdani Fuzzy Inference Expert System

Authors: Naila Samar Naz, Sagheer Abbas, Muhammad Adnan Khan, Benish Abid, Nadeem Tariq, Muhammad Farrukh Khan

PAGE 569 – 577

Paper 74: Performance Analysis of Multilayer Perceptron Neural Network Models in Week-Ahead Rainfall Forecasting

Authors: Lemuel Clark P. Velasco, Ruth P. Serquiña, Mohammad Shahin A. Abdul Zamad, Bryan F. Juanico, Junneil C. Lomocso

PAGE 578 – 588

Paper 75: Android based Receptive Language Tracking Tool for Toddlers

Authors: Sadia Firdous, Madhia Wahid, Amad Ud Din, Khush Bakht, Muhammad Yousuf Ali Khan, Rehna Batool, Misbah Noreen

PAGE 589 – 595

Paper 76: An Agent-based Simulation for Studying Air Pollution from Traffic in Urban Areas: The Case of Hanoi City

Authors: KAFANDO Rodrigue, HO Tuong Vinh, NGUYEN Manh Hung

PAGE 596 – 604

Paper 77: Spin-Then-Sleep: A Machine Learning Alternative to Queue-based Spin-then-Block Strategy

Authors: Fadai Ganjaliyev

PAGE 605 – 609

Paper 78: Triangle Hyper Hexa-cell Interconnection Network A Novel Interconnection Network

Authors: Asmaa Aljawawdeh, Esraa Emriziq, Saher Manaseer

PAGE 610 – 614

Paper 79: Growth Characteristics of Age and Gender-based Anthropometric Data from Human Assisted Remote Healthcare System

Authors: Mehdi Hasan, Rafiqul Islam, Fumuhiko Yokota, Mariko Nishikitani, Akira Fukuda, Ashir Ahmed

PAGE 615 – 619

Paper 80: Density based Clustering Algorithm for Distributed Datasets using Mutual k-Nearest Neighbors

Authors: Ahmed Salim

PAGE 620 – 630

Paper 81: Development of Talent Model based on Publication Performance using Apriori Technique

Authors: Zulaiha Ali Othman, Noraini Ismail, Mohd Zakree Ahmad Nazri, Hamidah Jantan

PAGE 631 – 640

LSB based Image Steganography by using the Fast Marching Method

Xiaoli Huan¹, Hong Zhou², Jiling Zhong³

Department of Computer Science, Troy University, Troy, Alabama, USA^{1,3}

Department of Mathematical Sciences, University of Saint Joseph, West Hartford, Connecticut, USA²

Abstract—This paper presents a novel approach for image steganography based on the Least Significant Bit (LSB) method. Most traditional LSB methods choose the initial embedding location of the cover image randomly, and the secret messages are embedded sequentially without considering the image pixels' values and positions. Our approach utilizes the user-selected seeds in the cover image to avoid the smooth/flat areas where cause a higher detection rate. Then the fast marching method is used to calculate T (the time of arrival of the front of the seeds) and propagate the seeds by computational dynamics. The front propagation process decides the embedding positions of the secret messages. The same algorithm can be used to retrieve the hidden information as well. The coordinates of the seeds are used as the shared key only known to the sender and receiver to add additional security protection. Peak Signal to Noise Ratio (PSNR) is evaluated to measure the quality of resulting images. The experiments show that the proposed approach generates results with high payload capacity and satisfied imperceptibility.

Keywords—Image steganography; LSB; the fast marching method; coordinates; PSNR

I. INTRODUCTION

Steganography has been an ancient practice to hide secret information within a media in such a way other people cannot easily detect the presence of the hidden contents. Cryptography and steganography are both techniques used to prevent the third party from reading the secret messages. However, they differ in the respect that cryptography makes the data exposable but not understandable without having the proper key to decode, while steganography hides the secret data inside a media and this modification of the original media cannot be easily perceived. In nowadays, steganography is used in many legal or illegal applications. For example, embedded digital watermarking techniques are developed to identify the ownership of the property. It is also reported that terrorist groups had used steganography to exchange information due to their affordability compared to dedicated secure networks [1].

The basic structure of image steganography is composed of the following:

- Secret-message: The information is to be hidden and delivered.
- Cover-image: An original image is used as a media to embed the secret-message.
- Stego-image: After the cover-image embeds the secret-message, the resulting image is known as the stego-image.

- Stego-key: Additional information is used for embedding and extracting the secret-message. The stego-key is a shared key known to the sender and receiver only.

II. RELATED WORK

Least Significant Bit (LSB) steganography is a popular technique in which the least significant bits (lowest bits) of pixels of the cover-image embed the secret-message. The changes to the cover-image are minimal and imperceptible to the human visual system [2]. However, the secret-message can be easily detected in the traditional LSB methods since the embedding positions are generated randomly and data are embedded sequentially [3]. These methods call for higher security features.

Steganographic methods which utilize a pixel's dependency on its neighborhood and psycho-visual redundancy to determine the smooth areas and edged areas in the gray level images are presented in [4]. However, in this method distortion is introduced and anyone is possible to recover the image due to its lack of stego-key protection. The approach in [5] uses a secret key to hide a secret-message in different channels of the LSB of a cover-image to protect it from unauthorized receivers. This method does not consider the pixels' values and positions in the cover-image. Therefore, the smooth/flat regions in the cover-image will be contaminated and cause low visual quality after data hiding. Edge adaptive schemes have been investigated. For example, the edge-detecting filter is used in [6]. Mean and standard deviation and canny edge detection are used in [7]. Methods hiding data around the edge boundary of an object are proposed in [8]. However, when the cover-image is mostly smooth or without sharp edges, the payload is limited in these approaches.

In our proposed method, we use the level set method to determine the embedding positions of the secret-message. The level set method (LSM) was proposed by S. Osher and J. Sethian in 1988 [9]. LSM is a computational technique for tracking interface motion over time and has various applications including image processing [10], fluid dynamics and physical modeling. LSM involves propagating a continuous scalar variable. "Considering $G(t)$ to be a moving closed curve in two dimensions. An Eulerian formulation for the motion of the interface is produced. The motion of the interface propagates along its normal direction with speed F , where F can depend on many factors, including the curvature, normal direction, shape, position of the front, or underlying fluid velocity. The interface $G(t)$ can thus be represented as the

zero-height level set of a function ϕ ". For a more detailed description of level set methods, the reader is referred to Sethian's published book [11].

Let's assume that the interface either moves "outward" ($F > 0$) or "inward" ($F < 0$) during the interface motion. The arrival time of the interface front at each grid point ($T(x,y)$) can be calculated and used to determine the propagating process of the front. This is the so-called fast marching method. In this method, all the arrival time values are composed of a function $T(x,y)$ which renders a surface. This surface tells the position of the interface front at any actual time T . "This surface is called the arrival time surface because it gives the arrival time of the interface passing at each grid point" [12].

The equation for the arrival time function is called boundary value formulation, which is

$$|\nabla T|F=1, F=e^{-\alpha|\nabla G_{\sigma}*(x,y,z)|} \quad (1)$$

$T=0$ on Γ , where Γ is the initial location of the interface. α is the fast marching method exponential coefficient which is set to 60 in our algorithm. T was discretized by the quadratic equation [12]:

$$\left[\begin{array}{l} \max(D_{ij}^{-x}T,0)^2 + \min(D_{ij}^{+x}T,0)^2 + \\ \max(D_{ij}^{-y}T,0)^2 + \min(D_{ij}^{+y}T,0)^2 \end{array} \right]^{1/2} = 1/F_{ij} \quad (2)$$

D^+ and D^- represent forward and backward difference operators. Equation (2) is solved at each grid point in the propagating process, and the root with the largest value is chosen as the correct viscosity result.

The advantages of using the fast marching method for LSB image steganography are the following:

- The seeds initially selected can be encrypted as the stego-key to add additional security protection.
- The user can choose seeds in non-smooth/flat regions in the cover-image to avoid low visual quality data hiding. The fast marching method enables image segmentation [13].
- The algorithm is straightforward to implement. The same algorithm can be used for embedding and retrieving the secret-message.

III. PROPOSED ALGORITHM

A. Finding the Embedding Positions by the Fast Marching Method

Equation (2) is applied in our image steganography algorithm. $T=0$ is assigned to the user-selected seeds in the cover-image. The user can select the seeds in the non-smooth/flat regions to avoid higher detection rate, and the seeds' positions can be encrypted as the stego-key. By solving (2), the front position at any time T can be obtained. This equation can be solved for each pixel in the cover-image until two times of the number of the hidden bytes is reached (one byte is hidden over two pixels). These pixels can then be mapped in a queue in the increasing order of T . The pixel with the smallest T is called first to hide the secret-message. In this way, the embedding

order of pixels in the cover-image is obtained. Fig. 1 shows the user-selected seeds in non-smooth/flat regions, and the seeds propagate by using the fast marching method.



Fig. 1. The user-Selected Seeds Propagate by the Fast Marching Method.

The scheme of FMM has been briefly described above. A detailed process is shown in the following:

1) Initialize four vectors: far_away, alive, try and neighbor.

2) Assign max T (e.g., DBL_MAX in C++) for all pixels in the cover-image and set their status as far-away (push them into the far_away vector).

3) For each user-selected seed point:

a) set the smallest T (zero) value.

b) Remove it from the far_away vector and set the status as alive (push it into the alive vector).

c) Check its four adjacent points (up, down, left and right) in the cover-image and set their status as try (push them into the try vector). Calculate their T values by the following equation:

$$T(x,y)=1/\exp(-1 * 60 * \text{grad_mag}[x][y])$$

grad_mag is the gradient magnitude value of the pixel. The cover-image first uses a Gaussian smoothing filter. Then the gradient magnitude values are computed in all color channels, and the values in the channel with the largest magnitude are picked [14].

4) For each point in the try vector:

a) Pick the point with the smallest T. Set the point as alive (push it into the alive vector) and remove it from the try vector.

b) Check its four adjacent points (up, down, left and right) in the cover-image. If the neighbor point is alive status, do nothing. If it is in the try vector, push it into the neighbor vector. If it is in far_away vector, push it into both the try and neighbor vectors and remove it from the far_away vector.

c) For each point (i, j) in the neighbor vector: Update its T. s1(a,b,c) and s2(a,b,c) are the functions to get the two roots

of a quadratic function $\frac{-b \pm \sqrt{b^2 - 4ac}}{2a}$. There are 16 possible roots to consider for (2) and the largest root is picked as T:

$$\text{double } F = 1.0 / \exp(-1 * 60 * \text{grad_mag}[i][j]);$$

$$\text{root}[0] = \text{s1}(2, -2 * (T[i][j-1] + T[i-1][j]), T[i][j-1] * T[i][j-1] + T[i-1][j] * T[i-1][j] - F * F);$$

$$\text{root}[1] = \text{s2}(2, -2 * (T[i][j-1] + T[i-1][j]), T[i][j-1] * T[i][j-1] + T[i-1][j] * T[i-1][j] - F * F);$$

$$\text{root}[2] = \text{s1}(2, -2 * (T[i][j-1] + T[i+1][j]), T[i][j-1] * T[i][j-1] + T[i+1][j] * T[i+1][j] - F * F);$$

$$\text{root}[3] = \text{s2}(2, -2 * (T[i][j-1] + T[i+1][j]), T[i][j-1] * T[i][j-1] + T[i+1][j] * T[i+1][j] - F * F);$$

$$\text{root}[4] = \text{s1}(2, -2 * (T[i][j+1] + T[i-1][j]), T[i][j+1] * T[i][j+1] + T[i-1][j] * T[i-1][j] - F * F);$$

$$\text{root}[5] = \text{s2}(2, -2 * (T[i][j+1] + T[i-1][j]), T[i][j+1] * T[i][j+1] + T[i-1][j] * T[i-1][j] - F * F);$$

$$\text{root}[6] = \text{s1}(2, -2 * (T[i][j+1] + T[i+1][j]), T[i][j+1] * T[i][j+1] + T[i+1][j] * T[i+1][j] - F * F);$$

$$\text{root}[7] = \text{s2}(2, -2 * (T[i][j+1] + T[i+1][j]), T[i][j+1] * T[i][j+1] + T[i+1][j] * T[i+1][j] - F * F);$$

$$\text{root}[8] = T[i][j-1] + F;$$

$$\text{root}[9] = T[i][j-1] - F;$$

$$\text{root}[10] = T[i][j+1] + F;$$

$$\text{root}[11] = T[i][j+1] - F;$$

$$\text{root}[12] = T[i-1][j] + F;$$

$$\text{root}[13] = T[i-1][j] - F;$$

$$\text{root}[14] = T[i+1][j] + F;$$

$$\text{root}[15] = T[i+1][j] - F;$$

d) Repeat step 4 until the number of points in the alive vector is greater than two times the number of hidden bytes. The pixel points in the alive vector are ordered by T ascendingly.

Fig. 2 shows an example of embedding orders with two user-selected seeds in a cover-image. T is calculated by using the fast marching method based on the image pixels' values and positions. The bands in the same color represent the pixels on the bands with the same T values. Pixels embed the secret-message in the increasing order of T.

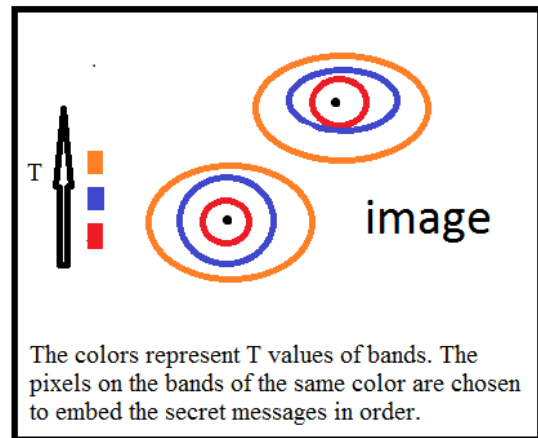


Fig. 2. Illustration of the Embedding Order with Two User-Selected Seeds.

B. Encoding the Secret-Message

After the embedding positions are obtained above, the algorithm starts the Least Significant Bit (LSB) encoding process. One byte of data is hidden into two adjacent points' R, G, B and Alpha channels in the alive vector. Any byte M from 0 to 255 can be extended to the form:

$$M = a_1 2^0 + b_1 2^1 + c_1 2^2 + d_1 2^3 + a_2 2^4 + b_2 2^5 + c_2 2^6 + d_2 2^7$$

If p^1 and p^2 are two adjacent elements in the alive vector of the cover-image and $(p_r^1, p_g^1, p_b^1, p_a^1)$ and $(p_r^2, p_g^2, p_b^2, p_a^2)$ are their RGB and Alpha values, the two new pixels' (p^{n1}, p^{n2}) values after M is embedded are:

$$p_r^{n1} = p_r^1 - p_r^1 \% 2 + a_1$$

$$p_g^{n1} = p_g^1 - p_g^1 \% 2 + b_1$$

$$p_b^{n1} = p_b^1 - p_b^1 \% 2 + c_1$$

$$p_a^{n1} = p_a^1 - p_a^1 \% 2 + d_1$$

$$p_r^{n2} = p_r^2 - p_r^2 \% 2 + a_2$$

$$p_g^{n2} = p_g^2 - p_g^2 \% 2 + b_2$$

$$p_b^{n2} = p_b^2 - p_b^2 \% 2 + c_2$$

$$p_a^{n2} = p_a^2 - p_a^2 \% 2 + d_2$$

C. Decoding the Secret-Message

Extracting the hidden data from the stego-image works similarly. The coordinates of the user-selected seed points can be encrypted as a shared stego-key. The extracting order is done by the fast marching method as the embedding process. If p^1 and p^2 are two adjacent elements in the alive vector of a stego-image and $(p_r^1, p_g^1, p_b^1, p_a^1)$ and $(p_r^2, p_g^2, p_b^2, p_a^2)$ are their RGB and Alpha values, the secret data can be constructed by:

$$M = (p_r^1 \% 2)2^0 + (p_g^1 \% 2)2^1 + (p_b^1 \% 2)2^2 + (p_a^1 \% 2)2^3 +$$

$$(p_r^2 \% 2)2^4 + (p_g^2 \% 2)2^5 + (p_b^2 \% 2)2^6 + (p_a^2 \% 2)2^7$$

IV. RESULTS AND ANALYSIS

The experimental results presented in this section compare the effectiveness of our proposed algorithm with existing methods. Several main factors affect an information hiding scheme: visual quality of the stego-images (HVS-human visual system) [15], embedding capacity, and error metrics such as PSNR.

Our experiment results show the proposed method achieves plausible HVS quality based on luminance similarity, structure correlation, edge similarity, and color similarity due to the nature of the fast marching method. It can have a larger payload capacity than methods such as [8].

We use the Mean Square Error (MSE) and the Peak Signal to Noise Ratio (PSNR) as the error metrics to evaluate stego-image quality. The MSE is computed by averaging the cumulative squared error between the original image and the stego-image, whereas PSNR represents a measure of the peak error. The following is the equation to compute MSE composed of d number of channels:

$$MSE = \frac{\sum_{m,n} [I_1(m,n) - I_2(m,n)]^2}{d \times m \times n}$$

The higher the value of PSNR, the closer is the stego-image to the cover-image. To compute the PSNR, the following equation is used:

$$PSNR = 10 \log_{10} \left(\frac{I_MAX^2}{MSE} \right)$$

I_MAX is the largest possible variation in the input image data type. It is 255 in case of the simple single byte per pixel per channel.

Table I is the results of PSNR on original LSB, edge-based LSB [7] and our method. Our method has higher PSNR values.

TABLE I. COMPARISON OF PSNR OF LSB, EG_LSB AND THE PROPOSED METHOD

Method	Image Size	Hidden bits	PSNR
LSB	512*512	36584	51.12
EG_LSB	512*512	36584	54.22
Our Method	512*512	36584	65.67

Fig. 3 shows the cover-images Lena, Baboon and Pepper, the secret-message (image Baboon) and stego-images by using the proposed method. Table II is the comparison of PSNR of LSB with Four Neighbor method [4], Secret Key [5] and our method.

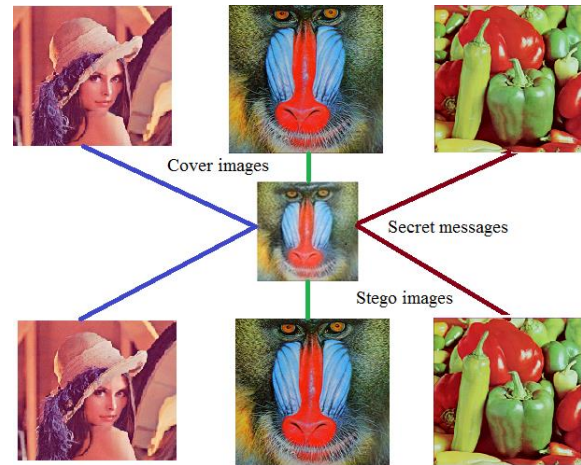


Fig. 3. Cover Images, Secret Messages and Stego Images by our Method.

TABLE II. COMPARISON OF PSNR OF LSB WITH FOUR NEIGHBOR METHOD [4], SECRET KEY [5] AND THE PROPOSED METHOD

Cover image	Hidden bits	PSNR neighbor	PSNR secretKey	PSNR Our method
Lena	392208	41.15	53.76	55.48
Baboon	435223	36.52	53.75	55.03
Pepper	393567	41.03	53.78	55.44

V. CONCLUSION

In this paper, a novel approach for LSB image steganography by using the fast marching method is presented. The approach can avoid non-smooth/flat regions and the user-selected seeds can be used as the stego-key. The embedding and extracting positions are determined by the computational technique fast marching method based on image pixels' values and positions. The experiments show that the proposed method has plausible visual quality and desirable PSNR. Future work can include testing by using different kinds of steganalysis algorithms and extend the proposed method to other steganographic medias such as audio/video.

REFERENCES

- [1] M. Conway, "Code Wars: Steganography, Signals Intelligence, and Terrorism," Knowledge, Technology and Policy, Vols. 16, No. 2, no. Technology and Terrorism, p. 45~62, 2003.
- [2] K. Bailey and K. Curran, "An Evaluation of Image Based Steganography," Multimedia Tools and Applications, vol. 30, no. 1, pp. 55-88, 2006.

- [3] A. Pfitzmann and A. Westfeld, "Attacks on steganographic systems," in Proc. 3rd Int. Workshop on Information Hiding, 1999.
- [4] M. Hossain, S. Haque and F. Sharmin, "Variable rate Steganography in gray scale digital images using neighborhood pixel information," in Proceedings of 2009 12th International Conference on Computer and Information Technology, Dhaka, 2009.
- [5] S. Masud Karim, M. Saifur Rahman and M. Ismail Hossain, "A New Approach for LSB Based Image Steganography using Secret Key," in Proceedings of 14th International Conference on Computer and Information Technology, Dhaka, 2011.
- [6] K. Hempstalk, "Hiding behind corners: Using edges in images for better steganography," in Proc. Computing Women's Congress, Hamilton, New Zealand, 2006.
- [7] A. Chaturvedi and K. Doeger, "A Novel Approach for Data Hiding using LSB on Edges of a Gray Scale Cover Images," International Journal of Computer Applications, vol. 86, no. 7, 2014.
- [8] M. Hussain and S. Haque, "Embedding data in edge boundaries with high PSNR," in 7th International Conference on Emerging Technologies, Islamabad, Pakistan, 2011.
- [9] Osher and Sethian, "Fronts propagating with curvature dependent speed: algorithms based on Hamilton-Jacobi formulations.," Journal of Computational Physics, pp. 79:12-49, 1988.
- [10] X. Huan, B. Murali and A. Ali, "Image restoration based on the fast marching method and block based sampling," Computer Vision and Image Understanding, vol. 114, no. 8, pp. 847-856, 2010.
- [11] J. Sethian, Level Set Methods and Fast Marching Methods, Cambridge Univ. Press, 1999.
- [12] J. Sethian, "A Fast Marching Level Set Method for Monotonically Advancing Fronts," in Proc. Natl. Acad. Sci., 1996.
- [13] N. Forcadell, C. Le Guyader and C. Gout, "Generalized fast marching method: applications to image segmentation," Numerical Algorithms, vol. 48, p. 189, 2008.
- [14] N. Dalal and B. Triggs, "Histograms of oriented gradients for human detection," in IEEE Computer Society Conference on Computer Vision and Pattern Recognition, San Diego, CA, 2005.
- [15] S. J. Thorpe, "Image Processing by the Human Visual System," in Advances in Computer Graphics, Berlin, Heidelberg, Springer, 1991, p. 309-341.

Developing Deep Learning Models to Simulate Human Declarative Episodic Memory Storage

Abu Kamruzzaman¹, Charles C. Tappert²

Seidenberg School of Computer Science and Information Systems
Pace University
Pleasantville, NY

Abstract—Human like visual and auditory sensory devices became very popular in recent years through the work of deep learning models that incorporate aspects of brain processing such as edge and line detectors found in the visual cortex. However, very little work has been done on the human memory, and thus our aim is to model human long-term declarative episodic memory storage using deep learning methods. An innovative way of deep neural network was created on supervised feature learning dataset such as MNIST to achieve high accuracy as well as storing the models hidden layers for future extraction. Convolutional Neural Network (CNN) learning models with transfer learning models were trained to imitate the long-term declarative episodic memory storage of human. A Recurrent Neural Network (RNN) in the form of Long Short Term Memory (LSTM) model was assembled in layers and then trained and evaluated. A Variational Autoencoder was also used for training and evaluation to mimic the human memory model. Frameworks were constructed using TensorFlow for training and testing the deep learning models.

Keywords—Convolutional neural network; long short term memory; Variational Autoencoder; deep learning; memory model; machine learning

I. INTRODUCTION

The aim of this research is to construct a deep learning model to simulate the human brain long-term declarative episodic memory storage, focusing primarily on the computer science perspective of the Rosenblatt Model for experiential storage in neural networks [1]. It is not known completely how human memory remembers past events. Previous work showed that Convolutional Neural Networks (CNN) models work well for classification of spatial data while CNN was unable to store the hidden layers for future predictions [2]. Our new hypothesis is that an integrated framework of CNN, Long Short Term Memory (LSTM) and Variational Autoencoder (VAE) adequately stores images for future recall.

Deep learning models can produce highly accurate results while trained and tested on datasets. However, the dataset might not generate accurate results while used inaccurately and larger dataset increase the amount of inconsistency of generating errors [3]. This issue can be resolved through additional training on the larger dataset.

The MNIST (Modified National Institute of Standards and Technology) is a well-known database of handwritten

characters for image processing comprised of 60,000 training set examples and 10,000 test set examples [4]. MNIST is a subset of NIST which have been size-normalized and have been aligned in the center [4]. The current test error rate for MNIST is very low reported to be 0.23% using CNN [5].

This research focuses on simulated deep learning memory models using simple CNN and pre trained CNN transfer learning VGG16, ResNet, Inception, MobileNet, LSTM and VAE to mimic the human brain's long-term declarative episodic memory of human mind. The research experiment and result show that the deep learning models built using TensorFlow API (Application Programming Interface) works well store the model for future usage. Our experiments in this journal uses CNN, LSTM, VAE conducted on MNIST handwritten dataset images with TensorFlow frameworks to simulate the human brain's long-term declarative episodic memory of human mind.

II. LITERATURE REVIEW

Deep learning is a subsection of machine learning where models are graph structures with multiple layers and typically non-linear. Both supervised and unsupervised methods are used for fitting models to data. Deep learning is used for prediction and generation and its application domains are image, audio and texts. Our literature review focuses on proving the similarities with human memory and deep learning model while also explaining on the deep learning algorithms such as CNN, LSTM, VAE which is the primary focus for this research to be used for storage mechanism to mimic human memory model.

Both human memory and deep learning models are mostly comprised of neurons. Hebb's states that the basics of human learning are that when a neuron accepts input from another neuron and if both neurons are highly active, the weight for both of the neurons should be strengthened [6].

A. Deep Learning and Memory Model Similarities

Human brain and deep learning core functionality is memory or storage [7]. Deep learning neural network contains input, weight parameters and works with calculated dataset and memory in brain acts similar way. Deep learning stores in dynamic RAM (DRAM), static RAM (SRAM) internally and externally which is the functionality of classical computers to save new data where as human brain dynamically and nomadically the patterns of neurons and synapses accomplish the behavior of neural networks storage mechanism [8].

Brain stores the input dataset of pattern recognizers in the hippocampus and learns from the frequency of the high-level features from cortical neurons and in similar fashion neural network store the complete dataset in the computer memory for frequent access to the dataset for learning the data behavior [9].

B. Long-Term Declarative Episodic Memory

Atkinson-Shiffrin memory model divided primarily into three categories named as sensory, short-term and long-term which are very popular for understanding memory as shown in Fig. 1. This research primarily studies the long-term declarative episodic (experiential) memory. This study is the focus of storing experiences and events that took place in different times in memory in a serial form and human can recreate these events and experiences that happened in a person lifetime that might have been forgotten for the time being. The permanent storage of the long-term declarative episodic (experiential) memory is infinite and limitless. The invention of Miller [11] discusses on the short-term memory that can hold only 5-9 chunks of information (seven plus or minus two) and a chunk is somewhat meaningful unit. The meaning of chunk is digits, words, chess positions, or people’s faces. All the following theories of memory after Miller’s chunk invention followed the concept of chunking and the limited capacity of short-term memory as a basic. The long-term memory comes from short-term memory once the memory saved permanently.

C. Convolutional Neural Network

Convolutional neural network known as CNN is very popular in deep neural networks aka deep learning for image processing and analysis. CNN apply multilayer perception with input, output, single or multiple hidden layers and does not require preloading of the images [12]. The CNN interprets images into pixels and features to classify the objects in the images during the training of the model. The images output classification allocated a probability from the numeric translation and learnt data as the training of the model completes.

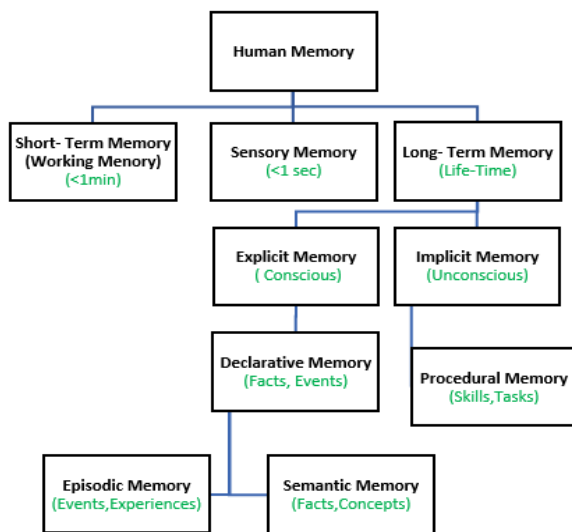


Fig. 1. Types of Human Memory (Adapted) [10].

CNN model training consists of several steps. Primarily the model takes an input from the image for sample analysis. Convolution is an evaluation of the sample area of pixels known as ‘features’ with the other parts of the image. The model uses a simple mathematical formula to select a match of these features. The network applies multiplication of each pixel to match the feature with is the source area. This method applied throughout the image to match every pixel. The model will apply these matches everywhere possible to attempt the highest accuracy of the image. The other subsamples are recognized and this technique repeated across the complete image. Pooling known to shrinking the large area of an image for calculation also applied. CNN also applies "Rectified Linear Units" which is known as ReLU where model swaps out negative calculations from convolution for a zero. ReLU helps identify the valuable units of the images and keeps the accuracy into stable position.

Fig. 2 below an input image (e.g. dog.jpg) sent to convolution layer for the CNN model to train. The CNN will train the model using the neural network hidden layers, acquire the features of the image, and extract the labels from the pre-trained weights to identify the output label of the image. We used VGG16, ResNet50, MobileNets and InceptionV3 pre-trained CNN transfer learning models with TensorFlow framework used in this research. However, these experiments are not presented in this journal.

D. Long Short-Term Memory (LSTM)

Long Short-Term Memory (LSTM) introduced in 1997 by Hochreiter & Schmidhuber is a branch derived from Recurrent Neural Network (RNN) [14]. LSTM remembers previously stored information into memory as needed. It has mechanism to forget and utilize the newly stored information or mix the newly stored input with the old stored memory information.

Fig. 3 below shows the architecture of RNN with three gates (input, forget and output) for LSTM. The input gate collects the new information and transfers to output gate with the current time stamp whereas forget gate deletes the information that is not required anymore.

The RNN gates act on incoming signals as to pass or block the data utilizing its strength and import that is similar to the neural network’s nodes. The filtering of RNN works with weights as well. The weights used through iterative process of guesses, backpropagation error. The input and output states monitored through weights using recurrent network learning mechanism. The weights adjusted through gradient descent.

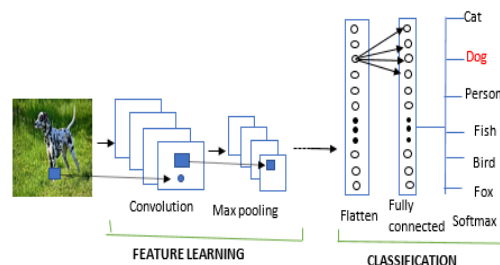


Fig. 2. A General Depiction of the Convolution Process (Adapted) [13].

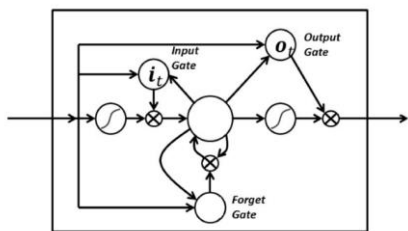


Fig. 3. RNN with Input, Output and Forget Gates [15].

Fig. 4 below shows the LSTM with inputs, outputs normalization and vector operations components in detail. The network takes three inputs. The LSTM network takes three inputs. The input is the X_t keeps track of current time step. h_t is the output and C_t is the memory of the current LSTM network. C_{t-1} is known to be the “memory” of the previous unit plays a very important role. h_{t-1} is the output of an LSTM.

Our research focus will be mostly on building an LSTM model to preserve episodic memory like the human brain. LSTMs can preserve the errors through time and layers using backpropagation. A supplementary constant error maintained through the recurrent nets learning using time steps that opens a channel to link sources and outcome remotely. This study looks through the LSTM deep learning model to imitate the episodic memory of human brain.

E. Variational Autoencoder (VAE)

Autoencoder is a function used in model to process the input data with restrictive sensitive manner. Variational Autoencoder (VAE) is a form of Autoencoder divided into two parts known as encoder and decoder. Encoder collects the input data and adds the most important data features to a vector form with a lower dimension than the original input. Decoder reconstructs the features vector to represent the output. Below Fig. 5 illustrates the VAE. VAE can take a principled Bayesian approach toward building systems. It's mostly used for semi-supervised machine learning. VAEs have one fundamentally unique property very useful for generative modeling different from vanilla autoencoders. VAEs contain latent spaces provide random sampling and interpolation with continuity by design.

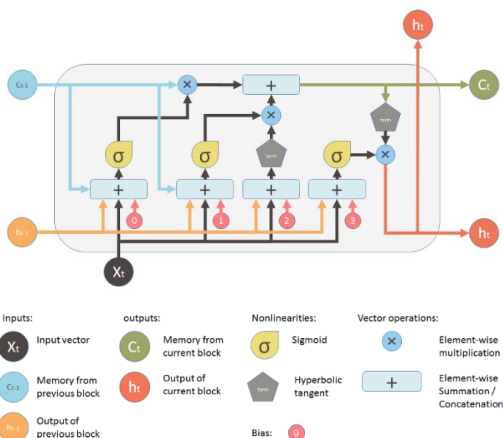


Fig. 4. Illustration of a Single LSTM Building Block [16].

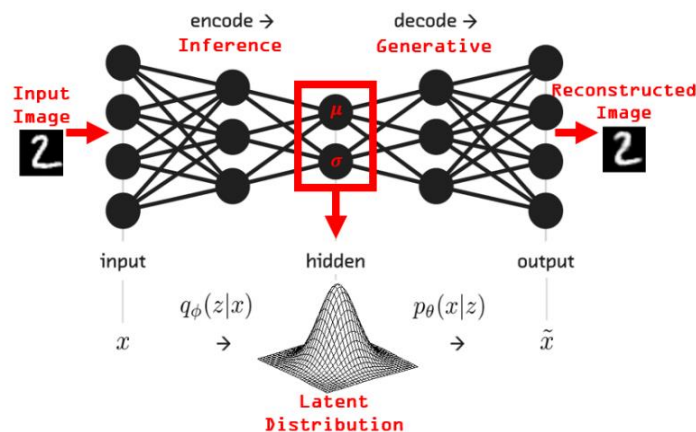


Fig. 5. Variational Autoencoder [17].

III. METHODOLOGY

The focus of this research is to learn and study the deep learning models with a c-system added on incorporated from the Rosenblatt Brain model [1] with storage mechanism. The deep neural network models are built from scratch using TensorFlow estimator framework. Experiments conducted on MNIST dataset to see how the representations work and stored for future predictions. In these experiments and results, CNN image classification and recognition tasks generated excellent output. In addition, CNN learning and storing of the model for future predictions were successful in these deep learning models.

Finally, we extended our MNIST experiments on LSTM and on VAE, using TensorFlow save and restore framework. In these experiments and results, MNIST image classification and recognition tasks generated excellent output and we were able to store the model for future predictions as well.

Our experiments and results focuses on the following:

A. Framework used to Store the Models for Future Extraction

The initial experiments were unable to store the dataset for future prediction using plain vanilla CNN and transfer learning CNN experiments. Therefore, our new deep learning experiments behave as long-term declarative episodic memory models using a framework with CNN, LSTM and VAE. The new experiments and results prove that the added framework combined with simple CNN model or pre-trained CNN models using input dataset MNIST handwritten dataset were able to classify the dataset and restore the output at later time.

Fig. 6 below depicts our architecture of the deep learning model in the visualization form that described below.

The newly proposed models collects input images from S-system, hidden layers shown in A-System and output layers are for R-System a normal display of a neural network classification model. The extended C-System works as the memory unit to store the output of the classification model for future retrieval. The C-system will maintain connections with both A-system (hidden layer) and R-system (output layer). We use different mechanisms to build our proposed C-system that explained later section in detail.

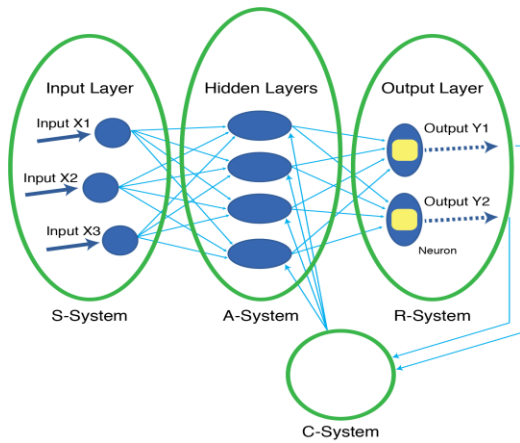


Fig. 6. Proposed Deep Learning Model Storage Architecture.

Our initial experiments were not able to store as complete memory model similar to human memory model while experiments conducted using CNN with MNIST images, LSTM with computer-generated numbers, ImageNet datasets applied on transfer learning CNN models such as ResNet, VGG16, InceptionV3 and MobileNet [2].

B. Proposed C-System

The proposed C-system is built using the TensorFlow Premade and Custom Estimators API and Save and Restore API frameworks. We also used the pre-trained ImageNet models transfer learning mechanism to test the C-system storage mechanism.

Google Brain team developed the TensorFlow framework which is an open source machine-learning framework [18]. TensorFlow bundles together multiple deep learning and machine learning models and algorithms to make the models useful. TensorFlow and open source platform helps to write lazy evaluation, imperative programs, graphs, sessions, variables, debug, etc. [1]. This framework is build using C++ works on Python. Tensorflow can train and run various deep learning models such as word embedding, image recognition, handwritten digit classification, recurrent neural networks, natural language processing, and sequence-to-sequence models for machine translation.

Our goal using the TensorFlow API to enable the C-System storage and retrieval feature as required. The Figure 7 below shows the hierarchy of TensorFlow API which is mostly divided into three levels. The top level of this hierarchy encapsulates the framework into a deep learning model. The mid-level APIs are a set of reusable packages to create computational graphs. The low level API give access to the runtime. In this level, tf.Session provides the flexibility to fine tune the models as needed. We customized the estimator of the High-level API to build our proposed C-system for majority of our experiments. We also use save and restore low-level API with tf.Session in our LSTM and VAE MNIST experiments to enable the C-system features. Below are the descriptions of high-level API Estimator and the low-level API Save and Restore that we used to build the C-system.

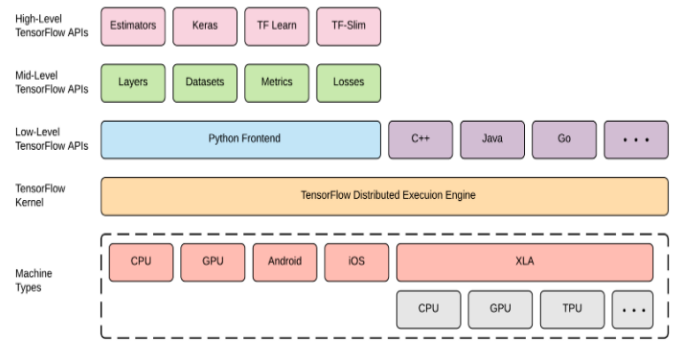


Fig. 7. Tensor Flow API Hierarchy [19].

C. Estimator API Framework

An Estimator API framework works well to specify, train, evaluate and deploy machine learning models and can be used with distributed platform utilizing the TensorFlow distributed training support [4]. This framework saves the complete deep learning neural network model if configured correctly. Google internally benefited introducing the TensorFlow Estimators where multiclass classification models perform 37% better accuracy and reduced required lines of code from 800 to 200 [4]. Estimators can be on the details of initialization, model save and restore, model logging, and other various features. The Estimator API used for training a model, estimating model accuracy, and generating predictions.

Cheng, Heng-Tze, et al. [4] mentions that an internal survey has shown that the Google codebase checked in with 1,000 Estimators and it is recorded that more than 120,000 experiments conducted within one year since Estimators framework is introduced and the prediction is that the true number of experiments are much higher. Fig. 8 below shows in percent usage of multiple Estimators at Google. Our MNIST CNN memory model experiment built showing both pre-made and custom Estimators. We used pre-made DNNClassifier in this experiment. The other pre-trained MNIST CNN memory models experiments using custom Estimators.

TensorFlow has a collection of tf.estimator to implement deep learning algorithms and the Estimator API comes from tf.estimator.Estimator. Estimator API has functions train(), evaluate(), or predict(). Fig. 9 shows how the Estimator is build. It automatically writes the checkpoints and the event files to the disk.

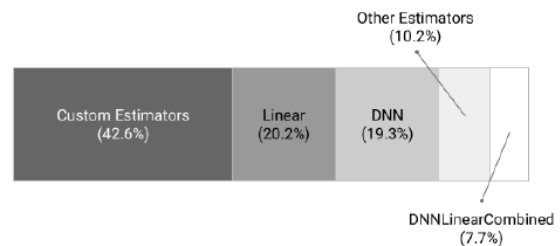


Fig. 8. Estimators Framework usage at Google [20].

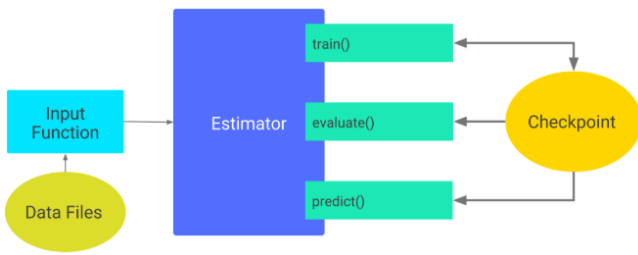


Fig. 9. Estimator Restore the Model [18].

Checkpoints created at training time are the versions of the model. Events files used for visualization on TensorBoard. The Estimator saves the model every 10 minutes (600 seconds) by default until model completely trained (if no steps are defined) in a custom directory defined by the developer through model_dir function call. We used /tmp/mnist_model as storing location for one of our experiment. The ls command in UNIX shows the objects in that directory. The Table 1 below \$ ls -l /tmp/mnist_model are the objects and descriptions are shown as comment as displayed in model_dir which is our proposed C-system. The directory retains five most recent checkpoints.

TABLE I. PROPOSED C-SYSTEM FILES DESCRIPTION

Object Name	Comments
checkpoint	model parameters will be reloaded from the checkpoint
events.out.tfevents.timestamp.hostname	TensorFlow events files with summary data; uses to create visualizations
graph.pbtxt	File saves the complete graph (meta + data). To load and use.
model.ckpt-1.data-00000-of-00001	stores the values of each variable
model.ckpt-1.index	identifies the checkpoint; store index of variables
model.ckpt-1.meta	Meta graph stores the graph structure

Our experiments used the default values and did not use the tf.estimator.RunConfig function. Estimator restore the model and saving to a specified directory. There exists two kinds of Estimators as shown in Fig. 10: Pre-made Estimators and custom Estimators. Pre-made Estimators and custom estimators displayed at a later discussion. The pre-made Estimators are plain vanilla models with default setups to build regular machine learning/ deep learning models such as Random Forests Classification/Regression and Linear Classification /Regression, and Deep learning models for classification and regression. Google YouTube Watch Next video recommender system (a user can choose a list of videos from a ranked list after watching the current video) uses a deep model with TensorFlow Estimators (DNNClassifier) framework where it takes multiple days to train a model and model training data are continuously updated [4]. The pre-made Estimators perform the tasks below:

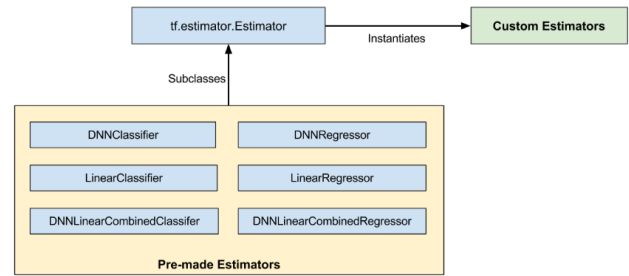


Fig. 10. Estimators API [18].

- Single or multiple input functions created.
- Feature columns for the model defined.
- Estimator defined with the feature columns and various hyperparameters.
- Estimator objects call single or multiple methods and with required input function for the source dataset.

Estimator requires customization built using custom estimators.

D. Custom Estimator API Framework

Custom Estimator API is a lower level method utilizes as a custom black-box model to reuse easily. We customize this API to build our C- system memory unit to store our deep learning models. The deep learning model is stored in a method called the model_fn(). A model_fn on a deep learning model illustrated in Fig. 11 below.

The function of the model has the code to outline the process of training the model. It may include identify the labels, loss function, model prediction, evaluation and training the model as well. Both pre-made and custom Estimator class contains three major methods, which are, the train(), evaluate(), predict().

- To train a dataset in the deep learning model train() method is called and this method is used for iteration through a set of training operations.
- To evaluate a dataset performance by iterating through a set of evaluation operations evaluate() method is called.
- To make predictions predict() method called on a trained model.

```
def model_fn(features, target, mode, params):
    predictions = tf.stack(tf.nn.softmax(tf.nn.conv2d(
        features, tf.nn.conv2d(
            [50, 50, 1])
        ),
        target,
        predictions)
    train_op = tf.train.create_train_op(
        loss, tf.train.get_global_step(),
        params['learning_rate'], params['optimizer'])
    return EstimatorSpec(mode=mode,
        predictions=predictions,
        loss=loss,
        train_op=train_op)
```

Fig. 11. Tensor Flow Framework Model_fn Pseudo Code.

Both pre-made and the custom Estimators require writing a method to input the dataset into the pipeline. Both training and evaluation of dataset require this method named `model_dir`. As `model_dir` method called during the estimator training, a checkpoint is stored using TensorFlow. This store in a folder in the hard disk storage initialized in `model_dir`. Every following call to `model_dir` during training, evaluation, or prediction the following happens:

- A model graph is being builds through estimator by running the `model_fn()`.
- The most recent checkpoint stores the weights of the new model initialized by the estimator.

It can also be said that using checkpoints TensorFlow rebuilds the model as the following function call `evaluate()`, `train()`, or `predict()`. Each model training should be built in separate directory to avoid the bad restoration of the model [21].

The model and checkpoint require being compatible for a model to be restore using checkpoint. For example, if a model trained on `DNNClassifier` as shown in Fig. 12 below Estimator using two hidden layers where each hidden layer have 10 hidden nodes:

Once the training is completed and checkpoints are created in `model_dir` and the hidden layer parameters are modified from 10 to 20 to retrain the model will fail because of the state of the checkpoint is incompatible with the new model. It will fail with the following error as shown in Fig. 13.

Different versions of a model should run from separate `model_dir`. This isolation helps the recovery of the checkpoints.

Estimator's checkpoints can easily save and restore models. Here developer can define the function parameter steps to train the model partially.

E. Save and Restore API Framework

Save and Restore API is a low-level TensorFlow method for saving and restoring deep learning models. Export and import of models using `SavedModel` is not language dependent, easily recovered, and works on serialization format.

- The graph variables saved and restored using the saver variable through the `tf.train.Saver()` object.
- To save the variables in a session, session instance run and stored in a directory passed through `save_path` method. `model.ckpt` is a prefix added to the checkpoint filename by system while storing the checkpoint files in model directory.
- `saver.restore` is called to restore the Graphs variables, build the graph and run the session instance.

Save and Restore low-level API with `tf.Session` is used in our LSTM and VAE MNIST experiments to enable the C-system storage and retrieval features.

```
classifier = tf.estimator.DNNClassifier(  
    feature_columns=feature_columns,  
    hidden_units=[10, 10],  
    n_classes=3,  
    model_dir='/tmp/mnist_model')  
  
classifier.train(  
    input_fn=lambda:train_input_fn(train_x,train_y, batch_size=100),  
    steps=200)
```

Fig. 12. Model Code with DNN Classifier Estimator.

```
InvalidArgumentError (see above for traceback): tensor_name =  
dnn/hiddenlayer_1/bias/t_0/Adagrad; shape in shape_and_slice spec [10]  
does not match the shape stored in checkpoint: [20]
```

Fig. 13. Tensor Flow Error Code.

IV. PROJECT REQUIREMENTS

To experiment all the proposed deep learning models, some programs and libraries installation required. It requires Python 3.5, Keras and TensorFlow 1.10 and numpy and matplotlib need to be installed. TensorBoard 1.10 required for graph visualization. Furthermore, a background knowledge of CNN, LSTM, pre-trained transfer learning, VAE, TensorFlow API and knowledge of Rosenblatt experiential storage model is required for the comparison of the architectures. We mostly used a local laptop environment to conduct all the experiments. Google Colab a free tool could be used for small experiments and Google cloud ML engine with VM instance and CUDA GPU can be utilized to achieve better performance for these experiments as well.

V. EXPERIMENTS AND RESULTS

Deep learning models such as CNN, LSTM or pre-trained CNN models without any framework unable to retrieved the complete c-system with storage mechanism [2]. Pre-trained CNN models transfer the weights of previously trained models but unable to replicate the proposed c-system. We needed a mechanism where we could store the complete model into c-system for future use. The new proposed TensorFlow framework added with CNN, pre-trained CNN (ResNet, VGG16, MobileNet, InceptionV3), LSTM or VAE provided the solution of storing the complete model. It also helps us visualize the model using TensorBoard.

Our new experiment models using TensorFlow Framework API on MNIST datasets elaborated in this journal include

- CNN memory model with Premade `DNNClassifier` Estimator
- CNN memory model with Custom Estimators
- LSTM MNIST Model with Save and Restore Framework API
- VAE Memory Model with Save and Restore Framework API

Often we had to train with a small dataset instead of the complete dataset. As deep learning models consumes enormous powerful resources and it takes significant amount of time running the complete dataset that makes the process very slow. For example, it would take us about 70 days to train ResNet model for 60,000 MNIST dataset in an ordinary machine. We ran for 2000 dataset for our experiment that took us more than 3 days.

MNIST CNN memory model contains two experiments. One experiment conducted using pre-made estimator while the other experiment was conducted using custom estimator. Both experiments were trained successfully for 2000 MNIST datasets as shown in Fig. 14 below. The evaluations conducted by restoring the trained model in both cases. In addition, the predictions were done from restoring the model in both cases to see if the correct images are predicted.

A. Experiment#1 CNN Memory Model with TensorFlow DNN Classifier Estimator

The purpose of building this MNIST CNN memory model with learning and training on MNIST hand written dataset to identify for image classification and recognition. The motivation of this experiment is to identify the sample images and store the model for future use. This experiment is to train a CNN deep learning model from scratch with learning and training on MNIST dataset and extend the model to build the proposed C-system for storing images or model for future prediction. We enhanced the model with tf.estimator.DNN Classifier using a 3-layer hidden units with 512, 256 and 128 units respectively for pre-made estimator. The model_fn() is built for custom estimator. Both experiments utilized the 70,000 MNIST dataset using training-set: 55000, validation-set: 5000 and test-set: 10000. Below is the snapshot of the input dataset with label before training. We trained the model up to 2000 datasets as our research interest is to build and test the storage mechanism for C-system. Therefore, it's not required to train the model for entire 55000 datasets. The C-system storing location was defined as model_dir = "./checkpoints_CNN_DNN" on pre-made DNNClassifier Estimator and model_dir= "./checkpoints_CNN_Custom/" for custom Estimator C-system storing location.

Initially the code calls the required imports and loads the MNIST data. Here is the high-level description for both pre-made and custom Estimator model experiments.

- Define functions for inputting data to the Estimator.
- Train the Estimator using the training-set defined in step 1.
- Evaluate the performance of the Estimator on the test-set defined in step 1.
- Use the trained Estimator to make predictions on other data.

We added the model implementation code of the model including comments in the Appendix section.

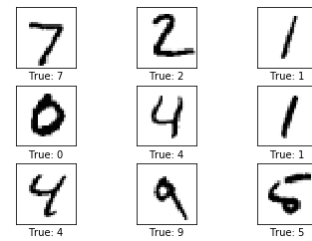


Fig. 14. MNIST Input Images and Labels used.

B. Experiment#1 Result

Fig. 15 below is the snapshot of DNNClassifier Estimator experiment image output with true and predicted label.

Fig. 16 below is the snapshot of DNNClassifier Estimator Model Evaluation result.

Fig. 17 below is the snapshot of C-system disk (./checkpoints_CNN_DNN) directory after training and evaluation for DNNClassifier Estimator.

Fig. 18 below is the snapshot of model graph visualization through TensorBoard for DNNClassifier Estimator from the C-system disk (./checkpoints_CNN_DNN /graph.pbtxt) directory.

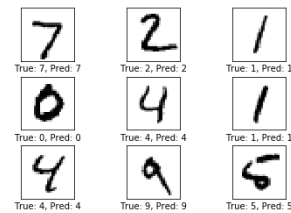


Fig. 15. MNIST Predicted Images and Labels after Training with Pre-Made DNNClassifier Estimator.

```
{'accuracy': 0.9677,
 'average_loss': 0.111842394,
 'loss': 14.157266,
 'global_step': 2000}
Classification accuracy: 96.77%
```

Fig. 16. Pre-Made Estimator Model Evaluation Result.

Name	Date modified	Type	Size
eval	10/13/2018 7:21 PM	File folder	
model.ckpt-0.data-00000-of-00001	10/13/2018 7:21 PM	DATA-00000-OF-00001 File	4,434 KB
model.ckpt-2000.data-00000-of-00001	10/13/2018 7:21 PM	DATA-00000-OF-00001 File	4,434 KB
checkpoint	10/13/2018 7:21 PM	File	1 KB
model.ckpt-0.index	10/13/2018 7:21 PM	INDEX File	1 KB
model.ckpt-2000.index	10/13/2018 7:21 PM	INDEX File	1 KB
events.out.tfevents.1539472891	10/13/2018 7:21 PM	LAPTOP-97D6GRAJ File	524 KB
model.ckpt-0.meta	10/13/2018 7:21 PM	META File	116 KB
model.ckpt-2000.meta	10/13/2018 7:21 PM	META File	116 KB
graph.pbtxt	10/13/2018 7:21 PM	PBTEXT File	262 KB

Fig. 17. Pre-Made Estimator C-System Disk Directory.

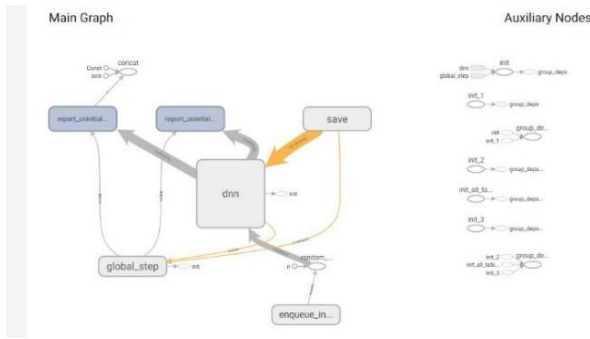


Fig. 18. Pre-Made Estimator Model Graph Visualization.

C. Experiment#2 CNN Memory Model with TensorFlow custom Estimator

Fig. 19 below is the snapshot of custom Estimator experiment image output with true and predicted label.

Fig. 20 below is the snapshot of custom Estimator Model Evaluation result:

C-system disk (./checkpoints_CNN_Custom) directory was created after training and evaluation for custom Estimator and graph visualization through TensorBoard for custom Estimator from the C-system disk (./checkpoints_CNN_Custom/graph.pbtxt) directory:

D. CNN Memory Model Summary

The MNIST CNN memory model classify the images well and stores the model where there is a mechanism for future prediction while combined with TensorFlow Estimator framework if this model needed to be retrieved at a later time.. In conclusion, based on the above experiments and results, even though CNN deep learning models alone cannot be used to replicate long-term declarative episodic memory. However, we can achieve the research objective while a CNN model is combined with a deep learning framework like Estimator API.

We also conducted custom estimator experiments on pre trained CNN deep learning models such as ResNet, VGG16, InceptionV3 and MobileNet and enable storage capability in similar fashions.

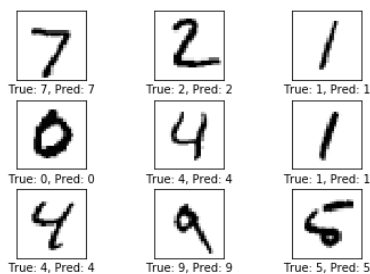


Fig. 19. MNIST Predicted Images and Labels after Training with Custom Estimator.

```
{'accuracy': 0.9789, 'loss': 0.06929768, 'global_step': 2000}
Classification accuracy: 97.89%
```

Fig. 20. Custom Estimator Model Evaluation Result.

E. Experiment#3 LSTM Memory Model with TensorFlow Save and Restore Framework

This experiment is to train a LSTM deep learning model from scratch on MNIST dataset and extend the model to build the proposed C-system for storing the model for future prediction. This experiment uses TensorFlow low level API framework tf.train.Saver to save and restore a model by utilizing the tf.Session. We build the LSTM model and pass it to the framework using tf.Session. The model is saved in “/tmp/lstm/” to be our C-system and restored from the same location. The following steps are required to build this model:

- 1) Make the environment ready through importing the needed libraries.
- 2) Define the configuration variables
- 3) Define the Functions
- 4) Load and preprocess the MNIST dataset and other input parameters to build the Model
- 5) A functioning Model implementation by TensorFlow
- 6) Model training on the prepared data
- 7) Results analysis

F. Save and Restore API Require of the following Steps

- 1) creating an instance of tf.train.Saver() class
- 2) save the model inside a session
- 3) Define the Saving Location
- 4) Call the tf.train.Saver.restore() to restore the model

We added the model implementation code of the model including comments in the Appendix section.

G. Experiment#3 Result

Model was trained successfully for 1000 datasets. The evaluation was conducted by restoring the trained model. In addition, the restored model was tested to see if the correct data are preserved. We also captured saver session and restore session log snapshot to observe the memory consistency. Similar to CNN model we observed the C-system disk (/tmp/lstm/) directory after training on MNIST using LSTM. Also, we were able to visualize graph through TensorBoard for LSTM from the C-system disk (/tmp/lstm/) directory.

In conclusion, the LSTM MNIST memory model satisfies the requirement of classifying the images and store the model for future retrieval.

H. LSTM Memory Model Summary

The LSTM MNIST memory model classify the images well and stores the model where there is a mechanism for future prediction while combined with TensorFlow Save and Restore framework if this model needed to be retrieved at a later time. Therefore, it is an ideal model to use independently for the objective of this research. In conclusion, based on the above experiment and result, even though LSTM deep learning model alone cannot be used to replicate long-term declarative episodic memory. However, we can achieve the research objective while a LSTM model is combined with a deep learning framework like TensorFlow Save and Restore API.

I. Experiment#4 VAE Memory Model with TensorFlow Save and Restore Framework

This experiment is to train a VAE deep learning model from scratch on MNIST dataset and extend the model to build the proposed C-system for storing the model for future prediction. VAE MNIST uses TensorFlow low level API framework `tf.train.Saver` to save and restore a model by utilizing the `tf.Session`. We build the VAE model and pass it to the framework using `tf.Session`. The model is saved in `"/tmp/lstm/"` to be our C-system and restored from the same location.

J. Experiment#4 Result

Model was trained successfully for 10000 datasets. The evaluation was conducted by restoring the trained model. In addition, the restored model was tested to see if the correct data are preserved. We observed the Saver session and Restore session C-system disk (`/tmp/vae/`) directory was created after training on MNIST using VAE. We observed the graph visualization through TensorBoard for VAE from the C-system disk (`/tmp/vae/`) directory.

In conclusion, the VAE MNIST memory model satisfies the requirement of classifying the images and store the model for future retrieval.

K. VAE Memory Model Summary

The VAE MNIST memory model classify the images well and stores the model where there is a mechanism for future prediction while combined with TensorFlow Save and Restore framework if this model needed to be retrieved at a later time. Therefore, it is an ideal model to use independently for the objective of this research. In conclusion, based on the above experiment and result, even though VAE deep learning model alone cannot be used to replicate long-term declarative episodic memory. However, we can achieve the research objective while a VAE model is combined with a deep learning framework like TensorFlow Save and Restore API.

Finally, we can draw a conclusion based on all these experiments and results that we can produce a desired C-system which can remember and replicate the previous events that occurred while building the deep learning model. Therefore, we can draw a conclusion that deep learning models can be replicated to incorporate human long-term declarative episodic memory storage.

We also conducted experiments on TensorFlow Custom Estimators Framework API on MNIST datasets for CNN ResNet, VGG16, InceptionV3 and MobileNet and enhance the models to be used as storage mechanism.

VI. DISCUSSION

Was a correlation found with human brain?

We assume there is a keen relationship and similarities with human brain long-term episodic memory storage and c-system memory storage unit we built using Tensorflow API. Human long-term episodic memory illustrates events and experiences of previous occurrences. Our deep learning models with c-system storage also originate on events and experiences. Here an event is triggered when a deep learning

model is being trained. In addition, the model gathers the experience from the behavior of the data is being trained on. After model gains the experience meaning trained on the data we store the model permanently into the c-system which is a permanent storage location of a disk specified by the framework. In our case, we used our C drive folder to be the replica of the c-system storage unit. In the event, we want the system to bring back the memory we connect the model using framework and the model is able to retrieve the information correctly. We can claim that our model storage capacity is much bigger than a human brain. Herbert Simon's chunk or George A. Miller's magic chunk [11] as illustrated before are very small in comparison to our deep learning memory storage. Here we can store the entire model that may have learn for days and worked on a large set of chunks or numbers. Therefore, we can draw the conclusion that we are able to find a correlation with our deep learning models and the human long-term declarative episodic memory.

VII. FUTURE WORK

We have explored into building a framework to build our proposed c-system storage mechanism. However, there are still other different techniques can be applied to build c-system storage mechanism. Below are some recommendations.

- Combine the CNN and LSTM together to build the c-system. CNN will work as the classification model and LSTM will work as the storage unit.
- Other dataset besides MNIST dataset can be tested and evaluated to check how the storage mechanism behaves.
- Our research was to work with images. This research can be enhanced to work with video frames.
- More work can be done to build comparison between human memory storage and the proposed c-system storage.
- Our research was limited to CNN, RNN-LSTM and VAE or pre trained CNN models. This can be expanded to work with other deep learning/ machine learning algorithms.
- We focused into TensorFlow framework for storage. Other frameworks can be evaluated to build the storage mechanism.
- TensorFlow framework low level API allows coding into other languages besides python. This research can be enhanced into multiple directions such as visualization to the web integrating other languages as well.
- TensorFlow.js also can be used to implement web mechanism to connect to the c-system.

VIII. CONCLUDING REMARKS

Finally, we reached into conclusion that deep learning models require building a framework to build the c-system to achieve the storage mechanism for an image classification

model. In addition, we can replicate the human memory model by enhancing the deep learning classification to model with storage unit.

REFERENCES

- [1] Rosenblatt, F. "A model for experiential storage in neural networks". Washington, DC: Spartan Books, 1964.
- [2] Abu Kamruzzaman, Yousef Alhwaiti, and Charles C. Tappert "Developing a Deep Learning Model to Implement Rosenblatt's Experiential Memory Brain Model" Future of Information and Communication Conference (FICC) IEEE 2019.
- [3] Karayev, S., Jia, Y., Shelhamer, E., Donahue, J., Long, J., Girshick, R., Guadarrama, S., and Darrell, T. "Caffe: Convolutional Architecture for Fast Feature Embedding", UC Berkeley EECS, Berkeley.
- [4] LeCun, Y., Bengio, Y., & Hinton, G. (2015). Deep learning. *nature*, 521(7553), 436.
- [5] Cireş, D., Meier, U., and Schmidhuber, J., "Multi-column Deep Neural Networks for Image Classification", IDSIA / USI-SUPSI, Manno, Switzerland, 2012.
- [6] D. O. Hebb, *The Organization of Behavior*. New York: John Wiley & Sons, 1949.
- [7] Teresa Nicole Brooks, Abu Kamruzzaman, Avery Leider and Charles C. Tappert "A Computer Science Perspective on Models of the Mind" Intelligent Systems Conference (IntelliSys), IEEE, 2018.
- [8] S. Nahal, *The Relationship Between Deep Learning and Brain Function: Proceedings of Student-Faculty Research Day*. Pleasantville, NY, USA: CSIS, Pace University, 2017, vol. May 5.
- [9] A. Fontana, "A deep learning-inspired model of the hippocampus as storage device of the brain extended dataset," arXiv preprint arXiv:1706.05932, 2017.
- [10] Mastin, L. (2010). Types of memory. *The human memory*.
- [11] Miller, George A. "The magical number seven, plus or minus two: Some limits on our capacity for processing information." *Psychological review* 63.2 (1956): 81.
- [12] Zhu, W., Lan, C., Xing, J., Zeng, W., Li, Y., Shen, L., & Xie, X. (2016, February). Co-Occurrence Feature Learning for Skeleton Based Action Recognition Using Regularized Deep LSTM Networks. In AAAI (Vol. 2, p. 8).
- [13] CNN workflow image - adeshpande3.github.io
- [14] Hochreiter, Sepp, and Jürgen Schmidhuber. "Long short-term memory." *Neural computation* 9.8 (1997): 1735-1780.
- [15] Wikipedia "Long short-term memory" https://en.wikipedia.org/wiki/Long_short-term_memory, 2018
- [16] Cheng, Heng-Tze, et al. "Tensorflow estimators: Managing simplicity vs. flexibility in high-level machine learning frameworks." *Proceedings of the 23rd ACM SIGKDD International Conference on Knowledge Discovery and Data Mining*. ACM, 2017.
- [17] "Visualizing MNIST with a Deep Variational Autoencoder" <https://www.kaggle.com/rvislaywade/visualizing-mnist-using-a-variational-autoencoder>, 2018
- [18] "TensorFlow" <https://www.tensorflow.org/>, 2018
- [19] "Tensorflow Estimator API" <https://blog.10yung.com/tensorflow-estimator-api-note/>, 2017
- [20] Cheng, Heng-Tze, et al. "Tensorflow estimators: Managing simplicity vs. flexibility in high-level machine learning frameworks." *Proceedings of the 23rd ACM SIGKDD International Conference on Knowledge Discovery and Data Mining*. ACM, 2017.
- [21] "TensorFlow: A proposal of good practices for files, folders and models architecture" <https://blog.metaflow.fr/tensorflow-a-proposal-of-good-practices-for-files-folders-and-models-architecture-f23171501ae3>, Apr 28, 2017

Automatic Control of Colonoscope Movement for Modern Colonoscopy

Helga Silaghi¹, Viorica Spoiala², Alexandru Marius Silaghi³, Tiberia Ioana Ilias⁴, Cornelia Györödi⁵, Claudiu Costea⁶,
Sanda Dale⁷, Ovidiu Cristian Fratila⁸

Faculty of Electrical Engineering and Information Technology, University of Oradea, Oradea, Romania^{1,2,3,5,6,7}
Medicine and Pharmacy Faculty, University of Oradea, Oradea, Romania^{4,8}

Abstract—The paper presents the mathematical realization of the trajectory that the colonoscope should have in the medical intervention, as well as the mathematical demonstration of the functions that make up the colonoscope. The goal of this work is finding a method for reducing the medical doctor's effort, by using intelligent control of colonoscope movement for improving the comfort of the patient subjected to a classical colonoscopy and reducing the risk of perforation of the colon. Finally, some experimental results are presented, validating the model and the control solutions adopted in the paper.

Keywords—Intelligent control; colonoscope movement; classical colonoscopy; mathematical model

I. INTRODUCTION

Colon cancer is rarely seen before the age of 45. After this age the mortality increases in 5 years with a ratio of 50%. Statistically, this type of cancer occupies second place on the rate of death in both women (after breast cancer) and men (after lung cancer) [1] [6].

Colonoscopy is considered the reference exam because it allows to visualize the total colon surface and performs, if biopsy is required, by taking samples of polyps. Two elements predispose to the development of colon cancer: polyps with a particular clinical form and inflammatory diseases (hemorrhagic colitis, Chron malady). In addition to the two elements mentioned above, there are certain factors that predispose to the appearance of polyps: eating, the environment, sedentary, genetic factors, etc.

The goal of this work is finding a method for reducing the medical doctor's effort, by using intelligent control of colonoscope movement for improving the comfort of the patient subjected to a classical colonoscopy and reducing the risk of perforation of the colon.

II. ARCHITECTURE AND FUNCTIONS OF COLONOSCOPE

The human colon is a muscular organ of 1250 mm in length, which contributes to three major functions of the human body: the absorption of non-digested foods, the digestion and concentration of faeces, their storage and evacuation [6]. Functionally, the colon can be divided into two parts separated by the transverse portion (right colon and left colon), as shown in Fig. 1.

The right colon (or cecum and ascending colon) plays a major role in the absorption of water and electrolytes, but also in the fermentation of undigested sugar. The left colon (the

colon, the sigmoid colon and the rectum) interfere primarily in stopping and evacuating salt from food.

Colon cancer is mainly located in the sigmoid region and the colorectal junction (65% of the localizations) and very rarely in the transverse portion [6].

It supports the cecum being the widest of the human colon allowing the development of the tumors before the symptoms occur. There is obviously a classification of the stages of evolution of these cancers: cancer with a survival period of 5 years (category A) 90% of the cancers are classified in this type, type D (hepatic metastasis) 5% types of cancer.

The colonoscope consists of four main parts: the connectors, the universal cord, the clamping system and the distal end [7].

The colonoscope has an operator channel that allows the passage of medical instruments such as for sampling, of coagulation or a laser fiber. Changing the angle of the colonoscope is done with a cable system inserted into the extremities of the device and is driven by two wheels that allow the endoscope head to move in two orthogonal directions that roughly can make all angles of the three-orthogonal system [4].

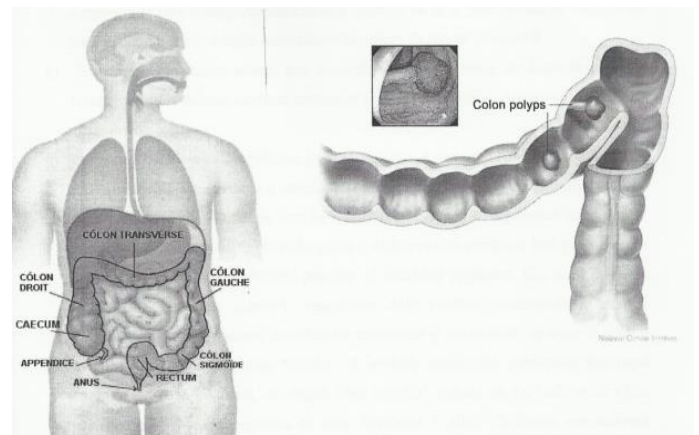


Fig. 1. The Anatomy of the Colon and the Sigmoid Region with Polyp.

III. MATHEMATICAL MODEL OF THE COLON

The paper presents the mathematical realization of the trajectory that the colonoscope should have in the medical intervention, as well as the mathematical demonstration of the functions that make up the colonoscope. We achieved the mathematical model of these functions with Matlab [4].

This simplistic mathematical model of the colon could diminish the perforations achieved by the colonoscope collision with the walls of the colon [2], [3]. Practically these equations could represent a trajectory of the geometric site where the colonoscope would not touch the walls of the intestine, as shown in Fig. 2.

The mathematical model of the colon was performed in four steps:

- We performed the projection on a vertical plane and tried to find the size of the colon.
- We wrote the equations for each portion.
- We split the graph into mathematical continuously functions, and then we set the points of discontinuity.
- We have set the conditions of continuity at the intersection points of the arc.

Mathematical functions:

a) *The left curve:* The curve is of the form $x = ay^2 - 24$, it must intersect points A (-20 -13); B (-20-13).

Final equation is:

$$x = \frac{4}{169}y^2 - 24 \quad \begin{cases} \frac{13}{2}\sqrt{x+24} \\ -\frac{13}{2}\sqrt{x+24} \end{cases} \quad (1)$$

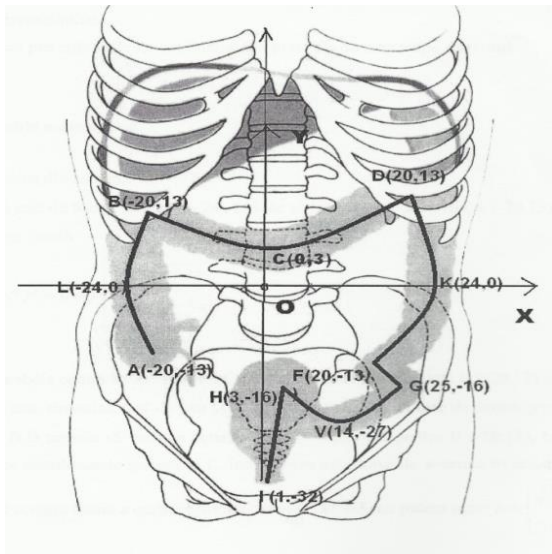


Fig. 2. Colon Mathematical Model.

b) Central parabola BCD with the top C(0,3) and other two points B(-20 -13); D(20 13)

The parabola is symmetrical with respect to the OY axis, which will result in the shape $y = ax^2 + c$ but the points B, D should verify the equation $\Rightarrow 13 = 400a + c$ for B (-20,13), the equation must verify the coordinates of the point C, in the above equation resulting in the final equation of the central curve $y = \frac{1}{40}x^2 + 3$ or we can write:

$$x = \begin{cases} \sqrt{40y-120} \\ -\sqrt{40y-120} \end{cases} \quad (2)$$

c) The DFK curve is symmetrical to the ALB parabola resulting in the direct writing of the equation:

$$4\frac{y^2}{169} = -x + 24 \quad \text{or } y = \begin{cases} \frac{13}{2}\sqrt{-x+24} \\ -\frac{13}{2}\sqrt{-x+24} \end{cases} \quad (3)$$

D(20 13); K(24 0); F(20 -13)

d) FG curve with points F (20 -13) and G (25-16)

$$m_{FG} = \frac{-16+13}{5} = \frac{3}{5} \Rightarrow y = -\frac{3}{5}x - 1 \quad (4)$$

e) The HVG curve is symmetrical with the axis parallel to OY at the point V(14 -27)

The equation is form $y = ax^2 + bx + c$ with the tipe V $\left(-\frac{b}{2a}, -\frac{\Delta}{4a}\right)$ and H(3 -16), G(25-16)

These two points must verify the initial equation.

The final equation of the HVG curve is:

$$y = -\frac{x^2}{11} + \frac{28}{11}x - \frac{251}{11} \quad (5)$$

f) The IH segment I(1 -32), H(3 -16)

$$m_{IH} = \frac{-32+16}{1-3} \Rightarrow m_{IH} = \frac{-16}{-2} = 8 \Rightarrow y=8x-40 \quad (6)$$

Because the graph was approximated with six mathematical functions, their number should be reduced [5], [8]. According to the mathematical analysis theorem to define a continuous function over an interval, it should be no parallel to the OY axis that intersects the graph into a single point.

- The LBCDK portion can be approximated by a single function by discontinuity points B, D. The equation of the LB arch is:

$$y = \frac{13}{12} * \sqrt{x+24} \quad (\text{the positive side of BLA arch}) \quad (7)$$

Equation of DK arch is:

$$y = \frac{13}{12} * \sqrt{x-24} \quad \text{(the positive side of DKF arch)} \quad (8)$$

First of the four continuous functions is:

$$f_1(x) = \begin{cases} \frac{13}{2} * \sqrt{x+24} & \text{for } x \in [-24-20] \dots \text{LB} \\ \frac{1}{40} * x^2 + 3 & \text{for } x \in [-20,20] \dots \text{BCD} \\ \frac{13}{2} * \sqrt{-x+24} & \text{for } x \in [20,24] \dots \text{DK} \end{cases} \quad (9)$$

Arch KF of the equation (10) for $x \in (20,24]$:

$$f_2(x) = \frac{13}{2} * \sqrt{-x+24} \quad (10)$$

A linear FG for $x \in [20,24]$:

$$f_3(x) = -\frac{3}{5} * x - 1 \quad (11)$$

The fourth continuous functions is:

$$f_4(x) = \begin{cases} \frac{13}{2} * \sqrt{x+24} & \text{for } x \in [-24-20] \\ 8 * x - 40 & \text{for } x \in [1,3] \\ \frac{x^2}{11} + \frac{28}{11} * x - \frac{251}{11} & \text{for } x \in [3,25] \end{cases} \quad (12)$$

So we approximated the graph with four continuous mathematical functions, as presented in Fig. 3.

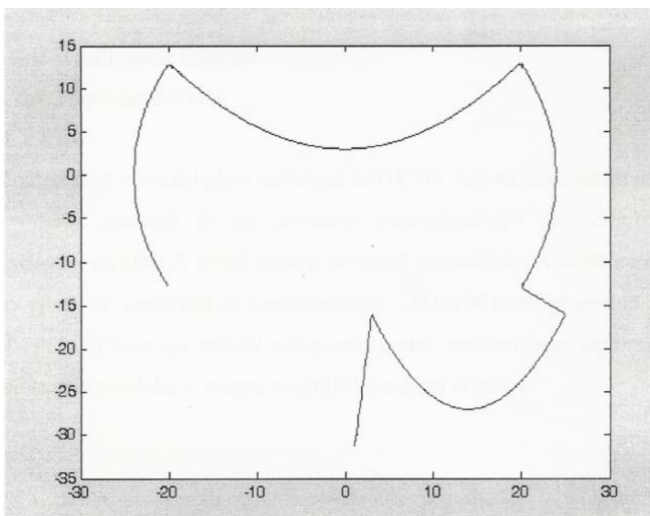


Fig. 3. Graph of the Function Performed in Matlab.

IV. EXPERIMENTAL RESULTS

The acquisition board of this practical application is called DSPACE DS 1104, this component can deliver in real-time communication between the external environment and the

computer. It has a fully programmable processor, and it is possible to program it even with the block diagram programming language (Fig. 4).

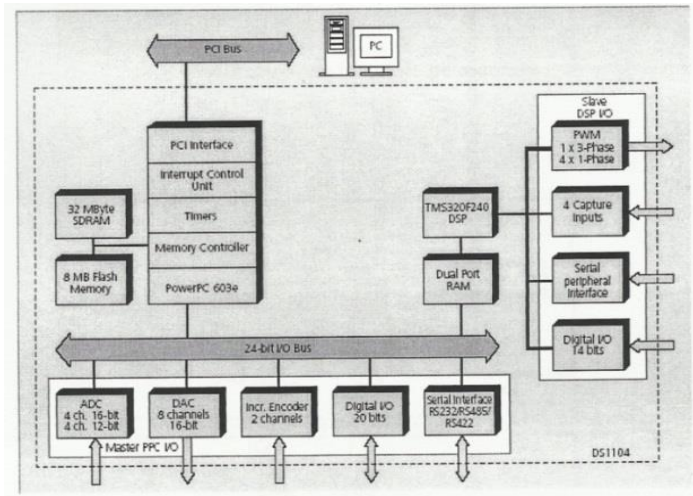


Fig. 4. Block Diagram of DS1104.

At the end of each engine attached to the colonoscope there is an encoder. Incremental encoders are of real use in automated driving processes. They have under construction a light source that penetrates phototransistors in order to have numerical signals on the three channels A, B, I.

The programs of this application are executed in Simulink using Matlab's compiler C and are generated for Control Desk, the latter being a purely experimental program that can handle different parameters and various automation functions.

Control Desk is the central module of this experimental work. Allows the tools listed above to be managed in the most comfortable way possible. This program has a purely experimental goal using Control Desk we can use the same experimental environment for multiple purposes.

Fig. 5 presents the control panel obtained with Control Desk. The acquisition board provides two MLI signals to the converter that feeds the two engines, but at the same time it generates a predefined information of the colonoscope on the predefined trajectory. The two imaginary voltages of circular currents in the two motors are measured by the analogue converter integrated into the acquisition plate. The encoders are connected directly to DSPACE to give the real-time information needed to keep the colonoscope on the predefined trajectory.

In the above diagram from Fig. 6 we can see that it is not necessary for all the blocks to be connected. These were the orders to pilot the colonoscope. In order to be able to make a connection with the Control Desk, we need to give the building command and then reopen with Control Desk.

V. CONCLUSIONS

This paper has achieved the goal of finding a method for reducing the medical doctor's effort, improving the comfort of the patient subjected to a classical colonoscopy and reducing the risk of perforation of the colon.

The central idea of this paper was to achieve the mathematical model of the colon's axes and to try to maintain the colonoscope on the given trajectory. With this hypothesis, we can diminish the contact points with the intestinal walls.

The entire paper was commissioned by an interface created under the Control Desk program that can control the DSpace acquisition board. We have implemented a program that complies with this trajectory, with compiler C in MATLAB.

The practical work was done with 8 Simulink-compatible function blocks and the DSpace library included in this software.

Of course, this mathematical model cannot answer all the problems that exist in the case of a traditional colonoscopy. For better realization of this model, more studies are needed on the human body, to find a common trajectory for all people; there are problems of different conformation of different people.

It is achieved the goal of making an alternative model to traditional colonoscopy and diminishing contact points with the intestinal walls. If there was an emphasis on more scientific research on this subject, there might be a solution to achieve a totally automated or partially computer-controlled colonoscopy. All technical implications in medicine that can improve the condition of the patient and make the medical doctor's task easier can be considered a success.

REFERENCES

- [1] L.M.Matica, C. Gyorodi, H.M. Silaghi, S. Abrudan Caciora, "Real time computation for robotic arm motion upon a linear or circular trajectory", International Journal of Advanced Computer Science and Applications IJACSA, Volume 9, Issue 2, ISSN: 2158-107X, WOS:000426979500004, Pages: 15-19, 2018.
- [2] J.Y. Fiset, Human-Machine Interface Design for Process Control Applications, ISA Press, USA, 2008.
- [3] L.M. Matica, H. Oros, "Speed computation in movement followed by accurate positioning" International Journal of Computers Communications & Control, ISSN 1841-9836, 12(1):76-89, 2017
- [4] L.M.Matica, C. Gyorodi, H. Silaghi, A. Silaghi, "Mixed profile method of speed and location for robotic arms motion used for precise positioning", International Journal of Advanced Computer Science and Applications IJACSA, Volume 9, Issue 5, 2018.
- [5] A. De Sabata, L. Matekovits, A. Silaghi, I. Peter, "Anisotropic dielectric devised by metamaterials-related technique", IEEE 11th International Conference on Communications (COMM), Bucharest, Romania, pp. 133-136, 2016.
- [6] O. Fratila, A. Maghiar, T. Ilias, M.A. Silaghi, "Analysis of the colonoscopic findings in patients with the acute gastrointestinal tract bleeding", Journal of Computer Science and Control Systems, University of Oradea, Romania, ISSN 1844-6043, pp. 135-140, 2008.
- [7] M. Wan, Z. Liang, Q. Ke, L. Hong, "Automatic centerline extraction for virtual colonoscopy", IEEE Transactions on Medical Imaging, Vol.21, Issue 12, Dec.2, ISSN: 0278-0062, pp. 133-136, 2016.
- [8] H. Silaghi, V.Spoiala, M.Silaghi, Acțiunări electrice, Editura Mediamira, Cluj-Napoca, ISBN 978-973-759-819-6, 314 pp., 2009.

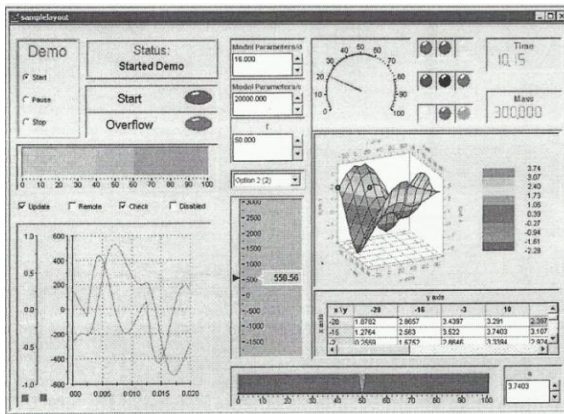


Fig. 5. Control Panel Obtained with Control Desk.

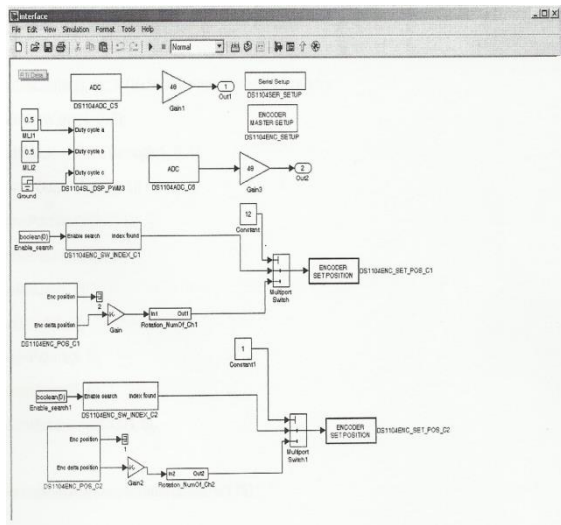


Fig. 6. The Colonoscope Movement with SIMULINK.

After the operating scheme was performed in SIMULINK, a second Control Desk interface was created for changing the direction of colonoscope movement. So, the positioning interface from Fig. 7 was created.

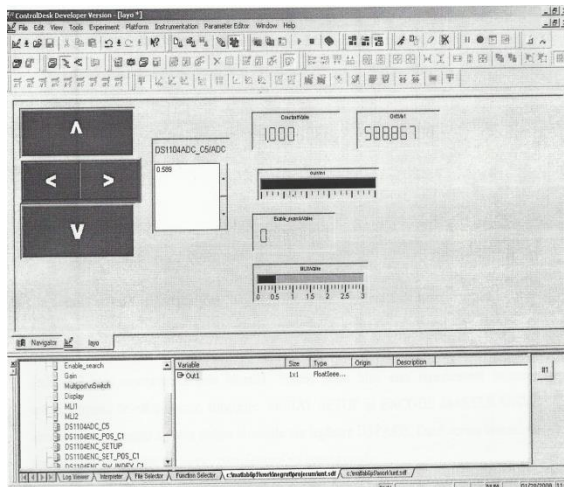


Fig. 7. The Colonoscope Positioning Interface.

Performance Analysis of Open Source Solution “ntop” for Active and Passive Packet Analysis Relating to Application and Transport Layer

Sirajuddin Qureshi¹, Dr Gordhan Das² Saima Tunio³, Faheem Ullah⁴, Ahsan Nazir⁵, Ahsan Wajahat⁶

Faculty of Information Technology, Beijing University of Technology, Beijing 100124, China¹

Information Technology Centre, Sindh Agriculture University Tandojam, Sindh, Pakistan^{2,3}

Faculty of Information Technology, Beijing University of Technology, Beijing, 100124, China^{4,5,6}

Abstract—A key issue facing operators around the globe is the most appropriate way to deal with spotting black in networks. For this purpose, the technique of passive network monitoring is very appropriate; this can be utilized to deal with incisive problems within individual network devices, problems relating to the whole LAN (Local Area Network) or core network. This technique, however, is not just relevant for troubleshooting, but it can also be castoff for crafting network statistics and analyzing network enactment. In real time network scenarios, a lot of applications and/or processes simultaneously download and upload data. Sometimes, it is very difficult to keep track of all the uploaded and downloaded data. Wireshark is a tool that is normally used to track packets for analysis between two particular hosts during two particular sessions on the same network. However, Wireshark as some limitations such as it is not a good tool for keeping track of bulky network data transferred among various endpoints. On the other side, an open source solution “ntop” offers active as well as passive packet analysis which can be handy for system administrators, networkers and IT managers. Additionally, with ntop VoIP traffic can also be monitored. In this research work, the ntop solution has been deployed to a network facility and performance analysis of ntop solution for various application processes (on application layer) such as HTTP, SSDP (based on HTTP) against their associated protocols such as TCP/IP, UDP, and VoIP have been analyzed. Additionally, above said processes and protocols have been comprehensively analyzed relating with their client/server breakdown, duration of the connection, actual throughput, total bytes (bytes received and sent) and total bandwidth consumed. This study has been helpful to see the weakest and strongest areas of a particular network in terms of analyzing and deploying network policies. This research work will help the research community to deploy ntop solution for real-time monitoring actively and passively.

Keywords—*ntop; network monitoring; packet analysis; the application layer; transport layer*

I. INTRODUCTION

Today’s internet-enabled infrastructure has resulted in the vast majority of applications to require networks of some sort [1–9]. All kinds of networks require essential security ensure communication is transmitted through appropriately protected

means [10–13]. Fig. 1 shows the difference between intranet and extranet.

Tracking and investigating traffic can be carried out for various reasons (Fig. 2) to examine the usage of network resources, measure the performance of network applications, adjust Quality of Service (QoS) policies in the network, log the traffic to fulfil the law, or create accurate models of traffic for academic reasons [14–21].

In order to examine where network resources are being consumed, there are a number of steps. The first step is to analyze the performance levels of network applications, adjusting Quality of Service network policies, recording the details of traffic according to regulations, or create accurate models of incoming and outgoing traffic for the purposes of academic objectives.

In order to fulfil all objectives, the scope and extent of research questions need to be identified. This concerns methods for appropriately classifying traffic, which may be applied to process big data near instantly, with reduced CPU and memory means. Other questions may be related to techniques related to the real-time approximation of the application of Quality of Service.

It is essential for all network operators to be aware of the performance levels of their network, in order to deliver reliability on the services they offer their customers.

Active and passive measurements are also a tool to troubleshoot their networks, in addition to simply measuring performance [22–27]. In certain instances, network faults may result in traffic being routed the wrong way. One way to tackle this can be through faults generating artificial traffic flows to inspect the behavior of traffic.

The Internet services are deep-seated part of higher education institutes [28–46]. Access to higher education is always beneficial for the public since higher education institutions maintain a foundation mission of research that is available through Internet high speed in higher education’s environments. Table I shows some of the Popular Online Education Initiatives taken so far recently.

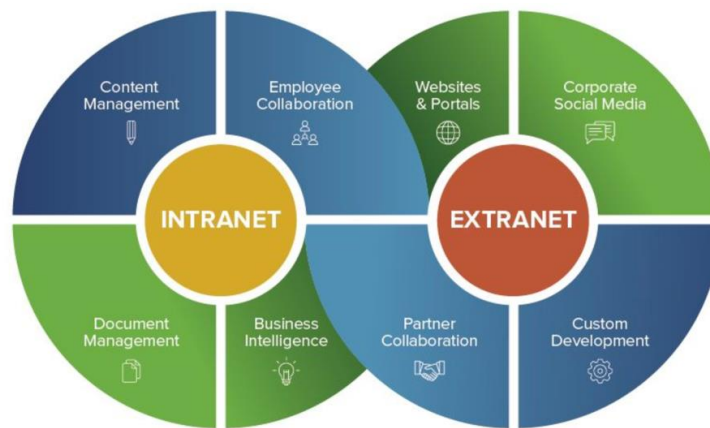


Fig. 1. Difference between Intranet and Extranet.

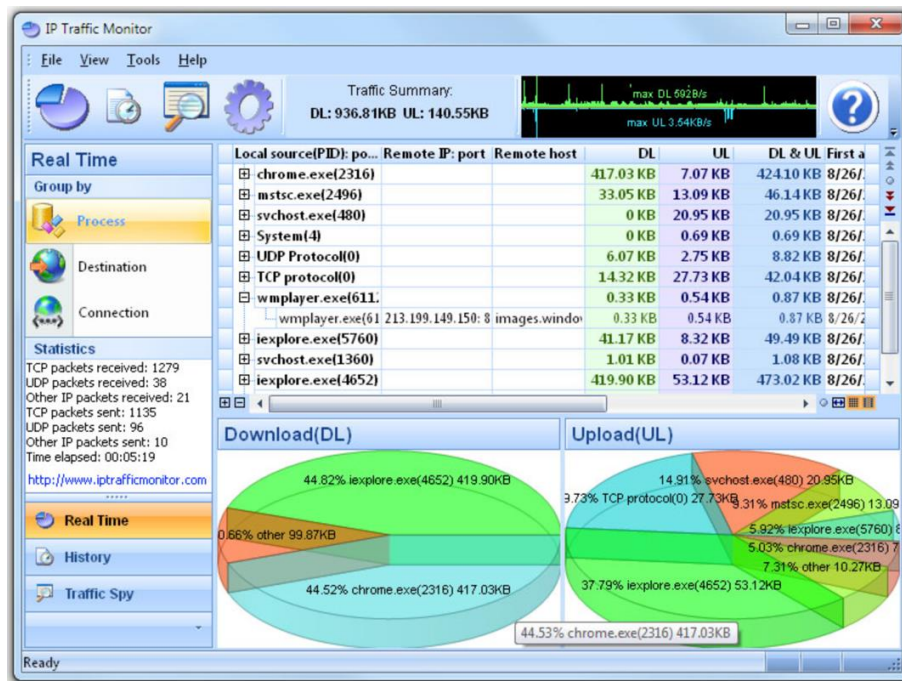


Fig. 2. Analysis of Internet Traffic in Real Time.

Nowadays, a new educational system introduced in the real-world distance education system, Virtual Education System, online education system, actual state and trends for the future education system. Education can become transformative when teachers and students synthesize information across subjects and experiences, critically weigh significantly different perspectives, and incorporate various inquiries. Educators are able to construct such possibilities by fostering critical learning spaces, in which students are encouraged to increase their capacities of analysis, imagination, critical synthesis, creative expression, self-awareness, and intentionality.

As a result of these approaches, there are bonus benefits that can help the global community at large, as seen in the creation of online courses from the United States. Called Massively Open Online Courses (MOOCs), these are now increasingly common at online platforms. Platforms offer

these in a fully online, or through blended options that combine online and classroom learning. The Pew Research Centre (2011) shows statistics that nearly 90% of American colleges or universities offered some courses of this nature.

Wireshark is a tool that is normally used to track packets for analysis between two particular hosts or between two particular sessions on the same network [47–50]. Fig. 3 shows the Wireshark Network Analyzer display windows. A typical network analyzer displays captured traffic in three panes:

1) *Summary*: This pane displays a one-line summary of the capture. Fields include the date, time, source address, destination address, and the name and information about the highest-layer protocol.

2) *Detail*: This pane provides all of the details (in a tree-like structure) for each of the layers contained inside the captured packet.

3) *Data*: This pane displays the raw captured data in both hexadecimal and text format.

Wireshark open source data packet analyzer. It is used for software, communication protocols, Ethernet and whole network analysis monitoring does not provide all features for analysis of the same network on Wireshark tool. However, Wireshark has some limitations such as it is not a good tool for keeping track of bulky network data transferred among various endpoints. Wireshark is not for intrusion detection system IDs, someone strange things on your network not show for warm. Wireshark doesn't manipulate on the network.

A network analyzer is a combination of hardware and software. Although there are differences in each product, a network analyzer is composed of five basic parts:

Hardware: Most network analyzers are software-based and work with standard operating systems (OSes) and network interface cards (NICs). However, some hardware network analyzers offer additional benefits such as analyzing hardware faults (e.g., cyclic redundancy check (CRC) errors, voltage

problems, cable problems, jitter, jabber, negotiation errors, and so on). Some network analyzers only support Ethernet or wireless adapters, while others support multiple adapters and allow users to customize their configurations. Depending on the situation, you may also need a hub or a cable tap to connect to the existing cable.

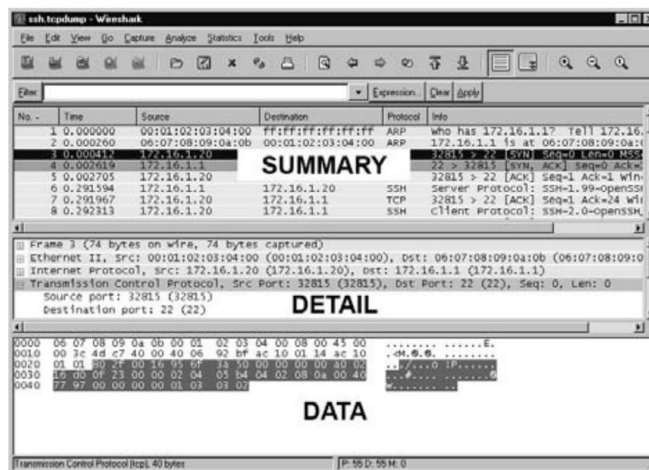


Fig. 3. Network Analyzer Display.

TABLE I. SOME POPULAR ONLINE EDUCATION INITIATIVES

Name	Sponsor	Year	Fees
Coursera	Joint efforts by Princeton University, Stanford University, University of California Berkeley, University of Michigan-Ann Arbor, & University of Pennsylvania	2011	private
eduMOOC	University of Illinois Springfield	2011	Free
edx	Harvard University & MIT	2012	Non -profit
iTunes U	Apple Corporation	2012	For-profit
Khan Academy	Salman Khan (Hedge Fund manager)	2007	Non-profit
Minerva	Minerva project and Keck Graduate Institute (KIG). (Larry Summers, former Harvard University President & United States Secretary Of the Treasury, chaired its first advisory board)	2012	Private
MITx	Joint efforts by Harvard University and edX	2001	Non-profit
Peer 2 Peer University (P2PU)	Funding from the Hewlett Foundation & the Shuttle worth Foundation	2009	Non-profit
Saylor	Michael J. Saylor (Chairman, CEO, & President Of the business intelligence company MicroStrategy)	2008	Non-profit
TED-Ed	Sapling Foundation	1984	Private Non-profit
Udacity	Sebastian Thrun	2012	For-profit
Udemy	Eren Bali	About 2010	Some are free; some are for a tuition fee
University Of the people	Shai Reshef (educational entrepreneur)	2009	Non-profit

Sources: Schroeder, 2012; official websites of individual initiatives

II. RELATED WORK

Gupta, U. [51] conducted the development of Monitoring in IOT enabled devices. He has developed Internet of things technologies complex network and heterogeneous environment. Monitoring the multi-router traffic, management information base, Zenoss, NTOP and Nagios implantation applications, process, events and logs observations are better in case of IOT.

Kokila S., Sathish, A., & Shankar, R. [52] conducted survey of a Comparative Analysis of Internet Traffic Identification Methods. They survey the main techniques and problems of IP packet based traffic analysis and focuses on application detection. Internet-based applications used more bandwidth increase of news user of Internet provider ISP increase network bandwidth interest of the user.

Nilsson, S., & Eriksson, J. [53] proposed the studied test Estimating Application Energy Consumption through Packet Trace Analysis. Their analysed power consumption utilised different applications calculating more accurate estimation mean power. Samsung Galaxy S4 battery 3G developing application transmission improvement the maximum through packet traces analysis.

Antichi, G., et al. [54] proposed a system architecture studied Enabling open-source high-speed network monitoring on netfpga. The monitoring system based on cooperative netfpga architecture positively with widely-recognised commercial system traffic considerably low cost. It provided open source instruments devices for capable high-performance monitoring system supporting 10 Gigabit per post base.

Garcia-Dorado, J. L. et al. [55] conducted survey High-performance network traffic processing systems using commodity hardware. Their studied compared successful implementations of packet capture engines required throughput and availability of processing cores in the system. High-performance network system used equipment to limitation and bottlenecks solutions packet processing.

Leung, C. M, & Schormans, J. A. [56] proposed methodology of Measurement-based traffic characteristic estimation for QoS-oriented IP networks. They studied two major points facilitate accurate perditions of network performance loss and delay through the measured buffer, and packet traffic bandwidth provided the best network performance. It used an algorithm for IP packets Internets WAN connectivity loss and delay less affected customers.

III. CAPTURE DRIVER

The capture driver is responsible to capture raw network traffic from the data cable. It filters unwanted traffic, and stores the remaining in a buffer. This is the most important, core element of a network analyzer, without data collection is impossible.

1) *Buffer*: The buffer stores captured data until its entire storage capacity has been reached. An alternative storage method is the rotation method when most recent data replaces

previously stored data. Buffers are memory-based or disk-based.

2) *Real-time Analysis*: This is a tool to analyze data, as soon as it is received off the cable. It can be used to find network performance issues and even applied to intrusion detection systems to investigate suspicious activity within networks.

3) *Decode*: The Decode part shows and explains the contents of the network traffic in order to ensure it is readable. These are unique to every protocol, as a result of which network analyzers offer different numbers of supported decodes. These lists are renewed constantly to include more decodes.

This research has been helpful to see the weakest and strongest areas of a particular network in terms of analyzing and deploying network policies. This research work will further help to deploy the ntop solution for real-time monitoring actively and passively.

IV. EXPERIMENTAL DETAILS

“ntop” is basically a web-based application user-friendly environment. The range of options “ntop” includes a graphical user interface as well as command line options, which make ntop as a priority of the network administrator who is already working in the Linux network environment. Based on the friendliness of ntop application, it easily installed the application and after configuration, it will start of packet capturing without wasting any time. Open source entities are getting importance in users day by day. It is almost easier to add plugins for the ntop to increase their functionality. The IP range is fully supported by ntop including IPV version 4 and 6.

A packet monitoring stage has been presented where different stages of packet monitoring have been depicted. The first stage is the network part where packets are captured.

Network part contains observation points. Observation points could anything ranging from network cards/interfaces to monitoring devices that forward packets to other points in the network under study. The second point in the network is server machines which work a packet aggregator. As data about a stream that was seen at a perception point, which may incorporate both trademark properties of a stream (e.g., IP addresses and port numbers) and measured properties (e.g., parcel and byte counters). They can be envisioned as records or lines in a common database, with one section for every property.

The metering and exporting procedures are by far the same which are normally taken to achieve this type of work and by firmly related exporting of data. Therefore, in this connection, we present these procedures. In Fig. 4, the process after achieving the data capture procedure has been presented. After capturing packet, all packets are time stamped and truncation is performed. After this packet sampling and packet filtering flow of a loop starts. In this research study, packet observing flow has been followed through this procedure.

This research work is done based on the IPV4 based network configuration. Easy installation and configuration process effortlessly open sources both window based and Linux based platform installation. Hardware requirement of 2.4 GHz process, 1GB RAM, 20 MB minimum hard desk.

Normally, network applications and their associated protocols are not studied together relating to network parameters. In earlier studies, network connectivity was done through standard switching environment as can be seen in Fig. 1.

However, in this work, not only network applications but their associated hosts (which are using the application) shall be analyzed against network protocols and network activities are monitoring through router environment. Routing tables perform excellent help in the ntop environment and fully supported through NetFlow. It can be seen in the Fig. 5, that P0 and P1 are points where network monitoring could be possibly studied. This is the added advantage of the ntop which offers the great facility to actively perform monitoring even sitting many miles away from the network. The client environment is also supported through VPN Client/Server breakdown is also very important to study, since bandwidth before not reflect any particular application, process or

protocol responsible for its consumption. This client/server breakdown shall help to optimize server resources for a number of clients/nodes attached to it at any given time. Conclusively, this study shall be handy to explore new analysis techniques grouped together under one plate form “ntop” for taking informed network decision and network policies in the coming years.

Distinctive instruments for framework checking, for instance, network monitoring tests offer impelled programming vernaculars for separating framework streams and building quantifiable event records. Appallingly, these gadgets have been planned for analyzing comprehended framework streams. However, it is not for the most part easy to consider what mastermind resources will be attacked. Nearby a couple of exclusions, for instance, security-related inspections various security contraptions available on the Internet are by and large planned for recognizing attacks against a lone host regularly the one where the device has been incited. This infers they don't give sort out/subnet area/protection nor incorporate development watching and estimation workplaces. Subnets are the most vulnerable part of the network which can be attacked while performing network monitoring options.

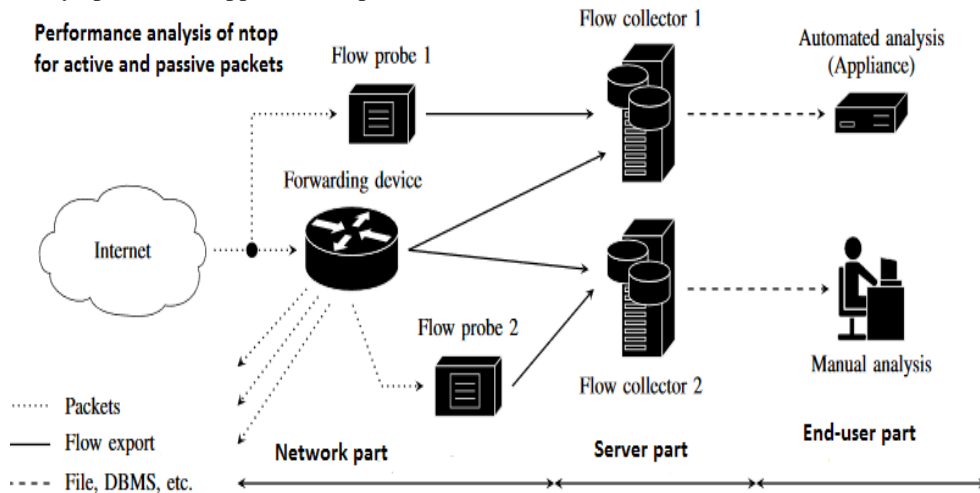


Fig. 4. Performance Analysis of Ntop for Active and Passive Packets.

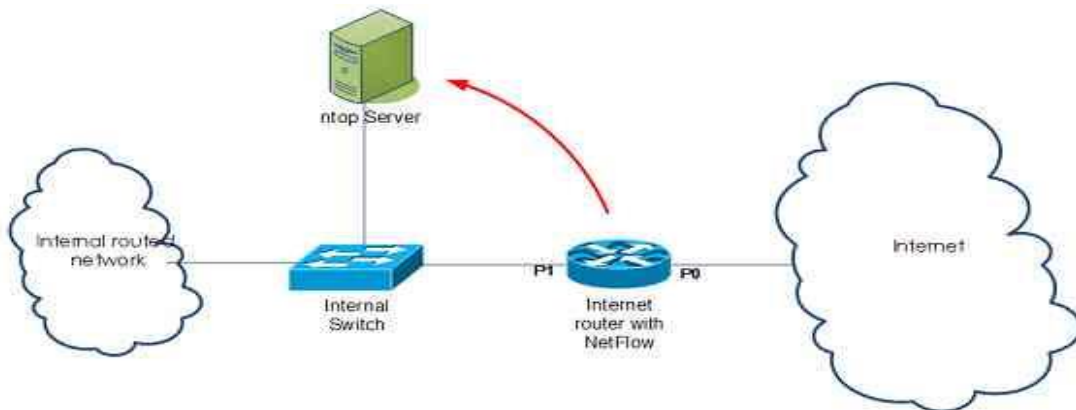


Fig. 5. Network Architect Scenario of Ntop Server Along with Applications within Routing and Switching Environment.

V. RESULTS AND DISCUSSION

The data has been taken after implementing *ntop* software network environment at Sindh Agriculture University Tandojam. In the following, the active flow has been described as per data set of *ntop* parameters shown in Fig. 6.

In Fig. 7, it can be easily deduced that whether data is related with client or server, *ntop* regardless of its type captures the details for further workout.

In this research work, *ntop* has been implemented to achieve run time monitoring of the whole network. Active flows of network connection along with the detail throughput details have been presented.

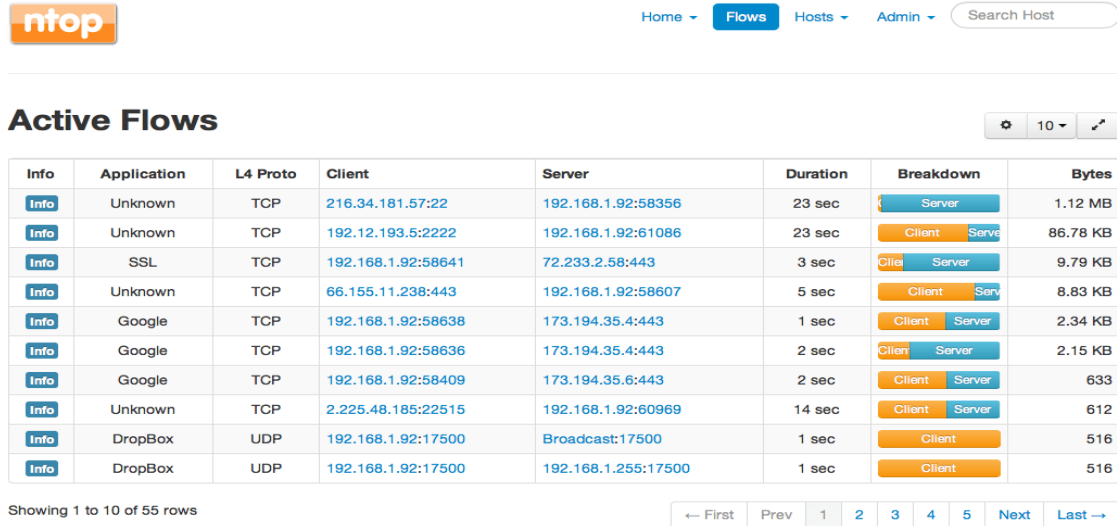


Fig. 6. Data Related with Active Flow has been Captured During the Experimentation Phase of thesis Works.

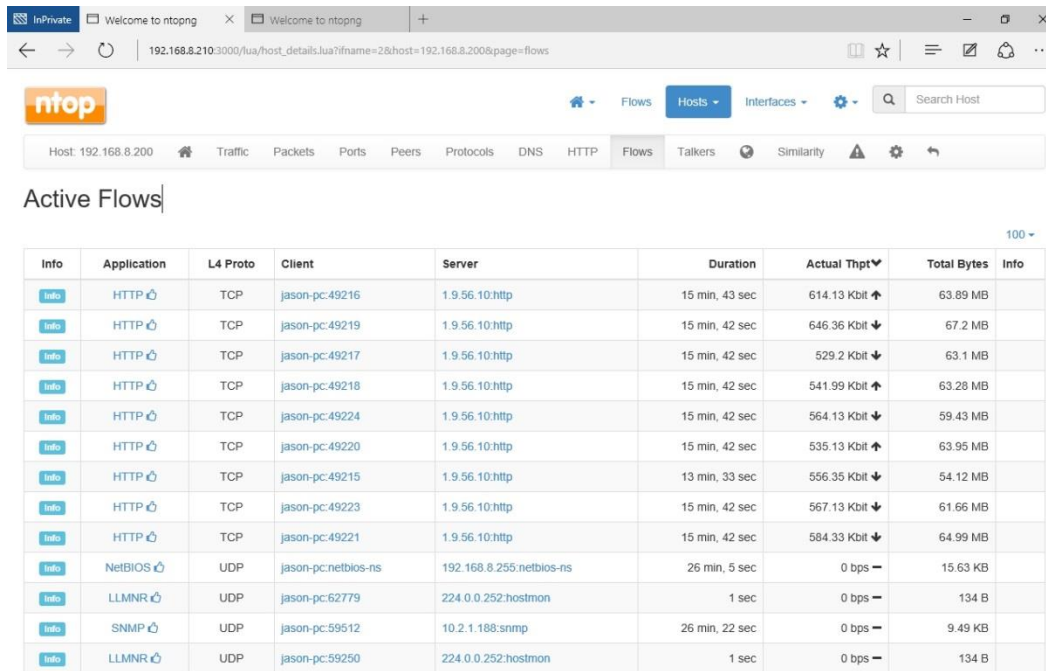


Fig. 7. Active Flows of Network Connection along with details of throughput and Duration of the Connections.

VI. CONCLUSION

It is the worst thing for a network administrator or manager to receive a call from an end user complaining about the health of the network. Additionally, we only know that any particular node is down on our network until someone complains about that. After receiving the complaint, the time to resolve that issue starts tickling. All the presented arguments are normally part of IT companies. Furthermore, performance analysis of any network is the key area for any organization. However, effective network monitoring gives you an added advantage of knowing the faults, congestion, and outage within the network in real time. In this research work, a practical approach for network analysis based on active and passive packet analysis is taken into consideration with the support of network monitoring tool called *ntop*. To achieve this research work "*ntop*" open source solution has been deployed and configured to a network facility under study which is the Information Technology Centre (ITC). Normally, network applications and their associated protocols are not studied together relating to network parameters. Particularly, a packet monitoring process has been well defined in this research work where different stages of packet monitoring have been properly outlined. The network monitoring process outlined in this research work is so flexible that can easily be modified for a different network architecture as per need. Conclusively, this research study proved handy to explore new analysis techniques grouped together under one platform "*ntop*" for taking informed network decision and network policies in the coming years.

REFERENCES

- [1] C. G. Bell, A. N. Habermann, J. McCredie, R. Rutledge, and W. Wulf, "Computer Networks," Computer (Long Beach, Calif.), 1970.
- [2] J. Yick, B. Mukherjee, and D. Ghosal, "Wireless sensor network survey," *Comput. Networks*, 2008.
- [3] P. M. Buscema, G. Massini, M. Breda, W. A. Lodwick, F. Newman, and M. Asadi-Zeydabadi, "Artificial neural networks," in *Studies in Systems, Decision and Control*, 2018.
- [4] R. M. Neal, "Pattern Recognition and Machine Learning," *Technometrics*, 2009.
- [5] J. Ahmad, H. Farman, and Z. Jan, "Deep Learning Methods and Applications," in *SpringerBriefs in Computer Science*, 2019.
- [6] A. L. Caterini and D. E. Chang, "Recurrent neural networks," in *SpringerBriefs in Computer Science*, 2018.
- [7] Y. Igarashi, T. Altman, M. Funada, and B. Kamiyama, "Computer Networks," in *Computing*, 2014.
- [8] J. Sen, "A survey on wireless sensor network security," *Int. J. Commun. Networks Inf. Secur.*, 2009.
- [9] N. M. M. K. Chowdhury and R. Boutaba, "A survey of network virtualization," *Comput. Networks*, 2010.
- [10] M. A. Mahmood, W. K. G. Seah, and I. Welch, "Reliability in wireless sensor networks: A survey and challenges ahead," *Computer Networks*, 2015.
- [11] M. A. Devmane and N. K. Rana, "Security issues of online social networks," in *Communications in Computer and Information Science*, 2013.
- [12] B. Galloway and G. P. Hancke, "Introduction to industrial control networks," *IEEE Commun. Surv. Tutorials*, 2013.
- [13] R. Zhang, J. Q. Chen, and C. A. Jaejung Lee, "Mobile commerce and consumer privacy concerns," *J. Comput. Inf. Syst.*, 2013.
- [14] V. Paxson, "Bro: A system for detecting network intruders in real-time," *Comput. Networks*, 1999.
- [15] M. A. Kafi, Y. Challal, D. Djenouri, M. Doudou, A. Bouabdallah, and N. Badache, "A study of wireless sensor networks for urban traffic monitoring: Applications and architectures," in *Procedia Computer Science*, 2013.
- [16] M. A. Kafi, Y. Challal, D. Djenouri, A. Bouabdallah, L. Khelladi, and N. Badache, "A study of wireless sensor network architectures and projects for traffic light monitoring," in *Procedia Computer Science*, 2012.
- [17] G. Padmavathi and D. Shanmugapriya, "A Survey of Attacks, Security Mechanisms and Challenges in Wireless Sensor Networks," *J. Comput. Sci.*, 2009.
- [18] A. Cecil, "A Summary of Network Traffic Monitoring and Analysis Techniques," in *Computer Systems Analysis*, 2006.
- [19] A. K. Marnerides, A. Schaeffer-Filho, and A. Mauthe, "Traffic anomaly diagnosis in Internet backbone networks: A survey," *Computer Networks*, 2014.
- [20] F. Olivier, G. Carlos, and N. Florent, "New Security Architecture for IoT Network," *Procedia Comput. Sci.*, 2015.
- [21] X. Laisheng, P. Xiaohong, W. Zhengxia, X. Bing, and H. Pengzhi, "Research on traffic monitoring network and its traffic flow forecast and congestion control model based on wireless sensor networks," in *2009 International Conference on Measuring Technology and Mechatronics Automation, ICMTMA 2009*, 2009.
- [22] S. Lee, K. Levanti, and H. S. Kim, "Network monitoring: Present and future," *Computer Networks*, 2014.
- [23] E. Marín-Tordera, X. Masip-Bruin, J. García-Almiñana, A. Jukan, G. J. Ren, and J. Zhu, "Do we all really know what a fog node is? Current trends towards an open definition," *Comput. Commun.*, 2017.
- [24] H. Zhang, Y. Xiao, S. Bu, D. Niyato, F. R. Yu, and Z. Han, "Computing Resource Allocation in Three-Tier IoT Fog Networks: A Joint Optimization Approach Combining Stackelberg Game and Matching," *IEEE Internet Things J.*, 2017.
- [25] E. Vaadia and N. Birbaumer, "Grand challenges of brain computer interfaces in the years to come," *Front. Neurosci.*, 2009.
- [26] V. Mohan, Y. R. J. Reddy, and K. Kalpana, "Active and Passive Network Measurements : A Survey," *Comput. Sci. Inf. Technol.*, 2011.
- [27] J. Wang, *Computer Network Security Theory and Practice*, 2009.
- [28] A. Forkosh-Baruch and A. Hershkovitz, "A case study of Israeli higher-education institutes sharing scholarly information with the community via social networks," *Internet High. Educ.*, 2012.
- [29] T. Govindasamy, "Successful implementation of e-Learning Pedagogical considerations," *Internet High. Educ.*, 2001.
- [30] R. J. C. Chu and C. C. Tsai, "Self-directed learning readiness, Internet self-efficacy and preferences towards constructivist Internet-based learning environments among higher-aged adults," *J. Comput. Assist. Learn.*, 2009.
- [31] E. D. Cassidy, A. Colmenares, G. Jones, T. Manolovitz, L. Shen, and S. Vieira, "Higher education and emerging technologies: Shifting trends in student usage," *J. Acad. Librariansh.*, 2014.
- [32] C. Jones and B. Shao, "The Net Generation and Digital Natives Implications for Higher Education," *High. Educ. Acad.*, 2011.
- [33] A. Y. Noaman, A. H. M. Ragab, A. I. Madbouly, A. M. Khedra, and A. G. Fayoumi, "Higher education quality assessment model: towards achieving educational quality standard," *Stud. High. Educ.*, 2017.
- [34] M. H. Harun, "Integrating e-Learning into the workplace," *Internet High. Educ.*, 2001.
- [35] H. E. Institutes, "A Framework for Supporting Adults in Distance Learning," *Adult Learn. Irish J. Adult Community Educ.*, 2004.
- [36] J. B. Roberts, L. A. Crittenden, and J. C. Crittenden, "Students with disabilities and online learning: A cross-institutional study of perceived satisfaction with accessibility compliance and services," *Internet High. Educ.*, 2011.
- [37] A. P. Rovai, "A practical framework for evaluating online distance education programs," *Internet High. Educ.*, 2003.
- [38] L. Shen, T. Manolovitz, G. Griffin, J. Britsch, E. D. Cassidy, and L. Turney, "Higher Education and Emerging Technologies," *Ref. User Serv. Q.*, 2013.

- [39] P. Krish, S. Hussin, M. R. Manap, and Z. Amir, "Mobile learning readiness among Malaysian students at higher learning institutes," *Asian Soc. Sci.*, 2012.
- [40] A. Kukulska-Hulme, "How should the higher education workforce adapt to advancements in technology for teaching and learning?," *Internet High. Educ.*, 2012.
- [41] K. Bohle Carbonell, A. Dailey-Hebert, and W. Gijsselaers, "Unleashing the creative potential of faculty to create blended learning," *Internet High. Educ.*, 2013.
- [42] A. Usman, "The Impact of Service Quality on Students' Satisfaction in Higher Education Institutes of Punjab," *J. Manag. Res.*, 2014.
- [43] R. Jain, G. Sinha, and S. Sahney, "Conceptualizing service quality in higher education," *Asian J. Qual.*, 2011.
- [44] S. Hussin, M. Radzi Manap, Z. Amir, and P. Krish, "Mobile Learning Readiness among Malaysian Students at Higher Learning Institutes," *Asian Soc. Sci.*, 2012.
- [45] R. Afreen, "Bring Your Own Device (BYOD) in Higher Education: Opportunities and Challenges," *Int. J. Emerg. Trends Technol. Comput. Sci.*, 2014.
- [46] J. J. Kidwell, K. M. V. Linde, and S. L. Johnson, "Knowledge Management Practices in Higher Education," *Educ. Q.*, 2000.
- [47] S. Akhuria, "Wireshark," *Jar. Komput.*, 2013.
- [48] J. F. Kurose and K. W. Ross, "Wireshark Lab: Getting Started," *Comput. Networking A Top - Down Approach*, 2010.
- [49] U. Banerjee, A. Vashishtha, and M. Saxena, "Evaluation of the Capabilities of WireShark as a tool for Intrusion Detection," *Int. J. Comput. Appl.*, 2010.
- [50] P. T. Files, "Wireshark Network Analysis The Official Wireshark Network Analyst Study Guide," *Analysis*. 2010.
- [51] Gupta, Udit. "Monitoring in IOT enabled devices." *arXiv preprint arXiv:1507.03780* (2015).
- [52] Kokila, S., A. Sathish, and R. Shankar. "Comparative Analysis of Internet Traffic Identification Methods." In *Proceedings of the UGC Sponsored National Conference on Advanced Networking and Applications*. 2015.
- [53] Nilsson, Samuel, and Joakim Eriksson. "Estimating Application Energy Consumption Through Packet Trace Analysis." (2014).
- [54] Antichi, Gianni, Stefano Giordano, David J. Miller, and Andrew W. Moore. "Enabling open-source high speed network monitoring on NetFPGA." In *2012 IEEE Network Operations and Management Symposium*, pp. 1029-1035. IEEE, 2012.
- [55] García-Dorado, José Luis, Felipe Mata, Javier Ramos, Pedro M. Santiago del Río, Victor Moreno, and Javier Aracil. "High-performance network traffic processing systems using commodity hardware." In *Data traffic monitoring and analysis*, pp. 3-27. Springer, Berlin, Heidelberg, 2013.
- [56] Leung, C. M., and John A. Schormans. "Measurement-based traffic characteristic estimation for QoS-oriented IP networks." *JOURNAL-COMMUNICATIONS NETWORK* 1, no. 2 (2002): 14-18.

Achieving Flatness: Honeywords Generation Method for Passwords based on User Behaviours

Omar Z. Akif¹

Department of Computer
College of Education for Pure Science (Ibn al-Haitham)
University of Baghdad
Iraq, Baghdad

Ann F. Sabeeh²

Department of Computer
College of Education for Pure Science (Ibn al-Haitham)
University of Baghdad
Iraq, Baghdad

G. J. Rodgers³

Department of Mathematics
College of Engineering, Design and Physical Sciences
Brunel University London
Uxbridge, London, UK

H. S. Al-Raweshidy⁴

Electronic and Computer Engineering Department, WNCC
College of Engineering, Design and Physical Sciences
Brunel University London
Uxbridge, London, UK

Abstract—Honeywords (decoy passwords) have been proposed to detect attacks against hashed password databases. For each user account, the original password is stored with many honeywords in order to thwart any adversary. The honeywords are selected deliberately such that a cyber-attacker who steals a file of hashed passwords cannot be sure, if it is the real password or a honeyword for any account. Moreover, entering with a honeyword to login will trigger an alarm notifying the administrator about a password file breach. At the expense of increasing the storage requirement by 24 times, the authors introduce a simple and effective solution to the detection of password file disclosure events. In this study, we scrutinise the honeyword system and highlight possible weak points. Also, we suggest an alternative approach that selects the honeywords from existing user information, a generic password list, dictionary attack, and by shuffling the characters. Four sets of honeywords are added to the system that resembles the real passwords, thereby achieving an extremely flat honeywords generation method. To measure the human behaviours in relation to trying to crack the password, a testbed engaged with by 820 people was created to determine the appropriate words for the traditional and proposed methods. The results show that under the new method it is harder to obtain any indication of the real password (high flatness) when compared with traditional approaches and the probability of choosing the real password is $1/k$, where k = number of honeywords plus the real password.

Keywords—Honeywords; user behaviours; worst password list; dictionary attack

I. INTRODUCTION

When any user wants to access a network for security purposes, he or she is prompted to enter credentials [1]. A password is the popular authentication technique being used today despite many newer ones, such as biometric based techniques and dual factor authentication [2]. Users tend to use small simple passwords and for this reason as well as their somewhat universal use, they are vulnerable to being compromised. Hence, it has become important to make progress in combatting cracking techniques [3]. Since these

are becoming increasingly sophisticated, has become a salient issue [4].

Intruders are increasingly eavesdropping on communication between legitimate users and servers as well as masquerading as authorised users or remote servers so as to be able to steal sensitive information [5]. A good password has to have two features: a user can remember it and it is difficult to guess [6]. Unfortunately, these two work against each other such that a password that is easy to remember is generally short and hence, easy to guess. Moreover, most people choose to use a single password for multiple accounts, because one is easy to remember. Invariably, people have a hierarchy of passwords, for example, they do not use the same password for email as they do for their bank account [7], in particular, because the bank requires more stringent security.

The idea behind honeywords is to create a relation between the real password and decoy hashed passwords, such that for every user the latter look like real passwords. The honeywords are these decoys. An attacker can recognise the presence of honeywords in a password file, as it is very unusual to have multiple passwords for a single user account. However, even if the attacker can crack multiple passwords associated with a user, he or she does not know which are honeywords, and which are the real ones [8]. What is the main focus of honeywords generation is the way in which they are produced. Currently, there are some problems regarding this, which are discussed later in this paper and a new generation method will be proposed to overcome these.

II. RELATED WORK

Passwords are especially vulnerable to hash chain based and effective dictionary attacks. A sample of 19 million passwords, of different lengths, available online, have been studied according to the distribution of the symbols in the password strings. The results have shown that the native language of the user can affect the distribution of symbols in passwords [9].

Hashing the plaintext or password is a one-way function, which makes it hard to find the required password [10]. However, rainbow tables, which are massive tables filled with hash values and can be used to find a required password, whereby a hacker employs them to find the password by reversing the hashing function. Despite of a rainbow table taking up a lot of storage when holding it, attackers can usually crack the password in a shorter amount of time than when applying the brute force technique [11].

Most existing biometric template protection schemes (BTPS) do not offer as strong security as cryptographic tools. Moreover, they are unable to determine whether or not a probe template has been downloaded the database by an imposter or an authentic user. Consequently, the “honeywords” idea was proposed to detect the cracking of hashed password databases. In particular, an extra layer of protection is needed with biometric feature schemes, as these have been shown to be flawed. A honey template protection scheme relating to faces has been proposed and evaluated as representing an improvement on existing schemes [12].

Many researchers have pointed out that most password hashes are not safe against hackers and hence, the method of honeywords (decoy passwords) has been used to detect attacks against hashed password databases. Furthermore, cracking hashed passwords has become easier for an intruder, who wants to enter the account through an authenticated user. In addition, a user’s password can be recovered by an intruder through using a brute-force attack on the hashed password. A user’s real password can be distinguished among honeywords for each user by using a secure server called a “honeychecker”, which triggers an alarm when a honeyword is used. [13].

III. REVIEW OF HONEYWORDS

The concept of honeywords is to provide a technique to detect whether an intruder into password files has been originally invited in. Essentially, the scenario of honeywords is based on any user u_i being provided with a list of k called “sweetwords”, which are denoted as $W_i = \{w_1, w_2, w_3, \dots, w_k\}$. One of these sweetwords (for instance w_j) is the right user’s password, while the rest of the list ($k - 1$) are fake and called *honeywords*. The main architecture feature is a new server, “the honeychecker”, which contains a database, for each user u_i and the index $c(i) = j$, where $w_j \in W_i$ is the correct password of u_i . The right password is referred to as the “real” password in line with the person who introduces honeywords.

The real password of the authorised user will be generated and entered during the registration stage, while on the basis of such a password; the system generates and adds ($k - 1$) honeywords. Moreover, the honeywords generation algorithm is targeted at creating decoy passwords that are the same as the real one, so that an intruder will not be able to recognise them from the real password. Accordingly, the system chooses a random $1 \leq j \leq k$, gives the real password to w_j and populates the set W_i with the generated honeywords. Finally, the password along with the honeywords are “hashed” and saved in the password file in the form $H_i = \{h_1 =$

$\text{hash}(w_1), \dots, h_k = \text{hash}(w_k)\}$, while the index $c(i) = j$ is stored by the honeychecker.

TABLE I. RELATED NOTATION

Notations	Meaning
u_i	i^{th} user in system
P_i	password of i^{th} user
W_i	Tuple of passwords stored for u_i
k	Number of elements in W_i
$c(i)$	index of correct password in W_i
sweetword	each element of W_i

When u_i logs-in the system, he or she should enter the password and then, the system will check $\text{hash}(p)$ against each hashed sweetword in H_i . If the password that has been entered does not match with any elements of H_i , the connection is rejected. In contrast, let j be such that $\text{hash}(p) = h_j$, then the pair u_i, j will be sent to the honeychecker. Hence, if $j = c(i)$, then the authentication succeeds, and the honeychecker will send back its “approval”, whilst otherwise an alarm is triggered, as the password file has probably been attacked. Table I illustrates the related notation [14].

IV. LIMITATIONS OF HONEYWORDS

Despite of the fact that current honeyword based methodologies can provide security against brute force attacks, they do have some limitations, are described below.

1) *Co-relational hazard*: If a relationship exists between the username and password, then the real password of the user can easily be recognised from the list W_i . In such cases honeywords cannot protect the original password, because of this association.

2) *Distinguishable well-known password patterns*: If a user chooses a password linked to some well-known object/fact, then an adversary can simply recognise the real password. For example, some of the passwords belonging to this category are bond007, james007, 007bond and 007007, which were found in a list of 10,000 most common passwords (these will be used to generate the honeywords in this paper).

3) *Issue related to DoS resistivity*: If an adversary knows the real password of the user, then he or she can recognise the honeywords and then, can intentionally submit honeywords to produce a false negative feedback signal by the “honeychecker”. If the adversary obtains these honeywords from several accounts, then all the web server may become blocked. This is known as a Denial-of-Service (DoS) attack and the real password of user should be not giving any knowledge about system generated honeywords to avoid one.

4) *The issue relating to multiple system vulnerability*: If a user uses the same password in two (or more) different systems, and if two systems are employing the same honeyword generation algorithm, when an adversary gets access to both systems, then Multiple System Vulnerability can occur. In this case, the adversary may obtain two lists of

W_i for the user u_i . Let $W_i^{S_j}$ refer to the list of sweetwords for user u_i in the system S_j . So, if honeywords that have been generated belong to $W_i^{S_p}$ and $W_i^{S_q}$ (where $p \neq q$) are different (probability of which is close to 1), then by performing the connection operation $W_i^{S_p} \cap W_i^{S_q}$ the unauthorised user can obtain the real password. This is known as Multiple System Vulnerability (MSV) of the honeyword based authentication technique [15].

V. PASSWORD ATTACKS

Password attacks include different character combinations being tried until a match with the correct password is found. There are several types of password attacks, some of the most important of which are described next.

1) *Brute force attacks*: In this type of attack, all the possible combinations of the password are applied to break it. It can also be applied to crack encrypted passwords wherever they are saved in the form of encrypted text [16].

2) *Dictionary attack*: A dictionary attack is applied to verification data by trying every word in the dictionary. This kind of attack is targeted at sites with a high probability of success, such as those with weak passwords or with only a few key combination numbers. This attack is faster than an attack of brute force and is more successful when a weak, public or short password is used [17].

3) *Phishing attack*: This is where an attacker attempts to retrieve legitimate users' confidential and sensitive credentials fraudulently by mimicking electronic communications from a trustworthy or public organisation in an automated fashion. The aim of phishing is to steal sensitive information, such as online banking passwords and credit card information from Internet users [18]. These attacks use a combination of social engineering and technical spoofing techniques that persuade users into giving away sensitive information that the attacker then uses to make a financial profit [19].

4) *Password guessing attack*: In this attack, the adversary steals the file of the password from the main server, and also obtains plaintext passwords by reversing the hash values detected [20].

VI. PERSONAL INFORMATION IN PASSWORDS AND HUMAN BEHAVIOURS

A text-based password is the most common authentication method and is likely to remain so for the foreseeable future. Whilst users have been recommended different types of authentication mechanisms, passwords are still considered the best way to protect access to a system. That is, none of the alternative technique can provided all the benefits of passwords without introducing extra burden to the users. However, passwords have been criticised as being one of the weakest techniques in relation to authentication. One of the key reasons for this weakness can be put down to the limitations of the human memory. For, as a consequence, most passwords rather than being real random strings and hence, quite strong, are simple so they are easy to remember [21].

Basically, people prefer to create passwords according on their personal information, because of the limitation of their memory capacity and a random password can be difficult to remember [22]. From the other side, some people have exceptional skills when it comes to predicting human behaviour and they use these skills to launch attacks through password hacking this can cause serious problems, which have become the focus of much research [23].

VII. LIST OF THE WORST PASSWORDS

Not only do most users create an easy password because they can easily remember it, for they often also use the same one in several systems. Whatever the case, frequently they are easy to guess by the intruder. A list of the 500 worst passwords has been created by researchers to help users avoid selecting them. Unfortunately, one in nine users employ one from this list and one in 50 use a password from the top 20 [24].

VIII. HONEYWORDS GENERATION METHODS AND DISCUSSION

In this section, some of the honeywords generation methods are discussed.

1) *Chaffing-by-tweaking*: This method involves tweaking the real password by selecting the character positions that will be tweaked to produce the honeywords, so the user password will be the seed of the generator algorithm. The same type of character will be selected: letters are replaced by letters, digits by digits, and special characters by special characters. For instance, when $t = 3$ and the last t characters have been selected for tweaking, the method for the generator algorithm is $Gen(k, t)$. While another approach called "*chaffing-by-tweaking-digits*" is carried out by tweaking the last t positions that contain digits. For instance, if the last algorithm has been used, then for the password *42hungry* and $t = 2$, the honeywords *12hungry* and *58hungry* may be generated.

Remark 1. Most people prefer to choose the numbers involved in passwords relating to a special date (birthday, anniversary or an important historical event). For this reason, it is highly probable that such a password includes a digit sequence like *19xx*, *20xx* or *xx*, where *xx* represents the last two digits of the date. Hence, for those passwords that involve applying the *chaffing-by-tweaking-digits* method, the date digits will be replaced with randomly selected digits. Basically, an adversary will recognise the true password easily among the honeywords. For example, assume the honeywords are generated with $t = 4$ and $k = 9$ for the password *alex1992*. It can clearly be seen that the digits in the honeywords do not relate to a specific date and hence the correct password, *alex1992*, is logically deducible by an adversary [25].

alex6323 alex9058 alex1992
alex1270 alex0976 alex2785
alex5469 alex8147 alex9705

2) *Chaffing-with-a-password model*: In this technique, the generator algorithm takes the password from the user, and then a probabilistic model of the original passwords is relied

- 4- This type of honeywords is made by shuffle and then some letters or digits from the ID user mixed. Subsequently, the real password together with some digits and letters are generated to be inserted in the honeywords, with meaningless words then being generated. In this step, 10 honeywords are created (This group is called G4).

Special cases

- 5- If there is a special character(s) included in the password, then the honeywords will contain the same number of these generated randomly.
- 6- The number of upper case letters in the password will equal the number in the honeywords.
- 7- If there are two words the same in list W_i for the user u_i , then the algorithm explained in Fig. 2 will be applied. Basically, if the original password is one of these two words then the honeyword will be replaced

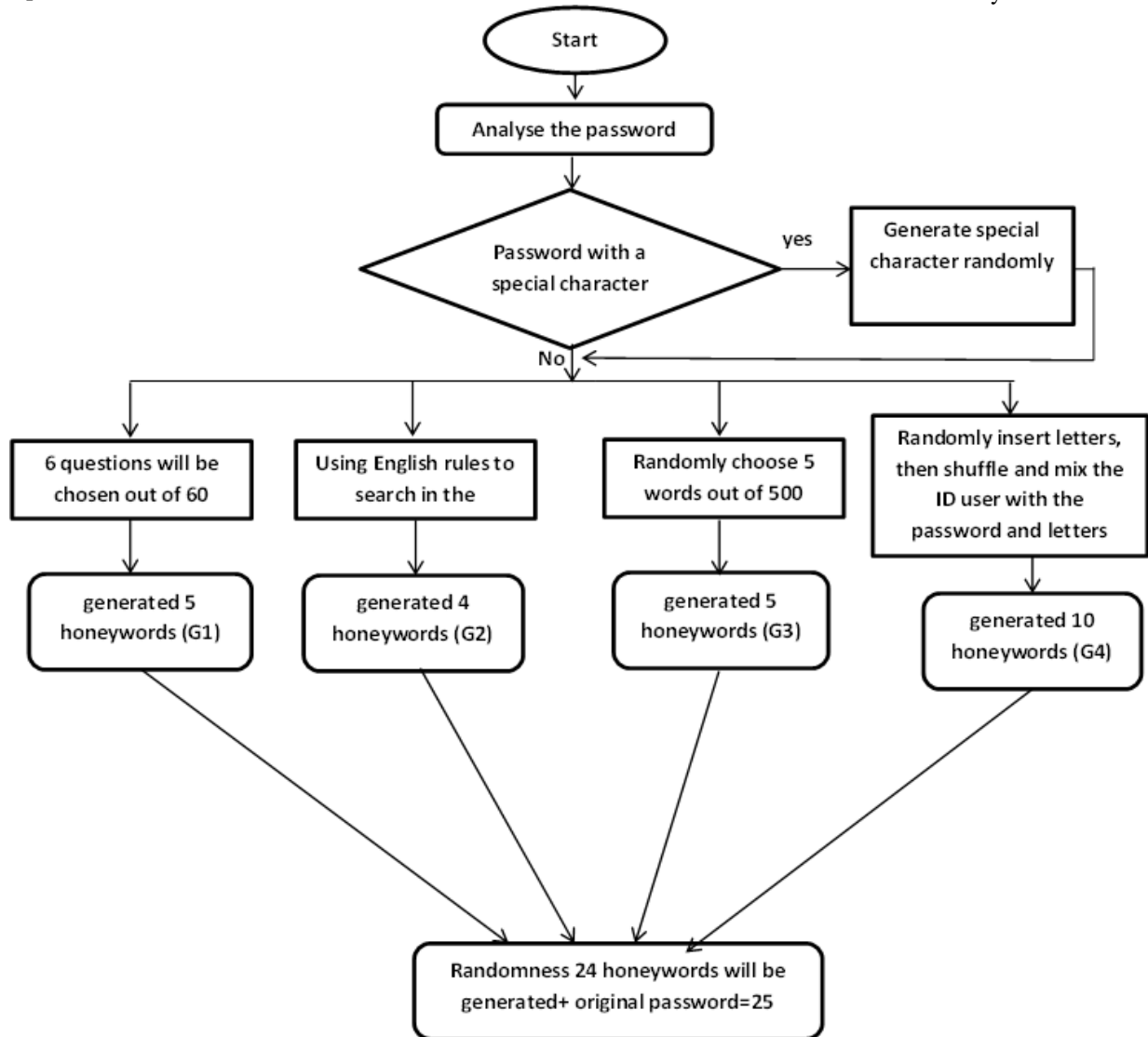


Fig. 1. Illustration of the Whole Structure of the Proposed Honeywords Generation Method.

XI. ANALYSIS OF THE SECURITY OF THE PROPOSED GENERATION METHOD: DENIAL OF SERVICE ATTACK

Using the proposed method will partially reduce the number of DoS attacks, but this is an improvement on current method, because it provides greater resistance, that is, increasing the flatness in the list of honeywords and the real password W_i makes the proposed method stronger than the traditional methods against these attacks. Because w_j in W_i

can be either a honeyword or the real password, the flatness will make the attacker confused when trying to guess the real one. In the existing methods, an attacker has to know how the honeywords pertaining to a particular password have all been generated by random tweaking, which is possible and then he/she can run a DoS attack. With the proposed method the honeywords are generated according to several procedures, and not randomly.

XII. ANALYSING THE FLATNESS IN THE NEW HONEYWORDS GENERATING METHOD

The flatness in the proposed method and how an adversary tries to analyse the honeywords in W_i for each u_i is discussed in this section. Obviously, the adversary does not have any predefined information about the password; however, he/she will try to analyse W_i to find any information about c_i . The honeywords created in this first group are associated with personal questions will most probably lead to personal answers. In this case, six answers, which are either in letter or digit form and the letters and digits are then randomly mixed to produce five honeywords. The high level of association of these honeywords with a user u_i 's real answers will make it difficult for the adversary to identify which one is the real password, i.e. this increases the flatness. In contrast, the traditional methods do not take into consideration whether there is a personal password, because all the honeywords are generated by tweaking some letters or digits in the real password.

It is clear that *chaffing-by-tweaking* has many problems; the first relates to when a digit is replaced by another. That is, generation of a honeyword does not relate to the human dates, starting either with 19xx or 20xx. The second problem is that not only is the digits tweaking easily recognised by the adversary, but also, he/she can be easily find the password when letters are replaced. For instance, when $t=3$, this means three letters will be replaced randomly by others, which results in the meaning of the original password not being present in the honeywords and hence they are completely distinct from the former. So, recognising the original password, which is the meaningful word among meaningless ones, will be very easy. For these reasons, the first group has been generated based on personal information, because most users continue to use this when they create their passwords.

Dictionary attacks are commonly used to break passwords, but in the proposed method they are used to generate the honeywords. Such an attack involves most of the passwords that have been created by users around the world, by using an algorithm based on English language rules to make the search in this dictionary to find honeywords very close to the original password. This algorithm tries to find words in the dictionary attack with the most same letters or digits with up to plus or minus three characters or digits. The first priority to find the different words will be regarding the digits if they are present, otherwise the four words with the closest letter sounds to the actual password are applied. For example, **ch** is mostly pronounced either as /k/, as in **character**, **chord**, or as /tʃ/, as in **chicken**, **chest**. Almost all words containing “chi” or “che” are pronounced with /tʃ/ (note exceptions like “chiropractor” /ˈkaɪrəʊpræktə/ **kaay**-roh-præk-tə and “chemistry” /ˈkɛmɪstri/ (**kem**-ist-ree), but there’s no reliable rule for “cha”, “cho”, and “chu”. The main benefit of using a dictionary attack is that all the honeywords that will be chosen are real passwords generated by users in the past, so the flatness will be very high in this group of honeywords as well.

As aforementioned, there are some passwords that are used commonly by users and researchers have collated them into one list, calling it the worst passwords in the world. Choosing

some of them randomly and making a combination of them is a popular procedure for adversaries. Consequently, group three will be generated according to this list.

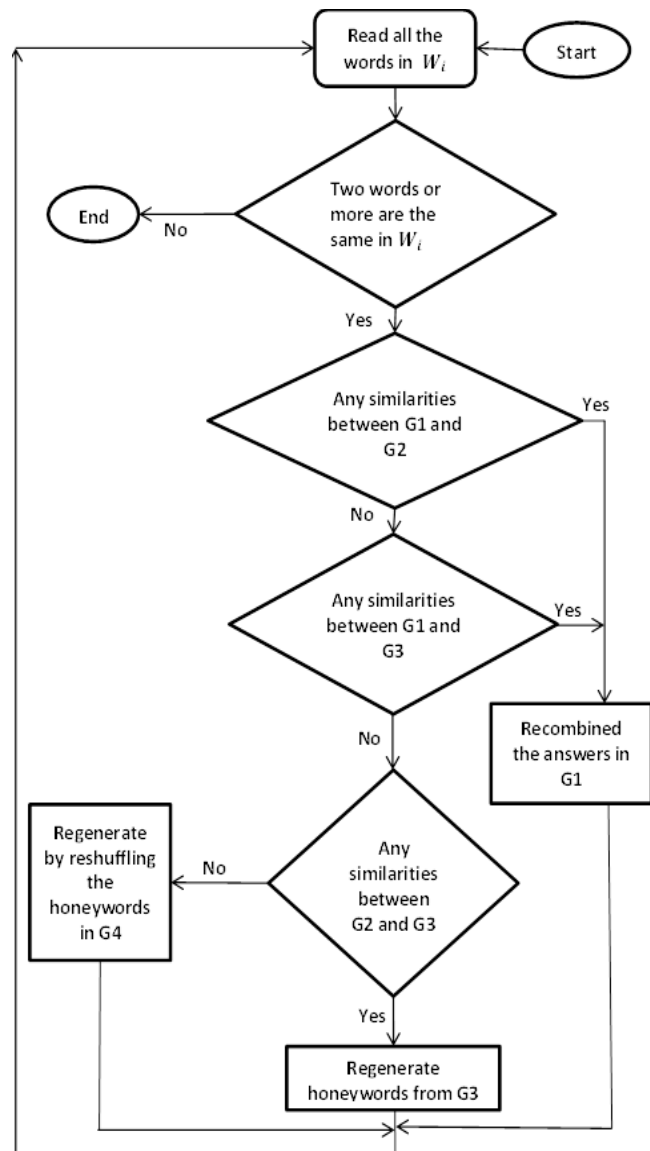


Fig. 2. Illustration of the Algorithm when Two or more Honeywords are the Same in W_i .

In addition, a minority of users have a strong password, whereby they select some letters randomly and create a meaningless one. However, most users in this group still select letters or digits from their names and/or personal dates. To avoid these types of passwords, with the proposed method and the goal of flatness, the fourth group is created. Some characters are chosen from the original password and ID and then some digits and letters are generated randomly to be inserted in the honeywords.

XIII. DISCUSSION ON ATTACKS ON THE NEW METHOD

Table II illustrates how an attacker could compromise the password by nominating some words from the honeywords table and then, analysing the results.

TABLE II. DISCUSSION ON THE TYPES OF ATTACKS AGAINST PASSWORDS

	Good Password	Personal Password	Generic Password
Dictionary Attack	Not Working	Not Working	Not Working
Brute-Force Attack	Not Working	Not Working	Not Working
Password Guessing Attack	If the attacker chooses all good honeywords with the password, then he/she will obtain 11 words, one of which is the real password (1/11). In addition, If the attacker is going to choose just the meaningful words, he will obtain 14 words and fortunately the real password is not one of them (0/14). This type of password is not popular, because most users prefer to use passwords are easy to remember.	If the attacker chooses just the meaningful words. he/she will obtain 15, among which the real password will be included. However, the flatness is very high because the honeywords are coming from real passwords lists; some of them relating to the user, some of them chosen from the dictionary attack and the final set is chosen from the public list of passwords (1/15). As a result, the guessing method will be chosen by the attacker..	If the attacker chooses just the meaningful words, he will obtain 15, among which the real password will be included. However, the flatness is very high because the honeywords are coming from real passwords lists, some of which are related to the user, some are chosen from the dictionary attack, and the final set is selected from the public list of passwords (1/15). As a result, the guessing method will be chosen by the attacker.
Clever Attacker	If the attacker chooses all good honeywords with the password, then he/she will obtain 11 words, one of which is the real password (1/11). In addition, If the attacker is going to choose just the meaningful words he will obtain 14 words, but fortunately the real password is not one of them (0/14). This type of password is not popular to be used due to most users are prefer to use passwords are easy remembering.	If the attacker chooses just the meaningful words, he/she will obtain 15, among which the real password will be included. However, the flatness is very high, because the honeywords are coming from real passwords lists, some of which are related to the user, some are chosen from the dictionary attack and the final set is selected from the public list of passwords (1/15). Now the attacker has just one choice, which is to try to analyse the words and nominate some of them as real password.	If the attacker chooses just the meaningful words, he will obtain 15, among which the real password will be included. However, the flatness is very high, because the honeywords are coming from real passwords lists, some of which are related to the user, some of them are chosen from the dictionary attack, and the final set was chosen from the public list of passwords (1/15). Now the attacker has just one choice, which is to try to analyse the words and nominate some of them as real password.

XIV. TESTBED AND RESULTS

It is a difficult to measure how people are thinking when they are creating a password, because it depends on unpredictable user behaviour. To address this, a testbed engaged with by 820 people was developed to determine whether users can recognise the real password among honeywords. The scenario involved dividing the passwords into three groups: good, personal, and generic. Then, the participants were provided with the W_i , and ask to nominate words that could be passwords, this column being titled "nomination". The idea behind this step was to ascertain how many people would nominate the real password among the honeywords, and how many words they would choose amongst which they believed the password would be found. Having chosen their words, they were asked to identify the single one that they thought was the real password and if they got it wrong then Intrusion Detection System IDS would trigger attempted intrusion, but if successful access was granted. The first type, namely the good password, was strong, being created with random letters, digits, and special characters. The results showed that this type of password is very strong, as most people who participated in the testbed

experiment did not choose it among the honeywords, i.e. no one was able to guess the real password when it was good and random.

The second type of password is the personal password, which was created based on information relating to the users. The testbed revealed that the new method is better than the traditional methods. Finally, with the same scenario, the third type of password, i.e. the generic password, was applied.

Fig. 3 illustrates the results of the strong password for the new method, with the total nominated representing how many words the participants chose, while the frequency is how many people selected a particular amount of passwords. For example, the number of people who nominated 14 words was 224 (27.317%), whereas 11 words were nominated by 78 (9.512%). No one guessed the real password, even if they had nominated it, which shows it was very strong and flat.

Fig. 4 shows the results of the proposed method when the real password is the personal information type and clearly, the number of people who nominated the password amongst their choices increased, being 502 out of 820 (61.219%). Moreover, there were two people who guessed the correct password (0.244%).

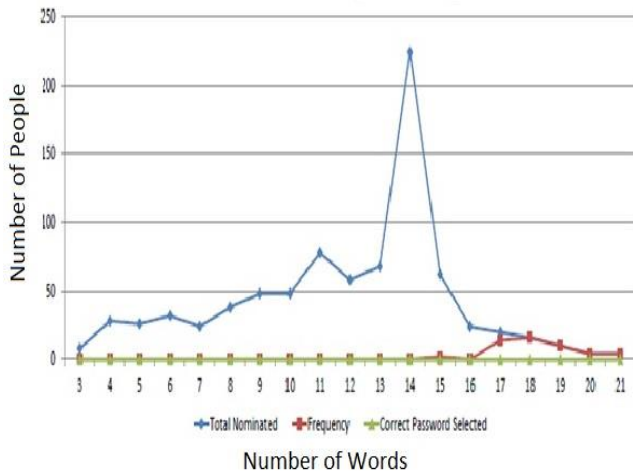


Fig. 3. The Results of the Proposed Method when a Strong Password was Applied.

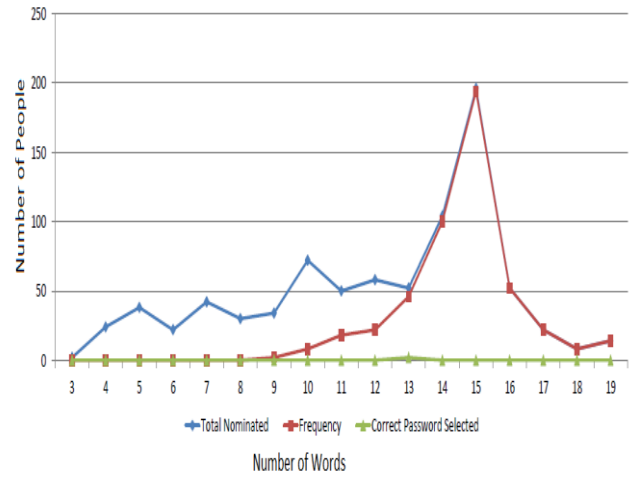


Fig. 5. The Testbed Results for the Proposed Method when the Real Password is Generic.

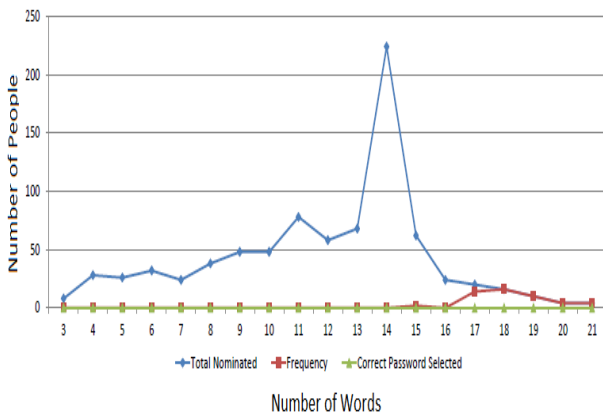


Fig. 4. The Testbed Results when the Real Password Contained Personal Information.

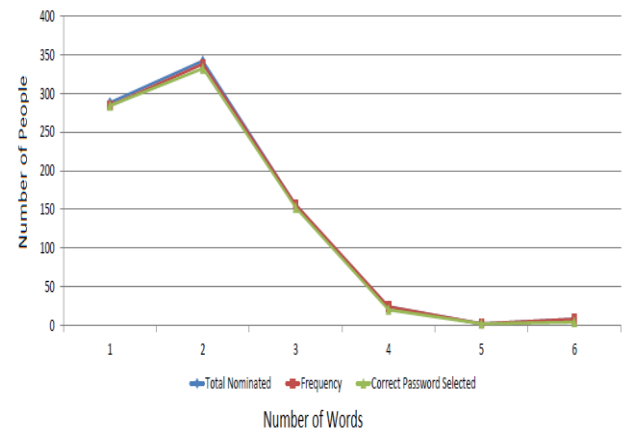


Fig. 6. The Testbed Results for the Traditional Method of "Chaffing-by-Tweaking".

Fig. 5 illustrates the new method when a generic password was the real password and the results show that this type provides the worst outcomes of the three, but the new method still gives better results than with the traditional one. Specifically, the total number who chose this password was 630 out of 820 (76.829%), and it was guessed correctly 21 times (2.561%). This implies that most attackers focus on generic words.

In Fig. 6, showing the outcomes when Chaffing-by-Tweaking was applied in the testbed, it is clear that the number of participants guessing the real password was very high, standing at 794 times out of 820 (96.829%), whilst the number who nominated was 812 (99.024%). Moreover, most people nominated just one or two words out of 25 (3.048%) in W_i and no one nominated more than six, which suggests that many were confident they from the beginning which was the correct password.

In Fig. 7, the results for the traditional method of Chaffing-by-Tweaking-Digits are shown. This method provides slightly better results than Chaffing-by-tweaking in that the password was guessed correctly 756 times out of a possible 820 (92.195%). To give an example of how the proposed method generates the honeywords, in Table III the password is "Ujemgzae91#e". Clearly, the first row contains honeywords generated based on personal information, while the second row has those created based on the worst passwords list. The rest of the table was generated by shuffle the letters and digits. A dictionary attack was not used in this table, because no word is similar this password.

Table IV illustrates an example when the testbed was applied with the generic password, "password222", being drawn from the list of worst passwords. The honeywords in the second row were generated based on a dictionary attack.

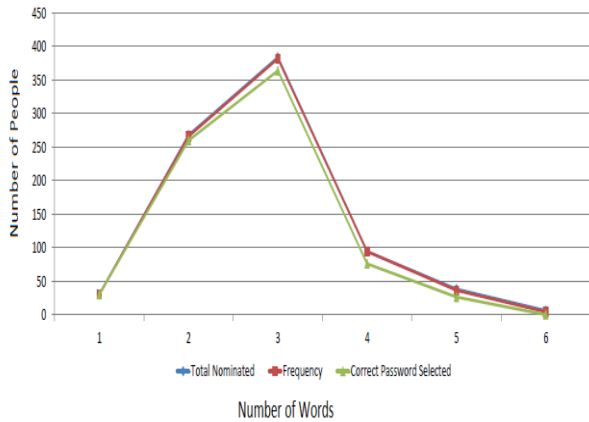


Fig. 7. The Testbed Results for the Traditional Method of "Chaffing-by-Tweaking-Digits".

TABLE III. TESTBED WITH THE NEW METHOD AND A GOOD PASSWORD

Prestol#70	Jordy\$86	Steves@75	Mechai1l\$81	Anna^1945
Liverpool@2005	Football&1234	Password*1111	Music@6666	bond@007
Booboo&75	Love&2014	Mustang@16	Zme1qo@55req	Epalm#1999ks
Pufna*37xy	Msac^hs31	Neadjg_69	Vlpheo\$10r	Kp#12zxme
Ltcbas!00j	Tg36\$ewba	Ujemgzae91#e	Rpnq#fxg	Lsczyr&12

TABLE IV. TESTBED WITH THE NEW METHOD AND A GENERIC PASSWORD

StationRoad1960	Church2016	Morgan2010	Stevs1958	Andy2000
Alunaliceza	Andralice2004	Anasialice1977	Anaalice85	Hello131313
Nicholas123	Andrew1212	Password222	Welcome777	Alice1974
ElArzd204	O9lefc7ss	Oxsr15dox	Z7erpmc0	Enm12q
Movxg20w	Qica12r00	Hvagjr4193	Nlpqroo1870	Zaqu2w88

XV. CONCLUSION

In this paper, a new honeywords generation method has been proposed. This method was developed to overcome the problems that exist with the traditional methods. The proposed method is based on personal information, dictionary attacks, the worst password list (generic passwords) and shuffling the characters. User behaviour is the underpinning principle the new method, because creation of the passwords differs from one user to another. Some limitations regarding the extant honeywords methods were mentioned in this have been discussed and these have been overcome by the proposed method have been explained. A testbed has been applied to obtain the results using 820 participants and these have shown that the new method is better than the traditional ones.

REFERENCES

- [1] S. M. Gurav et al., "Graphical password authentication: Cloud securing scheme," in 2014 International Conference on Electronic Systems, Signal Processing and Computing Technologies, 2014, pp. 479-483.
- [2] D. Mishra et al., "A secure password-based authentication and key agreement scheme using smart cards," Journal of Information Security and Applications, vol. 23, pp. 28-43, 8, 2015.
- [3] S. Houshmand, S. Aggarwal and R. Flood, "Next Gen PCFG Password Cracking," IEEE Transactions on Information Forensics and Security, vol. 10, pp. 1776-1791, 2015.
- [4] B. Gurung et al., "Enhanced virtual password authentication scheme resistant to shoulder surfing," in 2015 Second International Conference on Soft Computing and Machine Intelligence (ISCMI), 2015, pp. 134-139.
- [5] Siqiong Fan, Zhenfu Cao and Xiaolei Dong, "Cryptanalysis and improvement of a smart card-based identity authentication scheme," in ICINS 2014 - 2014 International Conference on Information and Network Security, 2014, pp. 152-157.
- [6] J. Ma et al., "A study of probabilistic password models," in 2014 IEEE Symposium on Security and Privacy, 2014, pp. 689-704.
- [7] S. M. Taiabul Haque, M. Wright and S. Scielzo, "Hierarchy of users' web passwords: Perceptions, practices and susceptibilities," International Journal of Human-Computer Studies, vol. 72, pp. 860-874, 12, 2014.
- [8] Dr. Ari Juels RSA, Professor Ronald L. Rivest MIT. Dr. Ari Juels RSA, Professor Ronald L. Rivest MIT., "For Stronger Password Security, Try a Spoonful of Honeywords," 2013.
- [9] D. Vishwakarma and C. E. V. Madhavan, "Efficient dictionary for salted password analysis," in 2014 IEEE International Conference on Electronics, Computing and Communication Technologies (CONECCT), 2014, pp. 1-6.
- [10] H. Kumar et al., "Rainbow table to crack password using MD5 hashing algorithm," in 2013 IEEE Conference on Information & Communication Technologies, 2013, pp. 433-439.
- [11] H. M. Ying and N. Kunihiro, "Decryption of frequent password hashes in rainbow tables," in 2016 Fourth International Symposium on Computing and Networking (CANDAR), 2016, pp. 655-661.
- [12] E. Martiri, B. Yang and C. Busch, "Protected honey face templates," in 2015 International Conference of the Biometrics Special Interest Group (BIOSIG), 2015, pp. 1-7.
- [13] M. J. Bhole, "Honeywords: A New Approach for Enhancing Security," International Research Journal of Engineering and Technology (IRJET), vol. 02, pp. 1563, 2015.
- [14] L. Catuogno, A. Castiglione and F. Palmieri, "A honeypot system with honeyword-driven fake interactive sessions," in 2015 International Conference on High Performance Computing & Simulation (HPCS), 2015, pp. 187-194.
- [15] N. Chakraborty and S. Mondal, "A New Storage Optimized Honeyword Generation Approach for Enhancing Security and Usability," arXiv Preprint arXiv:1509.06094, 2015.
- [16] A. Jesudoss and N. Subramaniam, "A SURVEY ON AUTHENTICATION ATTACKS AND COUNTERMEASURES IN A DISTRIBUTED ENVIRONMENT,".
- [17] E. I. Tatli, "Cracking More Password Hashes With Patterns," IEEE Transactions on Information Forensics and Security, vol. 10, pp. 1656-1665, 2015.
- [18] L. Wu, X. Du and J. Wu, "Effective Defense Schemes for Phishing Attacks on Mobile Computing Platforms," IEEE Transactions on Vehicular Technology, vol. 65, pp. 6678-6691, 2016.
- [19] I. Uusitalo, J. M. Catot and R. Loureiro, "Phishing and countermeasures in spanish online banking," in Emerging Security Information, Systems and Technologies, 2009. SECURWARE '09. Third International Conference On, 2009, pp. 167-172.
- [20] S. Kharod, N. Sharma and A. Sharma, "An improved hashing based password security scheme using salting and differential masking," in 2015 4th International Conference on Reliability, Infocom Technologies and Optimization (ICRITO) (Trends and Future Directions), 2015, pp. 1-5.

- [21] Y. Li, H. Wang and K. Sun, "A study of personal information in human-chosen passwords and its security implications," in IEEE INFOCOM 2016 - the 35th Annual IEEE International Conference on Computer Communications, 2016, pp. 1-9.
- [22] J. Bonneau, "The science of guessing: Analyzing an anonymized corpus of 70 million passwords," in 2012 IEEE Symposium on Security and Privacy, 2012, pp. 538-552.
- [23] M. Burnett, Perfect Password: Selection, Protection, Authentication. Syngress, 2006.
- [24] Available: <http://www.whatsmypass.com/the-top-500-worst-passwords-of-all-time>.
- [25] I. Erguler, "Achieving Flatness: Selecting the Honeywords from Existing User Passwords," IEEE Transactions on Dependable and Secure Computing, vol. 13, pp. 284-295, 2016.
- [26] Ibrahim Salim M. and T. A. Razak, "A study on IDS for preventing denial of service attack using outliers techniques," in 2016 IEEE International Conference on Engineering and Technology (ICETECH), 2016, pp. 768-775.
- [27] Z. Tan et al., "A System for Denial-of-Service Attack Detection Based on Multivariate Correlation Analysis," IEEE Transactions on Parallel and Distributed Systems, vol. 25, pp. 447-456, 2014.

Robust Recurrent Cerebellar Model Articulation Controller for Non-Linear MIMO Systems

Xuan-Kien Dang¹

Ho Chi Minh University of Transport
Ho Chi Minh City, Vietnam

Van-Phuong Ta²

HCMC University of Technology and Education
Ho Chi Minh City, Vietnam

Abstract—This research proposes a H^∞ robust recurrent cerebellar model articulation control system (RRCMACS) for MIMO non-linear systems to achieve the robustness of the system during operation. In this system, the superior properties of the recurrent cerebellar model articulation controller (RCMAC) are incorporated to imitate an ideal sliding mode controller. The H^∞ robust controller efficiently attenuates the effects of uncertainties, external disturbances, and noises to maintain the robustness of the system. The parameters of the controller were updated in the sense of the Lyapunov-like Lemma theory. Therefore, the stability and robustness of the system were guaranteed. The simulation results for the micro-motion stage system are given to prove the effectiveness and applicability of the proposed control system for model-free non-linear systems.

Keywords—Robust controller; MIMO non-linear systems; linear piezoelectric motor (LPM); recurrent network; Cerebellar model articulation controller

I. INTRODUCTION

Most of the practical applications are non-linear systems. The reason for this comes from the effects of friction and damping coefficients, cross-coupling, hysteresis phenomenon, and time-varying parameters [1-4]. The completely dynamic model of the practical systems can't be obtained. Therefore, the model-based controllers cannot achieve good performance for the non-linear MIMO systems [5-6].

To cope with the drawbacks of the model-based controllers, many modern controllers have been developed such as Fuzzy Logic Controller (FLC), Sliding Mode Controller (SMC), Neural Networks (NNs), and Cerebellar Model Articulation Controller (CMAC). In particular, the FLC was considered an effective control method for the uncertainties, free-model and non-linear systems. The essential property of the FLC is that the non-linear and uncertain parts are described as fuzzy sets and rules [7-9]. Consequently, the FLC overcomes the shortcomings of the model-based controllers in dealing with the non-linear, uncertainties systems. However, the performance of the FLC depends utterly on the selection of fuzzy sets and the number of rules. There are not specific methods that ensure the optimal selections of fuzzy sets and rules for the controllers so far. To achieve good performance for the practical applications, the fuzzy sets and rules were mostly selected by trial and error.

To deal with the effects of uncertainties, disturbances, and noises in non-linear systems, the SMC was developed and applied [10-11]. The SMC guarantees response of the system becomes insensitive to disturbances and noise in the sliding phase. Consequently, the robustness of the system can be guaranteed. The disadvantages and limitations of the SMC are the chattering phenomena and the selection of the boundary of uncertainties or disturbances. These problems are serious difficulty and impossible tasks in realistic applications.

Along with the SMC, the neural network (NN) was used to approximate non-linear functions to arbitrary precision. Therefore, it has been proposed for dealing with non-linear systems and obtained good results in realistic applications [12-13]. The NNs, however, have shortcomings that attracted much attention from the researchers so far. In particular, all weights in the structure of the neural network are updated each learning cycle, this is unsuitable for the problems requiring real-time learning; the selection of the number of neurons and hidden layers to achieve good performances is very difficult to obtain in the practical applications.

In recent decades, the Cerebellar Model Articulation Controller (CMAC) has been developed and adopted for the complex non-linear MIMO systems due to it has superior properties to NNs [14-17]. To improve learning capability and dynamic response of the CMAC, the wavelet function and recurrent technique were incorporated into the CMAC to improve the performance of the system [18].

Although the above researches achieved good results in designing the controllers to cope with the high non-linear MIMO systems, the robustness of the system in the presence of disturbances and sensor noise were not totally mentioned.

In this research, a H^∞ robust recurrent cerebellar model articulation control system (RRCMACS) is proposed for the non-linear MIMO system. Therein, the RCMAC is used to imitate the ideal sliding mode controller to minimize error surface and the H^∞ robust controller is utilized to attenuate the effects of disturbances, uncertainties, and sensor noise acting on the system to achieve the H^∞ robustness performance for the overall system.

The paper is organized as follows: Section 2 presents non-linear system and proposed control system. Section 3 describes the structure of the RCMAC and the H^∞ robust controller. The simulation results are provided in Section 4. Section 5 presents conclusions and future works.

II. PROBLEM FORMULATION AND PROPOSED CONTROL SYSTEM

In general, the dynamic equation of MIMO non-linear systems including disturbances, uncertainties, and noise is described below:

$$\begin{cases} \dot{\mathbf{x}}^n = \mathbf{F}_0(\mathbf{x}) + \Delta\mathbf{F}(\mathbf{x}) + (\mathbf{G}_0(\mathbf{x}) + \Delta\mathbf{G}(\mathbf{x}))\mathbf{u} + \mathbf{d}\mathbf{n}(\mathbf{x}) \\ = \mathbf{F}_0(\mathbf{x}) + \mathbf{G}_0(\mathbf{x})\mathbf{u} + \mathbf{UD}(\mathbf{x}) \\ \mathbf{y} = \mathbf{x} \end{cases} \quad (1)$$

where $\mathbf{y} = \mathbf{x} = [x_1, x_2, \dots, x_{n_0}]^T \in \mathbb{R}^{n_0}$ is the system output vector, $\mathbf{x} = [x^T, \dot{x}^T, \dots, x^{(n-1)T}]^T \in \mathbb{R}^n$ is the system state vector, $\mathbf{u} = [u_1, u_2, \dots, u_{n_0}]^T \in \mathbb{R}^{n_0}$ is the control input vector, $\mathbf{F}_0(\mathbf{x}) \in \mathbb{R}^{n_0 \times n_0}$ in the nominal non-linear function, $\mathbf{G}_0(\mathbf{x}) \in \mathbb{R}^{n_0 \times n_0}$ is the nominal gain matrix, $\Delta\mathbf{F}(\mathbf{x})$ and $\Delta\mathbf{G}(\mathbf{x})$ are the changes in parameters of the $\mathbf{F}_0(\mathbf{x}) \in \mathbb{R}^{n_0 \times n}$, and $\mathbf{G}_0(\mathbf{x}) \in \mathbb{R}^{n_0 \times n_0}$, respectively. $\mathbf{d}\mathbf{n}(\mathbf{x}) = [dn_1, dn_2, \dots, dn_{n_0}]^T \in \mathbb{R}^{n_0}$ stands for external disturbances and noise $\mathbf{UD}(\mathbf{x}) = \Delta\mathbf{F}(\mathbf{x}) + \Delta\mathbf{G}(\mathbf{x})\mathbf{u} + \mathbf{d}\mathbf{n}(\mathbf{x})$ is lumped uncertainties, disturbances, and noise. The objective of the control system is designed so that the output signals \mathbf{x} can only track desired trajectories $\mathbf{x}_d \in \mathbb{R}^{n_0}$ but also satisfy robust performance in the presence of the uncertainties, disturbances, and noise

For the high-order system, the sliding error manifold is defined [18] to reduce the order of variables during designing and computation the control system, the sliding error manifold has the following form:

$$\mathbf{S} = \mathbf{e}^{n-1} + \mathbf{K}\mathbf{e} \quad (2)$$

Therein, $\mathbf{e} = \mathbf{x}_d - \mathbf{x}$ and $\mathbf{e} = [\mathbf{e}, \dot{\mathbf{e}}, \dots, \mathbf{e}^{n-1}]^T$ are the tracking error and error vector of the system, respectively. Derivative both sides of \mathbf{s} and combination with the dynamic equation (1), yields.

$$\begin{aligned} \dot{\mathbf{S}} &= \mathbf{e}^n + \mathbf{K}\dot{\mathbf{e}} = \mathbf{x}_d^n - \mathbf{x}^n + \mathbf{K}(\dot{\mathbf{e}}) \\ &= \mathbf{x}_d^n - \mathbf{F}_0(\mathbf{x}) - \mathbf{G}_0(\mathbf{x})\mathbf{u} - \mathbf{UD}(\mathbf{x}) + \mathbf{K}(\dot{\mathbf{e}}) \end{aligned} \quad (3)$$

In case of the nominal values $\mathbf{F}_0(\mathbf{x}) \in \mathbb{R}^{n_0 \times n_0}$, $\mathbf{G}_0^{-1}(\mathbf{x}) \in \mathbb{R}^{n_0 \times n_0}$, the lumped of external disturbances, uncertainties, and noise $\mathbf{UD}(\mathbf{x})$ are exactly known, an ideal sliding mode (ISM) controller is designed to guarantee the stability of the system as follows [19]:

$$\mathbf{u}_{ISM} = \mathbf{G}_0^{-1}(\mathbf{x}) \left[\mathbf{x}_d^n - \mathbf{F}_0(\mathbf{x}) - \mathbf{UD}(\mathbf{x}) + \mathbf{K}(\dot{\mathbf{e}}) + \eta \text{sgn}(\mathbf{S}) \right] \quad (4)$$

Proof: According to the sliding mode control [9-10], the Lyapunov function candidate is selected to prove the stability of the system as follows:

$$\mathbf{V}(\mathbf{t}) = \frac{1}{2} \mathbf{S}^2 \quad (5)$$

Derivative two sides of Lyapunov function candidate, and replacing \mathbf{u} in (5) by \mathbf{u}_{ISM} in (4), yields

$$\dot{\mathbf{V}}(\mathbf{t}) = \mathbf{S}\dot{\mathbf{S}} = -\mathbf{S}\eta \text{sgn}(\mathbf{S}) \leq -\eta |\mathbf{S}| \quad (6)$$

The stability of the system is guaranteed in case of any $\eta > 0$

However, for the complex high non-linear systems, the external disturbances, uncertainties, and noise $\mathbf{UD}(\mathbf{x})$ cannot be defined, measured or estimated exactly in practical applications. Consequently, the \mathbf{u}_{ISM} cannot satisfy the stability and robust performance of the system. To handle these problems, a H^∞ robust recurrent cerebellar model articulation control system (RRCMACS) is proposed and depicted in Fig. 1. In this system, superior properties of the recurrent cerebellar model articulation controller (RCMAC) are incorporated to imitate the ideal sliding mode controller and the H^∞ robust controller efficiently attenuates the effects of external disturbances, noise, and uncertainties to a prescribed level to maintain the robustness of the system. The proposed control system has the following form:

$$\mathbf{u}_{RRCMACS} = \mathbf{u}_{ISM} - \mathbf{u}_{RC} - \mathbf{u}_{RCMAC} \quad (7)$$

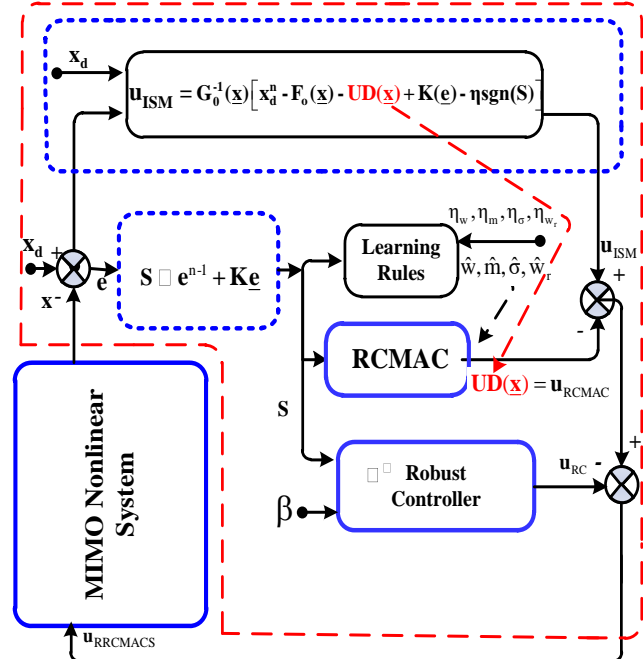


Fig. 1. Structure of the Proposed Control System.

III. THE RRCMAC SYSTEM DESIGN

A. The RCMAC

The \mathbf{u}_{RCMAC} with its fast learning, good generalization, and dynamic response capability of the CMACs [18] were utilized to mimic the ideal sliding mode controller, \mathbf{u}_{ISM} in the presence of the uncertainties, disturbance, noise to minimize the error sliding manifold, \mathbf{S} .

The structure of the **RCMAC** is depicted in Fig. 2 including input Space \mathbf{S} , association memory space \mathbf{A} , receptive field space \mathbf{R} , weight memory space \mathbf{W} , and output spaces \mathbf{O} .

The signal propagation in the RCMAC is described as follows:

$$S_{ri}(k) = S_i(k) + w_{rik}\mu_{ik}(k-1), i = 1, 2, \dots, n \quad (8)$$

$$\mu_{ik}(S_{ri}) = \exp\left[-\frac{(S_{ri} - m_{ik})^2}{\sigma_{ik}^2}\right], k = 1, 2, \dots, n_b \quad (9)$$

$$b_{ik} = \prod_{i=1}^n \mu_{ik}(S_{ri}), i = 1, 2, \dots, n, k = 1, 2, \dots, n_b \quad (10)$$

$$O_j = \sum_{j=1}^{n_0} \sum_{k=1}^{n_b} w_{jk} \prod_{i=1}^n \mu_{ik}(S_{ri}) = \mathbf{w}^T \mathbf{b}, j = 1, 2, \dots, n_0 \quad (11)$$

Where n , n_o , and n_b are the number of inputs, outputs, and blocks in receptive space; S_r , μ , b , and O are the input data including recurrent elements, Gaussian function, overlapped receptive space, and output data, respectively; m and σ are mean and deviation of Gaussian function; w_r and w are recurrent and output weights.

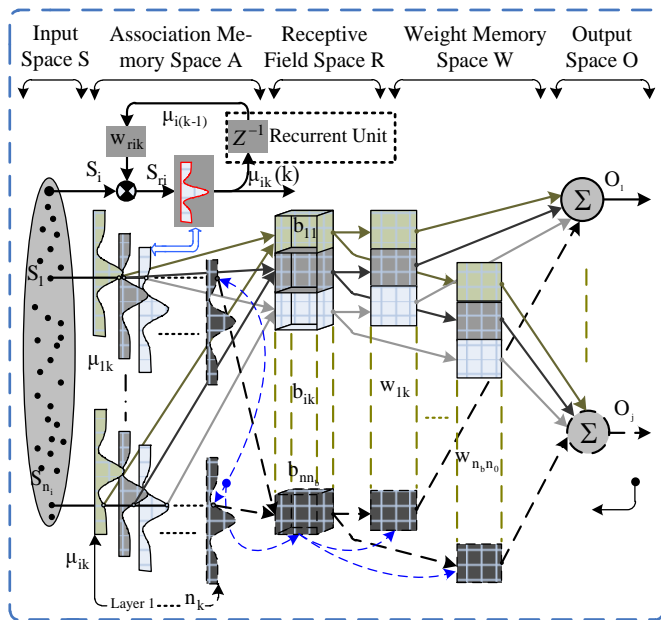


Fig. 2. The Structure of the RCMAC.

B. The Robust Controller Design

The RCMAC aims to imitate \mathbf{u}_{ISM} in (4). In the case of ideal designing, meanwhile, the parameters of the system are exactly known, external disturbances and uncertainties are absent. An ideal approximation controller can be described as follows:

$$\mathbf{u}_{RCMAC}^0(\mathbf{S}^0, \mathbf{m}^0, \boldsymbol{\sigma}^0, \mathbf{w}_r^0, \mathbf{w}^0) = \mathbf{w}^{0T} \mathbf{b}^0 + \boldsymbol{\varepsilon} \quad (12)$$

However, defining exactly the nominal parameters of the system is unobtainable in practical applications. Furthermore, the disturbances and noise always exist in the non-linear systems. Consequently, the estimated parameters are used instead of nominal parameters in designing the $\mathbf{u}_{RRCMACS}$ as follows:

$$\mathbf{u}_{RRCMACS}(\hat{\mathbf{S}}, \hat{\mathbf{m}}, \hat{\boldsymbol{\sigma}}, \hat{\mathbf{w}}_r, \hat{\mathbf{w}}) + \mathbf{u}_{RC} = \hat{\mathbf{w}}^T \hat{\mathbf{b}} + \mathbf{u}_{RC} \quad (13)$$

Therein, $\hat{\mathbf{S}}, \hat{\mathbf{m}}, \hat{\boldsymbol{\sigma}}, \hat{\mathbf{w}}_r, \hat{\mathbf{w}}$ is an estimation of the nominal parameters $\mathbf{S}^0, \mathbf{m}^0, \boldsymbol{\sigma}^0, \mathbf{w}_r^0, \mathbf{w}^0$ and \mathbf{u}_{RC} is the robust controller which attenuates the effects of the uncertainties, disturbances, and noise to guarantee the robustness of the system. Comprising (4) and (3), the error dynamic is rewritten as follows:

$$\dot{\mathbf{S}} = \mathbf{G}_0(\mathbf{x})(\mathbf{u}_{ISM} - \mathbf{u}) - \eta \text{sgn}(\mathbf{S}) \quad (14)$$

By replacing (12) and (13) into (14), yields

$$\begin{aligned} \dot{\mathbf{S}} &= \mathbf{G}_0(\mathbf{x})(\mathbf{u}_{RCMAC}^0 - \mathbf{u}_{RRCMACS}) - \eta \text{sgn}(\mathbf{S}) \\ &= \mathbf{G}_0(\mathbf{x})(\mathbf{w}^{0T} \mathbf{b}^0 - \hat{\mathbf{w}}^T \hat{\mathbf{b}} + \boldsymbol{\varepsilon} - \mathbf{u}_{RC}) - \eta \text{sgn}(\mathbf{S}) \\ &= \mathbf{G}_0(\mathbf{x})(\tilde{\mathbf{w}}^T \mathbf{b}^0 + \hat{\mathbf{w}}^T \tilde{\mathbf{b}} + \boldsymbol{\varepsilon} - \mathbf{u}_{RC}) - \eta \text{sgn}(\mathbf{S}) \end{aligned} \quad (15)$$

Where $\tilde{\mathbf{w}} = \mathbf{w}^0 - \hat{\mathbf{w}}, \tilde{\mathbf{b}} = \mathbf{b}^0 - \hat{\mathbf{b}}$ is an error of estimation.

According to the linearization technique, Taylor series expansion is used to transform the multi-dimension receptive-field space into a partially linear form. A linear approximation of $\tilde{\mathbf{b}}$ in three variables $\mathbf{m}, \boldsymbol{\sigma}$ and \mathbf{w}_r has the following form:

$$\begin{aligned} \tilde{\mathbf{b}} = \begin{bmatrix} \tilde{b}_1 \\ \vdots \\ \tilde{b}_k \\ \vdots \\ \tilde{b}_{nb} \end{bmatrix} &= \begin{bmatrix} \left(\frac{\partial b_1}{\partial \mathbf{m}}\right)^T \\ \vdots \\ \left(\frac{\partial b_k}{\partial \mathbf{m}}\right)^T \\ \vdots \\ \left(\frac{\partial b_{nb}}{\partial \mathbf{m}}\right)^T \end{bmatrix} (\mathbf{m}^0 - \hat{\mathbf{m}})_{\mathbf{m}=\hat{\mathbf{m}}} + \begin{bmatrix} \left(\frac{\partial b_1}{\partial \boldsymbol{\sigma}}\right)^T \\ \vdots \\ \left(\frac{\partial b_k}{\partial \boldsymbol{\sigma}}\right)^T \\ \vdots \\ \left(\frac{\partial b_{nb}}{\partial \boldsymbol{\sigma}}\right)^T \end{bmatrix} (\boldsymbol{\sigma}^0 - \hat{\boldsymbol{\sigma}})_{\boldsymbol{\sigma}=\hat{\boldsymbol{\sigma}}} \\ &+ \begin{bmatrix} \left(\frac{\partial b_1}{\partial \mathbf{w}_r}\right)^T \\ \vdots \\ \left(\frac{\partial b_k}{\partial \mathbf{w}_r}\right)^T \end{bmatrix} (\mathbf{w}_r^0 - \hat{\mathbf{w}}_r)_{\mathbf{w}_r^0=\hat{\mathbf{w}}_r} + \mathbf{T}_{ho} \end{aligned}$$

$$\begin{bmatrix} \vdots \\ \left(\frac{\partial \mathbf{b}_{nb}}{\partial \mathbf{w}_r}\right)^T \end{bmatrix} = \mathbf{C}^T \tilde{\mathbf{m}} + \mathbf{E}^T \tilde{\boldsymbol{\sigma}} + \mathbf{F}^T \tilde{\mathbf{w}}_r + \mathbf{T}_{ho} \quad (16)$$

where $\tilde{\mathbf{b}} = \mathbf{b}^0 - \hat{\mathbf{b}}$, $\tilde{\boldsymbol{\sigma}} = \boldsymbol{\sigma}^0 - \hat{\boldsymbol{\sigma}}$, $\tilde{\mathbf{w}} = \mathbf{w}_r^0 - \hat{\mathbf{w}}_r$, and \mathbf{T}_{ho} is higher-order terms of Taylor series expansion.

$$\mathbf{C}^T = \left[\frac{\partial b_1}{\partial \mathbf{m}}, \dots, \frac{\partial b_k}{\partial \mathbf{m}}, \dots, \frac{\partial b_{nb}}{\partial \mathbf{m}} \right]_{\mathbf{m}=\hat{\mathbf{m}}} \in \mathfrak{R}^{n_1 n_b \times n_b} \quad (17)$$

$$\mathbf{E}^T = \left[\frac{\partial b_1}{\partial \boldsymbol{\sigma}}, \dots, \frac{\partial b_k}{\partial \boldsymbol{\sigma}}, \dots, \frac{\partial b_{nb}}{\partial \boldsymbol{\sigma}} \right]_{\boldsymbol{\sigma}=\hat{\boldsymbol{\sigma}}} \in \mathfrak{R}^{n_1 n_b \times n_b} \quad (18)$$

$$\mathbf{F}^T = \left[\frac{\partial b_1}{\partial \mathbf{w}_r}, \dots, \frac{\partial b_k}{\partial \mathbf{w}_r}, \dots, \frac{\partial b_{nb}}{\partial \mathbf{w}_r} \right]_{\mathbf{w}_r=\hat{\mathbf{w}}_r} \in \mathfrak{R}^{n_1 n_b \times n_b} \quad (19)$$

Substitution $\mathbf{C}^T \tilde{\mathbf{m}} + \mathbf{E}^T \tilde{\boldsymbol{\sigma}} + \mathbf{F}^T \tilde{\mathbf{w}}_r + \mathbf{T}_{ho}$ and $\mathbf{b}^0 = \hat{\mathbf{b}} + \tilde{\mathbf{b}}$ into error dynamic equation (15), yields

$$\begin{aligned} \dot{\mathbf{S}} &= \mathbf{G}_0(\underline{\mathbf{x}})(\tilde{\mathbf{w}}^T \mathbf{b}^0 + \tilde{\mathbf{w}}^T \tilde{\mathbf{b}} + \boldsymbol{\varepsilon} - \mathbf{u}_{RC}) - \boldsymbol{\eta} \text{sgn}(\mathbf{S}) \\ &= \mathbf{G}_0(\underline{\mathbf{x}})(\tilde{\mathbf{w}}^T (\hat{\mathbf{b}} + \mathbf{C}^T \tilde{\mathbf{m}} + \mathbf{E}^T \tilde{\boldsymbol{\sigma}} + \mathbf{F}^T \tilde{\mathbf{w}}_r + \mathbf{T}_{ho}) \\ &+ \tilde{\mathbf{w}}^T (\mathbf{C}^T \tilde{\mathbf{m}} + \mathbf{E}^T \tilde{\boldsymbol{\sigma}} + \mathbf{F}^T \tilde{\mathbf{w}}_r + \mathbf{T}_{ho}) + \boldsymbol{\varepsilon} - \mathbf{u}_{RC}) - \boldsymbol{\eta} \text{sgn}(\mathbf{S}) \\ &= \mathbf{G}_0(\underline{\mathbf{x}})(\tilde{\mathbf{w}}^T \hat{\mathbf{b}} + \tilde{\mathbf{w}}^T (\mathbf{C}^T \tilde{\mathbf{m}} + \mathbf{E}^T \tilde{\boldsymbol{\sigma}} + \mathbf{F}^T \tilde{\mathbf{w}}_r) \\ &+ \tilde{\mathbf{w}}^T (\mathbf{C}^T \tilde{\mathbf{m}} + \mathbf{E}^T \tilde{\boldsymbol{\sigma}} + \mathbf{F}^T \tilde{\mathbf{w}}_r) + \mathbf{w}^{0T} \mathbf{T}_{ho} + \boldsymbol{\varepsilon} - \mathbf{u}_{RC}) - \boldsymbol{\eta} \text{sgn}(\mathbf{S}) \\ &= \mathbf{G}_0(\underline{\mathbf{x}})(\tilde{\mathbf{w}}^T \hat{\mathbf{b}} + \tilde{\mathbf{w}}^T (\mathbf{C}^T \tilde{\mathbf{m}} + \mathbf{E}^T \tilde{\boldsymbol{\sigma}} + \mathbf{F}^T \tilde{\mathbf{w}}_r) - \mathbf{u}_{RC} \\ &+ \mathbf{UD}(\underline{\mathbf{x}}) - \boldsymbol{\eta} \text{sgn}(\mathbf{S})) \end{aligned} \quad (20)$$

where $\mathbf{UD}(\underline{\mathbf{x}}) = \tilde{\mathbf{w}}^T (\mathbf{C}^T \tilde{\mathbf{m}} + \mathbf{E}^T \tilde{\boldsymbol{\sigma}} + \mathbf{F}^T \tilde{\mathbf{w}}_r) + \mathbf{w}^{0T} \mathbf{T}_{ho} + \boldsymbol{\varepsilon}$ stands for the external disturbances, noises, and uncertainties

In other to prove the stability and robustness of the system under the effects of disturbances, noises, and uncertainties, the Lyapunov function is chosen as follows:

$$\begin{aligned} \mathbf{V}(\mathbf{S}, \tilde{\mathbf{w}}, \tilde{\mathbf{m}}, \tilde{\boldsymbol{\sigma}}, \tilde{\mathbf{w}}_r) &= \frac{1}{2} \mathbf{S}^T \mathbf{G}_0^{-1}(\underline{\mathbf{x}}) \mathbf{S} + \frac{1}{2\eta_w} \tilde{\mathbf{w}}^T \tilde{\mathbf{w}} \\ &+ \frac{1}{2\eta_m} \tilde{\mathbf{m}}^T \tilde{\mathbf{m}} + \frac{1}{2\eta_\sigma} \tilde{\boldsymbol{\sigma}}^T \tilde{\boldsymbol{\sigma}} + \frac{1}{2\eta_{w_r}} \tilde{\mathbf{w}}_r^T \tilde{\mathbf{w}}_r \end{aligned} \quad (21)$$

By selection the adaptive rules as (22)-(25), the \mathbf{H}^∞ robustness performance of the system are satisfied.

$$\dot{\hat{\mathbf{w}}} = \frac{1}{\eta_w} \hat{\mathbf{b}} \mathbf{S}^T \quad (22)$$

$$\dot{\hat{\mathbf{m}}} = \frac{1}{\eta_m} \mathbf{C}^T \hat{\mathbf{w}} \mathbf{S} \quad (23)$$

$$\dot{\hat{\boldsymbol{\sigma}}} = \frac{1}{\eta_\sigma} \mathbf{E}^T \hat{\mathbf{w}} \mathbf{S} \quad (24)$$

$$\dot{\hat{\mathbf{w}}}_r = \frac{1}{\eta_{w_r}} \mathbf{F}^T \hat{\mathbf{w}} \mathbf{S} \quad (25)$$

Proof: Taking derivative two sides of the Lyapunov function (21), yields

$$\begin{aligned} \dot{\mathbf{V}} &= \mathbf{S}^T \mathbf{G}_0^{-1}(\underline{\mathbf{x}}) \dot{\mathbf{S}} + \eta_w \tilde{\mathbf{w}}^T \dot{\tilde{\mathbf{w}}} + \eta_m \tilde{\mathbf{m}}^T \dot{\tilde{\mathbf{m}}} + \eta_\sigma \tilde{\boldsymbol{\sigma}}^T \dot{\tilde{\boldsymbol{\sigma}}} + \eta_{w_r} \tilde{\mathbf{w}}_r^T \dot{\tilde{\mathbf{w}}}_r \\ &= \mathbf{S}^T (\tilde{\mathbf{w}}^T \hat{\mathbf{b}} + \tilde{\mathbf{w}}^T (\mathbf{C}^T \tilde{\mathbf{m}} + \mathbf{E}^T \tilde{\boldsymbol{\sigma}} + \mathbf{F}^T \tilde{\mathbf{w}}_r) - \mathbf{u}_{RC} + \mathbf{UD}(\underline{\mathbf{x}})) \\ &- \mathbf{S}^T \mathbf{G}_0^{-1} \boldsymbol{\eta} \text{sgn}(\mathbf{S}) - \eta_w \tilde{\mathbf{w}}^T \dot{\tilde{\mathbf{w}}} - \eta_m \tilde{\mathbf{m}}^T \dot{\tilde{\mathbf{m}}} - \eta_\sigma \tilde{\boldsymbol{\sigma}}^T \dot{\tilde{\boldsymbol{\sigma}}} - \eta_{w_r} \tilde{\mathbf{w}}_r^T \dot{\tilde{\mathbf{w}}}_r \end{aligned} \quad (26)$$

Due to $\mathbf{S}^T \tilde{\mathbf{w}}^T \hat{\mathbf{b}} = \tilde{\mathbf{w}}^T \hat{\mathbf{b}} \mathbf{S}^T$ and $\mathbf{S}^T \mathbf{G}_0^{-1} \boldsymbol{\eta} \text{sgn}(\mathbf{S}) \geq \mathbf{0}$, therefore, the equation (26) can be rewritten as below:

$$\begin{aligned} \dot{\mathbf{V}} &\leq \tilde{\mathbf{w}}^T (\hat{\mathbf{b}} \mathbf{S}^T - \eta_w \dot{\tilde{\mathbf{w}}}) + \tilde{\mathbf{m}}^T (\mathbf{C}^T \hat{\mathbf{w}} \mathbf{S} - \eta_m \dot{\tilde{\mathbf{m}}}) \\ &+ \tilde{\boldsymbol{\sigma}}^T (\mathbf{E}^T \hat{\mathbf{w}} \mathbf{S} - \eta_\sigma \dot{\tilde{\boldsymbol{\sigma}}}) + \tilde{\mathbf{w}}_r^T (\mathbf{F}^T \hat{\mathbf{w}} \mathbf{S} - \eta_{w_r} \dot{\tilde{\mathbf{w}}}_r) \\ &+ \mathbf{S}^T \mathbf{UD}(\underline{\mathbf{x}}) - \mathbf{s}^T \mathbf{u}_{RC} \end{aligned} \quad (27)$$

By replacing the adaptive rules from (22)-(25) into (27), yields

$$\begin{aligned} \dot{\mathbf{V}}(\mathbf{S}, \tilde{\mathbf{w}}, \tilde{\mathbf{m}}, \tilde{\boldsymbol{\sigma}}, \tilde{\mathbf{w}}_r) &\leq \mathbf{S}^T \mathbf{UD}(\underline{\mathbf{x}}) - \mathbf{S}^T \mathbf{u}_{RC} \\ &= \sum_{i=1}^n (\mathbf{S}_i \mathbf{UD}_i(\underline{\mathbf{x}}) - \mathbf{S}_i \mathbf{u}_{RC}) \end{aligned} \quad (28)$$

Selecting control law for the robust controller as follows:

$$\mathbf{u}_{RC} = \frac{(\beta_i^2 + 1) \mathbf{S}_i}{2\beta_i^2} \quad (29)$$

By replacing the \mathbf{u}_{RC} into (28), yields

Integrating two sides of equation (30) from $t = 0$ to $t = \infty$, yields $t = 0$

$$\begin{aligned} \dot{\mathbf{V}} &\leq \sum_{i=1}^n (\mathbf{S}_i \mathbf{UD}_i(\underline{\mathbf{x}}) - \mathbf{S}_i \frac{(\beta_i^2 + 1) \mathbf{S}_i}{2\beta_i^2}) \\ &\leq \sum_{i=1}^n (\mathbf{S}_i \mathbf{UD}_i(\underline{\mathbf{x}}) - \frac{1}{2} \mathbf{S}_i^2 - \frac{1}{2\beta_i^2} \mathbf{S}_i^2) \\ &\leq \sum_{i=1}^n (-\frac{1}{2} \mathbf{S}_i^2 - \frac{1}{2} (\frac{\mathbf{S}_i}{\beta_i} - \beta_i \mathbf{UD}_i(\underline{\mathbf{x}}))^2) \\ &+ \frac{\beta_i^2 \mathbf{UD}_i(\underline{\mathbf{x}})^2}{2} \\ &\leq \sum_{i=1}^n (-\frac{1}{2} \mathbf{S}_i^2 + \frac{\beta_i^2 \mathbf{UD}_i(\underline{\mathbf{x}})^2}{2}) \end{aligned} \quad (30)$$

$$V(T) - V(0) \leq \sum_{i=1}^n \left(-\frac{1}{2} \int_{t=0}^{t=\infty} S_i^2 dt \right) + \frac{\beta_i^2}{2} \int_{t=0}^{t=\infty} UD_i(\underline{x})^2 dt \quad (31)$$

Because of the value of the Lyapunov function, $V(T) \geq 0$, the inequality in (31) can be described as follows:

$$V(T) + \sum_{i=1}^n \left(\frac{1}{2} \int_{t=0}^T S_i^2 dt \right) \leq V(0) + \sum_{i=0}^{i=n} \frac{\beta_i^2}{2} \int_{t=0}^T UD_i(\underline{x})^2 dt \quad (32)$$

$$\Downarrow$$

$$\sum_{i=1}^n \frac{1}{2} \int_{t=0}^T S_i^2 dt \leq V(0) + \sum_{i=0}^{i=n} \frac{\beta_i^2}{2} \int_{t=0}^T UD_i(\underline{x})^2 dt$$

Basing on the equation of the Lyapunov function in (21), the inequality in (32) is equivalent to the following form:

$$\sum_{i=1}^n \left(\frac{1}{2} \int_{t=0}^T S_i^2 dt \right) + S^T(0)G_0^{-1}(\underline{x})S(0) + \frac{1}{\eta_w} \tilde{w}^T(0)\tilde{w}(0) + \frac{1}{\eta_m} \tilde{m}^T(0)\tilde{m}(0) + \frac{1}{\eta_\sigma} \tilde{\sigma}^T(0)\tilde{\sigma}(0) + \frac{1}{\eta_{w_r}} \tilde{w}_r^T(0)\tilde{w}_r(0) + \sum_{i=0}^{i=n} \frac{\beta_i^2}{2} \int_{t=0}^T UD_i(\underline{x})^2 dt \quad (33)$$

If the system starts with initial conditions $\mathbf{S} = \mathbf{0}$, $\tilde{\mathbf{w}} = \mathbf{0}$, $\tilde{\mathbf{m}}(\mathbf{0}) = \mathbf{0}$, $\tilde{\sigma}(\mathbf{0}) = \mathbf{0}$, $\tilde{\mathbf{w}}_r(0) = 0$ then the H^∞ robust performance can be obtained as follows [20-21]:

$$\sup_{UD_i \in L_2[0,T]} \sum_{i=1}^{i=n} \left(\frac{\|S_i\|}{\|UD_i\|} \leq \beta_i \right) \quad (34)$$

Where $\|S_i\|^2 = \int_{t=0}^T S_i^2 dt$, $\|UD_i\|^2 = \int_{t=0}^T UD_i^2 dt$ and β_i is the prescribed attenuation level.

IV. SIMULATION AND RESULTS

To verify the effectiveness of the proposed control system, a micro-motion stage powered by the linear piezoelectric motor (LPM) was used to investigate the stability and robustness of the system. The dynamic equation of LPM including hysteresis and stiffness behavior is described as follows [10, 18]:

$$\ddot{\mathbf{x}} = -\frac{\mathbf{D}}{\mathbf{M}}\dot{\mathbf{x}} + \frac{\mathbf{K}}{\mathbf{M}}\mathbf{u} - \frac{\mathbf{F}_H + \mathbf{F}_L}{\mathbf{M}} \quad (35)$$

where \mathbf{x} stands for displacement of the x-axis, y-axis respectively; \mathbf{M} is the effective mass of the moving stage; \mathbf{D} is the friction coefficient; \mathbf{F}_L is external disturbance forces;

\mathbf{K} is the voltage-to-force coefficient; \mathbf{u} is the control volt of the LPMs; \mathbf{F}_H is the hysteresis frictional force given as below:

$$\mathbf{F}_H = \alpha \mathbf{b} + \delta |\dot{\mathbf{x}}| + \gamma \dot{\mathbf{x}} \quad (36)$$

Where $\alpha, \mathbf{b}, \delta, \gamma$ and \mathbf{x} are parameters depending on the hysteresis loop and structure of the linear piezoelectric motor.

In general, the LPM is a complex and high non-linear system. According to the dynamic equation of the non-linear MIMO system (1), the dynamic equation of the LPM can be rewritten as follows:

$$\ddot{\mathbf{x}} = -\frac{\mathbf{D}_o}{\mathbf{M}_o}\dot{\mathbf{x}} + \frac{\mathbf{K}_o}{\mathbf{M}_o}\mathbf{u} + \mathbf{UD}(\underline{\mathbf{x}}) \quad (37)$$

where \mathbf{D}_o , \mathbf{M}_o , and \mathbf{K}_o are nominal values of \mathbf{D} , \mathbf{M} and \mathbf{K} , respectively.

$\mathbf{UD}(\underline{\mathbf{x}}) = -\frac{\mathbf{F}_{H0} + \mathbf{F}_{L0}}{\mathbf{M}_o} + f(\mathbf{D}, \mathbf{F}_H, \mathbf{F}_L, \mathbf{K}, t)$ denotes the uncertainties due to change in parameters, disturbances, and noises. This equation is used to build the simulation program for the proposed control system.

The initial parameters are used in simulation as follows:

$$\mathbf{M}_o = 5\text{kg} \quad \mathbf{D}_o = 66 \cdot 10^{-6} [\text{N} \cdot \text{sec} / \text{m}] \quad \mathbf{K}_{Eo} = 3 [\text{N} / \text{Volt}],$$

$$\eta_w = \eta_m = \eta_\sigma = \eta_{w_r} = 0.01, \quad n = 2, n_b = 11, n_o = 2, \quad \mathbf{K} = 0.5,$$

$$\beta = 0.1 \text{ and } 1.$$

$$\mathbf{w} = \begin{bmatrix} 0.1, 0.1, 0.1, 0.1, 0.1, 0.1, 0.1, 0.1, 0.1, 0.1, 0.1, 0.1 \\ 0.1, 0.1, 0.1, 0.1, 0.1, 0.1, 0.1, 0.1, 0.1, 0.1, 0.1, 0.1 \end{bmatrix},$$

$$\mathbf{m} = \begin{bmatrix} -1, -0.8, -0.6, -0.4, -0.2, 0, 0.2, 0.4, 0.6, 0.8, 1 \\ -1, -0.8, -0.6, -0.4, -0.2, 0, 0.2, 0.4, 0.6, 0.8, 1 \end{bmatrix}$$

$$\boldsymbol{\sigma} = \begin{bmatrix} 0.3, 0.3, 0.3, 0.3, 0.3, 0.3, 0.3, 0.3, 0.3, 0.3, 0.3, 0.3 \\ 0.3, 0.3, 0.3, 0.3, 0.3, 0.3, 0.3, 0.3, 0.3, 0.3, 0.3, 0.3 \end{bmatrix},$$

$$\mathbf{w}_r = \begin{bmatrix} 0.1, 0.1, 0.1, 0.1, 0.1, 0.1, 0.1, 0.1, 0.1, 0.1, 0.1, 0.1 \\ 0.1, 0.1, 0.1, 0.1, 0.1, 0.1, 0.1, 0.1, 0.1, 0.1, 0.1, 0.1 \end{bmatrix}$$

The effects of uncertainties, external disturbances, and noise, $\mathbf{UD}(\underline{\mathbf{x}})$ was generated by a random signal with mean = 5 and variance = 5. Sample time = 0.01s.

The simulation results of the RRCMACS due to periodic step commands were represented in Fig. 3 for the X-axis and the Fig. 4 for the Y-axis.

Fig. 5 and Fig. 6 represent the simulation results of the RARCMAC due to sinusoidal command in the X-axis and the Y-axis, respectively.

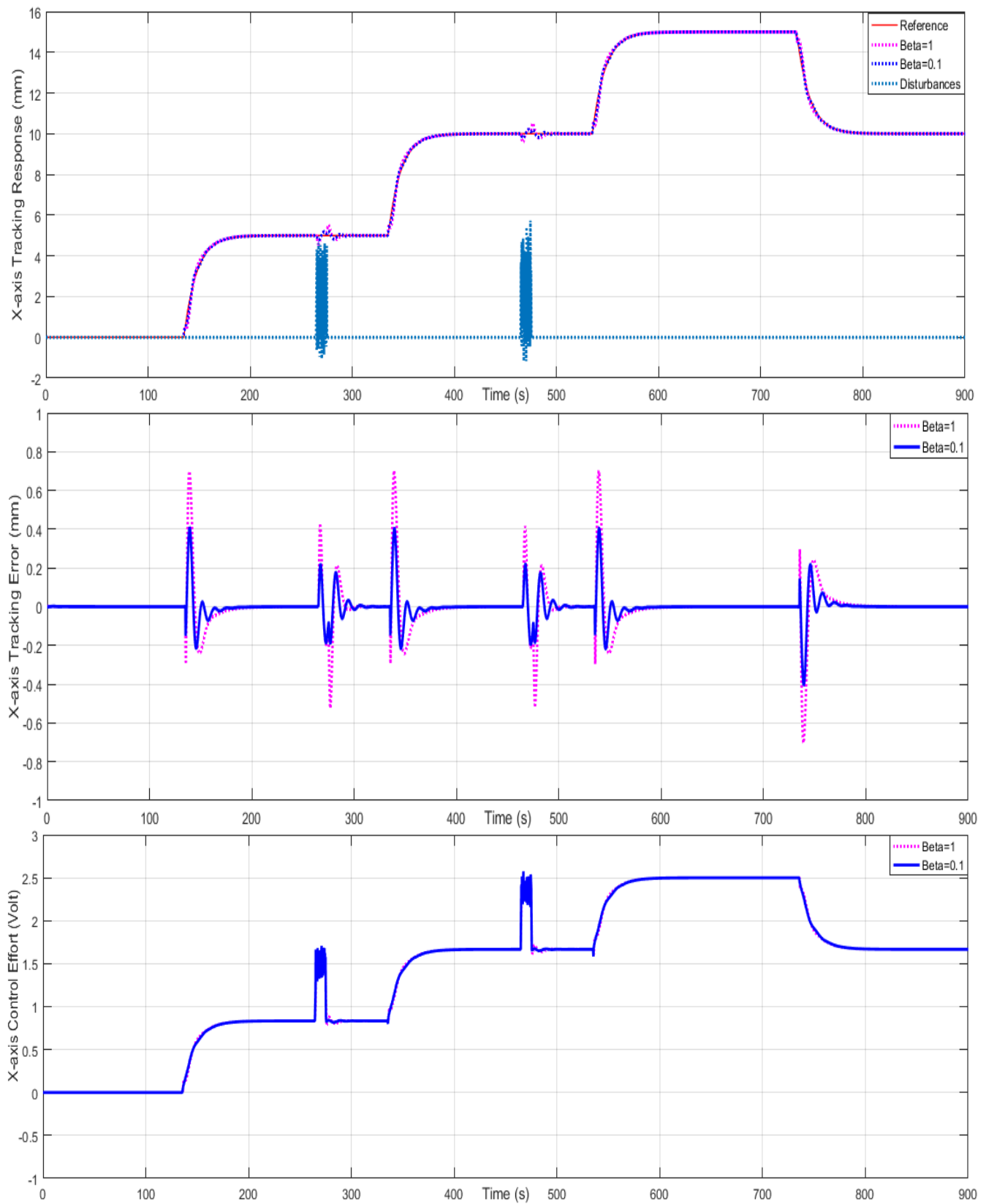


Fig. 3. Tracking Response, Tracking error and Control Effort of RRCMACS Due to Periodic Step Command in the X-Axis in Case of $\beta = 0.1$ and $\beta = 1$.

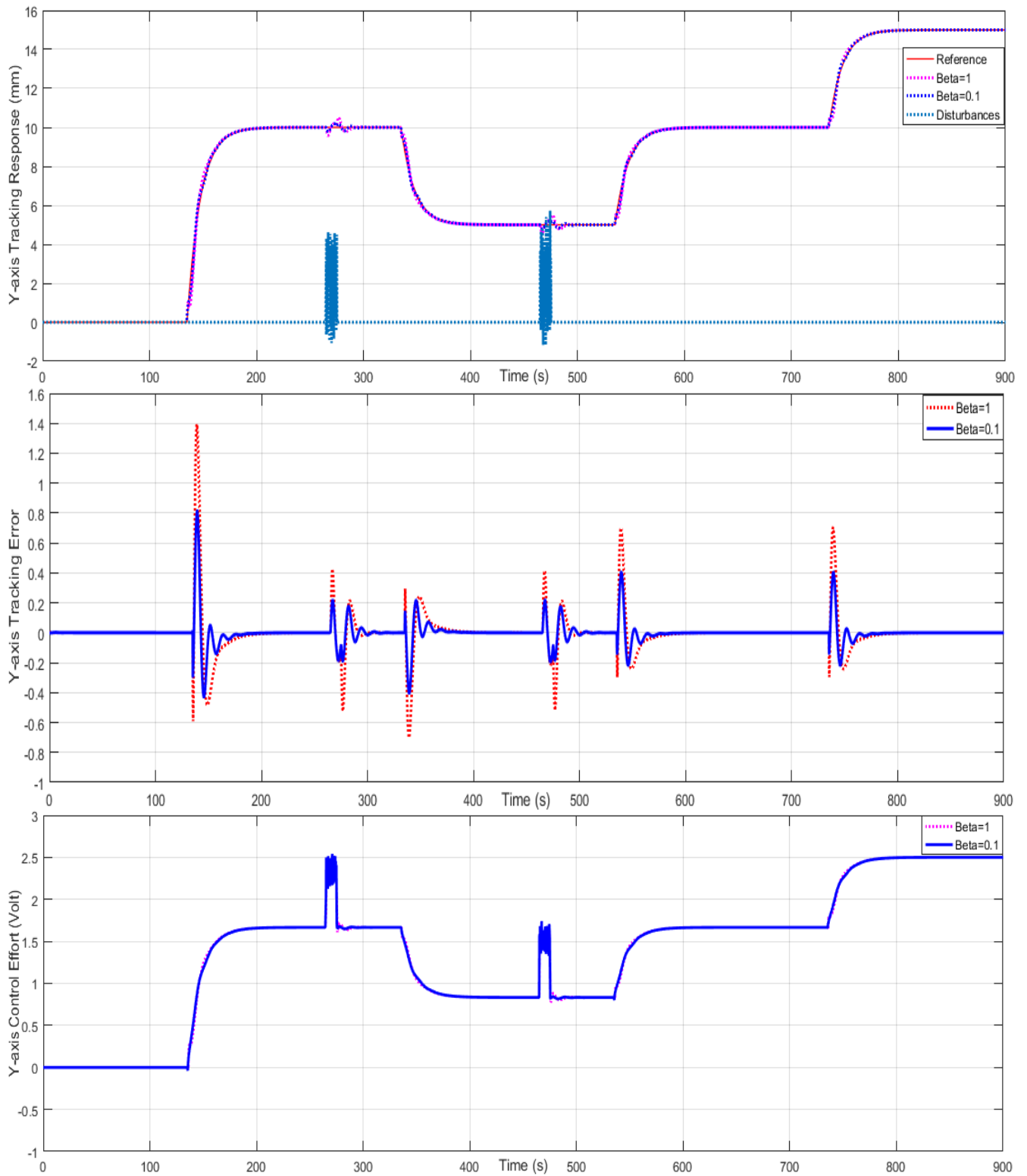


Fig. 4. Tracking Response, Tracking Error and Control Effort of RRCMACS Due to Periodic Step Command in the Y-Axis in Case of $\beta = 0.1$ and $\beta = 1$.

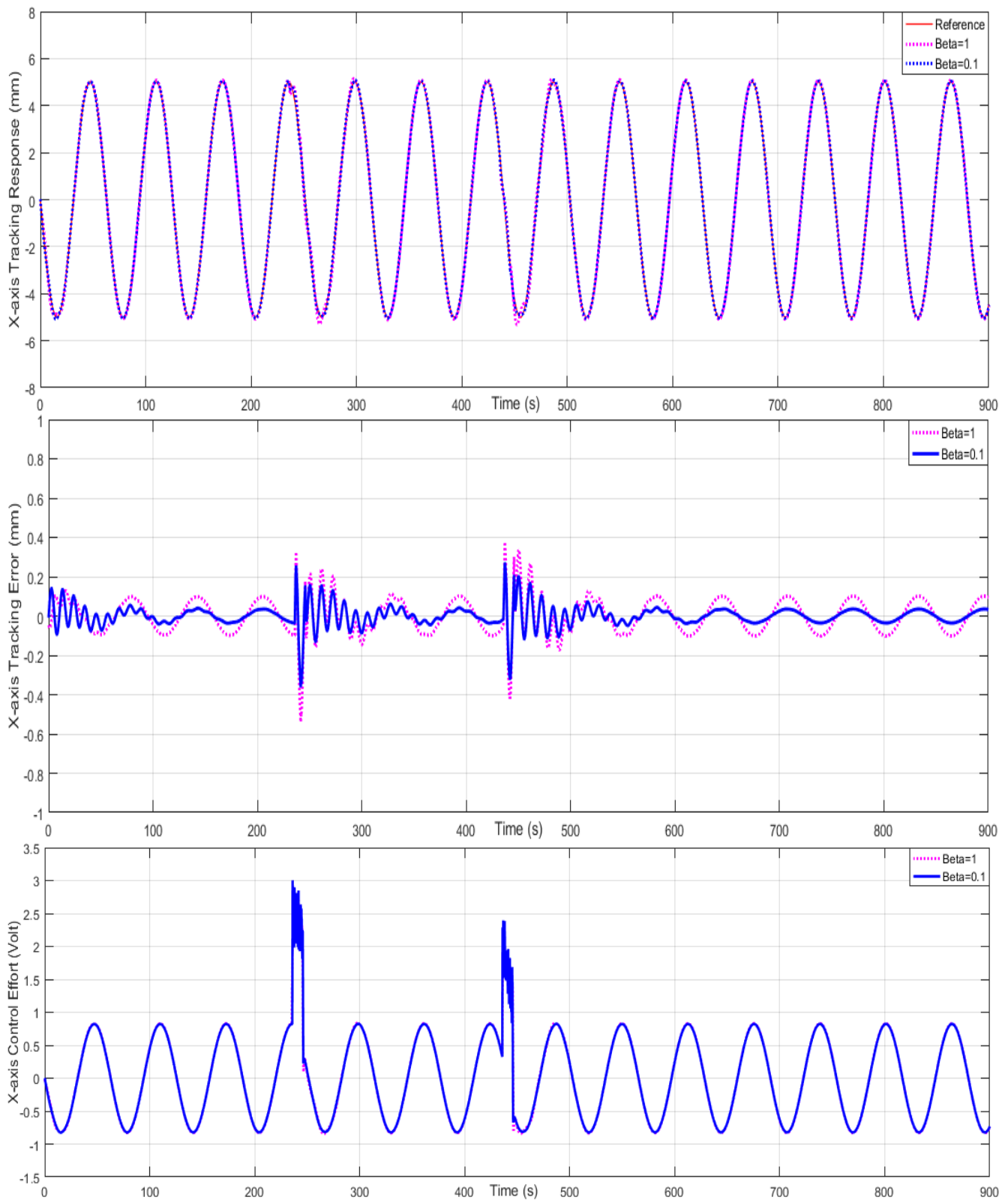


Fig. 5. Tracking Response, Tracking Error and Control Effort of RRCMACS Due to Sinusoidal Command in the X-Axis in Case of $\beta = 0.1$ and $\beta = 1$.

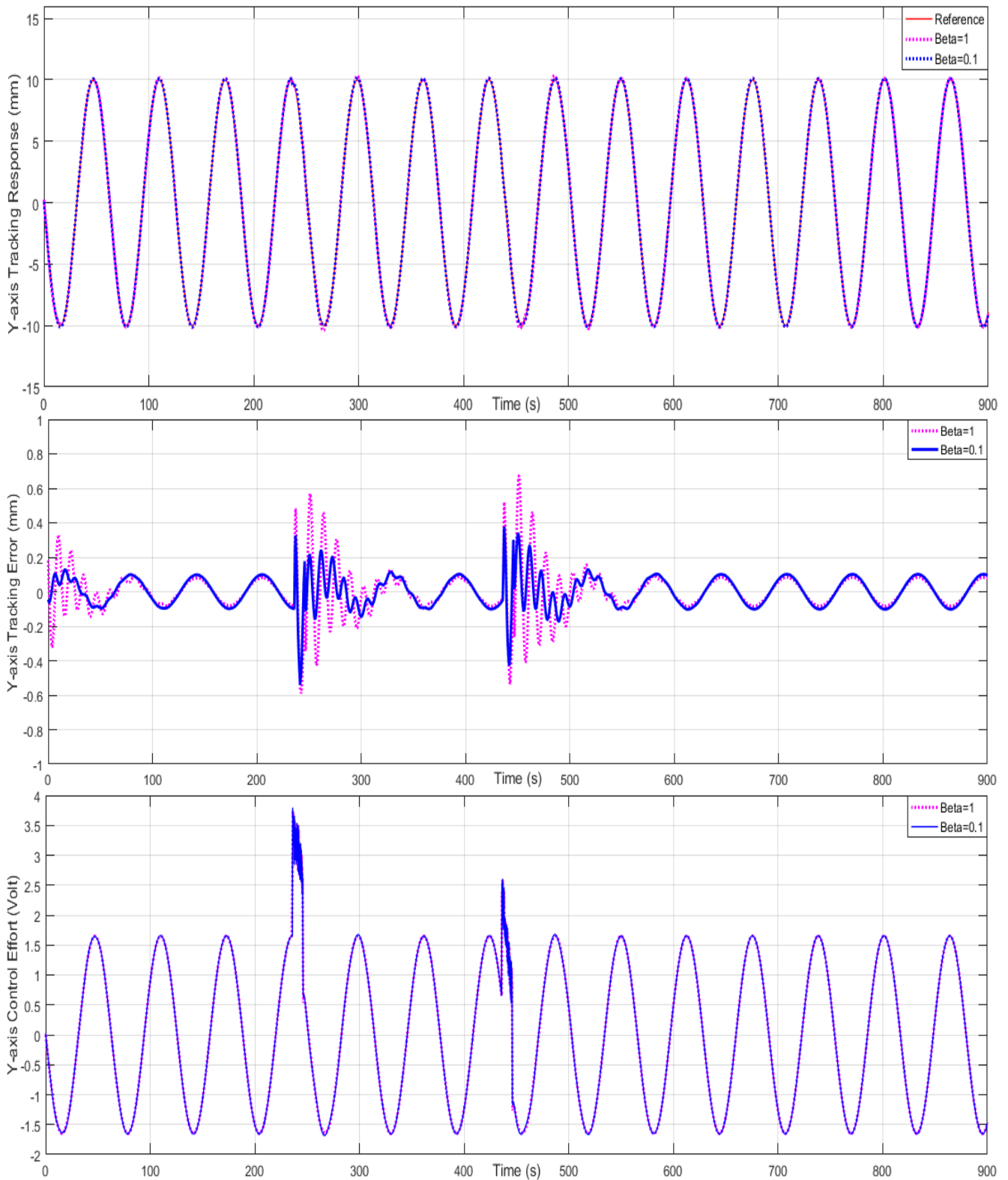


Fig. 6. Tracking Response, Tracking Error and Control Effort of RRCMACS Due to Sinusoidal Command in the Y-Axis in Case of $\beta = 0.1$ and $\beta = 1$.

The simulation results showed that the RRCMACS achieved good tracking responses in the X-axis and the Y-axis. The control system obtained the stability and robustness in the presence of uncertainties, $\mathbf{UD}(\mathbf{x})$ at $t_1 = 235s$ to $t_2 = 245s$ and $t_3 = 465s$ to $t_4 = 475s$ for both periodic step command and sinusoidal command. The performance of the control system was better as the attenuation level of the H^∞ robust controller smaller.

V. CONCLUSION AND FUTURE WORKS

In this paper, the RRCMACS was proposed for the non-linear MIMO system to achieve the stability and robustness in the presence of uncertainties, external disturbances, and noise, $\mathbf{UD}(\mathbf{x})$. The proposed control system comprised the RCMAC and the H^∞ robust controller. Therein, the RCMAC was utilized to imitate the ideal sliding mode controller to minimize the error sliding manifold, and the H^∞ robust controller aims to attenuate the effects of uncertainties, external disturbance, and noise to the prescribed attenuation level. The simulation results of the LPM powered micro-motion stage proved the effectiveness of the proposed control system. In addition, the $\mathbf{UD}(\mathbf{x})$ stands for the inherent complex properties of the non-linear MIMO systems. Therefore, the proposed control system can handle other non-linear MIMO systems. However, this research needs to mention the responses of the hardware equipments to apply for the real-time control system.

REFERENCES

- [1] Al-Ghanimi and J. Zheng, and Z. Man, A Fast Non-Singular Terminal Sliding Mode Control Based on Perturbation Estimation for Piezo Actuators Systems, *International Journal of Control*, 2017, vol.3. pp 1-22.
- [2] J.S. Mo, Z.C. Qiu, J.Y. Wei, X.M. Zhang, Adaptive positioning control of an ultrasonic linear motor system, *Robotics, and Computer-Integrated Manufacturing*, 2017, vol.44, pp 156-173.
- [3] Shuhui Bi, Lei Wang, Yongguo Zhao, and Mingcong Deng, Operator-based Robust Control for Non-linear Uncertain Systems with Unknown Backlash-like Hysteresis, *International Journal of Control, Automation and Systems*, 2016, pp.469-477.
- [4] Xinghua Zhang, Yantao Wang, and Xiaofei Fan, Stability Analysis of Linear Systems with An Interval Time-varying Delay – A Delay-range-partition Approach, *International Journal of Control, Automation and Systems*, 2017, pp.518-526.
- [5] V.Balaji, Dr. L.Rajaji, Shanthini K, Comparison Analysis of Model Predictive Controller with Classical PID Controller for pH Control Process *Indonesian Journal of Electrical Engineering and Informatics (IJEI)*, Vol. 4, No. 4, December 2016, pp. 250-255
- [6] Tarun Varshney, Improved NN-PID control of MIMO systems with PSO-based initialization of weights, *Int. J. Automation and Control*, Vol. 8, Nos. 2, 2014, pp. 158-172.
- [7] Sundarapandian Vaidyanathan, Takagi-Sugeno fuzzy logic controller for Liu-Chen four-scroll chaotic system, *Int. J. Intelligent Engineering Informatics*, Vol. 4, No. 2, 2016, pp. 135-150.
- [8] Garima Sinha, Pankaj Kumar Goswami, Sudhir Kumar Sharma, A Comparative Strategy Using PI & Fuzzy Controller for Optimization of Power Quality Control, *Indonesian Journal of Electrical Engineering and Informatics (IJEI)*, Vol. 6, No. 1, 2018, pp. 118-124.
- [9] G.Muni Reddy, T.Gowri Manohar, Fuzzy Logic Controller for Grid Connected Wind Energy Conversion System, *Indonesian Journal of Electrical Engineering and Informatics (IJEI)*, Vol. 6, No. 1,2018, pp. 37-44.
- [10] A. Al-Ghanimi, J. Zheng, and Z. Man, A Fast Non-Singular Terminal Sliding Mode Control Based on Perturbation Estimation for Piezoelectric Actuators Systems. *International Journal of Control*, Vol 90, 2017, pp. 480-491.
- [11] Abdelhak Msaddek, Abderraouf Gaaloul, and Faouzi M'sahli, Adaptive fuzzy supervision of the gain of the higher order sliding mode control, *Int. J. Automation and Control*, Vol. 9, Nos. 3, 2015, pp.228-246
- [12] S. Jung, Stability Analysis of Reference Compensation Technique for Controlling Robot Manipulators by Neural Network, *International Journal of Control, Automation and Systems*, Vol. 15, no. 2, 2017, pp. 952-958.
- [13] C. M. Lin and H. Y. Li, A novel adaptive wavelet fuzzy cerebellar model articulation control system design for voice coil motors', *IEEE Trans. Ind.Electron*, vol. 59, no. 4, 2012, pp. 2024-2033.
- [14] C. M. Lin and H. Y. Li, TSK fuzzy CMAC-based robust adaptive backstepping control for uncertain non-linear systems, *IEEE Trans. Fuzzy Syst.*, vol. 20, no. 6, 2012, pp. 1147-1154.
- [15] Thanh Quyen Ngo, Ta Van Phuong, Robust Adaptive Self-Organizing Wavelet Fuzzy CMAC Tracking Control for Deicing Robot Manipulator, *International Journal of Computers communication & Control*, Volt 10,2015, pp.567-578.
- [16] S. Y. Wang, C. L. Tseng, and S. C. Chien, Adaptive fuzzy cerebellar model articulation control for switched reluctance motor drive, *IET Elect.Power Appl.*, vol. 6, no. 3, 2012, pp. 190-202.
- [17] V.P. Ta, X.K. Dang, and T.Q. Ngo, Adaptive Tracking Control Based On CMAC for Non-linear Systems, *Proceedings of the International Conference on System Science and Engineering*, 2017, pp 494-498.
- [18] Van-Phuong Ta and Xuan-Kien Dang, An Innovative Recurrent Cerebellar Model Articulation Controller For Piezo-Driven Micro-motion Stage, *International Journal of Innovative Computing, Information and Control*, Volume 14, Number 4, 2018, pp. 1527-1535.
- [19] M. Bahita, Neural Stable Adaptive Control For a class of non-linear systems, *Journal of Engineering Science and Technology*, vol. 7, no. 1, 2012, pp. 97-18.
- [20] P C Chen, C W Chen and W L Chiang , Linear Matrix Inequality Conditions of Nonlinear Systems by Genetic Algorithm-based H Adaptive Fuzzy Sliding Mode Controller, *Journal of Vibration and Control*, Jan 25, 2011.
- [21] Alireza Alfi, Chaos suppression on a class of uncertain nonlinear chaotic systems using an optimal H infinity adaptive PID controller, *Nonlinear Science, and Nonequilibrium and Complex Phenomena*, Elsevier 2012.

Empirical Assessment of Ensemble based Approaches to Classify Imbalanced Data in Binary Classification

Prabhjot Kaur¹, Anjana Gosain²

Department of Information Technology, MSIT Research Scholar¹
USICT, Guru Gobind Singh Indraprastha University, New Delhi, INDIA^{1,2}

Abstract—Classifying imbalanced data with traditional classifiers is a huge challenge now-a-days. Imbalance data is a situation wherein the ratio of data within classes is not same. Many real life situations deal with such problems e.g. Web spam detection, Credit card frauds, and fraudulent telephone calls. The problem exists everywhere when our objective is to identify exceptional cases. The problem is handled by researchers either by modifying the existing classifications methods or by developing new methods. This paper review ensemble based approaches (Boosting and Bagging based) designed to address imbalance in classes by focusing on binary classification. We compared 6 Boosting based, 7 Bagging based and 2 hybrid ensembles for their performance in imbalance domain. We use KEEL tool to evaluate the performance of these methods by implementing the methods on seven imbalance data having class imbalance ratio from 1.82 to as high as 129.44. Area Under the curve (AUC) parameter is recorded as the performance metric. We also statistically analyzed the methods using Friedman rank test and Wilcoxon Matched Pair signed rank test to strengthen the visual interpretations. After analysis, it is proved that RusBoost ensemble outperformed every other ensemble in the imbalanced data situations.

Keywords—Ensemble approaches; boosting; bagging; hybrid ensembles; imbalanced data-sets; classification

I. INTRODUCTION

Classification process is very important in solving many real time problems. Various types of classifiers have been proposed in research field to solve classification problems. These classifiers only gives satisfactory results where the real time problems are represented by balanced data-set (the proportion of size of data classes is same). But sometimes, there are circumstances wherein we want to do the classification when the data-set is not balanced (proportion of size of data classes is not same) e.g. Web Spam Detection, Credit Card Frauds, Fraudulent Telephone calls etc. In such cases, if we apply the classification methods which are designed to classify balanced data sets, we will not get the accurate results. The major problem with imbalanced data set is that the data points belong to majority class (bigger class) impacts the classifier decision boundaries at the cost of minority class (smaller class) which is represented by very few points compare to majority class. This concern is known with the name as class imbalance problem in the research community. The extent of imbalance in data can be measured with class imbalance ratio (CIR). CIR is the percentage of size of majority class to the size of minority class. CIR value is indirectly related to the size of minority class. CIR with high

value is considered as highly imbalanced data. Various types of solutions are developed by research community to handle this problem. Methods developed to resolve this issue can be divided into three major categories. Data level, algorithm level and the combination of data and algorithm level (hybrid) approaches. In data level approaches, data is pre-processed for balancing the dataset before classification. The biggest benefit of this category is that one can use the existing classification methods which are developed to classify balanced data-sets. Researchers have applied different logics for balancing the data. Some methods balance the data by synthetically generating the data-points within minority class either randomly copying the existing data or by applying some intelligent process to generate synthetic data [1-11]. These types of methods come under the category of oversampling methods. The limitation with random oversampling by copying the existing data may lead to overfitting. In case of the noisy data-sets, random oversampling may lead to the increase of noise within the data-set [12, 13]. Some methods balance the data by removing data points from majority class either randomly or by using some intelligent concept before classification [13-19]. The biggest limitation with random undersampling is the loss of some important information. These type of methods are called undersampling methods. There is another sub-type of data-level methods wherein we combine the concept of oversampling and undersampling to balance the dataset before classification. These types of methods are known as hybrid data level methods [20, 21]. In algorithm level category, the researchers either modified the existing classification methods by working on the biasness of classifier towards the bigger class or by developing new methods to handle imbalanced data [22-38]. The third category, known as hybrid methods, combines data-level and algorithm level methods to boost the classifiers performance for imbalance data [39-53]. Many researchers combine data-level methods and algorithm level methods using ensemble concept to enhance the performance of earlier classification methods which were using only single classifier for getting results. Ensemble concept uses multiple classifiers for better predictive results compare to the methods which uses only single classifier to obtain the results. In this paper, we review ensemble based classification techniques which uses Bagging and Boosting concept to handle imbalance data-sets. We empirically assessed the methods using KEEL tool [54, 55] and statistically analyzed the results using Friedman [56] and Wilcoxon Matched pair signed rank [57] tests. Section II explains the idea of ensembles and review Boosting based and Bagging based ensembles designed to resolve class imbalance

issue. It also describes the performance criteria used in this paper to assess the performance of methods. Empirical calculation of ensembles approaches and their statistical analysis is discussed in Section III followed by conclusions in Section IV.

II. REVIEW OF ENSEMBLE APPROACHES

A. Fundamentals of Ensemble Approach

Ensemble approaches train more than one classifiers to resolve the same issue. This method is also named committee-based learning or learning through more than one classifier systems. Fig. 1 describes the model of ensemble approach. The area of ensemble approaches actually generated from three sections i.e. combining more than one classifiers, ensembles of weak classifiers and combination of experts [58]. Combining classifiers concept was mostly studied under pattern recognition area wherein the researchers works on strong classifiers and try to design powerful combining rules to get stronger combined classifiers. Ensemble of weak classifier is mostly studied by machine learning community wherein the researchers work upon weak classifiers to design powerful procedures for boosting the performance from weak to strong. This area has designed vary famous ensemble methods like AdaBoost [59] and Bagging etc. Combination of experts is studied by neural network community wherein the researchers usually consider a divide-and-conquer scheme to learn a combination of parametric prototypes jointly.

Ensemble methods are popular learning paradigm [58] since 1990's. It is because of two main pioneering work proposed in literature. One, which has empirically proved [60], analyzed that the outcomes resulted from a set of learners are found more precise than the results given by a single finest classifier as displayed in Fig. 2. The other, theory concept proven by Schapire [61] is that the weak base learners can be enhanced to strong learners. As strong classifiers are needed to solve many real time problems which are not possible to solve using weak classifiers, this need has motivated the researchers to generate strong classifiers by using ensemble methods. Ensemble methods use multiple classification procedures to attain better predictive results. Under this approach, various classifiers are trained either parallel or sequentially to resolve the same problem. An ensemble is created using two steps, by selecting the base classifier and then joining them to make ensemble of classifiers. Performance of ensemble methods can be decided by two factors: Accuracy of the individual learner and diversity among all classifiers. Ensemble's accuracy is directly related to the selection of base classifier. It is widely accepted [62] that improvement in the overall predictive accuracy by the ensemble can occur only if there is diversity among its components i.e. if individual classifiers don't always agree. Diversity is the measure to which a classifier can make different decisions on a single problem. Various ways can be used to measure diversity like by manipulating training patterns (cross-validation, bagging, boosting), by manipulating input features (by considering subset of features for classifier learning) and by incorporating random noise. Major research in literature belongs to homogeneous ensembles than heterogeneous ensembles wherein we use combinations of

different classifiers to produce results. But heterogeneous ensembles can produce more diversified results than homogeneous ensembles [66]. Computational complexity is very high in case of generating a single classifier than the ensemble. Because, while generating single classifier, for better performance it is essential to design various versions and tuning parameters for better model selection, whereas, the computational complexity in combining different classifiers is very less. Ensemble approaches reviewed in the paper are shown in Fig. 3.

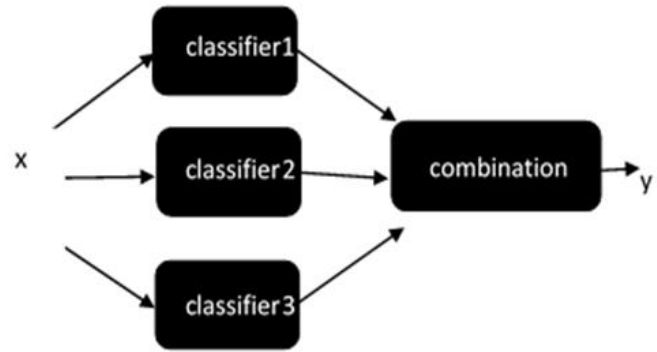


Fig. 1. A Common Ensemble Architecture [58].

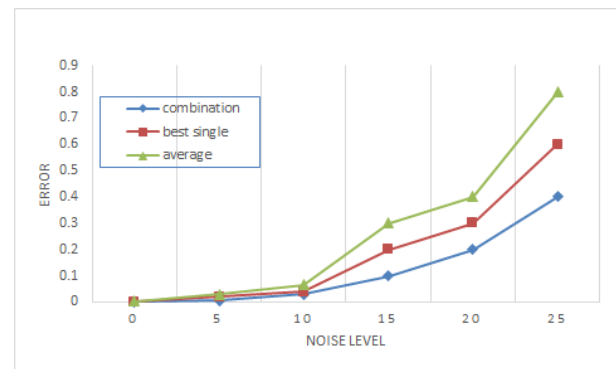


Fig. 2. Salamon and Hansen's Observation [58].

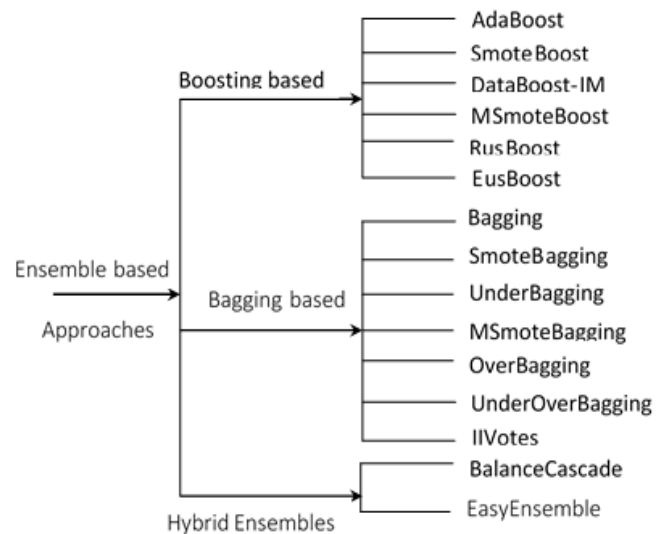


Fig. 3. Ensemble Approaches under Study.

B. Ensembles based upon Boosting Concept

Ensembles are categorized into two models namely Boosting and Bagging, based on the methodology of joining base classifiers. Boosting method converts the weak classifier to strong classifier by sequentially generating the base classifier hence it goes in the category of sequential ensemble paradigm [58]. In a boosting process, initially a model is build using initial training data, then another model is created whose purpose is to correct the errors from the model generated from previous model. This process is repeated until the perfect prediction is done or a maximum number of models are generated. Various ensembles, based upon boosting concept, reviewed during current study are described as below:

1) *Adaptive boosting method (AdaBoost)*: AdaBoost, [59] the first successful algorithm proposed by Freund and Schapire in 1996 using boosting concept for binary classification. In AdaBoost, we used complete data-set for training every classifier serially. After every iteration, the method assigns more weight to the misclassified data points, with the objective of accurately classifying the misclassified data points recognized during current iteration, in the next iteration. Hence, its main objective is to emphasize on the data points whose classification is predicted as hard. Weight allocated to the misclassified data points after every iteration is directly related to the status of misclassified data i.e. How hard it is to classify that data point. Weight is initially equally assigned to all the data. After every iteration, the weights allocated to misclassified data points are increased and allocated to correctly classified data points are decreased. Lastly, when an unknown data point is submitted, every classifier vote for it and the data point is finally allocated to the class based upon the majority votes. It is named adaptive as it is build using multiple repetitions for creating a strong classifier. The drawback of AdaBoost is that it allocates equal weights to the classes and is internally developed to detect equal size of classes (for balanced data-sets). In imbalanced scenarios, its results are always in the favor of majority class. Therefore, to handle this biasness towards majority class, many researchers updated equal weight situation of Adaboost method so as to modify the method to detect minority class accurately. Fig. 4 shows the procedure of AdaBoost.

2) *Smoteboost*: N. V. Chawla in 2002 proposed SmoteBoost [3] by modifying AdaBoost to address imbalance problem in classes. SmoteBoost combines an oversampling method SMOTE with standard boosting process. It generates synthetic data inside minority class using SMOTE process during every iteration of AdaBoost. The weights assigned to synthetically generated data remains constant and depend on the aggregate sum of information in the new data-set, whereas the weights assigned to the original data points are normalized so as to form a distribution with the new generated data points. When the classifier is trained, the weights assigned to the original data points are updated. Again the synthetic data is

generated in another phase and weights are modified so as to match the weight distribution. This process repeats itself till we get the required predictions or extreme number of classifiers are build. Limitation with the method is that it uses oversampling method to balance the data by generating synthetic data points therefore it is more computationally expensive compare to the methods that are based on undersampling approaches. Another limitation of SmoteBoost is that in case of noisy data-sets it may end up by increasing noisy data-points by random selection of the noise points as a candidate to produce synthetic data-points [12, 13].

3) *Databoost-IM*: Guo and Victor in 2004 proposed another boosting based method, namely DataBoost-IM [49], by combining boosting with data-generation to improve the predictive capabilities of classifiers for binary imbalance data-sets. Its working principle is unlike SmoteBoost as it, firstly, identify and separate data points which are hard to predict, from both minority as well as majority class, to produce synthetic data-points. It also considers bias information towards hard to predict data points to produce synthetic data on which the classifier from next iteration needs to focus. In this process, the weights assigned to both the classes in the new training set are re-balanced so that boosting procedure can focus on both the classes. Hence, this method focused on refining the prediction ability of both the majority and minority class. The principle drawback [63] of this procedure is that it can't manage very high imbalanced situations in light of the fact that it creates an extensive amount of data points which are troublesome toward oversee by the base classifier.

Algorithm: AdaBoost

Input: Data set $D = \{(x_1, y_1), (x_2, y_2), \dots, (x_m, y_m)\}$;

Base Classifier χ ; Number of learning rounds \forall .

Process:

1. $D_1(x) = 1/m$ //Initialize the weight distribution
2. **for** $t = 1, \dots, \forall$:
3. $h_t = \chi(D, D_t)$; // train a classifier h_t from D under distribution D_t
4. $\epsilon_t = P_{x \sim D_t}(h_t(x) \neq f(x))$; // Evaluate the error of h_t
5. **if** $\epsilon_t > 0.5$ **then break**
6. $\alpha_t = \frac{1}{2} \ln \left(\frac{1 - \epsilon_t}{\epsilon_t} \right)$;
7. $D_{t+1}(x) = \frac{D_t(x)}{z_t} \times \begin{cases} \exp(-\alpha_t) & \text{if } h_t(x) = f(x) \\ \exp(\alpha_t) & \text{if } h_t(x) \neq f(x) \end{cases}$
 $= \frac{D_t(x) \exp(-\alpha_t f(x) h_t(x))}{z_t}$ // update the distribution, where z_t
// is the normalization factor which
// enables D_{t+1} to be a distribution
8. **end**

Output: $H(x) = \text{sign}(\sum_{t=1}^T \alpha_t h_t(x))$

Fig. 4. AdaBoost Algorithm.

4) *Modified smoteboost (MSmoteBoost)*: To handle the noise sensitivity of SmoteBoost in 2009, Ma and He gave an intelligent boosting approach, MSmoteBoost [41], which incorporates MSmote data level method in every iteration of AdaBoost. Unlike Smote, MSmoteBoost remove noise data-points and consider the distribution of minority class. Minority class data is divided into three groups as border, security and latent noise points. The data points are categorized based on the distance from other data points, before generating synthetic points. Security data points are those which can strengthen the performance and noise points can reduce the performance of classifier. Hard to predict data are recognized as border category. The method processes the data differently with these categories while producing synthetic data points. The weights assigned to the new data points are based on the total number of points in the new data-set. Hence, their weights always remain constant, whereas original data-set's data point's weights are normalized so that they form a distribution with the new generated data points. The assigned weights of the original data points are updated after training the classifier.

The process repeats itself till the strong classifier is build. As this classifier is also using oversampling approach, Its computational cost is also high compare to the ensembles based on undersampling.

5) *Random undersampling boosting (RusBoost)*: In 2010, another boosting based ensemble is proposed. It is dissimilar from SmoteBoost because it incorporates undersampling data level method (Rus) in every iteration of AdaBoost with the motive of proposing a simple classifier which can work with fast speed than using any oversampling approach. RusBoost [39] removes data points randomly from majority class in every iteration of AdaBoost. RusBoost doesn't allocate new weights to the data points. It is sufficient to normalize the weights of the remaining data points in the new data-set according to the total sum of weights. After the classifier is trained, the process updates the weights of the original data-set. The process is repeated till we get the strong classifier. The inspiration of combining Random undersampling and boosting method is its simplicity, performance and speed. As the data set is balanced by removing data therefore time needed to build a model is low compare to oversampling models. Loss of required information is the major limitation because no intelligent method is used to eliminate data from the majority class. Another disadvantage is during noisy environments, it may end up removing good data from classes due to which there is more impact of noise on the classifier's performance [12, 13].

6) *Evolutionary undersampling boosting (EusBoost)*: In 2013, an intelligent undersampling based ensemble, EusBoost, is proposed which incorporates EUS [40] preprocessing method in every iteration of AdaBoost. The basis of EusBoost [40] is RusBoost, which is simplest method compare to other oversampling approaches. EuaBoost enhances the classifier

performance by the using the evolutionary undersampling approach. The key principle of EusBoost is diversity mechanism by considering different subset of data in every iteration.

C. Ensembles based upon Bagging (Bootstrap Aggregation) Concept

Bagging, like Boosting, also build a strong classifier by combining multiple weak classifiers for the better performance compare to using single classifier. Bagging [64] gives the best results if the problem using single classifier is overfitting. Unlike Boosting, any data point in bagging has the same probability to appear in a new data-set. The process of bagging starts by creating sub-sets from the data-set. Then each sub-set of data-set is trained independently using classifier that results in ensemble of different models. Then average of all these different models are used to build a strong classifier. It brings diversity by using different data-sets for every classifier. Hence, bagging comes under the category of parallel ensemble methods. The inspiration behind these ensemble methods is to exploit the independence between the weak classifiers [58]. Fig. 5 shows the bagging algorithm.

1) *Smotebagging*: SmoteBagging [65] combines oversampling of minority class using Smote with bagging. In this method both the classes participate in creating each bag. A Smote oversamples the data with a% rate during every iteration and increased the rate with the multiple of 10 with every next iteration. This proportion characterizes the measure of positive data points which are arbitrarily resampled from the first data-set amid each iteration. The remaining positive data is generated by Smote algorithm till the data is balanced. Bootstrapping negative data points are created to make the ensemble more diverse.

2) *Underbagging*: This approach [65] does undersampling after creating subset of data from original data-set. Therefore, in place of removing data from the whole data-set, it does it before training each classifier. Undersampling is done by using nearest neighbor principle for balancing the data before training the classifier.

3) *MSmotebagging*: MSmoteBagging [65, 67] is the variation of SmoteBagging wherein minority class is oversampled using MSmote data level method. Oversample minority class data points using MSMOTE preprocessing algorithm.

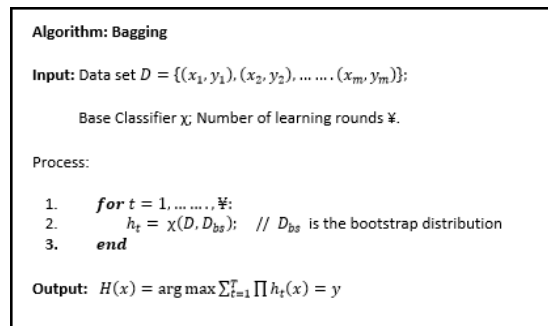


Fig. 5. Bagging Algorithm.

4) *Overbagging*: In this method [65], data-set is balanced when the bags are randomly picked from the original data-set. Therefore, in place of removing the data randomly from whole data-set, the data is generated randomly within minority class of sub-set before every classifier is trained. This method includes all the majority class data points in the new bootstrap.

5) *Underoverbagging*: UnderBagging to OverBagging (UnderOverBagging) [65] method uses the combination of oversampling and undersampling process. It considers the resampling rate 'a%' in every iteration which is ranged from 10% to 100%. Resampling rate is the multiple of 10. Therefore, the number of data points trained by every classifier in the subsequent iterations will be different. This method introduce diversity in the process.

6) *Imbalanced ivotes (IIVotes)*: IIVotes is the combination of SPIDER [68] and IVotes [69]. SPIDER is the preprocessing method. .IVotes is a variation of Bagging where the sampling is done according to the importance of each data point. Although SPIDER method improves the sensitivity of minority class but decrease the specificity at the same time. IIVotes modified SPIDER method by incorporating IVotes for improving the trade-off between specificity and sensitivity. The main purpose of this method is to acquire a balance between the specificity and sensitivity for the minority class in contrast to a single classifier combined with SPIDER.

D. Ensembles based upon Hybrid Ensemble Concept (Bagging and Boosting)

Hybrid Ensemble based methods are the combination of bagging, boosting and pre-processing methods. Liu, Wu, and Zhou in 2009 proposed EasyEnsemble [53] and BalanceCascade [53] and named these methods as exploratory undersampling methods. These methods follow different approaches to tackle negative data points after every iteration. These methods used bagging as the key concept in building ensemble and used AdaBoost technique in place of the weak classifier. In BalanceCascade the classifiers are trained sequentially because it works in a supervised manner. During bagging iteration after the AdaBoost classifier is trained, the correctly classified majority data are removed from the data-set and is not processed in the next iterations. As EasyEnsemble approach does not execute any operation on the data from the original data-set after every AdaBoost iteration. So the classifiers are trained in parallel.

E. Performance Criteria

In case of imbalanced data-sets, the main objective is to identify the minority class so we are considering minority class as the positive class. Table I shows the confusion matrix for imbalance data-sets.

TABLE I. CONFUSION MATRIX

	Positive (Minority)	Negative (Majority)
True	True Positive	True Negative
False	False Positive	False Negative

We are using Area under the ROC Curve (AUC) [70, 71] as the performance metric to assess the methods. AUC is a standout amongst the most famous execution metric used to assess the execution of classifiers intended for imbalanced data sets. It is a curve in which false-positive rate and true positive rate are plotted on x-axis and y-axis respectively. AUC is the finest tool for comparing different classifiers. A classifier's performance is directly proportional to its location towards the upper left corner. AUC portrays ROC quantitatively. It is calculated as the arithmetic mean of True Positive rate and True Negative rate.

$$AUC = \frac{TP_{Rate} + TN_{Rate}}{2} \quad (1)$$

Where TP_{Rate} is characterized as the quantity of positive data points that are accurately categorised as positive and TN_{Rate} is the total quantity of negative data points that are accurately categorised as negative. AUC reveals the global performance of every classifier for all conceivable estimation of False Positive rate.

III. EMPIRICAL ASSESSMENT OF ENSEMBLES

We have compared 15 ensemble approaches with 7 imbalanced data with the class imbalance ratio from 1.82 to 129.44. The characteristics of these data-sets are recorded in Appendix A. We used KEEL tool [54, 55] for comparing the performance of ensemble approaches by considering Decision Tree method (C4.5) as the weak classifier. C4.5 is the widely used classifier by many people to compare the algorithms in imbalance domains [72, 73]. The AUC of the methods is recorded with the following initial settings of the KEEL tool (Table II). Tables III and IV listed AUC values along with the variance. Results are visually displayed in Fig. 6, Fig. 7 and Fig. 8. Average performance of all the ensembles is shown in Fig. 9.

A. Visual Interpretations and Discussions

It is witnessed from the figures that for Boosting based approaches (Fig. 6), RusBoost stands out and outperformed every other method for extremely imbalanced data (Abalone19 having imbalance ratio of 129.44). In other cases, SmoteBoost and RusBoost almost performed equally. In case of Bagging based approaches (Fig. 7), Underbagging outperformed other methods for highly imbalanced data-set whereas the performance of SmoteBagging and UnderBagging is almost equal for other data-sets. Hybrid ensembles performed equally well for all the data-sets with minor differences for some data-sets. In case of Ecoli4, Balancecascade outperformed EasyEnsemble whereas in case of Abalone19, EasyEnsemble outperformed Balancecascade.

TABLE II. PARAMETER SETTING OF KEEL TOOL

Parameter Description	Value
Base Classifier	Decision Tree (C4.5)
Cross Validation	5 Fold
Data points per leaf	2
Confidence Level	0.25
Number of Classifiers	10
Pruning	True

TABLE III. AUC VALUES OF ENSEMBLE APPROACHES

Techniques	Data-Sets (Class Imbalance ratio :: 1.82 to 129.44)							
	Glass1(1.82)		Vehicle3 (2.99)		Yeast3 (8.10)		Ecoli4 (15.80)	
	AUC	Variance	AUC	Variance	AUC	Variance	AUC	Variance
Adaboost	0.8093	±0.0020	0.6812	±0.0004	0.8351	±0.0011	0.8449	±0.0115
SmoteBoost	0.7839	±0.0034	0.7442	±0.0009	0.8917	±0.0004	0.8826	±0.0057
DataBoost-IM	Not Performing		0.6917	±0.0020	0.8919	±0.0009	0.8489	±0.0065
MSmoteBoost	0.7625	±0.0061	0.7386	±0.0002	0.9176	±0.0010	0.8489	±0.0059
RusBoost	0.7703	±0.0041	0.7643	±0.0001	0.9198	±0.0004	0.9146	±0.0015
EusBoost	0.7836	±0.0036	0.7713	±0.0014	0.9321	±0.0004	0.8760	±0.0096
Bagging	0.7556	±0.0010	0.6602	±0.0008	0.8529	±0.0010	0.8906	±0.0069
SmoteBagging	0.7444	±0.0050	0.7488	±0.0020	0.9350	±0.0003	0.8996	±0.0030
UnderBagging	0.7547	±0.0038	0.7410	±0.0005	0.9354	±0.0003	0.8598	±0.0018
MSmoteBagging	0.7219	±0.0038	0.7678	±0.0003	0.9291	±0.0003	0.8632	±0.0040
OverBagging	0.7580	±0.0034	0.7207	±0.0004	0.9073	±0.0025	0.8853	±0.0069
UnderOverBagging	0.7286	±0.0024	0.7535	±0.0004	0.9293	±0.0005	0.8566	±0.0040
IVotes	0.6745	±0.0044	0.7330	±0.0016	0.8908	±0.0004	0.8879	±0.0018
BalanceCascade	0.7491	±0.0025	0.7282	±0.0008	0.9135	±0.0008	0.9093	±0.0028
EasyEnsemble	0.7491	±0.0025	0.7282	±0.0008	0.9135	±0.0008	0.8650	±0.0022

TABLE IV. AUC VALUES OF ENSEMBLE APPROACHES

Techniques	Data-Sets (Class Imbalance ratio :: 1.82 to 129.44)						
	Abalone 9-18 (16.40)		Yeast5 (32.78)		Abalone19 (129.44)		Average Performance out of 7 data-sets
	AUC	Variance	AUC	Variance	AUC	Variance	AUC
Adaboost	0.7327	±0.0239	0.8174	±0.0013	0.5095	±0.0006	0.7471
SmoteBoost	0.7939	±0.0238	0.9554	±0.0030	0.5291	±0.0015	0.7972
DataBoost-IM	0.7226	±0.0240	0.9071	±0.0009	0.5000	±0.0000	0.7603
MSmoteBoost	0.7290	±0.0139	0.9142	±0.0004	0.4989	±0.0000	0.7728
RusBoost	0.8105	±0.0085	0.9633	±0.0005	0.6888	±0.0060	0.8330
EusBoost	0.7957	±0.0133	0.9471	±0.0005	Not Performing		0.8509
Bagging	0.6510	±0.0086	0.8744	±0.0003	0.5000	±0.0000	0.7407
SmoteBagging	0.7961	±0.0149	0.9670	±0.0007	0.5467	±0.0008	0.8054
UnderBagging	0.7733	±0.0030	0.9592	±0.0004	0.6894	±0.0048	0.8161
MSmoteBagging	0.7303	±0.0117	0.9340	±0.0011	0.4996	±0.0000	0.7780
OverBagging	0.7377	±0.0198	0.8788	±0.0033	0.5488	±0.0008	0.7767
UnderOverBagging	0.7527	±0.0210	0.9413	±0.0020	0.5264	±0.0033	0.7841
IVotes	0.7456	±0.0228	0.8328	±0.0031	0.4990	±0.0000	0.7520
BalanceCascade	0.7456	±0.0185	0.9552	±0.0005	0.6667	±0.0069	0.8096
EasyEnsemble	0.7456	±0.0185	0.9552	±0.0005	0.6685	±0.0066	0.8036

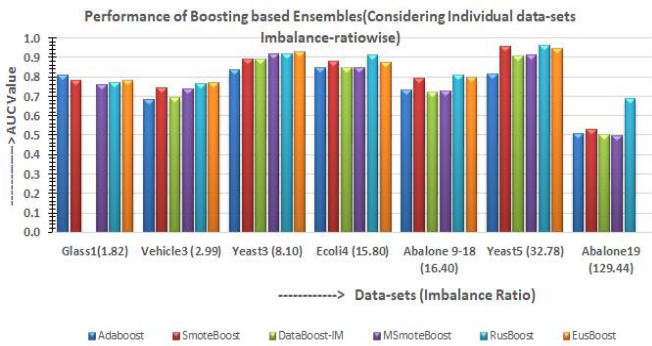


Fig. 6. AUC Results of Boosting based Ensembles.

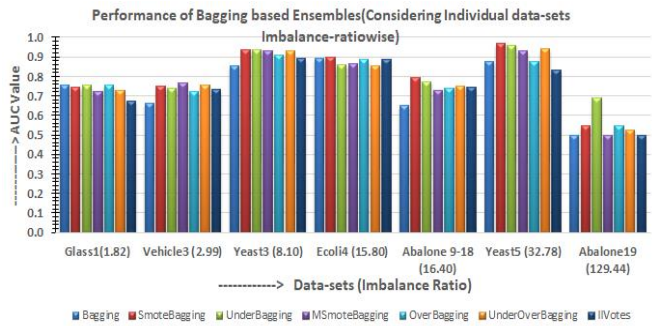


Fig. 7. AUC Results of Bagging based Ensembles.

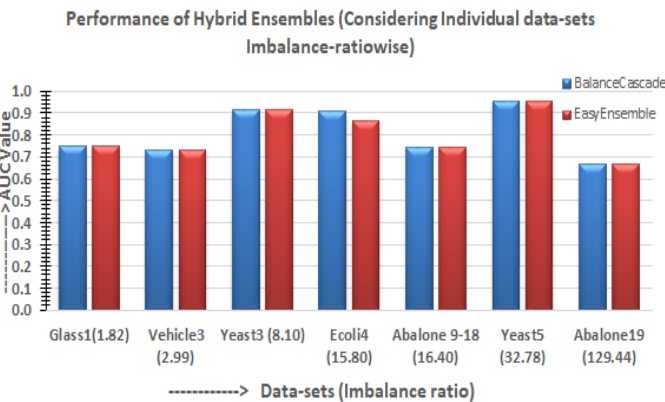


Fig. 8. AUC Results of Hybrid Ensembles.

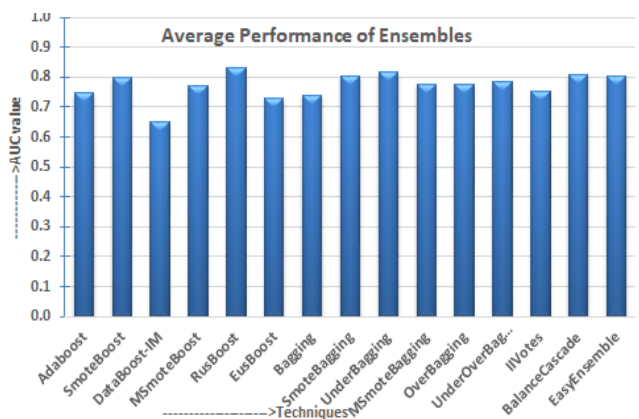


Fig. 9. Average AUC Results of all the Ensembles.

Considering the overall average performance of ensembles, it is observed that RusBoost outperformed other ensemble methods. The performance of SmoteBagging, UnderBagging, BalanceCascade and SmoteBoost performed equally well with the minor variations.

The visual interpretation about performance of these ensembles is not satisfactory and sufficient. So to prove these interpretations, we have done statistical validations.

B. Statistical Validations

It is very difficult to judge the performance of algorithms when their performance is tested with multiple data-sets and best performing method is not the same for every case. Statistical validation is an efficient tool when we have to compare the performance of methods with very little variation. To do better analysis we are using non-parametric tests as per the recommendation given in [72-74]. We are conducting two types of non-parametric tests. We are using Friedman rank test [75] to compare multiple methods and to know if there are any significant differences between the methods. If the ‘Null hypothesis is rejected’ then we are using Holm post-hoc test [75] to check if the control method (having rank 1) is significantly better than other methods (1 x N comparisons). This test computes ranks for every algorithm as per the following equation:

$$F_{AR} = \frac{(c-1) \left[\sum_{j=1}^c \hat{R}_j^2 - \frac{(cn)^2}{4} \right]}{\{[cn(cn+1)(2cn+1)]/6\} - (1/c) \sum_{i=1}^n \hat{R}_i^2} \quad (2)$$

Where ‘c’ is the total number of algorithms, \hat{R}_i is equal to the rank total of the i^{th} data-set and \hat{R}_j is the rank total of the j^{th} algorithm. As per the equation the best performing algorithm will have the lowest rank. To compare two methods, we are using Wilcoxon Matched Pair signed rank test [57] to find the significant differences between two methods.

1) *Statistical framework:* We applied the statistical tests on the AUC performance metric as per following steps In the first step, Best performer method is selected from every group of ensembles (Boosting, Bagging and Hybrid) using Friedman test and Holm post-hoc analysis. After this step, we left with only three best methods out of all the groups. In the second step, 3 methods are assessed using Friedman test to find the final method which outperformed every other ensemble to classify imbalanced data.

2) *Analysis and discussions:* Firstly, we apply Friedman test on Boosting based ensembles. Fig. 10 shows the ranks assigned by Friedman test. As per the ranking, RusBoost outperformed in the family of Boosting ensembles whereas DataBoost-IM is the worst performer. Table V lists the Friedman test statistic for Boosting ensembles.

TABLE V. TEST STATISTICS USING FRIEDMAN TEST (BOOSTING ENSEMBLES)

N	07
Chi-Square (F_{AR})	16.55
Degree of Freedom (K-1)	5
p-value	0.005435

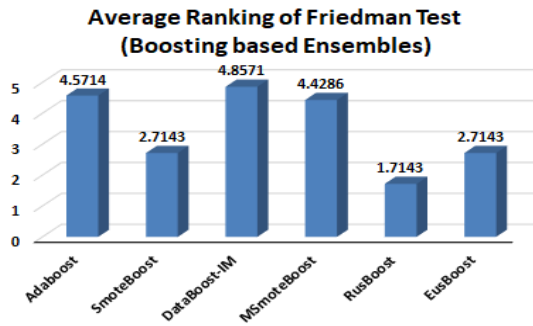


Fig. 10. Ranks Assigned by Friedman Test.

In the table, ‘N’ is the number of data-sets. ‘k-1’ is the degree of freedom (which is equal to number of algorithms minus 1). The table value of chi-square (χ^2) test for ‘5’ degree of freedom is 11.0705, which is lesser than the F_{AR} calculated value 16.55102 and the p-value is less than 0.05. Hence the null hypothesis (There is no significant difference between these groups of algorithms) is rejected. To know the difference, we did Holm post-hoc analysis by considering RusBoost as the control method (having rank 1). Holm statistics is given in Table VI. As per the statistic, the hypothesis for no significant differences is rejected for DataBoost-IM, AdaBoost, MSmoteBoost and EusBoost with the control method ‘RusBoost’ because the p-value is each case is less than 0.05. As the p-value of SmoteBoost is equal to 0.05, hence there are no significant differences between RusBoost and SmoteBoost. We further analyze these two algorithms using Wilcoxon Matched Pair signed rank test. The test statistics is given in Table VII. R^+ is the sum of ranks for the data-set in which the number of times first algorithm (RusBoost) outperformed other (SmoteBoost). R^- rank specify the number of times second algorithm (SmoteBoost) outperformed the other (RusBoost). It is clearly seen from the table that RusBoost performed better than SmoteBoost. So RusBoost is selected as the best performer from the Boosting based ensemble group. Friedman Test ranking for Bagging based ensembles is shown in Fig. 11 and Test statistics are shown in Table VIII. SmoteBagging outperformed other ensembles with first rank and IIVotes is the worst performer. As chi-square (χ^2) table value for 6 degree of freedom is 12.5916 which is lower than chi-square (F_{AR}) calculated value and p-value is less than 0.05, the null hypothesis is rejected. To know the difference between these ensembles, Holm post-hoc test is conducted with SmoteBagging as the control method. Table IX shows the Holm test statistics. All the methods except UnderBagging reject the null hypothesis, which means that we have to further analyze SmoteBagging and Underbagging for any significant differences. To closely analyze these two methods, we performed Wilcoxon Matched pair test. The test statistics (Table X) shows that p-value is more than 0.05 so null hypothesis for no significant differences is accepted. But the higher rank in favor of SmoteBagging proves its better performance compare to UnderBagging. Hence, SmoteBagging is selected as the best performer in the category of bagging based ensembles. As we have only two methods in hybrid ensemble category so we are performing Wilcoxon Matched pair test to analyze these methods. From the test statistics (Table XI), it is observed that

the hypothesis is accepted as the p-value is more than 0.05 but the higher rank score of BalanceCascade confirms its superiority from EasyEnsemble. So, BalanceCascade is selected as the best performer from hybrid ensemble category.

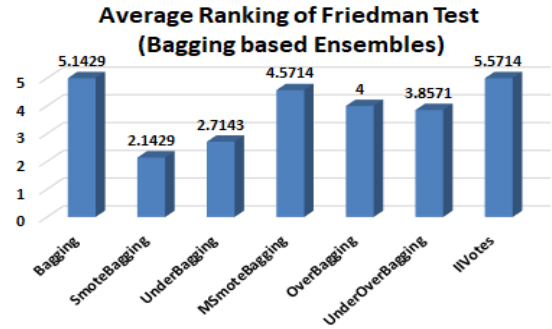


Fig. 11. Ranks Assigned by Friedman Test.

TABLE VI. STATISTICS USING HOLM TEST FOR COMPARING BOOSTING BASED ENSEMBLES

Control method: RusBoost (1.7143)				
I	Methods	Z Value	Holm (p-value)	Hypothesis ($\alpha=0.05$)
5	DataBoost-IM	3.142857	0.01	Rejected
4	AdaBoost	2.857143	0.0125	Rejected
3	MSmoteBoost	2.714286	0.016667	Rejected
2	EusBoost	1	0.025	Rejected
1	SmoteBoost	1	0.05	Not Rejected

TABLE VII. STATISTICS USING WILCOXON TEST FOR COMPARING RUSBOOST AND SMOTEBOOST

Methods	R^+	R^-	Hypothesis ($\alpha=0.05$)	p-value
RusBoost Vs SmoteBoost	26.0	2.0	Rejected, Significant differences between methods	0.04688

TABLE VIII. TEST STATISTICS USING FRIEDMAN TEST (BAGGING ENSEMBLES)

N	07
Chi-Square (F_{AR})	13.8367
Degree of Freedom (K-1)	6
p-value	0.031514

TABLE IX. STATISTICS USING HOLM TEST FOR COMPARING BAGGING BASED ENSEMBLES

Control method: SmoteBagging (2.1429)				
I	Methods	Z Value	Holm (p-value)	Hypothesis ($\alpha=0.05$)
6	IIVotes	2.96923	0.0083	Rejected
5	Bagging	2.59807	0.01	Rejected
4	MSmoteBagging	2.10320	0.0125	Rejected
3	OverBagging	1.60833	0.016667	Rejected
2	UnderOverBagging	1.48461	0.025	Rejected
1	UnderBagging	0.49487	0.05	Not Rejected

TABLE X. STATISTICS USING WILCOXON TEST FOR COMPARING SMOTEBAGGING AND UNDERBAGGING

Methods	R ⁺	R ⁻	Hypothesis ($\alpha=0.05$)	p-value
SmoteBagging Vs UnderBagging	16.0	12.0	Accepted, No significant differences	0.67260

TABLE XI. STATISTICS USING WILCOXON TEST FOR COMPARING BALANCECASCADE AND EASYENSEMBLE

Methods	R ⁺	R ⁻	Hypothesis ($\alpha=0.05$)	p-value
BalanceCascade Vs EasyEnsemble	11.0	10.0	Accepted, No significant differences	0.83393

Next step is to analyze these three best performer methods. We again performed Friedman Test with these three methods. Ranks assigned by the test shows (Fig. 12) that RusBoost is the best performer and Balancecascade is the worst performer and Friedman Test statistic (Table XII) reveals that chi-square (χ^2) table value for 2 degree of freedom (5.9915) is less than calculated value (6.0), hence there are no significant differences between the methods. We further analyze the methods with Holm post-hoc analysis. Test statistics (Table XIII) shows that RusBoost and SmoteBagging are similar as the null hypothesis for no significant differences is accepted. As a last step to find the best performer out of all ensemble methods, we closely analyzed RusBoost and SmoteBagging with Wilcoxon matched pair test. Although, the p-value of the test statistic shown in the table (Table XIV) is more than 0.05, which means that there are no significant differences between these pair of methods but the higher rank value of RusBoost shows that its performance is better than SmoteBagging. Another advantage of RusBoost is that as it is using undersampling approach within the boosting process to classify the data-set so it is computationally less expensive compare to SmoteBagging which follows oversampling approach and bagging process for classification.

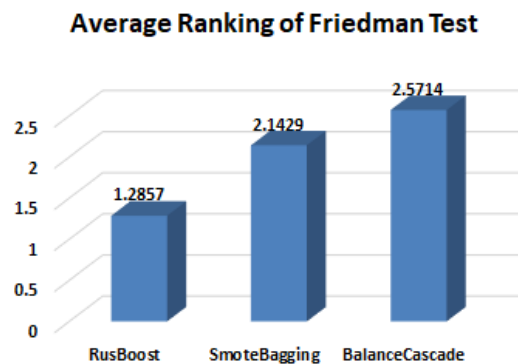


Fig. 12. Ranks Assigned by Friedman Test.

TABLE XII. TEST STATISTICS USING FRIEDMAN TEST (BEST PERFORMER ENSEMBLES)

N	07
Chi-Square (F_{AR})	6.0
Degree of Freedom (K-1)	2
p-value	0.049787

TABLE XIII. STATISTICS USING HOLM TEST FOR COMPARING THE CANDIDATE METHODS FOR BEST PERFORMER ENSEMBLES

Control method: RusBoost (1.2857)				
I	Methods	Z Value	Holm (p-value)	Hypothesis ($\alpha=0.05$)
2	BalanceCascade	2.405351	0.025	Rejected
1	SmoteBagging	1.603567	0.05	Not Rejected

TABLE XIV. STATISTICS USING WILCOXON TEST FOR COMPARISON BETWEEN RUSBOOST AND SMOTEBAGGING

Methods	R ⁺	R ⁻	Hypothesis ($\alpha=0.05$)	p-value
RusBoost Vs SmoteBagging	23.0	5.0	Accepted, No significant differences	0.108319

From the visual interpretations and the statistical analysis, we can say that RusBoost outperformed other ensemble based methods in the imbalance domains.

IV. CONCLUSION

In the current study, we review various boosting and bagging based ensemble approaches for their performance in imbalanced domains by focusing on binary classification. We empirically assessed 15 approaches using 7 imbalanced data sets (KEEL repository) with the class imbalance ratio from 1.82 to as high as 129.44. After analyzing the results through statistical analysis methods (Wilcoxon matched signed rank and Friedman test), it is reported that RusBoost has outperformed other 14 methods considering any level of imbalance ratio. In future, we are planning to propose an ensemble approach which can work efficiently in the presence of other data impurities like noise, etc. along with data-set.

APPENDIX A

TABLE AI. PROPERTIES OF DATA SETS

Sr. No	Data sets	Imbalance Ratio	Number of Dimensions	Minority Class %	Size of data-set
1	Glass1	1.82	9	35.51	214
2	Vehicle3	2.99	18	25.06	846
3	Yeast3	8.10	8	10.98	1484
4	Ecoli4	15.80	7	5.95	336
5	Abalone9-18	16.40	8	5.75	731
6	Yeast5	32.78	8	2.96	1484
7	Abalone19	129.44	8	0.77	4174

REFERENCES

- [1] A. Fernandez, V. L6Pez, M. Galar, M. J. Del Jesus and F. Herrera, "Analysing the classification of imbalanced data-sets with multiple classes: Binarization techniques and adhoc approaches", Knowledge Based Systems, Vol. 42, pp 97-110, 2013.
- [2] G. E. A.P.A Batista, R. C. Prati, and M. C. Monard, "A study of the behaviour of several methods for balancing machine learning training data", SIGKDD Expl. Newl., Vol 6, No. 1, pp 20-29,2004.
- [3] N. V. Chawla, K. W. Bowyer, L. O. Hall, and W. P. Kegelmeyer, "SMOTE:Synthetic Minority Over Sampling Technique", Journal of Artificial Intelligence Research, Vol. 16, pp 321-357, 2002.

- [4] J. A. Saez, J. Luengo, J. Stefanowski, and F. Herrera, "Managing Borderline and Noisy examples in Imbalanced Classification by combining SMOTE with Ensemble Filtering", IDEAL2014, LNCS, Vol. 8669, pp. 61-68, 2014, Springer.
- [5] R. Akbani, S. Kwek, and N. Japkowicz, "Applying Support Vector Machines to Imbalanced Datasets", ECML 2004, LNAI 3201, pp. 39-50, 2004. Springer-Verlag Berlin Heidelberg.
- [6] H. Han, W. Wang, and B. Mao, "Borderline-SMOTE: A new oversampling method in Imbalanced Data-sets Learning", In. ICIC 2005. LNCS, Vol. 3644, pp. 878-887. Springer, Heidelberg, 2005.
- [7] J. Stefanowski and S. Wilk, "Selective Preprocessing of imbalanced data for improving classification performance", Datawarehousing and Knowledge Discovery (Lecture Notes in Computer Science Series 5182, pp 283-292), 2008.
- [8] S. Hu, Y. Liang, L. Ma, and Y. He, "MSMOTE: Improving classification performance when training data is imbalanced", In *procc. 2nd Int. Workshop Computer Sci. Eng.*, Vol. 2, pp. 13-17, 2009.
- [9] C. Bunkhumpornpat, K. Sinapiromsaran, and C. Lursinsap, "Safe-Level-SMOTE: Safe Level- Synthetic Minority Over-Sampling Technique for handling the Class Imbalance Problem", PADD2009, LNAI, Vol. 5476, pp. 475-482, 2009, Springer.
- [10] Ying Mi, "Imbalanced classification based on Active Learning SMOTE", *Research Journal of Applied Sciences, Engg. And Tech.*, Vol. 5, issue 3, pp. 944-949, 2013.
- [11] P. Kaur and A. Gosain, "FF-SMOTE: A Metaheuristic Approach to Combat Class Imbalance in Binary Classification", *Applied Artificial Intelligence*, 2019, Tayler & Francis. DOI: 10.1080/08839514.2019.1577017.
- [12] P. Kaur and A. Gosain, "Comparing the behaviour of Undersampling and Oversampling of Class Imbalance Learning by combining Class Imbalance problem with noise", A.K. Saini et al. (eds.), *ICT Based Innovations, Advances in Intelligent Systems and Computing* 653, pp. 23-30, 2018. https://doi.org/10.1007/978-981-10-6602-3_3.
- [13] P. Kaur and A. Gosain, "An Intelligent Undersampling technique based upon Intuitionistic Fuzzy sets to alleviate Class Imbalance Problem of Classification with noisy environment", *International Journal of Intelligent Engineering Informatics*, Vol. 6, No. 5, pp. 417-433, 2018.
- [14] M. Kubat and S. Matwin, "Addressing the curse of imbalanced training sets:one-sided selection", *International Conference on Machine Learning*, Vol. 97, pp. 179-186, July 1997.
- [15] Y. M. Chyi, "Classification analysis techniques for skewed class distribution problems", Department of Information Management, National Sun Yat-Sen University, 2003.
- [16] S. Garcia and F. Herrera, "Evolutionary undersampling for classification with imbalanced data-sets: proposals and taxonomy", *Evolutionary Computation*, Vol. 17, pp 275-306, 2009.
- [17] Show-jane Yen and Yue-Shi Lee, "Cluster-based under-sampling approaches for imbalanced data distributions", *Expert Systems with Applications*, Vol. 36, pp 5718-5727, 2009.
- [18] M. M. Rahman and D. N. Davis, "Cluster based undersampling fAHCOR unbalanced Cardiovascular Data", WCE 2013, July 3-5, Vol III, London, UK, 2013.
- [19] T. Maruthi, B. S. Raju, R. N. Hota, and P. R. Krishna, "Class imbalance and its effect on PCA pre-processing", *International Journal of Knowledge engineering and Soft Data Paradigms*, Vol. 4, No. 3, pp. 272-294, 2014.
- [20] D. Li, S. S. Wu, T. I. Tsai, and Y. S. Lina, "Using mega-trend diffusion and artificial samples in small data-set learning for early flexible manufacturing system scheduling", *Knowledge, Computers and Operational Research*, Vol. 34, pp. 966-982, 2007.
- [21] E. Ramentol, Y. Caballero, R. Bello and F. Herrera, "SMOTE-RS B*: a hybrid pre-processing approach based on Oversampling and Undersampling for high imbalanced data-sets using SMOTE and Rough set theory", *Knowledge Information Systems*, Springer, 2011. DOI 10.1007/s 10115-011-0465-6.
- [22] G. Wu and E. Chang, "Kba: Kernel Boundary alignment considering imbalanced dataset distribution", *IEEE Transactions on Knowledge and Data Engineering*. Vol. 17, No. 6, pp. 786-795, 2005.
- [23] T. Iman, K. Ting, and J. Kamruzzaman, "z-SVM: An SVM for improved classification of imbalanced data", In *proceedings of the 19th Australian joint conference on Artificial Intelligence*, pp. 264-273, springer-verlag, 2006.
- [24] X. Hong, S. Chen, and C. J. Harris, "A kernel based two class classifier for imbalanced data-sets", *IEEE Transactions on Neural Networks*, Vol. 18, No. 1, pp. 28-41, 2007.
- [25] A. Fernandez, S. García, M. J. del Jesus, and F. Herrera, "A study of the behaviour of linguistic fuzzy rule base classification systems in the framework of imbalanced data-sets", *Fuzzy Sets and Systems*, Vol. 159, issue 18, pp. 2378-2398, 2008.
- [26] C-Y Yang, J-S Yang, and J-J Wang, "Margin calibration in svm class imbalanced learning", *Neurocomputing*, Vol. 73, No. 1-3, pp. 397-411, 2009.
- [27] A. Fernandez, M. J. del Jesus, and F. Herrera, "Hierarchical fuzzy rule base classification system with genetic rule selection for imbalanced data-sets", *International journal of Approximate reasoning*, Vol. 50, pp. 561-577, 2009.
- [28] R. Batuwita and V. Palade, "FSVM-CIL: Fuzzy Support vector machine for class imbalanced learning", *IEEE Transactions on Fuzzy Systems*, Vol. 18, No. 3, pp. 558-571, 2010.
- [29] Z. Zhao, P. Zhong, and Y. Zhao, "Learning SVM with weighted maximum margin criterion for classification of imbalanced data", *Mathematical and Computer Modelling*, Vol. 54, pp. 1093-1099, 2011.
- [30] X. Gu, T. Ni, and H. Wang, "New Fuzzy Support Vector machine for the Class Imbalance Problem in Medical data-sets Classification", *The Scientific World Journal*. Vol. 2014, pp. 1-12, Hindawi Publishing Corporation.
- [31] P. Domingos, "Metacost: a general method for making classifiers cost sensitive", In: *Fifth International Conference on Knowledge Discovery and Data Mining*, Vol. 99, p. 155-164, Aug. 1999.
- [32] W. Fan, S. J. Stolfo, J. Zhang, and P. K. Chan, "Adacost: Misclassification cost-sensitive boosting", *6th Inter. Conf. Of machine learning*, pp 97-105, SFO, CA, 1999.
- [33] Y. Sun, M. S. Kamel, A. K. Wong, and Y. Wang, "Cost sensitive boosting for classification of imbalanced data", *Pattern recognition*, Vol. 40, No. 12, pp. 3358-3378, 2007.
- [34] K. M. Ting, "A comparative study of cost-sensitive boosting algorithms", In *proc. 17th Int. Conf. On mac. Learning*, Stanford CA, pp. 983-990, 2000.
- [35] P. K. Chan and S. J. Stolfo, "Toward Scalable Learning with non-uniform class and Cost Distribution: A case Study in Credit Card Fraud Detection", In. *Proceedings of the fourth international Conference on Knowledge Discovery and Data Mining*, pp. 164-168, 2001.
- [36] M. Joshi, V. Kumar and R. Agarwal, "Evaluating Boosting algorithms to classify rare classes", In *proc. IEEE International Conference on data Mining*, pp. 257-264, 2001.
- [37] S-C Lin, I. C. Yuan-chin, and W. N. Yang, "Meta-learning for imbalanced data & classification ensemble in binary classification", *Neurocomputing*, Vol. 73, pp. 484-494, 2009.
- [38] Y. Yang and G. Ma, "Ensemble based active learning for Class imbalance problem", *J. Biomedical Science and Engineering*, Vol. 3, pp.1021-1028, 2010.
- [39] C. Seiffert, T. M. Khoshgoftaar, J. Van Hulse, and A. Napolitano, "RUSBoost: A Hybrid Approach to Alleviating Class Imbalance", *IEEE Trans. On Sys. Man and Cyber.-Part A*, Vol. 40, No.1, pp 185-197, 2010.
- [40] M. Galar, A. Fernández, E. Barrenechea, and F. Herrera, "EUSBoost: Enhancing ensembles for highly imbalanced data-sets by evolutionary undersampling", *Pattern Recognition*, Vol. 46, pp 3460-3471, 2013.
- [41] S. Hu, Y. Liang, L. Ma, and Y. He, "MSMOTE: Improving classification performance when training data is imbalanced", In *procc. 2nd Int. Workshop Computer Sci. Eng.*, Vol. 2, pp. 13-17, 2009.
- [42] R. Barendela, J. S. Sánchez, and R. M. Valdovinos, "New applications of ensembles of classifiers", *Patterns Anal. Appl.*, vol 6, pp. 245-256, 2003.
- [43] R. Yan, Y. Liu, R. Jin, and A. Hauptmann, "On predicting rare classes with SVM ensembles in scene classification", *IEEE International*

- Conference on Acoustics, Speech and Signal processing, Vol. 3, pp. 21-24, 2003.
- [44] D. Tao, X. Tang, X. Li, and X. Wu, "Asymmetric Bagging and Random subspace for support vector machines-based Relevance feedback in Image retrieval", *IEEE Transactions on Pattern analysis and machine intelligence*. Vol. 28, No. 7, 2006.
- [45] S. Wang and X. Yao, "Diversity analysis on imbalanced data-sets by using ensemble models", *IEEE symp. Cmpmut. Intell. Data Mining*, 2009, pp. 324-331.
- [46] S. Hido, H. Kashima, and Y. Takahashi, "Roughly balanced bagging for imbalanced data", *Statistical analysis of Data Mining*, Vol. 2, pp. 412-426, 2009.
- [47] J. Blaszczynski, M. Deckert, J. Stefanowski, and S. Wilk, "Integrating Selective pre-processing of imbalanced data with ivotes ensemble", *Rough sets and Current trends in Computing (Lecture notes in Computer Science Series 6086)*, Springer-Verlag, pp. 148-157, 2010.
- [48] N. V. Chawla, A. Lazarevic, L. O. Hall, and K. W. Bowyer, "SMOTBoost: Improving prediction of the minority class in boosting", *In proc. Knowledge Discovery databases*, 2003, pp. 107-119.
- [49] H. Guo and H. L. Viktor, "Learning from imbalanced data-sets with boosting and data generation: The Databoost-IM approach", *SIGKDD Expl. Newsl.*, Vol. 6, pp. 30-39, 2004.
- [50] B. X. Wang and N. Japkowicz, "Boosting Support Vector machines for imbalanced data-sets", *Knowledge Information Systems*, Vol. 25, Issue 1, pp. 1-20, 2010.
- [51] M. J. Kim, "Geometric mean based boosting algorithm to resolve data imbalance problem", *DBKDA2013, The fifth International conf. On Advances in databases, knowledge and data applications*, pp. 15-20, 2013.
- [52] K. Lokanayaki and A. Malathi, "A prediction for classification of highly imbalanced medical dataset using Databoost.IM with SVM", *International journal of Advanced Research in Computer Science & Software Engg.*, Vol. 4, Issue 4, April 2014.
- [53] X. Y. Liu, J. Wu, and Z. H. Zhou, "Exploratory Undersampling for class imbalance learning", *IEEE Tran. Systm. Man and Cyber. B, Appl. Rev.* Vol. 39, No. 2, pp. 539-550, 2009.
- [54] J. Alcalá-Fdez et al., "KEEL data-mining software tool: data set repository, integration of algorithms and experimental analysis framework", *Journal of Multiple- Valued Logic and Soft Computing*, Vol 17, No. (2-3), pp. 255-287, 2011.
- [55] J. Alcalá-Fdez et al., "KEEL: a software tool to assess evolutionary algorithms for data mining problems", *Soft Computing*, Vol. 13, No. 3, pp. 307-318, 2008.
- [56] J. L. Hodges and E. L. Lehmann, "Rank methods for combination of independent experiments in analysis of variance", *Annals of Mathematical Statistics*, Vol. 33, pp. 482-497, 1962.
- [57] F. Wilcoxon, "Individual comparisons by ranking methods", *Biometrics Bulletin*, Vol. 1, No. 6, pp. 80-83, 1945.
- [58] Z-H Zhou, "Ensemble Methods-Foundations and Algorithms", CRC Press, Tayler and Francis Group, 2012.
- [59] Y. Freund and R. Schapire, "Experiments with a new boosting algorithms", *In Proc.13th Int. Conf. Machine Learning*, pp. 148-156, 1996.
- [60] L. K. Hensen and P. Salamon, "Neural Network Ensembles", *IEEE Transactions on Pattern Analysis and Machine Intelligence*, Vol. 12, No. 10, pp. 993-1001, 1990.
- [61] R. E. Schapire, "The strength of weak learnability", *Machine Learning*, Vol. 37, No. 2, pp. 197-227, 1990.
- [62] R. Barendela, J. S. Sa' nchez, and R. M. Valdovinos, "New applications of ensembles of classifiers", *Patterns Anal. Appl.*, Vol 6, pp. 245-256, 2003.
- [63] K. M. Ting, "An instance-weighting method to induce cost sensitive trees", *IEEE Trans. Of knowledge and data Engg.*, Vol. 14, issue 3, pp. 659-665, 2002.
- [64] L. Breiman, "Bagging predictors", *Machine Learning*, Vol. 24, pp. 123--140, 1996.
- [65] S. Wang and X. Yao, "Diversity analysis on imbalanced data sets by using ensemble models", *in IEEE Symposium Series on Computational Intelligence and Data Mining*, 2009, pp. 324-331.
- [66] R. Barendela, J. S. Sa' nchez, and R. M. Valdovinos, "New applications of ensembles of classifiers", *Patterns Anal. Appl.*, vol 6, pp. 245-256, 2003.
- [67] M. Galar, A. Fernandez, E. Barrenechea, H. Bustince, and F. Herrera, "A Review on Ensembles for the Class Imbalance Problem: Bagging-, Boosting-, and Hybrid-Based Approaches", *IEEE Transactions on Systems, Man, and Cybernetics, Part C: Applications and Reviews*, Vol. 42, No. 4, pp. 463-484, 2012. doi: 10.1109/TSMCC.2011.2161285.
- [68] J. Stefanowski and S. Wilk, "Selective Preprocessing of imbalanced data for improving classification performance", *Datawarehousing and Knowledge Discovery (Lecture Notes in Computer Science Series 5182)*, pp 283-292), 2008.
- [69] L. Breiman, "Pasting small votes for classification in large databases and on-line", *Machine Learning*, Vol. 36, pp. 85-103, 1999.
- [70] C. E. Metz, "Basic Principals of ROC Analysis", *Seminars in Nuclear Medicine*. 8(4), pp 283-298, 1978.
- [71] J. A. Hanley and B. J. McNeil, "A method of comparing the areas under receiver operating characteristic curves derived from the same cases", *Radiology*, 148(3), pp 839-843, 1983.
- [72] J. Demšar, "Statistical comparisons of classifiers over multiple datasets", *Journal of Machine Learning Research*, Vol. 7, pp. 1-30, 2006.
- [73] S. García and F. Herrera, "An extension on statistical comparisons of classifiers over multiple datasets for all pairwise comparisons", *Journal of Machine Learning Research*, Vol. 9, pp. 2677-2694, 2008.
- [74] S. García, A. Fernández, J. Luengo, and F. Herrera, "Advanced non parametric tests for multiple comparisons in the design of experiments in computational intelligence and data mining: experimental analysis of power", *Information Sciences*, Vol 180, pp. 2044-2064, 2010.
- [75] S. Holm, "A simple sequentially rejective multiple test procedure", *Scandinavian Journal of Statistics*, Vol. 6, pp. 65-70, 1979.

Applying Diffie-Hellman Algorithm to Solve the Key Agreement Problem in Mobile Blockchain-based Sensing Applications

Nsikak Pius Owoh¹, Manmeet Mahinderjit Singh²

School of Computer Sciences, Universiti Sains Malaysia, USM 11800, Penang, Malaysia

Abstract—Mobile blockchain has achieved huge success with the integration of edge computing services. This concept, when applied in mobile crowd sensing, enables transfer of sensor data from blockchain clients to edge nodes. Edge nodes perform proof-of-work on sensor data from blockchain clients and append validated data to the chain. With this approach, blockchain can be performed pervasively. However, securing sensitive sensor data in a mobile blockchain (client/edge node architecture) becomes imperative. To this end, this paper proposes an integrated framework for mobile blockchain which ensures key agreement between clients and edge nodes using Elliptic Curve Diffie-Hellman algorithm. Also, the framework provides efficient encryption of sensor data using the Advanced Encryption Standard algorithm. Finally, key agreement processes in the framework were analyzed and results show that key pairing between the blockchain client and the edge node is a non-trivial process.

Keywords—Internet of Things; mobile crowd sensing; edge computing; sensor data encryption; mining; smart contract

I. INTRODUCTION

Mobile crowd sensing (MCS) has become an attractive method of gathering personal and environmental data [1]. It takes advantage of sensors (accelerometer, gyroscope, GPS, camera, etc.) and the communication capability of smart devices such as smartphones to collect and transmit large scale sensor data at low cost [2]. These sensors acquire useful data in several domains, including but not limited to environmental monitoring [3], healthcare [4], traffic monitoring [5]. Basically, a crowd sensing platform consists of a cloud-based system and a group of sensing devices (mobile users). The platform publishes a set of sensing task with various purposes, while the mobile users participate in the sensing task [6]. Mobile crowd sensing also plays a key role in the actualization of smart cities [7]. Cities are considered “smart” when they have among other things: intelligent versatility, smart administration, smart citizens, intelligent economics and intelligent life [8]. Most importantly, such cities should also be able to share data using information and communication technology (ICT) [9].

Despite the benefits of MCS, challenges such as incentivizing participants [10, 11], quality and reliability of sensed data [12], energy usage of mobile sensing devices [5], sensor data annotation [13], security and privacy [14, 15] still exist. Due to the sensitive information of users gathered and transmitted by sensing devices, different mechanisms have

been proposed to ensure secure sensing in MCS applications [16]. Unfortunately, security and privacy still remain a pressing issue as an active attacker can intercept and modify transmitted sensor data (data in motion) from a mobile sensing device like the smartphone [17] and/or can alter stored data (data at rest).

Recently, the inherent attributes of blockchain technology have been harnessed to provide security and privacy in IoT [18] and specifically MCS applications [19]. The adoption of this technology for these purposes is not surprising, as its previous application in cryptocurrency has recorded some success. The gains of blockchain based cryptocurrency technology include; transformed payments, as middlemen are taken out of the loop and reduce merchant payment fees to below 1%, as well as the removal of delays, as users receive transferred funds instantly without having to wait for days [20]. Apart from its use in cryptocurrencies and smart contracts, blockchains have been applied in social services [21], smart living applications [22], supply chain management [23], intelligent transportation systems [24], data storage [25], identity management [26], smart cities [2].

Blockchain is a technology that reads, stores and validates transactions in a distributed database system [27]. The stored data can be cryptocurrency (Bitcoin) [28], a contract [29] or even personal data [30]. Another definition of blockchain is that, it is a security mechanism that ensures immutability, anonymity and auditability of electronic transactions [16]. It acts as a distributed ledger (a virtual book that stores previous transactions) allowing data to be shared among a network of peers by implementing a chain of timestamped blocks that are connected by cryptographic hashes. With this mechanism, untrustworthy participants (such as those in mobile crowd sensing) can reach a consensus and perform transactions without the involvement of third-parties. Blockchain can either be public (permissionless), private (permissioned), or consortium. Any user with internet access can join the network by taking part in block validation and smart contracts creation in public blockchains. Private blockchains on the other hand, controls users’ right to validate block transactions and develop smart contracts [31]. Private blockchain offers privacy and efficiency of transactions. Consortium blockchains are somewhat private and grant selected nodes full access.

However, before using a blockchain, a peer-to-peer network with all interested nodes must be created. All

participating nodes are allocated a pair of private and public keys used for transactions [20]. When a transaction is performed by a node, it signs (using the private key) and broadcasts the transaction to the nearest peer. This ensures authentication as the transaction can only be signed by a user with the exact private key. Integrity is also maintained as data modification is easily detected on signed transactions. Received transactions are verified by miners and validated using consensus algorithms (such as proof-of-work, proof-of-stake, etc.), then added to the chain [32].

The much-needed security services in any system (confidentiality, privacy, integrity, availability and non-repudiation) are provided by blockchain. As regard confidentiality, this technology secures data (transaction details, account and wallet balances, assets, price, and smart contracts' business logic) from unauthorized persons (third parties) and can be achieved using encryption. Meanwhile, privacy secures the identity of blockchain users (participants) against disclosure and is actualized with the use of pseudonyms (64-bit addresses). On the other hand, integrity guarantees the immutability of transactions using cryptographic mechanisms such as hash functions and digital signature. Availability ensures that users of a certain system can use it at any time as such service is always available for legitimate users. Blockchain-based systems achieve this by implementing multiple connections with several users and ensuring that blocks are decentralized and replicated across the network. Non-repudiation ensures that an individual cannot deny any action performed in a system as evidence of actions such as money transfer, purchase authorization and sent messages are digitally signed. In blockchain, this security service is achieved using the Elliptic Curve Digital Signature (ECDSA). Blockchain implements mechanisms that ensure stringent integrity and availability of data. However, ensuring confidentiality has been difficult [20].

Despite all the advantages and uses of blockchain, this technology still faces some challenges. Firstly, scalability is a lingering problem owing to the proliferation of its usage and the increase in the number of daily transactions [33]. The block size in blockchain increases transaction latency especially in small transactions as preference is given to transactions with bigger transactional fees by miners. Thus, implementing blockchain in IoT becomes difficult since IoT applications deal with large sensor data that require high speed processing. However, redesigning of blockchains and storage optimization are proposed solutions to scalability issues in blockchain [34].

Secondly, security has always been an issue in open networks such as public blockchains and confidentiality which is a key security element is low in distributed systems such as this [20]. In addition, integrity which is an important function of blockchain offered by its immutability feature has a number of issues. Another strength of this technology is the duplication of data blocks to all nodes ensuring availability of data. Although this makes a single point of failure impossible, it is theoretically proposed that a 51% attack is still possible [20]. Privacy leakage is another weakness of blockchain as details and balances of all public keys can be seen by everyone in the network. This could lead to leakage of users'

sensitive information when blockchain is employed in sensing applications. Mixing and anonymous techniques have been proposed as solutions to privacy leakage issues. Unfortunately, [35, 36] showed that de-anonymization is possible. Meanwhile, third-party is mostly needed with mixing techniques which introduces bottlenecks. Lastly, blockchains are faced with the issue of selfish mining, where a block is vulnerable to cheating when a minimal hashing power is used. In selfish mining, miners hoard mined blocks without broadcasting them to the network and generate a private branch which is broadcasted only when specific requirements are satisfied. This allows selfish miners to continue mining the private chain while honest miners waste their time and resources.

The use of blockchain as an underlying technology in IoT-based applications has gained acceptance both in the academia and industry. However, its practical use in mobile applications (mobile blockchain) has not been fully explored. A major reason being that, mining which requires high computational resources cannot be performed on resource-constrained mobile devices (such as smartphones) [21, 37]. In an effort to bridge this gap, edge computing approach is employed [33]. This integration allows mobile users to run the mobile blockchain application with the aid of edge computing nodes; serving as miners to mobile users and tagged by a service provider. Using this approach, blockchains can be implemented in mobile crowd sensing applications hence utilizing its full potentials on sensor data.

Edge computing supports blockchain and blockchainless Directed Acyclic Graph (DAG) applications [38] using one or more high-end computers (cloudlets) acting like a cloud [20]. These cloudlets respond swiftly to compute-intensive tasks requested by the node layer (blockchain node). Mobile blockchain together with edge computing has been used to improve social welfare [21]. Also, Xiong et al., Zhu et al. [37, 39] employed edge computing for mobile blockchain. These works focus on improving services rendered by the edge computing service providers such as enhancing pricing [40], or placement of mobile edge applications. However, secure data transmission between the mobile blockchain client (smartphones) and the edge nodes (miners) using effective key agreement and data encryption mechanisms have received little attention. Motivated by this, we propose a framework that secures sensor data transmitted between mobile and edge nodes during sensing activities. Different from the approach used in Conoscenti et al., Dorri et al., Zyskind and Nathan [18, 44, 49] where symmetric keys are transmitted with the encrypted data which makes sensor data susceptible to attack, we employ public key cryptography for key establishment between blockchain nodes.

The following contributions are made in this paper:

- We present a key agreement protocol using public key cryptography for secure key exchange between mobile blockchain clients and edge nodes in an MCS scenario.
- We present a technique to secure sensor data transmitted between mobile nodes and edge nodes (miners) using symmetric data encryption.

- We evaluate the proposed framework based on the computational time of the ECDH key agreement protocol and the execution time of the AES encryption scheme.

In this paper, we use the word “client” interchangeably with “mobile blockchain client”. The rest of this paper is structured as follows: Section II presents a review of related works on blockchain-based security schemes for Internet of Things as well as frameworks for mobile blockchain. In Section III, we present the methodology and implementation of our proposed secure mobile blockchain framework for MCS. Further discussion on the results of the implementation of the proposed framework is presented in Section IV. We conclude the paper in Section V.

II. RELATED WORKS

Blockchain enhances the security of IoT devices for example in remote attestation which deals with the verification of trustworthiness of underlying Trusted Computer Base (TCB) [41]. Blockchain based systems do not depend on a specific central server or cloud due to the vulnerabilities that exist in traditional cloud-centered IoT architectures. For instance, the cloud being a single point of failure (due to attacks, maintenance and other software issues) [23, 42]. This section presents some works that employ blockchain to enhance security and privacy in IoT-based applications.

A. Blockchain-based Security and Privacy Preservation Schemes for IoT

To solve the problem of identity certification in IoT, where a provider in charge of authorizing entities can also block them, Kravitz and Cooper [43] proposed the use of permissioned blockchain for the management and security of IoT nodes. With the proposed system, asymmetric keys are rotated thereby offering security against attacks. To protect users’ privacy, a blockchain-based decentralized personal data management system that maintains ownership of data by users was proposed in Zyskind and Nathan [44]. The system addresses privacy issues such as data ownership, data transparency and auditability. Similarly, a privacy-aware blockchain connected gateway was proposed for privacy preferences management in Cha et al. [45]. The blockchain gateway employs blockchain technology to ensure that user preferences are not modified thereby improving user privacy protection in legacy IoT devices. The owners of IoT devices, the blockchain gateway administrators and the end users are the three participants that can use the proposed blockchain gateway. The authors employed the Ethereum blockchain platform which allows the administrator to develop smart contract for the device as well as manage privacy policies.

In an effort to secure Electronic Health Records (EHR), Zitta et al. [46] employed smart contracts on an Ethereum blockchain to develop intelligent EHR that are stored in individual nodes. Garman et al. [47] proposed an anonymous credential authentication scheme that does not require a trusted credential issuer rather uses a public append-only ledger (blockchain). Using this system, privacy of users is preserved without the need for trusted third parties. Name value mappings are offered using Namecoin (a system

developed on Bitcoin’s Blockchain) for the storage of public keys with the associated credential.

A blockchain-based two-factor authentication scheme was proposed in Wu et al [48]. With this scheme, security of sensitive data is guaranteed through authentication and authorization. Furthermore, the proposed scheme uses two smart contracts: the device contract for the storage of device profiles and the relationship contract for the storage of associated device pairing information. Authors evaluated the performance of the scheme by measuring the memory and CPU usage of individual nodes in the system. Privacy issues experienced when third party mobile services were employed were addressed in Zyskind and Nathan [44] using a blockchain-based application. For the application to function effectively, a set of permissions (location, list of contacts, camera, etc.) needs to be granted when initially signing up to any mobile application. Three entities including: mobile phone users, service providers and the nodes maintaining the blockchain make up the proposed decentralized system. Only two types of transactions are permitted in the proposed blockchain network; T_{access} for access control management and T_{data} for data storage and retrieval. The identity and corresponding permission of each user of a service is transmitted to the blockchain in a T_{access} transaction. Encryption is performed on data collected from the user’s mobile phone and then stored off-chain while storing only the hashes of the data in the private blockchain. Data in a T_{data} transaction can be queried by the user and service.

Also, a blockchain-based smart home system was proposed in Dorri et al. [18]. The system consists of three tiers namely: smart home tier, overlay tier and the storage tier. The smart home tier includes as its core components transactions, home miner and the local storage. Confidentiality, integrity and availability are offered in the smart home tier. The system offers security against Distributed Denial of Service (DDoS) and linking attacks. Furthermore, packet overhead, time overhead and energy usage were metrics used to evaluate the performance of the proposed system. The authors concluded that encryption and hashing operations performed by the miner on all transactions are non-trivial processes compared to the encryption operation done by individual devices. The work in Conoscenti et al [49] uses blockchain technology in place of a centralized server for sensor data storage. Like cryptocurrencies, sensor data in the proposed system are managed by users via a distributed database. Also, symmetric keys are used for encryption of data to ensure data confidentiality. However, sending shared keys together with generated data for verification of data contents by miners undermines privacy and security.

To ensure privacy and confidentiality of shared data in blockchain-based IoT, Rahulamathavan et al [50] proposed the use of attribute-based encryption (ABE). Similar to the work in [51], the authors also employed a hierarchical IoT network method that dedicates a cluster head for certain set of IoT sensors. The cluster head in this case has resources enough to carry out data processing and encryption. Proposed works in Conoscenti et al. [49], Dorri et al. [18], and Zyskind and Nathan [44] all focused on the use of symmetric encryption where shared keys are transmitted with encrypted

data to participants. Unfortunately, an eavesdropper can decrypt encrypted data using the captured keys when such encryption schemes are employed. However, a countermeasure is the use of public key cryptography for key agreement between participants.

B. Blockchain-based Access Control Schemes for IoT

Controlling access to IoT resources can be achieved using blockchain technology. For instance, a blockchain-based scheme that controls access to medical records was proposed in Xia et al. [52]. The scalable system grants legitimate users access to Electronic Health Record (EHR), from a pool of shared data, after performing identity and cryptographic key verification using a permissioned blockchain. The proposed system functions well in areas where conventional access control approaches like firewalls, passwords and intrusion detection systems fail. Similarly, in Ouaddah et al [53], access to IoT applications is controlled via a proposed FairAccess system that hybridizes the Bitcoin blockchain and the Ethereum smart contracts technology. The system provides access control management in an IoT-based environment.

To ensure end-to-end (E2E) security for IoT data in motion, Vućinić et al. [54] proposed the Object Security Architecture (OSCAR) for the IoT. The important issues with the Datagram Transport Layer Security (DTLS) protocol were addressed in the proposed architecture by securing the payload at the application layer using blockchain. Using this model, resource servers can either store their resources locally or on a proxy server after encrypting and signing them. On the other hand, Alphan et al. [55] proposed an End-to-End scheme that ensures authorized access to IoT resources by hybridizing OSCAR [54] and ACE (Authentication and Authorization for Constrained Environments) frameworks. The authors employed a trustless authorization blockchain in place of the single trusted authorization server in the ACE framework. This enhances the ACE authorization model as resource access control becomes secure, and flexible.

Another blockchain-based architecture for access control of IoT devices was proposed in Pinno et al. [56]. The authors claim that the proposed architecture which is decentralized and transparent, solves the FairAccess problem associated with traditional architectures and can be integrated with several IoT access control models. To ensure distributed and trustworthy access control for IoT, Zhang et al. [57] employed smart contract-based blockchain technology that consists of several access control contracts (ACCs), a single judge contract (JC) and one register contract (RC). In the proposed framework, managing data records is the main goal of the smart contracts.

C. Mobile Edge Node Blockchain

Recently, blockchain has been implemented in mobile applications using the edge computing concept [21]. Some Android applications such as Easy Miner [58], LTC and Scrypt Miner PRO [59] have been developed for performing mining operations on mobile devices. However, they currently lack full implementation. On the other hand, a novel mobile-commerce application called MobiChain which employs

blockchain technology for secure transactions was presented in Suankaewmanee et al. [32]. The authors developed a Mobile Blockchain Application Programming Interface (MBAPI) for effective mining operations on mobile devices. Computation time, energy consumption, and memory utilization were metrics used to evaluate the performance of the proposed module.

Edge computing for mobile blockchain was introduced in [40]. In the presented prototype, IoT or mobile devices (Android devices) carry out mining on an edge computing server. The nodes (using Ethereum) serve as miners that install mobile client applications. Internal sensors such as accelerometer and GPS are used to record data (transactions) of mobile peer-to-peer communication by the application. In Jiao et al. [21], the authors also employed edge computing services for mobile blockchain applications and proposed an auction-based market model which comprises of the blockchain owner, edge computing service provider (ESP) and miners. The proposed model enhances social welfare and simulation results show the efficiency of the proposed model in solving the social welfare maximization problem.

Edge computing has made it possible for mobile blockchain to reach its full potentials, as edge nodes (miners) supported with edge computing service provider (ESP) can solve the PoW puzzle offloaded by the mobile blockchain client. The edge computing concept makes it practical to employ blockchain in mobile crowd sensing applications that deal with large chunks of sensor data from numerous sensing devices. However, the security of sensed data offloaded to edge nodes from blockchain clients remains a major challenge, which this paper aims to solve.

III. METHODOLOGY

There are four phases in the proposed Mobile Blockchain Security Framework (MBCSF) as shown in Fig. 1. In what follows, we provide details of each phase.

A. Key Agreement

This is the first phase of the framework where a variant of Elliptic Curve cryptography (i.e. EDCH) algorithm is employed for key establishment between the blockchain client (smartphone) and miners. First, we provide a brief description of the Elliptic Curve Cryptography (ECC) and its Elliptic Curve Diffie Hellman (ECDH) variant.

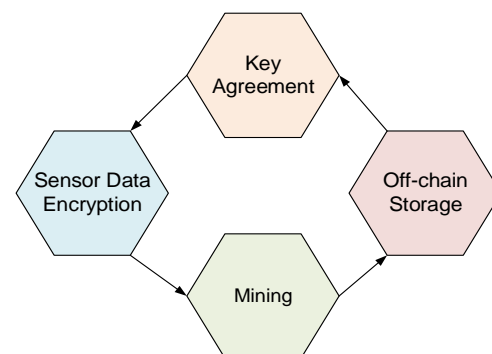


Fig. 1. The Proposed Mobile Blockchain Security Framework (MBCSF).

1) *Elliptic Curve Cryptography (ECC)*: Elliptic Curve Cryptography (ECC) is one of the public key cryptography (PKC) primitives, which is based on discrete logarithm (DL) [60]. Its popularity stems from its small key size and low computational overhead, which justifies why it is appropriate for mobile devices and delay-sensitive applications such as mobile crowd sensing. For instance, a 160 bit key in ECC provides equivalent security as a 1024 bit key in RSA [61]. ECC's mathematical operations are defined over the elliptic curve as shown in (1):

$$y^2 \equiv x^3 + ax + b \pmod{p} \quad (1)$$

where $4a^3 + 27b^2 \neq 0 \pmod{p}$. Each generated value of 'a' and 'b' produces a unique elliptic curve. All points (x, y) which satisfy the equation above and a point at infinity lies on the elliptic curve [61]. The private key is a randomly generated number while the public key is a point on the elliptic curve. The multiplication of the private key with the primitive element (generator) P generates the public key. The primitive element P, the curve parameters 'a' and 'b' make up the domain parameter of ECC [62].

2) *Elliptic Curve Diffie Hellman (ECDH)*: ECDH is a key agreement protocol that allows two communicating entities establish a shared secret key. This ensures exchange of public information between both parties (using parameters). The available public data and their respective private data are used to compute the shared secret. This ensures that an attacker (such as an eavesdropper) without knowledge of the private keys of each party, cannot compute the shared secret from the available public information. Using ECDH, a shared secret between two communicating parties (A and B) can only be generated after both parties agree on Elliptic Curve domain parameters. With this in mind, we integrate ECDH algorithm in our proposed framework. The major aim of our proposed framework is to eliminate the key distribution problem between the blockchain client and edge node. Descriptions of mathematical notations used in this paper are presented in Table I.

TABLE I. MATHEMATICAL NOTATIONS

Notations	Description
A	Blockchain client (smartphone)
B	Blockchain miner
S_A	Public key of the blockchain client
S_B	Public key of the blockchain miner
T_A	Private key of the blockchain client
T_B	Private key of the blockchain miner
P	Primitive element
E	Elliptic Curve
X, Y	Elliptic curve coordinates
K_{AB}	Shared secret key
P_T	Plaintext sensor data
C	Ciphertext

To securely establish keys, both the blockchain client and edge node (miner) must generate their private keys as shown in (2) and (3) from agreed domain parameters (E, P) using a 96-bits key generator.

$$T_A = K_{pr,A} \in \{2,3,\#E\} \quad (2)$$

$$T_B = K_{pr,B} \in \{2,3,\#E\} \quad (3)$$

Thereafter, the blockchain client computes (4) as its public key:

$$S_A = K_{pr,A} = S_A \cdot P \quad (4)$$

and sends S_A, E, P (public key, and domain parameters) to the miner.

The miner on the other hand, computes (5) as its public key:

$$S_B = K_{pr,B} = S_B \cdot P \quad (5)$$

and sends S_B, E, P to the blockchain client. Both S_A and S_B are points on the elliptic curve and are computed using the point multiplication. With S_A and S_B , both the blockchain client and the miner compute (6) and (7) as joint secret:

$$K_{AB} = T_A \cdot S_B = (X_{AB}, Y_{AB}) \quad (6)$$

$$K_{AB} = T_B \cdot S_A = (X_{AB}, Y_{AB}) \quad (7)$$

Fig. 2 illustrates the key agreement process between the blockchain client and the miner node.

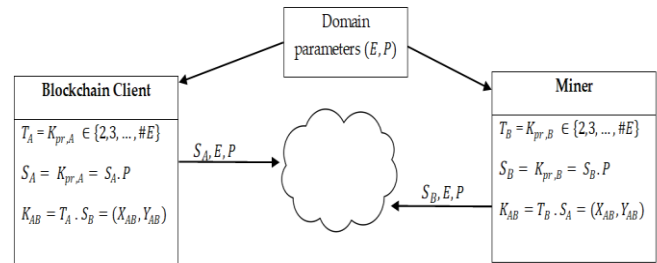


Fig. 2. Key Agreement Process in Proposed MBCSF using Elliptic Curve Diffie-Hellman.

B. Sensor Data Encryption

Encryption of sensor data only happens after a shared secret is established between the blockchain client and edge (miner) node. Encrypting large chunks of data such as those obtained from mobile sensors (blockchain client) with public key cryptography can be non-trivial even with ECC. Thus, a symmetric primitive such as AES is preferred as it requires lesser computations compared to ECC and RSA. To this effect, we employed AES with a 128 key bit length for encryption of sensor data in our proposed framework. Nevertheless, the shared secret K_{AB} from the key agreement phase is used to derive a session key which serves as the AES encryption key. Since only 128 key bit length can be used with AES, the last 32 bits of the 160 bit key of ECDH were dropped; using only the first 128 bits. Using this key, the blockchain client (smartphone) performs encryption on data from GPS, accelerometer and gyroscope sensors as shown in Fig. 3.

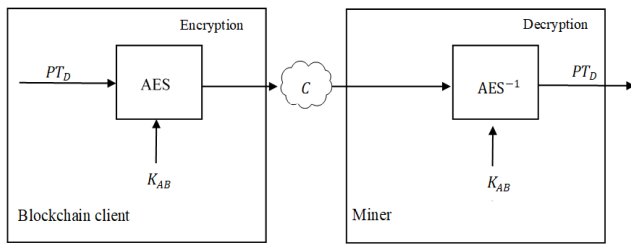


Fig. 3. Encryption and Decryption of Sensor Data in Proposed MBCSF using Advanced Encryption Standard.

Encrypted data are queued in a pool of unprocessed data awaiting validation by miners. Miners with the joint secret can derive the session key which is used to decrypt sensor data and commence the mining process. The algorithm for the encryption process is presented in Table II.

TABLE II. ALGORITHM TO ENCRYPT SENSOR DATA ON BLOCKCHAIN CLIENT (SMARTPHONE)

Algorithm 1: Encrypt Sensor data using AES-CBC
Input: Sensor data from blockchain client
<ol style="list-style-type: none"> 1. Initialize IV 2. $CT_1 \square Enc_{K_{AB}}(PT_1) \oplus IV$ 3. $CT_n \square Enc_{K_{AB}}(PT_n) \oplus CT_{n-1}$ for $n \geq 2$ 4. Repeat for all n
Output: Encrypted sensor data to miner node

C. Mining

Mining and blockchain updates are performed at this stage of the framework. Integrity and validity in blockchains are ensured using the compute-intensive process referred to as mining [40]. To add a new block of data to existing blockchain, a miner has to solve a proof of work (PoW) to get a hash value that links the preceding block to the current block. On completion of the PoW, a broadcast of the result is made to other miners in the network for validation. The new block is then appended to the blockchain only when a consensus is reached by majority of the miners. Thereafter, a reward is given to the miner who successfully solved the PoW. The entire mining process (PoW) requires computational power which makes it difficult for resource-constrained devices such as smartphones to either take part in the mining or consensus process. Based on this fact, we adopted the Mobile Edge Computing (MEC) architecture [63] in our framework, which enables the deployment of local data centers and servers by an edge computing service provider (ESP) at the “edge” of mobile networks. The ESP in our framework supports offloading of proof-of-work puzzle by blockchain clients (smartphones) using the uniform pricing scheme. It also handles data storage and request distribution from several end users.

From the previous stage where data were encrypted and offloaded to the edge node, the miner willing to solve the PoW first decrypts the sensor data using the derived session key from the shared secret computed in (6). On successful mining and validation of sensor data, the hash value of the data block is stored in the blockchain while the sensor data is encrypted

again by the miner and sent to the off-chain storage. Furthermore, we ensured that each hashed value points to the respective encrypted data in the off-chain storage. Indeed, the approach is preferred since large amount of sensor data from mobile crowd sensing users cannot be stored in the blockchain. More so, MCS stakeholders might need to reuse certain sensor data for decision making purposes.

With this framework, transaction details (sensor readings) in smart contracts are not transmitted in plaintext and this secures sensitive information from eavesdroppers. Also, the proposed framework ensures that sensor readings (transaction details) cannot be gathered or analysed with “off-chain” metadata to disclose any information about participants. This therefore maintains the confidentiality of sensitive information such as location details of users.

D. Off-Chain Storage

The data storage stores encrypted sensor data containing location information of MCS users. These data can be queried by users when sensing information need to be shared among sensing participants and blockchain members. We integrated cloud storage to achieve larger storage space while maintaining access control mechanisms on stored data. The proposed framework provides a cloud storage option where users’ profile and environmental data from peers such as servers, smartphone sensors can be stored.

The proposed framework was implemented both on the blockchain client and the edge node (miner). For the blockchain client, we used a Samsung Galaxy S4 (GT19500) smartphone running Android version 5.0.1. Table III summarizes hardware and software features of the mobile and miner node used in our experiment. Android studio was used for implementation of the mobile blockchain client. The application gathers data from GPS, accelerometer and gyroscope sensors. On the client-side, we implemented the ECDH from the Spongy castle library using the JCE (Java Cryptography Extension).

We initialized the *KeyAgreement* class with the blockchain client’s (smartphone) private key and the public key of the miner and then obtained the shared secret bytes by calling the *generateSecret()* function. The standard EC curve was used in our implementation. The generated keys are stored externally, and the key exchange performed successfully. With the secret key, sensor data offloaded for mining was encrypted using AES-CBC mode.

TABLE III. IMPLEMENTATION ENVIRONMENT FOR BLOCKCHAIN CLIENT AND EDGE NODE

Samsung Galaxy S4 (client)	Android 5.0.1
	2GB RAM, 16/32 GB storage
	Quad-core 2.3 GHz Krait 400 CPU, Adreno 330 GPU
Intel Xeon E5-2650	Ubuntu 16.04 LTS
	32 B DDR4 RAM, 1 TB Storage
	8 CPU cores, 16 threads

For the edge computing server, we employed the Intel Xeon E5-2650V4. The edge computing server is connected to the mobile device via a gateway (network hub). Ethereum smart contract was implemented using the solidity scripting language in a private blockchain network. We used the web3.js [64] (the official Ethereum Javascript API) for the object side to communicate with the matching geth client through HTTP connections. ECDH, ECDSA and AES algorithms run on the miner node as well. The shared secret generated at the point of connection with the mobile node is used for the decryption of transaction (sensor data) before mining is performed. This key is also used to encrypt sensor data after block validation by other miners.

IV. RESULTS AND DISCUSSION

Architecturally, the proposed framework consists of three layers: the user layer, the management layer and the storage layer as shown in Fig. 4. Smart devices (such as smartphones and tablets) carried by users are classified under the user layer. Forming a peer-to-peer network, smart devices (referred to as blockchain clients) are connected to the blockchain via the Ethereum smart contract. In this layer, sensor data are acquired from users and the environment. The management layer on the other hand offers data distribution and decentralization to other layers in the framework. Edge node computing and security are some of the services offered in this layer.

The storage layer serves as an off-chain storage for validated (mined) sensor data. The off-chain solution is chosen in our framework to avoid challenges that exist with storing large amount of data in the blockchain, especially when dealing sensor data from numerous devices in MCS [65].

Blockchain technology has played a major role in the success of cryptocurrency. Recently, blockchains together with smart contracts has been implemented in other areas such as IoT, supply chain, healthcare, mobile crowd sensing, etc. However, its adoption in mobile crowd sensing is still in its early stage. Immutability, auditability, transparency and anonymity are some of the characteristics of blockchain. These features make it possible for blockchain technology to ensure security services such as data integrity, availability, non-repudiation and confidentiality. In reality, confidentiality in blockchain is only provided via anonymity, where addresses are used for transactions.

Applying blockchain in mobile crowd sensing applications implements the mobile blockchain concept where mobile users perform sensing activities, mining and block validation pervasively. However, since mining and block validation are non-trivial activities, we implemented our framework using edge computing. Mobile crowd sensing users can gather sensor data from their smartphones (mobile nodes) and offload encrypted data to the edge node. The edge node (miner) uses the shared secret computed using ECDH to decrypt sensor data and perform PoW. Data confidentiality is ensured as only the miners with the shared secret can decrypt encrypted data. Meanwhile, edge computing service providers cannot decrypt transactions which maintains security at the edge computing sub layer. Encryption using symmetric keys as employed in Coscenti et al.; Dorri et al.; Zyskind and Nathan [18, 44, 49] does not guarantee effective data confidentiality, since keys are transmitted together with sensor data. An eavesdropper who listens to traffic between communicating parties can successfully capture encryption keys hence decrypt data meant for either party. Consequently, sensitive information of users are disclosed with the success of such an attack.

The need for an effective key agreement and distribution mechanism cannot be overemphasized especially when mobile blockchain is adopted for crowd sensing applications. Owing to the fact that mobile crowd sensing applications such as smart city applications gather sensitive information of users e.g. location data from GPS sensor, the robust key agreement protocol employed in the proposed framework ensures that the shared secret between communicating parties cannot be brute-forced by an attacker.

One major function of the proposed framework is the generation and distribution of secret keys between client and miner nodes in the blockchain. This process is implemented in the key agreement phase of the framework. Using the Elliptic Curve Diffie-Hellman algorithm, the framework ensures that only communicating nodes in the blockchain at any given time can compute the joint secret (session key) from their respective private keys. Sensor data are then encrypted using the computed keys. Employing encryption keys from a secure shared secret enhances the security of sensor data. Even when communication between the blockchain client and edge node is performed through a wireless channel which is susceptible to attacks, the proposed framework secures sensor data in mobile blockchain from attacks such as information disclosure and false data injection.

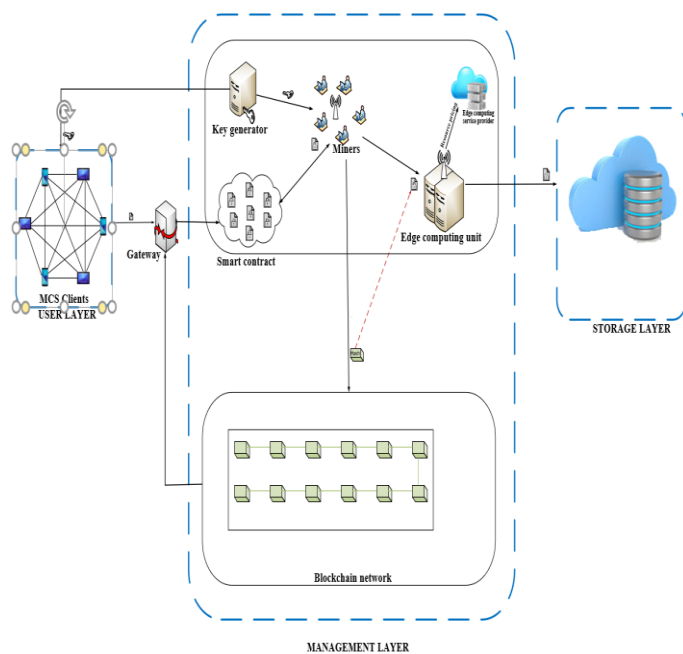


Fig. 4. Architecture of Proposed Mobile Blockchain-based Security Framework (MBCSF).

A. Security Analysis and Performance Evaluation

A proof of correctness of the key agreement algorithm (ECDH) adopted in the framework is given as follows:

The blockchain client computes its private key as (8), which is derived from (6):

$$T_A \cdot S_B = S_A(T_B P) \tag{8}$$

At the same time, the miner node computes its (9) which is the private key obtained from (7):

$$T_B \cdot S_A = S_B(T_A P) \tag{9}$$

As a result of this, both the blockchain client and the miner node compute similar keys represented in (10):

$$K_{AB} = T_B \cdot S_A \tag{10}$$

The private keys of the blockchain client and the miner node T_A and T_B respectively are large integers used to generate their associated public keys S_A and S_B . Resultantly, only the two communicating parties with the matching private keys can compute the shared secret, hence the session key. That way, a secure key is established between blockchain nodes even when an unsecure channel is used. Consequently, when the encryption key is derived from the shared secret, sensor data are protected against information leakage. The proposed framework offers the following security services:

1) *Confidentiality*: Symmetric encryption of sensor data from blockchain clients (smartphones) to edge (miners) nodes guarantees data confidentiality in the proposed framework. Sensitive information of users are protected from eavesdroppers as only ciphertext messages are transmitted between nodes.

2) *Integrity*: This is a fundamental security service provided by blockchain technology as they are designed to store immutable information. In our proposed framework, hashes of sensor data are stored in the blockchain, making it difficult to modify any data content that have been validated and added to the chain.

3) *Non-repudiation*: Using the Ethereum smart contract, all transactions are digitally signed using the ECDSA algorithm. The proposed framework in this paper ensures that sensor data are signed by the sending device.

To evaluate the performance of the proposed framework, we calculated the computational cost using a Java program to obtain the running time in milliseconds (ms) of the key agreement component of the framework. Table IV and Fig. 5 shows that, key pairing between the blockchain client (smartphone) and the miner node takes longer time than other key agreement processes.

Also, we evaluated the execution time of the AES algorithm on both blockchain client and (edge) miner node. From the presented results in Fig. 6, encryption of sensor data is faster on the edge node when compared to blockchain client (smartphone). The high computing power of the edge node justifies this result.

TABLE IV. COMPUTATIONAL COST OF SECURITY COMPONENTS IN THE PROPOSED (MBCSF)

Security Component	Computational cost
Private key generator (96 bits)	0.5ms
ECDH pairing (160 bits)	95ms
Secret key generation (160bits)	0.9ms
EC point multiplication (160 bits)	1ms
EC point addition (160 bits)	0.8ms

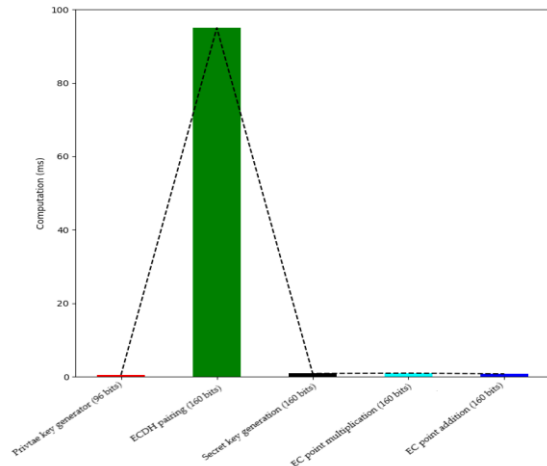


Fig. 5. Computational Cost of Security Components in the Proposed MBCSF.

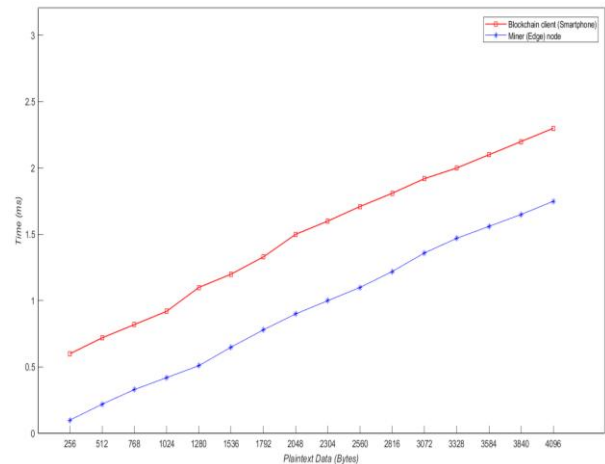


Fig. 6. Encryption Process in Blockchain Client and Miner Node.

V. CONCLUSION

In this paper, a security framework for mobile blockchain was presented. The framework designed for mobile crowd sensing applications consists of five steps (key agreement, sensor data encryption, mining and off-chain storage). With the framework, key agreement is achieved between mobile blockchain clients (smartphones) and edge (miner) nodes. Using ECDH as the key agreement algorithm, both communicating parties (blockchain client and miner node) employ public key cryptography for key generation. Adopting

elliptic curve cryptography enables the use of smaller key sizes to obtain maximum security level using a shared secret. The shared secret was used to derive the session key for the encryption of sensor data. Encrypted data in the proposed framework is secure as an attacker cannot obtain the private keys of the communicating parties.

REFERENCES

- [1] Capponi, A., et al., A cost-effective distributed framework for data collection in cloud-based mobile crowd sensing architectures. *IEEE Transactions on Sustainable Computing*, 2017. 2(1): p. pp. 3-16.
- [2] Biswas, K. and V. Muthukkumarasamy. Securing smart cities using blockchain technology. in *High Performance Computing and Communications; IEEE 14th International Conference on Smart City; IEEE 2nd International Conference on Data Science and Systems (HPCC/SmartCity/DSS)*, 2016 IEEE 18th International Conference on. 2016. IEEE.
- [3] Cardone, G., et al., Fostering ParticipAction in Smart Cities: A Geo-Social Crowdsensing Platform., *IEEE Communications Magazine*, Vol. 48, No. 14, pp.32–39., 2013.
- [4] Khan, W.Z., et al., Mobile Phone Sensing Systems: A Survey. *Ieee Communications Surveys & Tutorials*, Vol. 15, No. 1, pp. 402-427., 2013.
- [5] Ganti, R.K., F. Ye, and H. Lei, Mobile crowdsensing: Current state and future challenges. *IEEE Commun. Mag.*, Vol. 49, No. 11, pp. 32–39., 2011.
- [6] Nie, J., et al., A Stackelberg Game Approach Towards Socially-Aware Incentive Mechanisms for Mobile Crowdsensing. *arXiv preprint arXiv:1807.08412*, 2018: p. pp. 1-30.
- [7] Cardone, G., et al., The participact mobile crowd sensing living lab: The testbed for smart cities. *IEEE Communications Magazine*, 2014. 52(10): p. pp.78-85.
- [8] Gori, P., P.L. Parcu, and M.L. Stasi, Smart cities and sharing economy. 2015.
- [9] Sharma, P.K., S.Y. Moon, and J.H. Park, Block-VN: A distributed blockchain based vehicular network architecture in smart City. *Journal of Information Processing Systems*, 2017. 13(1): p. pp.84.
- [10] Wen, Y., et al., Quality-driven auction-based incentive mechanism for mobile crowd sensing. *IEEE Transactions on Vehicular Technology*, 2015. 64(9): p. pp.4203-4214.
- [11] Jin, H., et al. Inception: Incentivizing privacy-preserving data aggregation for mobile crowd sensing systems. in *Proceedings of the 17th ACM International Symposium on Mobile Ad Hoc Networking and Computing*. 2016. ACM.
- [12] Talasila, M., R. Curtmola, and C. Borcea, Mobile crowd sensing. *Google Scholar*, 2015: p. pp.
- [13] Pius Owoh, N., M. Mahinderjit Singh, and Z.F. Zaaba, Automatic Annotation of Unlabeled Data from Smartphone-Based Motion and Location Sensors. *Sensors*, 2018. 18(7): p. pp.2134.
- [14] He, D., S. Chan, and M. Guizani, User privacy and data trustworthiness in mobile crowd sensing. *IEEE Wireless Communications*, 2015. 22(1): p. pp.28-34.
- [15] Zhang, D., et al., 4W1H in mobile crowd sensing. *IEEE Communications Magazine*, 2014. 52(8): p. pp.42-48.
- [16] Jesus, E.F., et al., A Survey of How to Use Blockchain to Secure Internet of Things and the Stalker Attack. *Security and Communication Networks*, 2018. 2018: p. 1-28.
- [17] Owoh, N.P. and M.M. Singh, Security analysis of mobile crowd sensing applications. *Applied Computing and Informatics*, 2018: p. pp. 1-11.
- [18] Dorri, A., et al. Blockchain for IoT security and privacy: The case study of a smart home. in *Pervasive Computing and Communications Workshops (PerCom Workshops)*, 2017 IEEE International Conference on. 2017. IEEE.
- [19] Tanas, C., S. Delgado-Segura, and J. Herrera-Joancomartí, An Integrated Reward and Reputation Mechanism for MCS Preserving Users' Privacy, in *Data Privacy Management, and Security Assurance*. 2015, Springer. p. pp.83-99.
- [20] Fernández-Caramés, T.M. and P. Fraga-Lamas, A Review on the Use of Blockchain for the Internet of Things. *IEEE Access*, 2018.
- [21] Jiao, Y., et al., Social welfare maximization auction in edge computing resource allocation for mobile blockchain. *arXiv preprint arXiv:1710.10595*, 2017: p. pp. 1-6.
- [22] Han, D., H. Kim, and J. Jang. Blockchain based smart door lock system. in *Information and Communication Technology Convergence (ICTC)*, 2017 International Conference on. 2017. IEEE.
- [23] Kshetri, N., Can blockchain strengthen the internet of things? *IT Professional*, 2017. 19(4): p. pp. 68-72.
- [24] Lei, A., et al., Blockchain-based dynamic key management for heterogeneous intelligent transportation systems. *IEEE Internet of Things Journal*, 2017. 4(6): p. pp.1832-1843.
- [25] Ateniese, G., et al. Accountable storage. in *International Conference on Applied Cryptography and Network Security*. 2017. Springer.
- [26] Wilson, D. and G. Ateniese. From pretty good to great: Enhancing PGP using bitcoin and the blockchain. in *International conference on network and system security*. 2015. Springer.
- [27] Bozic, N., G. Pujolle, and S. Secci. A tutorial on blockchain and applications to secure network control-planes. in *Smart Cloud Networks & Systems (SCNS)*. 2016. IEEE.
- [28] Nakamoto, S., Bitcoin, A peer-to-peer electronic cash system, <https://bitcoin.org/bitcoin.pdf>. 2008.
- [29] Wood, G., Ethereum: A secure decentralised generalised transaction ledger. *Ethereum project yellow paper*, 2014. 151: p. pp. 1-32.
- [30] Yue, X., et al., Healthcare data gateways: found healthcare intelligence on blockchain with novel privacy risk control. *Journal of medical systems*, 2016. 40(10): p. 218.
- [31] Han, M., et al. Privacy reserved influence maximization in gps-enabled cyber-physical and online social networks. in *Big Data and Cloud Computing (BDCloud), Social Computing and Networking (SocialCom), Sustainable Computing and Communications (SustainCom)(BDCloud-SocialCom-SustainCom)*, 2016 IEEE International Conferences on. 2016. IEEE.
- [32] Suankaeawmanee, K., et al. Performance analysis and application of mobile blockchain. in *2018 International Conference on Computing, Networking and Communications (ICNC)*. 2018. IEEE.
- [33] Joshi, A.P., M. Han, and Y. Wang, A survey on security and privacy issues of blockchain technology. *Mathematical Foundations of Computing*, 2018. 1(2): p. pp. 121-147.
- [34] Zheng, Z., et al. An overview of blockchain technology: Architecture, consensus, and future trends. in *Big Data (BigData Congress)*, 2017 IEEE International Congress on. 2017. IEEE.
- [35] Narayanan, A. and V. Shmatikov, How to break anonymity of the netflix prize dataset. *arXiv preprint cs/0610105*, 2006.
- [36] De Montjoye, Y.-A., et al., Unique in the crowd: The privacy bounds of human mobility. *Scientific reports*, 2013. 3: p. pp.1376.
- [37] Xiong, Z., et al. Optimal pricing-based edge computing resource management in mobile blockchain. in *2018 IEEE International Conference on Communications (ICC)*. 2018. IEEE.
- [38] Yeow, K., et al., Decentralized consensus for edge-centric internet of things: A review, taxonomy, and research issues. *IEEE Access*, 2018. 6: p. 1513-1524.
- [39] Zhu, H., C. Huang, and J. Zhou, EdgeChain: Blockchain-based Multi-vendor Mobile Edge Application Placement. *arXiv preprint arXiv:1801.04035*, 2018: p. pp. 1-9.
- [40] Xiong, Z., et al., When mobile blockchain meets edge computing. *IEEE Communications Magazine*, 2018. 56(8): p. pp. 33-39.
- [41] Park, J. and K. Kim. TM-Coin: Trustworthy management of TCB measurements in IoT. in *Pervasive Computing and Communications Workshops (PerCom Workshops)*, 2017 IEEE International Conference on. 2017. IEEE.
- [42] Li, X., et al. An IoT Data Communication Framework for Authenticity and Integrity. in *Internet-of-Things Design and Implementation (IoTDI)*, 2017 IEEE/ACM Second International Conference on. 2017. IEEE.

- [43] Kravitz, D.W. and J. Cooper. Securing user identity and transactions symbiotically: IoT meets blockchain. in Global Internet of Things Summit (GloTS), 2017. 2017. IEEE.
- [44] Zyskind, G. and O. Nathan. Decentralizing privacy: Using blockchain to protect personal data. in Security and Privacy Workshops (SPW), 2015 IEEE. 2015. IEEE.
- [45] Cha, S.-C., et al., A Blockchain Connected Gateway for BLE-Based Devices in the Internet of Things. IEEE Access, 2018. 6: p. pp.24639-24649.
- [46] Zitta, T., M. Neruda, and L. Vojtech. The security of RFID readers with IDS/IPS solution using Raspberry Pi. in Carpathian Control Conference (ICCC), 2017 18th International. 2017. IEEE.
- [47] Garman, C., M. Green, and I. Miers. Decentralized Anonymous Credentials. in NDSS. 2014. Citeseer.
- [48] Wu, L., et al. An out-of-band authentication scheme for internet of things using blockchain technology. in 2018 International Conference on Computing, Networking and Communications (ICNC). 2018. IEEE.
- [49] Conoscenti, M., A. Vetro, and J.C. De Martin. Peer to Peer for Privacy and Decentralization in the Internet of Things. in Proceedings of the 39th International Conference on Software Engineering Companion. 2017. IEEE Press.
- [50] Rahulamathavan, Y., et al. Privacy-preserving blockchain based IoT ecosystem using attribute-based encryption. in 2017 IEEE International Conference on Advanced Networks and Telecommunications Systems (ANTS). 2017. IEEE.
- [51] Dorri, A., S.S. Kanhere, and R. Jurdak. Smart city architecture and its applications based on IoT. in Proceedings of the Second International Conference on Internet-of-Things Design and Implementation. 2017. ACM.
- [52] Xia, Q., et al., BBDS: Blockchain-based data sharing for electronic medical records in cloud environments. Information, 2017. 8(2): p. pp. 44.
- [53] Ouaddah, A., A.A. Elkalam, and A.A. Ouahman, Towards a novel privacy-preserving access control model based on blockchain technology in IoT, in Europe and MENA Cooperation Advances in Information and Communication Technologies. 2017, Springer. p. pp. 523-533.
- [54] Vučinić, M., et al., OSCAR: Object security architecture for the Internet of Things. Ad Hoc Networks, 2015. 32: p. pp. 3-16.
- [55] Alphan, O., et al. IoTChain: A blockchain security architecture for the Internet of Things. in Wireless Communications and Networking Conference (WCNC), 2018 IEEE. 2018. IEEE.
- [56] Pinno, O.J.A., A.R.A. Gregio, and L.C. De Bona. ControlChain: Blockchain as a Central Enabler for Access Control Authorizations in the IoT. in GLOBECOM 2017-2017 IEEE Global Communications Conference. 2017. IEEE.
- [57] Zhang, Y., et al., Smart Contract-Based Access Control for the Internet of Things. arXiv preprint arXiv:1802.04410, 2018.
- [58] EasyMiner, Easy Miner, Available at: <https://play.google.com/store/apps/details?id=com.mr.app.ui&hl=en>. 2017.
- [59] LTC, LTC and Scrypt Miner PRO, Available at: <https://play.google.com/store/apps/details?id=com.miner.scrypt&hl=en>. 2017.
- [60] Paar, C. and J. Pelzl, Understanding cryptography: a textbook for students and practitioners. 2009: Springer Science & Business Media.
- [61] Lee, Y.S., E. Alasaarela, and H. Lee. Secure key management scheme based on ECC algorithm for patient's medical information in healthcare system. in Information Networking (ICOIN), 2014 International Conference on. 2014. IEEE.
- [62] Shou, Y., H. Guyennet, and M. Lehsaini. Parallel scalar multiplication on elliptic curves in wireless sensor networks. in International Conference on Distributed Computing and Networking. 2013. Springer.
- [63] Abbas, N., et al., Mobile edge computing: A survey. IEEE Internet of Things Journal, 2018. 5(1): p. pp. 450-465.
- [64] Javascript, Web3 javascript api to interact with ethereum nodes. [Online]. Available: <https://github.com/ethereum/wiki/wiki/JavaScript-API>. 2018.
- [65] Lazarovich, A., Invisible Ink: blockchain for data privacy. 2015, Massachusetts Institute of Technology.

Optimizing the Hyperparameter of Feature Extraction and Machine Learning Classification Algorithms

Sani Muhammad Isa¹, Rizaldi Suwandi², Yosefina Pricilia Andean³

Computer Science Department,
BINUS Graduate Program Master of Computer Science
Bina Nusantara University Jakarta,
Indonesia 11480

Abstract—The process of assigning a quantitative value to a piece of text expressing a mood or effect is called Sentiment analysis. Comparison of several machine learning, feature extraction approaches, and parameter optimization was done to achieve the best accuracy. This paper proposes an approach to extracting comparison value of sentiment review using three features extraction: Word2vec, Doc2vec, Terms Frequency-Inverse Document Frequency (TF-IDF) with machine learning classification algorithms, such as Support Vector Machine (SVM), Naive Bayes and Decision Tree. Grid search algorithm is used to optimize the feature extraction and classifier parameter. The performance of these classification algorithms is evaluated based on accuracy. The approach that is used in this research succeeded to increase the classification accuracy for all feature extractions and classifiers using grid search hyperparameter optimization on varied pre-processed data.

Keywords—Sentiment analysis; word2vec; TF-IDF (terms frequency-inverse document frequency); Doc2vec; grid search

I. INTRODUCTION

Google Play is an online service that developed and operated by Google. This is an official app store for Android-based mobile phone. The entire google play service can be accessed through the Play Store app. Google Play sells Android apps, games, movies, and even e-books. Google play store apps data chosen because have enormous potential to drive app-making business to success. This research focused on apps review.

In recent years, the opinions of friends, domain experts are our consideration for decision making in our life. For example, which app is best to download, games to play, or e-book to read. Sentiment analysis or opinion mining plays an important role in this process [1]. The sentiment (expressions) states in natural language form.

With the increasing development in e-commerce, the needed to extract valuable information from consumer comment also increasing. It is important for the organization (Google Play developer company) to automatically identify each customer review whether it is positive, negative, or neutral [2]. The product comments contain a wealth of information about product evaluation from customers [3]. With the main form of information from the internet is text [4], text processing is needed the most. Text processing is needed for extracting the value of sentiment review.

Text classification research started from design the best feature extraction method to choose the best classifiers. Almost all techniques of text classification based on words [5]. For sentiment classification, this paper uses a machine learning based method because it has been widely adopted due to their excellent performance.

Word2vec, Doc2vec, and Terms Frequency-Inverse Document Frequency (TF-IDF) feature extractions that used in this research were implemented by python algorithm using the Sklearn library (TF-IDF) and the Gensim library (Word2vec & Doc2vec). Word2vec is a new open source feature extraction method based on deep learning [3]. Word2vec can learn the word vector representation and calculate the cosine distance in the high dimensional vector space. This research used word2vec because this approach can find the semantic relationships between words in the document.

TF-IDF is very important in this research. Balancing the weight between the less commonly used words and most frequent or general words is one of the capabilities of TF-IDF feature extraction. TF-IDF can calculate the frequency of each token in the review. This frequency shows the importance of a token to a document in the corpus [6].

To extend the learning of embeddings from word to word sequences, this research uses a Doc2vec as a simple extension to Word2vec. Many types of texts used this feature. They are word n-gram, sentence, paragraphs or document [7]. Refer to the embedding of the word sequence; we used the term document embedding that supported by Doc2vec.

The classification method was done with 3 classifier NB (Naive Bayes), SVM (Support Vector Machine), and DT (Decision Tree). SVM can be used to create the highest accuracy results in text classification problems [1]. The NB has high accuracy than other followed by the DT classifier.

This research dedicated to select the best feature extraction and choosing the best model for multiclass classification by comparing the TF-IDF, Word2vec, Doc2vec feature extraction and increase the accuracy using hyperparameter optimization. Hyperparameter optimization used to search the best parameter that produces the best classification accuracy. To selects, a point in space (in linear or log space) hyperparameter space using grid search is suitable in this case. Hyperparameter tuning is well-suited to use in some

derivative-free optimization, it is reflecting characteristic grid search to solve this problem [8].

This paper consisted of several parts of the section, there are: Section II to gives literature review, Section III describes the methodology of some techniques used in the research, Section IV describes result and analysis in this research, and Section V will conclude the paper.

II. RELATED WORK

To know what is the mood or effect from text expressing, it can use sentiment analysis with assigning a quantitative value (positive, negative, and neutral). Previous research has shown that sentiment analysis has a good accuracy, such as, Twitter [2], application reviews [9], documents [10], texts [3], [4], [11], newsgroup [12], and news article [13], IMDB [14]. The Google Play review dataset from Kaggle was used in this research. Kaggle is an online web service that provides a series of a dataset that can be used to research. Data has filtered for noise and null review user's data also contain the sentiment for each review.

Sentiment analysis is a good candidate for analyzing sentiments in text classification. Using machine learning, the classification of documents was done. This machine learning automatically classifies the document into categories that have been labeled before. It can see as a supervised learning task

because of the objective [12].

In Table I, there is attached some research about sentiment analysis from Google Scholar. This literature search using some keywords such as "Sentiment Analysis using Word2vec and TF-IDF", "Sentiment Analysis Google Play Review", "Sentiment Analysis using Doc2vec".

Based on the literature review, most of the research is focused on getting better accuracy. The method was designed according to the characteristics of the text. To represent the rank among the best approach in retrieving documents and labeling document, TF-IDF was used, Word2vec to obtain more accurate word vector, Doc2vec is one of the easiest ways is using an average of all words in the document to represent the feature of this document [18].

SVM, NB, and DT classifier were used in this paper for text classifier. In the classification process, many classification methods and machine learning techniques have been used. Using machine learning can increase accuracy by using optimization algorithm, i.e. hyperparameter optimization using a grid search. By adding a hyperparameter optimization, will get a better result with to determine hyperparameter efficiency in choosing parameter [19]. The methods have been used by [12] and [4] both methods produce a high level of accuracy with more than 80%. Then using this method will get a high accuracy [16].

TABLE I. LITERATURE REVIEW

Author	Dataset	Method	Result
J. H. Lau and T. Baldwin [7]	Document	Doc2vec	Better accuracy
R. Ju, P. Zhou, C. H. Li, and L. Liu [15]	Newsgroup	Latent Semantic Analysis + Word2vec	Better accuracy
D. Zhang, H. Xu, Z. Su, and Y. Xu [3]	Text (Chinese comments)	Word2vec and SVM-perf	Excellence accuracy
J. Lilleberg, Y. Zhu, and Y. Zhang [12]	Newsgroup	Word2vec, Terms Frequency-Inverse Document Frequency	Word2vec is the best solution
D. Rahmawati and M. L. Khodra [13]	Article	Word2vec	Better accuracy
S. K. R. Abinash Tripathy, Ankit Agrawal [14]	IMDb	Naïve Bayes, Max Entropy, SVM, SGD	Get better accuracy
P. Vateekul and T. Koomsubha [2]	Twitter	Long Short Term Memory and Dynamic Convolutional Neural Network	Better than Naïve Bayes and SVM
W. Zhu, W. Zhang, G.-Z. Li, C. He, and L. Zhang [16]	Text	Word2vec and Terms Frequency-Inverse Document Frequency	Better than Latent Semantic Analysis and Doc2vec
Y. Xi, Jin Gao, Yahao He, Xiaoyan Zhang [4]	Text	Word2vec, Terms Frequency-Inverse Document Frequency	Comparison
S. Fujita [17]	Newspaper	Contextual Specificity Similarity, K-Nearest	Contextual Specificity Similarity good in long text
L. Lin, X. Linlong, J. Wenzhen, Z. Hong, and Y. Guocai [11]	Text	CD_STR, TF-IDF weighted vector space model	Comparison
Q. Shuai, Y. Huang, L. Jin, and L. Pang [18]	Review	Doc2vec, Support Vector Machine, LogReg	Support Vector Machine, Logreg show a better result

III. METHODOLOGY

In the classification task using machine learning, the main important thing is the feature selection [18]. This research using 10.000 data of Google Apps from Kaggle. The reviews are divided into three class categories: positive, neutral and negative. The data then divided into train and test data with 80% of train data. The research methodology can be represented in Fig. 1.

A. Dataset

In this paper, dataset consisted of user reviews from Google Play complete with the sentiment analysis (Positive, Neutral, and Negative) for each review. Google Play stores allow users to write reviews about the downloaded applications. The data set contains 64,294 reviews, consists of the name application, review, sentiment, sentiment popularity, and sentiment subjectivity. This research used 10.000 reviews, it is consists of name applications, sentiments, and reviews because wanted to evaluate our approach against reviews containing diverse vocabularies, and sentiment as parameter classification. From the original, data are filtered by removing noise and null data using python NLTK library. Moreover, words that typo also deleted and modified the spelling of words using class Spelling Replacer.

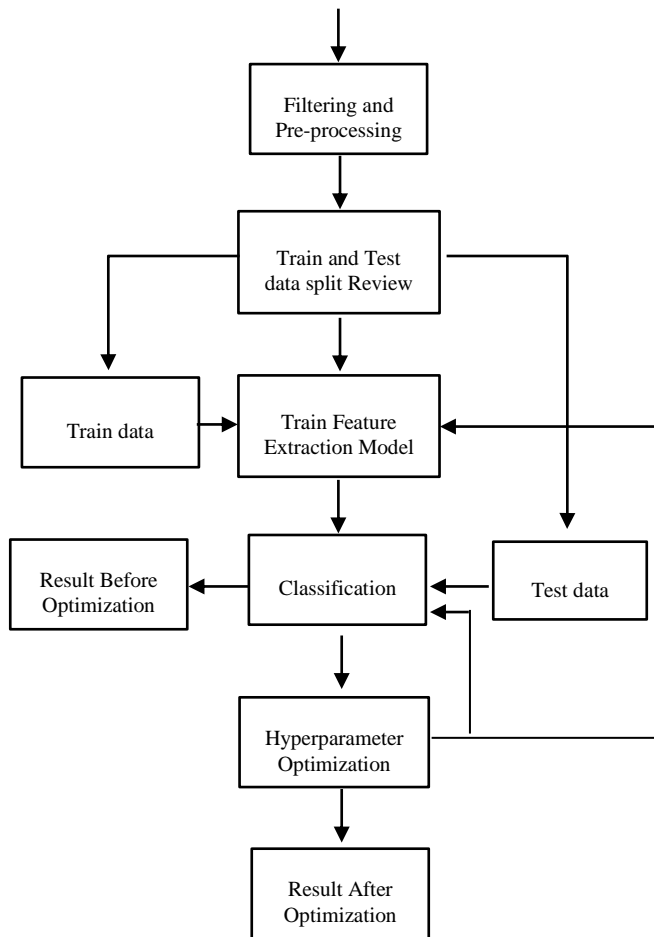


Fig. 1. Experiment Process.

B. Filtering

Preprocessed reviews were done by these techniques

1) *Stopword removal*: To eliminate term that is very common in the English language, we delete the stopwords (e.g., “such”, “was”, “any”, ”then”, etc). By using library NLTK corpus, the words we added to the stopwords list are “ ‘m ” and “ ‘s ”, also deleted the stopwords list are “y”, “o”, “s”, “i”, “d”. We remove punctuation at the end of the sentence (in the end the alphabet (upper & lower letters) or punctuation (@#\$\$%^&*()-_+=+~!{}|\\:;<,>./).

2) *Spelling replace*: We use spell method from the autocorrect library to checking out all of the words. This library is able to correct the words which are not in accordance with the English word dictionary. For example, the word before corrected is “lke” and after corrected will be “like”.

3) *Noise & null removal*: We remove a column if the data has an empty row from name application, review, and sentiment. Moreover, we used enchant from the NLTK library to delete the typo word. By using enchant, it will be checked one by one word. When checking the words, there is no word in the English dictionary, the word will be deleted.

For example, this is an example processed data from Kaggle “A big thanks ds I got bst gd health”, by using a stopwords removal, noise character removal, and remove punctuation, the result is “big thanks ds got bst gd health” with remove “A” and “I”.

We tried to correct the words and the result is “big thanks ds i got BST gd health”. In this case, “bst” fixed by English word dictionary become “BST” (British Summer Time) because “BST” is in the English dictionary. The final step is to delete the typo words using enchant, the result is “big thanks i got health”. In enchant some words removed because there are not in the English dictionary.

C. Feature Extraction

For feature extracting the user’s review, the method provided by the NLTK toolkit was used.

1) *Word2vec*: Two main learning algorithm for Word2vec are skip-gram and bag-of-words. Bag-of-words will predict the word based on the content and the order of the words in history does not influence the projection. However, skip-gram will predict the surrounding words given the current word. The bag of words used a distributed representation of the context that different bag of words with skip gram. It is important to state that the weight matrix between the projection layer and input was shared for all the words positions. This paper used a modified Word2vec to calculate the document vector. For each word in the document will calculate the vector of a word and calculate the average of the document vector. This research used 300 dimensions for the word vector dimension size. The 300 vectors have calculated the mean for the number of words in the review.

1. $R(d_i) = \sum_t w_2v(t)$ where $t \in d_i$
2. $w_R(d_i) = \sum_t w_t w_2v(t)$ where $w_t = \text{tf-idf weight of } t$
3. $C(d_i) = \text{concatenate}(\text{tf-idf}(d_i), w_R(d_i))$

Fig. 2. Step Word2vec.

Utilization of word2vec and TF-IDF for feature classification is the same as [12]. In Fig. 2, d_i represents the document, the vector representation from Word2vec denoted as $w_2v(t)$, and t represents the term that exists in the document. The following step was done for each document. The first step is using Word2vec to summing the vector representation of a document, the second step is to calculate the TF-IDF value and the value applied in Word2vec, the last step is merging value of the TF-IDF and Word2vec which is weighted by TF-IDF from the second step [13].

2) *TF-IDF*: TF-IDF was used to specify the most common and used word in a corpus. TF-IDF used the word frequency to specify it. TF-IDF calculate the inverse proportion of the document to which the word appears in. More high the value of the TF-IDF, the more connection a word had for each other and the frequency of occurrence is also high. TF-IDF approach can be expressed as the equation below:

$$w_{t,d} = tf_{t,d} \cdot \log \frac{|D|}{|\{d' \in D | t \in d'\}|} \quad (1)$$

where $tf_{t,d}$ is a term frequency of term t in document d , $\log \frac{|D|}{|\{d' \in D | t \in d'\}|}$ is inverse document frequency. $|D|$ is the total number of documents in the documents set, $\{t \in d'\}$ is the number of documents containing the term t . When a word that repeatedly comes up is considered important words in the TF-IDF. As a result, the term TF-IDF is used to calculate the TF-IDF weights at the same time [10].

3) *Doc2vec*: For learning document embeddings, Doc2vec can be used as an extension to Word2vec. Dbow (Distributed Bag of Words version of Paragraph Vector) and dmpv (Distributed Memory version of Paragraph Vector) are two approaches of Doc2vec. Dbow and skip-gram works in the same way. The input in both approaches was replaced by a special token that represents the document. The words order in the document is ignored in this architecture. Dmpv has similarities with cbow. In the process, dmpv require an additional token document in addition to the word yet at this not conclude cbow but incorporating. The objective is again to predict a context word given the concatenated document and word vectors.

Fig. 3 shows two architectures from [18], the first is DMPV, and it will add a paragraph id to be trained with word vectors. This paragraph id contains information that is missing from the current word.

Fig. 4 shows ways to input into the DBOW model is a paragraph id, predicting randomly sampled words in this document [18].

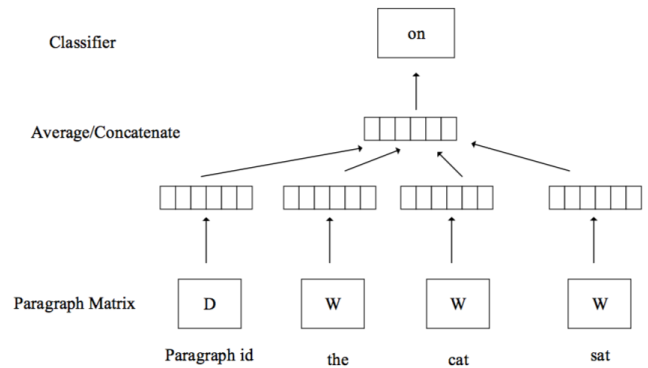


Fig. 3. DMPV

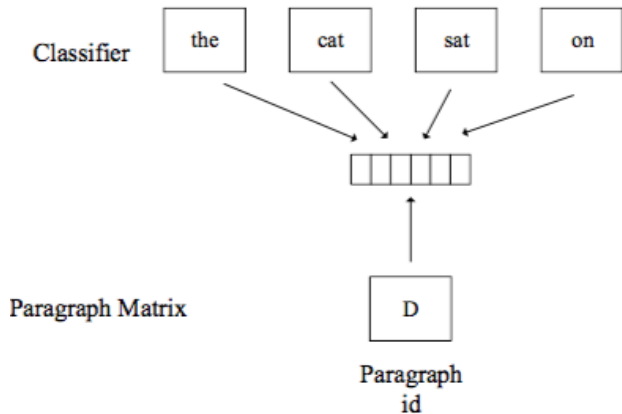


Fig. 4. DBOW

D. Classification

Using TF-IDF, Word2vec, and Doc2vec feature extraction, our initial approach was a summation of vectors in a particular document and then using linear Support Vector Machine (SVM), Naive Bayes, and Decision Tree to help classify them. It was implemented using the Sklearn library.

1) *Support vector machine*: Support Vector Machine (SVM) as a classifier is fully determined by a relatively small subset of the training instances, it is suitable for discrete data [18]. LinearSVC was used in this research as it is similar to SVM but with a kernel 'linear' parameter and implemented in terms of liblinear rather than libsvm. To analyze the complete vectorized data and the key idea behind the training of model that also known as SVM and to refine hyperplane. Equation represented by w was used [6].

$$\vec{w} = \sum_j a_j c_j \vec{d}_j, a_j \geq 0 \quad (2)$$

Dual optimization problem gives the value for a_j 's. c_j (1,-1) be the class (positive, negative, neutral) for a document d_j All the d_j such that a_j is greater than zero are termed as support vectors as they are the only document vectors which are contributing to \vec{w} .

2) *Naive bayes*: This research using a Naive Bayes as a classifier. Bayes Theorem is the based properties of Naive

Bayes algorithm. This classifier works with assuming that each of every feature was standing as an independent individual. Though, this algorithm requires a small amount of data training that used for calculating the parameter for prediction and represented by P(c|d).

$$P(c | d) = \frac{P(d | c) * P(c)}{P(d)} \quad (3)$$

For a given textual review ‘d’ and for a class ‘c’ (positive, negative, neutral).

3) *Decision Tree*: Decision tree works with the three main components. The edges, internal nodes, and leaf nodes. Each of these components represents an item in text classification. The edges, internal nodes, and leaf nodes represent the test for feature weights, the feature, and categories resulted from the test. When the final node or the leaf nodes was reached, this represents the final category for the document. Decision tree had been used in many application in speech and language processing [1].

Classifier performance results will be generated as a confusion matrix. This matrix shows predictions of positive, negative, neutral predicted reviews. The number of correctly predicted negative reviews are called with True Negative, The False Negative Predicted Neutral is a false prediction that supposed to be a Negative but predicted as Neutral. False Negative Predicted Positive is a false prediction that a negative falsely predicted as positive. The False Neutral Predicted Negative and False Neutral Predicted Positive are the false prediction that supposed to be Neutral, but predicted as Negative and Positive. Last, The False Positive Predicted and False Positive Predicted Neutral is a false prediction that supposed to be positive but predicted as Negative and Neutral. The paragraph can be represented in Table II.

E. Parameter Optimization

Improvement or additional optimization is needed in the search strategy to get better performance when testing each new machine. This optimization still needed even though when the first run on a new machine gives a reasonable performance [20]. Hyperparameter optimization has strategies, they are grid search and manual search. Using this grid search will increase accurate by doing the checking of the parameters that are in the servant list, it will compare for the best accuracy. In this implementation, the results are not everything improves accuracy, there is some accuracy down.

TABLE II. CONFUSION MATRIX FOR CLASSIFIER

Correct Labels			
	Negative	Neutral	Positive
Negative	True Negative	False Negative Predicted Neutral	False Negative Predicted Positive
Neutral	False Neutral Predicted Negative	True Neutral	False Neutral Predicted Positive
Positive	False Positive Predicted Negative	False Positive Predicted Neutral	True Positive

Most widely used strategies for hyperparameter optimization are grid search and manual search [21]. Only one Hyperparameter that grid search can handle and the hyperparameter names and values have to be specified by the user [22].

The parameters used in this research are defined for the feature extraction parameters TF-IDF and BernoulliNB Classifier. feature extraction used a hyperparameter such as use_idf, and ngram_range for the vectorizer. For the classifier, this research used an alpha parameter for the BernoulliNB classifier. Many possible parameters can be used in this feature extraction and classifier such as ‘dual’, ‘tol’, ‘C’, and ‘multi_class’ for LinearSVC classifier; ‘criterion’, ‘splitter’, ‘max_depth’, and ‘max_features’ for the Decision Tree classifier; ‘size’, ‘window’ and ‘min_count’ for the Word2vec and Doc2vec feature extractions but limited by the computer resources.

This research used a different technique of hyperparameter optimization. For the Word2vec and Doc2vec, this research used an empty parameter. Only the TF-IDF and BernoulliNB that used a predefined hyperparameter as described in Fig. 5. Fig. 1 describes the experiment process about the hyperparameter optimization and the step that optimize with this optimization. The Train feature extraction and classification are those two that optimized with grid search.

The empty parameter might succeed to increase classification accuracy. This was possible because the model runs for the second time using the processed data. This might double trained the model and generate better and much higher accuracy for sentiment analysis classification.



Fig. 5. Predefined Hyperparameter Example.

F. Evaluation

Evaluation in this research was done by calculating the classification accuracy score. The accuracy score calculates using The Sklearn library accuracy_score that calculate the number test data prediction that corrects divided by total testing data. T and F in the formula represent the True and False prediction. The Pos, Net, and Neg represent Positive, Neutral, and Negative.

$$Accuracy = \frac{TPos+TNet+TNeg}{TPos+FPos+TNet+FNeg+TNeg+FNeg} \quad (4)$$

IV. RESULT AND DISCUSSION

This section will discuss the results and describe the limitations, threats to validity, and implication

A. Experiment Result

The experiment was done using 3 feature extractions as mentioned in Section 3. The TF-IDF generate the biggest feature size that contains all the vocabulary that exists the dataset and act as the columns. The Word2vec feature

extraction requires the most time to execute because it calculated each word vector and averages all the word vector in the same review to be the review/document vector.

In Table III, the experiment result shows that classification accuracy with data normal, data delete typo, and data spelling replaces that classified with LinearSVC, BernoulliNB, and Decision Tree classifiers. The classification in Table II was done using the default parameter. From the feature extraction point of view, TF-IDF produced the best accuracy for the default parameter with 81% average accuracy. From the classifier’s point of view, LinearSVC has shown the best result with more than 84% in average accuracy much higher than Naïve Bayes and Decision Tree classifiers.

TF-IDF and LinearSVC can produce high accuracy rate is 85.66% in an average of 3 datasets. This result followed by the Decision Tree with TF-IDF feature extraction is 0.33% lower than TF-IDF while LinearSVC has resulted in 85.33% for the average of accuracy.

Table IV shows results from optimization with grid search optimization using the empty hyperparameter and predefined hyperparameter. The result has shown a better result for most feature extraction and classifier and changes from TF-IDF to Doc2vec as the best feature extraction accuracy with 85.33% on average. This result includes the predefined hyperparameter in Fig. 5 for the TF-IDF feature extraction and BernoulliNB classifier.

The result has shown that the predefined parameter succeeded in increased the accuracy for the TF-IDF and BernoulliNB classifier. In Table IV, accuracy for A-NB using normal data has succeeded increased by 1%. The result has shown a different result for Typo data and Spell data with 3% and 1% decreased each. The Bernoulli with TF-IDF also calculated using the empty hyperparameter and shows worse result than the predefined hyperparameter with 70%, 72%, and 70% for the normal, typo and spell data as present in Table V.

TABLE III. BEFORE OPTIMIZATION RESULT (A: TF-IDF, B: WORD2VEC, DOC2VEC)

Classification Results									
	Normal (%)			Typo (%)			Spell (%)		
	A	B	C	A	B	C	A	B	C
SVM	86	77	81	85	73	81	86	76	80
NB	73	63	75	76	58	77	74	62	79
DT	85	68	78	85	64	78	86	67	78

TABLE IV. AFTER OPTIMIZATION USING GRID SEARCH RESULT (A: TF-IDF, B: WORD2VEC, C: DOC2VEC)

Classification Results									
	Normal (%)			Typo (%)			Spell (%)		
	A	B	C	A	B	C	A	B	C
SVM	89	77	88	89	77	87	88	76	88
NB	74	62	84	73	60	82	73	60	85
DT	89	66	85	89	68	84	89	68	85

TABLE V. GRID SEARCH OPTIMIZATION DIFFERENCE RESULT USING PREDEFINED HYPERPARAMETER AND AN EMPTY PARAMETER

BernoulliNB with TF-IDF			
	Normal (%)	Typo (%)	Spell (%)
Empty Parameter	70	72	70
Predefined Parameter	74	73	73

Grid search hyperparameter is shown the best parameter with the best accuracy for the normal, typo and spell data. All normal, typo and spell data showed the same best parameter for grid search optimization with ‘alpha’: 0.01 , ‘use_idf’: True and ‘ngram_range’: (1,1). as mentioned before, not all data accuracy increased with this parameter, this possibly because of the small number of parameter that predefined for the grid search optimization. There might be another parameter combination that shown better result but can’t achieve in this research cause of some limitations.

After optimization using empty parameter, the result has shown that TF-IDF and Decision Tree produces the best accuracy with 89% on average higher 0.33% from LinearSVC using the same TF-IDF feature extraction. The best feature extraction in this problem depends on the classifier that used. In average, the Doc2vec is the best on average for three classifiers. But for Decision Tree classifier, TF-IDF produces higher accuracy than Doc2vec.

Types of datasets we have though are divided into three parts, there are normal data, typo data, spell data. Normal data is the data that not preprocess using spell check and typo deletion, typo data is the review that preprocessed using the NLTK library to delete typo words, and spell data is the review data that pre-processed using the Autocorrect to correcting the misspelled words.

Fig. 6 represents the increasing accuracy rate of normal data using grid search hyperparameter optimization. Hyperparameter optimization succeeded to increase the classification accuracy by a combination of available parameters. The most promising result is Doc2vec with an 8.9% increase for the BernoulliNB classifier.

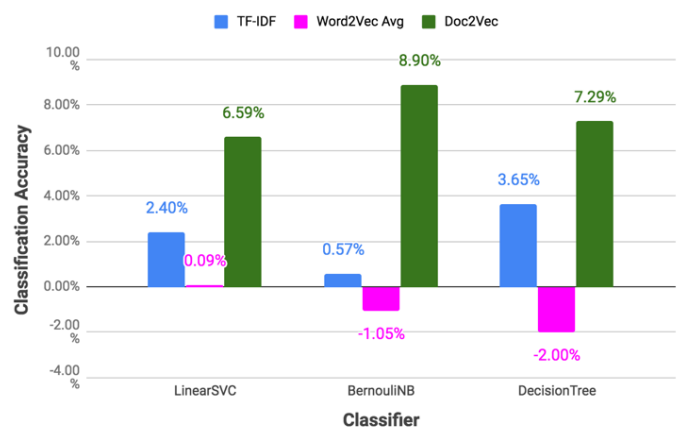


Fig. 6. Accuracy Chart using Normal Data.

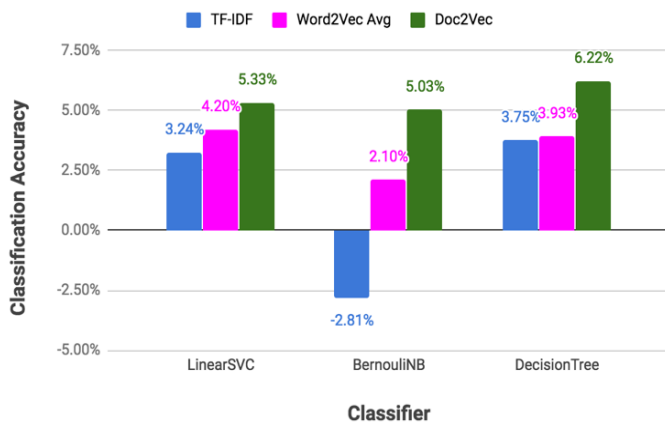


Fig. 7. Accuracy Chart using Typo Data.

Fig. 7 represents the increment accuracy rate using typo data. The chart showed all feature extraction and classifier has increased in a quite significant rate except for the Word2vec with BernoulliNB. The result showed that this method decreases 2.81% in accuracy from the original result.

Fig. 8 describes the increment accuracy rate with Spell data. In this chart, can be seen clearly that Doc2vec has increased the most. The summary for the optimization result is the Doc2vec has increased the most with 6.77% on average using normal, typo and spell data. Hyperparameter optimization using grid search manage to optimize the Doc2vec feature extraction for Google Play Review data.

B. Limitation

This research is limited by the computer resource to execute a calculation using bigger data and more complex optimization method. The computer used for this research has a relatively low spec with 16 RAM and just 2 CPU cores. These specs are low compared with [5] that supported with 2 Tesla K40 GPU. Other limitations for this research are the number of data available for google play apps review and available Python library. This research can be improved with better English spell replacer to fix the typo and much bigger dataset.

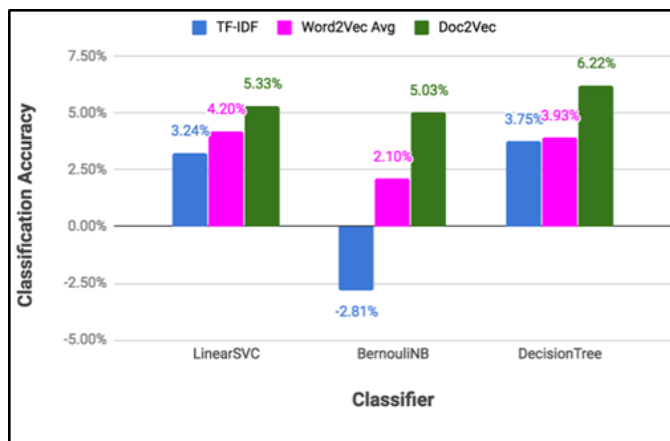


Fig. 8. Accuracy Chart using Spell Data.

C. Threats to Validity

The qualitative evaluation of the topic that relevant to the requirement engineering was done by the authors of the paper is one of the threats to validity. This is a threat as the evaluator could have an incomplete knowledge or misunderstanding about the specific information. Another threat to validity is the possibility of human error during the coding task. This human error can minimize with the second coder that double checking the code used for this research.

For text classification, many factors can influence the research. Data, method, variable, parameters and many more can make a different result. This result shows for normal data that included a typo and misspelled words, TF-IDF is the best feature extraction with SVM or Decision Tree Classifier. But, after optimizing the hyperparameter, the result shows that Doc2vec is the better result than others. The normal, typo and spell words do have a slight impact on the accuracy but did not have a significant influence. The typo and misspelled word only make around 2% in accuracy difference result.

V. CONCLUSION

This work presents a comparison between three feature extraction and a way to increase the classification accuracy for sentiment analysis. Before route optimization accuracy; TF-IDF using LinearSVC in normal data, TF-IDF using LinearSVC in spell data, and TF-IDF using DecisionTree in spell data have the same results is 86%. It can be concluded, in this study TF-IDF has the highest value. After hyperparameter optimization, the result has shown a different accuracy. After the optimization, there are accuracies up and down. TF-IDF using LinearSVC in normal data, TF-IDF using LinearSVC in spell data, TF-IDF using DecisionTree in spell data, and TF-IDF using DecisionTree in normal data have the same result i.e. 89%. Changes of accuracy made the Doc2vec to has the best accuracy results in total mean average. The increase in classification by hyperparameters optimization on the highest is Doc2vec using BernoulliNB in normal data increased by 8.9%.

REFERENCE

- [1] N. S. Joshi and S. A. Itkat, "A Survey on Feature Level Sentiment Analysis," vol. 5, no. 4, pp. 5422–5425, 2014.
- [2] P. Vateekul and T. Koomsubha, "A study of sentiment analysis using deep learning techniques on Thai Twitter data," 2016 13th Int. Jt. Conf. Comput. Sci. Softw. Eng. JCSSE 2016, 2016.
- [3] D. Zhang, H. Xu, Z. Su, and Y. Xu, "Chinese comments sentiment classification based on word2vec and SVMperf," Expert Syst. Appl., vol. 42, no. 4, pp. 1857–1863, 2015.
- [4] Y. Xi, Jin Gao, Yahao He, Xiaoyan Zhang, "Duplicate Short Text Detection Based on Word2vec," pp. 3–7, 2017.
- [5] X. Zhang, J. Zhao, and Y. Lecun, "Character-level Convolutional Networks for Text Classification," pp. 1–9, 2015.
- [6] A. Tripathy, A. Agrawal, and S. K. Rath, "Classification of Sentimental Reviews Using Machine Learning Techniques," Procedia - Procedia Comput. Sci., vol. 57, pp. 821–829, 2015.
- [7] J. H. Lau and T. Baldwin, "An Empirical Evaluation of doc2vec with Practical Insights into Document Embedding Generation," 2014.
- [8] E. R. Sparks et al., "Automating Model Search for Large Scale Machine Learning," pp. 368–380.

- [9] E. Guzman and W. Maalej, "How Do Users Like This Feature? A Fine Grained Sentiment Analysis of App Reviews," vol. 200, Table V, pp. 86–87, 2014.
- [10] R. Ju, P. Zhou, C. H. Li, and L. Liu, "An efficient method for Document categorization based on Word2vec and latent semantic analysis," Proc. - 15th IEEE Int. Conf. Comput. Inf. Technol. CIT 2015, 14th IEEE Int. Conf. Ubiquitous Comput. Commun. IUCC 2015, 13th IEEE Int. Conf. Dependable, Auton. Se, pp. 2276–2283, 2015.
- [11] L. Lin, X. Linlong, J. Wenzhen, Z. Hong, and Y. Guocai, Text Classification Based on Word2vec and Convolutional Neural Network, vol. 3316. Springer International Publishing, 2018.
- [12] J. Lilleberg, Y. Zhu, and Y. Zhang, "Support Vector Machines and Word2vec for Text Classification with Semantic Features," 2015.
- [13] D. Rahmawati and M. L. Khodra, "Word2vec semantic representation in multilabel classification for Indonesian news article," 4th IGNITE Conf. 2016 Int. Conf. Adv. Informatics Concepts, Theory Appl. ICAICTA 2016, pp. 0–5, 2016.
- [14] S. K. R. Abinash Tripathy, Ankit Agrawal, "Classification of Sentiment Reviews using N-gram Machine Learning Approach," 2016.
- [15] R. Ju, P. Zhou, C. H. Li, and L. Liu, "An Efficient Method for Document Categorization Based on Word2vec and Latent Semantic Analysis," 2015.
- [16] W. Zhu, W. Zhang, G.-Z. Li, C. He, and L. Zhang, "A study of damp-heat syndrome classification Using Word2vec and TF-IDF," 2016.
- [17] S. Fujita, "Text Similarity Function Based on Word Embeddings for Short Text Analysis," vol. 3406, pp. 391–402, 2018.
- [18] Q. Shuai, Y. Huang, L. Jin, and L. Pang, "Sentiment Analysis on Chinese Hotel Reviews with Doc2Vec and Classifiers," 2018 IEEE 3rd Adv. Inf. Technol. Electron. Autom. Control Conf., no. Iaeac, pp. 1171–1174, 2018.
- [19] S. R. Young, D. C. Rose, T. P. Karnowski, S. Lim, and R. M. Patton, "Optimizing Deep Learning Hyper-Parameters Through an Evolutionary Algorithm," 2008.
- [20] J. Bilmes and J. Demmel, "Author Retrospective for Optimizing Matrix Multiply using PHiPAC : a Portable High-Performance ANSI C Coding Methodology," 2014.
- [21] J. Bergstra and Y. Bengio, "Random Search for Hyper-Parameter Optimization," vol. 13, pp. 281–305, 2012.
- [22] L. Kotthoff and K. Leyton-brown, "Auto-WEKA 2.0 : Automatic model selection and hyperparameter optimization in WEKA," vol. 18, pp. 1–5, 2017.

Stabilizing Average Queue Length in Active Queue Management Method

Mahmoud Baklizi¹

The World Islamic Science & Education University W.I.S.E
Department of Computer Networks Systems
Amman, Jordan

Abstract—This paper proposes the Stabilized (DGRED) method for congestion detection at the router buffer. This method aims to stabilize the average queue length between allocated `minthre_shold` and `doublemaxthre_shold` positions to increase the network performance. The SDGRED method is simulated and compared with Gentle Random Early Detection (GRED) and Dynamic GRED active queue management methods. This comparison is built on different important measures, such as dropping probability, throughput, average delay, packet loss, and mean queue length for packets. The evaluation aims to identify which method presents better simulation performance measurement results when non-congestion or congestion situations occur at the router buffers in congestion control. The results show that at high packet arrival probability, the proposed algorithm helps provide lesser queue length values, delayed time, and packet loss compared with current methods. Furthermore, SDGRED generates adequate throughput at high packet arrival probability.

Keywords—Congestion control methods; GRED; dynamic GRED; random; simulation; active queue management method

I. INTRODUCTION

The worldwide broadcast of computer networks connects a huge number of devices, from personal computers to multi-branch organization networks [1, 2]. Enormous amounts of data are sent and received between network devices in the form of packets. When several senders send the data over the same intermediary link, packets are stored in the routers' buffer and spend a lot of time waiting for transmitted. However, in view of the buffer size disadvantages in whole network resources [3-5], incoming packets are dropped after the number of packets more than the resource size of the router buffer. Fig. 1 illustrates a possibly congested router buffer. Every packet arriving at the router buffer is considered overflow and dropped as well as causing congestion [6-8]. Of average delay (D) and mean queue length (mql) of packets in the router buffer which also decreases the amount of packets going in the router buffer (T) [9-11].

Enormous congestion control algorithms, such as Gentle Random_Early_Detection (GRED) [12], Enhanced Adaptive GRED (EAGRED)[13] and Markov-Modulated Bernoulli Dynamic GRED [6] have been proposed. However, these algorithms have failed to adjust dynamically to provide the best solution based on the mql status.

Generally, the disadvantages of existing congestion control algorithms can be summarized as follows. Existing algorithms

use static probability for packet dropping, and several propose an addition target value that leads to a large number of packet drops when the probability value is high and bursting traffic is present. However, the parameterization problem still exists in most dynamic methods. Bursting traffic causes a heavy congestion signal, which then leads to significant packet drops. Conversely, network performance becomes degraded when the probability of packet dropping is set too low. Specifically, Dp, PL, mql, and D increases, and T decreases. Consequently, a dynamic mechanism is required to implement packet dropping based on the congestion status. This paper proposes an enhance method, Stabilized Dynamic GRED (SDGRED), to address the aforementioned disadvantages and to improve network performance. The latter objective involves alleviating PL and obtaining more acceptable performance measurement results with regard to D and mql when heavy congestion takes place at the router buffers [14].

The paper is summarized as follows. Related work is presented in Section 2. The proposed SDGRED method is covered in Section 3. Section 4 presents the details of simulation experimental environment. The performance results of the developed simulation are discussed in Section 5. Section 6 presents the summary of the proposed paper.

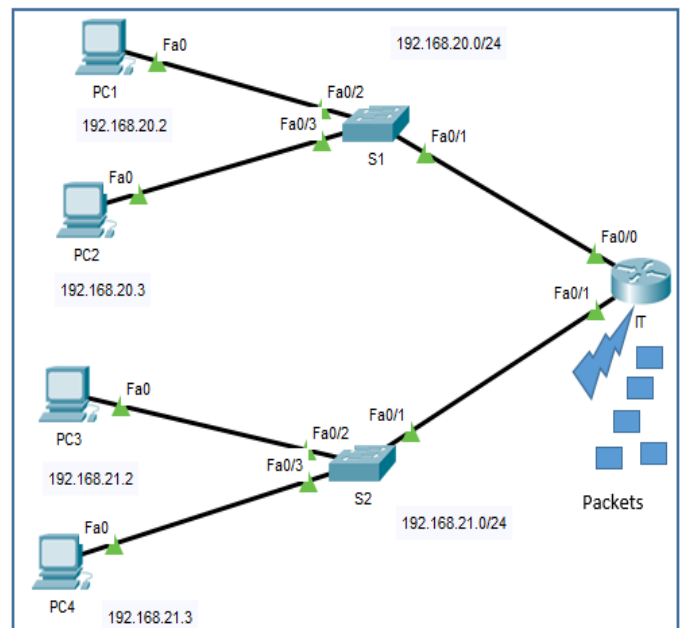


Fig. 1. Congestion in Router Buffer.

II. RELATED WORK

Several studies have explored controlling congestion and handling the aforementioned problems [15-20]. The Drop-Tail (DT) method [21] aims to control congestion employing a stable router buffer size to optimize queuing delay. The size of the router buffers is set to a maximum and all incoming packets are dropped when the router buffers overflow. There are several disadvantages of DT. Such as, increase the packet delay, decreases the throughput (T), an increase in the packet loss rate, and global synchronization [22].

Average Queue Management Methods (AQM) methods are a solution to overwhelm drawbacks of DT method. Unlike the DT method that starts dropping packets only after the router buffers overflow [13, 14, 23], AQM methods are depend on dropping the packets in the router buffer in early stages. So, early congestion control mechanism notifies the sources sender to start decrease their transmission packets early before the buffers are occupied completely and becomes full. AQM methods control the congestion in the router buffer, so as to increase the throughput, decreases the time delay, decreases the packet loss values, and keeps mql at a lowest value. AQM emerges with an adaptable utilization buffer size. Packet droppings are initiated based on a calculated threshold value to prevent buffer overflow. AQM calculates the current value of aql according to the number of packets then compares it.

(AQM) methods are a solution to overwhelm drawbacks of DT method. Unlike the DT method that starts dropping packets only after the router buffers overflow [13, 14, 23], AQM methods are depend on dropping the packets in the router buffer in early stages. So, early congestion control mechanism notifies the sources sender to start decrease their transmission packets early before the buffers are occupied completely and becomes full. AQM methods control the congestion in the router buffer, so as to increase the throughput, decreases the time delay, decreases the packet loss values, and keeps mql at a lowest value. AQM emerges with an adaptable utilization buffer size. Packet droppings are initiated based on a calculated threshold value to prevent buffer overflow. AQM calculates the current value of aql according to the number of packets then compares it with the set threshold. When the aql value arrives to defined threshold, all the incoming packets that arrive at the router buffer are dropped with main factor called the probability in order to preventing router buffer overflow and becomes full [24-26]. Enormous methods for congestion control, such as AGRED [22], EAGRED [27], DGRED [14], and FLGRED have been built based on AQM.

Floyd [27] proposed the GRED to make less some disadvantages in random early detection (RED)[12]. Comparable to RED, the GRED method chiefly purposes to control the congestion in router buffer at an early stage. GRED implements its algorithm by stabilizing the aql at a certain level. GRED uses a familiar approach used by RED in calculating the dropping. Conversely, GRED uses minimum, maximum, and double maximum threshold. Commonly, GRED responds to the arriving packets at router buffer according to the subsequent steps (Fig. 2):

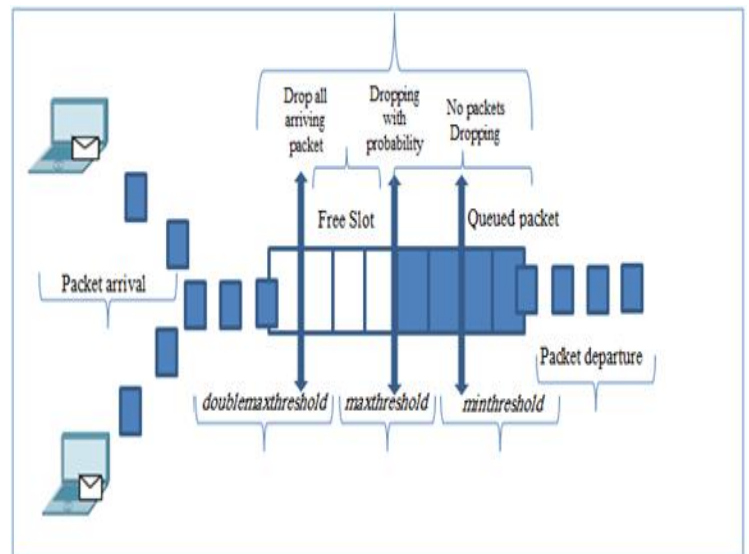


Fig. 2. GRED Buffer.

- When the current value of aql is less than the *minthre_shold* value, allow receiving packets.
- When the aql is greater than the *minimumthreshold* value and less than *maxthre_shold* value, the GRED method start drop the packets in the router buffer in random manner, as RED.
- When the aql is reach the *maxthre_shold* value and less than the *doublemaxthre_shold* value, the GRED method start drops the packets with based on higher probability scenario.
- Finally, if the aql value is arriving the *doublemaxthre_shold* value, the GRED method drops every arriving packets and the *Dp* is set one.

However, GRED has several disadvantages. Such as, GRED contains numerous threshold values, GRED parameters are set to exact values to gain satisfactory performance. This causes parameterization problem. And when the current aql value is below the *minthre_shold* value and heavy congestion occurs in the router buffer, the aql will take a long time to modify; the result the router buffer overflows and becomes full. Therefore, no dropping for packets even with the overfull GRED router buffer.

Dynamic GRED (DGRED) is a development of GRED method. DGRED uses a dynamic *maxthre_shold* position and *doublemaxthre_shold* to control the dropping policies mechanism in the router buffer at the early time earlier it overflows[14]. This algorithm aims to stabilize the aql value at the router using an original defined value called Target aql (Taql) that is calculated and set between the *minthre_shold* and *maxthreshold*. In addition, the proposed DGRED intends to provide better performance results than other AQM methods, such as RED and two of its variants, GRED and AGRED[14]. These results are represented by the results of mql, packet loss, and delay when congestion happens at the buffer, see Fig. 3.

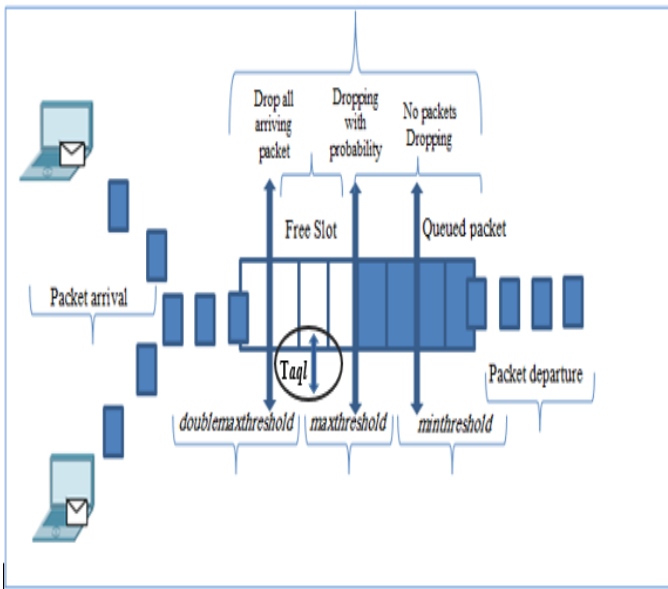


Fig. 3. DGRED Buffer.

DGRED furthermore changes the `maxthre_shold` and `doublemaxthre_shold` parameters setting at the buffer to improve performance measures. DGRED method employs `minthre_shold` and `doublemaxthre_shold` as set in GRED method.

However, DGRED has some limitations. DGRED involves several threshold values and `Taql`, which means using parameters to control the congestion in the router buffer (parameterization).

III. PROPOSED SDGRED METHOD

Fig. 4 shows SDGRED's processing stages. The parameter setting initialization step (Step 1) ensures that parameters are actually specified when the packets reach the router buffer. SDGRED method uses the `minthre_shold` and `maxthre_shold` values as that in DGRED method [14]. The `doublemaxthre_shold` in SDGRED method is considered the same value as that in DGRED[14], see Fig. 5. The initial value of `aql` is set zero and the counter sequence value starts from -1.

The SDGRED method then receives packets (Step 2) using a Bernoulli model, $\epsilon \in [9]$, $n = 0, 1, 2, 3, 4, 5 \dots$, wherever n refers to the arrival packets number in the router buffer in specific slot n . the Bernoulli process is appropriate when the buffer has a static length slot.

SDGRED then observes the queue status in the router buffer (Step 3) and calculates the `aql` value depend on status the buffer either contain packets or not contain packets, as shown in Fig. 6. Thus, in the case of empty router buffer queue, the `aql` value is considered according to idle time (n) and computed using Equation (1). Meanwhile, in the case of router buffer queuing, the `aql` is computed using Equation (2).

$$average\ ql = average\ ql \times (1 - average\ w)^n \quad (1)$$

$$average\ ql = average\ ql \times (1 - qw) + qw \times q_inst \quad (2)$$

Next (Step 4), the SDGRED method matches the `aql` value with the thresholds position values and subsequently updates

`maxthre_shold` and `doublemaxthre_shold` positions in the router buffer to increase network performance (Fig. 7). Both `maxthre_shold` and `doublemaxthre_shold` values set according to the `aql` value.

In Fig. 7, the `maxthre_shold` and `doublemaxthre_shold` values increased and decreased around the `minthre_shold` by Equations (3) to (5) to prevent congestion at the router buffers. Thus, the `aql` value stabilizes around the `minthre_shold` and prevents the saturation of router buffers. As a result, fewer packets are dropped. Furthermore, the calculations can cause changes in `aql` value in a slow mode. Therefore, the Equations (3) to (5) are derived.

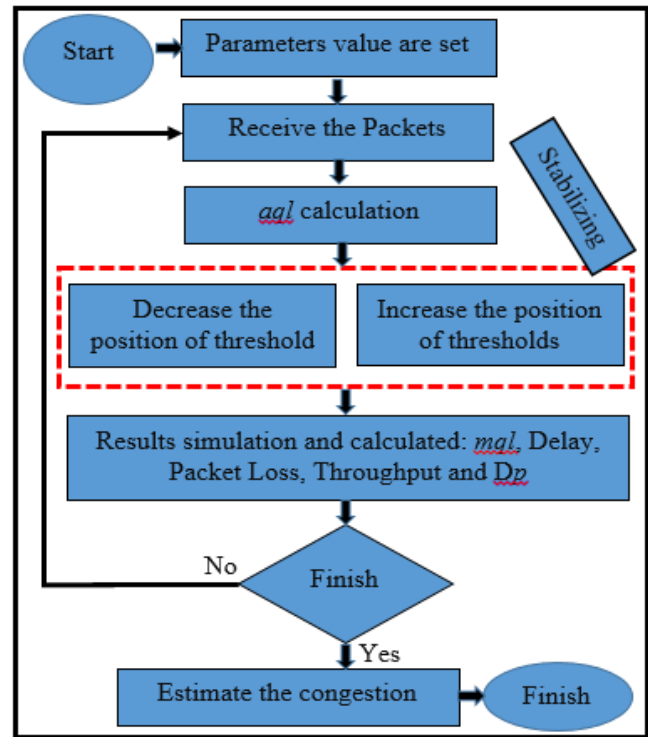


Fig. 4. SDGRED Stages.

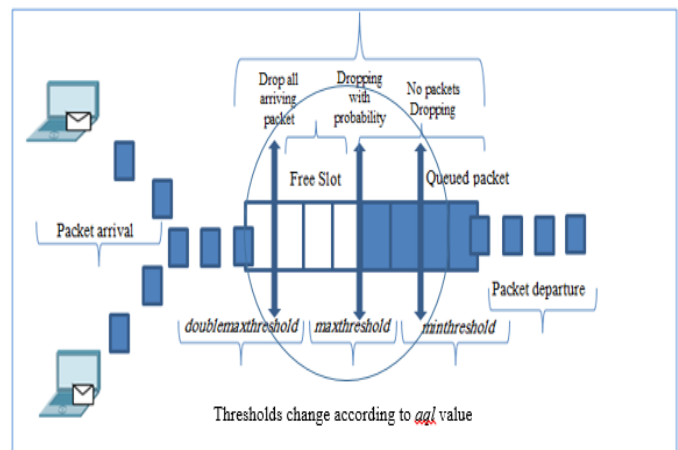


Fig. 5. The Proposed SDGRED Buffer.

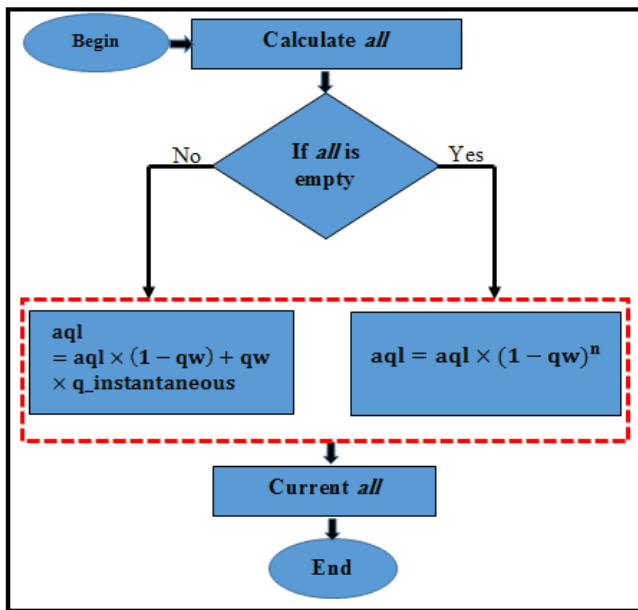


Fig. 6. Average Queue Length Status.

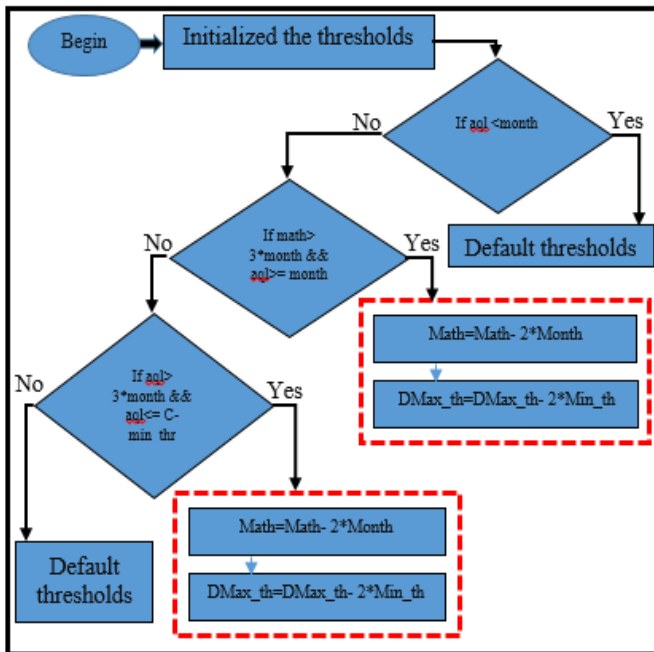


Fig. 7. Thresholds Stabilizing Stages.

As such, when the aql value is below min_threshold, no change occurs and the min_threshold, maxthre_shold and doublemaxthre_shold values will initialize [27]. Conversely, when the aql value is below the minthre_shold multiply two according Also maxthre_shold is reach greater than or equal to the position of minthre_shold multiply three, then the maxthre_shold and doublemaxthre_shold values change using Equations:

$$\text{maxthreshold} - 2 * \text{Minthre_shold} \quad (3)$$

$$\text{Doublemaxthreshold} - 2 * \text{Minthre_shold} \quad (4)$$

$$\text{maxthreshold} + \text{Minthre_shold} \quad (5)$$

Thus, the aql value arises rapidly and stabilizes at the min_threshold. Also, if the aql is greater than the minthre_shold multiply three and less than or equal to the buffer capacity min_threshold, the maxthre_shold and double maxthre_shold values will set as shown by Equation. Thus, they become the same and prevent the double maxthre_shold value to go over the buffer capacity. Subsequently, the maxthre_shold and doublemaxthre_shold values increase to push the aql near the minthre_shold and decrease the probability the router buffer becomes full and over flows. In the last, in a case none of previous scenario happen, the maxthre_shold and doublemaxthre_shold is set to the same values as in the DGRED method [22].

(Step5) of the SDGRED method, the congestion is assessed and packet dropping is applied. aql plays a main role in congestion estimation according to dropping polices. In case the aql value is not reach the min_threshold, no event for congestion is presented at the SDGRED router buffer and no packet is dropped. In addition, Dp is fixed to zero and C is fixed to-1. Hence, no packet is reached to the boundary of threshold. If the aql value is between the minthre_shold and maxthre_shold values, the SDGRED router buffer operates as DGRED for dropping the arrival packets. Dropping packets based on increasing C by 1 and calculating Dp for arriving packets. If the aql value is between the doublemaxthre_shold and maxthreshold, the SDGRED router buffer starts drop the incoming packets based on DGRED method, which involves initializing the C value and set one and calculating Dp for current arriving packets. Lastly, if the aql value is reach the doublemaxthre_shold value, the proposed SDGRED router buffer drops every arriving packet with Dp equal 1 and sets C to zero. Subsequently, in case the SDGRED router buffer becomes empty, the value of idle time is set to current time directly.

IV SIMULATION

GREED, DGRED, and the proposed stabilize DGRED are simulated depend on a discrete time queue model which uses a time as a slot [28, 29]. Each slot time may contain packet arrival (alpha) and packet departure (beta). Simulation is implemented by applying the compared methods in a network environment involving a lone router buffer hop. Particularly, both packet arrival and departure are implemented in single hope on a first packet arrival first packet departure basis. GREED, DGRED, and SDGRED simulations are applied in Java with i5 processor device, 1.68 GHz and 8 GB RAM. In this simulation, the probability value for both alpha and beta for the router buffer in a specific slot time is called alpha and beta, respectively [23, 29].on the other hand, the Packet arrivals and packet departures are demonstrated using a Bernoulli process and a geometrical distribution, respectively [29].

IV. EVALUATION RESULTS

The performance results of the SDGRED method is compared with DGRED and GREED AQM methods. The performances are implemented in simulation environment 10 runs, each run getting different seeds value as an input to the random number producer. This scenario eliminates likely bias in the output performance results and yields confidence intervals value. The performance results are calculated after the

system becomes stable to collect the results which means a steady state.

For the parameters are set in GRED, DGRED, and the proposed SDGRED are introduced using equal parameters at most. In order, to make congestion and non-congestion situations at the router buffer, the packet arrival was set to the following values[7].0.18,0.33, 0.48, 0.63, 0.78 and 0.93 respectively; each value of them goes to generate congestion or non-congestion station. The buffer size room was set 20 packets to guarantee the congestion at small buffer sizes. A total slot was set to 2000000 were used in the simulations. The minthre_shold is set 3, the maxthre_shold is set 9, doublemaxthre_shold is set 18, Dmax, is set 0.1 and qw is set 0.002, as recommended in DGRED[14]. Table I lists all the utilized parameters. The simulation performance results are stately using numerous performance metrics. Such as, Throughput, Delay, mql, packet loss, and dropping probability, which are discussed in the following subsection.

TABLE I. PARAMETERS SETTING

Parameter	DGRED	DGRED	SDGRED
alpha	0.18,0.33,0.48,0.63,0.78,0.93	0.18,0.33,0.48,0.63,0.78,0.93	0.18,0.33,0.48,0.63,0.78,0.93
beta	1/2	1/2	1/2
Buffer size	20	20	20
Q_w	0.002	0.002	0.002
D_max	0.1	0.1	0.1
# of slots	2 millions	2 millions	2 millions
Mint_hreshold	3	3	3
Max_threshold	3*min	3*min	3*min
Double_maxthreshold	2*max	2*max	2*max
Target aql	parameter	-----	dynamic

Mean Queue Length, Throughput, and Delay Results.

Respectively, Fig. 8, 9 and 10 explain the output performance results for GRED, DGRED, and the proposed SDGRED using different probabilities of packet arrivals as mention above. Specifically, Fig. 8 shows the mql and the probability of packet arrival.

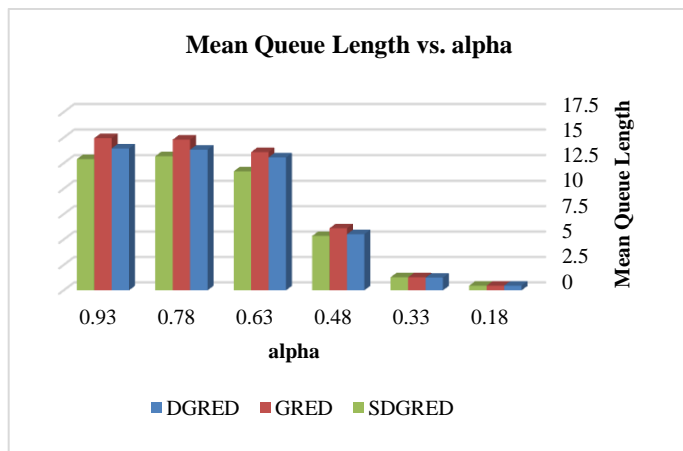


Fig. 8. Mean Queue Length.

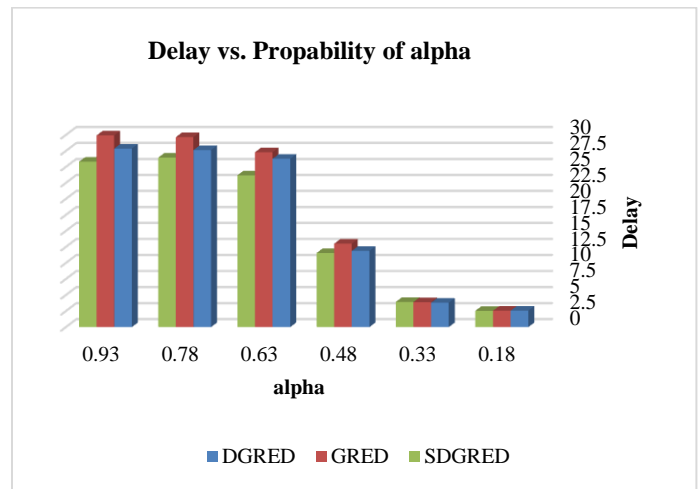


Fig. 9. Delay Performance Results.

The mean queue length for all methods and SDGRED method is the same up to a certain value of the probability of alpha 0.18, 0.33 and 0.48. Such a small probability value reasons bright congestion at most because the probability of packet departure was set 0.5 greater than that of alpha ($\alpha > \beta$). So, all compared methods gain satisfied and stable mean queue length values. On the other hand, for a higher probability values, such as, 0.63, 0.78 and 0.93 congestion is more likely to occur at the router buffers. Thus, the mean queue length of the AQM methods arises exponentially. In such a case, the proposed SDGRED performs better than the DGRED and GRED methods because fewer packets are dropped and the router buffer space available for new packets arrival.

Fig. 9 illustrates a comparison of the delays in all algorithms. Although DGRED shows good performance in terms of the average delay, the proposed SDGRED performs better because of the fewer dropped packets in SDGRED.

Finally, Fig. 9 shows the throughput performance measure in all the packet arrival probabilities were set. The proposed SDGRED and compared methods gain the same throughput results either light congestion or heavy congestion, the packets arrival probability are set to 0.18, 0.33, and 0.48 which means lower probability or higher than that of packet departure, such as, 0.63, 0.78 and 0.93. Fig. 10 refers a probability of packet arrival arrive 0.18, 0.33 and 0.48 increases to arrive to the packet departure value. On the contrary, when the alpha arrives the value of beta, all the compared methods stabilize at the packet departure probability which equals 0.5 when congestion happens.

A. Packet Loss and Dp

The proposed SDGRED method is likewise compared with the DGRED and GRED methods in regards of PL performance measures and DP performance measures to display the amount of dropped packets in the buffer. The results of PL and DP are computed after the simulation becomes stable and steady. The method simulations are run 10 times with various random seeds and the mean is determined. The results of GRED, DGRED, and the proposed SDGRED algorithms in means of PL and DP are clarified in Fig. 11 and 12, in that order.

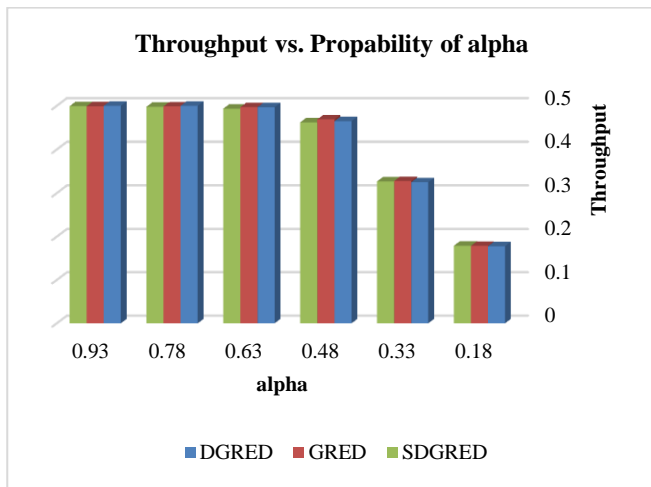


Fig. 10. The Throughput.

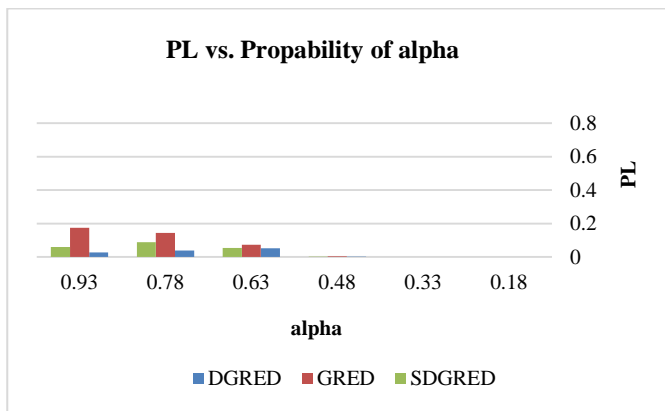


Fig. 11. Packet Loss Result.

In Fig. 11, GRED, DGRED, and the proposed SDGRED algorithm marginally produce the same PL performance result when the beta probability is greater than that of alpha. The DGRED introduces better PL performance at heavy congestion because the router buffer overflows earlier compared with those in the GRED and SDGRED methods.

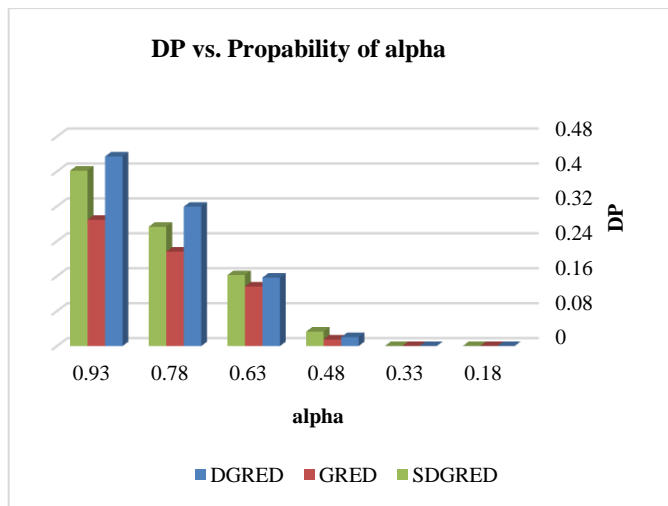


Fig. 12. Dropping Probability.

Fig. 12 shows that for the same reason, the proposed SDGRED algorithm evidently drops more packets when the beta probability is lower than that of alpha.

Therefore, the proposed method reveals the following improvements:

- GRED, DGRED, and the proposed SDGRED methods the same performance measure results when the alpha equals 0.18, 0.33, and 0.48.
- The SDGRED method offers a marginally better mql and Delay than the DGRED, and GRED methods when the alpha arrive to the 0.63, 0.78 and 0.93. In addition, when the alpha less than 0.5, the GRED, DGRED, and the proposed SDGRED methods gain similar T performance results.
- DGRED method slightly outperforms the SGRED and GRED methods for PL when heavy congestion. Moreover, at such values of packet arrival probability, SDGRED drops fewer packets (Dp) at their router buffers.

V. CONCLUSIONS

The current paper proposed an enhanced AQM method depend on the DGRED called the SDGRED. The proposed SDGRED aims to keep the aql between the minthre_shold position and doublemaxthre_shold position by changing the maxthre_shold and doublemaxthre_shold positions according to current aql value. This aql change helps stabilize the aql at minthre_shold position in order to prevent the congestion. SDGRED employs maxthre_shold and doublemaxthre_shold positions in adaptive manner to keep the aql value around the minthre_shold value, which may lead to fewer packet losses and queuing delay. The SDGRED technique is compared with the GRED and DGRED methods with the following performance measures such as, T, mql, D, PL, and Dp, to present which method offers better performance result in regards of packet arrival probability. The results show the SDGRD method is competitive to the compared methods.

REFERENCES

- [1] Welzl, M., Network Congestion Control: Managing Internet Traffic. 1 ed. 2005.
- [2] Adeeb alsaaidah, et al., Markov-Modulated Bernoulli-Based Performance Analysis for Gentle Blue and Blue Algorithms under Bursty and Correlated traffic. Journal of Computer Sciences, 2016. 12(6): p. 289-299.
- [3] Senthikumar, T. and V. Sankaranarayanan, Dynamic congestion detection and control routing in ad hoc networks. Journal of King Saud University - Computer and Information Sciences, 2013. 25(1): p. 25-34.
- [4] ABDEL-JABER, H., et al., Random Early Dynamic Detection Approach for Congestion Control Baltic J. Modern Computing, 2014. 2(1): p. 16-31
- [5] Ababneh, j., et al., Derivation of Three Queue Nodes Discrete-Time Analytical Model Based on DRED Algorithm, in The Seventh IEEE International Conference on Information Technology: New Generations (ITNG 2010),USA.2010. . 2010.
- [6] BAKLIZI, M., et al., MARKOV-MODULATED BERNOULLI DYNAMIC GENTLERANDOM EARLY DETECTION. Journal of Theoretical and Applied Information Technology, 2018. 96(20).
- [7] BAKLIZI, M., J. ABABNEH, and N. ABDALLAH. PERFORMANCE INVESTIGATIONS OF FLRED AND AGRED ACTIVE QUEUE MANAGEMENT METHODS. in Proceedings of Academicsera 13 th International Conference. 2018. Istanbul, Turkey.

- [8] Mulla, A.S. and B.T. Jadhav, Fuzzy Based Queue Management Policies – An Experimental Approach. International Journal of Current Engineering and Technology 2014. 4(1).
- [9] NSKI, A.C. and L. CHRÓST, ANALYSIS OF AQM QUEUES WITH QUEUE SIZE BASED PACKET DROPPING. Int. J. Appl. Math. Comput. Sci. 2011. 21(3): p. 567–577.
- [10] Abualhaj, M.M., A.A. Abu-Shareha, and M.M. Al-Tahrawi, FLRED: an efficient fuzzy logic based network congestion control method. The Natural Computing Applications, 2016.
- [11] Kusumawardani, M., Active queue management (aqm) and adaptive neuro fuzzy inference system (anfis) as intranet traffic Control. Academic Research International 2013. 4(5).
- [12] Floyd, S. Recommendations On Using the Gentle Variant of RED. <http://www.aciri.org/floyd/red/gentle.html> 2000.
- [13] Baklizi, M. and J. Ababneh, Performance Evaluation of the Proposed Enhanced Adaptive Gentle Random Early Detection Algorithm in Congestion Situations International Journal of Current Engineering and Technology 2016. 6(5).
- [14] Baklizi, M., et al., DYNAMIC STOCHASTIC EARLY DISCOVERY: A NEW CONGESTION CONTROL TECHNIQUE TO IMPROVE NETWORKS PERFORMANCE. International Journal of Innovative Computing, Information and Control, 2013. 9(4).
- [15] Ababneh, J., et al. Derivation of Three Queue Nodes Discrete-Time Analytical Model Based on DRED Algorithm. in Information Technology: New Generations (ITNG), 2010 Seventh International Conference on. 2010.
- [16] Abdel-jaber, H., et al. Traffic Management for the Gentle Random Early Detection Using Discrete-Time Queueing. in Proceedings of the International Business Information Management Conference 2008. Marrakech, Morocco.
- [17] Abdel-Jaber, H., et al., Performance evaluation for DRED discrete-time queueing network analytical model. Journal of Network and Computer Applications, 2008. 31(4): p. 750-770.
- [18] Abdel-jaber, H., et al. Modelling BLUE Active Queue Management Using Discrete-Time Queue. in Proceedings of the 2007 International Conference of Information Security And Internet Engineering (ICISIE'07). 2007. London.
- [19] Moarefianpour, A. and V.J. Majd, Input-to-State Stability in Congestion Control Problem of Computer Networks with Nonlinear Links. International Journal of Innovative Computing Information and Control 2009. 5(8): p. 2091-2105.
- [20] Chen, X., T. Liu, and J. Zhao, A LOGIC-BASED SWITCHING CONTROL APPROACH TO ACTIVE QUEUE MANAGEMENT FOR TRANSMISSION CONTROL PROTOCOL. International Journal of Innovative Computing, Information and Control 2008. 4(7): p. 1811—1820.
- [21] Brandauer, C., et al., Comparison of Tail Drop and Active Queue Management Performance for Bulk-Data and Web-Like Internet Traffic, in Proceedings of the Sixth IEEE Symposium on Computers and Communications. 2001, IEEE Computer Society.
- [22] Floyd, S. and V. Jacobson. Random early detection gateways for congestion avoidance. in Networking, IEEE/ACM Transactions on. 1993.
- [23] Baklizi, M., J. Ababneh, and A Survey in Active Queue Management Methods According to Performance Measures. International Journal of Computer Trends and Technology (IJCTT), 2016. 38 (3): p. 145.
- [24] Bitorika, A., et al. A Comparative Study of Active Queue Management Schemes. in Proceedings of IEEE ICC 2004, Congestion Control Under Dynamic Weather Condition 103. 2004.
- [25] Ryu, S., Active Queue Management (AQM) based Internet Congestion Control. October 1, 2002: University at Buffalo.
- [26] Salim, J.H., U. Ahmed, and J. 2000, Performance evaluation of explicit congestion notification (ECN) in IP networks, N.W. Group, Editor. 2000, RFC 2884.
- [27] Floyd, S. Recommendations On Using the Gentle Variant of RED. 2000; Available from: <http://www.aciri.org/floyd/red/gentle.html>.
- [28] Abdel-Jaber, H., et al., Performance evaluation for DRED discrete-time queueing network analytical model. J. Netw. Comput. Appl., 2008. 31(4): p. 750-770.
- [29] Woodward, M.E., Communication and Computer Networks: Modelling with discrete-time queues. 1993: Wiley-IEEE Computer Society Press.

Survey on Human Activity Recognition based on Acceleration Data

Salwa O. Slim¹, Ayman Atia², Marwa M.A. Elfattah³, Mostafa-Sami M. Mostafa⁴

Department of Computer Science, HCI lab

Faculty of Computers and Information, Helwan University, Cairo, Egypt^{1, 2, 3, 4}
Misr International University, Cairo, Egypt²

Abstract—Human activity recognition is an important area of machine learning research as it has many utilization in different areas such as sports training, security, entertainment, ambient-assisted living, and health monitoring and management. Studying human activity recognition shows that researchers are interested mostly in the daily activities of the human. Therefore, the general architecture of HAR system is presented in this paper, along with the description of its main components. The state of the art in human activity recognition based on accelerometer is surveyed. According to this survey, Most of the researches recently used deep learning for recognizing HAR, but they focused on CNN even though there are other deep learning types achieved a satisfied accuracy. The paper displays a two-level taxonomy in accordance with machine learning approach (either traditional or deep learning) and the processing mode (either online or offline). Forty eight studies are compared in terms of recognition accuracy, classifier, activities types, and used devices. Finally, the paper concludes different challenges and issues online versus offline also using deep learning versus traditional machine learning for human activity recognition based on accelerometer sensors.

Keywords—Human activity recognition; accelerometer; online system; offline system; traditional machine learning; deep learning

I. INTRODUCTION

Human Activity recognition (HAR) is the root of many applications, such as those which deal with personal biometric signature, advanced computing, health and fitness monitoring, and elder-care, etc. [1]. The input of HAR models is the reading of the raw sensor data and the output is the prediction of the user's motion activities [2].

A. Sensor Approaches

There are two types of sensors to recognize the human activities; using external or wearable sensors. In the past, the sensors were settled in predetermined points of interest, therefore the detecting of activities is essentially based on the interaction of the users with the sensors. One of the examples of external sensors applications is the intelligent home [3-7], which has a capability to identify the complicated activities, eating, taking a shower, washing dishes, etc., because they depend on data that is collected from various sensors which are placed in specific objects. Those objects are supported by peoples' interaction with them (e.g., stove, faucet, washing machine, etc.). However, there is no useful response if the user is out of the sensor area or the activities of the user do not need

to interact with those objects. Moreover, the composition and servicing of sensors require high costs.

Also, some of the extensive researches [8-11] have been focused on the recognition of activities and gestures from video sequences. This is most appropriate for security and interactive applications. Microsoft developed the Kinect game console that let the user interact with the game using the gestures without any controller devices. However, there are some issues in video sequences of HAR such as [2]:

- The privacy, as no one wants to be always monitored and recorded by cameras.
- The pervasiveness, it is difficult to attach the video recording devices to the target of individuals in order to collect the images of their entire body during daily living activities.
- Video processing techniques are comparatively costly and consuming time.

The above-mentioned limitations motivate to use a wearable sensor in HAR. Where the measured attributes almost depend on the following: environmental variables (such as temperature and humidity), movement of the user (such as using GPS or accelerometers), or physiological signals (such as heart rate or electrocardiogram). These data are indexed over the time dimension.

Accelerometer sensors sense the acceleration event from mobile phone, WII remote, or wearable sensors. The raw data stream from the accelerometer is the acceleration of each axis in the units of g-force. The raw data is represented in a set of 3D space vectors of acceleration. A time stamp can also be returned together with the three axes readings. Most of the existing accelerometers provide a user interface to configure the sampling frequency so that the user have to choose the best sampling rate which match his needs. There are many causes that encourage to develop new techniques for enhancing the accuracy under more factual conditions. However, the first works on HAR date back to the late 90's [12], [13].

B. Challenges Face HAR System Designers

Any HAR system design relies on the activities to be recognized. The activities kinds and complexity are able to affect the quality of the recognition. some of challenges which face researches are (1) how to select the attributes to be measured, (2) how constructing the system with portable, unobtrusive, and inexpensive data acquisition, (3) how

extracting the features and designing the inference methods, (4) how collecting the data in the real environment, (5) how recognizing activities of the new users without the need of re-training the system, and (6) how can be implemented in the mobile devices which meeting energy and processing limitations [14].

Oscar et al. [2] distinguished activities into seven groups such as Ambulation, Transportation, Phone usage, Daily activities, Exercise/Fitness, Military and Upper body. However, according to our survey eight different groups of activities can be distinguished by reorganizing the activities categorization in [2] such as the activities of phone usage were combined into Daily activities category, upper body and military categories are removed because they were not used in our survey, Household activities, Kitchen activities, Self-care activities, and Transitional activities were added. Those eight categories and the individual activities that belong to each category are summarized in Table I. The abbreviations and acronyms are defined in Table V.

C. Offline Versus Online HAR Systems

The recognition of human activity could be done using offline or online techniques. Whenever online processing is not necessary for the application, the offline processing can always be used. For example, if the tracking of person's daily routine is the goal such as in [15], the data was collected during the day by using the sensors and then it could be uploaded to a server at the end of the day. The data can be processed offline for classification purposes only.

However, some of the applications such as fitness coach where the user applies the given program which contains on a

set of activities with sequence and duration. It is widely required to identify what the user is currently doing [16]; therefore it requires to use online technique.

Another application can be the recruitment for participatory sensing applications [17]. For instance, the application aimed to collect the information from users during walking in a specific location in the city. Thus, online recognition of activities becomes significant. Some researches on human activities, which works on offline recognition, are using machine learning tools such as WEKA [18-20]. Nowadays, some of clouding systems are being used for online recognition [21] [22].

D. Machine Learning Techniques

The success of HAR process depends on which machine learning technique is suitable in the problem case. There are two different approaches: first approach depend on traditional machine learning such as KNN, Naïve Bayes, Bayes Net, IBK, J48, Random forest, SVM, DTW, etc., the second approach depend on deep learning such as convolution neural network, recurrent neural network, vanilla RNN forward, and Gated Recurrent Unit RNNs, etc.

Recognize the human activity is mission. The paper surveys the state of the art traditional machine learning and deep learning for HAR. Section II presents the general components of HAR system. Section III explores the difference between online and offline systems. Section IV compares between traditional and deep learning techniques. Section V shows the main issues for recognizing activities and the most important solutions to each one of them. Finally, a general conclusion is presented in Section VI.

TABLE I. THE CATEGORIZATION OF ACTIVITIES

Category	Activities	Related Ref.
Daily Activities	Ironing, Eating, Drinking, Using phone, Watching TV, Using computer, Reading book/magazine, Listening music/radio, Taking part in conversations, Getup bed, Sleeping, Note-pc, Carrying a box, Getting up	[29][32-35][46][53][56][60][64][77]
Household Activities	Sorting files on paperwork, Wiping tables, Vacuuming, Taking out trash, Cleaning a dining table, Washing dishes, Sweeping with broom, Cleaning up	[29][32][33][42][53][55-56][60][64]
Transportation	Riding a bus, Cycling, Driving	[24][28][38][40][47][53][55-56][58][61][63-64][67]
Ambulation	Running, Sitting, Standing, Lying, Ascending stairs, Descending stairs, Riding escalator, Riding elevator, Falling, Stopping, Casual movement	[23][24][26-28][36-50][52-56][58][59][61-71][75][76] [77] [81]
Kitchen Activities	Fill kettle, Pour boiling water into the mug, Add tea-bag, Add sugar, Add milk, Remove tea-bag, Pour milk outside the mug, Pour boiled water outside the mug, Making coffee, Making tea, Making oatmeal, Frying eggs, Making a drink, Cooking, Checking tools and utensils in the kitchen, making a sandwich, cooking pasta, cooking rice, Feed Fish.	[32-35][42][46][53][57][60][64]
Exercise/fitness	Walking in treadmill, Running in treadmill, Aerobic dancing, Jumping, Jogging, Playing basketball, Playing football, Rowing	[23][24][26][37][42][45][47][48][50][53] [56][68][70][75][77]
Self-care Activities	Applying makeup, Brushing hair, Shaving, Toileting, Flushing the toilet, Getting dressed, Brushing teeth, Washing hands, Washing face, Washing clothes, Drying hair, Taking medication	[29] [32-35][53][60]
Transitional Activities	lying down and getting up, Sitting down and getting up, walking up and down stairs	[52][53]

II. GENERAL STRUCTURE OF HAR SYSTEMS

The Human Activity Recognition process consists of four main phases: Data Acquisition, Pre-Processing, Feature Extraction, and Classification. As shown in Fig. 1, HAR systems consist of several phases which are:

Data Acquisition: It is the first phase in the activity recognition for collecting the data by using the sensors.

Pre-processing: It is the second phase after the data is collected. It has important roles such as removing the noise of the raw data, using windowing or segmentation schema on the collected data. Using the raw sensor data in the classification process may be not a suitable decision, therefore, the raw data needs some transformations such as breaking the continuous raw sensor data into the windows of a certain duration. For the sake of the energy efficiency, it is serious to take a low sampling frequency in order to reduce the time of sensors working. The work time for the powerful sensor is low when the low sampling frequency is used. However, using of the low sample frequency to recognize the activities is still an open question. According to Kwapisz et al. [23], the sampling rate might be no less than 20 Hz for detecting daily activities. Some of the sampling data may be lost when using a low sampling frequency as well as it is hard to recognize the activities when

the sensing device has low-resolution. Thus there is a trade-off between consumption of the energy and the rate of recognition. Liang et al. [24] proposed a method for energy-efficient. That method is based on tri-axial accelerometer which embedded in a smartphone in order to recognize the user's activities. They aimed to reduce the likelihood of time-consuming frequency-domain features for lower computational complexity and modify the sliding window size for improving the accuracy of recognition.

Feature extraction: The segmented data is collected as a series of pattern containing three values 3D acceleration components. It converts the signal into the most significant features which are unique for the activity. It is better to extract features of the data which is based on a temporal window rather than using the raw data which depend on classifying every single data point. Using the features, rather than the raw data, leads to reduce the effects of noise and also reducing the computational load of classification algorithms. Standard features are divided into time and frequency domain. Janidarmian et al. [25] stated that the time or frequency domain and heuristic features are the most effective in the context of activity recognition. Table II displays the details of those features.

TABLE II. LIST OF FEATURES

Feature	Description	Feature	Description
Mean	$\mu_s = \frac{1}{n} \sum_{i=1}^n S_i$	Skewness	$\frac{1}{n\sigma_s^3} \sum_{i=1}^n (S_i - \mu_s)^3$
Minimum	$\min(S_1, S_2 \dots S_n)$	Kurtosis	$\frac{1}{n\sigma_s^4} \sum_{i=1}^n (S_i - \mu_s)^4$
Maximum	$\max(S_1, S_2 \dots S_n)$	Signal Power	$\sum_{i=1}^n S_i^2$
Median	$\text{median}(S_1, S_2 \dots S_n)$	Root Mean Square	$\sqrt{\frac{1}{n} \sum_{i=1}^n S_i^2}$
Standard Deviation	$\sigma_s = \sqrt{\frac{1}{n} \sum_{i=1}^n (S_i - \mu_s)^2}$	Peak Intensity	<i>The number of signal peaks within a certain period of time</i>
Coefficients of Variation	$\frac{\sigma_s}{\mu_s}$	Person's Correlation Coefficient	$\frac{\text{cov}(a, b)}{\sigma_a \sigma_b}$
Peak-to-Peak Amplitude	$\max(s) - \min(s)$	Inter-axis Cross-Correlation	$\frac{\sum_{t=1}^n (a_t - \mu_a)(b_t - \mu_b)}{\sum_{t=1}^n (a_t - \mu_a)^2 \sum_{t=1}^n (b_t - \mu_b)^2}$
Percentiles	$\text{percentile}(s, p_i) = (1 - f)S_k + fS_{k+1}$	Autocorrelation	$R(k) = \frac{1}{(n - k)\sigma_s^2} \sum_{i=1}^{n-k} (S_i - \mu)(S_{i+k} - \mu) \forall K$
Interquartile Range	$\text{percentile}(s, 75) - \text{percentile}(s, 25)$	Trapezoidal Numerical Integration	$\int_1^n s(x) dx$ using multiple segment trapezoidal Rule
Pitch Angle	$\arctan\left(\frac{x_1}{\sqrt{y^2 + z_1^2}}\right)$	Signal Magnitude Area	$\frac{1}{n} \sum_{i=1}^n (x_i + y_i + z_i)$
Roll Angle	$\arctan\left(\frac{y_1}{\sqrt{x^2 + z_1^2}}\right)$	Signal Vector Magnitude	$\frac{1}{n} \sum_{i=1}^n \sqrt{x_i^2 + y_i^2 + z_i^2}$
Median crossings	$t = s - \text{median}(s)$ $MC = \sum_{i=1}^n \text{sgn}(t_i \cdot t_{i+1})$ $\text{sgn}(a, b) = \{1 \text{ if } (a, b) < 0; 0 \text{ if } (a, b) > 0\}$	Power Spectral Density	$\frac{1}{n} \sum_{i=1}^{n-1} \left(S_i \cos \frac{2\pi f i}{n} \right)^2 + \left(S_i \sin \frac{2\pi f i}{n} \right)^2$

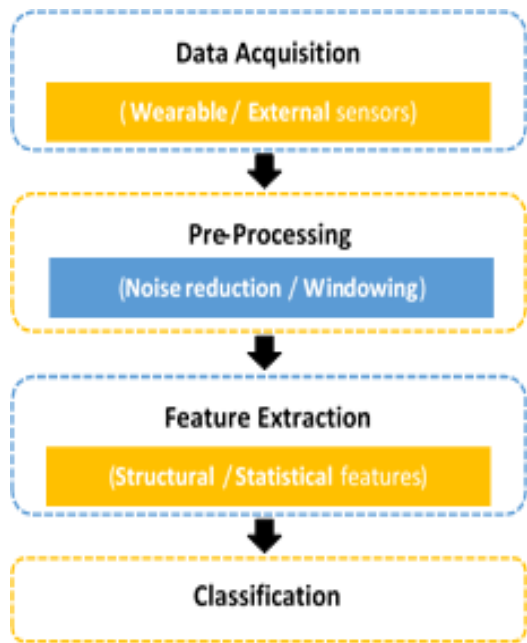


Fig. 1. Human Activity Recognition Flow.

Classification: It is the final phase of the human activity recognition process. The trained classifiers are used for classifying the various activities. The classification can be done either offline or online. A machine learning tool build on powerful processing may be used offline processing and the mobile phone itself or the cloud server may be used in the online processing.

III. ONLINE VS. OFFLINE HAR SYSTEMS

In the first, the training data are used for training the classifiers [25]. The human activities classifier can be trained online or offline as well as the classification process itself can be done online or offline. Offline classification (non-real-time) is sufficient solution when the user does not find an urgent need to receive immediate feedback. In the other side real-time classification (online) assists user for receiving real-time feedback. Liang et al. [24] proposed a framework for activity recognition using offline data training and online classification.

A. Online vs. Offline Training Phase

Online training means that the classifiers are trained on the hosting device, such as mobile, cloud, or Raspberry Pi, in real time. On the other hand, on offline training, a desktop machine is usually used for training the classifiers beforehand. As well as the raw data of the activities, which is collected by sensors, is stored and in later time these data are used for training the classification model as shown in Fig. 2. In the online training phase the raw data are not stored for later use but instead they are immediately processed for training to save time.

According to our readings, as shown in relevant references in Fig. 2, most of researchers prefer offline training. Only 8 out of all 45 studies were using online training in real time. One of the reasons for using offline method is that the training process is computationally expensive.

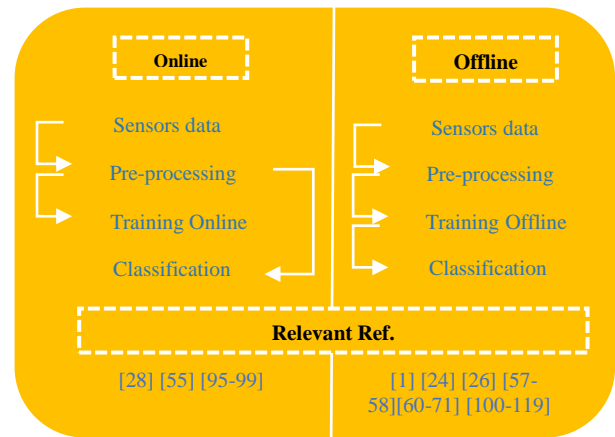


Fig. 2. Two Approaches of Training Phase.

B. Online vs. Offline Classification

In the final stage of classification, there are two ways to classify the activity for a specific label, which are online or offline, according to the training data. The most semi-supervised classification has been implemented and evaluated offline [2]. As well as there are more studies for supervised classification online and offline. All studies of the online and offline classification, which are described in details in the following two sections, are summarized in Fig. 3.

Fig. 3 shows the body sensors positions and related sensor type, device type, classifier type, and reference noted. The circles in Fig. 3 display two pieces of information, the types of devices which are used and the interior sensors. For example point 6 (the palm of the right hand) have three shapes which means some of the studies were used in this position for classification human activities by using three devices that are described in the following:

a) A red circle contains (A): Smartphone was used for sensing the accelerometer data in the reference [26] and [27]. The reference [26] used NB and KNN for classification human activities but the reference [27] used logitBoost classifier.

b) A red circle contains (A and G): Smartphone was used to collect Accelerometer and Gyroscope data for classifying human activities.

c) A green circle contains (A): WAS device was used for collecting the Accelerometer data.

The lines in Fig. 3 display two pieces of information, the point number and the location. For example point 20 has a red line which means this point is in a position on the back of the body. But when the line is a black color this means the point is in the front of the body position. The point 18 has a yellow line because the studies used the side pocket for holding the devices. The back pockets (point 10 and 11) were used in the same studies; therefore, their lines are merged.

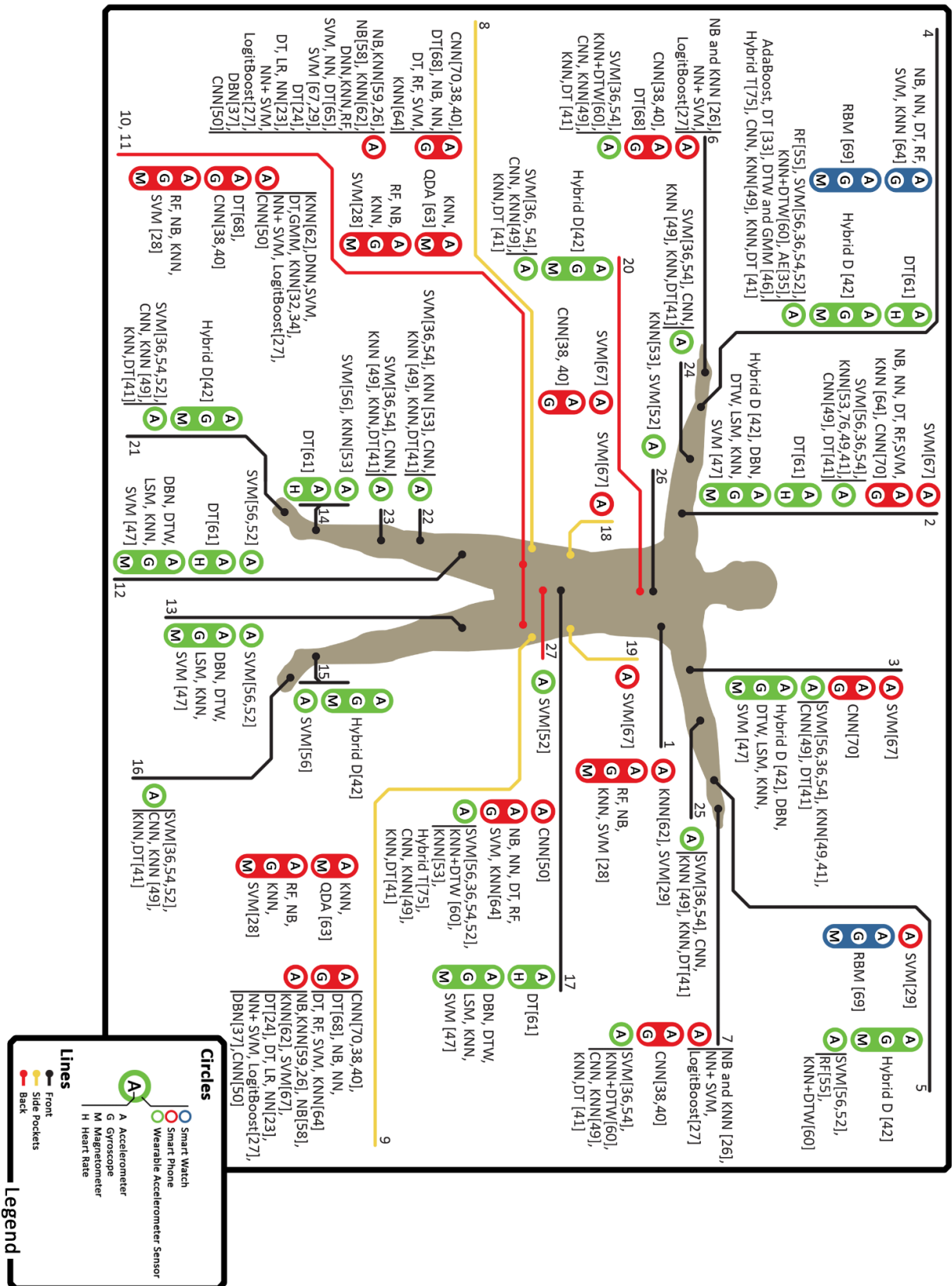


Fig. 3. Locations and Specifications of Different Sensors Devices, Interiors Sensors, and Classifiers which used in the HAR Studies.

1) *Online classification*: Online HAR systems are needed in the healthcare field for continuously monitoring to the patients with physical or mental pathologies in order to their protection, safety, and recovery. A lot of studies are based on giving real-time feedback for assisting people; some of them are summarized in Table III. In this survey, 20 studies in Table III were compared for displaying the activities which were classified, the classifier that was used, and accuracy which was achieved by using that classifier, the window length, overlap, and latency time of feedback, the type of training, reference of used dataset, and finally the type of devices which were used in collecting data.

According to our reading, there are 14 studies out of 20 focused to recognize the physical daily activities such as walking, running, sitting, and standing. One study [28] from 20 reviewed studies depends on online training. The mobile phone has become more robust in the available resources, such as battery, memory, CPU.

In online activity recognition, the mobile phone is used locally for collecting the data, pre-processing and classification; therefore, there are 12 out of 20 reviewed studies using the smart phone.

TABLE III. ON-LINE CLASSIFICATION OF HAR

Ref	Activities	Classifier	Accuracy	Wind. length	Overlap	Training	DS	Device	Latency time
[55]	AMB (2),HOS(1),TRSP(1)	RF	89.6 ± 3.9%	13 S	90%	offline		WAS	
[56]	AMB(5),DLY(4), HOS(3), TRSP(1), EXF(1)	SVM	95%	12.8 s	50%	offline		Wocket	4s
[57]	KIT(8)	HMM	85.6%	-	75%	offline	-	CogWatch , Kinect	1s
[26]	AMB(4), EXF(1)	NB, KNN	78%, 69%	10s	-	offline		Smartphone	-
[58]	AMB(3), TRSP(1)	NB	97%	1s	-	offline	-	Smartphone	
[59]	AMB(4)	NB,KNN	47.6%,92%	1s		offline		Smartphone	
[60]	KIT(6),SELF(9), DLY(8), HOS(3)	KNN+DTW	81%	1s	-	offline		IMOTE2,RFID	5.7s
[61]	AMB(7), TRSP(1)	DT	80%	4.2S	50%	offline		5 WAS	
[62]	AMB(6)	KNN	80%	-	-	offline		Smartphone	
[63]	AMB(4), TRSP(2)	KNN, QDA	94.9%, 95%	7.5S	-	offline		Smartphone	
[64]	AMB(4), TRSP(1), DLY(3), HOS(1), KIT(1)	NB, NN, DT, RF, SVM, KNN	The better MLP and RF	6S	-	offline	[20] [72]	Smart phone Smart watch	
[28]	AMB(2), TRSP(1)	RF, NB, KNN, SVM	90.3%, 79% 83.7%, 70.2%	4s		online		Smartphone	2S
[65]	AMB(6)	DNN,KNN,RF SVM, NN, DT.	98.6%, 97.6% 96%, 95.4%, 95.9%, 91.3%	1s	50%	offline		Smart phone	133ms
[66]	AMB(3)	DT	92.6%	5s	50%	offline		Smartphone	395 ms
[67]	AMB(4), TRSP(2)	SVM	90%	3.5 s		offline		Smartphone	
[68]	AMB(5), EXF(1)	DT	92.3%	3S	-	offline		Smartphone	
[69]	AMB (3)	RBM	93%	2S	50%	offline	[73]	smartwatch	
[70]	AMB(5), EXF(1)	CNN	97%	3S	-	offline	[23] [74]	Smart phone	3S
[71]	AMB(5)	DT	90.8%	1s	-	offline	-	WAS	-
[24]	AMB(7), TRSP(2), EXF(1)	DT	85%	variable	-	offline		smartphone	

2) *Offline classification*: When the online activity recognition (real-time activity recognition) is not critical for the application, the offline recognition is the best choice. In the offline classification, the user doesn't wait for the feedback of the recognition system in real-time. The user receives the results of the recognition after offline analysis and classification. For example, if the goal is monitoring the elderly person's activities of daily living [29], the data were collected during the day using sensors and then at the end of the day, it can be uploaded to a server for analysis and sending feedback to care manager or relatives etc. A lot of researchers use offline HAR system as a research base for examining their new techniques that are proposed to be used in the designing of an efficient HAR system, such as the techniques which are proposed for data collecting, pre-processing, feature extraction, or classification.

For example in [30], the offline classification was used for comparing seven classifiers in order to find the optimal one. Also in [31], a new classifier was developed for achieving appropriate accuracy in the child's behaviors detection. Some of researchers used offline classification for studying the efficiency of using accelerometer alone or to be combined with another sensor in the data collection phase. Studies included in our survey mainly used triaxial acceleration signal, while some of them used additional signals to improve recognition accuracy such as [29], [32-34].

The acceleration signal, which is recorded from the object, depends on the location of sensor and the activity being performed. In general, the magnitude of acceleration signal increase from the head to ankle. Vertical accelerations produced during level walking range from -2.9 m/s^2 to 7.8 m/s^2 at the lower back, to 16.7 m/s^2 to 32.4 m/s^2 at the tibia [51]. What is an appropriate position for a single tri-axial accelerometer to detect the kind of activities? This is an open question and some of the researchers tried to answer that question [52] [53]. Cleland et al. [52] collected the data from

six various locations on the body, (lower back, chest, left wrist, left hip, left thigh, and left foot). SVM is used to determine which position is best to place accelerometers for detecting the activities.

The training dataset affects the classification efficiency; therefore, some of the researchers used offline classification to focus on developing a methodology to extract the appropriate candidates for building the training dataset such as in [54]. Davila et al. proposed a new method to classify human activities (e.g., sit, walk, lie and stand) by using a data-driven architecture which depends on an iterative learning framework. Their suggested solution optimizes the performance of the model by selecting the most appropriate training dataset for non-linear multi-class classification that makes use of an SVM classifier, while also reducing the computational load. They achieved 76.1% when using WAV-F in the pre-processing phase. As well as they tried to improve the accuracy and reached to 81.9% when using band-pass Finite Impulse Response (FIR) with a WAV-F [36]. Table IV displays the activities, Pre-processing and feature extraction techniques, classifier and its accuracy, and devices which are used in the activity recognition for some of offline researches.

IV. TRADITIONAL AND DEEP LEARNING TECHNIQUES

In recent years the intelligent machine techniques is advanced very quickly such as smartphones, smartwatch, and wearable sensors. Those devices can now use applications provided with Artificial Intelligence for predicting human activity, depending on the raw accelerometer sensor signal. The primary goal of HAR is using machine learning models with high accuracy when predicting the human activity. Many traditional learning techniques like Decision Tree, Random Forest, AdaBoost, Support Vector Machine, K-nearest neighbor, Naïve Bayes, etc. achieved good accuracy. However, deep learning is highly used in HAR. After studying a lot of researches we found that there are three different strategies for building machine learning model as shown in Fig. 4.

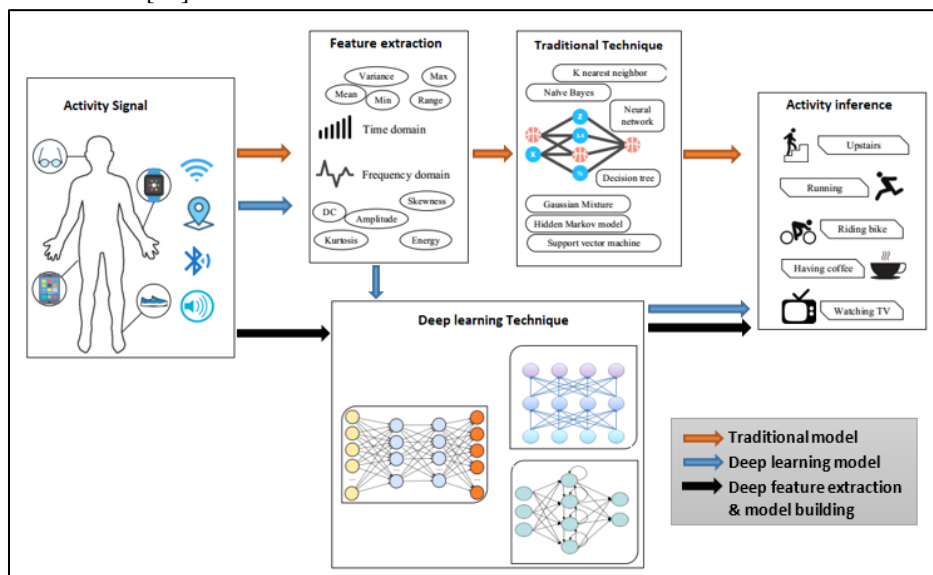


Fig. 4. General Structure of Traditional and Deep Learning Models.

- **Traditional model flow:** The data is collected by the sensors, extracting the features, then using one of traditional techniques, and finally extract the activity label.
- **Deep learning model flow:** Collecting the data, extracting the features, then using one of deep learning technique, and finally extract the activity label such as in [32] [34] [49]
- **Deep feature extraction and model building flow:** Collecting the data, then deep learning technique for automatic extracting features, and finally using softmax layer such as in [35] [37-39] [45] to predict the label of activity.

Arifoglu et al. [86] compared three variants of Recurrent Neural Networks, Which is one of deep learning algorithm, With 5 traditional techniques, SVMs, Naïve Bayes, HMMs, Hidden Semi-Markov Models, and Conditional Random Fields (CRFs), on public dataset collected by van et al. [87]. The data capture daily-life activities such as sleeping, cooking, leaving home, etc. using sensors placed at the homes in less than a month. The results obtained indicate that deep learning is competitive with those traditional methods.

By investigating 48 different research, it is found 56.25% of researches focused on using traditional algorithms for classification, some of those researches adapting the traditional algorithm for achieving high accuracy, 33.33% using deep learning, and 10.4% using algorithms (deep learning or/and traditional) for examining their proposed system but they didn't focus on the algorithm such as in [33][26]. Maekawa et al. [33] compared two traditional algorithms, AdaBoost and DT, for examining the efficiency of classifier when collecting the data from heterogeneous sensors. Hayashi et al. as well as Hammerla et al. [41] proposed a new method that called the empirical cumulative distribution function (ECDF) to representing sensor data for improving the efficiency of feature extraction phase. Ayu et al. [26] proposed a system for real-time activity recognition and compared two traditional classifiers (NB and KNN) for exploring the influence of training data size on recognition accuracy. Nhac et al. [28] comparing four traditional classifiers (RF, NB, KNN, SVM) for examining their proposed Mobile Online Activity Recognition System (MOARS) to automatically recognize several activities of smartphone users. Kwapisz et al. [23] focused on developing a public dataset that is collected with the smartphone for human activity recognition. DT, MLP, and Logistic Regression are compared for testing the quality of their collected dataset. The average accuracy of all traditional algorithms, which are listed in Table III and Table IV, is

displayed in Fig. 5 as well as the frequency of applying each algorithm. The algorithm frequency means the number of using algorithm.

The most frequently traditional classifier that is used in those studies is KNN as illustrated in Fig. 5. KNN may be used more frequently for classifying the researcher's proposed system or just for comparing with the main classifier. However, the frequency (the number of papers that used KNN classifier) of applying KNN reached 90.1%, its average accuracy is 75.48%. QDA and SR achieved high average accuracy, 95% and 96.1% respectively, in spite of the number of papers that used them are small. Some of researchers developed a new classifier based on combining different traditional classification algorithms such as in [27] [60] [75] and that is called "Hybrid T". Neural networks are a powerful biologically-inspired programming paradigm which enables a computer to learn from observational data and Deep learning, a powerful set of techniques for learning in neural networks. Neural network (NN) achieved accepted average accuracy 93.23% as shown in Fig. 5.

Deep learning has various architectures such as DBN [37] [65] [69], RNN [43], CNN [38-40] [45] [49] [50] [70], etc. Therefore, Fig. 6 displayed the average accuracy of all kinds of deep learning architectures and its frequency in this study. It is found that the average accuracy of all deep learning architectures are mostly close however the most frequently used is CNN.

According to this study, the overall average accuracy of traditional machine learning algorithms is 83.3%, which is less than the average accuracy of deep learning algorithms that can reach 94.9%, although the number of studies used traditional machine algorithms are more than those used deep learning.

Traditional machine learning algorithms are typically linear, in that they can be represented by only one node that linearly transforms input to output. Previously called artificial neural networks, deep learning uses multiple nodes, organized like the neural networks to model how human brains work. The more nodes and layers in a neural network, the more sophisticated its learning capabilities can become. Although people still use the term "neural networks", today deep learning networks represent how information flows across nodes which are like how information in the human brain flows across neurons. In the recent years, researches tend to use deep machine learning rather than traditional as illustrated in Fig. 7.

According to all studies investigated in this paper, using deep learning appears in the year 2014 till 2018. After 2014 the using deep learning in activity recognition is more than using traditional algorithms up to now.

TABLE IV. OFF-LINE CLASSIFICATION OF HAR

Ref	Activities	Pre-processing	Feature Extraction	classifier	Accuracy	Device	DS
[35]	AMB(5),SELF(2),DLY(5),KIT(1)	-	NNMF	AE	Precision 99.6%	WAS	[46]
[36]	AMB(4)	FIR, WAV-F	PCA, RPY, NAC	SVM	81.9%	12 WAS	[78]
[32]	DLY(6),HOS(1), KIT(1), SELF(1)	MED-F, SPINT	MFCC, RMS, ZCR, MEN, VAR, ENG, ETP, CCO	DNN,SVM DT,GMM, KNN	f-measure 92%,86% 85%,77%,63%	Smartphone	
[42]	AMB(4),KIT(3), HOS(1),EXF(1)	W-SEG	Auto-FE	Hybrid D	F1 score 91%	WAS	[79]
[23]	AMB(4), EXF(1)	W-SEG	AVG,STD,AAD,ARA, TBP, BD	DT, LR, NN	85.1%,75.1%, 91.7%	Smartphone	
[29]	SELF(4),HOS(2),DLY(1)	-	NAM, AVG, MIN, MAX, VAR	SVM	F-measure (91.4%)	Smartphone	
[33]	KIT(7),DLY(1),HOS(1),SELF(1)	-	MEN, ENG, FETP , FF	AdaBoost, DT	Precision 58.1%,75%	WAS in wrist	
[34]	DLY(5),KIT(1),SELF(1)	W-SEG	MEN, VAR, ENG, FENT,CCO	DNN, SVM, DT,GMM, KNN	91.7%,86% 85%,81.5%,62%	Smartphone	[80]
[54]	AMB(4)	WAV-F	PCA , RPY, NAC	SVM	76.1%	13 WAS	[78]
[53]	AMB(3),DLY(3),EXF(2),HOS(2),KIT(1),SELF(1),TRSI(2),TRSP(1)		VAR,ENT,FF	KNN	Precision 70%	6 WAS	
[27]	AMB(5)	LP-F	MEN,TBP, APF, VAPF, RMS, SD, MIN	NN+ SVM, LogitBoost.	91.5%	Smartphone	
[46]	AMB(4), DLY(2), KIT(1)	MED-F	4GR, \$AC	DTW	TN (81.8%)	WAS	
[75]	AMB(5),TRSP(1), EXF(1)	-	MEN,VAR,SKW,KUR,PF P, SPF	Hybrid T	89%	WAS	
[43]	AMB(5)	W-SEG	-	RNN	96.7%	Smartphone	[81]
[44]	AMB(5)	No-F, W-SEG	SAE, DAE , PCA, FFT, STM	SVM	92%	Smartphone	[81]
[76]	AMB(4)	-	AUTO-FE	KNN	65%	12 WAS	
[47]	AMB(7),EXF(4),TRSP		MEN, MAD, SKW, and CCO,CPCO, APF	DBN, DTW, LSM, KNN, SVM	99.3%,83.2%,89.6% %,98.7%,98.8%	5 WAS	[82]
[48]	AMB(6), EXF(1)	W-SEG	MEN, VAR, CCO, ENT, ZCR,FOD,MOI, EGV	SPR,NB, KNN,SVM	96.1%,89.4%,91.3% %,94.8%	WAS	
[37]	AMB(4), EXF(1)	W-SEG	SPEC	DBN	98.23%	Smartphone	[23]
[45]	AMB(3), EXF(1)	W-SEG		CNN	96.88%	Smartphone	[83]
[50]	AMB(5), EXF(1)	W-SEG	skip feature extraction	CNN	93.8%	Smartphone	
[49]	AMB(4)	LP-F, SMO-F	MEN, VAR	CNN,KNN	85.5%,80%	WAS	[78]
[38]	AMB(5), TRSP(1)	W-SEG	SPEC	CNN	95.1%	Smartphone	[84]
[39]	AMB(5)	W-SEG	DFT	CNN	95.18%	Smartphone	[81]
[77]	AMB(6), EXF(1), DLY(1)	NORM	MEN, VAR, ENT	LSM,SVM, ANN, DT,KNN	95.6%,92.1%,92.9% %,91.9%	WAS	[85]
[40]	AMB(5), TRSP(1)	W-SEG	SPC and SHF	CNN	95.7%	Smartphone	[84]
[41]	AMB(4)	-	ECDF	KNN, DT	F-measure 0.62,0.43	12 WAS	[78]
[52]	AMB(5), TRSI(1)	W-SEG	MEN, AVG, SDs, AVG-SD, SKW, AVG-SKW ,KUR, AVG-KUR, ENG, AVG-ENG, CCO	SVM	96.6%	6 WAS	

TABLE V. LIST OF ABBREVIATIONS AND ACRONYMS

4-Dimensional Features, Gravity (Gx, Gy, Gz, K)	4GR	Hidden Markov Model	HMM	Statistical Metrics	STM
4-Dimensional Features, Body Acceleration (Bx, By, Bz, K)	4AC	Household Activities	HOS	Support Vector Machine	SVM
Ambulation	AMB	Hybrid Deep	Hybrid D	The Norm Of The Axial Components	NAC
Auto-Encoder	AE	Hybrid Traditional	Hybrid T	Time Between Peaks	TBP
Automatic Feature Extraction	Auto-FE	Kinematics Features, Such As Roll, Pitch, Yaw	RPY	Transitional Activities	TRSI
Average	AVG	Kitchen Activities	KIT	Transportation	TRSP
Average Absolute Difference	AAD	K-Nearest Neighbour	KNN	Variance	VAR
Average Energy	AVG-ENG	Kurtosis	KUR	Variance Of APF	VAPF
Average Kurtosis	AVG-KUR	Least Square Method	LSM	Wavelet Filter	WAV-F
Average Of Peak Frequency	APF	Logistic Regression	LR	Window Segmentation	W-SEG
Average Resultant Acceleration	ARA	Low Pass Filter	LP-F	Zero-Crossing Rate	ZCR
Average Skewness	AVG-SKW	Maximum	MAX	Restricted Boltzmann Machine	RBM
Band-Pass Finite Impulse Response	FIR	Mean	MEN	Root Mean Square	RMS
Binned Distribution	BD	Mean Absolute Deviation	MAD	Self-care Activities	SELF
Cepstrum Coefficients	CPCO	Median	MED	Shallow Features	SHF
Convolution Neural Network	CNN	Median Filter	MED-F	Signal Power In Different Frequency Bands	SPF
Correlation Coefficients	CCO	Mel Frequency Cepstral Coefficients	MFCC	Skewness	SKW
Daily Activities	DLY	Minimum	MIN	Smoothing Filter	SMO-F
Decision Tree	DT	Movement Intensity	MOI	Sparse Representation	SPR
Deep Belief Networks	DBN	Naïve Bayes	NB	Spectrogram Representation	SPEC
Discrete Cosine Transform	DCT	Namely	NAM	Spline Interpolation	SPINT
Discrete Fourier Transform	DFT	Neural Network	NN	Standard Deviation	STD
Dynamic Time Wrapper	DTW	Noise Filter	No-F	Frequency Entropy	FETP
Eigenvalues Of Dominant Directions	EGV	Non-Negative Matrix Factorization	NNMF	Average Standard Deviation over 3 axes	AVG-SD
Energy	ENG	Normalization	NORM	Wearable Accelerometer Sensor	WAS
Entropy	ETP	Power Of The Frequency Peak	PFP	Recurrent Neural Network	RNN
Exercise/Fitness	EXF	Power Spectral Density	PSD	Gaussian Mixture	GMM
Fast Fourier Transform Coefficients	FFTC	Principle Component Analysis	PCA	Random Forest	RF
First-Order Derivative	FOD	Quadratic Discriminant Analysis	QDA	Frequency Features	FF

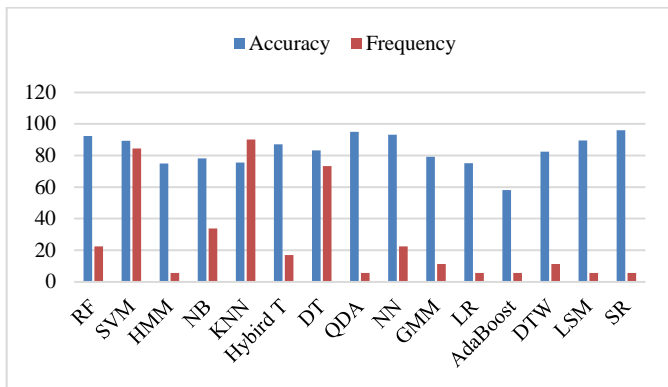


Fig. 5. Traditional Classifiers: Average Accuracy and Frequency Percentage.

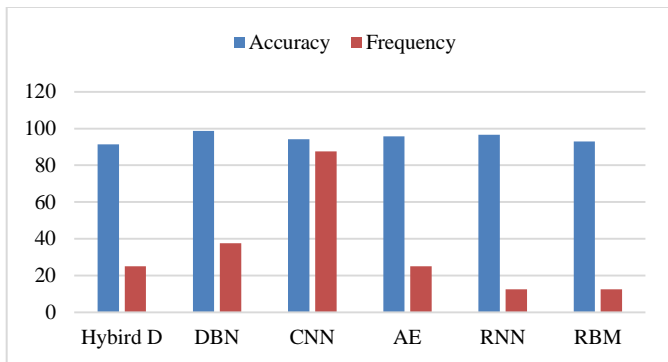


Fig. 6. Deep Learning Models: Average Accuracy and Frequency Percentage.

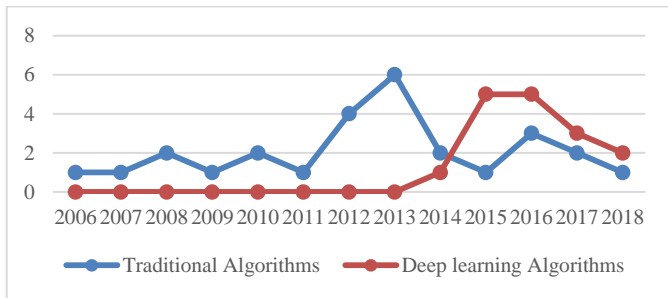


Fig. 7. Traditional and Deep Learning Algorithms used Per Year.

V. ISSUES AND CHALLENGES

Some of various sensors are used to collect the raw data for activities recognition. There are three categories of sensors: video sensors [8-11], environmental-based sensors [3-8], and wearable sensors. Camera is the video sensor which is located in the specific places. RGB camera received less focus in HAR research, probably because of its tradition in scene capture and Human movement in 3D space [88]. As well as identifying the human from the image requires more constraints because the process needs the high machine processing [89]. Therefore, the quality of the real-time HAR system should be affected [90].

The wearable sensor systems should deal with occlusion and restriction challenges that happen in HAR system which uses RGB camera. However, the main drawback of the wearable sensor is the accuracy of recognition. Because the

HAR system, which based on a wearable sensor, needs to the subject for wearing and attaching with several sensors on the different body parts. That is too much of hassle, uncomfortable for the users. As well as VO et al., [91] mentioned that the quality of HAR system, which based on wearable sensors, could not be effective because the subject can forget to use the dedicated sensor.

The location of wearable sensor or smartphone is more sensitive because it effects on the accuracy of the recognition. Reading raw data of accelerometer, which is embedded in the smartphone or wearable sensor, rely on the position and the orientation of the sensor on the subject's body. For example, the moving data reading is totally different when a user walking while holding a phone in his/her hand or pocket. Therefore many of the research faced this issue in their attempt to find the optimal solution [52].

Online HAR systems require continuous sensing and updating the classification model and both of them are energy consuming. Updating the data online may require significant computing resources (e.g., mobile phone memories). In general, various activities have different sampling frequency. There is a trade-off between sampling rate (which affects quality of feature extraction) and the efficiency of recognition. Ustev et al. [92] attempted to reduce both computing energy and resource cost by selecting the optimal sampling frequency and classification features. This enabled him to remove the calculation of time-consuming and frequency-domain features. Online classification system main concern is time consumed on the process as endpoint user is expecting an instant result. As for Offline systems are more concerned with processing power. Offline classification systems depends on the processing power of the setup in hand which - in case of mobile devices - very weak, while in Online systems classification is done on high processing servers that enables quick classification and instant result to the endpoint user.

In traditional machine learning, the features have to be extracted from the raw sensor data by any domain expert to reduce the complexity of the data as well as making the patterns more clearly for learning algorithm. Deep learning try to learn high-level features from the data in an incremental way and that is the major advantage when using deep learning algorithms. Therefore there is no need for domain expertise and hard-core feature extraction. Regarding problem-solving approach, machine learning techniques break the problem into different parts to be solved first then their results are combined at the final stage while deep learning aims to solve the problem end to end. For example, for a multiple object detection problem, Deep Learning techniques like Yolov2 system [93] takes the image as input and provide the location and name of objects at the output. In the other side machine learning algorithms like SVM, a bounding box object detection algorithm is required first to identify all possible objects to have the specific object as input to the learning algorithm in order to recognize relevant objects.

High-end machines are required for applying deep learning and that is the opposite requirements of traditional machine learning algorithms. The important part of executing deep learning is GPU which its algorithms take a long time because

there is a large number of parameter. For example Popular Deep Residual Networks algorithm takes about two weeks to train completely from scratch [94] while the training of traditional Machine Learning algorithms takes few seconds to few hours. In the testing phase, the scenario is completely opposite. Deep learning algorithm takes much less time to run in test time whereas, if you compare it with KNN (a type of traditional machine learning algorithm), testing time is increasing whilst the size of data is increasing. Although this is not applicable to all machine learning algorithms, as some of them have small testing times.

VI. CONCLUSION

This paper surveys the state-of-the-art in human activity recognition based on measured acceleration components. We stated the general structure of activity recognition system online and offline, traditional and deep learning machine learning algorithms. Moreover, those studies focus on recognizing the number of activities and different classification methods used for the recognition process. Forty-eight researches are qualitatively compared in regards to the activities, devices that are used, learning models, dataset, and recognition accuracy. Finally, we discuss the different challenges and issues of these studies. As well as this survey has shown that recently deep learning was used more than traditional machine learning, it also showed that CNN deep learning is mostly used; even though RNN [43] and AE [35] achieved a satisfying accuracy which is higher than 96%.

REFERENCES

- [1] Zhao, K.; Du, J.; Li, C.; Zhang, C.; Liu, H.; Xu, C. Healthy: A Diary System Based on Activity Recognition Using Smartphone. In Proceedings of the 2013 IEEE 10th International Conference on Mobile Ad-Hoc and Sensor Systems (MASS), Hangzhou, China, 14–16 October 2013; pp. 290–294.
- [2] Oscar. D. Lara and M. A. Labrador, "A Survey on Human Activity Recognition using Wearable Sensors," in IEEE Communications Surveys & Tutorials, vol. 15, no. 3, pp. 1192-1209, Third Quarter 2013.
- [3] T. van Kasteren, G. Englebienne, and B. Krse, "An activity monitoring system for elderly care using generative and discriminative models," J. Personal and Ubiquitous Computing, 2010.
- [4] A. Tolstikov, X. Hong, J. Biswas, C. Nugent, L. Chen, and G. Parente, "Comparison of fusion methods based on dst and dbn in human activity recognition," J. Control Theory and Applications, vol. 9, pp. 18–27, 2011.
- [5] J. Yang, J. Lee, and J. Choi, "Activity recognition based on rfid object usage for smart mobile devices," J. Computer Science and Technology, vol. 26, pp. 239–246, 2011.
- [6] J. Sarkar, L. Vinh, Y.-K. Lee, and S. Lee, "Gpars: a general-purpose activity recognition system," Applied Intelligence, pp. 1–18, 2010.
- [7] J. Hong and T. Ohtsuki, "A state classification method based on space time signal processing using svm for wireless monitoring systems," in 2011 IEEE 22nd International Symposium on Personal Indoor and Mobile Radio Communications (PIMRC), pp. 2229–2233, sept. 2011.
- [8] P. Turaga, R. Chellappa, V. Subrahmanian, and O. Udrea, "Machine recognition of human activities: A survey," IEEE Trans. Circuits Syst.Video Technol., vol. 18, no. 11, pp. 1473–1488, 2008.
- [9] J. Candamo, M. Shreve, D. Goldof, D. Sapper, and R. Kasturi, "Understanding transit scenes: A survey on human behavior-recognition algorithms," IEEE Trans. Intell. Transp. Syst., vol. 11, no. 1, pp. 206–224, 2010.
- [10] C. N. Joseph, S. Kokulakumaran, K. Srijevanthar, A. Thusyanthar, C. Gunasekara, and C. Gamage, "A framework for whole-body gesture recognition from video feeds," in International Conference on Industrial and Information Systems (ICIIS), pp. 430–435, 2010.
- [11] M. Ahad, J. Tan, H. Kim, and S. Ishikawa, "Human activity recognition: Various paradigms," in International Conference on Control, Automation and Systems, pp. 1896–1901, 2008.
- [12] O. X. Schmilch, B. Witzschel, M. Cantor, E. Kahl, R. Mehmke, and C. Runge, "Detection of posture and motion by accelerometry: a validation study in ambulatory monitoring," Computers in Human Behavior, vol. 15, no. 5, pp. 571–583, 1999.
- [13] F. Foerster, M. Smeja, and J. Fahrenberg, "Detection of posture and motion by accelerometry: a validation study in ambulatory monitoring," Computers in Human Behavior, vol. 15, no. 5, pp. 571–583, 1999.
- [14] E. Kim, S. Helal, and D. Cook, "Human activity recognition and pattern discovery," IEEE Pervasive Computing, vol. 9, no. 1, pp. 48–53, 2010.
- [15] Jun Yang. 2009. Toward physical activity diary: motion recognition using simple acceleration features with mobile phones. In Proceedings of the 1st international workshop on Interactive multimedia for consumer electronics (IMCE '09). ACM, New York, NY, USA, 1-10.
- [16] E. Munguia Tapia. "Using Machine Learning for Real-time Activity Recognition and Estimation of Energy Expenditure". Ph.D. Thesis, Massachusetts Institute of Technology, 2008.
- [17] S. Reddy, D. Estrin, M. Srivastava. Recruitment Framework for Participatory Sensing Data Collections, in proceedings of the International Conference on Pervasive Computing (Pervasive), May 2010.
- [18] Fahim, M.; Fatima, I.; Lee, S.; Park, Y.T. EFM: Evolutionary fuzzy model for dynamic activities recognition using a smartphone accelerometer. Appl. Intell. 2013, 39, 475–488.
- [19] Shoaib, M.; Scholten, H.; Havinga, P. "Towards Physical Activity Recognition Using Smartphone Sensors.", In Proceedings of the 2013 IEEE 10th International Conference on and 10th International Conference on Autonomic and Trusted Computing (UIC/ATC), Ubiquitous Intelligence and Computing, Vietri sul Mare, Italy, 18–21 December 2013; pp. 80–87.
- [20] Shoaib, M.; Bosch, S.; Incel, O.D.; Scholten, H.; Havinga, P.J. "Fusion of smartphone motion sensors for physical activity recognition". Sensors 2014, 14, 10146–10176.
- [21] Rodriguez, Camilo C., Diego C., William L., Jose V., Nicolas, Julian M., Luis, "IoT system for Human Activity Recognition using BioHarness 3 and Smartphone ", In Proceedings of International Conference on Future Networks and Distributed Systems (ICFNDS), Cambridge, United Kingdom, pp. 40-62, 2017.
- [22] P. Kumari, M. López-Benítez, G. M. Lee, T. S. Kim and A. S. Minhas, "Wearable Internet of Things from human activity tracking to clinical integration," 2017 39th Annual International Conference of the IEEE Engineering in Medicine and Biology Society (EMBC), Seogwipo, 2017, pp. 2361-2364.
- [23] J.R. Kwapisz, G.M. Weiss, and S.A. Moore, "Activity recognition using cell phone accelerometers," ACM SigKDD Explorations Newsletter, vol. 12, no.2, pp.74–82, 2011.
- [24] Y. Liang, X. Zhou, Z. Yu and B. Guo, "Energy-Efficient Motion Related Activity Recognition on Mobile Devices for Pervasive Healthcare", Mobile Networks and Applications, vol. 19, no. 3, pp. 303-317, 2013.
- [25] Bulling, A.; Blanke, U.; Schiele, B. A tutorial on human activity recognition using body-worn inertial sensors. ACM Comput. Surveys (CSUR) 2014, 46, doi:10.1145/2499621.
- [26] M. A. Ayu, S. A. Ismail, T. Mantoro and A. F. A. Matin, "Real-time activity recognition in mobile phones based on its accelerometer data," 2016 International Conference on Informatics and Computing (ICIC), Mataram, 2016, pp. 292-297.
- [27] A. Bayat, M. Pomplun, and D. A. Tran, "A study on human activity recognition using accelerometer data from smartphones," Procedia Computer Science, vol. 34, pp. 450–457, 2014.
- [28] L. Nhac & T. Nguyen & T. Ngo& T. Nguyen& H. Nguyen, "Mobile Online Activity Recognition System Based on Smartphone Sensors". Advances in Information and Communication Technology: Proceedings of the International Conference, ICTA, pp. 357-366, 2017.
- [29] K. Ouchi and M. Doi, "Smartphone-based monitoring system for activities of daily living for elderly people and their relatives etc.," ACM

- Conference on Pervasive and Ubiquitous Computing Adjunct Publication, pp.103–106, ACM, 2013.
- [30] Slim S.O., Atia A., Mostafa MS.M. (2016) An Experimental Comparison Between Seven Classification Algorithms for Activity Recognition. In The 1st International Conference on Advanced Intelligent System and Informatics (AISII2015), November 28-30, 2015, Beni Suef, Egypt. Advances in Intelligent Systems and Computing, vol 407. Springer, Cham.
- [31] S. O Slim, A. Atia and M. Sami M. Mostafa, "DTWDIR: An Enhanced DTW Algorithm for Autistic Child Behaviour Monitoring", International Journal of UbiComp, vol. 7, no. 2, pp. 01-11, 2016.
- [32] T. HAYASHI, M. NISHIDA, N. KITAOKA, T. TODA and K. TAKEDA, "Daily Activity Recognition with Large-Scaled Real-Life Recording Datasets Based on Deep Neural Network Using Multi-Modal Signals", IEICE Transactions on Fundamentals of Electronics, Communications and Computer Sciences, vol. 101, no. 1, pp. 199-210, 2018.
- [33] T. Maekawa, Y. Yanagisawa, Y. Kishino, K. Ishiguro, K. Kamei, Y. Sakurai, and T. Okadome, "Object-based activity recognition with heterogeneous sensors on wrist," International Conference on Pervasive Computing, pp.246–264, Springer, 2010.
- [34] T. Hayashi, M. Nishida, N. Kitaoka, and K. Takeda, "Daily activity recognition based on dnn using environmental sound and acceleration signals," European Signal Processing Conference, pp.2306–2310, IEEE, 2015.
- [35] B. Chikhaoui and F. Gouineau, "Towards Automatic Feature Extraction for Activity Recognition from Wearable Sensors: A Deep Learning Approach," 2017 IEEE International Conference on Data Mining Workshops (ICDMW), New Orleans, LA, 2017, pp. 693-702.
- [36] J. Davila, A. Cretu and M. Zaremba, "Wearable Sensor Data Classification for Human Activity Recognition Based on an Iterative Learning Framework", Sensors, vol. 17, no. 6, p. 1287, 2017.
- [37] Alsheikh, M.A.; Selim, A.; Niyato, D.; Doyle, L.; Lin, S.; Tan, H.-P. Deep Activity Recognition Models with Triaxial Accelerometers. In Proceedings of the AAAI Workshop: Artificial Intelligence Applied to Assistive Technologies and Smart Environments, Phoenix, AZ, USA, 12 February 2016.
- [38] Ravi, D.; Wong, C.; Lo, B.; Yang, G.-Z. "Deep learning for human activity recognition: A resource efficient implementation on low-power devices". In Proceedings of the IEEE 13th International Conference on Wearable and Implantable Body Sensor Networks (BSN), San Francisco, CA, USA, 14–17 June 2016; pp. 71–76.
- [39] Jiang, W. "Human Activity Recognition using Wearable Sensors by Deep Convolutional Neural Networks". In Proceedings of the 23rd ACM International Conference on Multimedia, Brisbane, Australia, 26–30 October 2015; pp. 1307–1310.
- [40] Ravi, D.; Wong, C.; Lo, B.; Yang, G.-Z. A deep learning approach to on-node sensor data analytics for mobile or wearable devices. IEEE J. Biomed. Health Inform. 2017, 21, 56–64.
- [41] Hammerla, N.; Kirkham, R. On Preserving Statistical Characteristics of Accelerometry Data using their Empirical Cumulative Distribution. In Proceedings of the 2013 International Symposium on Wearable Computers, Zurich, Switzerland, 9–12 September 2013; pp. 65–68.
- [42] F. J. Ordez and D. Roggen, "Deep convolutional and lstm recurrent neural networks for multimodal wearable activity recognition," Sensors, vol. 16, no. 1, 2016.
- [43] A. Murad and J. Pyun, "Deep Recurrent Neural Networks for Human Activity Recognition", Sensors, vol. 17, no. 11, p. 2556, 2017.
- [44] Y. Li, D. Shi, B. Ding, and D. Liu, Unsupervised Feature Learning for Human Activity Recognition Using Smartphone Sensors. Springer International Publishing, 2014, pp. 99–107.
- [45] Y. Li, D. Shi, B. Ding, and D. Liu, Unsupervised Feature Learning for Human Activity Recognition Using Smartphone Sensors. Springer International Publishing, 2014, pp. 99–107.
- [46] B. Bruno, F. Mastrogiovanni, A. Sgorbissa, T. Vernazza, and R. Zaccaria, "Analysis of human behavior recognition algorithms based on acceleration data," in Robotics and Automation (ICRA), 2013 IEEE International Conference on, 2013, pp. 1602–1607.
- [47] L. Wang, "Recognition of human activities using continuous auto-encoders with wearable sensors," Sensors, vol. 16, no. 2, 2016.
- [48] M. Zhang and A. A. Sawchuk, "Human daily activity recognition with sparse representation using wearable sensors," IEEE Journal of Biomedical and Health Informatics, vol. 17, no. 3, pp. 553–560, 2013.
- [49] Yang, J.B.; Nguyen, M.N.; San, P.P.; Li, X.L.; Krishnaswamy, S. "Deep convolutional neural networks on multichannel time series for human activity recognition". In Proceedings of the 24th International Joint Conference on Artificial Intelligence (IJCAI), Buenos Aires, Argentina, 25–31 July 2015.
- [50] Chen, Y.; Xue, Y. A Deep Learning Approach to Human Activity Recognition Based on Single Accelerometer. In Proceedings of the IEEE International Conference on Systems, Man, and Cybernetics, Hong Kong, China, 20 June 2015; pp. 1488–1492.
- [51] athie, M.J.; Coster, A.C.F.; Lovell, N.H.; Celler, B.G. Accelerometry: Providing an integrated, practical method for long-term, ambulatory monitoring of human movement. Physiol. Meas. 2004, 25, R1–R20.
- [52] Cleland, I.; Kikhia, B.; Nugent, C.; Boytsov, A.; Hallberg, J.; Synnes, K.; McClean, S.; Finlay, D. Optimal Placement of Accelerometers for the Detection of Everyday Activities. Sensors 2013, 13, 9183–9200.
- [53] L. Atallah, B. Lo, R. King, and G. Z. Yang, "Sensor placement for activity detection using wearable accelerometers," in Body Sensor Networks (BSN), 2010 International Conference on, 2010, pp. 24–29.
- [54] Davila, J.; Cretu, A.-M.; Zaremba, M. Iterative Learning for Human Activity Recognition from Wearable Sensor Data. In Proceedings of the 3rd International Electronic Conference on Sensors and Applications, Barcelona, Spain, 15–30 November 2016.
- [55] M. Saeed, J. Pietilä, and I. Korhonen. "An Activity Recognition Framework Deploying the Random Forest Classifier and A Single Optical Heart Rate Monitoring and Triaxial Accelerometer Wrist-Band." Sensors (Basel, Switzerland), 18(2), 2018.
- [56] Manini A., Intille S.S., Rosenberger M., Sabatini A.M., Haskell W. "Activity recognition using a single accelerometer placed at the wrist or ankle", Med Sci Sports Exerc; 45(11), pp. 2193–2203, 2013.
- [57] R. Nabieci, M. Najafian, M. Parekh, P. Jančovič and M. Russell, "Delay reduction in real-time recognition of human activity for stroke rehabilitation," 2016 First International Workshop on Sensing, Processing and Learning for Intelligent Machines (SPLINE), Aalborg, pp. 1-5, 2016.
- [58] Saponas T, Lester J, Froehlich J, Fogarty J, and Landay J. "iLearn on the iPhone: Real-time human activity classification on commodity mobile phones", University of Washington CSE Tech Report UW-CSE, 2008.
- [59] Kose, Mustafa.; Incel, O.D.; Ersoy, C. Online Human Activity Recognition on Smart Phones. In Proceedings of the Workshop on Mobile Sensing: From Smartphones and Wearables to Big Data, Beijing, China, 16 April 2012; pp. 11–15.
- [60] L. Wang, T. Gu, H. Chen, X. Tao and J. Lu, "Real-Time Activity Recognition in Wireless Body Sensor Networks: From Simple Gestures to Complex Activities," 2010 IEEE 16th International Conference on Embedded and Real-Time Computing Systems and Applications, Macau SAR, pp. 43-52. 2010.
- [61] E. M. Tapia et al., "Real-Time Recognition of Physical Activities and Their Intensities Using Wireless Accelerometers and a Heart Rate Monitor," 2007 11th IEEE International Symposium on Wearable Computers, Boston, MA, pp. 37-40, 2007.
- [62] Brezmes, T., Gorricho, J.L., and Cotrina, J. Activity Recognition from accelerometer data on mobile phones. In IWANN '09: Proceedings of the 10th International WorkConference on Artificial Neural Networks, 796-799, 2009.
- [63] P. Siirtola, J. Röning. "Recognizing Human Activities User-independently on Smartphones Based on Accelerometer Data". International Journal of Interactive Multimedia and Artificial Intelligence. No(1), pp.38-45, 2012.
- [64] M. Shoaib, O. D. Incel, H. Scolten and P. Havinga, "Resource consumption analysis of online activity recognition on mobile phones and smartwatches," 2017 IEEE 36th International Performance Computing and Communications Conference (IPCCC), San Diego, CA, 2017, pp. 1-6.

- [65] L. Zhang, X. Wu and D. Luo, "Real-Time Activity Recognition on Smartphones Using Deep Neural Networks," 2015 IEEE 12th Intl Conf on Ubiquitous Intelligence and Computing and 2015 IEEE 12th Intl Conf on Autonomic and Trusted Computing and 2015 IEEE 15th Intl Conf on Scalable Computing and Communications and Its Associated Workshops (UIC-ATC-ScalCom), Beijing, pp. 1236-1242, 2015.
- [66] Lara, O.; Labrador, M. A mobile platform for real-time human activity recognition. In Proceedings of the 2012 IEEE Consumer Communications and Networking Conference, Las Vegas, NV, USA, 14–17 January 2012, pp. 667–671.
- [67] Siirtola, P.; Roning, J. Ready-to-use activity recognition for smartphones. In Proceedings of the 2013 IEEE Symposium on Computational Intelligence and Data Mining (CIDM), Singapore, 16–19 April 2013; pp. 59–64.
- [68] Schindhelm, C. Activity recognition and step detection with smartphones: Towards terminal based indoor positioning system. In Proceedings of the 2012 IEEE 23rd International Symposium on Personal Indoor and Mobile Radio Communications (PIMRC), Sydney, Australia, 9–12 September 2012; pp. 2454–2459.
- [69] S. Bhattacharya and N. D. Lane, "From smart to deep: Robust activity recognition on smartwatches using deep learning," in IEEE International Conference on Pervasive Computing and Communication Workshops (PerCom Workshops). IEEE, 2016, pp. 1–6.
- [70] I. Andrey, "Real-time human activity recognition from accelerometer data using Convolutional Neural Networks". Applied Soft Computing, Vol. 62, 2018, pp. 915-922
- [71] D. M. Karantonis, M. R. Narayanan, M. Mathie, N. H. Lovel, and B. G. Celler, "Implementation of a real-time human movement classifier using a triaxial accelerometer for ambulatory monitoring," Information Technology in Biomedicine, IEEE Transactions on, vol. 10, no. 1, pp. 156–167, 2006.
- [72] M. Shoaib, H. Scholten, P. J. Havinga, and O. D. Incel, "A hierarchical lazy smoking detection algorithm using smartwatch sensors," in IEEE 18th International Conference on e-Health Networking, Applications and Services (Healthcom), IEEE, 2016, pp. 1–6.
- [73] A. Stisen, et al. Smart Devices Are Different: Assessing And Mitigating Mobile Sensing Heterogeneities For Activity Recognition. SenSys '15.
- [74] Human activity recognition using smartphones data set. <https://archive.ics.uci.edu/ml/machine-learning-databases/00240>, (Accessed on Oct 2018).
- [75] M. Ermes, J. Parkka, J. Mantyjarvi, and I. Korhonen, "Detection of daily activities and sports with wearable sensors in controlled and uncontrolled conditions," Information Technology in Biomedicine, IEEE Transactions on, vol. 12, no. 1, pp. 20–26, 2008.
- [76] T. Pfotz, N. Y. Hammerla, and P. Olivier, "Feature learning for activity recognition in ubiquitous computing," in Proceedings of the Twenty-Second International Joint Conference on Artificial Intelligence – Volume Volume Two, ser. IJCAI'11, 2011, pp. 1729–1734.
- [77] Zheng, Y. Yuhuang, Human Activity Recognition Based on the Hierarchical Feature Selection and Classification Framework. J. Electr. Comput. Eng. 2015, 2015, 34.
- [78] Activity Recognition Challenge. Available online: <http://opportunity-project.eu/challenge> (accessed on 10 October 2016).
- [79] Roggen, D.; Calatroni, A.; Rossi, M.; Holleczeck, T.; Förster, K.; Tröster, G.; Lukowicz, P.; Bannach, D.; Pirkel, G.; Ferscha, A.; et al. Collecting complex activity data sets in highly rich networked sensor environments. In Proceedings of the 7th IEEE International Conference on Networked Sensing Systems (INSS), Kassel, Germany, 15–18 June 2010; pp. 233–240.
- [80] M. Nishida, N. Kitaoka, and K. Takeda, "Development and preliminary analysis of sensor signal database of continuous daily living activity over the long term," in Proc. APSIPA, 2014.
- [81] Anguita, D.; Ghio, A.; Oneto, L.; Parra, X.; Reyes-Ortiz, J.L. A Public Domain Dataset for Human Activity Recognition Using Smartphones. In Proceedings of the European Symposium on Artificial Neural Networks, Bruges, Belgium, 24–26 April 2013; pp. 24–26.
- [82] Altun, K.; Barshan, B.; Tuncel, O. Comparative study on classifying human activities with miniature inertial and magnetic sensors. Pattern Recognit. 2010, 43, 3605–3620.
- [83] J. W. Lockhart, G. M. Weiss, J. C. Xue, S. T. Gallagher, A. B. Grosner, and T. T. Pulickal. Design considerations for the wisdm smart phone-based sensor mining architecture. In Proceedings of the Fifth International Workshop on Knowledge Discovery from Sensor Data, pages 25–33. ACM, 2011.
- [84] Ravi et al. ActiveMiles: Dataset available on. <http://hamlyn.doc.ic.ac.uk/activemiles/> Access (May 2018)
- [85] M. Zhang and A. A. Sawchuk, "USC-HAD: a daily activity dataset for ubiquitous activity recognition using wearable sensors," in Proceedings of the ACM International Conference on Ubiquitous Computing (UbiComp '12), International Workshop on Situation, Activity and Goal Awareness, Pittsburgh, Pa, USA, September 2012.
- [86] Arifoglu, D. and Bouchachia, A. "Activity Recognition and Abnormal Behaviour Detection with Recurrent Neural Networks". Procedia Computer Science, 110, pp.86-93, (2017).
- [87] T. Van Kasteren, G. Englebienne, and B. J. A. Kröse. "Human activity recognition from wireless sensor network data", Benchmark and software. Activity Recognition in Pervasive Intelligent Environments, pages 165–186, 2011.
- [88] L. Xia, C. Chen, and J. K. Aggarwal, "View invariant human action recognition using histograms of 3D joints," in 2012 IEEE Computer Society Conference on Computer Vision and Pattern Recognition Workshops, 2012, pp. 20–27.
- [89] A. T. Nghiem, E. Auvinet, and J. Meunier, "Head detection using Kinect camera and its application to fall detection," in 2012 11th International Conference on Information Science Signal Processing and their Applications (ISSPA), 2012, pp. 164–169.
- [90] M. Javan Roshtkhari and M. D. Levine, "Human activity recognition in videos using a single example," Image Vis. Comput., vol. 31, no. 11, pp. 864–876, Nov. 2013.
- [91] Q. V. Vo, G. Lee, and D. Choi, "Fall Detection Based on Movement and Smart Phone Technology," in 2012 IEEE RIVF International Conference on Computing & Communication Technologies, Research, Innovation, and Vision for the Future, 2012, pp. 1–4.
- [92] Y. E. Ustev, O. Durmaz Incel, and C. Ersoy, User, device and orientation independent human activity recognition on mobile phones: Challenges and a proposal, in Proc. 13th Int. Pervasive and Ubiquitous Computing Adjunct Publication Conf., Zurich, Switzerland, 2013, pp. 1427- 1436.
- [93] Redmon, J., Farhadi, A.: Yolo9000: Better, faster, stronger. In: Computer Vision and Pattern Recognition (CVPR), 2017 IEEE Conference on, IEEE (2017) 6517– 6525.
- [94] Kaiming He, Xiangyu Zhang, Shaoqing Ren, & Jian Sun. "Identity Mappings in Deep Residual Networks". arXiv 2016.
- [95] Anguita, D.; Ghio, A.; Oneto, L.; Parra, X.; Reyes-Ortiz, J.L. Energy Efficient Smartphone-Based Activity Recognition using Fixed-Point Arithmetic. J. UCS 2013, 19, 1295–1314.
- [96] Frank, J.; Mannor, S.; Precup, D. Activity Recognition with Mobile Phones. Lect. Notes Comput. Sci. 2011, 6913, 630–633.
- [97] Ouchi, K.; Doi, M. Indoor-outdoor Activity Recognition by a Smartphone. In Proceedings of the 2012 ACM Conference on Ubiquitous Computing, Pittsburgh, PA, USA, 5–8 September 2012; pp. 600–601.
- [98] Stewart, V.; Ferguson, S.; Peng, J.X.; Rafferty, K. Practical automated activity recognition using standard smartphones. In Proceedings of the IEEE International Conference on Pervasive Computing and Communications Workshops, Los Alamitos, CA, USA, 19–23 March 2012; pp. 229–234.
- [99] Gomes, J.; Krishnaswamy, S.; Gaber, M.; Sousa, P.; Menasalvas, E. MARS: A Personalised Mobile Activity Recognition System. In Proceedings of the 2012 IEEE 13th International Conference on Mobile Data Management (MDM), Bengaluru, Karnataka, 23–26 July 2012; pp. 316–319.
- [100] Lane, N.D.; Mohammad, M.; Lin, M.; Yang, X.; Lu, H.; Ali, S.; Doryab, A.; Berke, E.; Choudhury, T.; Campbell, A. Bewell: A smartphone application to monitor, model and promote wellbeing. In Proceedings of the 5th International ICST Conference on Pervasive Computing Technologies for Healthcare, Dublin, Ireland, 23–26 May 2011; pp. 23–26.

- [101] Reddy, S.; Mun, M.; Burke, J.; Estrin, D.; Hansen, M.; Srivastava, M. Using Mobile Phones to Determine Transportation Modes. *ACM Trans. Sens. Netw. (TOSN)* 2010, 6, 1–27.
- [102] Anjum, A.; Ilyas, M. Activity recognition using smartphone sensors. In *Proceedings of the 2013 IEEE Consumer Communications and Networking Conference, Las Vegas, NV, USA, 11–14 January 2013*; pp. 914–919.
- [103] Liang, Y.; Zhou, X.; Yu, Z.; Guo, B.; Yang, Y. Energy Efficient Activity Recognition Based on Low Resolution Accelerometer in Smart Phones. *Lect. Notes Comput. Sci.* 2012, 7296, 122–136.
- [104] Lu, H.; Yang, J.; Liu, Z.; Lane, N.D.; Choudhury, T.; Campbell, A.T. The Jigsaw Continuous Sensing Engine for Mobile Phone Applications. In *Proceedings of the 8th ACM Conference on Embedded Networked Sensor Systems, Zurich, Switzerland, 3–5 November 2010*; pp. 71–84.
- [105] Martin, H.; Bernardos, A.M.; Iglesias, J.; Casar, J.R. Activity logging using lightweight classification techniques in mobile devices. *Pers. Ubiquitous Comput.* 2013, 17, 675–695.
- [106] Miluzzo, E.; Lane, N.D.; Fodor, K.; Peterson, R.; Lu, H.; Musolesi, M.; Eisenman, S.B.; Zheng, X.; Campbell, A.T. Sensing Meets Mobile Social Networks: The Design, Implementation and Evaluation of the CenceMe Application. In *Proceedings of the 6th ACM Conference on Embedded Network Sensor Systems, Raleigh, NC, USA, 4–7 November 2008*; pp. 337–350.
- [107] Ryder, J.; Longstaff, B.; Reddy, S.; Estrin, D. Ambulation: A Tool for Monitoring Mobility Patterns over Time Using Mobile Phones. In *Proceedings of the International Conference on Computational Science and Engineering, Vancouver, BC, Canada, 29–31 August 2009*; Volume 4, pp. 927–931.
- [108] Wang, Y.; Lin, J.; Annavaram, M.; Jacobson, Q.A.; Hong, J.; Krishnamachari, B.; Sadeh, N. A Framework of Energy Efficient Mobile Sensing for Automatic User State Recognition. In *Proceedings of the 7th International Conference on Mobile Systems, Applications, and Services, Krakow, Poland, 22–25 June 2009*; pp. 179–192.
- [109] Yan, Z.; Subbaraju, V.; Chakraborty, D.; Misra, A.; Aberer, K. Energy-Efficient Continuous Activity Recognition on Mobile Phones: An Activity-Adaptive Approach. In *Proceedings of the 2012 16th International Symposium on Wearable Computers (ISWC), Newcastle, Australia, 18–22 June 2012*; pp. 17–24.
- [110] Khan, A.M.; Tufail, A.; Khattak, A.M.; Laine, T.H. Activity Recognition on Smartphones via Sensor-Fusion and KDA-Based SVMs. *Int. J. Distrib. Sens. Netw.* 2014, 2014, 1–14.
- [111] Kim, T.S.; Cho, J.H.; Kim, J.T. Mobile Motion Sensor-Based Human Activity Recognition and Energy Expenditure Estimation in Building Environments. *Smart Innov. Syst. Technol.* 2013, 22, 987–993.
- [112] Das, S.; Green, L.; Perez, B.; Murphy, M.; Perring, A. Detecting User Activities Using the Accelerometer on Android Smartphones; Technical Report; Carnegie Mellon University: Pittsburgh, PA, USA, 2010.
- [113] Siirtola, P. Recognizing Human Activities User-independently on Smartphones Based on Accelerometer Data. *Int. J. Interact. Multimed. Artif. Intell.* 2012, 1, 38–45.
- [114] Thiemjarus, S.; Henpraserttae, A.; Marukat, S. A study on instance-based learning with reduced training prototypes for device-context-independent activity recognition on a mobile phone. In *Proceedings of the 2013 IEEE International Conference on Body Sensor Networks (BSN), Cambridge, MA, USA, 6–9 May 2013*; pp. 1–6.
- [115] Das, B.; Seelye, A.; Thomas, B.; Cook, D.; Holder, L.; Schmitter-Edgecombe, M. Using smart phones for context-aware prompting in smart environments. In *Proceedings of the 2012 IEEE Consumer Communications and Networking Conference (CCNC), Las Vegas, NV, USA, 14–17 January 2012*; pp. 399–403.
- [116] Vo, Q.V.; Hoang, M.T.; Choi, D. Personalization in Mobile Activity Recognition System Using K-Medoids Clustering Algorithm. *Int. J. Distrib. Sens. Netw.* 2013, 2013, 1–12.
- [117] Khan, A.M.; Siddiqi, M.H.; Lee, S.W. Exploratory Data Analysis of Acceleration Signals to Select Light-Weight and Accurate Features for Real-Time Activity Recognition on Smartphones. *Sensors* 2013, 13, 13099–13122.
- [118] Guiry, J.J.; van de Ven, P.; Nelson, J. Orientation independent human mobility monitoring with an android smartphone. In *Proceedings of the IASTED International Conference on Assistive Technologies, Innsbruck, Austria, 15–17 February 2012*; pp. 800–808.
- [119] Berchtold, M.; Budde, M.; Gordon, D.; Schmidtke, H.; Beigl, M. ActiServ: Activity Recognition Service for mobile phones. In *Proceedings of the 2010 International Symposium on Wearable Computers (ISWC), Seoul, Korea, 10–13 October 2010*; pp. 1–8.

A Systematic Review of Domains, Techniques, Delivery Modes and Validation Methods for Intelligent Tutoring Systems

Aized Amin Soofi¹, Moiz Uddin Ahmed²
Department of Computer Science
Allama Iqbal Open University, Islamabad, Pakistan

Abstract—An Intelligent Tutoring System (ITS) is a computer software that help students in learning educational or academics concepts in customized environment. ITSs are instructional systems that have capability to facilitate user by providing instantaneous feedback and instructions without any human intervention. The advancement of new technologies has integrated computer based learning with artificial intelligence methods with aim to develop better custom-made education systems that referred as ITS. One of the important factors that affect students learning process is self-learning; all students cannot have similar experience of learning scholastic concepts from same educational material. Because students have individual differences that make some topics difficult or easy to understand regarding taken subjects. These systems have capability to improve teaching and learning process in different educational domains while respecting individual learning needs. In this study an attempt is made to review the research in field of ITSs and highlight the educational areas or domains in which ITSs have been introduced. Techniques, delivering modes and evaluation methodologies that have been used in developed ITSs have also been discussed in this work. This work will be helpful for both academia and new comers in the field of ITSs to further strengthen basis of tutoring systems in educational domains.

Keywords—ITS; intelligent tutoring system; intelligent learning; adaptive learning; intelligent tutoring; ITS review

I. INTRODUCTION

Information and communication technologies (ICT) have become necessary part of educational system in order to replace traditional teaching system with modern teaching system [1]. Modern information resources like hypermedia, multimedia, internet and intranet are contributed together to provide advanced learning pedagogies [2-4]. The new educational model is learner centered model in which flexibility is provided to learner to learn according to their ability and requirements in simple words this new model is oriented toward learner or student [5, 6]. To increase efficiency of these learning model factors like adaptability, interactivity, intelligence and dynamically generated web contents are added to these models that leads them towards development of intelligent tutoring system (ITS).

Many factors have been highlighted in previous studies that reflect importance of ITSs in educational domain, such as time limitations and individual meeting with students make it

difficult for teacher for provide feedback to individual student in large class [7]. In private tutoring system, usually tutor provide help to student as much as he/she can but providing as many tutors to facilitate number of students is not feasible option from economic point of view [8]. ITSs are a solution that can solve these kind of problems in education. The most important feature of ITSs is their ability to customize instructional strategies and activities according to learner's requirements and characteristics [9, 10]. Many researchers contribute their efforts for refining student's ability to solve different problems in education [11-14]. The first ITS named SCHOLAR tutor was introduced in 1970 [15]. This system was developed to review student's knowledge about South America geography. SCHOLAR tutor began two way interaction with students by using facts of knowledge and semantic network of concepts to appraise student's knowledge in geography [16].

The traditional ITSs consist of four main modules i.e. expert module, student or learner module, pedagogical or tutor module and user interface module [17]. The expert module deals with domain knowledge that learner or student wants to learn [18]. The methods for problem solving and evaluating students activities in learning process are also considered in this module [19]. The student module completely depends on student attributes such as learning style, activities, behavior and knowledge deficiency. All relevant information about student is gathered and updated in system to refine learning process [20]. Additional information such as past learning experiences and learning preferences may also be stored in system to provide adaptability in teaching process [10].

The pedagogical module identifies students deficiencies in specific topic or subject based on learner module and focus on the strategies to provide best material that overcome the deficiencies of student in specific area or subject or topic [21]. The user interface module is communication part of the ITS it provides interaction facility between system and user [22]. The aim of present study is to review the developed ITSs across educational fields and gather comprehensive information about their development techniques, purpose, delivery modes and evaluation methods. This paper is organized as following; in section II methodology of review is presented, results are presented in section III. The answers of posed questions are discussed in sub sections of section III and work is concluded in section IV.

II. METHODOLOGY

One of the most common ways to evaluate and understand all available research literature related to specific research problem or question is systematic literature review. In literature, numbers of methodologies are available for systematic review. The methodology adopted for this systematic literature review was based on guidelines presented in [23]. The review process consists of three phases which contain ten sub activities. The details of activities conducted in these phases are shown in Fig. 1 and discussed under.

In first phase of review the following questions were posed:

Q1: What are the subjects or domains for which ITSs have been designed?

Q2: What types of techniques or tools have been used in development of ITSs?

Q3: What type of delivery modes have been used by developed ITSs?

Q4: How the techniques have been validated?

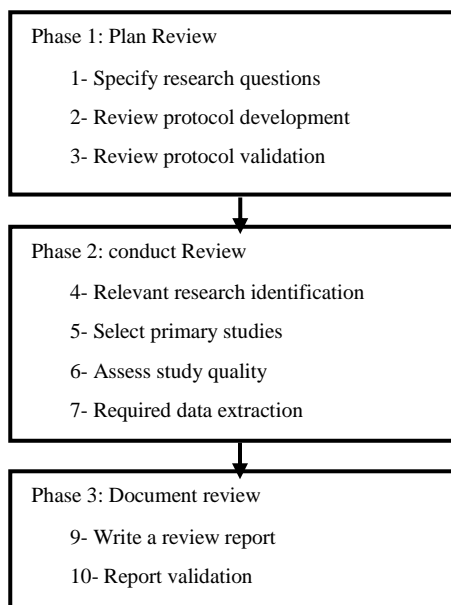


Fig. 1. Review Process Adapted from [23].

TABLE I. REVIEW PROTOCOL

Year	Sources	Keywords
2014-2018	IEEE Xplore, science direct, google scholar, ACM portal digital library, springer	ITS, intelligent tutoring system, intelligent learning, adaptive learning, intelligent tutoring, ITS review

The questions were formulated in order to complete first sub activity of phase 1. In second sub activity of phase 1 a review protocol was developed. The review protocol includes considered time span of published papers, publication sources and keyword used to find required data. The research focus on the articles published in last five years and repositories used to

find out required data include IEEE xplorer, science direct, ACM, Google scholar, springer and web of science. The final review protocol is given in Table I. The developed protocol is reviewed and validated after making some necessarily changes by researchers.

The execution of search chain on selected sources provides us a set of 82 articles. These articles were screened on basis of their title and abstract. After initial review according to inclusion criteria these 82 articles were filtered and only 39 articles were left that meet our inclusion criteria. For strengthen the search related to relevant articles, backward snowballing guidelines presented in [24] was also adopted to find out cited papers in selected articles that meet our inclusion criteria; this was done to make sure that no articles related to our research questions were left to considered.

In second phase of review a literature search was conducted in pre-defined databases by using keywords mention in Table I. These keywords were used in combination and alone for initial collection of research material related to our specified research questions. The inclusion criteria of this study is strictly based on posed research questions. Only those articles that contain material related to our research question were considered in this review.

III. RESULTS

The results of review are presented in this section. A year wise representation of results is given in Table II. These results are characterized with research questions posed earlier in this study. The variables of selected studies are presented in Table III.

A. What are the Subject/Domains for which ITSs have been Designed?

The result of review Table IV shows educational domains for which ITS have been designed. The frequency of each educational field in selected papers is demonstrated in Fig. 2. These domains were divided into six basic categories include; computer science, health/ medical science, mathematics, physics, language and others. Computer science was leading field in which ITS have been widely used to provide help in learning process. In computer science, programming was major area in which these systems were used. The frequency of systems that were designed for programming purposes in computer science domain was 61.11 %. Majority of the users of these systems were university level students.

TABLE II. YEAR WISE SEARCH RESULTS

year	No. of papers
2014	7
2015	8
2016	6
2017	8
2018	10
Total	39

TABLE III. VARIABLES OF SELECTED PAPERS

Publication year	Title	domain	purpose	Technique/tools	Delivery mode	Validation
2018	[8]	computer science	Problem solving in computer programming	Bayesian network & multi agent system	Web based	Experimental study (comparison between groups)
2018	[25]	mathematics	Personalization algebra teaching	Cognitive Tutor Algebra (CTA), Rule based	Computer based (proprietary) application software	Experimental study
2018	[14]	mathematics	Modeling mathematics learning	ALEKS (Assessment and Learning in Knowledge Spaces)	Web based	Observation study
2018	[26]	Others	Find metacognitive prompt in ITS	iSTART (Interactive Strategy Training for Active Reading and Thinking) , NLP	Web based	Experimental study (pretest and posttest)
2018	[27]	computer science	teaching programming	Bayesian Network	web based	Experimental study
2018	[28]	Computer science	Enhancing object oriented programming	Naive Bayes algorithm	Software prototyping	Simulated student model (prototype testing)
2018	[29]	Computer science	teaching programming language	ITSB tool (Delphi IDE)	Computer based application software	User feedback
2018	[30]	Computer science	Android application development	Rule based reasoning	Web based	Experimental study
2018	[31]	medical	Learning platform for Autism Spectrum Disorder childs	Chatbot using machine learning techniques (Convolution Neural Network)	Theoretical Framework	No validation
2018	[32]	Computer science	Solving multimedia problems	MyST (my science tutor), Intelligent multi agents	Web based	Experimental study
2017	[33]	Computer science	Self-learning in computer engineering	Artificial Neural Network based technique & Vortex Optimization Algorithm	Computer based application software	Experimental study & user feedback
2017	[34]	Others	Engineering students assessment	Open learning environment (StuDiAsE), fuzzy rule based system	Web based	Student diagnostic test
2017	[35]	Physics	Teaching basic electronics	Bayesian-based technique (Bayesian knowledge tracing)	Proposed model	No validation
2017	[36]	Computer science	Deductive logic	Bayesian-based & data mining (classification) techniques	Web based	Experimental study (learner performance)
2017	[37]	Computer science	fundamental computer programming	-	Theoretical framework	Experimental study (student response)
2017	[38]	medical	Cardio metabolic risk assessment	Artificial Neural Network	Web based	Experimental (Comparative analysis between two groups)
2017	[39]	mathematics	Provide support in basic mathematics learning	PGBM-COMPS tutor program, Rule based reasoning	Theoretical framework	Experimental (pretest–posttest comparison)
2017	[40]	Computer science	Teaching programming language	ITSB authoring tool (Delphi IDE)	Computer based application software	User feedback

Publication year	Title	domain	purpose	Technique/tools	Delivery mode	Validation
2016	[41]	medical	Cryosurgery prototype	Hybrid modeling approach (rules and constraints)	Computer based application software	Experimental (Comparative analysis between two groups)
2016	[42]	Computer science	Platform to teach MS word and PowerPoint	Type-2 fuzzy rule based reasoning	Web based	Student performance
2016	[43]	mathematics	Mathematical experiment	Bayesian technique	Web based	Experimental study (student performance on different conditions)
2016	[44]	medical	Understanding genetic breast cancer risk	Fuzzy-Trace Theory	Computer based application software (using Auto Tutor)	Experimental study
2016	[45]	Computer science	Problem solving (programming) by game base assessment	Bayesian network & multi agent system	Web based	Experimental study (controlled groups)
2016	[46]	language	Teaching English grammar	ITSB authoring tool (Delphi IDE)	Computer based application software	User feedback
2015	[12]	Computer science	Improve problem solving skills of novice programmer	Intelligent multi agent, Bayesian network and NLP algorithm	Web based	Learner knowledge (pretest and posttest) & performance
2015	[47]	medical	Human circulatory and emotional state	Meta Tutor (Intelligent multi agents)	web based	Correlation between emotional measurement methods
2015	[48]	Others	Multiple domain learning	Intelligent agents	Web based	Experimental study (student performance)
2015	[49]	Computer science	Slide presentation	Feature extraction & clustering, rule based reasoning	Web based	User feedback
2015	[50]	other	Cultural awareness Content delivery	Fuzzy rule based reasoning	prototype	User feedback
2015	[51]	language	Voice conversion in english	rule based reasoning	Web based	Experimental study (group experiment)
2015	[52]	Computer science	Basic computer skill improvement	Intelligent multi agents	Web based	Experimental study (learner knowledge and performance)
2015	[53]	Physics	Physics education	deep ANN & clustering analysis	framework	Comparison study
2014	[19]	Computer science	Debugging help for novice cs students	Case based reasoning	Computer based application software	Student performance (pretest and posttest) & log evaluation
2014	[54]	Physics	Automatic feedback in basic electronic	NLP based technique and rule based reasoning	Web based	User feedback & experiment (student performance)
2014	[55]	mathematics	Instructional method in mathematics	rule based reasoning	Computer based application software	Proto type testing, learner and teacher feedback
2014	[56]	mathematics	Peer tutoring in algebra	Bayesian knowledge tracing & rule based reasoning	Computer based application software	Student feedback & performance (pretest & posttest)

2014	[57]	Computer science	Analyze program in PHP	Bayesian-based technique	Computer based application software	Student feedback & performance (pretest & posttest)
2014	[58]	language	English language	UoLmP (rule based reasoning, if then rule)	Web based	User feedback
2014	[59]	Computer science	Controller programming	Case based reasoning	Computer based application software	Experiment (pretest & posttest)

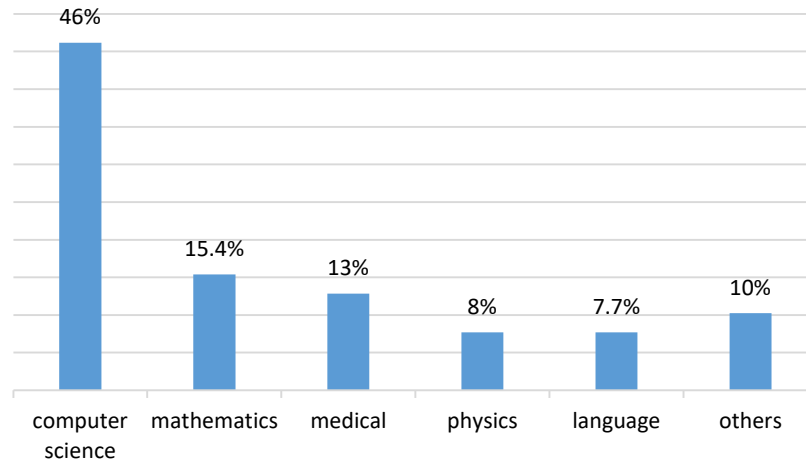


Fig. 2. Frequency of educational field in ITSs.

TABLE IV. CATEGORY WISE RESULTS OF QUESTION 1

Question	Category	No. of papers
What are the subject/ domains for which ITSs have been designed?	Computer Science	18
	medical	5
	mathematics	6
	physics	3
	language	3
	others	4

The second major field in which ITSs were used was mathematics, majority of ITSs (66.66%) were designed for school level students in this field to provide help in basic mathematics. The medical science field is at third rank, in which most of the system provides theoretical help to the students in understanding concepts about different topics, diseases and their management. In physics these systems were designed to provide theoretical concepts about different topics with focus on electronics. In languages domain all found ITSs were designed to teach English language or grammar.

B. What Type of Techniques or Tools have been used in Development of ITSs?

The review results of question 2 are presented in Table V and frequency of techniques used in development of tutoring systems is showed in Fig. 3. The techniques used for designing ITSs are categorized into eight different categories that are listed in Table V. Rule based reasoning technique was leading approach in designed ITSs. Rule based techniques increase trace of system reasoning for specific case with background familiarity [60]. This method was used in 28.21% studies to design ITSs, in computer science domain 66.66%

designed ITSs were based on rule based reasoning out of which most systems were designed for programming purpose. In mathematics domain 50% ITSs used rule based reasoning method for system designing. It seems that rule based method could be a suitable choice for decision making in computer programming fields and mathematics fields to deal with structure, patterns and numbers.

Bayesian technique was second widely used technique is designing of ITSs. These techniques based on probabilistic association between set of variables [61]. Bayesian method was used in 15.38% studies and majority of these studies were related to computer science, mathematics and physics domains. Bayesian technique is good method to deal with problems that deals with uncertainties [62]. In 12.28% studies intelligent agent systems were used in designed ITSs, intelligent agent system used to solve problems that are difficult to solve by an individual [63]. These systems were used for skill improvement, multi domain learning and problem solving in computer programming. In computing field intelligent agent techniques can be used to support its users in process of communication with system [64]. Frequency of data mining and Artificial Neural Network (ANN) techniques was almost similar.

Case based reasoning technique was least used technique in developed ITSs. This technique is usually used to solve new problems by finding most similar problem and updating the existing case according to found model [65]. However this technique was only used in two works that were related to computer programming. Case based reasoning can be beneficial in medical domain for design of tutoring systems [66].

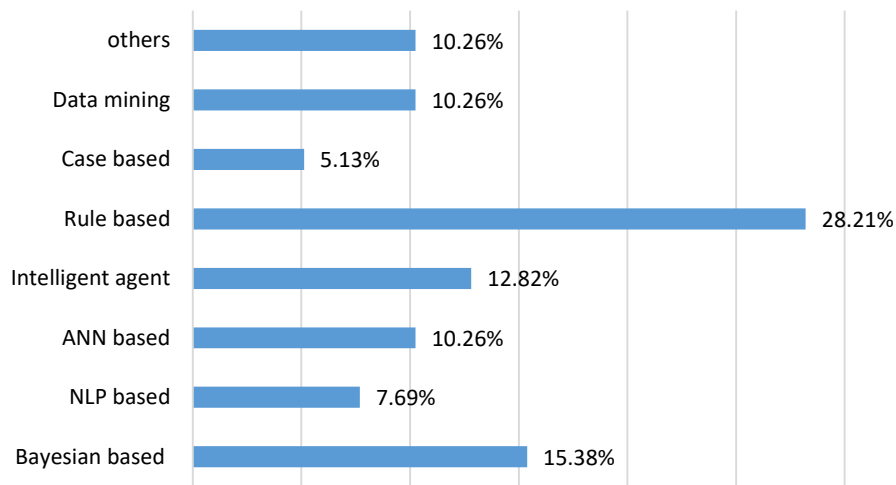


Fig. 3. Frequency of ITSs Development Techniques.

TABLE V. CATEGORY WISE RESULTS OF QUESTION 2

question	Techniques	No. of papers
What type of techniques or tools have been used in development of ITSs?	Bayesian based	6
	NLP based	3
	ANN based	4
	Intelligent agent	5
	Rule based	11
	Case based	2
	Data mining	4
	others	4

TABLE VI. CATEGORY WISE RESULTS OF QUESTION 3

question	Delivery mode	No. of papers
What type of delivery modes have been used by developed ITSs?	Web based systems	20
	computer based application software	12
	prototype	2
	proposed model	1
	framework	4

C. What Type of Delivery Modes has been used by Developed ITSs?

The results of question 3 are presented in Table VI and frequency of ITSs delivery modes is shown in Fig. 4. These results show that web based mode was leading mode in delivering by tutoring systems. 51% of selected papers were relied on web based systems for delivering educational material to learner. In computer science domain 55.55% intelligent tutoring systems were web based. The frequency of web based tutoring systems in mathematics and medical domains were 50% and 45%, respectively.

Computer based application software for intelligent tutoring was used in 30.77% studies. In mathematic domain 50% developed ITSs were computer based application software while frequency of application software in computer science and medical domain were 33.33% and 40%, respectively. In 10.26% studies researchers provides a conceptual or theoretical framework for tutoring systems. While model was proposed in only one study that was related to physics domain. These results reveal the fact that web based and computer application based modes are most popular infrastructure for the development of tutoring systems.

In our selected articles we do not found any ITSs which can provides mobile based content delivery to facilitate learner. However, mobile devices are considered as emerging technologies and its use in society is part of daily routine [67]. These devices can facilitate the implementation of tutoring systems independent of location and time [58].

D. How the Techniques have been Validated?

The results of question 4 are presented in Table VII and percentile results of question 4 are shown in Fig. 5. The method that was used widely for validation of the developed ITSs was experiment (59%). In experimental validation different type of techniques were used out of which 74% experiments were performed on basis of user or learner performance in which pretest and posttest were conducted to evaluate the system. 17% experiments were based on comparative analysis between groups of ITSs users and non-users, while remaining experimental approaches were based on learner knowledge and skills for system validation. Experimental methods were widely used in the field of computer science and medical. The frequency of these methods in computer science and medical were 61.11% and 60%, respectively.

In validation of any ITS, learner plays an important role, learner experience of using system or feedback is one of the most common method that could address the problems related to usability of specific system [68]. In this review we found only 15.38% studies in which systems were evaluated on basis of user feedback. While 10.25% studies use both experimental and feedback methods for system validation. The remaining validation method includes prototype testing, simulation and observation. Only one study in medical science domain was found in which not any kind of validation method was adopted for system evaluation.

TABLE VII. CATEGORY WISE RESULT OF QUESTION 4

Question	Validation method	No. of paper
How the techniques have been validated?	experiment	23
	user feedback	6
	Experiment & user feedback	4
	Prototype testing	3
	simulation	1
	observation	1
	No. evaluation	1

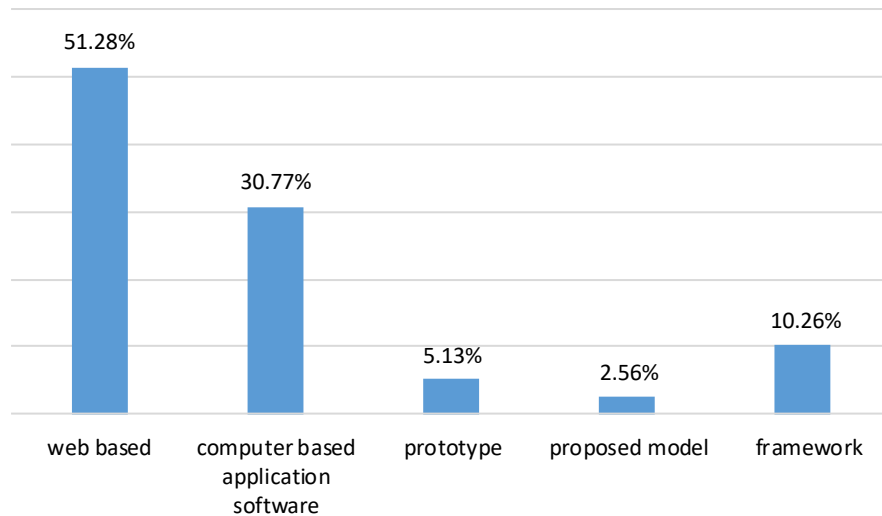


Fig. 4. Frequency of ITSs Delivery Modes.

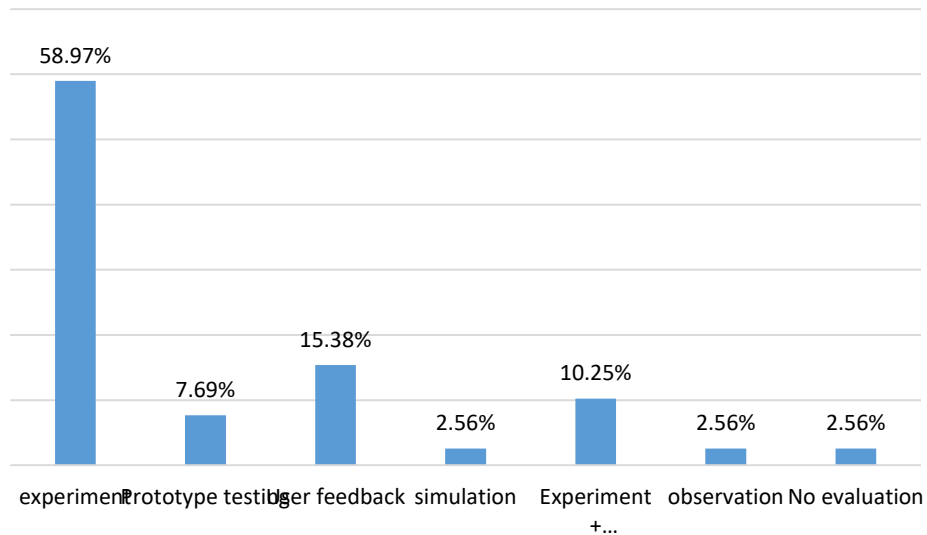


Fig. 5. Methods of Evaluation in ITSs.

IV. CONCLUSIONS

Intelligent Tutoring Systems have capability to replace traditional teaching method with modern adaptive teaching method in which every student get knowledge according to his/her requirement. The main feature of these systems is their ability to customize instructional strategies and activities according to learner's requirements and characteristics. In this study ITSs educational domains, purpose of ITSs in specific domain, technique for ITSs development, delivery modes of ITSs and methods of validating designed ITSs were reviewed. Computer science was a major area in which these systems were used for teaching programming subjects. Rule based and Bayesian techniques were most frequent used techniques in design of ITSs and most of the developed systems provide web based services. In addition, learner performance was major method for validation of designed system. User feedback plays important role in evaluation of any system but we found that user feedback was not considered at high level in these studies for validation of ITSs. As use of mobile devices increase, these devices can facilitate learner in personalized learning in more customized way. We also observe in this study that none of system focus on mobile based tutoring, so on the basis of this study we recommended development of mobile based ITSs.

REFERENCES

- [1] P. DAŠIĆ, J. DAŠIĆ, B. CRVENKOVIĆ, and V. ŠERIFI, "A Review of Intelligent Tutoring Systems in E-Learning," *Ann. Oradea University– Fascicle of Management and Technological Engineering*, vol. 15, pp. 85-90, 2016.
- [2] P. Phobun and J. Vicheanpanya, "Adaptive intelligent tutoring systems for e-learning systems," *Procedia-Social and Behavioral Sciences*, vol. 2, pp. 4064-4069, 2010.
- [3] M. C. Rosatelli and J. A. Self, "A collaborative case study system for distance learning," *International Journal of Artificial Intelligence in Education*, vol. 14, pp. 97-125, 2004.
- [4] J. Zhang, "Intelligent tutoring systems: research status and its development in China," in *Natural Language Processing and Knowledge Engineering, 2005. IEEE NLP-KE'05. Proceedings of 2005 IEEE International Conference on*, 2005, pp. 683-689.
- [5] M. C. Handa, "Learner-centred differentiation model: A new framework," *Australasian Journal of Gifted Education*, vol. 18, p. 55, 2009.
- [6] C. M. Reigeluth, S. Aslan, Z. Chen, P. Dutta, Y. Huh, D. Lee, et al., "Personalized integrated educational system: Technology functions for the learner-centered paradigm of education," *Journal of Educational Computing Research*, vol. 53, pp. 459-496, 2015.
- [7] T. Buchanan, "The efficacy of a World-Wide Web mediated formative assessment," *Journal of Computer Assisted Learning*, vol. 16, pp. 193-200, 2000.
- [8] D. Hooshyar, R. B. Ahmad, M. Yousefi, M. Fathi, S.-J. Horng, and H. Lim, "SITS: a solution-based intelligent tutoring system for students' acquisition of problem-solving skills in computer programming," *Innovations in Education and Teaching International*, vol. 55, pp. 325-335, 2018.
- [9] A. Keleş, R. Ocak, A. Keleş, and A. Gülcü, "ZOSMAT: Web-based intelligent tutoring system for teaching-learning process," *Expert Systems with Applications*, vol. 36, pp. 1229-1239, 2009.
- [10] A. M. Latham, K. A. Crockett, D. A. McLean, B. Edmonds, and K. O'Shea, "Oscar: An intelligent conversational agent tutor to estimate learning styles," in *Fuzzy Systems (FUZZ), 2010 IEEE International Conference on*, 2010, pp. 1-8.
- [11] F. Caviglia and M. Delfino, "Foundational skills and dispositions for learning: an experience with Information Problem Solving on the Web," *Technology, Pedagogy and Education*, vol. 25, pp. 487-512, 2016.
- [12] D. Hooshyar, R. B. Ahmad, M. Yousefi, F. Yusop, and S. J. Horng, "A flowchart-based intelligent tutoring system for improving problem-solving skills of novice programmers," *Journal of Computer Assisted Learning*, vol. 31, pp. 345-361, 2015.
- [13] G.-J. Hwang and F.-R. Kuo, "An information-summarising instruction strategy for improving the web-based problem solving abilities of students," *Australasian Journal of Educational Technology*, vol. 27, 2011.
- [14] D. Azcona, I.-H. Hsiao, and A. F. Smeaton, "Modelling Math Learning on an Open Access Intelligent Tutor," in *International Conference on Artificial Intelligence in Education*, 2018, pp. 36-40.
- [15] B. P. Woolf, *Building intelligent interactive tutors: Student-centered strategies for revolutionizing e-learning*; Morgan Kaufmann, 2010.
- [16] J. R. Carbonell, "AI in CAI: An artificial-intelligence approach to computer-assisted instruction," *IEEE transactions on man-machine systems*, vol. 11, pp. 190-202, 1970.
- [17] W. J. Clancey, "Methodology for building an intelligent tutoring system," *Methods and tactics in cognitive science*, pp. 51-84, 1984.
- [18] W. Ma, O. O. Adesope, J. C. Nesbit, and Q. Liu, "Intelligent tutoring systems and learning outcomes: A meta-analysis," *Journal of educational psychology*, vol. 106, p. 901, 2014.
- [19] E. E. Carter, "An Intelligent Debugging Tutor For Novice Computer Science Students," 2014.
- [20] Q. Brown, "Mobile intelligent tutoring system: moving intelligent tutoring systems off the desktop," 2009.
- [21] M. C. Polson and J. J. Richardson, *Foundations of intelligent tutoring systems*; Psychology Press, 2013.
- [22] C. C. Hugh Burns, *Foundations of intelligent tutoring systems: An introduction*; Texas Laboratory, 1989.
- [23] P. Brereton, B. A. Kitchenham, D. Budgen, M. Turner, and M. Khalil, "Lessons from applying the systematic literature review process within the software engineering domain," *Journal of systems and software*, vol. 80, pp. 571-583, 2007.
- [24] C. Wohlin, "Guidelines for snowballing in systematic literature studies and a replication in software engineering," in *Proceedings of the 18th international conference on evaluation and assessment in software engineering*, 2014, p. 38.
- [25] C. Walkington and M. L. Bernacki, "Personalizing Algebra to Students' Individual Interests in an Intelligent Tutoring System: Moderators of Impact," *International Journal of Artificial Intelligence in Education*, pp. 1-31, 2018.
- [26] K. S. McCarthy, A. D. Likens, A. M. Johnson, T. A. Guerrero, and D. S. McNamara, "Metacognitive Overload!: Positive and Negative Effects of Metacognitive Prompts in an Intelligent Tutoring System," *International Journal of Artificial Intelligence in Education*, pp. 1-19, 2018.
- [27] D. Hooshyar, R. B. Ahmad, M. Wang, M. Yousefi, M. Fathi, and H. Lim, "Development and evaluation of a game-based bayesian intelligent tutoring system for teaching programming," *Journal of Educational Computing Research*, vol. 56, pp. 775-801, 2018.
- [28] M. Dlamini and W. S. Leung, "Enhancing Object-Oriented Programming Pedagogy with an Adaptive Intelligent Tutoring System," in *Annual Conference of the Southern African Computer Lecturers' Association*, 2018, pp. 269-284.
- [29] M. J. Mosa, I. Albatish, and S. S. Abu-Naser, "ASP. NET-Tutor: Intelligent Tutoring System for leaning ASP. NET," 2018.
- [30] H. A. Al Rekhawi and S. Abu Naser, "An Intelligent Tutoring System for Learning Android Applications Ui Development," 2018.
- [31] A. Vijayan, S. Janmasree, C. Keerthana, and L. B. Sylva, "A Framework for Intelligent Learning Assistant Platform Based on Cognitive Computing for Children with Autism Spectrum Disorder," in *2018 International CET Conference on Control, Communication, and Computing (IC4)*, 2018, pp. 361-365.
- [32] R. Cole, C. Buchenroth-Martin, T. Weston, L. Devine, J. Myatt, B. Holding, et al., "One-on-one and small group conversations with an intelligent virtual science tutor," *Computer Speech & Language*, vol. 50, pp. 157-174, 2018/07/01/ 2018.
- [33] U. Kose and A. Arslan, "Optimization of self-learning in Computer Engineering courses: An intelligent software system supported by

- Artificial Neural Network and Vortex Optimization Algorithm," *Computer Applications in Engineering Education*, vol. 25, pp. 142-156, 2017.
- [34] M. Samarakou, P. Prentakis, D. Mitsoudis, D. Karolidis, and S. Athinaios, "Application of fuzzy logic for the assessment of engineering students," in *Global Engineering Education Conference (EDUCON)*, 2017 IEEE, 2017, pp. 646-650.
- [35] R. Britto, W. G. de Oliveira Filho, C. G. Barros, and E. C. Lopes, "Intelligent tutor system model applied to basic electronics," in *Information Systems and Technologies (CISTI)*, 2017 12th Iberian Conference on, 2017, pp. 1-5.
- [36] B. Mostafavi and T. Barnes, "Evolution of an intelligent deductive logic tutor using data-driven elements," *International Journal of Artificial Intelligence in Education*, vol. 27, pp. 5-36, 2017.
- [37] N. Bosch and S. D'Mello, "The affective experience of novice computer programmers," *International Journal of Artificial Intelligence in Education*, vol. 27, pp. 181-206, 2017.
- [38] G. Fontaine, S. Cossette, and M. A. Maheu-Cadotte, "Development and Evaluation of an Intelligent Learning Environment for the Assessment and Management of Cardiometabolic Risk by Acute Care Nurses: A Research Protocol," *Canadian Journal of Cardiology*, vol. 33, p. S212, 2017/10/01/ 2017.
- [39] Y. P. Xin, R. Tzur, C. Hord, J. Liu, J. Y. Park, and L. Si, "An intelligent tutor-assisted mathematics intervention program for students with learning difficulties," *Learning Disability Quarterly*, vol. 40, pp. 4-16, 2017.
- [40] M. W. Alawar and S. S. A. Naser, "CSS-Tutor: An intelligent tutoring system for CSS and HTML," *International Journal of Academic Research and Development*, vol. 2, pp. 94-98, 2017.
- [41] A. Sehwat, R. Keelan, K. Shimada, D. M. Wilfong, J. T. McCormick, and Y. Rabin, "Simulation-based cryosurgery intelligent tutoring system prototype," *Technology in cancer research & treatment*, vol. 15, pp. 396-407, 2016.
- [42] K. Almohammadi, H. Hagra, D. Alghazzawi, and G. Aldabbagh, "Users-centric adaptive learning system based on interval type-2 fuzzy logic for massively crowded e-learning platforms," *Journal of Artificial Intelligence and Soft Computing Research*, vol. 6, pp. 81-101, 2016.
- [43] B. Grawemeyer, M. Mavrikis, W. Holmes, S. Gutierrez-Santos, M. Wiedmann, and N. Rummel, "Affecting off-task behaviour: how affect-aware feedback can improve student learning," in *Proceedings of the sixth international conference on learning analytics & knowledge*, 2016, pp. 104-113.
- [44] C. R. Wolfe, V. F. Reyna, C. L. Widmer, E. M. Cedillos-Whynott, P. G. Brust-Renck, A. M. Weil, et al., "Understanding genetic breast cancer risk: Processing loci of the BRCA Gist intelligent tutoring system," *Learning and individual differences*, vol. 49, pp. 178-189, 2016.
- [45] D. Hooshyar, R. B. Ahmad, M. Yousefi, M. Fathi, S.-J. Horng, and H. Lim, "Applying an online game-based formative assessment in a flowchart-based intelligent tutoring system for improving problem-solving skills," *Computers & Education*, vol. 94, pp. 18-36, 2016/03/01/ 2016.
- [46] M. I. Alhabbash, A. O. Mahdi, and S. S. A. Naser, "An Intelligent Tutoring System for Teaching Grammar English Tenses," 2016.
- [47] J. M. Harley, F. Bouchet, M. S. Hussain, R. Azevedo, and R. Calvo, "A multi-componential analysis of emotions during complex learning with an intelligent multi-agent system," *Computers in Human Behavior*, vol. 48, pp. 615-625, 2015.
- [48] K. Dolenc and B. Aberšek, "TECH8 intelligent and adaptive e-learning system: Integration into Technology and Science classrooms in lower secondary schools," *Computers & Education*, vol. 82, pp. 354-365, 2015.
- [49] V. Echeverria, B. Guaman, and K. Chiluiza, "Mirroring Teachers' Assessment of Novice Students' Presentations through an Intelligent Tutor System," in *Computer Aided System Engineering (APCASE)*, 2015 Asia-Pacific Conference on, 2015, pp. 264-269.
- [50] P. Mohammed and P. Mohan, "Dynamic cultural contextualisation of educational content in intelligent learning environments using ICON," *International Journal of Artificial Intelligence in Education*, vol. 25, pp. 249-270, 2015.
- [51] D. P. Vinchurkar and M. Sasikumar, "Intelligent Tutoring System for Voice Conversion in English," in *Advanced Learning Technologies (ICALT)*, 2015 IEEE 15th International Conference on, 2015, pp. 314-316.
- [52] D. Wang, H. Han, Z. Zhan, J. Xu, Q. Liu, and G. Ren, "A problem solving oriented intelligent tutoring system to improve students' acquisition of basic computer skills," *Computers & Education*, vol. 81, pp. 102-112, 2015.
- [53] A. Smith, W. Min, B. W. Mott, and J. C. Lester, "Diagrammatic student models: Modeling student drawing performance with deep learning," in *International Conference on User Modeling, Adaptation, and Personalization*, 2015, pp. 216-227.
- [54] M. Dzikovska, N. Steinhäuser, E. Farrow, J. Moore, and G. Campbell, "BEETLE II: Deep natural language understanding and automatic feedback generation for intelligent tutoring in basic electricity and electronics," *International Journal of Artificial Intelligence in Education*, vol. 24, pp. 284-332, 2014.
- [55] G. A. Khachatryan, A. V. Romashov, A. R. Khachatryan, S. J. Gaudino, J. M. Khachatryan, K. R. Guarian, et al., "Reasoning Mind Genie 2: An intelligent tutoring system as a vehicle for international transfer of instructional methods in mathematics," *International Journal of Artificial Intelligence in Education*, vol. 24, pp. 333-382, 2014.
- [56] E. Walker, N. Rummel, and K. R. Koedinger, "Adaptive intelligent support to improve peer tutoring in algebra," *International Journal of Artificial Intelligence in Education*, vol. 24, pp. 33-61, 2014.
- [57] D. Weragama and J. Reye, "Analysing student programs in the PHP intelligent tutoring system," *International Journal of Artificial Intelligence in Education*, vol. 24, pp. 162-188, 2014.
- [58] S. Gómez, P. Zervas, D. G. Sampson, and R. Fabregat, "Context-aware adaptive and personalized mobile learning delivery supported by UoLmP," *Journal of King Saud University-Computer and Information Sciences*, vol. 26, pp. 47-61, 2014.
- [59] S.-J. Hsieh and Y.-T. Cheng, "Algorithm and intelligent tutoring system design for programmable controller programming," *The International Journal of Advanced Manufacturing Technology*, vol. 71, pp. 1099-1115, 2014.
- [60] W. R. Swartout, "Knowledge needed for expert system explanation."
- [61] T. N. Phyu, "Survey of classification techniques in data mining," in *Proceedings of the International MultiConference of Engineers and Computer Scientists*, 2009, pp. 18-20.
- [62] A. R. Masegosa and S. Moral, "An interactive approach for Bayesian network learning using domain/expert knowledge," *International Journal of Approximate Reasoning*, vol. 54, pp. 1168-1181, 2013.
- [63] P. Stone and M. Veloso, "Multiagent systems: A survey from a machine learning perspective," *Autonomous Robots*, vol. 8, pp. 345-383, 2000.
- [64] J. Psotka, L. D. Massey, and S. A. Mutter, *Intelligent tutoring systems: Lessons learned*: Psychology Press, 1988.
- [65] M. Pantic, "Introduction to machine learning & case-based reasoning," London: Imperial College, 2005.
- [66] A. Holt, I. Bichindaritz, R. Schmidt, and P. Perner, "Medical applications in case-based reasoning," *The Knowledge Engineering Review*, vol. 20, pp. 289-292, 2005.
- [67] L. Briz-Ponce, J. A. Juanes-Méndez, F. J. García-Peñalvo, and A. Pereira, "Effects of mobile learning in medical education: a counterfactual evaluation," *Journal of medical systems*, vol. 40, p. 136, 2016.
- [68] C. Mulwa, S. Lawless, M. Sharp, and V. Wade, "A web-based framework for user-centred evaluation of end-user experience in adaptive and personalized e-learning systems," in *Proceedings of the 2011 IEEE/WIC/ACM International Conferences on Web Intelligence and Intelligent Agent Technology-Volume 03*, 2011, pp. 351-356.

Personalized Recommender by Exploiting Domain based Expert for Enhancing Collaborative Filtering Algorithm: PReC

Mrs. M. Sridevi¹

Anurag Group of Institutions
Hyderabad, Telangana, India

Dr. R. Rajeswara Rao²

JNTU Kakinada
Vizianagaram, Andhra Pradesh, India

Abstract—The large amount of information available on the internet initiated various Recommender algorithms to act as an intermediate between number of choices and internet users. Collaborative filtering is one of the most traditional and intensively used recommendation approaches for many commercial services. Despite providing satisfying outcomes, it does have some issues that include source diversity, reliability, sparsity of data, scalability and cold start. Thus, there is a need for further improvement in the current generation of recommender system to achieve a more effective human decision support in a wide variety of applications and scenarios. Personalized Expert based collaborative filtering (PReC) approach is proposed to identify domain specific experts and the use of experts preference enhanced the performance of collaborative filtering recommender systems. A unified framework is proposed that integrates similar users rating data, experts rating and demographic data to reduce the number of pairwise computations from the search space to ensure scalability and enabled fine grained recommendations. The proposed method is evaluated using accuracy metrics MAE, RMSE on the data set collected from MovieLens datasets.

Keywords—Recommender system; collaborative filtering; domain based experts; demographic data

I. INTRODUCTION

With an overwhelming growth of information available over the internet in recent years, Recommender systems [1], [2] have proven to be a powerful tool whose aim is to guide users with personalized recommendations and alleviate the potential problem of information overload. However, the performance of these systems in dynamic environments remain unsatisfactory, thereby making Recommender systems inefficient, inaccurate and less robust to the changes of user preferences thereby motivating for further research in the field.

Despite the success of several Recommendation approaches such as Collaborative filtering [3], [4], Content based [5], [6] and Hybrid filtering [7], there have been several limitations increasing the need to provide effective and accurate recommendations. Collaborative filtering is one of the most traditional and intensively used recommendation approach for many commercial services like Movies recommendation, Music Recommendation, News Recommendation, Book Recommendation, etc., as it is

content independent and easy to implement. In this approach, recommendations are generated based on user ratings and the similarity measures between users (User-based CF) and/or items (Item-based CF). Despite providing satisfying outcomes, existing collaborative filtering methods does have some issues that include source diversity, reliability, sparsity of data, scalability and cold start. Thus, there is a need for further improvement in the current generation of recommender system to achieve a more effective human decision support, in a wide variety of applications and scenarios.

In order to address the aforementioned problems, existing solutions in the literature have been explored and an effective recommendation approach is proposed that can outperform traditional algorithms. A Personalized Expert based collaborative filtering (PReC) is proposed for domain specific expert identification by analyzing each user and item subgroups to predict relevant unseen preferences and improve the performance of the system in terms of source diversity and recommender reliability. A novel use of expert's preference elicitation enabled fine grained recommendations thereby, solving sparsity and cold start issues. Intelligent Demographic filtering mechanism is introduced to reduce the number of pairwise computations from the search space to ensure scalability. Finally, a versatile unified framework is proposed in which all the aforementioned approaches have been integrated to handle the challenges of current generation Recommender systems.

II. RELATED WORK

Recommender system has come into existence to overcome the choice option by providing recommendations that are tailored to individual user preferences. Research shows that Recommender systems [1] [2] have increased the sales and customer satisfaction. It guides users by providing personalized information in a large space of options. Collection of input data is one of the important components of Recommender system. It considers user preferences in the form of explicit rating i.e., providing 5-star ratings or implicit data by clicking, browsing, etc. Since the inception of Recommender systems, today we have many Recommendation strategies/algorithms based on the user ratings, content of the item, location, content, etc.

A. Collaborative Filtering

Collaborative filtering [3] [4] is one of the widely used technique to predict users preference or generate list of user preferences. However, there exists several issues which need to be addressed that include the complex computation for large dataset of users, understand the diversity of different information sources and understanding user preferences when there is sparsity of data. Prior research in Collaborative Filtering Recommender systems focus only on the accuracy of the recommendations at the cost of scalable and reliable recommendations. Among the various Recommender systems used, early systems that used collaborative filtering approaches are Grundy System a book recommender, Ringo [8] which recommended personalized music, Tapestry [9], a document recommender, an article recommender GroupLens [10], Amazon.com [11] recommender which recommends the relevant items, etc., In [12] improved collaborative filtering approach is used by extending user-item rating matrix that could alleviate the data sparsity issue but could not solve cold start problem and user interest shifted with time. In [13] Regularized Matrix Factorization is used to develop an Incremental Collaborative Filtering Recommender system.

B. Content-Based Recommender System

Content based recommender systems [5], [6] can be used in a wide variety of domains ranging from recommending news articles, hotels, movies and items for sale. Also referred as cognitive filtering, the key idea of content based recommender is to recommend items to the user according to relevant attributes of the item and user preferences by attributes. Content based recommender system [6] compares the items to others in the collection. Items with a high degree of similarity are presented as recommendations. This is called as “item-to-item correlation”. The information source used by the content-based filtering systems is text documents. These items are typically described with keywords and weights. By analyzing the keywords and document the system recommend a suitable item using probabilistic methods, for e.g., Naïve Bayes, decision trees [14], clustering, nearest neighbor, etc., There are many ways to build a user profile which involves (i) inferring profile from user actions (implicit). It includes read, buy, click, etc. and (ii) inferring profile from explicit user ratings, which includes feedback technique by selecting a value of range, filling out forms, etc., Both implicit actions and explicit ratings are processed against the database of content attributes to build the content profile. Content based recommender systems have been applied in various applications. The Fab system [5], which recommends Web pages to users, [15] represents documents, DailyLearner system [16] filter out news items too similar to those already seen by the user, etc. Content based recommender is effective in recommending accurate items when they are better described. The profiles of other users do not influence the recommendations of the target user as the recommendations are based on individual preferences. Content-based recommender systems always need to consider the following issues:

1) *Partial content analysis*: It is difficult to recommend about the user’s profile if only partial content available.

2) *High specialization*: It restricts the users to rate the items by identifying the similar items defined in their corresponding profiles and so new items and other options are not revealed to rate.

C. Hybrid Recommender System

Hybrid Recommender system [17] combines both collaborative filtering and content based filtering approach in different ways: i) Implementation of algorithms separately and combining the results [18]; ii) Utilizing some capabilities of content based into collaborative based approach [19]; iii) Utilizing some capabilities of collaborative based into content based approach [20]; and iv) Constructing a unifying model using different approaches [21].

Hybrid Recommender system integrates various RSs which helps us to overcome the disadvantages and improve the performance. Therefore the quality of the recommendations provided to the end user or customer. Empirically, several studies compared the performance and quality of hybrid approach [22] and proved that the hybrid approaches provide recommendations more accurately than original recommender approaches. The very common issues cold start and sparsity are also eliminated.

D. Expert based Recommender Systems

A series of algorithms have been described in the literature to identify the experts and exploit their opinion to demonstrate their effectiveness. Earlier research expert is judged by comparing with a set of predefined keywords [22], that is time-consuming and also the profile becomes outdated that no longer reflects in future. This resulted an increased demand for automating and more focused towards the development of personalized expert based Recommender systems. To capture the expert, a number of approaches exist in the literature, like Probabilistic models [23] that can estimate the association between domain and expert users, discriminative models [24] that directly estimate the conditional probability to find the relevance, voting models [25] use voting mechanism to vote the users, graph based models [26] determine the associations by inference on a graph consisting items, users, etc., and there are some other models that make use of latent variables that correspond to a theme. In [27], expert ranking is considered as a voting problem using data fusion techniques. Author in [28] used context dependent expertise information to reduce the number of users. In [29], Ranking SVM is applied to rank the experts by using pairwise approach to rank and predict the candidates. In [30] an evaluation of Learning to Rank algorithms is proposed for expert search on the DBLP database. In [31] a supervised learning approach is proposed to aggregate ranking and apply the same to search the experts and their blogs. An expert user is identified through the blog entries in [32] to generate recommendations. Experts identified from the user community dynamically proved to be time consuming in [33].

E. Demographic based Recommender System

Demographic Recommender system [34] considers demographic data in collaborative filtering when providing recommendations. In [35], recommendations are generated based on the product demographic data learned from online

reviews and blog entries. The demographic features of the tourist are taken in [36] without any rating data to generate the predictions but it can only achieve limited accuracy. A framework is developed by evaluating demographic attributes to solve cold start problem in [37].

III. PROPOSED METHODOLOGY

In this paper, we proposed personalized expert based collaborative filtering (PReC) to identify domain specific experts and use of demographic data with expert's preference in order to improve the performance of traditional collaborative filtering recommender systems. Initially, EUCF is proposed that integrates collaborative filtering features and clusters similar users and similar items thereby promoting experts based on the user profile and exploit their opinions thus addressing the reliability issue and enables fine grained recommendations. Secondly, an intelligent demographic filtering mechanism is introduced that integrates demographic features and user based collaborative filtering to reduce the number of pairwise expensive similarity computations from the search space to ensure scalability and cold start issue. And finally, a unified framework is proposed that integrates similar users rating data, experts rating and demographic data to deal source diversity, sparsity and enable fine grained accurate recommendations.

A. Expert user based Collaborative Filtering (EUCF)

Based on the study, we developed a framework as given in Fig. 1 to identify the experts from users' responses having similar preferences to improve recommendation quality. While traditional systems compare users profile with other users to recommend unseen movies, our proposed system compare expert users profile with target user and use the experts' opinion that eventually results in better recommendations to the target user.

1) *Neighborhood formation:* Once the rating profile of the user is constructed, similar users are identified by analyzing user profile (User-Item Rating Matrix) and by applying the similarity measure, Pearson correlation coefficient, equation (1).

$$s(x, y) = \frac{\sum_{i=1}^n (x_i - \bar{x})(y_i - \bar{y})}{\sqrt{\sum_{i=1}^n (x_i - \bar{x})^2} \sqrt{\sum_{i=1}^n (y_i - \bar{y})^2}} \quad (1)$$

where x_i, y_i is the rating of user x and y on 'i', \bar{x} mean of all x 's ratings, \bar{y} , mean of all y 's ratings and n is the number of items

Likewise, the similarity between items is computed by using the user item ratings and discovering similar items. For computation of similarity between items, Pearson correlation coefficient is used as given in equation (2).

$$s(t, r) = \frac{\sum_{i=1}^n (R_{it} - \bar{A}_t)(R_{ir} - \bar{A}_r)}{\sqrt{\sum_{i=1}^n (R_{it} - \bar{A}_t)^2} \sqrt{\sum_{i=1}^n (R_{ir} - \bar{A}_r)^2}} \quad (2)$$

where R_{it}, R_{ir} is the rating of user i on item 't' and item 'r' respectively, \bar{A}_t the average rating of item 't', \bar{A}_r , average rating of item 'r' and n is the number of users.

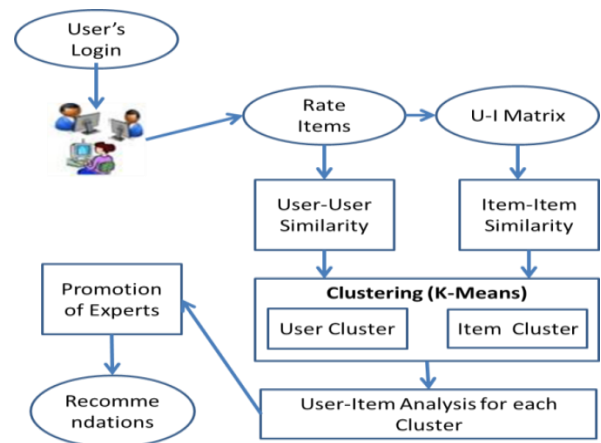


Fig. 1. Framework of EUCF.

2) *Expert identification and generating recommendations:* Designing a framework for expert identification involves collecting user rating data from user – item profile that contributes in identifying users with highest access factor and most similar to the average ratings opinion in exchange of high quality personalization. A pseudo rating profile is generated by taking the average ratings of the users in that cluster.

Once the identification of similar users and similar items is completed, the selection of the right expert during identification phase is critical. Expert user is a user who is most similar to the average ratings and whose access factor is greater than the other users. An expert user may vary from one domain to another domain and there may exist more than one expert user for the same domain. The task of expert finding usually involves taking the user rating data as input, denoting the heavy access factor and finding similarity with average ratings and returning the list of users ordered by their expertise level. User's expertise is characterized by the heavy access factor i.e., more number of ratings for a given domain and is given in equation (3).

$$\forall_{u \in U} \forall_{i \in I} i_{HA}^{(u)} = \frac{\log(|I_u|+1)}{\max_v \log(|I_v|+1)} \quad (3)$$

Where I_u set of items 'u' accessed, $HA = 1$ if 'u' has heavy access. The features of user profile related to the number of items rated associated with each domain and also identifying the user profile who is most similar to the average rating assuming that the users with such profiles are likely to be considered as experts. The average rating similarity is calculated as shown in equation (4).

$$\forall_{u \in U} \forall_{i \in I} d(u) = \sqrt{\sum_{i \in I} \sum_{i=1}^n \left((R_{u,i}) - \bar{R}_{U,i} \right)^2} \quad (4)$$

Where U, I are the user set and item sets respectively, n is the number of items, $\bar{R}_{U,i}$ average rating of users who rated item 'i'. Thus, the expertise can be measured by the following equation (5).

$$E(u) = i_{HA}^{(u)} * \left(\frac{1}{1+d(u)} \right) \quad (5)$$

In selecting the experts, threshold value of fixed size can be defined. Small threshold value often results in high precision but low recall in experts finding, whereas large threshold value results in low precision but high recall. We assume that there may exist more than one candidate expert for every domain. Formally, given the user ratings, candidate experts are identified and the similarity of expert user and the target user is computed as shown in equation (6).

$$s(e, a) = \frac{\sum_{i=1}^n (R_{e,i} - R_{\bar{e}})(R_{a,i} - \bar{R}_a)}{\sqrt{\sum_{i=1}^n (R_{e,i} - R_{\bar{e}})^2} \sqrt{\sum_{i=1}^n (R_{a,i} - \bar{R}_a)^2}} \quad (6)$$

and then finally predictions are generated based on similar experts recommendations. The expert scores are averaged to generate predictions by the following equation:

$$E(i) = \hat{R}_a + \frac{\sum_{e=1}^n (R_{e,i} - \hat{R}_e) s(e, a)}{\sum_{e=1}^n s(e, a)} \quad (7)$$

Where \hat{R}_a average rating of target user, $R_{e,i}$ rating of expert user on target item, \hat{R}_e average rating of target user to the items, $s(u, e)$ similarity of target user 'u' and expert user 'e'. An expert candidate is assessed by considering how many items (movies) have been rated, how many are related to the particular domain, and how similar the user with the average opinions.

B. Demographic User based Collaborative Filtering (UCFD)

We studied the difficulty in computing the similarity among different users from a large dataset. A novel approach is proposed for efficient computations of similar users based on demographic data of the user. We use demographic features of users to partition the set of users having similar demographic features i.e., age and gender and from the subset again, by analyzing the ratings of the user, similar users are identified by their ratings preferences. We assume that users with similar demographic features have similar user preferences that will effectively improve the time and performance in traditional Collaborative filtering system.

Thus a unified framework is proposed that utilizes both rating data and demographic data to compute the similarity between users thus bypasses the scalability issue. Formally, the profile of a user is represented as a vector where the elements of the vector correspond to the demographic features of the user as shown in Table I. The input contains a demographic feature vector space of each single user and the output is the relevant similarity score of the users. By selecting a set of well-designed features i.e., age and gender, our proposed approach outperforms the traditional models in terms of scalability on the dataset extracted from MovieLens dataset. After data selection, pairwise computations are performed to partition the users into clusters. The demographic filtering of users mainly reduces the pairwise similarity computations that are performed during user similarity computation. Our proposed approach has the advantage of overcoming the sparsity when there is sparsity of data. The framework combines demographic based and user based collaborative filtering recommendations in order to derive benefits.

TABLE I. DEMOGRAPHIC DATA

Attributes	Demographic vector description
age<=18	slot takes value 0
18<age<=35	slot takes value 1
36<age<=49	slot takes value 2
age>50	slot takes value 3
Male	slot describing gender takes 1
Female	slot takes value 0

Similarity of users based on demographic data can be computed using the following equation:

$$\text{dem}_{u,a} = \cos(u, a) = \frac{\vec{u} \cdot \vec{a}}{\|\vec{u}\| \|\vec{a}\|} = \frac{\sum_{i=1}^n u_i a_i}{\sqrt{\sum_{i=1}^n u_i^2} \sqrt{\sum_{i=1}^n a_i^2}} \quad (8)$$

and the similarity based on user rating data of similar demographic users is computed using Euclidean distance measure as shown in equation (9):

$$d(u, a) = \sqrt{\sum_{i=1}^n (R_{u,i} - R_{a,i})^2} \quad (9)$$

where, $R_{u,i}, R_{a,i}$ rating of user u and a on item 'i' and 'n' is the number of items and the similarity between the users is given by the equation (10).

$$s(u, a) = \frac{1}{1+d(u, a)} \quad (10)$$

Finally, as a result our proposed enhanced correlation is based on demographic correlation and similarity rating based correlation given by the following equation (11):

$$\text{dem_rat_sim}(u, a) = \alpha \text{dem}_{u,a} + \beta s_{u,a} + \gamma (\text{dem}_{u,a} * s_{u,a}) \quad (11)$$

UCFD generates prediction for the target user based on the enhanced correlation given by

$$\text{Pred_dem_rat_sim}(a, i) = \hat{R}_a + \frac{\sum_{u=1}^n (r_{u,i} - \bar{r}_u) * \text{dem_rat_sim}(u, a)}{\sum_{u=1}^n \text{dem_rat_sim}(u, a)} \quad (12)$$

where $\text{Pred_dem_rat_sim}(a, i)$ predicted rating for target user a for item i, $\text{dem_rat_sim}(u, a)$ similarity between user u and a, \hat{R}_a is average ratings of target user, $r_{u,i}$ rating of user u on item i, \bar{r}_u average ratings of user u and n is the number of similar neighbors.

C. Expert user based CF with Demographic Filtering (EUCFD)

A novel recommendation algorithm is proposed that fuses the opinions from similar users based on rating data, expert users (EUCF), and similar users based on demographic features (UCFD). A typical recommender system considers only one's judgment i.e., similar user, whereas our proposed system considers two more sources i.e., Expert users and demographic similar users in addition to similar users predictions to generate efficient output as shown in Fig. 2.

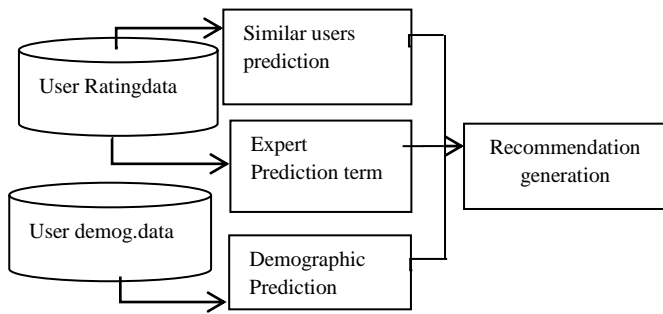


Fig. 2. Architecture of Proposed EUCFD.

The EUCF method extracts expert users from each item category and exploits their ratings rather than similar neighbors. In addition, the similarity between the target user and the users is considered based on demographic features in the prediction of ratings when there is sparsity of rating data and cold start issue and finally we fuse all the variants i.e., EUCF and UCFD to form EUCFD that utilizes domain based experts opinion by considering both demographic and ratings data.

Initially, we identify expert users from an independent user data set based on the number of ratings given to each item category. The demographic features of the active user are considered if there is sparsity of rating data. Recommendations are generated by considering the prediction terms of expert user and the accumulative values of similar users based on demographic data and similar users rating data.

1) *Enhanced prediction term for target user:* Finally, given a user's choice of preference, personalized recommendations are generated based on their preferences from the movies space. The algorithmic approaches are ensemble to generate recommendations by considering three varying factors: similar users prediction term, expert based prediction term, demographic based prediction term as given in the following equations:

$$SP(a,i) = \hat{R}_a + \frac{\sum_{u=1}^n (R_{u,i} - \bar{R}_u) * s(u,a)}{\sum_{u=1}^n s(u,a)} \quad (13)$$

$$EP(a,i) = \hat{R}_a + \frac{\sum_{e=1}^n (R_{e,i} - \bar{R}_e) * s(e,a)}{\sum_{e=1}^n s(e,a)} \quad (14)$$

$$DP(a,i) = \hat{R}_a + \frac{\sum_{u=1}^n (r_{u,i} - \bar{r}_u) * dem(u,a)}{\sum_{u=1}^n dem(u,a)} \quad (15)$$

From equation (13)(14)(15), we compute enhanced prediction term for target user as:

$$P(a,i) = \bar{R}_a + \alpha * SP(a,i) + \beta * EP(a,i) + \gamma * DP(a,i) \quad (16)$$

Where $\alpha + \beta + \gamma = 1$, \bar{R}_a is the average of target user ratings, $SP(a,i)$ is the user similarity prediction term, $EP(a,i)$ is the expert users prediction term and $DP(a,i)$ is demographic prediction term. Parameter α, β, γ is used to tune between the three values. We aggregate the recommendations generated from each module by considering the weights. When there is an absence in the explicit user input ratings, thus resulting in the sparsity of data thereby resulting inaccurate recommendations, then the canonical proposed approach is to consider the demographic features of the users retrieved from

the user profile and use these features to find the similarity between the users and to set recommendations for the target user.

D. Experimental Evaluation

1) *Datasets:* In this study, we considered MovieLens datasets. MovieLens dataset consists of approximately 100,000 ratings, 943 users and 1682 movies, where each user has rated atleast 20 movies and the ratings are on a 1-5 scale with '1' representing least and '5' representing highest. MovieLens is a web based Recommender system. The data used by Movie Lens is collected by GroupLens Research Project at Minnesota University. (<http://grouplens.org/datasets/movielens/100k/>). The statistics of the datasets are detailed in Table II.

2) *Evaluation metrics:* In order to evaluate our system, the data is divided into two sets with 80% - 20% split ratio of training set and testing set. Let 'x' be a variable that give the percentage of training and test data. If x=0.8, then it indicates that 80% of data is used as training set and 20% of data is used as test set. The performance of the proposed system can be evaluated by employing Recommendation Accuracy Metrics. In this paper, we use Mean Absolute Error (MAE) and Root Mean Square Error (RMSE) most frequently used Metrics to measure the accuracy.

$$MAE = \frac{1}{n} \sum_{i=1}^n |p_i - r_i| \quad (17)$$

$$RMSE = \sqrt{\frac{\sum_{i=1}^n (p_i - r_i)^2}{n}} \quad (18)$$

Where p_i prediction ratings for item 'i', r_i actual ratings for item 'i' and n is number of rated items. The lower the MAE value, the more accurate are the recommendations. The other metrics used in this study are precision and recall.

$$\text{Precision} = \frac{|relevant_items_recommended_items|}{|recommended_items|} \quad (19)$$

$$\text{Recall} = \frac{|relevant_items_recommended_items|}{|relevant_items|} \quad (20)$$

There is a certain ambiguity exists while using these measures. For an instance, increasing the total number of recommended items N, which directly effects on increase in recall but decreases precision. To overcome this ambiguity, we use another metric F1-Measure. It gives equal weightage to both precision and recall. All these measures are defined in equations (19), (20) and (21) individually.

$$F1 = 2 * \frac{precision * recall}{precision + recall} \quad (21)$$

TABLE II. DATASET STATISTICS

Statistics	MovieLens
No.of Users	943
No.of Movies	1682
No.of Ratings	100,000
Min-Max values	1 - 5

3) *Experimental results:* Finally, we evaluate our results and experiments on MovieLens datasets. The experiments proved that our proposed algorithms generate efficient and accurate predictions when compared to existing traditional User based Collaborative Filtering. The Mean Absolute Error of our proposed algorithms is lower than that of UCF. The outcomes from all the proposed algorithms are analyzed and

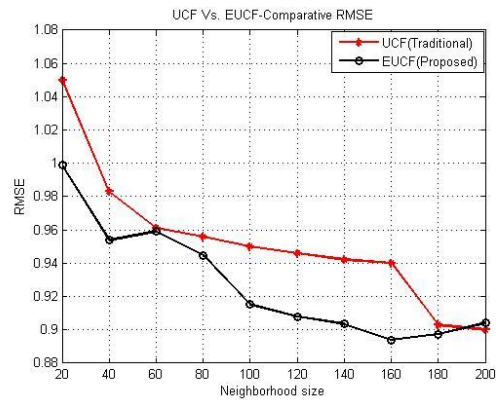
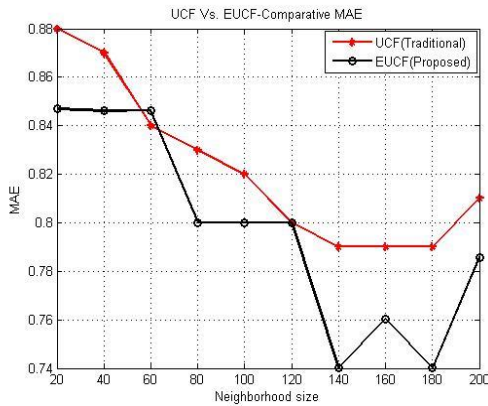
compared based on MAE. Table III gives the comparison of MAE values for all the proposed algorithms for different sizes of neighborhood. In order to make the improvement even prominent, the results are also compared for root mean square error formats given in Table IV. The outcomes are also analyzed graphically in Fig. 3, Fig. 4 and Fig. 5.

TABLE III. MAE VALUES OF PROPOSED ALGORITHMS BASED ON NEIGHBORHOOD SIZE

Algorithm	Neighborhood size									
	20	40	60	80	100	120	140	160	180	200
UCF	0.88	0.87	0.84	0.83	0.82	0.8	0.79	0.79	0.79	0.81
EUCF	0.8469	0.8462	0.8463	0.8001	0.8001	0.8001	0.7401	0.7601	0.7401	0.7857
UCFD	0.7381	0.7381	0.7381	0.6578	0.6595	0.6588	0.5693	0.5693	0.5693	0.6386
EUCFD	0.716	0.7254	0.7071	0.6025	0.5957	0.5689	0.5186	0.5061	0.5494	0.5498

TABLE IV. RMSE VALUES OF PROPOSED ALGORITHMS BASED ON NEIGHBORHOOD SIZE

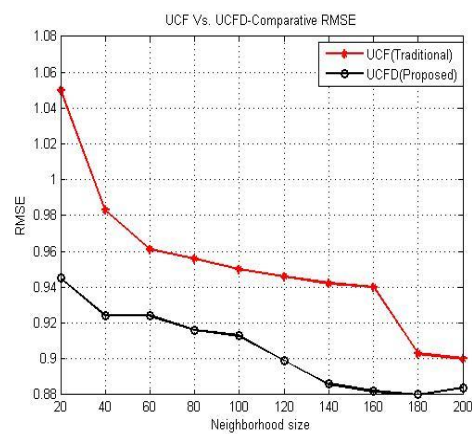
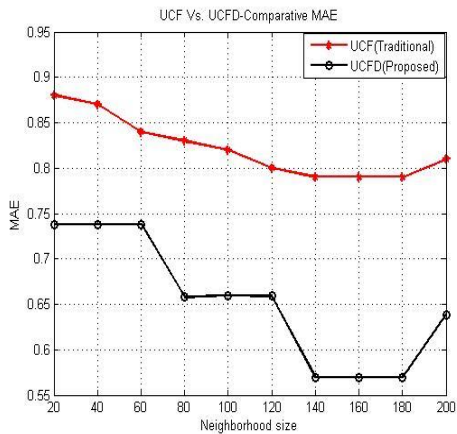
Algorithm	Neighborhood size									
	20	40	60	80	100	120	140	160	180	200
UCF	0.7744	0.7569	0.7056	0.6889	0.6724	0.64	0.6241	0.6241	0.6241	0.6561
EUCF	0.7172	0.716	0.716	0.6401	0.6401	0.6401	0.5477	0.5777	0.5477	0.6173
UCFD	0.5448	0.5448	0.5448	0.4327	0.435	0.4341	0.3241	0.3241	0.3241	0.407
EUCFD	0.512	0.5263	0.5	0.363	0.3549	0.323	0.269	0.256	0.301	0.302



(a) UCF vs. EUCF- MAE

(b) UCF vs. EUCF- RMSE

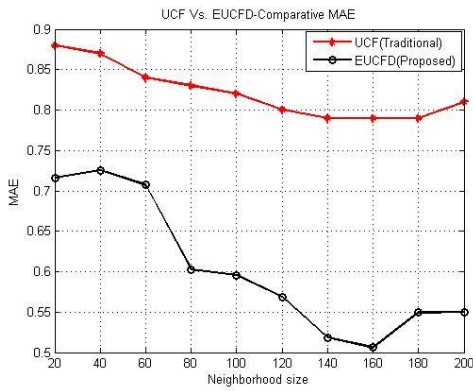
Fig. 3. Performance vs. Neighborhood Size, MovieLens Dataset.



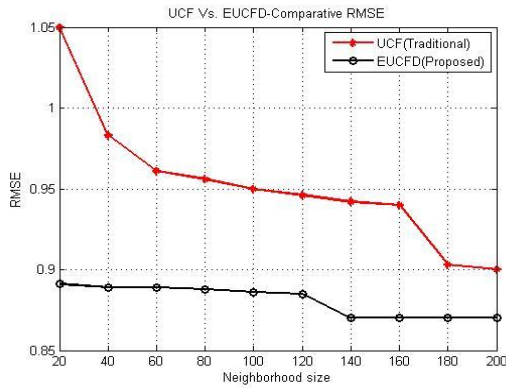
(a) UCF vs. UCFD- MAE

(b) UCF vs. UCFD- RMSE

Fig. 4. Performance vs. Neighborhood Size, MovieLens Dataset.



(a) UCF vs EUCFD MAE



(b) UCF vs. EUCFD RMSE

Fig. 5. Performance vs. Neighborhood Size, MovieLens Dataset.

We compared all three algorithms with the traditional algorithm and is summarized in Table V. It has been observed from Fig. 6 that EUCFD is more accurate than traditional user based collaborative filtering (UCF), item based collaborative filtering (ICF) and proposed UCFD, EUCF algorithms and the results proved that our proposed EUCFD algorithm outperformed remaining algorithms and our proposed method shows a significant increase in prediction performance when compared to a traditional single source model.

The results in Fig. 7 demonstrates the higher relevancy of the final EUCFD algorithm recommendations and the significant improvements made over UCF, EUCF and UCFD algorithms for MovieLens datasets. The F-Measure results of EUCF, UCFD and EUCFD are also analyzed graphically as well.

TABLE V. SUMMARY OF MAE AND RMSE (MOVIELENS)

S. No.	Algorithm	MAE	RMSE
1	User based CF (UCF)	0.8220	0.739
2	Item based CF (ICF)	0.8154	0.711
2	Expert user based CF(EUCF)	0.7966	0.636
3	Demographic user based CF (UCFD)	0.6537	0.432
4	Expert user based Demographic CF(EUCFD)	0.6040	0.372

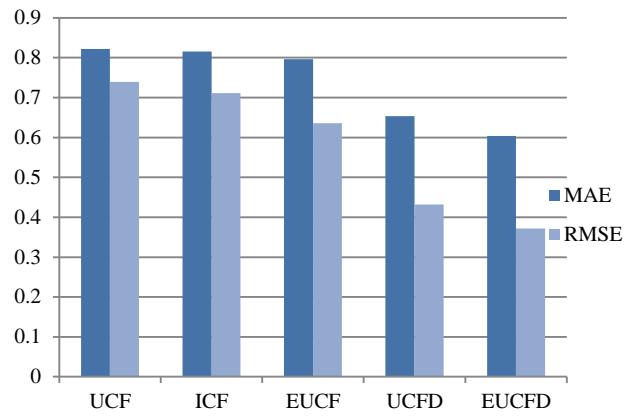
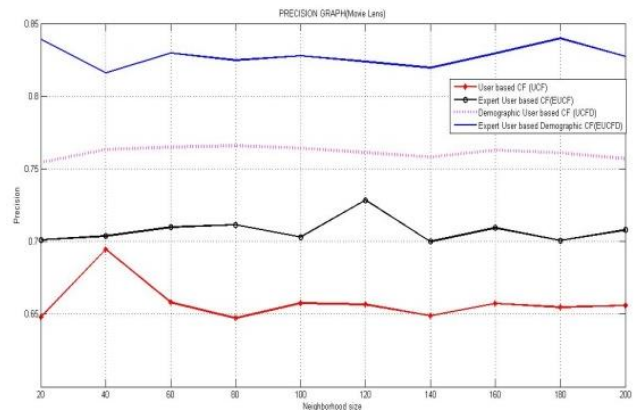
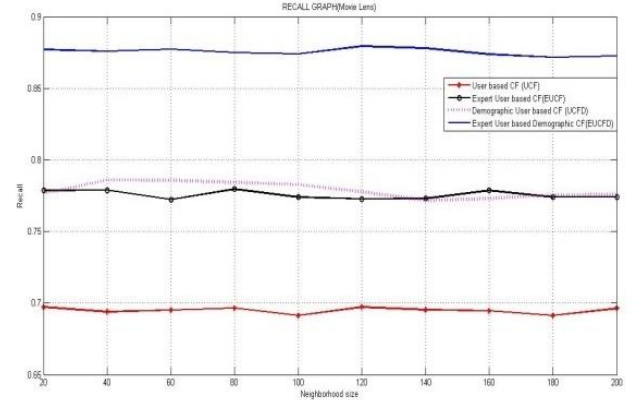


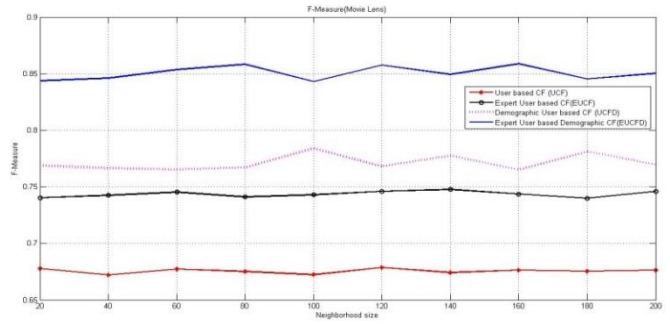
Fig. 6. MAE of UCF, EUCF, UCFD and EUCFD in MovieLens.



a) Precision



b) Recall



c) F Measure

Fig. 7. Performance vs. Neighborhood Size, MovieLens Data Set.

IV. CONCLUSION

This paper introduced the benefits to the users of information systems in retrieving their personalized preferences by considering rating data, experts' opinion and demographic data of the user to generate personalized preferences. Furthermore, we introduced novel methods in identifying domain based experts and integrated similar users' opinion with experts' opinion to improve the recommendation quality. This paper focus on the issues of Collaborative filtering that includes data sparsity, scalability and reliability. Initially, we contributed three approaches that significantly improved the recommendation quality. Results proved that our approach can increase the scalability and generate an accurate prediction that is more suitable for large data sets. Thus, our proposed approach works towards the development of an efficient recommender system.

REFERENCES

- [1] Adomavicius G., Tuzhilin, A. Toward the next generation of recommender systems: a survey of the state-of-the-art and possible extensions, *IEEE TKDE*, 17(6), 2005, pp.734-749.
- [2] JoeranBeel, BelaGipp, Stefan Langer, and CorinnaBreitinger"Research-Paper Recommender Systems: A Literature Survey", *International Journal on Digital libraries*, 2015.
- [3] Yue Shi, Martha Larson, And Alan Hanjalic Collaborative Filtering beyond the User-Item Matrix: A Survey of the State of the Art and Future Challenges, *ACM*, 2014.
- [4] J.B.Schafer,D.Frankowski,J.Herlocker,S.Sen, Collaborative filtering recommender systems. *The Adaptive Web*, 291-324, 2007.
- [5] Pasquale Lops, Marco de Gemmis and Giovanni Semeraro ' Content based Recommender systems: State of the art and trends', *Recommender Systems Handbook*, Springer Science+Business Media, LLC 2011.
- [6] Balabanović, M. and Shoham, Y. Fab: content-based, collaborative recommendation. *Communications of the ACM* 40 (3) (1997) 66-72.
- [7] Robin Burke. Hybrid Recommender Systems: Survey and Experiments. *User Modeling and User Adapted*.
- [8] U. Shardanand, P. Maes. Social information filtering: algorithms for automating word of mouth". *Proceedings of the SIGCHI conference on Human factors in computing systems*, pp. 210-217, (1995).
- [9] D. Goldberg, D. Nichols, B. Oki and D. Terry. "Using Collaborative Filtering to Weave an Information Tapestry." in *ACM*. New York. 1992.
- [10] P. Resnick, N. Iacovou, M. Sushak, P. Bergstrom, and J. Riedl,"GroupLens: An Open Architecture for Collaborative Filtering of Netnews," *Proc. 1994 Computer Supported Collaborative Work Conf.*,pp. 175-186, 1994.
- [11] G. Linden, B. Smith, J. York. Amazon.com Recommendations, Item-to-Item Collaborative Filtering. *IEEE Internet Computing*, Volume 7, Issue 1, (2003).
- [12] Li Zhang, Tao Qin PiQiangTeng, "An Improved Collaborative Filtering Algorithm Based on User Interest" *Journal of Software*, 2014.
- [13] Luo, X., Xia, Y., and Zhu, Q, Incremental Collaborative Filtering Recommender based on Regularized Matrix Factorization, knowledge based systems,2012.
- [14] L. M. de Campos, J. M. Fern_andez-Luna, J. F. Huete, and M. A. Rueda-Morales, Combining content-based and collaborative recommendations: A hybrid approach based on Bayesian networks," *International Journal of approximate Reasoning*, vol. 51,pp. 785{799, Sept. 2010.
- [15] Degemmis, M., Lops, P., Semeraro, G.: A content-collaborative recommender that exploits wordnet-based user profiles for neighborhood formation. *User Modeling and User-Adapted Interaction*17(3), 217–255 (2007).
- [16] Billsus, D. and M. Pazzani. User modeling for adaptive news access. *User Modeling and User-Adapted Interaction*, 10(2-3):147-180, 2000.
- [17] Wenfulin, Yingli,Shuangfeng, Yongbin Wang," The optimization of weights in Weighted Hybrid Recommendation algorithm, *ICIS/IEEE*, 2014.
- [18] M GhazanfarAPrugel-Bennett "An Improved Switching Hybrid Recommender System Using Naive Bayes Classifier and Collaborative Filtering- 2010.
- [19] L. M. de Campos, J. M. Fern_andez-Luna, J. F. Huete, and M. A. Rueda-Morales, Combining content-based and collaborative recommendations: A hybrid approach based on Bayesian networks," *International Journal of approximate Reasoning*, vol. 51,pp. 785{799, Sept. 2010.
- [20] M. Tiemann and S. Pauws, (Towards ensemble learning for hybrid music recommendation," in *Proceedings of the 2007 ACM conference on Recommender systems, RecSys '07*, (New York, NY,USA), pp. 177{178, ACM, 2007.
- [21] Thomas HornungCai-Nicolas Ziegler Simon Franz Martin Przyjaciel-Zablock Alexander Schatzle Georg Lausen "Evaluating Hybrid Music Recommender Systems" *IEEE* 2013.
- [22] M.J. Pazzani, A Framework for Collaborative, Content-based and Demographic Filtering. *Artificial Intelligence Review*, 13(5-6), 393-408, 1999.
- [23] Amatrian, X., Lathia, N., Pujol, J.M., Kwak, H., Oliver, N.: The Wisdom of The Few: A Collaborative Filtering Approach Based On Expert Opinions From The Web. In: *32nd International Conference ACM Special Interest Group on Information Retrieval*, New York, pp. 532–539 (2009).
- [24] Kumar, A. and Bhatia, M.P.S. Community expert based recommendation for solving first rater problem. *International Journal of Computer Applications* 37 (10) (2012) 7-13.
- [25] Craig Macdonald and IadhOunis, "Learning Models for Ranking Aggregates" *LNCIS*, Springer, Vol. 6611, 2011.
- [26] Zhou Zhao, Lijun Zhang, Xiaofei He, and Wilfred Ng "Expert Finding for Question Answering via Graph Regularized Matrix Completion", *IEEE Transactions On Knowledge And Data Engineering*, Vol. 27, No. 4, April 2015.
- [27] Song, S., Lee, S., Park, S., Lee, S.G.: Determining User Expertise For Improving Recommendation Performance. In: *6th International Conference on Ubiquitous Information and Communication 2012*, New York (2012).
- [28] V.Carchiolo, A.Longhue, M.Malgeri,G.Mangioni Searching for experts in a context-aware recommendation network, *Elsevier*, Vol.51, 2015
- [29] Catarina Moreira, PavelCalado, Bruno Martins "Learning to Rank Academic Experts in the DBLP Dataset", *Expert systems: Journal of Knowledge Engineering archive*, Vol 32, Issue 4 August 2015.Pg. 477–493.
- [30] W.S.Hwang, Ho-Jong Lee,S.W.Kim, Y.Won, M.Lee, Efficient recommendation methods using category experts for a large dataset", *Information fusion*, Elsevier, 2016.
- [31] Kibeom Lee and KyoguLee,"Using Dynamically Promoted Experts for Music Recommendation", *IEEE*, 2014.
- [32] K. Lee and K. Lee, "Using experts among users for novel movie recommendations" *Journal of Computer Science & Engineering*, 2013.
- [33] Yi Fang, LuoSi, Aditya "Discriminative probabilistic models for expert search in heterogeneous information sources" *ACM* 2011.
- [34] Gupta, J. and Gadge, J. Performance analysis of recommendation system based on collaborative filtering and demographics. *IEEE International Conference on Communication, Information & Computing Technology (ICCICT)*, 2015, 1-6.
- [35] Wayne Xin Zhao, YanweiGuo, Yulan He, Han Jiang, Yuexin Wu and Xiaoming Li," we know what you want to buy: A Demographic-based System for Product Recommendation on Microblogs", *ACM*, 2014.
- [36] Yuanyuan Wang,Stephen Chi-Fai Chan,Grace Ngai"Applicability of Demographic Recommender System to Tourist Attractions: A Case Study on Trip Advisor", *IEEE* 2012.
- [37] LailaSafoury and Akram Salah" Exploiting User Demographic Attributes for Solving Cold-Start Problem in Recommender System", *Lecture Notes on Software Engineering*, Vol. 1, No. 3, August 2013.

Model Reference Adaptive Control Design for Nonlinear Plants

Wafa Ghazlane¹, Jilani Knani²

Research Laboratory in Automatic Control LA.R.A

National Engineers School of Tunis, ENIT, University of Tunis El Manar, BP 37, Le Belvédère, 1002, Tunis, Tunisia

Abstract—In this paper, the basic theory of the model reference adaptive control design and issues of particular relevance to control nonlinear dynamic plants with a relative degree greater than or equal to one with unknown parameters are detailed. The studied analysis was motivated through its application to a robot manipulator with six degrees of freedom. After linearization using the input-output feedback linearization and decoupling algorithm, the nonlinear Multi-input Multi-output system was transformed into six independent single-input single-output linear subsystems each one has a relative degree equal to two, the obtained results in different simulations shows that the augmented reference model adaptive controller has been successfully implemented.

Keywords—Model reference adaptive control; nonlinear dynamic plants; relative degree; unknown parameters; robot manipulator; input-output feedback linearization

I. INTRODUCTION

Nowadays, a great performance of industrial control systems are under adaptive control techniques [1], these include a high scale of tasks in aerospace, robotics, process control, ship steering, and automotive and biomedical plants.

Specially, for robotic control, a control designer can be faced with joint flexibilities, unknown manipulator dynamic parameters, nonlinear joint interactions, and dynamics changing due to unknown and varying loads. Traditional robotic control algorithms have depended on specific knowledge of the robotic parameters and dynamic equations [2]. When a designer has limited knowledge of these parameters and interactions, it can be advantageous to exploit adaptive control approaches to reduce the effects of these problems.

Generally, the model reference adaptive control system (MRAC) was initially developed to adjust the problems in which the performance specifications are given in terms of a reference model [1, 3, 4]. This model tells how the process output ideally should deal to the command signal. The structure of the control system is given in Fig. 1.

The controller may be thought of as composed of two loops, the inner loop is a regular feedback loop consisting of the plant and the controller, the outer loop error, which determines the difference between plant output and model output is small [1, 5]. The MRAC was originally introduced for advanced control. The crucial importance with MRAC is to analyse the adjustment mechanism so that a stable system which brings the error to zero, is obtained.

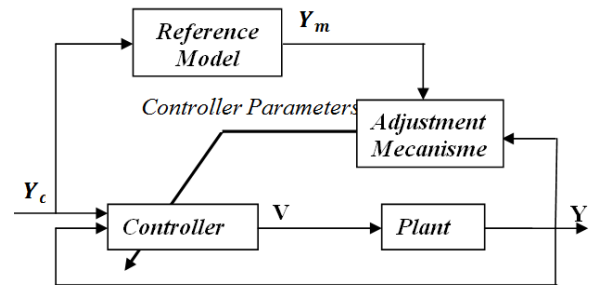


Fig. 1. A Model-Reference Adaptive Control System [1].

The organization of this paper is as follows: It is designed by five parts. In Section 2, the adaptive control statement is presented. In Section 3, the structure of the model reference adaptive control system with relative degree greater than or equal to one is explained. In Section 4, the control approach is applied to a robot manipulator with six degrees of freedom and the simulation results are developed. Finally, the conclusion was detailed in Section 5.

II. PROBLEM STATEMENT

The problem under consideration [5], is the control of a single-input single-output (SISO) discrete time linear system which is elaborated by the input output $\{V(k), Y(k)\}$ and can be formulated by the transfer function of the form:

$$G_p(q^{-1}) = q^{-d} K_p \frac{B(q^{-1})}{A(q^{-1})} \quad (1)$$

Where $A(q^{-1})$ denotes a monic polynomial with degree n , $B(q^{-1})$ represents a monic stable polynomial with degree $m < n$, the term $d=n-m$ is designed the relative degree of the system and K_p is called a constant gain parameter.

A model reference is represented by the input output $\{Y_c(k), Y_r(k)\}$ and can be described by the transfer function.

$$G_m(q^{-1}) = q^{-d} K_m \frac{B_m(q^{-1})}{A_m(q^{-1})} \quad (2)$$

Where $A_m(q^{-1})$ and $B_m(q^{-1})$ represent respectively a monic stable polynomial with degrees n and $m < n$, K_m denotes a constant gain parameter.

Therefore as [6], the relative degree of the model is supposed to be greater than or equal to that of the system.

The purpose of the MRAC design is to determine a control law $V(k)$, and an adaptation law, such that [6, 7] the resulting model following error $Y(k) - Y_r(k)$ asymptotically converges to zero, such that relation (3).

$$\lim_{k \rightarrow +\infty} |e(k)| = \lim_{k \rightarrow +\infty} |Y(k) - Y_r(k)| = 0 \quad (3)$$

III. STRUCTURE OF THE MODEL REFERENCE ADAPTIVE CONTROLLER

The general structure of the model reference adaptive control system can be detailed as shown in Fig. 2 by the block diagram below.

Two identical block for generating auxiliary filter signal FSA1 and FSA2 both with dimension n , $W^{(1)}(k)$ and $W^{(2)}(k)$ with dimension $(n-1) \times 1$ denote the vectors of state variables and $V(k)$ and $Y(k)$ represent respectively, the inputs of the designed controller as detailed in Fig. 2.

Consider the following state space representation of the SISO plant dynamics, together with two "signal filter generators" formed by a controllable pair (Λ, B) are given as.

$$\begin{cases} X_p(k+1) = A_p X_p(k) + B_p V(k) \\ Y(k) = C_p X_p(k) \end{cases} \quad (4)$$

$$\begin{cases} W^{(1)}(k+1) = \Lambda W^{(1)}(k) + B V(k) \\ V_F(k) = C^T W^{(1)}(k) \end{cases} \quad (5)$$

$$\begin{cases} W^{(2)}(k+1) = \Lambda W^{(2)}(k) + B Y(k) \\ Y_F(k) = \bar{D}^T W^{(2)}(k) + d_0 Y(k) \end{cases} \quad (6)$$

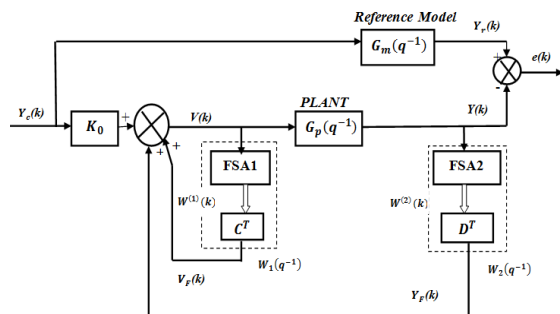


Fig. 2. Block Diagram of Model Reference Adaptive Control.

where,

$$\Lambda = \begin{bmatrix} 0 & 1 & 0 & \dots & 0 \\ \vdots & \ddots & \ddots & \ddots & \vdots \\ 0 & \dots & 0 & 0 & 1 \\ -n_{n-1} & \dots & \dots & -n_2 & -n_1 \end{bmatrix}, \quad B = \begin{bmatrix} 0 \\ \vdots \\ 0 \\ 1 \end{bmatrix},$$

$$C^T = [c_{n-1} \ \dots \ c_1] \quad \bar{D}^T = [d_{n-1} \ \dots \ d_1]$$

$$C^T = [c_1 \ \dots \ c_{n-1}] \quad \text{and} \quad D^T = [d_0 \ \dots \ d_{n-1}]$$

represents the controller parameters.

According to the block diagram of the control system, the control law can be put in the following form:

$$V(k) = K_0 Y_c(k) + W_1(q^{-1})V(k) + W_2(q^{-1})Y(k) \quad (7)$$

The expression (7) can be formulated as follows:

$$V(k) = \theta^T(k) \phi(k) \quad (8)$$

Where

$$\theta^T(k) = [K_c(k) \ c^T(k) \ D^T(k)] = [K_c(k) \ c_1(k) \ \dots \ c_{n-1}(k) \ d_0(k) \ \dots \ d_{n-1}(k)]$$

$$\phi^T(k) = [Y_c(k) \ V_F(k) \ Y_F(k)]$$

Finally, the calculation of the control law requires knowledge of the parameters of the system. However, in practice, these parameters are unknown and variable in time. So, the online estimation of the control parameters is therefore necessary [6, 7, 8, 9, 10]. In this case, the control law is written in the following form:

$$V(k) = \hat{\theta}^T(k) \phi(k) \quad (9)$$

As described in [8], depending on the relative degree r of the system and the nature of the transfer function of the reference model, two cases are considered:

Case i: $r = 1$ and the transfer function $G_m(q^{-1})$ must be strictly positive real (SPR).

Case ii: $r > 1$ and the transfer function $G_m(q^{-1})$ must be non-strictly positive real (NSPR).

A. Synthesis of the Control Law in the Case of the Relative Degree of the Plant $r = 1$ and $G_m(q^{-1})$ is Strictly Positive Real.

In this case, we assumed that the relative degree r of the plant is one and the transfer function $G_m(q^{-1})$ is (SPR). So, the MRAC system can be described as shown in Fig. 3 by the block diagram below.

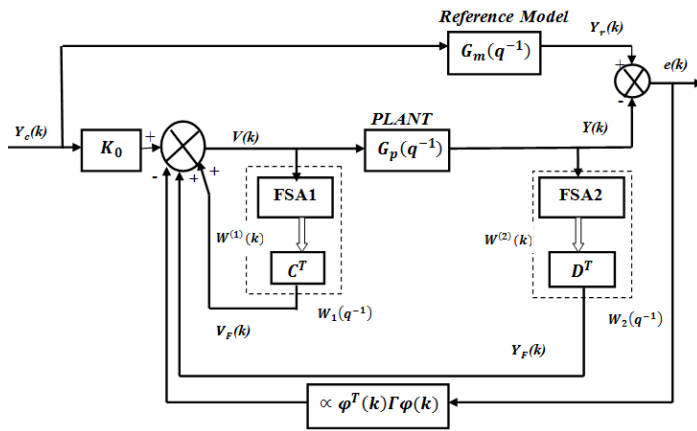


Fig. 3. A Model-Reference Adaptive Control System for Relative Degree $r = 1$.

The controller designed by $(2n + 1)$ adjustable parameters, which represented the elements of the parameter vector $\theta(k)$ formulated by relation (10)

$$\theta^T(k) = \begin{bmatrix} K_C(k) & C^T(k) & \bar{D}^T(k) d_0(k) \end{bmatrix} \quad (10)$$

If a vector $\varphi(k)$ is defined as

$$\varphi^T(k) = \begin{bmatrix} Y_C(k) & W^{(1)T}(k) & W^{(2)T}(k) & Y(k) \end{bmatrix} \quad (11)$$

The control law is written as:

$$V(k) = \theta^T(k) \varphi(k) - \alpha \varphi^T(k) \Gamma \varphi(k) e(k) \quad (12)$$

where $\alpha > 0$ and $\Gamma = \Gamma^T$ is a positive definite diagonal matrix

The parameters vector $\theta^T(k)$ can be written as follows:

$$\theta^T(k) = \theta^{*T}(k) + \theta^T(k) \quad (13)$$

Where $\theta^{*T} = \begin{bmatrix} K_0^*(k) & C^{*T} & \bar{D}^{*T} & d_0^*(k) \end{bmatrix}$ is the

vector with optimal parameters, and $\theta^T(k)$ is the vector of errors on control parameters. Then the expression of the command law is rewritten, as follows:

$$V(k) = \left(\theta^{*T}(k) + \theta^T(k) \right) \varphi(k) - \alpha \varphi^T(k) \Gamma \varphi(k) e(k) \quad (14)$$

In this case, a constant vector θ^* exists such that if $\theta^T(k) = \theta^{*T}(k)$, then $\theta^T(k) = 0$. So, it can be shown that the transfer function of the system will be equal to that of the reference model, and this term $\alpha \varphi^T(k) \Gamma \varphi(k) e(k)$ is seen to tend to zero.

Finally, in this condition the algorithm of adaptation parameters is given by the following equations:

$$e(k) = Y(k) - Y_r(k) \quad (15)$$

$$\theta(k+1) = \theta(k) - \Gamma e(k) \varphi(k) \quad (16)$$

$$V(k) = \theta^T(k) \varphi(k) - \alpha \varphi^T(k) \Gamma \varphi(k) e(k) \quad (17)$$

Synthesis of the Control Law in the Case of the Relative Degree $r > 1$ and $G_m(q^{-1})$ is Non Strictly Positive Real.

In this section, we discussed the MRAC approach for the case when the relative degree $r > 1$ and $G_m(q^{-1})$ is NSPR as described in [8], an auxiliary signal has to be fed into the reference model and the corresponding structure is described in Fig. 4.

In the condition of the relative degree r is equal to one, it is easy to define a SPR reference model $G_m(q^{-1})$. However, if the relative degree of the system $r > 1$, this assumption is not always satisfied. In this case, we assumed that there exists a urwitz polynomial $L(q^{-1})$ of degree $(n-1)$ such that $G_m(q^{-1})L(q^{-1})$ is SPR.

In this case, the error $e(k)$ denotes the tracking error between the output of the system $Y(k)$ and a fictitious output $Y_r^*(k)$ which is called auxiliary error or augmented error.

$$e(k) = Y(k) - Y_r^*(k) \quad (18)$$

or

$$Y_r^*(k) = Y_r(k) + Y_a(k) \quad (19)$$

$Y_a(k)$ is the auxiliary output of the reference model given by the following equation:

$$Y_a(k) = L(q^{-1})G_m(q^{-1}) \left[\left[L^{-1}(q^{-1})\bar{\theta}^T(k) - \bar{\theta}^T(k)L^{-1}(q^{-1}) \right] \bar{\varphi}(k) + \alpha \bar{\zeta}^T(k) \Gamma \bar{\zeta}(k) e(k) \right] \quad (20)$$

where

$$\bar{\zeta}(k) = L^{-1}(q^{-1})\bar{\varphi}(k) \quad (21)$$

$$\bar{\theta}^T(k) = \begin{bmatrix} C^T(k) & \bar{D}^T(k) & d_0(k) \end{bmatrix} \quad (22)$$

$$\bar{\varphi}^T(k) = \begin{bmatrix} W^{(1)T}(k) & W^{(2)T}(k) & Y(k) \end{bmatrix} \quad (23)$$

Finally [6, 7, 8, 9, 10], in this case the algorithm of adaptation of the parameters is given by the following equations as:

$$e(k) = Y(k) - Y_r(k) - Y_a(k) \quad (24)$$

$$\bar{\theta}(k) = \bar{\theta}(k-1) - \Gamma e(k) \bar{\xi}(k) \quad (25)$$

$$V(k) = \bar{\theta}^T(k) \bar{\varphi}(k) + Y_c(k) \quad (26)$$

IV. SIMULATION RESULTS

A. Dynamic Modelling and Linearization of a Robot Manipulator

In this section, a nonlinear six degrees of freedom robot manipulator model is employed to demonstrate the performance of the proposed MRAC approach, which is a serial open chain composed of seven rigid links connected with six rotoid joints as discussed in our recent works [11, 12, 13]. Therefore, controlling the motion of robot is a complicated operation due to the wide number of degrees of freedom and the high nonlinearities introduce in this plant. The dynamic equations of motion for the manipulator can be expressed by the following equations:

$$\Gamma = f(q, \dot{q}, \ddot{q}, f_e) \quad (27)$$

$$\Gamma_i = \sum_{j=1}^n d \frac{d}{dt} \left(\frac{\partial L_j}{\partial \dot{q}_j} \right) - \frac{\partial L_j}{\partial q_i} \quad i, j = 1, \dots, n \quad (28)$$

where $\Gamma, q, \dot{q}, \ddot{q}$ depicting Torques, articular positions, articular velocities and articular accelerations, f_e represents the external force and L_j denotes the lagrangian of the j^{th} joint.

So, we have applicated the formalism of Euler-Lagrange [13], such that equation (28), we obtained this relation (29):

$$\Gamma = A(q)\ddot{q} + C(q, \dot{q})\dot{q} + Q(q) \quad (29)$$

where $A(q)$ represents the matrix of kinetic energy ($n \times n$); $C(q, \dot{q})\dot{q}$ defines the vector of coriolis and centrifugal forces/torques ($n \times 1$); $Q(q)$ represents the vector of torques/forces of gravity.

Hence, the dynamic model of the above system was described by n second order differential equations [12, 13]. So, if the inertia matrix A is invertible for $q \in R^n$, we can determine the articular accelerations vector \ddot{q} of each joint as relation (30).

$$\ddot{q} = f(q, \dot{q}, \Gamma) \quad (30)$$

$$\ddot{q} = -A(q)^{-1} [C(q, \dot{q})\dot{q} + Q(q) - \Gamma] \quad (31)$$

Where q is the angular positions vector (6×1); \dot{q} is the angular velocities vector (6×1); \ddot{q} is the angular accelerations vector (6×1); Γ is the input torques vector (6×1).

For the goal of linear control design, we used the input output feedback linearization approaches as [14, 15, 16, 17], to linearize the nonlinear robot dynamics model. First, we assumed that the state variables of the plant changed into state space as:

$$x_1 = q_1, x_2 = \dot{q}_1, x_3 = q_2, x_4 = \dot{q}_2, x_5 = q_3, x_6 = \dot{q}_3$$

$$x_7 = q_4, x_8 = \dot{q}_4, x_9 = q_5, x_{10} = \dot{q}_5, x_{11} = q_6, x_{12} = \dot{q}_6$$

According to the above, to design the affine form of model dynamic for the robot manipulator which represents multivariable and nonlinear plant, we have derived each above state variables as formulated by the system (32):

$$\begin{cases} \dot{X}(t) = f(X(t)) + \sum_{i=1}^p g_i(X(t))U_i(t) \\ Y_i(t) = h_i(X(t)) \\ i = 1, 2, \dots, 6 \end{cases} \quad (32)$$

Where $X = [x_1, x_2, \dots, x_n]^T \in R^n$ defines the state vector; $U = [u_1, u_2, \dots, u_p]^T \in R^p$ denotes the control input vector; $Y = [y_1, y_2, \dots, y_p]^T \in R^p$ represents the output vector; $h_i(X)$ is a scalar function; $f(X)$ and $g_i(X)$ are n -dimensional smooth vector fields, with $i=1, 2, \dots, n$.

Second, for the purpose of linearizing and decoupling the model dynamics of the system and transforming it to six linear subsystem, the feedback linearization approach as [18, 19, 20, 21] consists essentially of applied the lie derivative to each output until one or more inputs arise, as formulated in the expression (33).

$$\text{Joints positions} \begin{cases} y_1 = h_1(x) = x_1 = q_1 \\ y_2 = h_2(x) = x_3 = q_2 \\ y_3 = h_3(x) = x_5 = q_3 \\ y_4 = h_4(x) = x_7 = q_4 \\ y_5 = h_5(x) = x_9 = q_5 \\ y_6 = h_6(x) = x_{11} = q_6 \end{cases}$$

For each joint position above, assume that the relative degree r_i represents the smallest integer such that fully one or more of the inputs appear in the new output $y_j^{(r_j)}$, $j=1\dots 6$.

$$y_j^{(r_j)} = L_f^{r_j} h_j(x) + \sum_{i=1}^p L_{g_i} (L_f^{(r_j-1)} h_j(x)) u_i \quad i, j=1, 2, \dots, p \quad (33)$$

Where $L_f^i h_j$ and $L_{g_i} h_j$ are the i^{th} Lie derivatives of $h_j(x)$ respectively in the direction of f and g .

$$L_f h_j(x) = \frac{\partial h_j}{\partial x} f(x), L_{g_i} h_j(x) = \frac{\partial h_j}{\partial x} g_i(x) \quad (34)$$

So, rewriting the expression (33) for each subsystem, we obtained that each one have a relative degree r_i equal to 2, are given by (35);

$$\left\{ \begin{array}{l} y_1 = h_1(x) = x_1 \\ \dot{y}_1 = L_f h_1(x) = \dot{x}_1 = x_2 \\ y_1^{(2)} = L_f^2 h_1(x) + L_{g_1} L_f h_1(x) u \\ r_1 = 2 \\ y_2 = h_2(x) = x_3 \\ \dot{y}_2 = L_f h_2(x) = \dot{x}_3 = x_4 \\ y_2^{(2)} = L_f^2 h_2(x) + L_{g_2} L_f h_2(x) u \\ r_2 = 2 \\ \vdots \\ y_6 = h_6(x) = x_{11} \\ \dot{y}_6 = L_f h_6(x) = \dot{x}_{11} = x_{12} \\ y_6^{(2)} = L_f^2 h_6(x) + L_{g_6} L_f h_6(x) u \\ r_6 = 2 \end{array} \right. \quad (35)$$

Finally, the nonlinear control law $u_i(t)$ applied to each joint of the robot manipulator system is formulated as the relation (36):

$$u_i(x(t)) = -\frac{L_f^{r_i} h_i(x(t))}{L_{g_i}^{r_i-1} L_f h_i(x(t))} + \frac{v_i(t)}{L_{g_i}^{r_i-1} L_f h_i(x(t))} \quad i=1\dots 6 \quad (36)$$

By using the input-output linearizing control law given by the above relation (36), the nonlinear plant dynamic system is transformed into six decoupled and linear subsystems [22, 23, 24, 25]. Each one was discretized to facilitate the linear reference model adaptive controller design.

B. Application of Control Strategy

As the linearized plant with input output feedback linearisation is constructed, we designed a linear controller by synthesising the proposed model reference adaptive controller in the case of the relative degree $r > 1$ and $G_m(q^{-1})$ is NSPR.

The joint1 represents a second-order and time-varying system, with relative degree ($r_1=2$) as described by the following equation:

$$y_1(k) = -a_{11}(k)y_1(k-1) - a_{12}(k)y_1(k-2) + k_{p1}(k)b_{10}(k)v_1(k-2) \quad (37)$$

$a_{11}(k)$, $a_{12}(k)$ and $b_{10}(k)$ are the unknown and time-varying parameters of model 1 that is estimated with a recursive least-squares algorithm as illustrated in figure 5.

$y_{c1}(k)$ denotes a reference input for the joint 1, described by the following relation:

$$y_{c1}(k) = 1 \forall k \geq 0 \quad (38)$$

The joint 2 represents a second-order and time-varying system, with relative degree ($r_2=2$) as described by the following equation:

$$y_2(k) = -a_{21}(k)y_2(k-1) - a_{22}(k)y_2(k-2) + k_{p2}(k)b_{20}(k)v_2(k-2) \quad (39)$$

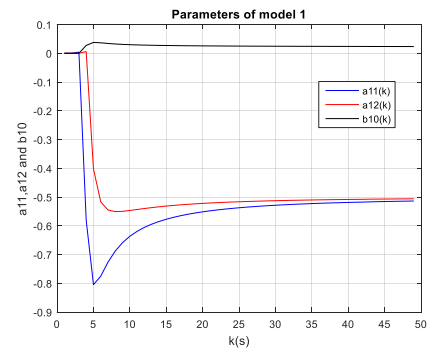


Fig. 4. The Estimated unknown and Time-Varying Parameters of Model 1.

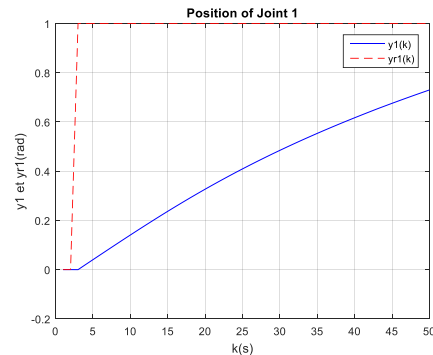


Fig. 5. The Evolutions of the Joint 1 Output $y_1(k)$ and Reference Model Output $y_{r1}(k)$.

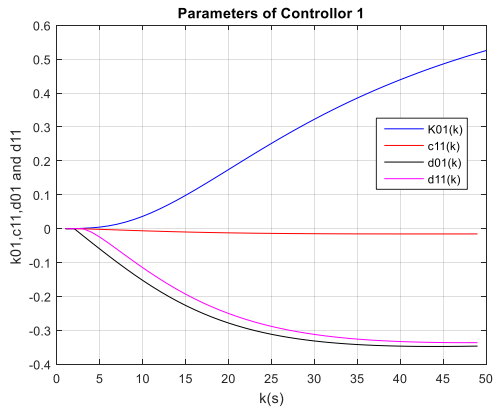


Fig. 6. Evolutions of the Controller Parameters 1.

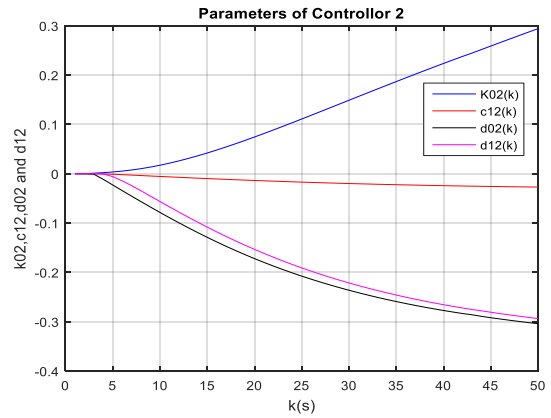


Fig. 9. The Adjustment Parameters of the Controller 2.

$a_{21}(k)$, $a_{22}(k)$ and $b_{20}(k)$ are the unknown and time-varying parameters of model 2 that is estimated with a recursive least squares algorithm as shown in Fig. 8.

$y_{c2}(k)$ is a reference input for the joint 2, described by the following relation:

$$y_{c2}(k) = 1 \forall k \geq 0 \quad (40)$$

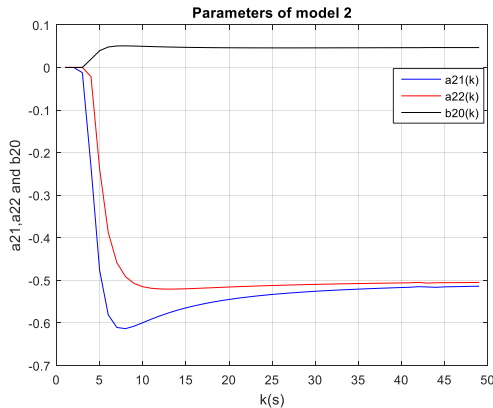


Fig. 7. The Estimated unknown and Time-Varying Parameters of Model 2.

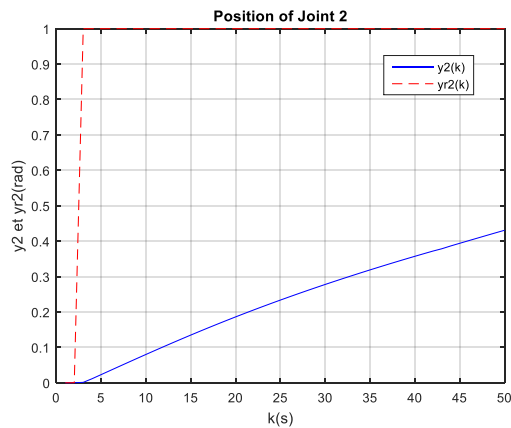


Fig. 8. The Evolutions of the Joint1 Output $y_2(k)$ and Reference Model Output $y_{r2}(k)$.

The joint 3 represents a second-order and time-varying system, with relative degree ($r3=2$) as determined by the following equation:

$$y_3(k) = -a_{31}(k)y_3(k-1) - a_{32}(k)y_3(k-2) + k_{p3}(k)b_{30}(k)y_3(k-2) \quad (41)$$

$a_{31}(k)$, $a_{32}(k)$ and $b_{30}(k)$ are the unknown and time-varying parameters of model 3 that is estimated with a recursive least-squares algorithm as shown in Fig. 11.

$y_{c3}(k)$ is a reference input for the joint 3, is given by the following relation:

$$y_{c3}(k) = 1 \forall k \geq 0 \quad (42)$$

The joint 4 represents a second-order and time-varying system, with relative degree ($r4=2$) as formulated by the following equation (43):

$$y_4(k) = -a_{41}(k)y_4(k-1) - a_{42}(k)y_4(k-2) + k_{p4}(k)b_{40}(k)y_4(k-2) \quad (43)$$

$a_{41}(k)$, $a_{42}(k)$ and $b_{40}(k)$ are the unknown and time-varying parameters of model 4 that is estimated with a recursive least squares algorithm as demonstrated in Fig. 14.

$y_{c4}(k)$ is a reference input for the joint 4, was elaborated by the following relation (44):

$$y_{c4}(k) = 1 \forall k \geq 0 \quad (44)$$

The joint 5 represents a second-order and time-varying system, with relative degree ($r5=2$) as given by the following equation (45):

$$y_5(k) = -a_{51}(k)y_5(k-1) - a_{52}(k)y_5(k-2) + k_{p5}(k)b_{50}(k)y_5(k-2) \quad (45)$$

$a_{51}(k)$, $a_{52}(k)$ and $b_{50}(k)$ are the unknown and time-varying parameters of model 5 that is estimated with a recursive least squares algorithm as shown in Fig. 17.

$y_{c5}(k)$ is a reference input for the joint 5, represented by the following relation (46):

$$y_{c5}(k) = 1 \forall k \geq 0 \quad (46)$$

The joint 6 represents a second-order and time-varying system, with relative degree ($r_6=2$) as determined by the following equation (47):

$$y_6(k) = -a_{61}(k)y_6(k-1) - a_{62}(k)y_6(k-2) + k_{p_6}(k)b_{60}(k)v_6(k-2) \quad (47)$$

$a_{61}(k)$, $a_{62}(k)$ and $b_{60}(k)$ are the unknown and time-varying parameters of model 6 that is estimated with a recursive least-squares algorithm as shown in Fig. 20.

$y_{c6}(k)$ is a reference input for the joint 6, denoted by the following relation (48):

$$y_{c6}(k) = 1 \forall k \geq 0 \quad (48)$$

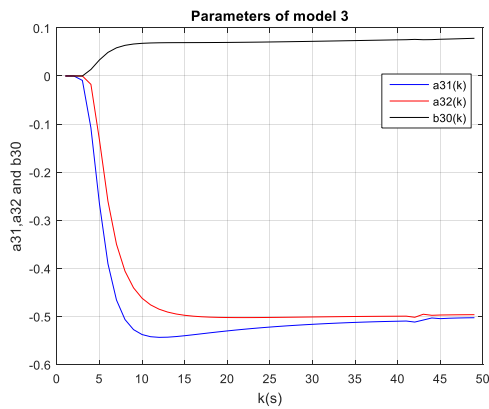


Fig. 10. The Estimated unknown and Time-Varying Parameters of Model 3.

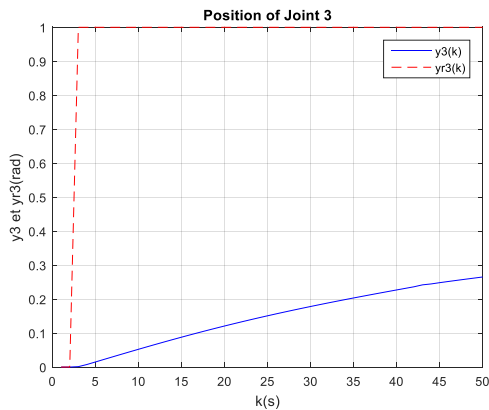


Fig. 11. The Evolutions of the Joint1Output $y_3(k)$ and Reference Model Output $y_{r3}(k)$.

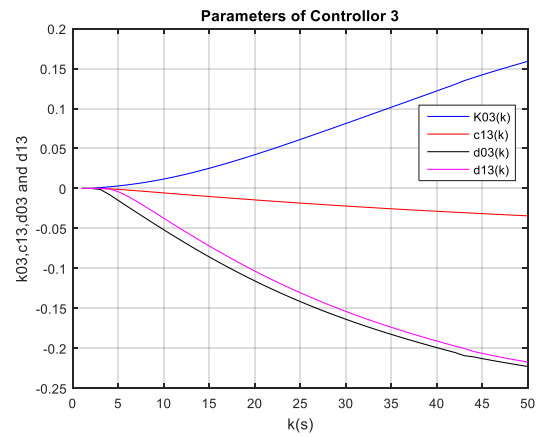


Fig. 12. The Adjustment Parameters of the Controller 3.

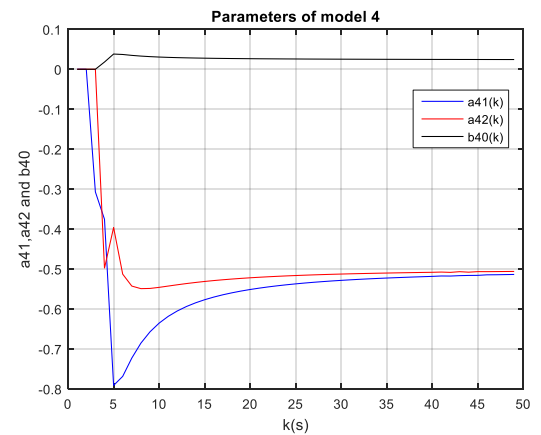


Fig. 13. The Estimated unknown and Time-Varying Parameters of Model 4.

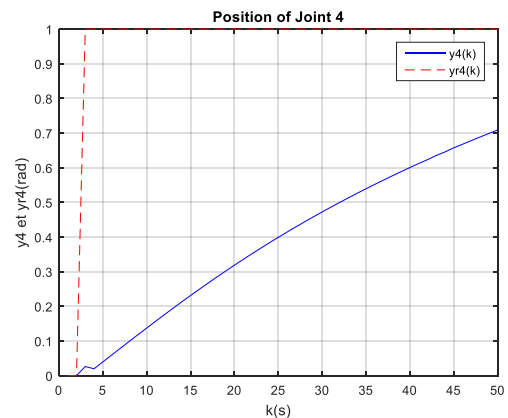


Fig. 14. The Evolutions of the Joint1Output $y_4(k)$ and Reference Model Output $y_{r4}(k)$.

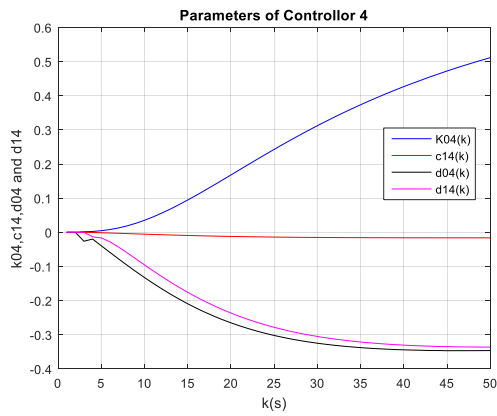


Fig. 15. The Adjustment Parameters of the Controller 4.

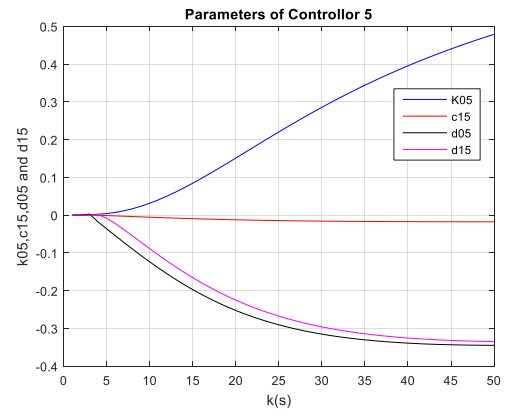


Fig. 18. The Adjustment Parameters of the Controller 5.

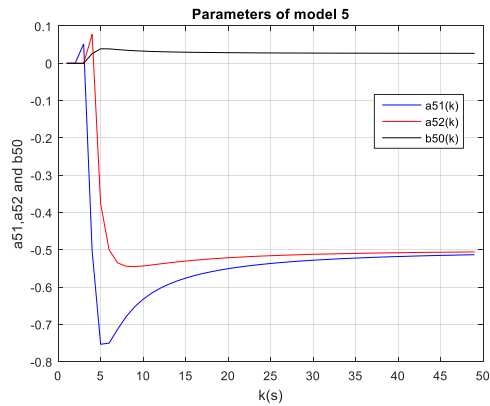


Fig. 16. The Estimated unknown and Time-Varying Parameters of Model 5.

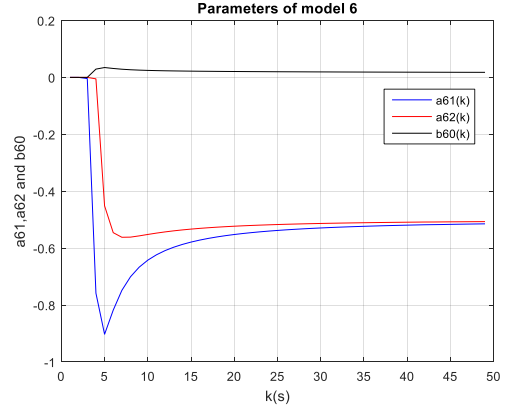


Fig. 19. The Estimated unknown and Time-Varying Parameters of Model 6.

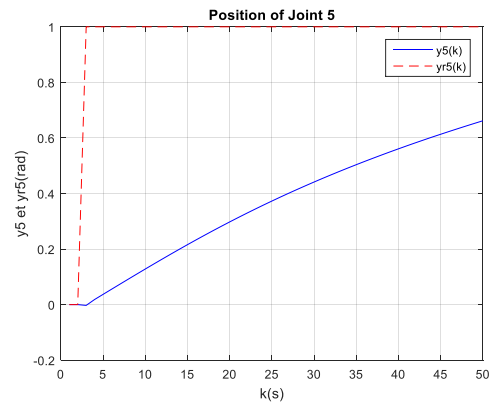


Fig. 17. The Evolutions of the Joint1 Output $y_5(k)$ and Reference Model Output $y_{r5}(k)$.

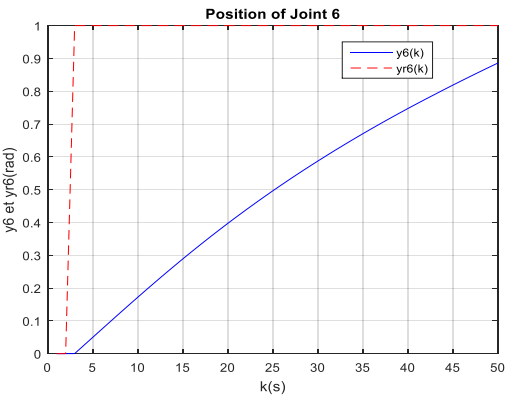


Fig. 20. The Evolutions of the Joint1 Output $y_6(k)$ and Reference Model Output $y_{r6}(k)$.

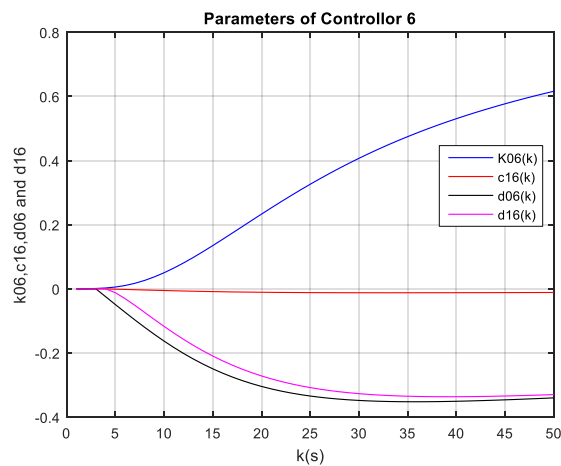


Fig. 21. The adjustment parameters of the controller 6.

Through the simulation results, as illustrated in figures 6,9,12,15,18,21, each one represents the evolution of the joint output and reference model output, one notes that each joint output converge to the reference model output, so each adaptive controller designed by parameters illustrated respectively in figures 7,10,13,16,19,22 was demonstrated a satisfactory tracking performance.

V. CONCLUSION

In this paper, a general class of discrete time adaptive control algorithms has developed and has illustrated that, under suitable cases, they will be convergent. This algorithm is used for SISO and MIMO plants. Two fundamental cases of controller design techniques are discussed in detail when the relative degree of the system equal to one and the transfer function of the reference model is assumed to be strictly positive. Also, the condition denotes that the relative degree greater than one and the transfer function supposed to be non-strictly positive real was called an augmented control architecture.

The contribution of this paper consists of motivated the studied analysis through its appliance to a robot manipulator with six degrees of freedom that is represents nonlinear, dynamic, multivariable and decoupled system. After linearization using the input-output feedback linearization and decoupling method, the nonlinear MIMO system was transformed into six independent SISO linear subsystems each one was represented by a relative degree equal to two with unknown and time-varying parameters. So, each linear subsystem has discretized to facilitate the linear MRAC design. However, the unknown and time-varying parameters of each model are estimated with a recursive least-squares algorithm. Finally, the control law of the augmented MRAC has been successfully implemented to each model as shown in the above simulation results.

As a perspective of our work, we will extend these researches for the plants with disturbances.

REFERENCES

- [1] K.J. Aström et B. Wittenmark, "Adaptive control", Addison-Wesley, 1989.
- [2] MW. Spong, S.Hutchinson, and M. Vidyasagar. "Robot Dynamics and Control", Second Edition. January 28, 2004.
- [3] I. D. Landau, R. Lozano, M. M'Saad and A. Karimi. "Adaptive Control Algorithms, Analysis and Applications," Second Edition. © Springer-Verlag London Limited 2011.
- [4] I. D. Landau, R. Lozano, M. M'Saad. "Adaptive Control," Springer Verlag, 1997.
- [5] I.D.Landau, "From robust control to adaptive control," Control Eng. Practice, vol.7, N10, pp.1113-1124, April 2002.
- [6] K. S. Narendra, L. S. Valvani. "Stable discrete adaptive control," IEEE Transactions on Automatic Control, vol. 25, 1980.
- [7] K. S. Narendra, Y. H. Lin. "A new error model for adaptive systems," IEEE Transactions on Automatic Control, vol. 25(3), 1980.
- [8] K.S.Narendra and A.M. Annaswamy. "Stable Adaptive Systems," Englewood Cliffs, NJ: Prentice Hall. 1989
- [9] S.S. Sastry et M. Bodson, "Adaptive Control: Stability, Convergence, and Robustness," Prentice Hall, Englewood Cliffs, NJ, 1989.
- [10] H. Kaufman, I. Barkana, and K. Sobel. "Direct adaptive control algorithms," Springer, New York, 1994
- [11] W.Ghozlane and J.Knani."Modelling and Simulation Using Mathematical and CAD Model of a Robot with Six Degrees of Freedom," CEIT-2016, 4thInternational Conference on Control Engineering & Information Technology.16-18 December 2016-Hammamet, Tunisia. ISBN: 978-1-5090-1055-4 © 2016.On IEEE.
- [12] W.Ghozlane and J.Knani."Nonlinear Control of MIMO System Using Feedback Linearization Control Method and PD Controller for Tracking Purpose," CEIT-2017, 5thInternational Conference on Control Engineering & Information Technology on IEEE.17-19 December 2017-Sousse, Tunisia.
- [13] W.Ghozlane and J.Knani. "Non Linear Control via Input-Output Feedback Linearisation of a Robot Manipulator," Advances in Science, Technology and Engineering Systems Journal Vol.3, No.5, 374-381.2018.
- [14] L. Sciacivco and B. Siciliano, "Modeling and control of robot manipulators," 2nd edition, Springer-Verlag London Limited, 2000.
- [15] A. Isidori. "Nonlinear Control Systems," Springer Verlag, 1989.
- [16] W. Li J. J. E. Slotine. "Applied Nonlinear Control," Prentice Hall, 1991.
- [17] H. Khalil. "Nonlinear Systems," Prentice Hall, Upper Saddle River, Second Edition, 1996
- [18] Nelles. O, "Nonlinear system identification," Springer, 2001.
- [19] A. Astolfi, D. Karagiannis, and R. Ortega. "Nonlinear and adaptive control with applications, Communications and Control Engineering," Springer-Verlag, 2007.
- [20] J.P. Corriou. "Process Control Theory and Applications," Springer-Verlag London 2004.
- [21] S. Skogestad and I. Postlethwaite. "Multivariable Feedback Control. Analysis and Design," Wiley, Chichester . New York . Brisbane. Toronto . Singapore, Second Edition . 2001.
- [22] Ortega and M.W. Spong. "Adaptive motion control of rigid robots," In Proc. IEEE 27th Conf. Decision and Control, pp. 1575-1584. 1988 (Austin, TX).
- [23] J.E.Slotine and W. Li, "On the adaptive control of robot manipulators," Int. J. Robot. Res.6:49-59. 1987.
- [24] W. Li, and J.J.E. Slotine, "An indirect adaptive controller," Sys. Control Lett. 12:259-266. 1989.
- [25] J.J. Craig, P.Hsu, and S.S. Sastry. "Adaptive control of mechanical manipulators," Int. J. Robot. Res. 6:16-28. 1987.

Diagnosis of Parkinson's Disease based on Wavelet Transform and Mel Frequency Cepstral Coefficients

Taoufiq BELHOSSINE DRISSE¹, Soumaya ZAYRIT², Benayad NSIRI³, Abdelkrim AMMOUMMOU⁴

Laboratory Industrial Engineering, Information Processing and Logistics (GITIL)^{1,2,4}

Faculty of Science Ain Chok, University Hassan II, Casablanca, Morocco

Research Center STIS, M2CS, Higher School of Technical Education of Rabat (ENSET)³

Mohammed V University in Rabat, Morocco

Abstract—The aim of this study presented in this paper is to determine the choice of the appropriate wavelet analyzer with the method of extraction of MFCC coefficients for an assistance in the diagnosis of Parkinson's disease. The analysis used is based on a database of 18 healthy and 20 Parkinsonian patients. The suggested processing is based on the transformation of the speech signal by the wavelet transform through testing several sorts of wavelets, extracting Mel Frequency Cepstral Coefficients (MFCC) from the signals, and we apply the support vector machine (SVM) as classifier. The test results reveal that the best recognition rate, which is 86.84%, is obtained by the wavelets of level 2 at 3rd scale (Daubechie, Symlet, ReverseBior or BiorSpline) combination-MFCC-SVM.

Keywords—Parkinson disease; discrete wavelet transform; MFCC; Support Vector Machine (SVM)

I. INTRODUCTION

The history of Parkinson's disease began in 1817 by James Parkinson [1]. It results in a slow and gradual destruction of neurons of the brain's dark substance. It is the second most common neurodegenerative disease, behind Alzheimer's disease. The most obvious motor symptoms of the Parkinson's disease are trembling, rigidity, slowness of movement, difficulty with walking, and communication.

Signal processing techniques have evolved swiftly in the last few years in the biomedical field such as respiratory sound analysis, electrocardiography (ECG), and even for the diagnosis of Parkinson's disease.

The acoustic treatment has been used recently in the diagnosis of many diseases. The MFCC for the extraction of cepstral coefficients has been used in the identification of diseases in newborns by Yasmina Kheddache and Chakib Tadj [2] also Takaya Taguchi et al. [3] for the major depressive disorder discrimination and for stress recognition from speech Salsabil Besbes and Zied Lachiri work with a multitaper MFCC features[4], whereas Zied Lachiri had also works on emotion recognition [5,6]. Always at the acoustic treatment we found also Nawel SOUSSI and Adnane CHERIF they work on voice disorders identification [7].

We can opt for some approaches for the detection of Parkinson's disease by the use of different characteristics of speech: work on the short time jitter and shimmer parameters by Mohammad Shahbakhi et al. [8] and by Athanasios Tsanas et al. [9], who has an exactitude of over 90% reported to

discriminate against Parkinson's disease compared to healthy patients.

Many researches have also been used on speech characteristics for the diagnosis of Parkinson's disease such as PLP, MFCC and Rasta-PLP [10-14].

Savitha S. Upadhyaa et al. [10] worked on the detection of Parkinson's disease from the extraction of MFCCs using the multitaper Thomson windowing technique. Orozco - Arroyave et al. [11], obtained a 60% accuracy by extracting the MFCC coefficient as recognition accuracy. Achraf Benba et al. [12] obtained a percentage accuracy (80%) by the combination of MFCC and the SVM [12], on a database of 17 healthy patients and 17 Parkinson patients.

We are interested in the Mel Frequency Cepstral Coefficients (MFCC) method [15], which is a method of extracting parameters according to the Mel scale. In fact, the perception of speech by the human auditory system is based on a frequency scale similar to the Mel scale [16]. The diagnosis of Parkinson's disease from the detection of vocal disorders using MFCC was first suggested by Fraile et al. [17, 18].

In this work, we develop the diagnostic model of Parkinson's disease [12] by the introduction of vocal signal compression of a database [19], which is composed of 18 healthy patients and 20 patients by wavelet transform through the testing of numerous sorts of wavelets, then we will extract the Mel scale cepstral coefficients (MFCC) of the transformed signals, and at the end classification study by vector machine (SVM) which is one of the algorithm of machine learning [20]. We will create a learning base that shows the percentage of 73% of the database and test the entire database to confirm whether patients are ill or not of each wavelet in order to choose the accurate one.

II. WAVELET TRANSFORM

Wavelets were introduced in the early 1980s by Morlet and Grossmann [21]. Then Mallat [22], Daubechies [23] and Meyer [24] established their own mathematical basis for wavelets. The wavelet transform decomposes the signals from a mother wavelet on a family of wavelets dilated by a coefficient of scale "a" inversely proportional to the frequency that enables to get different versions: dilated ones or compressed ones of the window, and translated by a translation coefficient "b" which characterizes the displacement of the window along the time

axis. The continuous wavelet transform (CWT) of a signal $s(t)$ is defined by [25]:

$$W_s(a,b) = \frac{1}{\sqrt{a}} \int_{-\infty}^{+\infty} s(t) \Psi^* \left(\frac{t-b}{a} \right) dt \quad (1)$$

Where $\Psi(t)$ is the mother wavelet, and $\Psi^*(t)$ is the complex conjugate of $\Psi(t)$. In this study, we are interested in discrete wavelets (DWT) because of their simplicity and their reduction of computation time and because, in the CWT, the coefficients of scales and dilations vary in a continuous way in the frequency and time domain of the signal analysed, which involves a significant consumption of the factor of time.

Mallat [22] had proposed an algorithm for the wavelets coefficients calculation which is based on multi-resolution analysis that conceives discrete wavelet transform such as sequence of filter application.

In fact, every signal consists of low frequency components called approximations and high frequency components called details. According to Mallat (1989), we can separate the details and approximations by using a pair of filters H and G which are a complementary low pass filter and a high pass filter. The low pass filter is a scaling function while the high pass filter is a wavelet function. Thus, the multi-resolution analysis allows a multi-scale decomposition of the starting signal by separating, at each level of resolution, the low frequencies (approximations) and the high frequencies (details) of the signal (Fig. 1).

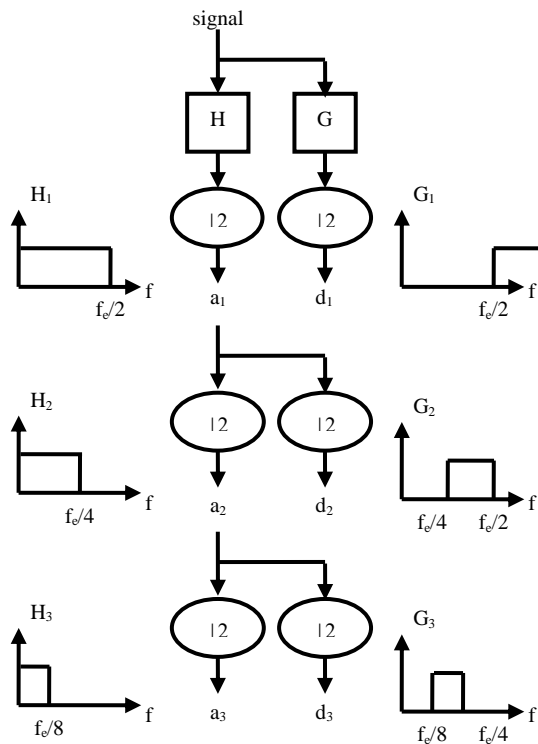


Fig. 1. Multi-Resolution Analysis at 3 Levels of Scales (A_i: Approximations and D_i: Details).

III. MFCC

The MFCC method proposed by Davis and Mermelstein [26] aims at extracting the characteristics parameters of vocal signal.

MFCC analysis consists of exploiting the properties of the human auditory system by transforming the linear scale of frequencies into the Mel [27] scale which provides the most efficient representation of the voice. The block diagram in the following Fig. 2 roughly describes the process of generating MFCC coefficients.

Now that we know the general operation of this procedure, we will explain the main blocks that constitute it.

A. Préaccentuation

The pre-emphasis is a filtering operation of a voice signal $\{s_n, n = 1, \dots, N\}$ in a first-order finite impulse response digital filter whose transfer function $H(z)$ is given by [28].

$$H(z) = 1 - k z^{-1} \quad (2)$$

In this study, we experimentally set the pre-emphasis coefficient k at 0.97 [26].

Thus, the pre-emphasized signal is linked to the signal by the following formula:

$$s'_n = s_n - k s_{n-1} \quad (3)$$

This operation permits to accentuate the high frequencies of the signal.

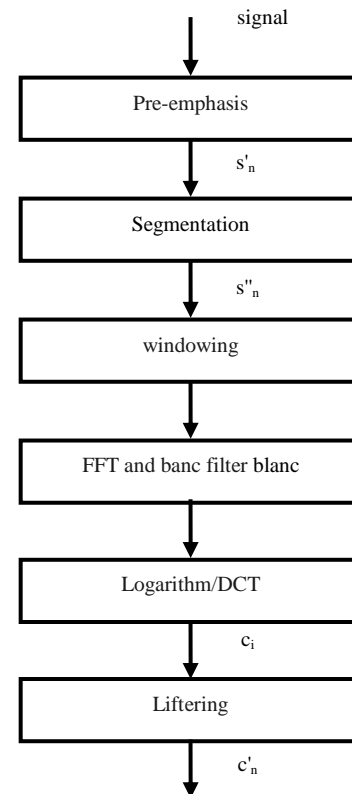


Fig. 2. Process of the Extraction of the Cepstral Coefficients.

B. Segmentation

The voice signal is of a non-stationary nature whereas the signal processing methods use stationary signals. It is therefore necessary, before extracting the parameters of the recognition, to cut the signal into frames of N speech samples in the interval. From 10 to 30 ms, this step enables us to obtain, for each speech segment, a quasi-stationary signal. The two adjacent frames are overlapped to avoid abrupt frame-to-frame transitions [12].

C. Windowing

The discontinuities at the ends of the frames are produced by the segmentation. The purpose of the windowing is to reduce these discontinuities of the signal by multiplying the samples $\{n = 1, \dots, N\}$ of each frame of the vocal signal by a window of hamming. The Hamming window is given by the following equation [29, 30]:

$$s'_n = \left\{ 0,54 - 0,46 \cos\left(\frac{2\pi n}{N-1}\right) \right\} s_n \quad (4)$$

This advantage of this window is that its frequency resolution is high and its secondary spectral lobe is very small compared to its primary lobe (attenuation of -43 dB) [31].

D. FFT

This phase turns the speech signal into a frequency domain [26] with the formula (5), with $n = 0, \dots, N-1$.

$$S_n = \sum_{k=0}^{N-1} s_k e^{-j2\pi \frac{kn}{N}} \quad (5)$$

E. Mel Filtering with Filter Bank

The MFCC method is a method for extracting parameters according to the Mel scale in the frequency domain. Indeed, the perception of speech by the human auditory system is based on a frequency scale similar to the Mel scale. This scale is linear at low frequencies and logarithmic at high frequencies and is given according to the following equation:

$$\text{Mel}(f) = 2595 \log_{10} \left(1 + \frac{f}{700} \right) \quad (6)$$

F. Logarithm and DCT

The MFCC coefficients can be calculated directly by applying the discrete cosine transform (DCT) of the logarithms of the energies obtained by M triangular filters (In this study we have set M to 20) [29, 30]:

$$c_i = \sqrt{\frac{2}{N}} \sum_{j=1}^M m_j \cos\left(\frac{\pi i}{N}(j-0,5)\right) \quad (7)$$

With i as the number of coefficients to extract, and N as the number of triangular filters

G. Liftering

The higher order of the cepstral coefficients is too small. To overcome this problem, we use the liftering in order to raise the cepstrum which consequently increase the amplitudes so that they become quite similar [29, 30].

$$c'_n = \left(1 + \frac{L}{2} \sin\left(\frac{\pi n}{L}\right) \right) c_n \quad (8)$$

Where, L is the Cepstral sine lifter parameter. In this study we used $L = 22$ [29].

IV. CLASSIFIER SVM

Support Vector Machine (SVM) is a class of machine learning method (kernel learning method [32]) developed by Vapnik and al. in the early 1990s [33]. In the classification problems with small samples, the SVM is considered as one of the most powerful tool.

SVM can transform a nonlinear separable problem into a linear separable problem with different kernel functions by projecting the training set into the feature space and then constructing a hyperplane that maximizes the margin between the data [34, 35] for classifying the test samples. The function of the hyperplane can be described as:

$$f(x) = wx + b \quad (9)$$

Where w is a normal vector of the hyperplane and b is a variable.

Supposing that the training set can be described as:

$$S = \{(x_1, y_1), (x_2, y_2), \dots, (x_n, y_n)\}$$

$x_i \in R_n, i=1, 2, \dots, n, y_n \in \{-1, 1\}$ is the class label for x_i and n is the number of the training sample.

With the training set S, the optimal w and b can be obtained by solving the following optimal problem by associating a multiplier of Lagrange [36]:

$$\left\{ \begin{array}{l} \min \psi(w) = \frac{1}{2} \|W\|^2 + C \sum_{i=1}^N \xi_i \\ y_i [W \times K(x_i, x_j) + b] + \xi_i \geq 1; i=1, 2, \dots, N \end{array} \right\} \quad (10)$$

Where W is the weight vector and b is the bias, both of which are determined only by the training samples. The regular parameter C is a penalty factor, which can balance the model complexity and empirical risk. In addition, ξ_i 's are positive parameters called slack variables, which represent the distance between the misclassified sample and the optimal hyperplane.

Function $K(x_i, x_j)$ is the kernel function, we represent among them:

- Linear kernel (simple produit scalaire):

$$K(x_i, x_j) = (x, x_i) \quad (11)$$

- Radial Basis Function (RBF) kernel:

$$K(x_i, x_j) = \exp\left(-\gamma \|x_i - x_j\|^2\right) \quad (12)$$

- Polynomial kernel:

$$K(x_i, x_j) = (x_i \cdot x_j + c)^2 \quad (13)$$

Then $f(x)$ can be computed with the following formula:

$$f(x) = \sum_{i=1}^n \alpha_i * y_i K(x_i, x_j) + b \quad (14)$$

Where α_i^* are the no nulls α when $\alpha = (\alpha_1, \dots, \alpha_T)$ and T is the Lagrange multiplier vector.

V. METHODOLOGY

This study intends to determine the performance of the SVM classifier by implanting a block based on the wavelet transform before the extraction of the MFCC coefficients for an accurate diagnosis of the Parkinson's disease (see Fig. 3):

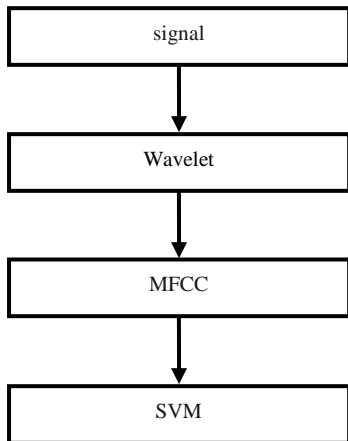


Fig. 3. Process of Diagnosis of Parkinson's Disease.

Our methodology for fulfilling the objectives of this study, which is based on the combination of wavelet choice, MFCC and the classifier SVM, functions in two phases: learning phase and test phase, as shown in Fig. 4, from a database [19] composed of 18 healthy patients and 20 Parkinson's patients. During the learning phase, the vocal signals, after the wavelet application and the extraction of the MFCC coefficients, enables us to obtain a model for the sick patients and sound ones. During the test phase and even after the application of the wavelets and the extraction of the MFCC coefficients, the classifier makes the membership decision based on the similarity between the model established during the training and the test.

VI. RESULTS

This study intends to choose the analyst wavelet. The criterion of choosing the best wavelet remains a problem to be determined. Unfortunately, there is no wavelet that is better than the others. It all depends on the application. In some cases,

the simplest wavelet (Haar) will be optimal. For other applications, it will be the worst choice.

To determining the performance of the SVM classifier, we implant a block based on the discrete wavelet transform before the extraction of the MFCC coefficients in order to have an accurate diagnosis of Parkinson disease (see Fig. 4).

We make use of the database [19] which consists of 20 recordings of patients affected by Parkinson disease and 18 sound ones. They all utter the vowel "a".

We apply the multi-resolution analysis algorithm of Mallat (Fig. 1) by using different analysts wavelets (see Table I) with this vocal signals, then the extraction of the cepstral coefficients at the Mel scale, and at the end as classification by SVM.

Fig. 5 presents wavelet and scaling functions of each wavelet in Table I, at the level 2 (db2, coif2, sym2 ...).

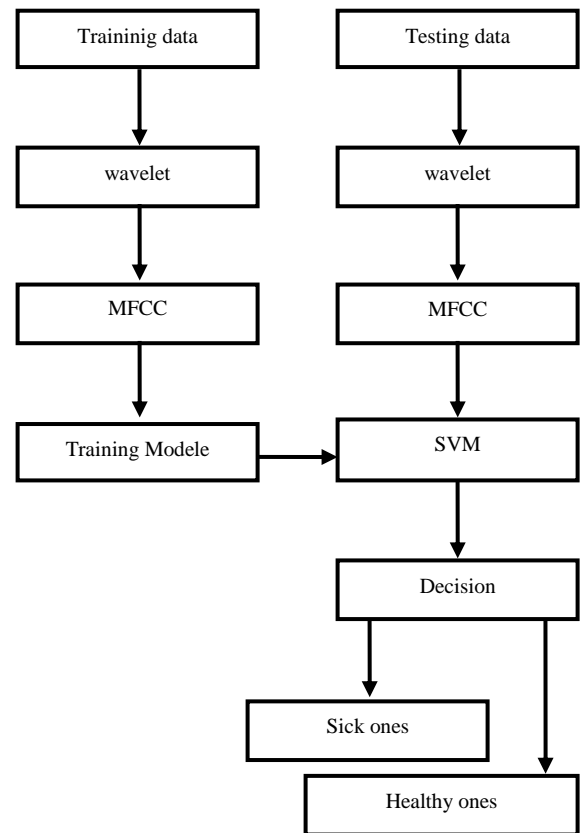


Fig. 4. The Pricipe of Parkinson's Disease Classification.

TABLE I. WAVELETS FAMILIES

Wavelet Families	Wavelets
Daubechies	db1, db2 and db3
Coiflets	coif1, coif2 and coif3
Symlets	sym1, sym2 and sym3
Discrete Meyer	dmey
BiorSplines	bior1.1, bior1.3 and bior1.5
ReverseBior	rbio1.1, rbio1.3 and rbio1.5

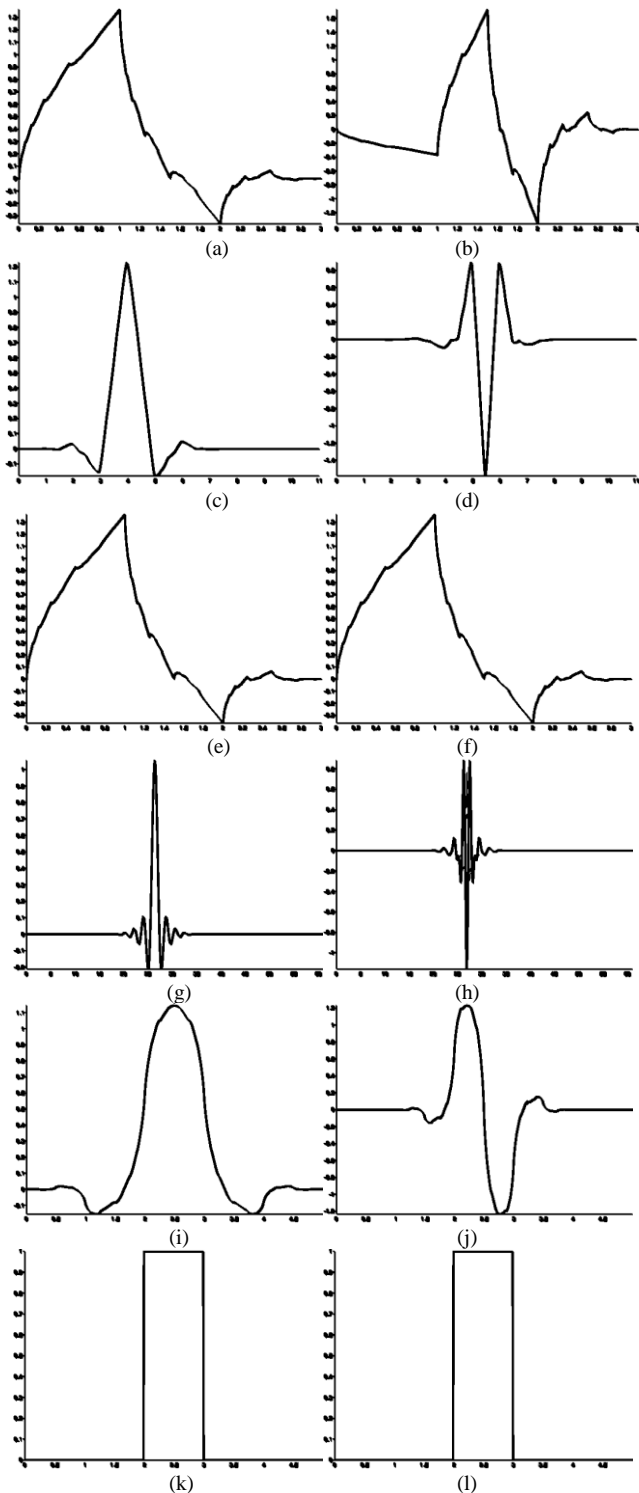


Fig. 5. Wavelet and Scaling Functions Respectively (a, b: Daubechies – c, d: Coiflets – e, f: Symlets – g, h: Discrete Meyer – i, j: BiorSplines – k, l: ReverseBior).

In the first phase, we transform these recordings using the discrete wavelets. Fig. 6(a) presents the vocal signal of one patient before the compression and after using the different types of DTW; (b) presents a zoom at the two representations of the signal.

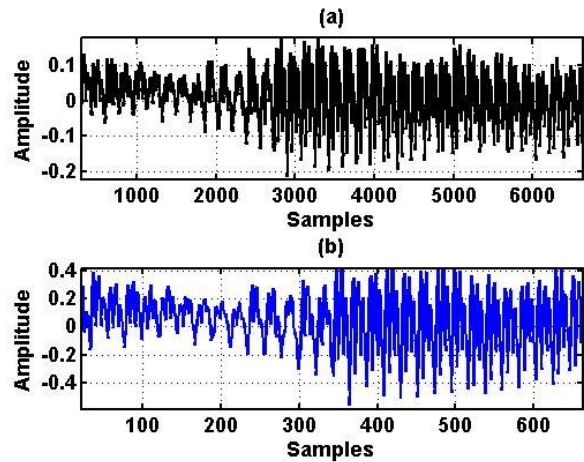


Fig. 6. (a) A Zoom of Speech before Compression. (b) A zoom of Speech after Compression using.

At the second phase, the approximation a_3 of each DWT will be the input to the MFCC block in which we extract the first 12 MFCC coefficients of each patient using the program "Htk mfcc matlab" [37]. We take only the 12 first coefficients because after that the Accuracy starts to decrease [12]. These coefficients are the characteristics on which we will rely to make a classification in order to have an accurate diagnosis. The MFCC contains a large number of frames that require significant processing time for classification and that prevent an accurate diagnosis [27]. To solve this problem, we calculated the average value of these images to get the voiceprint. Fig. 7(a) presents the 12 coefficients of MFCC and voiceprint for a healthy patient, whereas; (b) presents coefficients of MFCC and voiceprint for a patient affected by Parkinson disease.

The third phase aims at classifying sick and sound patients. To achieve the goal, we create training base (73%) of the database. Then we do a diagnostic test on the whole data using the training base of (73%), with SVM classifier with the linear kernel.

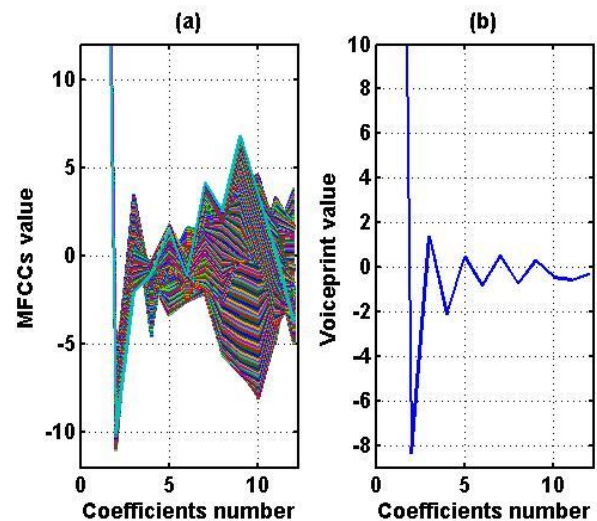


Fig. 7. (a) MFCC Value of Patient. (b) Voiceprint Value of Patient.

Measures such as accuracy, sensitivity and specificity were calculated using the following formula in order to measure the performance of the classifier [38, 39]:

$$\text{Accuracy} = \frac{\text{TN} + \text{TP}}{\text{TP} + \text{TN} + \text{FP} + \text{FN}} \quad (15)$$

$$\text{Sensitivity} = \frac{\text{TP}}{\text{TP} + \text{FN}} \quad (16)$$

$$\text{Specificity} = \frac{\text{TN}}{\text{TN} + \text{FP}} \quad (17)$$

With:

- TP a true positive (sound patients who were correctly classified).
- TN a true negative (patients affected by Parkinson disease who were correctly classified).

- FP a false positive (patient affected by Parkinson disease who was incorrectly classified).
- FN a false negative (sound patients who were incorrectly classified).

Percentage calculations of accuracy, sensitivity, and specificity of all the recordings from the training base that was created between the MFCC block output and the Input of the SVM block (of 73%) are given in following Table II.

Former process of diagnosis of Parkinson's disease published in the studies of Achraf [12] who based his study on MFCC without using wavelet reached 80% of accuracy whereas our study that used several wavelets before the extraction of the cepstral coefficients achieved an accurate more than 80% as shown in Table II.

The accurate of 86.84% as reached at the level 2 and at the 3rd scale of some wavelet which are: daubechie, symlet, Bior Splines and Reverse Bior.

TABLE II. ACCURACY, SENSITIVITY AND SPECIFICITY OF THE DIFFERENT WAVELETS AT THE FIRST 5 SCALES

Scale wavelet	Accuracy (%)					Sensitivity (%)					Specificity (%)				
	1	2	3	4	5	1	2	3	4	5	1	2	3	4	5
db1	28,95	65,79	84,21	81,58	78,95	33,33	55,56	94,44	94,44	94,44	25,00	75,00	75,00	70,00	65,00
db2	76,32	78,95	86,84	81,58	81,58	83,33	77,78	94,44	94,44	100,00	70,00	80,00	80,00	70,00	65,00
db3	73,68	76,32	78,95	84,21	76,32	83,33	77,78	94,44	94,44	94,44	65,00	75,00	65,00	75,00	60,00
coif1	76,32	73,68	84,21	84,21	78,95	88,89	83,33	100,00	94,44	100,00	65,00	65,00	70,00	75,00	60,00
coif2	76,32	76,32	81,58	78,95	78,95	88,89	77,78	94,44	88,89	88,89	65,00	75,00	70,00	70,00	70,00
coif3	76,32	84,21	84,21	81,58	78,95	88,89	88,89	94,44	94,44	100,00	65,00	80,00	75,00	70,00	60,00
sym1	71,05	81,58	81,58	81,58	78,95	83,33	94,44	94,44	94,44	94,44	60,00	70,00	70,00	70,00	65,00
sym2	76,32	78,95	86,84	81,58	81,58	83,33	77,78	94,44	94,44	100,00	70,00	80,00	80,00	70,00	65,00
sym3	73,68	76,32	78,95	84,21	76,32	83,33	77,78	94,44	94,44	94,44	65,00	75,00	65,00	75,00	60,00
dmey	76,32	68,42	78,95	81,58	73,68	77,78	72,22	88,89	94,44	100,00	75,00	65,00	70,00	70,00	50,00
bior1.1	71,05	65,79	81,58	78,95	76,32	83,33	55,56	94,44	88,89	88,89	60,00	75,00	70,00	70,00	65,00
bior1.3	73,68	78,95	86,84	78,95	78,95	83,33	88,89	94,44	88,89	94,44	65,00	70,00	80,00	70,00	65,00
bior1.5	73,68	73,68	78,95	81,58	81,58	83,33	77,78	94,44	94,44	94,44	65,00	70,00	65,00	70,00	70,00
rbio1.1	71,05	65,79	81,58	81,58	78,95	83,33	55,56	94,44	94,44	94,44	60,00	75,00	70,00	70,00	65,00
rbio1.3	78,95	71,05	86,84	81,58	81,58	83,33	77,78	94,44	94,44	100,00	75,00	65,00	80,00	70,00	65,00
rbio1.5	76,32	76,32	78,95	78,95	78,95	83,33	77,78	94,44	94,44	100,00	70,00	75,00	65,00	65,00	60,00

VII. CONCLUSION

In this article, we have presented a sample of Parkinson's disease based the extraction of MFCC coefficients from a database of recordings of sick patients and sound ones. The transformation of vocal signals is treated by numerous types of DWT by the first five scales approximation which will be injected into the MFCC block in order to extract the 12 cepstral coefficients each time. These coefficients are applied in the classification using the SVM classifier with a learning base which is 73% of the database. When we do a test with testing data that contain all the recording we obtain an accuracy of 86% which is higher than the results achieved in the block without wavelet. From that we can conclude that working with the discrete wavelet transform increases the accuracy of the classifier at the level 2 and at the 3rd scale while using daubechie, symlet, biorsplines and Reverse Bior. We conclude that there is no need to work with the 4 and 5 scale because from the 3rd scale, the accuracy starts to decrease.

REFERENCES

- [1] James Parkinson "Anonymous an Essay on the Shaking Palsy". 1817. London Medical and Physical Journal. 1817: 38.
- [2] Yasmina Kheddache, Chakib Tadj "Identification of diseases in newborns using advanced acoustic features of cry signals", BiomedicalSignalProcessingandControl April 2019, Pages 35-44.
- [3] Akaya Taguchi, Hirokazu Tachikawa, Kiyotaka Nemoto, Masayuki Suzuki, Toru Nagano, Ryuki Tachibana, Masafumi Nishimura and Tetsuaki Arai, "Major depressive disorder discrimination using vocal acoustic features", Journal of Affective Disorders, 1 January 2018, Pages 214-220.
- [4] Salsabil Besbes and Zied Lachiri, "Multitaper MFCC Features for Acoustic Stress Recognition from Speech" International Journal of Advanced Computer Science and Applications(ijacsa), 8(3), 2017.
- [5] Farah Chenchah and Zied Lachiri, "Acoustic Emotion Recognition Using Linear and Nonlinear Cepstral Coefficients". (IJACSA) International Journal of Advanced Computer Science and Applications, Vol. 6, No. 11, 2015.
- [6] Asma Mansour and Zied Lachiri, "SVM based Emotional Speaker Recognition using MFCC-SDC Features". (IJACSA) International Journal of Advanced Computer Science and Applications, Vol. 8, No. 4, 2017.
- [7] Nawel SOUISSI and Adnane CHERIF, "Artificial Neural Networks and Support Vector Machine for Voice Disorders Identification". (IJACSA) International Journal of Advanced Computer Science and Applications, Vol. 7, No. 5, 2016.
- [8] Mohammad Shabbakhi, Danial Taheri Far, Ehsan Tahami "Speech analysis for diagnosis of Parkinson's disease using genetic algorithm and support vectormachine". J. Biomed. Sci. Eng. 7 (March) (2014) 147-156. Speech analysis for diagnosis
- [9] Athanasios Tsanas, Max A. Little, Patrick E. McSharry, Jennifer Spielman, Lorraine O. Ramig "Novel speech signal processing algorithms for high-accuracy classification of Parkinson's disease". IEEE Trans. Biomed. Eng. 59 (No. 5 (May)) (2012) 1264-1271.
- [10] Savitha S. Upadhyaya, A.N. Cheeranb, J.H. Nirmal "Thomson Multitaper MFCC and PLP voice features for early detection of Parkinson disease" Biomedical Signal Processing and Control 46, 293-301
- [11] J.R. Orozco-Arroyave, et al. "Perceptual Analysis of Speech Signals From People With Parkinson's Disease". IWINAC 2013, Part I, LNCS 7930, Springer-Verlag Berlin Heidelberg, 2013, pp. 201-211.
- [12] Achraf Benba, Abdelilah Jilbab, H. Ahmed, Sara Sandabad "Voiceprints analysis using MFCC and SVM for detecting patients with Parkinson's disease". IEEE 1st International Conference on Electrical and Information Technologies ICEIT'2015, 2015, pp. 300-304.
- [13] Achraf Benba, Abdelilah Jilbab, Ahmed Hammouch "Discriminating between patients with Parkinson's and neurological diseases using cepstral analysis". IEEE Trans. Neural Syst. Rehabil. Eng., 24 (10) (2016), pp. 1100-1108
- [14] Laureano Moro Velázquez, Jorge Andrés Gómez-García, JuanIgnacio Godino-Llorente, Jesús Villalba, Juan Rafael Orozco-Arroyave, Najim Dehak, "Analysis of speaker recognition methodologies and the influence of kinetic changes to automatically detect Parkinson's Disease", Applied Soft Computing, January 2018, Pages 649-666.
- [15] S. Davis and P. Mermelstein "Comparison of parametric representations for monosyllabic word recognition in continuously spoken sentences" IEEE Transaction On Acoustics, Speech and Signal Processing, vol28, pp. 357-366, August 1980.
- [16] J. W. Picone "Signal Modeling Techniques in Speech Recognition" Proceeding of the IEEE, vol. 81, pp. 1215-1247, 1993.
- [17] R. Frail, JI. Godino-Llorente, N. Saenz-Lechon, V. Osma-Ruiz, C. Fredouille, "MFCC-based remote pathology detection on speech transmitted through the telephone channel" Proc Biosignals, Porto, 2009.
- [18] A. Jafari, "Classification of Parkinson's disease patients using nonlinear phonetic features and Mel-frequency cepstral analysis" Biomed. Eng. Appl. Basis Commun, Vol. 52, no. 4, 2013.
- [19] Erdogdu Sakar, B. Isenkul, M., Sakar, C.O., Sertbas, A., Gurgun, F., Delil, S., Apaydin, H., Kursun, O., "Collection and Analysis of a Parkinson Speech Dataset with Multiple Types of Sound Recordings", IEEE Journal of Biomedical and Health Informatics, vol. 2013 Jul; 17(4):828-34.
- [20] Alzubi, J., Nayyar, A., & Kumar, A. "Machine learning from theory to algorithms: an overview". In Journal of Physics: Conference Series (Vol. 1142, No. 1, p. 012012). IOP Publishing. (2018, November).
- [21] A. Grossman and J. Morlet, "Decomposition of hardy functions into square integrable wavelets of constant shape" SIAM, pp. 723-726, 1984.
- [22] S. G. Mallat, "A theory for multiresolution signal decomposition: the wavelet representation". IEEE trans on pattern anal. and machine intell., Vol. PAMI-11, N°7 (1989) pp 674-693
- [23] Daubechies I. "ten lectures on Wavelets". SIAM Publications, 1992
- [24] Yves Meyer "Les ondelettes : Algorithmes et Applications", Edition Armand Colin, 1994.
- [25] Chui CK. "An introduction to wavelets", San Diego, CA: Academic Press, 1992.
- [26] Davis, S., & Mermelstein, P. (1980). "Comparison of parametric representations for monosyllabic word recognition in continuously spoken sentences". Acoustics, Speech, and Signal Processing [see also IEEE Transactions on Signal Processing], IEEE Transactions on, 28(4), 357-366.
- [27] Abdenour Hacine-Gharbi. "Sélection de paramètres acoustiques pertinents pour la reconnaissance de la parole". Thèse d'Université d'Orléans, 2012.
- [28] Furui, S. "Digital speech processing, synthesis, and recognition" (2nd ed.). New York: Marcel Dekker. (2001).
- [29] Achraf BENBA, Abdelilah JILBAB and Ahmed HAMMOUCH. "Voice analysis for detecting persons with Parkinson's disease using MFCC and VQ." The 2014 International Conference on Circuits, Systems and Signal Processing, Saint Petersburg State Polytechnic University, Saint Petersburg, Russia, September 23-25, 2014.
- [30] S. Young, G. Evermann, T. Hain, D. Kershaw, X. Liu, G. Moore, J. Odell, D. Ollason, D. Povey, V. Valtchev, P. Woodland, "The HTK Book (for HTK Version 3.4)," Copyright. 2001-2006, Cambridge University Engineering Department.
- [31] FILIPE VELHO, "SPEAKER RECOGNITION USING THE CONTINUOUS WAVELET TRANSFORM", MONTRÉAL, QUÉBEC university, the 8 MARS 2006.
- [32] Xiao, J., Liu, Y. "Traffic incident detection using multiple-kernel support vector machine". Transportation Research Record: Journal of 171 the Transportation Research Board (2012) 44-52
- [33] V.N. Vapnik, V. Vapnik, "Statistical learning theory", Wiley New York, 1998.
- [34] X.-Y. Wang, H.-Y. Yang, C.-Y. Cui, "An SVM-based robust digital image watermarking against desynchronization attacks", Signal Process. 2008, 88 (9), pp. 2193-2205.

- [35] R. Wang, W. Li, R. Li, L. Zhang, "Automatic blur type classification via ensemble SVM", *Signal Processing: Image Communication* 2018.
- [36] J. Xiao, "SVM and KNN ensemble learning for traffic incident detection", *Physica A* 2018.
- [37] Wojcicki, k. writehtk. In: *Voicebox Toolbox* (2011). <http://www.mathworks.com/matlabcentral/fileexchange/32849-htk-mfcc-matlab/content/mfcc/writehtk.m>
- [38] Achraf BENBA, Abdelilah JILBAB and Ahmed HAMMOUCH. "Hybridization of best acoustic cues for detecting persons with Parkinson's disease," 2nd World conference on complex system (WCCS'14), IEEE, Agadir November 10-12, 2014.
- [39] Achraf BENBA, Abdelilah JILBAB and Ahmed HAMMOUCH. "Voiceprint analysis using Perceptual Linear Prediction and Support vector machines. for detecting persons with Parkinson's disease.", the 3rd International Conference on Health Science and Biomedical Systems (HSBS '14) Florence, Italy, November 22-24, 2014.

Risk Factors for Software Requirements Change Implementation

Marfizah A.Rahman¹, Rozilawati Razali², Fatin Filzahti Ismail³

Center for Software Technology and Management, Faculty of Information Science and Technology
Universiti Kebangsaan Malaysia, Malaysia

Abstract—Requirements change has been regarded as a substantial risk in software development projects. The factors that contribute to the risk are identified through impact analysis, which later determine the planning of the change implementation. The analysis is however not straightforward as the risk factors that constitute requirements change implementation is currently not much explored. This paper identifies the risk factors by firstly collating them qualitatively through a review of related work and a focus group study. The factors are then confirmed quantitatively through a survey in which data is analysed by using Partial Least Squares Structural Equation Modelling (PLS-SEM). The survey comprise of 276 practitioners from software industry who are involved in the impact analysis. The results indicate that User, Project Team, Top Management, Third Party, Organisation, Identification of Change, Existing Product and Planning of Change Implementation are the significant risk factors in planning of requirements change implementation.

Keywords—Requirements change; risk factor; structural equation modeling

I. INTRODUCTION

Changes in system requirements have negative and positive impacts on system development projects. The changes will have a negative impact if the processes are not properly managed [1]. Errors in managing the change requirements may result in project's cost increases, delay in the system development and affecting the system quality [2]. On the other hand, the process will have a positive impact if the changes conducted to the system are successfully implemented. System improvements can improve the level of user trust in the system [3].

Requirements change is one of the crucial risks in software projects [4], [5]. Requirements changes are inevitable in software system development projects. The addition of new requirements and changes to the existing requirements can occur at all stages of the system development process [6]. New requirements come in tandem with technological developments. As such, consumer needs are changing to meet the organisation's policies and operating and business operations environments. The changes occur due to several factors such as errors in original requirements, evolving customer needs, technological changes, and changes in the business environment or organisational policy [6].

Requirements change is proposed through change requests. Dealing with requirements change requests is a decision-intensive process [7], as it involves cost and resources [8].

Deciding whether or not to accept the change request is done by an important team called Change Control Board (CCB). CCB conducts impact analysis before the decision is made by comparing cost and risk [9], [10]. Impact analysis has great benefit in reducing the risks of implementing requirements change [11], [12]. By identifying potential impacts before making a change, the risks of embarking on a costly change can be greatly reduced [11], [13]. To ensure an accurate decision, CCB should be able to analyse the impacts of the identified factors holistically and assess their risk levels. Also, in order to ensure informed decision during impact analysis, CCB needs a predetermined risk factors or criteria to evaluate a requirements change request [14].

The risk factors to be considered in assessing the requirements change requests are however still indeterminate. Previous studies have shown that there are several risk factors that influence the change requirements and thus contribute to the successfulness of their implementation [15], [16]. The studies are more focused on technical aspects [17], instead of the non-technical aspects [18]. This resulted in unreliable and inaccurate decision making in the change request implementation.

Hence, the aim of this paper is to present the risk factors of the requirements change implementation. It focuses on change impact elements. The study uses a partial least square structural equation modelling (SEM) technique. The identified risk factors discussed in this paper were acquired through series of work conducted previously, reported in [19].

The paper is organized as follows: Section 2 provides the related work on the subject matter. Section 3 elaborates the research model and hypothesis. Section 4 briefly explains the methodology used. Section 5 provides the results. Finally, Section 6 concludes the paper with a summary that outlines the main findings and future work.

II. RELATED WORK

Requirements change has been recognised as a major issue in software development projects. One main issue is about how to assess a requirements change request before deciding either to accept or reject it for implementation [20]. The decision has to be made after impact analysis [21], [22], by which the affected elements are identified and scrutinised [23].

Over the past decade, impact analysis has become a major concern among practitioners and researchers in software engineering [8], [20], [24], [25]. For instance, a study has

proposed a tool to ensure an accurate impact analysis by identifying the hardware and software in the current system that are likely to be impacted by the proposed change [26], [54]. Another study developed a tool to determine the planning strategies in assigning human resources to change activities [27]. Both tools however have lack of functions which are to store and retrieve information of past changes [28].

The system is developed for users and based on user requirements. Change requests are triggered by users based on the experiences that they had with the system. When requesting a change, the users must provide information about the current system and clarify the change that they request to the project team [29]. Users must be involved in the process so that they are aware of the system operations after the requested change has been made [30], [54]. Among the identified risks involved is the less user involvement during systems development and inadequate user's knowledge regarding the developed systems [31]. The users also often lack of cooperation with the project team when needed [31], [32], less commitment towards the systems and has a negative attitude towards the system [32].

Later, project team is responsible to bring forward the request to CCB meeting for them to analyse and assess its impacts [54]. The project team plays an important role in system development. Among the risks involved with the project team are low-skilled capability in the development of the system [32]. As such, new members that are involved in the project may have less knowledge about the system that is being developed [32]. This might be due to the limited training given to the project team [33]. Besides that, the project team is also identified to have less experience in system development projects [31]. Experience gives the project team confidence to develop systems. On the other hand, there is also issue regarding the project team's lack of commitment in the system development [31]. During impact analysis, it is important to assess the project team's capability such as experience, motivation, skill and knowledge in order to ensure the feasibility of the change [34].

Besides that, support and commitment from the top management are also essential [31], [32]. Top management is responsible for the implementation of system development. The top management commitment is needed to make the decision of a subject matter. The absence of specific communication channel among the top management may lead to lack of commitment in the project [32]. Besides that, support from top management is also crucial. It is identified that there are top managements that failed to give support when needed, affecting the change requirement process [31].

Furthermore, the degree of dependency on the third party [32] and their involvement in the project [31] also contribute to the risks. The project development also involves third parties such as suppliers and external organisations related to the system. The risk factors that arise are the number of third parties involved [31]. When the number of third parties is large, related management becomes difficult. In addition, the high levels of dependence by the project team to third parties also pose a risk to system development projects [32].

The change request might affect the existing software components such as source code [35], [36], documentation [37], tools [38] and architecture [36], as well as the hardware components such as memory usage [39], performance [12] and platform [40]. There are also risks of complex architecture [4]. Out of all the components, the technology component is identified to have highest risk. Due to that reason, the analysis of a change request must consider not only the people involved but also the hardware and software used in the current system.

The costs and schedules are also important for project implementation. Determining the estimated cost and the schedule is not easy [32]. The cost to implement requirements change is influenced by the number of project team members and consultants as well as project duration, size and scope [41]. In fact, the incorrect or insufficient estimation of cost and schedule may contribute to more risk to the project [31]. On the other hand, optimising the schedule for implementing any requirements change schedule can result in significant time saving [42]. Therefore, it is important to judge the affected and affecting elements accurately to ensure an adequate allocation of time and cost in implementing the change [33], [31]. Strategic planning and technology standards imposed by the organisation also have been found to influence the change implementation [19], [43].

The goal of requirements change is to improve the value of the current software system. However, it triggers the risks in terms of late delivery, cost overrun, low product quality and sometimes failure to the entire software project [44]. As requirements change effort is considered as a project, the risk factors concerning projects also apply to them. Some instances of project risks are inexperienced project team members [33], commitment from team members towards the project and effective communication between team members and users [31].

The review above indicates that there are various elements that are deemed necessary when managing requirements change. As the elements contribute to the success or failure of a requirements change project, they are considered as risk factors. To date, it is uncertain how CCB should analyse the impacts of those risks and subsequently decide the way forward [45]. There are interrelationships between the risks [46]. The significance of these interrelationships needs to be confirmed objectively [4], [5] so that an accurate impact analysis can be made [20].

III. METHODOLOGY

The methodology for this study is the combination of qualitative and quantitative approach (mixed-method) [47], [48]. Fig. 1 illustrates the research design which contains the main activities involved in the study. The qualitative part consists of literature review and focus group study which have been conducted earlier to gather the identified risk factors as well as to confirm them. The findings have been reported in [19]. However, the findings from empirical study was only validated solely through opinion-based perspective, thus it should be refined and strengthen further by confirming the risk factors quantitatively through a large scale survey.

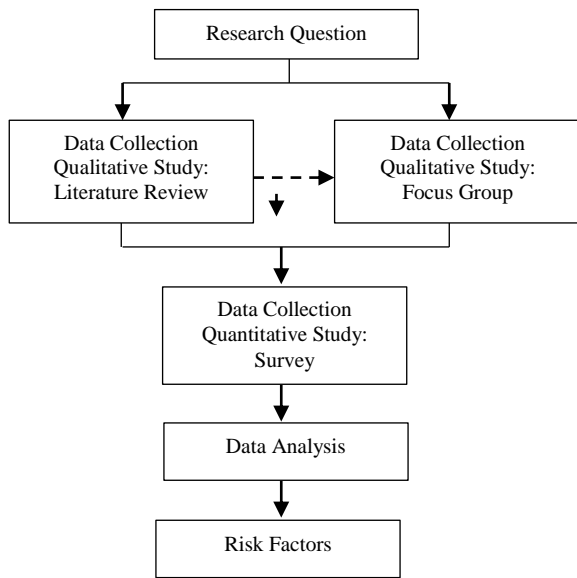


Fig. 1. Research Design.

Hence, a survey was conducted to confirm the existence and significance of the risk factors as the continuation work of one of the stage in the study. The questionnaires consisted of 37 questions covering the identified risk factors. The questions used a 7-point Likert agreement scale from (1) strongly not important to (7) strongly important. A panel of software experts validated the questions. Then, a pilot study was conducted involving 50 software practitioners from the University’s Computer Centre and 10 postgraduate students from the University. The questionnaires were then improved based on the findings received from both exercises.

TABLE I. DEMOGRAPHIC INFORMATION OF RESPONDENTS

Demographic Information	Percentage (%)
Organisation Type	
Government agencies	69.9
Semi-government	17.8
Private companies	12.3
Role	
Project managers	12.0
Project leaders	13.4
Project teams	72.1
Others	2.5
Working Experience Duration	
Less than 5 years	43.8
5-10 years	37.7
11–15 years	10.5
More than 15 years	8.0
Number of project	
Less than 5 projects	51.4
5-10 projects	29.0
More than 10 projects	19.6

The questionnaires were distributed to a number of information technology (IT) and software organisations in Malaysia within the period of 3 months. The organisations comprised of public and private sectors as well as local and multinational companies. There were 400 questionnaires disseminated but only 287 questionnaires were returned. However, 11 out of 287 questionnaires were omitted from the analysis due to incomplete answers. Therefore, analysis was made towards a number of 276 questionnaires which were answered completely. This caused the response rate to be 69.

The demographic information of the 276 respondents are listed in Table I.

The collected data were then analysed by using Partial Least Squares Structural Equation Modelling (PLS-SEM).

IV. MODEL AND HYPOTHESES

Fig. 2 below illustrates a conceptual model of requirements change implementation which was based on previous conceptual model work [19]. The conceptual model was updated with the empirical output from the focus group to produce the model. The model contains eight essential components: User, Project Team, Top Management, Third Party, Organisation (Strategic Planning, Technology Standard), Identification of Change, Existing Product (Software, Hardware) and Planning of Change Implementation.

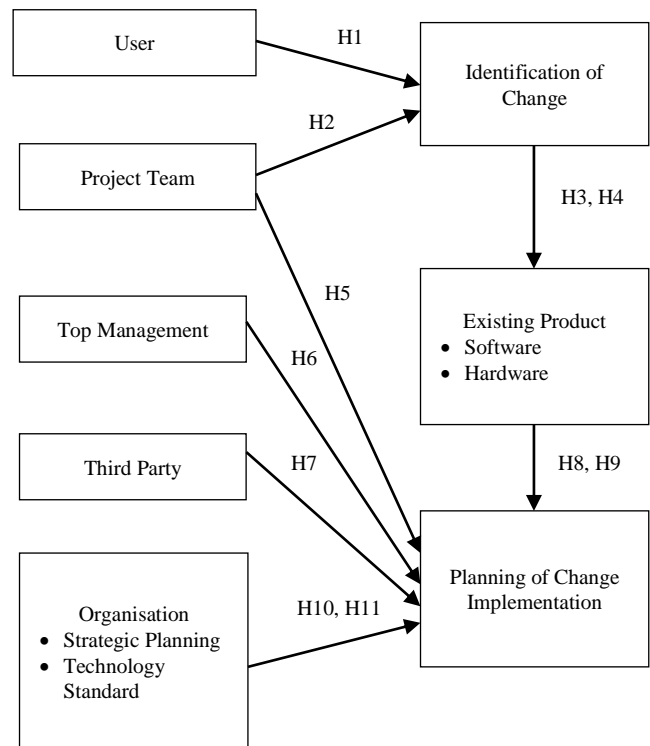


Fig. 2. Conceptual Model of Requirements Change Implementation.

Based on the conceptual model, the hypotheses were derived as depicted in Table II. The related works that support the hypotheses are also included in the table.

TABLE II. HYPOTHESES

	Hypothesis	Related Work
H1	User is positively associated with Identification of Change	[33][31][54]
H2	Project Team is positively associated with Identification of Change	[33][31][54]
H3	Project Team is positively associated with User	[33]
H4	Identification of Change is positively associated with Software	[32]
H5	Identification of Change is positively associated with Hardware	[32], [54]
H6	Software is positively associated with Planning of Change Implementation	[32]
H7	Hardware is positively associated with Planning of Change Implementation	[32]
H8	Software is positively associated with Hardware	[32]
H9	Project Team is positively associated with Planning of Change Implementation	[33][31]
H10	Top Management is positively associated with Planning of Change Implementation	[31]
H11	Third Party is positively associated with Planning of Change Implementation	[31]
H12	Strategic Planning is positively associated with Planning of Change Implementation	[19]
H13	Technology Standard is positively associated with Planning of Change Implementation	[19]

V. RESULTS

The common analysis conducted in PLS-SEM approach comprises of two stages [47]. The first stage is the analysis of measurement model. The purpose of measurement model is to examine the relationships between the latent constructs and their measures. This is to ensure the reliability and validity of the model. On the other hand, the goal of structural model is to assess the relationships between the latent constructs. The following paragraphs explain each model and its analysis, respectively.

A. Measurement Model

The measurement model refers to the relationships between the constructs and the items used to measure them. The analysis evaluates the convergent validity and discriminant validity of the constructs [48]. The convergent validity of a construct is established when the reliability level of the individual items that measure the construct is above 0.70, the composite reliability (CR) of the construct exceeds 0.70 and the average variance extracted (AVE) of the construct exceeds 0.5 [49]. The discriminant validity of a model is assessed by comparing each construct's square root of AVE against its bivariate correlations with other constructs as well as checking cross-loading cases [50].

The results of measurement model are shown in Table III. The descriptions of items used for the measurement are listed in Table IV. According to [51], the factor loading for items

that exceed the level of 0.6 is acceptable in exploratory research, whereas the factor loading of 0.70 to 0.90 is satisfactory [52] and above 0.90 indicates that the items measure the phenomenon accurately. The table shows that most items are satisfactory and above. There are only two items below 0.70, namely PT4 and PL2. They are still retained because they are within the acceptable level.

Convergent validity is the degree to which multiple items measure the same construct under the study. The common approach to examine convergent validity is the factor loadings and AVE. In this study, the AVE values are greater than 0.50. This suggests convergent validity is at the construct level. In addition, the CR values are greater than 0.70. This indicates the reliability is acceptable.

Discriminant validity is the degree to which the measures of different concepts are distinct. The discriminant validity is established between two constructs if the square root of AVE of each one is higher than the shared variance. The shared variances are compared to AVEs as shown in Table V. Since the AVE values of the two constructs are higher than the squared correlation, the discriminant validity among the latent constructs is supported [51].

TABLE III. MEASUREMENT MODEL

Construct	Item	Convergent Validity		
		Loading	CR	AVE
Top Management	TM1	0.942	0.884	0.792
	TM2	0.834		
Third Party	TP1	0.915	0.927	0.864
	TP2	0.944		
Technology Standard	TG1	0.973	0.972	0.945
	TG2	0.972		
Project Team	PT1	0.840	0.899	0.641
	PT2	0.842		
	PT3	0.782		
	PT4	0.670		
	PT5	0.853		
Planning	PL1	0.718	0.856	0.602
	PL2	0.631		
	PL3	0.871		
	PL4	0.858		
Identification	ID1	0.855	0.918	0.789
	ID2	0.910		
	ID3	0.898		
User	US1	0.830	0.894	0.629
	US2	0.820		
	US3	0.786		
	US4	0.819		
	US5	0.703		
Software	SW1	0.801	0.898	0.596
	SW2	0.784		
	SW3	0.707		
	SW4	0.780		
	SW5	0.717		
	SW6	0.835		
Hardware	HW1	0.902	0.895	0.826
	HW2	0.911		
	HW3	0.914		
Strategic Planning	SP1	0.941	0.842	0.863
	SP2	0.917		

TABLE IV. ITEM DESCRIPTION

Construct	Item	Item Description
Top Management	TM1 TM2	Commitment Support
Third Party	TP1 TP2	Number of third party involved Dependency to external agents
Technology Standard	TG1 TG2	Software Hardware
Project Team	PT1 PT2 PT3 PT4 PT5	Skill Commitment Motivation Experience Knowledge
Planning	PL1 PL2 PL3 PL4	Schedule Cost Hardware Resource
Identification	ID1 ID2 ID3	Reasons Type Resource
User	US1 US2 US3 US4 US5	Cooperation Readiness Commitment Knowledge Involvement
Software	SW1 SW2 SW3 SW4 SW5 SW6	Tools Interface Documentation Integration Source code Architecture
Hardware	HW1 HW2 HW3	Memory Platform Performance
Strategic Planning	SP1 SP2	Goal Policy

B. Structural Model

The structural model describes the dependency relationships between the constructs, as presented in Fig. 2. The analysis was done on the explanatory capacity of the model and the statistical significance of the various structural factors. Based on the results, the coefficient of determination (R^2) value of planning (0.4879) was considered as moderate [53]. However, R^2 value of change identification (0.2206), software (0.2725) and hardware (0.2020) was weak.

Apart from R^2 , Q^2 coefficient was also used as a threshold for predictive relevance [51]. The Q^2 coefficient in PLS-SEM was generated from a technique called blindfolding. The generated result of Q^2 for this model was 0.2927. Q^2 values were considerably above zero. This indicates the model's predictive relevance for the construct [51].

After evaluating the explanatory capacity of the structural model, the statistical significance of the various structural coefficients was tested through technique called bootstrapping to generate t-statistic value associated with each path. The outcomes are showed in Table VI.

The results showed that User and Project Team had significant relationship with Identification of Change. These results were similar with [33]. It means that the identification of change highly depended on user and project team. The Identification of Change also had significant relationships with Hardware and Software, which were also supported by [39].

The Project Team, Top Management, Strategic Management, Hardware and Software had significant relationships with Planning of Change Implementation. It means that planning of change implementation should consider the impact of change on project team, top management, strategic management, hardware and software. On the other hand, the relationship between Third Party and Technology Standard with Planning of Change Implementation was not significant.

TABLE V. DISCRIMINANT VALIDITY

	TM	TG	TP	PT	ID	US	PL	SW	HW	SP
Top Management (TM)	0.890									
Technology Standard (TG)	0.439	0.972								
Third Party (TP)	0.155	0.183	0.930							
Project Team (PT)	0.426	0.429	0.080	0.800						
Identification (ID)	0.382	0.436	0.120	0.442	0.888					
User (US)	0.387	0.313	0.070	0.589	0.348	0.793				
Planning (PL)	0.475	0.477	0.152	0.491	0.564	0.404	0.776			
Software (SW)	0.384	0.381	0.110	0.430	0.517	0.372	0.526	0.772		
Hardware (HW)	0.310	0.422	0.115	0.297	0.417	0.293	0.517	0.577	0.909	
Strategic Planning (SP)	0.347	0.541	0.178	0.436	0.429	0.244	0.470	0.339	0.298	0.929

TABLE VI. RESULTS OF PATH COEFFICIENT AND T-VALUE

Hypothesis	Path Relationship	Path Coefficient	t-value	Decision
H1	US → ID	0.135	2.005	Supported
H2	PT → ID	0.362	5.879	Supported
H3	PT → US	0.589	13.360	Supported
H4	ID → SW	0.517	9.242	Supported
H5	ID → HW	0.162	2.408	Supported
H6	SW → PL	0.163	2.649	Supported
H7	HW → PL	0.236	3.370	Supported
H8	SW → HW	0.493	7.585	Supported
H9	PT → PL	0.172	2.916	Supported
H10	TM → PL	0.173	2.733	Supported
H11	TP → PL	0.025	0.637	Not Supported
H12	SP → PL	0.167	2.348	Supported
H13	TG → PL	0.070	0.885	Not Supported

The factors that are significant are important during impact analysis. Therefore, they are considered as risk factors for requirements change implementation. This finding provides empirical evidence that the risks factors can decrease the degree of project success [31].

VI. CONCLUSION AND FUTURE WORK

This study aimed to confirm the risk factors for requirements change implementation. A survey was conducted to collect the data, which were then analysed using PLS-SEM approach. The results showed that user, project team, top management, identification of change, strategic management, hardware and software were significant factors for planning of change implementation. On the other hand, two factors were found not significant for the planning of change implementation; namely the third party and technology standard. As these findings were obtained through quantitative study, the reason of the insignificant results could not be determined clearly. Hence, future work on qualitative approach could be conducted to investigate the underlying reason behind those opinions.

The analysis focused on impact analysis. Therefore, the analysis can be replicated to other determinant risk factors for requirements change implementation. The model could then be extended as a risk measurement model for requirements change initiatives.

ACKNOWLEDGMENT

This work was funded by Fundamental Research Grant Scheme (FRGS/2/2013/ICT01/UKM/02/02).

REFERENCES

- [1] V. Yadav and M. Adya, "Control , Process Facilitation , and Requirements Change in Offshore Requirements Analysis : The Provider Perspective," *Jounal Inf. Technol. Theory Appl.*, vol. 14, no. 3, pp. 30–47, 2013.
- [2] Z. Jiayi, L. Yunjuan, and G. Yuesheng, "The Requirements change Analysis for Different level users," in *International Symposium on Intelligent Information Technology Application Workshops*, 2008, pp. 987–989.
- [3] P. Palvia, A. Patula, and J. Nosek, "Problems and Issues in Application Software Maintenance Management," *J. Inf. Technol. Manag.*, vol. 4, pp. 17–28, 1995.
- [4] Y. Fu, "Impact Propagation and Risk Assessment of Requirement Changes for Software Development Projects based on Design Structure Matrix," *Int. J. Proj. Manag.*, vol. 30, no. 3, pp. 363 – 373., 2012.
- [5] M. R. Strens and Sugden, "Change Analysis : A Step towards Meeting the Challenge of Changing Requirements," in *IEEE*, 1996, pp. 278–283.
- [6] N. Nurmuliiani, D. Zowghi, and S. P. Williams, "Requirements Volatility and Its Impact on Change Effort : Evidence-based Research in Software Development Projects," *AWRE 2006*, 2006.
- [7] A. Aurum and C. Wohlin, "The fundamental nature of requirements engineering activities as a decision-making process," *Inf. Softw. Technol.*, vol. 45, no. 14, pp. 945–954, Nov. 2003.
- [8] B. B. Chua and J. Verner, "Examining Requirements Change Rework Effort: A Study," *Int. J. Softw. Eng.*, vol. 1, no. 3, pp. 48–64, Jul. 2010.
- [9] M. Sirota, "Conceptual Decision Model," *IEEE Int. Work. Intell. Data Acquis. Adv. Comput. Syst. Technol. Appl.*, pp. 69–72, 2003.
- [10] J. Li, M. Li, D. Wu, and H. Song, "An integrated risk measurement and optimization model for trustworthy software process management," *Inf. Sci. (Ny)*, vol. 191, no. 15, pp. 47–60, May 2012.
- [11] S. I. Mohamed, I. a. M. Elmaddah, and A. M. Wahba, "Hybrid-Based Maintainability Impact Analysis for Evolving Systems," *Int. J. Softw. Eng. Knowl. Eng.*, vol. 19, no. 08, pp. 1131–1149, Dec. 2009.
- [12] B. J. Williams and P. B. J. Williams, "Change Risk Assessment : Understanding Risks Involved in Changing Software Requirements," *2006 Int. Conf. Softw. Eng. Res. Pract.*, 2006.
- [13] R. S. Arnold and S. a. Bohner, "Impact analysis-Towards a framework for comparison," *IEEE*, pp. 292–301, 1993.
- [14] P. Rovegard, L. Angelis, and C. Wohlin, "An Empirical Study on Views of Importance of Change Impact Analysis Issues," *IEEE Trans. Softw. Eng.*, vol. 34, no. 4, pp. 516–530, 2008.
- [15] Y. Li, J. Li, Y. Yang, and M. Li, "Requirement-Centric Traceability for Change Impact Analysis: A Case Study," *Springer-Verlag Berlin Heidelb.*, pp. 100–111, 2008.
- [16] S. Park, H. Kim, and D. H. Bae, "Impact Analysis of a Software Process Using Process Slicing," *2009 Ninth Int. Conf. Qual. Softw.*, 2009.
- [17] B. Michalik and D. Weyns, "Towards a Solution for Change Impact Analysis of Software Product Line Products," *Ninth Work. IEEE/IFIP Conf. Softw. Archit.*, pp. 290–293, 2011.
- [18] B. J. Williams and J. C. Carver, "Characterizing Software Architecture Changes : A Systematic Review," *Inf. Softw. Technol.*, vol. 52, pp. 31–51, 2010.
- [19] M. A. Rahman, R. Razali, and D. Singh, "A Risk Model of Requirements Change Impact Analysis," *J. Softw.*, vol. 9, no. 1, pp. 76–81, 2014.
- [20] H. O. Ali, M. Z. A. Rozan, and A. M. Sharif, "Identifying challenges of change impact analysis for software projects," *Int. Conf. Innov. Manag. Technol. Res.*, pp. 407–411, May 2012.
- [21] M. W. Bhatti, F. Hayat, and S. Ahmed, "A Methodology to Manage the Changing Requirements of a Software Project.," in *Information Systems*, 2010, pp. 319–322.
- [22] B. B. Chua and J. Verner, "Examining Requirements Change Rework Effort: A Study," *Int. J. Softw. Eng.*, vol. 1, no. 3, pp. 48–64, 2010.

- [23] S. Park and D. Hwan Bae, "An Approach to Analyzing the Software Process Change Impact Using Process Slicing and Simulation," *J. Syst. Softw.*, vol. 84, pp. 528–543, 2011.
- [24] Y. Ge and L. Bai, "Probability-based Safety Related Requirements Change Impact Analysis," *IEEE*, pp. 719 – 722, 2010.
- [25] H. Hindmarch, A. W. Gale, and R. E. Harrison, "A Support Tool for Assessing the Impact of Design Changes During Built Environment Projects," *IEEE*, pp. 1583–1587, 2010.
- [26] S. Nadi, R. Holt, and S. Mankovskii, "Does the past say it all? Using history to predict change sets in a CMDB," *IEEE 14th Eur. Conf. Softw. Maint. Reengineering*, pp. 97–106, 2010.
- [27] R. C. Lunardi, F. G. Andreis, W. Luis da Costa Cordeiro, and J. Araujo Wickboldt, "On Strategies for Planning the Assignment of Human Resources to IT Change Activities," *IEEE Netw. Oper. Manag. Symp.*, pp. 248–255, 2010.
- [28] M. Rahmouni, C. Bartolini, and H. P. Labs, "Learning from Past Experiences to Enhance Decision Support in IT Change Management," *IEEE*, pp. 408–415, 2010.
- [29] Z. Jiayi, L. Yunjuan, and G. Yuesheng, "The Requirements change Analysis for Different level users," *Int. Symp. Intell. Inf. Technol. Appl. Work.*, pp. 987–989, 2008.
- [30] J. F. Hoorn, E. A. Konijn, H. van Vliet, and G. van der Ver, "Requirement Change: Fear Dictate the Must Haves; Desires the Won't Have," *J. Def. Softw. Eng.*, vol. 80, pp. 328–355, 2007.
- [31] L. Wallace and M. Keil, "Software project risks and their effect on outcomes," *Commun. ACM*, vol. 47, no. 4, pp. 68–73, Apr. 2004.
- [32] R. Schmidt, K. Lyytinen, M. Keil, and P. Cule, "Identifying Software Project Risk: An International Delphi Study," *Jounal Manag. Inf. Syst.*, vol. 17, no. 4, pp. 5–36, 2001.
- [33] W.-M. Han and S.-J. Huang, "An empirical analysis of risk components and performance on software projects," *J. Syst. Softw.*, vol. 80, pp. 42–50, 2007.
- [34] B. B. Chua, "Rework Requirement Changes in Software Maintenance," *Int. Conf. Softw. Eng. Adv.*, pp. 252 – 258, 2010.
- [35] H. Kaiya, K. Hara, K. Kobayashi, A. Osada, and K. Kaijiri, "Exploring How to Support Software Revision in Software Non-intensive Projects Using Existing Techniques," in *IEEE 35th Annual Computer Software and Applications Conference Workshops*, 2011, pp. 327–334.
- [36] U. Vora, "Change Impact Analysis and Software Evolution Specification for Continually Evolving Systems," *2010 Fifth Int. Conf. Softw. Eng. Adv.*, pp. 238 – 243, 2010.
- [37] T. M. Pigoski, "Software Maintenance," in *The Guide to the Software Engineering Body of Knowledge (SWEBOK)*, no. May, 2001, pp. 1–16.
- [38] N. F. Schneidewind, "Predicting risk as a function of risk factors," *Innov. Syst. Softw. Eng.*, vol. 1, pp. 63–70, Mar. 2005.
- [39] N. F. Schneidewind, "Investigation of the Risk to Software Reliability and Maintainability of Requirements Changes," *Proceedings. IEEE Int. Conf. Softw. Maint.*, pp. 127–136, 2001.
- [40] N. Nurmuliani, D. Zowghi, and S. P. Williams, "Using card sorting technique to classify requirements change," *Proceedings. 12th IEEE Int. Requir. Eng. Conf. 2004.*, pp. 224–232, 2004.
- [41] R. Lagerstrom, L. M. von Wurtemberg, H. Holm, and O. Luczak, "Identifying factors affecting software development cost and productivity," *Softw. Qual. J.*, pp. 1 – 23, 2011.
- [42] R. Reboucas, J. Sauve, A. Moura, C. Bartolini, and D. Trastour, "A decision support tool to optimize scheduling of IT changes," *10th IFIP/IEEE Int. Symp. Integr. Netw. Manag.*, pp. 343 – 352, 2007.
- [43] M. A. Rahman, R. Razali, and D. S. V. Singh, "Model Analisis Impak Perubahan Keperluan Perisian," *Asia-Pacific J. Inf. Technol. Multimed.*, vol. 3, no. 1, pp. 33–42, 2014.
- [44] S. Foo and A. Muruganatham, "Software risk assessment model," *IEEE*, pp. 536 – 544, 2000.
- [45] B. Alenljung and A. Persson, "Portraying the practice of decision-making in requirements engineering: a case of large scale bespoke development," *Requir. Eng.*, vol. 13, no. 4, pp. 257–279, Aug. 2008.
- [46] M. A. Rahman, R. Razali, and D. Singh, "A Conceptual Model of Impact Analysis for Requirements Change," *AWERProcedia Inf. Technol. Comput. Sci.*, vol. 03, pp. 763–770, 2013.
- [47] J. C. Anderson and D. W. Gerbing, "Structural Equation Modeling in Practice: A Review and Recommended Two-Step Approach," *Psychol. Bull.*, vol. 103, no. 3, pp. 411–423, 1988.
- [48] D. Gefen and D. Straub, "A Practical Guide To Factorial Validity Using PLS- Graph : Tutorial And Annotated Example," *Commun. ACM*, vol. 16, pp. 91–109, 2005.
- [49] J. Henseler, C. M. Ringle, and R. R. Sinkovics, "The Use Of Partial Least Squares Path Modelling In International Marketing," *Adv. Int. Mark.*, vol. 20, pp. 277–319, 2009.
- [50] W. W. Chin, *The Partial Least Squares approach to Structural*. London, UK: Erlbaum Associates, 1998.
- [51] J. F. Hair, G. T. M. Hult, C. M. Ringle, and M. Sarstedt, *A Primer on Partial Least Squares Structural Equation Modelling (PLS-SEM)*. Thousand Oaks: SAGE Publications, Inc, 2014.
- [52] J. C. Nunnally and I. H. Bernstein, *Psychometric theory*, 3rd Ed. New York: McGraw Hill, 1994.
- [53] J. Cohen, *Statistical Power Analysis for the Behavioral Sciences*. New Jersey: Lawrence Erlbaum Associates, 1988.
- [54] N. Nurmuliani, D. Zowghi, and S. P. Williams, "Requirements Volatility and Its Impact on Change Effort : Evidence-based Research in Software Development Projects.," in *AWRE 2006*, 2006.

Managing and Reducing Handoffs Latency in Wireless Local Area Networks using Multi-Channel Virtual Access Points

Kamran Javed¹, Fowad Talib², Mubeen Iqbal³, Asif Hussain Khan⁴
Faculty of Computing and Information Technology
University of Sialkot, Sialkot, Pakistan

Abstract—The time is era of computer technology and relevant hybrid disciplines to emerge as a multi impact entity in the technological world. In the same stream where user of technology is increasing the expectation from the technology are also expedite, thus users need to have high speed network to support high speed devices, especially in the technical world where palm computers hit the market at its excel. High data transfer rate should be enough supportive to the environment of next generation wireless networks. Mobility is another added factor to high speed connectivity issues. Users for enormous application would like to use a network which is heterogeneous in nature, such as high availability and high bandwidth to avoid issues in real time applications, video streaming and including VoIP and multi-media over the mobile networks. Thus mobile communication access massively relies on the continuous network availability which is done through handoffs, ensures the seamless transfer of device from one AP to another. In this paper, I have extracted the novel approach of multi-channel virtual access points which will nullify or reduce the handoffs latency.

Keywords—Technology; mobility; heterogeneous; bandwidth; video streaming; mobile network; VoIP; handoffs

I. INTRODUCTION

Mobility of the nodes is obsessive compulsion of today's wireless networking system. Mobility requires the mechanism of handoffs for the continuous connectivity. During handoffs the mobile nodes change their connection from one AP to the other and this actually changes the channel of the communication with that particular AP. Changing the channel means that altering the frequency, time slot and code spreading, or combination of them as in TDMA, FDMA, CDMA and hybrid schemes. Changing the channel during the use of multi-media, VoIP, streaming, data or voice calls interruption is experienced or may be in some cases crashing the ongoing communication. The mobile nodes can get connected to any wireless network subject to the availability such as GPRS or WI-Max. These networks requires high data rate to provide good services to mobile nodes, for this purpose a handoff technique called vertical handoff is required to switch between the networks seamlessly, but the focus of this study is handoff between APs rather than inter-network transition [1].

The focus of the study requires the certain parameters to be fulfilled for the seamless switching between the APs for easy

configuration, cheap hardware and for the sake of rapid deployment in the existing system. IEEE 802.11 standards of wireless networks can do the best job for the purpose taking in account the above mentioned requirements. It is well established and well learned fact that the APs transport traffic between the clients (or nodes) and network infrastructure (which is mostly based on the wired network) to establish communication sessions between the nodes.

When a station (in this paper “station” refers to nodes on the move) moves away from an AP, after attaining certain distance, the signal strength drops below the threshold level of the connectivity, the station immediately starts searching for the next nearest AP to sustain its connectivity, unless found, its transceivers stops working means nor sending neither receiving anything, this “blackout” of signals impact the communication going on and multi-media applications. Threshold of the signal strength and finding the new AP's signal majorly depends upon the service range of the AP. Many solutions have been proposed till now for avoiding this problem. Vertical handoffs, as mentioned earlier and the Horizontal handoffs techniques are the alike but differentiated based on the network type being used while transition from one AP to another. Virtual access point is another approach to handle and overcome the issue in wireless networking and is focus of this study. (Grunenberger and Rousseau, 2010). Virtual access points with multi channels will support the purpose of this study, i.e. to provide seamless handoff in wireless networking. Added advantages are increased network capacity and interference avoidance along with its main feature that is handing off station from one AP to another without network traffic disruption. To support network traffic exchange between nodes through multi channels virtual access points a Distributed system protocol (inter-AP) will be helpful to achieve the purpose. Inter-AP protocol specifically in WLANs is supportive in changing the channels while transmitting packets and without interrupting the communication between station and AP.

II. EASE OF USE HANDOFFS PROCESS IN IEEE 802.11 AND RELATED WORK

If the handoffs delay is significant or longer than some milliseconds, it certainly will introduce a disordered behavior and hence will bring up sizeable and considerable disruption in the network traffic. According to (ITU,2003) if the handoff delay excels 150 millisecond it will not be able to provide good quality services or specifically good voice quality in case of

VoIP, as some times searching a new AP in the neighboring location, finding the channel of that AP ready to associate itself with the station can take up to 2 seconds. The handoffs procedure of a station can be depicted in two points.

Letting client search for the new AP available to get itself associated with. Station searching for the AP will send a probe request to locate the vacant channel operating on the AP in range.

On successful acknowledgment the AP then associated with the station through the determination of re-authentication process of association of the new AP for the station.

In this case the MAC handoff is initiated by the station. The above handoffs procedure is based on the Shin et al 2004, which proposed the reduction of latency in handoffs at the MAC layer of OSI Model. In terms of delay there are three components of the MAC layer as probe, authentication & association.

A scheme was proposed for the handoffs through selecting and caching mechanism is focused on the behavior of the station, because in this case the handoffs process is controlled by the mobile station. However proposed method helps in reduce the latency and ascertained that the seamless communication can be achieved in wireless networks. The probing process or channel scanning is the time taken by the AP can be proactive or selective scanning eavesdropping and can be reduced for the authentication information through proactive distribution. (Wu et al, 2007) (Liao and Gao, 2006).

Channels with less network traffic, not overlapped, increased network capacity, reduced interference and latency can be used for the communication between the APs and thus can listen to the neighboring APs. So the virtual access point concept can be used to lever handoffs in multichannel WLANs.

III. VAP CONCEPT

Virtual access point is underneath part of the actual access point and can be thought as an extensible access point as it seems different AP to the node because it ought to be with different identity i.e. SSID that is because the VAP works at the MAC level to replicate the functioning of the real Access point. The real AP can transmit as much VAPs as required, i.e. broadcasting different SSIDs from same physical AP, but here as an example an AP is broadcasting 3 SSIDs (VAPs) this means that information of nodes can be transmitted to 3 other real APs, that is why it can transfer the control visitors of three separate APs, one for the each separate VAP it facilitates. [2].

Virtual access point imitates and behaves like a physical access point. Based on the per radio system a private or dedicated entry way is designed. As already discussed, we can achieve the hand off by introducing two stereos as gadgets of APs to reduce the latency, where one stereo will keep verifying the next and new AP while keeping the connection between node and BSSID on the other stereo. Each stereo can have 16 virtual access points, each with unique entry way ranging from 0 to 15. However only one entry way is allowed according to standards and that is VAP 0. As we know that each entry way is uniquely associated to premeditated user configured service

set identifier and basic service set identifier. Apart from VAP 0 the VAP 1-15 is virtual access Factor x i.e. unique entry way ID. On each stereo every VAP can be independently allowed or impaired apart from the by default used VAP 0 which is always allowed. VAP 1-15 must be configured to be allowed or disconnected however to impair VAP 0 from the BSSID the stereo itself must be impaired from the BSSID because VAP 0 is actually assigned to the BSSID of the actual AP.

The concept and use of VAP is well learned and needs least explanation as of this article is concerned, based on the knowledge base assumption. However nominal explanation of limitations of VAP would be considered to lay solidity in the use of Multi-channel VAPs. As same channel is shared between all APs if client management is concerned. It means that if one station is moving away from one AP, then, that AP will start searching for neighboring AP to proceeds with the handoff, and for this both AP have to share the same channel on both APs, where probability of interference is quite high. In this article the use of VAP with multi-channel techniques is proposed because it addresses the handoff problem just as it wanted to be in seamless handoff and connectivity disruption. In this technique the APs will search for the neighboring AP using different channel from the one it is using to send beacons to the station.

Fig. 1 shows the handoff procedure of a moving station. This shows when a station decided to get away from an AP and moving closer towards neighboring AP, the handoff procedure will initiated and the station which is originally connected to the AP through a dedicated VAP will communicate with the neighboring AP with the aim of shifting the association state to the new AP. This virtual operation will be proceed with the seamless handoff, as station will be receiving the beacons reception from another channel of the same VAP and the shifting of association will occur through the different channel.

Channel Switch Announcement is the mechanism of sending a message encapsulated in AP beacon by AP to the moving station which lets the station know about its intention to change the channel. Normally station stop receiving data from the AP until it re-associates itself to the new AP. In normal circumstances, the station changes its channel when the channel is too noisy, high on traffic or has greater probability of interference. This CSA is element of 802.11 standards. [3].

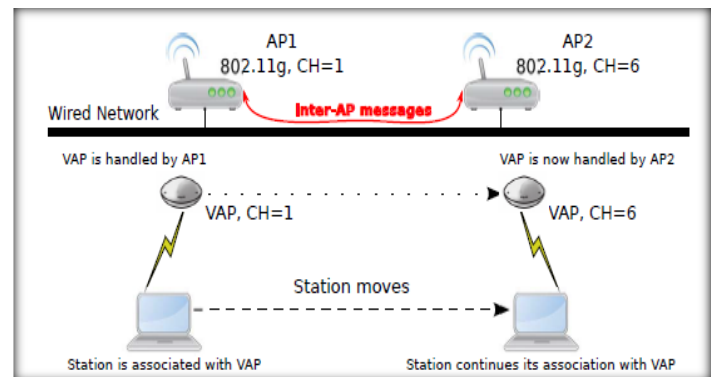


Fig. 1. Mobility Management Handoff and Inter-AP Messages.

Logically when a station is already associated with an AP and moves out of the range of it, it has to re-authenticate, re-associate to the new AP on same or may be on different channel, so the old AP thus changes its channel to transmit the data to the channel of new AP. During this the station will face a downtime as it will not be receiving any beacon from the older or new AP until the handoff procedure is completed and same will be with the APs.

So having virtual access points working not using multiple channels for the transmission will not solve the problem of latency and downtime in handoff procedure. This is why the multi-channel virtual access points are suggested as discussed earlier. Even after this, if there will be no AP at the new location of the station, the standard handoff procedure will be initiated which will also be true for the legacy of 802.11 WLAN devices.

In this section MVAP protocol is analyzed with great details, the communication between Station and both APs will occur in the following manner as shown in the figure (Fig. 2) below.

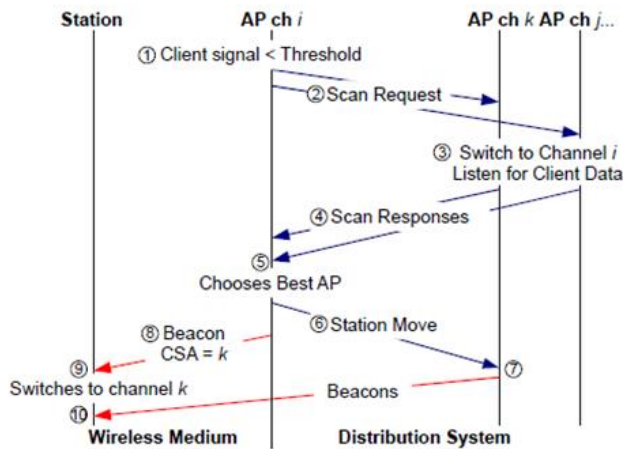


Fig. 2. Multi-Channel VAP.

1) A station (STA) starts moving from the AP_i to which it was associated through channel say (i), AP_i will start recognizing the motion of STA and its dropping signal strength which is decreasing than the threshold.

2) Using Distributed system the AP_i will send a Re-Scan beacon to the neighboring APs, as all the APs have the information about its neighboring APs like MAC address and IP.

3) All APs except (i) will tune themselves to same channel as of AP(i) which is been sent to them by AP(i) in this case channel i. All APs will start listening to the packets receiving from STA.

4) Any AP which will successfully receive beacons from the STA will send a response to Scan Request to AP(i) using the same Distributed System Technique.

5) AP(i) receives the Scan Responses and analyze them according to the direction of the motion of STA, and will choose best AP with better signal strength than its own.

6) Again using Distributed System, AP(i) will send Station Move message to the chosen AP(k), as shown in figure.

7) As soon as AP(k) will receive the Station Move message from AP(i), it will start sending beacons to the station STA.

8) Now AP(i) being nice to the STA will send the beacon of channel switch announcement CSA to switch its channel to k. Thus CSA will force the STA to switch its channel to k where further communication will take place.

9) STA receives the CSA element from AP(i) and switch its channel to k.

10) STA changes its AP and channel consequently without losing connectivity.

IV. IMPLEMENTATION

The implementation of the suggested solution of mVAP will be done using PACMAC i.e. packet manipulation framework tool, designed to capturing and manipulating the 802.11 frames in the network. This tool allows monitoring and injects the manipulated frames for quick prototyping of adaptation or alteration of IEEE 802.11 management and data functions. Maria Eugenia Berezin, Franck Rousseau, Andrzej Duda, updated this tool for the implementation of mVAP scheme in it. This tool is available for download at <http://pacmap.ligforge.imag.fr/> (Maria Eugenia Berezin, 2014).

MadWiFi driver was introduced in this tool, which listens to all the packets in monitoring mode, without filtering them, and at the same time MadWifi injects the manipulated frames in the network and sends them over the wireless medium.

Virtual network kernel interface TUN/TAP interface, used for providing packet reception and transmission for user space programs. [4] TUN stands for network tunnel and TAP is the network tap, network layer and link layer devices respectively. Tap network device used to inject or retrieve the frames from the network, while, here PACMAC uses the TAP tool to inject the incoming data packets over WLAN network in to the kernel space from user space and finally in to the kernel network or IP stack for further processing as shown in Fig. 3. While inter-AP messages uses a normal TCP socket for the exchange of packets.

As per this situation, the question of IP change may arises if there is a change in switching the AP because each access point have its own IP leasing mechanism which is updated in the ARP table of the access point, but here all access points are in the same sub-network [5].

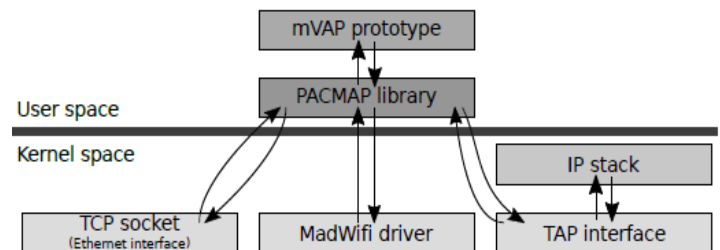


Fig. 3. PACMAP Architecture and M-VAP Implementation.

A. AP to AP Communication and Inter-AP Protocol

As far as communication between different devices is concerned not only the network mechanism among them is concerned but also protocols are to be defined. Protocols are the set of instruction, rules and standards which are to be defined that on what conditions the devices must communicate, likewise, FTP, SMTP, X.25 and still growing list. The communication between APs, between same or multi-vendor devices also needs the protocols to be defined in order to make them communicated with each other.

IAPP (inter access point protocol) or 802.11F provides wireless access point communication and maybe taken as an optional extension to 802.11. The IEEE 802.11 does not postulate the communication between APs as in case of user's roaming displacement from one AP to another AP. According to the requirement of this research, during handoff period the STA's security is vandalized, thus this protocol specifies the implementation of unique association throughout the BSS and ESS and for the secure exchange of STA from one AP to another [6].

Ethernet wired network normally interconnects access point in current settings likewise Distributed system are responsible for the inter AP communication. TCP is the reliable medium of sending messages between APs and includes the following information:

1) *Scan request*: Scan request is initiated by the AP(i) to which station STA is connected with before handoff procedure as shown in Fig. 2 and is sent to the neighboring APs it knows around it. This scan request included all information about the station STA like, MAC address, IP address and station channel currently tuned on, and also BSSID.

2) *Scan response*: Scan Response is acknowledgement or the response from the neighboring APs in turn of receiving scan request from AP(i). This response beacon will contains information about the MAC address & IP address of the station STA, RSSI Received Signal Strength Indicator (to let the AP(i) know whether the signal STA will receive are better than the old AP or below its threshold) and also the channel of itself i.e. channel of the new AP.

3) *Station move*: when the AP(i) will find out an AP with the better RSSI than itself it will choose the best AP and send the station move beacon to that AP. This beacon will include the information about STA MAC & IP addresses along with the beacon interval and channel count.

TCP sockets are used between the AP Ethernet interfaces to implement the inter-AP communication. So that each AP listens on the dedicated port and the communication of messages to other APs is carried out through these sockets.

B. Channel Switch Announcement

As detailed earlier, Channel Switch Announcement is used to by the AP to advertise its channel switching activity [7]. The information included in the CSA beacon transmitted by the AP is as follows:

1) *Channel switch count*: Associated devices with an AP must know that the AP is switching to another channel and it is mandatory to know that when it will switch, for this purpose before switching to new channel, beacons transmitted by the AP includes beacon counts, which decreases respectively with each transmitted beacon.

2) *Channel switch mode*: Channel switch mode includes information about the restrictions and limitation on transmission before switching like band selection and interference due to traffic on adjacent channels.

3) *New channel number*: It must include and advertise information that to which channel number it is switching and the neighboring APs and STAs should re-associate itself to this new channel now.

The channel switch announcement element is formatted is as follows in Fig. 4.

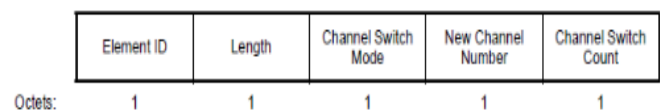


Fig. 4. Beacon Contains CSA Information.

The discussion above is to establish the fact that the each station STA is associated with its own Virtual Access Point and receives custom beacons from the AP and not the normal or universal one which are being transmitted to other APs of course. This element will be the part of beacon only after the new AP is chosen. According to the scenario of this research the AP will transmit 3 consecutive beacons, with the decrement of each transmitted beacon in the CSA count. The interval between the transmitted beacons will be 100ms. When the value after 3 beacons will reach to 0 to 300ms the AP will stop transmitting beacons to the station.

V. EVALUATION AND RESULTS

The scenario chosen to carry out the experiment, three laptops and one desktop is configured to work as per the requirement of the experiment. Two laptops are configured to work as Access Points, however, real access points can also be used in place of laptops, but the results from each node are required so laptops are configured as AP1 and AP2. The third laptop is configured as station STA which is mobile and will move away from one AP towards the other AP to let it undergo handoff process. The desktop computer on a wired network is used to provide internet access to the laptops which are being used as Aps.

Fig. 5 demonstrated the movement of the client (mobile station STA) from AP1 to AP2 this is clear that the STA was first associated to AP1 on channel 1 and then starts moving towards AP2 where it will be receiving beacon on channel 6 which will now become its new default AP. As shown in the diagram it flows back to near AP1 where it is not in range of AP2 and then associated itself back to AP1.

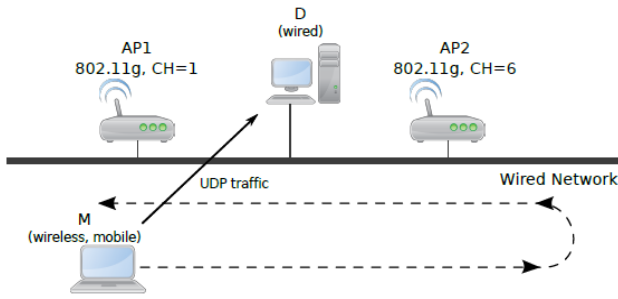


Fig. 5. Experimental Setup.

During all this transition from AP1 to AP2 and then back to AP1, the performance of the handoff can be monitored on Desktop terminal D, where we will receive the UDP from the station. For the sake of experiment, we will consider the packets of VoIP; these packets will be sent in continuous stream of UDP packets not be actual but mimicry of the original VoIP packets and are generated by different audio codecs like G729 & G.728. Voice codecs used for the evaluation in this research are as in Table I.

TABLE I. VOICE CODECS AND BEACON INTERVAL USED IN EVALUATION

Codec	Bit Rate(Kbps)	Voice Payload Size (Bytes)	Interval (ms)
G.728	8kbps	20	20
G.729	16kbps	60	30
G.711	64kbps	160	20

IPref tool is used for the generating the traffic of UDP packets, IPref tool is a network tool for monitoring and tuning. This tool can be used in cross platform tool that can produce standardize performance measurements for very network. The final frame of the UDP packet contains actual payload of audio codec plus 12 bytes reserved for the Real Time Protocol (RTP) as a header.

A. Performance Analysis

The performance in handoffs directly influenced by the latency of the packets arrived when the STA switches the AP and channel. So the time taken between the packet arrivals will be the latency due to handoff procedure. Such analysis is called packet inter-arrival Time or IAT. In terms to equation, this will be denoted by the nth packet and preceding packet n-1.

$$IAT = IAT(n) - IAT(n-1)$$

As shown in Table I, the inter arrival time of the packets is not more than 30ms which justifies the threshold of maximum 150ms of delay which is been thought complementary for the VoIP communication. It is also been noticed that only packet is lost during handoff process due to ARP table actualization. Consequently the transition from AP1 to AP2 or back to AP1 shows no interruption in the VoIP communication. A same situation can be observed in the CDF (cumulative Distribution Function of inter-Arrival Time (IAT) of the UDP packets in the Fig. 6(a,b,c) below, there are three different results for three different audio codec i.e. G.729, G.728 and G.711, respectively.

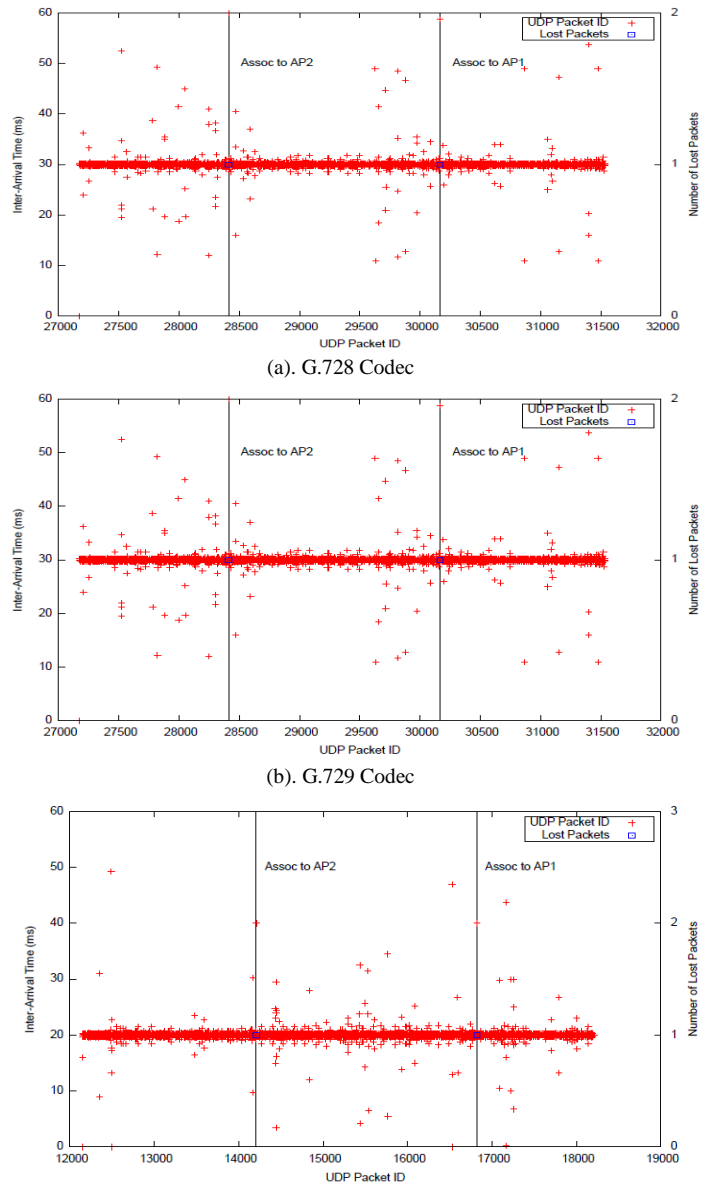


Fig. 6. (c) G.711 Codec.

It can be observed that none of the value of latency in the IAT passes the 20ms, 30ms and 20ms respectively. Statistical analysis will show its, mean, 90th percentile and standard deviation of the noted readings is shown in Table II.

The results in Table II shows the hypothesis developed in the research that multi-channel virtual access points can manage and handle the handoff procedure without interruption in the connectivity of the station to the transmitting APs.

TABLE II. IAT DISTRIBUTION FOR EACH CODEC USED

Codec	Mean	90 th percentile	Std. Deviation
G.728	0.02001	0.02024	0.00072
G.729	0.03001	0.03023	0.00163
G.711	0.02001	0.02024	0.00076

VI. DISCUSSION AND FUTURE WORK

As in this research the solution proposed to use multi-channel virtual access points instead of virtual access points, the proposed solution emphasize on switching the channel while switching the AP. However, it can also be done in a different way that may include some different protocols and techniques. One such solution can be switching the AP without changing the channel, which will produce more reliable results and the IAT can be even better. This can also be done by introducing another wireless card which will be always listening to the packets receiving from the moving station. With new wireless card AP will be able to exchange packets with its client without any interruption while it is scanning for the AP.

The approach used in the solution proposed in this research is based on the better signal strength and reception which is being received by the station at that very instant i.e. instantaneous signal strength, which can arise issue in case of any emergent change of direction of the moving station. For this to overcome, complete analysis of the most likely movement of the station can be helpful for performing handoff. For this Displacement Vector & Pointing Vector from Station to AP it is connected to and the next possible AP to be connected can give somehow deep information such as: historical information and trends about the movement of the station [8].

Finally, a recommendation on the security issues is mandatory at this stage. Authentication process must be included for the new AP, because in most the WLAN technologies, security is the major concerns in the current deployments [9]. The suggestion for the researchers is to ponder on this aspect of security, specifically 802.11i authentication protocol.

VII. CONCLUSION

In this research paper a solution has been presented which emphasizes on the use of multi-channel virtual access points for the 802.11 WLANs. In result of this latency of the handoff procedure is decreased to carry on continuous communication between AP and mobile station. The advantage of low latency will influence in expedite communication especially in stations

using multi-media applications or VoIP communications. This solution is also supported with the inter-AP protocol to send Scan Request to the neighboring AP to let them know about the movement of the station.

Other technicalities to carry out real world experiment included PACMAP framework to monitor and analysis the transmitted beacons and mimicking the VoIP UDP packets. The wireless card used in this experiment was Atheros based chipset, and the PACMAC was supported by the MadWifi driver, in user's space. As shown, three types of codecs used for the experiment, and results shows that the IAT doesn't cross the threshold of 150ms while performing handoff, hence, creating no disruption in the communication.

Concluding arguments included the suggestion of multi-radio environment, adding security features and suggesting a mechanism to trigger the scanning of the neighboring AP and various election routines of the APs. Our next research will be focusing these points, as well as will include vertical handoff techniques and impact of handoffs on the performance of 802.11 in WLANs to build full-bodied solution.

REFERENCES

- [1] Mishra, M. S. a. W. A., 2003. An Empirical Analysis of the IEEE 802.11 MAC Layer Handoff Process. SIGCOMM Comput. Commun, 33(2), pp. 93-102
- [2] Kim, H.-S., Park, S.-H., Park, C.-S., Kim, J.-W. and Ko, S.-J., (2014). Selective Channel Scanning for Fast Handoff in Wireless LAN using Neighbor Graph. Proceedings of ITC-CSCC, Sendai/Matsushima. (), pp.303-316
- [3] Developer Network, 2013. [http://msdn.microsoft.com/en us/ library /aa292197\(v=vs.71\).aspx](http://msdn.microsoft.com/en us/ library /aa292197(v=vs.71).aspx). [Online] Available at: [http://msdn.microsoft .com/enus/library/aa292197\(v=vs.71\).aspx](http://msdn.microsoft .com/enus/library/aa292197(v=vs.71).aspx)
- [4] Anon., 2013. Configuring Virtual Access Points, s.l.: s.n.
- [5] ITU, (2003). International Telephone Connections and International Telephone Circuits. International Telecommunication Union-TG 114.
- [6] Mhatre and K. Papagiannaki, "Using smart triggers for improved user performance in 802.11 wireless networks," in *MobiSys*, 2016.
- [7] Y. Liao and L. Gao, "Practical Schemes for Smooth MAC Layer Handoff in 802.11 Wireless Networks," in *WoWMoM*, 2016.
- [8] Raghavendra, Ramya, Elizabeth M. Belding, Konstantina Papagiannaki and Kevin C. Almeroth, (2017). Understanding Handoffs in Large IEEE 802.11 Wireless Networks. *IMC'07*, October 24-26, 2017, San Diego, California, USA.
- [9] H. Velayos and G. Karlsson, "Techniques to reduce the ieee 802.11b handoff time," in *IEEE ICC*, 2014.

An Enhancement on Mobile Social Network using Social Link Prediction with Improved Human Trajectory Internet Data Mining

B. Suryakumar¹

Ph.D. Research Scholar, Department of Computer Science
NGM College, Pollachi
Tamilnadu, India

Dr. E. Ramadevi²

Associate Professor, Department of Computer Science
NGM College, Pollachi
Tamilnadu, India

Abstract—Generally, the mobile social network has missing and unauthentic links. The prediction of those links is one of the major problems to understand the relationship between two nodes and recommends the potential links to the users derived from the history of user-link interactions and their contextual information. The recommendation problem can be modeled as prediction of the future links between users. Many research works have been developed to understand the relationship between the nodes and construct the models for missing or suspicious links prediction. Among those, Improved Multi-Context Trajectory Embedding Model with Service Usage Classification Model (IMC-TEM-SUCM) has better enhancement on human trajectory data mining by classifying the internet traffic. However, this method requires the prediction of the relationship between the nodes and social links. Hence in this article, the IMC-TEM-SUCM is proposed with the Social Link Prediction (SLP) mechanism for identifying the relationship between two nodes and predicting the stable links. In this technique, a number of nodal features are considered and their influence on the link prediction problem of Foursquare and Gowalla are examined. This extended network is used for computing two features such as optimism and reputation that depict node's characteristics in a signed network. After that, meta-path-based features are considered and their influence of the route length on the problem of link prediction is examined. Moreover, a link prediction process is performed by using the machine learning classification algorithms that use the extracted node-based and meta-path-based features. Also, Cosine coefficient and Jaccard coefficient similarity-based techniques are used for computing the similarity index between any two nodes. A higher similarity indicates a higher chance of forming links between them. Finally, the performance effectiveness of the proposed model is evaluated through the experimental results using different real-world datasets.

Keywords—Mobile social network; improved multi-context trajectory embedding model with service usage classification model; social link prediction; machine learning; cosine coefficient; Jaccard coefficient

I. INTRODUCTION

In modern years, location-based social networks have increased due to the emerging of site-enabled mobile devices. Generally, location-based social networks are a digital mirror to human mobility in physical world since it offers a chance to completely understand the spatial and temporal

activities/behaviors of people's lifestyles [1]. As a result, the popularity of mobile social Apps can support people to communicate with each other, share photos, information and connect with commercial activities. Different mobile industries monetize their services in messaging Apps. Thus, the service usage analytics in messaging Apps or location-based social network becomes essential for commerce since it can support recognize in-App behaviors of end users and so several applications are enabled. Though it provides in-depth analysis into end users and App performances, a primary process of in-App usage analytics are classifying Internet traffic of messaging Apps into different usage types such as services, locations, etc., and outlier or unknown combination of usage.

Many traffic classification methods have been developed by analyzing TCP/UDP port numbers of an IP packet or recreating protocol signatures in its payload [2-3]. But, the challenges were addressed for examining IP packet content since messaging Apps use unpredictable port numbers. Additionally, several mobile Apps use the Secure Sockets Layer (SSL) and its successor Transport Layer Security (TLS) as a building block for encrypted transmissions. Such challenges were tackled by developing data mining solutions to classify the encrypted Internet traffic data generated by messaging Apps into different service usage types. In previous researches, MC-TEM was proposed to analyze the human trajectory data [4]. In this model, CNN was used to learn the parameters. Moreover, IMC-TEM was proposed that uses a frog-leaping optimization algorithm for tuning the parameters which are needed to improve the accuracy of the contextual model and social link prediction [5]. On the other hand, it considers only the characterization of types of contexts for different Apps. It requires Internet traffic classification to jointly analyze service usage behaviour as well to enhance the location recommendation and social-link prediction performances. As a result, IMC-TEM-SUCM was proposed [6] by classifying internet traffic using Random Forest (RF) classifier. However, this method requires the prediction of the relationship between the nodes and social links to find any link failure between two nodes.

Therefore in this paper, the proposed SLP-IMC-TEM-SUCM is proposed to predict the social links for a better understanding of the relationship between two nodes. In this technique, a number of nodal features are considered and their

influence on the link prediction problem of Foursquare and Gowalla are examined. This extended network is used for computing two features such as optimism and reputation that describe nodes characteristics in a network. After that, meta-path-based features are considered and their route length influence on the problem of link prediction is also examined. Moreover, a link prediction process is performed by using the machine learning classification algorithms that use the extracted node-based and meta-path-based features. Also, Cosine coefficient and Jaccard coefficient similarity-based techniques are used for computing the similarity index between any two nodes. A higher similarity indicates a higher possibility of making links between them. Thus, the stable link is predicted to reduce the average delay during packet reception in mobile social networks.

The remaining article is prepared as follows: Section II presents the works related to the social link prediction techniques. Section III explains the proposed methodology. Section IV shows the performance evaluation of the proposed technique. Section V concludes the research work.

II. LITERATURE SURVEY

Efficient routing in mobile social networks [7] was proposed by exploiting friendship relations. In this technique, a new metric was introduced to detect the value of friendships between nodes accurately. According to this metric, the neighbourhood of each node was defined as the set of nodes having close friendly relations with that specific node either directly or indirectly. Moreover, a friendship-based routing was presented to periodically differentiate the friendship relations used in the broadcasting of messages. However, the complexity and maintenance cost of this model was high.

The problem of search with local information was addressed [8] in joint social and communication networks. In this model, the end-to-end delay distribution and success probability were derived to differentiate the delay and success probability on different social links. Moreover, greedy routing algorithms were used to enhance the delay and chain completion success. Next, this analysis was extended to the joint social and communication networks. However, the complexity of this analysis was high.

A link prediction algorithm [9] was proposed on the social network. In this study, two improved algorithms were proposed such as CNGF algorithm based on neighbourhood information and KatzGF algorithm based on the overall information of the network. Moreover, the link prediction algorithm was proposed based on the information about nodes multiple attributes which defects the inactive social network. However, it does not consider the service usage types to improve the LBSN recommendation.

User's location prediction method [10] was proposed in LBSN. In this study, a model was proposed that influences the global temporal preferences and spatial correlation for predictions. Here, global temporal preferences were used to exploiting the historical check-ins of other users that models the temporal reputation of locations. The spatial correlation was used to estimate the distance that a user was willing to stay a site based on his/her current site. However, the effectiveness

was less and required to further improvement based on the user's location.

Characterization of user behavior in the mobile internet [11] was studied. In this study, the mobile user behaviors were classified from three characteristics such as data use, mobility patterns and application use. Also, the traffic heavy users and the mobility pattern were observed as nearly associated with the application access characteristic of the users. Users may be clustered via their application use characteristic and application types may be recognized through an interaction of the users. However, fairness was less and network congestion was not controlled.

A link prediction method in LBSN [12] was proposed by developing social and mobility patterns. In this study, three new methods were proposed by merging social and mobility patterns such are: interior and exterior of commonplaces, familiar neighbours of places and total and partial overlapping of places. However, the location prediction was required to suggest locations that users could stay.

III. PROPOSED METHODOLOGY

In this section, the proposed IMC-TEM-SUCM with SLP algorithm is explained in brief. In this technique, node and meta-paths-based features are considered for predicting the social network links. The link prediction problem of considered datasets is solved based on the following process:

The link prediction problem is modeled as the classification process where there are two classes in which one class is used for the existence of future links and the other class is used for the non-existence of future links. For this case, a number of features namely node-based and meta-path-based features should be defined for utilizing in the classifiers.

- **Node-based Features:** The node-based features are applied on the Foursquare (G_F) and Gowalla (G_G) layer wherein the network infrastructure is modified via giving appropriate signs to the links. Every link in G_F or G_G is given a positive or negative sign by considering two nodes n_1 and n_2 in G_F or G_G . If they pursue each other, then there are two directed links between them and a positive sign is assigned on both directions. If one node follows the other node, then a positive sign is assigned in the actual direction and a negative sign is assigned in the opposed direction. According to this, G_F or G_G becomes a network with both positive and negative signs.

For a given network structure, a priori information on the link existence between a source and the destination node, the difficulty is to understand the sign of this link. Node-based feature involves the reputation that refers to the reputation of a node in the mobile social network. A higher reputation for a node indicates the node becomes more tolerable by other users and is expected to be followed. The reputation value for node n_1 is calculated by considering the positive and negative incoming links to the node. Consider, the number of positive incoming links and the number of negative incoming links to n_1 are $d_{in}^+(n_1)$ and $d_{in}^-(n_1)$. The Normalized Reputation (NR) of n_1 is computed as follows:

$$NR = \frac{d_{in}^+(n_1) - d_{in}^-(n_1)}{d_{in}^+(n_1) + d_{in}^-(n_1)} \quad (1)$$

Another node feature is optimism that can be calculated related to the reputation. Nodes with higher optimism values indicate that they are expected to follow others. The number of positive outgoing links and the number of negative outgoing links from n_1 are denoted as $d_{out}^+(n_1)$ and $d_{out}^-(n_1)$. The Normalized Optimism (NO) of n_1 is computed as follows:

$$NO = \frac{d_{out}^+(n_1) - d_{out}^-(n_1)}{d_{out}^+(n_1) + d_{out}^-(n_1)} \quad (2)$$

Here, the link between n_1 and n_2 are predicted by using common neighbors of these nodes $\{CN(n_1, n_2)\}$ that refers to the number of nodes with links to both n_1 and n_2 . Thus the reputation and optimism values of n_1 and n_2 such as $NR(n_1), NR(n_2), NO(n_1)$ and $NO(n_2)$ are utilized as node-based features.

- **Meta-Path-based Features:** This feature is used for capturing the interlayer connectivity information. A route between two users in a mobile social network has important data about their link such as relationship. Initially, meta-paths between two target nodes are mined up to a fixed path length according to the traversing the target network method like breadth-first search. By using cluster-based meta-path, a meta-path with length 2 from n_1 to n_2 in cluster C is defined as n_1 follows n_x ($x \neq 2$) which is friends with n_2

In this proposed technique, cluster-based meta-paths with length 2, 3 and 4 are employed as features. For each pair of nodes n_1 and n_2 , all cluster-based meta-paths of different lengths that pass via every cluster in G_F or G_G are computed with having one of the following conditions:

- A route from n_1 to C has not more than a length i and located in G_F or G_G . Additionally, there exists a route from C with length 1 which is located on G_F or G_G .
- A route from n_1 to C has not more than a length 1 and located in G_F or G_G . As well, there exists a route from C with not more than length i and is located on G_F or G_G .

Three different lengths are considered for the cluster-based meta-paths along with the above conditions. As a result, a set of six features is obtained for every pair of nodes. Once all features are extracted, Support Vector Machine (SVM), Naive Bayes and K-Nearest Neighbor (KNN) classifiers are used to predict the stable social links. Among these classifiers, SVM creates a set of hyperplanes in a high dimensional space and splits different classes by optimizing the space to the functional margins. Also, Gaussian kernel function maps the actual finite dimensional space into a higher dimensional space. Similarly, Naive Bayes generates the number of algorithms in which the particular feature value is considered as an independent of other features. To train the parameters of this model, maximum-likelihood estimation is used. Another classification method KNN has the K nearest training samples in the feature space and locally approximates the function. A weighted average

of the functions is computed and the value of K is optimized to train this classifier.

Finally, the performance of these classifiers is compared with a number of baseline links prediction methods such as cosine coefficient and Jaccard coefficient similarity methods. These methods compute a similarity index between any two nodes and a higher similarity indicates a higher possibility of making links between them. Thus, the stable link is predicted to reduce the average delay during packet reception in mobile social networks.

IV. EXPERIMENTAL RESULTS

This section presents the experimental results of the proposed SLP-ICM-TEM-SUCM by considering Cosine coefficient and Jaccard coefficient similarity techniques using MATLAB 2018a and compared in terms of accuracy, Mean Squared Error (MSE) and Mean Absolute Error (MAE). Here, two open geo-social networking datasets namely *Foursquare_s* [13] and *Gowalla* [14] are used for link prediction. Table I gives the basic statistics of the considered datasets.

A. Accuracy

It is computed based on the True Positive (TP) and True Negative (TN) among the total number of social links predicted.

$$Accuracy = \frac{TP+TN}{TP+TN+False\ Positive\ (FP)+False\ Negative\ (FN)} \quad (3)$$

Fig. 1 shows the comparison of SLP-ICM-TEM-SUCM for different similarity-based techniques such as cosine coefficient and Jaccard coefficient techniques in terms of accuracy (%). When considering *Gowalla* dataset, the accuracy of the Jaccard coefficient technique is 12.21% higher than Cosine coefficient technique. Similarly, the Jaccard coefficient technique achieves 11.91% higher accuracy than the Cosine coefficient technique. From the analysis, it is observed that the SLP-ICM-TEM-SUCM using Jaccard coefficient-based similarity technique has high accuracy than the Cosine coefficient-based similarity technique for both datasets.

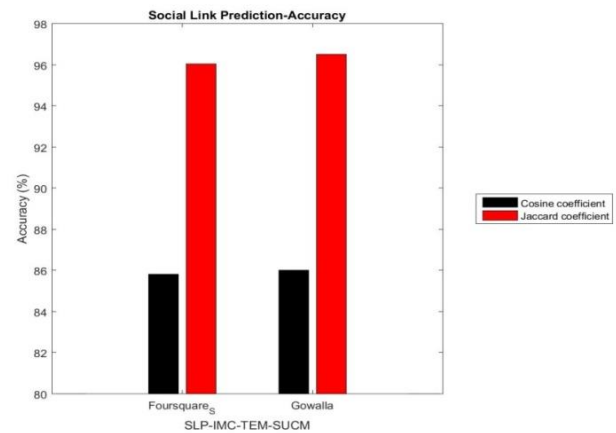


Fig. 1. Comparison of Accuracy.

TABLE I. STATISTICS OF DATASETS

Dataset	No. of Users	No. of Check-ins	No. of Links	No. of Locations
Foursquare _s	4163	483814	32512	121142
Gowalla	216734	12846151	736778	1421262

B. Mean Squared Error (MSE)

It is the expected variation of the errors between the real and predicted values.

Fig. 2 shows the comparison of MSE for SLP-IMC-TEM-SUCM using different similarity-based techniques such as cosine coefficient and Jaccard coefficient techniques. When considering Gowalla dataset, the MSE of the Jaccard coefficient technique is 47.58% less than Cosine coefficient technique. Similarly, the Jaccard coefficient technique achieves 46.22% less MSE than the Cosine coefficient technique. From the analysis, it is observed that the SLP-IMC-TEM-SUCM using Jaccard coefficient-based similarity technique has less MSE than the Cosine coefficient-based similarity technique for both datasets.

C. Mean Absolute Error (MAE)

It defines the mean absolute variation between the real and predicted values.

Fig. 3 shows the comparison of MAE for SLP-IMC-TEM-SUCM using different similarity-based techniques such as cosine coefficient and Jaccard coefficient techniques. When considering Gowalla dataset, the MAE of the Jaccard coefficient technique is 47.37% less than Cosine coefficient technique. Similarly, the Jaccard coefficient technique achieves 46.55% less MAE than the Cosine coefficient technique. From the analysis, it is observed that the SLP-IMC-TEM-SUCM using Jaccard coefficient-based similarity technique has less MAE than the Cosine coefficient-based similarity technique for both datasets.

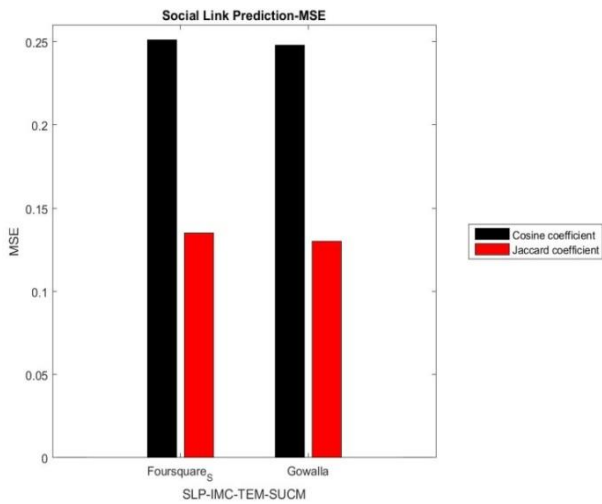


Fig. 2. Comparison of MSE.

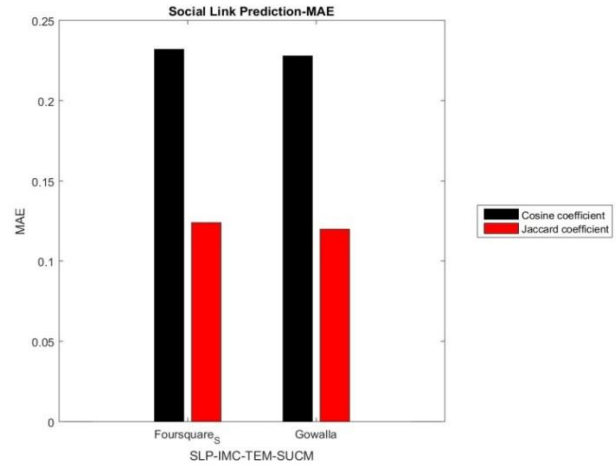


Fig. 3. Comparison of MAE.

V. CONCLUSION

In this article, SLP-IMC-TEM-SUCM is proposed to predict the missing or suspicious links. In this technique, the problem of link prediction in social networks is modeled as the classification process using two classes; one is for the existence of forthcoming links and other one is for the non-existence of forthcoming links. To achieve efficient classification, node and meta-path-based features are considered and extracted. After that, different classifiers are applied to classify these features. Further, the outcomes of each classifier are analyzed based on the similarity measure such as Cosine and Jaccard coefficient. A higher similarity indicates the higher probability of creating links between two users. Thus, the stable link is predicted to reduce the average delay during packet reception in mobile social networks. Finally, the experimental results demonstrate that the proposed SLP-IMC-TEM-SUCM using Jaccard coefficient technique achieves better performance than the Cosine coefficient-based similarity technique for predicting the social links.

REFERENCES

- [1] N.J. Yuan, F. Zhang, D. Lian, K. Zheng, S. Yu and X. Xie, "We know how you live: exploring the spectrum of urban lifestyles," in Proc. 1st ACM Conf. Online Soc. Netw., pp. 3-14, 2013.
- [2] S. Sen, O. Spatscheck, and D. Wang, "Accurate, scalable in-network identification of p2p traffic using application signatures," in ACM Proc. 13th Int. Conf. World Wide Web, pp. 512-521, 2004.
- [3] P. Haffner, S. Sen, O. Spatscheck, and D. Wang, "ACAS: automated construction of application signatures," in Proc. ACM SIGCOMM Workshop Min. Netw. Data, pp. 197-202, 2005.
- [4] B. Suryakumar and E. Ramadevi, "A multi context embedding model based on convolutional neural network for trajectory data mining," Int. J. Comput. Sci. Mob. Appl., vol. 5, no. 9, pp. 1-9, 2017.
- [5] B. Suryakumar and E. Ramadevi, "An improved multi-context trajectory embedding model using parameter tuning optimization for human trajectory data analysis," Int. J. Appl. Eng. Res., vol. 13, no. 22, pp. 1-9, 2018.
- [6] B. Suryakumar and E. Ramadevi, "Human trajectory data and internet traffic mining using improved multi-context trajectory embedding service usage classification model," Int. J. Eng. & Technol., vol. 7, no. 4, pp. 1-9, 2018.

- [7] E. Bulut and B. K. Szymanski, "Exploiting friendship relations for efficient routing in mobile social networks," *IEEE Trans. Parallel Distrib. Syst.*, vol. 23, no. 12, pp. 2254-2265, 2012.
- [8] K. Neema, Y. E. Sagduyu, and Y. Shi, "Search delay and success in combined social and communication networks," in *IEEE Glob. Commun. Conf.*, pp. 3077-3082, 2013.
- [9] L. Dong, Y. Li, H. Yin, H. Le, and M. Rui, "The algorithm of link prediction on social network," *Math. Probl. Eng.*, 2013.
- [10] J. Manotumruksa, "Users location prediction in location-based social networks," in *Proc. 6th Symp. Future Dir. Inf. Access*, pp. 44-47. BCS Learning & Development Ltd., 2015.
- [11] J. Yang, Y. Qiao, X. Zhang, H. He, F. Liu, and G. Cheng, "Characterizing user behavior in mobile internet," *IEEE Trans. Emerg. Top. Comput.*, vol. 3, no. 1, pp. 95-106, 2015.
- [12] J. Valverde-Rebaza, M. Roche, P. Poncelet, and A. de Andrade Lopes, "Exploiting social and mobility patterns for friendship prediction in location-based social networks," in *23rd IEEE Int. Conf. Pattern Recognit.*, pp. 2526-2531, 2016.
- [13] H. Yin, Y. Sun, B. Cui, Z. Hu, and L. Chen, "LCARS: a location-content-aware recommender system," in *Proc. 19th ACM SIGKDD Int. Conf. Knowl. Discov. Data Min.*, pp. 221-229, 2013.
- [14] A. Noulas, S. Scellato, N. Lathia, and C. Mascolo, "A random walk around the city: New venue recommendation in location-based social networks," in *IEEE Int. Conf. Priv. Secur. Risk Trust Soc. Comput.*, pp. 144-153, 2012.

Using FDD for Small Project: An Empirical Case Study

Shabib Aftab¹, Zahid Nawaz², Faiza Anwer³, Munir Ahmad⁴, Ahmed Iqbal⁵, Ashfaq Ahmad Jan⁶, Muhammad Salman Bashir⁷

Department of Computer Science, Virtual University of Pakistan, Lahore, Pakistan

Abstract—Empirical analysis evaluates the proposed system via practical experience and reveals its pros and cons. Such type of evaluation is one of the widely used validation approach in software engineering. Conventional software process models performed well till mid of 1990s, but then gradually replaced by agile methodologies. This happened due to the various features, the agile family offered, which the conventional models failed to provide. However besides the advantages, agile models lacked at some areas as well. To get the extreme benefits from any agile model, it is necessary to eliminate the weaknesses of that model by customizing its development structure. Feature Driven Development (FDD) is one of the widely used agile models in software industry particularly for large scale projects. This model has been criticized by many researchers due to its weaknesses such as explicit dependency on experienced staff, little or no guidance for requirement gathering, rigid nature to accommodate requirement changes and heavy development structure. All these weaknesses make the FDD model suitable only for large scale projects where the requirements are less likely to change. This paper deals with the empirical evaluation of FDD during the development of a small scale web project so that the areas and practices of this model can be identified with empirical proof, which made this model suitable only for large projects. For effective evaluation, the results of FDD case study are compared with a published case study of Extreme Programming (XP), which is widely used for the development of small scale projects.

Keywords—Agile models; feature driven development; FDD; empirical evaluation; comparative analysis

I. INTRODUCTION

Today the agile methodologies have taken over the conventional models in software industry [13-15]. It happened due to the features agile family offers, which the conventional models failed to provide. The conventional models performed well till the mid 1990s but in last two decades, software industry faced various challenges which were ultimately resolved by the agile models [19-22]. The limitations of conventional models include long development duration, less user interaction, no adaptability, high cost, and no response to the frequently change in user requirements [13-16]. Agile models valued those factors which were neglected in traditional models and ultimately diverted the focus from process to people [23-26]. Several agile models are used in software industry now-a-days including Scrum, Extreme Programming (XP), Dynamic System Development Model (DSDM), Crystal Method, Test Driven Development (TDD), and Feature Driven Development (FDD) [13-18]. Each agile

model contains its own development architecture and is suitable for particular type of projects (small, medium, large) [15-16]. However all the models work under one umbrella and follows the practices, values, and principles suggested by “Agile Manifesto” [24-26]. This manifesto is considered as a parent document of all the agile process models and consists of twelve basic rules of software development [14-15]. These principles include: frequent team communication, customer satisfaction, and managing frequent changing requirements [13]. The agile teams are self-organized, in which members work in a close collaboration. Moreover agile manifesto also focuses on simple design and timely delivery with reliable and qualitative product [14]. The agile models follow the iterative nature where each iteration brings a working module of the upcoming product, also known as partial working software [27-28]. Iterative development is very helpful to satisfy the customer as well as for the developers as it brings the customer feedback earlier which keeps the development team on track. FDD is one of the widely used agile development models by the software industry [13], [15], [19]. It is considered a process oriented and client centric development model, which mainly focuses on designing and building aspects of software development [15], [19], [31-32]. FDD follows the well-known pattern called ETVX and consists of five phases, also known as processes [19], [29-30]. The phases include: 1) Develop an Overall Model, 2) Build a Feature List, 3) Plan by Feature, 4) Design by Feature and 5) Build by Feature. Each phase further includes various activities and tasks. Besides the advantages, the FDD process model has always been criticized by many researchers due to its heavy structure. It is claimed that its explicit dependency on experienced staff and rigid nature to handle changing requirements make it only suitable for medium to large scale projects [13], [15], [19]. Due to these limitations, many researchers have proposed its customizations and integrations with other software models. This research deals with an empirical experience of using FDD for the development of small scale project. The empirical results are compared with a published research which used XP for the development of small scale project. Comparison is performed so that it can be evaluated that how FDD is not suitable for small scale project? Such empirical comparison can also guide the researchers towards an exact route for the modifications as well as for the integration of FDD with other models to achieve the maximum benefits. The empirical results presented in this research can be used as a baseline for further empirical comparisons.

II. RELATED WORK

FDD has been modified by many researchers due to its limitations such as heavy structure and rigid nature to handle small scale projects. However no significant analysis with empirical results is found which could identify those factors that why FDD is not suitable for small project? However many researches are available which have either customized the FDD model or integrated it with other models to reduce its limitations and to improve the results. Some of the studies are discussed here. Researchers in [1] presented Competitor Driven Development (CDD) which is a hybrid process model that integrated the practices from Extreme Programming (XP) and Feature Driven Requirement Reuse Development (FDRD). According to Authors the proposed CDD is a self-realizing requirement generation model which keeps track of market trends as well as competitor's next product launch to extract requirements. This model considers the market orientation of product to guess the product's success rate. In [2], authors proposed SCR-FDD by integrating the Scrum and FDD. This model has eliminated the weaknesses of both models by taking schedule related activities from Scrum and quality related activities from FDD. The proposed solution has resolved the issues regarding schedule, quality and deployment, which were considered as the big obstacles during the development and release of software product. In [3], the authors presented Feature-Driven Methodology Development (FDMD), a modified version of Feature Driven Development. The proposed model incorporated the features of object oriented approach with Situational Method Engineering (SME). In FDMD requirements are represented as features which are based on object oriented principles and defined by using action, result and object. Researchers in [4] proposed a modified version of FDD called Secure Feature Driven Development (SFDD). The proposed solution tried to cover security related issues of FDD by making some changes in classical FDD process model. The model has added an activity in each phase called "In-phase Security". Moreover two additional phases are also incorporated called "Build security by feature" and "Test security by feature". To ensure secure software development, proposed model also introduced a new role called security master. In [5], researchers introduced the feature of reusability in FDD and proposed Feature Driven Reuse Development (FDRD). This model considers re-useable feature sets along with the new requirements. In [6], authors introduced an ontology based feature driven development model for semantic web application. This model used domain ontology concepts which are widely known in domain knowledge modeling. Each phase of the proposed model has ontology as a basic building block. Ontology languages like RDF and OWL helped to overcome language ambiguity and inconsistency. In [7], a case study is

conducted to check the suitability of FDD process model for secure web site development. According to authors, integration of more iterative activities along with security practices in FDD can make it a suitable candidate for secure software development. Authors in [8] presented a framework to handle changing requirements efficiently which is based on Adaptive Software Development and Cognizant Feature Driven Development (CFDD). The proposed model is simple and easy to implement however it remained silent on other issues of FDD. In [9], researchers have presented software architecture evaluation method (SAEM) by integrating Quality Attribute Workshop (QAW), Architecture Trade off Analysis Method (ATAM) and Active Review for Intermediate Designs (ARID) with FDD. This model only deals with architecture evaluation issues and remained silent on other issues of FDD. In [10], researchers presented a supporting tool to implement FDD. This tool allows the implementation in a multi-user web based environment in the form of sub processes. The proposed tool has ability to track the changes in requirements and map these modifications in design classes. In [11], the authors have performed a comparative analysis between Feature Driven Development and Adaptive Software Development. The comparison mainly focused on two aspects; software requirements and software construction. The primarily purpose of this comparison was to evaluate the degree of agility in these two agile models. According to this study, no specific practices are used for requirement elicitation and software construction in ASD however in FDD some predefined practices are available for that purpose. In [12] the authors introduced the security relevant features in Feature Driven Development by following the four step security strategy in FDD. According to authors, after successful integration of these security steps, FDD can be used for the development of security critical software.

III. FDD PROCESS MODEL

FDD (Fig. 1) is one of the widely used agile models, particularly for the development of large and complex projects [13], [15]. This model develops the software according to client valued features. It follows eight best practices including: domain object modeling, development by feature, individual class ownership, feature teams, inspection, configuration management, regular builds and progress reporting. FDD consists of following phases [19].

"Develop an Overall Model" is the first phase in which context and scope of the project is finalized, for this purpose a high level walk through meeting is conducted [15]. After this activity, multiple object models are developed for the project by different domain experts, then one model is selected after detailed and critical review, in some cases more than one model are selected but then merged into a single one.

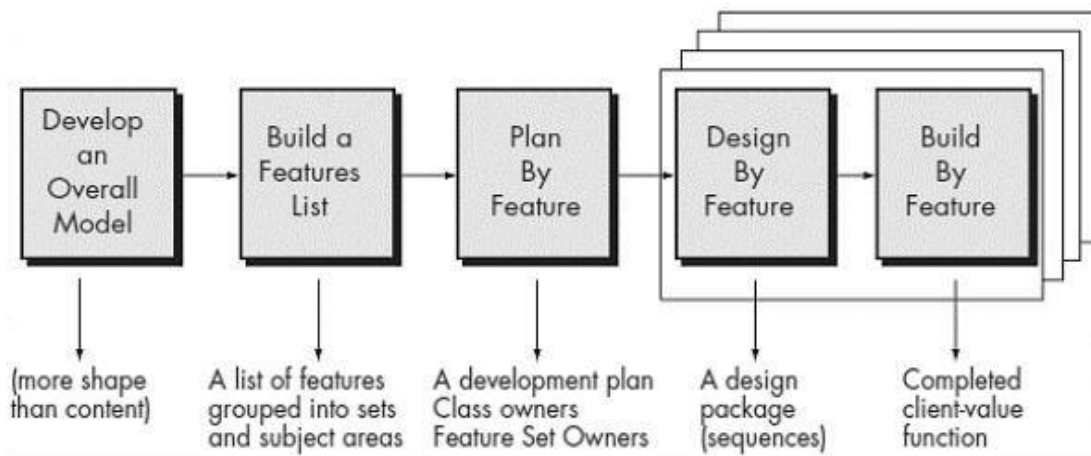


Fig. 1. Feature Driven Development (FDD) Process Model.

The selected model is called domain model which can be further refined in later stages of development life cycle. “Build a Features List” is the second phase which deals with the development of feature list. As its name shows, FDD focuses on features, a feature is a valuable function which has some business value in software [19]. After the selection of domain object model in first phase, it is easier for the team to define a comprehensive list of features to be developed. These features are then grouped into a feature set, which is a collection of related features [19, 27]. Two weeks is the maximum time for the implementation of any feature, if it feels difficult to implement any particular feature within two weeks then it would be broken into two or more sub features. Finally all the documented features are approved by the customer. Plan by Feature is the third phase which deals with the planning to implement the features. The key activity of this phase is to assign priorities to features, so that the higher priority feature would be considered in early iterations. After priority assigning, each feature is checked against its business need which verifies that the features are according to the project’s requirements. In this phase followings things are also identified in features: dependencies, risk involved, complexity and team workload. Moreover features are assigned to developers which are known as Class Owners. Design by Feature is Fourth phase of the model and first phase of the iteration. An iteration can consist of one day to two weeks [15], [19]. This phase focuses on different activities such as: designing the sequence diagrams, writing the classes and refining the overall model. Moreover different design packages are also produced against each class in this phase. Build by Feature is the second phase of iteration and last phase of FDD development life cycle. This phase deals with the actual implementation of features. After coding, code inspection and unit testing is performed. Classes are built in the sequence which was defined in plan by feature phase. When an iteration is completed successfully, the developed features are integrated with previously developed modules. FDD defines six key roles, five supporting roles and three additional roles. Key roles include: project manager, chief architect, development manager, chief programmer, class owner and domain experts. Supporting roles are: release manager, language guru, build engineer, tool smith and system

administrator [15], [19]. Additional roles include: tester, deployer and technical writer. Document and artifacts produced during FDD life cycle are Features list, Design packages, Track by feature chart and Burn up chart.

IV. EMPIRICAL EVALUATION

The purpose of this research is to evaluate the FDD process model with an empirical analysis during the development of small scale project. In order to effectively highlight the weaknesses of FDD, the empirical results are compared with the results of another published case study in which XP is used to develop small web based project. XP is one of the widely used agile models particularly for the development of small scale projects. This comparison would help us to pin point the issues which are limiting the use of FDD only for large projects. Characteristics of both the selected case studies are given in Table I.

TABLE I. CASE STUDIES DETAIL

Characteristics	FDD	XP
Product Type	Human Resource Management	Real Estate Management
Size	Small	Small
Iterations	4	3
Programming Approach	Object Oriented	-
Language	C#, ASP.NET	PHP
Documentation	MS Office	MS Office
Testing	Browser Stack	-
Web Server	IIS	Apache Wamp Server
Project Type	Average	Average
Team Size	5 Member	3 Member
Feedback	Weekly	-
Development Environment	Visual Studio 2012	Macromedia Dream Viewer and Net Beans
Other Tools	MS Visio	MS Visio
Reports	Crystal Report	-

The FDD case study which is discussed in this research was the part of an academic research project, in which agile models were implemented to develop the client oriented projects for empirical analysis. That project was implemented in a software development company situated in Islamabad city, capital of Pakistan. The software company had experienced staff with higher degrees of computer science disciplines as well as with the dominating knowledge of software development. The development teams in that software company were using agile models for most of the projects. XP case study is taken from [26], in which one project is developed with three different models. FDD case study is implemented by the team which had significant experience of agile development as required by the model. On the other hand, XP case study was implemented by the computer science students of BS and MS programs, where the team had less or no experience of agile development however training session of 10 days was organized. The empirical results of both the case studies are presented in Table II.

Aggregated and Partial results of the developed project with FDD are already discussed in [15]. However this study reflects the complete experiment including detailed empirical results of all iterations by keeping in view the guidelines extracted from [13], [16], [33-35]. The reason of choosing the XP for comparison is it's widely acceptance by the software industry particularly for small projects. In this way it would be easy to identify the practices of FDD which need the customization or modification to effectively deal with small projects. In Table II, first column shows the numbers in series and second column represents the metrics/attributes which are observed and measured for both the models in each release. These metrics are used to analyze the developed product from various aspects including development time, cost, working, productivity, quality, effectiveness and efficiency [13], [16], [36-39]. The last column shows average/cumulative values of the attributes from all releases. The remaining columns (release 1 to release 4) reflect the values of attributes from column 2 in each release for both the models.

TABLE II. EMPIRICAL RESULTS

Sr. No	Software Metric	Release 1		Release 2		Release 3		Release 4	Total	
		FDD	XP	FDD	XP	FDD	XP	FDD	FDD	XP
1	Completion Time (weeks)	1	2	1	1	1	1	1	4	4
2	Number of Modules	2	2	1	1	2	1	1	6	4
3	No of User Stories	21	17	12	13	15	11	9	57	41
4	Budgeted Work Effort (h)	200	240	200	120	200	120	200	800	480
5	Actual Work Effort (h)	175	210	175	90	175	90	175	700	390
6	Number of User Interfaces	5	2	3	1	2	1	2	12	4
7	No of Classes	5	46	5	34	4	30	4	18	110
8	Lines of Code	4200	4500	3300	3200	2760	3300	2550	12810	11000
9	KLOC	4.2	4.5	3.3	3.2	2.7	3.3	2.5	12.8	11
11	No of Code Integrations	12	20	12	12	10	12	8	42	44
12	Post Release Defects	4	2	3	2	3	4	2	12	8
13	Post Release defects / KLOC	0.952	0.44	0.909	0.625	1.111	1.212	0.8	0.937	0.727
14	Productivity (= line of code/ actual time spent in hours)	24	21.4	18.9	35.6	15.8	36.7	14.6	18.3	28.2
16	No of Pre-release Change Requests	4	3	2	2	3	2	1	10	7
17	Total Change requests/KLOC	0.952	0.66	0.606	0.62	1.11	0.60	0.4	0.781	0.636
18	Time to Implement Changes (h)	5	4	4	3	3	1	2	14	8

V. CRITICAL ANALYSIS

The detailed empirical results are shown in Table II, which reflect the significant differences in some of the important software metrics. The size, nature and complexity level of both the projects were same however FDD model showed poor performance as compared to XP. KLOC of the application which is developed using FDD are 12.8 with the actual effort of 700 hours. However with XP model, 11 KLOC are produced in 390 hours (Fig. 2, 3). Actual effort in each release of both the models is also shown in Fig. 4.

There were five members in FDD project as compared to three in XP. Moreover the team members in FDD were experienced with agile development as that case study was implemented in a software house, however on the other hand members in XP project were hardly familiar with agile and got the training of ten days just before the development. This reflects the poor performance of FDD process model in small project. The KLOC produced in FDD project were higher than XP project with the difference of 1.8 but this does not justify the difference of 310 hours in actual effort which FDD team consumed even after having two more members than the XP team. These factors point out the heavy structure of FDD process model due to which it consumes more resources in small project.

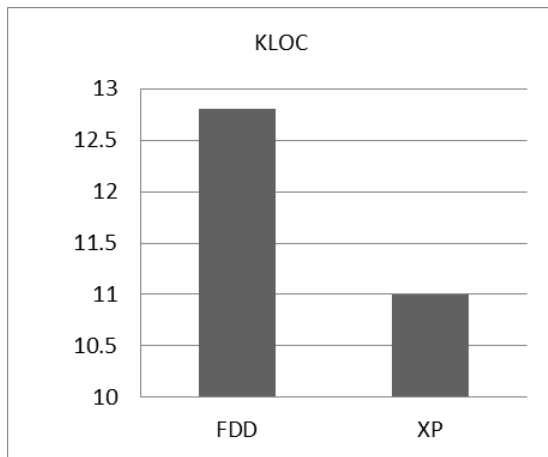


Fig. 2. KLOC.

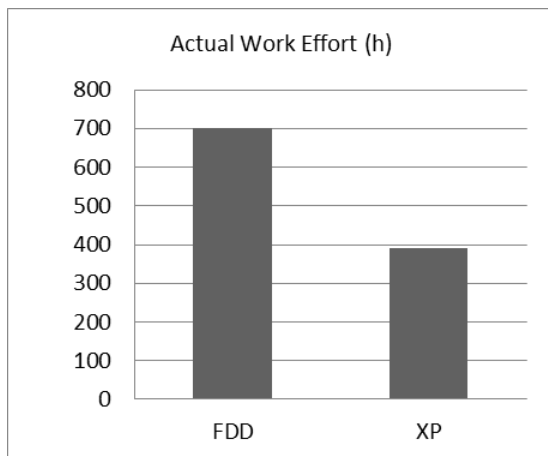


Fig. 3. Actual Work Effort.

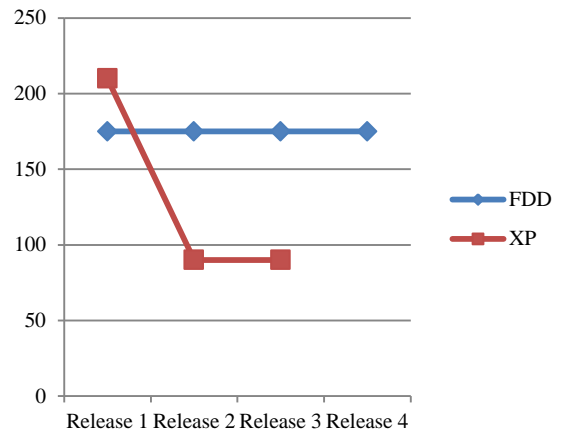


Fig. 4. Release wise Actual Work Effort.

The no of user stories (requirements) implemented in FDD project are 57 and with XP this no is 41 (Fig. 5). Moreover the no of code integrations in FDD are 42 whereas in XP this no is 44. There are more requirements in FDD project but less code integrations as compared to XP case study.

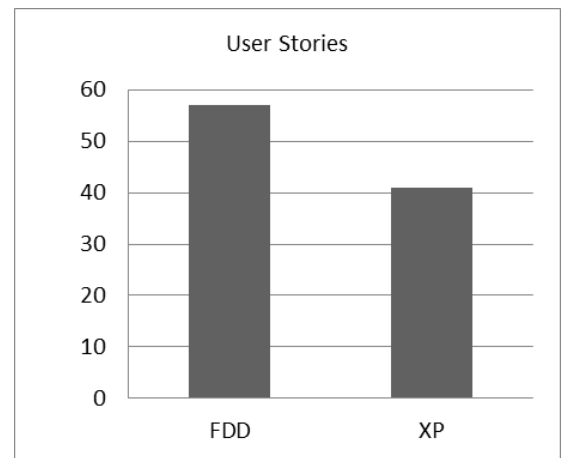


Fig. 5. No of user Stories.

The no of design classes shows the development approach adopted by the team particularly when viewed along with KLOC, implemented user stories, no of code integrations and designed interfaces. FDD team implemented 18 classes whereas XP team completed the development with 110 no of classes (Fig. 6). The no of user interfaces designed in FDD are 12 and in XP this no is 4. In comparison with XP, FDD completed the development with 16 more requirements, 8 more interfaces but with 92 no of less designed classes. This shows that the FDD team did not performed well in design by feature phase where classes are written as no of code integrations are almost same in both the projects.

The defects which appear at the client side after the release is also considered an important quality parameter which contributes to the ultimate satisfaction of the customer. The application developed with FDD showed 12 defects whereas with XP the no of defects are 8 (Fig. 7). This metric also raises the question on the quality aspect of FDD as it took much

more time for development with experienced and large team as compared to XP.

Software productivity is an important metric which shows the whole team effort during the development period. It reflects that how much work the team has done in a particular time interval (actual effort) to achieve the desired goal. However to judge the efficiency and effectiveness of the model this single parameter is not enough. All the parameters included in Table II collectively contribute to reflect the quality of the model. FDD team showed the productivity of 18.3 and XP showed 28.2 (Fig. 8). The release wise productivity of both the models is shown in Fig. 9. FDD showed poor productivity because it has taken more time for development (Actual effort) as compared to XP.

The overall results show the poor performance of FDD as compared to XP. The projects implemented in both case studies have same complexity level, nature (web based) and size however environment, team size, coding language and development tool are different.

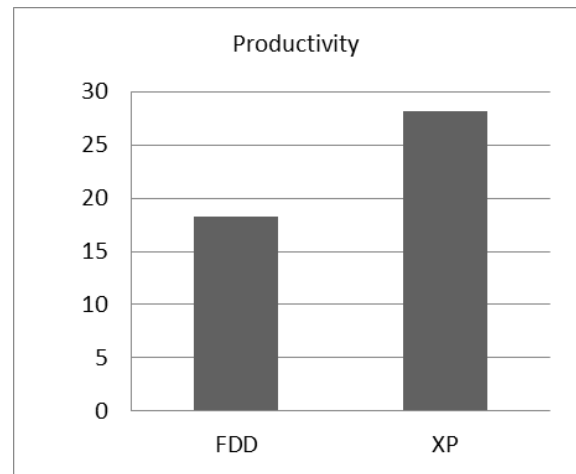


Fig. 8. Productivity.

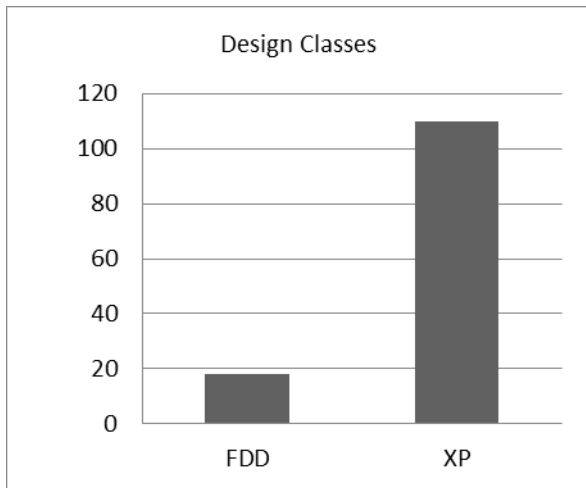


Fig. 6. No of Design Classes.

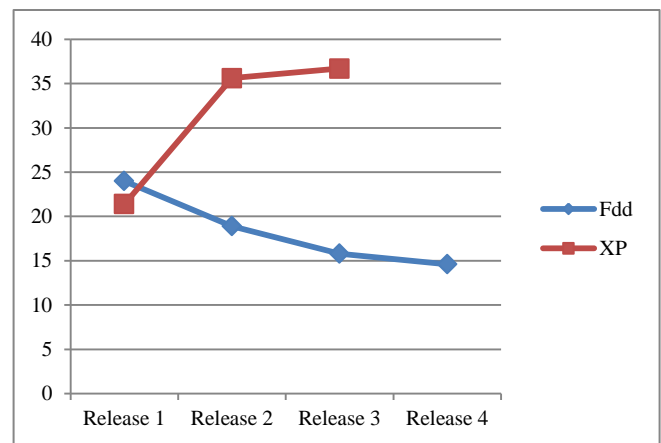


Fig. 9. Release wise Productivity.



Fig. 7. No of Post Release Defects.

There may be various causes of the poor performance of FDD process model. One is definitely the heavy structure due to which it could not perform well even with the more team members and with more time for development as compared to XP. The Complexity level of both the projects were same according to best of our knowledge however there may be a chance that FDD project was more difficult as it had more user interfaces but if its complexity level was higher than XP project even then the debatable thing is that the FDD team consisted of 5 experienced members with agile as compared to 3 non experienced members of XP. Moreover FDD project was developed in a software house with professional environment whereas XP project was implemented by graduate and undergraduate students in a lab. And finally after all the extra resources the FDD model consumed, the released product showed more defects as compared to XP. The communication issue or miss management can also be the reasons for poor performance in FDD as it has been seen that FDD team has designed very less classes as compared to XP and definitely the change management procedure, defect removal process and component based development as well as testing could be easy with appropriate no of classes.

VI. CONCLUSION AND FUTURE WORK

FDD is one of the widely used agile models in software industry particularly for large scale projects. This model is criticized by many researchers due to its weakness such as: dependency on experienced staff due to its complex structure, rigid nature to accept requirement changes at later stages, little or no guidance for requirement extraction, and heavy development structure. All these limitations make this model only suitable for large scale projects where requirements are less likely to change. This paper evaluated the FDD process model on a small scale project through an empirical case study. The purpose of this study is to identify those areas and practices through empirical analysis which are limiting the use of FDD model to the large projects. In this study, the results of FDD case study is compared with a published case study of Extreme Programming (XP), which is a well-known agile model for the development of small projects, so that the performance of FDD can be evaluated effectively. According to the empirical analysis the performance of FDD is poor in almost every important quality metric as compared to XP. There could be many reasons of poor performance of FDD including heavy development structure, complex project, mismanagement of practices and communication issues among team members. However in our point of view the root cause of poor performance directly or indirectly is the heavy and rigid structure as well as the complex practices of FDD. This research can be used as a baseline for further empirical comparisons of FDD.

REFERENCES

- [1] V. P. Doshi and V. Patil, "Competitor driven development: Hybrid of extreme programming and feature driven reuse development," 1st Int. Conf. Emerg. Trends Eng. Technol. Sci. ICETETS 2016 - Proc., pp. 1–6, 2016.
- [2] S. S. Tirumala, S. Ali, and A. Babu, "A Hybrid Agile model using SCRUM and Feature Driven Development," Int. J. Comput. Appl., vol. 156, no. 5, pp. 975–8887, 2016.
- [3] R. Mahdavi-Hezave and R. Ramsin, "FDMD: Feature-Driven Methodology Development," Proc. 10th Int. Conf. Eval. Nov. Approaches to Softw. Eng., pp. 229–237, 2015.
- [4] A. Firdaus, I. Ghani, and S. R. Jeong, "Secure Feature Driven Development (SFDD) Model for Secure Software Development," Procedia - Soc. Behav. Sci., vol. 129, pp. 546–553, 2014.
- [5] S. Thakur and H. Singh, "FDRD: Feature driven reuse development process model," Proc. 2014 IEEE Int. Conf. Adv. Commun. Control Comput. Technol. ICACCCT 2014, no. 978, pp. 1593–1598, 2015.
- [6] F. Siddiqui and M. Afshar Alam, "Ontology based application model for feature driven development," Proc. 5th Indian Int. Conf. Artif. Intell. IICAI 2011, pp. 1125–1137, 2011.
- [7] A. Firdaus, I. Ghani, and N. I. M. Yasin, "Developing Secure Websites Using Feature Driven Development (FDD): A Case Study," J. Clean Energy Technol., vol. 1, no. 4, pp. 322–326, 2013.
- [8] K. Kumar, P. K. Gupta, and D. Upadhyay, "Change-oriented adaptive software engineering by using agile methodology: CFDD," ICECT 2011 - 2011 3rd Int. Conf. Electron. Comput. Technol., vol. 5, pp. 11–14, 2011.
- [9] F. Kanwal, K. Junaid, and M. A. Fahiem, "A {Hybrid} {Software} {Architecture} {Evaluation} {Method} for {FDD} - {An} {Agile} {Process} {Model};" 2010 {International} {Conference} {Computational} {Intelligence} {Software} {Engineering}, pp. 1–5, 2010.
- [10] M. Rychlý and P. Tichá, "A tool for supporting feature-driven development," Lect. Notes Comput. Sci. (including Subser. Lect. Notes Artif. Intell. Lect. Notes Bioinformatics), vol. 5082 LNCS, pp. 196–207, 2008.
- [11] A. F. Chowdhury and M. N. Huda, "Comparison between adaptive software development and feature driven development," Proc. 2011 Int. Conf. Comput. Sci. Netw. Technol. ICCSNT 2011, vol. 1, pp. 363–367, 2011.
- [12] M. Siponen, R. Baskerville, and T. Kuivalainen, "Integrating Security into Agile Development Methods," Proc. 38th Annu. Hawaii Int. Conf. Syst. Sci., vol. 00, no. C, p. 185a–185a, 2005.
- [13] S. Aftab, Z. Nawaz, F. Anwer, M. Salman, M. Ahmad, and M. Anwar, "Empirical Evaluation of Modified Agile Models," Int. J. Adv. Comput. Sci. Appl., vol. 9, no. 6, pp. 284–290, 2018.
- [14] F. Anwer, S. Aftab, M. S. Bashir, Z. Nawaz, M. Anwar, and M. Ahmad, "Empirical Comparison of XP & SXP," IICSNS Int. J. Comput. Sci. Netw. Secur., vol. 18, no. 3, pp. 161–167, 2018.
- [15] S. Aftab, Z. Nawaz, M. Anwar, F. Anwer, M. S. Bashir, and M. Ahmad, "Comparative Analysis of FDD and SFDD," Int. J. Comput. Sci. Netw. Secur. (IICSNS), vol. 18, no. 1, pp. 63–70, 2018.
- [16] S. Ashraf and S. Aftab, "Pragmatic Evaluation of IScrum & Scrum," I.J. Mod. Educ. Comput. Sci. Mod. Educ. Comput. Sci., vol. 1, no. 1, pp. 24–35, 2018.
- [17] F. Anwer and S. Aftab, "Latest Customizations of XP: A Systematic Literature Review," Int. J. Mod. Educ. Comput. Sci., vol. 9, no. 12, pp. 26–37, 2017.
- [18] S. Ashraf, "Scrum with the Spices of Agile Family: A Systematic Mapping," Int. J. Mod. Educ. Comput. Sci., vol. 9, no. 11, pp. 58–72, 2017.
- [19] Z. Nawaz, S. Aftab, and F. Anwer, "Simplified FDD Process Model," Int. J. Mod. Educ. Comput. Sci., vol. 9, no. 9, pp. 53–59, 2017.
- [20] S. Ashraf, "IScrum: An Improved Scrum Process Model," Int. J. Mod. Educ. Comput. Sci., vol. 9, no. 8, pp. 16–24, 2017.
- [21] F. Anwer, S. Aftab, and I. Ali, "Proposal of Tailored Extreme Programming Model for Small Projects," Int. J. Comput. Appl., vol. 171, no. 7, pp. 23–27, 2017.
- [22] S. Ashraf and S. Aftab, "Latest Transformations in Scrum: A State of the Art Review," Int. J. Mod. Educ. Comput. Sci., vol. 9, no. 7, pp. 12–22, 2017.
- [23] F. Anwer and S. Aftab, "SXP: Simplified Extreme Programming Process Model," Int. J. Mod. Educ. Comput. Sci., vol. 9, no. 6, pp. 25–31, 2017.
- [24] F. Anwer, S. Aftab, S. Shah Muhammad, S. Shah Muhammad Shah, and U. Waheed, "Comparative Analysis of Two Popular Agile Process Models: Extreme Programming and Scrum" Int. J. Comput. Sci. Telecommun., vol. 8, no. 2, 2017.
- [25] F. Anwer, S. Aftab, U. Waheed, and S. S. Muhammad, "Agile Software Development Models TDD , FDD , DSDM , and Crystal Methods : A Survey," Int. J. Multidiscip. Sci. Eng., vol. 8, no. April, 2017.
- [26] G. Rasool, S. Aftab, S. Hussain, and D. Streitferdt, "eXRUP: A Hybrid Software Development Model for Small to Medium Scale Projects," J. Softw. Eng. Appl., vol. 06, no. 09, pp. 446–457, 2013.
- [27] S. R. Palmer and M. Felsing, "A practical guide to feature-driven development," Pearson Education, 2001.
- [28] P. Coad, E. Lefebvre, and J. De Luca Java, "Modeling In Color With UML," Enterprise Components and Process. Prentice Hall International, (ISBN 013011510X), 1999
- [29] S. R. Palmer and M. Felsing, A Practical Guide to Feature Driven Development. 2002.
- [30] B. Boehm, "A Survey of Agile Development Methodologies," Laurie Williams, pp. 209–227, 2007.
- [31] P. Abrahamsson, O. Salo, J. Ronkainen, and J. Warsta, "Agile Software Development Methods: Review and Analysis," 2017.
- [32] D. Ph, "Major Seminar on Feature Driven Development Agile Techniques for Project Management Software Engineering By Sadhna Goyal Guide : Jennifer Schiller Chair of Applied Software Engineering," p. 4, 2007.
- [33] M. R. J. Qureshi, "Estimation of the New Agile XP Process Model for Medium-Scale Projects Using Industrial Case Studies," Int. J. Mach. Learn. Comput., vol. 3, no. 5, pp. 393–395, 2013.

- [34] S. U. Nisa and M. R. J. Qureshi, "Empirical Estimation of Hybrid Model: A Controlled Case Study," *Int. J. Inf. Technol. Comput. Sci.*, vol. 1, no. July, p. 8, 2012.
- [35] M. Qureshi, "Empirical Evaluation of the Proposed eXSCRUM Model: Results of a Case Study," *Int. J. Comput. Sci. Issues.*, vol. 8, no. 3, pp. 150–157, 2012.
- [36] N. E. Fenton, and S. L. Pfleeger, "Software Metrics: A Rigorous and Practical Approach: Brooks," 1998.
- [37] S. H. Kan, *Metrics and models in software quality engineering.* Addison-Wesley Longman Publishing Co., Inc. 2002.
- [38] C. Jones, "Applied Software Measurement", McGraw Hill, 1991.
- [39] N. Fenton and J. Bieman, "Software Metrics: Roadmap," *It Prof.*, vol. 2, pp. 38–42, 2014.

Opinion Mining: An Approach to Feature Engineering

Shafaq Siddiqui¹, M. Abdul Rehman², Sher M. Daudpota³, Ahmad Waqas⁴

Department of Computer Science
Sukkur IBA University
Sukkur, Sindh, Pakistan

Abstract—Sentiment Analysis or opinion mining refers to a process of identifying and categorizing the subjective information in source materials using natural language processing (NLP), text analytics and statistical linguistics. The main purpose of opinion mining is to determine the writer’s attitude towards a particular topic under discussion. This is done by identifying a polarity of a particular text paragraph using different feature sets. Feature engineering in pre-processing phase plays a vital role in improving the performance of a classifier. In this paper we empirically evaluated various features weighting mechanisms against the well-established classification techniques for opinion mining, i.e. Naive Bayes-Multinomial for binary polarity cases and SVM-LIN for multiclass cases. In order to evaluate these classification techniques we use Rotten Tomatoes publicly available movie reviews dataset for training the classifiers as this is widely used dataset by research community for the same purpose. The empirical experiment concludes that the feature set containing noun, verb, adverb and adjective lemmas with feature-frequency (FF) function perform better among all other feature settings with 84% and 85% correctly classified test instances for Naive Bayes and SVM, respectively.

Keywords—Opinion mining; feature engineering; machine learning; classification; natural language processing

I. INTRODUCTION

Sentiment analysis or opinion mining is a process of recognizing and categorizing people’s sentiments, opinions, attitudes, and emotions from the text written in natural language. Because of the proliferation of text data on web and social media, opinion mining has gained a lot of attention and has in this way turned into an active research area in natural language processing NLP, which exploits systems and techniques from data mining.

Every hour, millions of messages are posted on social media like twitter, rotten tomatoes and Facebook. These messages cover numerous topics including public opinion about various topics such as products, current affairs, politics, and movies and so on. The public opinions or sentiments against a product in fact impact the market trends. For instance, [1] found a strong correlation between positive sentiments on twitter and the box-office collection of the movies. The polarity ration regarding a movie has an influence on movie revenue. For example, in the first week of release of “*New Moon*” movie polarity ratio was 6.29 and box-office collection was 142M. In the second week the ratio dropped to 5 and the box-office collection also dropped to 34M. The polarity ration of tweets can be measured as under:

$$PNratio = \frac{|Tweets_with_positive_sentiments|}{|Tweets_with_negative_sentiments|}$$

In the opening week of “*The Blind Side*” movie, the box-office collection as 34M with the polarity ratio of 5.1 and then in the second week polarity ratio increased to 9.61 and the collection also increased to 41M.

Recently, the increased demand of employing opinion mining for decision making in various application domains has drawn a considerable attention of research community from computer science towards the development of practical solutions. For instance, in [2] authors reported a strong correlation between public mood on social media and political as well as cultural events like the Presidential Election and Thanksgiving Day. There are a lot of example of real world use cases where sentiment analysis has been exploited for decision making [2, 3,4]. Thus, many algorithms and methods for sentiment analysis evolved in recent years [5]. In order to get deeper understanding into strengths and shortcomings of these methods, it is important to evaluate them in different settings with a variety of preprocessing choices.

In this paper, we empirically performed the evaluations of two well established classification methods, i.e. Naive Bayes-Multinomial for binary polarity cases and SVM-LIN for multiclass cases. These methods are evaluated by means of three different feature settings in preprocessing phase. The feature settings include Feature Presence (FP), which represents binary values, Feature Frequency (FF) and Term Frequency–Inverse Document Frequency TF-IDF both represent real values. We have validated the evaluation using publicly available dataset of movie reviews taken from Rotten Tomatoes. The empirical evaluation revealed an interested conclusion that the feature-frequency (FF) setting performed better among all other feature settings with 84% and 85% accuracy for Naive Bayes and SVM, respectively.

The rest of the paper is organized as follows. The background section contains some related and technical knowledge about the domain. The Literature Review section contains previous research which relates to the experiment. The Methodology section introduces the specifics of the experiment. The Results section presents the results of the work. Lastly, the Conclusion section presents the conclusion.

II. BACKGROUND

A. Natural Language Processing

Natural Language Processing (NLP) is a framework to support an interaction between computers and human (natural) languages by providing processing capability of a text written in natural language using the methods and techniques stemming from various fields like computer science, computational linguistics and artificial intelligence. Natural language processing provides us various algorithms for understanding and recognizing the patterns of human language especially statistical algorithms, which are based on machine learning. The machine-learning algorithms learn different rules through the analysis of large corpora (A hand-annotated documents with their respective polarity values to be learned by algorithm) of typical real-world. These algorithms take a large set of features generated from corpora as input. Research in natural language processing is now focused towards soft and probabilistic predictions based on assigning weight to all features. Such models have an advantage of expressing the relative certainty of many different possible answers rather than only one, thus they provide more reliable and accurate results when such kind of a model is included as a component of larger systems some of these algorithms are Naive Bayes, Maximum Entropy Measure and SVM [6].

B. Finding Appropriate Features

Sentiment Analysis is a task of performing text classification. In supervised classification different machine learning algorithms can be used to classify the text. In supervised learning the major focuses are features selection and choosing appropriate classification algorithm. In Natural language processing the terms features and token are used interchangeably. Finding best features are very important when text mining is performed using machine learning algorithms. Features which tend to be consistent in text of a certain class are generalized as a good indicator of that class [6, 8]. For example the word bad may be a good indicator to identify a text as negative. However, many features such as unigrams, bigrams, trigrams, POS tagged unigrams, dependency trees and several other have been used in sentiment analysis [1, 2, 5]. The purpose of finding these features is to find good indicators to generalize for text classification.

Some of the several feature types are discussed below:

- N-grams

We use n-grams to capture the dependencies between all words which appear in a sentence structure sequentially; n-grams combination does not preserve the words' syntactical or semantic relations. An n-gram is a probabilistic language model which predicts next word conditioned on the occurrence of previous word. The probabilistic expression is $P(x_i|x_{i-(n-1)} \dots, x_{i-1})$.

N-grams can be of size 1 (unigrams) size 2 (bigrams), size 3 (trigrams) and so on.

Finding of Pang et al. (2002) research states that unigrams perform better than bigrams [10, 11].

- Parts of Speech Tagging

POS tagging has been used for a long time in text classification and Natural Language Processing (NLP). POS tagging differentiates syntactic meaning of words in a sentence by using some specific tags, such as tags for noun, pronoun, verb, adjective, adverb, conjunction and others.

In sentiment analysis POS tagged words are used as features for classification as the adjective can provide good clues about the polarity of the sentence. In 2011 Mejova et al. conducted a study in which they tested POS tagged features effectiveness in supervised learning separately and with combinations of POS tags. The combinations of adjectives, adverbs and nouns performed better than other combinations when treated as features and all individual POS tagged features were outperformed by adjective when used as features. In this study we have applied Apache OPENNLP Maxent POS tagger model. Some POS tags are defined in Table 1 below.

- Syntactic Dependency Tree Patterns

A syntax dependency tree is a syntax tree structure that captures the dependency between a word (root) and its dependents (Childs) it identifies useful semantic relationships. In syntax tree the relation among nodes are based on their grammatical dependency. Dependency parsing identifies parts of speech and syntactic relations and then determines the grammatical structure of sentence. Many researches have been conducted for determining the efficient and accurate parsing tree pattern for sentiment analysis.

Except that appropriate feature selection, assignment of numerical feature values to selected feature is also important. This value assigning method is called the weighting method and most widely used weighting methods are term frequency (TF) and presence.

C. Feature Selection Methods

Feature selection methods are techniques to reduce the size of features space and to choose small set of features to capture relevant properties or classification of dataset.

An effective feature selection method can increase the efficiency of classifier.

TABLE I. POS TAGS

Tag	Parts of Speech
JJ	Adjective
NN	Noun, singular or mass
RB	Adverb
VB	Verb, base form
NNS	Noun, Plural

Many feature selection method has been proposed such as Information Gain (IG), Mutual Information (MI), X2 test (CHI), term strength (TS) and term presence.

Normally the size of feature vectors for a document and sentence is usually bif specially when unigram features are used and these large sized vectors can slow down the system performance one way to get rid of these large vector which contains less efficient features is to pre-process the data such as removal of stop word

D. Naive Bayes Classifier

Bayesian classifier, a statistical technique, predicts the probability of an event to belong to a particular class. The classifier is based on Bayes Theorem [7] which states that the probability of an event is based on the prior (conditional) knowledge of the event. It can mathematically be stated as under:

$$P(A | B) = \frac{P(B | A)P(A)}{P(B)} \quad (1)$$

where

A and B are events and $P(B) \neq 0$.

$P(A)$ and $P(B)$ are the probabilities of A and B without considering their conditional interaction.

$P(A | B)$ is a conditional probability of event A given a condition that the B is true.

$P(B | A)$ is a conditional probability of event B given a condition that the A is true.

given sample to belong to a particular class.

E. Support Vector Machine Classifier

Support Vector Machines are based on the idea of decision planes for defining decision boundaries. We used decision planes for separating the objects having different class memberships. A decision plane creates a boundary between them.

III. LITERATURE REVIEW

Due to the rapid growth of text data on web and social media, opinion mining has gained a lot of attention and has thus become an active research area in natural language processing, which exploits techniques and methods from data mining. The sentiment Analysis is not only limited to computer science domain but it has also spread to management sciences and social sciences application domains due to its importance and applications to business areas and society. In fact, the importance of opinion mining is proportional to the growth of social media such as Facebook, social discussion forums, Twitter and product review websites. With the growth of social media we now have huge stores of raw datasets which can be analyzed to find different informative patterns [8, 9].

A simple use case for sentiment analysis is to discover what people feel about a particular topic and what their attitude about a particular topic is. For example:

Do people on a social chat group think that the recently released movie was a block buster or flop one?

The newly opened restaurant is serving best sea foods?

What is the public opinion for a particular election candidate?

By analyzing tweets for sentiments will answer these questions. Furthermore, we can also learn why people think that the movie was a hit or flop by extracting the exact words indicating why people did or didn't like the movie. For example, poor plot, and or bad casting.

This is the kind of insight one hopes to find when conducting market research. Now one can easily decide that in which particular direction he/she need to work more in next film either on plot or cast.

From many years research has been focusing on different levels of classification either document level classification, sentence level classification or phrase level classification using supervised or unsupervised learning. For supervised learning selection of features, feature weight assignments and features selection methods play an important role in classification performance.

Prior to the text polarity classification which identify that the document as positive or negative several research studies were conducted for subjectivity classification of document that whether the document or sentence is subjective or objective?

In 2002, Pang and lee conducted a sentiment analysis study using movie review data. In that document level supervised learning they classify the document using Naïve Bayesian, SVM and Maximum Entropy. They choose several token such as POS tags, adjectives and n-grams as features and they found that the machine learning methods outperformed the human classification (they asked their two students to classify the documents). They also found that SVM outperformed other machine learning algorithms and unigrams perform better than bigrams [10].

In 2004, Bo Pang and Lillian Lee again conduct a study in which they perform Sentiment Analysis Using Subjectivity Analysis Based on Minimum Cuts [11]. In this study they examined the relationship between subjectivity detection and polarity classification. Their findings show that text subjectivity detection can compress it into small and much shorter extracts but retaining polarity information at a comparable level to that of full review.

Their work identifies that subjectivity extracts classified by Naïve Bayes are more effective inputs. Their work also shows that utilizing context based information via minimum-cut framework can see statistically significant improvement in

polarity-classification accuracy. In [12], Eguchi et al. proposed methods in which he define some assumptions that sentiment expressions are related to their topics. As for example, a negative view for a politician may be indicated using reckless or negative review for a voting event may be indicated by Flaw. In their research Eguchi combined topic relevance models and sentiment relevance models. They create a training dataset by annotating S (sentiment) and T (topic) to sentiment. Then these S, T and polarities of sentiment together formed a triangular relationship and they obtained high performance.

In [13], Riya et al. introduce a hybrid approach on Sanders analytics dataset. The classification was a combination of both Knowledge base and machine learning approach in which each word was first classified using knowledge based approach with the help of SentiWordNet then the complete tweets was classified using different classifiers. The hybrid approach results in 100% accuracy, the Naïve Bayes classifier with a total accuracy of 75%. The paper concludes that in sentiment classification the machine learning techniques are easier than symbolic techniques.

The approach of Tirath, Sanjeev [14] was more focused on calculating some robust features. The features having information gain (IG) score greater than zero where considered for classification.

Asha et al. [15] used three different dataset to report the accuracy of Naïve Bayes and SVM classifiers. The features selection approach was based on the extraction of TF, TF-IDF, opinion oriented keywords using SentiWordNet. The features were then assigned a weight using GINI index. The results show that both classifiers performed better on large movie review data set SAR14.

Dhiraj Gurkhe's [5] dataset was an amalgamation of tweets, movie reviews dataset, hand classified tweets from Sanders, emoticons dataset and sentiment lexicons. Three different features vectors were used for classification having unigrams, bigrams and unigrams+bigrams. The classification results show that the Naïve Bayes performs better by using unigrams features.

IV. METHODOLOGY

In this study an experiment on Rotten Tomatoes movies reviews dataset was performed. This dataset contains 1500 positive reviews and 1500 negative reviews. The purpose behind choosing the movie reviews dataset is that they are more detailed and often considered as good material for subjectivity and polarity classification. Typical comments are usually very short such as tweets that are only one or two sentences long. These comments are narrowly focused on a single topic of interest expressed. Whereas movie reviews tend to be more detailed and focused on whole story, acting, actors and give an overall impression about the movie.

For performing machine learning, the focus is to find some relatively correct clues from the text which can lead to correct classification. These clues about the original data are called features and are stored as a feature vector, $F = (f_1, f_2, \dots, f_n)$

in feature vectors each coordinate represent one clue say feature f_i of the original text.

Features selection strongly influences the classifier learning. In feature selection this study goal is to capture desired properties of text in some numerical form. The choice of features is based upon their relevancy with sentiment analysis task. The algorithms for extracting best feature sets does not exist, thus we only rely over research intuitions, expertise in field, domain knowledge and performing various experiments for choosing the best set of features [17, 18].

In this study we have focused on unigrams and we used Apache OPENNLP an open-source java library for extracting the relevant linguistic features from the corpora. OPENNLP is a set of classifiers which work on word level. As we are working on word level we removed all the punctuations and emotions from the text. Table 2 below summarizes the types of word level features we used for classification. We experiment with different combination of above mentioned features and along with these features we have also used three different weighting functions and then choose the feature set and weighting function which performed best for the Sentiment Analyzer.

A. Negation Handling

Negation handling is an important part of polarity analysis. Some of the sentences such as "it was not a good movie" has the opposite polarity from the sentence "It was a good movie". Word influenced by the negation especially adverbs and adjectives should be treated differently. One way to handle negation is to use a bigram dictionary including special feature word NOT for every adverb and adjective [16].

Another way could be to perform parsing of all sentences, but this approach is computationally expensive and may cause inaccuracies if the corpus is not completely tagged. Another approach is to construct training dataset having all possible negation sentences, but this requires time and efforts to construct an optimal dataset.

In this approach we have dealt with some simple cases of negation such as not, do not, doesn't. We have performed POS tagging and have defined some rules for checking the pre-determiner of adverbs and adjectives this approach has increase the performance a little better, it would possible to define more extensive rule for more better performance that would deal with noun and verbs instead.

TABLE II. FEATURES USED FOR CLASSIFICATION

Feature	Definition	Example
Word	All words in text	Come, world
Lemma	Word entry in dictionary	Watching = watch children = child, players = player
Parts of Speech (POS) tags	Noun, Verb, Adjective	The girl was very beautiful In this sentence the word beautiful is adjective

B. Weighting Functions

The three weighting functions we used in this experiment are:

1) *Feature presence (FP)*: It represent a binary value, these binary values indicate the absence and presence of a feature in text (e.g. in the text–“good day”, only the features “good” and “day” are set to 1) and all the other remaining words in the vocabulary (set of words we see in corpus) are set to 0.

2) *Feature frequency (FF)*: It represents a real value, which indicates the occurrences (frequency) of a feature in a given example, the frequency value is normalized according to the size of the text (in words).

3) *TF-IDF*: It represents a real value, which indicates the occurrences (frequency) of the feature in a given text; this frequency value is then divided by the logarithm of the number of examples from the corpus containing this feature. This can be explained as for features f_i ,

$$TF - IDF(f_i) = \frac{FF_i}{\log(DF_i)} \quad (2)$$

Where FF_i denotes feature frequency of f_i , and " DF_i " denotes the document frequency of f_i (number of documents containing f_i). The purpose of using this weighting function was to give a larger weight to features that were seen less in the corpus than the common ones. In other words, we increase the impact of rare words over common words.

C. Classification

After determining the best features we performed classification. In performing classification task each sentence is considered as conditionally independent. In this study we performed supervised classification. Classifier learning or training is done using cases from training set and later the quality of training is evaluated using the cases from the test set. The labels of interest are polarity labels “Positive” and “Negative” for Naïve Bayes and SVM classifier.

We have taken the following steps for performing classification:

1) *Data preprocessing*: Training dataset was preprocessed by applying POS tagging, location and subject tagging, removing stop words and punctuations.

2) *Feature extraction*: Suitable features were extracted for classification using different combinations of word level features and weighting functions discussed above.

3) *Model building*: Using features the classifiers were trained and a model was created.

4) *Model evaluation*: The classifiers were evaluated by mean of confusion matrix and ROC analysis.

5) *Classification*: The test cases were classified using the classification models. The test dataset for classifiers had 1500 positive and 1500 negative reviews. The algorithm 1 describe our approach to data cleaning and training dataset preparation before performing classification.

D. Algorithm

Algorithm 1: Training dataset preparation

```
1. Start [input: raw dataset with labels, output: training dataset (features with labels)]
2. foreach review r in dataset do
3.   stemming(r)
4.   stopping(r)
5.   case_normalization(r)
6.   POS_tagging(r)
7.   tokenize(r)
8.   foreach token t in r do
9.     IF t is not subjective & t ∈ {verb, adverb, adjective and noun} then
10.      feature ← feature U t
11.    END IF
12.  END LOOP
13.  write(feature, label)
14. END LOOP
15. END
```

V. RESULTS AND DISCUSSION

In this experimental setup we try to see how each classifier perform on the dataset when using different features settings. We have defined the five different feature settings for each of the weighting function. These settings are defined in Table 3.

We have compiled the results for all five different features setting with all three different weighting functions for both classifiers Naive Bayes and SVM.

Fig. 1, 2 and 3 shows the result (Percentage of correctly classified test instances) of running Naïve Bayes and SVM classifier on testing dataset with weighting functions FP, FF, TF-IDF, respectively.

TABLE III. FEATURE SETTINGS

Features Settings	Description
Unigram (U)	Using words without subject words
Lemma (L)	Using the lemmas from WordNet Subject words are not considered
Lemma + POS tags (L+P)	All lemma concatenated with their respective parts-of-speech tag. Such as (beautiful_adjective). Subject words are not considered
Selected Lemma (SL)	Only selected lemmas whose parts of speech are adjective and adverb because it has been observed that the subjective sentiments of an author are reflected mostly on adverbs and adjectives. Subject words are not considered
Selected Lemma 2 (SL2)	Only selected lemmas whose parts of speech are adjective, adverb, noun and verb so that the dependencies can be captured. Subject words are not considered

Fig. 1 depicts the performance graph of both SVM and Naïve Bayes algorithm using different features and feature presence weighting function. The graph show that when adjective, adverbs, nouns and verbs were extracted as features the SVM classifier outperformed the Naïve Bayes classifier with overall accuracy of 85%, when tested on test dataset while the Naïve Bayes classifier gave 84% accuracy.

Fig. 2 depicts the performance graph of both SVM and Naïve Bayes algorithm using different features and feature frequency weighting function. The graph show that when adjective, adverbs, nouns and verbs were extracted as features the SVM classifier again outperformed the Naïve Bayes classifier with overall accuracy of 85.5%, when tested on test dataset while the Naïve Bayes classifier gave 84.5% accuracy. The weighting function feature presence increased the performance of both classifiers.

Fig. 3 depicts the performance graph of both SVM and Naïve Bayes algorithm using different features and Term frequency-inverse document frequency weighting function. The graph show that the SVM gave an accuracy of 83% when adjective, adverbs, nouns and verbs were extracted as features but the performance of Naïve Bayes classifier depletes badly. Naïve Bayes classifier gave 83% accuracy when lemmas were extracted as features.

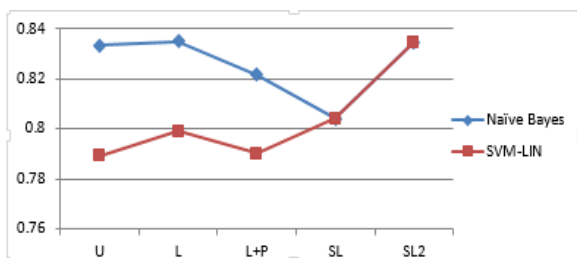


Fig. 1. Accuracy Results using Test Dataset with TF-IDF.

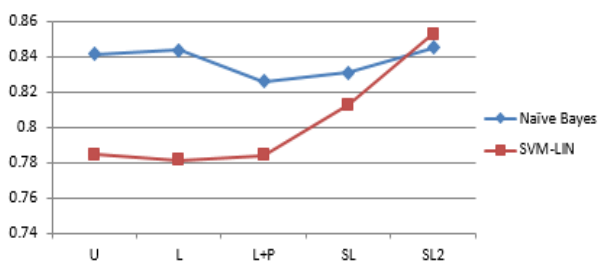


Fig. 2. Accuracy Results using Test Dataset with Feature-Frequency (FF).

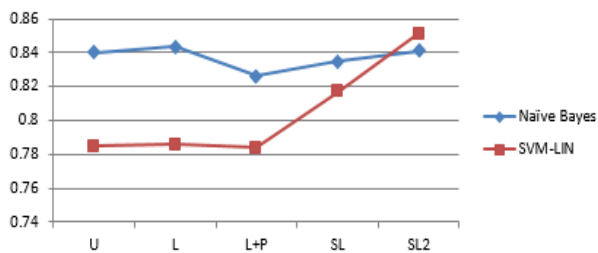


Fig. 3. Accuracy Results using Test Dataset with Feature-Frequency (FF).

TABLE IV. CONFUSION MATRIX

Confusion Matrix		Target			
		Positive	Negative		
Model	Positive	1279	221	Positive Predicted Values	0.852
	Negative	203	1297	Negative Predicted values	0.864
		Sensitivity	Specificity	Accuracy = 0.858	
		0.86	0.854		

After analyzing the results of the experiment we can conclude that the features setting SL2 which includes only adverb, adjective, verb and noun lemmas perform good using all three weighting functions when used by both classifiers.

As it is now clear that the models build using feature set of adverb, adjective, verb and noun lemmas performed best when used with feature-frequency weighting functions with accuracies 84% and 85% for Naïve Bayes and SVM-LIN respectively we evaluate the models using a test dataset of 1500 positive, 1500 negative movie reviews. The confusion matrix in Table 4 shows the positive predicted rate, negative prediction rate, sensitivity, specificity and accuracy of Naïve-Bayes classifiers. The F-score of test results was 0.85.

The true positive rate of the build was 86% while the true negative rate was 85%. The overall accuracy achieved was approximately 85%. The performance of both classifiers was also evaluated using ROC curve analysis. The ROC curve analysis is shown in Fig. 4 and 5. The ROC curve shows an excellent classification test accuracy for Naïve Bayes classification model with value 0.93 while the ROC curve accuracy for SVM classification model was 0.72.

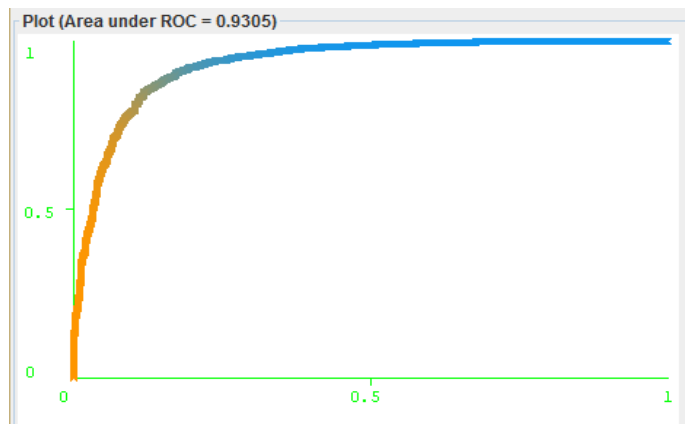


Fig. 4. ROC Curve of Naïve Bayes Classifier.

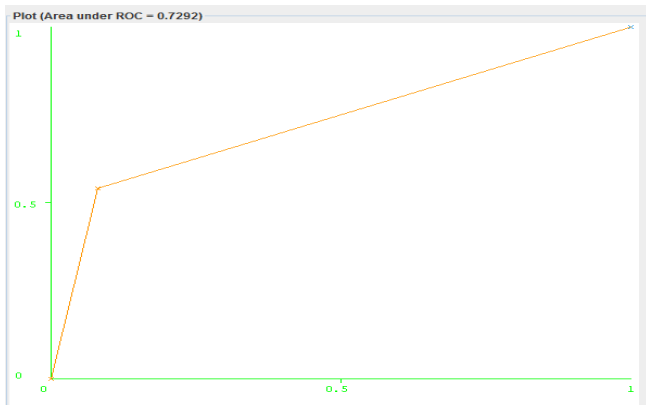


Fig. 5. ROC Curve of SVM Classifier.

VI. CONCLUSION

We have performed classification on two different datasets and calculated simple word based features for classification. To find most appropriate feature set we defined five different feature settings and use three different weighting functions and then calculated the accuracies of features for each feature setting and identified that the feature set containing noun, verb, adverb and adjective lemmas with feature-frequency (FF) function perform better among all other feature settings with 84% and 85% correctly classified test instances for Naïve Bayes and SVM, respectively.

REFERENCES

- [1] Bollen, Johan, Huina Mao, and Xiao-Jun Zeng. (2011) Twitter mood predicts the stock market, *Journal of Computational Science*
- [2] Asur, S., & Huberman, B. A. (2010, August). Predicting the future with social media. In *Proceedings of the 2010 IEEE/WIC/ACM International Conference on Web Intelligence and Intelligent Agent Technology-Volume 01* (pp. 492-499). IEEE Computer Society.
- [3] A. Mittal, A. Goel, (2011) Stock prediction using Twitter sentiment analysis, Stanford University, CS229
- [4] Diakopoulos, N. A., & Shamma, D. A. (2010). Characterizing debate performance via aggregated Twitter sentiment. In *Proceedings of the*

- 28th international conference on Human factors in computing systems (pp. 1195-1198). New York, NY: ACM Press.
- [5] Dhiraj Gurkhe, Niraj Pal, Rishit Bhatia. (2014). Effective Sentiment Analysis of Social Media Datasets. *International Journal of Computer Applications*, 4.
- [6] Julian Brooke, 2009, A Semantic Approach to Automated Text Sentiment Analysis. Springer-Verlag Berlin Heidelberg, 478-483.
- [7] Walaa Medhat, Ahmed Hassan, Hoda Korashy: Sentiment analysis algorithms and applications: A survey, *Ain Shams Engineering Journal*, Elsevier, p. 1093-1113, Volume 5, Issue 4, December 2014
- [8] J. Han, M. Kamber, and J. Pei. 2006 *Data mining: concepts and techniques*. Morgan kaufmann series,
- [9] Yessenov K, Misailovic S. (2009). Sentiment analysis of movie review comments, 1-17 <http://people.csail.mit.edu/kuat/courses/6.863/report.pdf>.
- [10] Pang, B. and Lee, L, 2004, A Sentimental Education: Sentiment Analysis Using Subjectivity Summarization Based on Minimum Cuts.
- [11] Pang, B., Lee, L., and Vaithyanathan, S, 2002, Thumbs up? Sentiment Classification Using Machine Learning Techniques.
- [12] Koji Eguchi, Victor Lavrenko. (2006). Sentiment retrieval using generative models, *Proceedings of the 2006 Conference on Empirical Methods in Natural Language Processing*. Sydney, Australia
- [13] Riya Suchdev, Pallavi Kotkar, Rahul Ravindran, Sridhar Swamy. (2014). Twitter Sentiment Analysis using Machine Learning and Knowledge-based Approach. *International Journal of Computer Applications*, 36-40.
- [14] Tirath Prasad Sahu, Sanjeev Ahuja. (2016). Sentiment Analysis of Movie Reviews: A study on feature selection and classification algorithms. *IEEE*.
- [15] Asha S Manek, P Deepa Shenoy, M Chandra Mohan, Venugopal., (2015). Aspect term extraction for sentiment analysis in large. Springer Science.
- [16] Akshay Amolik, Niketan Jivane, Mahavir Bhandari, Dr.M.Venkatesan. (2015). Twitter Sentiment Analysis of Movie Reviews using Machine Learning Techniques.
- [17] M. K. Elhadad, K. Badran and G. I. Salama, "A novel approach for ontology-based dimensionality reduction for web text document classification," in *2017 IEEE/ACIS 16th International Conference on Computer and Information Science (ICIS)*, pp. 373-378, Wuhan, China, 2017.
- [18] Mazandu, G. K., Chimusa, E. R., & Mulder, N. J. (2016). Gene ontology semantic similarity tools: survey on features and challenges for biological knowledge discovery. *Briefings in bioinformatics*, 18(5), 886-901.

Cloud Server Security using Bio-Cryptography

Zarnab Khalid¹, Muhammad Rizwan², Aysha Shabbir³, Maryam Shabbir⁴, Fahad Ahmad⁵, Jaweria Manzoor⁶

Department of Computer Science
Kinnaird College for Women, Lahore, Pakistan

Abstract—Data security is becoming more important in cloud computing. Biometrics is a computerized method of identifying a person based on a physiological characteristic. Among the features measured are our face, fingerprints, hand geometry, DNA, etc. Biometric can fortify to store the cloud server using bio-cryptography. The Bio-cryptography key is used to secure the scrambled data in the cloud environment. The Bio-cryptography technique uses fingerprint, voice or iris as a key factor to secure the data encryption and decryption in the cloud server. In this paper, the security of the biometric system through cloud computing is discussed along with improvement regarding its performance to avoid the criminal to access the data. Biometric is a genuine feature for the cloud provider. Cryptography algorithm will be explained using blockchain technology to overcome security issues. The blockchain technology will provide more protection through cryptographic keys to secure biometric data.

Keywords—Cloud computing; biometrics; fingerprints; encryption and decryption methods; cryptography keys; bio-cryptography; blockchain

I. INTRODUCTION

Cloud Computing is mainly a spotlight of the computer industry today. Cloud computing is an evolving model with new aspects and capabilities, maintaining the data of cloud is dominant. There are many techniques and approaches to maintain the data and secure in the cloud server [1]. In a cloud computing environment, the entire data exist in a set of networked resources. Cloud service is available all around the world using standard network protocol accessible from every device with internet connection (laptops, mobile phone, tablets). Authenticating is necessary for validating one to part by an interactive party that is usually implemented in client-server side where sever needs to confirmed who is accessing their information and needs to be authenticated. The main drawback of cloud computing technology is lack of confidence they gained from possible receivers specially internet users [4].

Biometry technology provides verification of identity and sensitive security level, while in cryptography key management is a necessary for key storage. Biometric is combined with cryptography because biometry feature is admissibly unique, as a result bio-cryptography was put to secure the cloud server using key binding to create cryptographic key. Key binding is the main concept in bio-cryptography [2] that combines user biometrics with the existing cryptography keys to form biometric encryption process. Biometric is basically used for security and networking system.

The Cryptography key is entirely independent on biometrics. The main idea of cryptography is to avoid the unauthorized operations on documents, text ad storage base [3].

Cloud Computing Architecture comprehends components and subcomponents that are mandatory for cloud computing. The architecture contains front end platforms called clients, these clients are servers, e.g. Mobile laptop, printer, tab, etc. The back-end platforms are mostly servers for storage, database, software applications and operating system within a cloud and a network counting the internet, intercloud combines to form a cloud computing architecture. The front and the back end of cloud usually connect each other to form a network and is named as internet. If cloud computing has many clients then it is high demanded for a lot of storage data. The architecture of cloud computing has been shown in Fig. 1.

The Biometric system is raised its increasing and has become the promising way to identify users [7] and authentication methods based upon password, identification cards and is considered to be more reliable. The biometric system consists of three steps. The first step involves enrollment in which the user can store basic information about the user id and user number, then identifies an image of specific trait and check the specific characteristic being used e.g. fingerprint. The second step is to read information from the system. The system analyses the characteristics and perform actual comparison to match the pattern of given input. After comparison, the user can either accept or reject the procedure present in the file.

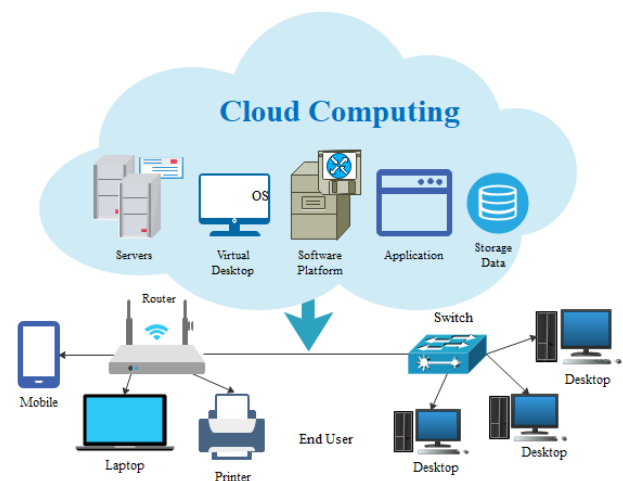


Fig. 1. Cloud Computing Architecture [7].

Cloud computing is an evolving model with new aspects and capabilities, maintaining the data of cloud is dominant. There are many techniques and approaches to maintain the secure data in the cloud server. Cloud computing undergoes many attacks and can be secured using methods and techniques to overcome the problems related to the security [12]. Cloud service is available all around the world using standard network protocol accessible from every device with internet connection (laptops, mobile phone, tablets) [13]. Cloud computing security is based upon authentication and verification of some parameters that can help in measuring the right amount of data security in the cloud server.

Biometry technology provides verification of identity and sensitive security level, while in cryptography the key management is necessary for storing key. [8] Inception and deception are two phases of network analysis to determine network traffic stream, biometric data is secured using secret key sharing among encryption and decryption parties. The original biometric data is extracted by generating a key. The Cryptography key is entirely independent on biometrics. [6]

The biometrics can secure passcodes more effectively [9] and authenticate the uniqueness in an individual to grant access to the computer or system using fingerprint scanner technology.

The Blockchain essential is an evolutionary internet protocol. It is an open source cryptography asymmetric mechanism and distributed architecture. Many aspects of technology are found in the blockchain peer to peer technology, cryptography [10] distributed over a network, the security of blockchain relies on these technologies. The Blockchain technology is completely different from traditional database structure. Peer to peer network that accomplished blockchain collectively following protocol for communicating inner-node and authenticating new nodes. Each block holds a valid transaction that is distributed over a network.

This blockchain technology uses a script to deal with the sudden pattern transaction in the system. Blockchain is made of three technologies private key cryptography, peer to peer network and blockchain's protocol. The blockchain is simply a cryptographically provable list of data [11]. The primary advantage of the blockchain technology is that data itself can be dispersed. The blockchain undergoes many attacks from third party to access the files in cloud server [14] and can be prevented by using technologies and blockchain security to protect the data from theft. In this paper cryptography keys will be discussed along with blockchain technology that will help in securing the biometric data in cloud server. Bigger blockchains user with more users has lower risk of getting attacked by the hacker because of the large number of complexities required to breach such a network

In Section II, Literature Review is discussed. In Section III, problem statement of the paper is deliberated. In Section IV, the proposed solution of the paper is elaborated and explained through biometrics, cryptography keys and blockchain technology that explain how the data is secure more effectively in the cloud server. In the end, Section V will designate the conclusion and discussion regarding the paper. The security of blockchain depends upon cryptography peer to

peer technology. The Cloud server for storing information is given below to explain how the data is being stored and protected through encryption and decryption of cryptographic keys, identification through biometric technology and at last blockchain transaction that holds blocks of data. The data is stored forming chains inside the block. The data is processed to be fit in a block and each block is represented by using cryptographic hash. The architecture of securing data in cloud computing has been shown in Fig. 2.

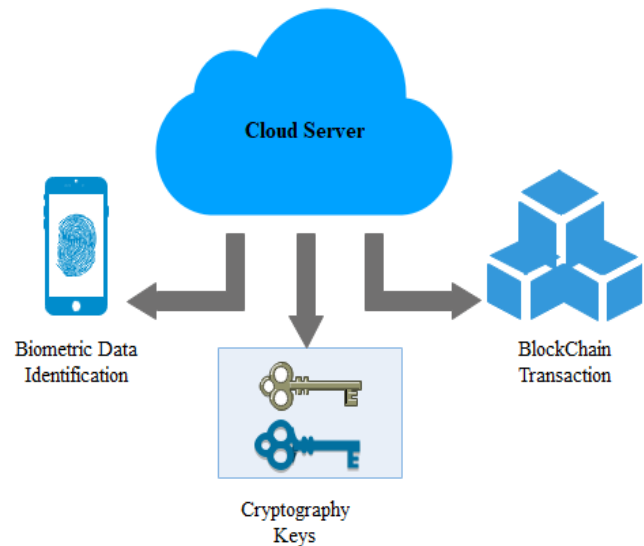


Fig. 2. Cloud Computing for Securing Data.

II. LITERATURE REVIEW

The last researchers finding and investigation have been written previously. Cloud computing security importance and techniques [1] are used to overcome data privacy issues and problems handled by cloud server provider. Author in [2] proposes two methods to decrease bio-cryptography computational complexity using fuzzy vault technique to rehearse error-correcting codes in the secret key. Author in [3] explains multiple methods to secure data using cryptographic keys and comparison between cryptography methods. Different methods are discussed to secure data using cryptography process. The multimedia data are high dismissal of large capacities and requires real time analysis for better results. Author in [4] proposed protective biometric identification scheme that can attack conspiracy tossed by the users and the cloud server. The proposed result can accomplish an essential level of protection by resisting the attacks and to provide lesser estimation costs in identification procedures. Author in [5] proposed user authentication points on bases of fingerprint authentication and comparing with previous method. Author in [6] used existing techniques to organize in different types of solutions. Using previous techniques error control methods in bio-cryptography will be discussed. Author in [7] proposed scheme is to secure cloud if the invader can falsify identification demand and to secure the cloud from the attackers and comparisons with previous protocols to get results more effectively. In [8], author provides evidence to detect cryptography procedures by their unique key exchange. The methods of generating

cryptography protocols to detect high entropy data by the method of fingerprint were proposed. Author in [9] proposed extracting features and matching procedures through fingerprint system to secure hardware techniques, categorizes different part of including techniques for extracting its features and matching of the procedures. Author in [10] implements digital signature scheme through blockchain. A method to apply similar concept and data structure with distributed method was introduced. In [11], the author proposes unsolved problems of blockchain community. The problems were analyzing in ranges from organizing newer cryptography primitives on bitcoin to enable use-case privacy protection of

file storage. In [12] various security threats are explained in cloud computed and needed to be resolved. In [13] cloud computing security is measured on bases of parameters. Parameters are recognized to measure the data security of cloud. Author in [14] explains many attacks on the blockchain and provides assured data derivation of cloud. Author in [15] proposes set of cryptographic protocols confirming privacy of cryptographic procedures with public and private keys.

The prototype system is implemented using smart bonds. The comparison between previous research work has been shown in Table I.

TABLE I. COMPARISON BETWEEN PREVIOUS RESEARCH WORK

Year	Topic	Proposed Solution	Strength	Weakness
2014	Methods of Reducing bio-cryptography algorithms [2]	A technique to rehearse error correcting codes in secret key	Using methods for reducing bio-cryptography algorithms and providing flexibility to reduce the errors for security	High consumption of computational resources, caused by various mathematical processing and the huge amount of data
2014	Bio cryptography Authentication in cloud sharing [4]	Providing essential level of protection by lessening the attacks	Novel implementation for bio-cryptographic infrastructure and recovery of shared storage encryption	Culpabilities for storing encryption key within cloud platforms Password security is not upgraded
2015	Bio-cryptography authentication protocol improvement [5]	Fingerprint authentication and previous method comparison	Biometric authentication is improved against the fake device attacker for stealing biometric data and password	A method proposed by a researcher that was weak against the attacker with high time complexity
2015	Security threats in cloud computing [12]	Security threats to be resolved in cloud	Examine the various security issues that are defenseless to the cloud computing and needed to be resolved	The cloud computing brings critical challenges that cannot be avoided by the consumer, if security of clouds is concerned
2017	Multimedia cryptography [3]	Multiple method to secure the data using cryptography keys and their comparison	Using bio-cryptography to enhanced security of data or image while transmitting, this will be efficient for improving multimedia data encryption	Multimedia encryption is hard to understand due to conversion of original data into another data
2017	Security and privacy on Blockchain [11]	Unsolved problem in blockchain community	Cooperation between academia and blockchain community to resolved unsolved problems	Problem in security and privacy Research and problems related to industry to analyze glitches ranging from organizing new cryptographic primitives
2018	Privacy-preserving biometric identification in cloud computing [7]	Secure the cloud if the invader demands false identification	Secures and offer high level of privacy protection. Real experiments on the Amazon cloud, over databases with different scopes	Tremendous amount of cost in the system that depends on conformist cryptographic primitives
2018	Blockchain access control system for cloud storage [15]	Privacy of cryptography procedures with public and private keys	Blockchain provides security in the cloud sharing and access control over the data stored in the cloud without provider participation	Security and copyright issues, Transfer of file to other users, Problems for encrypting the data.

III. PROBLEM STATEMENT

Bio-cryptography secures the data by encrypting and decrypting in the cloud server. As the security of cryptography keys are weak for remembering pass codes so a method is required to secure the data more accurately. Cryptography keys are not secure. There are many privacy issues regarding this procedure so a technique is needed to provide full protection in cloud server.

IV. PROPOSED SOLUTION

To secure the data more accurately and precisely biometric-based cryptography is combined with the blockchain technology to secure the data in the cloud server. Cryptography keys are usually weak to secure large data. Blockchain technology uses the cryptography encryption and decryption keys to secure network and to store values in it. Blockchain is linked with public cryptographic key to protect the data from the hackers accurately. The data in the blockchain is stored in form of record or text file.

A. Methodology

In This paper we will provide security of data saved in cloud server by the blockchain technology that helps the cryptography keys to implement secure data. Blockchain is also an internet distributed database method based on distributed architecture, Asymmetric cryptographic component. Blockchain technique used advanced block as data component through which data is stored in the form of record, text file. Blockchain contains three elements, one for data storing, other one for hash value that works like fingerprint. Cryptography is the main part of the blockchain where transaction must be kept private. Methods to store data in cloud server using bio-cryptography and block chain have been shown in Fig. 3. When biometric data is encrypted and secured in blockchain, it cannot be altered. Even if somehow the data gets altered, the entire chain of the network is also changing accordingly, this mean at every alternation or change in data is tracked and absolutely no data will be lost because the user can always look through the previous versions of blocks to find out the difference in the latest version. In this process the user enters the data through biometric identification scanner the data is encrypted into the blockchain for security and decrypt into the cloud server. The following steps explain the procedure to store biometric data in cloud server with the help of cryptography keys and blockchain.

1) The digital image of fingerprint is pre-processed to recover the image quality. This enhanced image is approved through fingerprint algorithm to identify unique details. The details of recognizing unique features of fingerprints are known as minutiae. A template is generated after the post-processing of fingerprint image.

2) After the fingerprint detection the biometric data is encrypted using cryptography keys. The encrypted data is then passed through blockchain transaction, each block holds the data.

3) The data is secured more effectively using blockchain that is linked with cryptography storing information in a form of chunks forming a chain that can hold transaction of data.

4) The secured data is then decrypted using private key so it can be read more effectively.

5) All the secured data is stored in cloud server after decryption. The stored information is secured and can only be accessed by server and user.

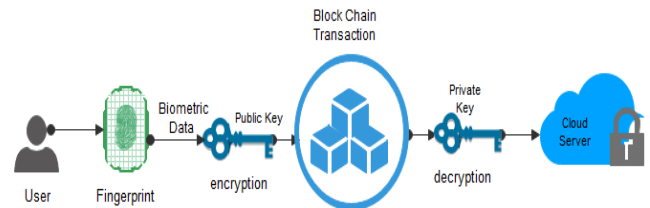


Fig. 3. Methods to Store Data in Cloud Server using Bio-Cryptography and Blockchain.

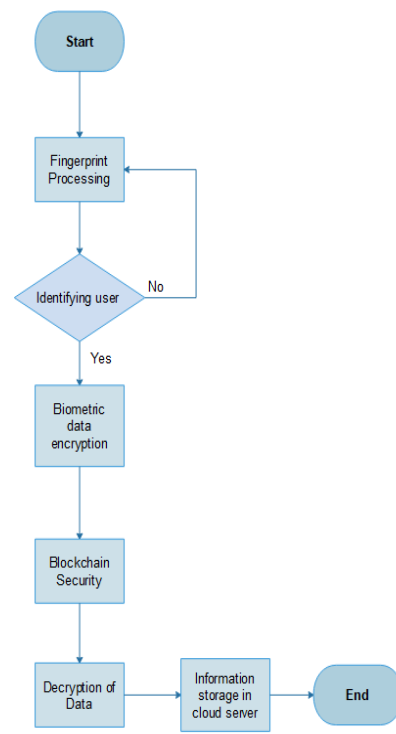


Fig. 4. Flowchart of Proposed Solution.

Flowchart of the following methodology is illustrated in Fig. 4. The flow chart describes the procedure to secure the data in the cloud server using cryptography and blockchain.

B. Biometric

Biometric is used in computer science for identification and access control. Biometric identification is calculable characteristics to identify distinctiveness. Biometric is identified by behavioural characteristics that includes fingerprint, veins, palm, DNA, iris recognition. A secure way to authenticate its user is to ensure functionality of data and

data stored in cloud server biometric authentication is used secure the cloud and its data. Biometric is not a new technology nowadays but many of them neglects its unused potential. This Technology is growing rapidly. Organizations are adopting biometric to update passports. Biometric system can be updated in two methods verification and identification, for identification none of the approaches are claimed from the user while the goal of verification is to control whether the person is the one to be claimed.

Biometric is basically used for security and networking system. The biometric system has methods for identification linking PIN numbers and passwords. A fingerprint is a pattern of ridges on the surface of fingertip. The pattern of distinct remains unchanged throughout life. The fingerprints pattern is also unique in an individual. The details of fingerprint image are scanned into biometric system including the amount of pressure applied, dryness of skin or presence of any cuts or other deformities present on fingertip. Biometric are making smart phone more useful and might be a key for helping others by protecting the data with growing internet of things. The connected devices (laptops, computers, tablets) can be measured and the profile can be derived from biometrics from the resulted data. Biometric system contains three different components, sensor that records the information, a computer for storing biometric information, a software that connects computer hardware to the sensor. Biometric is in a form of identification and access control in computer science. Fig. 5 shows the working of finger identification through biometrics.

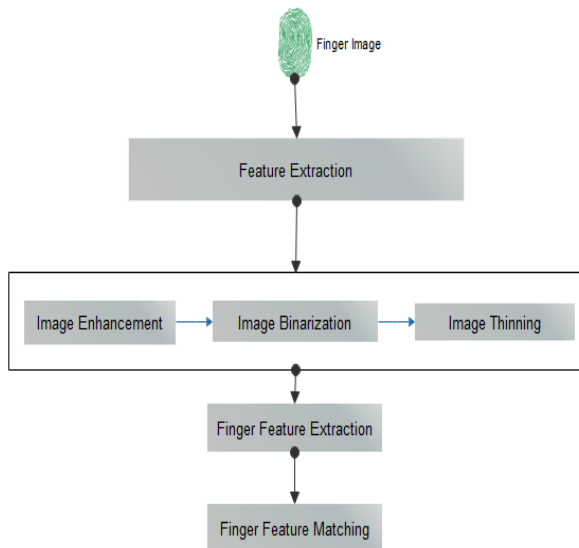


Fig. 5. Working of Finger Identification Through Biometrics.

C. Blockchain Technology

Blockchain provides a distributed, absolute data store that can be used across network of users. It is a distributed database that supports continuously increasing list of transaction information accounts, cryptographically protected from meddling and reviewing. The transaction data is kept in the blockchain. Blockchain consists of three elements first for data storage, second one is used as hash value that works like fingerprint and always unique to identify the block. The

process of adding new block to blockchain by transaction of hash verification is known as mining. The new added block is linked with previous block. The third element is hash of previous block is chain of blocks to make blockchain more secure. The main drawback of blockchain is high consumption of hardware, energy and time required for mining process.

Blockchain has surged from a technology with slight applications associated with digital currencies. The security in blockchain is important to protect from the attackers. The data is protected through blockchain and kept in the cloud server. The data is stored forming chains inside the block. The data is processed to be fit in a block and each block is representing by using cryptographic hash usually known as digital fingerprint. When underlying cryptographic algorithms are broken, the impression of blockchain is analysed. The structure of the blockchain is given below. The blockchain is the underlying cryptographic protocol; each technology of blockchain is a factor to achieve the requirements. The security of cryptographic hash functions is essential part for the security of blockchain and its nature should be secure for a very long time. The blockchain technology used the chunks of data to store the data in it and to provide security of data by chaining them. Cryptography is the main essential for blockchain privacy where transaction needs to be private. The industrial benefits of blockchain are to improve discoverability, reduce costs and complexity and can be trusted in keeping records of files. Blockchain increases accessibility, improve efficiency in business networks. The structure of Blockchain has been shown in Fig. 6.

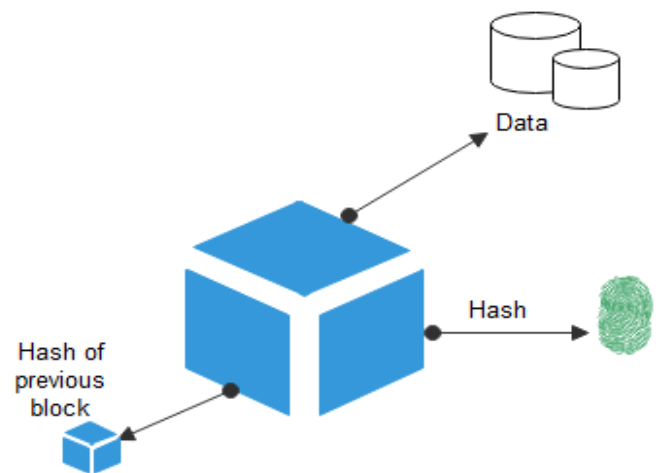


Fig. 6. Structure Diagram of Blockchain.

Blockchain is composed of three core parts: block, chain and network

1) *Block*: The block in blockchain is the main core of blockchain. A list of transaction recorded into a report over a given time. The size event and activation are different for every blockchain. Blockchain controls the movement of their token. The block header contains last block hash, transaction, time, target and version that describes the structure of the data inside the blockchain. When a block is completed it creates a

unique secure code, that is tied with next block, creating chains of block.

2) *Chain*: The hash that links one block to another, chains them together. It is most difficult thought to perceived in blockchain. The hash in block is created from data from previous block. The hash is fingerprint of that data and links blocks in order. Hashing increases the security of the data. Hash pointers are where the blockchain sets itself in terms of certainty as pointers not only contains address of previous block, but also hash data of the block for attaining blockchain.

3) *Peer to peer network*: The network composes of nodes. The nodes work as a computer running an algorithm that secures the network. Each node contains entire records of transaction that are recorded in blockchain, in case of full node the whole blockchain is copied into the device, while device is being connected to the network. Peer to peer network in blockchain differs from traditional client-servers model, as there is no central point of storage and information is constantly shared, recorded between all applicants of the network.

D. Cryptography Algorithm

The Cryptography key is completely independent on biometrics. Cryptography algorithms include public and private keys for encryption and decryption of data. Bio-cryptography is used to avoid scrambling data in the cloud environment. Biometric authentication identifies users on the basis of their behavioral characteristics. Cryptography algorithm keeps data safe and secure when communicating through a network. Cryptography algorithm alters the data from readable form to a protected form. Cryptographic keys keep authentication and keep information private. Cryptography is used to secure information from unauthorized revelation. It has two fundamental types symmetric and asymmetric and has various properties like length and depends on proposed functions.

Cryptography converts ordinary information into scrambled incomprehensible clutter. This process of conversion is called encryption. The second process of cryptography is decryption which takes the cyphertext and recreates the plain text. The process of encryption and decryption is controlled by the key. The key is shared between two communicating parties. A technique derived from mathematical concepts and rule-based calculation known as algorithm that transfer messages that are hard to cipher so cryptography algorithms are generated for protection of data privacy, web surfing on internet and deliver confidential statements [16].

Cryptosystem uses a set of cryptographic algorithms to encrypt and decrypt messages among computer system, devices including smartphones and other applications. One algorithm is used to encryption; another algorithm is used for message authentication and another one for key exchange.

The process is embedded in protocols and run on network systems and operating systems, involving public and private key generation, message verification and key exchange [17]. Process of cryptography has been shown in Fig. 7.

1) *Symmetric key encryption*: Symmetric key is also known as private key. In this encryption a secret key is used for encryption and decryption. In the encryption process the information is locked using cryptography and can only be accessed by the user and server. The key is advanced by either the client or the both side (client and server). Distribution of keys is a big problem in this technique as encryption and decryption of data is done by a single key. Symmetric key is much faster than asymmetric encryption. Symmetric key is considered for transferring large number of files. Symmetric key must be kept secret and has to be transmitted to receiving end yet, that means it has to be captured by a spy to illegally decrypt the message. To establish the shared key using only symmetric key is a way difficult so the asymmetric key is recognized for sharing of key between two parties. Some examples of symmetric key include AES, DES, etc.

2) *Asymmetric key encryption*: Asymmetric or public key cryptography uses two key one public key for encryption of data and one private for decryption of data. It is the newer encryption as compared to symmetric key. It is computationally infeasible to figure the private key based upon public key, due to this public keys can be shared freely, allowing users for easy and suitable method for encrypting content, while private keys are kept secret The authentication claims that it's belong to the user and have not being altered or swapped by any malicious file, Due to computational complication of asymmetric encryption it is only used for small chunks of data. There are two security benefits for encryption. Asymmetric key does not allow the hacker to forge licences for others. The security services provided by asymmetric key is authenticated, confidentially and non-repudiation [18]. Symmetric key for delivering confidential, integrity and security, users should be certain that public key is authenticated, that it belongs to the user and has not been tampered or replaced by the third party. The data should be protected and kept safe. One key in the pair can be shared with everyone, that's why it's called a public key [19].

a) *Confidentially*: An individual's content is encrypted in specific public key, it can only be decrypted using specific private key, confirming that only proposed receipt can decrypt can used the data. Confidential data can only be accessed, used and copied by authorized users.

b) *Integrity*: It is a part of decryption process that verifies contents of original encrypted message with new decrypted match, so even a little change in the original content can cause failure to decryption.

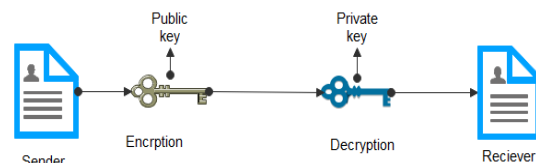


Fig. 7. Process of Cryptography [16].

V. CONCLUSION AND DISCUSSION

In this paper the information about the biometric data security over cloud computing is discussed by storing data on the cloud server to protect it from the criminal, hacker, etc. Cloud computing is an evolving model with the new aspects and capabilities, for maintaining the data of cloud is dominant. Blockchain technology utilizes cryptography for securing data of the user, ensuring that the transaction is done safely and storing all the secure information. The public key cryptography key is used in the blockchain to encrypt the data in the form of chunks and creating chains for holding transaction of data and afterward decrypting using private key, the secure information is stored in the cloud server to be accessed only by the user and the server.

REFERENCES

- [1] R. Kaur and J. Kaur, "Cloud computing security issues and its solution: A review," 2015 2nd International Conference on Computing for Sustainable Global Development (INDIACom), New Delhi, 2015, pp. 1198-1200.
- [2] M. Velciu and V. Patriciu, "Methods of reducing bio-cryptographic algorithms computational complexity," 2014 IEEE 15th International Symposium on Computational Intelligence and Informatics (CINTI), Budapest, 2014
- [3] B. Dhanalaxmi and S. Tadisetty, "Multimedia cryptography—A review," 2017 IEEE International Conference on Power, Control, Signals and Instrumentation Engineering (ICPCSI), Chennai, 2017
- [4] M. Fadil and A. M. Barmawi, "M. Velciu, A. Pătrașcu and V. Patriciu, "Bio-cryptographic authentication in cloud storage sharing," 2014 IEEE 9th IEEE International Symposium on Applied Computational Intelligence and Informatics (SACI), Timisoara, 2014
- [5] Improving bio-cryptography authentication protocol," 2015 9th International Conference on Telecommunication Systems Services and Applications (TSSA), Bandung, 2015.
- [6] H. S. G. Pussewalage, J. Hu and J. Pieprzyk, "A survey: Error control methods used in bio-cryptography," 2014 11th International Conference on Fuzzy Systems and Knowledge Discovery (FSKD), Xiamen, 2014
- [7] L. Zhu, C. Zhang, C. Xu, X. Liu and C. Huang, "An Efficient and Privacy-Preserving Biometric Identification Scheme in Cloud Computing," in IEEE Access, vol. 6, pp. 19025-19033, 2018.
- [8] S. Luo, J. D. Seideman and S. Dietrich, "Fingerprinting Cryptographic Protocols with Key Exchange Using an Entropy Measure," 2018 IEEE Security and Privacy Workshops (SPW), San Francisco, CA, 2018, pp. 170-179.
- [9] S. Hosseini, "Fingerprint vulnerability: A survey," 2018 4th International Conference on Web Research (ICWR), Tehran, 2018, pp. 70-77
- [10] M. Sato and S. Matsuo, "Long-Term Public Blockchain: Resilience against Compromise of Underlying Cryptography," 2017 26th International Conference on Computer Communication and Networks (ICCCN), Vancouver, BC, 2017, pp. 1-8.
- [11] H. Halpin and M. Piekarska, "Introduction to Security and Privacy on the Blockchain," 2017 IEEE European Symposium on Security and Privacy Workshops (EuroS&PW), Paris, 2017, pp. 1-3
- [12] N. Kajal, N. Ikram and Prachi, "Security threats in cloud computing," *International Conference on Computing, Communication & Automation*, Noida, 2015, pp. 691-694.
- [13] R. A. R. Shaikh and M. M. Modak, "Measuring Data Security for a Cloud Computing Service," 2017 International Conference on Computing, Communication, Control and Automation (ICCUBEA), Pune, 2017, pp. 1-5.
- [14] D. K. Tosh, S. Shetty, X. Liang, C. A. Kamhoua, K. A. Kwiat and L. Njilla, "Security Implications of Blockchain Cloud with Analysis of Block Withholding Attack," 2017 17th IEEE/ACM International Symposium on Cluster, Cloud and Grid Computing (CCGRID), Madrid, 2017, pp. 458-467.
- [15] I. Sukhodolskiy and S. Zapechnikov, "A blockchain-based access control system for cloud storage," 2018 IEEE Conference of Russian Young Researchers in Electrical and Electronic Engineering (EIConRus), Moscow, 2018, pp. 1575-1578.
- [16] A. Arora, A. Khanna, A. Rastogi and A. Agarwal, "Cloud security ecosystem for data security and privacy," 2017 7th International Conference on Cloud Computing, Data Science & Engineering - Confluence, Noida, 2017, pp. 288-292.
- [17] M. Derfouf, A. Mimouni and M. Eleuldj, "Vulnerabilities and storage security in cloud computing," 2015 International Conference on Cloud Technologies and Applications (CloudTech), Marrakech, 2015, pp. 1-5.
- [18] S. Rajeswari and R. Kalaiselvi, "Survey of data and storage security in cloud computing," 2017 IEEE International Conference on Circuits and Systems (ICCS), Thiruvananthapuram, 2017, pp. 76-81.
- [19] P. Tasatanattakool and C. Techapanupreeda, "Blockchain: Challenges and applications," 2018 International Conference on Information Networking (ICOIN), Chiang Mai, 2018, pp. 473-475.

Enhanced Physical Document Management using NFC with Verification for Security and Privacy

Z. Zainal Abidin¹, N.A. Zakaria², Z. Abal Abas³, A.A. Anuar⁴, N. Harum⁵, M.R. Baharon⁶, Z. Ayop⁷

Information Security Forensics and Computer Networking

Universiti Teknikal Malaysia Melaka (UTeM), Melaka, Malaysia^{1, 2, 4, 5, 6, 7}

Optimization Modelling Analytic and Simulation, Universiti Teknikal Malaysia Melaka (UTeM), Melaka, Malaysia³

Abstract—This study focuses on implementation of physical document management for an organization using Near-Field Communication (NFC) since it provides faster detection on tracking items based on location. Current physical document management operates using bar-codes. However, barcodes are able to be duplicated, which make it not secure that lead to forgery and unauthorized modification. Therefore, the purpose of the proposed physical document management system is to produce a better administration control in an organization through the use of verification mechanism. Nonetheless, the current NFC based system is lack of verification process. Thus, an enhancement in physical document management with verification process is proposed and self-developed system is built using C#, SQLite, Visual Studio, NFC tag and NFC reader (ACR122U-A9). Moreover, the new system required employee to log in to the system by scanning ID tag and followed by the physical document File tag, which both tags scanned at the NFC reader. Then, information of the physical file coordinator and the status of the location of the physical document file is displayed. The significant of this study is to protect confidential document and improve administrative control through dual verification; and produce a database to monitor the real-time data detection.

Keywords—Document file management system; physical document files detection; near-field communication (NFC)

I. INTRODUCTION

Physical document management system contains a collection of hardcopy documents that has been an important record and evidence in most organizations. The printed document may consist of high classified document or need a right of permission to distribute [1]. The security of the classified hardcopy documents need a systematic filling system and safe implementation [2] due to high reliability on most working procedures. In fact, the crucial hardcopy document must be protected from threats and attacks such as forgery [3], falsification and unauthorized modification.

With the aid of technology adapted into the physical document management system, the integration of autonomous system contributes to faster access to information, more efficient, safe environment and convenient for user [4] in obtaining the printed version of document for further process.

Moreover, a significant change in technological, social and economic system is happening and would be evolved due to

industrial revolution [5]. The change in industrial revolution is evaluated with the consequences method for measuring the indicator performance in the implementation phase that aligned with the 21st century. [6], [7].

Thus, this paper proposes an verification as one of the security feature, which making the revolution of industry 4.0 as a reality. The development phase is done at the document and employee databases. The employee database is linked together with document database in searching for a “match” information between employee who holds the document file and the NFC tag that contain information of the physical document. The new method reduces the time consumed in searching the document file and increase the satisfaction when the employee who wants to find the current position of the physical file at instance.

Additionally, the matching method with verification helps the document management system to be more efficient, effective, avoid human error and reduce time for searching the document folder at the document room. In fact, the system is convenient as the employee needs to tap his or her ID for verification at the NFC reader and scan the document file’s NFC tag for searching the “match” data.

In this study, an experiment has been implemented for detecting the availability of document in the folder, folder’s name and the employee in-charge who holds the folder of the document at the current location.

Thus, this paper introduces the implementation of physical document detection using NFC for physical document management system. Each of the existing studies on technology used for physical document management is introduced in section 2.0, the related work. The barcode, RFID and NFC is explained in sections A, B and C.

II. RELATED WORK

A. Barcode

Barcode is a machine-readable, data representation in the form of bars and spaces on a surface. Furthermore, barcode is an identification code that contains a well-defined combination of parallel lines [8]. Barcode is useful for automatic identification using endpoint devices such as Point of Sales (PoS) as shown as in Fig. 1.

A Special thanks to Malaysia Research Assessment (MyRA) and Universiti Teknikal Malaysia Melaka (UTeM) for giving a sponsor.



Fig. 1. Barcode [9].

A barcode is machine-readable optical label that can be captured by the PoS terminals, smartphones or computer at retail stores for retrieving information about the item to which it is attached [10], [11]. In fact, barcodes decode fast and most barcodes standards provide redundant information for error correction purpose [12], [13].

There are two types which are linear barcodes and matrix barcodes [12]. Linear barcode is the first generation of barcode ever created and it is in one-dimensional, 1D barcode that is made up from lines and spaces that its own specific pattern. Meanwhile, matrix barcode is also known as 2D barcode that uses two-dimensional way to present the information [9], which is improved from the one-dimensional barcode that presents data more per unit area.

The 1D barcodes consists of code 39, code 128, EAN-13 and ISBN meanwhile 2D barcodes are such as QR code, PDF417, Data Matrix and Maxi code as shown in Fig. 2.

However, using barcode, identification method is not a good idea because barcode can be reprinted for later usage [14] as illustrated as in Fig. 3.

1D barcodes	Code 39 	Code 128 	EAN-13 	ISBN
2D barcodes	QR Code 	PDF417 	DataMatrix 	Maxi Code

Fig. 2. 1D and 2D Barcodes [9].

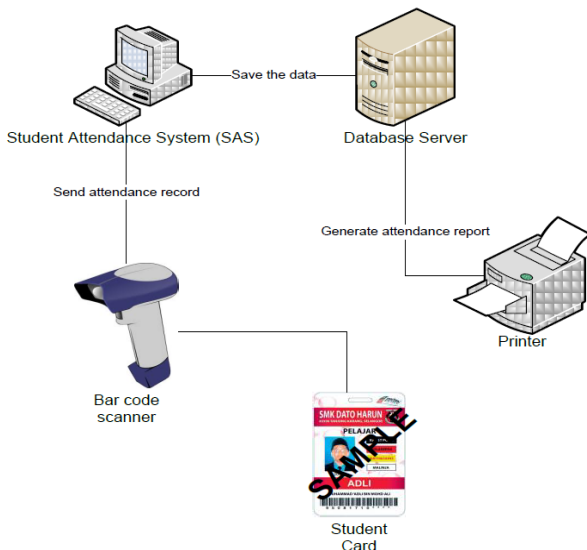


Fig. 3. Barcode System [14].

B. Radio-Frequency Identification (RFID)

The Radio Frequency Identification (RFID) is a technology that uses a radio waves to automatically identify people or objects from a distance [15] and it is developing drastically [16] in various industries. The RFID technology is designed by developers not only in traditional applications for instance asset or inventory tracking [17], but also in security services such as electronic passports and RFID-embedded credit cards.

Moreover, RFID technology is a non-contact, automatic identification technology to detect, track, sort and distinguish a variety of objects including people, vehicles, goods and assets [18] without the need for direct contact as the magnetic stripe technology or line of sight contact (as found in bar code technology).

RFID technology tracks the activities of objects through a network of radio enabled scanning devices over a several meters of distance. There are three different stages of frequency of RFID in Fig. 4, which is low, high and ultra-high frequency [19] that operated at difference distance.

The RFID system consists of three elements, which is an RFID tag or transponder, RFID tag reader and back-end database which stores record associated with tag information [20] as illustrated in Fig. 5, which each tag contains a unique identity code.

An RFID reader releases a low-level radio frequency magnetic field that energizes the tag. The tag responds to the reader's query and states its presence via radio waves, transmitting its unique identification data. This data is decoded by the reader and passed to the local application system via middleware. The middleware acts as an interface between the reader and the RFID application system. The system examines and verify the identity code with the information stored in the host database [20] or backend system. In this way, accessibility or authorization for further processing can be granted or refused, depending on results received by the reader and processed by the database.

However, current NFC's data privacy is exposed when other user has the same NFC device, which he or she able to read the data using scan random tag number [17]. In order to overcome the data privacy problem, the verification is implemented [12] for better security.

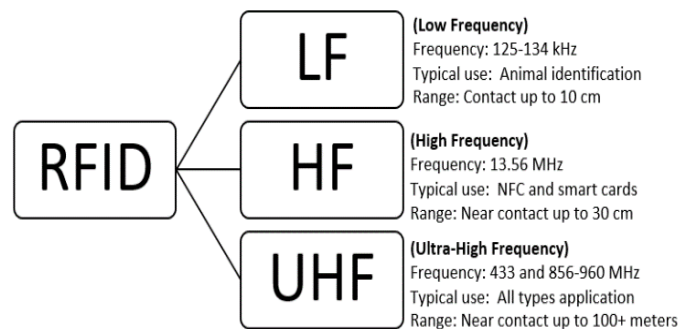


Fig. 4. RFID System [19].

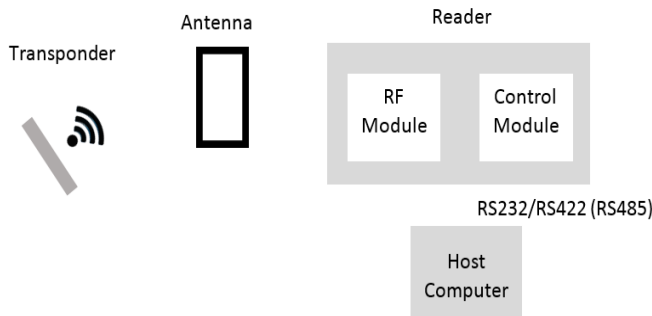


Fig. 5. How RFID Work.

RFID technology increases a number of fears regarding privacy, security and law enforcement. Current RFID's data privacy is exposed when other user has a same NFC device he or she can also read the data and tend to scan random tag number. To overcome data exposure problem, this study is to improve the security of data transmission. Therefore, a new method is proposed for matching the availability of document file which search the information with NFC based on basic system developed. In fact, the new matching method with verification mechanism helps to reduce time when searching the document file at the document room which the employee may not know where the current files are. Furthermore, it is convenient since the process of searching the data is smooth and tend to avoid human mistake that could be stolen or misplace. RFID is chosen since it cannot be easily replicated. It is based on the component content in that RFID which is a small chip that contains its own unique identification and address. Therefore, we use Near Field Communication, NFC technologies to improve its security and make it more systematic.

C. Near Field Communication (NFC)

Near Field Communication, NFC is a technology that allows a device to communicate with another hardware at a maximum distance of around less than 10 cm [21]. NFC is based on RFID that used same working principles, which has interface technology for short-range data communication working in the frequency band of 13.56 MHz [22] with ISO/IEC 18092 standard, compatible to ISO/IEC standards 14443 (proximity cards) and 15693 (vicinity cards) and to Sony's FeliCa contactless smart card system.

A basic principle of the NFC technology is "it's all in a touch". This means that simply touching an object or an NFC device with another NFC device immediately triggers an action. Objects can be equipped with NFC tags. These tags are used to store content like file name, file type or file id number. As shown on Fig. 6, when the NFC based reader tag the NFC-tagged that were attached at the item, such as cloth, it shows the detail information about the cloth and the sales assistant has to verify its identity to prove that the customer purchases the cloth.

Thus, NFC can be used with existing infrastructures based on the standards, excluding the need for a separate NFC infrastructure, which is make it easier and more convenient to make transactions, exchange digital content, and connect electronic devices with a touch. Moreover, NFC has been developed between NXP Semiconductors formerly Philips Semiconductors and Sony Corporation since it has the ability to read and write to devices, it is believed that they have a wider use in the future than standard smart cards.

NFC involves an initiator and a target. The initiator, as follows from the name, initiates and actively generates an RF signal and controls the exchange of data where the request is answered by a passive target. The NFC protocol also distinguishes between two modes of communication: active and passive.

Active communication is the initiator and target both communicate by making their own electric fields. The communication is done at half duplex; disengaging their RF field until no other device is transmitting. In this mode, both devices are typically having power supplies.

On the other hand, Passive mode is more common application where the initiator is the only device that generates the RF signal and having a backup key recognition [23]. The presence of the correct key is checked by the wireless link generated between the initiator and key generator. For instance, payment, public parking and toll stations are the application of Passive mode NFC.

Therefore, the proposed system is developed the verification feature to improve the security and the expiry date detection system using NFC. The tag and target device answers that call by modulating the current RF field which the initiator device listens out for, and then processes the signals, later transferring the data. The data rates currently supported are 106, 212, 424 or 848 Kbit/s.

The methodology of the proposed system is explained in Section 3.0. Also, section 4.0 demonstrates the results and findings and section 5.0 concludes the study.

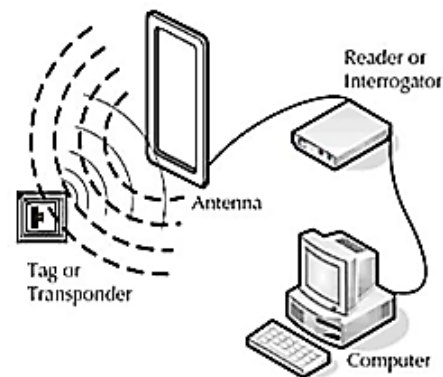


Fig. 6. NFC Topology [20].

III. METHODOLOGY

The implementation of the document file detection system is using waterfall model as shown in Fig. 7 that consists of six phases, that commonly used in software development and applicable for prototype system.

A. Project Planning and Feasibility Study

In the phase 1, the project planning is laid out. The feasibility study is implemented to gathered information and requirement such as the objective project is determined, identify and understand what type of current technology used in document file management and determine the suitable software and hardware that planning to use to make the development executed as expected. In this phase, the implementation idea that involves NFC need to be done, functionality and system requirement to accomplish the study. For the hardware specifications, a NFC reader, a smartphone with NFC integrated, a NFC tag and a personal computer is needed for the experiment setup. On the other hand, the software requirements consist of PHPMyAdmin, WAMP server and go to tags for windows are useful for the prototype development.

B. Identify and Analyze Problem

In the phase 2, the problem is identified and analysed, which is decision to either enhance or propose a method into the physical document management. Moreover, the process to collect data, identify the problem and recommend some suggestions for improving the existing system is also laid out. This phase involves in gathering data, finding solution for overcoming the limitation of the current system and identifying the target users in developing NFC technology. The main objective of this phase is to produce a solution for the proposed system and evaluate other techniques used in other application on data gathering and problem solving.

C. Propose Network Design

In phase 3, the requirement and analysis are designed according to topology design, software and hardware selection. Based on the analysis conducted, a new system needs to be proposed and designed. In this phase, planning is designed on network design on physical and logical; and the flow design. Also in this phase, the selection of the software and hardware that going to be use is properly designed. In this phase, we designed the web based application to be developed using personal computer.

D. Implementation

In phase 4 shows the installation and configuration of hardware and software which is using NFC and implemented in the real system. A database is created to store the required data and integrated with the NFC reader, NFC tags for the secure system. For the database design, there are two types of database that is conceptual and logical design. Fig. 8 shows the entity relationship diagram (ERD) that refers to the conceptual database. The development of system used the hardware and software required which is NFC reader (hardware), a set of workstation which is PC, CPU, keyboard and mouse (hardware), NFC tag (hardware), GoToTag application (software), PhpMyAdmin (software).

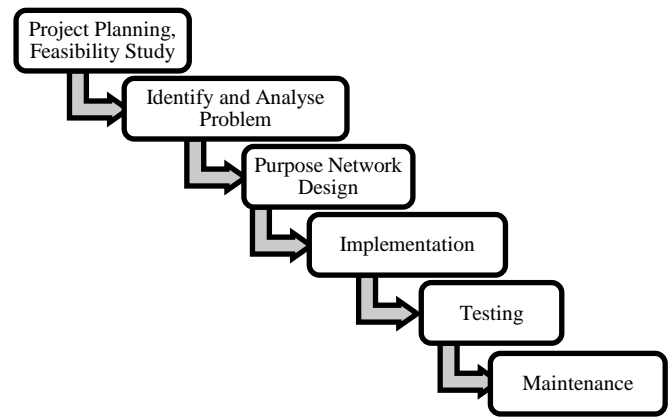


Fig. 7. Waterfall Model Life Cycle.

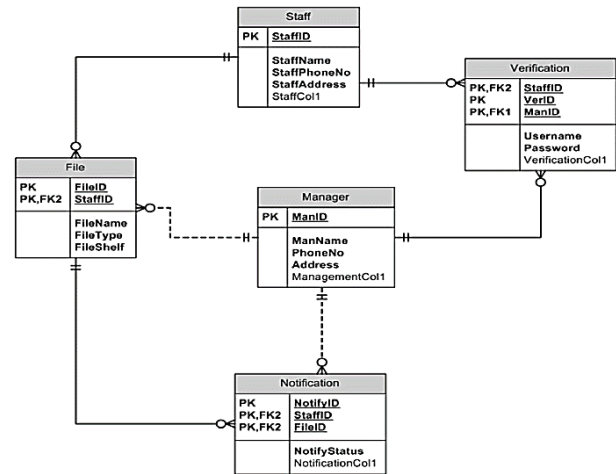


Fig. 8. ERD for the Database Design.

E. Testing

In phase 5, for testing phase, unit testing, integration testing, and system testing is performed. The unit testing is to ensure that NFC reader is switched on by looking at the green light at the upper right corner of the device and the reader is ready to scan the NFC tag. Besides, the integration testing is determined that the combination of NFC writer, NFC tag, database and developed interfaces are functioned well. At this stage, when the NFC tag is scanned at the NFC reader, then there is a sound of “beep” to indicate that the NFC tag is acknowledged by the NFC reader. After that, the information is appeared on the interfaces showing the details data about the physical files. The system is tested by going through the data validation and error-handling. All testing is to ensure the document file tracking system using NFC environment is working properly.

F. Maintenance

In phase 6, the requirement statement need to be accomplished by researchers and any changes need to be updated and recorded for future reference. The effectiveness of the system application is based on the level of reliability and validity of a recorded data. The hardware and software is setup as shown in Fig. 9.

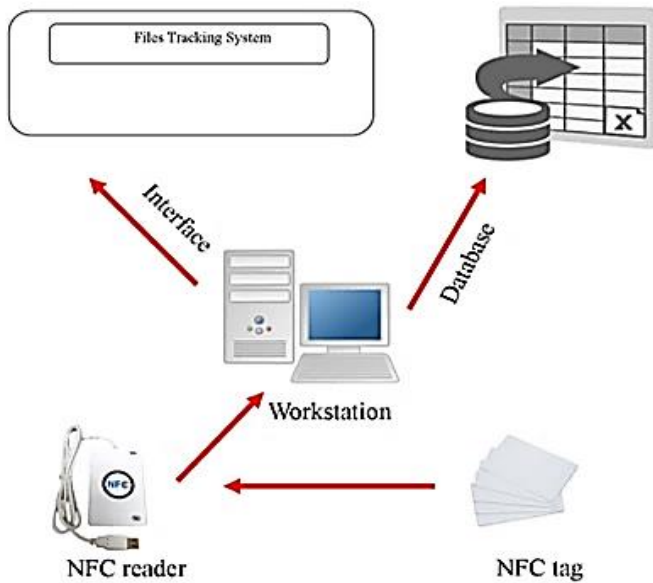


Fig. 9. Hardware and Software Setup of the Proposed System.

IV. RESULTS AND FINDINGS

In this paper, experiments are shown during the proposed system development, which is the verification and detection of document file detection. The first experiment is to develop the verification feature, which is integrated with databases, Document File Detection System Interfaces and NFC reader as shown as in Fig. 10. The main page displayed that dual verification has occurred when the employee need to scanned his or her ID to the NFC reader to indicate that the employee is the authorized user and the ID number will display on the main page. Then, the NFC tag at the physical document is tapped to scan information about the physical document and the data is appeared on the File ID section by displaying the subject code, semester rack and subject name as in Fig. 11 in order to conform that this physical document belongs to the respective employee.

Then, click the button SAVE to store information into the database. After the data is saved, the pop up menu with "DATA SAVED!" indicates that the data have been safely stored in the database as in Fig. 11. The admin clicked a button "Exit" to end the session.

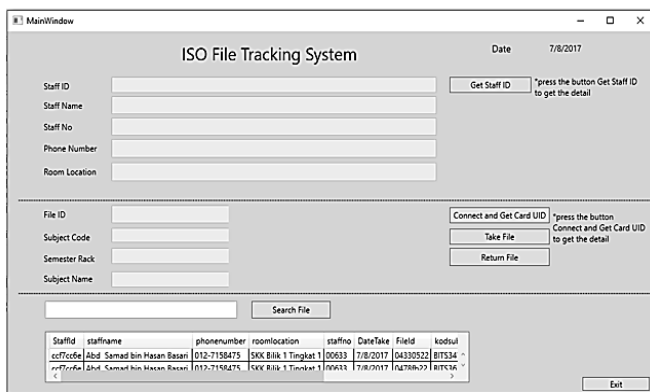


Fig. 10. Main Page.

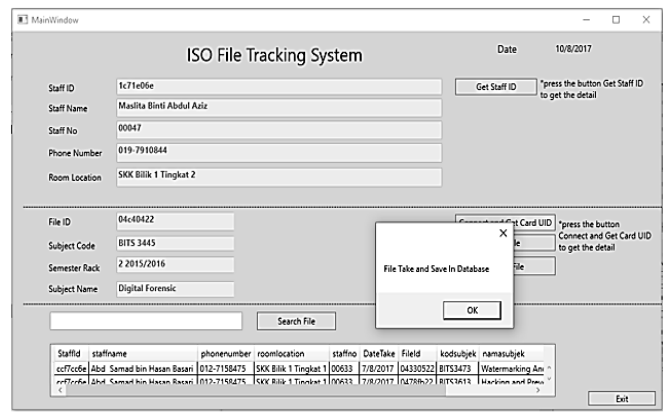


Fig. 11. The Status of Physical Document File.



Fig. 12. Physical File Search for Verification.

Fig. 12 shows the user interface as when the user wants to take the physical document out from physical document room, the search file button is used to search the location of the file and the output shows if the physical document is in the room or not. If the physical document is in the room, the information shows the location and employee who currently holds the document file, the information is displayed at the screen.

Based on our findings, employee can view expired or not, which display the items information, the name of the employee who access the system and show the expiry date about the food product from the proposed system.

Another outcome from the findings is the user interface of this proposed system, displayed the list of items tag information with time remaining and status of the current food expiry date, which is operated during the data processing between the NFC tag and the database. This function can be enhanced to be more effective and efficient system with the additional features of automatic read and save data into the database or cloud based database.

The recommendation for future development is there is no need to display the owner of employee's name at record bar because it creates a redundancy with the record displayed at top of the interface and only show the current or latest location of the document file.

V. CONCLUSION

In this paper, we proposed a file management detection using NFC (short range) for file management system. The combination of NFC with file management, helps organizations to be more effective and efficient in operation. The proposed system named as Document File Detection integrates security characteristics such as verification feature for making the system more robust and efficient. As a conclusion, the proposed system is recommended to produce a

better performance and operates in cloud based file tracking system for faster detection. The future system is planning to design that aligned with 4th Industrial Revolution.

ACKNOWLEDGMENT

Thank you to the Center of Applied Computing Technology (C-ACT), Fakulti Teknologi Maklumat dan Komunikasi (FTMK), Universiti Teknikal Malaysia Melaka (UTeM) and MyRA.

REFERENCES

- [1] Mathioudakis, I. Rousalova, A.A. Gagnat, N. Saad, G. Hardavella, "How to keep good clinical records", *Breathe (Sheff)*, vol. 12 no. 4, pp. 369–373 doi: 10.1183/20734735.018016, 2016.
- [2] S.S Zainal Abidin and M.H. Husin, "Improving accessibility and security on document management system: A Malaysian case study", *Applied Computing and Informatics*, open access journal, DOI: 10.1016/j.aci.2018.04.002, 2018.
- [3] A. Husain, M. Bakhtiari and A. Zainal, "Printed Document Integrity Verification using Barcode", *Jurnal Teknologi*, vol. 70, no. 1, pp. 99–106, 2014.
- [4] P. Tan, H. Wu, P. Li and H. Xu, "Teaching Management System with Applications of RFID and IoT Technology" *Education Sciences*, vol. 8, no. 26, pp. 1-13, 2018.
- [5] M. Gaspar, J. Julião, M. Cruz, "Organizational Strategies Induced by the Fourth Industrial Revolution: Workforce Awareness and Realignment", *Innovation, Engineering and Entrepreneurship. HELIX 2018. Lecture Notes in Electrical Engineering*, vol. 505. pp. 330-336, Springer, 2018.
- [6] A. Alqarni, M. Alabdulhafith and S. Sampalli, "A Proposed RFID Authentication Protocol based on Two Stages of Authentication", *Procedia Computer Science*, vol. 37, pp. 503–510, 2014.
- [7] U.A. Pozdnyakova, V.V. Golikov, I.A. Peters and I.A. Morozova, "Genesis of the revolutionary transition to industry 4.0 in the 21st century and overview of previous industrial revolutions. In E. Popkova, Y. Ragulina and A. Bogoviz A. (eds) *Industry 4.0: Industrial Revolution of the 21st Century*", Springer, vol. 169, pp.11-19, 2019.
- [8] M. Akshatha, K.P. Alankrutha, A. G. Janitha, M. Lavita, V. G. Smitha, "Student Authentication and Verification System using Barcode Scanner", *International Journal of Internet of Things*, vol. 6, no. 2, pp. 71-74, 2017.
- [9] A. Shaikh, S. Mali, S. Tambe and A. Yadav, "Mobile barcode system with inventory management and employee work tracking using Google Analytics", *International Journal of Engineering and Computer Science*, vol. 4, no. 2, pp. 10547-10549, 2015.
- [10] M. Gangurde, P. Ghule, P. Kasar, A. Satpute and S. Tupe, "Business Logistics System by using Robust Barcode Scanner", *Imperial Journal of Interdisciplinary Research*, vol. 3, no. 4, pp. 1528-1530, 2017.
- [11] N.M.Z. Hashim, N. Ibrahim, N.M Saad, F. Sakaguchi and Z. Zakaria "Barcode Recognition System", *International Journal of Emerging Trends & Technology in Computer Science*, vol. 2, no. 4, pp. 278–283, 2013.
- [12] P. Bodnar, & L.G. Nyul. (2012). Improving Barcode Detection with Combination of Simple Detectors. [Online]. Available FTP: <https://doi.org/10.1109/SITIS.2012.52>.
- [13] H. Subramaniam, M. Hassan, and S. Widyarto. "BarCode Scanner Based Student Attendance System (SAS)", *Journal of Technology of Information and Communication (Jurnal TIKOM)*, vol. 1, no.3, pp. 173–177, 2013.
- [14] S.W. Park and I.Y. Lee, "Anonymous Authentication Scheme Based on NTRU for the Protection of Payment Information in NFC Mobile Environment", *Journal of Information Process System*, vol. 9, pp. 461–476, 2013.
- [15] D. Parkash, T. Kundu and P. Kaur, "The RFID Technology and Its Applications: A Review", *International Journal of Electronics, Communication and Instrumentation Engineering Research and Development*, vol. 2, no. 3, pp. 109-120, 2012.
- [16] G. Arcese, G. Campagna, S. Flammini and O. Martucci, "Near-field Communication: Technology and Market Trends", *Technologies*, vol.2, pp. 143-163, 2014.A. Yewatkar, F. Inamdar,
- [17] R. Singh, A. Ayushya and A. Bandal, "Smart Cart with Automatic Billing, Product Information, Product Recommendation Using RFID & Zigbee with Anti-Theft", *Procedia Computer Science*, vol. 79, pp. 793–800, 2016.
- [18] D.B. Datta. "Radio Frequency Identification Technology: An Overview of its Components, Principles and Applications", *International Journal of Science, Engineering and Technology Research*, vol. 5, no. 2, pp. 565–574, 2016.
- [19] Atlas RFID Store. (2012). The basics of an RFID system, [Online]. Available FTP: <http://rfid.atlasrfidstore.com/hs-fs/hub/300870/file-252314647pdf/Content/basics-of-an-rfid-system-atlasrfidstore.pdf>.
- [20] K. Curran, A. Millar and C.M. Garvey, "Near Field Communication", *International Journal of Electrical and Computer Engineering*, vol. 2, no 3, pp. 371-382, 2012.
- [21] W. Suparta, "Application of Near Field Communication Technology for Mobile Airline Ticketing", *Journal of Computer Science*, vol. 8, no. 8, pp. 1235-1243, 2012.
- [22] G. Arcese, G. Campagna, S. Flammini and O. Martucci, "Near Field Communication: Technology and Market Trends", *Technologies*, vol.2, pp. 143-163, 2014.
- [23] R. Steffen, J. Preißinger, T. Schöllermann, A. Müller and I. Schnabel, "Near Field Communication in an Automotive Environment use cases, architecture and realization", *Second International Workshop on IEEE*, pp. 15-20, 2010.

A Machine Learning Approach for Predicting Nicotine Dependence

Mohammad Kharabsheh¹

Computer Information System, The Hashemite University
The Hashemite University, Zarqa, Jordan

Omar Meqdadi²

Software Engineering, Jordan University of Science and
Technology Jordan University of Science and Technology
Irbid, Jordan

Mohammad Alabed³

Bio-Medical Engineering, The Hashemite University
The Hashemite University, Zarqa, Jordan

Sreenivas Veeranki⁴

Medical Science, University of Texas Medical Branch
University of Texas Medical Branch, USA

Ahmad Abbadi⁵

MD, Tobacco Control Intern,
World Health Organization
Amman, Jordan

Sukaina Alzyoud⁶

Community & Mental Health Nursing,
The Hashemite University, Zarqa, Jordan

Abstract—An examination of the ability of machine learning methodologies in classifying women Waterpipe (WP) smoker's level of nicotine dependence is proposed in this work. In this study, we developed a classifier that predicts the level of nicotine dependence for WP tobacco female smokers using a set of novel features relevant to smokers including age, residency, and educational level. The evaluation results show that our approach achieves a recall of 82% when applied on a dataset of female WP smokers in Jordan.

Keywords—Machine learning; nicotine dependency; Women; Waterpipe; classification

I. INTRODUCTION

Bioinformatics is offered as a multidisciplinary field that helps researchers improving methods and software tools in order to understand biological data for several purposes under consideration by human beings. Bioinformatics is based on the employment of biology, computer science, mathematics and statistics to examine and interpret biological data. That is, bioinformatics is considered as a term for the body of biological researches that use computer programming and techniques as a part of their methodology. Additionally, the reference to some analysis "pipelines" is commonly used in the field of genomics.

Tobacco smoking is one of the most problematic public health problems that requests research, policy, and program initiatives [1]. Tobacco smoking behavior is related to several dimensions such as personal, social, community factors. Thus, knowing these factors is useful in developing a classification model for that behavior. For instance, solutions for waterpipe smoking cessation could be enriched by developing of models that classify smoker behaviors and thus may generate new hypotheses for clinical research. To do this, an accurate selection of variables that are strongly related to the behavior of smokers is required.

Unfortunately, to the best of our knowledge, there is not much support for automated generation of nicotine dependency levels from clinical datasets using machine learning classifiers. This study aims at determining whether machine learning approaches can assist in classifying waterpipe smoking behaviors of women. In this paper, we apply machine learning techniques to a corpus of women tobacco smoking questionnaires, which were previously developed by the authors of this work in [2], to discover and detect *Nicotine Dependence level* of Jordanian women. One of the long-term goals of the authors is to provide knowledge-rich environment that improves the quality of clinical decisions.

In particular, we formulate our study in the form of two research questions:

RQ1: Can we accurately predict if nicotine dependence level using classification factors?

Our obtained results show that we can build highly accurate prediction models for detecting women waterpipe smokers' level of nicotine dependence. For instance, we developed a machine learning classifier that achieves a recall of 81% recall and a precision of 75%.

RQ2: Which factors are the most important as predictors of nicotine dependence level?

We constructed a decision tree classifier and performed a Top Node analysis to identify the most informative factor for predicting nicotine dependence level. Nicotine dependence is a state of dependence upon nicotine [3].

The remainder of this paper is organized as follows. Section II reviews related. Section III discusses the methodology we follow in this study. Section IV presents the obtained results of our study. Section V discusses our obtained results. Section VI introduces the main threats to validity of

this work followed by Section VII with the conclusion of the paper and some plans for future research.

II. RELATED WORKS

The capability of using databases in order to extract useful information for quality health care is a vital for the success of healthcare institutions [4]. Historically, there are a several studies of investigations that necessity of using learning classifiers with Healthcare application and health informatics classifications.

Shouman et al. [5] performed nearest neighbor approach on benchmark data set to explore the performance of such approach in the diagnosis of heart diseases. Their approach achieves an accuracy of 97.4%. Brown et al. [6] apply SVMs on gene expressions in order to classify genes based on functionality. The obtained results show that SVMs are well performed with the problem of microarray gene classification. Nahar et al. [7] examined the effectiveness of classifier with predictive apriority for classifying heart disease in men and women.

The effectiveness of decision tree, neural network and naïve Bayes network in predicting heart attack were explored in [8]. The obtained results claim that the Naïve Bayes fared outperformed decision Trees as it could identify all the significant medical predictors. The study in [9] proposed and evaluates the effectiveness of a learning classifier on Pima Indian diabetes dataset. The results claimed that the machine learning is effective to detect diabetes disease diagnosis. The performance of neural network, Fuzzy logic and decision tree in diagnosing diabetes were examined in [10].

Kampourakia et al. [11] have introduced a web-based application that is based on SVMs to makes automatic diagnoses about health problems. Razzaghi et al. [12] have proposed multilevel SVM-based algorithms. They evaluate the proposed approach on public benchmark datasets with imbalanced classes and missing values in health applications. Their results show that multilevel SVM-based method produces accurate and robust classification performance. Yu et al. [13] present SVM approach to classify persons with and without common diseases. The approach shows effectiveness in detecting persons with diabetes and pre-diabetes in a sample of the U.S. population. The study in [14] proposed SVM approach that was trained using several terminological features to assign protein function and then choose passages based on the assignments.

To the best of our knowledge, this is the first work in the area of investigating the role of machine learning in detecting the nicotine dependence level of smoking women.

III. PROPOSED METHODOLOGY

In this section, we describe the design of our study. Initially, we introduce the dataset that is used in our study, and next we list the factors that are considered in our classification approach. Finally, we provide the prediction models and the performance metrics that is used in the evaluation of proposed models.

A. Studied Dataset

Our study was conducted among a sample of Jordanian women. A total of 108 women participated in the study with an age range of 18 to 56 years (mean = 26, $SD \pm 9$). Almost all participants 94.5% reside in an urban setting. More than two third 69.7% had a university degree. Thirty eight percent of study participants were students.

To produce concrete results, we collected our dataset over three points of time (two weeks before, two weeks into-, and two weeks after Ramadan. Objective measures were collected over three times before-, once during-, and after Ramadan. The study was conducted in the gynecology- obstetric clinics of two hospitals (one governmental and one private) in Amman city - Jordan. On average 35 patients are seen on daily basis at the clinics. All the gynecology- obstetric clinics of both hospitals were included to recruit none-pregnant study participants. In addition, all antenatal clinics affiliated with Hiba hospital were visited to recruit pregnant women. Inclusion criteria was women who are 18 years or older; able to read and write Arabic; absence of serious illness or being identified as high-risk patient.

The Women Tobacco Smoking Questionnaire (WTSQ): developed by the Principle Investigator, which is designed as a single measure to assess pattern of tobacco smoking among women. The questionnaire consist of four sections: (1) Demographics which includes age, educational level, marital status, etc., (2) tobacco smoking status asking about history of smoking habits, waterpipe smoking habits, (3) depression symptoms scale [15], this scale includes 6 items that assess the presence of depression, (4) Waterpipe Nicotine Dependence Scale [11], this scale measures level of nicotine dependence among waterpipe smokers, (5) waterpipe smoking during Ramadan, this part ask participants about their waterpipe smoking during Ramadan. Response options in the questionnaire vary based on the construct and items measuring that construct. They range from Likert-type responses; yes/no responses, fill in the blank, to a multiple-choice question.

B. Classification Factors

To classify and predict women waterpipe smokers' level of nicotine dependence, we considered 19 factors as shown in Table I. We use these factors since they perform well in traditional tobacco prediction research and represent standard factors for the desire for women to smoke waterpipe [2, 16]. Another rational is that these factors also cover experiencing cravings that leads them to smoke waterpipe [17, 20]. It was demonstrated that young initiation age of smoking linked to being a regular smoker at a later age [17, 18, 19]. Moreover, it was shown that number of tobaccos smoked significantly related to level of nicotine dependence [17, 21, 25, 29, 30].

C. Creating the Corpus

The primary step involved in performing our classification purpose is creating the corpus that represents the input of machine leaning classifiers. For this work, the corpus includes the extracted values relevant to every classification factor for each instance of our studied dataset. These values are extracted from the women's responses of WTSQ.

TABLE I. SUMMARY OF CLASSIFICATION FACTORS

Classification Factor	Definition
Age	Participants age should be 18 years or older
Residence	place of residence
Education-Level	The highest level of education of the participants.
Work-Status	Type of work
Current-Tobacco	Number of tobaccos of any type smoked in the last 30 days even if one puff
Past-Tobacco	Have you smoked tobacco in the past
Tobacco-Age	How old were you when you first started smoking tobacco
Tobacco-Type	Type of tobacco products currently smoke
Number-of-Cigarette	Number of cigarettes smoked
Current-Waterpipe	Number of waterpipe of any type smoked in the last 30 days even if one puff
Waterpipe-Week	Number of waterpipe of any type smoked in the last seven days even if one puff
Waterpipe-Inhale	Do you inhale the smoke when you smoke waterpipe
Waterpipe-Stop	How many times could you stop waterpipe for more than 7 days
Waterpipe-Month	Same as current tobacco smoke
Waterpipe-Alone	Do you smoke waterpipe alone
Waterpipe-Need	Have you ever felt that you actually need to smoke waterpipe
Waterpipe-Income	The percentage of income that you regularly spend for waterpipe smoking
Waterpipe-Days-Without	Number of days you could spend avoiding waterpipe
Waterpipe-Cigarette-Instead	When I feel the need to smoke waterpipe and it is not available, I smoke a cigarette instead

Next, we label each instance of the corpus with the associated nicotine dependency level by finding the summation of all participant answers and divided to three groups (A-High Score, B, C) with equal participants in each group. Table II summarizes the corpus information.

D. Prediction Models and Evaluation Metrics

There are numerous machine learning techniques such as Support Vector Machines (SVM) that can help the achievement of our classification goals. In this study, we chose to use the below classification approaches, which have been used with relative success in prior classification work [5, 22, 23, 27] with different domains and problems.

TABLE II. SUMMARY OF CORPUS INFORMATION

Total number of instances	Number of Level A	Number of Level B	number of Level C
108	36	36	36

- Support Vector Machine Learner (SMVL): is an approach that increases the dimensionality of data until the data points are differentiable in some dimension.
- Bayesian Learner (Naïve Bayes): is a Bayesian learner, which is like the techniques that are used in classifying email spam.
- K-Star: is a nearest neighbor algorithm that utilizes a distance metric such as the Mahalanobis distance.
- IBk: is a single-nearest-neighbor algorithm, which classifies data entities via using the closest associated vectors in the training set through distance metrics.

Several good quality implementations of SVM are available. We use the WEKA toolkit implementation [21, 31] to build our model.

With supervised classifiers, the dataset is divided into two sets: a training set and a test set. The training set is used to train the classifier, while the accuracy of the model is measured using the test set. In our study, the decision of which subset is used as a training set or a test set is controlled by 10-fold cross-validation [23] technique, which was widely used.

We used four performance metrics to evaluate the efficacy of each classifier: Precision that represents the percentage of retrieved instances that are relevant ($P = \text{True Positives} / (\text{True Positives} + \text{False Positives})$). Recall represents the percentage of relevant instances that are retrieved ($R = \text{True Positives} / (\text{True Positives} + \text{False Negatives})$). F-Measure is metric that is calculated by a combination of precision and recall ($(2 * R * P) / (R + P)$), and thus its value is between 0 and 1. ROC represents the area under the Receiver Operating Characteristic (ROC) curve, which is based on the plotting of true positives versus false positives.

IV. STUDY RESULTS

We now present the details behind the results and the outcomes of our study that were obtained by answering our research questions posed before.

A. RQ1: Can we Accurately Predict Nicotine Dependence Level using Classification Factors?

To answer this question, we want to build prediction models to help classifying women waterpipe smokers' level of nicotine dependence, and we want to know if we can accurately predict these dependencies using the factors that we examined early.

As we mentioned earlier, we used several SVM approaches to build our prediction models. Also, we used the 10-fold cross validation approach to divide our inputted dataset into training and test sets. The effectiveness of our models is evaluated using the recall, precision, ROC, and F-measure metrics. Now let us look at our proposed classifiers that were trained using a combination of all factors that are given in Table I. The performance results of our classifiers are shown in Table III.

It is observed that our obtained results show the prediction improvement when comparing our developed classifier with the baseline model in terms of all evaluation measures. For instance, when comparing our SMO classifier to the baseline

model, the improvement ratio is 0.82 in terms of recall and 0.43 in terms of precision. *That is, we can build highly accurate prediction models for detecting women waterpipe smokers' level of nicotine dependence.* Thus, our results demonstrate that several factors of a person such as age, level of education, and the number of cigarettes impact the nicotine dependence level of Jordanian women.

Our second observation is that SMO and Naïve Bayes offer better classification accuracy than the rest of the machine learning classifiers. For instance, Naïve Bayes computes a probability for each class based on the probability distribution in the training dataset. Therefore, with each training example, the prior and the probability can be updated dynamically to achieve flexibility and robustness to classification errors. On other hand, the SMO learner achieves better accuracy because of increasing the dimensionality of data until the data points are differentiable in some dimension. Additionally, the space usage needed for SMO is linear in the size of training set; therefore it allows SMO to handle very large training sets with higher accuracy.

B. RQ2: Which Factors are the Most Important as Predictors of Nicotine Dependence Level?

Here, we try to evaluate the performance of different factor group combinations for performing our classification. To do this, we combined related factors into four groups, as follows:

- Group1. Age, Residence, Level_Education, Work Status, Waterpipe-Income
- Group2. Tobacco Past, Tobacco Age, Tobacco-Type, Number-of-Cigarette
- Group3. Current-Waterpipe, Waterpipe-Week, Waterpipe-Month, Waterpipe-Need, Waterpipe-Cigarette-Instead
- Group4. Waterpipe-Inhale, Waterpipe-Stop, Waterpipe-Alone, Waterpipe-Cigarette-Instead

To answer RQ2, a classification model is trained using factors from each factor group and then its precision and recall are measured. We developed these classification models using the SMO approach since, as we discussed early, it has outperformed other classification approaches in term of recall and precision.

Group4 produced poor results, see Table IV. One reason could be contributed to the fact that waterpipe mostly smoked in gatherings and not alone. Another interpretation could be that women did not think to stop waterpipe smoking since previous studies [24] showed that they do not perceive it as harmful to health. Group1 produces the best results. One explanation might be as indicated in previous findings that nicotine dependence increases with age. Additionally, living in urban and sub-urban settings could facilitate smokers' access to places that serve waterpipe or sell waterpipe tobacco. Working and having personal income could enable individuals to be economically independent to spend money on waterpipe smoking.

In an attempt to get a zoomed-in picture, we also evaluate the effectiveness of each factor independently as a predictor of

nicotine dependence level. Instead of measuring the performance of each factor in predicting nicotine dependence level, we chose to use a decision tree to rebuild a classifier that is trained using all classification factor given in Table I.

The essential algorithm that builds the decision tree is the C4.5 algorithm [26]. C4.5 follows the greedy divide and conquer approach using the training data, where it begins with an empty tree, and then it adds decision nodes (leaf) at each level. Moreover, the information obtained using a specific factor/attribute is calculated, and then the attribute with the highest information gain is chosen. Additional analysis is performed to determine the threshold (e.g., cut-off) value at which to split the attribute. This process is recursively repeated at each level until the number of records in the leaf reaches the specified threshold.

With decision trees, we could perform the Top Node analysis [28] to order factors based on their effectiveness in predicting nicotine dependence level. The Top Node approach examines the structure of a decision tree [18], and counts the appearance of each factor at each level of the tree. Then, the importance rank of each factor is determined by the combination of the tree level in which the factor appears and the occurrence count of the factor. That is, the root node of the decision tree represents the most important factor and so the factors become less important as we move down the tree. The performance of our decision tree classifier that was trained using the combination of all factors and was build using the C4.5 algorithm is given in Table V. As we could observe, SMO and Naive Bayes have produced better results than decision tree.

On the other hand, the results of the Top Node analysis are shown in Table VI. The table shows the top factors that appear in the first three levels (e.g., levels 0, 1, and 2) of the created tree along with number of occurrences of each top factor. *For our dataset*, the age factor is the most influential than other considered factors. This finding could be contributed to the assumption that women have more ability to smoke water pipe more freely with age. Interestingly previous studies demonstrated that nicotine dependence level increase with age [15]. Moreover, we would assume that with age it becomes more difficult for women to decrease or quit smoking.

TABLE III. CLASSIFICATION RESULTS OF NICOTINE DEPENDENCE DETECTION USING MACHINE LEARNING ALGORITHMS

Learner	Recall	Precision	F-Measure	ROC
SMO	0.82	0.43	0.56	0.90
Naïve Bayes	0.79	0.42	0.55	0.91
K-Star	0.47	0.21	0.29	0.69
IBk	0.64	0.29	0.41	0.74

TABLE IV. CLASSIFICATION RESULTS OF NICOTINE DEPENDENCE DETECTION USING COMBINATION OF FACTORS

Group	Recall	Precision	F-Measure	ROC
Group1	0.75	0.38	0.51	0.84
Group2	0.63	0.28	0.39	0.74
Group3	0.45	0.16	0.24	0.65
Group4	0.42	0.15	0.22	0.61

TABLE V. CLASSIFICATION RESULTS OF NICOTINE DEPENDENCE DETECTION USING C4.5 ALGORITHM

Learner	Recall	Precision	F-Measure	ROC
C4.5	0.69	0.33	0.45	0.76

TABLE VI. RESULTS OF TOP NODE ANALYSIS FOR THE DECISION TREE ALGORITHM

Level	Frequency	Attribute
0	7	age
	3	Work-Status
1	9	Tobacco Past
	6	Level_ Education
2	12	Tobacco Current
	9	Tobacco-Type
	2	Residence

V. DISCUSSION ON FINDINGS

In this study, we have used the supervised classifiers to develop our approach. We showed the effectiveness of our classification approach in predicting women Waterpipe smoker's level of nicotine dependence. Our results provide the performance of the studied factors and attributes. The results suggest that our approach would help researchers in the planning for health management of female smokers.

We could conclude that the developed model outperforms a random guessing approach that would result in an overall misclassification rate. That is, comparing with random guessing would verify the strength of our model. We correctly achieved a recall of 82% and a precision of 43%. However, the produced model is based on a dataset that is extracted from answers of female smokers, and thus it is possible that includes false negative answers. Such sampling may be subjective and so could affect the classification performance. Therefore, we do not claim that our evaluation is without faults. Moreover, although our model achieves higher recall, the model does not achieve high precision values. This could be a main weakness of our model since it represents a troubling finding. Other weaknesses are discussed as threat to validity in the next section. Possible future work could study how selection of study dataset of habits impact the ability of our approach, and study how to improve the precisions of our model by dealing with possible threats of validity of this study.

The research was undertaken using the supervised classifiers with specific classification approaches such as Bayesian Learner and decision trees. This research could be undertaken using other classification approaches or through the usage of unsupervised classifiers. However, we believe that unsupervised classifying model could be much difficult to understand and use in practice for health care planning where we are looking for simple and basic rules that practitioners could use. Also, it is shown in the literature that the used approaches, such as decision trees, outperforms other supervised classification approaches [28].

VI. THREATS TO VALIDITY

We now examine threats. We use datasets of 108 Jordanian women age range of 18 to 56 years, and thus it might not be

representative of all women out there. There may be other factors that we did not consider in our work, such as family and friends waterpipe smoking, waterpipe smoking sessions, waterpipe smoking heads, and psychological status such as depressive modes. We plan to evaluate the effectiveness of other factors and dimensions in future.

In this work, we used several commonly used machine learning techniques such as support vector machine learner and decision trees. However, each of these techniques has its own limitations that could affect the validation of our obtained results. More research using other techniques might be part of our future work.

VII. CONCLUSION AND FUTURE WORK

The current study exploited the effectiveness of machine learning techniques in classifying and predicting nicotine dependence level of waterpipe smoking women. We have performed a study based on a set of factors obtained from a dataset of 108 women with an age range of 18 to 56 years.

This work presents machine learning classifiers based on support vector machine, Bayesian learner, nearest neighbor algorithm, and decision trees for predicting nicotine dependence level of Jordanian women. To build our models, we used a set of factors such as age, level of education, and working status.

Our results show that the presented prediction models have reasonable accuracy with 82% recall in the best case and 47% recall in the worst case. In addition, a precision of 43% is achieved in the best case and 21% in the worst case. Top Node analysis shows age is the most important factor in our classification.

We aim to explore more classification factors and study the effectiveness of other machine learning techniques in predicting nicotine dependencies in future studies in order to achieve better prediction performance. We plan to enrich our study by investigating more varies datasets from different countries and environments.

ACKNOWLEDGMENT

The current study was funded by the Deanship of Scientific Research at the Hashemite University. We would also like to thank Hiba Privet Hospital for approving the study and providing access to their out-patient's clinics.

REFERENCES

- [1] WHO. (2018). WHO global report on trends in prevalence of tobacco smoking 2000–2025 (Second Edition ed.). Geneva: World Health Organization.
- [2] Alzyoud, S., Veeranki, S.P., Kheirallah, K., Shotar, A.M., Pbert, L. (2016). Validation of the Waterpipe Tolerance Questionnaire among Jordanian School-Going Adolescent Waterpipe Users. *Global Journal of Health Science* 8(2): 8(2):198-208. doi: 10.5539/gjhs.v8n2p198.
- [3] D'souza, M. S., & Markou, A. (2011). Neuronal mechanisms underlying development of nicotine dependence: implications for novel smoking-cessation treatments. *Addiction science & clinical practice*, 6(1), 4.
- [4] Eapen, A. G. (2004). *Application of Data mining in Medical Applications*. Ontario, Canada, 2004: University of Waterloo.
- [5] Shouman, M., Turner, T., & Stocker, R., "Applying k-Nearest Neighbour in Diagnosing Heart Disease Patients," *International Conference on Knowledge Discovery (ICKD 2012)*, 2012.

- [6] Brown MP, Grundy WN, Lin D, Cristianini N, Sugnet CW, Furey TS, Ares M Jr, Haussler D., "Knowledge-based Analysis of Microarray Gene Expression Data using Support Vector Machines". Proceedings of the National Academy of Sciences, 2007.
- [7] Nahar, J., Imama, T., Tickle, K., Chen, Y., "Association rule mining to detect factors which contribute to heart disease in males and females," Elsevier, 2013.
- [8] Ms. Ishtake S.H ,Prof. Sanap S.A., "Intelligent Heart Disease Prediction System Using Data Mining Techniques", International J. of Healthcare & Biomedical Research,2013.
- [9] S. W. Pumami, A. Embong, J. M. Zain and S. P. Rahayu, "A New Smooth Support Vector Machine and Its Applications in Diabetes Disease Diagnosis," Journal of Computer Science, Vol. 5, No. 12, pp. 1006-1011.
- [10] Rashedur M. Rahman, Farhana Afroz, Comparison of Various Classification Techniques Using Different Data Mining Tools for Diabetes Diagnosis, Journal of Software Engineering and Applications, 2013.
- [11] A. Kampourakia, D. Vassisa, P. Belsisb, C. Skourlasa, "e-Doctor: A Web Based Support Vector Machine for Automatic Medical Diagnosis," The 2nd International Conference on Integrated Information..
- [12] Talayeh Razzaghi, Oleg Roderick, Ilya Saфро, Nick Marko, "Fast imbalanced classification of healthcare data with missing values," 18th International Conference on Information Fusion (Fusion), 2015.
- [13] Wei Yu, Tiebin Liu, Rodolfo Valdez, Marta Gwinn, Muin J Khoury, " Application of support vector machines modeling for prediction of common diseases: the case of diabetes and pre-diabetes," BMC Medical Informatics and Decision Making2010.
- [14] Rice SB, Nenadic G, Stapley BJ: Mining protein function from text using term-based support vector machines. BMC Bioinformatics. 2005
- [15] Haddad, Linda G., Ali Shotar, Janet B. Younger, Sukaina Alzyoud, and Claudia M. Bouhaidar. "Screening for domestic violence in Jordan: validation of an Arabic version of a domestic violence against women questionnaire." International journal of women's health 3 (2011): 79.
- [16] E. Aboaziza and T. Eissenberg, "Waterpipe tobacco smoking: what is the evidence that it supports nicotine/tobacco dependence?," *Tobacco Control*, vol. 24, no. Suppl 1, pp. i44-i53, 12/09,09/16/received,11/20/accepted 2015.
- [17] R. Bahelah et al., "Waterpipe smoking patterns and symptoms of nicotine dependence: The Waterpipe Dependence in Lebanese Youth Study," Addictive Behaviors, vol. 74, pp. 127-133, 2017/11/01/ 2017.
- [18] W. Maziak, K. D. Ward, and T. Eissenberg, "Factors related to frequency of narghile (waterpipe) use: the first insights on tobacco dependence in narghile users," *Drug & Alcohol Dependence*, vol. 76, no. 1, pp. 101-106, 2004.
- [19] Alzyoud, S., Kheirallah, K. A., Weglicki, L. S., Ward, K. D., Al-Khawaldeh, A., & Shotar, A. (2014). Tobacco smoking status and perception of health among a sample of Jordanian students. *International journal of environmental research and public health*, 11(7), 7022-7035.
- [20] R. A. Auf, G. N. Radwan, C. A. Loffredo, M. El Setouhy, E. Israel, and M. K. Mohamed, "Assessment of tobacco dependence in waterpipe smokers in Egypt," *The international journal of tuberculosis and lung disease : the official journal of the International Union against Tuberculosis and Lung Disease*, vol. 16, no. 1, pp. 132-137, 2012.
- [21] D. Mays, K. P. Tercyak, K. Rehberg, M.-K. Crane, and I. M. Lipkus, "Young adult waterpipe tobacco users' perceived addictiveness of waterpipe tobacco," *Tobacco Prevention & Cessation*, vol. 3, no. December, 2017 2017.
- [22] Witten IH, Frank E, Hall MA, Pal CJ. Data Mining: Practical machine learning tools and techniques. Morgan Kaufmann; 2016 Oct 1.
- [23] Efron, B., " Estimating the error rate of a prediction rule: improvement on cross-validation ", *Technical Journal of the American Statistical Association*, vol. 78, no. 382, pp. 316–331, 1983.
- [24] Akl, E.A.; Jawad, M.; Lam, W.Y.; Co, C.N.; Obeid, R.; Irani J. Motives, beliefs and attitudes towards waterpipe tobacco smoking: a systematic review. *Harm Reduct J*. 2013, 10(1), 12, doi: 10.1186/1477-7517-10-12.
- [25] Martinasek, M.P.; McDermott. R.J.; Martini, L. Waterpipe (hookah) tobacco smoking among youth. *Curr Probl Pediatr Adolesc Health Care*. 2011, 41, 34–57. doi:10.1016/j.cppeds.2010.10.001.
- [26] Quinlan, J., " C4.5: programs for machine learning", Morgan Kaufmann Publishers Inc., 1993.
- [27] Garcia, H., Shihab, E.," Characterizing and predicting blocking bugs in open source projects," In Proceedings of the 11th Working Conference on Mining Software Repositories (MSR'14), New York, NY, USA, pp. 72 - 81, 2014.
- [28] Hassan, A., Zhang, K.," Using decision trees to predict the certification result of a build," In Proceedings of the 21st IEEE/ACM International Conference on Automated Software Engineering (ASE '06), pp. 189–198, 2006.
- [29] Kheirallah, Khalid A., Sukaina Alzyoud, and Kenneth D. Ward. "Waterpipe use and cognitive susceptibility to cigarette smoking among never-cigarette smoking Jordanian youth: analysis of the 2009 Global Youth Tobacco Survey." *Nicotine & Tobacco Research* 17.3 (2014): 280-284.
- [30] Valdivia-Garcia H, Shihab E, Nagappan M. "Characterizing and predicting blocking bugs in open source projects". *Journal of Systems and Software*. 2018 Sep 1;143:44-58.
- [31] <https://www.cs.waikato.ac.nz/ml/weka/>.

The Opportunities and the Limitations of using the Independent Post-Editor Technology in Translation Education

Burcu TÜRKMEN¹, Muhammed Zahit CAN²

Lecturer, Zonguldak Bulent Ecevit University, Applied English and Translation Programme, Zonguldak, TURKEY¹

PhD. Student, Sakarya University, The Institute of Social Sciences, Translation Studies Department, Sakarya, TURKEY¹

Assistant Professor, Sakarya University, The Institute of Social Sciences Translation Studies Department, Sakarya, TURKEY²

Abstract—A new mechanical function known as post-editing, which helps to correct the imperfections of raw machine translation output, is introduced in the translation market. While this function is commonly used as an integral part of the machine translation, it can also be used for correcting non-translated texts on its own. The main purpose of this study is to find an answer to the question of which contributions could be made to the competences of translation students by using independent post-editors during academic translation education. A model course application and survey are conducted with the participation of students from translation studies departments. The interrater reliability is used in this study. In accordance with the results, it is found that most of the students have not known the usage of the independent post-editors during the translation process. The research provides new insights into the contributions of post-editor technology to the translation education. The findings of the research also reflect the contributions of post-editor technology to the translation quality in terms of the speed-time management, the accuracy of punctuations, abbreviations, and grammar rules. It is also determined that the post-editors contribute to the competencies of the translation students. As a result, it is suggested that the post-editors may be used as an educational material in translation education. Indeed, the results require other studies about the usage of post-editors as educational materials.

Keywords—Post-editors; machine translation; translation education; computer-assisted translation

I. INTRODUCTION

Using machine translation systems and the significance of the localization industry cannot be ignored in order to meet ever-increasing demands for translation services. Different translation service providers and customers are aware that using such systems is a viable solution for translation. Certain projects need to be completed within a short time and with a low budget. In this context, translation service providers' aim is to increase the translation efficiency, improve delivery of work and customer feedback times, and keep their work in a competitive environment.

According to TAUS [1], the quality of the translated texts received from the machine translation programs and the followed post-editing processes are at two different levels. According to the first level of quality (limited post-editing), the text is called "good enough" if it can convey the meaning

of the source text accurately and comprehensibly without making any grammatical or formal corrections. At this level, the editor must be sure that there is no mistaken addition or subtraction of the translation text in terms of its semantic correctness and in such a way that the meaning complexity in the target text can be created. The second level of quality (full post-editing), "publishable quality" means to be the same as expected from human translation. In addition to clarity and correctness, the translation output must be grammatically and formally correct. In this context, there are standards updated continuously by the International Organization for Standardization (ISO) [2].

Today's technology does not have a machine translation system that can be equal to the human translation output. Therefore, the quality of the translation obtained in the target language depends on human translators rather than machine translation. ISO, which is an international standards federation worldwide, working in partnership with a large number of state-owned and independent agencies and organizations (the International Organization for Standardization) published a standard Translation Services- Post-Editing of Machine Translation Output Requirements in 2017. This standard covers issues such as machine translation concepts, language and content creation concepts, the concepts about people and institutions, the concepts related to translation, the issues related to post-editing process, post-editing requirements of machine translation outputs, tasks of post-editors¹. It can be said that these studies will continue and in this way, the interest on the post-editors will increase.

In this research, especially the independent post-editors are analysed. Under the literature review and discussion section, the studies and researches on post-editors integrated into machine translation and the systems of independent post-editors are introduced. Under the methodology section, research design, study group/the participants, the validity and the reliability of the research, procedures, data collection tools and data analysis steps are introduced. Then, the post-editors used in the research are introduced in a separate section. Under the results and discussions section, the survey questions and their results received from 140 Translation Studies

¹ Full version of the standard is not open, information about the context is given. <https://www.sis.se/api/document/preview/8027889/>, accessed: 04.20.2018.

students from English and German minors, are evaluated and displayed. Under the self-control of students and evaluation of post-editors section, two different evaluations about post-editors are given. The evaluations are carried out by the students. The first evaluation is carried out before using the post-editors, the second one is carried out after using the post-editors while they were translating the chosen texts. Under the conclusion section, the contributions of the post-editors during the translation process are given and it is suggested to use post-editors during the translation education.

II. LITERATURE REVIEW AND DISCUSSION

In Translation Studies field, the neural machine translation has been seen as a revolution since its contributions to the high quality of the translated texts and saving the effort during the translation process. In this concern, post-editing systems offer a unique opportunity for improving neural machine translation systems [3]. Post-editing is also determined as the modification process of the machine translation output with a minimum labour effort rather than re-translation of the text. Automatic post-editing aims to correct the systematic and repetitive errors found in the output of machine translation [4]. In this concern, in another research, online automatic post-editing system is introduced as trained on generic data and its exploiting user feedback to develop its performance. Online automatic post-editing system is evaluated on the output of neural machine translation systems. As indicated in the results of this research, from the view of resources and the technical expertise requirements, the current automatic post-editing technology in the typical setting of most Language Service Providers (LSPs) is seen effective [5].

According to García, the first recorded post-editor usage was blocked in the early 1960s. During the 1960s the post-editors were used by USA Airforce Foreign Technology Department and Euratom. However, when the financial support in the United States expired partially with a report prepared by Automatic Language Processes Committee (ALPAC) in 1966 if the post-editors are compared with human translation, was ended since it was thought that the post-editors are not worth the effort in terms of quality and usage difficulty. It is stated that during the 1970s, machine translation and post-editors were used by different European Union organizations and certain companies [6]².

In the research of Federico Gaspari and others, a survey was conducted with the participation of 438 stakeholders in the translation and localization sector and 30% of those reported using machine translation. While 38% of those using machine-translation indicated that their translation had already been through post-editing, 30% of them indicated that they did not use the post-editors at all, and 32% of the participants used post-editor at different levels [7]. The survey results indicate that using machine translation and post-editors in the direction of increasing demands is increasing day by day, and it is predicted that this will continue in the future [8], [9], [10].³

Full version post-editors are often used in the texts that are more important and intended for publication on the market

and are integrated with Computer Aided Translation (CAT) tools, translation memories, or dictionaries. On the other hand, limited post-editors are not often integrated with CAT tools. The limited post-editors which are generally available free of charge, may be used as the full version and fulfil more extensive functions when they are purchased. It is not a surprise that machine translation (MT) is often seen during business negotiations when the intensive pressures of localization services and the delivery of products to foreign markets are considered. It is known that a machine translation tool can translate faster. By using such tools, it is possible to translate thousands of words in a day in a cheaper way.

Since no human intervention is required in machine translation, it is the cost of these tools/programs only. However, when there is no human touch, the linguistic quality of the target text and the level of loyalty will be doubtful. The quality of the translation content received by using the machine varies and depends on many factors such as the quality and standardization level of the source material, the terminology suitability used to train the translation machine, the quality and size, the level of applied post-editing, the customer's low-quality definition and language pairs.

According to ISO 17100: 2015, post-editing means "editing and correcting the machine translation output" [11]. Allen noted the separation among the different levels of post-editing. First, it describes the determinants of post-editor levels and suggests using translation input and output to categorize these levels. It is possible for machine translation in three different levels for translation output. These can be classified as 1) translation delivered without post-editing, 2) translation delivered with limited post-editing, and 3) translation delivered with full end-format [12]. Correspondingly to the ISO standard, the students translate a common text without using machine translation, then they use the independent post-editor programs on these translated texts, and the aforementioned limited and full post-edited texts are obtained [13].

Guerberof Arenas discusses the views and thoughts on post-editing of professional translators, especially those using machine translation in a competitive environment required by modern times, in a survey supported by a survey application. It is noted that the majority of professional translators participating in the survey are satisfied with the use of post-editors in terms of workflow and timing [14]. However, some of the translators expressed that they did not like to use post-editors. They stated the reasons for this as while getting a good machine translation, some machine translation programs have been experiencing problems such as low quality, the high number of instructions to complete small tasks, maintenance of terminology, the large number of reference materials and complicated matching. The disadvantages mentioned above vary according to the types of machine translation and post-editors used by the translators. Although post-editors have the disadvantages, professional translators consider that these programs will develop over time in the localization sector and have a considerable share of machine translation output and terminology qualities.

² The post-editors are the ones integrated in machine translation.

³ For further information read and compare.

According to another study, it is stated that the post-editing process is known as its contribution to the translation quality, and this quality extremely depends on automatic metrics of machine translation. Post-editor systems do not take the translator experiences into consideration, even though the translation processes of the professional and inexperienced translators are different. However, it is seen that, besides the punctuation, spell-check results and etc., the meaning shifts and the structural issues are shown to be good indicators of post-editing effort [15].

In this study, different from machine translation software, the post-editors were used by a specific group of students who were trained in English and German translation by giving information about the types and uses of independent post-editors, suggestions about the using post-editors. It is seen in the studies related to post-editors, they mainly analyse the programs integrated with machine translation. However, under this research, researches on independent programs (which are not integrated with machine translation) have been carried out. However, the students who use the post-editors express that they get positive results on their target texts and these opinions are supported with the evaluations of the survey data.

III. RESEARCH QUESTIONS

The research questions of the study are:

- 1) Whether the students who will work as translators/interpreters know the names of certain computer-assisted translation tools, and the post-editors and their functions.
- 2) Whether the students (professional translator candidates) benefit from the post-editors by using them - independent of the native languages- into German and English foreign languages.
- 3) Whether using such technologies while translating into a foreign language contributes to professional translator competences.

IV. METHODOLOGY

A. Research Design

The purpose of the descriptive research is to describe a phenomenon and its characteristics [16]. Descriptive research includes certain types of research methods such as survey, correlation study, qualitative study, and content analysis. All this kind of types are different from the view of their data collection/analysis procedures, but not in data availability [17]. As it is seen, according to the descriptive research method, the current situation that is what has happened rather than how or why something has happened is concerned. Therefore, in order to collect data from the students and describe the results received from them, the survey has been conducted. The results are described and they indicate the current position of post-editors in translation education. The suggestion is given for improving the quality of translated texts into foreign languages and using post-editors as educational materials during translation education.

B. Study Group/ Participants

In the research, a survey has been applied to two different student groups from English and German translation departments to determine the knowledge and perceptions about post-editors. 52 students from Sakarya University [18] and 88 students from Zonguldak Bulent Ecevit University [19], totally 140 students, participated in this survey and the research voluntarily. It can be stated that the results obtained from this sample group can include other translation studies students who translate from Turkish, their native language, into German and English. By using a slightly weaker claim, it can also be advocated that the translators who translate from Turkish native language into German and English can be included to the research universe.

C. The Validity and Reliability of the Research

The qualitative research method is used in this research. Furthermore, with the purpose of indicating the validity and the reliability of the assessment, expert opinions are consulted. Common criteria are determined for the interrater reliability, and for the internal validity of the research, the triangulation technique (the consistency among the analysis of data from the survey, application/observation and self-evaluation) is followed. The interrater reliability is related to the kappa statistic. According to interrater reliability, the data is collected in the study and correct representations of the variables are measured. Measurement of the extent to which data collectors (raters) assign the same score to the same variable is called interrater reliability [20]. The questions of the survey are submitted to two Assistant Prof. Dr., as raters, in The Translation Studies Department at Sakarya University. In the simple correlation calculated between two raters, at a higher level and positive 0.97 relation is determined.

D. Procedures

The process for revealing the perceptions and applications of the students in a realistic and integrated approach is followed. In this research, translating from native languages into foreign languages is preferred because of the opinion of making more mistakes during the text production process in foreign language. The reason of preferring post-editors in foreign language is their potential for receiving an independent research result from native language, and in this framework, the international dimension increase of the research. Shortly after the translations are completed, a survey is prepared in order to find out whether the students use any program or tools for determining the reasons of faults while translating texts from Turkish into English or German, and to check the accuracy of the target texts. In the event that they use such programs and/or tools, it is aimed to learn what they are. In this concern, 7 survey questions are asked to the students.

E. Data Collection Tools and Data Analysis

Within the scope of qualitative research, the method of observation was collected via using the survey technique. The steps of the model application with post-editors are seen as below:

Step 1: At first, a joint Turkish source text is required to be translated from Turkish native language into English and German languages.

Step 2: The translated texts are checked by using the post-editors.

Step 3: Finally, via a survey, the self-checking/ evaluation of the usability and the advantages of these programs before and after the usage of post-editors has been done.

Step 4: By the favour of the survey, views of students about their own translations before using the post-editors are received.

Step 5: Thus, at the second level, the students evaluate their own target texts after using the post-editors, and the differences occurred after the usage of post-editors in the target texts are determined. In the first application, the students are not informed about the post-editors, and it is controlled whether they know anything about these programs without having an education. At the end of the first application, right after the survey, students are informed about the post-editors and they are required to check their target texts via certain post-editors.

In the last part of the research, 4 questions are asked to the students (right after translating the joint text, they are required to evaluate their target texts by using post-editors). In the light of these questions, the students are required to

- 1) Score their target texts between 1-10 before using post-editors.
- 2) Score their target texts between 1-10 after using post-editors.
- 3) Answer whether the post-editors are beneficial in terms of translation quality.
- 4) Answer in what aspects the post-editors are beneficial.

Right after making the evaluations of the translated and checked texts by using the post-editors, it is seen that the aforementioned post-editors provide an improvement on the target texts. Through the data analysis of the survey results, the results of the spell-checker and the post-editors on the translations of joint texts, the final evaluations for quality and benefits of the post-editors and self-controls of students, the descriptive analysis are followed. The results of this descriptive analysis are correlated with the related studies in literature.

V. POST-EDITORS USED IN THE RESEARCH

In the context of the research, certain post-editors and spell-checkers are used for the translation practice and then for the supervision of the translated target texts of the students in English and German. The post-editor and spell-checker programs analyse the texts to find possible typos in the target texts obtained after the machine translation. These online programs offer more than 20 correction suggestions on their memories. In addition to the suggestions for corrections, thanks to the translation tabs in the same programs, machine translation databases such as Google Translate are also available. Some of these programs can also be used as a digital dictionary. Under this research, the online GoogleSEO, Duden

and LanguageTool post-editors have been used in the translation control application carried out by German translators. During the translation control application carried out by Applied English and Translation Program students, they used the online LanguageTool and Reverso post-editors and the Spell Checker and Translate programs which can be downloaded to mobile phones. The information about how these programs work will be shared below. It is important for two reasons: firstly, it will be more transparent about how the research is conducted, and secondly, a general view of the working principles of the post-editors will be obtained.

VI. RESULTS AND DISCUSSION

In this section, the data obtained from the survey and self-evaluation questions asked to the students who are studying Translation Studies, are described. Certain evaluations are combined and evaluated in the light of more than one data. Totally 140 Students, participating in the survey and translation application carried out within the scope of the current scientific research, continue their education in Bulent Ecevit University Applied English and Translation Program (88 students) and Sakarya University Department of Translation Studies- German (52 students). The students attend to the survey and translation practices on the basis of volunteerism.

A. The Evaluations of Translation before using Post-Editors

Question 1 of the survey is intended to determine the language pairs in which students' study. Question 2 is "Please indicate the reason for making mistakes in your translations from Turkish source language into English or German target language". In addition, more than one option offered by the response to the students. The reasons of making mistakes of students while they are translating are 1) to feel weakness in making preference words on target language, 2) to be unsure of the grammatical rules of the target language, 3) to be unsure of the writing rules on the target language, and 4) to be unsure about tense usages in the target language. Except for these reasons, they indicated the reasons for lack of attention and time problem. It is seen that the students have problems in preferring words while making translating texts from Turkish source language into English or German languages. It can be said that this results from not to know certain usages except for grammatical rules in the foreign languages, and not be sure about preferring the appropriate word.

In the question 3, the students are asked to answer "Which of the options do you prefer in order to create an accurate text in terms of spelling and grammatical rules, on a foreign language?". In addition, more than one option was offered by the response to the students. Under this question, it is desired to know what might be the reasons for creating sentences with missing points. It is aimed to receive the answers to this problem classified as auditory memory, visual memory and rule knowledge. 69.3% of the participant students answered that they remember the spelling of the words as a picture, that is, they use visual memories, 38.6% remember the grammatical rules and 37.1% answered that I remember the auditory spelling of the words. In the answers to this question, it is seen that most of the students stated that they remember words and uses thanks to their visual memories.

In the question 4, students are asked to rank the answers according to their priority order. The 4th question is "List the items which help to the right usage of spelling and grammatical rules in order to obtain a complete text in the foreign language". In order to facilitate classification of the answers, three reasons such as Auditory Memory, Visual Memory and Rule Knowledge are given to the students. For these three answers, the priorities are given separately. According to the answers, it is depicted that 78 people, 55.7% of all students, choose the Visual Memory option as the first priority among the items that help to the right usage of both spelling and grammatical rules in order to create complete text on the foreign language. In this context, it is understood that students keep the words in their minds as a picture. It can be concluded that the creation of complete text on foreign language is directly related to the visual memory of the students. It can also be thought that in the context of translation education, it is possible for the translation instructors to use the visual elements to help them develop their students' skills for the creation of complete texts in foreign languages.

The answers reveal that 38 people, 27.1% of all students, choose Auditory Memory as the first priority among the items which help to use both spelling and grammatical rules in order to create complete text on the foreign language. According to the answers, it is seen that 36 people, 25.7% of the students, choose Rule Knowledge as the first priority among the items that help to use both spelling and grammatical rules in order to create complete text on the foreign language. In this context, it is understood that students keep the words in their minds depending on their spelling and grammar rules. Questions 3 and 4 are directed to the students in an interconnected manner. In this context, it can be concluded that visual materials as learning material in translation education are more helpful to students. In contrast to the use of visual materials, it is also important that students who are studying foreign languages and translation have problems in pronunciation/phonetics. To make it clearer, Table I is set out below that summarizes the answers to questions 3 and 4 together.

TABLE I. GRAMMAR AND SPELLING ERROR PREVENTERS AND PRIORITIES

	Quesiton 3: Preventer	Question 4: Priority
visual memory	69.3%	55.7%
rule knowledge	38.6%	25.7%
auditory memory	37.1%	27.1%

For question 5, students are asked to rank the answers according to their priority order. Question 5 is "What do you use to check the correctness of your target texts (translations) while translating into foreign languages?". In this question, "four different options such as Parallel Texts, Computer Programs, The Person Whom I Trust His/Her Foreign Language and I Don't use Spell Checkers", are given to the students in order to facilitate the classification of the answers. For these four answers, the priorities are given in separately. According to the answers, parallel texts mean intending to control structures such as patterns and sentence structure through texts similar to translation texts completed into the

source language and target language. According to the answers, the computer programs mean the spell-checking applications that are included in the Word Office Program and the spell-checkers in the machine translation programs such as Google Translate and/or Trados.

Here, the people who are trusted in their foreign language competences mean the teachers, teaching staff, sometimes family members or friends, who are considered to be at a higher level of knowledge of foreign language (English or German) than students. According to the answers, it is seen that only 6 of the 140 students who participated in the survey know and/or use the spell-checker programs. In this context, the majority of students are not aware of the spell-checkers. They frequently check the accuracy of the translations by using computer programs, then they search for parallel texts and consult with the teachers, teaching staff, successful friends, etc. to check their translations. It should be noted that the using of computer-aided supervision made by students will not be confused with the using of post-editors. When asked about the utilities that are used for translation, translation utilities such as Google Translate are expressed. This indicates that the learners are unaware of the post-editors. On the other hand, it is worth remembering that some translation machines or dictionaries, such as Google Translate, also provide spell checking and provide certain fixes, and in this respect, they can actually do spell-checking during the machine translation process.

In question 6, students are required to order their priorities "What kind of supporters did you use for the translation (English / German)?" Six different options to facilitate the classification of answers are offered in this question. These are, Online Dictionaries, searching on Google, Translation Software, Printed Dictionaries, People Whom I Trust on Their Foreign Language and Using Spell-Checker Programs. For these six answers, the priorities are given in separately. As it is seen from the answers, 124 people, 88.6% of the students, choose "I'm using Online Dictionaries" such as Google Translate, Tureng, Beluka, etc. as a 1st priority in response to the question. According to the answers, 24 people, 17.1% of the students, choose Searching on Google as the 1st priority in response to the 6th question, and 82 people, 58.6% of the students as the 2nd priority. According to the data of this answer, most of the students, who have translation education, do not use translation software such as Trados, Google Toolkit and Wordfast or they use rarely. The obtained results indicate that most of the students do not give priority to using published (book) dictionaries, or they use rarely. The results reflect that students prefer using online dictionaries since their easy usages, being fast and facilitating to saving time. According to the data received from the question, it is seen that the students, even if rarely, students consult to the people whom they trust their foreign languages such as teachers, friends or family members, who are thought better educated or experienced than the students are.

It is seen that 8 people, 5.7% of the students, choose spell-checkers, and more than 70% of them do not use such programs or use rarely. According to the answers of this question, it is seen that the student check their translations in the target language on the basis of the meanings of the words,

and they use the online translation programs, mainly the Google Translate application, to translate directly the sentences or phrases. The students state that while translating into the target language and then in the checking process of the translations, they search the texts as in sentences or by their titles from Google Search Engine since they think that comparing parallel texts and the similar structures may be useful. Below, the data is simplified and made clearer through Table II.

TABLE II. USED SUPPORTERS AS 1ST AND 2ND PRIORITY DURING THE TRANSLATION PROCESS

	1 st priority	2 nd priority
Online Dictionaries	88.6%	10.7%
Searching on Google	17.1%	58.6%
Using spell-checkers	5.7%	8.6%

Under the research, it is obtained that most of the students are unaware of the spell-checkers, which are important for the translation quality, and they have not used such kind of programs before. The 7th question is prepared as in open-ended form. They are asked to answer the question “What are the translation utility software while translating from Turkish into foreign languages? How do you check your translations’ correctness? The answers to this question are classified and evaluated. Within the context of this question, it is aimed to learn the translation utilities, software, programs such as online dictionaries, translation programs, websites and etc. which provide the usage opportunities in digital environments during the translation process. However, it is aimed to learn how the students check the correctness of their translations completed in the target language.

Within the context of this scientific research, two different student groups are available. The first group is from Applied English and Translation Program. It is seen that the aforementioned student group uses the online dictionaries such as Tureng, Sesli Sözlük, English-Turkish Dictionary, and Google Translate and Yandex Translate. However, they state that they use the parallel texts by searching from various search engines, consult to the people who have translation education and translation teaching staff and teachers from different forums in order to check the final forms of the translated texts.

On the other hand, the same question is asked to the second group which is from Translation Studies (German) Department. They stated that they use online dictionaries such as Tureng, Sesli Sözlük, Pons, Verbformen, Google.de, Cambridge, abkuerzungen.de, Beluka, canoonet, TDK, Glosbe, WordReference.com, bab.la, Langenscheidt Online-Wörterbuch, Konjugation.de, and Google Translate. Besides these, they stated that in order to check the accuracy of the translations, they search the parallel texts to find similar texts. They also consult with the people who have translation education and translation teaching staff from different forums in order to check the final forms of the translations. The answers of the students indicate that the methods, which students prefer for checking of the translations and the

auxiliary tools during the translation process, corresponds the similar results. As a result of the first survey, it can be said that the students are not able to perform their own audits, they only use various online dictionaries and translation programs such as Google Translate among the auxiliary translation programs. However, it is clear that students don’t check their texts’ correctness for spelling and grammatical rules, and they don’t use post-editors.

The students also stated that they check their translations by asking the people whom they trust their foreign language competences such as their teachers, translation lecturers or translators. Among the aims of this study, the importance of spell-checkers and post-editors in the translation education becomes clear. By using such programs during the translation education curriculums, the students can make their own audits on sentence structures, grammar and spelling rules, and can obtain more qualified texts in the target languages.

B. The Self-Control of Students and Evaluation of Post-Editors

The students in two groups (English and German) are asked to translate a joint text. During the text translation process, all students are free to use translation utilities, online dictionaries, etc. After collecting the first target texts, the survey above is applied to them and then, they are informed about the post-editors and they are asked to check their translations by using these post-editors.

The students are asked to evaluate themselves (their own translations) and the post-editors that they learn and use during the course with 4 questions. Firstly, the students are asked to “score their own translations between 1-10 before using post-editors (10 point means the best)”. Students are asked to translate from Turkish source language to English or German target language. During the translation process, they are free to use every kind of online sources and applications that they know. The scores of students for their own evaluations are seen in a wide range between 3 and 10. 10% of the students score between 3-4, 55% scores between 5-7, and 35% scores between 8-10 point. According to this result, the average evaluation of their translation is 7.

After completing the translations and self-evaluation, students are informed about post-editors and they are asked to check and edit their translations by using post-editors. Then, they are asked to “score their texts on which they use post-editors between 1 and 10”. By completing the evaluation of the second target texts (before using post-editors), the students can see the differences between their first texts (after using post-editors).

Compared with the first evaluations, it is observed that there is a positive change. 8% of the students score 5-7, whereas 92% of the students score 8-10. There is a significant difference between the translation of students that they don’t use and use post-editors. In the light of this data, for the general evaluation of the translations, for the students, it can be said that the post-editors are satisfactory and give positive results. Table III will allow comparing the results more easily and highlighting the results.

TABLE III. EVALUATION OF TARGET TEXT BEFORE AND AFTER USING POST-EDITORS

	Percentage of Students	Score of Translations
Before Using Post-Editors	55%	5-7
	35%	8-10
After Using Post-Editors	8%	5-7
	92%	8-10

When the translation audits by using, post-editors are completed, the students participated in the research are asked what they think about the post-editors in respect of the translation quality in the target language.

For using post-editors, 0.7% of the students choose Neutral, 2.9% choose I think it is useless, 5% choose I think it is a bit useful, quite a large group of student 91.4% choose I think it is useful (Table IV). It is seen that the data obtained from the previous question are parallel with the data of this question. While a general evaluation is asked in the previous question, more tangible data about the quality of the translations getting by using post-editors is tried to be obtained. According to this, it is seen that about 95% of the students agree that the post-editors make a positive contribution to the quality of the target text. It can be said that such data reveals the need for the post-editors to be analysed in terms of translation education.

TABLE IV. BENEFITS OF USING POST-EDITORS IN THE EYES OF THE STUDENTS

Neutral	0.7%
I think it is useless	2.9%
I think it is a bit useful	5%
I think it is useful	91.4%

Finally, the students are asked to answer the question of in which aspects do they think the post-editors are beneficial. The students are asked to order the benefits of post-editors in terms of their importance. As a result, they are agreed that the post-editors are beneficial: 113 students in the 1st line indicates the importance of translation quality, 2nd line indicates the speed-time for the delivery process of translation, 3rd line indicates the correct writing of the words, 4th line indicates the punctuation and spelling rules, 5th line indicates the grammatical rules, 6th line indicates the abbreviations, separate and compound writing rules. The 7th line indicates the number of students who think that the post-editors should be in the translation education curriculums, and the 8th line indicates that post-editors make sense of being successful, competent and being independent of the outside of the translators during the translation process. According to the answers, it is seen that the post-editors are effective for providing the benefits above.

Based on the data received above, the advantages of the post-editors are determined. At this stage, the question to which extend the independent post-editors take place in the translation education curriculum, is asked. Under this research, the translation education curricula of 15 different European universities from 9 countries are analysed from their

websites. It is seen that they include the translation technologies in their curricula, but especially any content about post-editors are not seen. This indicates that the translation studies departments in Europe neither give places in their curricula nor give details for post-editors.

VII. CONCLUSION

Considering the survey and evaluations conducted under this research, it is determined that the independent post-editors are beneficial for the translation departments' students from the point of punctuation and spelling, grammar rules and have a positive effect on the quality of the translation into foreign languages. It is found that the post-editors are useful in terms of "speed-time" in order to contribute to the delivery process since they can quickly determine the mistakes of the text at the correction stage. However, it is seen that it helps with abbreviations, separate, contiguous writing rules, and the use of a high language instead of daily language. However, there is no way to check the correctness of the translation text in independent post-editors, a comparison with the source text is not possible. In this respect, it is also necessary to be careful about post-edited texts in terms of translation. Because each proposal does not guarantee that the original manuscript will remain true for its meaning.

As in the research, about the detailed evaluation of technological developments in terms of translators/interpreters and the translation profession, carried out by Ersoy and Balkul, it is emphasized to integrate the contemporary technological changes and the new practices into the curricula of translation departments [21]. Therefore, translator trainees should not only prepare themselves for cultural and language-based conditions but also for future technologies and their advantages like using the independent post-editors as course materials during their educations. It is revealed under this research that the post-editors have different functions beyond the editing of the target text such as making sense of independence from the outside of the post-editors during the translation process. In this respect, making the post-editors a part of translation education should be emphasized in any native languages. Since the students are unaware of post-editors, it is necessary to integrate such programs into the courses related translation and technology such as Computer Assisted Translation. When the professional translator qualifications are considered, it can be said that translator candidates develop their technological, research and development competencies through the post-editors. It can be predicted that the translations can reach certain standards at this point. Literature review indicates that many researchers examine the post-editors integrated with the machine translation, whereas the post-editors can be used independently from the machine translation by the translators.

The research reveals that the post-editors are not known yet by the candidate translators. However, the translation application and the survey results indicate that the post-editors have important functions for completing texts in foreign languages. This necessitates another research about the post-editors being a translation education material. As a result of this study, it is indicated that using the post-editors during the

translation process from any native language into English and German, as a foreign language, may give similar results.

Overall, it needs to be stressed that the findings of this research are limited to the evaluations of the practices and the questionnaires. However, further studies can illustrate the issue better. Certain research topics as given below could be the further research topics about the independent post-editors:

The research about the effects of the independent post-editors on translation quality: A research on different text types could be carried out and the performances of the independent post-editors on different types of texts, and the speed of the translators by translating with the post-editors could be studied.

The research about how could the independent post-editors be more functional in translation education and language education: A research about, beyond the post-editing function, how could the independent post-editors be more functional as education material if they had certain didactical purposes.

The research about how could the independent post-editors be more functional by using audible reading, attaching visuals and vocalising, adding sample sentences.

REFERENCES

- [1] TAUS: (2016). TAUS Post-Editing Guidelines, Retrieved 21.04.2018, from <https://www.taus.net/think-tank/articles/postedit-articles/taus-post-editing-guidelines>.
- [2] KOPONEN, M. (2016), Is Machine Translation Post-editing Worth The Effort? A Survey of Research Into Post-editing and effort, The Journal of Specialised Translation, Issue 25- January 2016, University of Helsinki.
- [3] PERIS, A.; CEBRIAN, L.; CASACUBERTA, F. (2017). Online Learning for Neural Machine Translation Post-Editing, Retrieved 25.12.2018, from <https://www.groundai.com/project/online-learning-for-neural-machine-translation-post-editing/>.
- [4] VU, T.T.; HAFFARI, G. (2018). Automatic Post-Editing of Machine Translation: A Neural Programmer-Interpreter Approach, Proceedings of the 2018 Conference on Empirical Methods in Natural Language Processing, p. 3048-3053. Brussels, Belgium, October 31-November 4 2018. 2018 Association for Computational Linguistics.
- [5] NEGRI, M.; TURCHI, M.; BERTOLDI, N.; FEDERICO, M. (2018). Online Automatic Post-editing for Neural Machine Translation, Italian Conference on Computational Linguistics, Torino, Italy 10-11 December 2018. Vol. 2253, Retrieved from (25.12.2018) <http://ceur-ws.org/Vol-2253/>.
- [6] GARCIA, I. (2012), "A Brief History of Postediting and of Research on Postediting." Anthony Pym and Alexandra Assis Rosa (eds) (2012) New Directions in Translation Studies. Special Issue of Anglo Saxonica 3(3), 292–310.
- [7] GASPARI, F.; HALA, A.; DOHERTY, S. (2015). "A Survey of Machine Translation Competences: Insights for Translation Technology Educators and Practitioners." Perspectives: Studies in Translatology, p. 1–26. Retrieved 25.05.2018, from <http://dx.doi.org/10.1080/0907676X.2014.979842>.
- [8] DEPALMA, D. (2013). Post-editing in practice, Retrieved 21.04.2018, from <http://www.tcworld.info/e-magazine/translation-and-localization/article/post-editing-in-practice/>.
- [9] EDMUNDSON, H. P. and DAVID, G. H. (1958). "Research Methodology for Machine Translation." Mechanical Translation 5(1), 8-15.
- [10] GUERBEROF, A. A. (2010). "Project Management and Machine Translation." Multilingual 21(3), 1–4.
- [11] ISO Translation services -- Post-editing of Machine Translation Output Requirements, Retrieved 05.04.2018, from <https://www.iso.org/standard/62970.html>.
- [12] HU, K.; CADWELL, P. (2016). A Comparative Study of Post-editing Guidelines, Baltic J. Modern Computing, Vol. 4 (2016), No. 2, 346-353, Retrieved 21.04.2018, from https://pdfs.semanticscholar.org/b01f/c3b465c02c0174262bbfbd67987fca1222be.pdf?_ga=2.151871418.209486593.1527164074-584386589.1527164074.
- [13] ALLEN, J. (2003). Post-editing. Computers and Translations: A Translator's Guide. 35, 297-317.
- [14] GUERBEROF, A. (2009). Productivity and quality in MT post-editing, In Proceedings of MT Summit XII-Workshop: Beyond Translation Memories: New Tools for Translators MT, AMTA 2009 (26-30 Aug. 2009, Ottawa, Canada).
- [15] DAEMS, J.; VANDEPITTE, S.; HARTSUIKER, R.J.; MACKEN, L. (2017). Identifying The Machine Translation Error Types with The Greatest Impact on Post-Editing Effort, Frontiers in Psychology, August 2017, Vol. 8, Article 1282.
- [16] NASSAJI, H. (2015). Qualitative and Descriptive Research: Data Type Versus Data Analysis, Language Teaching Research, Vol. 19 (2) 129-132.
- [17] ATMOWARDYOYO, H. (2018). Research Methods in TEFL Studies: Descriptive Research, Case Study, Error Analysis, R & D, Journal of Language Teaching and Research, Vol.9 No.1, 197-204, January 2018.
- [18] SAKARYA UNIVERSITY Department of Translation Studies, Retrieved 04.04.2018, from <http://www.ceviribilim.sakarya.edu.tr/>.
- [19] BULENT ECEVIT UNIVERSITY Çaycuma Vocational High School Applied English and Translation Program, Retrieved 04.04.2018, from <http://cmyo.beun.edu.tr/yabanci-diller/1/uygulamali-ingilizce-ve-cevirimenlik-programi.html>.
- [20] MCHUGH, M. L. (2012). Interrater Reliability: The Kappa Statistic, Retrieved 24.12.2018, from https://www.researchgate.net/publication/232646799_Interrater_reliability_The_kappa_statistic
- [21] ERSOY, H.; BALKUL, H. I. (2012). "Teknolojik Gelişmelerin Çevirmen ve Çeviri Mesleği Açısından Olumlu ve Olumsuz Etkileri: Çeviri Alanında Yeni Yaklaşımlar", Akademik İncelemeler Dergisi (Journal of Academic Inquiries) Volume: 7, Number: 2, Year: 2012, Retrieved 15.12.2018, from [https://www.academia.edu/3588396/Teknolojik_Geli%C5%9Fmelerin_%C3%87evirmen_ve_%C3%87eviri_Mesle%C4%9Fi_A%C3%A7ısından_Olumlu_ve_Olumsuz_Etkileri_%C3%87eviri_Alan%C4%Bİnda_Yeni_Yakla%C5%9F%C4%Bİmler](https://www.academia.edu/3588396/Teknolojik_Geli%C5%9Fmelerin_%C3%87evirmen_ve_%C3%87eviri_Mesle%C4%9Fi_A%C3%A7ısından_Olumlu_ve_Olumsuz_Etkileri_%C3%87eviri_Alan%C4%B1nda_Yeni_Yakla%C5%9F%C4%Bİmler).

On Telemedicine Implementations in Ghana

E. T. Tchao¹, Isaac Acquah², S. D. Kotey³, C. S. Aggor⁴, J. J. Kponyo⁵

Department of Computer Engineering, KNUST, Ghana^{1, 2, 3, 4}

Department of Electrical and Electronic Engineering, KNUST, Ghana⁵

Abstract—Most Sub-Saharan Africa countries including Ghana experience a shortage of medical professionals, especially in the rural areas. This is mainly caused by the low-intake of students into medical schools due to inadequacy of facilities to train students. Also, a number of medical students graduate and emigrate to foreign countries to seek new opportunities and enhanced living standards. To reduce the effect of this, telemedicine is being implemented in certain areas to provide healthcare. Much as advances are being made in information and communication technologies, the advancement of telemedicine in developing countries still needs to be upgraded and extended to cover more areas. Some categories of telemedicine have little to no implementation in Ghana due to lack of resources, little government support as well as the absence of structured frameworks and policies to ensure their implementation. This paper seeks to present telemedicine applications and implementations in Ghana till date as well as suggest some recommendations to mitigate some of the challenges impeding the advancement of telemedicine.

Keywords—Telemedicine; Ghana; m-health; store-and-forward; information and communication technology

I. INTRODUCTION

A substantial percentage of the population in most developing countries is not assured access to good quality healthcare, especially those in rural areas. The conventional primary healthcare in Ghana refers to primary healthcare through the Community-based Health Planning and Services (CHPS) compound, health post and health center. This usual mode of delivery is besieged by a number of challenges. Health facilities find it difficult to employ enough trained health professionals to manage the staggering number of people needing care due to limited budgetary allocation. According to the World Bank, rural dwellers constituted about 45% of the country's population in 2016 [1]. Unfortunately, this section of the populace is the worst affected in terms of the inequitable distribution of healthcare resources [2]. The Ghana Health Service in 2017 revealed that the average doctor and nurse to population ratio are one doctor to 8,431 and one nurse to 627 [3], and these ratios are even more predominant in rural healthcare delivery. The healthcare to population ratio for the 10 regions in Ghana is shown in Table I. The quality of healthcare delivery differs to a large extent across different regions of Ghana.

Urban areas have a good number of pharmacies, clinics and hospitals while rural areas often lack or have fewer of these facilities readily available. This causes patients in most rural areas to depend, to large extent, on traditional African medicine or travel long distances to access modern healthcare [4].

Furthermore, specialist physicians are mostly stationed at the urban centers. This implies cases which cannot be handled by physicians in the rural areas have to be referred to the urban facilities.

It is estimated by the Ghana Statistical Service [5] that about 6.8 million (23.4%) people living in Ghana are poor and cannot afford to spend GHS 4.82 (~USD 1) per day (GHS 1,760) in 2016/2017. Within that same period, it was estimated that 2.4 million people (8.2%) are extremely poor and cannot afford to spend GHS 2.69 per day and a greater part of these people are rural dwellers. Low level of income of rural dwellers means some patients may end up not following up on treatment of their ailments due to the associated cost of travelling to urban health facilities to seek medical intervention. To improve the delivery of quality healthcare in these deprived areas, there is the need for a system which will reduce cost while ensuring patients receive satisfactory healthcare. With the advances being made in information and communication technologies, telemedicine serves as a solution to these issues. Investments in large scale telecommunication infrastructure across Africa has been inadequate, partly as a result of wars and civil unrests in some parts of the continent. This development has been estimated to slow down economies and infrastructure building by up to seven years for each year in which there is unrest. Besides, in rural areas, where telemedicine will be most beneficial to the poor, the likelihood of it being provided is very low due to enormous infrastructural requirements and connectivity costs [6]. Internet connectivity is also low in locations outside the urban expanse [7].

Telemedicine technologies have been in use for some time in the developing world, but on a relatively smaller scale compared to developed countries. One major challenge for this is the relatively little contribution of governments in promoting telemedicine implementations, especially privately initiated telemedicine projects. Another challenge is low investment in fast internet and data transmission infrastructure, especially in the rural areas. Funding is also a challenge when it comes to telemedicine with a number of successfully piloted projects grinding to halt due to lack of funds to implement the project on a large scale.

Telemedicine initiatives in Africa receive lots of press coverage but often, few are sustained after the trial stages to be incorporated into the existing medical system. As a consequence, there is also very little published data on their operation [6]. There is relatively very little scholarly work proving the existence of telemedicine implementations in developing countries as compared to the developed world [8]. Thus, studies and reports on telemedicine in Africa are desirable.

TABLE I. HEALTHCARE STATISTICS FOR RESPECTIVE REGIONS OF GHANA [9]

Region	Population (2017)	Number of Health Facilities (2016)	Population to Doctor Ratio (2017)	Population to Nurse Ratio (2017)	Population (2019)
Ashanti	5,490,543	1501	6482	689	5,792,187
Brong Ahafo	2,723,048	725	11,891	670	2,850,607
Central	2,507,668	429	9,219	547	2,563,228
Eastern	3,099,637	884	14,219	704	3,244,834
Greater Accra	4,721,891	694	3,751	637	4,943,075
Northern	2,927,959	579	13,877	590	3,062,883
Upper East	1,216,681	337	29,675	422	1,273,677
Upper West	811,122	311	20,278	388	849,123
Volta	2,491,439	598	12,094	674	2,607,996
Western	2,954,789	757	26,862	728	3,093,201

II. TELEMEDICINE

Telemedicine is the application of information and communication technology to provide healthcare access remotely [10]. It includes diagnosing, treating and evaluating patients through information exchange remotely. It considerably cuts down the cost associated with providing quality healthcare especially in rural areas by eliminating the need to construct and staff new facilities, which developing countries like Ghana generally lack. Telemedicine systems normally consist of a communication device with software to support sharing of information as well as a secure network channel for communication. A secure channel is necessary to ensure confidentiality and privacy of patient information and health records. It is generally believed that ICT has the potential to improve clinical care and public health. In addition to helping with medical education, administration and research, appropriate use of ICT can improve access to healthcare, improve the quality of healthcare service delivery and also reduce the effect of global shortage of healthcare professionals. However, a number of questions still remain about the potential value to people in resource-constrained settings such as the developing world [11].

Telemedicine applications can be divided into three main categories. The first is the store-and-forward in which medical records and data (digital images, etc.) for non-emergencies are stored and sent to a specialist for diagnosis and prescriptions at convenient times. The second is the real-time interactive consultation. With this, services are provided in real-time using videoconferencing equipment at both ends for a variety of services including consultation and diagnosis. The third is remote monitoring, which helps the medical specialist monitor the condition of a patient using various devices remotely. Offering patient care over distance and possibly from another country raises issues such as liability, licensure, jurisdiction, quality and continuity of care, confidentiality, data security, consent, authentication and remuneration. The current practice in many telemedicine services is that the referring doctor keeps the responsibility of ensuring care is provided to the referred patient. The consulted doctor only offers second opinion advice which can either be accepted or rejected by the referring doctor [7]. Jurisdiction and liability remain with the referring doctor and his or her country in the case of cross border practice.

A. Store and Forward Technology

The store and forward technology involves a non-simultaneous communication between the patient and healthcare provider in which medical information, such as medical images are put together and sent to a doctor or medical specialist for evaluation offline at a convenient time. This category of telemedicine does not require the patient and healthcare provider to meet. A medical record in electronic form is included in the data sent, if possible. A key difference between the face-to-face patient-doctor meetings and store and forward telemedicine is the absence of a regular physical assessment. In the store-and-forward process, the doctor depends largely on a pre-recorded report, which could be in the form of a text message or email with images with or without audio or video data of a physical assessment. The store-and-forward technology is cheaper and simpler to implement than other forms of telemedicine. Medical information and clinical queries of patients can also be sent and responded to by healthcare providers at their convenience. This technology however, could reduce the level of diagnostic accuracy than a real-time system due to the possible difference in time between symptoms' occurrence and diagnosis [12, 13].

B. Real-Time Interactive

Real-time telemedicine involves a simultaneous communication channel between the patient and healthcare provider in real time. The patient transmits medical information and the healthcare provider receives it instantly. This technology involves over-the-phone conversations, online communication and visits to the patients' homes. A variety of medical activities such as physical tests, psychiatric assessments and medical history assessment can be done much like with the traditional face-to-face treatments. The real-time interactive technology allows healthcare providers to diagnose conditions of patients in remote locations in real time. However, it is more expensive to implement than the store-and-forward technology. A timing schedule is also required between the healthcare provider and the patient or a colleague healthcare provider for a successful consultation [12, 13].

C. Remote Patient Monitoring (RPM)

Remote patient monitoring, also called 'self-monitoring/testing', is a category of telemedicine application

which enables healthcare providers to check up on a patient remotely using various technological equipments. This application of telemedicine is mainly used for managing chronic diseases or specific conditions like heart disease, diabetes mellitus, or asthma. These services can be comparable to conventional face-to-face patient consultations and can also be economical [13]. Remote patient monitoring enables patients to be monitored outside the clinical setting to reduce cost of healthcare whilst increasing the quality of care [14]. The major features of RPM include remote monitoring and trend analysis of physiological parameters and early detection of deterioration which reduce the number of emergency department visits, hospitalizations and shortens duration of hospital stays [15]. Different applications of RPM introduce a number of variations in RPM system architecture. However, most RPM systems consist of four main components: a sensor to measure physiological parameters, data storage at the patients' end (an optional requirement), a central data storage and a diagnostic software [16].

III. METHODOLOGY

Literature was collected by searching indexing databases. Cited papers in articles considered for review were also collected. Papers and articles included for consideration provided information on telemedicine implementations in Ghana. Papers and articles presenting case studies of telemedicine implementations without describing the implementation itself were excluded due to the fact that we seek to discuss the telemedicine implementations in this paper.

IV. APPLICATIONS IN GHANA

There are a number of telemedicine applications which have been implemented in Ghana. We take a look at some of these applications based on the technologies used in deploying them in this section.

A. Store and Forward Applications

The following projects discussed below are examples of store and forward application Telemedicine implementation in Ghana.

1) *Asynchronous remote medical consultation*: Remote Asynchronous Communication for Healthcare (ReACH) was set up to resolve the failures in the existing patient referral infrastructure, by presenting an online system in which rural doctors in Ghana can input case information as text or images, and forward, or "assign" that case to a specialist in one of the central hospitals. The store-and-forward nature of the entire system makes it an inexpensive tool that does not require high speed internet connections and functions effectively over e-mail as well as through a web-based portal. A further step is taken to leverage the delay-tolerant networking (DTN) architecture, which would allow computers without intranet or internet connection to be updated via a USB key. The shortage of medical specialists in the country is addressed by enabling volunteer specialists around the world to access the system, to provide a second-tier group of consultants in the event that the medical specialists in Accra are unable to handle a particular case due to their lack of time or expertise. Doctors are also

allowed to easily communicate with colleagues in a non-case-specific manner. To ensure accountability for specialists in the system, information seekers are allowed to assign their cases to a few potential specialists, while the system does the final assignment to one of the specialists (to balance load automatically between the specialists). The system is capable of using already existing social connections between information-seekers and specialists to ensure seekers know the specialist attending to them to make specialists more responsive to persons, instead of to a system. On the other hand, information-seekers have a publicly available profile with uniquely identifying data, making them accountable in the system. This makes it easy for a specialist know the outcome of a particular case. All cases were allowed to pass through a first assignment tier with Ghanaian specialists before foreign specialists were engaged when there was an overload of work on the Ghanaian specialists. Participants in the system as much as possible had some amount of field knowledge of the medical practice in Ghana, to ensure they were familiar with the conditions and the people they would be working with. In cases where this was not possible, a full-day training session was proposed with the local doctors and made available to specialists abroad [17, 18].

2) *Web-based tele-ophthalmology system*: A web-based tele-ophthalmology system was set up to allow eye practitioners to share photos with a case history online to receive help on the case from a specialist at Moorfields Eye Hospital in London. It involved a number of referring centers across Africa including Korle-Bu Teaching Hospital in Accra. The online platform uses a secure method based on SSL encryption for information sharing, to preserve data privacy. As part of ethical requirements for research, patient participating in the teleconsultation provides a signed consent form before participating. The doctor seeking help provides a brief case history of the patient which includes the current problem, planned treatment of the problem and research undertaken concerning the problem. A maximum of four images can be uploaded with the case history file. Internet access was provided in each participating center as well as training on capturing images. Digital cameras are used to capture images. When a practitioner uploads a case on the system seeking help, an email is sent automatically to the specialist from whom help is sought, notifying them to respond on the system. When a case is also responded to, an email is sent to the practitioner stating the case has been responded to. The site supervisor and doctors related to the case are the only ones with access to that case [19].

3) *Sene PDA*: The Sene PDA project was aimed at improving healthcare delivery at the Community-based Health Planning and Services (CHPS) zones via the use of information technology. It was one of the early mobile health initiatives in Ghana and was first deployed in 2004. It was introduced to enable reports used to make decisions by Community Health Officers and District Health Managers to be generated accurately with the aid of technology and to

reduce the time spent by the concerned parties to generate monthly reports on services provided. It also helps to better increase following up of mothers and children who have registered for services and reduces the rate of dropouts for immunizations and safe motherhood services [20, 21].

4) *Mobile technology for community health (MOTECHE) in ghana*: MOTECHE was introduced to enable the quantity and quality of prenatal and neonatal care in rural Ghana to be increased with the aid of mobile phones. The goal of this was to improve healthcare for mothers and their new-born babies. It has two major components: Nurse Application and Mobile Midwife Application. The Nurse Application helps community health workers monitor and record the care given to newborns and women in the rural areas. Each rural facility was provided with low-end mobile phones with the Nurse application installed on it. With this application, the health worker is able to record data about a patient's visits to the clinic and also query the MOTECHE database to retrieve details of patients as well as lists of patients due for care and women due for delivery.

The Mobile Midwife application helps pregnant women and their families to receive voice messages or SMS messages with information about their pregnancy each week. Information provided through this channel includes reminders for seeking specific healthcare, advice to help with challenges associated with pregnancy and educational information to promote good health practices [20, 22-24].

5) *Onetouch medicareline*: The OneTouch MedicareLine program was developed to offer free calls and SMS messages between registered physicians and surgeons in Ghana. The main focus for its implementation was to reduce economic barriers associated with the use of mobile phones, and not on technological innovation. After registering with the system, a doctor is provided with a sim card. The sim card can be used to call other participants on the program free of any personal charges. This can save cost significantly, given the high cost of airtime especially in Ghana. As part of the program, the Ghana Medical Association was provided with a computer terminal to broadcast messages to participants of the program, alerting them of updates to the system. Future phases of the program envision new technological interventions. A second phase of the program was planned, which would include participants receiving free multimedia messaging service (MMS) to enable phone consultations be done with photos as well as the ability of the medical service and concerned government organizations to get data from participants via SMS messages. A third phase was also proposed to include a partnership with hardware mobile equipment vendors to provide each participating doctor with a smartphone preloaded with medical reference material [20, 25].

6) *mPEDIGREE technology*: The mPedigree technology was started to curtail the effects of counterfeiting in the health industry. Counterfeit drugs are a major concern in the health sector and have cost a lot of lives, jobs and revenue to genuine drug producers. The mPedigree system works with mobile

network providers in storing a central registry which contains information of product brands of participating pharmaceutical manufacturers. In collaboration with the participant manufacturers, each product produced by these manufacturers has a concealed 12-digit number which is revealed by the consumer at the point of purchase. This number is unique and serves as an identity for each product. To check for product authenticity, the consumer sends the 12-digit number to a short code at no personal cost. If the product is genuine, a reply will be given containing unique details of the product, else it will be confirmed as a counterfeit product. Aside pharmaceutical products, the technology works with various other products to authenticate them and counter the deleterious effects of counterfeit products on the end users [20, 26].

7) *The ghana consultation network (GCN)*: GCN was introduced in Ghana as a computer-based system providing medical consultation among doctors over a network. The aim was to enable doctors in Ghana to consult with each other, as well as with doctors across the world. Doctors are able to login into the system via a web-based user interface through a local server (located in participating hospitals) or through public servers hosted with Internet Service Providers. Provision of local servers enables availability of network connectivity in the event of unreliable internet connectivity. The system is presented as a social networking platform, one for medical consultation with both professional and social colleagues due to the fact that doctors already view consultation as reaching out to personal contacts. The system inculcates two modes of communication, a highly structured consultation mode for specific patients which works like an electronic case history and an unstructured discussion mode which works like an online forum. SMS messages and email messages have also been incorporated into the system for notifications of updates due to the widespread use of mobile phones. A number of doctors have been enrolled so far on the system, including doctors from Ghana, USA, South Africa and Nigeria. GCN was implemented after four iterative rounds of design and fieldwork. It began with an exploration of needs, some design exercises, a pilot deployment and the current deployment. Although the field survey focused more on rural hospitals in the northern part of Ghana, current deployment of the system is in the southern part of Ghana due to the ease of accessibility, with plans to extend the system to the north [20, 25].

8) *SATELLIFE PDA project*: The SATELLIFE PDA Project was setup to explore how Personal Digital Assistants (PDAs) could be used to address the digital divide between health professionals in Africa. Satellife conducted a pilot test in December 2001, in conjunction with the American Red Cross, to determine how effective PDAs were for field surveys related to measles in Ghana. Thirty volunteers from the Ghanaian Red Cross were trained over two days, and they encountered no challenges using the PDAs, even though a number of them had never used computers prior to that. Within the course of just three days, over 2,400 surveys were

completed, where previously only 200 surveys would have been completed with the traditional pen and paper method. The entire pilot deployment was finished within a week, with the ease and unprecedented speed of gathering data. The project produced very strong proof of the value of PDAs and technology for data gathering and reporting. A service known as Healthnet was also established at the medical school to provide access to medical information and electronic conferencing [20, 27].

9) *Vodafone healthline project*: Vodafone Ghana launched a medical health-oriented initiative named “Healthline”, aimed at educating and informing the Ghanaian public concerning important health matters. The project attempts to answer health questions from Ghanaians in the form of a television and radio shows. According to Vodafone Ghana, the project is expected to educate the Ghanaian public and clarify certain health related issues and practices. There is also a feature known as Healthline 255, where accurate expert medical advice is provided by medical experts to people in need of good quality healthcare by medical experts from the convenience of their phones [20].

10) *Electronic health information and surveillance system (eHISS)*: The Electronic Health Information and Surveillance System (eHISS) was developed and operated by Viamo, a Ghana-based company. The system was developed to assess the symptoms of sick children through mobile phones and also to provide tailored health advice to their caregivers. An automated interactive voice response system based on a clinical algorithm presents a number of questions sequentially to the caregiver to be answered, after which information on the disease symptoms and geographic location are gathered. The clinical algorithm was designed based on local assessments of clinicians’ reports and recommendations and the Integrated Management of Childhood Illness Chart Booklet (IMCI) [28]. The algorithm was developed over a period of two years with the help of communication researchers, biostatisticians, epidemiologists, public health experts and clinicians.

When a call is connected with the system, there is a brief introduction and instructions are given to the caregiver on what to press for a ‘yes’ or ‘no’ response on their mobile phones. The first set of questions posed to the caregiver seek to determine if there are any ‘danger signs’ as indicated in the IMCI guideline, taking into consideration the age of the child. The next set of questions aimed to determine the exact symptoms the child was exhibiting. Further questions sought to determine the severity of the child’s condition. A caregiver is required to give an answer to all the questions asked by the system, to enable all symptoms to be captured to ensure accurate advice is given after the symptoms are assessed [29, 30].

11) *District health information system (DHIS 2)*: The District Health Information System (DHIS 2) is a web-based health information system with a centralized database to enable generation of reports and use of health service data

from health centers. At the core of the system is a lightweight Microsoft Excel-based tool for ease of data input. Data in the database is stored in independent reporting forms according to the health facility the data is from. The system enables data to be analyzed from different health facilities or regions and to generate reports for centralized decision making by healthcare managers [31, 32].

B. Real-Time Interactive Applications

The following real-time interactive Telemedicine implementations have been piloted in Ghana:

1) *Millennium village health system*: The Millennium Village Health System (MVHS) is a core part of the Millennium Villages Project (MVP) to attain the Millennium Development Goals (MDGs) in low-income rural Africa. The MVHS is aimed at obtaining universal health coverage of primary health services to achieve the MDGs in healthcare, including a reduced child mortality rate and a reduced maternal mortality rate in relation to a baseline. The main strategy is to guarantee widespread access to health services without charge to patients at the point of care, with a continuous delivery of services between the household, clinic and the referral hospital. The MVHS encourages the continuous real-time collection and feedback of health data, including the recording of all the important events and verbal autopsies, to allow the continuous modification and improvement of methods to enhance health outcomes. Currently, the MVP is running the Millennium Village Global Network (MVG-Net). The aims of this network are to enable community health workers with the aid of MVP clinical facilities, to enhance the care given to patients continually, greatly improve the quality of data collection and reporting, and assist in the assessment of the MVP’s progress towards enhancing the healthcare provided at MVP community sites. The MVG-Net has an open-source electronic health delivery platform known as OpenMRS which stores data for managing patient care, program evaluation and monitoring, decision making, and management. It enables a facility-based data storage of individual-level data, community-based data capture of individual-level information, data storage of individual patient health records, and an automated scheme for aggregating data and generating reports and feedback to health care providers and managers. ChildCount+, a program running under MVG-Net, is an SMS-based system that helps collect data for community health workers to monitor pregnant women and children under 5 years of age. As part of the test, the mClinic software was designed for midwives in Bonsaaso of the Ashanti Region of Ghana, to use to enable them have access to the MVG-Net. mClinic works on inexpensive android-based devices and allows midwives to obtain data [20, 33, 34].

2) *Novartis*: Novartis pilot project was intended to extend access to quality healthcare for people living in remote rural areas, to reduce time and cost of transportation and to eliminate unneeded referrals. It was developed to allow for

centralization of healthcare expertise with digital technology. Later, the project was expanded in 2015 to cover the entire Amansie-West district in the Ashanti Region. Mobile technology is used to connect community health workers based in rural, remote areas to experienced healthcare professionals via 24-hour teleconsultation centers. These healthcare professionals guide and advise the community health workers in their patient care to improve the quality of healthcare patients receive. This helps to reduce unnecessary referrals and also allows for immediate support in the event of medical emergencies. The project was launched in cooperation with the Columbia University Earth Institute's Millennium Promise, the Ghanaian Ministry of Health, National Health Insurance Authority and Ambulance Services of Ghana, and Ghana Health Services [35].

3) *Pan african eNetwork*: The Pan African eNetwork is a project initiated to help impart quality education to 10,000 students across Africa over a period of five years. Students were to be taken through various disciplines from some of the best universities and educational institutions from India. Aside this, telemedicine services are provided through online medical consultation to medical practitioners in Africa by medical specialists in India in various specialties [20].

4) *Sanford*: Sanford Health Enterprise is a non-profit rural healthcare organization based in the USA. Sanford began operations in Ghana in 2012 to help with Ghana's health system and works with over 300 health professionals. Sanford operates through at least 360 clinics in Ghana in collaboration with the Ghana Health Service and the Ministry of Health, and offers a wide range of services which include education, specialty hospital care and primary health care. Sanford operates both real-time and store and forward telemedicine in Ghana. Sanford uses EMR (Electronic Medical Records) to create a paperless system with easy and effective access to patients' records across their working sites. Software of the system needs a dedicated internet connection, a camera, a transmitting stethoscope software and an audio-video call system capable of two-way interaction. Some challenges facing their telemedicine initiative in Ghana include limited availability of internet connectivity especially in the rural areas, unstable electricity in rural areas, many diverse languages and inadequate medical facilities in rural areas [36].

5) *Mahiri*: Mahiri Mobile Services began a project to equip healthcare givers in remote areas in Ghana with tablet devices from Telmedx. These tablet devices are capable of providing high quality live video connection to doctors in Tamale and Nsawam to seek medical advice without them having to travel to those locations. The system provides the ability to treat medical conditions of all forms that would normally not be handled by physicians.

Patients are attended to in their homes, in remote clinics, in schools, or during community gatherings by traveling nurses who have been trained to use the technology, which was developed by Telmedx, an organization in San Diego, California. The system allows a doctor to examine patients

over high-quality cameras of mobile devices using a web browser for real-time medical consultations. Doctors can also take high-quality photos of patient conditions from a web browser by controlling the backup cameras attached to the mobile devices remotely. The live video and still photos can be viewed beside each other on the computer screen, and can easily be saved to the medical records. The Telmedx mobile video platform also gives groups of doctors and specialists the ability to watch the same live video. Doctors are able to capture photos for closer analyses and efficient consultations. The mobile telemedicine program has been active in Ghana for quite a while, and has been lauded by doctors for its high quality of videos and photos [4, 20].

6) *Family health hospital telemedicine*: The Family Health Hospital in Accra launched a telemedicine center to grant patients access to medical experts and also to improve medical education in the country. The facility is furnished with video-conferencing systems and monitors, and is also aimed at enhancing medical training at Ghana's first private medical school, the Family Health Medical and Nursing Schools, which is a part of the Family Health Group. The center was set up as part of a collaboration between the Family Health Group Apollo Hospital in India and Airtel Ghana. The facility takes away the need for patients in the country to travel outside the country to seek specialist medical care. Patients only need to book an appointment with the hospital to have access to a live medical consultation with doctors in USA and India [37].

V. DISCUSSION

There have been a number of telemedicine applications implemented across Ghana. However, there is a scarcity of literature covering some of these implementations as shown in Table II. Most of these implementations were done using the store-and-forward technology. This development is attributed to the relatively low and ease of implementation of the store-and-forward method. It was seen to be convenient for both patients and healthcare givers because information was bundled together and forwarded to the specialist at a convenient time and analyzed by the specialist at a convenient time as well. Simple messaging applications on PCs and cell phones were also used to transmit the information, which eliminated the need for a high bandwidth internet connection. Other technologies are costly and requires high speed internet access, especially for the interactive technology. Though store-and-forward technologies are less costly to implement, they take away one important aspect of telemedicine, live remote diagnostics.

The real time interactive technology has been also implemented by some organizations as well. VoIP and video calls demanded the use of high bandwidth internet access. This proved a bit of a challenge because of the unavailability, or limited availability of high-speed internet connections in the rural areas. Specialized applications which provided the ability to make VoIP and video calls were also used, which meant either buying the software, or building it from scratch, in order to have a dedicated channel for communication, instead of relying on what is offered to the public for general use.

Equipment for this, which includes cameras, PCs, servers, also added to cost in implementing telemedicine with this technology.

Remote Patient Monitoring (RPM) with miniaturized devices was the technology not seen in use in Ghana. This form of RPM requires the use of miniature sensing devices which are wireless network aware to record and transmit data to be analyzed by a diagnostic application or by a medical specialist without the patient having to visit the clinic. The challenge here is the relative scarcity and cost associated with getting many of these devices for various medical conditions and maintaining them to ensure they are always functioning properly. This challenge, as well as the need for reliable internet connection for data transmission in real time when necessary and a diagnostic-capable software able to analyze data collected making it difficult to implement. The major challenges facing telemedicine implementations in Ghana are:

- Low investment in fast internet and data transmission infrastructure, especially in the rural areas.
- Funding to maintain and scale up telemedicine projects.
- Relatively little contribution by the government in promoting telemedicine implementations.
- Miniature devices which are used for Remote Patient Monitoring are scarce and expensive and are mostly specific-purpose devices.

Telemedicine is gradually gaining grounds in Ghana and the impressive data throughputs measured for deployed LTE and WiMAX networks in [38-39] show that state-of-the-art implementation of Telemedicine applications in Ghana is feasible with the connectivity possibilities 4G and 5G networks present. However, the pilot implementations reviewed in this study show that there is a lot more that can be done to improve it. Some recommendations that can be adopted to increase uptake of the technology include:

- More research should be done in the area of data transmission to provide the ability to have good quality VoIP and video calls in the presence of low speed internet connection. This will greatly reduce the bandwidth challenges associated with the Real-Time Interactive technology especially in the rural areas.
- The government and stakeholders should include and apportion funds in their budgets for the maintenance of telemedicine projects.
- The government should be more involved and formulate strong policies which will promote and ensure the sustainability of telemedicine applications.

Devices used in RPM should be generalized to be able to sense information for a larger number of conditions. This will eliminate the need to have different sensing devices for different medical conditions thereby reducing the costs.

TABLE II. SUMMARY OF TELEMEDICINE APPLICATIONS IN GHANA

Project	Area of activity	Period of activity	Population affected	Focus
ReACH	Upper West Region	2008 -	>50,000	General
Tele-Ophthalmology	Accra	2003 -	>100,000	Focused on eye care
Sene PDA	Sene	2004 -	>50,000	Focused on immunization
MOTECH	Kassena-Nankana, Awutu Senya, Gomoa West, Ada, South Tongu	2010-2014	>22, 237	Focused on pregnant women and newborns
MedicareLine	Accra	2007-2008	>100,000	General
mPEDIGREE	Nation-wide	2008-	N/A	Focused on pharmaceutical drugs
GCN	Northern Ghana	2007-2008	N/A	General
SATELLIFE	Accra	2001	>100,000	General
Vodafone Healthline	Nation-wide	2011 till date	>100,000	General
eHISS	Agogo (Asante Akim North)	2015	>45,870	General
DHIS 2	Nation-wide	2011 till date	>100,000	General
MVHS	Bonsaaso	2012 - 2014	>30,000	Focused on pregnant women
Novartis	Amansie-West	2015	>100,000	Focused on pregnant women
Pan-African eNetwork	Kumasi	2007	>100,000	General
Sanford		2012	>50,000	General
Mahiri			>30,000	General
Family Health	Accra	2016	>100,000	General

VI. CONCLUSION

Telemedicine is being adopted to solve a wide range of problems in the medical field. There are many benefits Ghana as a developing country can obtain from implementing telemedicine on a nation-wide basis. With the advances being made in information and communication technologies, telemedicine applications are most likely to expand to many more areas and solve many more of the pertaining problems. Though telemedicine is still in its developing stages in Ghana, it has the potential to be very useful in delivering healthcare, especially in rural areas, given the fact that there is a shortage of medical personnel in the country.

This paper sought to present some of the applications of telemedicine which have been implemented in Ghana. Several telemedicine applications have been implemented in Ghana till date and have been discussed in this paper. However, there is a scarcity of literature discussing some of the implementations. It was realized that some implementations did not gain grounds in Ghana due to lack of funds and little government support and these are some of the challenges facing telemedicine implementation in Ghana. With an increased involvement of the government in this country, advances in telemedicine will no doubt be sped up, thereby mitigating a lot of the challenges facing nationwide implementations of telemedicine projects. It was also noticed that Remote Patient Monitoring involving automated miniature devices was not seen in use in Ghana. If used, Remote Patient Monitoring involving miniaturized devices has the potential to reduce drastically patient visits to clinics as well as forgetfulness by patients to check their vitals, thereby eliminating congestion in medical facilities as well as reducing the workload on healthcare givers.

REFERENCES

- [1] Trading Economics. Ghana - Rural population [Internet]. Available from: <https://tradingeconomics.com/ghana/rural-population-percent-of-total-population-wb-data> [Last Accessed: 2019-02-11]
- [2] Benjamin Otsen, Peter Agyei-Baffour. Cost-effectiveness analysis of telemedicine for primary healthcare delivery in the amansie-west district, Ghana. *African Journal of Health Economics*. 2017
- [3] Ghana Health Service. The Health Sector in Ghana: Facts and Figures (Report). 2017
- [4] Clint Carney, JD. Delivering healthcare to rural Ghana: telmedx and mahiri mobile serve patients in remote areas. 2017. DOI: 10.30953/tmt.v2.67
- [5] Ghana Statistical Service. Ghana living standards survey round 7 (GLSS 7) (Report). 2018
- [6] Mars, Maurice. Telemedicine and advances in urban and rural healthcare delivery in Africa. *Progress in Cardiovascular Diseases*. vol 56 no. 3. 2013. pp 326-335. DOI: 10.1016/j.pcad.2013.10.006
- [7] Eric Tutu Tchao, Kwasi Diawuo, Willie K. Ofosu. Mobile telemedicine implementation with wimax technology: a case study of Ghana. *Journal of Medical Systems* 41: 17. 2017. DOI 10.1007/s10916-016-0661-8
- [8] Scott R, Mars M. Telehealth in the developing world: current status and future prospects. *Smart Homecare Technology and TeleHealth*. Vol. 25. 2015. DOI: 10.2147/SHTT.S75184
- [9] Ghana Statistical Service. Ghana's population by region, 2019 [Internet]. Available from: <http://www.statsghana.gov.gh> [Last Accessed: 2019-02-11]
- [10] Brown N.: A brief history of telemedicine. *Telemedicine Information Exchange (Book)*. 1995;105:833-5
- [11] Richard Wootton, Nivritti G Patil, Richard E Scott, Kendall Ho, editors. *Telehealth in the developing world*. Royal Society of Medicine Press Ltd. 2009
- [12] Yar-Ling Tan, Bok-Min Goi, Ryoichi Komiya. Real-time/store-and-forward telemedicine with patients' data protection by KP-ABE Encryption. 2011
- [13] Innovateus. What are the types of Telemedicine? [Internet]. Available from: <http://www.innovateus.net/health/what-are-types-telemedicine> [Last Accessed: 2019-02-08]
- [14] Bayliss E, Steiner J.F, Fernald D.H, Crane L.A, Main D.S. Descriptions of barriers to self-care by persons with comorbid chronic diseases. *Ann Fam Med* 2003; 1:15-21. DOI: 10.1370/afm.4
- [15] Center for Technology and Aging. Technologies for remote patient monitoring in older adults (Report). 2009
- [16] Smith T, Sweeney R. Fusion trends and opportunities. *Medical devices and communications (Report)*. 2010
- [17] Luk Rowena, Ho Melissa, M. Aoki Paul. A framework for designing teleconsultation systems in Africa. *Int'l Conf. on Health Informatics in Africa*. 2008. arXiv:0801.1925
- [18] Luk Rowena, Ho Melissa, M. Aoki Paul. Asynchronous remote medical consultation for Ghana. In: *Proceedings of the SIGCHI Conference on Human Factors in Computing Systems (CHI '08)*; 05-10 April 2008; ACM New York, NY, USA ©2008; Pages 743-752. DOI: 10.1145/1357054.1357173
- [19] Craig Kennedy, Richard Bowman, Nor Fariza, Edith Ackuaku, Christine Ntim-Amponsah, Ian Murdoch. Audit of web-based telemedicine in ophthalmology. *Journal of Telemedicine and Telecare*. Vol. 12. Pp. 88-91. 2006. DOI: 10.1258/135763306776084356
- [20] Afarikumah E. Electronic health in Ghana: current status and future prospects. *Online Journal of Public Health Informatics*. Vol. 5 no. 3. 230. 2014. DOI: 10.5210/ojphi.v5i3.4943
- [21] Ofosu A, Nyonaator F. Sene pda project-an ehealth initiative in Ghana (Report). 2013
- [22] Angela Afua Entsieh, Maria Emmelin, Karen Odberg Pettersson. Learning the ABCs of pregnancy and newborn care through mobile technology. *Global Health Action*. Vol. 8: 29340. 2015. DOI: 10.3402/gha.v8.29340
- [23] LeFevre et al. Mobile Technology for Community Health in Ghana: what happens when technical functionality threatens the effectiveness of digital health programs? *BMC Medical Informatics and Decision Making*. Vol. 17 no.27. 2017. DOI 10.1186/s12911-017-0421-9
- [24] Grameen Foundation. *MOTECH in Ghana: Lessons Learned (Report)*. 2012
- [25] R. Luk, M. Zaharia, M. Ho, B. Levine and P. M. Aoki. ICTD for healthcare in Ghana: Two parallel case studies. 2009 International Conference on Information and Communication Technologies and Development (ICTD), Doha, 2009, pp. 118-128. DOI: 10.1109/ICTD.2009.5426714
- [26] Myjoyonline.com. mPedigree a Ghanaian solution to global counterfeiting; the story of GTP [Internet]. 2015. Available from: <https://www.myjoyonline.com/business/2015/October-27th/mpedigree-a-ghanaian-solution-to-global-counterfeiting-the-story-of-gtp.php> [Last Accessed: 2019-02-08]
- [27] Osei Darkwa. An exploratory survey of the applications of telemedicine in Ghana. *Journal of Telemedicine and Telecare*. 2000. Vol. 6 no. pp 177-183.
- [28] World Health Organization. *Integrated management of childhood illness chart booklet*. [Internet]. 2014. Available from: http://www.who.int/maternal_child_adolescent/documents/IMCI_chartbooklet/en. [Last Accessed: 2019-02-08]
- [29] Mohammed Aliyu et al. Feasibility of electronic health information and surveillance system (eHISS) for disease symptom monitoring: A case of rural Ghana. *PloS one*. vol. 13. 2018. DOI: 10.1371/journal.pone.0197756
- [30] J. Brinkel et al. Mobile phone-based interactive voice response as a tool for improving access to healthcare in remote areas in Ghana—an evaluation of user experiences. *Tropical Medicine and International Health*. volume 22 no 5 pp 622-630. 2017. DOI: 10.1111/tmi.12864
- [31] Olav Poppe. *Health information systems in west Africa: implementing dhis2 in Ghana (Thesis)*. 2012

- [32] Reza Dehnavieh et al. The District Health Information System (DHIS2): A literature review and meta-synthesis of its strengths and operational challenges based on the experiences of 11 countries. *Health Information Management Journal* 1–14. 2018. DOI: 10.1177/1833358318777713
- [33] Olivia Vélez, Portia Boakye Okyere, Andrew S. Kanter, Suzanne Bakken. A usability study of a mobile health application for rural Ghanaian midwives. *Journal of Midwifery & Women's Health*. Vol 59. Pp. 184-191. 2014. doi:10.1111/jmwh.12071.
- [34] Patricia Mechael et al. Capitalizing on the characteristics of mhealth to evaluate its impact. *Journal of Health Communication: International Perspectives*, 17:sup1, pp. 62-66. 2012. DOI: 10.1080/10810730.2012.679847
- [35] Novartis Foundation. Novartis telemedicine factsheet (Report). 2016
- [36] Ministry of Health. Integrated national ict for health and development forum conference report (Report). 2016
- [37] Graphic Online. Family Health hospital launches telemedicine centre [Internet]. Available from: <https://www.graphic.com.gh/news/health/family-health-hospital-launches-telemedicine-centre.html>, [Last Accessed : 2019-02-11]
- [38] E. T. Tchao, J. D. Gadze and J. O. Agyapong: "Performance Evaluation of a Deployed 4G LTE Network" *International Journal of Advance Computer Science and Application*, 9(3):165 - 178, March 2018.
- [39] E. T. Tchao, W K Ofofu, K Diawuo: "Radio Planning and Field Trial Measurement of a Deployed 4G WiMAX Network in an Urban Sub-Saharan African Environment"; *International Journal of Interdisciplinary Telecommunications and Networking*. September, 2013; 5(5): pp 1-10.

V-ITS: Video-based Intelligent Transportation System for Monitoring Vehicle Illegal Activities

Vehicle Intelligent Transportation System by Abbas Q

Qaisar Abbas

College of Computer and Information Sciences,
Al Imam Mohammad Ibn Saud Islamic University (IMSIU), Riyadh 11432, Saudi Arabia

Abstract—Vehicle monitoring is a challenging task for video-based intelligent transportation system (V-ITS). Nowadays, the V-ITS system has a significant socioeconomic impact on the development of smart cities and always demand to monitor different traffic parameters. It noticed that traffic accidents are exceeded throughout the world with the percentage of 1.7%. The increase in accidents and the percentage of deaths are due to the people that don't abide by the traffic rules. To address these challenges, an improved V-ITS system is developed in this paper to detect and track vehicles and driver's activities during highway driving. This improved V-ITS system is capable to do automatic traffic management that saves traffic accidents. It provides the feature of a real-time detection algorithm for driver immediate line overrun, speed limit overrun and yellow-line driving. To develop this V-ITS system, a pre-trained convolutional neural network (CNN) model with 4-layer architecture was developed and then deep-belief network (DBN) model was utilized to recognize illegal activities. To implement V-ITS system, OpenCV and python tools are mainly utilized. The GRAM-RTM online free data sets were used to test the performance of V-ITS system. The overall significance of this intelligent V-ITS system is comparable to other state-of-the-art systems. The real-time experimental results indicate that the V-ITS system can be used to reduce the number of accidents and ensure the safety of passengers as well as pedestrians.

Keywords—Computer vision; intelligent traffic management system; traffic monitoring; vehicle tracking from video; image processing; deep learning

I. INTRODUCTION

An intelligent transportation system based on the video (V-ITS) automatically tracks the vehicle illegal driving activities is an active research area in the field of computer vision and socioeconomic development. Due to rapidly increase the vehicles, the intelligent system is required to control serious injuries caused by traffic-related accidents. This problem is widespread across the globe. In fact, the automatic tracking of a vehicle is required to monitor the roads and highways as well. To monitor the road or highways, there are many traffic parameters that should be calculated such as over-speeding, yellow-lane or off-road driving and detection of obstacles presented on the road. Such an expert system also facilitates driver assistance during automatic driving.

In particular, the statistics of accidents in Saudi Arabia is increasing rapidly during the last five months. In one estimation, there were 82.281 accidents in one month. These

accidents were due to not use of leaving enough safety distance between vehicles, run red traffic lights, sudden change of lane, and lack of commitment to the priorities. The system is predicted and discovered the mistakes of the drivers especially highway driving. A desktop application software was developed to detect and track both vehicle and driver's activities during highway driving, using a real-time video camera installed on highway road.

This V-ITS based system communicates with the respective authorities to apply strict measures when the driver exceeds the speed limit or track sudden change or leave out the yellow lane or stop in the left path. On the road, the activities tracking is a challenging and important task due to influence in surveillance or road site accidents. In the past studies, the surveillance cameras [1] on the road are increasing due to the negligence of the car or truck drivers during highway driving. Therefore, there is a great demand to increase surveillance systems.

The main goal of this paper is to propose the latest computational intelligence algorithms using deep-learning concept and to develop an effective and efficient system for providing vehicle illegal activities detection rate from video sequences. The use of video image processing and machine learning algorithms for traffic monitoring was initiated in many countries. When these algorithms have implemented on the hardware, there are different parameters calculated. All video detection systems used for traffic monitoring can be broadly classified in two categories: 1) Systems which rely on localized incident detections, and 2) Systems which track individual vehicles. The advantage of the first is that the computational requirements are quite low, and algorithms are relatively simple. In the case of vehicle tracking systems, sophisticated algorithms are needed and are usually computationally demanding. As a result of this project, our main objective is to track vehicle activities during highway driving time. Vehicle tracking systems offer a more accurate estimation of microscopic traffic parameters like lane changes, erratic motion etc.

In V-ITS system, detection and monitor is planning to develop to track activities of vehicles on the spot by using real-time video sequences. Generate a penalty if there is a traffic violation occur during the driving process on the highways. Automatically discover the most times and days accidents, and peak traffic violations. Predict accidents and congestion during highway driving. Automatic generation of Penalties to illegal drivers. If use ITS-V system then the drivers will try to control

the speed limits that will definitely reduce accidents on the road. Compare to the speed limit, the accidents are occurred to immediate line turn or driving on yellow-line to cross the vehicles very fast. In case of different weather conditions on the road, the chances of accidents will reduce to 70% due to the immediate line overrun, speed limit overrun and yellow-line driving.

II. RELATED WORK

Object tracking from live video sequences in Video surveillance [1] applications is an important and emerging research area, which is attracting many scientists. The object tracking is directly related to the domain of computer vision under image processing category. It has many applications in practice such as traffic control, security, and surveillance and mass events, etc. To effectively track an object, it is always a challenging task. During driving, some ways have to find out to track the vehicle activities so that the accidents should be minimized. Also, object tracking is required to highlights the role of humans in the next generation [2] of driver assistance and intelligent vehicles. It is important to detect and track the activities of human or robotic driving for safety reasons.

It noticed that the statistics of road-side accidents are rapidly increasing throughout the world especially in Saudi Arabia. According to estimation, there were 82.281 accidents occurred during a time period of one month. These accidents were due to not use of leaving enough safety distance between vehicles, run a red traffic light, sudden change of lane, and lack of commitment to the priorities. In this paper, an automatic system is developed to predict and discover the mistakes of the drivers, especially highway driving. A desktop application software is implemented to detect and track both vehicle and driver's activities during highway driving, using a real-time video camera installed on highway road. Real-time car detection and tracking are applied over hundreds of image frames. The proposed system will communicate with the respective authorities to apply strict measures when the driver exceeds the speed limit or track sudden change or leave out the yellow lane or stop in the left path.

In fact, the road, traffic lights and other drivers on the road [3] information are provided by the vision-based systems. It noticed that the number of vehicles increased nowadays and created a total burden on computer vision systems. Therefore, there is a dire need for developing effective and efficient solutions for tracking vehicle illegal activities on the road. Moreover, the security risks have significantly increased and that becomes an important subject for law enforcement authorities for surveillance highways. To solve these problems, there are lots of researchers who develop a tracking algorithm but still inefficient and un-effective.

Another requirement of these systems in public is to have a rationally large number of pixels on an objective. There are many different types of objectives which could be important and it is often not possible to get a large number of pixels on objective and robustness [4]. The road digital cameras must provide plenty related to uncommon events compared to just over speed information. For example, those digital cameras must include plenty of information related to immediate line overrun, speed limit overrun and yellow-line driving.

Automatic detection and identification of objects is the main importance of security systems and video surveillance applications. Automatic video surveillance is placed to provide coverage over the scenes of most interest. Within the scope of view of the camera, some areas are of greater importance than others and some areas are really of no interest at all.

For an automatic development of vehicle detection and tracking, it is an important subject in the domain of computer vision. Therefore in this paper, a system is trying to develop an application that can track vehicle activities from live video streaming during highway driving. The primary aim of this project (ITS-V) is to focus on the detection of moving vehicles for surveillance purposes. This problem is also related to the domain of artificial intelligence [5] due to recognizing moving objects from live video streams. When working on ITS-V problem, an accurate solution is required to track object and segment [6] it at the same time without losing time efficiency. Also, real-time vehicle activity tracking means that the tracking and segmentation step were integrated together. It is also important that the developed application must help to law enforcement agencies in case of discovering any vehicle violating laws and it helps in improving traffic safety levels and raise the quality of existing roads network.

The features of the system can achieve a better standard of safety on the roads to reduce the rate of accidents and deaths among drivers as less as possible. It can read the exceed speed limit of the vehicle. The system will work on highways only because according to statistics accidents often happen on the highways. To reduce the number of accidents, a system is developed that works in good control with the vehicle, so it can follow the driver's movements and behaviors. And the system processes the images of accidents in the video clips and adds them to a dataset to discover which roads have the most accidents.

The speed limit parameter for a traffic violation in KSA is varied from 120 km to 140 km per hour if the driver goes over it more than 10% the system will detect him. In the past studies, the authors utilized some image processing and machine learning algorithms to detect real-time driver's activities. Those machine learning techniques such as SVM [7], [8], PCA [9], Neural Networks [10] or Bayesian decision-making [11]. However, in this paper, the latest deep learning techniques are integrated together to develop this novel system.

Instead of driving activities control system, there is also a requirement for developing driving assistance systems and that is considered to be a challenging task [12, 13]. To do this task, there are many algorithms proposed to track the vehicles in the motorway driving [14]. The advantage of these systems is their real-time performance. There are many systems also talking about the problems related to detect and track real-time vehicle activities. These systems are explained below.

An intelligent transportation system based on the video (ITS-V) is providing an important solution for the problem of socioeconomic [15] impact on society. For tracking or segmentation of vehicles, there is a need to monitor different traffic parameters such as yellow-line, off-road or immediate line changing during highway driving. Since, there are lots of challenges of traditional video-based tracking systems such as

in case of vehicle drifting, occlusions, obstacles and detection still in various environmental conditions. To address these challenges, there are few studies that focused on all these problems during vehicle tracking.

Another paper [16], the authors developed a driving assistance system to track head-and eye-blinking. Whereas in [17], the authors presented a solution to detect a lane using a vision system on the vehicle. Though, they concluded that lane detection is a difficult problem because of the varying road conditions that one can encounter while driving. There are also some papers that talking about the techniques for monitoring and understanding of real-world human activities, in particular of drivers, from distributed vision sensors [18]. In order to achieve this goal, the authors used different parameters such as head pose estimation module, hand, and foot tracking, ego-vehicle parameters, lane, and road geometry analysis, and surround vehicle trajectories. The system is evaluated on a challenging dataset of naturalistic driving in real-world settings.

In contrast to these approaches, the authors developed an Intelligent Vehicle Monitoring System [19] that using Global Positioning System along with Google Maps and Cloud Computing which collects useful information about a vehicle. The detection of a vehicle is also a challenging task. In paper [20], the authors developed a video-based analysis system that detects, tracks and archives vehicles in video stream data at multiple resolutions. This step is important even for controlling activities of autonomous vehicle driving. Even in urban areas [21], the sensors utilized in the car to communicate with the clouds to given information about drivers activities during driving. In this study [22], the authors introduced an activity classification system based on activity class through random forests (RFs) classifier. Moreover, in [23], the authors discussed a human-centered perspective to develop an intelligent vehicle.

There are a lot of limitations and deficiencies of the current strengths and weaknesses of existing V-ITS approaches of video-based vehicle tracking, which are as under. Previous approaches did not provide effective traffic monitoring results due to the effects of occlusion and spillover. The state-of-the-art approaches utilized old fashion image processing and machine learning algorithms to track the vehicle illegal movements. In addition, large trucks often occlude neighboring vehicles and make them hard to recognize side-by vehicle activity. Though the approach is this paper to overcome these limitations. The past studies have the inability to detect vehicles due to headlight reflections and different weather situations such as dust storm. The dust storm is come in KSA and making the automatic system totally raise false positive to detect vehicle activities.

The accuracy of tracking is also affected by the distance of the camera from the closest lane. A larger pan angle is required to cover all lanes when the camera is placed far from the closest lane, so the camera should be placed as close to the closest lane as possible. By using previous techniques, the selection of key points of vehicles is crucial and those systems are sensitive to drift and occlusion. The other developed systems outside the KSA for automatically determining the

vehicle illegal activities are computationally expensive due to the increasing number of vehicles. It noticed from the literature that there is a dire need to develop a high-performance vehicle detection method.

To overcome these above-mentioned problems, an improved V-ITS system was presented through advanced deep learning algorithms to get robust results. In the past studies, the deep learning algorithms [24-36] have many variants to represent visual features such as the convolutional neural network (CNN), recurrent neural network (RNN), deep belief networks (DBN), restricted Boltzmann machine (RBM) and AutoEncoder. A four multilayer convolutional neural network (CNN) [38] model is trained in different roads samples along with diverse environmental conditions. Those samples were obtained from GRAM Road-Traffic Monitoring (GRAM-RTM) dataset [37]. The three layers in the CNN model were dedicated towards driver immediate line overrun, speed limit overrun and yellow-line driving along with one features extraction layer. After this CNN model, a deep belief neural network (DBN) [39] model was used to classify these three drivers' illegal activities.

III. METHODOLOGY

The systematic flow diagram of all steps of the proposed V-ITS system is displayed in Fig. 1. An increasing number of vehicles and environment conditions created a new interest in the development of new technologies in real-time video image processing. It noticed from the past studies that there are many commercial systems proposed but they have difficulties with congestion, shadows, dust storms, and lighting transitions. Also, there are some illegal driving activities such as yellow-lane driving that they are unable to detect. Therefore in this research study, a feature-based transform system is developed to overcome these difficulties by using advanced deep-learning algorithms to process real-time video sequences. The author of this paper entitled this system as a video-based intelligent transportation system (V-ITS).

In this paper, the vehicle features are tracked instead of tracking just entire vehicles to make it fit for various environmental conditions such as occlusion and lighting conditions. Also, the developed system can easily differentiate between cars and trucks through feature-based tracking. Moreover, there are some examples of training samples for traffic violations on a highway are shown in Fig. 2.

Overall the proposed vehicle tracking system is developed based on four main stages that are mentioned below. To develop this ITS-V system, the firsts step is to segment of the scene into individual vehicles and then tracking each vehicle inside a tracking zone. A simple background subtraction technique was utilized to segment vehicle from the background video frames. After detecting and segmenting the vehicle form a background scene, the next step is to compute traffic parameters such as vehicle speed in different lanes of the highway roads. After collecting local parameters thorough CNN model at the collection site, this intelligent data is then passed on to automated and operator assisted applications, which is developed through the DBN model for classification. In the end, plenty is generated according to the specific traffic

violation and stored in the somewhere distributed server to avoid further traffic violations.

The first step of this research study is to extract the video frames from the side of highway daily time driving. In this paper, a pre-train four multi-layer convolutional neural network (CNN) model was used to transform features for prediction of driver's illegal activities during highway driving. Those frames are extracted from a video in every 0.3 seconds. Afterward, a deep-belief network (DBN) model was applied to predict the final decision of the activity class of driver's illegal driving. The DBN model is trying to help pre-train CNN model to pool layer for defining an effective features map. In the proposed system, a single features map was utilized that was extracted from a single video frame. To perform the final prediction about the driver's illegal activities, a group of frames was used for recognition. From the video frames, fifteen feature maps are stored to generate by the pre-trained CNN model for prediction, the equivalent of three seconds of video. Afterward, this group of feature maps is concentrated into one single pattern, which will be the input of our proposed DBN model, to obtain the final classification of the traffic violation system.

To train the CNN model, the GRAM road-traffic monitoring (GRAM-RTM) dataset was utilized. In this dataset, the sample videos are selected according to different environmental conditions to make the system runs better compare to state-of-the-art systems. The methodological steps are explained in the upcoming subsection of this paper.

A. Acquisition of Datasets

GRAM Road-Traffic Monitoring (GRAM-RTM) dataset [37] was utilized in this paper to test and compare the performance of proposed V-ITS system. In fact, the GRAM-RTM dataset consists of multiple vehicles tracking ground truth during real-time video processing. The V-ITS system was tested and implemented on HP brand Laptop with an Intel core processor of the processing capability of i7 CPU @ 3.35 GHz and 8 GB of RAM with Windows XP. This program was programmed in OpenCV and Python tools. The experimental results were also statistical measured. The dataset of 1200 region-of-interest (ROI) video frame images including normal of 600 and traffic violation of 600 were acquired from GRAM-RTM to test and evaluate the performance of V-ITS system. An example of this dataset from urban second video is visually displayed in Fig. 2.

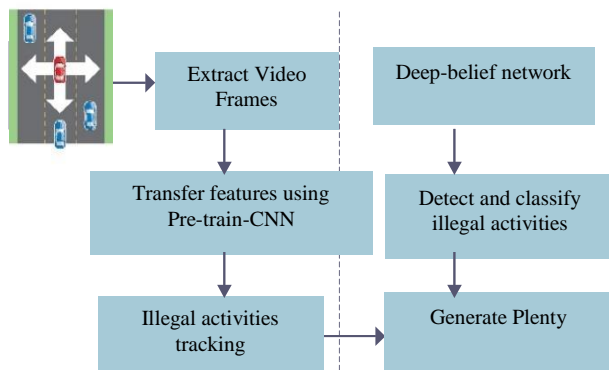


Fig. 1. A Systematic Diagram of Proposed V-ITS System for Detecting Vehicle Illegal Activities.

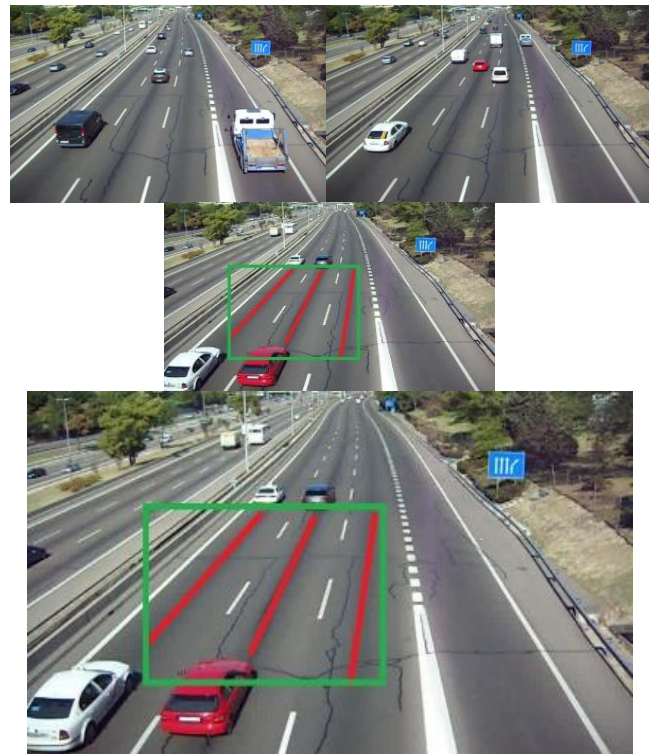


Fig. 2. An Example of Training a Convolutional Neural Network Model for Transfer Training Video Region-of-Interest (ROI).

The region-of-interest (ROIs) for each video frames from GRAM-RTM dataset is automatically defined to trained the convolutional neural network (CNN) [38] for transform features. In the video frames, the three-lines are drawn to defined vehicle tracking and checking illegal activities. This step is visually represented in Fig. 2. The high-level features are defined from these ROI video frames to effectively train the multilayers of the CNN model. The detailed description of this CNN model is defined in the next subsection.

B. Pretrain CNN Model

Convolutional neural network (CNN) model [38] is using in many applications to extract deep features and it has applications in many different fields. In practice, the CNN model is used to detect the pixel-level features using convolutional filters in different layers and then finally classify them through softmax linear classifier. In the past studies, the authors achieved significantly higher performance than manually tune machine learning algorithms.

To extract features from an image, a domain-expert knowledge is required to detect best features from image processing. However, if a convolutional neural network (CNN) model is applied to a digital image then it provides deep-invariant features. Those features are extracted from a different multilayer of CNN model. To recognize the objects from images, the features-map is responsible for the output layer. But the features-map created by CNN model is not optimized for real-time video processing. Therefore, a pre-train CNN model was utilized to get an effective features map.

In this paper, a pre-train CNN model is utilized to extract effective and optimize features from video frames. A pre-

training strategy was used to guide CNN for defining the features from video frames. The dataset is divided into three different groups such as immediate line overrun, speed limit overrun and yellow-line driving. The frames are extracted from GRAM Road-Traffic Monitoring (GRAM-RTM) dataset that defined the problems of immediate line overrun, speed limit overrun and yellow-line driving. In fact, the CNN network structure is learned to recognize the three different tasks for a traffic violation from labeled video sequences. At the top layer of the CNN model, the features are extracted and transformed into weights to train the next layer of the CNN model. A pre-training step for CNN multilayer architecture along with deep-belief network (DBN) is explained in the subsequent paragraphs.

The region-of-interest (ROIs) are extracted from video frame from fixed regions and then send to the four multilayer CNN architecture which has been already trained for high-level feature extraction in different frames from GRAM-RTM dataset video frames in three different categories. Those categories are related to a traffic violation. Convolution and max-pooling layers are added to the network for extracting and selecting the most important features. The two fully-connected deep belief network (DBN) layers are then added to the network after convolution and the pooling layers. In practice, a multi-layer RBM network is utilized for developing in a DBN unsupervised network. In deep learning algorithms, the DBN architecture proved to be an excellent generative model that can easily outperform for fine-tune parameters.

During the training stage, high-level features are learned simultaneously with the training of the proposed CNN network. After four layers of convolution, RBM, and pooling, the features are out of the last layer into the two-layer fully-connected network for further training. Finally, the trained feature matrix is taken as the input of DBN. DBN is trained and fully connected to the output of the network to predict saliency. In the inference stage, the full image was used as the input of the network. Similar to the training stage, the high-level features of the test video frame is extracted via the trained CNN network. Finally, using the trained DBN and the learned features, the plenty value was computed in each frame.

In order to develop a pre-train CNN model, the high-level features are learned or extracted together to train the multi-layer architecture of the network. In advance step, the pre-training step is applied to get and learn good informative features extracted from video frames. The dataset samples are divided into three category classes. The ROI regions are defined earlier from each video to do better initialization of the training step. These ROIs frames are visually represented in Fig. 2. In three different traffic violation, a set of informative features are defined to effectively train the CNN model. Then a single features map was generated from every single image, which is convolved with a Gaussian mask.

The first layer of convolution neural network (CNN) model was generated by following the DBN and max-pooling concepts. To develop this pre-train CNN model, the features are obtained at the first layer are additionally learned through the next three CNN network layers. Training Similar to the pre-training step, the training of the proposed CNN network is

performed with features from the pre-training step as the input on the same collected from target frame regions.

C. Driver's Illegal Activities Prediction

Given a frame region, the driver's illegal activity is predicted through the pre-train CNN model and classifies those activities by deep-belief network (DBN) multilayer architecture. In order to achieve the high-level traffic violation parameters, the ROI image region was used from the video frame to do perfect training of the CNN network. In fact, the convolutional filters are performed to each layer of the pre-train CNN network model. Afterward, the deep belief network (DBN) model was applied followed by the pooling layer to classify driver's illegal activities. In order to recognize driver's illegal activities, the last two layers are fully-connected layer and input to this layer is a feature map to the DBN architecture. After repeated running a DBN model, a weighted matrix is obtained that is conforming to the high-level video features of this frame. Hence, the traffic violation value of this frame can be obtained via multiplying the weight with the features and it is defined by the Eq. (1).

$$Plenty_{i=1,2,3}^n = \max_f(W_L x; 0) \quad (1)$$

Where w parameter is learned parameters from the deep-belief network (DBN) classifier for three categories of plenty class, and x is the high-level features matrix extracted by the well-trained a multilayer convolutional neural network (CNN) network model. In this equation, G parameter denotes the Gaussian masking template to detect driver immediate line overrun, speed limit overrun and yellow-line driving.

IV. EXPERIMENTAL RESULTS

Experimental results are described in this section to validate the performance of the proposed V-ITS system for detecting vehicle illegal activities without performing pre- or post- image processing techniques. The proposed V-ITS system based best variants of deep-learning multilayer architecture is proposed in this paper that is different from state-of-the-art detection systems.

The performance was evaluated based on the frames that are extracted from GRAM Road-Traffic Monitoring (GRAM-RTM) dataset. The multi-layer CNN architecture model was trained in three different samples from GRAM-RTM dataset. The three different samples driver's illegal activities are counted based on immediate line overrun, speed limit overrun and yellow-line driving. The samples datasets are considered to have different environments such as normal, sunny, and cloudy. To extract high-level features from video frames, the RBM layer was added to pre-train CNN model. To show the effectiveness of proposed pre-train CNN and DBN models, the comparisons with the CNN network is presented in Table I.

The V-ITS system was implemented in python and OpenCV tools in Windows XP 64-bit system. The learning rate for training the four-layer CNN is initialized as (10 x 6) with a batch size of 32. The training of the four-layer of CNN model for about 75 epochs and the training procedure costs nearly 12 hours in all. In the experiments, it averagely takes 0.254 seconds to train an image, and 0.152 seconds to test a video frame image. The performance detector calculates two kinds of

errors, namely to miss a true violation detection and to detect the false violation. The first error is measured by the detection rate while the second one is called the number of false accepts. These measures are represented in an average form in Table I.

To evaluate the performance of V-ITS system, different vehicles are considered in the experiments. The experimental results are shown in Table I. In this table, all types of environmental conditions are considered. As shown in this table, the proposed system is performed better results compared to a simple convolutional neural network (CNN) model with pre-training through principal component analysis (PCA) technique. On average, the proposed V-ITS system is getting 90% better detection rate compared to the 84% value obtained by CNN model. The V-ITS system is capable of detection and recognition the traffic violation up to four frames per second (fps), so at normal speed (i.e., 100 km/h), the system offers at least two opportunities to identify driver's illegal activities. In fact, the V-ITS will be upgraded in the future to add more traffic violation at lower speeds. The V-ITS system has been tested in a real-time environment mode during nighttime and daytime under different environmental conditions.

TABLE I. RESULTS CONCERNING THE AVERAGE PRECISION OF TRACKING METHODS FOR VEHICLES IN SELECTED DATASET FROM GRAM-RTM IN CASE OF IMMEDIATE LINE OVERRUN, SPEED LIMIT OVERRUN AND YELLOW-LINE DRIVING

No.	V-ITS Performance		
	Methods	CNN	Pre-train CNN & DBN
1	Line-overrun	0.751	0.890
2	Limit-overrun	0.845	0.920
3	Yellow-drive	0.821	0.945
Average Detection Rate		84.50%	90.01%

In this paper, a novel V-ITS system based on a new CNN framework is proposed to automatically detect driver's illegal activities during highway driving. To detect effective features, high-level features are learned and the classification results are predicted through the DBN model. The proposed pre-train model is distinct from the state-of-the-art techniques, an extra layer was added through DBN into the CNN framework to obtain more accurate features. Moreover, to avoid manual annotation of video frames data, Deep Belief Network (DBN) classifier was added to pre-train CNN model for recognizing of driver's illegal activities without using complex methods of image processing algorithms. The proposed V-ITS system outperforms compare to simple pre-train CNN model using PCA in the same selected dataset.

V. CONCLUSIONS

Tracking of vehicle illegal activities is a critical step for the development of an automatic traffic management system. In the past studies, there are many authors focus on extracting traffic parameters without focusing on environmental conditions. In this paper, an efficient V-ITS system is developed to predict the driver's illegal activities during

highway driving. The system was evaluated and tested on GRAM-RTM dataset. The experimental results indicate that the proposed V-ITS system outperformed compared to state-of-the-art video processing systems. It is happened due to use of pre-train CNN model to transform the features and then DBN is deployed to classify the vehicle illegal activities in multiple video frames. In this paper, the V-ITS system measured traffic parameters due to pre-train CNN deep learning algorithm to get robust results without any problem or delay. The main objective of this paper is to consider the latest deep learning algorithm to calculate traffic illegal parameters without focusing pre- or post-processing steps as done in many studies. In this study, the combination of transform features and multilayer architecture of deep learning algorithms (DBN) are effectively integrated for better classification results. To implement and test this V-ITS system, Python, computer vision OpenCV tools were utilized. In a future study, more traffic violation is added according to the type of vehicle.

ACKNOWLEDGMENT

The author would like to thank Deanship of Scientific Research at Al Imam Mohammad ibn Saud Islamic university, Saudi Arabia, for financing this project under the grant no. (380902).

REFERENCES

- [1] S. Ojha and S. Sakhare, "Image processing techniques for object tracking in video surveillance- A survey," International Conference on Pervasive Computing (ICPC), Pune, pp. 1-6, 2015.
- [2] E. Ohn-Bar and M. M. Trivedi, "Looking at Humans in the Age of Self-Driving and Highly Automated Vehicles," in IEEE Transactions on Intelligent Vehicles, vol. 1, no. 1, pp. 90-104, March 2016.
- [3] J. Wu and X. Zhang, "A PCA Classifier and its Application in Vehicle Detection," in Neural Networks, Proceedings. IJCNN '01. International Joint Conference on, vol. 1, 2001.
- [4] S. Sivaraman and M. Trivedi, "A General Active-Learning Framework for On-road Vehicle Recognition and Tracking," IEEE Trans. on ITS, vol. 11, no. 2, June 2010.
- [5] A. Broggi, P. Cerri, and P. Antonello, "Multi-resolution Vehicle Detection using Artificial Vision," in Intelligent Vehicles Symposium, 2004 IEEE, June 2004.
- [6] H. Grabner, M. Grabner, and H. Bischof, "Real-Time Tracking via On-line Boosting," in Proc. BMVC, pp. 6.1-6.10, 2006.
- [7] C. Papageorgiou and T. Poggio, "A Trainable System for Object Detection," Int. J. Comp. Vision, vol. 38, no. 1, pp. 15-33, Jun. 2000.
- [8] Z. Sun, G. Bebis, and R. Miller, "On-road Vehicle Detection using Gabor Filters and Support Vector Machines," in 14th Intern. Conf. on Digital Signal Processing (DSP), vol. 2, pp. 1019-1022, 2002.
- [9] J. Wu and X. Zhang, "A PCA Classifier and its Application in Vehicle Detection," in Neural Networks, Proceedings. IJCNN '01. International Joint Conference on, vol. 1, pp. 600-604 vol.1, 2001.
- [10] N. Matthews, P. An, D. Chamley, and C. Harris, "Vehicle Detection and Recognition in Grayscale Imagery," Control Engineering Practice, vol. 4, no. 4, pp. 473-479, 1996.
- [11] H. Schneiderman and T. Kanade, "A Statistical Method for 3D Object Detection applied to Faces and Cars," in IEEE Conf. on Computer Vision and Pattern Recognition, vol. 1, pp. 746-751, 2000.
- [12] A. Ess, K. Schindler, B. Leibe, and L. Van Gool, "Object Detection and Tracking for Autonomous Navigation in Dynamic Environments," The International Journal of Robotics Research, vol. 29, 2010.
- [13] E. Richter, R. Schubert, and G. Wanielik, "Radar and Vision-based Data Fusion - Advanced Filtering Techniques for a Multi-object Vehicle Tracking System," in Intelligent Vehicles Symposium, 2008 IEEE, pp. 120-125, June 2008.

- [14] NC Mithun, T Howlader, SMM Rahman, Video-based tracking of vehicles using multiple time-spatial images, *Expert Systems with Applications*, vol. 62, no. 15, pp. 17-31, 2016.
- [15] C. Braunagel, E. Kasneci, W. Stolzmann and W. Rosenstiel, "Driver-Activity Recognition in the Context of Conditionally Autonomous Driving," 2015 IEEE 18th International Conference on Intelligent Transportation Systems, Las Palmas, pp. 1652-1657, 2015.
- [16] A. A. Assidiq, O. O. Khalifa, M. R. Islam and S. Khan, "Real time lane detection for autonomous vehicles," 2008 International Conference on Computer and Communication Engineering, Kuala Lumpur, pp. 82-88, 2008.
- [17] Eshed Ohn-Bar, Ashish Tawari, Sujitha Martin, Mohan M. Trivedi, On surveillance for safety critical events: In-vehicle video networks for predictive driver assistance systems, *Computer Vision and Image Understanding*, vol. 134, pp. 130-140, May 2015.
- [18] Dimil Jose, Sanath Prasad, V.G. Sridhar, "Intelligent Vehicle Monitoring Using Global Positioning System and Cloud Computing", *Procedia Computer Science*, vol. 50, pp. 440-446, 2015.
- [19] W Wu, EA Bernal, RP Loce, ME Hoover, "Multi-resolution video analysis and key feature preserving video reduction strategy for (real-time) vehicle tracking and speed enforcement systems", *S Patent* 8,953,044, 2015.
- [20] M. Gerla, E. K. Lee, G. Pau and U. Lee, "Internet of vehicles: From intelligent grid to autonomous cars and vehicular clouds," *IEEE World Forum on Internet of Things (WF-IoT)*, Seoul, pp. 241-246, 2014.
- [21] Lijie Xu and Kikuo Fujimura, "Real-Time Driver Activity Recognition with Random Forests. In Proceedings of the 6th International Conference on Automotive User Interfaces and Interactive Vehicular Applications (AutomotiveUI '14). ACM, New York, NY, USA, Article 9 , 8 pages, 2014.
- [22] E. Ohn-Bar and M. M. Trivedi, "Looking at Humans in the Age of Self-Driving and Highly Automated Vehicles," in *IEEE Transactions on Intelligent Vehicles*, vol. 1, no. 1, pp. 90-104, March 2016.
- [23] Jianwei Ding, Yongzhen Huang, Wei Liu, and Kaiqi Huang, "Severely Blurred Object Tracking by Learning Deep Image Representations, *IEEE TRANSACTIONS ON CIRCUITS AND SYSTEMS FOR VIDEO TECHNOLOGY*", vol. 26, no. 2, FEBRUARY 2016.
- [24] Hong yang Xue, Yao Liu, Deng Cai, Xiaofei He, Tracking people in RGBD videos using deep learning and motion clues, *Neurocomputing* vol. 204, pp. 70-76, 2016.
- [25] Bohan Zhuang, Li jun Wang, Huchuan Lu, "Visual tracking via shallow and deep collaborative model", *Neurocomputing*, vol. 218, pp. 61-71, 2016.
- [26] Naiyan Wang, Dit-Yan Yeung, "Learning a deep compact image representation for visual tracking", *Proceeding NIPS'13 Proceedings of the 26th International Conference on Neural Information Processing Systems*, Lake Tahoe, Nevada, pp. 809-817, 2013.
- [27] Lijun Wang, Wanli Ouyang, Xiaogang Wang, and Huchuan Lu, "Visual Tracking with fully Convolutional Networks", *EEE ICCV* 2015.
- [28] Chao Ma, Jia-Bin Huang, Xiao kang Yang, Ming-Hsuan Yang, "Hierarchical Convolutional Features for Visual Tracking", *Proceeding ICCV '15 Proceedings of the 2015 IEEE International Conference on Computer Vision (ICCV)*, pp. 3074-3082 December 07 - 13, 2015.
- [29] H. Li, Y. Li and F. Porikli, "DeepTrack: Learning Discriminative Feature Representations Online for Robust Visual Tracking," in *IEEE Transactions on Image Processing*, vol. 25, no. 4, pp. 1834-1848, April 2016.
- [30] Charissa Ann Ronao, Sung-Bae Cho, "Human activity recognition with smartphone sensors using deep learning neural networks", *Expert Systems With Applications*, vol. 59, pp. 235-244, 2016.
- [31] Trumble, M., Gilbert, A., Hilton, A., Collomosse, "J.: Learning markerless human pose estimation from multiple viewpoint video", In: *Proc. ECCV Workshops*, 2016.
- [32] Lishen Pei, Mao Ye, Xuezhuan Zhao, Tao Xiang Tao Li, Learning spatio-temporal features for action recognition from the side of the video, *Signal, Image and Video Processing* January, vol. 10, no. 1, pp 199-206, 2016.
- [33] Konstantinos Charalampous, Antonios Gasteratos, "On-line deep learning method for action recognition", *Pattern Analysis & Applications*, vol. 19, no. 2, pp. 337-354, May 2016.
- [34] Cheng-Sheng Chan, Shou-Zhong Chen, Pei-Xuan Xie, Chiung-Chih Chang, Min Sun, "Recognition from Hand Cameras: A Revisit with Deep Learning", *Computer Vision – ECCV 2016 Volume 9908 of the series Lecture Notes in Computer Science* pp. 505-521, September 2016.
- [35] Yanming Guo, Yu Liu, Ard Oerlemans, Songyang Lao, Song Wu, Michael S. Lew, "Deep learning for visual understanding: A review, *Neurocomputing*", *Recent Developments on Deep Big Vision*, vol. 187, pp. 27-48, 26 April 2016.
- [36] Guerrero-Gómez-Olmedo, R., López-Sastre, R. J., Maldonado-Bascón, S., & Fernández-Caballero, A. "Vehicle tracking by simultaneous detection and viewpoint estimation", In *International Work-Conference on the Interplay Between Natural and Artificial Springer*, Berlin, Heidelberg, pp. 306-316, 2013.
- [37] G.W. Yang, and J. Hui-Fang, "Multiple Convolutional Neural Network for Feature Extraction," *International Conference on Intelligent Computing*, pp. 104-114. Springer International Publishing, 2015.
- [38] A. Qaisar, "DeepCAD: A Computer-Aided Diagnosis System for Mammographic Masses Using Deep Invariant Features," *Computers*, vol.5,pp.1-15,2016.
- [39] Qaisar Abbas, "Glaucoma-Deep: Detection of Glaucoma Eye Disease on Retinal Fundus Images using Deep Learning", *International Journal of Advanced Computer Science and Applications*, 8(6):, pp. 41-45 ,2017.

Analysis of Doppler Effects in Underwater Acoustic Channels using Parabolic Expansion Modeling

Ranjani G¹, Sadashivappa G²

Dept. of TCE RVCE
Bengaluru, India

Abstract—Underwater communication systems play an important role in understanding various phenomena that take place within our vast oceans. They can be used as an integral tool in countless applications ranging from environmental monitoring to gathering of oceanographic data, marine archaeology, and search and rescue missions. Acoustic Communication is the viable solution for communication in highly attenuating underwater environment. However, these systems pose a number of challenges for reliable data transmission. Nonnegligible Doppler Effect emerges as a major factor. In order to support reliable high data rate communication, understanding the channel behavior is required. As sea trials are expensive, simulators are required to study the channel behavior. Modeling this channel involves solution to wave equations and validation with experimental data for that portion of the sea. Parabolic expansion model is a wave theory based acoustic channel model. This model applies Pade coefficients and Fourier coefficients as expansion functions to solve the wave equations. This work attempts to characterize the impact of Doppler Effect in the underwater acoustic channel using parabolic expansion models.

Keywords—Doppler effect; underwater communication; acoustic channel models; parabolic expansion

I. INTRODUCTION

Wave equation is the theoretical basis of the mathematical models of acoustic propagation. It shows the relationship between sound pressure and vibration velocity of particle. Theory of acoustic propagation and solution to the frequency-domain wave equation are available in literatures [1-2]. There are different underwater acoustic propagation channel models available namely ray tracing, parabolic expansion models, normal mode propagation model multipath expansion model and fast field model. These models can be classified based on their range dependence into two types namely range independent models and range dependent models. Range independence indicates that the model considers a horizontally stratified ocean whose properties vary only as a function of depth. On the contrary, range dependence means that the model could consider some properties of the ocean medium that are allowed to vary as a function of range or the angle of the receiving antenna. According these definitions, normal-mode model, multipath expansion model and fast-field model are range independent while, ray-theoretical model and parabolic expansion model are range dependent.

Of the range dependent models, Ray-theoretical models characterize the propagation on the basis of geometry. Ray tracing techniques are available in literatures [3-5]. A multipath channel was modeled by Qarabaqi and Stojanovic, with ray

tracing method [6]. Doppler Effect is modeled in these literatures by direct variation of the frequency component in the pressure field function. Parabolic expansion model is based on wave theory. The field functions obtained at low frequencies is accurate and provides an insight into antenna design. In this model, Doppler Effect is modeled as variation in the wave number of the field function. Parabolic expansion based modeling techniques are available in literatures [7-13].

This work attempts to characterize the impact of Doppler Effect due to source receiver motion in the underwater acoustic channel with parabolic expansion models using two different expansion functions namely Pade coefficients and Fourier coefficients to solve wave equations and analyze them with the environment data obtained from one of the Indian sea trials. This paper is organized as follows. Section 2 provides review of the parabolic expansion model. Section 3 explains the modeling of Doppler Effect using the parabolic expansion model and Section 4 discusses the results obtained and the work concludes with the key findings.

II. PARABOLIC EXPANSION MODEL

For sinusoidal frequency f_0 , the wave equation for the acoustic pressure in an environment with azimuth symmetry is,

$$\left(\frac{\partial^2}{\partial r^2} + \frac{1}{r^2} \frac{\partial^2}{\partial \psi^2} + \frac{\partial^2}{\partial z^2} + k^2 \right) P = 0 \quad (1)$$

Here, P is the acoustic pressure propagating in the (r, ψ, z) plane in dB re μPa , k is the wave number, r is the range in meters and z is the depth in meters, ψ is the azimuth in radians. k is the wave number in radians/meter; c is the velocity of the sound in the medium in meters/second. The second term in (1) provides the azimuth coupling between different radial element sets and is very small in general and thus is neglected

Parabolic Expansion Model assumes the medium is stratified, propagation is in vertical direction alone and the ocean bottom is flat and horizontal. This assumption is valid for all short range shallow water communication and useful in reducing computational complexity.

At far field, spreading and horizontal reflections are weak in case of short range and shallow depth, At range independent regions (smaller range over which horizontal variation is considered to be small), only forward wave propagation exists. To handle range dependence, the range is divided into several smaller range independent regions and thus the assumption is that the energy contained in the backward wave propagation is

negligible. Thus the two dimension equation is reduced to one dimension.

For mathematical simplicity assume

$$P(r, z) = \left(\frac{1}{\sqrt{r}} \right) \phi(r, z) e^{ik_0 r} \quad (2)$$

$$Q = \left(\frac{\partial^2}{\partial z^2} + k^2 \right) \quad (3)$$

Then (1) can be written as

$$\frac{\partial \phi}{\partial r} = i(\sqrt{Q} - k_0) \phi \quad (4)$$

Obtaining solution to ϕ requires finding \sqrt{Q}

A. Split step Fourier Algorithm

In split step algorithm the square root operator is split into two operators, one involving wave number and the other involving velocity.

Let

$$q = \left(\frac{Q}{k_0^2} - 1 \right) \quad (5)$$

The solution to (4) can also be written in terms of operators as:

$$\psi(r + \Delta r, z) = e^{ik_0(Q_{op}-1)\Delta r} \psi(r, z) \quad (6)$$

$$(1 - Q_{op}) = T_{op} + U_{op}$$

$$T_{op} = 1 - \left[1 - \left(\frac{k_z}{k_0} \right)^2 \right]^{1/2}$$

$$U_{op} = 1 - \frac{c_0}{c(r, z)}$$

$$k_z = nk_0 \quad (7)$$

k_z is the depth dependant wave number, k_0 is the reference wave number and n is the refractive index; the operator Q_{op} is split into two terms viz T_{op} (velocity operator) and U_{op} (wave number operator).

Thus Split step Fourier Transform algorithm is implemented by (8).

$$\psi(r + \Delta r, z) = e^{-ik_0 \frac{\Delta r}{2} U_{op}(r + \Delta r, z)} \times IDFT \left\{ e^{-ik_0 \Delta r T_{op}(k_z)} \times DFT \left[e^{-ik_0 \frac{\Delta r}{2} U_{op}(r, z)} \times \psi(r, z) \right] \right\} \quad (8)$$

B. Split Step Pade Algorithm

In split step Pade algorithm the Square root operator is approximated with Pade solution

$$\sqrt{1+q} \approx \frac{A+Bq}{C+Dq} = 1 + \sum_{i=1}^{n_p} \frac{a_i q^i}{1+b_i q};$$

$$a_i = \frac{2}{2n_p + 1} \sin^2 \left(\frac{i\pi}{2n_p + 1} \right); b_i = \cos^2 \left(\frac{i\pi}{2n_p + 1} \right) \quad (9)$$

With this approximation, the solution to (4) reduces to the form which can be split into three terms each forming a matrix $H(1), H(2), H(3)$. The matrices so obtained will in general have three or less term at every depth grid and hence they are called Tri diagonal matrices.

$$(\mathbf{H}(1) + \mathbf{H}(2) + \mathbf{H}(3)) \phi(r + \Delta r, z) = \phi(r, z) \quad (10)$$

$$H_{i,j}(1) = \int_z h_i(z) f_1(z) h_j(z) dz \quad i = j-1, j, j+1; f_1 = \frac{1}{\rho} \quad (11)$$

$$H_{i,j}(2) = \int_z h_i(z) f_2(z) h_j(z) dz \quad i = j-1, j, j+1; f_2 = \frac{1}{\rho c^2} \quad (12)$$

$$H_{i,j}(3) = \int_z h_i(z) \frac{\partial}{\partial z} \left(f_3(z) \frac{\partial}{\partial z} (h_j(z)) \right) dz \quad i = j-1, j, j+1 \quad (13)$$

$$h_i(z) = \begin{cases} 0 & z \leq z_{i-1} \\ z - z_{i-1} / z_i - z_{i-1} & z_{i-1} \leq z \leq z_i \\ 1 - z - z_i / z_{i+1} - z_i & z_i \leq z \leq z_{i+1} \\ 0 & z \geq z_{i+1} \end{cases} \quad (14)$$

where $\phi(r, z)$ is the propagating field; ρ is the density; z is the depth, and $h_i(z)$ is the linear finite element basis function.

Gaussian elimination method is applied to solve the system of equations represented in Matrix form to obtain the numerical solution of the parabolic wave equation.

III. MODELING DOPPLER EFFECT USING THE PARABOLIC EXPANSION MODEL

Doppler Effect is caused by transceiver motion. When the source is moving and the receiver is stationary, the shift in transmit frequency along the various vertical angle of transmission is given by

$$f'_n \approx f_T \left(1 + \frac{v_s}{c} \cos(\theta_n - \phi_s) \right); n = 1, 2, \dots, N_z \quad (15)$$

f_T is the Transmit frequency in Hz; v_s is the source velocity in m/s and ϕ_s is the angle in radians θ_n the source makes with the horizontal while moving and are the discretely sampled vertical angle in radians along which the transmission loss is calculated.

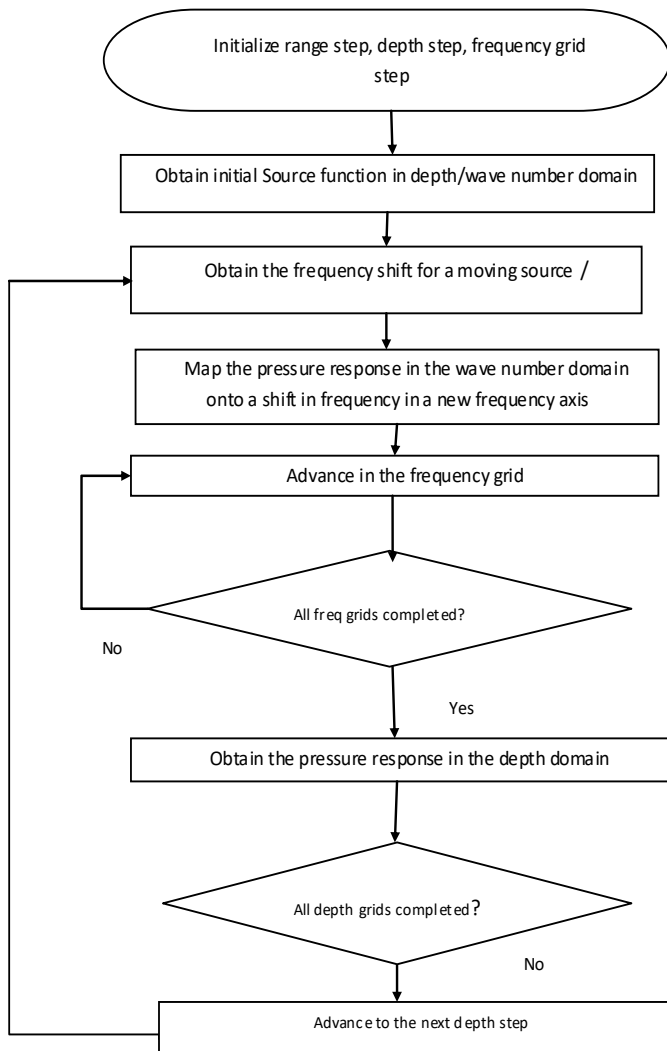


Fig. 1. Parabolic Expansion Method.

Consider the receiver is placed at the same depth and the source is moving along the horizontal axis. The spread in frequency by source motion is incorporated to the output field by distributing the source function into discrete frequency grids defined by (15) and applying smoothing between frequency cells through interpolation.

$$f_i = f_T - \frac{N_f}{2} \Delta f + (i-1) \Delta f; f_i = 1, 2, \dots, N_f, \quad (16)$$

Where N_f is the number of frequency grids and

$$\Delta f = \frac{f_{\max} - f_{\min}}{N_f}; \quad (17)$$

$$f_{\max} = \max(f_n); f_{\min} = \min(f_n);$$

The effect of receiver movement is incorporated by a shift in frequency in a new frequency axis that accounts for both source and receiver motion. The Doppler shift for each wave number and their maxima and minima are defined as:

$$\Delta F_n = f_T \frac{|v_r|}{c_0} \cos(\theta_n - \phi_r) \quad (18)$$

$$\Delta F_{\max} = \max_n(\Delta F_n);$$

$$\Delta F_{\min} = \min_n(\Delta F_n); \forall n = 1, 2, \dots, N_z$$

where the receiver speed and direction of motion are represented by v_r, ϕ_r respectively.

These Doppler shifts modify the extremes of the frequency axis depending on the direction of receiver motion. Thus the new frequency axis is defined as:

$$f''_{\max} = \begin{cases} f_{\max} + \Delta F_{\min} & v_r < 0 \\ f_{\max} & \text{otherwise} \end{cases} \quad (19)$$

$$f''_{\min} = \begin{cases} f_{\min} + \Delta F_{\max} & v_r > 0 \\ f_{\min} & \text{otherwise} \end{cases}$$

The new PE field is generated by interpolation across frequency grid. This is the initial field and it is propagated through each range cell by transforming it to wave number domain and the field at the receiver is calculated using Split step Pade and Split step Fourier algorithm. The steps involved in Doppler modeling are depicted in Fig. 1.

IV. RESULTS

Nominal values of the density of sea water for different depth and salinity are tabulated in Table I [14] and are depicted in Fig. 2.

TABLE I. DENSITY VALUES OF SEAWATER

Temperature (°C)	Salinity				
	5	10	20	30	35
0	3.97	8.01	16.07	24.10	28.13
5	4.01	7.97	15.86	23.74	27.70
10	3.67	7.56	15.32	23.08	26.97
15	3.01	6.85	14.50	22.15	25.99
20	2.07	5.86	13.42	20.98	24.78
25	0.87	4.62	12.10	19.60	23.36
30	0.57	3.15	10.57	18.01	21.75

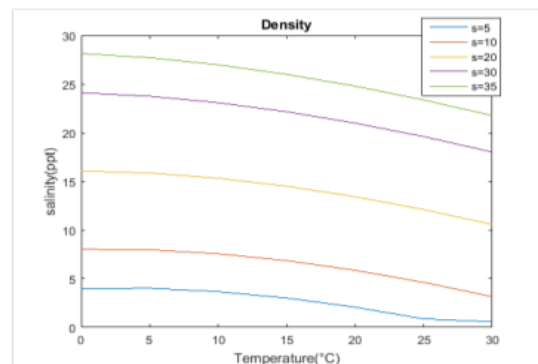


Fig. 2. Density Vs Temperature and Salinity.

ETOPO5 is the bathymetry derived for the Indian Ocean region (20°E to 112° E and 38°S to 32°N). The datasets are provided in ASCII, NETCDF and BINARY formats. [15].The data set is plotted in Fig.3 and the plot infers that the bathymetry is uniform.

Under INDMOD project, the ship ORV Sagar Kanya was deployed at (43° E) for the measurements of depth, Temperature, salinity, speed profile[16]. The observed datasets for duration of one hour is considered and the results are plotted in Fig. 4.

The sound speed profile obtained from the Sagar Kanya experiment data is used as a reference to define the environment profile for both the algorithms.

The input parameters considered is shown in Table II. The pulse shown in Fig. 5 is transmitted. Amplitude of the pulse is inversely proportional to the bandwidth considered.

The split step Fourier algorithm has an explicit wave number operator; the transmission loss across frequency component is shown in Fig. 6.

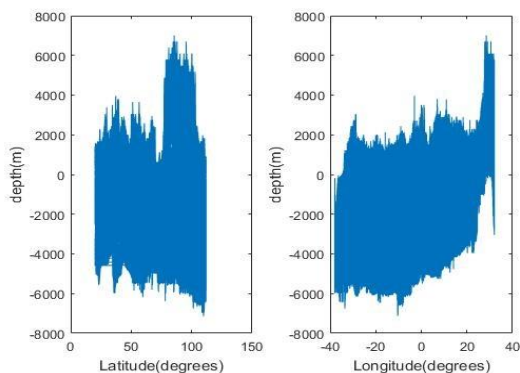


Fig. 3. (a) Latitude Vs Depth (b)Longitude Vs Depth Obtained from ETOPO5 Data.

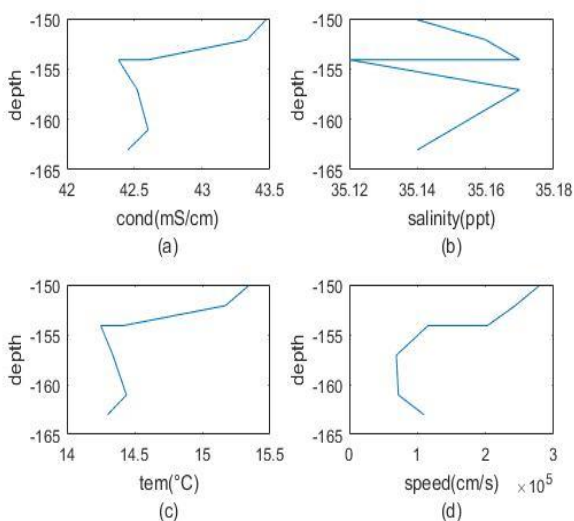


Fig. 4. Variation of (a) Temperature (b) Salinity (c) Conductivity (d) Speed with Respect to Depth Obtained from Sagar Kanya Experiment Data.

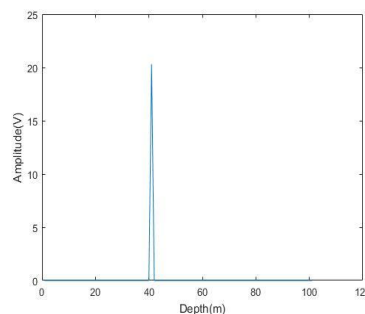


Fig. 5. Transmitted Pulse in Depth domain

The receiver is placed at different depths as shown in Fig. 7 to study the frequency range received by the receiver.

TABLE II. PARAMETERS OF SPLIT STEP FOURIER ALGORITHM

Parameters	Values
Range (r)	5Km
Max Depth (Zmax)	100m
Source Frequency (f_T)	3800Hz
Sound Speed C(Z)	1460-1540m/s
Source Depth (Zsrc)	40 m
Source Angle (Φ_s)	$\pi/4$
Source Velocity (V_s)	20m/s
Receiver Angle(Φ_r)	$\pi/4$
Receiver Velocity (V_r)	5m/s

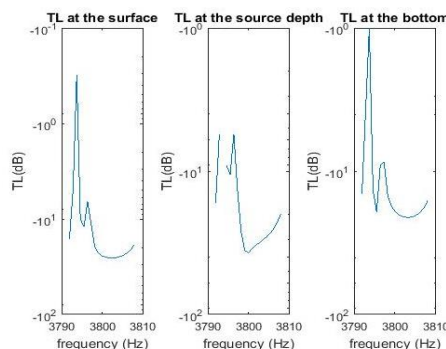


Fig. 6. Transmission Loss at 5Km with source frequency 3.8KHz; $v_r=5m/s$; $\phi_r=\pi/4$ rad

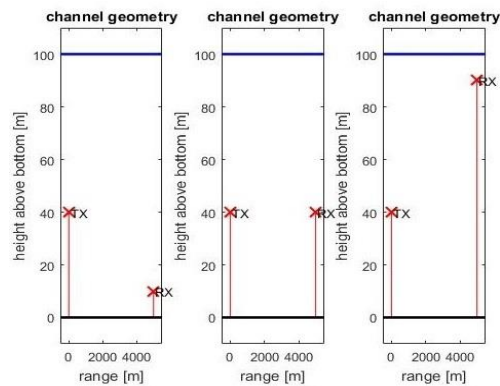


Fig. 7. Channel Geometry (a)Zg=10m; (b)Zg=40m; (c)Zg=90m;

Similar to the previous case, the pulse shown in Fig. 5 is transmitted from the source depth 40m. The input parameters considered are shown in Table III.

Fig. 8 shows the corresponding received pulse. Results show that when the receiver position (receiver depth) is near to the source depth, stronger signals are received.

Consider the source frequency in the lower, mid, high band say 5.3 Hz, 9.8 Hz, 14.2 Hz Fig. 9 depicts the attenuation in the amplitude of the received pulse as a function of depth.

Consider the receiver motion; Let the receiver be moving with the speed of 215 m/s, 2150 m/s 21500 m/s at an angle 45 degrees to the source. The corresponding Doppler shift from equation 11 is 1Hz, 10Hz, 100Hz, respectively. The frequency shift with respect to receiver motion is shown in Fig. 10.

TABLE III. PARAMETERS FOR SPLIT STEP PADE ALGORITHM

Parameters	Values
Range (r)	5Km
Max Depth (Zmax)	100m
Source Frequency (ft)	9.8Hz
Bandwidth	8.9Hz
Sound Speed C(Z)	1460-1540m/s
Coherence Bandwidth	0.01-0.89Hz

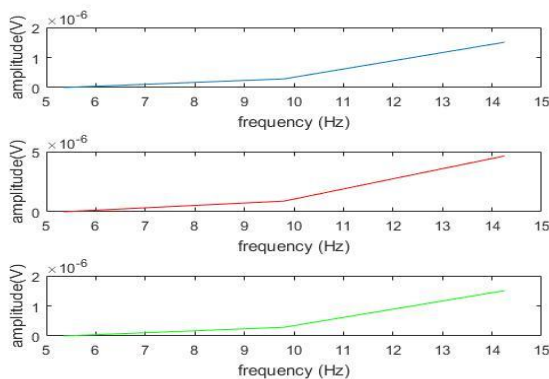


Fig. 8. Received Pulse at Depths $Z_g=10\text{m}$ (top); $Z_g=40\text{m}$ (mid); $Z_g=90\text{m}$ (bottom).

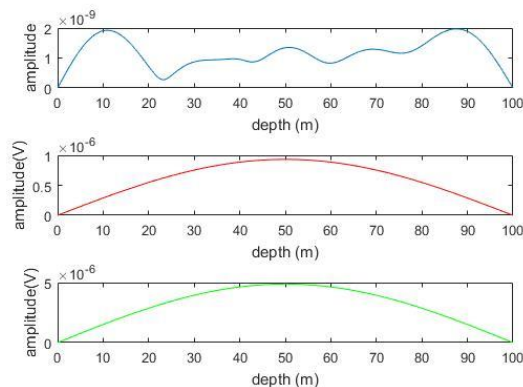


Fig. 9. Attenuation vs Depth Curve for the Source Frequencies 5.3Hz(Top), 9.8Hz(Mid), 14.2Hz(Bottom).

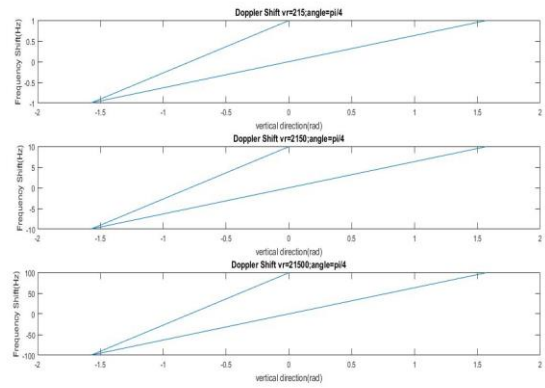


Fig. 10. Doppler Shift with Receiver Height =40m; Range=5Km (Top) vr=215 m/s;(Mid) vr=2150 m/s;(Bottom) vr=21500 m/s.

Fig. 11 depicts the fast fading scenario. The output power for various Doppler shifts is plotted against delay.

As the Doppler shift increases, coherence time decreases and hence more and more delayed components (resolvable multipath components) are received over the same symbol period.

Fig. 12 depicts the frequency selective fading scenario where different frequency components undergo different transmission loss. The transmission loss of frequency samples is plotted for various coherence bandwidths. It is observed that more samples undergo a flat fading when the coherence bandwidth is more as in Fig. 12 (bottom).

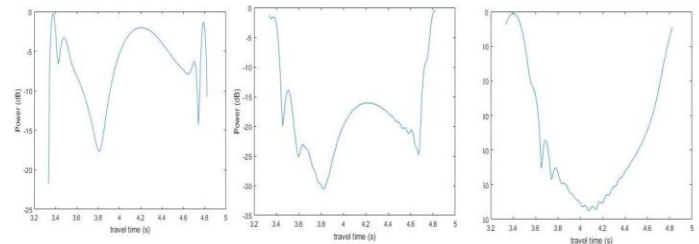


Fig. 11. Received Pulse with Receiver Height =40m; Range=5Km with Doppler Shift =100Hz; (Top); Doppler Shift =10Hz;(Middle); Doppler Shift =1Hz(Bottom).

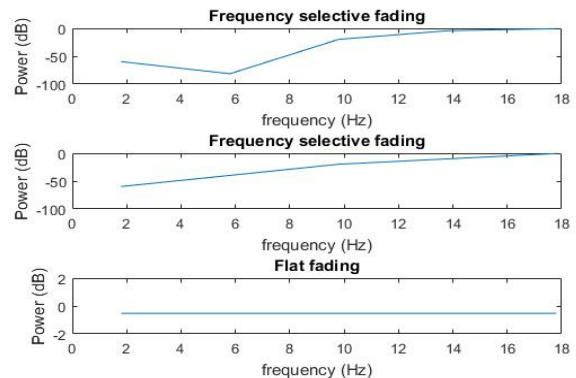


Fig. 12. Received Pulse with Receiver Height =40m; Range=5Km with Coherence Bandwidth =4.45 Hz; (top); Coherence Bandwidth =8.9 Hz (Middle); Coherence Bandwidth =20 Hz (Bottom).

V. CONCLUSIONS

This Paper analyses the parabolic expansion based modeling approach to model the Doppler Effect under the environment parameters that depicts the ocean scenario in India. The present data set depicts a flat environment as only a portion of the data set is considered. The future study is directed towards the analysis for environment data observed for a longer duration. The receiver picks up stronger signals when they are around the source depth. Split step Pade method characterize the platform motion through wave number variation at each depth grid. Unlike the previous work in [13], the present work considers a wider bandwidth. At increased frequency of operation, the inversion of tridiagonal matrix results in nearly singular values reducing the accuracy. The accuracy of the results can be enhanced by considering Split step Fourier coefficients as they have an explicit wave number domain operator. Future work is directed towards developing a beam forming algorithm for Doppler compensation.

REFERENCES

- [1] Etter(2003), "Underwater Acoustic Modeling and Simulation", 3rd ed., Spon Press.
- [2] F.B. Jensen, W.A. Kuperman, M.B. Porter, and H. Schmidt(2011), "Computational Ocean Acoustics", 2nd Ed., Springer,
- [3] Hanjiang, Luo et.al , "Simulation and Experimentation Platforms for Underwater Acoustic Sensor Networks: Advancements and Challenges", ACM Computing Surveys (CSUR), Vol 50 Issue 2, Article No. 28 ,2017
- [4] Aijun Song and Mohsen Badiey, "Channel Simulation for Underwater Acoustic Communication Network", WUWNet'12,2012
- [5] Xiaowei Guan, Lixin Guo, Qingliang Li , "A 3D parabolic equation method for knife-edge diffraction modeling", Applied Computational Electromagnetics Society Symposium (ACES) ,2017
- [6] Qarabaqi.P.,Stojanovic.M., "Statistical Characterization and Computationally Efficient Modeling of a Class of Underwater Acoustic Communication Channels," IEEE Journal of Oceanic Engineering, vol.38, no.4, pp.701-717, Oct. 2013
- [7] Wei Gu,1 Yanli Zhou,2 and Xiangyu Ge1,"A Compact Difference Scheme for Solving Fractional Neutral Parabolic Differential Equation with Proportional Delay", Hindawi Journal of Function Spaces ,Volume 2017, Article No. 8.,2017
- [8] Q. Zhang, M. Ran, and D. Xu, "Analysis of the compact difference scheme for the semi linear fractional partial differential equation with time delay," *Applicable Analysis: An International Journal*, vol. 96, no. 11, pp. 1867–1884,2017
- [9] Ruobing Jiang , Yanmin Zhu , Tong Liu , Qiuxia Chen, "Compressive detection and localization of multiple heterogeneous events in sensor networks," *Ad Hoc Networks*, v.65, p.65-77 , 2017
- [10] Akram Ahmed, Mohamed Younis, "Accurate Shallow and Deep Water Range Estimation for Underwater Networks", IEEE Global Communications Conference (GLOBECOM), 2015
- [11] Michael Zuba, Aijun Song,J.-H, " Exploring parabolic equation models for improving over underwater network simulations", UComms-2014
- [12] Smith, K.B", "Convergence, stability, and variability of shallow water acoustic predictions using a split-step Fourier parabolic equation model, *Journal of Computational Acoustics*, vol 9, 243–285, 2001
- [13] David J. Pistacchio,"Source/receiver motion-induced Doppler influence on the bandwidth of sinusoidal signals", Master's Thesis, Naval Postgraduate School Monterey, California,2003)
- [14] Ranjani.G, Dr. Sadashivappa.G "Acoustic Channel and Doppler Effect Modeling-A case study", Proceedings of the 7th IETE ICon RFW-2014, May 2014,
- [15] www.nio.org/index.php?option=com_projdisp &task=show&tid=2&sid
- [16] G. S. Bhat et al , "BOBMEX: The Bay of Bengal Monsoon Experiment", *Bulletin of the American Meteorological Society*, Vol. 82, No. 10, October 2001.

Automated Grading Systems for Programming Assignments: A Literature Review

Hussam Aldriye¹, Asma Alkhalaf², Muath Alkhalaf³

Computer Science at the Collage of Computer, King Saud University, Riyadh, Saudi Arabia^{1,3}
Computer Science at Alrass Collage of Science and Arts, Qassim University, Qassim, Saudi Arabia²

Abstract—Automated grading for programming assignments is becoming more and more important nowadays especially with the emergence of the Massive Open Online Courses. Many techniques and systems are being used nowadays for automated grading in educational institutions. This article provides a literature review of the many automated grading systems and techniques that are being used currently. It focuses on highlighting the differences between these systems and techniques and addressing issues, advantages and disadvantages. The review shows that these systems have limitations due to difficulty in usage by students as noticed by some course instructors. Some of these problems stem from UI/UX difficulties while other problems were due to beginner syntax errors and language barriers. Finally, it shows the need to fill the gap by building new systems that are friendlier towards beginner programmers, has better localization and easier user experience.

Keywords—Automated grading

I. INTRODUCTION

Innovation in education has come a long way in improving the speed and efficiency of grading. For example, the inventiveness behind the idea of the Scantron has significantly promoted the grading of tests for instructors and has consequently provided a better means for professors to check on students' knowledge of particular concepts. Homework and exams are the best way to determine student comprehension. However, grading programming assignments is time consuming and prone to errors especially with large number of students in the Massive Open Online Courses (MOOS) and complex programming assignments. This raises the need for a more consistent and efficient grading technique. This challenge has lead to the development of automated grading tools. This paper provides comparison and evaluation of different tools used for automated grading for programming assignments focusing on the effectiveness of these tools in learning process.

This article is organized as follows. Section 2 describes the software defects while Section 3 presents the literature review of the current automated grading techniques and the tools applying those techniques. Section 4 provides summary comparison of the reviewed tools. Finally, Section 5 concludes the article.

II. SOFTWARE DEFECTS

Before we review the literature on automated assignment grading techniques and systems, we would like to introduce the types of errors that are usually targeted by these techniques. In general, a software defect, failure or error is defined as producing wrong result or performing an action in an unintended way. However, Software defects can be classified as following syntax errors, logical errors, and runtime errors.

1) *Syntax error*: To This error is raised due to incorrect grammar/syntax in the programming language such as incorrect program structure, mistyped words (typos), missing semicolons. Moreover, this kind of errors can be detected by the programming language compiler while compiling the software code. This error is the easiest error to catch and fix since most of the compilers that used this day such as GCC or JRE provides a full description of the error (line number and message show what is missing).

2) *Logical errors*: In this error, the software compiles and runs fine, but the output of the software is wrong due to many reasons such as misunderstanding of the requirement or specification, logical-mathematical errors (divide by zero, adding when you should be subtracting) and opening and using data from the wrong source. These errors, unfortunately, cannot be detected by the compiler and this issue brings up a question, can we detect this kind of errors before launching the software? The short answer is yes, by using testing methods and other techniques, this will be described in detail in Section 2.2.

3) *Runtime errors*: This is an advanced error, and it is rare to introductory course students to fall in. Runtime error will only happen when the software is running. In fact, this is one of the most complicated issues to track down and lead to software crashes. There are several tools to track this kind of error such as NASA Java Pathfinder (JPF) to detect Deadlock, race problem, heap bounds checks, Null Pointer Exceptions and much more advance problem thus finding these problems may take hours, days or months it depends on the size and the complexity of the software.

III. EXISTING TECHNIQUES FOR AUTOMATED GRADING

A. Unit Testing

The main goal of any software testing approach is to check if the software contains errors, produces the right outputs, and follows the specification conducted by the Software tester or the QA team. However, unit testing has reached distinguished prominence in the area of computer science curriculum over the past years [1] and it is one of the most common approaches used nowadays to exam software units or features.

In this test, the targeted software should be clean of any syntax errors, by passing the targeted software to the compiler then apply the test. The output of this test provides the correct or wrong answer based on predetermined inputs derived from the specification document or assignment requirement. Moreover, unit testing is consisting of *test case* and *test methods*; each test case is consisting of one or more test methods that tests a unit or a part of the software code.

In an automated grading system, the instructor responsible for preparing the 'test case' or multiple test cases as a 'test suit'

(Student Assignment File)

```
import java.util.Scanner;
public class Numbers {

    public static void main(String[] args) {
        Scanner s = new Scanner(System.in);
        int x, y, z;
        System.out.print("Enter three numbers: ");
        x = s.nextInt();
        y = s.nextInt();
        z = s.nextInt();
        System.out.println("Sum = " + (x + y + z));
    }
}
```

that covers all the aspects that students should include in their assignment. Fig. 1 shows on the right side the multiple JUnit test cases that test a simple Java assignment on the left side written by an introductory student in Rwaq MOOC, each test case assigned to a certain method and has a weight or score.

A comparison between five unit testing tools is represented in Table I.

B. Sketching Synthesis and Error Statistical Modeling (ESM)

In [2], the authors introduced a new tool based on sketching synthesis and ESM to provide an instant feedback for introductory programming assignments. The introduced tool was applied on "Introduction to Computer Science and Python Programming Language" that offered by MIT. The key idea behind this method is to provide the system with a reference implementation (best answer) for a simple computational problem such as 'compute derivatives'. Fig. 2 is an example of a reference that is used as the specification for student submissions.

(Test case written by the instructor)

```
@Test
public void testNums1() throws Exception
{
    // first check if the class was loaded. if not issue an
    error.
    if (!NumbersFound)
        throw new Exception("class Numbers was not found or
        misspelled.");
    try {
        // prepare for I/O redirection from input/output stream
        to our own
        final ByteArrayOutputStream outContent = new
        ByteArrayOutputStream();
        PrintStream oldStdOut = System.out;

        // CHANGE INPUT VALUE. if program needs two input
        value then
        // separate by space.
        // For example: 1 2 ==> will give the two input values
        1 and 2
        final ByteArrayInputStream in = new
        ByteArrayInputStream(
            "1 5 7".getBytes());

        InputStream oldStdIn = System.in;
        System.setOut(new PrintStream(outContent));
        System.setIn(in);

        // load main method
        Method m = getMethod("Numbers", "main",
        String[].class);
        String[] params = null;
        m.invoke(null, (Object) params);

        // check assignment output
        assertTrue("Program output is not correct or
        misspelled. Here is the output:\n" +
        outContent.toString(),
        outContent.toString().matches("(?s).*13.*"));
    }
}
```

Fig. 1. Example of JUnit Test Cases.

TABLE I. UNIT TESTING TOOLS

Testing Tools	License	Reporting	Configuration/Setup	Error detection		
				Runtime	Syntax	Logical
Junit4	Open source	Clear and easy to read and parse	Include .jar file in test directory	N	N	Y
Parasoft JTest	Enterprise	HTML reports And charts	GUI-based unit testing tool	Y	N	Y
TestNG	Open source	Not easy to parse and simplify for student	XML configurations	N	N	Y
Powermock	Open source	Need someone familiar with the tool to read errors	extends other mock libraries such as EasyMock	N	N	Y
JWalk	**free	Not easy to parse and simplify for student	GUI-based unit testing tool	N	N	Y

** Only for research or evaluation purposes

```
1 def computeDeriv_list_int(poly_list_int):  
2     result = []  
3     for i in range(len(poly_list_int)):  
4         result += [i * poly_list_int[i]]  
5     if len(poly_list_int) == 1:  
6         return result # return [0]  
7     else:  
8         return result[1:] # remove the leading 0
```

Fig. 2. The Reference Implementation for Compute Derivative [2].

Therefore, the tool now shall process and analyze the equivalence of the submitted answers with the reference answer. This approach is using constraint-based synthesis technology [2], [3] to efficiently search over a huge space of programs. Precisely, they use the SKETCH synthesizer that uses the SAT-based algorithm [4] to complete program sketches, so that the students meet the given specification. Moreover, Using SKETCH synthesis system allows writing programs while leaving fragments of it undefined as holes. The synthesizer fills up the contents of these holes such that the program conforms to a specification provided regarding a reference implementation. The synthesizer uses the CEGIS algorithm [5] to compute the values for generated holes and uses bounded symbolic verification techniques for producing equivalence check of student submitted implementation and the reference implementation. Finally, the synthesizer passes the solution to the tool feedback generator to parse the error if found, and translates the output to natural language that students can understand, see Fig. 3.

The generated feedback takes around 40 seconds for each submission and successfully provides feedback on over 64% of wrong answers. The limitations of this tool are as following:

- The tool does not check the structural requirements
- The tool does not accept large constant value.

The tool does not support OOP

C. Peer-To-Peer Feedback

In this approach, the instructor makes the students randomly grade each other's answers. This approach may help students to identify and get used to errors causes, but many problems encountered [6] in systems using this approach such as no instance feedback (students may wait for a long time to get a feedback) and wrong or incomplete feedback due to students limited knowledge especially, introductory students. Finally, students trust and respond to their instructor's comments rather than their peer feedback. In addition, many students find peer feedback hard and not easy to gauge.

D. Random Inputs Test Cases

This approach is proposed in [7], were instructor prepares a set of independent inputs that used to check if the student assignment output is false positive or false negative. However, using this approach to grade students' assignments is very limited and weak since it does not give any feedback that shows the students error; if exist. The objective of this test is to check if the students have determined the correct output or not, so in this case, students will have only two possible grades 0 or 10.

E. Pattern Matching

In pattern matching [6], the instructor provides a specification of the output that a correct assignment will be assumed to generate, and system requests the Unix Lex and Yacc [7] tools (Yet Another Compiler) to create a program that verifies that the output from the student submitted solution meets the provided specification. This technique has many disadvantages since it only accepts and gives a grade to perfect matching solutions. Instructors cannot break down the pattern to distribute the grades on methods.

F. Comparison

The following comparison in Table II shows why Unit testing better than the other techniques.

Three different student submissions for computeDeriv

```

1 def computeDeriv(poly):
2     deriv = []
3     zero = 0
4     if (len(poly) == 1):
5         return deriv
6     for e in range(0, len(poly)):
7         if (poly[e] == 0):
8             zero += 1
9         else:
10            deriv.append(poly[e]*e)
11    return deriv

```

(a)

```

1 def computeDeriv(poly):
2     idx = 1
3     deriv = list([])
4     plen = len(poly)
5     while idx <= plen:
6         coeff = poly.pop(1)
7         deriv += [coeff * idx]
8         idx = idx + 1
9         if len(poly) < 2:
10            return deriv

```

(b)

```

1 def computeDeriv(poly):
2     length = int(len(poly)-1)
3     i = length
4     deriv = range(1,length)
5     if len(poly) == 1:
6         deriv = [0]
7     else:
8         while i >= 0:
9             new = poly[i] * i
10            i -= 1
11            deriv[i] = new
12    return deriv

```

(c)

Feedback generated by our Tool

The program requires 3 changes:

- In the return statement **return deriv** in line 5, replace **deriv** by **[0]**.
- In the comparison expression **(poly[e] == 0)** in line 7, change **(poly[e] == 0)** to **False**.
- In the expression **range(0, len(poly))** in line 6, increment **0** by **1**.

(d)

The program requires 1 change:

- In the function **computeDeriv**, add the base case at the top to return **[0]** for **len(poly)=1**.

(e)

The program requires 2 changes:

- In the expression **range(1, length)** in line 4, increment **length** by **1**.
- In the comparison expression **(i >= 0)** in line 8, change operator **>=** to **!=**.

(f)

Fig. 3. The a,b,c Shows Different Student Submission for the Same Problem and the Feedback for Each Submission Generated by the Feedback Generator [2].

TABLE II. COMPARISON OF TOOLS AND TECHNIQUES USED TO GRADE STUDENTS' JAVA ASSIGNMENTS

Tools and techniques	Sketching synthesis and error statistical modeling	Peer-to-peer feedback	Random input test cases	Pattern Matching	Unit testing
Execution time	Fast (less than 10 sec in many cases)	40-60 sec in average	Slow, takes hours in many cases	Fast (less than 10 sec in many cases)	Average, it takes 30 sec
Reliability	Accurate (depends on the written test case)	Can detect 64% of students errors	Not reliable it depends on student knowledge	In some case, if all possible inputs are covered	In some case, if all possible outputs are covered
Dependency Test	Supported	Supported	Supported	Not Supported	Not Supported
Instant Feedback	Yes	Yes	NO	Yes	Yes
Support Oop	Yes	No	Yes	No	No

IV. EXISTING SYSTEMS FOR AUTOMATED GRADING

The automated grading system of student work has been reviewed for decades. For example, automatic grading of short quizzes involves three types of questions, short answer, multiple-choice and true or false. These questions have been a typical feature of most e-learning system such as Web-Work (an online student homework system for sciences and math courses), Web-CAT (Automatic Grading Student programming assignment), Web-based Grading, and Class-Marker (Online test maker). Grading systems have been interesting in large-scale educational institutions with a substantial number of students. These systems can be classified into three categories [8] (a) Automatic grading systems (the grading and the feedbacks generated by the system) (b) Semi-Automatic grading system (grades generated by the system and feedback produced by human) (c) Manual grading system (the grading and feedbacks produced by human).

A. Automated Grading Systems

In [9], Edwards and Pérez-Quiñones from Virginia Tech have introduced a Web-CAT an extensible and customizable open-source and online automated grading system for students Java and C++ programming assignment. Web-CAT is a state of the art in automated grading system, and many instructors around the world including King Saud University (KSU) have used it with the standard Java-TDD integrated plugin to grade an introductory programming course assignment. The Java-TDD is a combination of jar files that help Web-CAT to manage JUnit test libraries. Web-CAT provides many services to students and instructors, such as assignment submission, automated feedback based on predefined test cases, hints that help to fix errors in the code, and generate grades based on the test case report produced by JUnit-Reporter.

However, while using Web-CAT at Dickinson College, department of mathematics and computer science, [10] in introduction to programming course (COMP131), the instructors frequently observed undesirable difficulties from students' side. The students cannot understand the feedback messages generated by the system regarding their submitted assignments. Most of the errors were general and do not reflect the reason of the actual error. Moreover, the same problem was discovered in Introduction to Java programming language at King Saud University, were 50.6% of the enrolled students were unhappy using the system because the generated feedback report was unclear and does not explain the errors type and also how the system generates their scores. Fig. 4 shows an example of a Web-CAT generated report. The system UI is not usable and most of the submitted assignments fail. Students got zero mark due to having syntax errors such as missing semicolon or missing brackets (Web-CAT does not compile the submissions before running the test cases).

On the other hand, instructors noticed that the system configuration is complex and cannot be accessed remotely from outside the college building since it has been installed on a local server. The students must submit their assignments using the college labs or connect to the system through the local network.

The system proposed by H. Kitaya and U. Inoue is another good example of automated grading system [11]. They provide a java assessment tool that conducts a test by using a regular expression application programming interface (API) to compare the student's java assignments with a reference implementation written by the instructors. The system is a web-based application using many technologies that helps to generate testing frameworks such as Java Servlet and JSP on Apache tomcat, see Fig. 5. Writing a regular expression has major drawbacks in grading systems. It is very restricted to a certain format and output type, and it is not easy to construct an expression pattern. Finally, the system generates only a Japanese feedback messages; this is not applicable in any international course.

B. Semi-Automatic Grading Systems

ASys [12] is a notable recent semi-automatic Java grading system, which focuses on checking the student Java assignment source code by applying three mainly phases: Compilation, Analysis, and Testing respectively. The compilation phase is to check if the source code has any syntax errors, and the output of this phase will be reflected by the programming language compiler. Secondly, if the assignment file passes the first phase the system will enter a crucial phase that is the analysis process that uses a domain specific language (DSL). In this phase, the system authors build an assessment template that consists of two libraries, the Java meta-programming library and a DSL on top of the assessment template. The Java library is composed of 70 methods in an 'Inspectors' class that can be used to examine and handle the source code to check the code properties. Therefore, instructors can check the students Java assignments' programmatically by invoking the DSL that allows the system to load and examine the assignment Java file whether the student has implemented it in a correct way or not.

For example, DSL can detect errors in using inheritance, abstract classes and interface by examining a set of evaluation code. If the evaluation code fails, it returns ZERO and transforms to semi-automatically mode to prompt the instructors with a source code that raises the problem, this is illustrated in Fig. 6.

Assessment system (ASSYST) [13] is an example of a legacy grading system built in 1997 on Linux environment machine. ASSYST uses pattern matching technique and black box testing approach to check and conforms that a student solution meets the specification. Furthermore, the system is not promising since it has many problem reported by the students who have used the system to grade their assignments as it freezes if the system face unknown errors either in student code or in the system core. Years later, David W. Juedes from Ohio University designed a new web based grading system (WBG) [14] inspired by ASSYST. WBG is originally written in Perl and Java in 2005 and in 2010 the system was redesigned in TCL/TK [15] scripting language and it works only under Linux and Sun Solaris.

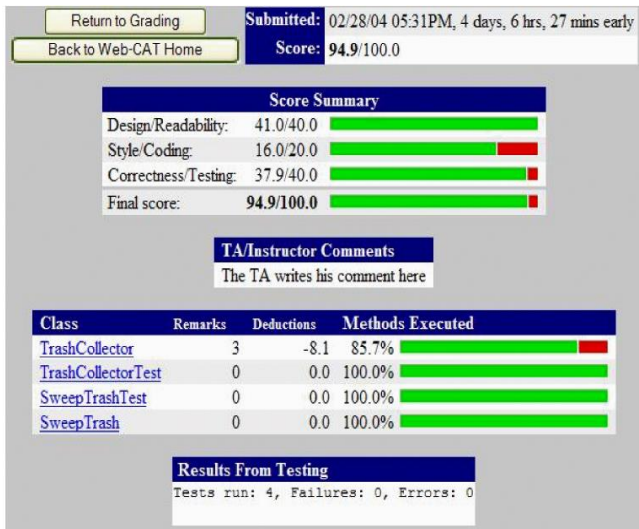


Fig. 4. Web-CAT Generated Report.

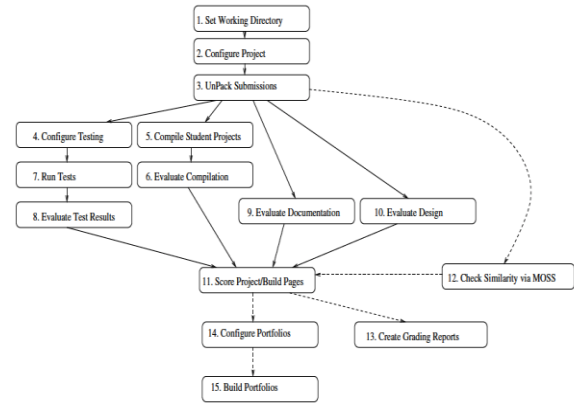


Fig. 7. WBG Overall Structure [14].

WBG uses Basic Comment File (BCMT) which provides the grading engine with a list of long and short predefined comments that used to report students through HTML web page of spelling mistakes, syntax errors (reported by the compiler) and output mismatching the random test values. Fig. 7 illustrates the structure of the WBG system.

While reviewing the system, we discovered many disadvantages such as manual project configuration as shown in Fig. 8. The system requires BCMT files for both, design and implementation, no section/course management, and no support for other Mac OS/Windows operating systems

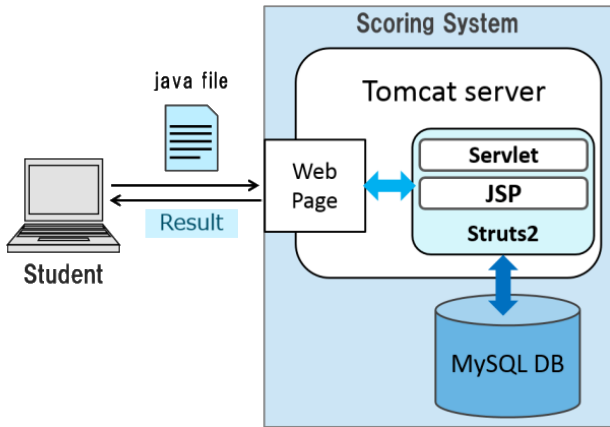


Fig. 5. [11] System Architecture.

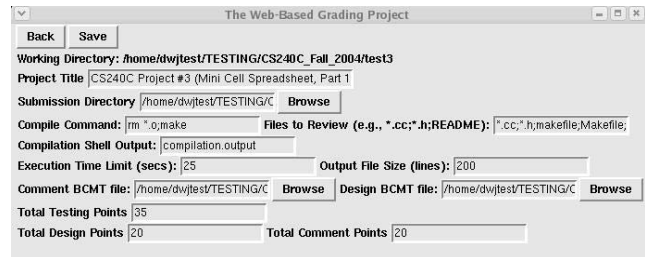


Fig. 8. Project Configuration.

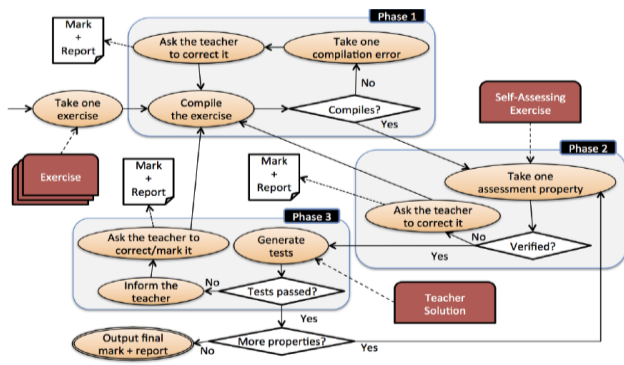


Fig. 6. Asys Data Flow Diagram [12].

The system provides multiple services in addition of grading students' assignments and projects. Services including (i) reporting students' performance and grading progress, (ii) "Measure Of Software Similarity" [16] tool developed by Alex Aiken at UC Berkeley to automatically detect all submitted assignments and projects for evidence of plagiarism.

C. Manual Grading Systems

A group of Professors, Teacher Assistants (TAs) and students from University of Toronto, Canada introduced a 'Markus' [17] web-based marking tool to simplify the assignments submission process. It replaces the usual submission approaches (sending emails or submit the assignments in CD/Memory stick, etc.). The main goal of the system is to provide instructors with a simple tool that helps them to give a clear and high- quality feedback to introductory students. The system depends on instructors provided comments or student peer reviews as students can review each other's assignments then instructors can use manual grade and correct the provided reviews/feedback. Markus allows instructors to create a kickoff code (reference implementation) for each assignment to help students solve a certain programming problem.

V. COMPARISON OF EXISTING GRADING SYSTEM

This section will present in Table III a comparison of all the existed grading systems that have been mentioned in this

article and showing the advantages and disadvantages of using these systems.

TABLE III. COMPARISON OF THE EXISTED GRADING SYSTEMS

	Web-CAT [7]	WebJavaScroing [8]	Markus [16]	ASys [11]	ASSYST [13]	WBGP [14]
Automated Testing? Automated=1, Semi=0.5, Manuel=0	Automated test suit	Automated, output matching	Manuel, peer review	Automated test cases	Automated test data (Black box testing)	Automated test and pattern matching
Automated Grading? Automated=1, Semi=0.5, Manuel=0	Grades assigned by the system	Grades assigned by the system	Grades assigned by Instructor or TA	Grades assigned by Instructor	Manuel grading by Instructor	Grades assigned by the system
System Usability and Interface USABLE=1, NOT USABLE=0	Not Usable, hard to configure tests and upload assignments	Not usable, no English interface	Usable, Web-based GUI, easy to upload, login, signup	Usable, GUI application, no registration	Not usable, Command base system	Not usable, bad interface design
Sections/Course Support Support=1, Not Supported=0	Supported	Not supported	Supported	Not supported	Not supported	Not supported
Easy to understand system feedbacks EASY=1, MEDIUM=0.5, HARD=0	Medium, as reflected by many students in KSU survey and [8][10]	Hard for non-Japanese actor	Easy, since all approved feedback are generated by Instructors and TA	Easy, feedback generated by Instructor	Hard, feedback generated by the system compiler.	Easy, pre-defined feedbacks by BCMT
Provide hints to correct errors PROVIDE = 1, IN SOME CASE=0.5, NOT PROVIDE=0	Not provided	provided	Provide in some cases (depend on the instructor or TA)	Provide in some cases (depend on the instructor)	Not provided	Provide hints
Main Advantages Over The Other Systems	Integrated with Eclipse and NetBeans IDE	Support multi-submissions	Support group assignments, sections and grade progress chart	precompiled assignments, automatically inform the instructor incase when tests fail.	Measures the code-efficiency by calculating execution time	Plagiarism check
Automated Testing? AUTOMATED=1, SEMI=0.5, MANUEL=0	Automated test suit	Automated, output matching	Manuel, peer review	Automated test cases	Automated test data (Black box testing)	Automated test and pattern matching
Automated Grading? AUTOMATED=1, SEMI=0.5, MANUEL=0	Grades assigned by the system	Grades assigned by the system	Grades assigned by Instructor or TA	Grades assigned by Instructor	Manuel grading by Instructor	Grades assigned by the system
System Usability and Interface USABLE=1, NOT USABLE=0	Not Usable, hard to configure tests and upload assignments	Not usable, no English interface	Usable, Web-based GUI, easy to upload, login, signup	Usable, GUI application, no registration	Not usable, Command base system	Not usable, bad interface design

VI. CONCLUSION

In this article, we have reviewed many automated grading systems and techniques. A particular attention was paid to the problem of how feedback is generated, to what limit the process is automated, and how much instructor interference needed. Some of the systems were semi-automated, supporting only automated grading or testing. Others are limited to a specific operating system or not appropriate for international courses where there is no proper localization. These limitations are showing a strong need for developing a new technique that fills the gap. As future work, we intend to build a system that provides a fully automated process with the ability to provide consistent grading, precise feedback, and better localization while reducing the time needed by instructor to configure the system.

REFERENCES

- [1] M. Wick, D. Stevenson, and P. Wagner, "Using Testing and JUnit Across the Curriculum," SIGCSE Bull, vol. 37, no. 1, pp. 236–240, Feb. 2005.
- [2] R. Singh, S. Gulwani, and A. Solar-Lezama, "Automated Feedback Generation for Introductory Programming Assignments," SIGPLAN Not, vol. 48, no. 6, pp. 15–26, Jun. 2013.
- [3] M. Ricken and R. Cartwright, "ConcJUnit: Unit Testing for Concurrent Programs," in Proceedings of the 7th International Conference on Principles and Practice of Programming in Java, New York, NY, USA, 2009, pp. 129–132.
- [4] A. Solar-Lezama, G. Arnold, L. Tancau, R. Bodik, V. Saraswat, and S. Seshia, "Sketching stencils," 2007, p. 167.
- [5] A. Solar-Lezama, R. Rabbah, R. Bodik, and K. Ebcioğlu, "Programming by sketching for bit-streaming programs," ACM SIGPLAN Not., vol. 40, no. 6, p. 281, Jun. 2005.
- [6] C. Kulkarni, "Learning design wisdom by augmenting physical studio critique with online self-assessment," Stanford University HCI Group.
- [7] D. Juedes, "WBG (Web-based Grading Project)," School of EECS, Ohio.
- [8] A. Pears, S. Seidman, C. Eney, P. Kinnunen, and L. Malmi, "Constructing a core literature for computing education research," ACM SIGCSE Bull., vol. 37, no. 4, p. 152, Dec. 2005.
- [9] S. H. Edwards and M. A. Perez-Quinones, "Web-CAT: Automatically Grading Programming Assignments," SIGCSE Bull, vol. 40, no. 3, pp. 328–328, Jun. 2008.
- [10] G. Braught and J. Midkiff, "Tool Design and Student Testing Behavior in an Introductory Java Course," in Proceedings of the 47th ACM Technical Symposium on Computing Science Education, New York, NY, USA, 2016, pp. 449–454.
- [11] Y. Akahane, H. Kitaya, and U. Inoue, "Design and Evaluation of Automated Scoring: Java Programming Assignments," Int. J. Softw. Innov., vol. 3, no. 4, pp. 18–32, Oct. 2015.
- [12] D. Insa and J. Silva, "Semi-Automatic Assessment of Unrestrained Java Code: A Library, a DSL, and a Workbench to Assess Exams and Exercises," 2015, pp. 39–44.
- [13] D. Jackson and M. Usher, "Grading student programs using ASSYST," ACM SIGCSE Bull., vol. 29, no. 1, pp. 335–339, Mar. 1997.
- [14] D. W. Juedes, "Web-based grading: Further experiences and student attitudes," in FRONTIERS IN EDUCATION CONFERENCE, 2005, vol. 35, p. F4E.
- [15] B. B. Welch, Practical programming in Tcl & Tk, 3rd ed. Upper Saddle River, NJ: Prentice Hall, 2000.
- [16] K. W. Bowyer and L. O. Hall, "Experience using 'MOSS' to detect cheating on programming assignments," 1999, vol. 3, p. 13B3/18-13B3/22.
- [17] MarkUs: Online marking. University of Toronto, Canada, 2009.

Supply Chain Modeling and Simulation using SIMAN ARENA[®] a Case Study

Azougagh Yassine¹, Benhida Khalid², Elfezazi Said³

Laboratoire Process, Signaux, Systèmes Industriels et Informatique (LAPSSII)
Ecole Supérieure de Technologie de Safi, Cadi Ayyad University, Marrakech, Morocco

Abstract—The control of supply chains passes often by identification of various constraints and optimization of the different links and parameters associated to the functioning of the supply chain. To attain these goals, it is vital to get the best knowing and understanding of the supply chain diversity and complexity also to anticipate its behavior, which requires, a pertinent modeling that will offer the necessary information to evaluate the supply chain performance. The present paper focuses on modeling and simulation of a case study of a supply chain using SIMAN ARENA[®] Rockwell software, mainly transport and different operations in this chain. The purpose is creating the simulation models and how to use in a case study to diagnose and master the operation and functioning of this supply chain. The objective is creating simulation models to determine the performance of the supply chain by calculating the transportation time in each travel, number of travels, number of transported fertilizers and sulfur wagons and unloaded acid talks and finally the waiting times in train station, in order to optimize this performance indicators.

Keywords—Supply Chain; transport; simulation; modelling

I. INTRODUCTION

Today in an uncertain economic context, the evaluation and analysis of models or experiments results allows firms in a supply chain context to measure and evaluate the performance of their supply chains and to predict their behavior and reactions to the fluctuations of their environment in terms of innovation, concurrence and competition. To evaluate this performance, it is important to use modeling and simulation techniques, which are powerful tools that have proven their ability to analyze complex systems specifically, supply chain. The performance evaluation is hard work, and the recourse of models reflecting the reality of systems and then simulating their behaviors, provides answers to conduct this work in Supply Chain. However, there is some related research of modeling using simulation especially in discrete event systems modeling and analyzing [1-5]. To the best of our knowledge, there is a deficiency of research works interesting in the modelling of supply chains, especially for a reel study case.

With regard to complete the existing works, this paper focuses to propose a conceptual approach which models the processes of a reel supply chain and developing simulation models using the simulator ARENA[®] [6,7]. Specifically, the logistics flows modelling in a supply chain of a real firm in the phosphate field. This study is realized by the development of models from a case study to show their interest in the analysis of logistics systems performance.

The present manuscript is organized as follows. The next section presents a basic terminology necessary to conduct this work. Third section exposes a review of different supply chains modelling approaches in the scientific literature. Fourth section shows a review of simulation approaches and tools. The Fifth section describes the conducted supply chain case study and, the adopted simulation models followed with Conclusion in Section Six.

II. BASIC TERMINOLOGY

In order to better understand and realize the context of this work and to provide the groundwork for the subsequent study, key terms are defined.

A. Logistic

Logistics is the management of the different flows (physical, information and financial) of an organization in order to prepare resources that correspond to well-defined needs [8,9]. Therefore, it is the set of operations that provide the right product, at the right time, in the right place and with the right cost.

B. Supply Chain

The supply chain is an evolution of the logistics concepts. It integrates management on upstream and downstream of the company (e.g. suppliers, manufacturers, distributors, third-party logistics providers, and retailers) to cover all the physical, information and financial flows [10, 11]. The supply chain is defined as the sequence of steps (see Fig. 1) in the production and distribution of a product from suppliers of suppliers of the producer to the customers of its customers.

The supply chain can be defined as a set of links or interdependent enterprises coordinating themselves in the execution of the supply, production and distribution activities [12] to ensure the products or services circulation from the conception to the end of life.

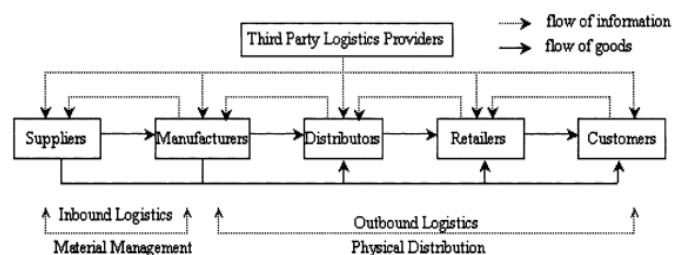


Fig. 1. The Supply Chain Structure.

III. REVIEW OF SUPPLY CHAINS MODELLING APPROACHES

In view of a wide choice of the supply chain notion, there are several taxonomies of modelling approaches used to describe and analyze the supply chains. Diverse researches in the literature interest to this kind of works [11, 13-22]. The principal classification of these modelling approaches is presented in the studies of Labarthe [18, 19] which classify these models in three main approaches as follows (see Fig. 2): the analytical approaches, the simulation approaches and the organizational approaches.

The study conducted in this paper presents a development of a simulation models for representing the comportment and dynamic of a reel supply chain. These models belong to the simulation approaches.

The simulation approaches [18, 19] represent supply chains using a set of methods, techniques, and mechanisms to present, to reproduce and to simulate, the behavior of a real system. Almost of supply chains simulation works is based on discrete event models.

The literature on modelling of many types of systems by simulations models is particularly wide. Several works and studies discuss this kind of problems on supply chains modelling and simulation. A few review researches are presented below:

- Chafik Razouk [1] proposes a new handling operation's design and simulation of empty containers using ARENA®.
- Bensmaine et al. [23] proposed a case study of supply chain simulation using ARENA®.
- Dhanan Sarwo Utomo [24] proposes a fuzzy chance-constrained programming model to include uncertainty in the biogas supply chain design problem.
- T.M. Pinho [25] proposes an approach and application to organize diverse planning levels and event-based models to control the forest-based supply chain using SimPy simulation tool.
- Malin Song [26] proposes a study to simulate a land green supply chain based on system dynamics and policy optimization.
- Sameh M Saad [27] proposes a framework integrated mathematical and simulation modelling techniques for planning and optimising petroleum supply chain.
- Fu [28], Boesel [29] and Abo Hamad [30] propose a framework using simulation and optimization in order to evaluate and ameliorate the supply chains performance.

The conducted review shows that supply chain modelling is of very interest to the researcher community. As a consequence, modeling, a case study of a reel supply chain using ARENA® simulation models are little used.

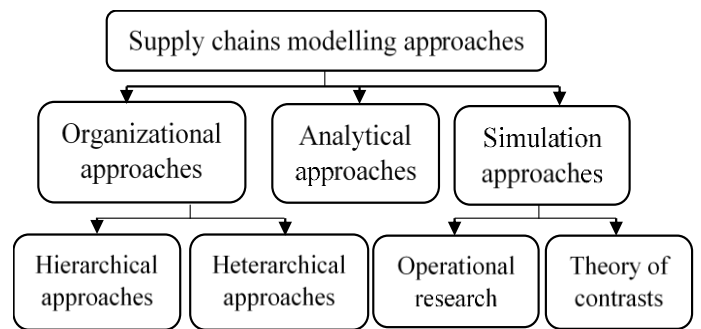


Fig. 2. Supply Chains Modelling Approaches.

IV. SIMULATION APPROACHES

A. Simulation Methodology

Simulation is a process with three mains iterative and interrelated components (see Fig. 3):

- System identifying: In this first step, the system is defined and the necessary data, of the system to simulate, are collected.
- Model design: It is about proposing the tools and structure of models using in the system to simulate.
- Model execution: In this step, the evolution of the conceived model is identified.
- Execution Analysis: Tests are done, on the model data, using specific analyzes. The most basic analysis would simply be to look at the data and derive conclusions from it.

B. Supply Chains Simulation Tools

Define the literature on supply chains modelling is mostly extensive, there are several tools and methods to approach simulation [31, 32] according to the case study, using:

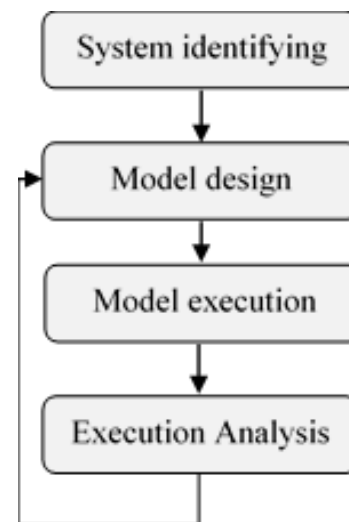


Fig. 3. Simulation Methodology.

- Specialized software: ARENA[®], SIMIO[®], WINISK[®], EXTENDSIM[®], Witness[®].
- Simulation languages: SIMULA, SIMAN, GPSS, QNAP2.
- Libraries for simulation: JAVASIM, C++ SIM
- General programming languages: C, JAVA, DELPHI

In this study, a specialized software is chosen, which offers the possibility to describe the models graphically, as a result avoid writing thousands of lines of programming code. For this purpose, the choice of simulation tool, depends on its characteristics beside the other simulation tools, discussed in the study of Dias et al. [33] and Yuri et al. [34], especially in the work of Tewoldeberhan [35] whose reports a benchmark survey of simulation tools by evaluating, a package of discrete-event simulation software, according to the following criteria: vendors, model development, input modes, testing and efficiency, execution, animation, output, user, experimental design and coupling simulation-optimization, as presented in Table 2.

According to Table 2, which presents the results of the benchmark study according to the selection criteria, it appears that ARENA[®] Rockwell Software [7] is the most powerful tool in this study, which justifies its use in many simulation studies. For these reasons, ARENA[®] is the tools to model and simulate the case study.

ARENA[®] is a simulation software based on the SIMAN language originating from two words "SIMulation and ANalysis". This language provides the ability to graphically describe the model using a scheme, which allows avoiding writing programming thousands of lines of code.

V. SUPPLY CHAIN CASE STUDY

A. Phosphate Case Study Description

The system studied in this paper is a phosphate supply chain constitute on multi-sites of production and a logistic

platform at seaport. The distance between those entities is 13 km. The following Fig. 4 presents the configuration of the studied supply chain.

The production sites transform the raw materials in goods (Phosphate and Sulfur to phosphoric acid and fertilizers) which are transported to and from the logistic platform, which are designed for exporting goods and importing raw materials [36, 37].

The products transportation is done normally by trains 24/24 hours. Exactly by 3 reams towed by 2 locomotives, the first one to transport fertilizers ream, the second ream is mixed to transport Sulfur and phosphoric acid. Table 1 summarizes the equipment available for transportation.

This supply chain is known for its logistical limitations due to many constraints. The main constraint is the distance between production sites and logistic platform, and existence of a single rail for transportation. The aims of this study of modeling is to control and diagnose the supply chain performance of the case study, by relying on the product transport process, which represents a bottleneck and restricts the supply chain ability to provide the necessary products in the various entities of this chain quantities.

B. Simulation Models

Using ARENA[®] SIMAN Rockwell software, the global simulation model of the phosphate supply chain (see Fig. 5) is constructed by connecting the appropriate blocks of the simulation tool, which shows the physical flows on this supply chain. In order to organize models, a various sub-model is used that constitute every part of the studied supply chain, and to avoid cluttering the models with links between the sub-models and the different blocks, a 'route' and 'station' blocks is used.

The initialization sub-model presented in Fig. 6 groups all modules responsible to generate the several entities in this supply chain exactly reams, locomotives, wagons, tankers and products that are presented in Table 1.

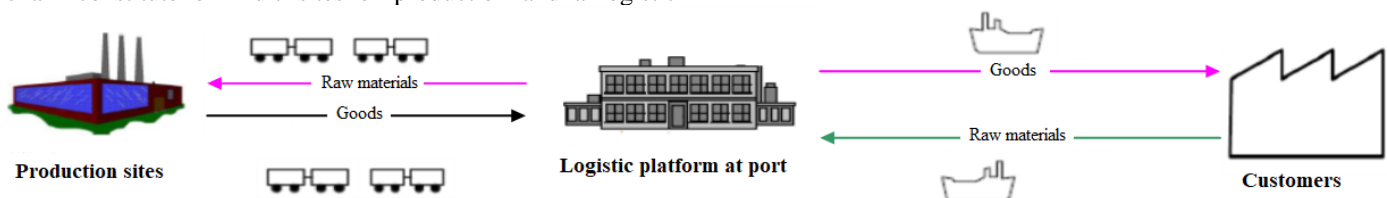


Fig. 4. The Supply Chain Studied.

TABLE I. TRANSPORTATION EQUIPMENTS

For the products	Available wagons	Divided reams	Transportation locomotives	Handling locomotives
Phosphoric acid	19	3	1	1 in production sites.
Sulfur	12	3		
Fertilizers	24	2,5	1	

TABLE II. RESULTS OF BENCHMARK STUDY OF SIMULATION TOOLS

Criteria	Weights	ANYLOGIC	ARENA	AUTOMOD	ENTREPRISE DYNAMICS	EXTEND	FLEXISIM	PROMODEL	QUEST	SIMUL8	WITNESSES
Vendors	5,70	1,10	3,10	2,51	2,00	2,68	2,01	2,01	3,01	2,23	3,01
Development of models & data inputs	9,40	2,99	2,61	2,29	2,60	2,70	2,69	2,01	3,01	2,50	2,49
Coupling simulation and optimization	8,00	2,50	2,50	2,70	2,60	2,50	2,50	2,70	2,50	2,50	2,50
Simulation execution	7,70	2,01	2,01	2,10	2,34	2,20	1,99	2,01	2,49	1,95	2,01
Animations	6,20	2,49	2,66	2,90	2,32	1,32	2,99	1,67	3,01	1,01	3,01
Testing and efficiency	7,50	1,90	2,39	2,60	2,40	2,29	1,49	2,01	2,49	1,8	2,01
Data Outputs (results)	6,70	2,59	2,32	1,90	1,66	2,23	2,69	2,01	2,01	2,69	2,01
Experimental design	5,80	2,01	2,99	2,10	2,01	2,11	2,03	3,01	2,01	2,01	2,01
Users experience	5,70	1,10	2,01	2,01	1,61	2,49	1,49	1,94	1,01	2,99	2,45
Points total		134,82	156,44	147,45	139,00	144,33	140,07	134,84	152,84	137,71	148,86
Benchmark rank		10	1	4	7	5	6	9	2	8	3

In order to minimize the influence of the initial conditions of the final results after simulation, that will affect the supply chain performance evaluation, all reams are assumed loaded and distributed in the entire supply chain, and both locomotives are in circulation.

Starting from the train station, the fertilizer ream goes to the production sites and the mixed ream to the port.

The fertilizer loading sub-model in production sites (see Fig. 7), is used to place empty wagons (Using the block 'dropoff') transported from the port to be loaded in factory station, also to tow the loaded wagons (Using the block 'pickup') to the port. In loading process, the wagons are placed 12 by 12 (Using the block 'decide') to be loaded one by one under two filling hoppers. Then, the full ream is placed to be connected to the locomotive (Using the block 'Hold') to route it to the port.

The fertilizer unloading sub-model in port (see Fig. 8), is used to place (Using the block 'Dropoff') the ream, divided on twelve wagons (Using the block decide), in the two unloading naves, and to connect (Using the block 'pickup') the empty

waiting ream (Using the block 'hold') to the locomotive in order to route it to the production sites.

The acid unloading and sulfur loading sub-model in port (see Fig. 9) regroups the following processes: the drop of the mixed ream (Using the block 'Dropoff') from the locomotive and separating it (Using the block 'decide') to two small reams acid and sulfur then the acid ream is directed to the unloading area (Using the block 'delay') and the sulfur ream to the loading area. At end, the locomotive tows both the full sulfur ream and the empty acid ream (Using the block 'pickup') which are waiting (Using the block 'hold') to be directed to the production site.

The acid loading and sulfur unloading sub-model in port (see Fig. 10) regroups the blocks responsible for sulfur unloading starting by introducing the full ream in the unloading area, and ends with the towing of the empty ream to form the mixed train. The process of acid loading is carried out according to two modes (Using the block 'decide') according to the quality to be loaded and the appropriate method (normal or special quality).

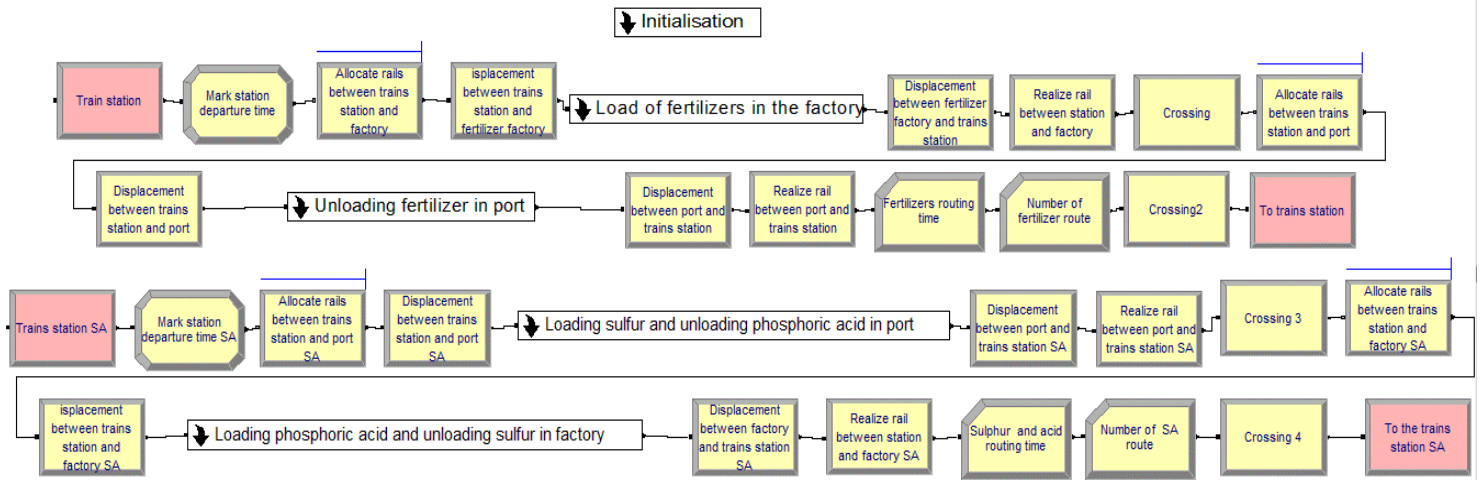


Fig. 5. Global Simulation Model.

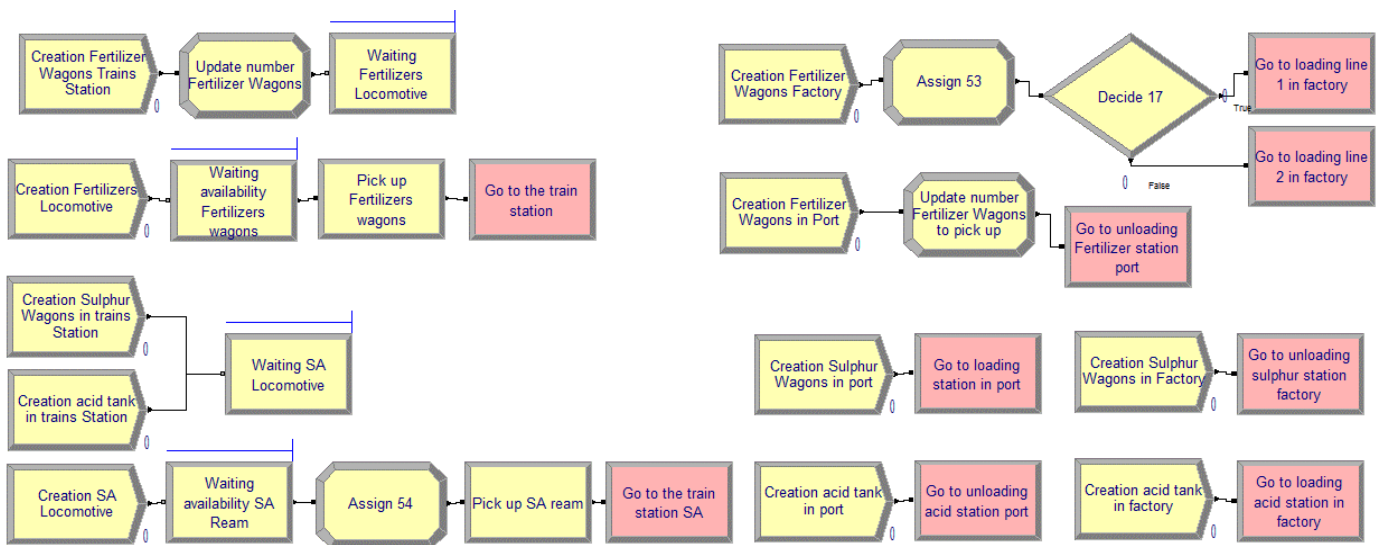


Fig. 6. Initialization Sub-Model.

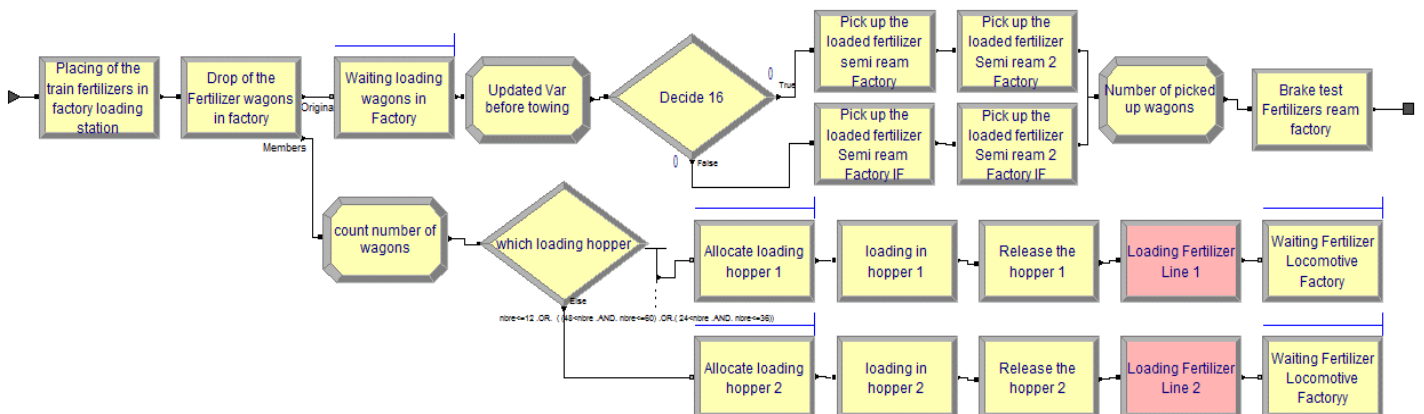


Fig. 7. Fertilizer Loading Sub-Model.

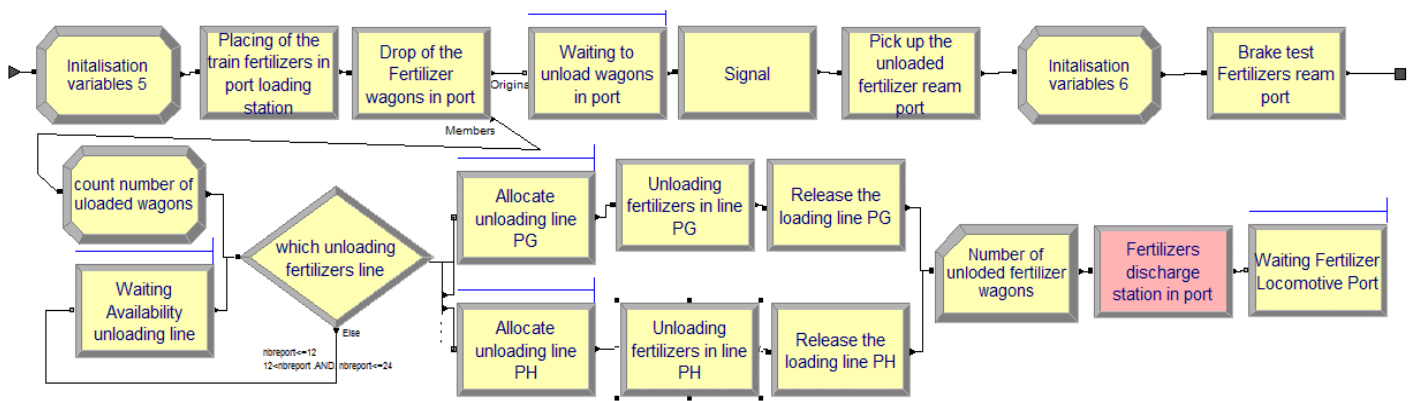


Fig. 8. Fertilizer unloading Sub-Model.

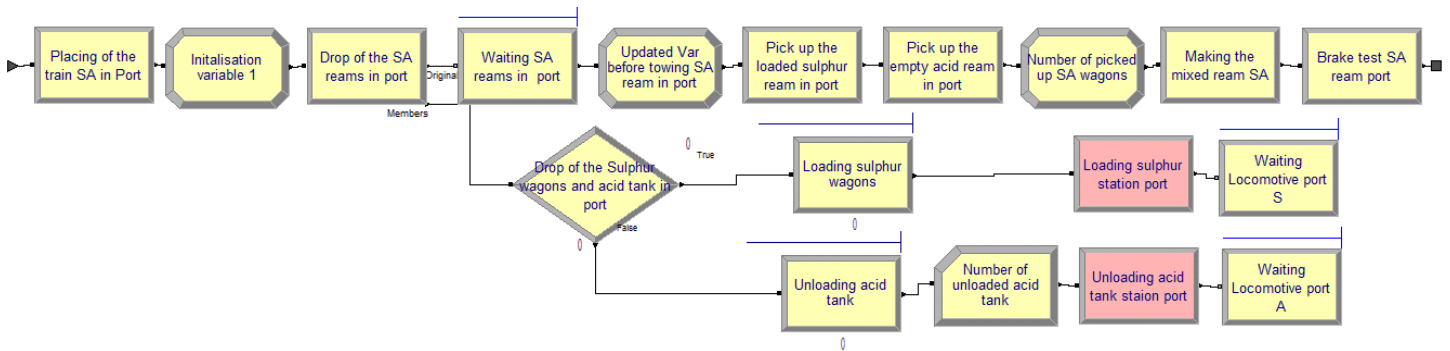


Fig. 9. Acid unloading and Sulfur Loading Sub-Model.

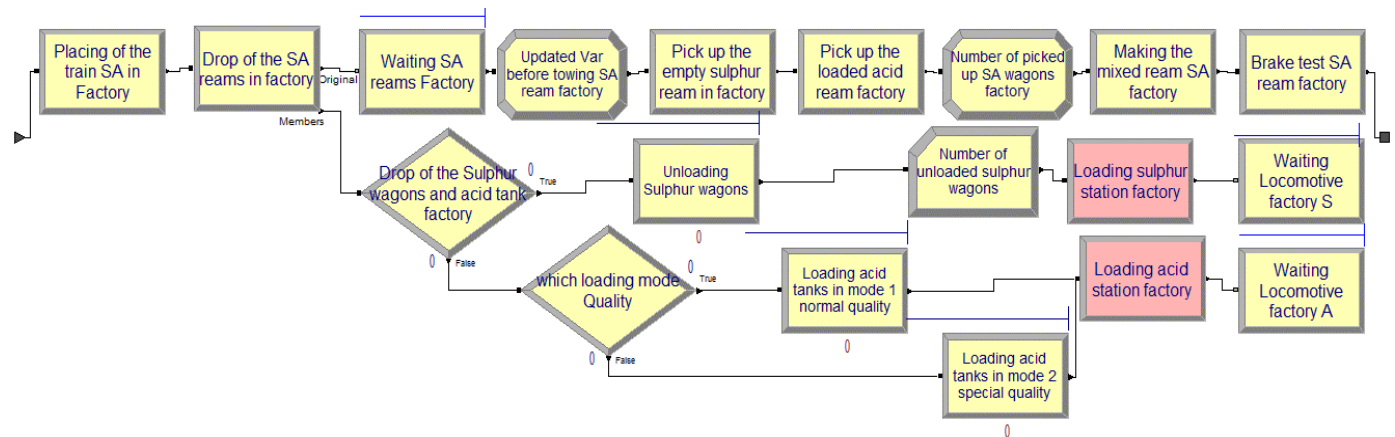


Fig. 10. Acid Loading and Sulfur unloading Sub-Model.

C. Simulation Model Validation

Before drawing any inferences from the statistical results of this simulation model, it must make sure that it is correct and represents the real supply chain. To do this, the simulation results are compared with theoretical results calculated from collected data of the lead time of each process in the studied supply chain. The compared results (see Table 3), concerns the transportation time in each travel and the number of travels done in 24 hours.

D. Simulation Results

The model was simulated over a month. The performance indicators evoked by this simulation model are the transportation time in each travel, number of travels, number of transported fertilizers and sulfur wagons and unloaded acid tanks and finally the waiting times in train station. The calculated times correspond to the average of the times. The simulation results of the studied supply chain are showed in Fig. 11 and 12.

TABLE III. COMPARING THEORETICAL RESULTS AND THE SIMULATION RESULTS

	Theoretical results		Simulation results
	Min	Max	
Transportation time in each travel	3,42	4,17	3,76
Number of travels	5	7	5

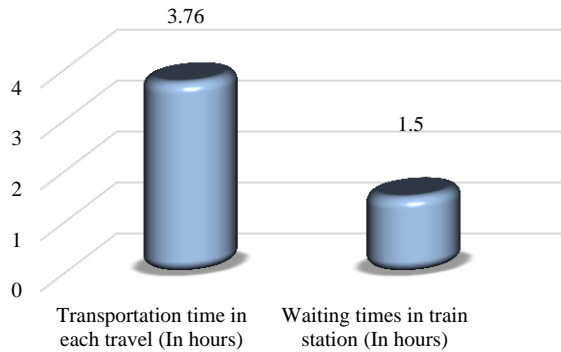


Fig. 11. Simulations results: Waiting and transportation times.

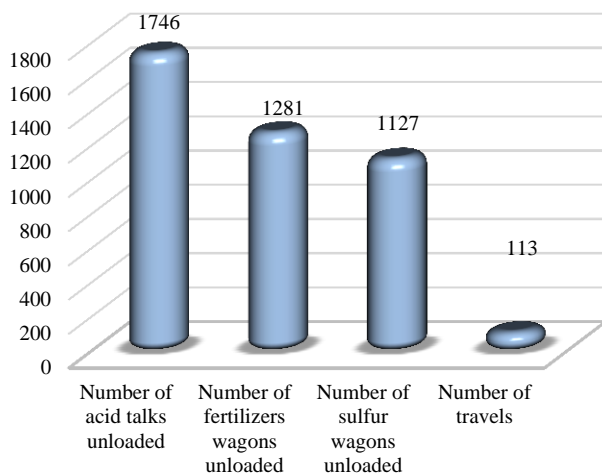


Fig. 12. Simulations results: The transported products.

Indeed, the established models are a very fine analysis of the current situation, allowing designing several optimization scenarios. The obtained results present the current performance of the studied supply chain that requires an improvement and optimization by studying several improvement scenarios in order to improve the simulation results. The mainly objective is to reduce the transportation time in each travel then to increase the number of travels, as well as the number of wagons / tanks transported, and finally reducing the waiting time in the train station.

VI. CONCLUSION

This work is a study describing simulation models of a real supply chain in operating phosphate industry using SIMAN ARENA® Rockwell software. The main objective of these models is determining a lot of performance indicators specifically the transportation time in each travel between entities of this chain, the number of travels, the number of products wagons transported, and the waiting time in the train station for the purpose to evaluate and improve the studied supply chain performance.

This work allows referring to the modeling and simulation according to the scale of complexity of the systems, with the aims to evaluate and check the system potential fluctuations and predict the future behavior.

Using the SIMAN ARENA® Rockwell software a tool for flows simulation, has become a necessity for the optimization of industrial processes and support for strategic decision-making.

Using these models, we are currently working on the study and simulation of several scenarios that can contribute to optimizing flows in this supply chain.

REFERENCES

- [1] Razouk C., Benadada Y., "Optimization and Simulation Approach for Empty Containers Handling", International Journal of Advanced Computer Science and Applications, Vol. 8, No. 11, 2017, pp. 520-525.
- [2] Ruomeng K., Chengjiang Y., "An Algorithm Research for Supply Chain Management Optimization Model", International Journal of Advanced Computer Science and Applications, Vol. 5, No. 5, 2014, pp. 147-150.
- [3] Masud Rana Md., Md. Jobayer Hossain Ratan Kumar Ghosh, Md. Mostafizur Rahman, "A Discrete Event Barber Shop Simulation", International Journal of Advanced Computer Science and Applications, Vol. 3, No.2, 2012, pp. 69-72.
- [4] Viswanadham N., Srinivasa Raghavan N. R., "Performance Analysis and Design of Supply Chains: A Petri Net Approach", Journal of the Operational Research Society, vol. 51(10), 2005, pp. 1158-1169.
- [5] Chen H., Amodeo L., Chu F., and Labadi K., "Performance Evaluation and Optimization of Supply Chains modelled by Batch Deterministic and Stochastic Petri", IEEE transactions on Automation Science and Engineering, pp. 132-144.
- [6] D. Waters, "Logistics - An Introduction to Supply Chain Management", Palgrave Macmillan, 2003.
- [7] Arena Rockwell Automation, URL: http://www.arenasimulation.com/Arena_Home.aspx
- [8] Christopher, M., "Logistics and supply chain management: creating value-added networks", Pearson education, 2005.
- [9] Council of Logistics Management, <http://www.clm1.org/mission.html>, 12 Feb 98.
- [10] Yan-Ling Wang. "Logistics supply chain coordination based on multi-agent system", 2010 IEEE International Conference on Management of Innovation & Technology, 06/2010.
- [11] Min H., Zhou G. "Supply chain modelling: past, present and future", Computers & Industrial Engineering, Vol. 43, 2002, pp. 231-249.
- [12] Gunasekaran, A., and Kobu, B., "Performance measurements and metrics in logistics and supply chain management: a review of recent literature for research and applications", International Journal of Production Research, vol. 45, 2007, pp. 2819-2840.
- [13] Harrel C., Tumay K., "Simulation made easy" Engineering & Management Press, 1994.

- [14] Ganeshan R., Jack E., Magazine M.J., Stephens P., "A Taxonomic Review of Supply Chain Management Research in Quantitative Models for Supply Chain Management" Kluwer Academic Publishers, Boston, 1998, pp. 841-880.
- [15] Beamon M., "Supply chain design and analysis: models and method" International Journal of Production Economics, vol. 5, 1998, pp 281-294.
- [16] Trilling L., Besombes B., Chaabane S., Guinet A., "Modeling practices: Investigation and Comparison of Methods and Analysis Tools for the Hospital Systems Study", HRP project report, Academic Press, 2004.
- [17] Kleijnen J.P.C., "Supply chain simulation tools and techniques: a survey", International Journal of Simulation & Process Modelling, vol. 1, 2005, pp. 82-89.
- [18] Labarthe, Olivier, Bernard Espinasse, Alain Ferrarini, and Benoit Montreuil. "A Methodological Approach for Agent Based Simulation of Mass Customizing Supply Chains", Journal of Decision System, 2005.
- [19] Labarthe O. "Agent-Oriented Modeling and Simulation of Supply Chains in a Context of Mass Customization: Models and Methodological Framework", « Modélisation et simulation orientées agents de chaînes logistiques dans un contexte de personnalisation de masse : modèles et cadre méthodologique », Phd thesis University Paul Cézanne Marseille, 2006, pp. 30-100.
- [20] Farideh Haghshenas Kashani, Mahsa Soleimani, "Evaluation of investment resources impact on development of formal education management system", International Journal of Advanced and Applied Sciences, Vol. 2, No. 10, 2015, pp. 52-61.
- [21] Swati Hira, Anita Bai, P. S. Deshpande, "Designing multidimensional model using relational schema", International Journal of Advanced and Applied Sciences, Vol. 3, No. 5, 2016, pp. 1-8.
- [22] Tan Ching NG, Morteza Ghobakhloo, "What derives lean manufacturing effectiveness: An interpretive structural model", International Journal of Advanced and Applied Sciences, Vol. 4, No. 8, 2017, pp. 104-111.
- [23] A. Bensmaine, L. Benyoucef and Z. Sari, "Simulation of a real supply chain using Arena", "Simulation D'une Chaîne Logistique À Echelle Réelle sous Arena", International Conference On Industrial Engineering and Manufacturing ICIEM'10, 2010, Batna, Algeria.
- [24] Dhanan Sarwo Utomo, Bhakti Stephan Onggo, Stephen Eldridge, Applications of agent-based modelling and simulation in the agri-food supply chains, European Journal of Operational Research, Volume 269, Issue 3, 2018, Pages 794-805.
- [25] T.M. Pinho, J.P. Coelho, P.M. Oliveira, B. Oliveira, A. Marques, J. Rasinmäki, A.P. Moreira, G. Veiga, J. Boaventura-Cunha, Routing and schedule simulation of a biomass energy supply chain through SimPy simulation package, Applied Computing and Informatics, 2018.
- [26] Malin Song, Xin Cui, Shuhong Wang, Simulation of land green supply chain based on system dynamics and policy optimization, International Journal of Production Economics, 2018.
- [27] Sameh M Saad, Elganidi H Elsaghier, David Ezaga, Planning and optimising petroleum supply chain, Procedia Manufacturing, Volume 17, 2018, Pages 803-810,
- [28] Fu M. C., "Optimization for simulation: Theory vs. practice", INFORMS Journal on Computing, Vol. 14, no. 3, 2002, p. 192-215.
- [29] Boesel J., Nelson B. L., Ishii N., "A framework for simulation-optimization software", IIE Transactions, Vol. 35, 2003, p. 221-229.
- [30] Abo-Hamad W., Arisha A., "Simulation-optimization methods in supply chain applications: a review", Irish Journal of Management, Vol. 551, 2011, p. 95-123.
- [31] S. Umed and Y. T. Lee, "Design specifications of a generic supply chain simulator", Proceedings of the 2004 Winter Simulation Conference, 2004.
- [32] Angerhofer, B.J. and ANGELIDES, M.C. "System Dynamics Modelling in Supply Chain Management: Research Review", Proceedings of the 2000 Winter Simulation Conference, 2000.
- [33] Dias, L.M.S., Pereira, G.A.B., Vik, P., Oliveira, J.A., "Discrete Simulation Tools Ranking—a Commercial Software Packages comparison based on popularity", Proceedings of the Industrial Simulation Conference, 2011, Venice.
- [34] Yuri M., Jelena P., « Discrete-Event Simulation: Methodology and Practice », Support de cours, Department of Modelling and Simulation, Riga Technical University, Latvia, 2005, pp. 41.
- [35] Tewoldeberhan T.W., Verbraeck A., Valentin E., Bardonnnet G., "An evaluation and selection methodology for discrete-event simulation software", Proceedings of the Winter Simulation Conference, 2002, San Diego, Calif.
- [36] Yassine Azougagh, Khalid Benhida, Said Elfezazi. "Contribution to the modelling and analysis of logistics system performance by Petri nets and simulation models: ", IOP Conference Series: Materials Science and Engineering, 2016.
- [37] Benhida Khalid, Yassine Azougagh, and Said Elfezazi. "Modelling a flows in supply chain with analytical models: Case of a chemical industry", IOP Conference Series Materials Science and Engineering, 2016.

An Agglomerative Hierarchical Clustering with Association Rules for Discovering Climate Change Patterns

Mahmoud Sammour¹, Zulaiha Ali Othman², Zurina Muda³, Roliana Ibrahim⁴

Center for Artificial Intelligence Technology, Faculty of Information Science and Technology
Universiti Kebangsaan Malaysia, Bangi, Selangor, Malaysia^{1,2,3}
Information Systems Department, Faculty of Computing⁴
Universiti Teknologi Malaysia, Skudai, Johor, Malaysia

Abstract—Ozone analysis is the process of identifying meaningful patterns that would facilitate the prediction of future trends. One of the common techniques that have been used for ozone analysis is the clustering technique. Clustering is one of the popular methods which contribute a significant knowledge for time series data mining by aggregating similar data in specific groups. However, identifying significant patterns regarding the ground-level ozone is quite a challenging task especially after applying the clustering task. This paper presents a pattern discovery for ground-level ozone using a proposed method known as an Agglomerative Hierarchical Clustering with Dynamic Time Warping (DTW) as a distance measure on which the patterns have been extracted using the Apriori Association Rules (AAR) algorithm. The experiment is conducted on a Malaysian Ozone dataset collected from Putrajaya for year 2006. The experiment result shows 20 pattern influences on high ozone with a high confident (1.00). However, it can be classified into four meaningful patterns; more high temperature with low nitrogen oxide, nitrogen oxide and nitrogen dioxide high, nitrogen oxide with carbon oxide high, and carbon oxide high. These patterns help in decision making to plan the amount of carbon oxide and nitrogen oxide to be reduced in order to avoid the high ozone surface.

Keywords—Hierarchical clustering; dynamic time warping; ground-level ozone; Apriori Association Rules

I. INTRODUCTION

Ozone, scientifically called trioxygen, is an inorganic molecule with the chemical formula O_3 . It is a pale blue gas with a distinctively pungent smell [1]. Reports suggest that ground level ozone can be rather harmful to the human respiratory system. In addition, there are also research reports that this can also result in several other detrimental diseases such as severe exposure to the ozone can negatively affect and upset lung function, and can potentially increase inflammation [2]. For instance, studies find that the mortality rate in urban areas is related to the effects of the ozone, and there is a correlation between them [3]. Other studies such as the one by [4] concluded that the effects of ozone can be non-linear, and specifically, extreme exposure to ground level ozone can be dangerous for the health. Therefore, in view of the dangers the ozone layer entails, it could be critical to research and determine the factors which cause the ozone layer to spread the most.

Several studies have been proposed for the task of predicting ozone levels [5], [6]. Such methods utilized the clustering techniques in order to group the spots that have a high level of ozone. However, the results of clustering sometimes would lead to inferior indications regarding the ozone. This is due to multiple reasons. First, the results of clustering significantly change based on the clustering technique and the distance measure used. There are several clustering techniques such as partitioning (e.g., k-means, k-medoids, etc.) and hierarchical (e.g., agglomerative and divisive). Besides that, there are different distance measures that can be utilized with the clustering technique such as Euclidean, Minkowski and Dynamic Time Warping (DTW). These choices lead to different results of clustering. On the other hand, evaluating the results of clustering is a challenging task in which different evaluation methods have been proposed for this purpose. All these mentioned reasons make the process of identifying significant patterns from ozone clustering results a difficult task.

This paper aims to propose the Apriori Association Rules algorithm in order to extract patterns from the clustering results and considered to be an extension of our study in [7]. Therefore, the next section of this paper discussed the existing techniques in the literature. In Section III introduces the proposed algorithm. While Section IV presented the performance and evaluation. A result and discussion are presented in Section V. Finally, Section VI concludes the finding of this study.

II. RELATED WORK

According to [8] who accommodated a review for the trends of ground-level ozone using data from the last century have concluded that the ground-level ozone has dramatically increased in the last three decades. As a response, the research community has attempted to propose statistical models that have the ability to predict the increasing ozone rates. For instance, [9] proposed an agglomerative hierarchical clustering to identify the most polluted area in Houston, Texas, in terms of ground-level ozone. In their study, the authors have declared multiple factors that have a significant impact on the ozone increment, such as wind speed, wind direction, and solar radiation.

In addition, [10] proposed a k-means clustering approach with Euclidean distance measure in order to identify the peaks of ozone rates in an industrial area in Central-Southern Spain. The authors have successfully identified several polluted plots. Another approach was proposed by [11] in which a statistical method of passive sampling was used to investigate the air pollution in Pakistan. Furthermore, [12] proposed a combination of statistical means of quantile regression and agglomerative hierarchical clustering in order to measure the pollution of air in terms of ground-level ozone.

Other researchers have attempted to identify characteristics of ground-level ozone such as [13] who proposed a Hybrid Single Particle Lagrangian Integrated Trajectory (HySPLIT) Model in order to characterize the ground ozone concentration in the gulf of Texas. In their study they figured out that the lowest ozone concentrations are associated with trajectories that remained over the central Gulf for at least 48 hours. On the other hand, higher concentrations are associated with trajectories that pass close to the Northern and Western Gulf Coast. Wang et al. addressed the problem of detecting ground-level ozone from a spatio-temporal aspect [14]. The authors proposed a nearest neighbor clustering approach in order to identify spatio-temporal patterns of the air pollution.

Another observational study was conducted by [15], which concentrated on the pollution in Tangshan, North China. This study mainly relied on statistical analysis. The study implied the dramatic expansion rates of ozone and nitrogen dioxide (NO_x) from 2008 to 2011. The study concluded the reason behind the increment rates as being due to the extent of industries that are located in the city. In addition, [16] accommodated a comparative study of three regression approaches including Neural Network (NN), Support Vector Machine (SVM) and Fuzzy Logic (FL) in terms of predicting ground-level ozone. Based on the Root Mean Square Error (RMSE), SVM has shown superior performance in predicting the ozone levels. Similarly, [17] have examined two NN models including Feed-forward NN and Back-propagation NN in terms of ozone prediction. Basically, multiple features have been encoded and fed into the network including temperature, humidity, wind speed, incoming solar radiation, sulfur dioxide and nitrogen dioxide. Feed-forward NN has outperformed the other model.

In addition, [5] accommodated a comparison among two linear regression methods including SVM and multi-layer perceptron NN to identify ozone levels in the Houston–Galveston–Brazoria area, Texas. The results showed superior performance for SVM. Tamas et al. used three clustering approaches in order to detect pollution in the air including Artificial Neural Network (ANN), Self-Organized Mapping (SOM) and K-means clustering. Using hourly data, the results showed two main sources of pollution including ozone (O_3) and nitrogen dioxide (NO_2) [6].

On the other hand, [18] did a long-term statistical study for ground-level ozone in Japan from 1990 to 2010. The study focused on identifying correlation for the increment rates of ozone. The authors identified three main causes, stated as: (i) the decrease of NO titration effect, (ii) the increase of

transboundary transport, and (iii) the decrease of situated photochemical production. Similarly, on an observational study of ozone level causes by [19], the authors indicated that the Asia continent is one of the main sources that affects the ground-level ozone in Western United States.

III. MATERIALS AND METHOD

The proposed method consists of Agglomerative Hierarchical Clustering with Dynamic Time Warping (DTW) as a distance measure. The reason behind selecting the clustering technique and distance measure lie in their superior performance according to the state of the art of ozone clustering. In addition, the Apriori Association Rules will be applied on the clustering results in order to discover knowledge. The following sub-sections will tackle the proposed method components.

A. Agglomerative Hierarchical Clustering

This phase aims to apply the hierarchical clustering technique. In general, hierarchical clustering algorithms work by aggregating the objects into a tree of clusters [20]. Hierarchical clustering can be categorized into two types, agglomerative and divisive. Such categorization is inspired from the mechanism of grouping the objects whether bottom-up or top-down approach. AHC is considered as a bottom-up hierarchical approach where each object is set in a separated cluster [21], then AHC will merge such clusters into larger clusters. The process continues until a specific termination has been reached. A complete linkage algorithm aims to identify the similarity between two clusters by measuring two nearest data points that are located in different clusters. Hence, the merge will be done between the clusters that have a minimum distance (most similar) between each other. In this paper, AHC has been applied as a maximum linkage.

B. Dynamic Time Warping (DTW)

DTW has been widely used to compare discrete sequences and sequences of continuous values [22]. Let $S = \{s_1, s_2, \dots, s_i\}$ and $T = \{t_1, t_2, \dots, t_j\}$ be a two time series sequences. DTW will minimize the differences among these series by representing a matrix of $n \times m$. In such a matrix, the distance/similarity between s_i and t_j will be calculated using Euclidean distance.

However, a warping path $P = \{p_1, p_2, \dots, p_k, \dots, p_K\}$ where $\max(m, n) \leq K \leq m + n - 1$ will be elements from the matrix that meet three constraints including boundary condition, continuity and monotonicity. The boundary condition constraint requires the warping path to start and finish in diagonally opposite corner cells of the matrix. That is $p_1 = (1, 1)$ and $p_K = (m, n)$. The continuity constraint restricts the allowable steps to adjacent cells. The monotonicity constraint forces the points in the warping path to be monotonically spaced in time. The warping path that has the minimum distance/similarity between the two series is of interest. Hence, the DTW can be computed as follows:

$$d_{DTW} = \min \frac{\sum_{k=1}^K p_k}{K} \quad (1)$$

C. Apriori Association Rules (AAR)

Apriori is an algorithm for frequent item set mining and association rule learning over transactional databases [23]. It proceeds by identifying the frequent individual items in the database and extending them to larger and larger item sets as long as those item sets appear sufficiently often in the database. The frequent item sets determined by Apriori can be used to determine association rules which highlight general trends in the database. In this manner, applying the Apriori algorithm on our dataset would reveal the interesting patterns that occur. In order to distinguish these interesting patterns or rules, it is necessary to consider the value of confidence which is being illustrated as follows:

Confidence: The confidence of a rule is defined as $\text{Conf}(X \text{ implies } Y) = \frac{\text{supp}(X \cup Y)}{\text{supp}(X)}$ in which $\text{supp}(X \cup Y)$ means "support for occurrences of transactions where X and Y both appear". Confidence ranges from 0 to 1, where the closeness to 1 indicates an interesting relation. Confidence is an estimate of $\text{Pr}(Y | X)$, the probability of observing Y given X. The support $\text{supp}(X)$ of an itemset X is defined as the proportion of transactions in the data set which contain the itemset.

IV. EXPERIMENT

First, the data was collected from LESTARI, which is the Institution for Environment and Development in Malaysia and the Asia Pacific. The institution has been established since 1994 with the structure of Universiti Kebangsaan Malaysia (UKM) in order to deal with environment and development issues. The data contain ozone levels for one year (i.e. 2006), particularly for the city of Putrajaya. The data are represented hourly as time intervals, which contain 8760 instances and consist of the following attributes: date, hours, O₃, NO_x, nitrogen dioxide (NO₂), temperature (Temp), non-methane hydrocarbons (NMHC), and carbon oxide (CO). Hence, the proposed AHC with DTW was applied on the dataset.

Two main approaches were used to validate the clustering process; external and internal validation of clusters [24]. External validation aims to validate the clusters based on the distribution in which the common information retrieval metrics are such as precision, recall and f-measure. However, the mechanism of validation relies on labeled data. Since the real-life data are usually unlabeled, applying external validation tends to be insufficient.

On other hand, internal validation aims to measure the correctness among objects within a cluster (i.e. intra-cluster) and the correctness among objects within multiple clusters (i.e. inter-cluster). Basically, the main aim of the clustering task is to make sure that the objects within a single cluster are mostly similar, while the objects within multiple clusters are mostly dissimilar. Hence, computing the Root Mean Square Error Standard Deviation (RMSE-SD) would measure the homogenous of the objects within a single cluster and multiple clusters, which can be computed as:

$$\text{internal RMSE} - \text{SD} = \frac{1}{n-1} \sum_{i=1}^n (x_i - x_{i+1})^2 \quad (2)$$

Where n is the number of objects inside a cluster and $x_i - x_{i+1}$ is the distance between two objects in the same

cluster. Similarly, RMSE-SD can be computed for the external clusters as:

$$\text{external RMSE} - \text{SD} = \frac{1}{n-1} \sum_{i=1}^n (x_i - \bar{x})^2 \quad (3)$$

Where n is the number of objects of two inter clusters and $x_i - \bar{x}$ is the distance between an object in one cluster and the other object in other cluster. Similarly, RMSE-SD can be computed for the external clusters as (3).

Note that, the smaller value of RMSE-SD between the objects within a single cluster leads to better performance in which the objects are very similar. In contrast, the bigger value of RMSE-SD between the objects within a single cluster leads to lower performance in which the homogenous among the objects is being maximized. Therefore, the best results associated with a smaller value of RMSE-SD among intra-cluster, and with a greater value of RMSE-SD among inter-clusters. Based on the latter mentioned explanation, the results of applying AHC with DTW can be depicted as in Table I. As shown in Table I, the best results of intra and inter cluster has been achieved at the number of cluster 9.

The US Office of Air and Radiation have discussed the factors that lead to air pollution. In their investigation, the ozone was one of the main factors that could harm the human health. For this matter, [25] provided five categories of air pollution which are shown in Table II.

In order to provide a more critical analysis of the acquired clusters, the best number of cluster based on the RMSE-SD, which is 9, will be considered. In addition, the categorization proposed by [25] also will be considered. Therefore, two number of clusters will be considered in the analysis which are 5 and 9; the next sections will tackle this analysis.

TABLE I. RESULTS OF INTRA AND INTER CLUSTER OF AHC

# Clusters	Intra-Cluster	Inter-Cluster
15	0.0042	0.3869
14	0.0041	0.3825
13	0.0041	0.3814
12	0.0042	0.3813
11	0.0045	0.3901
10	0.0045	0.4031
9	0.0039	0.4077
8	0.0039	0.3401
7	0.0041	0.3252
6	0.0066	0.3221
5	0.0068	0.3153
4	0.0073	0.3149
3	0.0054	0.3608

TABLE II. CATEGORIES OF AIR POLLUTION

# index	Unhealthy Level
1	Very Unhealthy
2	Unhealthy
3	Unhealthy for Sensitive Groups
4	Moderate
5	Good

V. RESULT AND DISCUSSION

A. Analysis when $K=5$

This section aims to provide a critical analysis of clustering when $k=5$, by identifying new patterns. This can be conducted by detecting anonymous or abnormal trends for the ground-level ozone rates. In this manner, each cluster included within the five clusters will be discussed separately.

The analysis tackles the days included in this cluster and is conducted based on three 8-hour intervals, according to [26]. Fig. 1 depicts the results of this experiment. Note that the values of the ozone have been measured using the particle per million recorded from the stations. For cluster 1, the first 8-hour interval began with 0.004 ppb and ended with 0.005 ppb, whereas the second interval showed a rise of the ozone values reaching to the peak of 0.061 ppb at 2 p.m. and ended with 0.050 ppb at 5 p.m. In the third interval, the ozone values gradually decreased reaching 0.008 ppb. This pattern is considered to be standard in accordance to the literature [27].

For cluster 2, the first interval began with 0.014 ppb and ended with 0.005 ppb. The second interval showed a rise of ozone values reaching the peak of 0.113 ppb at 2 p.m. and ended with 0.089 ppb. In the third interval, the values decreased to reach 0.014 ppb. A remarkable pattern could be noticed from this cluster, whereby this pattern represented the sharp increase and decrease of the ozone values.

For cluster 3, the first 8-hour interval began with 0.017 ppb and ended with 0.007 ppb. The second interval showed an increase of values reaching the peak of 0.058 ppb at 2 p.m., and this peak did not change until 4 p.m. In the third interval, the values gradually decreased reaching 0.012 ppb. A pattern can be shown as starting with a high value.

For cluster 4, the first 8-hour interval began with 0.005 ppb and ended with 0.006 ppb, whereas the second interval showed an increase of values reaching the peak of 0.037 ppb at 2 p.m., and this peak did not change until 3 p.m. In the third interval, the values gradually decreased reaching 0.005 ppb. A remarkable pattern could be noticed from this cluster, whereby this pattern represented the lowest values of the ozone for the whole day.

For cluster 5, the first 8-hour interval began with 0.033 ppb and ended with 0.016 ppb, whereas the second interval showed an increase of values reaching the peak of 0.059 ppb at 3 p.m. and ended with 0.051 ppb. In the third interval, the values sharply decreased reaching 0.019 ppb at 8 p.m. and ended with 0.017 ppb. A remarkable pattern could be noticed from this cluster, whereby this pattern represented a high value of starting and unusual decline of the ozone values.

B. Analysis when $K=9$

This section aims to provide a critical analysis of clustering when $k=9$, by identifying new patterns. This can be conducted by detecting anonymous or abnormal trends for the ground-level ozone rates. In this manner, each cluster included within the nine clusters will be discussed separately. The analysis tackles the days included in this cluster and is conducted based on three 8-hour intervals, according to [26]. Fig. 2 depicts the results of this experiment. Note that, the

values of the ozone have been measured using the particle per million recorded from the stations.

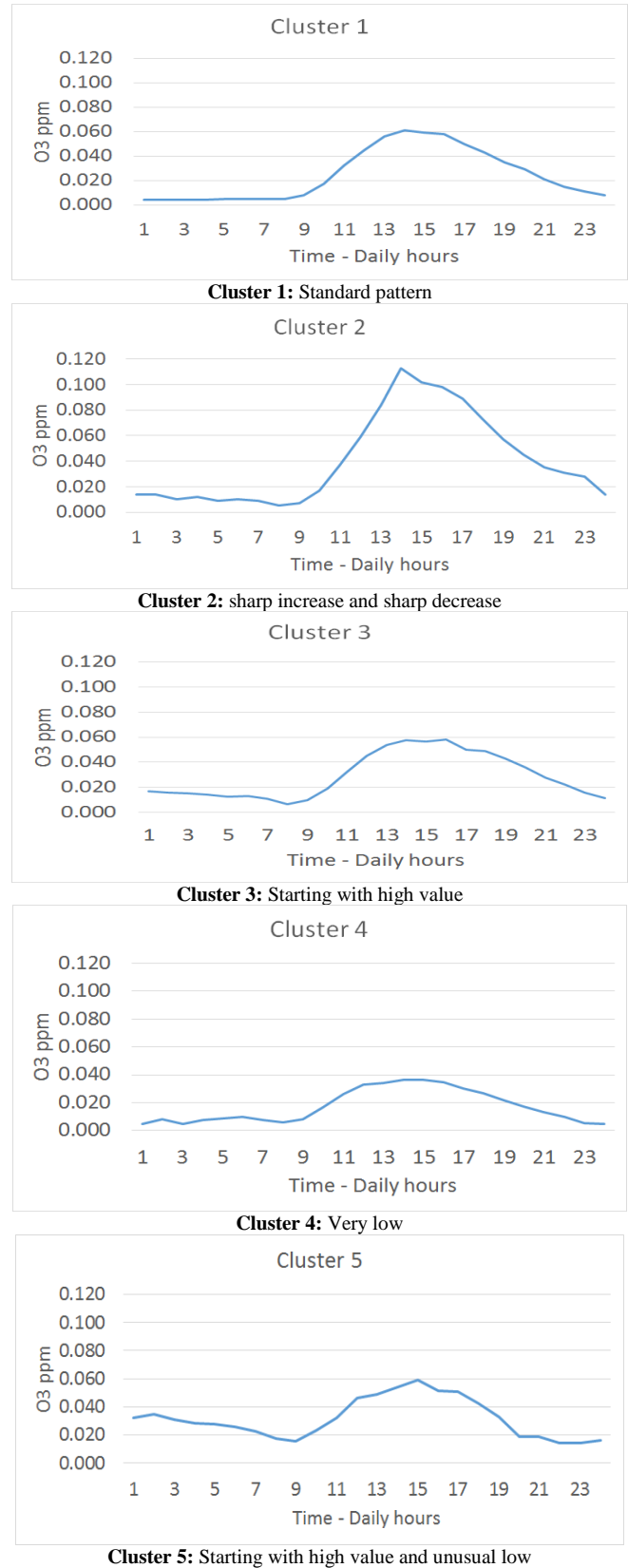


Fig. 1. Results of clustering when $K=5$.

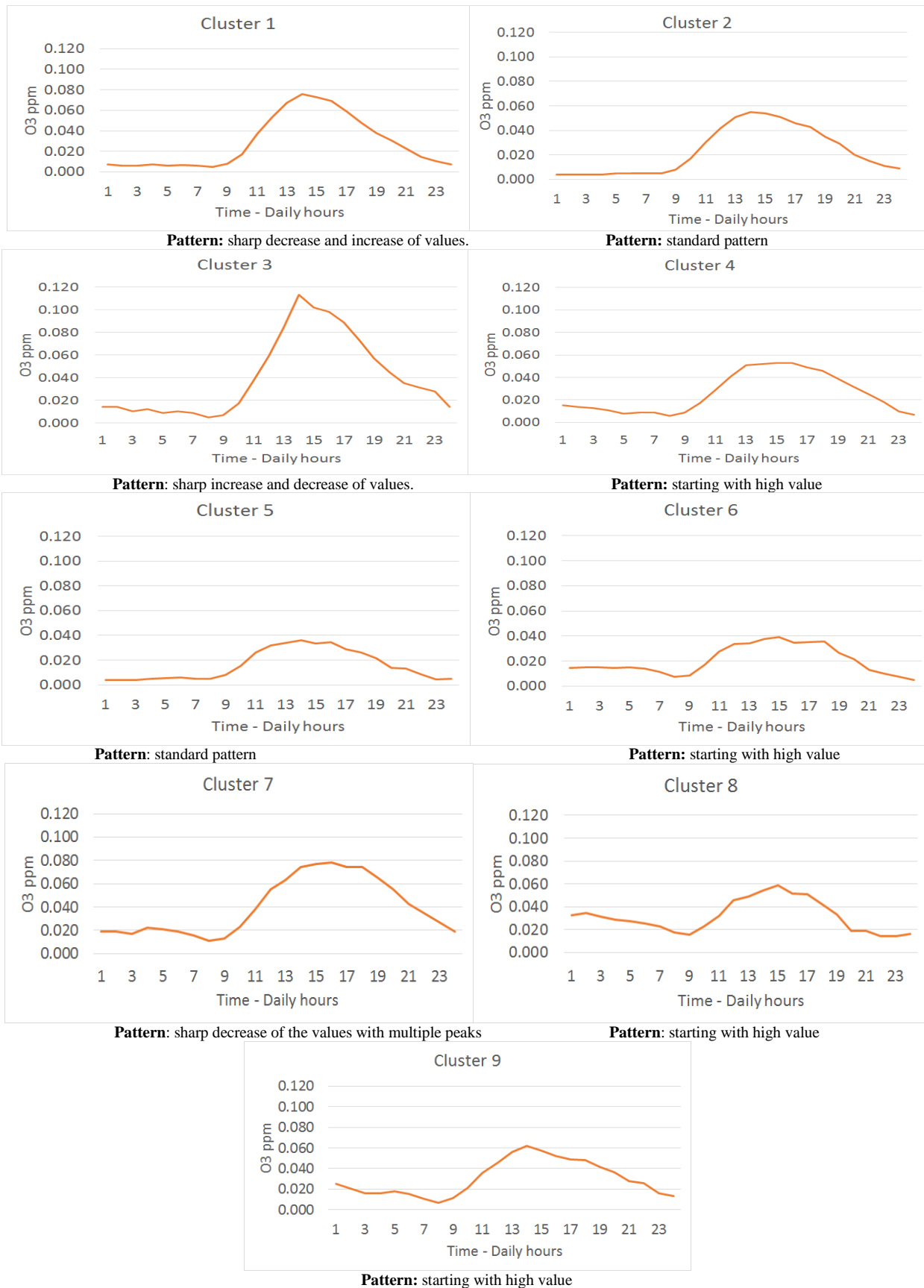


Fig. 2. Results of Clustering when K=9.

For cluster 1, the first 8-hour interval began with 0.008 ppb and ended with 0.005 ppb. Whereas, second interval showed a rise of ozone values reaching the peak of 0.076 ppb at 2pm, then ended up with 0.059 ppb at 5pm. In the third interval, the values gradually decreased reaching 0.007 ppb. A remarkable pattern could be noticed from this cluster, whereby this pattern represented the sharp decrease and increase of ozone values.

For cluster 2, the first interval began with 0.004 ppb and ended with 0.005 ppb. The second interval began with 0.008 ppb and sharply increased to the maximum peak of 0.055 ppb at 2 p.m., then decreased to 0.046 ppb at 5 p.m. The third interval decreased and reached 0.009 ppb. This cluster has a standard pattern

For cluster 3, the first interval began with 0.014 ppb and ended with 0.005 ppb. The second interval showed an increase of values reaching the peak of 0.113 ppb at 2 p.m. and ended with 0.089 ppb. In the third interval, the values decreased to 0.014 ppb. A remarkable pattern could be noticed from this cluster, whereby this pattern represented the sharp increase followed by a sharp decrease of values.

For cluster 4, the first interval began with 0.015 ppb and ended with 0.006 ppb. The second interval showed multiple peaks in which the values at 4 p.m. reached 0.053, and 0.049 ppb at 5 p.m. The third interval showed a decrease of values that reached 0.007 ppb.

For cluster 5, the first interval began with 0.004 ppb and ended with 0.005 ppb. The second interval showed three peak stated as; 0.032 ppb at 12 p.m., 0.036 at 2 p.m., and 0.035 ppb at 4 p.m., and ended with 0.029 ppb. The third interval showed an unstable decrease that reached 0.005 ppb. This cluster has a standard pattern.

For cluster 6, the first interval began with 0.015 ppb then showed a stable decrease until 8 a.m. reaching 0.008 ppb. The second interval showed two peaks of 0.034 at 12 p.m. and 0.039 at 3 p.m. The third interval showed a gradual decrease of the values reaching 0.005 ppb. The pattern embedded in the cluster has a high value of the starting point.

For cluster 7, the first interval began with 0.019 ppb and ended with 0.011 ppb. The second interval showed two peaks of 0.078 ppb at 4 p.m. and 0.074 ppb at 2 p.m. The third interval showed a gradual decrease reaching 0.019 ppb. A remarkable pattern could be noticed from this cluster, whereby this pattern represented a sharp decrease of the values with multiple peaks.

For cluster 8, the first interval began with 0.033 ppb and ended with 0.016 ppb. The second interval showed a maximum peak of 0.059 ppb at 3 p.m. and then ended with 0.051 ppb. The third interval showed a sharp decrease of values reaching 0.017 ppb. The pattern embedded in this cluster has a high value of the starting point.

For cluster 9, the first interval began with 0.025 ppb and ended with 0.007 ppb. The second interval showed a sharp increase of values reaching a maximum of 0.062 ppb at 2 p.m. and ended with 0.049 ppb. The third interval showed a gradual decrease of the values reaching 0.014 ppb. The pattern embedded in this cluster has a high value of the starting point.

C. Comparison between $K=5$ and $K=9$

This section aims to accommodate a comparison between the two numbers of cluster 9 and 5 which were analyzed in the previous sections. The comparison will be based on multiple variables including the starting values of ozone, maximum peak, maximum peak of median, and ending values. Table III shows the values of 5 number of clusters.

As shown in Table III, the number of days included in the 'unhealthy' category represents nearly half of the year which seems to be the overestimated categorization. This means that this category should be divided into more categories, whereas the 'moderate' category contains only eight days which seems to be the underestimated categorization. Generally, this category is supposed to contain more days.

However, Table IV shows the values of 9 number of clusters. As shown in Table IV, unlike the standard 5 categorization, the 9 categorization has the ability to provide a better description of the year's days. This can be represented by giving more categories. For instance, the 'unhealthy' category has been split into two categories, namely 'unhealthy' and 'very unhealthy for sensitive group'. These categories have shown a reasonable contained number of days. In addition, the category 'moderate' has been split into three categories, namely 'high moderate', 'moderate' and 'low moderate'. Similarly, these categories contained a reasonable number of days. Finally, the category 'good' has been also divided into two categories as 'very good' and 'good'.

D. Extracting Pattern using AAR

Basically, determining the factors that affect the ozone is a difficult task. Akimoto et al. conducted a study to analyze the causes of ground-level ozone in Japan using 20 years of data [18].

As a conclusion in their study, they have surprisingly found that even with the decrease of NO_x and NMHC (i.e. considered as the main causes of increasing the ozone rates), there is still an ongoing increment of ground-level ozone rates. Based on their judgment, they have referred the reason to transportation. Hence, it is a challenging task to identify the factors that would affect the ground-level ozone. However, this study attempts to present an analysis for specific cases of extreme growth of ozone rates. Therefore, the association rules approach has been used in order to clarify the factors that would increase rates of ozone in Putrajaya, Malaysia. Table V depicts the results of applying association rules by showing the most significant patterns with highest confidences.

As we can see in Table V, the first 12 rules are associated with two factors whereas the other rules are associated with a single factor. In particular, the first five rules (i.e. 1-5) are associated with NO_x and the temperature, where the increase of temperature with NO_x = 0.003 leads to an increase in the ozone rates. In addition, the following two rules (i.e. 6 and 7) are associated with NO_x and NO₂, where the decrease of NO₂ with an NO_x = 0.003 would lead to an increment in the ozone rates. The five following rules (i.e. 8-12) are associated with NO_x and CO, where the decrease of CO with NO_x = 0.003

(especially for rule 10 and 11) would lead to an increment in the ozone rates.

On the other hand, the remaining eight rules (i.e. 13-20) are associated with a single factor which is CO. In fact, these rules are related to the peak or highest rates of ozone. Although there is no direct relation between the CO values and the ozone rates, as a general view, CO is related to transportation. This can be evidenced in the findings of [18] study which implies that transportation is one of the main reasons behind the growth of ground-level ozone rates.

TABLE III. VALUES USING CLUSTER = 5

Days	K=5	Morning		Afternoon		Evening	Standard Category
	Class	Start	end	Max	Men Max	end	
60	4	0.005	0.006	0.09	0.037	0.005	Good
8	5	0.033	0.016	0.093	0.059	0.017	Moderate
104	3	0.017	0.007	0.105	0.058	0.012	Unhealthy for Sensitive Groups
173	1	0.004	0.005	0.115	0.061	0.008	Unhealthy
19	2	0.014	0.005	0.148	0.113	0.014	Very Unhealthy

TABLE IV. VALUES USING CLUSTER = 9

Days	K=9	Morning		Afternoon		Evening	Proposed Category
	Class	Start	end	Max	Men Max	end	
38	5	0.004	0.005	0.06	0.036	0.005	Very Good
22	6	0.015	0.008	0.09	0.039	0.005	Good
63	4	0.015	0.006	0.093	0.053	0.007	High Moderate
121	2	0.004	0.005	0.096	0.055	0.009	Moderate
8	8	0.033	0.016	0.093	0.059	0.017	low Moderate
20	9	0.025	0.007	0.077	0.062	0.014	Unhealthy for Sensitive Groups
52	1	0.008	0.005	0.115	0.076	0.007	Very Unhealthy for Sensitive Groups
21	7	0.019	0.011	0.105	0.078	0.019	Unhealthy
19	3	0.014	0.005	0.148	0.113	0.014	Very Unhealthy

TABLE V. SIGNIFICANT PATTERN EXTRACTED USING AAR

#	Factor 1	Factor 2	=>	Ozone	Confidence
1	NOx=0.003	Temp=33.7	=>	0.089	1.00
2	NOx=0.003	Temp=32.1	=>	0.088	1.00
3	NOx=0.003	Temp=30.4	=>	0.070	1.00
4	NOx=0.003	Temp=29.9	=>	0.061	1.00
5	NOx=0.003	Temp=29.2	=>	0.059	1.00
6	NOx=0.003	NO2=0.013	=>	0.059	1.00
7	NOx=0.003	NO2=0.002	=>	0.070	1.00
8	NOx=0.003	CO=1.7	=>	0.070	1.00
9	NOx=0.003	CO=1.61	=>	0.061	1.00
10	NOx=0.003	CO=0.31	=>	0.088	1.00
11	NOx=0.003	CO=0.27	=>	0.086	1.00
12	NOx=0.003	CO=0.16	=>	0.078	1.00
13	CO=0.75	-	=>	0.148	1.00
14	CO=0.91	-	=>	0.147	1.00
15	CO=0.7	-	=>	0.143	1.00
16	CO=0.44	-	=>	0.140	1.00
17	CO=0.63	-	=>	0.140	1.00
18	CO=0.60	-	=>	0.139	1.00
19	CO=0.59	-	=>	0.139	1.00
20	CO=0.78	-	=>	0.131	1.00

VI. CONCLUSION

This study has proposed a pattern extraction method for ground-level ozone using the Apriori Association Rules method. The data used in the experiment were collected from LESTARI, which is the Institution for Environment and Development in Malaysia and the Asia Pacific. In the beginning, AHC with DTW were applied on the dataset in order to cluster the days based on the ozone levels. Consequentially, the proposed AAR was applied to extract significant patterns. The experiment shows that the extracted patterns are related to CO which is an interesting relation in accordance to the literature. In fact, this study utilized a ground-level ozone data with a single year. Hence, using a dataset with multiple years in future researches has the ability to identify frequent patterns which may facilitate the determination of the important factors of the ozone. However, there is two limitations in this study which is the resources of hardware and time consuming. This is because, AHC requires

a high computational cost and time. Therefore, only one-year ozone data were selected in this study to avoid this limitation.

ACKNOWLEDGMENT

This study is supported by the Universiti Kebangsaan Malaysia (UKM) and funded by research grant (FRGS/1/2016/ICT02/UKM/02/8).

REFERENCES

- [1] H. Liu et al., "Ground-level ozone pollution and its health impacts in China," *Atmos. Environ.*, vol. 173, pp. 223–230, 2018.
- [2] L. Shen, L. J. Mickley, and E. Gilleland, "Impact of increasing heat waves on U.S. ozone episodes in the 2050s: Results from a multimodel analysis using extreme value theory," *Geophys. Res. Lett.*, 2016.
- [3] M. Ahmadi, Y. Huang, and K. John, "Application of spatio-temporal clustering for predicting ground-level ozone pollution," in *Advances in Geographic Information Science*, 2017, pp. 153–167.
- [4] W. Zhao, S. Fan, H. Guo, B. Gao, J. Sun, and L. Chen, "Assessing the impact of local meteorological variables on surface ozone in Hong Kong during 2000–2015 using quantile and multiple line regression models," *Atmos. Environ.*, vol. 144, pp. 182–193, 2016.

- [5] W. Sun et al., "Prediction of surface ozone episodes using clusters based generalized linear mixed effects models in Houston–Galveston–Brazoria area, Texas," *Atmos. Pollut. Res.*, 2015.
- [6] W. Tamas, G. Notton, C. Paoli, M. L. Nivet, and C. Voyant, "Hybridization of air quality forecasting models using machine learning and clustering: An original approach to detect pollutant peaks," *Aerosol Air Qual. Res.*, vol. 16, no. 2, pp. 405–416, 2016.
- [7] M. Sammour and Z. Othman, "An Agglomerative Hierarchical Clustering with Various Distance Measurements for Ground Level Ozone Clustering in Putrajaya , Malaysia," *Int. J. Adv. Sci. Eng. Inf. Technol.*, 2016.
- [8] M. Weber et al., "Total ozone trends from 1979 to 2016 derived from five merged observational datasets-the emergence into ozone recovery," *Atmospheric Chemistry and Physics*. 2018.
- [9] K. B. Ensor, B. K. Ray, and S. J. Charlton, "Point source influence on observed extreme pollution levels in a monitoring network," *Atmos. Environ.*, 2014.
- [10] J. A. Adame, A. Notario, F. Villanueva, and J. Albaladejo, "Application of cluster analysis to surface ozone, NO₂ and SO₂ daily patterns in an industrial area in Central-Southern Spain measured with a DOAS system," *Sci. Total Environ.*, 2012.
- [11] S. S. Ahmad and N. Aziz, "Spatial and temporal analysis of ground level ozone and nitrogen dioxide concentration across the twin cities of Pakistan," *Environ. Monit. Assess.*, vol. 185, no. 4, pp. 3133–3147, 2013.
- [12] A. Monteiro et al., "Trends in ozone concentrations in the Iberian Peninsula by quantile regression and clustering," *Atmos. Environ.*, 2012.
- [13] O. Connan, K. Smith, C. Organo, L. Solier, D. Maro, and D. Hébert, "Comparison of RIMPUFF, HYSPLIT, ADMS atmospheric dispersion model outputs, using emergency response procedures, with 85Kr measurements made in the vicinity of nuclear reprocessing plant," *J. Environ. Radioact.*, 2013.
- [14] M. Deng, Q. L. Liu, J. Q. Wang, and Y. Shi, "A general method of spatio-temporal clustering analysis," *Sci. China Inf. Sci.*, vol. 56, no. 10, pp. 1–14, 2013.
- [15] D. Ji et al., "The heaviest particulate air-pollution episodes occurred in northern China in January, 2013: Insights gained from observation," *Atmos. Environ.*, 2014.
- [16] P. Hájek and V. Olej, "Ozone prediction on the basis of neural networks, support vector regression and methods with uncertainty," *Ecol. Inform.*, 2012.
- [17] M. Kandil, A. Gadallah, F. Tawfik, and N. Kandil, "Prediction of Maximum Ground Ozone Levels using Neural Network," *Int. J. Comput. Digit. Syst.*, vol. 218, no. 1224, pp. 1–8, 2014.
- [18] H. Akimoto, Y. Mori, K. Sasaki, H. Nakanishi, T. Ohizumi, and Y. Itano, "Analysis of monitoring data of ground-level ozone in Japan for long-term trend during 1990-2010: Causes of temporal and spatial variation," *Atmos. Environ.*, 2015.
- [19] E. Manzini et al., "Northern winter climate change: Assessment of uncertainty in CMIP5 projections related to stratosphere-troposphere coupling," *J. Geophys. Res. Atmos.*, vol. 119, no. 13, pp. 7979–7998, 2014.
- [20] M. Aghagolzadeh, H. Soltanian-Zadeh, B. Araabi, and A. Aghagolzadeh, "A hierarchical clustering based on mutual information maximization," in *Proceedings - International Conference on Image Processing, ICIP, 2006*.
- [21] A. Bouguettaya, Q. Yu, X. Liu, X. Zhou, and A. Song, "Efficient agglomerative hierarchical clustering," *Expert Syst. Appl.*, 2015.
- [22] S. Salvador and P. Chan, "Toward accurate dynamic time warping in linear time and space," *Intell. Data Anal.*, 2018.
- [23] A. J. Doshi and B. Joshi, "Comparative analysis of Apriori and Apriori with hashing algorithm," *Int. Res. J. Eng. Technol.*, 2018.
- [24] Y. Zhang et al., "Multi-kernel extreme learning machine for EEG classification in brain-computer interfaces," *Expert Syst. Appl.*, vol. 96, pp. 302–310, 2018.
- [25] K. Kuklinska, L. Wolska, and J. Namiesnik, "Air quality policy in the U.S. and the EU – a review," *Atmos. Pollut. Res.*, 2015.
- [26] A. Zare, J. H. Christensen, A. Gross, P. Irannejad, M. Glasius, and J. Brandt, "Quantifying the contributions of natural emissions to ozone and total fine PM concentrations in the northern Hemisphere," *Atmos. Chem. Phys.*, 2014.
- [27] Y. Y. Toh, S. F. Lim, and R. von Glasow, "The influence of meteorological factors and biomass burning on surface ozone concentrations at Tanah Rata, Malaysia," *Atmos. Environ.*, 2013.

Regularization Activation Function for Extreme Learning Machine

Noraini Ismail¹, Zulaiha Ali Othman²

Center for Artificial Intelligence Technology
Faculty of Information Science and Technology
Universiti Kebangsaan Malaysia
Bangi, Selangor, Malaysia

Noor Azah Samsudin³

Jabatan Kejuruteraan Perisian
Fakulti Sains Komputer dan Teknologi Maklumat
Universiti Tun Hussein Onn Malaysia
Parit Raja, Johor, Malaysia

Abstract—Extreme Learning Machine (ELM) algorithm based on single hidden layer feedforward neural networks has shown as the best time series prediction technique. Furthermore, the algorithm has a good generalization performance with extremely fast learning speed. However, ELM facing overfitting problem that can affect the model quality due to the implementation using empirical risk minimization scheme. Therefore, this study aims to improve ELM by introducing an Activation Functions Regularization in ELM called RAF-ELM. The experiment has been conducted in two phases. First, investigating the modified RAF-ELM performance using four types of activation functions are: Sigmoid, Sine, Tribas and Hardlim. In this study, input weight and bias for hidden layers are randomly selected, whereas the best neurons number of hidden layer is determined from 5 to 100. This experiment used UCI benchmark datasets. The number of neurons (99) using Sigmoid activation function shown the best performance. The proposed methods has improved the accuracy performance and learning speed up to 0.016205 MAE and processing time 0.007 seconds respectively compared with conventional ELM and has improved up to 0.0354 MSE for accuracy performance compare with state of the art algorithm. The second experiment is to validate the proposed RAF-ELM using 15 regression benchmark dataset. RAF-ELM has been compared with four neural network techniques namely conventional ELM, Back Propagation, Radial Basis Function and Elman. The results show that RAF-ELM technique obtain the best performance compared to other techniques in term of accuracy for various time series data that come from various domain.

Keywords—Extreme learning machine; prediction; neural networks; regularization; time series

I. INTRODUCTION

Over the past decade, the use of Artificial Neural Networks (ANN) in time series prediction has been grown and evolved [1]. Although basically this technique is biologically inspired, ANN has been successfully implemented in various fields and performed very well [2], especially for the purpose of forecasting and classification. Compared to statistical-based forecasting techniques, the ANN approach has several unique features [3], such as: 1) non-linear and data driven; 2) not for explicit basic model (non-parametric); and 3) more flexible and universal which allowing the model to work with more complex time series. ANN model does not take the statistical data distribution into account because the suitable model is formed adaptively based on the data provided.

Recent discussions on new research in ANN for time series predictions has been presented by [4]. There are various ANN prediction models in literature. The most common and popular ANN are multi-layer perceptron based feedforward hidden layer network. This model has been proposed for non-linear time series forecasting by [5] and the result has overcome traditional statistical methods such as regression and Box-Jenkins approaches. Recurrent neural network based on feedforward hidden layer networks has also been tested for time series forecasting [6]. This model is very dynamic and allows forecasting for non-linear time series from various fields [7], [8]. Although ANN prove predictably well in multiple applications, however, it has some limitations such as black-box based learning [1], over-fitting models and easily trapped in local minimum.

In addition, the Support Vector Machine (SVM) technique also is often used in time series forecasting. It was introduced by [9]. This prediction method based SVM uses the general regression model class, such as Support Vector Regression and Least-Square [10]. SVM can be categorized as Linear, Gaussian or Radial Basis Functions (RBF) [11], polynomials [12], and multi-layer perceptron classifications. For time series prediction [13], linear Support Vector Regression is built by minimizing the risk reduction of the structure (bound to general error) that leading to better predictive performance than conventional techniques.

Due to continuous research, there are many suggestions for improvement on ANN and SVM structures in literature. This is because these techniques play an important role in machine learning and data analysis. However, these two popular techniques face some challenging issues such as slow learning abilities [1]. This is a major constraint in the analysis of time series data. The key factors involved in this problem are the use of slow learning gradient-based algorithm during training process. To address this problem, [14] has introduced a new ANN framework called Extreme Learning Machine (ELM). This technique shows very good performance in predictions and even better than conventional neural network methods, but still exist some shortcomings which need further development and perfection [15]–[17].

Therefore, this research work is an attempt to improve ELM by introducing an Activation Functions Regularization in ELM called RAF-ELM in the context of this paper. This paper is organized as follows. Section II discussed the existing

application using ELM based on literature review. In Section III discussed the proposed ELM and its implementation. Then, the dataset used and the result obtain are given and discussed in Section IV. Moreover, the performance of the investigated model also was analyzed and compared in Section IV. Finally, the paper is concluded in Section V.

II. RELATED WORK

In recent years, ELM has been used in various applications such as signal processing [18], image processing [19], [20], medical diagnosis [21], market analysis [22], aviation and aerospace [23], forecasting [24] and others [25]. In signal processing, [18] has applied the ELM algorithm to identify two different EEG (electroencephalogram) signals. This computer-based system can be used to determine the intention of a paralyzed patient by analyzing the recorded EEG signals from the patient's scalp. This study also uses non-linear character selection algorithms to eliminate less important features in the data set used. Whereas [26] use multiple kernel ELM to classify EEG signals called MKELM. The MKELM method is developed by integrating two types of kernel so that the algorithm can explore additional information from some non-linear feature space effectively for EEG classification. The experimental results confirm that the advantages of MKELM method for the EEG classification related with motor imaging in BCI applications provide high classification accuracy.

Furthermore, the new human face recognition algorithm based on the extraction of the histogram feature gradient and ELM oriented was proposed by [27]. The results show that the proposed algorithm performance is better than SVM and k-nearest neighbors algorithms. Additionally, the proposed algorithm also shows a significant increase in classification accuracy with short training time, one hundred times better and minimum dependence on the number of prototypes. In the same year, [28] proposed an effective ELM-based local scanning area for object recognition called MM-LRF-ELM. Experimental validation on the Washington RGB-D data set illustrates that the proposed combination method achieves better recognition performance. Whereas [19] proposed ELM based on local recruitment areas with three channels called 3C-LRF-ELM. This suggestion algorithm allows the hepatologic features to be automatically diagnose illness using a set of lungs, kidney and spleen image data sets. The study compares two types of neural network layers i.e. using a single and two hidden layer network. The results showed that 3C-LRF-ELM single layer neural network provided better classification performance.

ELM has also been successfully applied in medical diagnosis. Author in [29] proposed a novel hybrid diagnostic system called LFDA-RKELM which integrates character extraction techniques with ELM algorithms for the diagnosis of thyroid disease. The proposed method consists of three stages namely dimension reduction process based on feature extraction; data modeling using the ELM kernel; and lastly, the best classification model is used to perform thyroid disease diagnosis tasks using the most discriminatory subset of feature and optimum parameters. Experimental results indicate that

LFDA-RKELM overcame the basic method. In contrast to the study, [21] improves the ELM algorithm using the competitive swarm optimization technique. The proposed model has been tested based on 15 medical classification datasets. Experimental results show that the proposed model can achieved better generalized performance with smaller hidden neurons and with greater stability. However, it requires more training time than other ELM-based metaheuristic. While [30] submitted an application to predict the Huntington's disease several years earlier based on data from MRI brain scan. Experimental results show that the predictions are realistic with reasonable accuracy provided that the missing values are dealt with caution.

In addition, ELM has also been applied in market analysis, aviation and aerospace, but not so extensive. Market analysis is a documented investigation of company planning activities, in particular results involving inventory, purchasing, expansion or reduction of work, facility expansion, equipment purchasing capital, promotional activities, and many other aspects involving the company. In this domain, [31] has presented a design for stock index movement analysis using the ELM kernel. The findings suggest that the proposed method provides good results. However, researchers found that the ELM kernel needed more CPU resources than RBFN techniques and SVM that led to longer processing times. Next, [32] using ELM to forecast cash outflow for financial institutions. In this study, the ELM algorithm shows good predictive results in terms of accuracy, error rate and processing time. While in the field of aviation and aerospace, [23] has proposed ELM techniques to improve absolute position accuracy and solve complicated modeling and computing problems for aviation drilling robots. The study was carried out by considering the effect of geometric factor and non-geometric factor in building a predictive positional error model using ELM techniques. The results show that the accuracy of the absolute position and the maximum point of the robot center has increased by 75.89% and 80.93%. Finally, ELM is also used to solve problems in environment domain. Author in [33] used the ELM to predict the air quality index in Delhi, India. In the proposed model, the air pollution quality index and the previous day's meteorological conditions are used for predictions. The performance of this proposed model is compared with the existing forecasting system (SAFAR). The results show that ELM provides higher accuracy results than SAFAR.

Based on the state-of-the-art, it can be concluded that past studies have used various techniques in predicting and analyzing time series data. ANN techniques show satisfactory results, better than regular statistical methods. The popular technique in ANN is ELM, BP, RBFN and Elman. This study was focusing on the performance of ELM techniques in various fields. From the literature, it can be seen that ELM technique is able to overcome other ANN techniques. This technique has also been successfully applied in various fields and obtained very satisfactory results. However, this technique has a potential to generate over-fitting models and leads to a less stable when it comes to a certain condition. Therefore, this study proposed to enhance ELM performance. This paper is an extension of a previous study and further explorations of

This research was funded by Ministry of Higher Education using FRGS grant (FRGS/1/2016/ICT02/UKM/02/8).

the proposed enhancement in proceeding paper of International Conference on Intelligent and Interactive Computing entitled “Improved Ozone Pollution Prediction using Extreme Learning Machine with Tribas Regularization Activation Function”.

III. IMPROVED MODEL OF EXTREME LEARNING MACHINE

The ELM algorithm is well known for its fast speed capability and shows good generalization performance. However, ELM has several weaknesses as it tends to produce over-fitting model because ELM is developed based on the Empirical Risk Minimization principles. In addition, ELM also has a weak capacity control because it calculates the min least-square norms directly that may lead to a less robust estimation when dealing with unexpected or outliers. Therefore, this study proposes Activation Functions Regularization in ELM called RAF-ELM based on Structural Risk Minimization scheme that according to statistical learning theory.

In machine learning, the regularization function is defined as a process of introducing additional information to solve the over-fitting problem. Generally, regularization is a technique used for objective functions to solve optimization problems [34]. This optimization problem is a process for achieving ideal results. In addition, optimization can also be defined as a form of optimizing an existing solution, or designing and creating something optimally. Therefore, this study proposes improvements in ELM techniques by adding this regularization to make the activation function more balance and resilient to random non-uniform distribution, thus can improve ELM performance. A formula of RAF-ELM with an added regularization component $R(f)$ to the activation function $f(x)$ can be summarized in equation 1:

$$\sum_{i=1}^n \beta_i [f(z_i) + R(f_i)] = y$$

$$(f) = \lambda \sum_{k=1}^N \theta_k^2 \tag{1}$$

The function of $R(f)$ is added to the activation function $f(z)$. λ is the parameter to impose penalties on the complexity of $f(z)$ to improve the ability of the model to be learned. The parameter value can be adjusted to help the algorithm find the appropriate value for the model. However, if the $R(f)$ value is too small, its function may not do anything and if the value is too large, it can cause under-fit model and loss valuable information. Therefore, the aim of this learning problem is to find the appropriate parameter by predicting the possibility of input (label) and giving a minimum error.

In addition, the number of neurons in hidden layers is varied (usually set at random) and improper value setting will affect the accuracy of results [35]. Therefore, this study will improve the structure of the model by adding a neuron parameter tuning function from [5 to 100] to improve the performance of the ELM algorithm. The resulting models will be evaluated and the number of neurons that perform greatest for the time series data will be identified.

In addition, many recent studies focus only on the use of the Sigmoid activation function, regardless of the performance

of other activation functions such as Sin, Hardlim, and Tribas. This is because the Sigmoid activation function has easier math calculations and always gives excellent results [33]. Therefore, this study will compare the four activation functions of Sigmoid, Sin, Hardlim and Tribas to see the effect of different activation functions on RAF-ELM algorithm performance for time series data. The pseudo code for the RAF-ELM algorithm is shown in Fig. 1. The improvements are in line 16-18 where the regularization function is added to the activation function. The pseudo code for the activation functions of Sigmoid, Sin, Hardlim and Tribas can be seen in Fig. 2.

RAF-ELM Algorithm-Pseudocode

```

1 START
2 Input:
3   Sequence of training data, D = (x,t)
4   Type of activation function, f(x) =      5   Sigmoid, Sine, Tribas,
Hardlim
6   NeuronNum, i = [5,100]
7   Regularization function, j = [0.01,1]
8
9 Initialize input weight, wi and bias, bi
10 randomly
11
12 FOR EACH (int i = 0; i < NeuronNum; i++)
13   Compute the hidden output matrix
14   H(w1,...,wL, x1,...,xN, b1,...,bL)
15
16   FOR (int j = 0; j < NeuronNum; j++) 17   Calculate f(x)
18   END FOR
19
20   Compute output weight based on class
21   label
22
23 END FOR
24 repeat process until stoping condition
25 achieved
26 END
    
```

Fig. 1. Pseudo-Code of the RAF-ELM Algorithm.

```

1  if (func.startsWith("sig")) {
2      for (int j = 0; j < NumberofHiddenNeurons; j++) {
3          for (int i = 0; i < numTestData; i++) {
4              double temp = tempH_test.get(j, i);
5              temp = 1.0f / (1 + Math.exp(-temp));
6              H_test.set(j, i, temp + norm);
7          }
8      }
9  } else if (func.startsWith("sin")) {
10     for (int j = 0; j < NumberofHiddenNeurons; j++) {
11         for (int i = 0; i < numTestData; i++) {
12             double temp = tempH_test.get(j, i);
13             temp = Math.sin(temp);
14             H_test.set(j, i, temp + norm);
15         }
16     }
17 } else if (func.startsWith("hardlim")) {
18     for (int j = 0; j < NumberofHiddenNeurons; j++) {
19         for (int i = 0; i < numTestData; i++) {
20             Random rndom = new Random();
21             double d = rndom.nextBoolean() ? 1 : -1;
22             double temp = tempH_test.get(j, i) * d;
23             temp = (temp >= 0) ? 1 : 0;
24             H_test.set(j, i, temp + norm);
25         }
26     }
27 } else if (func.startsWith("tribas")) {
28     for (int j = 0; j < NumberofHiddenNeurons; j++) {
29         for (int i = 0; i < numTestData; i++) {
30             Random rndom = new Random();
31             double d = rndom.nextBoolean() ? 1 : -1;
32             double temp = tempH_test.get(j, i) * d;
33             temp = (temp >= -1 && temp < 1) ? 0 : 1 - Math.abs(temp);
34             H_test.set(j, i, temp + norm);
    
```

Fig. 2. Pseudo Code of Activation Function.

IV. EXPERIMENT AND RESULT

In ELM, there are four important variables including the number of neurons, the random ranges between the input layer and the hidden layer, the random range of hidden nodes, and the type of activation function. However, this study focuses on two main variables, namely the activation function using RAF and the number of neurons whereas the range between the input layer and the hidden layer, and the range of hidden nodes is determined randomly to maintain the fast learning concept of ELM technique. This is because if all variables are controlled by parameter tuning, the algorithm's learning speed will slow down [36], [37].

To test the effects of activation functions and neuron number on RAF-ELM performance, several experimental sets have been carried out. In this experiment, the parameter tuning of the neuron number in hidden layers is set to [5-100], a random range of values for hidden weights [-1, 1], and a random range of hidden node thresholds [0, 1]. The test variable (i.e., activation function of RAF) is set to Sigmoid, Sin, Hardlim, or Tribas.

For this experiment, the result of the error value obtained was calculated based on MAE. The small MAE values show the best model. This study will also take the processing time into consideration as an efficiency measurement of the model.

A. Dataset

This study is used the air quality data from UCI Machine Learning repository, where data sources are collected by Saverio De Vito from ENEA (National Agency for New Technologies, Energy and Sustainable Economic Development) in Italy. This original UCI data set comprises 9358 records which contain a gas response from multi-sensor devices that used to measure air quality within the city. This multi-sensor device is placed in a highly exposed area with high air pollution. The datasets are recorded from March 2004 to February 2005 (one year) which contains 15 attributes. The air quality estimation problem cannot be well solved with the lost precision over time due to the emergence of sensors drift and concept drifts caused by seasonal influence, human behavior and sensor aging. In our experiment, we mainly solved Carbon Oxide (CO) concentration estimation problem. The result will be compare with the study in [38] that improve Elman network to solve silimilar problem using same dataset.

B. The Effect of different Activation Functions on the Performance of RAF-ELM

Selecting the activation function that corresponds to the algorithm as well as the type of data is very important. Therefore, this study will compare 4 types of activation functions: Sigmoid, Sin, Hardlim and Tribas. Fig. 3 shows the average of the results for the activation function variable where the neuron number parameter setting is set to [5-100], the random range of the hidden weights [-1, 1], and random ranges of hidden node [0, 1].

Average results indicate that Sigmoid gives a smaller error value as a whole with a value of 0.042687 MAE, followed by Tribas (0.043940 MAE), Sin (0.045456 MAE) and Hardlim

(0.102183 MAE). The overall error value for Sigmoid and Tribas is approximately, with a difference of 0.001254 MAE. While Hardlim gives the highest average result with error value of 0.102183 MAE. For processing time, the activation function of Sin shows a shorter time duration than other activation functions with a value of 0.030715 s, Sigmoid with 0.040186 s and followed by Tribas (0.047390 s) and Hardlim (0.049683 s).

C. The Effect of different Number of Neuron on the Performance of RAF-ELM

In this phase, experiments were performed to see the best neurons for the proposed RAF-ELM method. According to [15], the number of neurons has a significant impact on the performance of ELM techniques. Therefore, the appropriate number of neurons should be identified because the determination of arbitrary number of neurons will affect the ELM's performance. The automatic tuning [39] should be used by setting neuron's initial value using additional constructive techniques. This experiment set the number of neurons to [5-100].

Fig. 4 illustrates optimal results for each number of hidden neurons. Based on this figure, the graph shows that the number of neurons that are too small gives poor performance for RAF-ELM forecasting model, while the RAF-ELM model stabilizes when the number of neurons is 35 and above for the activation function of Sigmoid, Sin and Tribas. RAF-ELM forecasting model for the number of neuron 99 for Sigmoid achieves best performance with error value 0.037955137 MAE. In addition, the Tribas activation function is seen to be performing well for the number of neurons 5 to 30 compared to other activation functions and thus providing similar results with the activation function of Sigmoid and Sin for the number of neurons of 31 to 100. This finding is similar in the study by proceeding paper that is mentioned before. However, Tribas activation function does not give an optimal result. While Hardlim provides a stable result for the number of neurons 5 to 100 with a small amount of difference, but unable to outperform other activation functions.

Table I is the summary of optimal error values for all activation fuvtion. Based on the result, it can be seen that the Sigmoid activation function provides optimal results with 0.037955 MAE error value, followed by Sin (0.038087 MAE), Tribas (0.03963 MAE) and Hardlim (0.101762 MAE). The optimal result gives the same result as the overall average value in Fig. 3 where sigmoid activation function is better than other activation functions.

TABLE I. SUMMARY OF OPTIMAL ERROR VALUES FOR ALL ACTIVATION FUNCTION

Activation Function	Num. of Neuron	MAE		Time (s)	
		Train	Test	Train	Test
Sig	99	0.037955	0.037955	15.312	0.014
Sin	97	0.038087	0.038082	14.953	0.014
Hardlim	20	0.101762	0.101285	3.14	0.016
Tribas	75	0.039630	0.039627	11.625	0.015

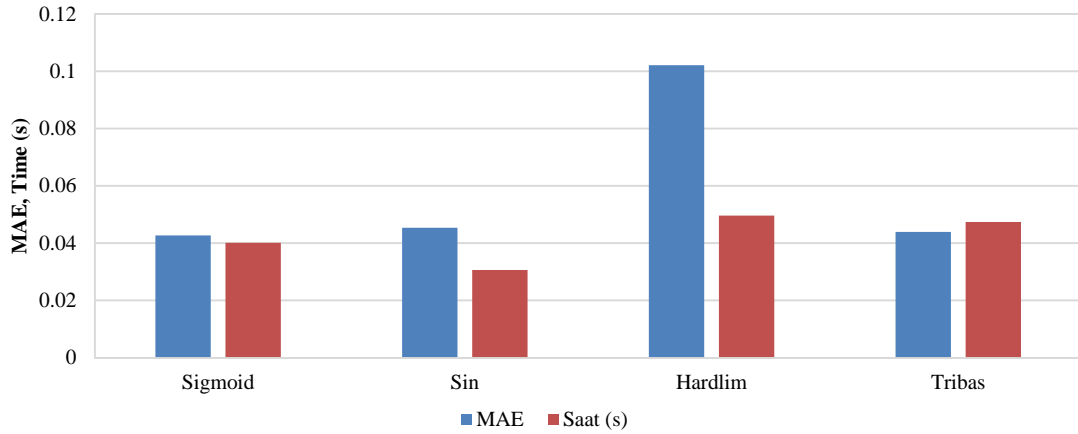


Fig. 3. Comparison of Average Results for four Types of Activation Functions based on MAE Error Rate.

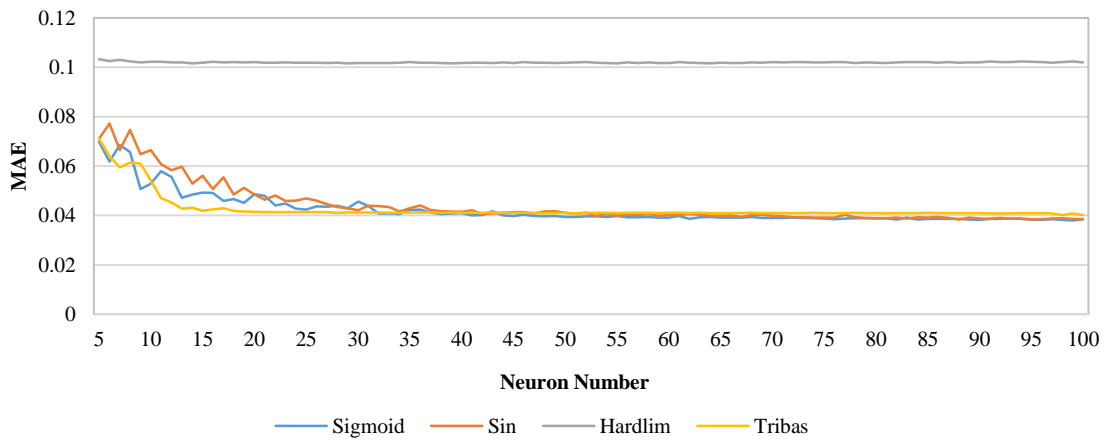


Fig. 4. Comparison of different Neuron Number for four Types of Activation Functions based on MAE Error Rate.

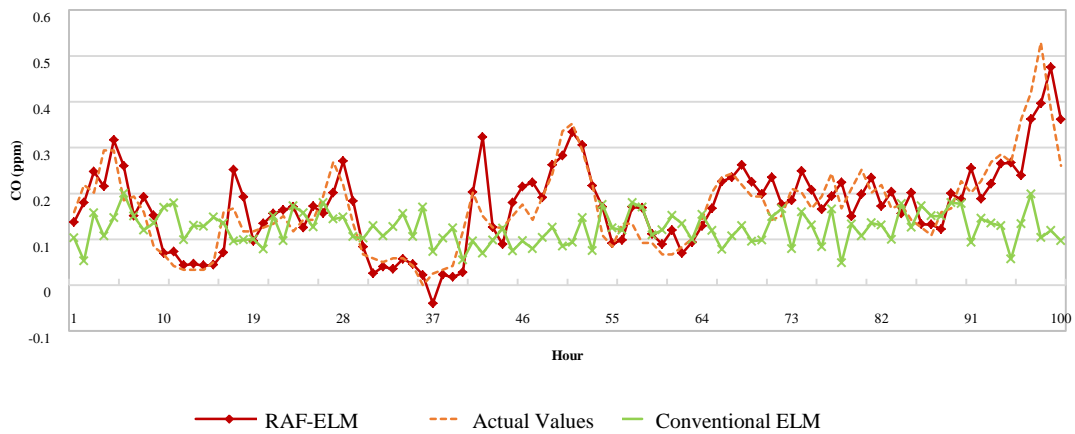


Fig. 5. Comparison of Actual Values with Predictive Values for the Optimal RAF-ELM and Conventional ELM within 100 Hours.

Fig. 5 shows the difference of actual value and predictive value between the optimal RAF-ELM techniques and the conventional ELM techniques. Based on the figure, RAF-ELM technique performs better than the conventional ELM with a small distinction between the non-linear lines of the actual value and the predicted value. Then, t-tests were conducted to see the significant differences between the conventional ELM and RAF-ELM neural network techniques. Table II shows, there was significant difference in the accuracy level of the conventional ELM and RAF-ELM performance ($t = 12.45$; $p < 0.05$).

Compared to previous studies using the same UCI data in forecasting, [38] has improved Elman's neural network technique and obtained better performance from BP techniques and original Elman with 0.0769 MSE results. Whereas, the optimal error rate for RAF-ELM is 0.0415 MSE and 0.03796 MAE. This shows that RAF-ELM technique was able to outperform the improved Elman technique in [38] with a difference of 0.0354 MSE, thus far better than the BP and the traditional Elman technique.

This study has suggested the best predictive techniques of ELM neural network techniques. The discussions on improvements and the selection of variables are described in detail. Proper parameter determination also contributes to good modeling. Therefore, a comprehensive study on the relationship between parameter determinations and performance of the proposed RAF-ELM algorithm is based on two test variables including type of activation function and number of hidden neurons. The results show that the activation function of Sigmoid achieves the best performance in most cases while the number of neurons is found to provide more stable prediction results at values of 35 to 100.

Overall, the forecasting model that provides optimal performance results is the proposed RAF-ELM technique where the activation function is Sigmoid and the number of neurons is 99.

TABLE II. T-TEST RESULT FOR RAF-ELM OVER CONVENTIONAL ELM

	T-test	Significat Level (p)	Significant Status (p<0.05)
RAF-ELM	12.45	<.0001	Yes
ELM			

V. VALIDATION

The validation phase was conducted to verify the effectiveness of proposed RAF-ELM techniques in various data environments.

As previously mentioned, the comparison of technical performance is based on the error result of MAE and processing time. The result of proposed RAF-ELM will be compare with other ANN techniques namely conventional ELM, BP, RBFN and Elman using 15 set of benchmark data have been selected from the OpenML repository (<https://www.openml.org>). Table III shows the list of names and data set information to be used. Based on Table IV, it can be concluded that the RAF-ELM technique provides better results for all sets of benchmark data. In addition, processing time also indicates that the RAF-ELM technique provides better results than BP, RBFN and Elman. This shows that the proposed RAF-ELM technique provides good performance on various time series data that come from various domains.

TABLE III. SPECIFICATION OF REAL-WORLD REGRESSION CASES

No.	Data Sets	Attributes	Total Record
1	SWD	11	1000
2	LEV	5	1000
3	USCrime	14	47
4	Sleuth	7	93
5	Vineyard	3	52
6	Elusage	3	55
7	Machine_cpu	7	209
8	Satellite_image	37	6435
9	GeographicalOriginalofMusic	118	1059
10	Analcatadata_vehicle	5	48
11	Wind	15	6574
12	Pol	49	15000
13	Bodyfat	15	252
14	Pollen	5	3848
15	Houses	9	20640

TABLE IV. PERFORMANCE COMPARISON RESULTS OF RAF-ELM WITH CONVENTIONAL ELM, BP, RBFN AND ELMAN OVER 15 REGRESSION BENCHMARK DATASETS

Data Sets	RAF-ELM		ELM		BP		RBFN		Elman	
	MAE	Time (s)	MAE	Time (s)	MAE	Time (s)	MAE	Time (s)	MAE	Time (s)
SWD	0.250285	0.015	0.328954	0.019	0.5408	1.11	0.5378	0.03	0.5029	0.75
LEV	0.211866	0	0.245896	0.013	0.544	0.31	0.7264	0.02	0.5221	0.47
USCrime	0.443344	0	0.761179	0	20.1735	0.09	23.5787	0	21.7713	0.06
Sleuth	1.052529	0	5.402610	0	57.1175	0.06	65.0199	0.02	84.7826	0.06
Vineyard	0.174844	0	3.017522	0	2.2966	0.03	1.5853	0.8408	2.6887	0.03
Elusage	6.491505	0	6.784657	0	8.4883	0.02	19.3721	0	16.3226	0.02
Machine cpu	2.982449	0.016	0.352996	0	26.4298	0.11	36.1974	0.02	21.1478	0.13
Satellite_image	0.20239	0.031	0.384473	0.07	0.9936	63.91	1.6722	0.75	0.7105	11.7
Geographical Original of Music	0.123212	0	0.176078	0.01	0.5124	99.54	0.7292	0.75	0.4824	5.25
Analcatadata vehicle	0.221790	0	0.534427	0	147.1069	0.02	176.611	0	185.5561	0.03
Wind	0.027079	0.04	0.06120	0.06	2.6852	11.97	3.9969	0.35	2.6666	5.83
Pol	0.373177	0.049	0.776129	0.012	13.9565	251.5	29.2806	3.29	11.6061	33.7
Bodyfat	0.298404	0	0.357808	0.015	0.407	0.47	5.7504	0.4101	0.6772	0.23
Pollen	0.113975	0.032	1.093838	0.019	1.2649	1.31	2.3506	0.17	1.2548	1.8
Houses	0.090348	0.091	0.508891	0.013	46560.93	16.29	91801.7	0.44	53696.89	12.9

VI. CONCLUSION

This study was conducted to suggest the best predictive model for time series data using neural network techniques. In achieving this objective, several sets of experiments have been implemented. The main phase of the experiment is to anticipate improvements to ELM techniques to improve predictive performance. In assessing the performance of a proposed ELM called RAF-ELM, a set of experiments was conducted based on several key variables ie the activation function type, the number of neurons and the value of the controlling function. Based on this experiment, the best forecasting method has been selected. The proposed RAF-ELM method provides an optimal predictive decision on Sigmoid activation function, the number of neurons 99 and the value of escort 0.7. This optimal RAF-ELM method has also been validated through validation experiments on 15 sets of regression data. The results show that the proposed RAF-ELM model provides excellent overall performance results. This proves that the proposed ELM model not only provides good performance on time series data, but also for many other types of data. However, there are several limitations in this study

that require further research. Among the suggestions for future studies is integration of RAF-ELM algorithms with other algorithms or technologies. In recent years, researchers often combine the best features in certain algorithms to improve the efficiency of an algorithm. This method is called hybridization method. Based on previous studies, genetic algorithms and Support Vector Machines often provide good research results and solve problems in various fields. Therefore, the combination of genetic algorithms, Support Vector Machines and RAF-ELM are seen to be able to produce better training models and this study is worth the effort to explore. The second suggestion is expanding the application of RAF-ELM algorithm. Although the ELM technique has the advantage in theory, the use in real-world applications is limited. This is because ELM is a new algorithm compared to other neural network techniques. Therefore, how to effectively implement ELM in daily life is an important aspect of future research.

ACKNOWLEDGMENT

This research was funded by Ministry of Higher Education using FRGS grant (FRGS/1/2016/ICT02/UKM/02/8).

REFERENCES

- [1] N. da Silva, D. Hernane Spatti, R. Andrade Flauzino, L. H. B. Liboni, and S. F. dos Reis Alves, *Artificial Neural Networks*, vol. 26, no. 9, 2017.
- [2] S. Walczak, "Artificial neural networks," in *Encyclopedia of Information Science and Technology*, Fourth Edition, IGI Global, 2018, pp. 120–131.
- [3] Z. Zhang, "Artificial neural network," in *Multivariate Time Series Analysis in Climate and Environmental Research*, Springer, 2018, pp. 1–35.
- [4] A. S. Weigend, *Time series prediction: forecasting the future and understanding the past*. Routledge, 2018.
- [5] A. S. Lapedes, E. W. Steeg, and R. M. Farber, "Use of Adaptive Networks to Define Highly Predictable Protein Secondary-Structure Classes," *Mach. Learn.*, vol. 21, no. 1, pp. 103–124, 1995.
- [6] C. de Groot and D. Würtz, "Analysis of univariate time series with connectionist nets: A case study of two classical examples," *Neurocomputing*, vol. 3, no. 4, pp. 177–192, 1991.
- [7] G. Grudnitski and L. Osburn, "Forecasting S&P and gold futures prices: An application of neural networks," *J. Futur. Mark.*, vol. 13, no. 6, pp. 631–643, 1993.
- [8] C. Kuan and T. Liu, "Forecasting exchange rates using feedforward and recurrent neural networks," *J. Appl. Econom.*, vol. 10, no. 4, pp. 347–364, 1995.
- [9] V. Vapnik, "Support vector machine," *Mach. Learn.*, vol. 20, no. 3, pp. 273–297, 1995.
- [10] R. M. Balabin and E. I. Lomakina, "Support vector machine regression (SVR/LS-SVM) - An alternative to neural networks (ANN) for analytical chemistry? Comparison of nonlinear methods on near infrared (NIR) spectroscopy data," *Analyst*, vol. 136, no. 8, pp. 1703–1712, 2011.
- [11] Caroline Kleist, "Time Series Data Mining Methods: A Review," *Eng. Appl. Artif. Intell.*, vol. 24, no. 533039, p. 61, 2015.
- [12] C. Chatfield, "Time-series forecasting," *Significance*, vol. 2, no. 3, pp. 131–133, 2005.
- [13] L. J. C. L. J. Cao, K. S. C. K. S. Chua, and L. K. G. L. K. Guan, "Combining KPCA with support vector machine for time series forecasting," 2003 IEEE Int. Conf. Comput. Intell. Financ. Eng. 2003. Proceedings., no. 1, pp. 325–329, 2003.
- [14] G. Huang, Q. Zhu, and C. Siew, "Extreme Learning Machine: A New Learning Scheme of Feedforward Neural Networks," *IEEE Int. Jt. Conf. Neural Networks*, vol. 2, pp. 985–990, 2004.
- [15] G. Huang, G. Bin Huang, S. Song, and K. You, "Trends in extreme learning machines: A review," *Neural Networks*, vol. 61, pp. 32–48, 2015.
- [16] S. Ding, H. Zhao, Y. Zhang, X. Xu, and R. Nie, "Extreme learning machine: algorithm, theory and applications," *Artif. Intell. Rev.*, vol. 44, no. 1, pp. 103–115, 2015.
- [17] X. Liu, S. Lin, J. Fang, and Z. Xu, "Is extreme learning machine feasible? A theoretical assessment (Part I)," *IEEE Trans. Neural Networks Learn. Syst.*, vol. 26, no. 1, pp. 7–20, 2015.
- [18] H. Zhao, X. Guo, M. Wang, T. Li, C. Pang, and D. Georgakopoulos, "Analyze EEG signals with extreme learning machine based on PMIS feature selection," *Int. J. Mach. Learn. Cybern.*, vol. 9, no. 2, pp. 243–249, 2018.
- [19] J. Fang, X. Xu, H. Liu, and F. Sun, "Local receptive field based extreme learning machine with three channels for histopathological image classification," *Int. J. Mach. Learn. Cybern.*, pp. 1–11, 2018.
- [20] J. X. Tang, C. W. Deng, G. B. Huang, and B. J. Zhao, "Compressed-Domain Ship Detection on Spaceborne Optical Image Using Deep Neural Network and Extreme Learning Machine," *Ieee Trans. Geosci. Remote Sens.*, vol. 53, no. 3, pp. 1174–1185, 2015.
- [21] M. Eshtay, H. Faris, and N. Obeid, "Improving Extreme Learning Machine by Competitive Swarm Optimization and its application for medical diagnosis problems," *Expert Syst. Appl.*, vol. 104, pp. 134–152, 2018.
- [22] P. P. Das, R. Bisoi, and P. K. Dash, "Data decomposition based fast reduced kernel extreme learning machine for currency exchange rate forecasting and trend analysis," *Expert Syst. Appl.*, vol. 96, pp. 427–449, 2018.
- [23] P. Yuan, D. Chen, T. Wang, S. Cao, Y. Cai, and L. Xue, "A compensation method based on extreme learning machine to enhance absolute position accuracy for aviation drilling robot," *Adv. Mech. Eng.*, vol. 10, no. 3, p. 1687814018763411, 2018.
- [24] Z. M. Yaseen et al., "Predicting compressive strength of lightweight foamed concrete using extreme learning machine model," *Adv. Eng. Softw.*, vol. 115, pp. 112–125, 2018.
- [25] M. Alizamir, O. Kisi, and M. Zounemat-Kermani, "Modelling long-term groundwater fluctuations by extreme learning machine using hydro-climatic data," *Hydrol. Sci. J.*, vol. 63, no. 1, pp. 63–73, 2018.
- [26] Y. Zhang et al., "Multi-kernel extreme learning machine for EEG classification in brain-computer interfaces," *Expert Syst. Appl.*, vol. 96, pp. 302–310, 2018.
- [27] S. Naik and R. P. K. Jagannath, "GCV-Based Regularized Extreme Learning Machine for Facial Expression Recognition," in *Advances in Machine Learning and Data Science*, Springer, 2018, pp. 129–138.
- [28] H. Liu, F. Li, X. Xu, and F. Sun, "Multi-modal local receptive field extreme learning machine for object recognition," *Neurocomputing*, vol. 277, pp. 4–11, 2018.
- [29] C. Ma, J. Guan, W. Zhao, and C. Wang, "An Efficient Diagnosis System for Thyroid Disease Based on Enhanced Kernelized Extreme Learning Machine Approach," in *International Conference on Cognitive Computing*, 2018, pp. 86–101.
- [30] E. Eirola, A. Akusok, K.-M. Björk, H. Johnson, and A. Lendasse, "Predicting Huntington's Disease: Extreme Learning Machine with Missing Values," in *Proceedings of ELM-2016*, Springer, 2018, pp. 195–206.
- [31] X. Li et al., "Empirical analysis: stock market prediction via extreme learning machine," *Neural Comput. Appl.*, 2016.
- [32] J. Xue, S. H. Zhou, Q. Liu, X. Liu, and J. Yin, "Financial time series prediction using t2,1RF-ELM," *Neurocomputing*, 2017.
- [33] M. Bisht and K. R. Seeja, "Air pollution prediction using extreme learning machine: A case study on Delhi (India)," vol. 79, 2018.
- [34] W. Zaremba, I. Sutskever, and O. Vinyals, "Recurrent Neural Network Regularization," *Iclr*, no. 2013, pp. 1–8, 2014.
- [35] W. Cao, J. Gao, Z. Ming, and S. Cai, "Some Tricks in Parameter Selection for Extreme Learning Machine," in *IOP Conference Series: Materials Science and Engineering*, 2017, vol. 261, no. 1.
- [36] J. Bergstra, JAMESBERGSTRA and U. Yoshua Bengio, "Random Search for Hyper-Parameter Optimization," *J. Mach. Learn. Res.*, 2012.
- [37] M. Williams et al., *Numerical Optimization*. 2013.
- [38] G. Mei, H. Zhang, and B. Zhang, "Improving Elman neural network model via fusion of new feedback mechanism and Genetic Algorithm," in *Progress in Informatics and Computing (PIC)*, 2016 International Conference on, 2016, pp. 69–73.
- [39] G.-B. Huang, H. Zhou, X. Ding, and R. Zhang, "Extreme learning machine for regression and multiclass classification.," *IEEE Trans. Syst. Man. Cybern. B. Cybern.*, 2012.

Energy-Aware Routing Hole Detection Algorithm in the Hierarchical Wireless Sensor Network

Najm Us Sama¹, Kartinah Bt Zen², Atiq Ur Rahman³, Aziz Ud Din⁴

Faculty of Computer Science and Information Technology, Universiti Malaysia Sarawak, 94300 Kota Samarahan, Sarawak¹

College of Computer and Information Sciences, Jouf University, Saudi Arabia¹

Faculty of Computer Science and Information Technology, Universiti Malaysia Sarawak, 94300 Kota Samarahan, Sarawak²

Faculty of Computing and Information Technology, Northern Border University, Rafha, Saudi Arabia³

Shaikh Zayed Islamic Center, University of Peshawar, Pakistan⁴

Abstract—To minimize the communication overhead with the help of optimal path selection in Wireless Sensor Network (WSN) routing protocols is the challenging issue. Hierarchical routing optimizes energy utilization by distributing the workload among different clusters. But many-to-one multi-hop hierarchical routing will result in the excessive expenditure of energy near the sink and leads to early energy exhaustion of the nodes. Due to this, the routing hole problem can be caused around the base station. Data routed along the hole boundary nodes will lead to premature exhaustion of energy. This will maximize the size of the hole in the network. Detection of holes saves the additional energy consumption around the hole and minimize the hole size. In this paper a novel energy efficient routing hole detection (EEHD) algorithm is presented, on the detection of routing hole, the periodic re-clustering is performed to avoid the long detour path. Extensive simulations are done in MATLAB, the results reveal that EEHD has better performance than other conventional routing hole detection techniques, such as BCP and BDCIS.

Keywords—Wireless sensor network; routing protocol; hierarchical routing; routing hole problem; routing hole detection

I. INTRODUCTION

Routing in sensor networks is an active research topic and the responsibility of routing protocol is to enable the sensor nodes to select routes among the source node and sink node [1]. Energy balancing is always the main goal in sensor networks. Some applications might be very harsh, and very unlikely to renew or recharge the batteries of nodes in the sensor network. Thus, in a sensor network is non-renewable battery provision is the most challenging issues. It is a dire need to develop energy-efficient routing strategies that minimize power requirements at the overall network. Because unbalanced energy consumption will lead to routing hole problems, which is one of the most challenging issues in the communication process. Routing hole acts as an obstacle to communication and also known as "communication voids" [2, 3] and results in network partitioned. Much research has been done for detection, avoidance, and mitigation of routing hole problems [4-7].

Many kinds of literature used the cluster based technique to achieve energy efficiency and energy balancing [8-10] but in multi-hop clustering, the cluster heads have to transmit its own data as well as forward the data of other CHs. Due to the dual

load, the lifetime of CH becomes lesser than others and leads to routing hole problem. Data routed along the hole boundary nodes will lead to premature exhaustion of energy of hole boundary nodes. This will maximize the size of the hole in the network. Detection of holes saves the additional energy consumption around the hole and minimize the hole size. It assures longer network lifetime and efficient use of nodes. Routing hole detection is the only solution to avoid the long detour. The routing hole should be detected in advance before to start the data transportation phase, and the nodes placed on the boundary of the hole announced the hole information to its neighbor nodes. Hence the long detour path can be avoided.

A novel energy efficient routing hole detection (EEHD) algorithm is presented, which compare the energy of cluster head (CH) with a threshold value and advertises itself as a critical node if the energy is equal or lower than the threshold. And the critical node is known as the routing hole in a network. When the routing hole is detected the algorithm performs periodic re-clustering to avoid the long detour path. The causes of routing hole are presents and some of the strategies from research for routing hole detection, avoidance and mitigation are also discussed.

The rest of the paper is categorized as follows. The background and causes of routing hole problems have been presented in Section 2. A novel routing hole detection algorithm is illustrated in Section 3. Section 4 presents the performance discussion. At last, the conclusion is summarized in Section 5, followed by References.

II. ROUTING HOLE PROBLEM

In literature, existing routing protocols may lead to routing hole problem due to some inefficiency of routing technique. A routing hole consists of an area in the sensor network where a group of sensor nodes stop functioning or disconnected from the network and do not participate in the routing of the data [11]. The routing holes are caused by the failure of sensor nodes such as defect, battery exhaustion or external event damage.

A. Causes of Routing Hole Problem

The routing holes can be caused by a few reasons, which are the failure of sensor nodes in a random deployment, lack of coverage and inefficient routing protocol.

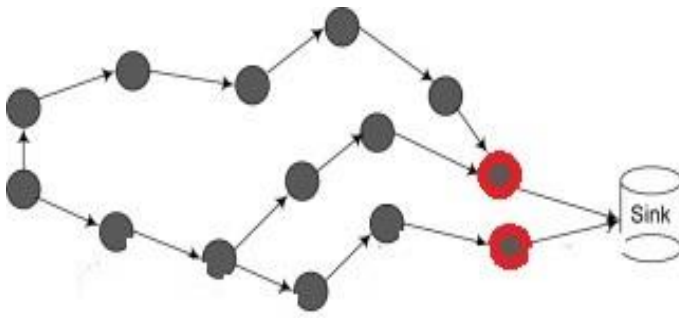


Fig. 1. Routing Hole Due to Random Deployment.

In random deployment, many-to-one multi-hop data routing pattern results in quicker loss of energy of nodes near the sink; this is referred to as routing hole problem.

As shown in Fig. 1 random deployment of nodes in wireless sensor networks, may lead to serious coverage overlapping among the nodes and due to critical nodes the network may suffer coverage hole problems. The presence of coverage-hole in the network area means that every point in the interested region is not being covered[12]. Coverage hole problem causes the network partitioned which leads to routing hole problem. In Fig. 2 the sensor node 2 is dying out, the area is now not covered by any sensor nodes and sensor node 1 cannot send its sense data to sensor node 3.

Routing holes also can be caused by energy unaware routing as shown in Fig. 3. In multi-hop cluster based routing algorithm the sensor nodes send its sense data to CH, then CH will send the aggregated data to its neighboring CH and so on till the packets received by the sink. But routing hole may occur because the CH near to base station has a maximum workload or due to worst path selection routing technique [13].

As regards the above-mentioned important challenge in WSNs, avoiding the routing hole problem is considered to be a crucial challenge for such networks and should definitely be taken into account. Many types of research have done on routing hole mitigation [14-23].

Routing hole detection is important because data routed along the hole boundary will lead to early exhaustion of energy at the boundary nodes. Early detection of holes avoids the additional energy consumption around the hole boundary and minimize the hole size. This pro-active early detection assures long network lifetime and nodes to be more energy efficient.

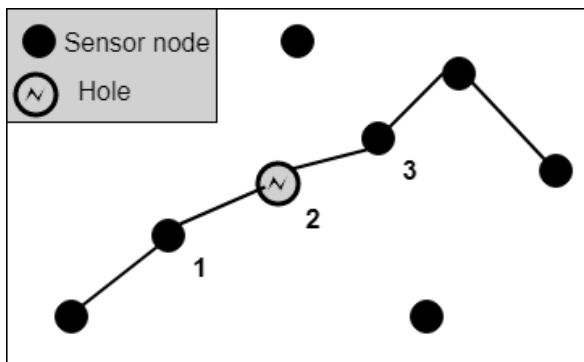


Fig. 2. Routing Hole Due to Lack of Coverage.

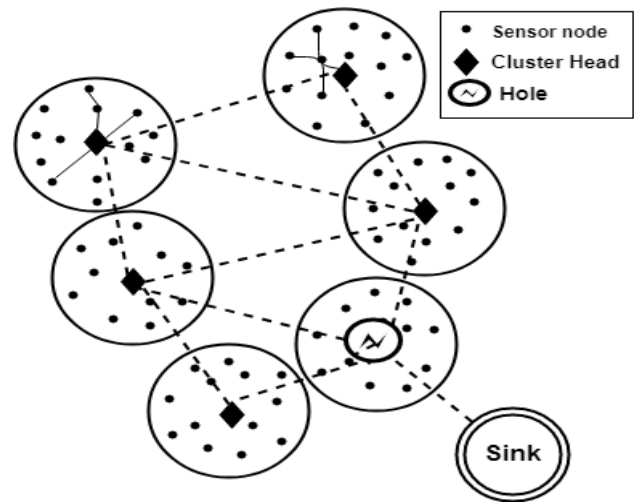


Fig. 3. Routing Hole in Multi-Hop Hierarchical WSN.

Authors in [24] proposed a distributed solution to detect the holes and their boundaries (BDCIS) in WSN. In the first step, each node collects connectivity information and builds its one-hop neighbors graph. In the second step independent sets are established, and then connect the independent sets in order to choose the best path in the last step. The simulation shows that this algorithm achieves enhanced performance in terms of minimum energy depletion, accuracy, and less communication overhead. Each node needs to share the connectivity information to construct independent sets from one-hop neighbor's graph, which make the proposed solution inefficient in terms of energy consumption. Coverage Protocol (BCP) is presented by authors in [25] that preserves both border and area coverage. The proposed strategy supposes that every node in the network has four sides. Simulation results illustrate that BCP achieves a high coverage ratio by replacing the border nodes with transfer nodes, but it has the extra overhead to find out the transfer nodes and then replace it. The recognition of the four sides of every node is the main drawback of BCP. The BDCIS and BCP are assisted as a comparison in the proposed work because these are an energy efficient routing hole detection algorithm with some deficiencies as discussed above.

Unfortunately, the time or space complexity of these existing algorithms is higher. The routing hole detection is necessary to avoid the long detour path, which is caused by forwarding packets via the hole boundary node. Hence, there is a dire need to detect a routing hole with less time and space complexity. A novel energy efficient routing hole detection (EEHD) is proposed for balanced energy consumption and less computational overhead.

III. ENERGY EFFICIENT ROUTING HOLE DETECTION (EEHD) ALGORITHMS

In proposed work, the sensor nodes are considered to have limited energy and can sense their own residual energy and all the nodes of the sensor network are equipped with the same amount of energy level in the beginning. Base Station (BS) is without energy restriction, but far away from the area of sensor nodes. All sensor nodes are static and have the same capabilities, just a subset of deployed sensor nodes is designed as CHs. In this architecture, multi-hop clustering is applied to

communicate with the BS. Sensor nodes sense the environment at a fixed rate and always have data to send to the BS. The energy required for transmitting a message is the same for all nodes because the radio channel is symmetric. It is required that every sensor node, with a unique identification number (ID), can monitor its own battery power level. CH performs data aggregation and sends the compressed data to BS via multi-hop as shown in Fig. 4.

The routing hole should be detected in advance before to start the data transportation phase, and the nodes placed on the boundary of the hole announced the hole information to its neighbor nodes. Hence the long detour path can be avoided.

Many detection techniques are presented in the literature which detects the boundary nodes to avoid the long detour path. But each has its weaknesses like computational overhead and maximum energy consumption. To avoid these drawbacks the proposed routing hole detection algorithm sets a threshold value for detecting the hole. CH mark itself as unavailable once its local energy fall behind a threshold. Then CH advertises itself as a critical node to its neighbor and re-clustering will take place. First, to start data transportation phase the routing hole is detected in advance, then the nodes located on the boundary of the hole advertises the hole information to its neighbor nodes. Hence the long detour route can be avoided for communication. The proposed routing hole detection algorithm detects the routing hole by the required energy threshold E_{Thr} . If the energy of CH is less than E_{Thr} , identified itself as routing hole and re-clustering will be done by the neighbor nodes of the hole. In order to heal the routing hole problem, the periodic re-clustering is necessary across all nodes.

According to EEHD flowchart shown in Fig. 6 before to start the transportation of data, each CH will calculate and compare its energy with the threshold value. The CH will advertise itself as a routing hole if its energy is equal or less than to the threshold.

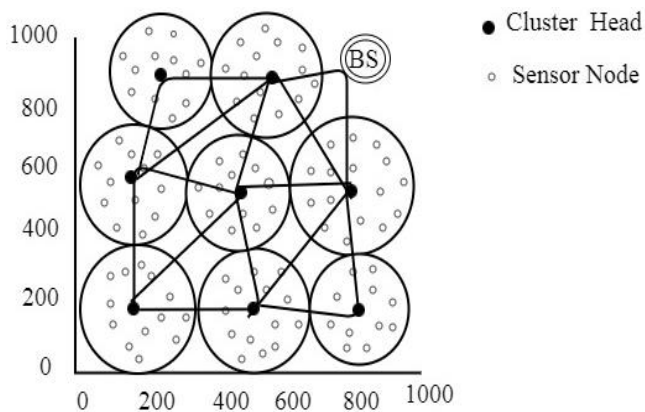


Fig. 4. Multi-Hop Clustering WSN.

A. An Example Scenario of EEHD

The routing hole detection algorithm can be better understood if we take the scenario for description. Let us take an example network of four CH's C1, C2, C3, and C4 as shown in Fig. 5.

The energy levels and member sensor nodes of each CH are given in Table I below. The energy level of CH's after every transportation is also given in Table I. The threshold value is supposed to be 1. After each transportation of packet, the CH will compare its energy with the threshold value if it's equal to 1, the CH will advertise itself as a routing hole and trigger the re-clustering. As we observe in Table I that after 3rd iteration the cluster head C3 energy level is 1 which is equal to the threshold. Hence C3 will advertise itself as a routing hole.

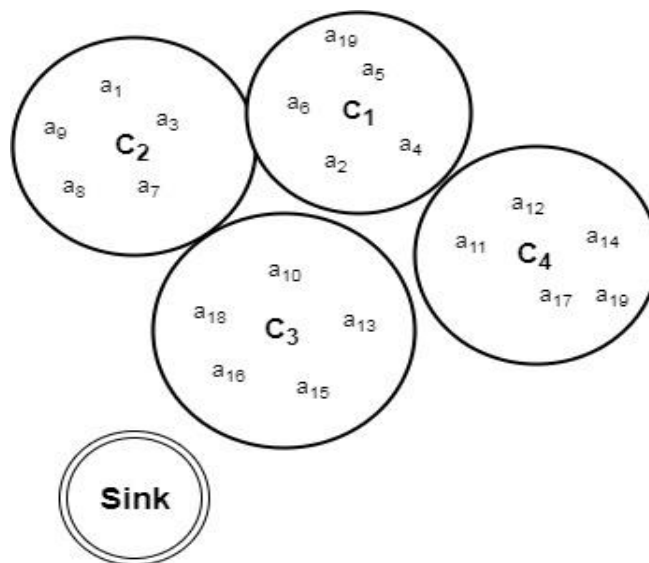


Fig. 5. EEHD Example Scenario.

TABLE I. ENERGY LEVEL OF CH'S

Cluster Heads	Energy	Neighbors	CH energy at each iteration of transportation		
			1st	2nd	3rd
C1	5	a2, a4, a5, a6	4	3	2
C2	6	a1, a3, a7, a8, a9	6	4	2
C3	4	a10, a13, a15, a16, a18	4	3	1
C4	8	a11, a12, a14, a17	8	7	5

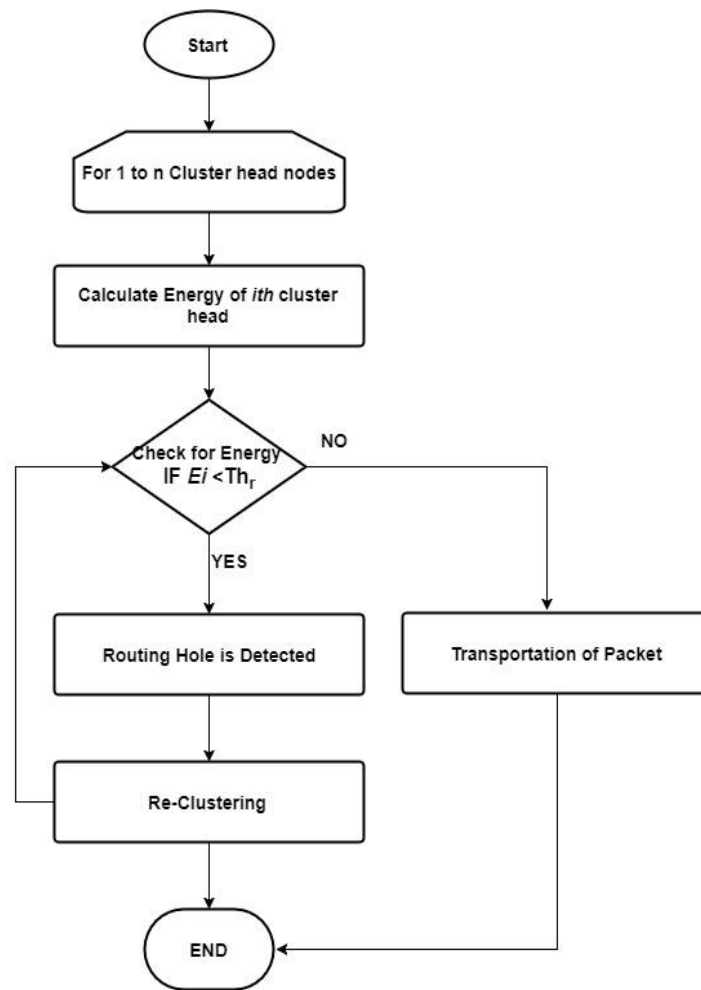


Fig. 6. Flowchart for Routing Hole Detection.

IV. PERFORMANCE DISCUSSION

In this section, the performance of proposed EEHD is evaluated on the basis of computation overhead, hole detection time, energy consumption and detection rate of holes. The proposed algorithm is compared with other existing hole detection algorithms such as BCP [25] and BDCIS [24]. The proposed algorithm is evaluated by answering the following questions:

- **Simulation Setup:** To explore the performance of the proposed detection algorithm, we generate a sensor network comprising of randomly deployed nodes and carry out extensive simulations in MATLAB R2014b. Random data traffic was generated from the sensor nodes having a transmission range of 150 meters and the sink node was kept outside of the topology.
- **Performance Metrics:** For assessment of the performance of the proposed routing hole detection algorithm, a set of performance metrics is used such as detection time, energy consumption and computation overhead. For best performance, a strategy is needed that uses the sensor nodes energy in a uniform manner, with minimum detection time and less computation overhead.

The simulation results are compared with existing detection techniques on the above-mentioned performance metrics are shown in figures.

A. Hole Detection Time

The proposed routing hole detection algorithm is evaluated by hole detection time as compared to other existing hole detection strategies like BCP and BDCIS shown in Fig. 7. The hole detection time of the proposed routing hole detection algorithm is minimum as compared to BCP and BDCIS. The hole detection time of BCP is less than BDCIS because the computation overhead BDCIS is more than BCP. However, in all three protocols, the hole detection time is increased with the increase in the number of holes.

For 10 holes, the detection time of a BCP and BDCIS is about 4200 and 3900 simulation seconds respectively, and for the proposed EEHD algorithm, it is about 3000 simulation seconds. There is a considerable decrease as compared to other detection strategies. The same decrease of time can be observed for 20 holes, i.e. 1000 simulation seconds. And for 30 holes the detection time of the proposed EEHD algorithm decreases about 1300 simulation seconds.

B. Energy Consumption

In this section, the energy consumption of proposed routing hole detection is compared with other detection techniques such as BCP and BDCIS as shown in Fig. 8. BCP has less energy consumption than BDCIS because every node receives only one message from its immediate neighbors to build its Localized Voronoi Polygons (LVP) and the minimum energy consumption is recorded for our proposed routing hole detection algorithm because it's don't need any computation like BDCIS or neighbor node information BCP.

For 10 holes, the energy consumption of a BCP and BDCIS is about 43 and 38 Joules while for the proposed EEHD algorithm, it is about 30 Joules. There is a considerable decrease in the energy consumption rate as compared to other detection strategies. The 10 Joules decrease in energy consumption can be noticed for 20 holes. As compared to BCP and BDCIS, for 30 holes the energy consumption rate of the proposed EEHD algorithm is decreased about 13 Joules.

C. Computation Overhead

The BCP has extra overhead to find out the transfer nodes and then replace with border nodes. Tow messages have to send by every node in BDCIS strategy, one for the neighbor node checking while the other contains the list of neighbor nodes. Hence, the computation overhead of BDCIS is more than BCP. It can be observed in Fig. 9 that our proposed EEHD algorithm has the lowest computation overhead because it just depends on one comparison of energy with the threshold.

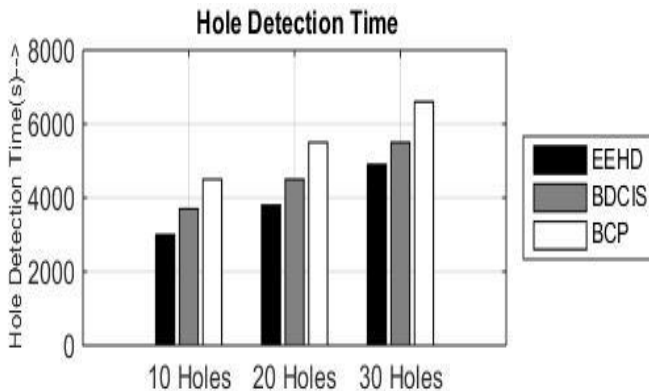


Fig. 7. Comparison of Routing Hole Detection Time.

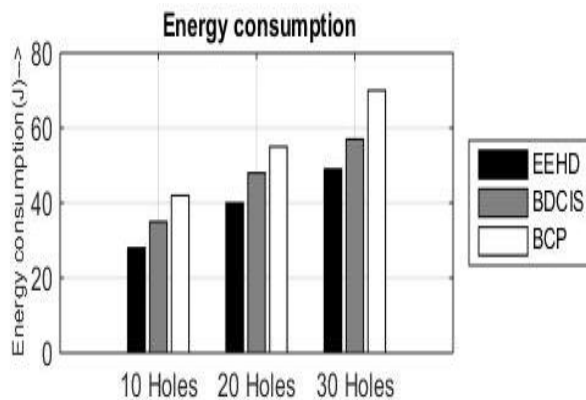


Fig. 8. Comparison of Average Energy Consumption.

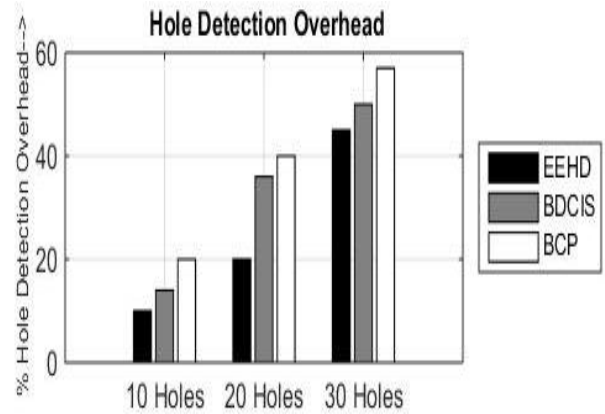


Fig. 9. Hole Detection Overhead.

For 10 holes, the detection overhead of proposed EEHD algorithm is 10% and 15% less from BDCIS and BCP, respectively. There is a considerable decrease in overhead as compared to other detection strategies. As compared to BCP and BDCIS, for 30 holes the overhead of the proposed EEHD algorithm is decreases by about 13%.

V. CONCLUSION

An energy efficient routing hole detection algorithm is proposed in which the energy of each CH is compared with threshold if the energy level of CH is equal to the threshold, CH will advertise itself as routing hole and member nodes will call to the re-clustering algorithm. Prior to the detection of the holes, it is assumed that the construction of clusters has been performed.

Simulation results show enhancement of the proposed detection algorithm in the comparison of existing routing holes detection techniques, such as BDCIS and BCP. It is proven that the proposed EEHD algorithm able to detect holes with less time and computational complexity, thus consumed minimum energy.

REFERENCES

- [1] Y. Ge, S. Wang, and J. Ma, "Optimization on TEEN routing protocol in a cognitive wireless sensor network," *EURASIP Journal on Wireless Communications and Networking*, vol. 2018, p. 27, February 01 2018.
- [2] N. Ahmed, S. S. Kanhere, and S. Jha, "The holes problem in wireless sensor networks: a survey," *SIGMOBILE Mob. Comput. Commun. Rev.*, vol. 9, pp. 4-18, 2005.
- [3] G. Ahmed, N. M. Khan, and M. M. Y. Masood, "A dynamic transmission power control routing protocol to avoid network partitioning in wireless sensor networks," in *Information and Communication Technologies (ICT)*, 2011 International Conference on, 2011, pp. 1-4.
- [4] P. Kumar Sahoo, M.-J. Chiang, and S.-L. Wu, "An Efficient Distributed Coverage Hole Detection Protocol for Wireless Sensor Networks," *Sensors* (Basel, Switzerland), vol. 16, p. 386, 03/17 12/21/received 03/11/accepted 2016.
- [5] P. Antil and A. Malik, "Hole Detection for Quantifying Connectivity in Wireless Sensor Networks: A Survey," *Journal of Computer Networks and Communications*, vol. 2014, p. 11, 2014.
- [6] H. Huang, H. Yin, G. Min, X. Zhang, W. Zhu, and Y. Wu, "Coordinate-Assisted Routing Approach to Bypass Routing Holes in Wireless Sensor Networks," *IEEE Communications Magazine*, vol. 55, pp. 180-185, / 2017.
- [7] A. Debnath and M. K. Debbarma, "Energy efficient-dynamic and self-optimized routing in a wireless sensor network based on ant colony

- optimization," *International Journal of Networking and Virtual Organisations*, vol. 20, pp. 184-194, 2019.
- [8] J. Wang, Y. Gao, W. Liu, A. K. Sangaiah, and H.-J. Kim, "An Improved Routing Schema with Special Clustering Using PSO Algorithm for Heterogeneous Wireless Sensor Network," *Sensors*, vol. 19, p. 671, 2019.
- [9] K. A. Darabkh, M. Z. El-Yabroudi, and A. H. El-Mousa, "BPA-CRP: A balanced power-aware clustering and routing protocol for wireless sensor networks," *Ad Hoc Networks*, vol. 82, pp. 155-171, 2019.
- [10] A. V. Bharathy and V. Chandrasekar, "A Novel Virtual Tunneling Protocol for Underwater Wireless Sensor Networks," in *Soft Computing and Signal Processing*, ed: Springer, 2019, pp. 281-289.
- [11] J. G. Q. Fang, and L. Guibas., "Locating and bypassing routing holes in sensor networks," *Mobile networks and applications*, vol. 11, pp. 187-200, 2006.
- [12] P. K. Sahoo and L. Wei-Cheng, "HORA: A Distributed Coverage Hole Repair Algorithm for Wireless Sensor Networks," *Mobile Computing, IEEE Transactions on*, vol. 14, pp. 1397-1410, 2015.
- [13] J. Yu, Y. Qi, G. Wang, and X. Gu, "A cluster-based routing protocol for wireless sensor networks with nonuniform node distribution," *AEU - International Journal of Electronics and Communications*, vol. 66, pp. 54-61, 2012.
- [14] A. U. Rahman, A. Alharby, H. Hasbullah, and K. Almuzaini, "Corona-based deployment strategies in wireless sensor network: A survey," *Journal of Network and Computer Applications*, vol. 64, pp. 176-193, 2016.
- [15] H. A. Hashim, B. O. Ayinde, and M. A. Abido, "Optimal placement of relay nodes in wireless sensor network using artificial bee colony algorithm," *Journal of Network and Computer Applications*, vol. 64, pp. 239-248, 2016.
- [16] C. Sha, H. Chen, C. Yao, Y. Liu, and R.-c. Wang, "A Type of Energy Hole Avoiding Method Based on Synchronization of Nodes in Adjacent Annuluses for Sensor Network," *International Journal of Distributed Sensor Networks*, vol. 2016, p. 14, 2016.
- [17] P. Kumar Sahoo, M. J. Chiang, and S. L. Wu, "An Efficient Distributed Coverage Hole Detection Protocol for Wireless Sensor Networks," *Sensors*, vol. 16, 2016.
- [18] W. An, N. Qu, F.-M. Shao, X. Xiong, and S. Ci, "Coverage hole problem under sensing topology in flat wireless sensor networks," *Wireless Communications and Mobile Computing*, vol. 16, pp. 578-589, 2016.
- [19] K. Latif, N. Javaid, A. Ahmad, Z. A. Khan, N. A. Alrajeh, and M. I. Khan, "On energy hole and coverage hole avoidance in underwater wireless sensor networks," *IEEE Sensors Journal*, vol. PP, pp. 1-1, 2016.
- [20] K. N. Kannan and B. Paramasivan, "Development of Energy-Efficient Routing Protocol in Wireless Sensor Networks Using Optimal Gradient Routing with On Demand Neighborhood Information," *International Journal of Distributed Sensor Networks*, vol. 2014, p. 7, 2014.
- [21] M. M. Umar, N. Alrajeh, and A. Mehmood, "SALMA: An Efficient State-Based Hybrid Routing Protocol for Mobile Nodes in Wireless Sensor Networks," *International Journal of Distributed Sensor Networks*, vol. 2016, p. 11, 2016.
- [22] J. Yang, Z. Fei, and J. Shen, "Hole detection and shape-free representation and double landmarks based geographic routing in wireless sensor networks," *Digital Communications and Networks*, vol. 1, pp. 75-83, 2015/02/01/ 2015.
- [23] A. Zahedi and F. Parma, "An energy-aware trust-based routing algorithm using gravitational search approach in wireless sensor networks," *Peer-to-Peer Networking and Applications*, pp. 1-10, 2019.
- [24] R. Beghdad and A. Lamraoui, "Boundary and holes recognition in wireless sensor networks," *Journal of Innovation in Digital Ecosystems*, vol. 3, pp. 1-14, 2016/06/01/ 2016.
- [25] A. Dabba and R. Beghdad, "BCP: A Border Coverage Protocol for wireless sensor networks," in *Science and Information Conference (SAI)*, 2014, 2014, pp. 632-640.

Microsatellite's Detection using the S -Transform Analysis based on the Synthetic and Experimental Coding

Soumaya Zribi¹

University of Tunis El Manar
SITI Laboratory National School of Engineers of Tunis
BP 37, le Belvédère, 1002, Tunis
Tunisia

Imen Messaoudi²

University of Carthage, Higher Institute of Information
Technologies and Communications
(ISTIC) Industrial Computing Department
Tunisia

Afef Elloumi Oueslati³

University of Carthage
National School of Engineers of Carthage (ENICarthage)
Electrical Engineering Department
Tunisia

Zied Lachiri⁴

University of Tunis El Manar
SITI Laboratory National School of Engineers of Tunis
BP 37, le Belvédère, 1002, Tunis
Tunisia

Abstract—Microsatellite in genomic DNA sequence, or Short tandem repeat (STR). It is a class of tandem repeat that have repeated pattern with size of 2- 6 base-pairs adjacent to each other. The detection of the specific tandem repeat is an important part of genetic diseases identification and it is also used in DNA fingerprinting and in evolutionary studies. Many tools based on string matching have been developed to detect microsatellites. However, these tools are based on prior information about repetitions in the sequence which cannot be always obtainable. For this, the signal processing techniques were suggested to overcome the limitations of the bioinformatic tools. In this paper, we use a new variant of the S-Transform which we apply to short tandem repeats signals. These signals are firstly obtained by applying different coding techniques to the DNA sequences. To further study the performance of the proposed method, we establish a comparison with different bioinformatics approaches (TRF, Mreps, Etandem) and three other methods of signal processing: The Adaptive S-Transform (AST), the Empirical Mode and Wavelet Decomposition (EMWD) and the Parametric Spectral Estimation (PSE) considering the AR model. This study indicates that our approach outperforms the earlier methods in identifying the short tandem repeat, in fact, our method detects the exact number and positions of trinucleotides present in the tested real DNA sequence.

Keywords—DNA sequence; microsatellites; synthetic and experimental coding; s-transform; bioinformatic tools; Empirical Mode and Wavelet Decomposition (EMWD); Parametric Spectral Estimation (PSE)

I. INTRODUCTION

Computational analysis of the DNA sequences is a fundamental subject, which aims to understand the biological functionality of all living organisms. A particular attention was turned to microsatellites, which ensure many biological functions. In fact, they are implicated in cell metabolism, mismatch repair system [1], regulation of chromatin

organization [2], genes activity and in many other functions [3].

A microsatellite sequence, also called Short Tandem Repeat (STR), represents two or more adjacent copies of a short nucleotide pattern unit [4]. The STR is defined by a specific period (pattern unit). The microsatellite's period is typically between 2 and 6 nucleotides per unit appointed di-, tri-, tetra-, penta- and hexa-nucleotides, respectively [5]. These elements (STRs) have a length less than 150 base pair [6]. Microsatellites considerably occur at different locations within the organism genome. They are very redundant, reduced and dispersed therefore, microsatellites are detected through automatic tools due to their importance on the one hand, for the human genome; approximately 10% of the DNA consists of microsatellites [7]. This special repeat can be a direct cause of many human diseases such as Huntington's chorea, spinal and bulbar muscular atrophy [8], myotonic dystrophy [9] and Friedreich's ataxia [10]. On the other hand, for other genomes, microsatellite elements are useful in many research domains such as DNA forensics [11], population genetic analysis [12], conservation biology and phylogenetics [13], [14].

Taking into account the importance of these regions, many researches focused on studying tandem repeats or microsatellites using the bioinformatic tools [15],[16]: the MISA [17], Sputnik [18], Mreps [19], EMBOSS (etandem and equitandem) [20], RepeatMasker [21], and TRF [22]. These tools use repeats candidates and compare them to DNA consensus sequences to detect microsatellites. These algorithms use a regular expression [21], the Hamming distance [15], the recursive match and the penalty scores [22]. They also use *k*-mers with suffix trees [23] and Heuristic alignment procedure [24].

Among these tools, Tandem Repeats Finder (TRF) is the most used one for detecting the short tandem repeats in DNA

sequences [22]. Nevertheless, it is not easy to use due the need to carefully choose settings. This is not only specific to this tool, as most bioinformatics tools need also prior information for the input parameters of the system such as [16]: pattern, pattern size, number of repeats, reference sequence or score [25]. However, sometimes, we do not have this prior information because of lack the short tandem repeats characteristics.

Aiming to overcome these limitations, scientists tried to find effective approach based on the signal processing techniques without prior information on targeted sequence. These approaches mainly use periodicity to detect STRs [26]. In this sense, the spectral analysis based on the exact periodic subspace decomposition and the autoregressive model (AR) were carried out [27]. On the other hand, methods providing a time-frequency representation have been proposed [29], [30]. Thus, the Short Time Fourier transform [28] and the Complex Morlet wavelet transform was used for patterns visualization [31], [32]. In an attempt to detect Microsatellites, the adaptive and modified S-transform has been also used [33], [34].

In this paper, we are interested in the microsatellite's identification in the genomic sequences. As part of the genomic signal processing domain, this work proposes a new method that combines the S-transform and a particular coding technique. Our detection system achieves accurate results without using any prior knowledge about the input data. This paper is organized as follows. Section 2 presents the S-Transform which we will use as a time-frequency representation technique. A coding step is recommended to directly apply the S-transform on the DNA sequence. The different coding techniques used for the genomic sequences coding are described in section 3. In Section 4, the STRs detection algorithm has been detailed and illustrative examples are included. Section 5 provides the experimental results and evaluates the short tandem repeat identification performance by comparison to other methods. Finally, Section 6 concludes this paper.

II. S-TRANSFORM AS ANALYSING TECHNIQUE

The S-Transform (ST) is a time–frequency distribution which was developed by Stockwel et al. in 1994 for analyzing geophysics data [35]. It is a hybrid technique of the Short Time Fourier Transform (STFT) and the Continuous wavelet Transform (CWT). It retains the phase information as in the STFT and provides a variable resolution similar to CWT. There are several ways to deal with these characteristics. Here, we present three existing variants of the S-Transform: The Standard S-Transform (SST) [35], the Generalized S-Transform (GST) [36] and the Width Window Optimized S-Transform (WWOST) [37]. Finally, we propose our S-Transform modification aiming to enhance the time-frequency resolution of microsatellites representations.

A. The Standard S-Transform (SST)

The S-Transform, in its standard form, consists in calculating the Fourier Transform of a signal $x(t)$ multiplied by a gaussian window. Therefore, the Standard S-Transform calculation formula is:

$$S(t, f) = \int_{-\infty}^{+\infty} x(\tau)w(\tau, f)e^{-j2\pi\tau} d\tau \quad (1)$$

Where f represents the frequency, τ represents the time, w is the gaussian window and t controls the position of w on the τ -axis.

In the time domain, the gaussian window is given by:

$$W(t) = \frac{1}{\sigma\sqrt{2\pi}} e^{-\frac{t^2}{2\sigma^2}} \quad (2)$$

Where σ is the gaussian standard deviation. It depends on the frequency as follows:

$$\sigma(f) = \frac{1}{f} \quad (3)$$

This function controls the window's width. The S-Transform can be defined as:

$$S(t, f) = \int_{-\infty}^{+\infty} x(\tau) \frac{|f|}{\sigma\sqrt{2\pi}} e^{-\frac{(\tau-t)^2 f^2}{2}} e^{-j2\pi f\tau} d\tau \quad (4)$$

With lowest frequency, S-Transform performs well in the frequency domain. While, with highest frequency, S-Transform gives better resolution in the time domain. The main drawback to the S-Transform is then the time–frequency resolution. More efficient representations were introduced by proposing several modifications [33]. The S-Transform optimization consists in controlling the gaussian window's width by adding new parameters [34].

B. The Generalized S-Transform (GST)

The Generalized S-Transform is proposed by McFadden [36] as a modified form of the Standard S-Transform. This modification consists in introducing a novel parameter α . This parameter controls the gaussian window's width as follows:

$$\sigma(f) = \frac{\alpha}{f} \quad (5)$$

Consequently, the Generalized S-Transform is written as follows:

$$S(t, f) = \int_{-\infty}^{+\infty} x(\tau) \frac{|f|}{\sigma\sqrt{2\pi} \alpha} e^{-\frac{(\tau-t)^2 f^2}{2\alpha^2}} e^{-j2\pi f\tau} d\tau \quad (6)$$

Width Window Optimized S-Transform (WWOST)

Sejdic and his team [38] have suggested another modification of the gaussian window width by introducing a new parameter p in the expression of $\sigma(f)$.

$$\sigma(f) = \frac{1}{f^p} \quad (7)$$

Thus, the S-Transform becomes as follows:

$$S(t, f) = \int_{-\infty}^{+\infty} x(\tau) \frac{|f|^p}{\sigma\sqrt{2\pi}} e^{-\frac{(\tau-t)^2 f^{2p}}{2}} e^{-j2\pi f\tau} d\tau \quad (8)$$

In order to enhance the energy concentration in the time-frequency representation by the S-Transform, we propose another way to control the window width.

C. Proposed Modification of the S-Transform

In this work, we propose a new variant of the S-Transform by combining the two modified versions of the S-Transform.

The gaussian standard deviation in this case will be defined as:

$$\sigma(f) = \frac{\alpha}{f^p} \quad (9)$$

The S-Transform becomes:

$$S(t, f) = \int_{-\infty}^{+\infty} x(\tau) \frac{|f|^p}{\sigma\sqrt{2\pi}\alpha} e^{-\frac{(\tau-t)^2 f^{2p}}{2\alpha^2}} e^{-j2\pi f\tau} d\tau \quad (10)$$

In Fig. 1, we represent the Gaussian window function around the frequency 0.33 (which is equivalent to periodicity 3 in DNA). We take into account different values of p and α and we provide the temporal and the spectral supports of the correspondent window. When $p = 1$ and $\alpha = 1$, we are in the case of the Standard S-Transform (SST). When $p = 1$ and $\alpha = 2.4$, it is a Generalized S-Transform (GST). For $p = 1.8$ and $\alpha = 1$, it is the Width Window Optimized S-Transform (WWOST). Finally, for $p = 1.2$ and $\alpha = 2.4$, we are in the presence of the proposed S-Transform.

The combination of the parameters p and α in the S-Transform offers more flexibility to the gaussian window to capture periodicity 3 than the anterior versions. It has the characteristic that it minimizes the band in both spatial and frequency domains.

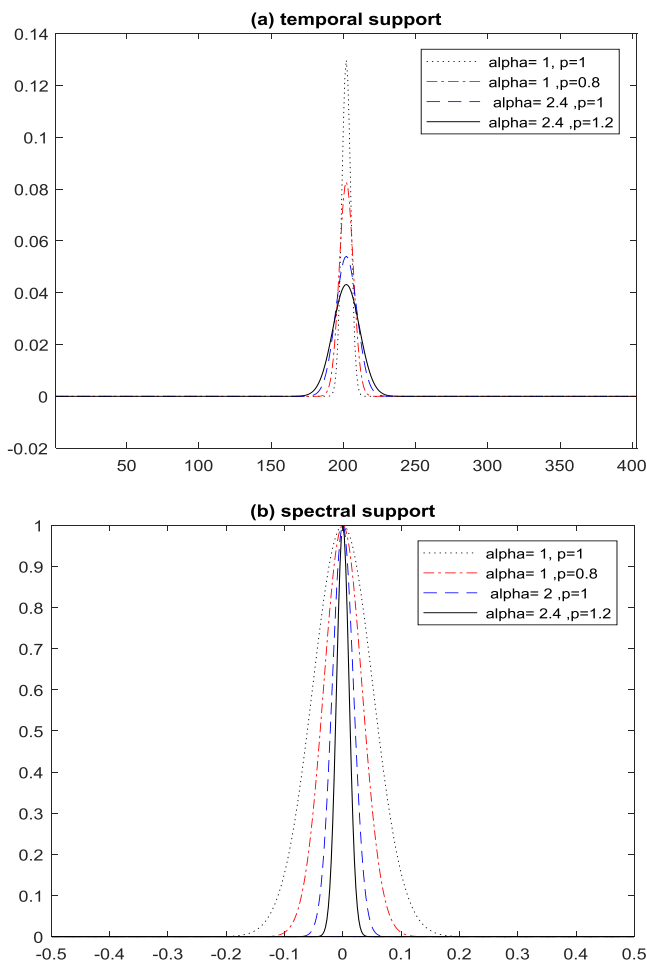


Fig. 1. The Gaussian Window with different Parameters Concentrated Around Periodicity 3; (a) Temporal Support, (b) Spectral Support.

Hence, the importance of this new variant of the S-Transform in terms of detecting the characteristic periodicities is in DNA especially in the microsatellite ones.

III. DNA CODING TECHNIQUES

To be able to apply suitable signal processing methods to the DNA sequence, we must first convert the ATCG string to numeric signal. We would point out that DNA is a character string combining 4 nucleotides: A, C, T and G.

To achieve this conversion operation, different coding techniques have been proposed. The choice of the coding technique is delicate since that each method must be tested to see if it can enhance particular useful information [39]. These techniques can be defined by the substitution of nucleotides by numerical values according to the user's choice. On the other hand, they can be based on statistical or structural properties of DNA; which will reflect interesting specificities of the sequence. Thus, two large DNA coding methods including synthetic and experimental coding.

A. Synthetic Coding

The synthetic coding principle consists in assigning a real or an imaginary value to a nucleotide base or a group of nucleotides. The most widely used synthetic mapping techniques are the binary coding, the complex binary [40] and the random walk [41].

1) *Binary coding*: The binary coding is based on simply assigning 0 or 1 to indicate the presence or the absence of a nucleotide base in the original sequence. For example, we can apply the following formula to seek the presence of the base A:

$$U(i) = \begin{cases} 1 & \text{if the base at position } i \text{ is } A \\ 0 & \text{otherwise} \end{cases} \quad (11)$$

2) *Binary complex coding*: The binary complex coding consists in giving an imaginary value to each nucleotide as follows:

$$U(i) = \begin{cases} 1 + j & \text{if the base at position } i \text{ is } A \\ 1 - j & \text{if the base at position } i \text{ is } T \\ -1 - j & \text{if the base at position } i \text{ is } C \\ -1 + j & \text{if the base at position } i \text{ is } G \end{cases} \quad (12)$$

3) *Random walks*: DNA nucleotide can be classified according to their chemical structure [41]. We found in the pyrimidine class the nucleotides (C, T) and (A, G) in the purine one. The random walk is based on assigning the value -1 if the base is C or T and 1 in case if the base A or G.

B. Experimental Coding

Experimental coding techniques make use of experimental tables to reflect the chemical and the structural properties of DNA in the produced signal. As examples, we present here the EIIP [42], EIIPc [43] and the PNUC coding [44].

1) *EIIP*: The EIIP mapping is based on the electrons energy measurement which is delocalized in nucleotides [42]. The energy values corresponding to each nucleotide are illustrated in Table I.

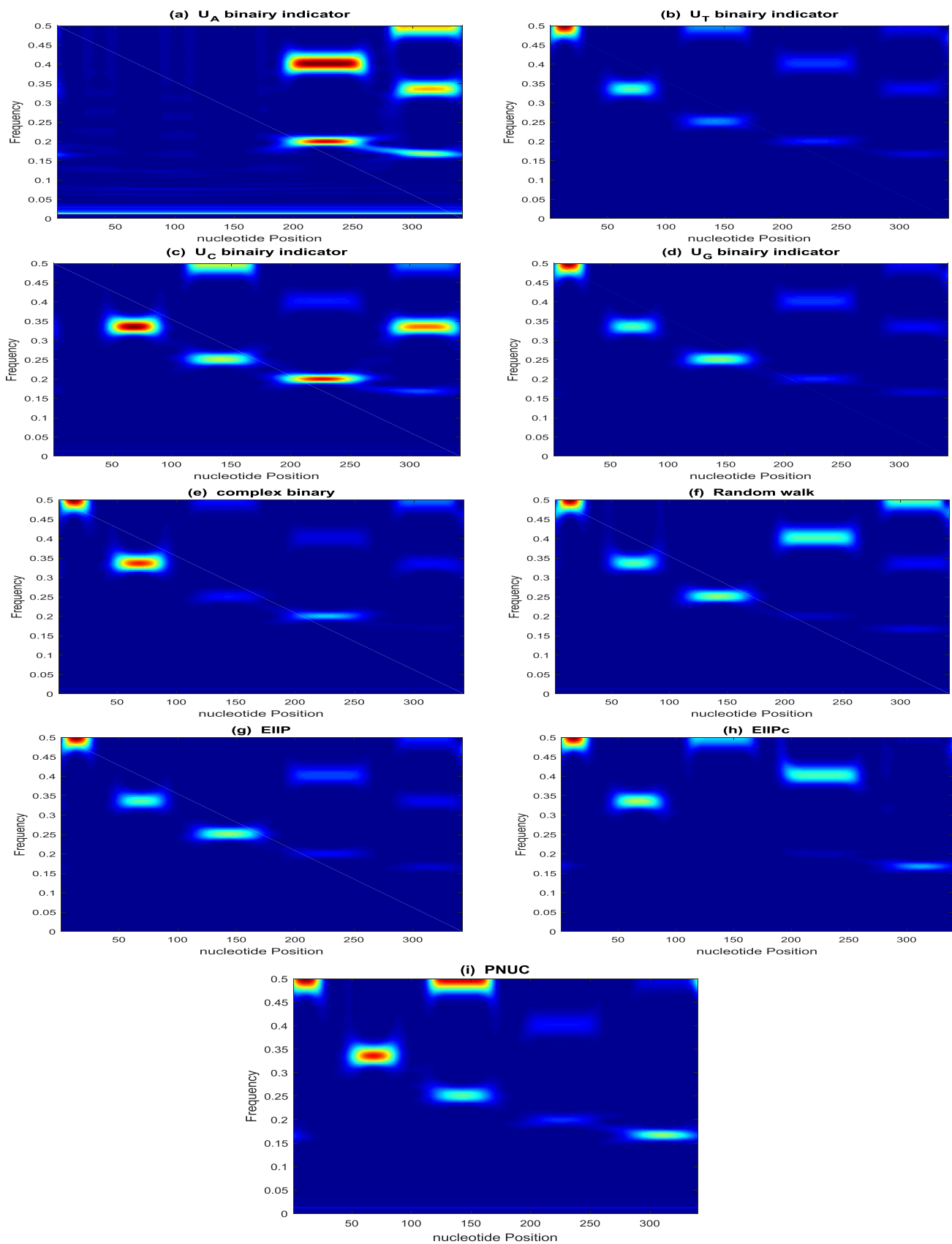


Fig. 3. Time-Frequency Representations of an Artificial Microsatellite Coded with Synthetic and Experimental Technique..

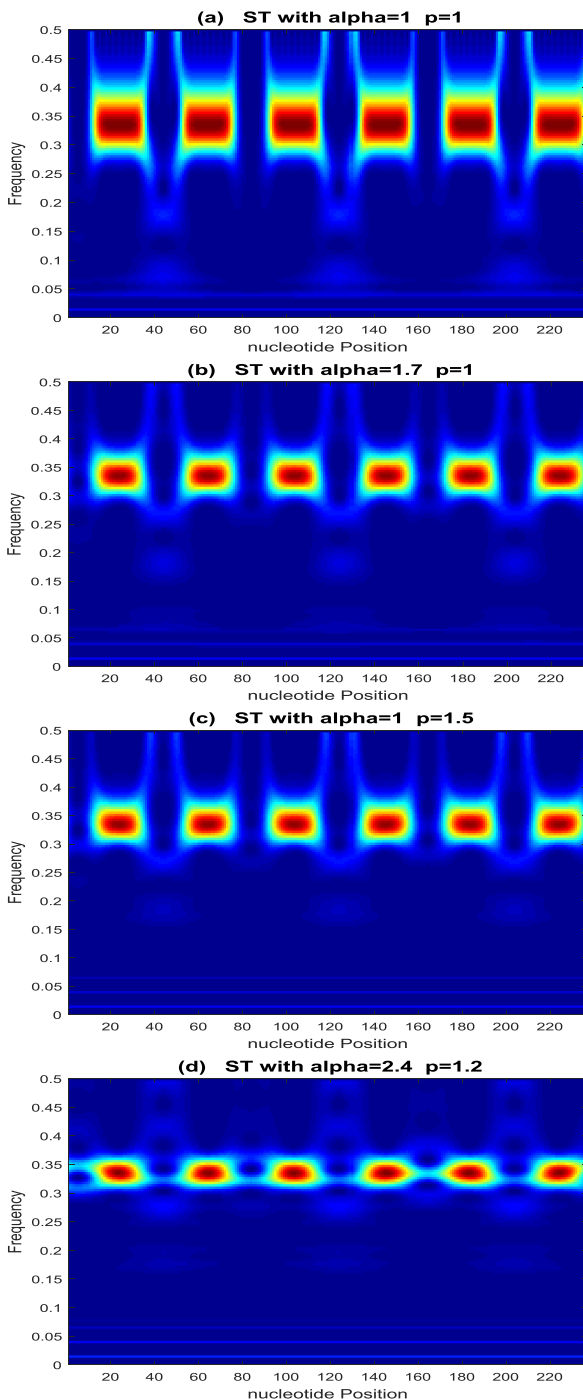


Fig. 5. Time Frequency Representation of Seq by: (a) SST, (b) GST, (c) WWOST and d) the New Variant of S-Transform.

D. Binarization

After enhancement of the microsatellite representation in the time-frequency plan with the particular values, we go on to the detection step. However, in order to delimit the start and the end of the short tandem repeat from the ST representation,

we must eliminate the noise existing in it. For this aim, we thought of transforming the time frequency representation into a binary one using a thresholding operation. The binarization step consists in giving the value of 0 or 1 to a pixel after comparing it to a threshold. In our work, we tested different threshold values. The optimal STRs detection was obtained for a threshold equal to 0.83. In Fig. 6, we present the time-frequency representation of *Seq* after binarization considering the best threshold value.

E. Extraction Pattern from Short Tandem Repeat

After identifying the microsatellite length and its periodicity. We want now to determine its specific pattern. So, we use an automatic algorithm to capture repetitive pattern.

The extraction pattern consists in comparing a DNA sequence of size p to DNA sequence of length n . The consensus repeat pattern is the most repeated pattern of the sequence.

In the previous example, the algorithm above gave us the results shown in Table V.

This table presents multiple short tandem repeats that exist in *seq* with its characteristics: (beginning, end, periodicity, pattern). And we notice that the patterns location is made with good precision.

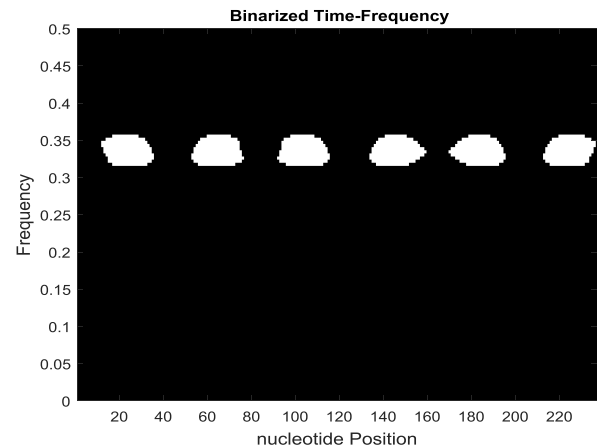


Fig. 1: The Binarized Time-Frequency Representation of Seq.

TABLE V. SHORT TANDEM REPEAT DETECTION IN SEQ

Start (bp)	End (bp)	Period	Pattern
12	37	3	CGT
53	78	3	TAC
92	117	3	CGT
133	160	3	TAC
169	196	3	CGT
212	237	3	TAC

V. EXPERIMENTAL RESULTS

In this section, we will test the performance of our algorithm in detecting STRs. The sequence X64775 of *Oryza sativa Indica Group* is selected for our experimentations. This DNA sequence is obtained from the NCBI database [46]. It has a short tandem repeat starting at 142 base-pairs and extending to 186 base-pairs. The repetition of the pattern ‘GGC’ is the characteristic of this repeat region. We chose this sequence Due to its common use in previous studies [27], [33].

The result obtained after applying each step of our algorithm is illustrated in Fig. 7. We also give the ST presentation of the sequence without applying the OTSU method (Fig. 7(b)).

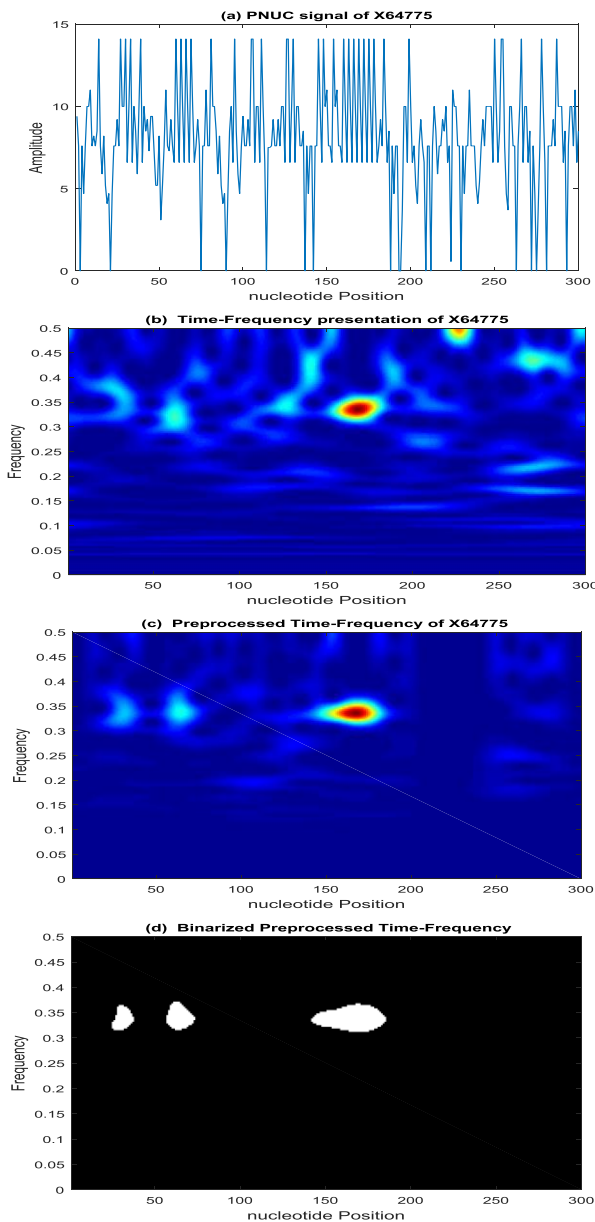


Fig. 6. (a) PNUC Signal Representation, (b) ST Representation of the PNUC Signal, (c) ST Representation after Preprocessing the PNUC Signal with OTSU, (d) Binarized time-Frequency Representation.

The sub-figures (b) and (c) demonstrate the role played by the OTSU method in smoothing the ST representation; which enhances the three regions with high energy around the frequency 0.33 (i.e. Periodicity 3). In fact, these zones represent repeats of trinucleotides motifs in the X64775 sequence. Periodicity 3 is well localised in both the time and the frequency domains. Hence, the importance of our algorithm is in characterizing microsatellites by the correspondent frequency and locating their position.

To evaluate the efficiency of the proposed method, we compared the obtained results, first, with bioinformatics tools. So, we chose: Mreps, Etandem and TRF.

For Mreps and Etandem, we kept the default parameters. For TRF, in the beginning we also kept the default settings. Then, we changed the settings as follow: match=2, mismatch=5 and indels=5, for the Minimum Alignment Score=30.

The obtained results are presented in Table VI.

We notice that periodicity 3 is detected one time by Etandem and TRF with the default setting. however, Mreps detects 2 regions of periodicities 3 and one region with periodicity 6. As for our method, it locates 3 regions with periodicity 3. Our results are the nearest to those of TRF considering the adjusted parameters; which are the most suitable.

We compared as well with analysis techniques as the Adaptive S-Transform (AST), the Empirical Mode Wavelet Decomposition (EMWD) and the Parametric Spectral Estimation (PSE) considering the AR model.

The results of the microsatellite detection in X64775 by the methods ATS, EMWD and PSE are detailed in [27] and [33].

From Table VII, Periodicity 3 is detected by EMWD only two times. The remaining techniques identify 3 regions with periodicity 3. These techniques succeed to identify the microsatellites listed in the NCBI database. Whereas, PSE and our method detect another short tandem repeat similar to one detected by TRF in terms of localization. Only our proposed method detected the same three microstatellites detected also by TRF, from the standpoint of periodicity and position.

TABLE VI. MICROSATELLITES DETECTION IN X64775 WITH BIOINFORMATIC TOOLS AND OUR PROPOSED METHOD

Method	Region	Period	Pattern	
Etandem	140-202	3	GCG	
Mreps	59-73	3	-	
	147-163	6	-	
	159-182	3	-	
TRF	Default settings	145-188	GGC	
	match=2, mismatch=5, indel=5, score=30	29-43	3	CGC
		59-73	3	CGG
145-188		3	GGC	
Proposed method	27-37	3	CGC	
	59-71	3	CGG	
	146-183	3	GGC	

TABLE VII. MICROSATELLITES DETECTION IN X64775 WITH ANALYSIS TECHNIQUES AND PROPOSED METHOD

Method	Region	Period	Pattern
AST	61-79	3	GGC
	108-116	3	CGG
	160-186	3	GGC
EMWD	57-72	3	CGG
	140-187	3	GGC
PSE	49-57	3	TAC
	59-76	3	CGG
	141-188	3	GGC
Proposed method	27-37	3	CGC
	59-71	3	CGG
	146-183	3	GGC

To conclude, we succeeded in finding an efficient method for STRs detection. Furthermore, the obtained results match those of bioinformatics tools with the advantage of being independent from any prior knowledge about the searched repeat.

VI. CONCLUSION

This study reveals the advantage of signal and image processing tools in highlighting short tandem repeats in DNA sequences instead of bioinformatics ones. The system, we proposed here, is based upon using a DNA coding technique and the S-transform.

First, we have investigated the role played by the coding technique in enhancing the time-frequency representation of microsatellites. Thus, we have tested six coding techniques which are: PNUC, EIIPc, EIIP, the binary coding, the complex binary coding and the random walk. The best resolution was obtained with the PNUC coding technique.

Next, we have presented our new approach for the microsatellites' detection. The algorithm consists of four steps.

As a first step, we encoded the DNA sequence into a numerical signal using the PNUC technique. Secondly, we preprocessed the obtained signal with the Otsu's method in order to maximize the useful information. Then, we applied a new variant of the S-Transform to get time frequency presentation of the sequence subject of study. The latter representation allowed us to easily localize the microsatellite position and periodicity after proceeding by a binarization step. The final step consists of extracting the pattern from the microsatellites, automatically.

To prove the effectiveness of our method, we have compared results with those of some bioinformatics tools: TRF, Mreps and Etandem. We have also established a comparison with other signal processing tools, which are: AST, Parametric Spectral Estimation and EMWD. In all cases, our approach outperforms these methods in terms of STR detection.

The main advantage of our algorithm consists in being independent from any prior knowledge of the repeat's characteristics. Moreover, it offers the possibility to get a simple graphic visualization of microsatellites.

In the future work, this approach can be extended to identify tandem repeats with higher repetitions unit length (minisatellites and satellites).

REFERENCES

- [1] LI, You-Chun, Korol, Abraham B., Fahima, Tzion, and al., "Microsatellites: genomic distribution, putative functions and mutational mechanisms: a review." *Molecular ecology*, vol. 11, no 12, p. 2453-2465, 2002.
- [2] LI, You-Chun, Korol, Abraham B., Fahima, Tzion, and al. "Microsatellites within genes: structure, function, and evolution." *Molecular biology and evolution*, vol. 21, no 6, p. 991-1007, 2004.
- [3] Kimura, Miyako, Sakamuri, Rama Murthy, Grothouse, Nathan A., and al. "Rapid variable-number tandem-repeat genotyping for *Mycobacterium leprae* clinical specimens." *Journal of clinical microbiology*, vol. 47, no 6, p. 1757-1766, 2009.
- [4] Charlesworth, Brian, Sniegowski, Paul, and Stephan, Wolfgang. "The evolutionary dynamics of repetitive DNA in eukaryotes." *Nature*, vol. 371, no 6494, p. 215, 1994.
- [5] Ellegren, Hans. "Microsatellites: simple sequences with complex evolution." *Nature reviews genetics*, vol. 5, no 6, p. 435, 2004.
- [6] Jarne, Philippe et Lagoda, Pierre JL. "Microsatellites, from molecules to populations and back." *Trends in ecology & evolution*, vol. 11, no 10, p. 424-429, 1996.
- [7] Pearson, Christopher E., Edamura, Kerrie Nichol, et Cleary, John D., "Repeat instability: mechanisms of dynamic mutations." *Nature Reviews Genetics*, vol. 6, no 10, p. 729, 2005.
- [8] P. Leeflang, Esther, Zhang, Lin, Tavare, Simon, et al. "Single sperm analysis of the trinucleotide repeats in the Huntington's disease gene: quantification of the mutation frequency spectrum." *Human Molecular Genetics*, vol. 4, no 9, p. 1519-1526, 1995.
- [9] Hannan, Anthony J. "Tandem repeats mediating genetic plasticity in health and disease." *Nature Reviews Genetics*, vol. 19, no 5, p. 286, 2018.
- [10] Jones, Lesley, Houlden, Henry, et Tabrizi, Sarah J. "DNA repair in the trinucleotide repeat disorders." *The Lancet Neurology*, vol. 16, no 1, p. 88-96, 2017.
- [11] Moretti, Tamara R., Baumstark, Anne L., Defenbaugh, Debra A., et al. "Validation of short tandem repeats (STRs) for forensic usage: performance testing of fluorescent multiplex STR systems and analysis of authentic and simulated forensic samples." *Journal of Forensic Science*, vol. 46, no 3, p. 647-660, 2001.
- [12] Kimura, Miyako, Sakamuri, Rama Murthy, Grothouse, Nathan A., et al. "Rapid variable-number tandem-repeat genotyping for *Mycobacterium leprae* clinical specimens." *Journal of clinical microbiology*, vol. 47, no 6, p. 1757-1766, 2009.
- [13] Jarne, Philippe et Lagoda, Pierre JL. "Microsatellites, from molecules to populations and back." *Trends in ecology & evolution*, vol. 11, no 10, p. 424-429, 1996.
- [14] Richard, Guy-Franck, Kerrest, Alix, et Dujon, Bernard, "Comparative genomics and molecular dynamics of DNA repeats in eukaryotes." *Microbiology and Molecular Biology Reviews*, vol. 72, no 4, p. 686-727, 2008.
- [15] Lim, Kian Guan, Kwoh, Chee Keong, Hsu, Li Yang, et al. "Review of tandem repeat search tools: a systematic approach to evaluating algorithmic performance." *Briefings in bioinformatics*, vol. 14, no 1, p. 67-81, 2012.
- [16] Zribi, Soumaya, Oueslati, Afef Elloumi, et Lachiri, Zied. "Tandem repeat search tools performance for the *Arabidopsis thaliana* genome." In *Advanced Technologies for Signal and Image Processing (ATSIP)*, 2016 2nd International Conference on. IEEE, p. 330-335, 2016.
- [17] Thiel, Teresa, Michalek, W., Varshney, R., et al. "Exploiting EST databases for the development and characterization of gene-derived SSR-markers in barley (*Hordeum vulgare* L.)." *Theoretical and applied genetics*, vol. 106, no 3, p. 411-422, 2003.
- [18] Abajian, Chris, "Sputnik - DNA microsatellite repeat search utility", 1994.

- [19] Kolkpakov, Roman, Bana, Ghizlane, et Kucherov, Gregory. "mreps: efficient and flexible detection of tandem repeats in DNA." *Nucleic acids research*, vol. 31, no 13, p. 3672-3678, 2003.
- [20] Sarachu, Martín et Colet, Marc. "wEMBOSS: a web interface for EMBOSS." *Bioinformatics*, vol. 21, no 4, p. 540-541, 2004.
- [21] Tarailo - Graovac, Maja et Chen, Nansheng. "Using RepeatMasker to identify repetitive elements in genomic sequences." *Current protocols in bioinformatics*, , vol. 25, no 1, p. 4.10. 1-4.10. 14 2009.
- [22] Benson, Gary, et al. "Tandem repeats finder: a program to analyze DNA sequences." *Nucleic acids research*, vol. 27, no 2, p. 573-580, 1999.
- [23] Saha, Surya, Bridges, Susan, Magbanua, Zenaida V., et al. "Computational approaches and tools used in identification of dispersed repetitive DNA sequences." *Tropical Plant Biology*, vol. 1, no 1, p. 85-96, 2008.
- [24] RIVALIS, Eric. "A survey on algorithmic aspects of tandem repeats evolution." *International Journal of Foundations of Computer Science*, vol. 15, no 02, p. 225-257, 2004.
- [25] Cao, Minh Duc, Balasubramanian, Sureshkumar, et Bodén, Mikael. "Sequencing technologies and tools for short tandem repeat variation detection." *Briefings in bioinformatics*, vol. 16, no 2, p. 193-204, 2014.
- [26] Tran, Thao T., Emanuele II, Vincent A., et Zhou, G. Tong. "Techniques for detecting approximate tandem repeats in DNA." In : *Acoustics, Speech, and Signal Processing*, 2004. *Proceedings.(ICASSP'04)*. IEEE International Conference on. IEEE.p. V-449, 2004.
- [27] Zhou, Hongxia, Du, Liping, et Yan, Hong. "Detection of tandem repeats in DNA sequences based on parametric spectral estimation." *IEEE transactions on information technology in biomedicine*, vol. 13, no 5, p. 747-755, 2009
- [28] Sharma, Deepak, Issac, Biju, Raghava, G. P. S., et al. "Spectral Repeat Finder (SRF): identification of repetitive sequences using Fourier transformation." *Bioinformatics*, vol. 20, no 9, p. 1405-1412, 2004.
- [29] Sussillo, D., Kundaje, A., & Anastassiou, D. "Spectrogram analysis of genomes." *EURASIP Journal on Advances in Signal Processing*, 2004(1), 790248,2004.
- [30] Touati, Rabeb, Messaoudi, Imen, Ouesleti, Afef Elloumi, et al. "Helitron's Periodicities Identification in *C. Elegans* based on the Smoothed Spectral Analysis and the Frequency Chaos Game Signal Coding." (IJACSA) *International Journal of Advanced Computer Science and Applications*, Vol. 9, No. 4, 2018.
- [31] Messaoudi, Imen, Oueslati, Afef Elloumi, et Lachiri, Zied. "Revealing Helitron signatures in *Caenorhabditis elegans* by the Complex Morlet Analysis based on the Frequency Chaos Game Signals." In : *IWBBIO*. p. 1434-1444, 2014.
- [32] Padole, Mamta C. "Recognizing Short Tandem Repeat Regions in Genomic Sequences Using Wavelet." In : *Mathematics and Computers in Sciences and in Industry (MCSI)*, 2014 International Conference on. IEEE. p. 288-294, 2014.
- [33] Sharma, Sunil Datt, Saxena, Rajiv, et Sharma, Sanjeev Narayan. "Identification of microsatellites in DNA using adaptive S-transform." *IEEE journal of biomedical and health informatics*, vol. 19, no 3, p. 1097-1105, 2015.
- [34] Sharma, S. D., Saxena, Rajiv, Sharma, S. N., et al. "Short tandem repeats detection in DNA sequences using modified S-transform." *International Journal of Advances in Engineering & Technology*, vol. 8, no 2, p. 233, 2015.
- [35] Stockwell, Robert Glenn, Mansinha, Lalu, and Lowe, R. P. "Localization of the complex spectrum: the S transform." *IEEE transactions on signal processing*, vol. 44, no 4, p. 998-1001, 1996.
- [36] Mcfadden, P. D., Cook, J. G., et Forster, L. M. "Decomposition of gear vibration signals by the generalised S transform." *Mechanical systems and signal processing*, vol. 13, no 5, p. 691-707, 1999.
- [37] Djurović, Igor, Sejdović, Ervin, et Jiang, Jin. "Frequency-based window width optimization for S-transform." *AEU-International Journal of Electronics and Communications*, vol. 62, no 4, p. 245-250, 2008.
- [38] Sejdovic, Ervin, Djurovic, Igor, et Jiang, Jin. "A window width optimized S-transform." *EURASIP Journal on Advances in Signal Processing*, vol. 2008, p. 59, 2008.
- [39] Zribi, Soumaya, Messaoudi, Imen, Oueslati, Afef Elloumi et Lachiri, Zied. "Tandem repeats detection based on S-transform applied on synthetic and experimental codings." In : *Control, Automation and Diagnosis (ICCAD)*, 2017 International Conference on. IEEE. p. 314-319, 2017.
- [40] A. Arneodo, C.Vaillant, B.Audit, F.Argoul, Y.d'Aubenton-Carafa, C.Thermes, Multi-scale coding of genomic information: from DNA sequence to genome structure and function. *Phys Rep* vol.498,no 2:45–188,2011.
- [41] .Bai, Y.Liu, T.Wang "A representation of DNA primary sequences by random walk", *Mathematical Biosciences*, Elsevier, Vol. 209, n°9, pp 282–291, 2007.
- [42] V.Parisi, V.De Fonzo,F. Aluffi-Pentini : finding tandem repeats in DNA sequences. *Bioinformatics* 19(14):1733–1738
- [43] M. Kobayashi, H. Toyozumi, "Genomic Sequence Analysis using Electron-Ion Interaction Potential", University of Aizu, Graduation Thesis. March, 2005.
- [44] D.S. Goodsell and R.E. Dickerson, "Bending and curvature calculations in B-DNA", *Nucleic Acids Research*, vol. 22, n° 24, pp: 5497-5503, Oxford University Press, 1994.
- [45] H.Chen and R. Gururajan. "Otsu's threshold selection method applied in de-noising heart sound of the digital stethoscope record." In : *Advances in Information Technology and Industry Applications*. Springer Berlin Heidelberg, p. 239-244,2012.
- [46] The NCBI GenBank database, 2014. Available: <http://www.ncbi.nlm.nih.gov/Genbank/>.

Location Prediction in a Smart Environment

Wael Ali Alosaimi¹, Ahmed Binmahfoudh², Roobaea Alroobaea³, Atef Zaguia⁴
Computer Engineering^{1,2}, Computer Science^{3,4}
College of Computing and Information Technology, Taif University, Taif, Saudi Arabia

Abstract—The context prediction and especially the location prediction is an important feature for improving the performance of smart systems. Predicting the next location or context of the user make the system proactive, so the system will be capable to offer the suitable services to the user without his involving. In this paper, a new approach will be presented based on the combination of pattern technique and Bayesian network to predict the next location of the user. This approach was tested on real data set, our model was able to achieve 89% of the next location prediction accuracy.

Keywords—Location prediction; context; pattern; Bayesian network

I. INTRODUCTION

Nowadays, we are witnessing an exponential advancement of technology. From the advent of the computers to the advent of laptops and tablets, technology has become an integral part of our daily life. Still, the evolution of computer networks and telecommunications marked the most important development enabling mobility and information sharing. This allowed the emergence of new systems that combine ubiquity and intelligence. Using such systems creates a smart environment, capable to have an autonomous decision making, an automatic adaption to the needs of the user without his intervention and provide comfort to the user.

An intelligent/smart system is based on the early idea of the ubiquitous computing [1]. It is a machine that integrates a computer connected to the network that can collect and analyze data and communicate with other systems. These systems are also characterized by their ability to learn from historic of user behaviour, security and connectivity. Their capability to adapt to the recent data extracted from the environment. This information extracted from the environment are the context [2].

During the previous years, most research topics were centered upon the concept of smart systems. The main goal of these researches is to divulge user's needs, to provide to user help and convenience to accomplish their daily activities and in different domains. The omnipresent system or ubiquitous system will be focused in this study [3]. To accomplish their goals, these systems should be sensitive to the context: context-aware [4]. Determine the contexts surrounded the user is the essential part in smart system. In this context, this research work is situated.

The main goal of this research work is to develop a dynamic adaptation system of services according to the context. This research paper is an extended work from previous work that was published in [18]. In this paper, an improved approach of user location prediction is presented based on the

current context features that are considered important for the prediction.

The paper is prearranged as follows. Section 2 presents related works and highlights the novelty of our work. Section 3 present the challenges and the proposed solution. Section 4 introduces our approach for location prediction based on integration of pattern and Bayesian Network. Section 5 the paper is concluded.

II. RELATED WORK

This section will present a summary of the existing research within the context prediction topic, specifically those that present the location prediction.

Firstly, a definition of the context is presented. In [5] and [6], they defined the context as any portion of information used to give information about any entity. This entity can be a person, a place or an object.

In [7], they used a clustering approach to predict the next location. This approach is based on kernel model using the point of interest of user behavior. In [8], [9], [10] and [11], they used a Markov chain to predict the future context. This approach is based on states or steps using the following equation:

$$P[X_{n+1} = j | X_n = i_n, \dots, X_0 = i_0] = P[X_{n+1} = j | X_n = i_n] = p_{ij}(n)$$

It means that if the chain or actual context is in state X_i then the next state or context is X_j . This transition is done by a probability p_{ij} that does not depend of the previous context or states. This approach depends on the calculation of the probability transition between states. It is used principally to report the short-term location problem [9]. In [12] the WhereNext system is proposed. According of the historic trajectory of a moving entity, the finest corresponding association rule is selected. The selected rule is used and then to predict the next location. Therefore, this approach is created by determining the ordered sequence of the locations and the association rules. To predict the future user mobility, a historical spatial-temporal movement patterns are used in [13] and [14]. They indicate that the preferences of the user's change unceasingly according two temporal proprieties which are non-uniformness and consecutiveness. In [15], they used a supervised learning classifier SVM (Support vector machine) to predict the next cell. This approach is based on the use both long- and short-term context information as CSI (Channel state information). Also [16] used SVM to predict the image features from dataset of 1000 images. In [17], they used neural network to predict the next location based on location updates of adjacent past. This approach uses a huge data set of users behaviour as training to guarantee a good result.

In [21], to determine the next location of a mobile object, a new leverage context information is presented. Combining many different contexts, they predict the next location of vehicles by using a context-aware location prediction algorithm. Their approach is based on the determination of the appropriate movement pattern according to the current context.

According to the cited works, we perceived that most of the research works used a limited number of contexts or only the user's behaviour to predict the next location of the user. Despite that using other contextual information will improve the prediction.

Consequently, this paper uses the combination of the Bayesian network and the pattern technique modeled on the ontology with contexts information. This will be an efficient approach.

III. CHALLENGES AND PROPOSED SOLUTION

The main purpose of this research paper is to develop a smart system capable to predict the user behaviour, which is aimed at providing the comfort and facilitate many of the complex tasks we face in our daily lives. Therefore, the system will be capable to detect any change of the context on the environment where the user exists. Then, according to these changes the system will offer the most adequate services to the user.

To accomplish our objectives, there is needed to define the challenges that should be taken in account to develop our system along with our proposed solution.

- What are the required components to design the architecture of a user feature prediction system?

At this point, all the necessary components of the system will be defined, specified and developed.

- How will we represent information concerning the feature of the user, patterns, Bayesians networks and rules of the feature prediction?
- How will the system manage uncertain or ambiguous data in the prediction process presented in [18]?

For question two and three, the new context-based method will be introduced using the pattern technique and a Bayesian network (BN) to resolve the uncertainty problem during the prediction process in a pervasive system.

IV. ARCHITECTURE OVERVIEW

In this section, an overview of the architecture is presented. To address the questions presented in Section 3, we have designed the context awareness architecture (Fig. 1). The main modules of the architecture are: pattern, Bayes and ontology.

As shown in Fig. 1, any change on the environment will trigger an event. This event is detected by the sensors installed on the environment. These captors send new information detected to the module pattern. The role of the module pattern is to determine the predicted location (in case of no ambiguity)

by interacting with the ontology. In case of ambiguity, the module Pattern sends a set of the different ambiguous locations to the module Bayes that will uses the Bayesians networks to determine the most probable location. This is done by sending the adequate information to the ontology

Once the next location is determined, the module adequate services determine the adequate services to offer bestowing to the location.

The ontology (Fig. 2) contains all information concerning the context (user, location, system and environment), the patterns, and the Bayesian networks.

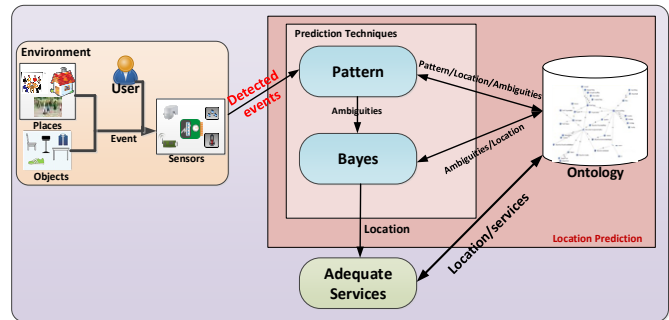


Fig. 1. Location Prediction Framework.

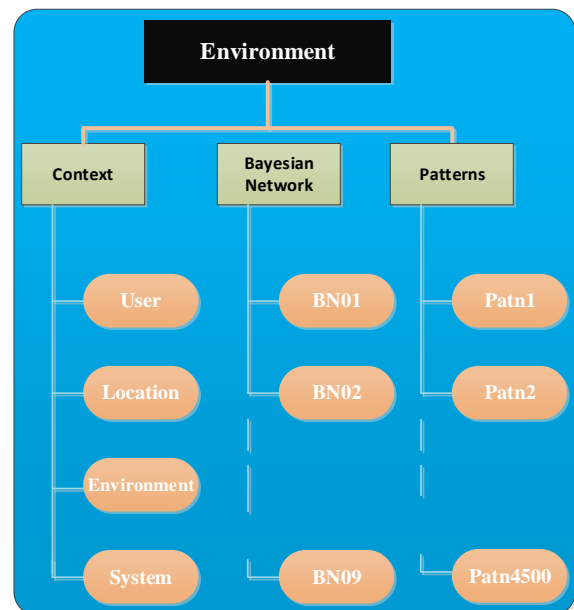


Fig. 2. The Classes of the Ontology.

V. LOCATION PREDICTION: COMBINATION OF PATTERN TECHNIQUE AND BAYESIAN NETWORKS

In this section, we will present in detail our approach and how we improved the approach presented in [18]. In the next section, we will present a brief detail about the approach presented in [18] and the inconvenient of this approach. Then in section Bayesian Network, we present the integration of Bayesian network with pattern to overcome the problem presented in [18].

A. Ontological Model

1) *Pattern technique*: In [18] they presented an approach based on patterns (Fig. 2). These patterns are presented on the form of problem and solution as showing in Fig. 3.

In their approach [18] they present the pattern problem as a set of; user behaviors and contexts; and pattern solution as the next location (predicted location) (Fig. 4).

This approach involves searching for similar pattern problem in the ontology (Fig. 2) and presenting the corresponding of pattern solution once the similar pattern problem has found. For instance, Fig. 5 shows how the approach is employed. As can be seen that the search system starts by creating a *patternSearch* composed of the actual user behaviour history and the contexts. Then, the system search for the matching of the patterns problems. When it is found, the adequate pattern solution (next location) is presented.

This approach was tested on real data and the achieved accuracy of the next location prediction was 86% (in the situation of no similar pattern). But this approach has shown a markable weakness in the case of the existing of similar pattern problem [18].

To resolve this problem, we integrate the Bayesian network to overcome the indecision cases (our approach).

2) *Bayesian network integration*: As mentioned in [18] during the prediction of the context, the system might face uncertainty or ambiguity. This is caused by the resemblance of many patterns that was created from user behaviour modeled on the ontology (Fig. 2). To avoid this problem and improve the results obtained in [18], the integration of the Bayesian network is introduced using context.

The Bayesian Network is a graphical model reasoning in the case of uncertainly [19]. It is a direct acyclic graph and all independencies are described using conditional probability distributions [20].

For instance, if the system finds that the possible next location is C1 or C3 or C6, the system cannot make decision about the possible solution (ambiguity). In this situation, comes the role of the Bayesian network to take decision according to the actual contexts. Fig. 6 shows an example of the Bayesian network with context information. As shown, every next location ambiguity has relations between every context information with a certain probability.

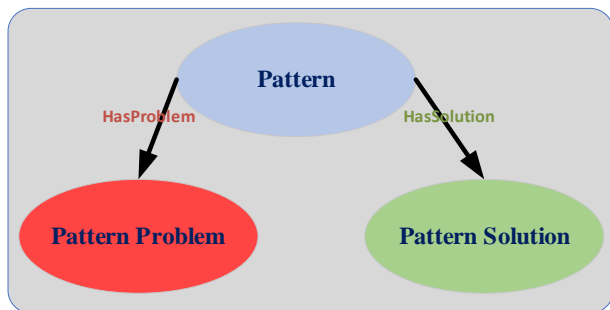


Fig. 3. Ontological Pattern Definition.

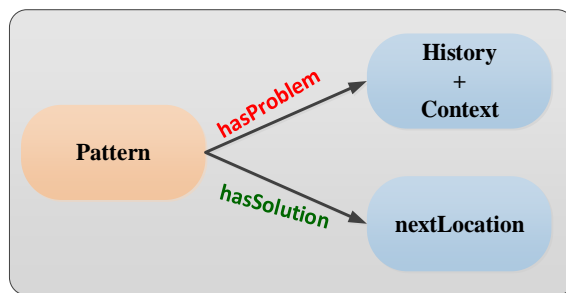


Fig. 4. Ontological Pattern Example.

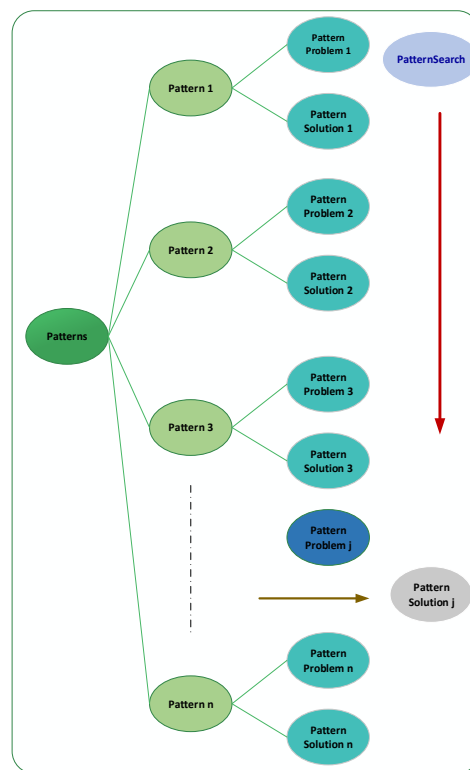


Fig. 5. Algorithm Pattern Search.

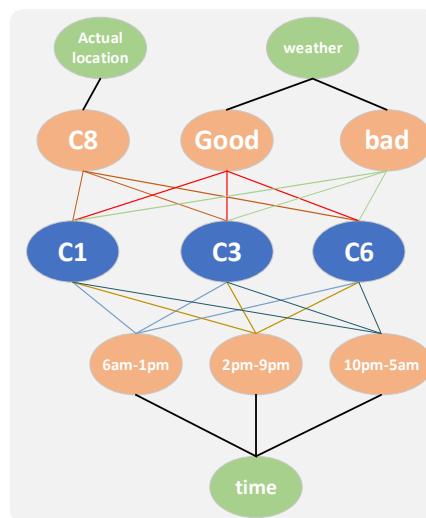


Fig. 6. Example of Bayesian Network with Context.

The adaptation of the Bayesian Network with context information such as (time, weather, actual location, etc.) is presented by following equation:

$$Cnt_j \xrightarrow{t} \rightarrow (l_i, P_i) \quad (1)$$

$$i = 1$$

Where t presents the number of ambiguous next location and $j \in [1..n]$ (n present the number of context)

As mentioned on the equation (1), every context (Cnt_j) is on relation between all the ambiguous next location (l_i) with a certain probability (P_i) (likelihood probability).

To make decision about the suitable next location, the equation (2) was used to calculate all a posteriori probability for every ambiguous next location and choose the one that has the greater probability.

$$P(C|M) = \frac{P(M|C)P(C)}{P(M)} \left\{ \begin{array}{l} C: \text{Concept: ambiguous next location} \\ M: \text{set of the context} \end{array} \right\} \quad (2)$$

Where:

$P(C|M)$: a posteriori probability

$P(M|C)$: likelihood

$P(M)$: evidence

$P(C)$: a priori probability

For the example presented in Fig. 6, suppose that likelihood probabilities are in the Table I. These probabilities usually estimated by an expert. The contexts presented in Table I are examples to explain our idea.

In this case the equation (2) is used to determine the next location by calculating the posteriori probabilities. Suppose that the actual time is 6:30 pm and the weather is bad.

$$P(C1|C8, Bad, 2pm - 9pm) =$$

$$P(C1) \times \frac{P(C8|C1) \times P(Bad|C1) \times P(2pm - 9pm|C1)}{P(C8, Bad, 2pm - 9pm)}$$

$$= 1 \times \frac{0.25 \times 0.26 \times 0.13}{P(C8, Bad, 2pm - 9pm)} = \frac{84.5 \times 10^{-3}}{P(C8, Bad, 2pm - 9pm)}$$

$$P(C3|C8, Bad, 2pm - 9pm) =$$

$$P(C3) \times \frac{P(C8|C3) \times P(Bad|C3) \times P(2pm - 9pm|C3)}{P(C8, Bad, 2pm - 9pm)}$$

$$= 1 \times \frac{0.29 \times 0.19 \times 0.22}{P(C8, Bad, 2pm - 9pm)} = \frac{0.0121}{P(C8, Bad, 2pm - 9pm)}$$

$$P(C6|C8, Bad, 2pm - 9pm) =$$

$$P(C6) \times \frac{P(C8|C6) \times P(Bad|C6) \times P(2pm - 9pm|C6)}{P(C8, Bad, 2pm - 9pm)}$$

$$= 1 \times \frac{0.34 \times 0.13 \times 0.01}{P(C8, Bad, 2pm - 9pm)} = \frac{4.42 \times 10^{-4}}{P(C8, Bad, 2pm - 9pm)}$$

TABLE I. LIKELIHOOD PROBABILITIES

Contexts \ Locations	C1	C3	C6
C8	0.25	0.29	0.34
Good	0.31	0.28	0.31
Bad	0.26	0.19	0.13
6am-1am	0.04	0.01	0.02
2pm-9pm	0.13	0.22	0.01
10pm-5am	0.01	0.01	0.19

As shown, the posteriori probability $P(C3|C8, Bad, 2pm - 9pm)$ has the highest probability therefor the next location is C3.

VI. USE CASE AND RESULTS

In this section, the experimental results are presented for the proposed approach. The used data set is introduced before presenting the evaluation of the approach.

A real data set was used named MDC (mobile data challenges) [22], it was created by Nokia. This data was recorded during 18 months by 200 voluntaries. They used smart phones to gather information about their speeds, their displacement, information on the use of the device, etc.

To test our approach, the dataset was spilt to 80% as training data and 20 % as testing. The patterns used in [18] were increased from 2500 to 4500 patterns to get more consistent results.

A java program was developed to send queries to the ontology. We randomly generate 1500 queries of user behaviour for each day. Fig. 7 shows the number of queries created randomly for every day to test our approach. The blue lines present the number of rejected queries and red lines are the number of the accepted queries.

The results obtained are presented in Fig. 8. The average of the prediction model was 89%, there is also more than 90% in some days as shown in the following diagram.

A competitive result was obtained a comparing to the approach presented in [18]. In [23], they used the same data set to test different algorithms, comparing to their results (Table II), motivating results were attained for the prediction of a user's next location using our approach based of the combination of pattern technique and Bayesian networks.

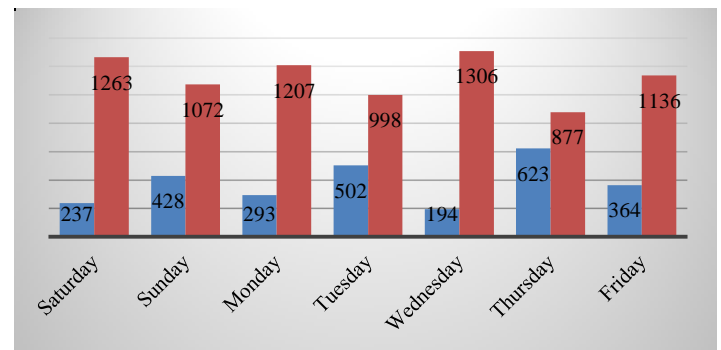


Fig. 7. Accepted and Rejected Queries.

TABLE II. LOCATION PREDICTION ACCURACY [23]

Day	Decision trees J48=C4.5%		SVM %		Nearest Neighbor Lbk (K=1) %	
	with noise	Without noise	with noise	Without noise	with noise	Without noise
Saturday	92.37	92.11	69.54	73.19	93.20	90.36
Sunday	91.22	88.22	59.56	58.32	92.46	87.84
Monday	88.06	83.94	65.43	66.27	89.47	86.10
Tuesday	87.58	86.37	55.69	60.81	89.74	88.42
Wednesday	92.11	89.71	65.04	71.78	93.98	91.95
Thursday	84.72	83.63	54.1	60.17	86.39	83.75
Friday	86.72	87.77	58.99	58.99	89.89	89.89

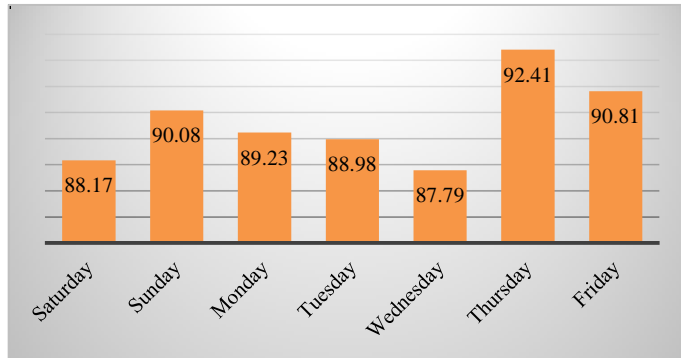


Fig. 8. Average of the Prediction Model.

VII. CONCLUSION

This research work is an entry point for the field of service adaptation in smart system by the prediction of the context using the contextual information collected from the sensors existing in the environment such as the current position of the user, time, day etc. The progress of smart system/pervasive system is related to the determination of user's behaviour and context. The prediction of the future context is one of the important elements in pervasive system /smart system to provide a proactive context-awareness adaptation.

This paper is presented a new approach based on pattern and Bayesian network to predict the next location of the user. At first, this approach uses the pattern technique to determine the next location and in the case of the ambiguity to take decision the Bayesian network is used to make decision about the adequate next location. From the experimental results, it can be seen comparing to other algorithms presented on the literature review that the competitive results are obtained.

However, some limitation should be noticed and should be taken into consideration in the future work. In our case study, the prediction of the location was limited to eight locations. Moreover, in a smart environment, the number of locations will not be limited to eight locations; in this case the size of the ontology will increase exponentially because for every location we will create a separate Bayesian network.

ACKNOWLEDGMENT

This study was funded by the Deanship of Scientific Research, Taif University, KSA [research project number 1-439-6054].

REFERENCE

- [1] Weiser, M., The Computer for the 21 st Century. Scientific american, 1991. 265(3): p. 94-105.
- [2] Bui, N., et al., A survey of anticipatory mobile networking: Context-based classification, prediction methodologies, and optimization techniques. IEEE Communications Surveys & Tutorials, 2017. 19(3): p. 1790-1821.
- [3] Krumm, J., Ubiquitous computing fundamentals. 2016: Chapman and Hall/CRC.
- [4] Dey, A.K., Context-Aware Computing, in Ubiquitous Computing Fundamentals. 2016, Chapman and Hall/CRC. p. 335-366.
- [5] Rosenberger, P. and D. Gerhard, Context-awareness in industrial applications: definition, classification and use case. Procedia CIRP, 2018. 72: p. 1172-1177.
- [6] Van Engelenburg, S., et al., What Belongs to Context?: A Definition, a Criterion and a Method for Deciding on What Context-Aware Systems Should Sense and Adapt to. 2018.
- [7] Do, T.M.T., et al., A probabilistic kernel method for human mobility prediction with smartphones. Pervasive and Mobile Computing, 2015. 20: p. 13-28.
- [8] Liu, J.S. and R. Chen, Sequential Monte Carlo methods for dynamic systems. Journal of the American statistical association, 1998. 93(443): p. 1032-1044.
- [9] Bar-David, R. and M. Last, Context-aware location prediction, in Big Data Analytics in the Social and Ubiquitous Context. 2014, Springer. p. 165-185.
- [10] Qiao, Y., et al., A hybrid Markov-based model for human mobility prediction. Neurocomputing, 2018. 278: p. 99-109.
- [11] Nizetic, I., K. Fertalj, and D. Kalpic. A prototype for the short-term prediction of moving object's movement using markov chains. in Information Technology Interfaces, 2009. ITI'09. Proceedings of the ITI 2009 31st International Conference on. 2009. IEEE.
- [12] Monreale, A., et al. Wherenext: a location predictor on trajectory pattern mining. in Proceedings of the 15th ACM SIGKDD international conference on Knowledge discovery and data mining. 2009. ACM.
- [13] Gao, H., J. Tang, and H. Liu. Mobile location prediction in spatio-temporal context..
- [14] Yuan, N.J., et al. Reconstructing individual mobility from smart card transactions: A space alignment approach. in Data Mining (ICDM), 2013 IEEE 13th International Conference on. 2013. IEEE.
- [15] Chen, X., F. Mériaux, and S. Valentin. Predicting a user's next cell with supervised learning based on channel states. in Signal Processing Advances in Wireless Communications (SPAWC), 2013 IEEE 14th Workshop on. 2013. IEEE.
- [16] Alroobaea, R., Alsufyani, A., Ansari, M.A., Rubaiee, S. and Algarni, S., 2018. Supervised Machine Learning of KFCG Algorithm and MBTC features for efficient classification of Image Database and CBIR Systems. International Journal of Applied Engineering Research, 13(9), pp.6795-6804.
- [17] Liu, Q., et al. Predicting the Next Location: A Recurrent Model with Spatial and Temporal Contexts. 2016.

- [18] Zaguia, A. and R. Alroobaea, Ontological Model to Predict user Mobility. *International Journal of Advanced Computer Science and Applications*, 2019. 10(2).
- [19] Jensen, F.V., *An introduction to Bayesian networks*. Vol. 210. 1996: UCL press London.
- [20] Boutilier, C., et al., Context-specific independence in Bayesian networks, in *Proceedings of the Twelfth international conference on Uncertainty in artificial intelligence*. 1996, Morgan Kaufmann Publishers Inc.: Portland, OR. p. 115-123.
- [21] R. Bar-David and M. Last, "Context-aware location prediction," in *Big Data Analytics in the Social and Ubiquitous Context*: Springer, 2015, pp. 165-185.
- [22] Laurila, J.K., et al. *The mobile data challenge: Big data for mobile computing research*. in *Pervasive Computing*. 2012.
- [23] Guessoum, D., M. Miraoui, and C. Tadj, Contextual location prediction using spatio-temporal clustering. *International Journal of Pervasive Computing and Communications*, 2016. 12(3): p. 290-309.

Low-fidelity Prototype Design for Serious Game for Slow-reading Students

Saffa Raihan Zainal Abidin¹, Siti Fadzilah Mat Noor², Noraidah Sahari Ashaari³

Faculty of Information Science & Technology, Universiti Kebangsaan Malaysia, Bangi, Malaysia

Abstract—Serious game is an alternative teaching aid that is getting a place of use by teachers and parents. Its widespread use has basically changed the way of life and learning of children and has a positive impact on achievement and increased the motivation of children in learning. However, not all serious game designs are suitable for slow-reading students. They are slightly different from other students in terms of cognitive potential and are struggling to meet academic demands in the class. Therefore, the main objective of this study is to produce low-fidelity prototypes involving target users as early as the design process. This study focuses on the production of storyboard contents suitable for slow-reading students to save time and cost of game model development. This study uses a child-centered design (CCD) method that involves paper prototypes, chauffeured prototype, think aloud protocols and observations. The results of this study are low-fidelity prototypes in the form of computerized storyboards that have been verified and will be used for heuristic assessments. These low-fidelity prototypes are expected to give an early look and help researchers in developing high-fidelity prototypes.

Keywords—Serious game; brain-based learning; low-fidelity prototype; paper prototype; chauffeured prototype; think aloud protocol; slow-reading students

I. INTRODUCTION

Serious game has grown rapidly over the last decade into becoming a popular and successful new technology in the 21st century. According to [1] and [2], serious game is built with a specific purpose besides just entertainment. The word 'serious' can be referred to as the role of the game in delivering inputs either in the form of education or training to players. Study [3] has shown the growing interest of the public in serious game review. The increasing number of research papers on serious games published in various fields from the late 1990s to 2013 showed a positive impact. Serious games have been used in various areas such as health, education, training, culture, defense and society [1].

Designs of a serious game vary according to target users. So, in designing a gameplay, it is very important to understand the needs of users [1]. Designing a serious game for children is a challenge as they are different from adults. Children see things from a different view [4]. According to [5], children should be involved in the design process because their expectations and meaningfulness of the product may not be the same as the designer's assumption since the worlds of children and adults are different. Hence, this study uses the child-centered design (CCD) method proposed by [6]. This method

is a repetitive process and is the same as user-centered design (UCD), with the difference being that the end users of this study are children [6].

However, most serious games on the market are designed for children with normal learning abilities. Only a limited number of software is designed to meet the needs of students with learning problems [7]. According to [8], the design principles for developing child technology are different from adults because the desire, the readiness and the needs of these people differ. The focus of this study is on children who are left behind in reading literacy. Reading skills are the basic skills that everyone must master because without reading skills, children will not be able to face challenges in their lives. According to [9], students with poor reading literacy, better known as slow-reading students (SRS), are those who fail in examinations and must follow the remedial classes provided by the school.

Humans are generally never aware of the complicated process of language in the brain. Teachers need to step up their role and innovate to make teaching and learning (T&L) more fun and meaningful, especially for SRS [9]. Brain-based learning (BBL) approach in a serious game is an innovation that is proposed in this model. BBL is not a new approach; in fact, it has been used daily by teachers during T&L. According to [10], BBL focuses on the overall brain function which can have a positive impact on student achievement. Individual self-potential can be enhanced when the function of the brain is optimally utilized with the help of teachers and teaching aids in a way they are most comfortable. According to [11], using game techniques is an approach that is well-liked by the students as games become a routine in which they play not only in the classroom, but also in their free time.

II. BACKGROUND STUDY

This section discusses backgrounds study related to the approach applied in this game model, which is brain-based learning (BBL), the technology used to help slow-reading students (SRS) which is serious game and low-fidelity prototypes covering paper prototypes, chauffeured prototype, think aloud protocols and observations.

A. Brain-Based Learning (BBL)

The approach or strategy used in game designs should be taken into account in designing the game model. Theoretical approaches and brain-based learning (BBL) strategies are applied in serious games. In the context of this study the BBL is defined as a technique that values the optimal function of the brain compared to the usual teaching method [12]. Optimal

This research was supported by the Universiti Kebangsaan Malaysia, Grant no. KRA-2018-025.

learning state integrating relaxed alertness, orchestrated immersion and active processing instructional techniques is the main feature of this approach [13]. BBL are seen as a technique that encourages the best way of learning and encouraging teachers to use this information when planning a teaching strategy to stimulate student motivation more effectively and to improve learning [13] [14].

Brain is the most important organ in supporting daily life. This BBL is based on the theory that learning is occur as long as human brain is not prevented from undergoing routine processes as opposed to traditional teaching. [12] [15]. According to [16], BBL can be seen as a technique used to improve teaching and learning (T&L) through the ability to learn to use the most comfortable ways they can. For the purposes of this study, students are required to i) be actively involved in all the seven brain compatible instructional phases listed below, [17], ii) have fun learning (serious games) and iii) Learn in their context and in related to existing knowledge. Seven brain compatible instructional phases are:

1) *Activation*: To stimulate the learning of a new concept, the existing knowledge of the student is activated. This is because prior knowledge always influences the teaching process by helping students to get rid of irrelevant things. Thus, the content developed should include the prior knowledge of SRS by involving their syllabus. This phase is where we activate student's memory processor system (prior knowledge) in order to stimulate their learning transfer process.

2) *Clarify the outcomes that need to be achieved and the learning process involved*: Teaching objectives as well as a comprehensive overview of new knowledge that students will learn will be shown. In this game model, players are introduced with learning objectives before players start a game session. This is to give an overview of the ideas taught to help students develop the desired understanding where students affirm for themselves their personal performance target, activate the right brain processor prior to the left brain, and alleviate anxieties over the accessibility and relevance of the material.

3) *Making connection*: Making connection and develop meaning is the stage where the topic or unit of work about to be completed is connected to what has been done before with what is yet to come. It builds on what the learners already know and understand. This process stimulates the student brain to make connections between newly learned and existing ideas. These three phases of teaching activities are thought to be able to create "Relaxed alertness" among students.

4) *Carry out learning activities*: This activity requires a thorough involvement by each student. Doing the learning activity is the stage for digesting, thinking about, reflecting on and making sense of experience utilizing visualization, auditory, kinesthetic in multiple contexts as well as to access all of the multiple intelligences. Here, students were encouraged to be in the state of "Orchestrated immersion", which immerses them in multisensory experiences.

5) *Demonstrating student's understanding*: Understanding demonstration activities provide opportunities for students to use their new knowledge or skills in new situations. This process gives students time to feel comfortable with the newly acquired concept and indirectly reinforces their conceptual understanding. This is the stage for brain-active processing. Through this game, it allows students to consolidate and internalize information effectively when they are actively engaged with the knowledge itself. Students can test their understanding and driving the transfer of information into the long-term memory of the students.

6) *Review for students' retention*: Evaluation and closing activities provide students with an opportunity to assess their understanding and stimulates working memory to summarize the lesson, which helps to strengthen the transfer process.

7) *Preview the next topic*: This activity is the experience that helps the brain pre-processor and the reptilian brain to focus on the new lesson and help improve the effectiveness of the learning process. This is important to prepare the brain for the new learning activities.

B. Serious Game and Slow-Reading Students

A serious game by definition [3] is an application with three main components: experience, entertainment and multimedia where serious game has a role to convey messages and inputs, knowledge, skills or general content to players. According to [18], serious game is designed interactively and has an educational goal of entertaining and creating an active learning environment available on any digital platform such as computers and smartphones. Its use is increasingly in various fields including in education. According to [19], a serious game is becoming increasingly popular not only as a game but as a convincing educational tool.

This study focuses on slow-reading students (SRS) where they are normal students but struggling to meet academic demands. They are slightly different from other students in terms of cognitive potential [9], understanding, thinking and they are not categorized as special needs students. According to [20], this computer-based learning technique can help slow learners learn to understand more easily in learning because of the use of multimedia elements and the ability to convey the same information but in different forms like sound, text, and images.

Serious game used because of the game potential that can have a positive impact on SRS. This SRS wants something fun while learning and at the same time lets them play [21]. This affects the emotions of the players, when they have fun in learning, memory space can be improved [22] [23] [24]. Past studies show that this serious game is capable of making learning more effective [25] [26] [27] and improving performance in learning [26] [28] [29] [30] [31]. While from the aspect of student psychology, serious games can increase motivation and students give more respond [25], [27], [29] [30] [31] [32] [33] [34] [35].

C. Low-Fidelity Prototype

In [36], author states that a prototype resembling an application developed on a real device is known as fidelity. The prototype used to rate applications can be simple as sketches on paper as well as complex fully interactive models on developed application devices. In [37], author refers prototype as low-fidelity and high-fidelity.

In [37], author states that normally a low-fidelity prototypes are made with paper, glue, cardboard and pen. Low-fidelity prototypes are very useful in the early stages of the design process for gathering needs and analysis. This prototype is useful in providing alternative design that can be produced quickly and valued [36] [38]. This prototype can also avoid misconceptions of communication between stakeholders in the early stages. Low-fidelity prototype is easy to recover and can sometimes be changed during the evaluation phase [36].

The purpose of this study is to get feedback in terms of the content and basic features of the software suitable for SRS. For paper-based sketches, storyboards have been created. This storyboard is then computerized using software like Photoshop and Microsoft Power Point. However, to understand the user's expectations and impressions, the chauffeured prototype, think aloud protocol and observation were used to get the feedback and improved storyboard.

III. RESEARCH METHODOLOGY

Users are involved as early in the game design process. Triangulation methods containing three research methods are used. Paper prototypes for producing storyboards are used and chauffeured prototype and think Aloud protocols (TAP) are carried out with observation. All tests are conducted at a school that runs the LINUS and remedial program. The results of the analysis are analyzed to produce storyboards that have been verified by users. This storyboard is used as a guide by researchers to conduct heuristic assessments before developing a high fidelity prototype.

The purpose of this study is to produce low-fidelity prototypes for serious games that have been verified. The researcher gets an approval by the school management first because it involves teachers and students as respondents. The study was conducted for two days. The first day involves only teachers who run paper prototypes while the second day involves teachers and students who run the chauffeured prototype, TAP and observation. The methodology of this study was developed as shown in Fig. 1.

The study participants consisted of teachers and slow-reading students (SRS) from a school running the LINUS and remedial program. Table I shows the number of teachers and students involved in low-fidelity prototypes. On the first day the prototyping test was carried out involved five teachers as respondents. The second day involved five respondents consisting of 3 teachers and 2 SRS.

This study involves three phase:

A. Phase 1: Design the Storyboard

Paper Prototype; According to [39], one of the fastest prototyping methods is to use paper. This prototype is cheap

and fast designed to illustrate models, ideas or features. This prototype is used in the early phase of the design because users can view the product description without having to use the code. Changes can also be made quickly and the results will continue to be seen. Three processes are involved in paper prototype.

The first process, the researchers sketches the storyboard using pen and paper. The initial sketch idea is obtained from literature studies and preliminary studies conducted earlier. The initial sketch proposed by the researcher is shown to the teacher. Five teachers were involved in this test and they briefed on the purpose of this test is to produce storyboards. Teachers then sketch their ideas on storyboards.

The second processes, all the sketches from teachers are collected and the assessments are done by researcher. The researcher justified the storyboard by teachers and decides which one to use after the discussion.

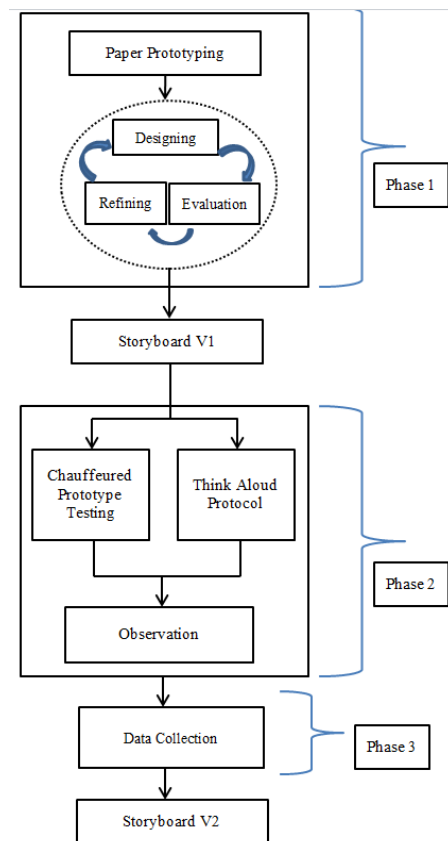


Fig. 1. Low-Fidelity Prototype Methodology.

TABLE I. NUMBERS OF TEACHERS AND STUDENTS

SK Bebuloh, W.P Labuan		
Techniques	No. of Teachers	No. of Students
Paper Prototype	5	-
Chauffeured Prototype	3 (Respondent 1, 2, 3)	2 (Respondent 4 and 5)
Think Aloud Protocol	3	-
Observation	3	2

The third process, the purification of the design in which the researcher improves the storyboard as required by the teacher. This process repeats until the teacher is satisfied with storyboard. In this study, two repetitions of paper prototypes were repeated by each teacher to get storyboard version 1.

B. Phase 2: Test and Improve Storyboards

Results from phase 1, which are storyboards, have been computerized using computer software Power Point and Photoshop with several functions that can be used. In this phase, chauffeured prototype, TAP and Observations are used to test and improve the storyboards.

1) *Chauffeured prototype*: According to [40], the chauffeured prototype is similar to the Wizard of Oz technique. The advantages of the chauffeured prototype are not all parts need to be together but interactivity can still be tested. Researchers directly can create the parts in storyboard based on user requirements. [39] the main difference between both techniques is for the chauffeured test, the user knows that the tested system is not a real and incomplete system. Users are aware of the existence of chauffeured where researchers or people who are aware of the prototype play a role as a driver or chauffeured. If a user tries a function that does not exist, chauffeured can add the function by drawing a new part directly in the prototype.

2) *Think Aloud Protocol (TAP)*: Simultaneously with the chauffeured prototype, the Think Aloud protocol (TAP) technique is used. Basically, TAP is a technique that requires users to express their thoughts when doing tasks or solving problems. According to [41], in TAP users are encouraged to tell their experiences, their thoughts, actions, and feelings when interacting with the interface. According to [42], TAP is a voluntary activity where respondents are required to speak what they feel loudly. However, SRS is not involved with TAP, only the teachers do. According to [43], in conducting tests with children, the assessor should use variations in the TAP as it is difficult for the child to follow the instructions for the TAP standard test. Teachers are required to express what they feel while testing the storyboard. In this study, researchers use the concurrent think aloud technique where players are required to state what they think when viewing storyboards. The objective is to identify usability issues and propose solutions to the issues raised.

3) *Observation*: In [44], author states qualitative methods for data collection such as interviews, observations and document analysis known as "Ethnographic Methods". Observation is performed when the user is running the chauffeured prototype and the TAP using the computer. This observation is done to see users reaction when interact with the storyboard and to record the player's sense of storyboard. Observations are performed with the help of visual recording. Observation data is recorded in the field note during the test session.

C. Collection of Data

The results of the triangulation test were collected and analysed. The results then are used to improve storyboards to produce storyboard version 2. This new version will be used for heuristic assessment tests.

IV. RESULTS AND DISCUSSION

The final result of the test is a validated computer storyboard. This storyboard is then used in conducting heuristic evaluation to see the suitability of the game interface. Table II below shows a summary of the results obtained from tests carried out.

In this study, researchers engaged users from the early phase of prototype design development to obtain immediate feedbacks before moving on to the next phase. Researchers and respondents are more focused on the development of game content. For paper prototypes, researchers and respondents started from scratch using pens and papers. The process is repeated twice for paper prototypes to produce a storyboard version 1. After researchers converted the sketches into computerized storyboards, the chauffeured prototype involved three teachers and two SRS executives to observe user interactions using storyboards.

Respondents 1 and 3 asked what happens if the player draws the right or wrong answer. Driver informed that an audio sound is implemented for correct and incorrect answers. Respondent 2 asked whether the pictures were given in order or at random to which the driver revealed that the pictures are given in order. Respondents 1 and 2 also asked what happens if the player clicks the image. The driver notified that the picture has an audio description. For example, if the player pressed the image of a ball, the audio "Ball" will be on. For both SRS respondents 4 and 5, they are only interested in pressing the buttons and menu that has functions, for instance, the 'Next' and 'Back' buttons. Respondent 4 went directly to the 'drag and drop' menu while Respondent 5 looked from the beginning of the storyboard before moving to the game menu. By showing a storyboard, both SRS respondents clicked the picture and repeated the driver's voice to say alphabet 'a', 'b', and so 'e'.

When respondents (teachers) conducted the chauffeured prototype, they also applied the think aloud protocol (TAP) where respondents expressed what they felt when they used the prototype. The researcher also conducted an observation with the aid of a visual recording of the respondents while carrying out the TA. In this technique, observations are performed and responses from respondents are recorded in the field note as well as with audio and visual help. Respondents 1 and 3 agreed that colourful contents can attract the attention of SRS to play longer. This is important because SRS have limited hearing and vision, a short focus and can quickly feel bored to a static thing [45]. Both respondents also stated that Times New Roman font did not correspond to SRS and suggested researchers review the appropriate font for SRS. Respondent 2 (Teacher) stated that this software is suitable for SRS. All

respondents agreed that the software and modules are easy to use, understandable, enjoyable, interesting and can be played anywhere and anytime, even at home with adult supervision. Respondent 2 (Teacher) also stated that the content of the game is the same as that used in the classroom, but the innovation of this computer game is able to attract students because it is something new. Respondents 1, 2 and 3 hope that this software can help SRS, improve their literacy skills and increase their passion in learning.

Through observation, Respondents 1, 2, and 4 have had no problem in using their computers and equipment but Respondents 3 and 5 had a little difficulty. Respondent 3 is a senior teacher who is not very skilled at using computer but had no further problem when assisted by the researcher. While Respondent 5 is an SRS who has never used computers but faced no further problems as she is used to playing games using smartphones. All teacher respondents (1, 2, and 3) concentrated on the content of the game so that it will suit SRS. For SRS respondents (4 and 5), they did not know which button to click because of their weakness in reading the instructions. So, SRS just clicked the buttons and pictures that were appealing to them. After the teacher explained to SRS, they understood what they need to do. For SRS respondents, they did not find using a computer and mouse difficult although, at first, they were a bit clumsy. All the respondents were also interested in seeing colourful storyboards with sound effects.

The researcher also explained that BBL strategy is applied in this serious game to the teacher respondents (1, 2 and 3) because the strategy has been used in their daily T&L in reality. They are seven brain-compatible teaching phases [17] that have been adopted in designing the BBL strategies in this game. This game is used by the remedial students who have basic reading skills. When a new concept is taught, students can link it to prior knowledge and thus, existing knowledge is activated. In [46], author stated that the BBL approach emphasizes the relevance of new and existing information to students to make them more prepared in T&L. Through games, information is obtained in various forms such as visual, audio and kinesthetic to give students the opportunity to link the information obtained to create profound meaning. This BBL approach is able to increase the understanding and achievement of students in learning [13], [17], [46]. For each game, the students are briefly explained about the activity objective to give an overview or idea about the activity. After the T&L session, a teacher repeats the topic taught previously and describes the new topic to be learned. This allows the brain to prepare for future lessons which can help improve the effectiveness of the learning process. After getting feedback and making improvements to produce storyboard version 2, researchers will use this new version to make heuristic evaluation of the game interface. In [47], author state that heuristic inspection methods are a method of engineering usability to identify the usability problems of a user interface design so that software can be improved in a recurring development process. These assessment results are used to make changes to the software before developing high-fidelity prototypes.

There may be some possible limitations in this study. This study is focused on SRS but one of the method uses not involved them as it is difficult for the SRS to follow the instructions without teachers help. SRS can only be involved with qualitative data collection because of their lack of understanding in written instructions if quantitative studies are carried out.

TABLE II. FINDINGS

Sekolah Kebangsaan Bebuloh W.P Labuan	
Category	Details
Issues	<ol style="list-style-type: none"> 1. The font used does not correspond to the slow reading student. 2. The font size is quite small. 3. The background for font should be contra to facilitate students to see the letters and words. 4. Students need guidance assistance because of their weakness in understanding the written instructions. 5. A teacher and a student need assistance in using a computer and mouse.
Advantages	<ol style="list-style-type: none"> 1. Contents used are appropriate and parallel to the student's syllabus of LINUS and remedial. 2. Game content is easy to understand and the game is easy to play. 3. Colorful interface can attract the students. 4. Ideally played anytime and anywhere with adult supervision. 5. Game is easy and playable by students. 6. Suitable for classroom use to attract students to play and learn. 7. Help students with a short period of concentration with colorful animations.
Observation	<ol style="list-style-type: none"> 1. Respondents are attracted to colorful graphic. 2. Respondents are attracted by sound effect. 3. Three out of five respondents had no problem using the computer and mouse. 4. For a functional menu, the respondent repeated several times to hear sound effects (Example: Next Button and Back Button). 5. Students repeat the voice by the chauffeured to say alphabet 'a', 'b', so 'e'.
Suggestions	<ol style="list-style-type: none"> 1. Create an avatar. 2. Have Menu "Let's Learn" and "Activity". 3. Menu "Let's learn" contains letter and word identification. 4. Activity and exercise menu are combined. 5. The menu for exercises is sorted by topic (letters, words, syllables). 6. Have Menu singing abc songs. 7. Separate instructions with the main interface. 8. Differentiate the syllable instructions with different colors. 9. For "Drag" and "Drop" exercises, the respondents suggested that the given picture was arranged instead of randomly. 10. Distinguish the sound for correct and wrong answers.
Hope	<ol style="list-style-type: none"> 1. Teachers hope to play a fully functional game. 2. Can improve students reading literacy skills. 3. Can encourage students to learn.

V. CONCLUSION

The study was aimed at developing a low-fidelity prototype of computerized storyboards. This storyboard is used for further development of the heuristic evaluation of the interface and subsequently the development of high-fidelity prototypes. In this study, users are involved from the initial phase of storyboard making from scratch. They contributed ideas about the content that are relevant to the target audience. Researchers also explained briefly about BBL strategies that are indirectly but commonly used by teachers in T&L daily as well as to get teachers' response about BBL. Not only is the game element important when designing a serious game but the strategy or approach used is also important. The game applies seven phases of the brain-compatible teaching [17] as well as strategy [48]. In conclusion, this low-fidelity prototype is expected to be an early reference for the development of a high-fidelity prototype for slow-reading students.

ACKNOWLEDGMENT

The authors would like to thank Sekolah Kebangsaan Bebuloh, W.P Labuan. The Ministry of Higher Education for the finance sponsored under program MyBrain15 (MyPhD). The Faculty of Information Science and Technology, Universiti Kebangsaan Malaysia for providing facilities and financial support under the university Grant with Project Number KRA-2018-025.

REFERENCES

- [1] A. Shapi, N. A. Abd Rahman, M. S. Baharuddin, and M. R. Yaakub, "Interactive Games Using Hand-Eye Coordination Method for Autistic Children Therapy," *Int. J. Adv. Sci. Eng. Inf. Technol.*, vol. 8, no. 4, pp. 1381–1386, 2018.
- [2] H. F. Md. Muslim, T. S. M. Tengku Wook, and N. A. Mat Zin, "Kajian awal permainan serius untuk warga emas mengidap diabetes," *Proceeding Glob. Summit Educ. GSE 2014*, vol. 2014, no. March, pp. 553–559, 2014.
- [3] F. Laamarti, M. Eid, and A. El El Saddik, "An Overview of Serious Games," *Int. J. Comput. Games Technol.*, vol. 2014, 2014.
- [4] C. M. Ruland, J. Starren, and T. M. Vatne, "Participatory design with children in the development of a support system for patient-centered care in pediatric oncology," *J. Biomed. Inform.*, vol. 41, pp. 624–635, 2008.
- [5] J. C. Read and S. Gilutz, "Research Methods for Child Computer Interaction," pp. 927–930, 2016.
- [6] S. Idler, "Child-Centered Design is User-Centered Design, But Then Different," *UXKids*, 2013. [Online]. Available: <http://uxkids.com/blog/child-centered-design-is-user-centered-design-but-then-different/>.
- [7] N. Abdollah, W. F. Wan Ahmad, and E. A. Patah Akhir, "Multimedia Design and Development in 'Komputer Saya' Courseware for Slow Learners," in *Second International Conference on Computer Research and Development*, pp. 354–358, 2010.
- [8] A. R. Mohd Salihan, M. A. Nazlena, and M. Masnizah, "Comelgetz Prototype In Learning Prayers Among Children," *Asia-Pacific J. Inf. Technol. Multimed.*, vol. 6, no. 1, pp. 115–125, 2017.
- [9] S. R. Zainal Abidin, S. F. Mat Noor, and N. Sahari, "Guidelines of Brain-based Learning through Serious Game for Slow Reader Students," in *2017 6th International Conference on Electrical Engineering and Informatics (ICEEI)*, 2017.
- [10] S. Saleh and A. D. Halim, "Kecenderungan Otak dan Hubungannya dengan Pencapaian dan Motivasi Pelajar," *J. Pendidik. Malaysia*, vol. 41, no. 1, pp. 65–70, 2016.
- [11] K. Squire and H. Jenkins, "Harnessing the power of games in education," *Insight*, vol. 3, pp. 5–33, 2003.
- [12] R. N. Caine and G. Caine, *Making Connections: Teaching and the Human Brain.*, no. 218, 1991.
- [13] S. Saleh, "The Effectiveness of the Brain Based Teaching Approach in Enhancing Scientific Understanding of Newtonian Physics among Form Four Students," *Int. J. Environ. Sci. Educ.*, vol. 7, no. 1, pp. 107–122, 2012.
- [14] A. Bawaneh, A. Nurulazam, and Salmiza Saleh, "The Effect of a Brain-Based Teaching Method on Conceptual Change in Students' Understanding of Electricity ChangeAgent," *Eurasian J. Phys. Chem. Educ.*, vol. 4, no. 2, pp. 79–96, 2012.
- [15] E. Jensen, "Brain-Based Learning: The New Paradigm of Teaching," 2nd Ed., Corwin Press, 2008.
- [16] J. D. Connell, "The Global Aspects of Brain-Based Learning," in *Educational Horizons*, vol. 88, 2009, pp. 28–39.
- [17] S. Saleh, "Kebekerkesanan Pendekatan Pengajaran Berasaskan Otak Dalam Menangani Masalah Berkaitan Motivasi Belajar Fizik Pelajar," in *Prosiding Seminar Jawatankuasa Penyelarasan Pendidikan Guru*, 2008.
- [18] M.-A. Maheu-Cadotte, S. Cossette, V. Dubé, G. Fontaine, T. Mailhot, P. Lavoie, A. Cournoyer, F. Balli, and G. Mathieu-dupuis, "Effectiveness of serious games and impact of design elements on engagement and educational outcomes in healthcare professionals and students: a systematic review and meta-analysis protocol," 2018.
- [19] G. Kokkalia, A. Drigas, A. Economou, P. Roussos, and S. Choli, "The Use of Serious Games in Preschool Education," *Int. J. Eng. Technol.*, vol. 12, no. 11, pp. 15–27, 2017.
- [20] N. Abdollah, W. F. Wan Ahmad, and E. A. Patah Akhir, "Development and Usability Study of Multimedia Courseware for Slow Learners: 'Komputer Saya,'" in *2012 International Conference on Computer & Information Science (ICCIS)*, 2012, pp. 1110–1114.
- [21] T. Y. Su, P. Gates, and I. Harrison, "Digital Games and Learning Mathematics: Student, Teacher and Parent Perspectives," *Int. J. Serious Games*, vol. 3, no. 4, pp. 55–68, 2016.
- [22] P. Felicia, *Digital Games in Schools*. European Schoolnet, 2009.
- [23] M. Liu, J. A. Rosenblum, L. Horton, and J. Kang, "Designing Science Learning with Game-Based Approaches," *Comput. Sch.*, vol. 31, no. 1–2, pp. 84–102, 2014.
- [24] N. Peirce, "Digital Game-based Learning for Early Childhood A State of the Art Report," 2013.
- [25] S. De Freitas and S. Jarvis, "Serious games - Engaging training solutions: A research and development project for supporting training needs," *Br. J. Educ. Technol.*, vol. 38, no. 3, pp. 523–525, 2007.
- [26] M. W. Martin and Y. Shen, "The Effects of Game Design on Learning Outcomes," *Comput. Sch.*, vol. 31, no. 1–2, pp. 23–42, 2014.
- [27] A. C. Siang and R. K. Rao, "Theories of learning: a computer game perspective," *Multimed. Softw. Eng. 2003. Proceedings. Fifth Int. Symp.*, pp. 239–245, 2003.
- [28] M.-E. Ntourlia, D. Gouscos, and M. Meimaris, "TuxMath: Is it Possible for a Game to Enhance Multiplication Skills?," in *4th European Conference on Games-Based Learning: ECGBL 2009*, 2009.
- [29] M. Kebritchi, A. Hirumi, and H. Bai, "The effects of modern mathematics computer games on mathematics achievement and class motivation," *Comput. Educ.*, vol. 55, no. 2, pp. 427–443, 2010.
- [30] N. Muhamad, J. Harun, S. Md Salleh, and M. A. Z. Megat Zakaria, "Penggunaan Game-Based Learning Bagi Meningkatkan Kemahiran Penyelesaian Masalah Kreatif Dalam Matematik," in *2nd International Education Postgraduate Seminar (IEPS 2015)*, 2015, pp. 1–9.
- [31] N. A. Mohamed Masrop, H. A. Mak Din, A. N. Zainal Ariffin, and I. F. Mohammed Salleh, Nur Muizz Ahmad, "Kesan Permainan Digital Dalam Pendidikan," *Proceeding Int. Conf. Inf. Technol. Soc.*, no. June, pp. 1–7, 2015.
- [32] L. P. Rieber, "Seriously considering play: Designing interactive learning environments based on the blending of microworlds, simulations, and games," *Educ. Technol. Res. Dev.*, vol. 44, no. 2, pp. 43–58, 1996.
- [33] M. Prensky, "The Digital Game-Based Learning Revolution," in *The Digital Game-Based Learning Revolution*, vol. 1, no. 1, 2001, pp. 1–19.
- [34] M. Papastergiou, "Digital Game-Based Learning in high school Computer Science education: Impact on educational effectiveness and

- student motivation,” *Comput. Educ.*, vol. 52, no. 1, pp. 1–12, 2009.
- [35] H. Tüzün, M. Yılmaz-Soylu, T. Karakuş, Y. Inal, and G. Kizilkaya, “The effects of computer games on primary school students’ achievement and motivation in geography learning,” *Comput. Educ.*, vol. 52, no. 1, pp. 68–77, 2009.
- [36] E. Bertou, “Low - fi Prototyping Tablet Apps for Children,” Tilburg University, 2013.
- [37] J. Sauer, H. Franke, and B. Ruettinger, “Designing interactive consumer products: Utility of paper prototypes and effectiveness of enhanced control labelling,” *Appl. Ergon.*, vol. 39, pp. 71–85, 2008.
- [38] J. Rudd, K. R. Stern, and S. Isensee, “Low vs. high-fidelity prototyping debate,” *Interactions*, vol. January, no. 1, pp. 76–85, 1996.
- [39] S. Hietala, “User Study of a Prototype for Mobile Work Time registration,” Luleå University of Technology, 2016.
- [40] J. F. Nunamaker, A. R. Dennis, J. S. Valacich, D. Vogel, and J. F. George, “Electronic meeting systems to Support Group Work.,” *Commun. ACM*, vol. 34, no. 7, pp. 40–61, 1991.
- [41] O. Alhadreti and P. Mayhew, “Rethinking Thinking Aloud: A Comparison of Three Think-Aloud Protocols,” in *Conference on Human Factors in Computing Systems*, 2018, pp. 1–12.
- [42] J. Cowan, “The potential of cognitive think-aloud protocols for educational action-research,” *Act. Learn. High. Educ.*, 2017.
- [43] J. Nielsen, “Usability Engineering,” in Academic Press, 1993.
- [44] B. B. Kawulich, “Participant Observation as a Data Collection Method,” *Forum Qual. Sozialforsch. / Forum Qual. Soc. Res.*, vol. 6, no. 2, 2005.
- [45] H. Azizeanna, M. Murni, and M. T. Abu Osman, “Tablet Technology Integration framework for Slow Learner Learning,” in *Information and Communication Technology for The Muslim World (ICT4M)*, 2014, pp. 3–7.
- [46] F. Fazil and S. Saleh, “Keberkesanan Pendekatan Pengajaran Berasaskan Otak Dalam Meningkatkan Kefahaman Pelajar Tingkatan Empat Terhadap Pembelajaran Konsep Dan Mekanisme Fotosintesis,” *Asia Pacific J. Educ. Educ.*, vol. 31, pp. 69–83, 2016.
- [47] N. Ashaari, H. Mohd Judi, A. A. Abdul Ghani, S. Mohd Hasan, and A. S. Md Yunus, “Skor Pengukuran Kebergunaan Perisian Kursus Matematik Berdasarkan Faktor Penilai,” *Sains Malaysiana*, vol. 39, no. 4, pp. 677–684, 2010.
- [48] S. Hileman, “Motivating Students Using Brain-Based Teaching Strategies,” *The Agricultural Education Magazine*, vol. 80, no. 2, pp. 1–28, 2006.

Experimentation for Modular Robot Simulation by Python Coding to Establish Multiple Configurations

Muhammad Haziq Hasbulah¹, Fairul Azni Jafar², Mohd. Hisham Nordin³, Kazutaka Yokota⁴

Faculty of Manufacturing Engineering, Universiti Teknikal Malaysia Melaka^{1, 2, 3}

Hang Tuah Jaya, 76100 Durian Tunggal, Melaka, Malaysia

Research Div. of Design and Eng. For Sustainability, Graduate School of Engineering⁴

Utsunomiya University 7-1-2 Yoto, Utsunomiya-shi, 321-8585, Japan

Abstract—Most of the Modular Self-reconfigurable (MSR) robots are being developed in order to have the capability of achieving different locomotion gaits. It is an approach of robotic system which involving a group of identical robotic modules that are connecting together and are able to perform specific tasks. In this study, a 3D-printed MSR robot named Dtto-Explorer Modular Robot was used to investigate the achievable propagation that can be made based on three of Dtto robot modules. As Dtto robot is developed based on Modular Transformer (M-TRAN), Dtto robot has the number of Degree of Freedom (DOF) same as M-TRAN which is 2 DOF. Hence, this study is done with the intentions to know the variation of configuration that can be made by multiple module robots which have only 2 DOF. The robot propagation was simulated in Virtual Robot Experimentation Platform (V-REP) software. The result of the simulation shows that the Dtto MSR robot can propagate multiple configurations after all the robot modules being connected to each other by different attachment orientation of the Dtto robot and it is suitable for the purpose of further research on MSR robot architecture.

Keywords—Dtto robot; simulation; configuration; locomotion; orientation

I. INTRODUCTION

The Dtto modular robot is developed based on M-TRAN robot which was first developed by Murata et al. [1]. The module consists of two semi-cylindrical parts that can be rotated about its axis and with a link. It possess 2 DOF [2], which resemble M-TRAN robot module ability. However, the Dtto modular robot is being designed so that each module can be minimized as much as possible to have a large free space in half of the robot. It is purposely done so that it can be used by users to set up their preferred sensor such as Infrared (IR) sensor or install more actuators. It is 3D printable and at low cost to be builds. This study is done by using Dtto robot, design by Alberto [2] because the result from this study will be used as a references to our next research purpose as this robot can be redesigned as it is an open-source robot and it is fabricated by using only 3D printer.

As it is being designed based on M-TRAN modular robot, a review summation of Dtto and M-TRAN modular robot

comparison has been performed and can be seen as in Table I.

The comparison between the robots is based on several characteristics which are CPU, Communication, Battery, Sensor-applied and Robot Connection Mechanism. M-TRAN robot is a Hybrid type MSR robot which is in the form of Chain and Lattice, same goes with Dtto robot. Hence, we believe that Dtto robot is able to propagate multiple configurations. However, with only 2 DOF, it might not have many movements ability to propagate multiple configurations. It is believe that the collective behavior of modular robot could establish more movements or propagate multiple configurations of different locomotion gaits [5], even though the movement is limited for one robot module.

Basically, most of the MSR robots that have been developed are able to propagate snake-like motion, which is minimal possible configuration for modular robot to have locomotion ability. It is known as Serpentinoid curve or Sinusoidal curve which was discovered in 1976 by Hirose for application of biomechanics of snake to robot construction [6][7], so the robot can propelled forward by sending Sine and Cosine value. Basically, its implementation for the locomotion mechanism for snake-motion propagation can be referred from research study done by Gómez [8]. The mechanism theory will be discussed in Section 2 of this paper. Besides that, other possible propagation for the Dtto modular robot were also established as this study is done to ensure the Dtto robot with 2 DOF is able to propagate multiple configurations with multiple robot modules. Besides snake-like motion, the other configurations being propagate are Cube-shaped, U-shaped, Cuboid-shaped and Chain-shaped. This study has been done by establishing simulation in V-REP software, controlled by Python coding.

In the sections to follow, we discuss the theoretical concepts of Snake-like locomotion where it is being implemented for establish multiple configuration of the Dtto modular robot. Then we discussed the methodology approach for conducting this experimentation in Section III. The simulation results are illustrated and discussed in the Section IV and this paper is concluded in Section V.

TABLE I. SUMMARIZATION OF COMPARISONS FOR DTTO AND M-TRAN MODULAR ROBOT

Characteristics	Comparisons Summarization			
	M-TRAN	M-TRAN II	M-TRAN III	Dtto
CPU	BasicStamp II	Neuron chip, Three PICs	HD64F7047, HD64F3687, HD64F3694	Arduino Nano v3.0
Communication	Asynchronous serial	LonWorks & RS-485, Asynchronous serial	Bluetooth wireless modem	Bluetooth wireless, HC-05, RF24L01
Battery	DC 12V	Li-ion	Lithium-polymer	Li-Po
Sensor Applied		Acceleration sensor	IR proximit, IR diode, IR sensor	InfraRed LED Emitter- Receiver (Optiona)
Robot Connection Mechanism	SMA (shape memory alloy) coil and magnet	SMA (shape memory alloy) coil and magnet	Mechanism based on latch connector	Permanent magnet (Neodymium magnet)
References	[1]	[3]	[4]	[2]

II. THEORETICAL FOR SNAKE-LIKE LOCOMOTION CONCEPTS

The theoretical concept for the robot to have Snake-like Locomotion needs to be unraveled so we can understand how the motion works. The angle of curvature that varies in sinusoidal with the distance along the curve [9] is based on the equation of curvature where it define the Serpentinoid curve or Sinusoidal curve. Equation (1) is the equation of curvature mentioned where k is the number of undulations, l is the length of the curve, s is the distance along the curve, and α is the value of angle that forms the tangent to the curve when $s = 0$ which determine the shape of the curve.

$$K(s) = -\frac{2\pi k}{l} \alpha \sin\left(\frac{2\pi k}{l} s\right) \quad (1)$$

The curvature definition can be defined by the rate of change of the vector unit tangent to the curve when it is provided with the Cartesian coordinates (x,y) of the points located in the Serpentinoid curve which depends on the temporal variable, t as in Equation (2) and (3).

$$x(s, t) = \int_0^s \cos\left(\alpha \cos\left(t + \frac{2\pi k}{l} s\right)\right) ds \quad (2)$$

$$y(s, t) = \int_0^s \sin\left(\alpha \cos\left(t + \frac{2\pi k}{l} s\right)\right) ds \quad (3)$$

However, according to Rodríguez [8] and Gómez [9], the mentioned equations, where it is proposed by Hirose, does not have analytical solution. Hence, it opened up various possibilities for establishing this configuration by coordinated the joints of the robot so that the serpentinoids wave can be reproduces. Hence, one of the alternative that we adopted in our study is by calculating the angles which will being applied to the robot's joints to reach the desired position. So, the reference of the robot movement will be based on joints target position according to a sinusoidal function.

Based on the simplified Serpenoid curve [10], the snake robot gaits generation way, arc length is defined as the curvature of the s , where b is constant:

$$p(s) = -ab \sin(bs) \quad (4)$$

Hence, for the generation of winding or oscillates movement gait, the relative angle of each joint has to be determined which will create a static configuration. However, for locomotion propagation for the robot to move, the s value has to be changed with respect to time sequentially. Hence, the corner of dynamic circumstances in the modular snake-like robot joint where φ is angle of rotation is as Equation (5) [7]:

$$\varphi_i(t) = A \sin(\omega t + (i - 1)\beta) \quad (5)$$

Hence, the Equation (5) is applied in our study for establishing this configuration where $i = 0,1,2,3 \dots$, is the number of modular robots series. The modular robot oscillates according to a sinusoidal function and its parameters such as amplitude, speed and phase shift is being determined at first.

III. METHODOLOGY

The robot control is established by interfacing with Python as we want to provide external control to the Dtto robot in simulation environment for each configuration. This communication is maintained via a while loop and the configuration of the robot changed based on the input, where the robot configuration is predetermined which one of the configurations and is based on the snake-like motion equation [6][7][11], so the robot can propelled and create motion for the robot to move in space. The following flowchart (Fig. 1) is the establishment of Python to V-REP communication so that the robots propagate multiple configurations. V-REP is integrated simulation environment where each object can be controlled individually by remote Application Program Interface (API) client.

Three following files are needed for using remote API functionality in Python script which are vrep.py, vrepConst.py and remoteApi.dll. Those files have to be in the same directory with Python script project. It is because those elements directory is need to be known by Python. The three mentioned files can be located in V-REP installation directory.

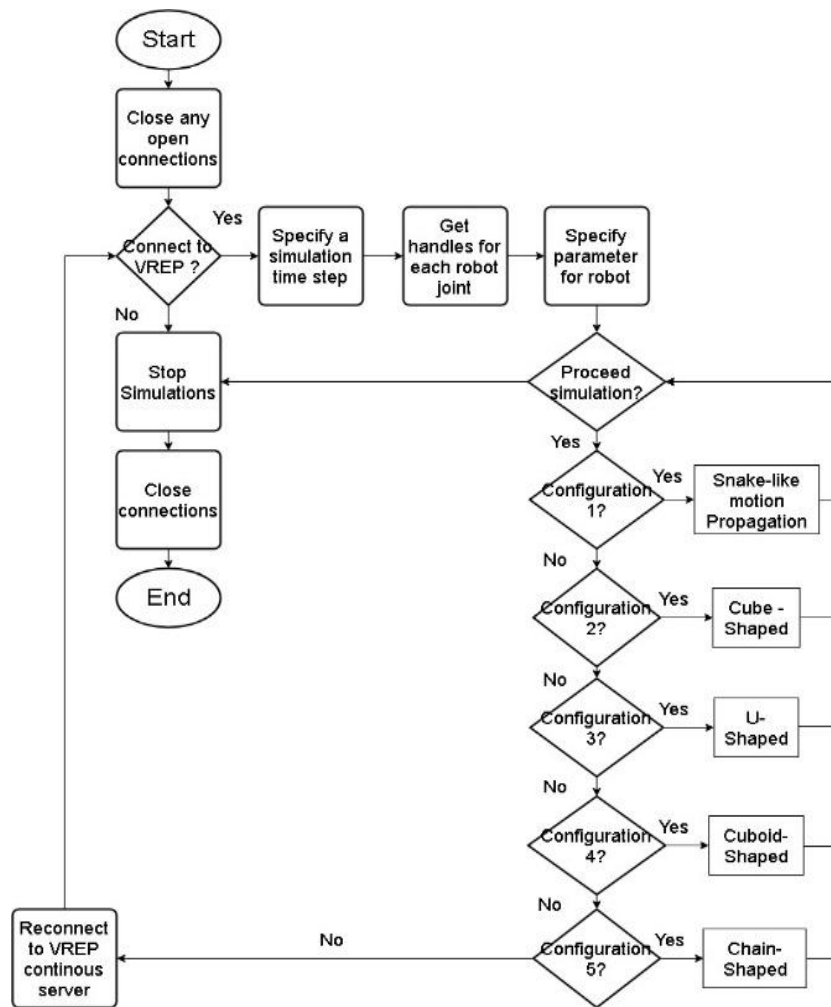


Fig. 1. All the Number of Joints for the Robot being Access in Python Coding.

For this research work, all the virtual Dtto modular robots will be controlled based on number of joints. Hence, as the robot has multiple of joints which is 2, by using the same name, the robot joint will be accessed based on the number. The Python list is created to access the elements of the list. As in this study, the number of module robot is 3 (which mean 3 elements in the list), the list will be accessed by indexing starting from 0 to 2 as in Fig. 2.

As the code is running, the while-loop code will start as the user enter the letter “Y” by the keyboard which indicate that the user want to proceed with the simulation. As the code running, user will need to enter the number ‘1’, ‘2’, ‘3’, ‘4’, and ‘5’ that indicate the configuration being simulated. The robot movement code in the while loop will keep running and the robot configuration can be changed from time to time based on the user input. In this methodology, Dtto MSR robot model is used and imported into V-REP. Besides that, time steps of V-REP simulation is specified for a small value which is 0.001. The increment of simulation time will be based on each of the simulation time step for each time the simulation is executed. Four pre-determined configurations were selected based on the three axis configurations that are achievable, which are Cube-shaped, U-shaped, Cuboid-shaped and Chain-shaped.

```

position(clientID, maleMotor[0],
((A_V[0] * (1 - s)) + (A_V[1] * s)) * (math.sin(t * (
((speed[0] * (1 - s)) + (speed[1] * s)) + (
0 * P_V[0] * (1 - s)) + (
P_V[1] * s))), vrep.simx_opmode_onesho
position(clientID, femaleMotor[0],
((A_H[1] * (1 - s)) + (A_H[0] * s)) *
(math.cos(t * (

```

Fig. 2. All the Number of Joints for the Robot being Access in Python Coding.

IV. RESULTS AND DISCUSSION

Discussion and interpretation based on the experimentation result are discussed in this sub-topic. The configurations propagate by the robot need to be discussed to have a better understanding on the capability of the Dtto modular robot to propagate multiple configurations.

It is believe that the main configuration for the Dtto robot propagation is the snake-like motion that has been discussed in Section 2. Dtto modular robot does not have specific item that give it mobile capabilities such as wheels. That is why snake-like motion is one of the configurations that is necessary to give Dtto modular robot an ability to move. This configuration

is chosen because it is suitable to be implemented to modular robot as it has similarity with snake type robot which is modularity that can be seen to snake robot for each of its segment. The other configuration possible with limited DOF is studied and all configurations are simulated by V-REP software.

To propagate multiple configurations for the robot, the approach as in Flowchart of Fig. 1 was followed to show that the robot is able to propagate multiple configurations with 3 modules of Dtto robot where one module only have 2 DOF.

Fig. 3(b) shows that to have 3 axis configuration (X, Y, and Z), one or more of the modular robot have to be in different position compare to the one in Fig. 3(a) whereas the modular robots is in same position attachment, it only have 2 axis configuration (X and Z). By having an ability to propagate configuration by 3 axis, it gives more possible configuration for the modular robots to propagate.

The first configuration being studied for Dtto modular robot is the ability to propagate a snake-like motion. At first, the robot will be studied as the robot has the same position attachment with 2 axis configuration as in Fig. 3(a). The robot orientation will be as Fig. 4 which at X and Z axis (Left) and X and Y axis (Right). Fig. 4 also shows the Axis-Time graph that shows the motion created for the robot. Axis-Time graph will be used to analyze the movement of the robot during its propagation in term of axis respected to simulation time. Based on the Equation (5), for the first configurations, the snake-like motion equation that being coded in Python language is as Equation (6) and (7) where *maleMotor* and *femaleMotor* is actually being specify for robot's joint.

$$maleMotor[i] = (A_{V[1]}(1 - s)) \sin(t(v_{[1]}(1 - s)) + i(P_{V[1]}(1 - s))) \quad (6)$$

$$femaleMotor[i] = (A_{V[2]}(1 - s)) \cos(t(v_{[1]}(1 - s)) + i(P_{V[2]}(1 - s))) \quad (7)$$

From Fig. 4 the modular robot at X-Z axis orientation create a caterpillar type motion and from the Axis-Time graph it shows that there is increasing value of the X-axis data. It means that, this configuration creates a propelled motion that move the 3 modular robot as one towards X-axis direction (propagate forward). For the modular robot at X-Y axis orientation, it creates a snake-like motion by sending a value of Sine and Cosine to the robot. We can see from the Axis-Time graph that the snake-like motion create a wave like graph that known as a serpenoid curve based on values of angles. However, for the modular robot at X-Y axis orientation, the graph shows unnoticeable changes for X-axis and Y-axis data. The simulation resulting as in Fig. 4(b), the motion of the robot for X axis is forward and reverse in serpenoid motion without propagate forward or backward. The motion for Y-axis is left and right in serpenoid motion, without propagating to left or right. Hence, this orientation is not suitable because we need

at least one configuration that gives movement to the robot. However, even though the configuration as Fig. 4(a) gives the movement ability to the robot, it only propagates by 2 axis of configuration which limits the number of configuration that is able to be made. That is why we choose to have the modular robots in attachment position as Fig. 3(b) so that the snake-like motion can be achieved with 3 axis configuration of the robot which give more possibilities for multiple configurations.

For simulating multiple configurations, as mentioned before, the first configuration simulated is the snake-like motion but with the orientation of modular robots as in Fig. 3(b). The simulation result can be seen in Fig. 5.

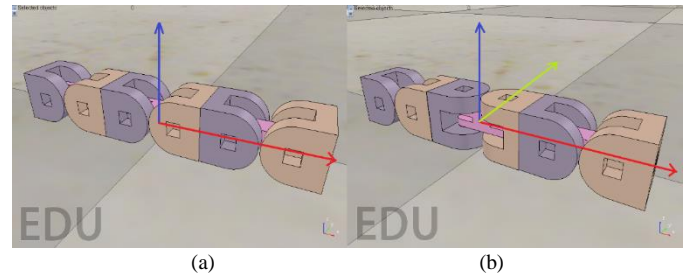


Fig. 3. Uniform Attachment Position (a) and Irregular Attachment Position of Robot (b).

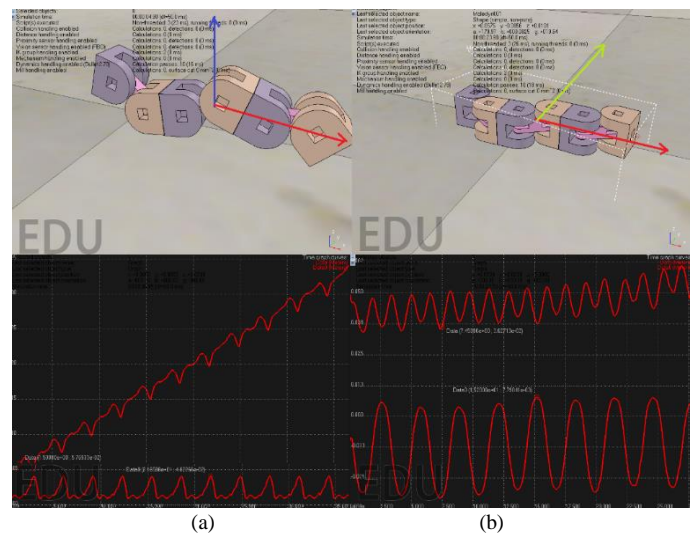


Fig. 4. Robot X-Z Axis Orientation (a) and X-Y axis orientation (b) with Axis-Time Graph.

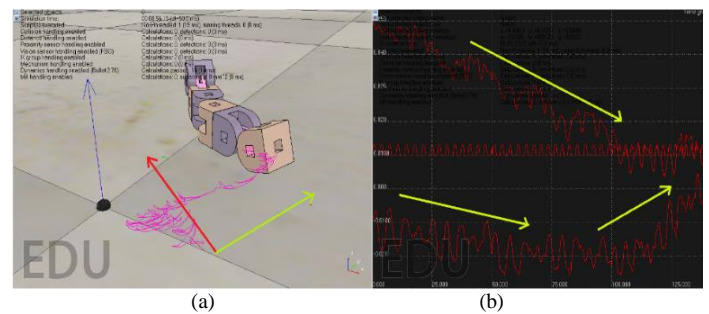


Fig. 5. Robot Snake-Like Motion Propagate (a) and Axis-Time Graph (b).

Based on Fig. 5, it can be seen that the robot is able to move towards right direction (Y-axis) and propagate backwards (X-axis) simultaneously which is proving that at this orientation, this configuration that provides locomotion to the Dtto modular robot can be achieved. Based on the Axis-time graph in Fig. 5(b), there are changes for X-axis data (downward direction) of the Sine and Cosine wave which means this configuration create a propelled motion that move the 3 modular robots as one towards X-axis direction but propagate backward. There are also changes for the Y-axis data and there is no change in Axis-time graph for Z-axis data which shows that the propagation of the robot for this orientation is at X-axis and Y-axis just as mentioned and shown in Fig. 5(a). Hence, it means that there is movement that the robot produces and it shows that this configuration is suitable for the purpose of robot locomotion. It is not necessary for the robot to propagate snake-like motion first, but we decided to have one propagation for robot mobility. The snake-like motion was studied first because it is complicated compared to other predetermined configurations that we decided. We decided for snake-like motion because it has similarity with normal snake robot (modular with redundant segment).

Then, the other propagation was simulated as we want to know whether the multiple configurations can be achieved with this configuration or not. As mentioned before, the other configurations being propagate are Cube-shaped, U-shaped, Cuboid-shaped and Chain-shaped. Fig. 6 shows that the other 4 predetermined configurations are able to be simulated which show that Dtto modular robot is able to propagate multiple configurations. The configuration as in Fig. 6 is being propagated in V-REP software by manipulating the equation coded as Equation (6) and (7). For configuration as Fig. 6(a), the value for *maleMotor* and *femaleMotor* is based on Sine value only. The propagation created is based on the Equation (8) and (9) that being coded in Python.

$$maleMotor[i] = (A_{V[1]}) \sin(t(v_{[1]}) + (P_{V[1]})) \quad (8)$$

$$femaleMotor[i] = (A_{V[2]}) \sin(t(v_{[1]}) + (P_{V[2]})) \quad (9)$$

Then the configuration as in Fig. 6(b) being developed for Dtto robot to propagate by having Sin and Cosine value for first *femaleMotor* and *maleMotor*, respectively for 1st robot module. The 2nd robot module have been specified with exactly 0 value for both *maleMotor* and *femaleMotor* and finally, the 3rd robot module being specify with Cosine and Sine value for *femaleMotor* and *maleMotor*, respectively.

$$maleMotor[0] = (A_{V[1]}) \sin(0(v_{[1]})) + (P_{V[1]}) \quad (10)$$

$$femaleMotor[0] = (A_{V[1]}) \cos(t(v_{[1]})) + (P_{V[1]}) \quad (11)$$

$$maleMotor[2] = (A_{V[1]}) \sin(t(v_{[1]})) + (P_{V[1]}) \quad (12)$$

$$femaleMotor[2] = (A_{V[1]}) \cos(0(v_{[1]})) + (P_{V[1]}) \quad (13)$$

The 4th configuration being developed by coded equation in which the value of Sine is being specified for

femaleMotor of the 1st robot module and for *maleMotor* of the 3rd robot module as in Equation (14) and (15).

$$maleMotor[0] = femaleMotor[1] = maleMotor[1] = femaleMotor[2] = (A_{V[1]}) \cos(0(v_{[1]})) + (P_{V[1]}) \quad (14)$$

$$femaleMotor[0] = maleMotor[2] = (A_{V[1]} + A_{V[2]}) \sin(t(v_{[1]} + v_{[2]} + (P_{V[2]}))) \quad (15)$$

Last but not least, the 5th configurations able to be propagating by specify the value 0 for *femaleMotor* of first module robot, *maleMotor* of third robot module. The Sine value being specify for *maleMotor* of first robot module and *femaleMotor* for third robot module. This propagation is being done as the Equation (16) being coded into Python language.

$$maleMotor[0] = femaleMotor[2] = (A_{V[1]}) \sin(0(v_{[1]})) + (P_{V[1]}) \quad (16)$$

All other configurations besides Serpentinoid configuration that being simulated by Python in V-REP simulation environment in this experiment can be seen as in Fig. 6.

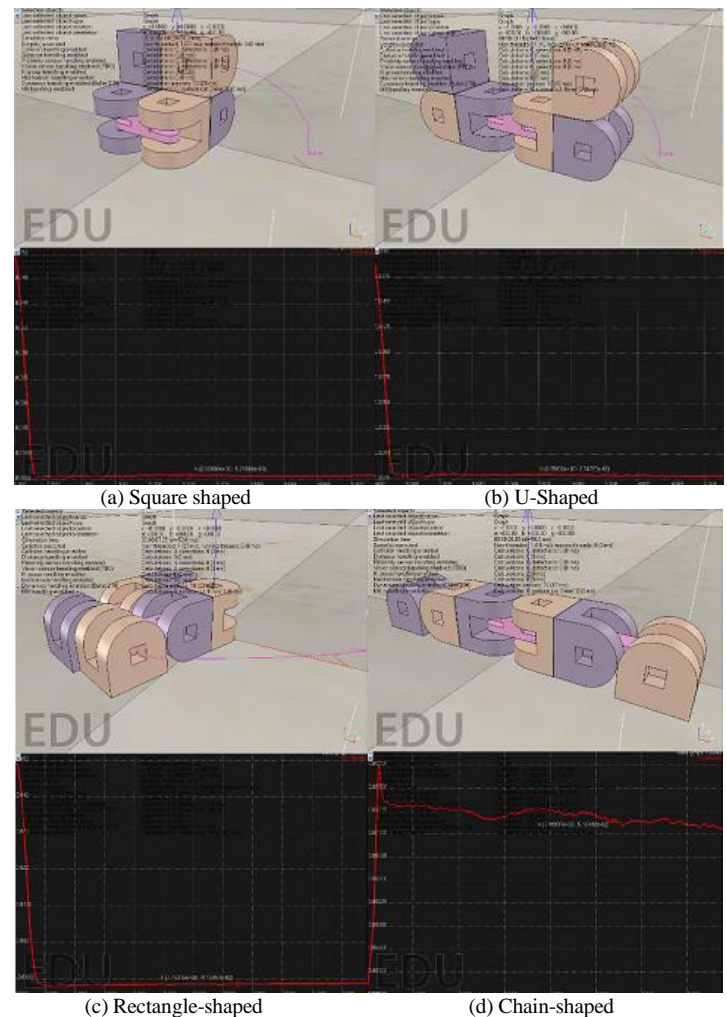


Fig. 6. Robot Snake-Like Motion Propagate (a) and Axis-Time Graph (b).

Based on Fig. 6, it shows that DTTTO modular robot able to propagate multiple configurations in state of orientation as in Fig. 3(b). As the axis-time graph in Fig. 6, it shows that there are movement for the robot to propagate its own configuration and the movement stop as shown in the graph where the axis data value is keep constant which shown the robot movement for propagation stop after it achieved the desired propagation shape.

V. CONCLUSION

In conclusion, this study is conducted to ensure that the Dtto modular robot is able to propagate multiple configurations and will provide significant information for future research work. The simulation created is maintained by while-loop in Python coding so the robot is able to propagate multiple configurations without reprogram. Due to the robot limitation where Dtto only have 2 DOF, with multiple number of module robot, it is necessary to establish possible position attachment, and by establish orientation of 3 axis configuration for the robots, it will establish more propagation of different configurations and locomotion for the modular robot.

REFERENCES

- [1] S. Murata, E. Yoshida, A. Kamimura, H. Kurokawa, K. Tomita, and S. Kokaji, "M-Tran: Self-Reconfigurable Modular," *Ieee/Asme Trans. Mechatronics*, Vol. 7, No. 4, PP. 431–441, 2002.
- [2] Alberto, "Dtto - Explorer Modular Robot," Hackaday, 2016. [Online]. Available: <https://hackaday.io/project/9976-dtto-explorer-modular-robot>. [Accessed: 04-Jul-2017].
- [3] H. Kurokawa, A. Kamimura, E. Yoshida, K. Tomita, S. Kokaji, and S. Murata, "M-TRAN II: Metamorphosis from a four-legged walker to a caterpillar," in *Proc. of the Int. Conf. on Intelligent Robots and Systems (IROS)*, vol. 3, pp. 2454–2459, 2003.
- [4] H. Kurokawa, K. Tomita, A. Kamimura, S. Kokaji, T. Hasuo, and S. Murata, "Distributed Self-Reconfiguration of M-TRAN III Modular Robotic System," *Int. J. Rob. Res.*, vol. 27, no. 3–4, pp. 373–386, 2008.
- [5] M. Yim, "New locomotion gaits," in *Proceedings of the 1994 IEEE International Conference on Robotics and Automation*, pp. 2508–2514, 1994.
- [6] S. Hirose, *Biologically inspired robots: snake-like locomotors and manipulators*, Illustrate. Oxford University Press, 1993.
- [7] W. Nan, P. Bo, and Z. Sha-Sha, "Simulation study of snake-like robot's serpentine locomotion based on recurdyn," *Res. J. Appl. Sci. Eng. Technol.*, vol. 7, no. 1, pp. 37–41, 2014.
- [8] J. G. Gómez, "SERPENTINOID CURVE," Jupyter nbviewer, 2015.
- [9] A.S.M., Rodríguez, "Diseño , construcción y control de una serpiente robótica," in *Congreso Nacional de Investigación en Grado INVESGRADO*, pp. 1–15, 2012.
- [10] S. Ma and N. Tadokoro, "Analysis of Creeping Locomotion of a Snake-like Robot on a Slope," *Auton. Robots*, vol. 20, no. 1, pp. 15–23, 2006.
- [11] J. Gonzalez-gomez and E. Boemo, "Motion of Minimal Configurations of a Modular Robot: Sinusoidal , Lateral Rolling and Lateral Shift Motion," in *Climbing and Walking Robots: Proceedings of the 8th International Conference on Climbing and Walking Robots and the Support Technologies for Mobile Machines (CLAWAR 2005)*, pp. 667–674, 2005.

A Novel Assessment to Achieve Maximum Efficiency in Optimizing Software Failures

An SRGM with Exponential Log-Normal Distribution

Jagadeesh Medapati¹, Prof Anand Chandulal J², Prof Rajinikanth T V³

Assistant Professor, Department of CSE, GITAM Institute of Technology, Visakhapatnam, Andhra Pradesh, India¹

Professor, Department of CSE, GITAM Institute of Technology, Visakhapatnam, Andhra Pradesh, India²

Professor, Department of CSE, SREENIDHI Institute of Science and Technology, Telangana, India³

Abstract—Software Reliability is a specialized area of software engineering which deals with the identification of failures while developing the software. Effective analysis of the reliability helps to signify the number of failures occurred during the development phase. This in turn aid in the refinement of the failures occurred during the development of software. This paper identifies a novel assessment to detect and eliminate the actual software failures efficiently. The approach fits in an exponential log normal distribution of Generalized Gamma Mixture Model (GGMM). The approach estimates two parameters using the Maximum Likelihood Estimate (MLE). Standard Evaluation metrics like Mean Square Error (MSE), Coefficient of Determination (R²), Sum of Squares (SSE), and Root Means Square Error (RMSE) were calculated. The experimentation was carried out on five benchmark datasets which interpret the considered novel technique identifies the actual failures on par with the existing models. This novel software reliability growth model which is more effectual in the identification of the failures significantly and facilitate the present software organizations in the release of software free from bugs just in time.

Keywords—Software reliability; failure rate; reviews; software cost; optimization

I. INTRODUCTION

Software reliability deals with the process of analyzing the failures obtained during the process of designing software. This methodology helps to evaluate the reliability of software grounded on the developed model and where it takes a generated failure into account and formulates a basis for the identification of reliability process. However, these methods help to underline the present methodology of the software, identifying the Mean Time To failure (MTTF), identify the Mean Absolute Error (MAE) and understand the Mean Square Error (MSE). However, no serious attempts were made to initiate software failures during the initial development phases that help in the total analysis of the system together with a procedure by minimizing the failures such that at the failure-free software can be released just in time. As the number of failures increases, the present literature formulates various strategies and presented diverse thoughts where different models have been constituted with the only objective to identify the software failures and develop strategies to refine the failures, which are entitled as review procedures in software industries with a core intention to minimize the software failures. If the number of failures increases the

number of reviews to diminish failures increase substantially making it difficult for the software to release just-in-time.

This increases the overheads of the software cost indirectly. Also in the approaches being followed by the traditional methods of estimating the reliability, the developers are only concentrating on the failures generate. However there is no serious attempt in analyzing the failure notified is a true fault or failure generated due to some of the inside errors such as network fault, data transmission failure, other failures at the internal source and because of the internal failures the end output may be tinted as a failure. Neglecting this basic ideology of analyzing a true failure and an accidental failure, the present traditional systems are evaluating the efficiency of the developed software.

Also, the traditional approaches being followed by software team in estimating the failures is totally dependent on the knowledge base present in the literature i.e., the failure rate is totally based on the supervised learning approach where the assessment is carried out mainly based on the knowledge source. However, whenever a new novel software is to be designed no such knowledge respiratory will be available and as such identification of the failure together with the clear-cut distinction among the true failure and actual failure seemed to be a potentially challenging task.

The present article makes an attempt in this direction by full filling the gaps and meeting the above two objectives listed viz., discrimination of true failures and actual failure, identification of the failure in the software where no such history is available. This article also proposes an approach wherein the failure rate can be minimized and the true failure is thereby reflected. This approach is totally based on the derived mathematical model based on Exponential Logarithmic Normal Distribution (ELND). This article is structured as follows:

Section 2, Background Study precisely highlights the numerous research carried out in the area of software reliability. Section 3 of the article gives zest of the ELND approach and its necessity; the datasets considered were presented in Section 4. The methodology is illustrated in Section 5 of the article, Section 6 deals with various performance metrics were considered in order to analyze the efficiency of the developed model. In Section 7 of the article, the results derived were summarized and discussed. In the

concluding Section 8, concludes the work presented in the above sections.

II. BACKGROUND STUDY

In order to drive the developed software's towards perfection, every software company tries to adopt the policies of software reliability life cycles with the objective to develop reliable software. In general practice after the software is developed and is assumed to be clear for implementation; the testing phase is conducted generally called as the review. In these reviews, the probability of the failures can be notified. If this failure probability is high steps are to be initiated to substantially bring down the failure rate considerably before releasing the software to the market. Many models are presented in the literature by taking this issue and formulating the objectives like developing user-friendly software, developing software which is fully functional, enhances the capability and ensures maintainability. With these objectives, the software developing should be carried out to prepare failure-free software satisfying the user's requirement. Of late many models showcased in the literature presents models that fulfil the objectives of the user requirements. Some of the predominant models in this area of research that are coined initially are from [1], by proposing the initial study of software reliability and have published and presented a good number of papers to benefit the potential researchers working in this field. Markov Birth death Process is utilized in shaping the failure probability and also suggested methodologies to identify the failure rate. The falls in this regard are identified by using the binomial distribution and Weibull distribution was considered for identifying the mean value function. The research in this area is further taken into life by [5], [6] and [7]. The errors if at all exeunt are fixed and failure intensity is proportional to the number of remaining failures[5]. A pictorial view of the failure rates and has thrown an insight to identify that the failure rate may decay during different time intervals[6]. Bayesian method of approach is followed by [7] which a derivation for estimating the effect of failures on the software cost. Every failure rate can be projected as a two-class discrete time model, where the first class represents the error detection process and the second class is utilized for estimating the future error. In these works, the authors have assumed that the failure rate formulates a geometric progression [14].

The second level of research in this direction was initiated by [16] and [17] in the research carried out by the authors the estimation of the failure rates were based on measures of dispersions and are limited to the central limit theorem. Authors have also formulated models based on hyper geometric distribution to derive a model that can find the optimal number of failures from a developed software product.

A new direction for estimating the reliability was proposed by [23], where the authors have developed a model namely Gompertz distribution and this methodology is proven to be a most validating method for estimation of the failures. Research is also extended not only using the Non-

Homogeneous Poisson Processes but other distributions like a family of Pareto distribution was carried out by [24], [25] and [26], where the authors have formulated new ideologies for estimating the failure rates and identify the mean time to failure. Latest studies were also published where most of the works are based on Weibull distribution, generalized Laplacian distribution, Raleigh distribution and Gaussian distribution. These models are also confined to the study of reliability basing on the error rates.

However, in spite of rigorous research in this area, most of the works presented by the earlier authors are confined to the study of the impact of failure rate and some articles tried to project the time between the failures. No serious attempt was witnessed in the literature to minimize the error rate or to discriminate the true error from the actual error. This article is framed to fulfil this objective in the most novel approach.

III. EXPONENTIAL LOGARITHMIC NORMAL DISTRIBUTION

In order to estimate the failures, it is necessary to understand the pattern of the failures. This analysis of the pattern helps to signify the true failures and the possible non-failures. However, it is to be notified exactly. For this purpose, many models have been present in the literature [2]-[4] [8] [11]-[15] [18]-[22]. However, these models failed to attribute the analysis of the true failure as it is evident that every initial data in the failure data model assumes exponential distribution and hence the article we have considered Exponential Logarithmic Normal Distribution. The Probability Density Function (PDF) for fitting the ELND is given by

$$f(p, q) = q(e^{-px}) \text{If } x > 0; \quad (1)$$
$$= 0 \text{ otherwise.}$$

Where 'x' represents a failure

Here the values of p and q are estimated using the methodology of lease square and by using the formulae

$$\sum \mu_i = np + q \sum t_i \text{ and} \quad (2)$$

$$\sum \mu_i t_i = p \sum t_i + q \sum t_i^2 \quad (3)$$

IV. DATASETS

In order to present the proposed methodology, we have considered two datasets, namely, [9] and [10] for highlighting the proposed model. The first dataset of Tandem consists of failure data executed in four releases, Release 1 to Release 4. Each of the releases consisted of the failures generated. In the second dataset considered for the experimentation namely, Brooks & Motely contain a failure data set. These datasets are considered for the presentation of the proposed model is given below.

Labels in the Table I, TW represents the Test Weeks, EH represents the Execution Hours and ND represents the No. of defects. Labels in the Table II, TW represents the Test Weeks, EH represents the Execution Hours and AD represents the No. of defects.

TABLE I. ORIGINAL FAILURES IN TANDEM DATASET

TW	Release 1		Release 2		Release 3		Release 4	
	EH	ND	EH	ND	EH	ND	EH	ND
1	519	16	384	13	162	6	254	1
2	968	24	1186	18	499	9	788	3
3	1430	27	1471	26	715	13	1054	8
4	1893	33	2236	34	1137	20	1393	9
5	2490	41	2772	40	1799	28	2216	11
6	3058	49	2967	48	2438	40	2880	16
7	3625	54	3812	61	2818	48	3593	19
8	4422	58	4880	75	3574	54	4281	25
9	5218	69	6104	84	4234	57	5180	27
10	5823	75	6634	89	4680	59	6003	29
11	6539	81	7229	95	4955	60	7621	32
12	7083	86	8072	100	5053	61	8783	32
13	7487	90	8484	104	9604	36		
14	7846	93	8847	110	10064	38		
15	8205	96	9253	112	10560	39		
16	8564	98	9712	114	11008	39		
17	8923	99	10083	117	11237	41		
18	9282	100	10174	118	11243	42		
19	9641	100	10272	120	11305	42		
20	10000	100						

TABLE II. ORIGINAL FAILURES IN BROOKS AND MOTELY DATASET

W	EH	AD
1	7.25	7
2	10.42	29
3	17.5	61
4	24.83	108
5	32.08	134
6	44.66	159
7	64.58	175
8	117.08	223
9	164.26	259
10	259.36	312
11	315.11	369
12	374.36	408
13	417.94	479
14	462.69	559
15	505.02	624
16	580.02	681
17	642.85	771
18	716.43	831
19	759.18	888
20	799.85	978
21	896.6	1024
22	985.18	1081
23	1041.93	1110
24	1121.18	1150
25	1194.68	1166
26	1260.01	1184
27	1327.84	1221
28	1444.76	1236
29	1532.84	1244
30	1610.92	1272
31	1648.84	1278
32	1689.92	1283
33	1744.42	1286
34	1807.42	1289
35	1846.92	1301

V. METHODOLOGY

The data for the experimentation of the proposed model is presented in the above section, each of these datasets is considered and for each dataset the initial estimates of the parameters of the proposed Exponential Logarithmic Normal Distribution, p and q are estimated. Using the method of Least Square Estimation and the values so obtained are presented below:

Using these estimates the analysis of the proposed model is considered.

Here the first dataset Tandem is considered containing four releases 1 to 4 is presented along with the second failure dataset considered Brooks & Motely in the above Tables I and II.

Against each of the dataset, the analysis is carried out in a phased manner wherein the first phase the true failures are estimated and the experimentation are processed to minimize the failure rate given in Tables III.

Against each of the data released, the number of the actual defects highlighted is considered and using these defects the actual failures are predicted and are presented as below:

Labels in Table IV to Table VIII, TW represent the Test Weeks, ND represents the No. of Defects, PD represents Predicted Defect, RES represents the Residual and Fault classifies whether the failure is a True failure or not.

TABLE III. ESTIMATED VALUES OF PARAMETERS P AND Q FOR THE DATASETS CONSIDERED

Datasets Considered	p	q
Tandem Release 1	135.845	0.078
Tandem Release 2	179.573	0.063
Tandem Release 3	49.339	0.237
Tandem Release 4	605.941	0.005
Brooks & Motely	11981.548	0.004

TABLE IV. ACTUAL FAILURES FOR TANDEM DATASET RELEASE-1

Observations	TW	ND	PD	RES	Fault
Failure 1	1	16	10.18	5.82	N
Failure 2	2	24	19.598	4.402	N
Failure 3	3	27	28.309	-1.309	Y
Failure 4	4	33	36.368	-3.368	Y
Failure 5	5	41	43.823	-2.823	Y
Failure 6	6	49	50.719	-1.719	Y
Failure 7	7	54	57.099	-3.099	Y
Failure 8	8	58	63	-5	Y
Failure 9	9	69	68.459	0.541	N
Failure 10	10	75	73.509	1.491	N
Failure 11	11	81	78.181	2.819	N
Failure 12	12	86	82.502	3.498	N
Failure 13	13	90	86.5	3.5	N
Failure 14	14	93	90.198	2.802	N
Failure 15	15	96	93.618	2.382	N
Failure 16	16	98	96.783	1.217	N
Failure 17	17	99	99.71	-0.71	Y
Failure 18	18	100	102.418	-2.418	Y
Failure 19	19	100	104.923	-4.923	Y
Failure 20	20	100	107.241	-7.241	Y

In this process, the residuals are identified where the actual notified errors are subtracted from the predicted errors and the process carried out on the two datasets namely Tandem and Brooks & Motely are tabulated in Table IV to Table VIII. The Fault column in every table specifies the outcome of the proposed model on the datasets and it clearly specifies how best the proposed model have identified the true failures and in turn reduce the failure rate when compared to the original dataset.

TABLE V. ACTUAL FAILURES FOR TANDEM DATASET RELEASE-2

Observations	TW	ND	PD	RES	Fault
Failure 1	1	13	11.036	1.964	N
Failure 2	2	18	21.393	-3.393	Y
Failure 3	3	26	31.114	-5.114	Y
Failure 4	4	34	40.238	-6.238	Y
Failure 5	5	40	48.801	-8.801	Y
Failure 6	6	48	56.837	-8.837	Y
Failure 7	7	61	64.38	-3.38	Y
Failure 8	8	75	71.459	3.541	N
Failure 9	9	84	78.104	5.896	N
Failure 10	10	89	84.34	4.66	N
Failure 11	11	95	90.192	4.808	N
Failure 12	12	100	95.685	4.315	N
Failure 13	13	104	100.84	3.16	N
Failure 14	14	110	105.679	4.321	N
Failure 15	15	112	110.22	1.78	N
Failure 16	16	114	114.482	-0.482	Y
Failure 17	17	117	118.482	-1.482	Y
Failure 18	18	118	122.237	-4.237	Y
Failure 19	19	120	125.76	-5.76	Y

TABLE VI. ACTUAL FAILURES FOR TANDEM DATASET RELEASE-3

Observations	TW	ND	PD	RES	Fault
Failure 1	1	6	10.397	-4.397	Y
Failure 2	2	9	18.603	-9.603	Y
Failure 3	3	13	25.08	-12.08	Y
Failure 4	4	20	30.192	-10.19	Y
Failure 5	5	28	34.227	-6.227	Y
Failure 6	6	40	37.411	2.589	N
Failure 7	7	48	39.925	8.075	N
Failure 8	8	54	41.909	12.091	N
Failure 9	9	57	43.474	13.526	N
Failure 10	10	59	44.71	14.29	N
Failure 11	11	60	45.685	14.315	N
Failure 12	12	61	46.455	14.545	N
Failure 13	13	36	47.063	-11.06	Y
Failure 14	14	38	47.542	-9.542	Y
Failure 15	15	39	47.921	-8.921	Y
Failure 16	16	39	48.22	-9.22	Y
Failure 17	17	41	48.455	-7.455	Y
Failure 18	18	42	48.641	-6.641	Y
Failure 19	19	42	48.788	-6.788	Y

TABLE VII. ACTUAL FAILURES FOR TANDEM DATASET RELEASE-4

Observations	TW	ND	PD	RES	Fault
Failure 1	1	1	2.863	-1.863	Y
Failure 2	2	3	5.713	-2.713	Y
Failure 3	3	8	8.549	-0.549	Y
Failure 4	4	9	11.372	-2.372	Y
Failure 5	5	11	14.182	-3.182	Y
Failure 6	6	16	16.978	-0.978	Y
Failure 7	7	19	19.761	-0.761	Y
Failure 8	8	25	22.531	2.469	N
Failure 9	9	27	25.288	1.712	N
Failure 10	10	29	28.031	0.969	N
Failure 11	11	32	30.762	1.238	N
Failure 12	12	32	33.48	-1.48	Y

TABLE VIII. ACTUAL FAILURES FOR BROOKS AND MOTELY DATASET

Observations	TW	ND	PD	RES	Fault
Failure 1	1	7	44.292	-37.29	Y
Failure 2	2	29	88.42	-59.42	Y
Failure 3	3	61	132.386	-71.39	Y
Failure 4	4	108	176.188	-68.19	Y
Failure 5	5	134	219.829	-85.83	Y
Failure 6	6	159	263.309	-104.3	Y
Failure 7	7	175	306.627	-131.6	Y
Failure 8	8	223	349.786	-126.8	Y
Failure 9	9	259	392.785	-133.8	Y
Failure 10	10	312	435.625	-123.6	Y
Failure 11	11	369	478.307	-109.3	Y
Failure 12	12	408	520.831	-112.8	Y
Failure 13	13	479	563.197	-84.2	Y
Failure 14	14	559	605.407	-46.41	Y
Failure 15	15	624	647.462	-23.46	Y
Failure 16	16	681	689.36	-8.36	Y
Failure 17	17	771	731.104	39.896	N
Failure 18	18	831	772.693	58.307	N
Failure 19	19	888	814.129	73.871	N
Failure 20	20	978	855.412	122.59	N
Failure 21	21	1024	896.541	127.46	N
Failure 22	22	1081	937.519	143.48	N
Failure 23	23	1110	978.346	131.65	N
Failure 24	24	1150	1019.02	130.98	N
Failure 25	25	1166	1059.55	106.45	N
Failure 26	26	1184	1099.92	84.079	N
Failure 27	27	1221	1140.15	80.853	N
Failure 28	28	1236	1180.23	55.775	N
Failure 29	29	1244	1220.15	23.846	N
Failure 30	30	1272	1259.94	12.065	N
Failure 31	31	1278	1299.57	-21.57	Y
Failure 32	32	1283	1339.06	-56.06	Y
Failure 33	33	1286	1378.4	-92.4	Y
Failure 34	34	1289	1417.6	-128.6	Y
Failure 35	35	1301	1456.65	-155.6	Y

VI. PERFORMANCE EVALUATION METRICS

In order to evaluate the outputs derived from the proposed model, we have considered the following metrics such as Mean Squared Error (MSE), R^2 , Sum of Squares Error (SSE) and Root Mean Squared Error (RMSE). The formulas for the calculation of the above metrics are given by

Mean Squared Error

$$MSE = \frac{\sum (|Actual Failure_i - Estimated Failure_i|)^2}{n-1} \quad (4)$$

Mean Absolute Percent Error

$$MAPE = \frac{\sum \frac{|Actual Failure_i - Estimated Failure_i|}{Actual Failure_i} \times 100}{n} \quad (5)$$

Error of Sum of Squares

$$SSE = \sum_{i=1}^n (x_i - \bar{x})^2 \quad (6)$$

Coefficient of Determination

$$R^2 = 1 - \frac{SSE_{res}}{SSE_{tot}} \quad (7)$$

Root Mean Square Error

$$RMSE = \sqrt{\frac{\sum (|Actual Failure_i - Estimated Failure_i|)^2}{n-1}} \quad (8)$$

VII. RESULTS AND DISCUSSIONS

The results of the performance evaluation metrics are showcased in the following Table IX.

From the above Table IX, it can be clearly seen that the MSE is less for the Release 1 and the R^2 , is almost approaching 1, which signify that the model performs better.

The SSE metrics and RMSE metrics also showcase significant measures. This showcases that the proposed methodology is delivering an outstanding performance in predicting the failures. The experimentation carried out across the two datasets namely, Tandem and Brooks & Motely were represented below. The figures showcase the experimentation carried out across the datasets with respect to the individual failure dataset.

TABLE IX. ACTUAL FAILURES FOR TANDEM DATASET RELEASE-4

Dataset Considered	MSE	R^2	SSE	RMSE
Tandem Release 1	11.317	0.988	192.388	3.364
Tandem Release 2	26.088	0.982	417.408	5.108
Tandem Release 3	116.630	0.664	1866.081	10.800
Tandem Release 4	3.861	0.980	34.749	1.965
Brooks and Motely	9659.621	0.966	309107.871	98.283

Fig. 1, Fig. 4, Fig. 7, Fig. 10 and Fig. 13 depict the actual failures of various datasets. It can be clearly seen that for the values which lie above the curve were reported as failures but not a failure in the original. The present model is novel to identify the true failures and thus drives our attempt in novel nature.

Fig. 2, Fig. 5, Fig. 8, Fig. 11 and Fig. 14 depict the predicted failures of various datasets. The same set of failures at the respective time were even predicted.

Fig. 3, Fig. 6, Fig. 9, Fig. 12 and Fig. 15 depict the residuals evaluated for various datasets. This clearly showcases the entire methodology and the results keep it on track so that the novelty of the entire concept is justified. The failures that are identified were displayed for the datasets considered. The residuals were calculated across every observation and were presented for the datasets considered.

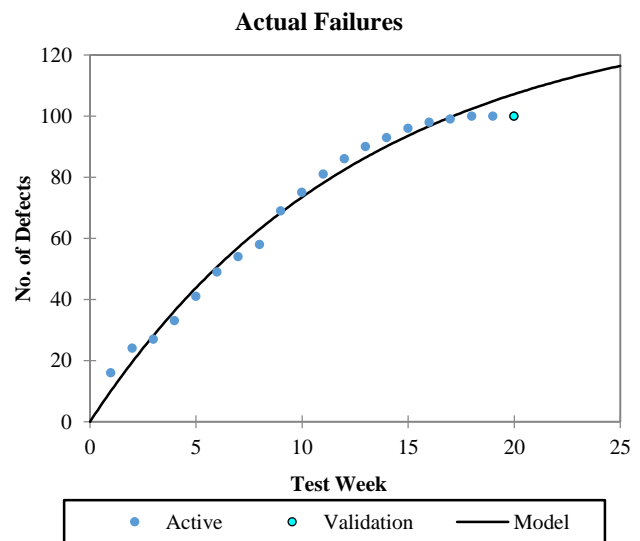


Fig. 1. Actual Failures vs No. of Defects for the TANDEM Release 1.

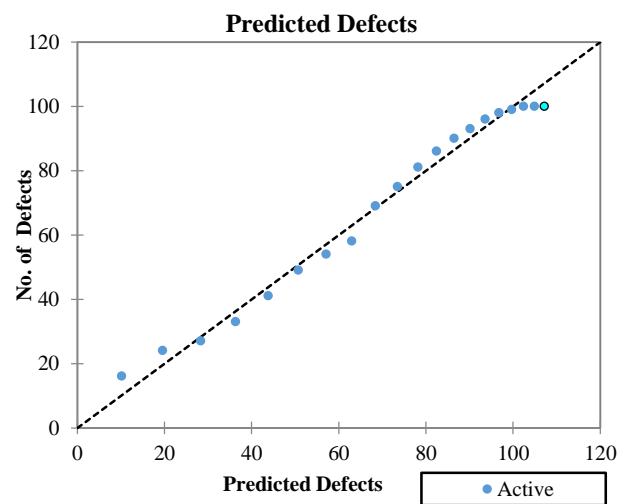


Fig. 2. Predicted Defects vs No. of Defects for the TANDEM Release 1.

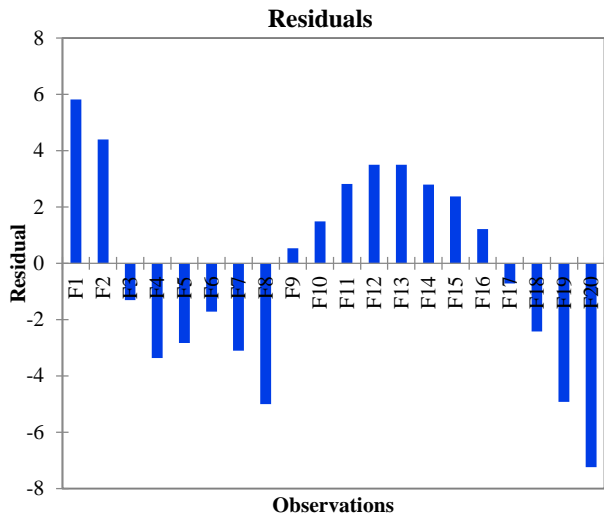


Fig. 3. Observations versus Residuals for the TANDEM Release 1.

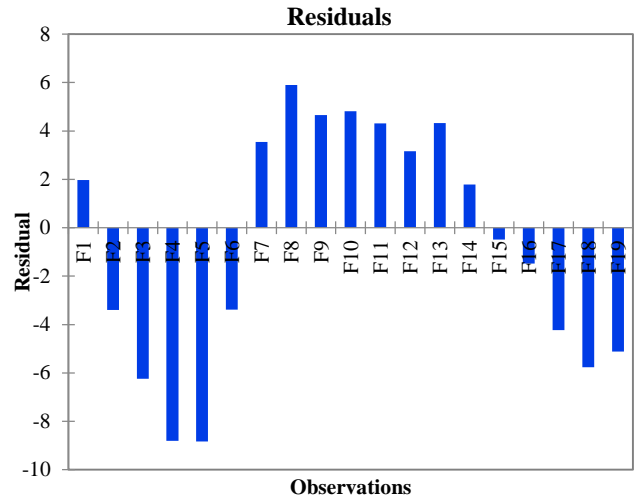


Fig. 6. Observations Versus Residuals for the TANDEM Release 2.

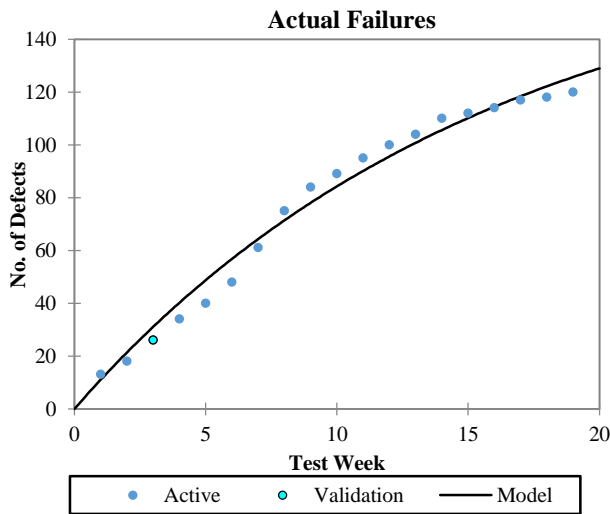


Fig. 4. Actual failures vs No. of Defects for the TANDEM Release 2.

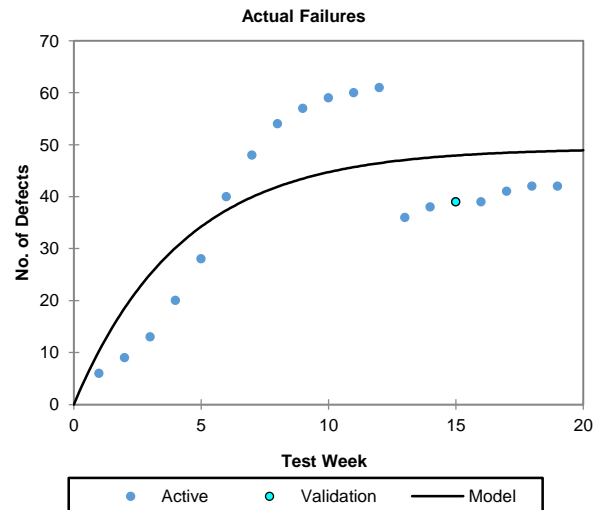


Fig. 7. Actual Failures vs No. of Defects for the TANDEM Release 3.

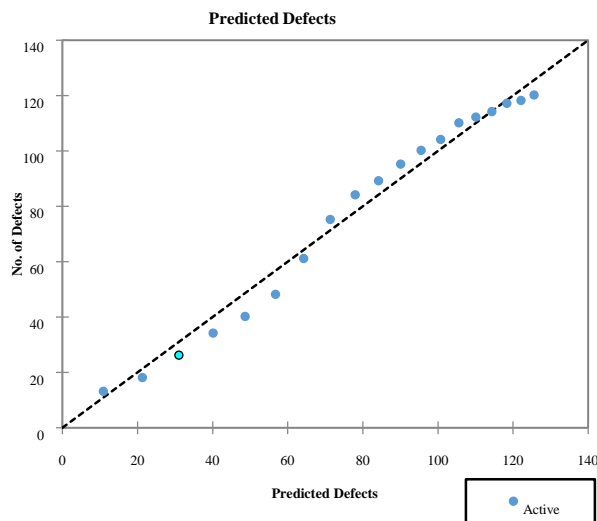


Fig. 5. Predicted Defects vs No. of Defects for the TANDEM Release 2.

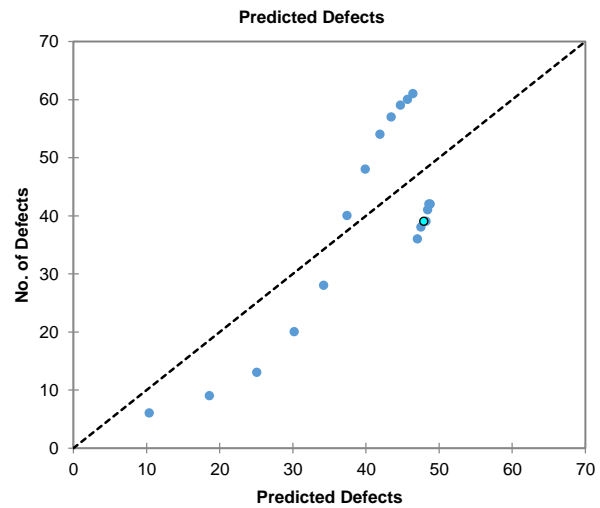


Fig. 8. Predicted Defects vs No. of Defects for the TANDEM Release 3.

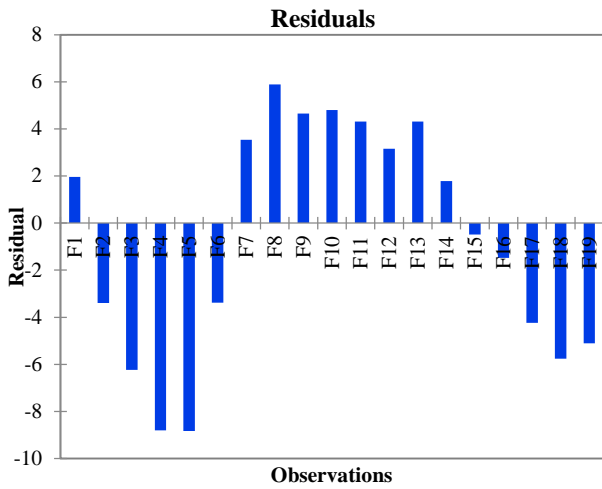


Fig. 9. Observations versus Residuals for the TANDEM Release 3.

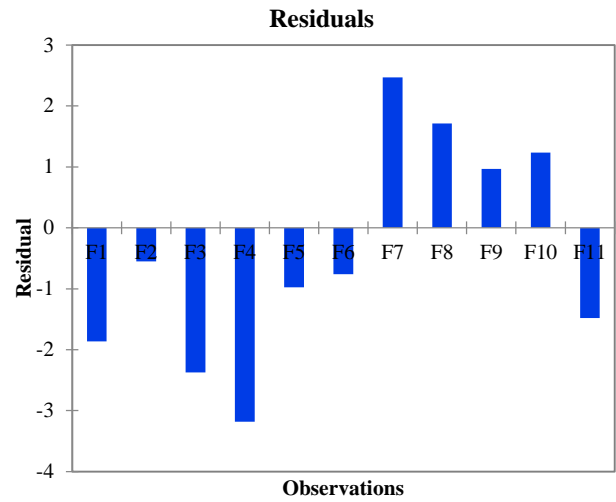


Fig. 12. Observations versus Residuals for the TANDEM Release 4.

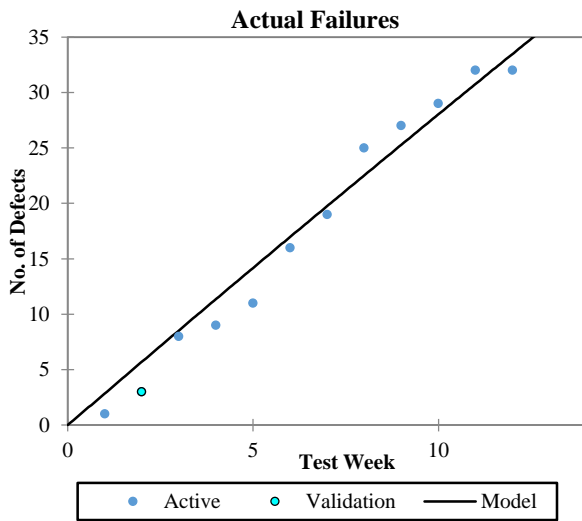


Fig. 10. Actual failures vs No. of Defects for the TANDEM Release 4.

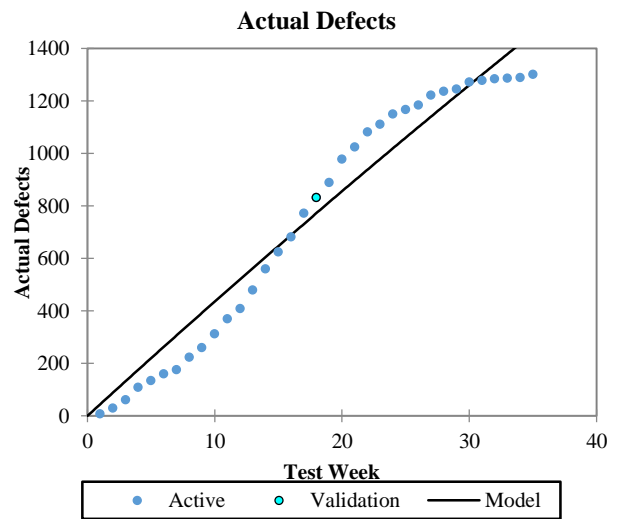


Fig. 13. Actual failures vs No. of Defects for Brooks & Motely.

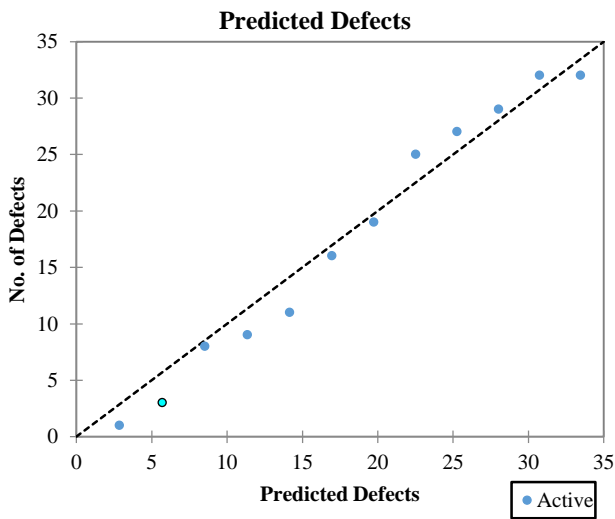


Fig. 11. Predicted Defects vs No. of Defects for the TANDEM Release 4.

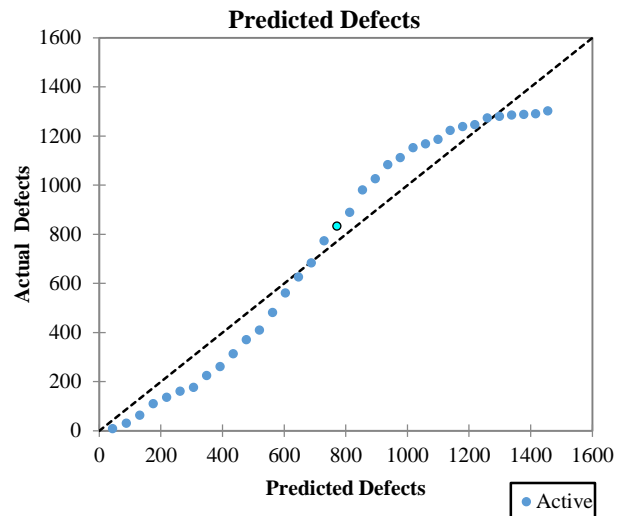


Fig. 14. Predicted Defects vs No. of Defects for Brooks & Motely.

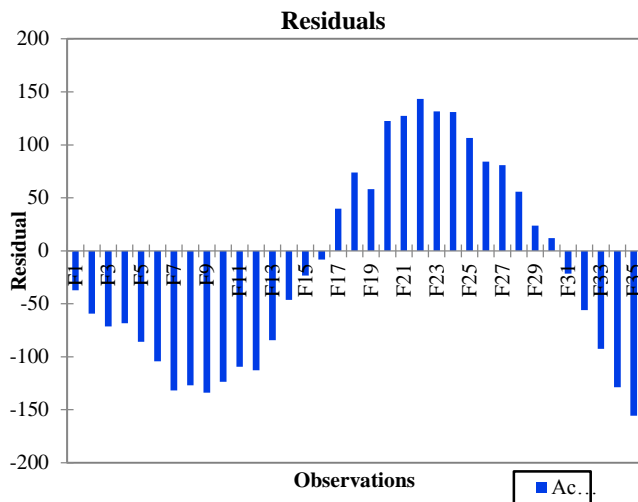


Fig. 15. Observations versus Residuals for Brooks & Motely.

VIII. CONCLUSION

In this article an ideology is presented which is novel for the minimization of failures and also facilitating the software developer to understand the actual failures that are derived from the project because of some of the technical flaws and also highlighted the predicted failures, which are not the failures but reported as failures due to the issues of technicality or human failures. The works presented in this article on two benchmark datasets helps to understand the potentiality of the model. The results also attribute the significance of the model and this model can be implemented into a software firm helps to not only minimize the review times but also helps to release the software just in time together with enhancing the profit budget.

ACKNOWLEDGMENT

We would also like to show our gratitude to *Dr Srinivas Yarramalla*, Professor, Department of Information Technology, GITAM Deemed to be University, Visakhapatnam for sharing his pearls of astuteness with us throughout the course of this research, and we are also enormously grateful to *Dr Naveen K Kuppilli* Assistant Professor, Department of Information Technology, GITAM Deemed to be University, Visakhapatnam for his remarks on a former adaptation of the manuscript, although any errors are our own and should not tarnish the reputations of these esteemed persons.

REFERENCES

[1] Hudson, G. R.; Programming Errors as a Birth-Death Process, Technical Report SP-3011, System Development Corp., 1967.
 [2] Pham, H., Software Reliability, Springer-Verlag, New York, 2000.
 [3] Michael R. Lyu; Handbook of software reliability and system reliability, McGraw-Hill, Inc., Hightstown, NJ, 1996.
 [4] John D. Musa, Software Reliability Engineering: More Reliable Software Faster and Cheaper, Authorhouse, 2004.
 [5] Jelinski, Z.; Moranda. P. B.; Software Reliability Research," (Statistical Computer Performance Evaluation), W. Freiberger, Ed., Academic Press, Inc., New York, 1972, 465-484.
 [6] Shooman, M. L.; W. Freiberger, ed., Statistical Computer Performance

Evaluation Academic Press, W.Freiberger (ed.), New York, 1972.
 [7] Littlewood, B.; Verrall, J. L.; A Bayesian Reliability Growth Model for Computer Software, Proceedings, IEEE Symposium on Computer Software Reliability, New York, 1973, 22, 332-346.
 [8] Goel, A.L.; Okumoto, K.; Time-Dependent Error Detection Rate Model for Software Reliability and Other Performance Measures, IEEE Transactions on Reliability, 1979, 28, 206-211.
 [9] A. Wood, Predicting software reliability, IEEE Computer, 11, 1996, 69-77.
 [10] Brooks WD.; Motley RW.; Analysis of discrete software reliability models – technical report, New York: Rome Air Development Centre; 1980.
 [11] Read, C.B.; Gompertz Distribution, Encyclopedia of Statistical Sciences, 1983, Wiley, New York.
 [12] Ohba, M, Software reliability analysis models," IBM Journal of Research and Development, IBM Journal, Research Development, 1984, 28, 428-443.
 [13] Ohba.M; Inflection S-shaped software reliability growth model, Stochastic Models in Reliability Theory, Springer- Verlag Merlin, 1984, 144 – 162
 [14] Yamada, S.; Osaki, S.; S-Shaped Software Reliability Growth Models and Comparisons, Applied Stochastic Models and Data Analysis, 1985, 11, 1431-1437.
 [15] Musa, J.D.; Iannino, A.; Okumoto, K.; Software Reliability: Measurement, Prediction and Application, McGraw-Hill, 1987.
 [16] Brown D. B., Correction to A Cost Model for Determining the Optimal Number of Software Test Cases, IEEE Transactions on Software Engineering, 15(6), 824, 1989.
 [17] Tohma, Y. ; Jacoby, R. ; Murata, Y. ; Yamamoto, M.; Hyper-geometric distribution model to estimate the number of residual software fault, Proc. COMPSAC-89, Orlando, 1989,610-617.
 [18] Kapur PK; Some modelling peculiarities in software reliability, International conference on quality, reliability and infocom technology, New Delhi, India; 2007, 155–65.
 [19] Kapur PK; On modelling failure phenomenon of multiple releases of a software in operational phase for product and project type software – a theoretical framework,International conference on quality, reliability and infocom technology; 2007, 605–18.
 [20] Pham, H., Software Reliability, Springer-Verlag, New York, 2000.
 [21] Kuo, S.Y.; Hung, C.Y.; Lyu, M.R.; Framework for modeling software reliability, Using Various Testing-Efforts and Fault-Detection Rates, IEEE Transactions on Reliability, 2001, 50, 310-320.
 [22] Khan, M. G. M.; Ahmad, N.; Rafi, L. S.; Modeling and analysis of software reliability with Burr type X testing-effort and release determination Proc of the CASON-2008, IEEE Computer Society, China, 2008, 759-762.
 [23] Ohishi, K.; Okamura, H.; Dohi, T.; J of Systems and Software, 2009, 82, 535-543.
 [24] SatyaPrasad, R.; Naga Raju, O.; Kantam, R.R.L.; SRGM with Imperfect Debugging by Genetic Algorithms I. J. of Software Engineering & Applications, 2010, 1, 66-79.
 [25] Satya Prasad, R.; Ramchand H Rao, K.; Kantam, R.R.L.; Software Reliability with SPC, International Journal of Computer Science and Emerging Technologies, 2(2),2011, 233-237.
 [26] Kantam, R.R.L; Subrahmanya Ravikumar, M.; Limited Failure Censored Life Test Sampling Plan in Burr Type X Distribution. Journal of Modern Applied Statistical Methods, 15, 2016, 428-454.

AUTHORS' PROFILE



Jagadeesh Medapati received M.Tech from GITAM Deemed to be University, Visakhapatnam in 2009, currently pursuing his PhD from JNT University, Hyderabad. He is currently working as an Assistant Professor in the Department of Computer Science & Engineering, GITAM Institute of Technology, GITAM Deemed to be University, Visakhapatnam, India. His research interest includes Software Reliability, Software Engineering, Theoretical Computer Science and Computational Intelligence.



Prof Anand Chandulal Jasti received M.Tech from JNT University, Hyderabad in 1992, PhD from JNT University, and Hyderabad in 2007. He is currently working as Professor in Department of Computer Science & Engineering, GITAM Institute of Technology, GITAM Deemed to be University, Visakhapatnam, India. He has several publications in national & International journals and conferences. his research interest includes Text Mining Security, Soft Computing and Optimization Technologies



Prof TV Rajanikanth received M.Tech from Osmania University, Hyderabad in 2001, PhD from Osmania University, and Hyderabad in 2007. He is currently working as Professor in Department of Computer Science & Engineering, and Dean for Research & Development of SREENIDHI Institute of Science and Technology, Hyderabad, Telangana, India. His contribution towards research made him to publish several research articles in renowned national & International journals and conferences. His research interest includes Data warehouse & mining, Semantic Web, Spatial Data mining, ANN.

Process Capability Indices under Non-Normality Conditions using Johnson Systems

Dr. Suboohi Safdar¹, Dr. Ejaz Ahmed², Dr. Tahseen Ahmed Jilani³, Dr. Arfa Maqsood⁴

Department of Statistics, University of Karachi, Karachi, Pakistan^{1,4}

Computer Science & Information Systems²

Karachi Institute of Business Management, Karachi, Pakistan

School of Computer Science, University of Nottingham, Nottingham, UK³

Abstract—Process capability indices (PCIs) quantify the ability of a process to produce on target and within specifications performances. Basic indices designed for normal processes gives flawed results for non-normal process. Numerous methods have been proposed for non-normal processes to estimate PCIs in which some of them are based on transformation methods. The Johnson system comprising three types that translate a continuous non-normal distribution to normal. The aim of this paper is to estimate four basic indices for non-normal process using Johnson system with single straightforward procedure. The efficacy of the proposed approach can be assessed for all three Johnson Curves (S_B, S_U, S_L) but result for S_U is presented in this paper. PCIs for a data set are estimated and percentiles are obtained by our proposed exact method based on selected Johnson density function which was earlier based on approximate methods without any prior knowledge of density function of non-normal process. We compare our results with other existing methods to estimate PCIs for non-normal process. From statistical analysis we have noted that this modification improve process capability indices.

Keywords—Johnson curve; percentiles; simulation; exact method

I. INTRODUCTION

Process capability analysis is conducted for a process which necessitate two conditions; first a controlled process and second the requirements pre-determined by product designer. Much of work has been performed for estimating PCIs for normal processes but these PCIs are inappropriate for non-normal because the estimators of PCIs for normal processes are not enough sufficient to characterize non-normal processes and deceive results. Several methods have been developed for PCIs of non-normal processes. Examples are Bates [1] discussed robustness of indices based on normal population, Pyzdek [2,3] showed that for non-normal processes standard process capability indices will give false process fallout rates and misled the results. Rivera [4] discussed C_{pk} index estimation using transformation technique. Safdar and Ahmed [5, 6] proposed procedures for estimating PCIs for non-normal processes and obtained capability estimates based on Weibull shape parameter. Piña-Monarrez *et al* [7] extended their work for estimating indices for Weibull and Lognormal distributions.

More precisely two basic approaches are discussed so far in published literature to estimate PCIs for non-normal

processes. First, translate non-normal process to normal using transformation and estimate PCIs from any existing method designed for normal processes. Few popular transformation methods are Burr percentile method [8], Johnson method [9] Box-Cox power transformation method [10] and Montgomery square root transformation method [11] Second approach to estimate PCIs is based on percentile methods and most applied is Clements percentile method [12]. His method is based on percentiles as process parameters to estimate C_p and C_{pk} indices for non-normal processes. Pearn and Kotz [13] extended his work for C_{pm} and C_{pmk} indices. Pearn and Chan [14] generalized a superstructure for all of these four indices. Zwick [15] Schneider and Pruett [16] and Chen [17-20] suggested various PCIs for non-normal processes.

In this present article we estimated PCIs for non-normal process under Johnson system of distribution. We presented one distribution S_U for estimating PCIs for non-normal data set of 100 measurements for a hypothetical process [21]. Our prime focus in this paper is to propose a uniform straightforward and easy approach to estimate PCIs for non-normal processes. We estimated these PCIs from Pearn and Chan [14] superstructure using Johnson system and the percentiles (0.00135, 0.5 and 0.99865) of non-normal processes for the superstructure are obtained from best fitted Johnson density function whereas Pearn and Chan [14] estimated these percentiles as the percentage points of non-normal processes.

We also emphasis on three assumptions of statistical process control (SPC) tools; First to manage the process in statistical control; second the parameters of the selected Johnson density function adequately fits the data and last the normality assumptions for the selected Johnson curve should not violated.

The paper structure is as follows: Section II presents existing PCIs for non-normal processes. Section III and IV briefly explains Johnson system of distribution and existing PCIs under Johnson distributions. In Section IV new capability computation procedures for non-normal distribution under Johnson system are proposed. Section VI comprehensively gives steps for obtaining modified PCIs using Johnson system with a brief flow chart. Section VII illustrates the proposed method explain with one example. After illustration of the proposed procedure a conclusion is made.

II. EXISTING PCIS FOR NON-NORMAL PROCESSES USING PEARSONIAN SYSTEM

For normal processes Vannman [22] constructed a superstructure form for four basic indices C_p, C_{pk}, C_{pm} and C_{pmk} ;

$$C_p(u, v) = \frac{d - u|\mu - m|}{3\sqrt{\sigma^2 + v(\mu - T)^2}} \quad u \geq 0; v \geq 0 \quad (1)$$

Such that,

$$C_p(0,0) = C_p, C_p(1,0) = C_{pk}, C_p(0,1) = C_{pm} \text{ and } C_p(1,1) = C_{pmk}$$

In this superstructure μ and σ are the process mean and process standard deviation respectively, T is target value, $d = (USL - LSL)/2$ is half length of specification interval and $m = (USL + LSL)/2$ is the midpoint between upper and lower specification limits.

The basic indices C_p, C_{pk}, C_{pm} and C_{pmk} are proved inappropriate for non-normal processes because for non-normal μ and σ are not enough sufficient for non-normal process further the distribution of sample variance is sensitive to departure from normality. To accommodate the cases where the underlying distribution may not be normal Clements [12] proposed estimation of C_p and C_{pk} indices using other process parameters which are not sensitive to normality. He replaced 6σ of C_p by length of interval between upper and lower 0.135 percentage points of non-normal data and process mean μ of C_{pk} by 0.5 percentage point-median of the data set. Pearn and Kotz [13] applied Clements method to estimate C_{pm} and C_{pmk} indices and Pearn and Chan [14] constructed a superstructure to design indices for non-normal processes as;

$$C_{NP}(u, v) = \frac{d - u|M - m|}{3\sqrt{\left(\frac{F_{0.99865} - F_{0.135}}{6}\right)^2 + v(M - T)^2}} \quad u \geq 0; v \geq 0 \quad (2)$$

Such that $C_{NP}(0,0) = C_{NP}, C_{NP}(1,0) = C_{Npk}, C_{NP}(0,1) = C_{Npm}$ and $C_{NP}(1,1) = C_{Npmk}$. Where $F_{0.135}, M$ and $F_{0.99865}$ are the 0.135th, 0.5th and 0.99865th percentage points of non-normal processes under Pearsonian system respectively. Zwick [15] and Schneider *et al.* [16] considered two generalizations of C_p and C_{pk} but they used process mean μ rather than process median M. Chang and Lu [23] applied Clements method to obtain percentiles for C_{NP}, C_{Npk}, C_{Npm} indices. Extending their methods Pearn and Chan [14] constructed another superstructure and obtained percentiles based on order statistics;

$$\hat{C}_{NP}(u, v) = \frac{d - u|\hat{M} - m|}{3\sqrt{\left[\frac{\hat{F}_{0.99865} - \hat{F}_{0.135}}{6}\right]^2 + v(\hat{M} - T)^2}} \quad u \geq 0; v \geq 0 \quad (3)$$

Such that

$$\hat{C}_{NP}(0,0) = \hat{C}_{NP}, \hat{C}_{NP}(1,0) = \hat{C}_{Npk}, \hat{C}_{NP}(0,1) = \hat{C}_{Npm} \text{ and } \hat{C}_{NP}(1,1) = \hat{C}_{Npmk};$$

$$\hat{F}_{0.135} = X_{(R_2)} + \left(\left[\frac{(0.135)n + 0.99865}{100} \right] - R_2 \right) \times (X_{(R_2+1)} - X_{(R_2)})$$

$$\hat{M} = X_{(R_3)} + \left(\left[\frac{n+1}{2} \right] - R_3 \right) \times (X_{(R_3+1)} - X_{(R_3)})$$

$$\hat{F}_{0.99865} = X_{(R_1)} + \left(\left[\frac{(99.865)n + 0.135}{100} \right] - R_1 \right) \times (X_{(R_1+1)} - X_{(R_1)})$$

Where $R_1 = [(99.865n + 0.135)/100]$, $R_2 = [(0.135n + 0.99865)/100]$ and $R_3 = [(n+1)/2]$. In this setting, the notation [R] is defined as the greatest integer less than or equal to the number R and $x_{(i)}$ is defined as i^{th} order statistic.

Pearn and Kotz [13] and Pearn and Chen [24] applied Clements [12] method to estimate PCIs of non-normal processes. The PCIs in which those estimators correspond to can be expressed as

$$C'_{NP}(u, v) = (1-u) \times \frac{USL - LSL}{6\sqrt{\left[\frac{F_{0.99865} - F_{0.135}}{6}\right]^2 + v(M - T)^2}} + u \times \min \left\{ \frac{USL - M}{3\sqrt{\left[\frac{F_{0.99865} - M}{3}\right]^2 + v(M - T)^2}}, \frac{M - LSL}{3\sqrt{\left[\frac{M - F_{0.99865}}{3}\right]^2 + v(M - T)^2}} \right\} \quad u \geq 0; v \geq 0 \quad (4)$$

Such that $C'_{NP}(0,0) = C'_{NP}, C'_{NP}(1,0) = C'_{Npk}, C'_{NP}(0,1) = C'_{Npm}$ and $C'_{NP}(1,1) = C'_{Npmk}$

Equations (1) to (4) are the existing superstructures to estimate PCIs for wide range of processes. Now we briefly describe the Johnson system of distributions and existing methods to estimate PCIs for non-normal processes in Section III.

III. JOHNSON SYSTEM OF DISTRIBUTION

The Johnson system of frequency curve was first developed by Johnson [9]. Farnum [21] has given a detailed description on the use of Johnson Curves. Chou *et al* [25] and Polansky *et al.* [26] proposed Johnson system of distribution to transform non-normal data sets. For complete description of this system, see Bowman Shenton [27], Johnson, Kotz and Balakrishnan [28], Stuart and Ord [29] and Kendall and Stuart [30]

Briefly, there are three distributions (S_B, S_U, S_L) of Johnson curves having two shape (γ and η), one location (ϵ) and one scale (λ) real parameters. S_B cover bounded distributions as gamma, beta and other distributions. It is bounded on lower end by \mathcal{E} , upper end by $\epsilon + \lambda$ or both. S_U are unbounded and cover t and normal distributions. S_L covers log-normal family and bounded only lower side by \mathcal{E} .

These three distributions are generated by transformations of the form

$$z = \gamma + \eta k_i(x; \lambda, \varepsilon) \tag{5}$$

Where $k_i(x; \lambda, \varepsilon)$ are chosen to cover a wide range of possible shapes and z is a standard normal variable. Johnson suggested these following functions for each distribution:

$$k_1(x; \lambda, \varepsilon) = \ln\left(\frac{x - \varepsilon}{\lambda + \varepsilon - x}\right) \quad \text{For } S_B \text{ distribution}$$

$$k_2(x; \lambda, \varepsilon) = \sinh^{-1}\left(\frac{x - \varepsilon}{\lambda}\right) \quad \text{For } S_U \text{ distribution}$$

$$k_3(x; \lambda, \varepsilon) = \ln\left(\frac{x - \varepsilon}{\lambda}\right) \quad \text{For } S_L \text{ distribution}$$

The three well known methods of estimation the parameters of Johnson System are the *moment matching method* by Draper [31], *the percentile matching method* by Slifker and Shapiro [32] and the *quantile estimation method* by Wheeler [33].

Table I comprises Johnson distributions (S_B, S_U, S_L) for X (Johnson variate) and (Standard normal Johnson variates). In Section IV we summarize the earlier developed methods to estimate PCIs using Johnson system for non-normal distributions.

IV. EXISTING PCIS FOR NON-NORMAL DISTRIBUTION USING JOHNSON SYSTEM

For normal processes the indices C_p and C_{pk} are defined as;

$$C_p = \frac{USL - LSL}{(\mu + 3\sigma) - (\mu - 3\sigma)} = \frac{USL - LSL}{6\sigma}$$

$$C_{pk} = \frac{\min\{USL - \mu, \mu - LSL\}}{3\sigma} \tag{6}$$

Pyzdek [2] worked on measurements of a hypothetical process to illustrate the use of Johnson transformation and

fitted S_B curve. He used λ (the scale parameter of S_B curve) as process spread 6σ with the reason that difference between lower ε and upper bound $\varepsilon + \lambda$ of the curve $(\varepsilon + \lambda) - \varepsilon$ may use as process spread.

$$C_p = \frac{USL - LSL}{(\varepsilon + \lambda) - (\varepsilon)} = \frac{USL - LSL}{\lambda} \tag{7}$$

Farnum [21] obtained C_p and C_{pk} using Johnson system and fitted S_U curve. He replaced process spread 6σ by $U_p - L_p$ for non-normal process and found L_p and U_p by putting $z = -3$ and $z = 3$ in equation of x for S_U curve (as displayed in Table I). These two indices are defined as:

$$C_p = \frac{USL - LSL}{U_p - L_p}$$

$$C_{pk} = \min\left\{\frac{USL - M}{U_p - M}, \frac{M - LSL}{M - L_p}\right\} \tag{8}$$

Extending Equation (8) the two other PCIs for non-normal processes under Johnson distribution are

$$C_{pm} = \frac{USL - LSL}{6\sqrt{\left[\frac{U_p - L_p}{6}\right]^2 + (M - T)^2}}$$

$$C_{pmk} = \min\left\{\frac{USL - M}{3\sqrt{\left[\frac{U_p - L_p}{6}\right]^2 + (M - T)^2}}, \frac{M - LSL}{3\sqrt{\left[\frac{U_p - L_p}{6}\right]^2 + (M - T)^2}}\right\} \tag{9}$$

Where M is the average of (L_p, U_p) and T is target value specified by product designer. In Section V standardized method to estimate (L_p, M, U_p) as process parameters for non-normal processes with new capability computation procedure is presented.

TABLE I. JOHNSON CURVES FOR X & Z VARIABLE

Johnson curve	X-variate	Z-variate
Bounded S_B	$\varepsilon + \frac{\lambda}{1 + e^{-\frac{z-\gamma}{\eta}}}$	$\gamma + \eta \log\left(\frac{x - \varepsilon}{\lambda + \varepsilon - x}\right) \quad (\varepsilon < x < \varepsilon + \lambda)$
Unbounded S_U	$\varepsilon + \lambda \sinh\left(\frac{z - \gamma}{\eta}\right)$	$\gamma + \eta \sinh^{-1}\left(\frac{x - \varepsilon}{\lambda}\right) \quad (-\infty < x < \infty)$
Lognormal S_L	$\varepsilon + \exp\left(\frac{z - \gamma}{\eta}\right)$	$\gamma + \eta \log(x - \varepsilon) \quad (\varepsilon < x)$

V. NEW CAPABILITY CALCULATION FOR NON-NORMAL DISTRIBUTION UNDER JOHNSON SYSTEM

A uniform SPC based procedure is presented to estimate PCIs for non-normal processes under Johnson system. We used superstructure form of Pearn and Chan [14] to estimate PCIs based on Johnson distributions.

For our new capability calculations we estimate these percentiles using density function $f(x)$ of selected Johnson distribution which is found to be the best fit for the given non-normal data set.

$$\int_{-\infty}^{\hat{F}_{0.135}} f(x)dx = 0.00135;$$

$$\int_{-\infty}^{\hat{F}_{99.865}} f(x)dx = 0.99865;$$

$$\int_{-\infty}^M f(x)dx = 0.5 \tag{10}$$

Based on our new capability calculations we named our capability indices as **JPCI** in computation tables.

Now we illustrate our procedure in steps to estimate PCIs easily.

VI. STEPS FOR OBTAINING MODIFIED PCIs USING JOHNSON SYSTEMS

The following steps are made for the proposed method.

Step 1: For the given data set obtain proportion non-conforming NC, process yield% and Vannman PCIs from Equation (1).

Step 2: Check whether process parameters (μ, σ) of Vannman superstructure misled the results. If no, there is no need to transform and if yes transform data set using Johnson transformation to select best fitted curve from (S_L, S_B, S_U)

Step 3: Superimpose the original and Johnson based fitted curve on probability histogram of original non-normal data sets to show that the chosen Johnson curve adequately fits the data.

Step 4: Simulate samples of size n=49, 99, 199, 499, 999, 1499 and 1999 for the fitted Johnson curve.

Step 5: From each simulated sample count (if any) number of observation(s) beyond the specification limits and exclude them for a statistical controlled process. Construct a grouped frequency distribution of controlled samples and apply chi-square goodness of fit test to asses that new samples are from the fitted Johnson distribution

Step 5: Transform x variates and predetermined specification limits (LSL, USL) of fitted Johnson curve in standard normal $Z = \frac{x - \mu}{\sigma}$ as (Z_l, Z_u) . Estimate proportion of process measurements, that exceeds the specification

limits as (p_l, p_u) . Find 0.135th, 0.5th and 0.99865th percentage points $(\hat{F}_{0.135}, \hat{F}_{99.865})$ for each data set by Farnum and based on our new computation procedure from the Johnson density function.

Step 6: For graphical assessment of normality construct probability histogram and draw normal probability plot (NPP) for each sample. For statistical assessment apply Shapiro-Wilk normality test for x and z variates.

Step 7: Estimate indices using Johnson system named as **JPCI** based on our computation procedure using superstructure from Equation (3) and percentiles for superstructure from Equation (10), **John (Z)** by Pyzdek and Farnum method from Equations (8) and (9). We also estimates PCIs by existing methods under Pearson distribution to check the efficacy of our method; Clements from Equation (2), Pearn and Chan from Equation (3), Pearn-Kotz-Chan from Equation (4).

VII. ILLUSTRATION OF PROPOSED METHOD

For illustration of proposed method the data consist of 100 measurements from a process earlier presented by Farnum [21] is taken. See Table II.

First we estimate the PCIs assuming that observations come from normal distribution for the given hypothetical process.

From Table III, we observe that PCIs assuming normal population are not satisfactory and misleading. We must use PCIs designed for non-normal processes. The best fitted equation as Farnum [21] found for data set is S_U

TABLE II. 100 MEASUREMENT OF PROCESS (LSL=5, USL=40, T=22.5)

6.3	6.8	9.3	10.4	11.1	11.6	12.2	12.5	12.5	12.6
12.9	13.2	13.2	13.3	13.3	13.5	13.5	13.9	14	14.4
14.8	14.8	15.2	15.4	15.7	15.8	15.9	16.2	16.3	16.5
16.5	16.7	16.9	17	17.1	17.7	17.8	17.9	18	18.1
18.1	18.1	18.1	18.1	18.1	18.4	18.4	18.7	18.7	18.8
19.1	19.3	19.3	19.5	19.6	19.7	19.7	19.9	20.2	20.3
20.6	20.6	20.7	20.8	21.4	21.5	21.9	22	22	22.1
22.3	22.6	22.7	22.9	23	23.3	23.3	23.5	24	24.2
24.7	25	25.1	25.5	25.5	25.7	25.9	26	26.1	29.3
29.4	29.6	29.6	29.8	29.9	29.9	31.4	34	34.9	40.6

TABLE III. PCIs ASSUMING NORMAL PROCESS

PCIs	Normal based PCIs	NC%	Process Yield%
C _p	0.957	0.41	99.59<99.73
C _{pk}	0.806	1.56	98.44<99.73
C _{pm}	0.872	0.89	99.11<99.73
C _{pmk}	0.734	2.77	97.23<99.73

$$Z = -1.767 + 2.519 \sinh^{-1} \left(\frac{x - 10.942}{10.826} \right); (-\infty < x < \infty) \quad (11)$$

The S_U distribution is an unbounded distribution so both transformed limits are possible for each sample. Now we constructed histogram for the data set and superimpose the fitted Johnson curve.

Fig. 1 shows that fitted Johnson curve adequately fits the original data.

For each simulated sample histograms and normal probability plots NPP are drawn to graphical examine the adequacy of model and normality assumption, see Fig. 2.

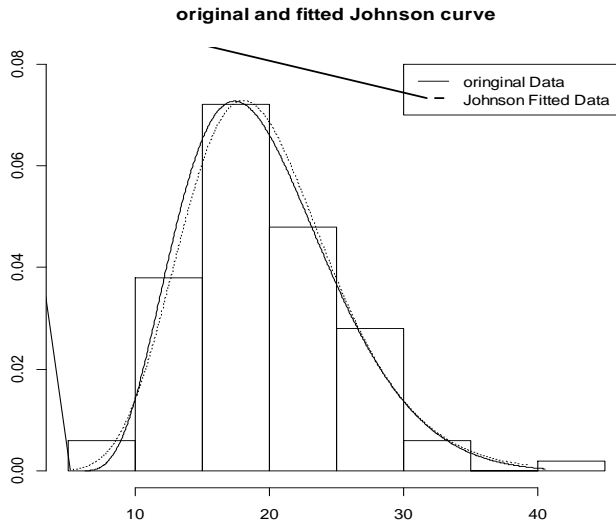


Fig. 1. Original and Best Fitted Johnson Curve with Probability Histogram.

For statistical test of normality Shapiro-Wilk normality test is performed and results are comprised in Table IV.

For original data and each sample transformed limits for S_U , proportion of non-conforming (NC) and 0.135th, 0.5th and 0.99865th percentiles (for Farnum method and our proposed method) are obtained. The results are given in Table V.

From Table VI, it is observed that capability calculations proposed under Johnson system for S_u distribution improve indices with those obtained by Pyzdek and Farnum theories using Johnson system and other existing methods under Pearsonion system.

TABLE IV. SHAPIRO-WILK NORMALITY TEST

Sample Size	Type	SW Statistics	P-value
Original data	X	0.975	0.055
	Z	0.994	0.938
49	X	0.980	0.545
	Z	0.972	0.281
99	X	0.973	0.040
	Z	0.975	0.055
199	X	0.971	0.000
	Z	0.988	0.099
499	X	0.976	0.000
	Z	0.993	0.017
999	X	0.976	0.000
	Z	0.993	0.000
1499	X	0.983	0.000
	Z	0.997	0.017
1999	X	0.984	0.000
	Z	0.998	0.010

TABLE V. ORIGINAL AND TRANSFORMED SPECIFICATION LIMITS, NC (PPM) AND PERCENTILES

Size	(USL,LSL)	Transformed Limits in Z	NC PPM	(L _p , U _p) (Farnum)	(L _p , U _p) (Our method)
original data	(5,40)	-6.356	0	8.13	13.83
		3.034	1206	39.76	46.04
49	(5,40)	-2	22750	-5.1	14.96
		3	1350	46.2	46.18
99	(5,40)	-2	22750	-3.6	14.74
		2	22750	54.7	54.74
199	(5,40)	-3	1350	2.6	14.2
		2	22750	52.6	52.6
499	(5,40)	-3	1350	1.8	14.38
		2	22750	53.6	53.55
999	(5,40)	-3	1350	0.5	14.18
		2	22750	56	56
1499	(5,40)	-3	1350	4.1	13.85
		3	1350	46.8	46.8
1999	(5,40)	-3	1350	5	13.84
		3	1350	46.6	46.63

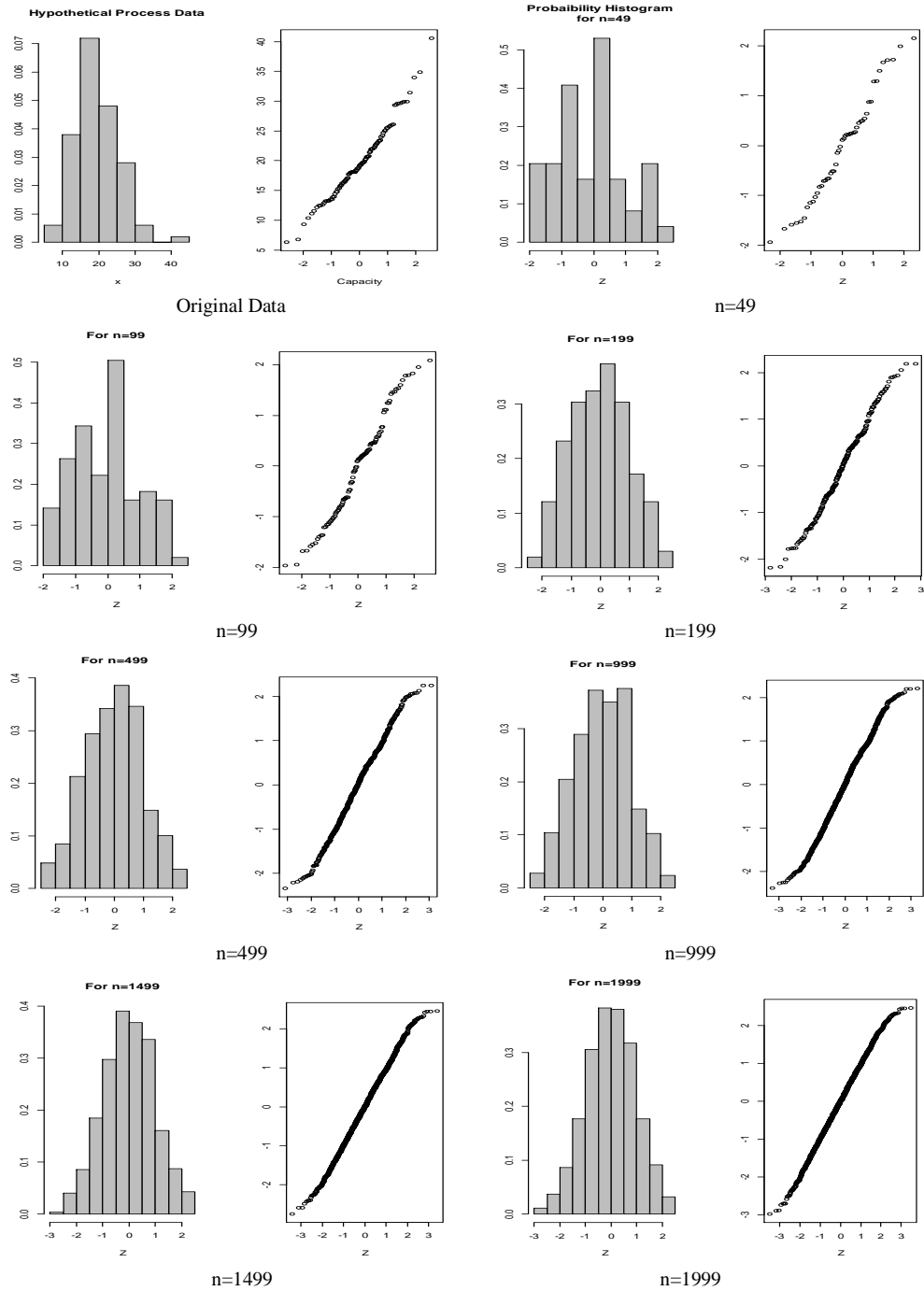


Fig. 2. Histogram and NPP of Best Fitted Johnson Curve.

TABLE VI. PCIS UNDER JOHNSON SYSTEM FOR SU DISTRIBUTION

Samples	Methods	Cp	Cpk	Cpm	Cpmk
Original data	PCI (Vannman)	0.956	0.806	0.872	0.734
	John(Z)(Pyzdek and Farnum)	0.862	0.704	0.779	0.637
	JPCIs (Modified)	1.086	0.879	0.923	0.748
	Clements	1.045	0.833	0.882	0.703
	Pearn & Chen	1.045	0.824	0.871	0.687
	PKC	1.045	1.007	0.882	0.846
n=49	JPCIs	1.121	1.051	1.097	1.029
	John(Z)	0.682	0.607	0.666	0.594
	Clements	1.278	1.241	1.27	1.234
	Pearn& Chen	1.278	1.241	1.27	1.234
	PKC	1.278	1.254	1.27	1.246
n=99	JPCIs	0.875	0.816	0.862	0.804
	John(Z)	0.6	0.495	0.572	0.471
	Clements	1.144	1.111	1.138	1.106
	Pearn& Chen	1.144	1.111	1.138	1.106
	PKC	1.144	1.065	1.138	1.061
n=199	JPCIs	0.911	0.781	0.849	0.727
	John(Z)	0.7	0.496	0.597	0.423
	Clements	1.134	0.98	1.03	0.89
	Pearn& Chen	1.134	0.972	1.02	0.874
	PKC	1.134	1.043	1.02	0.977
n=499	JPCIs	0.894	0.745	0.816	0.68
	John(Z)	0.676	0.475	0.579	0.407
	Clements	1.123	0.946	0.991	0.835
	Pearn& Chen	1.123	0.946	0.991	0.835
	PKC	1.123	1.044	0.991	0.96
n=999	JPCIs	0.837	0.687	0.764	0.628
	John(Z)	0.631	0.425	0.537	0.362
	Clements	1.102	0.906	0.95	0.78
	Pearn& Chen	1.102	0.906	0.95	0.78
	PKC	1.102	1.042	0.95	0.942
n=1499	JPCIs	1.062	0.867	0.917	0.749
	John(Z)	0.82	0.684	0.759	0.633
	Clements	1.074	0.876	0.923	0.753
	Pearn& Chen	1.074	0.875	0.923	0.753
	PKC	1.074	1.044	0.923	0.892
n=1999	JPCIs	1.067	0.869	0.917	0.747
	John(Z)	0.841	0.683	0.76	0.616
	Clements	1.065	0.867	0.916	0.745
	Pearn& Chen	1.065	0.867	0.916	0.745
	PKC	1.065	1.053	0.916	0.87

VIII. DISCUSSION AND CONCLUSION

The aim of this Paper is to focus attention on PCIs and their estimators and to emphasize their original basic purpose that of controlling the expected proportion outside specification limits based on engineering consideration. Earlier the percentiles of PCIs which are designed-modified for non-normal processes using Johnson system are estimated by approximate methods which do not require the knowledge of the density function of the data. We simulate the samples based on Johnson density function from the Johnson parameters estimated for the original non-normal process and then obtain the capability calculation for the indices. The percentiles of the PCIs are estimated by our modified method because the density function of the simulated samples is known.

In this paper we not only compare the results of PCIs based on Johnson systems with other existing methods for non-normal populations but list a program that can comprises the complete analysis step-by-step for choosing any of the Johnson curve. This program initially make the process in statistical control with the given specification limits, plot the density curve on original data to check the adequacy, and estimate PCIs based on new probability calculation as we execute the script for any non-normal or even normal data sets. All the computations are performed in R-console.

We observed in dealing with one non-normal data set that PCIs based on new probability calculation of simulated samples under Johnson system improve the indices estimated by Pyzdek and Farnum theories. We also noted 'over-the-sample' variations in each simulated sample based on fitted Johnson curve. We performed our capability calculation based on Pearn and Chan superstructure and obtain percentiles by exact method of selected Johnson distribution not by approximate method. We have also observed that new capability calculation improve the indices.

IX. FURTHER RECOMMENDATIONS

The authors are intended to do this program for estimating process capability indices for multivariate data.

REFERENCES

- [1] Bates TE, English JR. The robustness of modern process capability analysis. *Computers Ind. Eng.*1991; 21:45-49.
- [2] Pyzdek T. Process capability analysis using personal computers. *Quality Engineering* 1992; 4: 419-440.
- [3] Pyzdek. Why Normal distributions aren't [All that Normal]. *Quality Engineering* 1995; 7: 769-777.
- [4] Rivera LAR, Hubele NF, Lawrence FP. Cpk index estimation using data transformation. *Computers Ind. Eng.*1995; 29: 55-58.
- [5] Ahmed E, Safdar S. Process capability analysis for non-normal data. *Pakistan Business Review* 2010; 234-243.
- [6] Safdar S, Ahmed E. Process capability indices for shape parameter of Weibull distribution. *Open Journal of Statistics* 2014; 4: 207-219. doi: 10.4236/ojs.2014.43020.
- [7] Piña-MonarezMR, Ortiz-Yañez JF, Rodríguez-Borbón MI. Non-normal capability indices for the Weibull and Lognormal Distributions. *Quality and Reliability Engineering International* 2016; 32:1321-1329. doi: 10.1002/qre.1832.
- [8] Burr IW. Cumulative frequency distribution. *Ann Math Stat.* 1942; 13: 215-232.
- [9] Johnson NL. System of frequency curves generated by translation. *Biometrika*, 1949; 36: 149-176.
- [10] Box GEP, Cox DR. An analysis of transformation. *Journal of Royal Statistical Society.* 1964; 26: 211-243.
- [11] Somerville SE, Montgomery DC. Process capability indices and Non-normal distributions. *Quality Engineering* 1996-97; 19: 305-316.
- [12] Clements JA. Process capability calculations for Non-normal distributions. *Quality Progress.* 1989 September, 95-100.
- [13] Pearn WL, Kotz. S. Application of Clements' method for calculating second and third generation process capability indices for non-normal Pearsonian populations. *Quality Engineering* 1994; 7: 139-145.
- [14] Pearn WL, Chan KS. Capability indices for non-normal distributions with an application in electrolytic capacitor manufacturing. *Microelectronics Reliability Engineering.*1997; 37: 1853-185
- [15] Zwick D. A hybrid method for fitting distributions to data and it use in computing process capability indices. *Quality Engineering.*1995; 7: 601-613.
- [16] Schneider and Pruet J. Uses of process capability indices in the supplier certification process. *Quality Engineering* (1995-96); 9: 225-235.
- [17] Chen KS. Process capability indices for skew populations. *Journal of Management and Systems.* 1996; 3: 207-216.
- [18] Chen KS. A new process capability index for asymmetric tolerances. *Journal of the Chinese Institute of Industrial Engineers.* 1997; 14: 355-362.
- [19] Chen KS. Incapability index with asymmetric tolerance. *Statistica Sinica.* 1998;8: 253-262.
- [20] Chen KS. Estimation of the process incapability index. *Communications in Statistics: Theory and Methods.* 1998; 27(5):1263-1274.
- [21] Farnum NR. Using Johnson curves to describe Non-normal process Data. *Quality Engineering.* (1996-1997); 9: 329-336.
- [22] Vannman K. A unified approach to capability indices. *Statistica Sinica,* 1995; 5: 805-820.
- [23] Chang PL, Lu KH. PCI calculations for any shape of distribution with percentile. *Quality World,* technical section. 1994; September 110-114.
- [24] Pearn WL, Chen KS. Estimating process capability indices for non-normal Pearsonian populations. *Quality and Reliability Engineering International* 1995; 11: 386-388.
- [25] Chou YM, Turner S, Henson S, Mayer D and Chen KS. On using percentiles to fit data by a Johnson distribution. *Communication in Statistics-simulation and Computation.* 1998; 23:314-354
- [26] Polansky AM, Chou YM, Mason RL. Transforming non-normal data to normality in statistical process control, *Journal of Quality Technology* 1998; 30: 133-140.
- [27] Bowman KO, Shenton LR. Johnson's system of distributions. *Encyclopedia of Statistical Sciences.* 1983; 4: 303-314.
- [28] Johnson L, Kotz. S, Balakrishnan N. *Continuous Univariate Distribution* Vol. 1. John Wiley & Sons, New York, NY.
- [29] Stuart A, ORD JK. *Kendall's Advanced Theory of Statistics 1(5)* Oxford University press, New York, NY. 1987
- [30] Kendall MG, Stuart A. *The Advanced Theory of Statistics, Vol 1.* Macmillan: New York.1977
- [31] Draper J. Properties of distributions resulting from certain simple transformation of the Normal distribution. *Biometrika.*1952; 39: 290-301.
- [32] Slifker JF, Shapiro SS. The Johnson system: selection and parameter estimation. *Technometrics* 1980; 22: 238-246.
- [33] Wheeler RE. Quantile estimators of Johnson curve parameters. *Biometrika.* 1980; 67: 725- 728

Application of Artificial Neural Network and Information Gain in Building Case-based Reasoning for Telemarketing Prediction

S.M.F.D Syed Mustapha¹, Abdulmajeed Alsufyani²

Computer Science Department, College of Computer and Information Technology
Taif University, Taif, Saudi Arabia

Abstract—Traditionally, case-based reasoning (CBR) has been used as advanced technique for representing expert knowledge and reasoning. However, for stochastic business data such as customers' behavior and users' preferences, the knowledge cannot be extracted directly from data to build the cases in reasoning in making prediction. Artificial Neural Network that is known to be able to build model for predicting unprecedented business data is used together with Shannon Entropy and Information Gain (IG) to identify the key features. 8 attributes have been identified as key features from the 17 attributes which are based on the telemarketing data. These attributes are used to select the key features in building CBR. The weightage for the key features in the cases is obtained from the IG values. The mechanism of creating the cases based on the input from the ANN is discussed and the integration process between ANN and CBR is given. The process of integrating the ANN and CBR shows that both techniques complement each other in building a model in predicting a customer who would subscribe one of the promoted new banking services called "term deposit".

Keywords—Artificial neural network; prediction model; telemarketing; Shannon Entropy; feature selection; case-based reasoning

I. INTRODUCTION

Generally, marketing is an essential tool to increase sales and telemarketing is one of the marketing mechanisms since the advent of internet technology. There are two types of telemarketing, namely, the inbound and outbound [1]. The former describes the initiation made by the customer while the latter is managed by a group of telemarketing team that is designated to perform the systematic task in soliciting potential customers. In order to have an effective telemarketing communication, some background data are required to understand the potential of the customer in subscribing the proposed product prior to the teleconversation. The background data are related to the customer such as the age, profession, financial standing, prior marketing engagement with customers and even academic qualifications of the customers. These attributes are ought to be the ones that are significant to contribute to the final decision made by the customer whether to subscribe or otherwise on the proposed product.

In order to have a better prediction of the telemarketing situation, the attributes have to be selected based on its

relationship to the predictors (in this case the decision to be made by the customer on the subscription of the product). Each attribute will be measured based on the features of the attributes using Shannon Entropy and Information Gain (IG). The attributes are ranked based on IG values prior to feeding to the ANN for predicting the customer's response. We work on 45,212 data where about 10% is kept for testing and the remaining for training the neural network. The accuracy is reported based on the tested data against the actual result.

Our work is motivated by the past work in using machine learning techniques for making prediction mainly in sales, marketing and consumer behavior. According to Dilek et al. [2], marketing is an expensive operating cost for an organization that making a close to accurate forecasting on the potential market segment will be useful to reduce the cost of the production and materials, directly and indirectly. The ability to classify the consumer behavior using machine learning techniques such as regression, non-linear principal component analysis and classification was demonstrated by Richard et al. [3]. Modeling customer satisfaction has also resorted to ANN as its ability to determine the non-linear relationship between the consumer satisfaction and the factors that influence its behavior [4]. ANN is also used for volatile relationship like stock market on daily basis based on the index stock market indicator [5]. In market related application, ANN is able to predict housing prices by comparing ANN and hedonic economic model [6]. Similar work is done by Waheeb and Ghazali in predicting chaotic time series using high order neural network [15]. ANN was also proven to be able in predicting technical skills of potential soccer player [16].

Case-based reasoning (CBR) was introduced as a rapid approach in building expert's knowledge which is acquired from the past solvable cases [17]. Each case is presented with features and key features which are identified as discriminative factors to select suitable cases. Integrating CBR-ANN as complementing approach of both techniques has been shown by several works recently. Platon et al. deployed two machine learning techniques, ANN-CBR and a feature selection technique called PCA (Principal Component Analysis) to predict the power consumption on hourly basis [12]. The data that have readings with high variability is significant to be detected and to be used for prediction, it is captured using PCA. Electric consumption readings are random in nature, hence ANN would be the suitable method to model its behavior. Another proof of using a combined ANN-CBR is on

the design of green building based on the past successful building design. ANN is used to model the non-linear relationship of the key features in the cases and to predict the suitable case for a give case query [13]. Another suitable application of CBR-ANN integration is appraising the pricing for the domain name where the charges are based on arbitrary attributes such as length of domain name, words component, number of clicks, number of searches, etc. [14]. Biswas et al. took the advantage of using ANN to determine the feature weightage for the CBR cases. The ANN tree is pruned by taking into consideration of the four aspects in determining the feature weightages – sensitivity, activity, saliency and relevant [18].

Feature selection is one of the essential components prior to identifying key attributes that could enhance the accuracy in the prediction or classification using any machine learning techniques. Feature selection has been discussed and applied elsewhere in the literature. For example, feature selection using entropy has been successful for extracting the salient power consumption readings [7]. Another work reported on the usefulness of feature selection was on prediction of risks on hepatitis disease where feature selection had proven to be significant in enhancing the performance of the learning algorithm [8].

Our work in relation to the related work is on the application of feature selection on the telemarketing data using Shannon Entropy [9] and utilizing ANN and CBR for making prediction on the potential subscriber for the term deposit. In the following section, we describe the details in our research methodology.

This paper is organized in the following manner, Section 1, Introduction as discussed in this section, followed by Section 2, Materials and Methods, and finally Results and Discussion in the Section 3.

II. MATERIAL AND METHODS

In this project, neural network takes the input values within the range of 0 and 1 and the data was transformed accordingly as described in subsection Data Preparation. In the subsequent subsection, the application of Shannon Entropy and Information Gain on the 16 attributes (as the 17th attribute is the decision) is illustrated. The theoretical ANN model and CBR concept are expounded and demonstrated in terms of how these two techniques can be integrated.

A. Data Preparation

Data is obtained from UCI Machine Learning Website (<https://archive.ics.uci.edu/ml/datasets/Bank+Marketing>) which was made available since 14th Feb 2014. The data was first tested by Moro [10,11]. There were 17 attributes about a customer which are age, job type, marital status, education level, credit in default, housing loan, loan, personal loan, contact device, last contacted month and week as well as duration of the conversation by telemarketers, number of times the customer being contacted, the number of days lapse after the last contact, number of times the customer being contacted prior to the recent campaign, outcome of the previous campaign and finally the decision on whether the customer subscribes the term deposit product or not. The data provided

was in original format that it has to be converted to numerical scale between 0 – 1. For a qualitative categorical data (such as qualification – high school, tertiary, uneducated, etc.), the numerical is assigned in an even interval. For a binary category such as “Yes” or “No”, each is assigned at an extreme value, 0.9 and 0.1 respectively. For the attributes with numerical values, they are normalized and discretized between 0.1 and 0.9. This is important for data such as salaries or total saving amount which comes in infinite variations. The final outlook of the entire data is numerical values between 0 and 1. The decision whether to subscribe to the term deposit or not is valued as 0.9 and 0.1, respectively. There are 56,000 customer data in which 46,000 is separated as training data and the remaining is for testing.

B. Shannon Entropy and Information Gain the Shannon

Entropy of Q is Given as

$$Q(A) = -\sum_{i=1}^n p_i(a) \log_2 p_i(a) \quad (1)$$

where p_i is the probability of the features within a given attribute; and n is the number of features of the attribute in relation to the decision type “Yes” or “No”, hence $n = 2$. For the data being used in this project, the number of features varies for each attribute and the number of unique features are determined automatically. For example, the attribute *Occupation* has M features ($m_i \in M$ where $i = 3$, for example, $m_1 =$ B-blue-collar, $m_2 =$ W-white-collar and $m_3 =$ U-unemployed). Hence, $Q(A_m)$ is calculated as

$$\sum_{i=1}^2 -p_i \log_2 p_i = \left(-\frac{C(Y)}{C(Y+N)}\right) \log_2 \left(\frac{C(Y)}{C(Y+N)}\right) + \left(-\frac{C(N)}{C(Y+N)}\right) \log_2 \left(\frac{C(N)}{C(Y+N)}\right) \quad (2)$$

where C is the cardinality and m is one of the feature in M . When value Q is close or equal to 1, the feature is impure and hence is significant to the attribute. For each $m_i \in M$, $Q(A_{m_i})$ is calculated and the sum is $Q(A)$.

Each attribute (total of 16 attributes) is measured using IG (Information Gain) to determine discriminative value in determining the final decision. IG for an attribute is calculated as the followings:

$$Q(TA) = \left(\sum_{i=1}^{C(M)} \left(-\frac{C(Y)_i}{C(Y+N)_i}\right) \log_2 \left(\frac{C(Y)_i}{C(Y+N)_i}\right) + \left(-\frac{C(N)_i}{C(Y+N)_i}\right) \log_2 \left(\frac{C(N)_i}{C(Y+N)_i}\right) - Q(A)\right) \quad (3)$$

The entropy value for an attribute is calculated based on the total number of “Yes” and “No” for all features under the attribute. Hence, IG is $Q(TA) - Q(A)$.

C. Artificial Neural Network

We set our ANN with one hidden layer and sigmoid model as the transfer function. The output layer is set to be 0.9 to represent “Yes” or 0.1 as “No”. Sigmoid model is shown as follows:

$$y = \left(\frac{1}{1+e^{-x}} \right) \quad (4)$$

Every attribute that has been selected based on the Information Gain value will be coded as the input node. The number of hidden layer nodes is equal to the number of attributes. The entire network is depicted in Fig. 1. The initial values between 0 and 1 are fed into each input node which represents the attributes. The weights for the hidden layer are randomly computed as initial value. These values are propagated forward using sigmoid function. The final value is summed by totaling the values from all nodes from the hidden layer. The differences with the targeted value and total sum are computed in order to perform adjustment to the weightage. This is performed in many cycles until the sum error between the target and the computed weightage has reached to some threshold value. In our work, the stopping criteria is set to be error, $\epsilon < 0.001$ or 1000 cycles.

D. Case-Based Reasoning (CBR)

Traditional CBR has four fundamental phases which are performed on each case such as retrieval, reuse, revise and retain [18]. In retrieval phase, cases are retrieved based on the similarities to the problems being matched. The matching is performed by measuring the similarities of the key features between the cases and the posed problem. Hence, one or more cases could be retrieved, and this depends on the threshold being set as the minimum value for a case to be retrieved. Reuse phase is when the past cases have similar problems to the posed problem, and hence the recommended solution from the past cases can be recommended to be reused. However, not all cases have good matching that the recommended solution could be reused as it is. In this regard, some adaptations on the recommended solutions need to be performed based on the discrepancies on the key features and this led to revision. Revise phase involves the process of adjusting the recommended solution in the partially matched cases. The new adapted solution is done based on few strategies such as reference to ontology, heuristics rules or semantic database. Beside adaptation, cases which are not useable or obsolete, the recommended solution has to be changed or the entire cases have to be discarded as the problems are no longer relevant to the current context. Retain phase is performed on the cases where adjustment on the solution is made and the cases can be treated as new cases being created and retained in the case library.

E. Integrating ANN and CBR

The purpose of integrating ANN and CBR is to take the advantage of both machine learning techniques. Traditionally, during the creation of CBR case, the key features are determined by the expert who will also advise on the weightage based on the importance of each key feature in order to discriminate effectively the cases. However, in many domains where the data are unprecedented, the expert could not give his/her intuitive idea. Information gain is deployed as the feature selection method to determine the key attributes. Information Gain (IG) is measured based on the ratio of an attribute's entropy value against the entire entropy. The attributes that is considered are those where the data could be

categorized with maximum of four categories. Hence, attribute such as National Security Number, Phone number are not categorizable as each data is unique. IG generates the values that the selection of the suitable attributes is determined manually. The quality of attributes selection is determined by applying in ANN model. The performance of the ANN will determine the right selection of the attributes which are significant to be the considered as key features in case creation. Fig. 2 shows the entire process of determining key features for the cases using feature selection and ANN for CBR.

Business data may have physical meaning but the contribution to distinguish in decision making is not known. The attributes can only be signified by evaluating its contribution based on comparison of the information gain against all attributes. The result of the feature selection is discussed in Section III. The set of data with the selected attributes are performed on ANN to build the prediction model. A performance criterion of the ANN model is set (discussed in Section III) and if the results are unsatisfactory, the attributes will be reduced further. The adjustment of the feature selection is done iteratively until ANN model is able to meet the minimum required performance. Each feature selection has its IG value which is used to determine the weight for the key features in building the case.

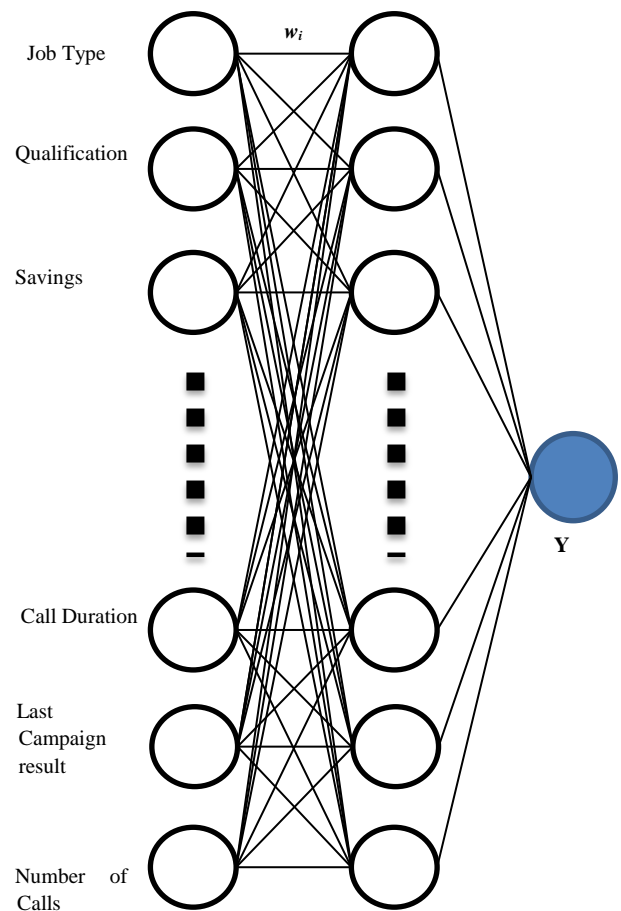


Fig. 1. Single Hidden Layer ANN.

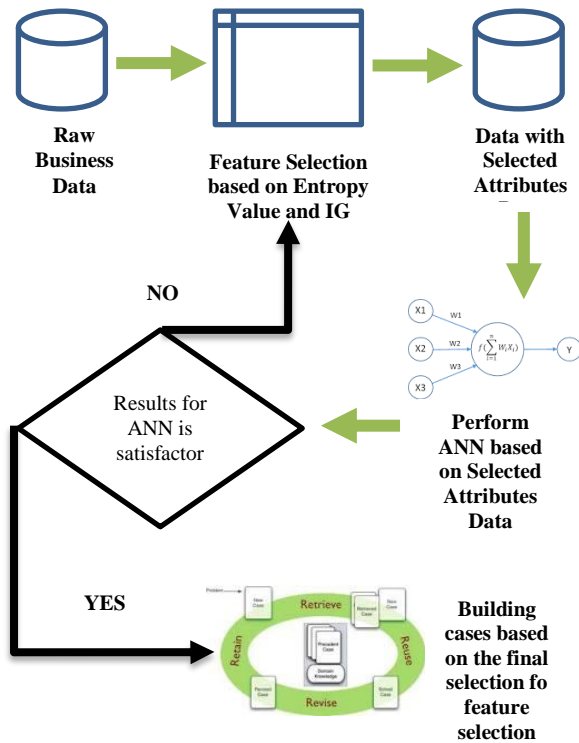


Fig. 2. Process of ANN-CBR Integration based on Feature Selection.

F. Building CBR

Building case for CBR has the advantage that each case can be built as independent case solving unit. Hence, each data can be treated as a case. This is called a linear case library which may not be efficient for a fast case retrieval. The cases have to be grouped by using clustering method. Since the data sets are labelled, the cases are segregated by the two main decision making, “Yes” or “No” to subscribe the term deposit. Heuristics algorithm using k-means can be applied to cluster the data sets for both sides (“Yes” and “No”) to few more sub-clusters. Each sub-cluster is created to allow the grouping of different class of cases based on the similarity values. The procedure in generating sub-cluster is given below:

Procedure to generate sub-cluster:

- 1) Given set of data, $N = \{n_1, n_2, \dots, n_k\}$
- 2) Choose a random centroid point, c where $c \in N$
- 3) Let c_1 and c_2 are two sub-clusters
- 4) Determine $d(c_1, c_2)$
- 5) Repeat
 - a) for each data n_i , determine $d_{i,1} = (c_1, n_i)$ and $d_{i,2} = (c_2, n_i)$
 - b) assign cluster to n_i based on the $d_{i,1}$ value
 - c) reassign the new points for c_1 or c_2 depending on which cluster gets a new member
 - d) execute step a with new points of c_1 or c_2

Until the centroid c_1 or c_2 converged to the same position.

The same procedure could be applied to generate smaller cluster within the two clusters and the number of clusters depending on the complexity of the attributes. Since, using the feature selection has reduced to 8 attributes, two clusters are sufficient. For each n , the value d is calculated using the following Euclidean distance:

$$d_{i,j} = (\sum_1^k \delta(n - c)^2)^{1/2} \tag{5}$$

where δ indicates the attributes value for each key feature. In this project, all attributes are normalized in order to allow numerical computation.

CBR is known as lazy learning in machine learning that its knowledge that are stored in the cases can grow through a simple comparison with the existing knowledge and stored when the new case does not match with the existing ones. Fig. 3 shows the process managing the case query. A case query could potentially be close to the centroid or far from any centroid. In the Cluster Assignment, the Case Query will be evaluated to determine its closest centroid. If it is found (new cluster is not needed), further search on case library is performed to find similar or partial match with the existing case. New cluster is recommended if no existing centroid have a close match. A close match value is determined if the Case Query falls within the boundary of the maximum and minimum distance of the case member within the same centroid. If none exist, then it is recommended that the Case Query needs a new cluster. The new Case Query will become the first centroid point. Cluster and sub-cluster avoid linear searching which can be $O(N)$ for a large case library while clustered case library will reduce to $O(\log N)$ depending on the number of clusters. For this purpose, other types of clustering algorithms such as AHC (Analytical Hierarchical Clustering [19]) is possibly used.

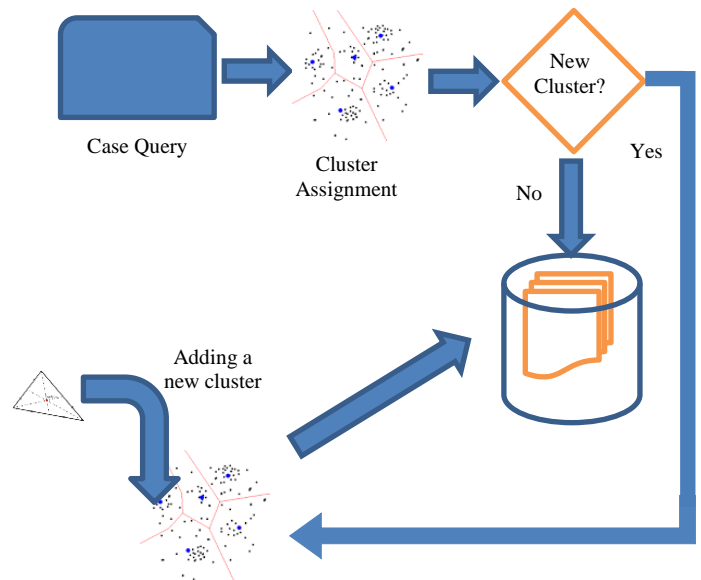


Fig. 3. Processing Case Query.

III. RESULTS AND DISCUSSION

We represent the results in two manners, the outcome of the Shannon Entropy and Information Gain and the success rate of applying ANN in performing the prediction. Table I shows the physical meaning of the attributes as explained in the UCI Machine Learning website.

Some of the attributes use qualitative or descriptive values that the values have to be manually converted to some distinct numerical values to differentiate between the optional values. Table II shows the entropy and the information gain values for each attribute. Only those attributes with $IG > 0.01$ will be considered as informative attributes (these attributes are bold).

The challenges that we are facing is that most of the attributes do not have high entropy value and they are not different from each other to make effective selection on the informative attributes. Hence, using information gain, we manage to reduce the attributes from 16 to 8.

The ANN program that we develop could take any number of attributes. For this experiment, we deploy only 8 attributes. There are 35,930 training data with the decision of “Yes” and 4760 data with “No”. The testing data for “Yes” and “No” are 3992 and 528 respectively. There are four experiments performed on the ANN, as shown in Table III.

TABLE I. ATTRIBUTE DESCRIPTIONS

Attribute No	Physical Meaning
Attribute 1	Age
Attribute 2	Employment Types (Student, Self-Employed, Retired, Management etc.)
Attribute 3	Marital Status
Attribute 4	Highest Education
Attribute 5	Credit in Default
Attribute 6	Balance in Saving
Attribute 7	Housing Loan
Attribute 8	Contact Mode (Mobile or Fixed Line)
Attribute 9	Last contact month
Attribute 10	Last contact day of the week
Attribute 11	Duration of the telemarketing conversation
Attribute 12	Number of times the customer being contacted
Attribute 13	Number of days lapse after the last telemarketing call
Attribute 14	Number of times being contact prior to the current campaign
Attribute 15	Number of days lapse since the last campaign
Attribute 16	Outcome of the previous marketing campaign
Attribute 17	Accept or Decline the term deposit

For each testing data, we apply the ANN model that has been built using the training data. Training data are separated based on the decision “Yes” or “No” and ANN is trained accordingly. The final weightage is computed to form the ANN model and the two sets of testing data (namely, with “Yes” and “No” decision) are applied for both ANN model with two different set of decision type. The targeted values of the decision for “Yes” and “No” are 0.9 and 0.1, respectively. Fig. 2 shows the sample of the results generated automatically in Excel using Visual Basic.

The “Computed Value” is the value generated from the ANN model. The “Difference” is the absolute value of the difference between the “Targeted Value” and the “Computed Value”. The “Difference” that is less than 0.001 and 0.01 are totaled on each of the testing data set on the two ANN model which is built on the two training data sets and the percentage shown in Table III represents the data with differences below 0.001 and 0.01. That means, if we set 0.01 as the threshold, we shall able to have at least 93% of testing data correctly predictable. If we set the threshold higher to 0.001 (smaller difference between the targeted and computed value), the percentages drop to 13% and 17% for the “Yes” and “No” cases. In the case of testing data that is executed on the ANN model which has opposite decision value, none of the testing data showed shows small differences, hence, it can be concluded that none of the testing data will be wrongly predicted. The testing data is not included as part of the data for training. Hence, the training data is considered as new.

TABLE II. ENTROPY AND IG VALUES

Attributes	Entropy values	Information Gain (IG)
Attribute 1	0.50725	0.013375
Attribute 2	0.50870	0.011922
Attribute 3	0.51783	0.002791
Attribute 4	0.51688	0.003748
Attribute 5	0.52020	0.000424
Attribute 6	0.51715	0.003475
Attribute 7	0.50670	0.013927
Attribute 8	0.51683	0.003794
Attribute 9	0.50097	0.019659
Attribute 10	0.52006	0.000563
Attribute 11	0.51406	0.006563
Attribute 12	0.45886	0.061762
Attribute 13	0.51743	0.003193
Attribute 14	0.50334	0.017283
Attribute 15	0.50334	0.017283
Attribute 16	0.04241	0.478219

TABLE III. RESULTS FOR THE ANN

Experimental Set Up		<0.001	<0.01
Training Data with "Yes"	Testing Data with "Yes"	13%	98%
Training Data with "Yes"	Testing Data with "No"	0%	0%
Training Data with "No"	Testing Data with "Yes"	0%	0%
Training Data with "No"	Testing Data with "No"	17%	93%

H	I	J	K
Attribute	Targeted value	Computed Value	Difference
16	0.2	0.9019777	0.0019777
	0.6	0.9056676	0.0056676
	0.4	0.9045856	0.0045856
	0.2	0.8956658	0.0043342
	0.6	0.9037097	0.0037097
	0.4	0.9040949	0.0040949
	0.2	0.8991377	0.0008623
	0.2	0.9011563	0.0011563
	0.6	0.9058895	0.0058895
	0.2	0.8967431	0.0032569
	0.6	0.9060655	0.0060655
	0.6	0.9050942	0.0050942

Fig. 4. Results generated using Excel Format.

IV. CONCLUSIONS

Business data like telemarketing is always large and the values of the attributes are not discernible as whether they should be included or excluded in the analysis. One may have attributes that may be seemed to be essential in terms of the functional aspects, but they do not carry any meaning in the data analysis. For example, the duration of the call in persuading the customer is an essential attribute but it may be meaningless if all of the values under the same attributes are the same. Hence, using Shannon Entropy and Information Gain will be useful in selecting attributes that could enhance in identifying the distinctive data. ANN model is proven to be useful to be used to model stochastic data such as telemarketing data as it has no standard model that can be used to model for making prediction. However, ANN is always be considered as black box where the decision being made is not transparent to the decision makers. Translating the black box model into white box model in the form of business rules and case presentation offer few benefits. The cases can be maintained and through periodical review of its decision without the need to rerun the ANN. The solution in the cases can be adapted to new situations. Practitioners could learn from the cases to understand the pattern in consumer behavior and preferences. Our work here shows that such model can be built using ANN and the prediction is reliable for certain threshold value.

The present work has few potential works for improvements. Adaptation is the powerful aspect in CBR as it allows the sustainability of the case library to be able to handle unprecedented situation. At present, adaptation which is done through adjustment to the parameters do not guarantee that the case is able to adapt to a more challenging situation. Deploying solid knowledge representation technique such as ontology shall allow reasoning and adaptation to new solution. Another aspect of improvement is the clustering in which the number of clusters is pre-fixed considering the number of attributes is small. For a larger set of attributes, the number of clusters and sub-clusters can be automatically determined to avoid as the behavior of the clusters cannot be determined manually.

REFERENCES

- [1] Kotler, P. and Armstrong, G. (2004). Principles of Marketing, 10Ed. Pearson Education Inc. New Jersey
- [2] Dilek Penpece and Orhan Emre Elma, (2014). Predicting Sales Revenue by Using Artificial Neural Network in Grocery Retailing Industry: A Case Study in Turkey. International Journal of Trade, Economics and Finance, Vol 5, No 5. October 2014, pp 435 – 440.
- [3] Richard Briesch and Priyali Rajagopal, (2010). Neural Network Applications in Consumer Behavior. Volume 20, Issue 3, July 2010, pp 381-389.
- [4] Nooshin Zeinalizadeh, Amir Abbas Shojaie, Mohammad Shariatmadar, (2015). Modeling and analysis of bank customer satisfaction using neural networks approach. International Journal of Bank Marketing. Vol 33, Issue 6, pp 717 – 732
- [5] Qiu M, Song Y (2016) Predicting the Direction of Stock Market Index Movement Using an Optimized Artificial Neural Network Model, PLoS ONE 11(5): e0155133. doi:10.1371/journal.pone.0155133
- [6] Limsonbunchai V, Gan C and Lee M. (2004). House price prediction: hedonic price model vs. artificial neural network. American Journal of Applied Sciences,1(3), pp 193-201
- [7] Sergio J., Àngela N., Fransisco M., Narcís A. (2015) Hybrid methodologies for electricity load forecasting: Entropy-based feature selection with machine learning and soft computing techniques, Energy, Vol 86, 15 June 2015, pp 276 – 291.
- [8] Pinar Yildirim (2015). Filter Based Feature Selection Methods for Prediction of Risks in Hepatitis Disease. International Journal of Machine Learning and Computing, Vol. 5, No. 4, August 2015, pp 258 – 263.
- [9] Shannon, Claude E. (July–October 1948). "A Mathematical Theory of Communication". Bell System Technical Journal. 27 (3): 379–423. doi:10.1002/j.1538-7305.1948.tb01338.x.
- [10] Moro, S., Cortez, P., and Rita, P. (2014). A Data-driven Approach to Predict the Success of Bank Telemarketing, Decision Support Systems, Elsevier, 62: 22 – 31, June 2014.
- [11] Moro, S. Laureano, R. and Cortez, P (2011). Using Data Mining for Bank Direct Marketing: An Application of the CRISP-DM Methodology. In P. Novais et al. (Eds), Proceedings of the European Simulation and Modelling Conference- ESIM'2011, pp. 117 – 121, Guimaraes, Portugal, October, 2011d. EUROSIS.
- [12] Platon, R, Dehkordi, V.R. and Martel, J. (2015). Hourly predictions of a building's electricity consumption using case-based reasoning, artificial neural networks and principal component analysis. Energy and Buildings, Vol 92, pp 10 – 18.
- [13] Cheng, J.C.P and Ma, L.J. (2015). A non-linear case-based reasoning approach for retrieval of similar case and selection of target credits in LEED projects. Building and Environment. Vol 93, pp 349 – 361.
- [14] Dieterle, S and Bergmann, R. (2014). A Hybrid CBR-ANN Approach to the appraisal of Internet Domain Names. In L. Lamontagne and E. Plaza (Eds.): ICCBR 2014, LNCS 8765, pp. 95–109.
- [15] Waheeb, W and Ghazali, R. (2016). Chaotic Time Series Forecasting Using Higher Order Neural Networks. International Journal on Advanced Science Engineering Information Technology, Vol 6, No.5, pp 624 – 629.

- [16] Nawi, N.M., Hussein, A.S., Samsudin, N.A., Hamid, N.A., Yunus, A.M., Aziz, M.F.A. (2017). The Effect of Pre-Processing Techniques and Optimal Parameters selection on Back Propagation Neural Networks. *International Journal on Advanced Science Engineering Information Technology*, Vol 7, No.3, pp 770 – 777.
- [17] Richter, M.M and Weber, R.O. (2013). *Case-based Reasoning*. Springer-Verlag.
- [18] Biswas, S.K., Chakraborty, M., Singh, H.R., Devi, D., Purkayashtha, B. and Das, A.K. (2017). Hybrid case-based reasoning system by cost-sensitive neural network classification. *Soft Computing*, 21, pp 7579 – 7596.
- [19] Murtagh, F. (2014) Ward's Hierarchical Agglomerative Clustering Method: Which Algorithms Implement Ward's Criterion? *Journal of Classification*, 31, pp 274- 295.

A Survey on Opportunistic Routing

Saleh A. Khawatreh¹, Mustafa Abdullah², Enas N. Alzubi³

Computer Engineering Dept., Faculty of Engineering, Al-Ahliyya Amman University, Amman-Jordan^{1,3}
Civil Engineering Dept., Faculty of Engineering, Al-Ahliyya Amman University, Amman- Jordan²

Abstract—Opportunistic Routing (OR) is attracted much in the research field of multi-hop wireless networks because it is different from traditional routing protocols [such as: Distance Vector (DV) and Link State (LS)], that it needs a lightweight protocol which is strong source routing basis]. In this paper, the development of opportunistic routing (OR) is presented, starting from the Selection Diversity Forwarding (SDF), Extended Opportunistic (ExOR), Proactive Source Routing (PSR), Cooperative Opportunistic Routing Scheme in Mobile Ad Hoc Networks(CORMAN), and the Zone-based Proactive Source Routing(ZPSR). The simulation tests using Network Simulator 2 (ns2) show the effectiveness of Opportunistic Routing protocols among various terms including control overhead, Packet Delivery Ratio (PDR), throughput, and end-to-end delay.

Keywords—Opportunistic routing; PSR; ExOR; proactive routing; source routing; tree-based routing; lightweight routing; wireless networks; ad hoc networks

I. INTRODUCTION

Mobile Ad Hoc Networks (MANET) is a challenging field due to its infrastructure which has less nature and time varying medium that effected by wireless medium propagation and multi-path fading, where nodes are free moving and self-configuring wireless communication links among them. There is no direct link to reach a node, so if any node wants to send a message to other node which it may not be its neighbor so in this case a multi hop communication is needed. In addition, wireless networks are soft links, that means, the link status change among the time, so the transmission power and the routing decisions are effected according to that, finally, Ad hoc networks has many applications such as: battlefield, health care, security, industry, environmental monitoring, and emergency operations in rescue and search. So many researches have been published since 1980s [1]. The most challenges in MANETs include end-to-end delay, security, and real-time multimedia sending.

Numerous routing protocols in the network layer have been created where everyone has its advantages and applications. Two distinct functions of the network layer are: routing and forwarding, forwarding is the process where nodes regulate the packets transfer from one link to another. Routing is a different process where nodes need to determine which path to select among transferring the packets to the destination and this need a control inputs, despite the huge efforts in data routing in MANETs, data forwarding is less challenging and follows the mechanism in Internet Protocol (IP), which was designed for wired networks. So the major goal in the research is to make wireless links as good as wired ones.

Opportunistic Routing (OR) has become the most attractive paradigm in wireless networks, due to its feature to develop the performance of wireless ad hoc networks. It takes advantage of broadcast characteristics and the spatial diversity, by packet transmit overhearing and the coordinating between relays nodes, OR sets a set of candidate nodes to act like a forwarding nodes to transmit packets to the destination. This dynamic sets of relays increase the performance of the network and the results improve that it increases the capacity, throughput, and decrease end-to-end delay, power consumption and control overhead [2]. In other words, OR is a routing techniques where a node broadcasts packets and the nodes which receive it correctly take the part of the data forwarding until the packets reach the destination, according to that, any node can participate in data forwarding based on the reception status of the packets, which differs from the traditional data routing IP where each intermediate node must check its routing table to take a decision which path to use.

Many categories of routing protocols are proposed in MANETs, the first category is proactive protocols (or named table-driven), in these protocols, every node has an information about the network topology, the nodes periodically flood its information about the link status to its all neighbors, so after certain time, all the nodes will have the whole topology of the network, the most popular protocols which belong to this category include Optimized Link State Routing (OLSR) [3] and Destination Sequenced Distance Vector(DSDV) [4]. The second category is reactive protocols (named as on-demand), in this protocols, nodes not always have routing information, instead that, routing information is constructed only when needed, and some examples include: Dynamic Source Routing (DSR) [5] and Ad-hoc On-demand Distance Vector (AODV) [6]. The third category is the hybrid routing, where nodes have entire routing information to some destinations and calculates routing information to others, it is a mixture between the first two ones, these routing protocols can be categorized into Link State (LS) and Distance Vector (DV), based on their algorithms, where in LS routing, every node exchanges information about itself among all nodes in the network where nodes in DV routing algorithm exchange the cost to each destination among neighbors.

To support opportunistic forwarding in MANETs, we need a routing facility that can offer source routing like DSR and gives robust information about the links like OLSR, but these protocols cannot be used due to their overhead, so a new routing protocol is proposed which is PSR that is described later.

In this paper, we present a survey of the improvements on OR starting with the Selective Diversity Forwarding (SDF), Extended-Opportunistic Routing (ExOR), Proactive Source Routing (PSR), Cooperative Opportunistic Routing Scheme in Mobile AD Hoc Networks (CORMAN), and the Zone-based Proactive Source Routing (ZPSR).

The remainder of the paper is organized as the following: Section II presents the Opportunistic routing protocols, Section III includes computer simulation for PSR and CORMAN, and finally, Section IV concludes the paper.

II. OPPORTUNISTIC ROUTING PROTOCOLS

In this section, different Opportunistic Routing (OR) protocols are presented, one of the first researches in OR proposed the Selective Diversity Forwarding (SDF) [7] where the transmitter chooses the best relays from multiple receivers that correctly receive its packets, then these selected relays take part of the data forwarding. However, it did not participate in real life due to its high control overhead. This inspired the researchers and led to propose an extension to OR which was ExOR by Morris and Biswas [8], they proposed anew cross-layer solution between the link and network layers. They take advantages of OR and DFS. In ExOR, the transmitter selects a set of forwarders which forward the data to the distinct destination according to the closeness to the destination, according to medium-access-control (MAC) sub layer it controls the contention and manage the data forwarding. To enhance the ExOR in wireless networks we need to know the nodes IDs and the topology of the networks and this needs to participate source routing protocol and link state routing protocol, and that results in a huge overhead, so a new routing protocol has proposed, a lightweight Proactive Source Routing (PSR) [9] where each node calculates a Breadth-First Spanning Tree (BFST) rooted at itself and includes all the nodes in the network. A Novel Cooperative Opportunistic Routing Scheme in Mobile Ad Hoc Networks (CORMAN) is presented in [10]. Finally, the new Zone-based Proactive Source Routing (ZPSR) [11] is proposed, where the network is divided into clusters and PSR is applied in the inter cluster, and outside, a Zone-based Routing Protocol (ZPR) [12] is used, and that improves the network performance. Here are the details:

A. Selection Diversity Forwarding (SDF)

In MANETs traditional routing schema is based on the shortest path to destination algorithms, such as, DV, LS. Many problems of these protocols include the instantaneous propagation and the exploitation less of the broadcast nature.

Larsson in his paper proposed SDF, it use the model of selection diversity in the framework in routing, it categorized as non-deterministic routing, and this is the first study of SDF according to fading and non-fading medium status. This method has three parts, described below:

1) *Network model*: Nodes broadcast the packets as slotted ALOHA, the nodes are half duplex type, and assumed distributed in uniform way on a square surface that density is λ

and the direction of the transmission is controlled by transmitting terminal, nodes can receive these packets according to the following equation:

$$P_i * \frac{G(R_o)}{N} = SNR_{min} \quad (1)$$

Where presents the transmitting power of node i , N is the receiving power, R_o is the distance between the nodes, $G(R_o)$ is the gain of the channel, and the SNR_{min} is the minimum signal to noise ratio that is accepted to successive reception.

Two scenarios were studied, the first when one node is transmitting and the others are receiving, and this is called as heterogenous traffic. On the other hand, a heavy loaded network is considered, and each node has one packet at least to send, and this system is considered as homogenous model.

2) *Capture model*: A capture model is proposed with the probability of the reception according to the following:

$$P_k = \begin{cases} 1, & \text{if } \frac{P_i G_{ik}}{N + \sum_{j \neq i,k} P_j G_{jk}} \geq CIR_{min} \\ 0, & \text{otherwise} \end{cases} \quad (2)$$

When node i sends a packet to node k , many interfered nodes denoted by j . G_{ik} and G_{jk} are link gains and CIR_{min} represents the minimum required signal carrier to interference ratio. The gain of the channel is assumed to be constant.

3) *Propagation models*: Here two channel models are experienced: a non-fading and a Rayleigh channel.

In the first model, the gain of the channel is based to the distance r as in the below equation:

$$G(r) = Constant * r^{-a} \quad (3)$$

In the second model, the Rayleigh fading is proposed uncorrelated from slot time and illustrated as the following:

$$fG(\gamma, R) = \frac{1}{G(r)} e^{-\frac{\gamma}{G(r)}} \quad (4)$$

Where γ represents a random variable of the gain.

The operation of SDF is shown in Fig. 1, according to it, the node broadcast the packets, then many nodes receive it and send acknowledgements sequentially to the sender then the sender sends a forwarding order then an acknowledgements are sent back.

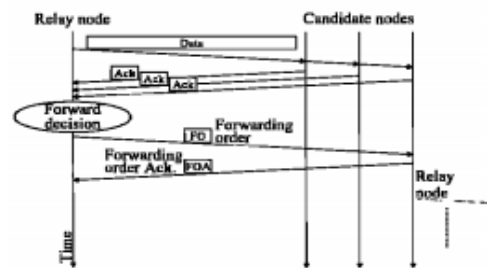


Fig. 1. Channel Access Mechanism in SDF.

It is fact that this protocol is not assumed to operate solely, it needs a protocol that provides the direction to the destination. One of the simplest connections is using Bellman Ford Routing [12], in which nodes select the relay nodes according to the cost to the destination. Other models can be used as power control; link rate could also be used to increase the performance. However, it increases the complexity of the design. Finally, SDF increased the network performance compared with the single path routing such as MFP and NFP. But the major drawbacks of this protocol are its overhead and cannot be used in sole model.

B. Extended-Opportunistic Routing (ExOR)

ExOR is an integrated extension and MAC protocol which improves the performance of big unicast data transmissions in MANETs. Here every hop is choosing after the transmission for this hop, and therefore, the paths are determined according to the real transmissions.

ExOR model has three challenges. The nodes which receive the packets need to be agreed on the nodes identities and pick one forwarder. This agreement should not cause a large overhead, so it need to be a lightweight, however, it should be robust to ensure that all the packets are received and don't need to retransmissions. Finally, the forwarder must be chosen as the closest to the destination.

A simple ExOR can be studied according to Fig. 2. In which a simple network is presented, suppose the source node wants to send packets to the destination. First, the source broadcasts the packets, the nodes then uses a protocol to know which nodes in the sub-set. The closest node to the destination is selected as a forwarder; the process is repeated until the destination receives the packets, back to Fig. 2. The probability to reach an intermediate node is 10%, and the probability to reach the destination from these intermediate is 100%. In traditional routing if the source node cannot transmit to the specific intermediate node then it must to retransmit until it reaches even though it reached other ones.

Fig. 3 shows another advantage of ExOR, according to this figure, a chain of nodes is considered, when the source wants to send a packet to the destination, in the traditional routing, the source first selects a certain path for example, src-B-D-dst. If node B didn't receive the packets, then the source must to retransmit the packets until node B receive it, however, other nodes received the packet where it may be near to node B (before or after it). In ExOR, the source does not need to retransmit the packets; any intermediate node can forward the packets.

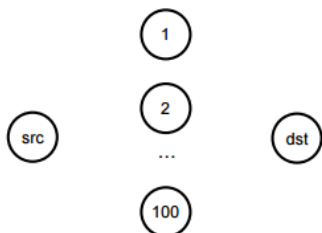


Fig. 2. Network Nodes Example.



Fig. 3. A Chain of Network Nodes Example.

The ExOR design has four challenges. First, the nodes should have an agreement, in which it contains the sub-set of the nodes that received each packet, since this agreement is a control messages it must be a lightweight control overhead but robust simultaneously. Second, the closest node to the destination must be chosen as a forwarder node. Third, if the network is large and dense, there will be a delay if many nodes are selected as participants, so it is better to choose the most effective ones only. Finally, ExOR should avoid simultaneous transmissions to avoid collisions.

To eliminate the control overhead, ExOR uses a patch of packets every transmission, so the agreement control messages will decrease to a significant ratio.

1) *Node state:* Every ExOR node maintains the state for every batch of the packets which is participating in the transmission, according to the node's presence in the batch's forwarder list. Nodes start keeping the state of the nodes after receiving the first packet. Then it stores the received packets in its batch.

The forwarder list includes a copy of the prioritized nodes list, which copied from a packet in the packet buffer. For a batch, all nodes contain the same forwarder list, which generated by the source.

The forwarding timer determines the time at when the node must forward its packets, and this must be set far from the receiving.

The transmission stalker tracks the measured rate at when the current node is sending, based on the expected packets numbers, which has left to send later. The nodes use this data to set the forwarding timer. The batch map shows, for every packet in the batch, the node which have the highest-priority to let it received a copy of the packet.

Ethernet Header			
Ver	HdrLen	PayloadLen	
Batch ID			
PktNum	BatchSz	FragNum	FragSz
FwdListSize		ForwarderNum	
Forwarder List			
Batch Map			
Checksum			
Payload			

Fig. 4. ExOR Packet Header.

2) *Packet format*: Fig. 4 presents the ExOR's packet header. It follows the Ethernet header, and the data follows the Ethernet header. All ExOR packets are broadcasted. The Ver field in Fig. 4 references to the ExOR version, this is used to future changes. The HdrLen field presents the size of the ExOR header and Payload Len presents the size of the payload. The BatchID field references to the batch the packets belong to. The PktNum represents the packet's offset in this batch. This offset represents the map of the batch entries for each packet. The BatchSz corresponds to the number of packets in each batch. FragSz presents the size of the current fragment (in packets), and FragNum presents current packet's offset of the fragment. The FwdListSize field presents the number of forwarders which are in the list. the forwarder num indicates the sender's offset among the list. Finally, The Batch Map is a batch map of the sending's node copy; to save space, every entry is an indicator to the forwarder List.

3) *Batch preparation*: The source collects a batch of packets which all estimated to the same destination. It picks a new batch ID and picks a list of forwarders. The source only has the all packets and that is illustrated in the batch map. Finally, the packets are broadcasted from source.

4) *Forwarder list*: The source indicates the forwarder list as a priority list accorded to the predictable cost of sending a packet between the nodes in the list until it reaches the destination. The cost parameter is the number of hops required to move a packet by the traditional routing from a node to a destination, including hops and retransmissions.

The source picks the forwarder list using the information about the network. The source gets this information via a periodic link-state message. ExOR is insensitive to fault or out-of-date bulks, because a packet's path is specified by status of the time of transmission.

5) *Packet reception*: Each node checks the header of each successful packet. If the list contains the node, the node put the packet into the buffer to a corresponding batch. For every item in the batch map included in the packet, then the node compares the item with the items in the batch map, and exchanges the older if the packet's item which is the highest priority node.

6) *Scheduling transmissions*: ExOR tries to manage when the nodes send their fragments so at a time only one node sends its packet. This manner allows the highest-priority nodes to send first. This scheduling avoids collisions.

7) *Completion*: When a node's batch map points that over 90% of the batch is received by the highest priority nodes, the node sends nothing. The last packets in the batch will be the most expensive to send, because it would need all the overhead of the transmission management, although, the overhead will be divided among few packets, and if the fragments are small, there is a greater probability that nodes will suppose their timers incorrect and then collide.

Because ExOR warranties to receive 90% of a batch, the destination requests the packets which remained by a traditional routing. The destination sends the batch map back to the source, then sends these packets by traditional routing, using link-level information to obtain a reliable delivery.

The major drawbacks of ExOR are it doesn't support reliable delivery, and there are many questions that are not answered; how to choose the candidate nodes? How many and which neighbors to select as forwarder lists?

C. Proactive Source Routing (PSR)

PSR supplies each node with a breadth-first spanning tree (BFST) about the whole network started in itself. To support that, nodes broadcast the tree structure every interval, to their neighbors, a node expand and refresh its information about the network by structure a longer and more recent BFST. This Information then will be flooded to its neighbors in the next period. When a neighbor is become lost, a technique is followed to remove its pertinent information from the topology of the detecting node.

1) *Route update*: Because of its proactive nature, all nodes exchange these BFST, with its neighbors and a star paradigm is obtained denoted as Sv . $N[v]$ presents the close neighbors and $N(v)$ presents the open neighbors. And this technique uses the following equation:

$$Gv = Sv \cup \bigcup_{u \in N(v)} (Tu - v) \quad (5)$$

In the above equation if $T-x=T$, we conclude that x is not in T , and if $T-x=0$, so that T is x .

2) *Neighborhood trimming*: These periodic broadcast flooding as a model as "hello" messages when a neighbor is considered lost, its tree to the network connectivity must be removed; this is named as neighbor trimming. Assume node v . The neighbor trimming technique is considered at v about node u that is a neighbor of v by one of the following ways:

- a) Routing updates or data packet has not been received from node u for a specific period of time.
- b) A transmission to node u has not succeeded, as denoted in the link layer.

Node v reacts by:

- Refreshing $N(v)$ by $N(v) - \{u\}$.
- then, computing the union paradigm with the information of u removed, i.e.,

$$Gv = Sv \cup (Tw - v) \quad (6)$$

3) Finally, constructing BFST Tv . and is not flood immediately to avoid extra messaging. This updating manner at v is ensuring avidness of sending packets by lost neighbors. So, many neighbors trimming techniques may be constructed in one period.

4) *Streamlined differential update*: Flooding route updates as hello messages in PSR, helps to replace the "full dump"

routing, with “differential updates.” and to send these full updated messages less than those short messages. In PSR, two methods are constructed to decrease the overhead; first, they used a compressed tree representation in both updated messages to decrease the size of it. Second, each node tries to keep a refreshed BFST in every change of the network so the differential updates are shorter.

5) *Compressed tree representation*: In this method we use binary tree representation such as shown below for the binary tree show in Fig. 5. A10B11C11D10E00F00G11H00I00

Stable BFST, by calculating the following equation:

$$(Tv - u) \cup_{w \in N(v)} (Tw - v) \quad (7)$$

D. *A Cooperative Opportunistic Routing Scheme in Mobile AD Hoc Networks (CORMAN)*

CORMAN is a pure network layer protocol based on opportunistic routing in MANETs. Its node communication mechanism is based on ExOR. First it is better to highlight the objectives and the challenges, and these objectives are: It extends the applicability of ExOR, and reduces the overhead of ExOR by choosing a shorter list of forwarders than in ExOR. The challenges are:

- 1) Overhead in calculating the route.
- 2) Adaptation of the forwarder list.
- 3) Robustness versus link variations.

CORMAN routes the packets in a batch manner similar as in ExOR. Data packets are collected into batches. And all packets in the batch have the same forwarder list before they transfer from the source. To boost CORMAN, they have a Proactive Source Routing (PSR) that provides every node with a complete routing knowledge to all the nodes in the network. So, the forwarding list includes the nodes identities on the path starting from the source until the destination. As long as, the packets forwarded among the nodes, the nodes which listed as forwarders can notice a change of the topology. This is named as *large-scale live updates*. And, in addition to that, CORMAN allows other nodes which are not considered as forwarders to retransmit packets if there some missing or fault, and this is referred to as *small-scale retransmission*.

Therefore, CORMAN has the following modules. Every module solves one of its challenges.

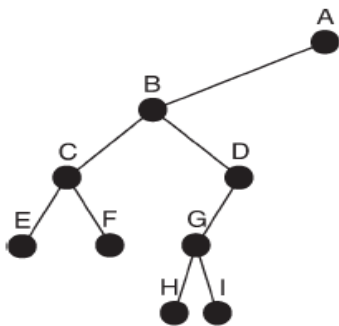


Fig. 5. Example of a Binary Tree.

1) Proactive source routing (PSR) used as a background and nodes periodically refresh its knowledge about network structure, by exchanging messages among the neighbors.

2) Large scale live updates. When the packet received in a forwarding node, this node can change the forwarder list, due to, its better knowledge about the destination as shown in Fig. 6.

3) Small scale retransmission. Because CORMAN uses a short forwarder list, it needs a mechanism to ensure the robustness among the transmission, to obtain this, the nodes which are not consider as a forwarder control the transmissions and retransmit the missed ones as shown in Fig. 7.

CORMAN has the following interesting ways to research:

- 1) It is better to further test CORMAN, such as, comparing it with ExOR model and IP forwarding.
- 2) The symmetry of multiple small-scale
- 3) Retransmissions could be obtained with better methods than RSSI.
- 4) Nodes in CORMAN transmit data packets in fragments. Among multiple nodes, it could allow nodes in different segments to operate at the same time.

E. *The Zone-based Proactive Source Routing (ZPSR)*

This is a hybrid protocol that combines the advantages of both PSR and ZRP. The basic idea of this protocol is to group the nodes in clusters and every cluster has a cluster head that is responsible of communicating with the outside world and to collect the data from the nodes members and send it outside. In the cluster the nodes perform the PSR, and in the outside the ZRP is used, that way gives the improvements to the performance.

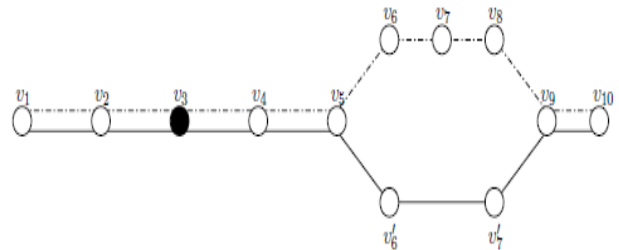


Fig. 6. Route updating Example.

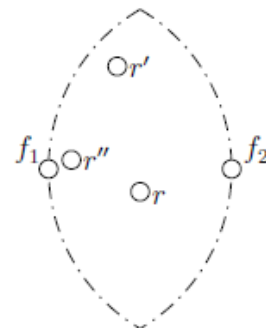


Fig. 7. Retransmission Region Example.

III. PERFORMANCE EVALUATION OF CORMAN

In this section, the performance of CORMAN is presented by doing computer simulation using Network Simulator ns-2 (version 2.34). It is compared with AODV in networks with different densities and mobility of the nodes. Then the performance explorations of these results are discussed. The PDR is plotted versus the network dimensions (Fig. 8) to show the performance relation between the CORMAN and AODV. The average delay is plotted versus the network dimensions (Fig. 9) to show the performance relation between the CORMAN and AODV. The delay jitter is plotted versus the network dimension (Fig. 10) to show the performance relation between the CORMAN and AODV.

The PDR is plotted versus the nodes mobility (Fig. 11) to show the performance relation between the CORMAN and AODV.

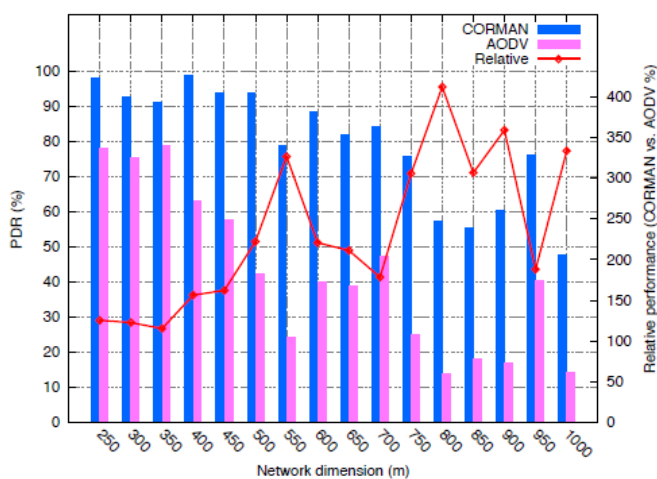


Fig. 8. PRD vs. Network Dimensions.

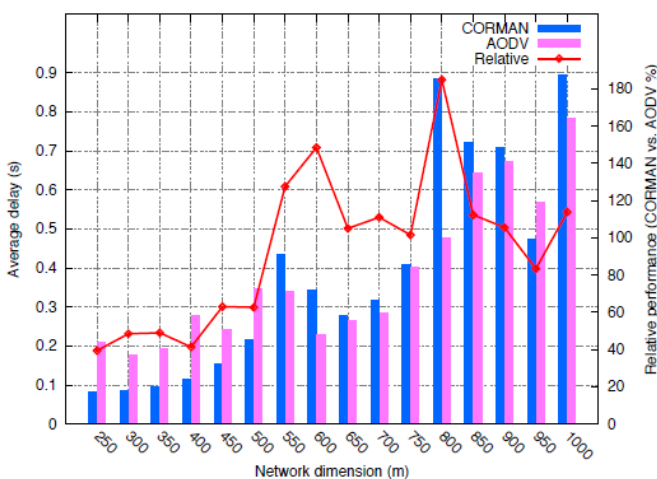


Fig. 9. Delay vs. Network Dimensions.

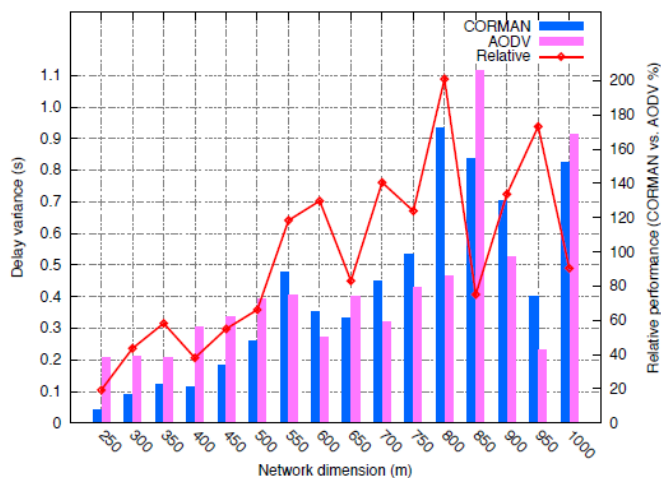


Fig. 10. Delay Jitter vs. Network Dimensions.

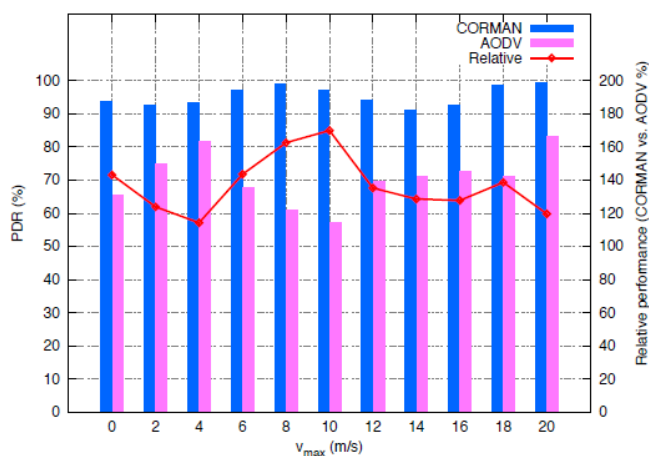


Fig. 11. PRD vs. Nodes Mobility.

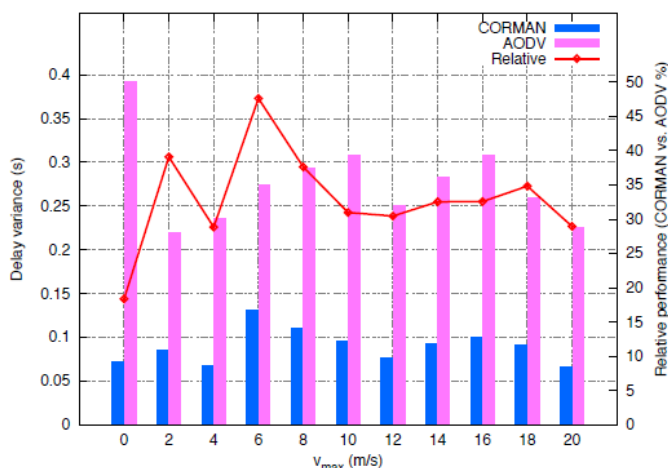


Fig. 12. Delay vs. Nodes Mobility.

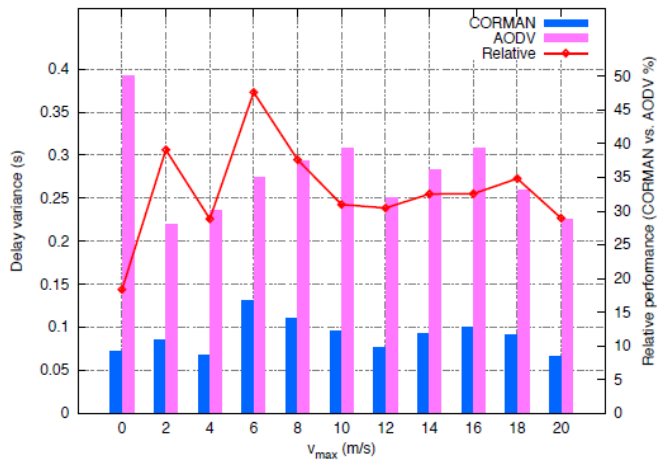


Fig. 13. Delay Jitters. Nodes Mobility.

The delay is plotted versus the network dimension (Fig. 12) to show the performance relation between the CORMAN and AODV. The delay jitter is plotted versus the network dimension (Fig. 13) to show the performance relation between the CORMAN and AODV.

IV. CONCLUSION

In this paper, a survey of the major types of opportunistic routing is presented. The first type of OR is SDF in 2001, after that ExOR in 2005 then PSR is presented in 2011, after one year a CORMAN is proposed in 2012, and recently in 2015 DPSR is proposed. These types have many drawbacks which can be a rich research area.

REFERENCES

- [1] Chlamtac, M. Conti, and J.-N. Liu, "Mobile ad hoc networking: Imperatives and challenges," *Ad Hoc Netw.*, vol. 1, no. 1, pp. 13–64, Jul. 2003.
- [2] R. Rajaraman, "Topology control and routing in ad hoc networks: A survey," *ACM SIGACT News*, vol. 33, no. 2, pp. 60–73, Jun. 2002.
- [3] T. Clausen and P. Jacquet, "Optimized Link State Routing Protocol (OLSR)," RFC 3626, Oct. 2003. [Online]. Available: <http://www.ietf.org/rfc/rfc3626.txt>
- [4] C. E. Perkins and P. Bhagwat, "Highly dynamic Destination-Sequenced Distance-Vector Routing (DSDV) for mobile computers," *Comput. Commun. Rev.*, vol. 24, pp. 234–244, Oct. 1994.
- [5] D. B. Johnson, Y.-C. Hu, and D. A. Maltz, "On The Dynamic Source Routing Protocol (DSR) for mobile ad hoc networks for IPv4," RFC 4728, Feb. 2007. [Online]. Available: <http://www.ietf.org/rfc/rfc4728.txt>
- [6] C. E. Perkins and E. M. Royer, "Ad hoc On-Demand Distance Vector (AODV) routing," RFC 3561, Jul. 2003. [Online]. Available: <http://www.ietf.org/rfc/rfc3561.txt>
- [7] P. Larsson, "Selection diversity forwarding in a multihop packet radio network with fading channel and capture," *ACM Mobile Comput. Commun. Rev.*, vol. 5, no. 4, pp. 47–54, Oct. 2001.
- [8] S. Biswas and R. Morris, "ExOR: Opportunistic multi-hop routing for wireless networks," in *Proc. ACM Conf. SIGCOMM*, Philadelphia, PA, USA, Aug. 2005, pp. 133–144.
- [9] Maleki, Morteza, Karthik Dantu, and Massoud Pedram. "Power-aware source routing protocol for mobile ad hoc networks." *Proceedings of the 2002 international symposium on Low power electronics and design*. ACM, 2002.
- [10] Wang, Zehua, Yuanzhu Chen, and Cheng Li. "CORMAN: A novel cooperative opportunistic routing scheme in mobile ad hoc networks." *Selected Areas in Communications*, *IEEE Journal on* 30.2 (2012): 289-296.
- [11] Sangheethaa, S., and P. V. Shyamili. "Zone-based Proactive Source Routing Protocol for Ad-hoc Networks." *Composoft* 4.1 (2015): 1477.
- [12] Haas, Zygmunt J., Marc R. Pearlman, and Prince Samar. "The zone routing protocol (ZRP) for ad hoc networks." (2002).

Optimal Design of a Variable Coefficient Fractional Order PID Controller by using Heuristic Optimization Algorithms

Omer Aydogdu¹

Department of Electrical and Electronics Engineering
Konya Technical University,
Konya, Turkey

Mehmet Korkmaz²

Department of Electrical and Electronics Engineering
Aksaray University, Faculty of Engineering
Aksaray, Turkey

Abstract—This paper deals with an optimal design of a new type Variable coefficient Fractional Order PID (V-FOPID) controller by using heuristic optimization algorithms. Although many studies have mainly paid attention to correct the performance of the system's transient and steady state responses together, few studies are interested in both transient and steady state performances separately. It is obvious that handling these two cases independently will bring out a better control response. However, there are no studies using different controller parameters for the transient and steady state responses of the system in fractional order control systems. The major contribution of the paper is to fill this gap by presenting a novel approach. To justify the claimed efficiency of the proposed V-FOPID controller, variable coefficient controllers and classical ones are tested through a set of simulations which is about controlling of an Automatic Voltage Regulator (AVR) system. According to the obtained results, first of all it was observed that proposed V-FOPID controller has superiority to the classical PID, Variable coefficient PID (V-PID) and classical Fractional Order PID (FOPID) controllers. Secondly, Particle Swarm Optimization (PSO) algorithm has shown its advantage compared to the Artificial Immune System (AIS) algorithm for the controller design.

Keywords—Artificial immune system; automatic voltage regulator; particle swarm optimization; variable coefficient fractional order PID controller

I. INTRODUCTION

Traditional PID controller and its offshoots are indispensable type of controllers for the industrial and academic studies. In many industrial applications, especially requiring feedback, it is benefited from the PI and PID controllers. PID controllers are widely used in industrial applications due to their simple structure and ability to meet the needs [1], [2]. Nevertheless, improved industrial and academic applications are in need of advanced control strategies, new controller types etc. With this idea, a new type of controller has been enhanced by Podlubny as the generalization of a traditional PID controller [3], [4]. Although the fractional calculus is not a new issue, FOPID controller based upon fractional calculus has become popular recently. Fractional calculus contains the non-integer order of the integral (λ) and derivative (μ) terms [5]-[7]. Although it is explored in the 1700s, it has not found application areas due to

its heavy calculation process up to last two decades [3], [4], [8]. Nowadays, thanks to the development of fast and high capacity processors, fractional calculations have been made easier. With this development, fractional calculus attracted the attention of scientists and found the opportunity to be applied to many fields [9]-[13].

Furthermore, fractional controllers have been applied in a large number of fields as a powerful controller that is more successful than traditional ones for disturbance rejection and fluctuation of input rates. Nonetheless, a determination of the fractional controller parameters is a challenge point in these days. Researchers still seek new methods to obtain best parameters for the fractional controllers. Luo have put forward new design techniques which are systematic ways for FOPID controllers [14]-[16]. In addition to this, heuristic optimization techniques have also been considered for obtaining fractional controller coefficients [17]-[21]. Additionally, Gaing have used PSO technique to obtain optimal solution for AVR control system [17]. Korkmaz benefited from genetic algorithm (GA) and PSO in the design of Ball and Beam control system [22]. Das has applied fuzzy logic based novel fractional controllers in the control of AVR system [23].

As distinct from the classical approaches, it might be possible to design nonlinear or variable parameter controller structures which affect the system not only by a constant parameter value but also online adjustable one. For instance, traditional PIDs or FOPIDs have always same controller parameters regardless of the change in the parameter uncertainties or any disturbances while the nonlinear ones vary the control signal with the rate of error. In literature, variable and nonlinear PID control method is applied to several processes such as main steam temperature control which is executed by means of two controllers, PID and non-linear PID control [24], [25]. Similarly, Korkmaz have compared PID and non-linear PID controllers on different plants which show the advantage of non-linear PID control over traditional one and they have utilized from the error function (also called Gaussian error function) [26].

Ibrahim has implemented non-linear PIDs' design using fuzzy logic [27]. The main idea of the nonlinear variable PID controllers is to supply adjustable parameters which are system error dependent. According to our researches, there is

no similar structure for FOPID controllers and a systematic parameter design procedure for them.

This study mainly targets to fill these gaps and main contributions of this study to the literature are as follows:

- Presenting a new type of variable fractional PID controller, whose gains are dependent to the system error so that it is possible to improve the transient response and provide a robust control structure.
- A systematic design procedure for the determination of the fractional and traditional controllers by using heuristic optimization methods such as artificial immune and particle swarm optimization algorithms.

II. FRACTIONAL CALCULUS

Fractional calculus has been thought a generalization of classical calculus in which $d^n y/dt^n$, n is accepted as a non-integer form, $n \in \mathbb{R}$. Generally, fractional order derivatives and integrals have been symbolized as a letter of D which represents the type of fractional calculus, defined as;

$${}_b D_t^\alpha = \begin{cases} \frac{d^\alpha}{dt^\alpha}, & \Re(\alpha) > 0 \\ 1, & \Re(\alpha) = 0 \\ \int_b^t (d\tau)^{-\alpha}, & \Re(\alpha) < 0 \end{cases} \quad (1)$$

Where, b represents the onset time value and α is a fractional order. Negative terms of α refers to fractional integral contrary to the positive numbers of it represents the fractional derivative. α can either be a complex number that provide us with defining systems in more powerful and effective way. For these extraordinary properties of fractional calculus many systems can be expressed in different ways. There are many types of definition indicated in the literature about fractional calculus, that three of the most widely used definition in the literature can be given as follows [7], [28]-[30].

A. Riemann Liouville Definition

The fractional derivative can be defined using the definition of the fractional integral as in (2),

$${}_b D_t^\alpha f(t) = \frac{1}{\Gamma(n-\alpha)} \frac{d^n}{dt^n} \int_b^t \frac{f(\tau)}{(t-\tau)^{\alpha-n+1}} d\tau \quad (2)$$

Where, $n - 1 < \alpha < n$ and $\Gamma(\cdot)$ is Euler Gamma function.

B. Grünwald Letnikov Direct Definition

The definition can be defined as in (3), by using the substitution $h \rightarrow -h$ in the reverse Grünwald-Letnikov derivative,

$${}_b D_t^\alpha f(t) = \lim_{h \rightarrow 0} h^{-\alpha} \sum_{j=0}^{\lfloor (t-b)/h \rfloor} (-1)^j \binom{\alpha}{j} f(t-jh) \quad (3)$$

Where, $\lfloor (t-b)/h \rfloor$ is a truncation coefficient and $\binom{\alpha}{j}$ is binomial coefficients.

C. Caputo Definition

Caputo fractional derivative defined as in (4),

$$\square {}_b D_t^\alpha f(t) = \frac{1}{\Gamma(n-\alpha)} \int_b^t \frac{f^n(\tau)}{(t-\tau)^{\alpha-n+1}} d\tau \quad (4)$$

where; $n - 1 < \alpha < n$. The Gamma function $\Gamma(m)$ can be defined for a positive real m as follows:

$$\Gamma(m) = \int_0^\infty e^{-u} u^{m-1} du \quad (5)$$

Laplace transformation has great importance for describing linear control system in terms of simplifying computations. Similar to classical calculus in Laplace domain, fractional calculus can also be convertible to Laplace domain in (6).

$$\mathcal{L} \left\{ \frac{d^m f(t)}{dt^m} \right\} = s^m \mathcal{L}\{f(t)\} - \sum_{k=0}^{n-1} s^k \left[\frac{d^{m-1-k} f(t)}{dt^{m-1-k}} \right]_{t=0} \quad (6)$$

According to this explanation, Riemann Liouville Definition in Laplace domain can be rewritten as (7).

$$\mathcal{L} [{}_b D_t^\alpha f(t)] \begin{cases} s^\alpha F(s), & \text{if } \alpha \in \mathbb{R}^- \\ F(s), & \text{if } \alpha = 0 \\ s^\alpha F(s) - \sum_{k=0}^{\alpha-1} s^k {}_0 D_t^{\alpha-k-1} f(0), & \text{if } \alpha \in \mathbb{R}^+ \end{cases} \quad (7)$$

In other respects, in literature various approaches have been suggested to realize fractional order systems [10], [31]-[33]. Here in the study, the well-known Oustaloup method which is utilized in all kind of fractional terms formulizes.

III. AUTOMATIC VOLTAGE REGULATOR (AVR) SYSTEM

Automatic voltage regulators (AVR) are practically used to maintain terminal voltage at the nominal level for synchronous alternator [21], [34], [35]. For this reason, it is important to keep voltage level at the desired value for power plants. Due to the system parameter uncertainties, controllers play a crucial role to have a robust control. As shown in Fig. 1, an AVR system without controller consists of four main parts; Amplifier, Exciter, Generator and Sensor. Linearized transfer functions of the AVR system is possible to express in Laplace domain and all mathematical models of the Amplifier, Exciter, Generator and Sensor blocks are defined in Fig. 1.

Where; K_a, K_e, K_g, K_s are gain values and $\tau_a, \tau_e, \tau_g, \tau_s$ are time constants of the Amplifier, Exciter, Generator and Sensor models respectively. Generally accepted parameters boundaries of the AVR system in literature for Amplifier, Exciter, Generator and Sensor model are shown in Table I [18]. AVR system parameters are also selected given in Table I for this study.

TABLE I. AVR SYSTEM PARAMETERS

AVR system	Parameter Boundaries	AVR Initial Parameters	AVR Changing Parameters
Amplifier	$10 \leq K_a \leq 400$, $0.02 \leq \tau_a \leq 0.1$	$K_a = 10, \tau_a = 0.1$	$K_a = 14, \tau_a = 0.07$
Exciter	$1.0 \leq K_e \leq 400$, $0.1 \leq \tau_e \leq 1.0$	$K_e = 1.0, \tau_e = 0.4$	$K_e = 1.2, \tau_e = 0.5$
Generator	$0.7 \leq K_g \leq 1.0$, $1 \leq \tau_g \leq 2$	$K_g = 1.0, \tau_g = 1.0$	$K_g = 0.7, \tau_g = 1.6$
Sensor	$K_s = 1.0$, $0.001 \leq \tau_s \leq 0.06$	$K_s = 1.0, \tau_s = 0.01$	-

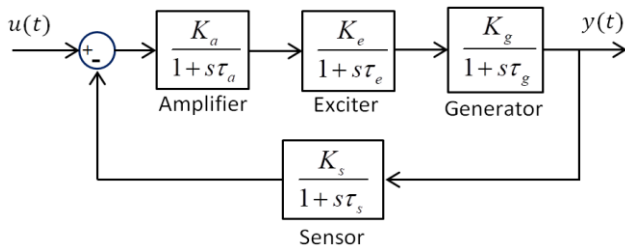


Fig. 1. An AVR System Block Diagram without Controller.

IV. IMPLEMENTED SYSTEM

In this study, a variable fractional order PID controller which is designed by using heuristic optimization techniques is proposed and implemented for the control of the automatic voltage regulator (AVR) system. The whole block diagram of the implemented system is shown in Fig. 2. As seen in figure, the proposed diagram consists of three parts; an AVR system, a variable controller and an optimizer.

According to the diagram, PSO or AIS optimizers get the reference input, control signal and system output data, seek the optimal value of necessary controller coefficient such as; $K_p, K_i, K_d, \lambda, \mu, c_1-c_6$ and send the obtained parameters to the controller.

A. Mathematical Model of the V-FOPID

The classical PID control given as in (8) and FOPID control given as in (9) have constant coefficient which are proportional gain (K_p), integral gain (K_i), derivative gain (K_d), fractional integral order (λ) and fractional derivative order (μ) to control the system. These parameters have the same value throughout the operation regardless of the system error. Because of this reason, as mentioned in the previous sections, it is not possible to interfere separately to the transient and steady states with the constant parameters. Therefore, the core of the study seeks the answer of the question that what kind of controller structure should be established that improves the transient state without affecting the steady-state response. Can it be possible to implement a variable PID (V-PID) scheme such as in (10) in the paper [26]. With this idea, a new type controller has been enhanced for fractional PID controllers such as variable coefficient fractional order PID (V-FOPID) controller given in (11).

$$G_{PID}(s) = K_p + \frac{K_i}{s} + K_d s \quad (8)$$

$$G_{FOPID}(s) = K_p + \frac{K_i}{s^\lambda} + K_d s^\mu \quad (9)$$

$$G_{V-PID}(s) = K_p' + \frac{K_i'}{s} + K_d' s \quad (10)$$

$$G_{V-FOPID}(s) = K_p' + \frac{K_i'}{s^\lambda} + K_d' s^\mu \quad (11)$$

It is clearly seen that the equations (9), (10) and (11) are derived from (8), which is a classical PID controller. However, the proportional, integral and derivative gains of the (10) and (11) differ from the classical PID and FOPID ones. The gains are symbolized by K_p', K_i', K_d' in (12), (13), (14)

which depend on the value of the errors. Thereby, the values of the controller parameters change in regard to the system error. This novel method for the fractional PIDs allows having better system response both in transient and steady-state.

$$K_p' = c_1 |e(t)| + c_2 \quad (12)$$

$$K_i' = c_3 |e(t)| + c_4 \quad (13)$$

$$K_d' = c_5 |e(t)| + c_6 \quad (14)$$

Where, $|e(t)|$ is the absolute error between reference signal and system output, c_1 through c_6 are the new tuning parameters of the V-PID or V-FOPID controller for varying coefficients.

As well as classical tuning parameters of the PID and FOPID controllers, the new types of controller have three more additional parameters to be optimized. The controller coefficients to be optimized by the PSO and AIS algorithm can be summarized as:

PID control parameters are K_p, K_i, K_d ,

V-PID control parameters are $c_1, c_2, c_3, c_4, c_5, c_6$,

FOPID control parameters are $K_p, K_i, K_d, \lambda, \mu$,

V-FOPID control parameters are $c_1, c_2, c_3, c_4, c_5, c_6, \lambda, \mu$.

For the system to be able to give the best response, all of these parameters are obtained and optimized by the PSO and AIS algorithms.

B. Optimal Design of the Control Systems

In the study, in order to obtain the best controller coefficients, it has been utilized by two different optimization techniques which are PSO and AIS algorithms. These heuristic methods are good alternatives when the system analytical solution is hard to find.

Variable coefficients of the controllers are determined by using the mentioned optimization techniques. The idea behind describing variable parameters is having a better transient response. A well transient response is always thought having a short rising and settling time and lower oscillation. To obtain get better transient response, the system needs higher proportional and derivative but lower integral effects on the transient situation. This condition is ensured if the value of the integral, proportional and derivative effects depends on the change in the system error as in our proposed scheme.

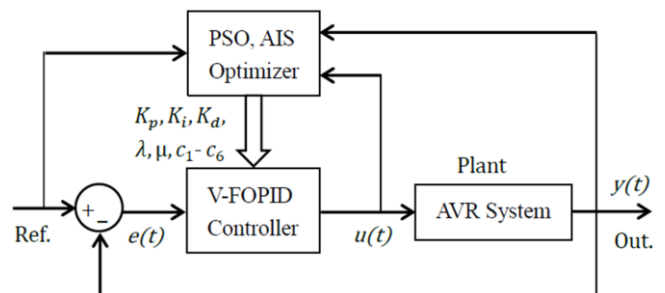


Fig. 2. Block Diagram of Implemented System with Variable Coefficient.

Performance criteria are the quantity measurements of the control systems which are based on different punishment such as Integrated Absolute Error (IAE), Mean Square Error (MSE), Integrated Square Error (ISE), Integral time Square Error (ITSE) and etc. It is benefited from multi-objective function by multiplying certain coefficients for designing process given in (15).

$$J = \int_0^t (w_1 |e(t)| + w_2 u^2(t)) dt \quad (15)$$

Where, $|e(t)|$ is the absolute error signal, $u(t)$ is the control signal. In this study, the performance index given in (15) is used in the calculation of the fitness values or affinity evaluation in the optimization algorithms. While specifying the best controller parameters, following systematic process is carried out by optimization algorithms for all controllers. In the optimization algorithms, all controller parameters as given above are optimized.

PSO method is a population based stochastic optimization technique proposed in 1995 by Kennedy and Eberhart, who were inspired by social behavior of bird flocking or fish schooling [36]. The algorithm is very effective, easy and understandable to apply on the search of optimization process in large solution space. These specialties of it have made possible to apply in the various engineering area and especially control engineering [19], [21], [35].

According to the PSO algorithm, positions of particles, which represent the individual solutions, are updated regarding to their local best position and this leads to find global best position. After each iteration, global position and velocities of particles are renewed and stored as a global best position if the value is better than before.

The PSO algorithm works as follows by stepwise:

- Step 1. Initialize a population of particles with random position and velocity in d dimensions.
- Step 2. Calculate the fitness value ($p_{id}(k)$) for each particle,
- Step 3. If the current fitness value is better than the best fitness value ($pBest$), set current value as the new ($pBest$).
- Step 4. Choose the global best fitness value of all the best fitness values as the ($gBest$).
- Step 5. Calculate particle velocity according to:
$$v_{id}(k) = v_{id}(k-1) + \gamma_1 \times rand \times (pBest - x_{id}) + \gamma_2 \times rand \times (gBest - x_{id}),$$
- Step 6. Update particle position according to:
$$x_{id}(k) = x_{id}(k-1) + v_{id}(k).$$
- Step 7. Repeat the procedure from “Step 2” until the convergence or the number of maximum iterations.

Where, id is particle index, k is discrete time index, $rand$ is a random number between (0, 1), γ_1 and γ_2 are learning factors defined usually as, $\gamma_1 = \gamma_2 = 2$.

In this study, another optimization method known as Artificial Immune System (AIS) is used for the optimization of the controller parameters. This method is originally based on the immune system of the vertebrates that immune system cells such as B and T , response to foreign matters, which are called antigens (Ag) to protect body. In this process, once antigens include the body, they are matched with the existing memory antibodies (Ab). The search process continues until the stopping criterion is reached. The stopping criterion is taken to reach the number of maximum iteration or exact matching between Ag and Ab . AIS usage as an optimization algorithm could be thought as a new area for control engineering. This type of algorithm is generally used in classification problems but recently, the application to optimization problem is frequently used, as well [37]-[39].

The AIS optimization algorithm works as follows by stepwise:

- Step 1. Initializations; generate a set of random population of individuals (P), composed of the subset of memory cells (M) added to the remaining population (Pr), considering of the equation $P = Pr + M$.
- Step 2. Affinity evaluation; determine the n best individuals P_n of the population P set, based on an affinity measure.
- Step 3. Clonal selection and expansion; the best n individuals are cloned and a temporary clone population (C) is produced. The number of clones is proportional to the affinity.
- Step 4. Affinity maturation; apply a hyper mutation method to the clone population (C^* : mutated population).
- Step 5. Metadynamics; re-select the improved individuals from the mutated population (C^*). Some members of the P set can be replaced by other improved members of C^* , replace d low affinity antibodies of the population, maintaining its diversity.
- Step 6. Repeat the procedure from “Step 2” until a certain stopping criterion is met.

The same procedure is applied in order to obtain the best parameters for all controllers. All parameters' upper-lower boundaries are specified as in the range of [+5, -5] and optimization algorithms are started to acquire best solution set for the controllers. Iteration numbers of optimization algorithms are set as 100. The optimal controller coefficients obtained with the PSO and AIS algorithms are given in the Table II for PID and FOPID controller and the Table III for V-FOPID controller.

TABLE II. PSO OR AIS OPTIMIZED PID AND FOPID PARAMETERS

Controller	K_p	K_i	K_d	μ	λ
PSO PID	0.9695	0.8125	0.4269	-	-
PSO FOPID	1.4228	0.5923	0.2693	1.2296	1.4655
AIS PID	0.8662	0.8076	0.4701	-	-
AIS FOPID	0.3915	1.4602	0.4268	1.0366	0.4238

V. EXPERIMENTAL RESULTS

AVR terminal voltage stabilization is targeted even in the presence of disturbance or parameter uncertainties for the modelled parts. For this purpose, PID, V-PID, FOPID and the proposed new type V-FOPID controllers are used to show results. As an example using the AVR parameters given in Table 1, Fig. 3 reveals the four types of controller response under the same conditions of which parameters are designed with PSO techniques.

Similarly, Fig. 4 shows the same controller response but that was designed with AIS algorithm.

Fig. 5 and Fig. 6 shows the FOPID and V-FOPID controllers effects when the amplifier gain and time constant are changed from the actual value $K_a=10, \tau_a=0.1$ to $K_a=14, \tau_a=0.07$. With similar thoughts, the same parameter uncertainty cases are considered for the exciter and generator models; changing from actual value $K_e=1.0, \tau_e=0.4$ to $K_e=1.2, \tau_e=0.5$ (response of the controller as shown in Fig. 7 and Fig. 8) and generator model parameters are distorted as $K_g=0.7, \tau_g=1.6$ from the real value $K_g=1.0, \tau_g=1.0$ (response of the controller as shown in Fig. 9 and Fig. 10).

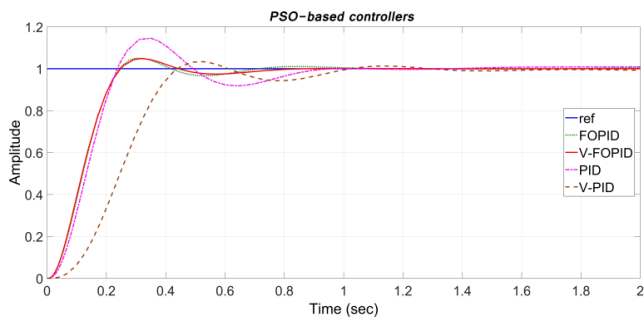


Fig. 3. Output Curves for All PSO-based Controllers.

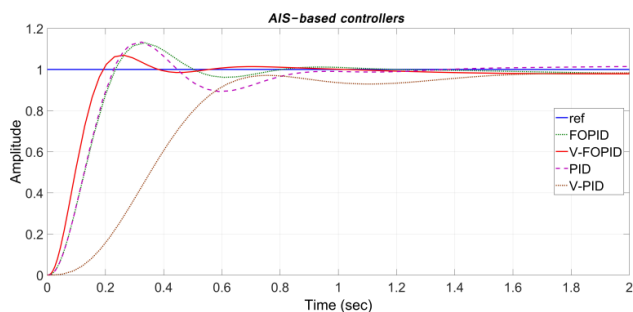


Fig. 4. Output Curves for All AIS-based Controllers.

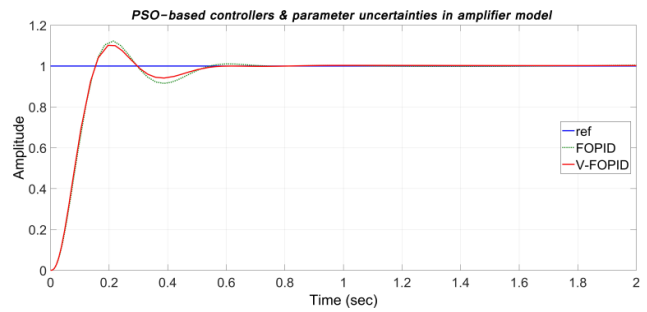


Fig. 5. PSO-based Output Curves in the Presence of Amplifier Uncertainties.

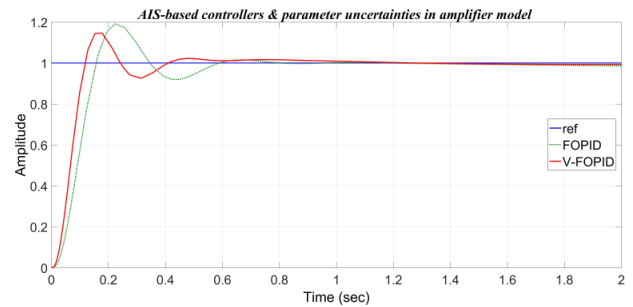


Fig. 6. AIS-Based Output Curves Existing Amplifier Uncertainty.

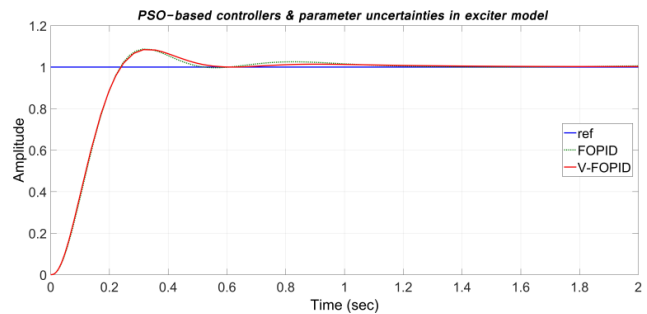


Fig. 7. PSO-Based Output Curves Existing Exciter Uncertainties.

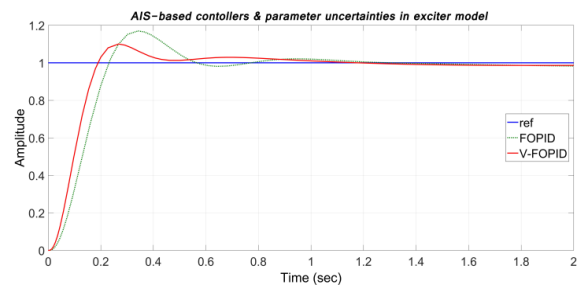


Fig. 8. AIS-Based Output Curves Existing Exciter Uncertainties.

Parameter changes in the generator model means the change of load conditions. In addition to these figures, Table IV and Table V point out the output characteristics of the control systems such as rise time (t_r), settling time (t_s), maximum overshoot (M_p), steady state error (ess). The others are the performance criteria, IAE , ISE and J which are referred above for PSO and AIS optimizer based controller, respectively.

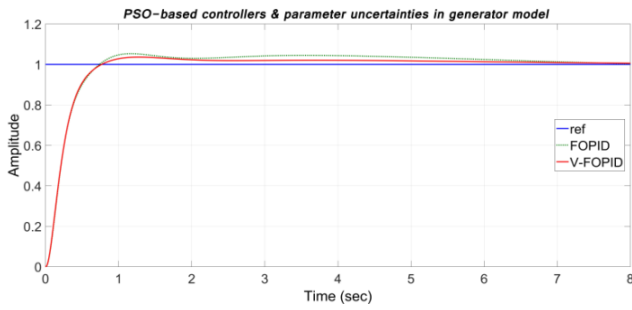


Fig. 9. PSO-Based Output Curves Existing Generator Uncertainties.

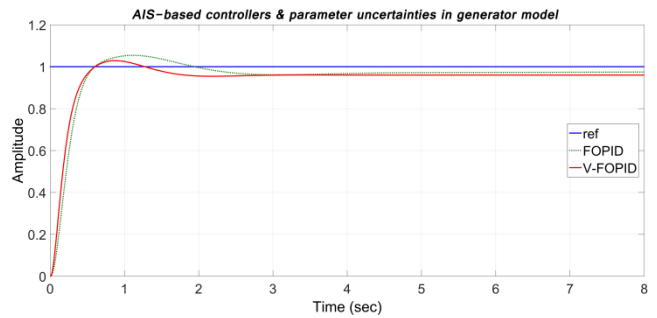


Fig. 10. AIS-Based Output Curves Existing Generator Uncertainties.

TABLE III. PSO OR AIS OPTIMIZED V-FOPID PARAMETERS

PSO / AIS Optimized Controller	K_p'		K_i'		K_d'		μ	λ
	c_1	c_2	c_3	c_4	c_5	c_6		
PSO V-FOPID	0.6157	1.3485	1.1132	-0.5134	0.5123	0.2872	1.2152	-1.2672
AIS V-FOPID	0.8403	1.1605	1.2686	-0.7165	0.4873	0.3147	1.3000	-0.0366

TABLE IV. OUTPUT CHARACTERISTICS OF PSO-BASED CONTROLLERS

Cases	Control	IAE	ISE	J	M_p	e_{ss}	t_r	t_s
AVR Initial Parameters	FOPID	0.1486	0.1006	0.1711	1.0499	-0.004692	0.1884	0.6424
	V-FOPID	0.1440	0.09888	0.1687	1.0486	-0.000625	0.1892	0.6530
Changing AVR Amplifier Parameter	FOPID	0.1202	0.07493	0.1437	1.1224	-0.00403	0.1173	0.5099
	V-FOPID	0.1135	0.07265	0.1392	1.1014	-0.002316	0.1176	0.5011
Changing AVR Exciter Parameter	FOPID	0.1582	0.1023	0.1806	1.0868	-0.005515	0.1845	0.4501
	V-FOPID	0.1565	0.1006	0.1812	1.0841	-0.002698	0.1855	0.4869
Changing AVR Generator Parameter	FOPID	0.4854	0.1793	0.5068	1.0530	-0.003767	0.5545	6.0354
	V-FOPID	0.3854	0.1717	0.4092	1.0361	-0.005858	0.5504	1.8210

TABLE V. OUTPUT CHARACTERISTICS OF AIS-BASED CONTROLLERS

Cases	Control	IAE	ISE	J	M_p	e_{ss}	t_r	t_s
AVR Initial Parameters	FOPID	0.1765	0.1084	0.1895	1.1296	0.01822	0.1771	1.1646
	V-FOPID	0.1361	0.08267	0.1950	1.0694	0.02147	0.1425	1.0621
Changing AVR Amplifier Parameter	FOPID	0.1427	0.0826	0.1564	1.1915	0.01332	0.1193	0.7579
	V-FOPID	0.1083	0.06162	0.1709	1.1463	0.006767	0.0901	0.8831
Changing AVR Exciter Parameter	FOPID	0.1869	0.1115	0.1999	1.1701	0.01713	0.1754	1.2485
	V-FOPID	0.1452	0.08444	0.2042	1.1003	0.01377	0.1434	1.0688
Changing AVR Generator Parameter	FOPID	0.4683	0.1804	0.4806	1.0541	0.02544	0.4050	2.2026
	V-FOPID	0.4857	0.1499	0.5419	1.0290	0.03991	0.3664	1.4914

VI. CONCLUSIONS

In this study the effect of the different controllers on the AVR plant has been investigated. The AVR system is an important and challenging plant that is frequently used in control engineering applications and it is needed to adjust the terminal voltage. The problems with this plant are the uncertainty of parameters and instability of the terminal voltage. In order to provide a stable control, a controller has to ensure the desired terminal voltage and must be robust despite the changes on the parameters. With regard to this purpose, it is designed with different type of controllers. The fractional controllers which are highly popular in recent years have been compared to the classical ones. Furthermore, a new type of fractional controller scheme (V-FOPID) has been proposed to get a worthy solution to the problem in the study. The comparison between the new type controller and other conventional controllers are given to demonstrate their effects on the AVR plant. In order to show the superiority of the proposed V-FOPID controller, similar design procedure is carried out for all mentioned controllers. To get optimal parameters of controllers, heuristic optimization techniques are employed considering the multi-objective performance function (J).

Consequently two noticeable results have been obtained. First of all, the results prove that proposed V-FOPID controller gives better results according to the PID, V-PID and FOPID ones. Also, the idea behind the improvement of a transient state response of a system without affecting the steady state response has worked successfully. In order to achieve this, changing parameters of the V-FOPID controller are given in Fig. 11. Secondly, better parameter set has been obtained by PSO algorithm. When the performance measurements (J) are examined in Table III and Table IV, it is seen that the PSO method is more effective than the AIS method in the optimization of such systems.

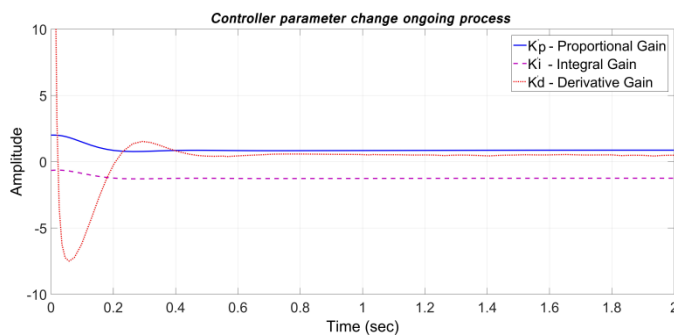


Fig. 11. Parameter Changes of PSO-Based Controllers During the Experiment.

REFERENCES

- [1] K.J. Åström, and T. Hägglund, Advanced PID control, ISA-The Instrumentation, Systems and Automation Society, 2006, ch. 6.
- [2] F. Ronilaya, and H. Miyauchi, "A new implementation of PID-type fuzzy controller for a battery grid-supporting inverter in an autonomous distributed variable-speed wind turbine", IEEJ Transactions on Electrical and Electronic Engineering, vol. 10(2), pp. 134-143, 2015.
- [3] I. Pdlubny, Fractional order systems and $PI^{\alpha}D^{\beta}$ controllers", IEEE Trans. Automatic Control, vol. 44(1), pp. 208-214, 1999.
- [4] I. Podlubny, Fractional differential equations, Acad. Press, London, 1999, ch. 9.
- [5] K. Oldham, and J. Spanier, The fractional calculus theory and applications of differentiation and integration to arbitrary order, Elsevier Science, vol. 111, 1974.
- [6] A. Oustaloup, La commande CRONE: commande robuste d'ordre non entiere, Paris : Hermès, 1991.
- [7] Z. Li, L. Liu, S. Dehghan, Y. Chen, and D. Xue, "A review and evaluation of numerical tools for fractional calculus and fractional order controls", International Journal of Control, vol. 90, no. 6, pp. 1165-1181, 2017.
- [8] K.S. Miller, and B. Ross, An introduction to the fractional calculus and fractional differential equations, Wiley-Interscience, 1993.
- [9] M. Caputo, Elasticità e dissipazione. Zanichelli, Bologna, 1969.
- [10] M. Caputo, and F. Mainardi, A new dissipation model based on memory mechanis, Pure and Applied Geophysics, vol. 91, pp. 134-147, 1971.
- [11] R.L. Magin, Fractional calculus in bioengineering, Redding: Begell House, 2006, pp. 269-355.
- [12] S. Manabe, "The non-integer integral and its application to control systems", Mitsubishi Denki laboratory reports, 1961, vol. 2.
- [13] L. Du, N. Ning, J. Zhang, Q. Yu, and Y. Liu, "Self-calibrated SAR ADC based on split capacitor DAC without the use of fractional-value capacitor", IEEJ Transactions on Electrical and Electronic Engineering, vol. 8, pp. 408-414, 2013.
- [14] Y. Luo, and Y. Chen, "Fractional order Proportional Derivative controller for a class of fractional order systems", Automatica, vol. 45, no. 10, pp. 2446-2450, 2009.
- [15] Y. Luo, Y.Q. Chen, C.Y. Wang, and Y.G. Pi, "Tuning fractional order Proportional Integral controllers for fractional order systems", Journal of Process Control, vol. 20, no. 7, pp. 823-831, 2010.
- [16] Y. Luo, Y. Chen, and Y. Pi, "Experimental study of fractional order Proportional Derivative controller synthesis for fractional order systems", Mechatronics, vol. 21, no. 1, pp. 204-214, 2011.
- [17] Z.L. Gaing, "A particle swarm optimization approach for optimum design of PID controller in AVR system", IEEE transactions on energy conversion, vol. 19, no. 2, pp. 384-391, 2004.
- [18] Y. Tang, M. Cui, C. Hua, L. Li, Y. Yang, "Optimum design of fractional order $PI^{\alpha}D^{\beta}$ controller for AVR system using chaotic ant swarm", Expert Systems with Applications, vol. 39, no. 8, pp. 6887-6896, 2012.
- [19] M. Zamani, M. Karimi-Ghartemani, N. Sadati, and M. Pamiani, "Design of a fractional order PID controller for an AVR using particle swarm optimization", Control Engineering Practice, vol. 17, no. 12, pp. 1380-1387, 2009.
- [20] H. Senberber, and A. Bagis, "Fractional PID controller design for fractional order systems using ABC algorithm", in Proc. (IEEE Electronics) 21st International Conference on ELECTRONICS, Lithuania , 2017, pp. 1-7.

- [21] N.R. Raju, and P.L. Reddy, "Robustness Study of Fractional Order PID Controller Optimized by Particle Swarm Optimization in AVR System", *International Journal of Electrical and Computer Engineering*, vol. 6, no. 5, p. 2033-2038, 2016.
- [22] M. Korkmaz, and O. Aydogdu, "Fractional Order Controller Design for Ball and Beam System", *Trans Tech Publications, Applied Mechanics and Materials*, vol. 313, pp. 544-548, 2013.
- [23] S. Das, I. Pan, S. Das, and A. Gupta, "A novel fractional order fuzzy PID controller and its optimal time domain tuning based on integral performance indices", *Engineering Applications of Artificial Intelligence*, vol. 25, no. 2, pp. 430-442, 2012.
- [24] J.J. Gu, Y.J. Zhang, and D.M. Gao, "Application of nonlinear PID controller in main steam temperature control", In *2009 Proc. APPEEC conf.*, pp. 1-5.
- [25] Y. Jiang, H.Y. Gao, S.P. Yu, and X.C. Luan, "Optimal genetic algorithm for the nonlinear PID controller", in *Proc. IEEE International Conference on Machine Learning and Cybernetics, 2007*, vol. 2, pp. 1014-1017.
- [26] M. Korkmaz, O. Aydogdu, and H. Dogan, "Design and performance comparison of variable parameter nonlinear PID controller and genetic algorithm based PID controller", in *Proc. IEEE International Symposium on Innovations in Intelligent Systems and Applications (INISTA), 2012*, pp. 1-5.
- [27] A.A.S. Ibrahim, "Nonlinear PID controller design using fuzzy logic", in *Proc. IEEE 11th Mediterranean Electrotechnical Conference (MELECON), 2002*, pp. 595-599.
- [28] A.J. Calderón, B.M. Vinagre, and V. Feliu, "Fractional order control strategies for power electronic buck converters", *Signal Processing*, vol. 86, no. 10, pp. 2803-2819, 2006.
- [29] D. Valério, and J.S. Da Costa, "Introduction to single-input, single-output fractional control", *IET control theory & applications*, vol. 5, no. 8, pp. 1033-1057, 2011.
- [30] C. Yeroglu, and N. Tan, "Note on fractional-order proportional-integral-differential controller design", *IET control theory & applications*, vol. 5(17), pp. 1978-1989, Nov. 2011.
- [31] A. Oustaloup, *La robustesse, analyse et synthèse de commandes robustes*, Paris : Hermès, 1994, pp.150-102.
- [32] A. Oustaloup, F. Levron, B. Mathieu, and F.M. Nanot, "Frequency-band complex noninteger differentiator: characterization and synthesis", *IEEE Transactions on Circuits and Systems I: Fundamental Theory and Applications*, vol. 47, no. 1, pp. 25-39, 2000.
- [33] B.M. Vinagre, I. Podlubny, A. Hernandez, and V. Feliu, "Some approximations of fractional order operators used in control theory and applications", *Fractional calculus and applied analysis*, vol. 3, no. 3, pp. 231-248, 2000.
- [34] A. Mandal, H. Zafar, P. Ghosh, S. Das, and A. Abraham, "An efficient memetic algorithm for parameter tuning of PID controller in AVR system", in *Proc. 11th International Conference on Hybrid Intelligent Systems, 2011*, pp. 265-270.
- [35] S. Panda, B.K. Sahu, and P.K. Mohanty, "Design and performance analysis of PID controller for an automatic voltage regulator system using simplified particle swarm optimization", *Journal of the Franklin Institute*, vol. 349, no. 8, pp. 2609-2625, 2012.
- [36] R. Kennedy, and J. Eberhart, "Particle swarm optimization", in *Proc. IEEE International Conference on Neural Networks IV, 1995*, pp. 1942-1948.
- [37] L.N. De Castro, and J. Timmis, *Artificial immune systems: a new computational intelligence approach*, Springer-Verlag, 2002.
- [38] R. Li, W. Zhan, and Z. Hao, "Artificial Immune Particle Swarm Optimization Algorithm Based on Clonal Selection", *Boletín Técnico*, vol. 55, no. 1, pp.158-164, 2017.
- [39] R. Syahputra, and I. Soesanti, "Power System Stabilizer Model Using Artificial Immune System for Power System Controlling", *International Journal of Applied Engineering Research*, vol. 11, no. 18, pp. 9269-9278, 2016.

Speaker Identification based on Hybrid Feature Extraction Techniques

Feras E. Abualadas¹

Computer Science
International Islamic University Malaysia
Ajloun National University, Jerash, Jordan

Akram M. Zeki²

Kulliyah of Information and Communication Technology
International Islamic University Malaysia
Kuala Lumpur, Malaysia

Muzhir Shaban Al-Ani³

College of Science and Technology- Computer Science
University of Human Development
Sulaymaniyah-KRG, Iraq

Az-Eddine Messikh⁴

Kulliyah of Information and Communication Technology
International Islamic University Malaysia
Kuala Lumpur, Malaysia

Abstract—One of the most exciting areas of signal processing is speech processing; speech contains many features or characteristics that can discriminate the identity of the person. The human voice is considered one of the important biometric characteristics that can be used for person identification. This work is concerned with studying the effect of appropriate extracted features from various levels of discrete wavelet transformation (DWT) and the concatenation of two techniques (discrete wavelet and curvelet transform) and study the effect of reducing the number of features by using principal component analysis (PCA) on speaker identification. Backpropagation (BP) neural network was also introduced as a classifier.

Keywords—*Speaker identification; biometrics; speaker verification; speaker recognition; text-independent; text-dependent*

I. INTRODUCTION

A biometric system is considered one of the most important patterns recognition that authenticates a person based on features extracted from physiological or behavioral characteristics [1].

Biometric identification method is preferred in comparison with conventional identification methods that contain passwords for different reasons; the speaker to be identified is needed to be physically present at the point-of-identification [2]. The identification based on biometric techniques does not require to carry a token, a smartcard and remember a password [3].

Human voice is one of the biological characteristics used to distinguish a person from his/her voice, thus we indicate to voice recognition systems [4]. Speaker recognition system is a process that used individuals sound to recognize/discriminate purposes, where it differs from speech recognition since it is concerned with the identity of a person while speech recognition is concerned with recognizing the word [4].

Speaker recognition systems have many applications for security purpose such as keys or passwords and database access [5].

Automatic Speaker recognition can be divided basically into two types: speaker identification (SI) and speaker verification (SV) [5].

Speaker verification is the task of verifying the identity of speakers based on information that contains in the speech signal to make sure that the person is the one who claimed [6]. Basic structure related to the speaker verification as shown in (Fig. 1).

On the other hand, speaker identification refer to the task that is interested in finding identity of the anonymous speakers by one-to-many (1: n) comparisons, where the speaker's voice is compared to the voice of speakers listed in a database, in which basic structure is concerned with speaker identification as explained in (Fig. 2). While in speaker verification the comparison is one-to-one (1:1) and a person is authenticated if it is the one who claims to be [7].

Speaker recognition system can be a text-independent and text-dependent system, depending on the speech used by a system. Text dependent systems are those systems that have prior knowledge of the text to be spoken where the same text is used in (training, testing) phase [8].

While in a text-independent system, recognition system does not possess previous knowledge concerned with spoken text (the text system is unconditional with the used text) [9].

This work concerns on the problem of speaker identification; we proposed a speaker identification system, which deals with defining the speaker's identity based on features extraction (discrete wavelet transformation and curvelet) including principal component analysis (PCA). For speaker identification, various recognizers can be used such as Hidden Markov Models (HMM), Random Forest (RF), Self-Organizing Map (SOM), statistical approaches, etc. In this research Backpropagation (BP) neural network is used as a classifier.

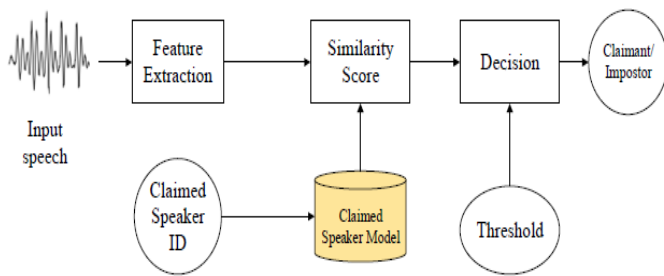


Fig. 1. The basic Structure Related to Speaker Verification.

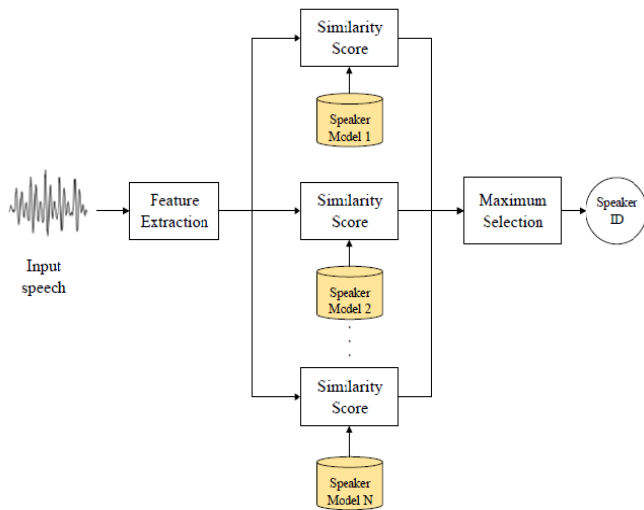


Fig. 2. The basic Structure Related to Speaker Identification.

The rest of the paper is organized as: the next section describes some of the researches in the last few years related to speaker recognition. In Section 3 presents the design and implementation of the developed system. Section 4 presents the result for speaker identification. Finally, paper concludes in Section 5.

II. RELATED WORK

There have been many studies and researches on speaker recognition, where some strategies have been suggested in the last few years.

For speaker recognition systems, these techniques can achieve high performances. Generally, some of these researches were summarized below with different techniques.

They presented a feature extraction method that depends on wavelet analysis for speaker identification system (SIS). Two Techniques combined with each other (Stationary Wavelet Transform (SWT) and Mel-Frequency Cepstral Coefficient) are used to overcome the discrete wavelet Transform drawbacks, these features are used as an input for a classifier, the data set consists of 200 speakers, where K-nearest neighbors (Knn) are used as a classifier. The experimental result showed that suggestion approach achieved better performance rate by using (SWT), where the drawbacks of DWT reduced [10].

They study a speaker identification system, where two systems designed and compared in terms of (computational

time and gender and identification rate). A Mel-frequency Cepstral Coefficients (MFCC) and bark frequency Cepstral coefficient (BFCC) as feature extraction are used with Gaussian Mixture Model (GMM), where the impact of filter coefficients number and speaker number are investigated. The experimental results showed that when the number of speaker and coefficient are increased the time of computational increases and the results show that use of MFCC with GMM is better than GMM based on BFCC [11].

They compared different features for text-dependent speaker recognition, where they used wavelet transforms under stressed condition; these conditions have been adopted from SUSAS database, Question, Neutral, Lombard and Anger. Vector quantization is used as a classification method with wavelet. Experimental results showed that Linear Predictive Cepstral Coefficients (LPCC) provide the best result among many features such as, Linear Frequency Cepstral Coefficients (LFCC), ARC, Log Area Ratio (LAR), CEP and Male Frequency Cepstral Coefficients (MFCC), where the improvement achieved in Neutral and Lombard case to 93% and 94% [12].

They study a Linear Predictive Cepstral Coefficients (LPCC) and Mel-frequency Cepstral Coefficient (MFCC) methods independently for speaker identification system and proposed a new feature based on the concatenation Linear Predictive Cepstral Coefficients and Mel-frequency Cepstral Coefficient (LMACC), where each of them recorded in clean and noisy environment based on multi-layer perceptron (MLP) neural network as classifier. The experimental result showed that concatenation of both features LMACC-MLP achieved height performance recognition rate in comparative with each method independently reach to 85% [13].

Authors have presented an approach for speaker identification based on fusion via samples and statistical approach. The data set collected by recorded from 20 male speakers of 5 samples each of 7 words, these samples are passing through a preprocessing phase which includes resizing, noise removal and windowing to be adequate for processing. Features vectors defined each speaker was generated by employing a statistical approach after principal component analysis (PCA) for feature extraction is used for performance evaluation. Features vector was partitioned into overlapping segments of feature vectors, where the percentage of the correct identified segments over all tested segment was used to calculate the performance. The Experimental results showed that this approach obtained a good result of recognition reaching 95% similarity [14]. developed a model for a text-independent speaker identification to obtain a features vector without losing information based on Mel Frequency Cepstral Coefficients (MFCC) with Vector Quantization (VQ), for speaker recognition a Gaussian Mixture Model (GMM) is adopted. To increase the efficiency of feature extraction the signal is passing through the preprocessing phase, which includes Pre-emphasis, silence removal and downsampling. To reduce the number of speaker during a test stage, gender detection algorithm is used. Experimental results show that the suggested algorithm reduced the time testing to almost half 0.10 51sec and gives 91% accuracy in comparison with VQ and GMM gives 88% and take 0.2242sec [15].

They presented an automatic speaker identification system (SID) based on Gaussian Mixture Model and Support Vector Machines (GMM-SVM), where data set consist of 360 speakers. Each one has 10 sentences adopted from TIMIT phone labeled database corpus. The extracted Features, Mean Hilbert Envelope Coefficients (MHEC) and Gammatone Frequency Cepstral Coefficients (GFCC) are modeled by Gaussian Mixture Model (GMM). Support Vector Machine (SVM) was used to train the corresponding super vectors. Experimental results showed that MHEC features are better in comparison with RASTA-MFCC and GFCC features in different noisy conditions [16].

Authors have used Mel Frequency Cepstral Coefficient (MFCC) as a feature extraction technique to study the performance of speaker recognition system in noisy environments, where noise is considered as one of the factors that affect the sound of a person. Three different techniques Back-Propagation Neural Network (BPNN), Euclidean distance and Self Organizing Map (SOM) are used as classifiers with different windowing, Hamming window, and Blackman window. Experimental results showed that SOM gives better performance in comparison with BPNN and Euclidean distance [17].

They study and compare different techniques for feature extraction and feature classification to get an optimal choice for automatic speaker recognition system (ASR). The experimental result showed that Mel frequency cepstral coefficients (MFCC) are preferred in comparison with Linear Predictive Cepstral Coefficients (LPCC), Linear Predictive Coefficients (LPC) and Wavelet decomposition techniques and Gaussian Mixture Model (GMM) gives better accuracy and less memory usage for feature classification in comparison with Vector Quantization (VQ), Dynamic Time Warping (DTW) and Hidden Markov Model (HMM) techniques [18].

Authors have presented a method based on Mel-Frequency Cepstral Coefficients (MFCCs) and Discrete Wavelet Transform (DWT) to design a speaker identification system that minimizes the probability of identification errors. For noisy speech signals (MFCC) based feature extraction with additive white Gaussian noise (AWGN), and to enhance the representation of signal features extracted from DWT vector synthesized features in MFCC. Vector Quantization using the Linde-Buzo-Gray (VQLBG) with MFCC is used to enhance the MFCC performances and to recognize the noisy speech. Experimental results showed that the proposed technique in comparison with MFCC gives a better performance where the use of DWT of degraded signal obtains more features and reduces the noise effect when dealing with signals like AWGN, this leads to higher identification rates and improves the recognition rate [19].

They Developed an automatic speaker recognition based on discrete wavelet transformation (DWT) for feature extraction with Back Propagation Network as classifier, where features extracted from approximation and detailed coefficients. Experimental results showed that wavelet is Appropriated for feature extraction where Discrete Meyer wavelet provides higher inter-class variance and lesser intra-class variance in

comparison with various wavelets such as Haar, Symlet and Reverse Biorthogonal [20].

Feature extraction technique Mel Frequency Cepstral Coefficient (MFCC), Dynamic Mel-Frequency Cepstral Coefficient (DMFCC) and the Plural between these two features are used to evaluate the performance of text-independent, multilingual speaker identification using Gaussian Mixture Model (GMM) as a classifier. The data set created consists of 120 speakers; each one has five sessions recorded for 20 seconds with a 16 KHz sampling rate using Gold Wave software in English and Tamil languages. The system performance was tested using a different length of segment. The experimental result showed that combination between DMFCC and MFCC features achieved better performance rate in comparison with using each one individually, where the Error Rate obtained for MFCC, DMFCC and (MFCC+ DMFCC) is 5.8%, 2.9% and 1.2% with MFCC respectively [21].

The effect of combining the features extracted from Mel-Frequency Cepstral Coefficients (MFCC) and Linear Predictive Cepstral Coefficients (LPCC) in comparison with using features individually for speaker identification system in case of cross, mono and multilingual. To do that, data of 30 speakers were created. Each one recorded his/her voice in three different languages (English, Hindi, and Canada) languages. The number of speakers identified by MFCC is 18 and 20 speakers by LPC while the number of speakers with a combination of features (MFCC and LPC) is 22. This concludes that using MFCC and LPC features combined instead of using (one at a time) improves the speaker identification performance about 30% for created dataset [22].

This work concerns with sound recognition techniques to identify individuals speakers. Each human has a singular feature in his sound; it is helpful to distinguish between person and another one using their own sound. The concept of voice recognition that is completely unlike speech recognition is to identify the person speaker versus a store sound pattern, to not perceive what's being aforesaid. Within the domain of sound recognition, several ways are developed like Neural Network, Hidden Markov Models, Genetic algorithms and Fuzzy logic.

III. METHODOLOGY OF DEVELOPED SYSTEM

This research focuses on creating the speaker identification system and then assessing the system performance and capabilities in speaker recognizing area of research where Back Propagation Neural Network is used to develop the system.

The determination of individuals who speak is the main attribute of any speaker recognition system, where it consists of different modules in an addendum to the classification engine. In this research, we proposed a system that includes (4 Modules) and these Modules are depicted in Fig. 3.

First, the resulted voice after processing goes over to the feature extraction module to extract features that are used to construct the dataset, where the resulted features passed to selection module include principal analysis component (PCA).

Finally, the extracted features resulting from two modules (feature extraction & feature selection) will be passed to the

final module, which is the recognition module, with separated forms. The testing and training phases together compose the recognition module, where the system is used to discriminate a speaker sound after it trained.

The dataset (sounds) as an input, where these sounds will pass through sample resizing operation during preprocessing module because there is no ability to control the amount of sample sounds during the recording process, wherein this work the number of samples was resized to 40000.

After reading the sound file, discrete wavelet transformation utilized then each voice fed to the NN. The speaker recognition module is called after extracting features, where these features represent the (coefficients) of different DWT, where BP Neural Network was designed to use the features extracted from singly and combined to train the designed classifiers. Two various datasets were formed are involved: a dataset of discrete wavelet transformation (DWT) features only, and a dataset of (DWT + Curvelet). Fig. 4 shows the classification operation, where it consists of two phases mainly, (training and testing) phase.

Initially, a group of patterns that represent discrete wavelet coefficients that was extracted from three various levels of wavelet are used to train the classifier at the first time. To divide space of feature in a method that allows maximizing the ability of recognition for Neural Network. To build appropriate weight vectors that can classify the training set in correctly within defined some error rate. The trained classifier: that uses these weight vectors that result from training phase are used for appoint the unknown input pattern to one of the class (speaker) depending on the feature vector that was extracted.

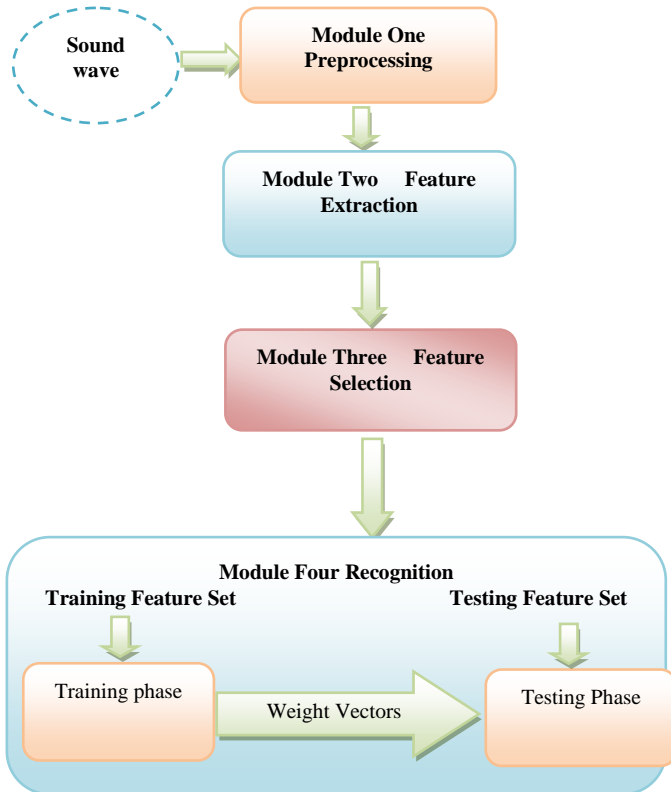


Fig. 3. Developed System Flow Control.

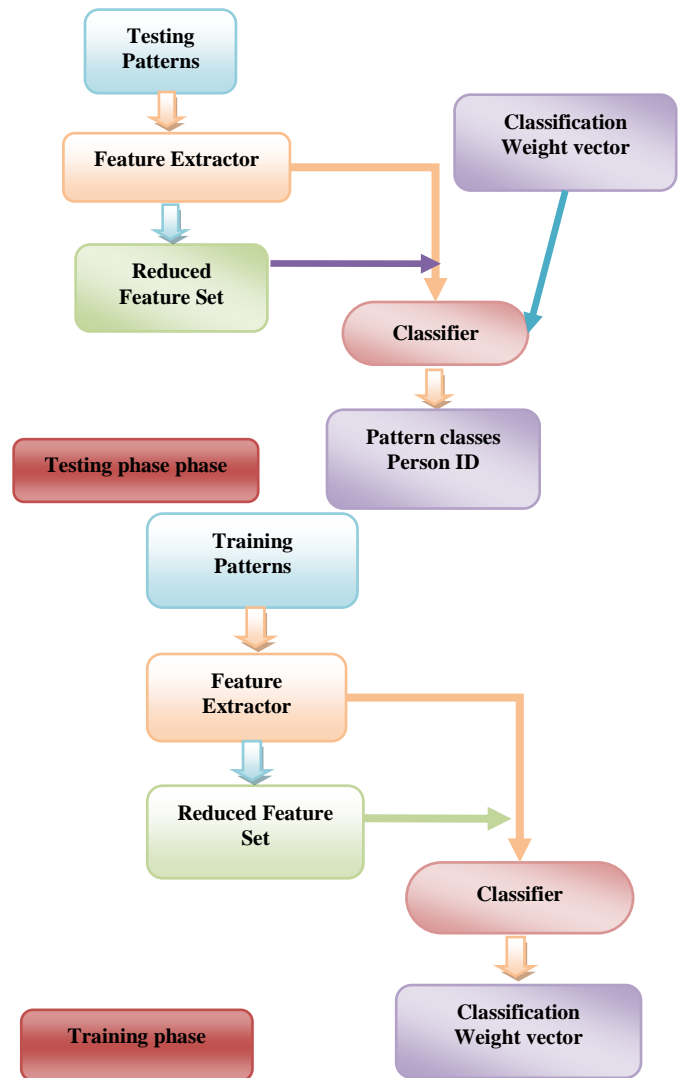


Fig. 4. Recognition System Phase.

IV. ASSESSMENT OF RESULTS

In this research, the dataset involves various sounds download from (<http://www.voxforge.org>) for fifty various persons (male and female), each one spoke ten various statements, where the dataset consists of 500 samples in total.

To minimize the loss of information in a signal speech, the parameters gaining from data must be chosen according to the speech signal nature to being processed. Signal of speech is used within this work, quantized with 16-bit quantization level and sampled with $F_s=8$ KHz.

For performance measurement of proposed system (use part of the data for training and whole it for testing, were the features that extracted from each level independently was used for training Neural Network that was suggested, to determine the level with best classification ability.

The accuracy of classification when a set of discrete wavelet coefficients extracted independently for different three wavelet levels that are used to train the BP NN is tabulated in Table I.

TABLE I. ACCURACY OF CLASSIFICATION FOR BP (DIFFERENT DISCRETE WAVELET LEVEL)

# of levels	Level 1	Level 2	Level 3
Testing accuracy	95	94	100

From Table I, it is inferred that level three achieved the best accuracy, where level one and level two shows acceptable discrimination ability. Fig. 5 shows the accuracy of classification for different discrete wavelet levels.

It is very necessary to study, the impact of concatenation (features extracted from various levels with other technique) to investigate if there is any impact on the classification ability in a form that can be positively or negatively done, where in this work curvelet transform is used with discrete wavelet transformation.

The accuracy of classification, in which the classifier can be trained over set of patterns, represent set of Discrete wavelet coefficients + curvelet), as shown in Table II.

From Table II, it is inferred that the accuracy was increased in level one and two when curvelet is concatenation with discrete wavelet transformation and gives the best classification accuracy, which is equal to the classification accuracy of level three. Fig. 6 shows the accuracy of classification when DWT and curvelet were combined.

The output of feature extraction has many features of which none is important for speaker discrimination, and the number of features should be also relatively low.

The process of feature selection is to select the best features that describe the speaker when dealing with hundreds of features that lead to increasing the workload of recognition. Selecting the best features set leads to reducing the classifier training time and as well as increasing the classification accuracy [23].

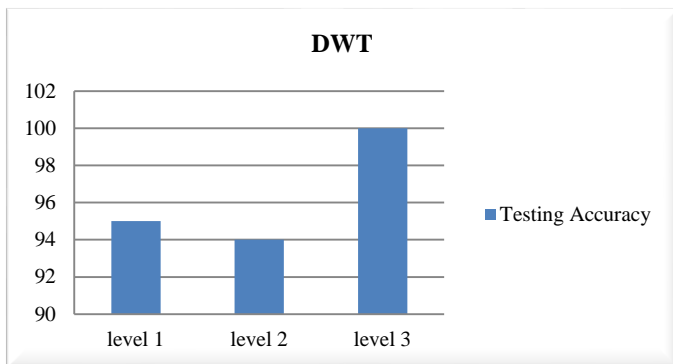


Fig. 5. Accuracy of Classification of different Discrete Wavelet Level.

TABLE II. ACCURACY OF CLASSIFICATION USING (FEATURES EXTRACTED FROM CONCATENATION DWT AND CURVELET)

# of levels	Level 1	Level 2	Level 3
Testing accuracy	100	100	100

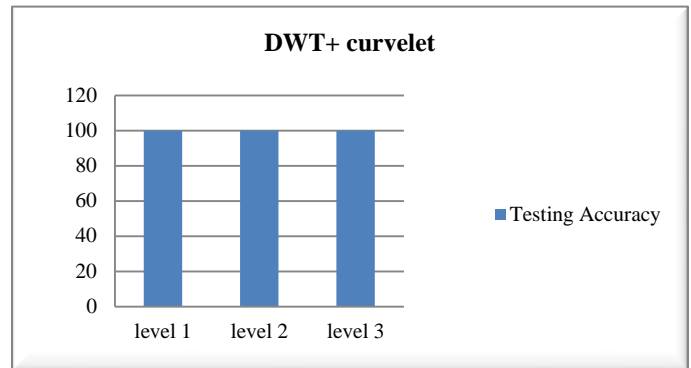


Fig. 6. Accuracy Classification of Combined different DWT Level with Curvelet.

The accuracy of classification using principal component analysis in addition to discrete wavelet + curvelet is shown in Tables III and IV.

From Tables III and IV, it is inferred that the accuracy was impacted positively and it is clear that reducing the features by using PCA did not affect the classification accuracy where the classification accuracy of level one and level two was increased to achieve the best classification and the accuracy of level three still 100%. Fig. 7 shows the accuracy of classification when PCA applied to DWT and (DWT + curvelet), respectively.

TABLE III. ACCURACY OF CLASSIFICATION USING PCA WITH (DWT + CURVELET)

# of levels	Level 1	Level 2	Level 3
Testing accuracy	100	100	100

TABLE IV. ACCURACY OF CLASSIFICATION USING PCA WITH DWT

# of levels	Level 1	Level 2	Level 3
Testing accuracy	100	100	100

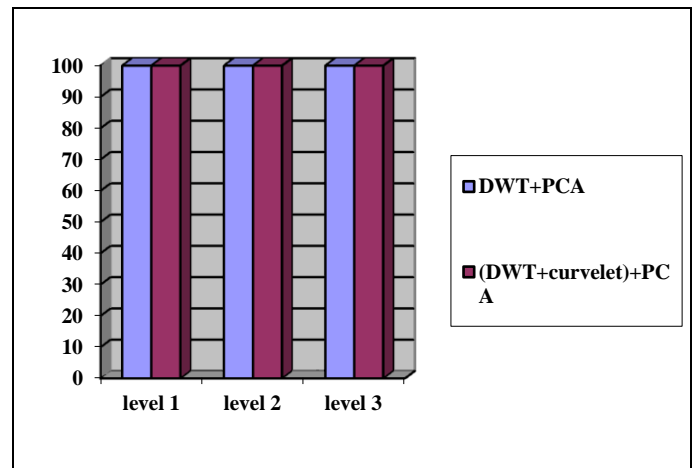


Fig. 7. The Accuracy of Classification of Applying PCA.

V. CONCLUSION

This paper concentrates on analyzing and studying the effect of using various levels of discrete wavelet transformation in addition to concatenation of different DWT level with curvelet technique to perform speaker identification. Also, the behaviors of classifier (Backpropagation Neural Network) were studied within the field of speaker recognition.

The practical results showed that level three of DWT gives the best accuracy where achieved to 100% and the accuracy was improved in level (1 and 2) when applying (DWT + curvelet).

In this approach, it is clear that introducing PCA with BP networks improved the accuracy. This approach is an effective method for speaker identification system, where it keeps the effective information and reduces the redundancy of characteristic parameters. Fig. 8 shows the effect of using different techniques of feature extraction using three different levels of discrete wavelet transformation.

Future work will focus on integrated some techniques with each other to increase the accuracy of speaker identification system such as DWT&LPC, LPC&MFCC were the development can be occurs in this stage that concentrated on reduces the number of features, removes irrelevant, noisy and redundant data, and results in acceptable recognition accuracy.

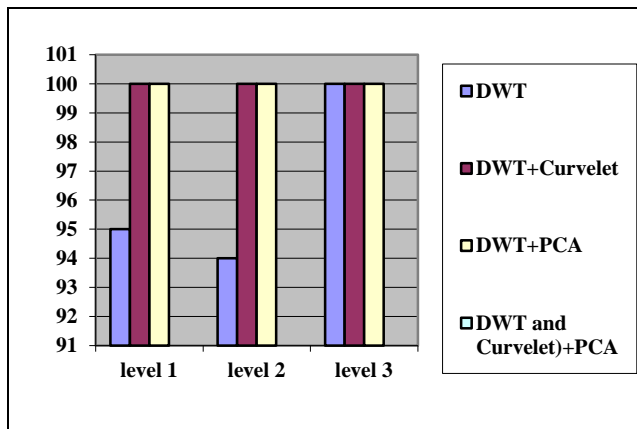


Fig. 8. Classification Accuracy of different Feature Extraction Technique.

REFERENCES

- [1] Prabhakar, S., S. Pankanti, and A.K. Jain, Biometric recognition: Security and privacy concerns. *IEEE security & privacy*, 2003. 99(2): p. 33-42.
- [2] Tripathi, K., A comparative study of biometric technologies with reference to human interface. *International Journal of Computer Applications*, 2011. 14(5): p. 10-15.
- [3] Woo, S.C., C.P. Lim, and R. Osman. Development of a speaker recognition system using wavelets and artificial neural networks. in 2001. *Proceedings of 2001 International Symposium on Intelligent Multimedia, Video and Speech Processing*, . 2001. IEEE.
- [4] Togneri, R. and D. Pulella, An overview of speaker identification: Accuracy and robustness issues. *IEEE Circuits and Systems Magazine*, 2011. 11(2): p. 23-61.

- [5] Shah, S.M. and S.N. Ahsan. Arabic speaker identification system using combination of DWT and LPC features. in 2014 International Conference on Open Source Systems and Technologies (ICOSST), 2014. IEEE.
- [6] Nemati, S. and M.E. Basiri, Text-independent speaker verification using ant colony optimization-based selected features. *Expert Systems with Applications*, 2011. 38(1): p. 620-630.
- [7] Powar, S.M. and V. Patil, Study of Speaker Verification Methods.
- [8] Singh, N. and R. Khan, Speaker Recognition and Fast Fourier Transform. *International Journal*, 2015. 5(7).
- [9] Gbadamosi, L., Text independent biometric speaker recognition system. *International Journal of Research in Computer Science*, 2013. 3(6): p. 9.
- [10] Sekkate, S., M. Khalil, and A. Adib. Fusing wavelet and short-term features for speaker identification in noisy environment. in, 2018 International Conference on Intelligent Systems and Computer Vision (ISCV). 2018. IEEE.
- [11] Kumar, C., et al. Analysis of MFCC and BFCC in a speaker identification system. in 2018 International Conference on Computing, Mathematics and Engineering Technologies (iCoMET), . 2018. IEEE.
- [12] Biswal, K.T. and J. Rout, Speaker Recognition System using Wavelet Transform under Stress Condition. *IJSEAT*, 2017. 4(12): p. 745-751.
- [13] Omar, N.M. and M. El-Hawary. Feature fusion techniques based training MLP for speaker identification system. in 2017 IEEE 30th Canadian Conference on Electrical and Computer Engineering (CCECE),. 2017. IEEE.
- [14] Al-Shayea, Q.K. and M.S. Al-Ani, Speaker Identification: A Novel Fusion Samples Approach. *International Journal of Computer Science and Information Security*, 2016. 14(7): p. 423.
- [15] AboElenein, N.M., et al. Improved text-independent speaker identification system for real time applications. in 2016 Fourth International Japan-Egypt Conference on Electronics, Communications and Computers (JEC-ECC),. 2016. IEEE.
- [16] Dhineshkumar, R., A.B. Ganesh, and S. Sasikala, Speaker identification system using gaussian mixture model and support vector machines (GMM-SVM) under noisy conditions. *Indian Journal of Science and Technology*, 2016. 9(19).
- [17] Sukhwal, A. and M. Kumar. Comparative study of different classifiers based speaker recognition system using modified MFCC for noisy environment. in 2015 International Conference on Green Computing and Internet of Things (ICGCIoT),. 2015. IEEE.
- [18] Kaur, K. and N. Jain, Feature Extraction and Classification for Automatic Speaker Recognition System-A Review. *International Journal of Advanced Research in Computer Science and Software Engineering*, 2015. 5.
- [19] Maged, H., A. AbouEl-Farag, and S. Mesbah. Improving speaker identification system using discrete wavelet transform and awgn. in 2014 5th IEEE International Conference on Software Engineering and Service Science (ICSESS), . 2014. IEEE.
- [20] Albin, A.J., N. Nandhitha, and S.E. Roslin. Text independent speaker recognition system using Back Propagation Network with wavelet features. in 2014 International Conference on Communications and Signal Processing (ICCSP). 2014. IEEE.
- [21] Nidhyanathan, S.S. and R.S.S. Kumari, Language and text-independent speaker identification system using GMM. *WSEAS Transactions on Signal Processing*, 2013. 9(4): p. 185-194.
- [22] Nagaraja, B. and H. Jayanna, Combination of Features for Multilingual Speaker Identification with the Constraint of Limited Data. *International Journal of Computer Applications*, 2013. 70(6): p. 1-6.
- [23] Srinivasan, V., V. Ramalingam, and V. Sellam, Classification of Normal and Pathological Voice using GA and SVM. *International Journal of Computer Applications*, 2012. 60(3): p. 34-39.

ATAM: Arabic Traffic Analysis Model for Twitter

Amani AlFarasani¹, Tahani AlHarthi², Sarah AlHumoud³

Computer Science Department, Al-Imam Mohammad Ibn Saud Islamic University (IMSIU)
Riyadh, Saudi

Abstract—Harvesting Twitter for insight and meaning in what is called sentiment analysis (SA) is a major trend stemming from computational linguistics and AI. Industry and academia are interested in maximizing efficiency while mining text to attain the most currently available data and crowdsourcing opinions. In this study, we present the ATAM model for traffic analysis using the data available on Twitter. The model comprises five components that start with data streaming and collection and ends with the road incident prediction through classification. The classification of data is done using a lexicon-based method. The predicted classes are as follows: safe, needs attention, dangerous, and neutral. The data were collected for three months in the city of Riyadh, Saudi Arabia. The model was applied on 10k tweets with an overall accuracy of the model classifying all four classes of 82%.

Keywords—Data mining; machine learning; sentiment analysis; unsupervised learning; lexicon-based; support vector machines

I. INTRODUCTION

The Kingdom of Saudi Arabia is one of the Gulf Cooperation Council (GCC) countries. It is divided into 13 regions; each region is divided into a number of governorates. Riyadh is the capital city of Saudi Arabia with a measured area of 1,554 km² [1] and a population of 6,505,509 [2].

According to statistics from the General Authority for Statistics in Kingdom of Saudi Arabia (GASTAT)¹, 242,851 driving licenses were issued in the Riyadh region in 2016. A total of 141,736 accidents occurred in the same year. Road conditions are to blame for many of the accidents in Riyadh city. Traffic jams, potholes, extreme weather conditions, gas explosions, and malfunctioning traffic lights contribute to the accidents. It is important for travelers to learn about these conditions before making a trip, to improve safety and driving efficiency. According to Internet World Stats statistics, the number of Internet users is over 4 billion, with more than 219 million of them being Arabic users. Also, in 2017, users who provided Arabic web content scored the fourth highest among all Internet users after English, Chinese, and Spanish. In 2018, more than 70% of the Saudi population used the Internet. That number is projected to increase.

Among all social media platforms, Twitter has relatively heavy usage in Saudi Arabia for expressing opinions, advertising, sharing photos, locating information, and discussing various topics. The number of active Twitter users in 2019 exceeded 50% of the total population². Harvesting

available data from Twitter to gain insight and transportation intelligence is a low-cost complementary solution to the infrastructure-based high-cost solutions [3], [4]. Gathering crowdsource opinion data from Twitter using the well-known methodology of Sentiment Analysis (SA) is cheaper and faster than other methods and covers a large number of users in real-time. It is better than using surveys and sensors in terms of cost and timeliness. SA applies supervised or unsupervised machine learning approaches and is implemented using one of the leading programming languages, such as Python or R, or other tools and environments, such as Orange and WEKA [5], [6].

With the high use of Twitter in the region and the raising concerns about road safety in the fast-growing city of Riyadh, Saudi Arabia, the ATAM project aims to provide a model for harvesting road conditions from Twitter. In addition, the lexicons needed to classify data are available upon request for reproducibility. The harvested data are analyzed using SA approaches to provide an instant glimpse of road conditions for drivers and road users. It could also help in instantaneously notifying authorities about road conditions that could result from weather damage or accidents that affect safety. The ATAM model consists of five components: data collection, data preparation, spam filtering, data annotation, and classification. In the next section, we provide background information with related works on SA in general, in the Arabic context, and in terms of traffic analysis. Then, in Section 3, we present the methodology. Section 4 presents the results and discussion. The conclusion of the work is then provided.

II. BACKGROUND AND RELATED WORK

Utilizing Twitter data to get instantaneous insights into traffic patterns could be done using SA techniques and methods.

A. Sentiment Analysis

SA is natural language processing (NLP) methodology used to analyze human opinions, emotions, attitudes, and sentiments. Its prominent growth has accompanied the high use of social media, providing vast amounts of data that are available in the public domain.

SA can be implemented using several approaches: Medhat et al. [7] explored these approaches and divided them into two main types. The first is based on machine learning, and the second is a lexicon-based approach. The lexicon-based approach is further divided into the dictionary-based and corpus-based approaches. A corpus-based approach can be statistical or semantic. The machine-learning approach is also divided into supervised learning and unsupervised learning. In the literature, [8, 9, 10, 11, 12] Arabic SA has been accomplished by the following three main steps:

¹ "The General Authority for Statistics": <https://www.stats.gov.sa/en>

² "Statista": <https://www.statista.com/statistics/284451/saudi-arabia-social-network-penetration/>

1) *Preprocessing*: After collecting data and before data classification, data need to be cleaned to remove noise. Preprocessing can be done by the following steps: First is data tokenization, which is an essential factor in understanding and manipulating data. This process aids in removing unrelated data, such as usernames and URLs. It also aids in fixing spelling and removing mistakenly repeated characters. This process also works to remove stop words or words that have no polarity significance in the sentences. Second is normalization; and it is a process to reduce the characters in each word to the minimum representable form and to modify multi-form words to a unified form. The former is done by removing diacritics, for example, and the latter is done by removing and replacing the characters that have more than one form to one of its forms [13].

2) *Features extraction*: This process comes after preprocessing, tokenization, and normalization. It mines features from data that can be used to categorize data entries to a class depending on its features [14]. Three types of features are mined [15]. First, morphological features and this consists of semantic, syntactic, or lexico-structural items. The second type is the frequent product feature, which is also referred to as hot features [16]. The third type is implicit features, which are not directly apparent.

3) *Classification*: Classification is the process of dividing and classifying data into two or more classes to facilitate and automate the understanding of data. In SA, data are mainly classified into positive and negative types. Data classification can be done, as stated earlier, using two approaches. First is the supervised learning approach, where data are divided into training data and testing data. Training data are annotated by a human expert labeling the data, which are provided to teach and train the classifier. Testing data are new data used to test and evaluate the performance of the classifier for accuracy. Second, is the unsupervised approach or the rule-based approach where data are classified according to the knowledge provided in labeled lexicons [17].

4) A plethora of researchers are interested in SA for publicly available data streams of social media, as summarized in Table I. Zhou et al. [18] collected a dataset containing 57,000 tweets in the form of 1,000 tweets split into 57 files. The data collection was done in two weeks on the topic of the Australian federal election in 2010. They distributed the data according to sentiment into three

categories: positive, negative, and neutral. Instead of using the “bag-of-words” traditional method, they opted to extract data that include sentiment or words that express a subjective opinion. Measured by category, 65.1% were positive tweets, 77.2% were negative, and 46.2% neutral. The authors were able to identify words with opinions using a rule-based approach with Wilson opinion lexicon [19]. They also measured the strength intensity of positive or negative opinions. They accomplished that using three modules: a feature selection module, which extracts the opinionated words from each sentence; a sentiment identification module, which associates expressed opinions with a relevant entity at each sentence level; and a sentiment aggregation and scoring module, which calculates the sentiment scores for each entity. The sentence intensity was divided into five classes: strong negative (SN), negative (N), neutral (Neu), positive (P), and strong positive (SP). The researchers used a primarily straightforward approach to SA; however, this approach needs to overcome some limitations in certain areas for it to reach its full potential. Some of these areas include distinguishing between parts of speech, taking emotion analysis into account, and utilizing more accurate entity recognition techniques. The authors claimed, “The TSAM model will yield much more accurate results with the above works implemented.” Although they presented the model and plotted the results, they did not provide accuracy data to validate and show the significance of the model.

An important part of SA is the readiness of the data collected, are which has a direct effect on the performance of the classifiers. This is described by Gokulakrishnan et al. [8], who focused on the preprocessing stage of SA, which includes the following steps: replacing emoticons, identifying uppercasing and lowercasing, extracting the URL, determining the punctuation, removing stop words and query terms, compressing words, and removing skewness in the dataset. The datasets collected included 17,000 tweets. The authors used three classifiers: neutral, polar, and irrelevant. They implemented more than one type of algorithm to classify the datasets and to compare them with each other’s performances. They noted that the sequential mining optimization algorithm (SMO) [20] had the best accuracy, where the positive measured 65.1%, the negative was 77.2%, and the neutral was 46.2%. When using the Synthetic Minority Oversampling Technique (SMOTE) [21], the average accuracy of SMO increased from 77.2% to 81.9%.

TABLE I. SENTIMENT ANALYSIS HIGHLIGHT IN ENGLISH LITERATURE

Paper	Context	Classifier	Data Size	Labels	accuracy
[18]	Australia	Lexicon-based SA	57,000	SN (Strong negative), N (Negative), Neu (Neutral), P (Positive) and SP (Strong Positive)	NA
[8]	Sri Lanka	Naïve Bayes, Random Forest, Support Vector Machines and Sequential mining optimization	17,000	Neutral, Polar (Positive/Negative) and Irrelevant	SMO 77.2%
[9]	South Korea	Knowledge generator, knowledge enhancer, and synonym binder	40,000	Positive, Negative and Neutral	accuracy was 55%.

Another work on precise classification was done by Batool et al. [9], proposed using Archivist, which is a service that uses Twitter API to find and archived tweets. Then they used Alchemy API, which utilizes NLP and machine-learning algorithms to analyze content. They collected a dataset of 40,000 tweets of different categories for testing and verification in 43 days. Then they divided these data depending on sentiment into three categories: positive, negative, and neutral. They used a knowledge-enhancer module, which adds additional knowledge that was not extracted as keywords by Alchemy API. Their accuracy score was 55%.

B. Arabic Sentiment Analysis

The Arabic language could be divided into three types [11]. First is classical Arabic, which is used in the Quran holy book and prayers. Second, is Modern Standard Arabic (MSA), which is used in formal contexts, such as in books, education, and news. The third is the Dialectal Arabic (DA), which is used informally in verbal communications and is used recently in written communication with the use of social media and short messages. These forms of the language result in lexical, morphological, and grammatical differences resulting in the difficulty of developing one Arabic NLP application to process data from the different varieties [22].

Besides, Arabic NLP applications face the challenge of encoding, which is the representation of the language symbols in computers, especially when representing the different shapes of the same letter or the diacritics. Unicode is the actual current standard for encoding a large number of language symbols including Arabic, such as the Arabic letter ك (U+0643) and the Persian ك (U+06A9) using the same shape ك, which adds confusion when the Arabic letter is written using a Persian keyboard [10] [23] [24] [11].

Another challenge to Arabic SA is the lack of gold-standard corpora, quality resources, accurate stemmers, and tools compared to English. For that, the research in Arabic NLP is still in its early stages, needing more resources and

efforts. This paper aims to provide a model to classify Arabic text in the traffic domain, contributing by enriching this field with the ATAM model.

In the following, we present the highlights of previous studies on Arabic SA, which are summarized in Table II. Ibrahim et al. [25] used ArSeLEX Lexicon with a collection of 5244 words. First, they used an AMIRA Part of Speech (POS) tag [26] to extract the words with a higher likelihood to be sentimental, such as adjectives, nouns, and verbs. Second, they removed redundant words. Then, each of the remaining words is translated, and all its synonyms are fetched. The output of the dataset was 300 positive, 2,829 negative, and 412 neutral terms. The Arabic variety was MSA and Arabic Egyptian dialect. The highest accuracy they reached using the SVM classifier measured 95%.

Khasawneh et al. [27] collected 1,500 Arabic comments and audio segments from the Twitter website. Then, the data were broken down according to news type into sports or economy. This was done using MSA analysis by manually constructing 13 dictionaries, 6 of which were for positive and negative Arabic text, 2 for audio files, 3 for positive or negative or neutral symbols, and 2 for special characters. The results were evaluated by using two machine-learning classifier techniques: the bagging and Boosting techniques. The bagging technique accuracy result was 82.95%, while the boosting technique's accuracy score was 64.52%.

Albraheem et al. [28] used the NODEXL tool to retrieve tweets and compiled 100 tweets with Saudi hashtags. This was a small number that could hardly be reliable enough to draw any learning conclusions. The number of positive words that their model found in the tweets was 33 while the number of positive words detected by human language experts was 40. The accuracy of positive words was 82.5%, while the accuracy of negative words was 71.01%. The accuracy of all tweets was 73%.

TABLE II. SENTIMENT ANALYSIS HIGHLIGHTS IN ARABIC LITERATURE

Paper	Lexicon	Tools/ Languages	Size	Sentiment Score	Arabic variety
[25]	ArSeLEX	AMIRA	5,244 word	Positive 300 Negative 2,829 Neutral 412	MSA & Egyptian dialectal Arabic
[27]	NA	NA	1,500 Arabic comments	Sports: Positive 369 Negative 171 News: Positive 83 Negative 316 Economics: Positive 234 Negative 327	MSA & dialectal Arabic
[28]	NA	NODEXL tool	100 Arabic tweets extracted from some of the Saudi hashtags	The positive words were 82.5% and the negative words were 71.01%	Dialectal Arabic
[29]	created by authors	R	3,000 tweets	The accuracy of the unsupervised approach was 81.70%.	MSA & dialectal Arabic

Alhumoud et al. [29] implemented a hybrid learning approach that combines lexicon and supervised approaches compared to the supervised and unsupervised learning approaches. Both the supervised classifier and the hybrid classifier trained on 3,000 tweets collected from three domains. The unsupervised approach has two dictionaries, positive and negative. The training dataset contains 3,690 sentimental words, which are built from rows of single sentimental words and their labels. The training datasets included 1,370 positive words, and 2,320 negative words, 1,000 MSA sentimental words, and 2,690 Saudi dialect sentimental words. The accuracy of the unsupervised approach was 81.70%.

C. Sentiment Analysis in Traffic

SA in traffic is concerned with tapping into the available datasets on traffic with the aim of inferring meaning, indicators, and safety signals that foster more efficient driving. The following related work highlights the available research on SA in the traffic domain with a Twitter dataset source.

Kurniawan et al. [30] collected data consisting of 110,449 tweets for seven days from official traffic accounts from the Indonesian province Yogyakarta. They used three algorithms for machine-learning, namely Naïve Bayes (NB), a Support Vector Machine (SVM), and a Decision Tree (DT). The data were classified into two categories: traffic and non-traffic tweets. The results show that the SVM provided the best performance, as its classification accuracy in balanced and imbalanced data was 99.77% and 99.87%, respectively.

Andrea et al. [31] aimed to detect real-time traffic accidents from data consisting of 2,649 tweets using n-labelled SUMs and classified according to Status Update Message (SUM), which is the user message shared in social networks and class labels related to traffic events. The highest value reached with the SVM classifier was 95.75%. One of the drawbacks of this study, which was conducted in Italy, is the lack of a data collection period or a list of the number of words.

Lee et al. [32] collected data from 22,353 Korean messages within three months in 2014. The number of Twitter messages (62,495) were collected from 5,247 users. They collected their data using Traffic Information Producers (TIPs) and Opinion Leaders (OLs) and keyword and network analysis. The data were classified into categories including traffic conditions, locations, and instructions and were measured at 90% accuracy.

Wang et al. [33] collected 245,568 tweets on traffic events in Chicago, USA. The classification was done using the EM algorithm to classify data into three classes: slow traffic, accidents, and other road conditions (e.g., construction). The dataset sizes were 163,742, 77,454 and 4,372, respectively, and the accuracy value was 85%.

Alhumoud [34] presents a framework for Arabic Twitter content analysis to gain traffic insight applied in the city of Riyadh, Saudi Arabia. The study was done with a dataset of more than 1 million tweets collected within three months. The proposed model comprised three main components: data acquisition, data analysis, and a reverse geotagging scheme (RGS). The data acquisition phase utilized AsterixDB to collect tweets and perform preliminary preprocessing. AsterixDB is a “highly scalable data management system that can store, index, and manage semi-structured data.” In the data analysis phase, the data were analyzed using the hazard classifier based on the transportation hazard index (THI), which is a lexicon provided by the author yielding one of four possible hazard intensities for each tweet. The hazards were classified into four types: accident incidents, weather incidents, negative road incidents, and positive road incidents. The results showed that 13% of the dataset reported traffic-related incidents with an overall precision of 55% and 87% for incidents identification prediction without and with reverse geotagging, respectively.

A summary of SA studies on traffic is depicted in Table III.

TABLE III. SENTIMENT ANALYSIS IN TRAFFIC

Paper	Data Size	Collection	Classification	Label	Accuracy
[30]	NA	Using Twitter Streaming API	NB & SVM and DT	Traffic tweets and non-traffic tweets	balanced and imbalanced data were 99.77% and 99.87%
[31]	NA	Using Twitter Streaming API	SVM	NA	SVM classifier 95.75 %
[32]	22,353	(API) & using a keyword analysis and a network analysis.	TIPs & OLs	NA	90%.
[33]	245,568	API	Sequential importance sampling-based EM algorithm	Tweets on slow traffic, accidents and other road conditions.	85 %.
[34]	1M	AsterixDB	Lexicon based using THI	Incidents: accident, weather, negative, positive	55% and 87%

III. METHODOLOGY

The ATAM system comprises five components. Those components include data collection using two methods to be explained in the next section. The second component is data preprocessing and denoising with state of the art text preprocessing techniques and normalization. The third component is the spam filtering according to the rules implemented in [35]. The fourth component is an annotation; that is, labeling the corpus by human experts into the desired four classes to train the model for correct classification. The fifth and final component is the classifier, that classifies data into four classes using a rule-based classifier. The ATAM system components are depicted in Fig. 1. Following is a more detailed explanation of the system.

A. Collecting Data

Twitter data were collected using R with Twitter API, which allows accessing tweets and collecting them using two approaches. First, a streaming function that allows the collecting of tweets in real time based on the provided street lexicon. The second approach involves collecting specific user tweets using the userTimeline function, which allows researchers to pull the latest 3,200 tweets from a user timeline. The accounts that are scrapped are known for traffic tweets and hazardous road conditions in the city of Riyadh. The number of collected tweets reached 292,965 by using 44 street keywords in a three months period from September 2017 to November 2017. The streets under consideration are in the city of Riyadh, Saudi Arabia.

B. Preprocessing

After streaming Twitter data, the data were prepared for analysis. Preprocessing involves nine actions: (1) removing repeated letters (i.e., converting “liiiiife” into “life”), except words that match the road lexicon are kept unchanged; (2) normalizing by converting multiple forms of a letter into one uniform letter [i.e., (ة to ة), (ة to ة), (ي to ي), and (أ/إ to ا)]; (3) removing numbers, spaces, and the tatweel, which is the Arabic letter (-), or (4) (المالك) removing any non-Arabic letters; (5) removing punctuation marks (e.g., “,:;?!), except hashes (#) (which is required in the spam filtering step, that classifies a tweet with more than four hashes as a spam tweet); (6) removing Arabic diacritics, such as َ; (7) removing stop words, which are provided in [36]; (8) removing words that have less than two letters; (9) and stemming.

The stemming process involves the extraction of a word root to enhance the classifier accuracy by merging many word forms into one root form [37]. The Arabic language has a composite morphology structure that makes root extraction more complicated and limits the stemming to removing prefixes and suffixes [38]. However, there are several algorithms can simplify extracting roots. These algorithms follow some rules for removing prefixes and suffixes to produce proper stemming, such as the AlKabi [39], Ghawanmeh [40], Hmeidi [41], Khoja [42] and WSS-Based algorithms [37].

The Light10 stemmer [43], which is claimed to be the best available stemmer, works by solely removing the initial letter

ها, ان, ات, ون, ين,), and suffix (ال, وال, بال, كال, فال, لل), prefix (و, ي, به, ية, م, ة, ي), and this may not result in an accurate root extraction. In the case of this research, the arabicStemR package in R developed by Nielsen in MIT was used. However, the stemmer included suffix and prefix elimination, and that changed the meaning of some important keywords, such as street names (e.g., “شارع الستين” was transformed into “شارع ست” after stemming). For this reason and because of the limited added value by stemming in the study’s dataset, the stemming step was ignored.

As for removing the stop words, it was postponed preceding the annotation step to preserve the meaning and clarity of the sentences and to enable correct annotation by the experts.

C. Spam Filtering

One of the significant challenges in studying datasets from Twitter is the high volume of noise or spam tweets. Spam data are unrelated data that are collected with the target data, including advertisements and news. As the dataset size was large, the need for an automated spam filtering was inevitable. We used the algorithm provided in [35] where tweets with URLs, phone numbers, more than four hashtags, and duplicated tweets are classified as spam. The algorithm also implements a rule-based classifier with a spam lexicon. Also, in this study, tweets that not related to streets or tweets with less than three words were classified as spam. The number of remaining tweets after spam filtering decreased by 96%, leaving 11,037 tweets.

D. Annotation

In this step, the resulting dataset from the previous step undergoes labeling by two expert Arabic speakers. The procedure of annotation was as follows. Using the instructions specified by the authors, the two experts labeled 5,781 data entry items into one of the following labels: neutral, safe, needs attention, and dangerous. By agreement of the two experts on a data entry label, a data entry was accepted with the given label. If they disagreed, the data entry was eliminated. After annotation, the number of safe tweets accounted for 8%, while the dangerous tweets accounted for 6%. Tweets that need attention accounted for 18%, while neutral tweets reached 68%.

E. Arabic Traffic Analysis Model for Twitter

The ATAM model implements a rule-based classifier that classifies data into four classes: safe, needs attention, dangerous, and neutral. The classifier utilizes three lexicons built using the gulf region dialect, which is commonly used by Saudi Twitter users. After applying the previous steps, the size of the dataset was 10,175 tweets. Technically, the ATAM model implements four counters that count the occurrences of the four different classes; in each tweet in the dataset by matching each keyword in the lexicon to the available dataset using the R language. Then, each tweet is classified according to the most repeated class label. If the labels from each class occur in one tweet equally, the highest occurring class in severity is assigned with the following priority: dangerous, needs attention, safe, and neutral. The algorithm is shown in Fig. 2.

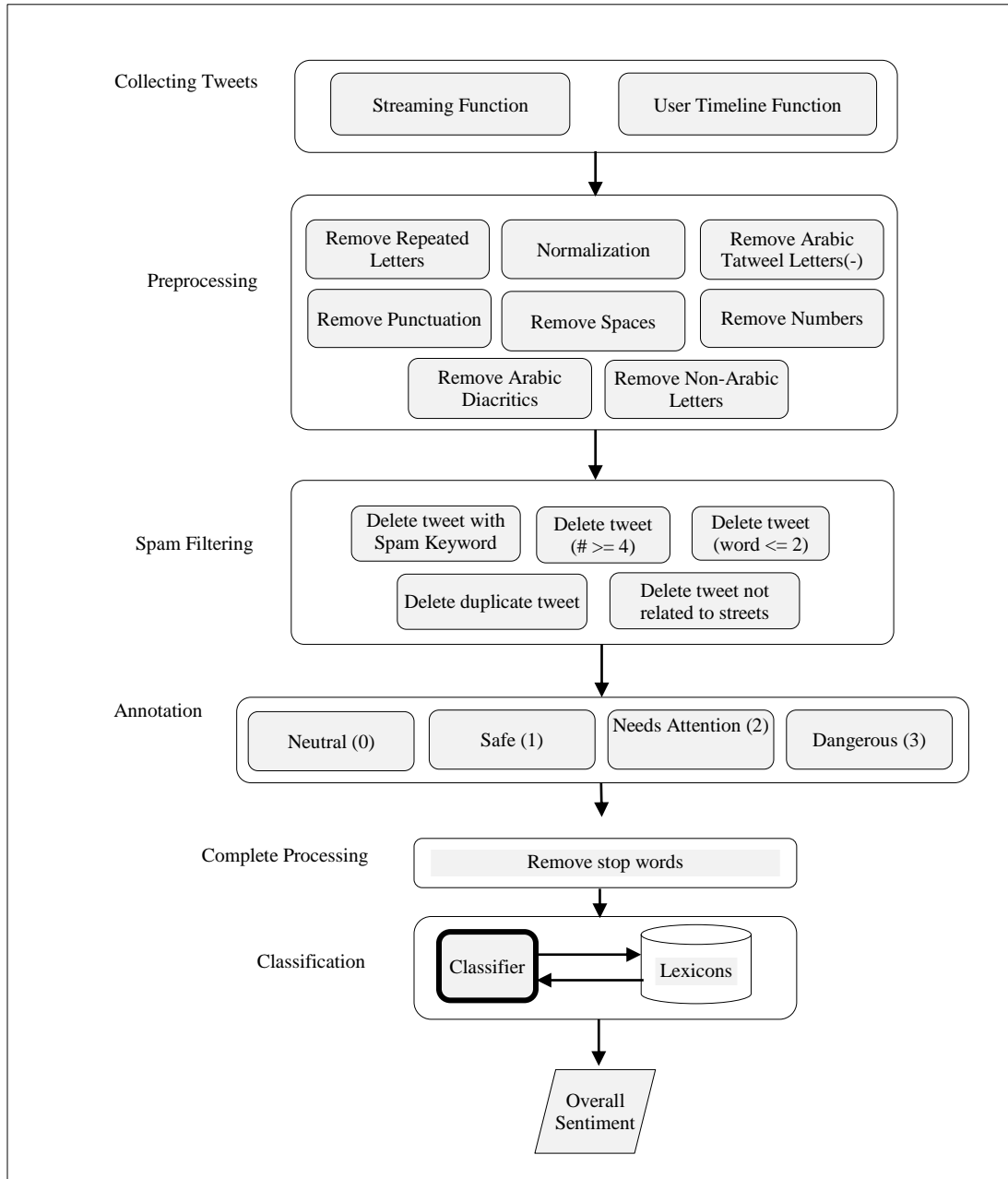


Fig. 1. ATAM System Architecture.

IV. RESULTS AND DISCUSSION

After building the ATAM model, we tested and evaluated the accuracy of this model using equation (1), which is one of the most common metrics used to measure performance. Accuracy was measured for all four classes: safe, dangerous, needs attention, and neutral over 300 tweets.

Equation 1 shows the accuracy formula, where TP, FP, TN, and FN are true positive, false positive, true negative, and false negative, respectively. True positive stands for test results that detect the condition when the condition is present. True negative is when it does not detect the condition when the

condition is absent. False positive is when it detects a condition when the condition is absent. Finally, false negative denotes when it does not detect the condition when the condition is present.

$$Accuracy = (TP + TN) / (TP + TN + FP + FN)$$

The ATAM model was applied to 10,175 tweets, and 300 of them were studied and tested to calculate the accuracy. The neutral data reached 44% of the total tweets, while safe data was 14%, needs attention data was 25%, and dangerous data was 17% of the total tweets. To calculate accuracy for the dataset under consideration, TP, TN, FP, and FN were

calculated for each label. Those values are depicted in Table IV. As the table shows, the maximum accuracy was for the class “needs attention,” with 88%. Then, the second highest was the “dangerous” class, scoring 86% for the accuracy. The “safe” class scored 85%, while the lowest accuracy score was for the “neutral” class, with 70% accuracy. The average

accuracy scored by the ATAM model was 82%. The low score for the neutral class could be explained by the incorrect classification of tweets of significant incident by the model. This could be improved by enlarging the lexicons to include more incident keywords.

ATAM Algorithm

INPUT: Tweets T, Safe Lexicon SL, Needs attention lexicons NL, Dangerous lexicons DL, Neutral N

OUTPUT: L = {Safe, Needs Attention, Dangerous, Neutral}

INITIALIZATION: L= 0, Lsafe = 0, Lneedsattention = 0, Ldangerous = 0, where Lsafe: Sum of safe words, Lneedsattention: Sum of the needs attention words, Ldangerous: Sum of the dangerous words, L: to get the highest between Lsafe, Lneedsattention or Lneedsattention

```
1. For each  $T_i \in T$ 
  1. For each  $SL_i \in SL$ 
    1. If  $SL_i \in T_i$  then
      1. Lsafe = Lsafe + 1
    2. End if
  2. End for
  3. For each  $NL_i \in NL$ 
    1. If  $NL_i \in T_i$  then
      1. Lneedsattention = Lneedsattention + 1
    2. End if
  4. End for
  5. For each  $DL_i \in DL$ 
    1. If  $DL_i \in T_i$  then
      1. Ldangerous = Ldangerous + 1
    2. End if
  6. End for
  7. If Lsafe > Lneedsattention and Lsafe > Ldangerous then
    1. L = Safe
  8. End if
  9. If Lneedsattention > Lsafe and Lneedsattention > Ldangerous then
    1. L = Needs Attention
  10. End if
  11. If Ldangerous > Lneedsattention and Ldangerous > Lsafe then
    1. L = Dangerous
  12. End if
  13. If Ldangerous == Lsafe or Ldangerous == Lneedsattention and Ldangerous != 0 then
    1. L = Dangerous
  14. End if
  15. If Lneedsattention == Lsafe and Lneedsattention > Ldangerous and Lneedsattention != 0 then
    1. L = Needs Attention
  16. End if
  17. If Lsafe == 0 and Lneedsattention == 0 and Ldangerous == 0 then
    1. L = Neutral
  18. End if
End For
Return L
```

End ATAM Algorithm

Fig. 2. Arabic Traffic Analysis Model.

TABLE IV. THE ACCURACY OF 300 TWEETS

Actual \ Predicted	Safe	Needs Attention	Dangerous	Neutral	Acc
Safe	24	1	0	0	85%
Needs Attention	3	43	2	1	88%
Dangerous	0	0	28	0	86%
Neutral	48	31	45	205	70%

The comparably high performance of these results could be due to the accuracy and lack of duplication of the keywords that were used in the lexicon dictionaries for each class. The ATAM model ensures that the tweets are appropriately categorized after calculating the number of lexicons' words that relate to a specific label in one tweet. As explained earlier, if more than one class is represented in a tweet, then the final classification result is assigned to the more severe class. For example, the tweet “ طريق عثمان فاضي بس يحتاج إعادة زفلة فهو مليون ” which means “Uthman road is not busy but needs construction; it has a lot of dangerous holes” holds two sentiments, dangerous and safe; therefore, we programmed our model to assign the final classification for this tweet as dangerous.

V. CONCLUSION

Twitter traffic analysis serves as a timely and complimentary solution to the costlier infrastructure-based sensors and GPS systems. English text analysis enjoys the abundance of gold-standard corpora and resources. However, in Arabic, text analysis is still in an early stage where the resources scarcity and language nature bring huge challenges to the research. This study presents an Arabic Traffic Analysis Model (ATAM) to tackle this area of research. This model aims to mine related Arabic texts from Twitter to present instantaneous pivots on traffic incidents. These incidents fall into four categories: safe, needs attention, dangerous, and neutral. For this study, we collected around 300k tweets in a period of three months. The tweets were subject to spam filtering, leaving a data size of 10,000 related tweets. Additionally, half of those tweets, were annotated by expert Arabic speakers to measure classifier accuracy. The results showed that the overall accuracy was 82% for all four classes. As a future work, we aim to build a web service for live streaming and classifications.

REFERENCES

[1] S. Alaamer, "Characterization of 137Cs in Riyadh Saudi Arabia," World Journal of Nuclear Science and Technology, vol. 2, no. 4, pp. 161-164, 2012.

[2] A. A. Salam, "Population and Household Census, Kingdom of Saudi Arabia 2010: Facts and," International Journal of Humanities and Social Science, vol. 3, no. 16, 2013.

[3] Y. Gu, Z. Qian and F. Chen, "From Twitter to detector: Real-time traffic incident detection using social media data," Transportation Research Part C: Emerging Technologies, vol. 67, pp. 321-342, 2016.

[4] S. Alhumoud, "Twitter Analysis for Intelligent Transportation," The Computer Journal, vol. 61, no. 12, 2018.

[5] S. Alhumoud, T. Albuhaire and M. Altuwajri, "Arabic sentiment analysis using WEKA a hybrid learning approach," in 7th International

Joint Conference on Knowledge Discovery, Knowledge Engineering and Knowledge Management (IC3K), Portugal, 2015.

[6] S. O. Alhumoud, M. I. Altuwajri, T. M. Albuhaire and W. M. Alohaideb, "Survey on Arabic Sentiment Analysis in Twitter," International Journal of Computer and Information Engineering, vol. 9, no. 1, 2015.

[7] W. Medhat, A. Hassan and HodaKorashy, "Sentiment analysis algorithms and applications: A survey," Ain Shams Engineering Journal, vol. 5, no. 4, pp. 1093-1113, 2014.

[8] B. Gokulakrishnan, P. Priyanthan, T. Ragavan, N. Prasath and A. Perera, "Opinion mining and sentiment analysis on a Twitter data stream," in International Conference on Advances in ICT for Emerging Regions (ICTer2012), 2012.

[9] R. Batool, A. M. Khattak, J. Maqbool and S. Le, "Precise tweet classification and sentiment analysis," in IEEE/ACIS 12th International Conference on Computer and Information Science (ICIS), Japan, 2013.

[10] A. Shoukry and A. Rafea, "Sentence-level Arabic sentiment analysis," in International Conference on Collaboration Technologies and Systems (CTS), USA, 2012.

[11] N. Y. Habash, Introduction to Arabic Natural Language Processing, Morgan & Claypool publishers, 2010.

[12] S. Alowaidi, M. Saleh and O. Abulnaja, "Semantic Sentiment Analysis of Arabic Texts," International Journal of Advanced Computer Science and Applications(IJACSA), vol. 8, 2017.

[13] B. Han, P. Cook and T. Baldwin, "Lexical normalization for social media text," Journal ACM Transactions on Intelligent Systems and Technology (TIST), vol. 4, no. 1, p. 5:1-5:27, 2013.

[14] J. Pereira, Handbook of Research on Personal Autonomy Technologies and Disability Informatics, IGI Global, 2010.

[15] M. Z. Asghar, A. Khan, S. Ahmad and F. M. Kundi, "A Review of Feature Extraction in Sentiment Analysis," Journal of Basic and Applied Scientific Research, vol. 4, no. 3, pp. 181-186, 2014.

[16] M. Hu and B. Liu, "Mining opinion features in customer reviews," in AAAI'04 Proceedings of the 19th national conference on Artificial intelligence, California, 2004.

[17] B. Liu, Sentiment Analysis and Opinion Mining, Morgan & Claypool Publishers, 2012.

[18] X. Zhou, X. Tao, J. Yong and Z. Yang, "Sentiment analysis on tweets for social events," in IEEE 17th International Conference on Computer Supported Cooperative Work in Design (CSCWD), Canada, 2013.

[19] T. Wilson, J. Wiebe and P. Hoffmann, "Recognizing contextual polarity in phrase-level sentiment analysis," in Proceeding HLT '05 Proceedings of the conference on Human Language Technology and Empirical Methods in Natural Language Processing, Canada, 2005.

[20] J. Platt, "Sequential Minimal Optimization: A Fast Algorithm for Training Support Vector Machines," Microsoft research technical report, 1998.

[21] C. Seiffert, T. M. Khoshgoftaar, J. V. Hulse and A. Napolitano, "Building Useful Models from Imbalanced Data with Sampling and Boosting," in FLAIRS Conference, 2008.

[22] A. Farghaly and K. Shaalan, "Arabic Natural Language Processing: Challenges and Solutions," ACM Transactions on Asian Language Information Processing, vol. 8, no. 4, p. 22, 2009.

[23] W. Salloum and N. Habash, "ADAM: Analyzer for Dialectal Arabic Morphology," Journal of King Saud University - Computer and Information Sciences, vol. 26, no. 4, pp. 372-378, 2014.

[24] S. AlOtaibi and M. B. Khan, "Sentiment Analysis Challenges of Informal Arabic Language," International Journal of Advanced Computer Science and Applications(IJACSA), vol. 8, no. 2, 2017.

[25] H. S. Ibrahim, S. M. Abdou and M. Gheith, "Sentiment Analysis For Modern Standard Arabic And Colloquial," International Journal on Natural Language Computing (IJNLC), vol. 4, no. 2, 2015.

[26] M. Diab, "Towards an optimal POS tag set for Modern Standard Arabic processing," in Proceedings of Recent Advances in Natural Language Processing (RANLP), Bulgaria, 2007.

[27] R. T. Khasawneh, H. A. Wahsheh, I. M. Alsmadi and M. N. Al-Kabi, "Arabic sentiment polarity identification using a hybrid approach," in

- International Conference on Information and Communication Systems (ICICS), Jordan, 2015.
- [28] L. Albraheem and H. Al-Khalifa, "Exploring the problems of sentiment analysis in informal Arabic," in Proceedings of the 14th International Conference on Information Integration and Web-based Applications & Services, Indonesia, 2012.
- [29] S. Alhumoud, T. Albuhairi and W. Alohaide, "Hybrid sentiment analyser for Arabic tweets using R," in 7th International Joint Conference on Knowledge Discovery, Knowledge Engineering and Knowledge Management (IC3K), Portugal, 2015.
- [30] D. A. Kurniawan, S. Wibirama and N. A. Setiawan, "Real-time traffic classification with Twitter data mining," in 8th International Conference on Information Technology and Electrical Engineering, Indonesia, 2016.
- [31] E. D'Andrea, P. Ducange, B. Lazzarini and F. Marcelloni, "Real-Time Detection of Traffic From Twitter Stream Analysis," IEEE Transactions on Intelligent Transportation Systems, vol. 16, no. 4, pp. 2269-2283, 2015.
- [32] H. P. Lee, D.-P. Hong, E. Han and S. H. K. Yun, "Analysis of the characteristics of expressway traffic information propagation using Twitter," KSCE Journal of Civil Engineering, vol. 20, no. 7, pp. 2587-2597, 2016.
- [33] S. Wang, F. Li, L. Stenneth and P. S. Yu, "Enhancing Traffic Congestion Estimation with Social Media by Coupled Hidden Markov Model," in Joint European Conference on Machine Learning and Knowledge Discovery in Databases, 2016.
- [34] S. Alhumoud, "Twitter Analysis for Intelligent Transportation," The Computer Journal, vol. 61, no. 12, 2018.
- [35] N. A. Twairesh, M. A. Tuwaijri, A. A. Moammar and S. A. Humoud, "Arabic Spam Detection in Twitter," in Language Resources and Evaluation Conference, Slovenia, 2016.
- [36] A. Alajmi and E. m. Saad, "Toward an ARABIC Stop-Words List Generation," International Journal of Computer Applications, vol. 46, no. 8, p. 6, 2012.
- [37] Q. Yaseen and I. Hmeidi, "Extracting the roots of Arabic words without removing affixes," Journal of Information Science, vol. 40, no. 3, pp. 376-385, 2014.
- [38] A. Alsaad and M. Abbod, "Arabic Text Root Extraction via Morphological Analysis and Linguistic Constraints," in 16th International Conference on Computer Modelling and Simulation, UK, 2014.
- [39] M. N. Al-Kabi and R. S. Al- Mustafa, "Arabic Root Based Stemmer," in International Arab Conference on Information Technology, Jordan, 2006.
- [40] S. Ghwanmeh, G. Kanaan, R. Al-Shalabi and S. Rabab'ah, "Enhanced Algorithm for Extracting the Root of Arabic Words," in Sixth International Conference on Computer Graphics, Imaging and Visualization, China, 2009.
- [41] I. Hmeidi, R. Al-Shalabi and D. A. T. Al-Taani, "A Novel Approach to the Extraction of Roots from Arabic Words Using Bigrams," Journal of the American Society for Information Science and Technology, p. 583-591, 02 12 2009.
- [42] S. Khoja and R. Garside, "Stemming Arabic Text," Computing Department, Lancaster University, 1999.
- [43] L. S. Larkey, L. Ballesteros and M. E. Connell, "Light Stemming for Arabic Information Retrieval," TLTB, vol. 38, pp. 221-243, 2007.

An Effective Approach to Analyze Algorithms with Linear $O(n)$ Worst-Case Asymptotic Complexity

Qazi Haseeb Yousaf ^{*1}, Muhammad Arif Shah^{*2}, Rashid Naseem³, Karzan Wakil⁴, Ghufraan Ullah⁵
Department of Computer Science, City University of Science and Information Technology, Peshawar, Pakistan^{1,2,3,5}
Research Center, Sulaimani Polytechnic University, Sulaimani 46001, Kurdistan Region, Iraq⁴

Abstract—A theoretical approach of asymptote analyzes the algorithms for approximate time complexity. The worst-case asymptotic complexity classifies an algorithm to a certain class. The asymptotic complexity for algorithms returns the degree variable of the algorithmic function while ignores the lower terms. In perspective of programming, asymptote only considers the number of iterations in a loop ignoring inside and outside statements. However, every statement must have some execution time. This paper provides an effective approach to analyze the algorithms belonging to the same class of asymptotes. The theoretical analysis of algorithmic functions shows that the difference between theoretical outputs of two algorithmic functions depends upon the difference between their coefficient of 'n' and the constant term. The said difference marks the point for the behavioral change of algorithms. This theoretic analysis approach is applied to algorithms with linear asymptotic complexity. Two algorithms are considered having a different number of statements outside and inside the loop. The results positively indicated the effectiveness of the proposed approach as the tables and graphs validates the results of the derived formula.

Keywords—Asymptotic complexity; interval analysis; in-depth analysis; Big-Oh; crossover point

I. INTRODUCTION

An algorithm is a set of instructions to specify a solution to the problem in a finite time. The single problem may have more than one algorithm. For instance, algorithms to search maximum value in one-dimensional array or methods to sort elements in an array. Given the number of algorithms for a problem, it is obligatory that every algorithm differs in the order of complexity. Considering the difference in complexity of algorithms, some algorithms perform better than others in the provided environment. The level of complexity effects in execution time, the memory space acquired and lines of code (LOC) for the algorithms. From the given three metrics of complexity, LOC has no direct impact on algorithm complexity and is not considered a good metric for analysis of algorithm [1]. Therefore, execution time and space acquired are metrics for analysis of algorithms. The run-time of the algorithm is measured either by approximate analysis or execution time on the machine. Real execution time requires computational resources to run algorithms in actual time. The computational resources are affected by the environmental factors like temperature, number of resources utilized, dimensions of used resources etc. In contrast, the approximate method follows a virtual computational model. The virtual computational model depends on certain fixed execution times for different programming structures. Random Access

Machine (RAM) is one of an adapted model for forming approximate algorithmic functions in terms of input size of the algorithm. RAM has three assumptions:

- Only one processor
- Infinite Memory
- Cost of one unit processor time for each binary operation and each array access.

A mathematical set-theoretic approach of asymptotes gives the time complexity of an algorithm. Asymptotic notations analyze algorithms for different time complexities. Generally, there are five asymptotic notations in mathematics. These are Big-Oh (O), Big-Omega (Ω), Theta (Θ), Small-Oh (o) and Small-Omega (ω). Big-Oh (O), Big-Omega (Ω) and Theta (Θ) are used asymptotes to analyze the algorithms [2].

Big-omega appears for asymptotic lower bound in analysis of algorithm. In computing, it is termed as best-case analysis. Leiserson et al. [1] defines Big-Omega mathematically as:

$$\Omega(f(n)) \geq \{ g(n) : \text{there exists } c > 0 \text{ and } n_0 \text{ such that } g(n) \leq c \cdot f(n) \text{ for all } n > n_0. \} \quad (1)$$

Big-Oh represents asymptotic upper bound for the analysis, when input size becomes so big that it tends to infinity, which is normally termed as worst-case analysis. Leiserson et al. [1] defines the equation of Big-Oh as follow:

$$O(f(n)) = \{ g(n) : \text{there exists } c > 0 \text{ and } n_0 \text{ such that } f(n) \leq c \cdot g(n) \text{ for all } n > n_0. \} \quad (2)$$

Theta shows tight bound for given function. It gives the average case analysis in computing. From mathematical definition stated by Leiserson et al. [1]

$$\theta(f(n)) = \{ g(n) \text{ if and only if } g(n) = O(f(n)) \text{ and } g(n) = \Omega(f(n)) \text{ for all } n > n_0. \} \quad (3)$$

Given in the above defined equations (1), (2) and (3), n is the input size for algorithm. It may be size of array, stack or basic data structure to hold memory. $f(n)$ represents mathematical function of algorithm and $g(n)$ is the comparable function or asymptote.

The algorithms are compared on their worst-case analysis [3]. If the results of the worst-case analysis for two algorithms are the same, then the second metric to analyze the algorithms is best-case analysis. The problem arises when the worst-case and best-case analysis gives the same time complexity. It becomes difficult with asymptotes to analyze the better

algorithm from the given pool [4]. The problem of analyzing the algorithm with the same time-complexity is discussed by [2,4,5] in their respective papers. Leiserson et al. [1] and Sedgewick et al. [3] in their books quoted a generalized statement for the above-discussed problem that “*Asymptotic big-Oh approximations are for the functions tend towards infinite large values*”. This means with asymptotes, analysis for small input values is not feasible. So this traditional approach is not enough to analyze and choose the best algorithm from the given set [2–4]. Moreover, the real-world problems work with a specific interval of inputs. While asymptotes give us peak value analysis. It ignores the in-between behavior of an algorithmic function. The alternative method to differentiate the same asymptotic time complexity algorithms is real-time analysis on RAM. The RAM technique is a theoretical analysis requires less time and is not affected by certain environmental factors. Rahman [4] proposed two theoretical approaches (i) graph analysis and (ii) interval analysis [4]. Interval analysis works on a mathematical point of intersections for two or more functions. Full mathematical implementation of point of intersection contains a number of calculating steps with an overload of undesirable results in many cases like imaginary values, negative integer values, and continuous values. To some extent, the point of intersection approach throws an idea to check for the positive integer where the *crossover* occurs between the two algorithmic functions. This paper suggests a solution, which will analyze algorithms with the same asymptotic complexity, but different algorithmic functions. The proposed method finds approximate number ‘ n_o ’, where n_o is the point from which the algorithmic functions start changing their behaviors.

II. LITERATURE REVIEW

Algorithms are analyzed and validated from the very start of programming, for example, Garey et al [6], discussed the memory allocation algorithms for complexity effecting running time. Similarly, Mackeorth and Freuder [7], discussed network consistency algorithms related to artificial intelligence and analyzed them for worst-case analysis resulting in the linear time for binary constraints. Vitter and

Flajolet [8] introduced average-case analysis: this technique worked well for small algorithms and data structures. The study was on statistical measurements and formulations. Analysis of algorithms is still a need of the day. The statement is supported by the recent studies of [9–15] on analysis of algorithms applied in different fields via different techniques. Adams and Aschheim (2016) compared algorithms for dental coding and ranking problems. The paper concluded with setting optimized (OPT) algorithm as best for large inputs with simple coding [13]. Schubert and Zimek [14] also discussed the analysis of algorithms technique separating implementation and evaluation. Most recently a study is conducted for the max-min filter on random inputs. The study focused on asymptotic analysis for the said problem on dynamic algorithms [15].

Analysis of algorithm is done considering different aspects of real-time evaluation, asymptotic analysis, non-asymptotic analysis, and sensitive analysis etc. Among the above asymptotic analysis is one of the easiest ways to get

approximated results theoretically but with accuracy payoff. Tarek [2] wrote on the set-theoretic approach of asymptotes i.e. asymptotic functions are relative functions than individual bare ones. This means asymptotic functions always depend on coefficient and exponents of input size n . The extended work of Decelle et al. [16] was an exact analysis of the stochastic block model. The author used an asymptotic approximation for analysis. A research study [17] on non-asymptotic analysis of machine learning algorithms may be in principle costly to generate results beyond a certain number of equations. Teng [18] discussed linear time algorithms for preconditioning and solving dominant linear systems. Xu et al. [19] explore the algorithms for Virtual Machine (VM) deployment and load balancing. The research included certain new metrics to conclude for the best performing algorithm in the deployment and load balancing of VM. The proposed and existed all metrics are environmental variables dependent on the applied platform. Pietri et al. [20] give the survey of VM deployment on Physical Machines (PM). The adopted techniques were proven correct but research was inconclusive about the best technique. Thi and Thi [21] published work on the same problem of approximated the complexity of algorithms using asymptotes. The work suggested statistical and probability formulas resulting in equivalent values that of asymptotes. The formula calculates sorting algorithms realistic complexity. The method is partially automated and most calculations are done manually. In addition, the method depends on the type and nature of input [21].

The above studies show that authors are inconclusive to decide between algorithms. For the same degree of two different algorithmic functions asymptotes failed to analyze them for small or large input sizes. Asymptotes treat them equally good for all input sizes, which is not exactly the case. The inference is to replace asymptotic analysis by realistic analysis specifically for same worst-case complexity algorithms, but the realistic analysis also bears the load of environmental factors and availability of physical resources. The problem of analyzing with the same time-complexity is discussed by [5] and [4] in their respective papers. Rahman et al. [4] suggested the analysis of algorithmic functions by graphs through drawing them. The author also gave an interval analysis to mark the point where the big value starts with the creation of threshold value (k) for n tends to infinity. The study considers the insertion sort as an example. Insertion sort is quadratic in nature. The worst-case analysis for insertion sort is $O(n^2)$. It was claimed algorithmic functions for two different implementations of insertion sort. The proposed methodology was to suppose a threshold point and then calculate values of ‘ k ’ for all inputs and mark the input point breaking a specific threshold. The problem in the study was the selection of a threshold point and then to find that input where the big value starts. Alternative for interval analysis is the graph method. It is very difficult to draw and analyze the graphs for infinite input values. Also, the input size is discrete in nature [3] while graphs of polynomials are continuous in nature [21,22]. Ferreira et al. [5] conducted a survey on memory allocation techniques. The article concluded that the malloc family has linear time complexity, but it is difficult to choose the best algorithm of the family because of the same time complexity. However, sensitivity analysis is suggested

for overcoming this problem. The sensitive analysis is not an efficient metric because the hardware and software vary too much from point to point and doing an analysis every time before implementation may not be easy. Most recently Schubert and Zimek [14] discussed the hurdles in algorithm evaluation and implementation on environment-sensitive metrics like machine execution time and platform dependent testing. The author argues with different techniques used to validate the efficiency of algorithms presented in research papers. Most of the time the current algorithm proved less efficient than presented in the previous research papers. The affecting factor is a run-time evaluation of algorithms, the most common technique used for analysis of research algorithms. Therefore, there must be a standard technique to check the algorithm and its implementation separately. The data mining algorithms are tested on different platforms with different datasets giving the changed result on every platform [14]. On the other side of the discussion, there are many sorting algorithms available. Merge sort, heap sort, insertion sort, bubble sort, selection sort, and many others. These algorithms are passing through advancements to reduce the overall complexity. Small improvements in algorithms are totally negligible due to discrete classes of asymptotes. Some of the recent work in advancement and analysis of sorting algorithms is the study of quadratic algorithms for sorting evolving data [24] and analysis of algorithms on the multi-threaded and multi-core environment. As the algorithms are advancing it is obligatory to make changes in the algorithm evaluation techniques. A review is conducted on sorting algorithms with respect to the size of the array. The review included all the used sorting algorithms of various complexities. The results proved some of the quadratic algorithms better over merge and quicksort in the provided conditions [25]. The time complexity of insertion sort, bubble sort, and selection sort is the same $O(n^2)$. It is difficult to analyze best among these three discussed. However, their algorithmic functions may be helpful to conclude some results.

III. METHODOLOGY

Interval analysis is the feasible theoretical technique to analyze the algorithms with the same worst-case analysis [2,3]. Observation of mathematical graphs and functions clarifies that there may be a point of intersection for two same degree mathematical curves [21–24]. Asymptote always considers a mathematical function of an algorithm termed as algorithmic function. It takes the highest power term or degree of algorithmic function. The highest terms show the worst-case scenario for the algorithm. However, in the real run-time, every line of code has an effect on time of execution. So, the conclusive statement may come as that every term and related coefficient of the algorithmic function is important and must be considered for theoretical analysis. The impact will be theoretical analysis close to real-time analysis of algorithms. For the implementation of the proposed method, few linear expressions are considered as algorithmic functions performing the same task in a different manner.

$$3n+7 \tag{4}$$

$$n+29 \tag{5}$$

$$2n+145 \tag{6}$$

The n in the above equations represents input size for the algorithm. The Big-Oh for the above defined algorithmic functions is $O(n)$. According to asymptotic analysis, algorithms are under the same curve of $O(n)$ but graph analysis shows the changing behavior of a function from interval to interval. Table I compares the input size to the output time of the algorithms. As the input size increases, the algorithm will consume more time.

From Table I it is seen that for input size $n=1$ to $n=10$ in (5) gives higher output values while the case reverses after input size $n=11$ and values start diverging. The value for (4) gets higher and higher due to the larger coefficient than (5). Consider some other examples from Table II and III.

Table II shows the comparison between (5) and (6). The output values show that the difference is constantly increasing due to the fact of the higher coefficient and the constant term of (6) in comparison with (5).

Table III compares the mathematical equation of (6) with (4) for input size n . It shows that the coefficient of n in (4) is greater than the coefficient of n in (6), while constant in (6) is greater than constant in (4). As a result, for input size $n=1$ to 137 the difference starts converging and after input size 138 it again starts diverging due to the higher coefficient of n for (4). The above results lead to the conclusion that output also depends on the coefficient of n and constant as it depends on n specifically, for small inputs. Further analysis shows that there must be a *crossover* point if coefficient for first and constant for second is larger and vice versa. This *crossover* is dependent on the difference or gap between the respective coefficient and constants. The formula to find the *crossover* point is proposed on the basis of these findings. The formula gives the *crossover* point where algorithmic functions change their behaviors. The functions in Tables I, II and III are all linear. Therefore, generalized forms of two linear algorithmic functions are assumed as shown in (7) and (8):

$$f(n)=a_1 n+b_1 \tag{7}$$

$$g(n)=a_2 n+b_2 \tag{8}$$

Where n_o is the *crossover* point, a_1 coefficient of n in $f(n)$, b_1 constant term in $f(n)$, a_2 coefficient of n in $g(n)$, b_2 constant term in $g(n)$

The following are the possible cases for relating the coefficients and constants of (7) and (8):

Case 1: If the coefficient of n and the constant term of the first function ($f(n)$) is greater than the coefficient of n and the constant term of the second function ($g(n)$) then second function ($g(n)$) will take less execution time throughout from 1 to infinity. Mathematically it can be represented as,

$$\text{if } a_1 > a_2 \text{ and } b_1 > b_2 \rightarrow g(n) \text{ is better than } f(n) \text{ for interval } [1, \infty) \tag{9}$$

Case 2: If coefficient of n of first function ($f(n)$) is greater than coefficient of n of second function ($g(n)$) while constant term of first function ($f(n)$) is smaller than constant term of the second function ($g(n)$) then *crossover* point n_o will decide the

intervals. The first function ($f(n)$) will take less execution time before n_o and second function ($g(n)$) will take less execution time after n_o . Mathematically it can be represented as:

if $a_1 > a_2$ and $b_1 < b_2$ then

$$n_o = \lfloor (b_2 - b_1) / (a_2 - a_1) \rfloor \quad (10)$$

So $f(n)$ is better than $g(n)$ for interval $[1, n_o)$ and for interval (n_o, ∞) $g(n)$ is better than $f(n)$

Case 3: If the coefficient of n and the constant term of the first function ($f(n)$) is smaller than the coefficient of n and the constant term of the second function ($g(n)$) then first function ($f(n)$) will take less execution time throughout from 1 to infinity. Mathematically it can be represented as:

if $a_1 < a_2$ and $b_1 < b_2 \rightarrow f(n)$ is better than $f(n)$ for interval $[1, \infty)$ (11)

Case 4: If coefficient of n of first function ($f(n)$) is smaller than coefficient of n of second function ($g(n)$) while constant term of first function ($f(n)$) is greater than constant term of the second function ($g(n)$) then *crossover* point n_o will decide the intervals. The second function ($g(n)$) will take less execution time before n_o and first function ($f(n)$) will take less execution time after n_o . Mathematically it can be represented as:

if $a_1 < a_2$ and $b_1 > b_2$ then

$$n_o = \lfloor (b_2 - b_1) / (a_2 - a_1) \rfloor \quad (12)$$

So $g(n)$ is better than $f(n)$ for interval $[1, n_o)$ and for interval (n_o, ∞) $f(n)$ is better than $g(n)$.

For two algorithmic functions with same worst-case analysis Big-Oh, the better will be “whose coefficient ‘a’ and constant ‘b’ is lesser”

If one of the two (‘a’ or ‘b’) for an algorithmic function is lesser while the second is higher than finding the *crossover* point by the given formula:

$$n_o = (\text{higher } b - \text{smaller } b) / (\text{higher } a - \text{smaller } a) \quad (13)$$

The algorithmic function with a greater coefficient of n will take less time before n_o and algorithmic function with a smaller coefficient of n will take less time after n_o .

The same technique can be helpful for higher order polynomial algorithmic functions, for example, quadratic and cubical.

IV. RESULTS

The proposed formula is validated on graphs and tables. The first step is to calculate intervals for (4), (5) and (6) by applying the proposed formula. The graphs for (4), (5) and (6) are drawn for small random intervals. The intersection point in the graph is compared with values in Tables I, II and III. Lastly, values of the intersection point of formula are validated through graph and table.

$$(4) \rightarrow 3n+7$$

$$(5) \rightarrow n+29$$

$$(6) \rightarrow 2n+145$$

TABLE I. CROSSOVER POINT AT INPUT SIZE 11

Input Size (n)	Output Time Eq 4 (3n+7)	Output Time Eq 5 (n+29)
1	10	30
2	13	31
10	37	39
.	.	..
11	40	40
12	43	41
.	.	.
71	220	100
72	223	101

TABLE II. NO CROSSOVER POINT

Input Size (n)	Output Time Eq 5 (n+29)	Output Time Eq 6 (2n+145)
1	30	147
2	31	149
.	.	.
98	127	341
99	128	343
.	.	.
174	203	493
175	204	495

TABLE III. CROSSOVER POINT AT INPUT SIZE 138

Input Size (n)	Output Time Eq 4 (3n+7)	Output Time Eq 6 (2n+145)
1	10	147
2	13	149
.	.	.
106	325	357
.	.	.
137	418	419
138	421	421
139	424	423
.	.	.
177	538	499
178	541	501

As from (4) and (5), the coefficient of n in (4) is higher than (5) but on contrary constant of (5) is greater. So, applying the proposed formula:

$$n_o = (\text{higher } b - \text{smaller } b) / (\text{higher } a - \text{smaller } a)$$

$$n_o = (29-7) / (3-1)$$

$$n_o = 11$$

The crossover point n_o is similar to that given in Table I. This shows that (4) is better before input size 11 and (5) performs better after input size 11. The graph shows the same results in Fig. 1.

Similarly, the graphical representation of (4) and (6) are given in Fig. 2. The graph changes behavior between 135 and 140 as shown in Fig. 2 (Graph with input size (n) 100-500). The value in Table III for the given equations is input size 138. To validate it with proposed formula, consider (4) and (6), the coefficient of n for (6) is smaller to (4) while vice

versa is the case if constants of both equations are observed. By applying the formula:

$$n_o = \frac{\text{higher } b - \text{smaller } b}{\text{higher } a - \text{smaller } a}$$

$$n_o = \frac{145 - 7}{3 - 2}$$

$$n_o = 138$$

It is concluded from the results that (4) has less execution time on RAM on the interval [1,138) as compare to (6). On the other hand, (6) performs better in the interval (138, ∞).

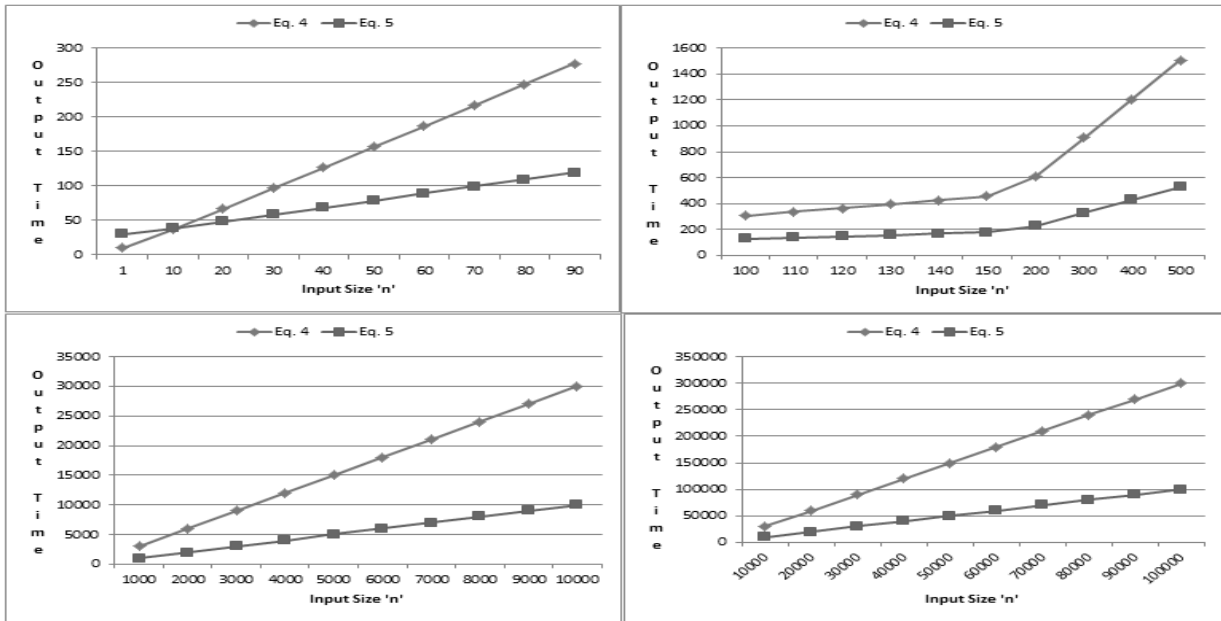


Fig. 1. Graphs Representing Eqs. (4) and (5) for Various Ranges of Input (n).

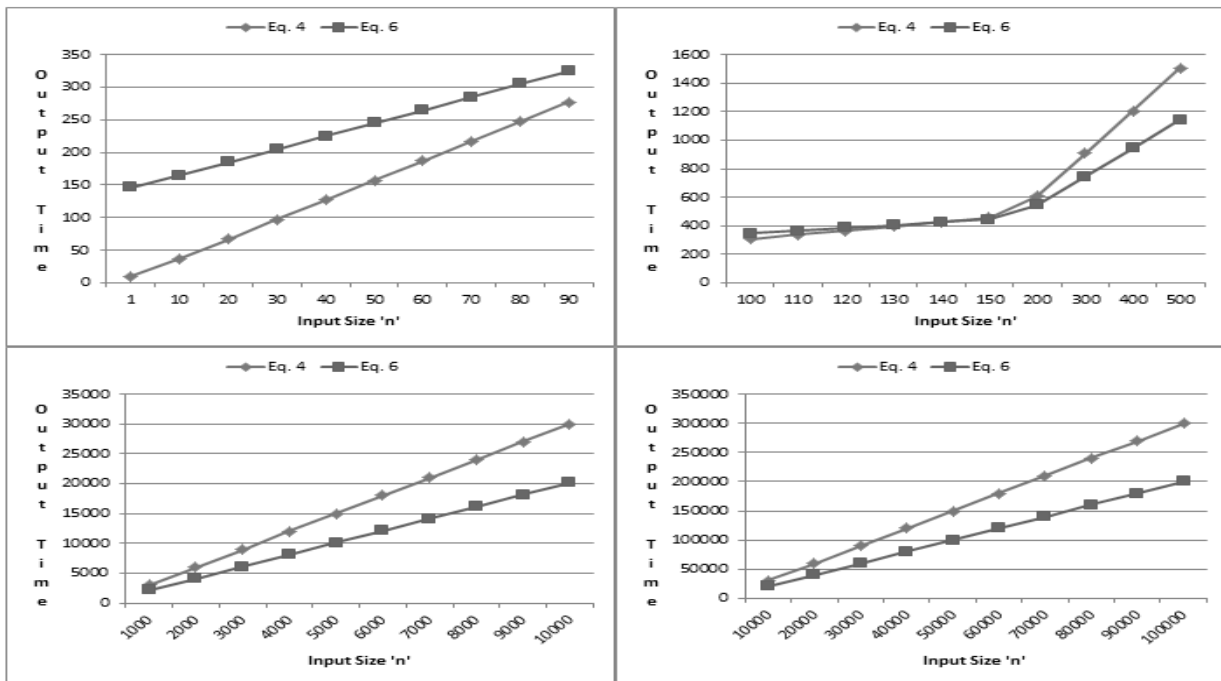


Fig. 2. Graphs Representing Eqs. (4) and (6) for Various Ranges of Input (n).

V. DISCUSSION

As suggested from the literature set-theoretic approach of asymptote is commonly used for analysis of algorithms. The approach gives an easier way to analyze algorithms in less time and effort as compared to run-time analysis. However, the technique of asymptotic complexity does not separate the algorithms with the same worst-case analysis. In reality, asymptotes assign a generic class of Big-Oh to each algorithmic function by focusing degree term thus ignoring lower terms. However, according to RAM assumptions each statement has some execution time. It is also to be noted that more and more statements inside and outside repetition structure increase the value of coefficient and constants respectively. Hence the impact falls as increased execution time. It is observed from the study that algorithmic functions of different algorithms with the same worst-case analysis relate to each other in terms of the corresponding coefficient and constant terms. Lesser the coefficient and constant term lower will be the execution time and vice versa. To calculate the relation between coefficient and constants of two algorithms a formula is proposed and validated in this study. As the results demonstrated that difference of coefficients of n and difference of *constant terms* of two algorithmic functions is nearer so a simpler formula generates the approximate *crossover* point for algorithmic functions. The *crossover* point forms the intervals for each given algorithm. Hence the method narrows the gap between theoretical and exact analysis for the algorithms.

VI. CONCLUSION

Analysis of algorithms is important to categorize algorithms on the basis of time and space. Algorithms are analyzed approximately by calculating their asymptotic complexity. The mathematical functions are discussed to relate two algorithms in order of statements inside and outside the repetition structures. The relation between terms of algorithmic functions leads to the formula for intersecting point. The intersecting point eventually forms intervals for performance behavior of algorithms. The analysis of linear algorithmic functions follows quadratic algorithmic functions as part of future work. The same formula works efficiently well for quadratic algorithmic function if constant terms c_1 and c_2 have a very small difference i.e. $|c_1 - c_2|$ is approximately equal to zero. For the large difference between constant terms of quadratic algorithmic functions, the formula requires slightest of changes. Besides this for future work, it is in the pipeline to generalize the formula for all the polynomial algorithmic functions. It is also set as a milestone to design a computational algorithm for the defined formula.

REFERENCES

- [1] C. C. E. Leiserson, R. R. L. Rivest, C. Stein, and T. H. Cormen, Introduction to Algorithms, Third Edition, vol. 7. 2009.
- [2] A. Tarek, "A generalized set-theoretic approach for time and space complexity analysis of algorithms and functions," 2006, vol. 2, pp. 316–324.
- [3] R. Sedgewick and P. Flajolet, An introduction to the analysis of algorithms. 2013.
- [4] L. Rahman, M. S. A. Khan, A. Kabir, and M. S. Miah, "A model for set-theoretic analysis of algorithm with asymptotic perspectives," in 2013 International Conference on Informatics, Electronics and Vision (ICIEV), 2013, no. 3, pp. 1–6.
- [5] T. B. Ferreira, M. A. Fernandes, and R. Matias Jr., "A comprehensive complexity analysis of user-level memory allocator algorithms," in 2012 Brazilian Symposium on Computing System Engineering, 2012, pp. 99–104.
- [6] M. Garey and R. Graham, "Worst-case analysis of memory allocation algorithms," STOC '72 Proc. fourth Annu. ACM Symp. Theory Comput., pp. 143–150, 1972.
- [7] A. K. Mackworth and E. C. Freuder, "The complexity of some polynomial network consistency algorithms for constraint satisfaction Problems," vol. 25, no. 1985, pp. 65–74.
- [8] J. S. Vitter and P. Flajolet, "Average-Case analysis of algorithms and data structures L'analyse en Moyenne des algorithmes et des structures de données," no. page i, 1990.
- [9] R. Goyal and D. K. Srivastava, "A study on cluster analysis technique - Hierarchical Algorithms," no. 9, pp. 1274–1279, 2016.
- [10] M. Wolfram, A. Marten, and D. Westermann, "A comparative study of evolutionary algorithms for phase shifting transformer setting optimization," in 2016 IEEE International Energy Conference (ENERGYCON), 2016, pp. 1–6.
- [11] K. S. Prado, N. T. R. B. V. F. Silva, L. B. Jr, L. A. Digiampietri, and E. M. Ortega, Human-Computer Interaction. Interaction Platforms and Techniques, vol. 4551. Berlin, Heidelberg: Springer Berlin Heidelberg, 2007.
- [12] C. Meshram, S. Gajbhiye, and D. Gupta, "Statistical analysis of an algorithm's complexity for Linear Equation 2 . statistical analysis on experimental results," vol. 8, no. 2, pp. 191–198, 2015.
- [13] B. J. Adams and K. W. Aschheim, "Computerized dental comparison : A critical review of dental coding and ranking algorithms used in victim identification," vol. 61, no. 1, pp. 76–86, 2016.
- [14] H. K. E. Schubert and A. Zimek, "The (black) art of runtime evaluation : Are we comparing algorithms or implementations?," Knowl. Inf. Syst., 2016.
- [15] M. Li, H. Liang, S. Liu, C. K. Poon, and H. Yuan, "Asymptotically optimal algorithms for running Max and Min Filters on random inputs," IEEE Trans. Signal Process., vol. 66, no. 13, pp. 3421–3435, 2018.
- [16] A. Decelle, F. Krzakala, C. Moore, and L. Zdeborov??, "Asymptotic analysis of the stochastic block model for modular networks and its algorithmic applications," Phys. Rev. E - Stat. Nonlinear, Soft Matter Phys., vol. 84, no. 6, p. 066106, Dec. 2011.
- [17] F. R. Bach and E. Moulines, "Non-asymptotic analysis of stochastic approximation algorithms for machine learning," Neural Inf. Process. Syst., no. 2, pp. 1–9, 2011.
- [18] S. Teng, "Nearly linear time algorithms for preconditioning and solving symmetric, diagonally dominant linear," vol. 35, no. 3, pp. 835–885, 2014.
- [19] M. Xu, W. Tian, and R. Buyya, "A survey on load balancing algorithms for virtual machines placement in cloud computing," pp. 1–20, 2016.
- [20] I. Pietri and R. Sakellariou, "Mapping virtual machines onto physical machines in cloud computing : A Survey," vol. 49, no. 3, 2016.
- [21] J. Clément, T. H. Nguyen Thi, and B. Vallée, "Towards a realistic analysis of some popular sorting algorithms," Comb. Probab. Comput., vol. 24, no. 01, pp. 104–144, Jan. 2015.
- [22] I. These, "Introduction to graph theory," Discrete Math., vol. 37, no. 1, p. 133, 1981.
- [23] J. L. Gross, J. Yellen, and P. Zhang, Handbook of graph theory. Second Edition. 2013.
- [24] J. J. Besa, W. E. Devanny, D. Eppstein, M. Goodrich, and T. Johnson, "Quadratic time algorithms appear to be optimal for sorting evolving data," pp. 87–96, 2018.
- [25] J. Totla, "Review on execution time of sorting algorithms- A Comparative Study," vol. 5, no. 11, pp. 158–166, 2016.

Implementation of Multi-Agent based Digital Rights Management System for Distance Education (DRMSDE) using JADE

Ajit Kumar Singh¹, Akash Nag², Sunil Karforma³, Sripati Mukhopadhyay⁴
Department of Computer Science, The University of Burdwan, Burdwan, India^{1,3}
Department of Computer Science, MUC Women's College Burdwan, India²

Abstract—The main objective of Distance Education (DE) is to spread quality education regardless of time and space. This objective is easily achieved with the help of technology. With the development of World Wide Web and high-speed internet the quality of DE is improved because now Digital Content (DC) can be easily and in no time distributed to many learners of different locations in text, audio and video formats. But, the main obstacle in digital publishing is the protection of Intellectual Property Rights (IPR) of DC. Digital Rights Management (DRM) that manages rights over any digital creation is the only solution to this problem. In this paper, we have made an attempt to implement a Digital Rights Management System for Distance Education known as DRMSDE. We have identified that Multi-Agent System (MAS) based technology is very popular for such type of implementations. Keeping that in mind, we have chosen one of the most popular Multi-Agent based tools, namely JAVA Agent Development Framework (JADE), for our system. This paper presents an overview and the system architecture for the proposed implementation.

Keywords—Distance Education (DE); Intellectual Property Rights (IPR); Digital Rights Management (DRM); Multi-Agent System (MAS); JADE

I. INTRODUCTION

The advancement of Information and Communication Technologies (ICT) touches every aspect of life [1], and knowingly or unknowingly we all are part of this technological revolution. The areas that are affected most are telecommunication, commerce, education, health and the media industry. Education with ICT reaches every corner of the globe within a fraction of a second under the domain of DE. DE is the most demanding and popular education system running in parallel to the traditional education system. The reason behind the popularity of DE is the flexibility of studying with respect to time and place. The main source of DE is DC that includes assignments and text tutorials along with advanced audio and video tutorials. DC may easily be copied and used by multiple users simultaneously. This advantage of DC sometimes becomes problematic because unauthorized users can also use and even modify DC, which is against the content-creators' IPR. Our main purpose is to protect IPR using the technology available with us, and thereby, preventing misuse of content.

Maintaining the rights of the different users in DE is a big challenge and it affects the quality of DE. DRM is the only

solution to this problem. DRM is a combination of hardware and software, collaborating to protect the rights of content creators. There are two generations of DRM [2]; in the first generation DRM, digital contents are locked and the users, who pay, then only use the content. Second Generation DRM includes identification, protection, monitoring, and tracking of all forms of rights, permissions etc.

In this study, we have designed and implemented a Distance Education System (DES) with DRM for protection of IPR for DC. Here we are using both approaches. For text tutorial, we are using second generation DRM and for advanced tutorial we are using first generation DRM. Our system is known as DRMSDE [3]. Here we are using MAS [4, 5] approach for the implementation of our system. An agent based approach is a new paradigm for software implementation. Agents are programs that take some input from systems as well as from some other agents, and perform actions for the system. In MAS at least two or more agents cooperate to achieve system goal. Real world problems can be successfully implemented using MAS. One of the major advantages of agent-based system is that we can easily upgrade the system by introducing a new agent. In case of DE, new experiments are done every time. MAS is good for domains like DE. There are so many tools to implement MAS but among all, JADE [6] is very popular. JADE, is a software framework that is used to build MAS. It is a middleware that includes a run-time environment, library and graphical tools. JADE is in compliance with FIPA specification, it has predefined programmable and extensible agent model that helps to develop MAS. JADE is the most popular agent development tool.

This paper is organized in six sections; Section 2 discusses some literature on agent-based DES. Section 3 describes the proposed DRMSDE system model in which we discuss the different components of our system. Section 4 presents the proposed system architecture, while Section 5 discusses implementation details. Finally, Section 6 concludes our work throwing some light on future applications and scope for improvement.

II. RELATED WORK

In the life cycle of DC we need to protect it from unauthorized users by DRM techniques [7]. DRM can be achieved in two ways [8]-using Right Expressions, and

through Authentication and Authorization. In Right Expressions, permissions and conditions are expressed in machine-readable form using Right Expression Language (REL) and right expressions follow DC throughout its life which is very essential for commercial distribution. In Authentication and Authorization technique, users are first authenticated based on their login credentials (usually a login ID and password). After successful authentication; the system checked whether they are authorized to perform certain actions on DC based on the type of user. The general architecture of a DRM-based educational system is shown in Fig. 1.

In a country DE is hosted by either public or private sectors. Regardless of who provides education, an effective DRM system is very much essential for fare use. We now list below some existing Education Systems based on DRM that are in use throughout the world:

A. BOKAHRI-IMBLS [9]

BOKHARI Intelligent Multi-agent based e-Learning System (BOKHARI-IMBLS) is a research model developed in Aligarh Muslim University in 2014 by Prof. Mohammad Ubaidullah Bokhari and his scholar Sadaf Ahmad. This is a web-based interactive E-Learning system designed for the distance learning environment using MAS. The main objective of the system is to incorporate intelligence, accessibility, interactivity, adaptability, collaborative and security into a single system. Its architecture has four levels which are user level that describes human agents, web level describes high interactive websites, system level has Seven interactive Agents (Student Interface Agent (SIA), Tutor Interface Agent (TIA), Collaboration Agent (CA), Intelligent Decision Support Agent (IDSA), Test/Evaluation Agent (TA), Lesson Planning Agent (LPA) and Security Agent (SA)) to achieved system goal and finally the storage level describes profile and content database. BOKHARI-IMBLS takes care of security issues of E-learning systems.

B. EDU-DRM

The Turkish government is taking an initiative to promote digital education in schools under a project called “Movement of Enhancing Opportunities and Improving Technology” known as FATIH in 2011 [1]. Under this project thousands of schools and classes are equipped with modern ICT tools. DC are created by many authors. FATIH project requires a DRM System to monitor and distribution of DC. EDU-DRM is a new DRM system for FATIH. In EDU-DRM, bitwise logic based encoding approach is used to implement REL that require minimal space in the database.

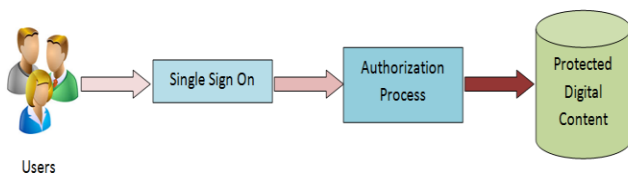


Fig. 1. General Architecture of DRM in Education.

C. Jorum

Though the dictionary meaning of ‘jorum’ is a large vessel, here it represents a large digital repository. The Joint Information Systems Committee (JISC) is designed as an e-Learning repository for staff in UK Universities and colleges to share, reuse and re-purpose e-learning and teaching resources (Jorum) in 2005. Teaching and supporting staff create the repository and use it for preparing a lesson plan for students. Parts of this repository use DRM for security. Some materials of JORUM are free but some are protected by DRM [8]. JORUM uses two licenses, one allows re-purposing of content and the other does not.

D. FDRM

Federated Digital Rights Management (FDRM) [10] is a DRM solution in the field of education and research. The purposes of the FDRM project are to support local and inter-institutional sharing of resources in a discretionary secure and private manner and protecting the rights of user and creator. In FDRM rights records are written in XML. The FDRM has Resource Attribute Authority, Object Attribute Resolver, License Service and Resource Manager Components for secure content delivery using PGP or JSP and an Apache module or in JAVA. In the next section we will now describe DRMSDE system model.

E. EduSource

eduSource is a project by Canadian public-private partnership for the network of learning objects in French and English language and accessible to all Canadians for DRM implementation in eduSource. New Brunswick Distance Education Network (NB DEN) one of the partners of eduSource plays a lead role [11]. eduSource is designed to support multiple DRM models, including free access, co-operative sharing, fee-based, subscription-based, etc. [8]. In eduSource Open Digital Rights Language (ODRL) and XML are used in implementing DRM.

F. COLIS

The Collaborative Online Learning and Information System (COLIS) is a distributed online learning project incorporated with DRM and funded by the Australian Federal Government Department of Education Science and Training (DEST) in the year 2002 [8]. The learner enters into the system with login ID and password and session length. After successful login, the learners see their names on the title and select course under courses. The learner chooses DC for access but before accessing the content an “End User License Agreement and Copyright notice” is displayed that show some copyright related terms and conditions. If the learner has the access right then he or she uses it. Otherwise, Digital Right Error will occur [12].

III. DRMSDE SYSTEM MODEL

The DRMSDE is a prototype model for securing DE in which the rights of different users are properly maintained. In our system, the major components are users, DC and roles/rights of users on Digital material. In this section we explain each component in details as follows:

A. Users

Presently in DRMSDE we allow following three types of users to use the system which are:

- 1) *Administrative manager*: An Administrative manager is a group of experts who control the entire system.
- 2) *Learner*: A group of knowledge-seekers/students, i.e. consumers of our system.
- 3) *Content creator*: Content Creators are a group of teachers who create content, i.e. they are producers of DC on different topic for different subject in a particular course and inform learners about their creations periodically.

B. Tutorial

The core component of DE is its tutorial. In our proposed system we broadly classify tutorials into two types: one is DE tutorial and another is advanced tutorial. The DE tutorials are provided by the DE authority to users that has valid DRM code. Advanced tutorials are also maintained by the DE authority but for accessing advanced tutorials, learners have to purchase a license key from DE authority. After getting the license key learners are able to use both tutorials related to his/her course because a DRM code is given to all registered users. The concept of DE tutorial and Advanced Tutorial are similar to textbooks and reference books for a particular subject.

C. Roles of Users

Roles of a user are determined on the basis of what the user may do. Roles of our users are:

- 1) *Administrative manager*: Administrative Managers are the super user of DE System. They assign Access rights to other users of the system and fully access the entire DC and other databases.
- 2) *Learner*: The Learners can view; download copy and print DC related to their course for a specified period of time but cannot erase and modify DC.
- 3) *Course creator*: Course creators are group of teachers responsible for creating, managing and modifying tutorials.

In the next section we will describe DRMSDE system Architecture.

IV. DRMSDE SYSTEM ARCHITECTURE

Proper rights management is essential for the implementation of DE successfully. The main objective of our proposed Multi-Agent based DRMSDE system is to provide a secure environment in which authorized Learners can freely access their own DC according to their rights, needs and their own convenience. Our proposed system is shown in Fig. 2. The agents of our system that perform various operations are Learner Agent, Content Creator Agent, Administrative Manager Agent and Authentication Agent.

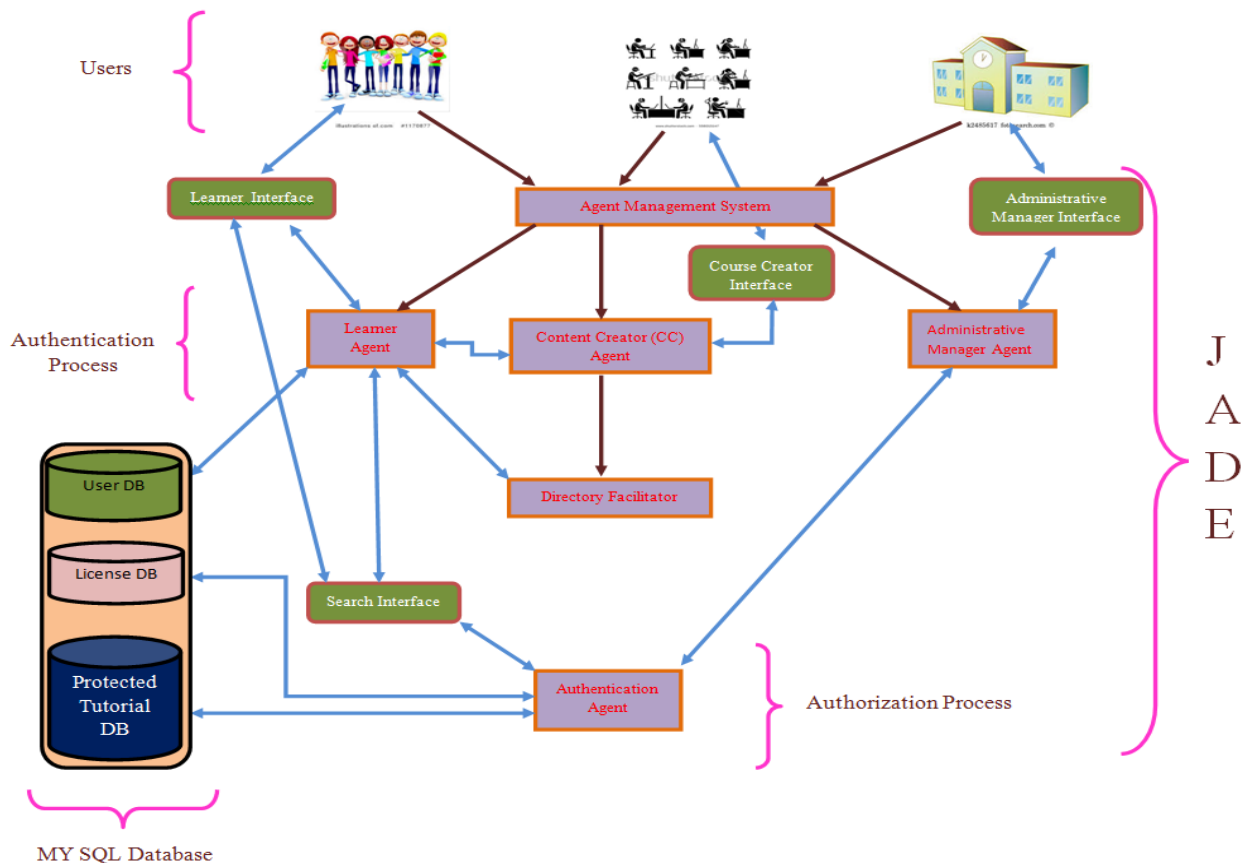


Fig. 2. DRMSDE System Architecture.

Each individual agent is now described below:

1) *Learner Agent*: It Receives UserId and Password from Learner interface and checks the authenticity of a user by communicating with the user database. The Learner Agent communicates with a Directory Service Agent for available Content Creator Agents and communicates with appropriate Agents for the tutorial requested by the Learner.

2) *Content Creator (CC) Agent*: CC Agent receives UserId and Password from CC Interface and matches these with the UserId and Password of Content Creator stored in the user database and display an appropriate message to CC. CC agents register to Directory Service Agent (DSA) so that Learner agent can find them when required. CC Agents create tutorials of a different type for different courses and inform the learners about the tutorial for access through DSA. Tutorials are available in two forms one is paid and other is free.

3) *Administrative Manager Agent (AMA)*: Like Learner and Content Creator Agent, Administrative Manager Agent also receives UserId and Password from its Interface and checks the authenticity of administrative Manager through User Database. AMA registers Learners and Content Creators. It also initiates Authorization Agent when Learner wants to access tutorial.

4) *Authorization Agent*: This agent is responsible for authorizing the learners when he or she tries to access the tutorial. Our system provides two modes of tutorial access one is free and another paid. To access the free tutorial, learners have to enter DRM code, which is a code given to the Learner by our system at the starting of each semester. DRM code is course and semester specific. Authorization agent matched DRM Code with free tutorial and after proper verification from database Agent allow learner for access. In case of paid tutorial Learners have to follow License procedure with AMA and with License Key Authorization Agent authorizes the Learner for the paid tutorial. Besides the above agents, when the main container is launched, two agents, which are Agent Management System (AMS) and Directory Facilitator (DF) are automatically started by JADE. All the user defined agents are initiated by AMS [13]

5) *Agent Management System (AMS)*: Basically AMS supervises the entire JADE platform. It is the contact point for all agents that need to interact in order to communicate with each other. All agents contact each other through AMS.

6) *Directory Facilitator (DF)*: DF is the agent that implements yellow page service used by any agent wishing to register its service for other available services. In our system agents are registered with DF and Learner request the DF for a list of active CC agents. The JADE DF accepts subscriptions from agents that wish to be notified whenever a service registration is made that match some specified criteria. In the next section we will now discuss DRMSDE system Implementation.

V. DRMSDE SYSTEM IMPLEMENTATION

MAS can be built with any programming language [14], but Object Oriented Programming Language is better because the concept of objects and agents is similar to some extent. Besides programming language, the software platforms and frameworks are key to implement MAS. The platform provides a middleware to support execution and other essential operations. For our System Implementation, we are using popular Windows 8.0 operating system. JAVA, a powerful Object Oriented Programming Language for system development, for the database we are using MYSQL and for agent interaction JADE 3.4 is used. We choose JADE [15] to build our system because of the following reasons:

- JADE is one of the best modern agent environments.
- JADE is capable to work on distributed and heterogeneous platform.
- JADE is open source software compliant with FIPA specification.
- JADE architecture matches with our system requirement.
- JADE simplifies development of agents and their communication.

A. System Execution [16, 17]

To see the working of agents in our DRMSDE we need to execute the system. When we run our Agent-Based DRMSDE system then JADE environment demanded user id and password for authentication of administrative manager agent. This creates administrative manager agent and start Administrative manager GUI (see Fig. 3) and JADE environment (see Fig. 4) are displayed.

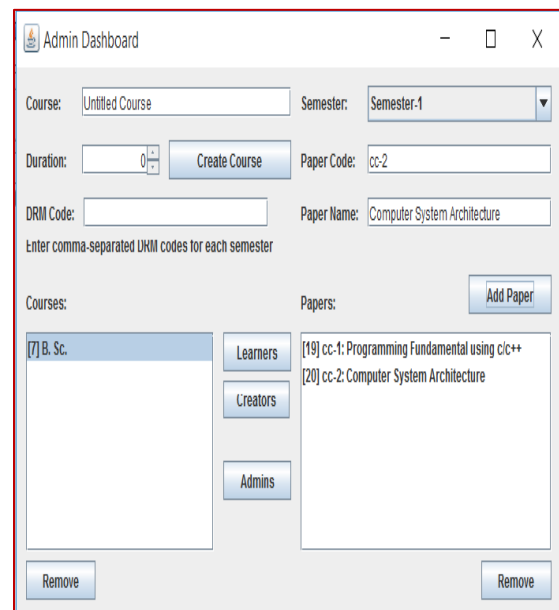


Fig. 3. Administrative Manager GUI.

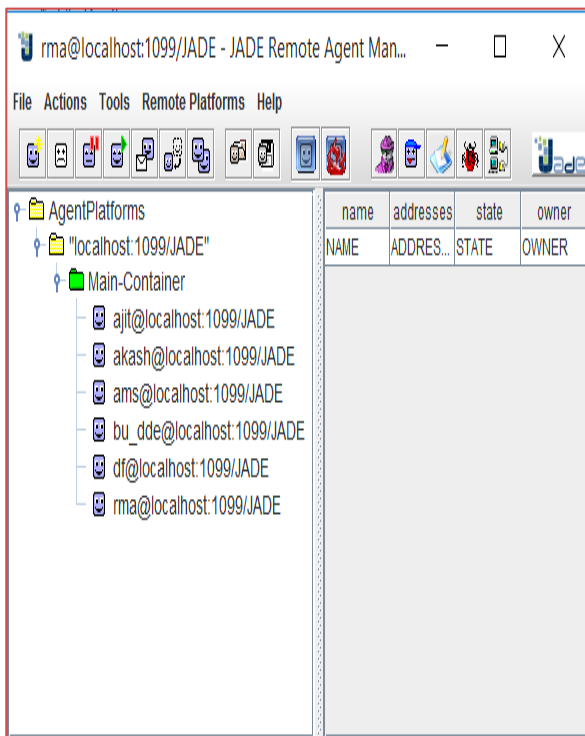


Fig. 4. JADE Environment.

From the administrative manager GUI, admin can create different courses, enroll Learners (see Fig. 5) to various courses and register content creators (see Fig. 6) into our system who provide audio, video and text tutorial in two modes free and paid.

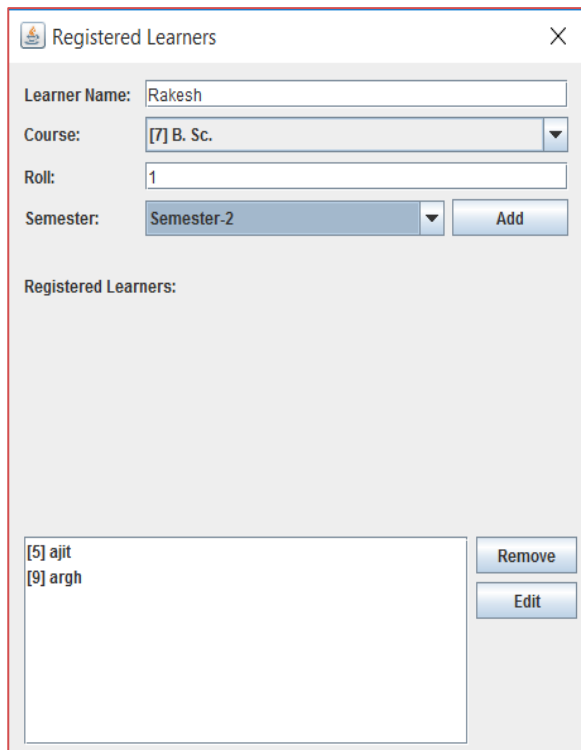


Fig. 5. Learner Enrollment.

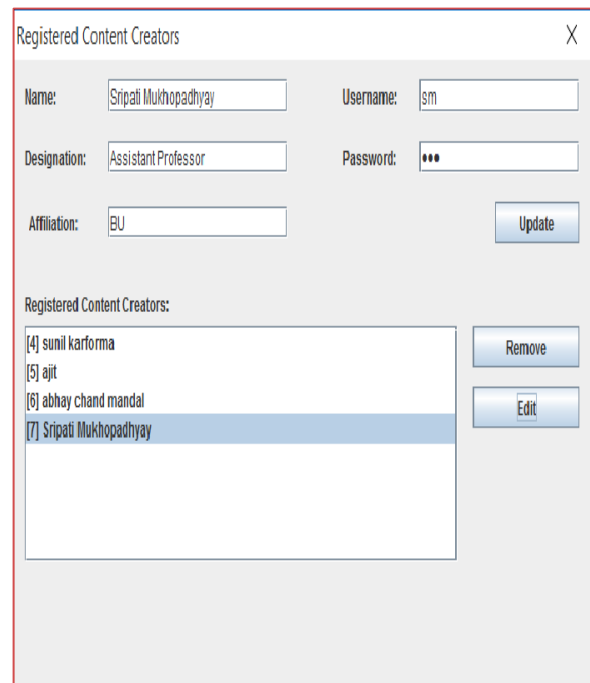


Fig. 6. Content Creator Registration.

After successful enrollment of Learners and registration of Content Creator each content creator prepares tutorials (see Fig. 7) on different topic of different courses and semester.

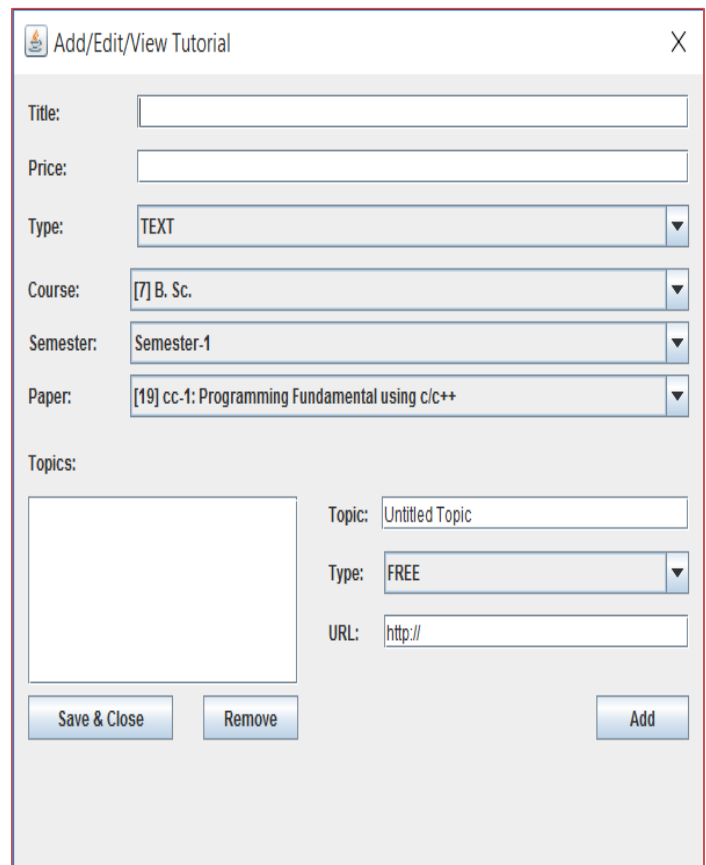


Fig. 7. Tutorial Management.

When tutorials are managed by different content creators then content creators' create their agent by using JADE environment and for authentication process, they provide valid user id and password. Now Learners have created their own agents by providing authentic user id and password to JADE environment. After entering into the system search tutorial GUI helps Learners to search tutorial (Fig. 8)

level view via dynamically created traceable workflow diagrams. The sniffer view of our DRMSDE system is shown in Fig. 10.

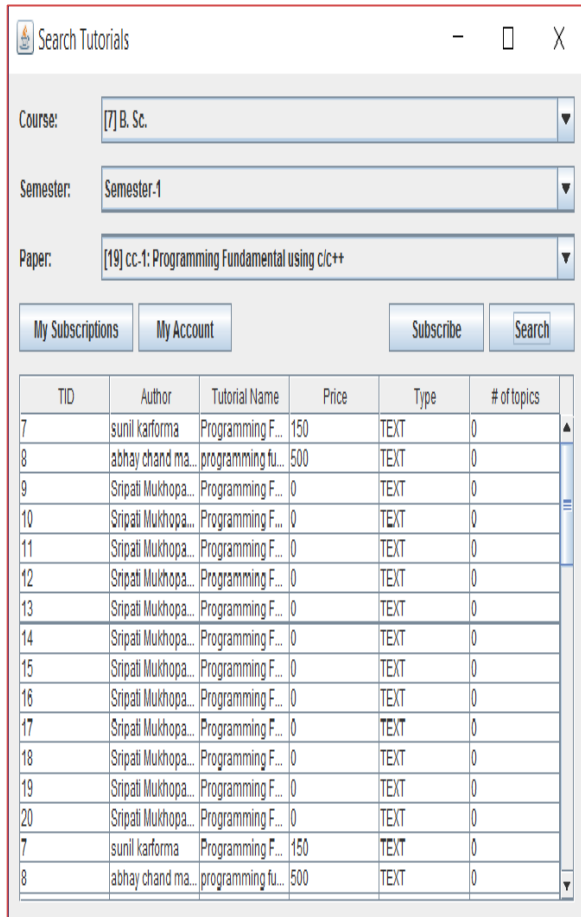
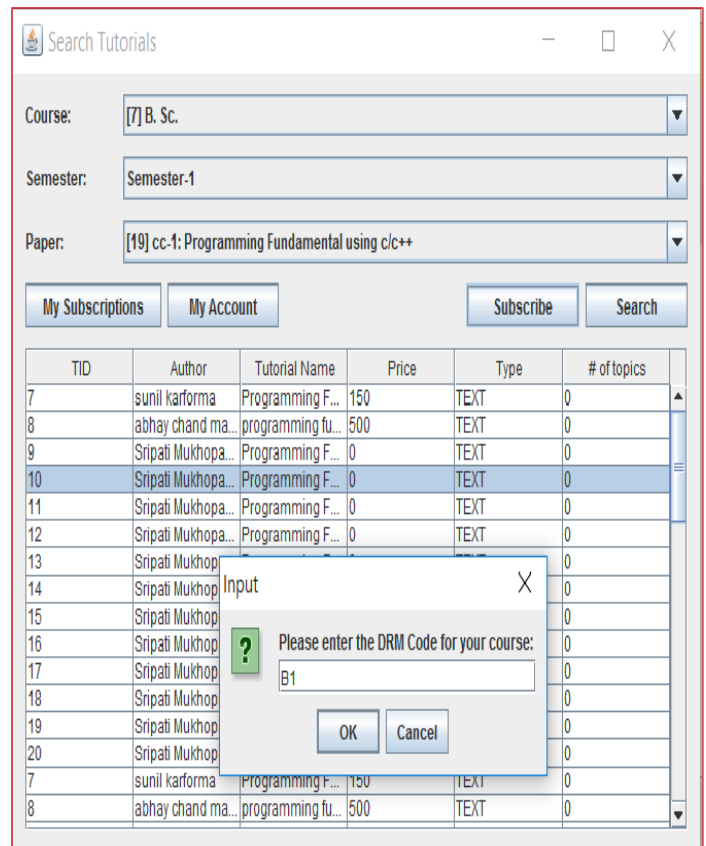


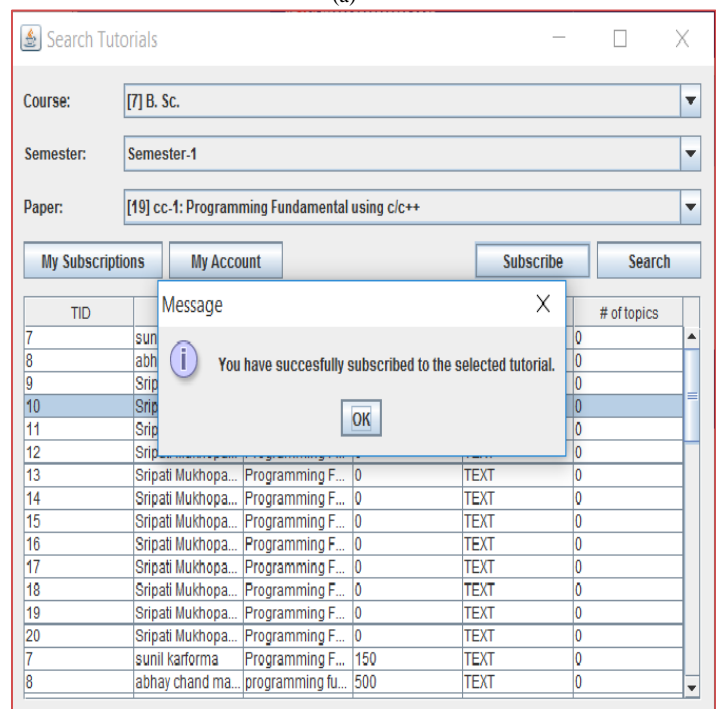
Fig. 8. Search Tutorial

When Learner enters their course, semester and paper for which tutorial is required then DF Agent provides all the details of the CC agents. It is up to the Learners to choose paid or free tutorials. After selecting tutorial if it is free, then learners need to enter DRM CODE (Fig. 9(a) & (b)) and for paid tutorial License Key is required for authentication process then only tutorials are accessed by Learners according to their rights. But if DRM CODE and License key are not matched which means Learner is not authorized to access tutorial then access denied message is displayed.

The most exciting property of Agent is their ability to communicate with each other. Agents are communicated with different agents by sending and receiving messages. These things can be easily expressed by JADE's built-in sniffer. This sniffer is a tool that receives messages from all agents in the system, reasons for the information, and presents it from different points of view. The tool is able to visualize messages as a low-level UML sequence diagram and provides a high-



(a)



(b)

Fig. 9. Authentication using DRM CODE.

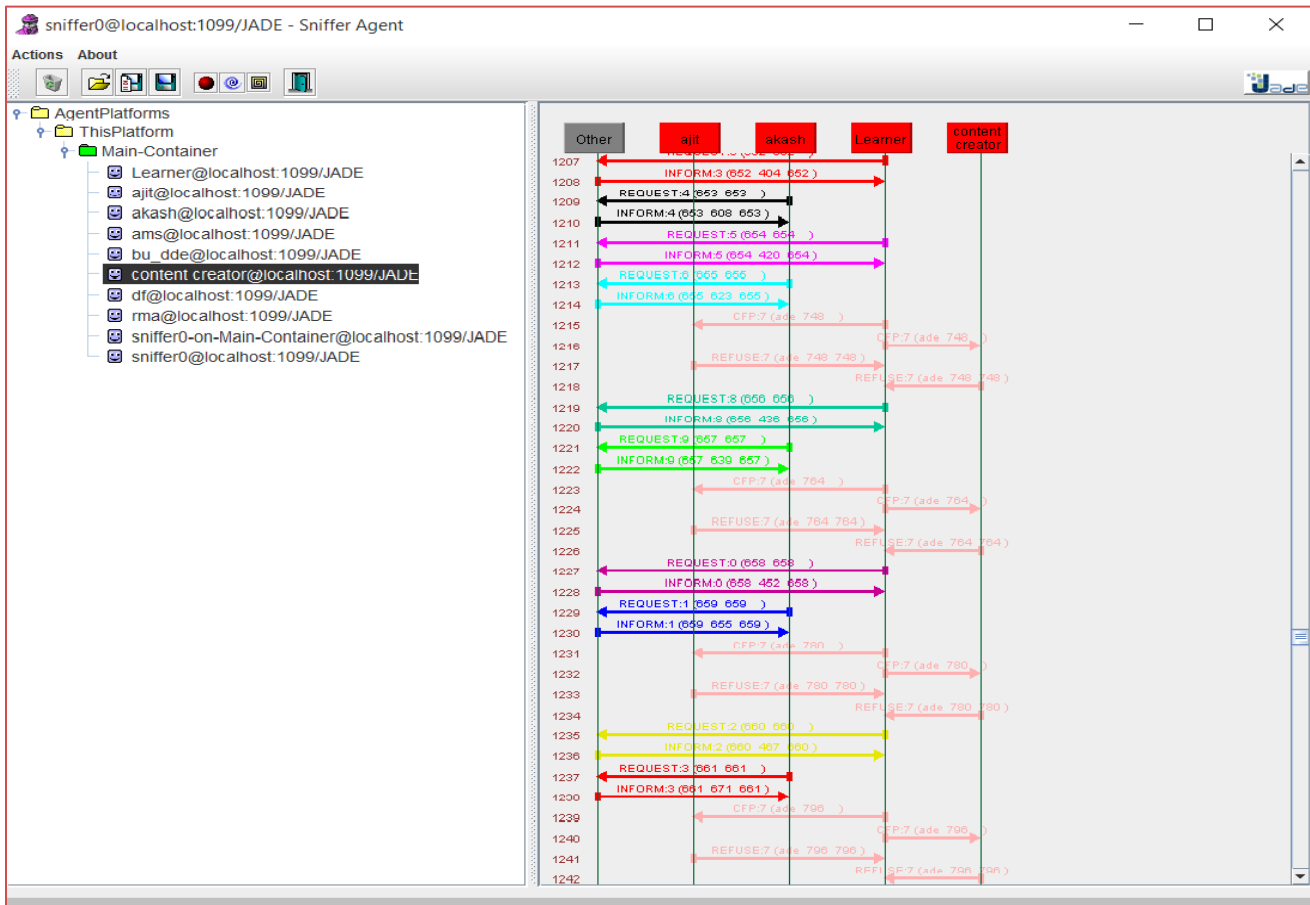


Fig. 10. Sniffer Agent.

B. System Classes

In our system we have implemented ContentCreatorAgent , LearnerAgent and UniversityAgent classes for creating ContentCreator , Learner and Administrative Manager Agent respectively with the help of JADE built in AMS agent . Agent communications are also initiated by AMS. Agents need interface to perform some action through actionPerformed(...) methods. ContentCreatorGUI, LearnerGUI and UniversityGUI classes are used for ContentCreator , Learner and Administrative Manager Agent respectively. TutorialRequestPerformer class implements a ticker behavior which executes the Learner request on every tick. TutorialRequestServer class catches all incoming requests from Learner agents and replies to them accordingly and DBHelperclass interacting with database. Fig. 11 shows all the classes of our system.

C. System Database Model

We are using MYSQL database to fulfill our database requirements. The records of different users, tutorials as well as rights of different users are very efficiently managed by MYSQL. The snapshot of different tables and their interactions are shown in Fig. 12.

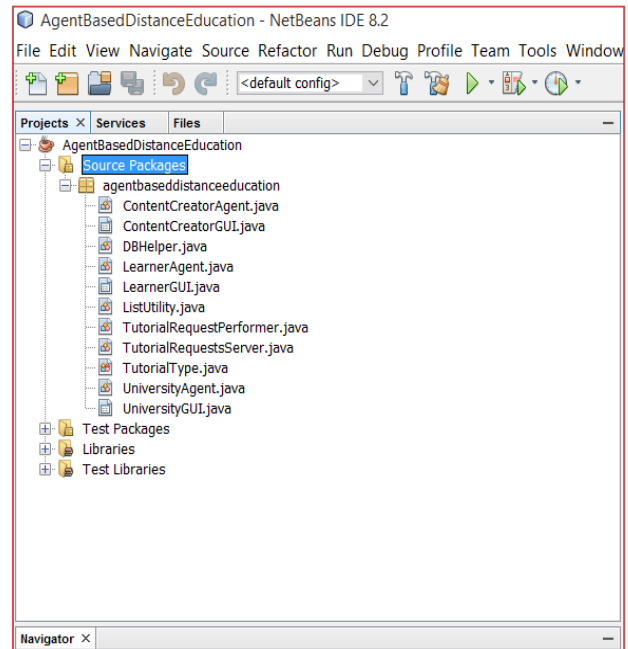


Fig. 11. System Classes.

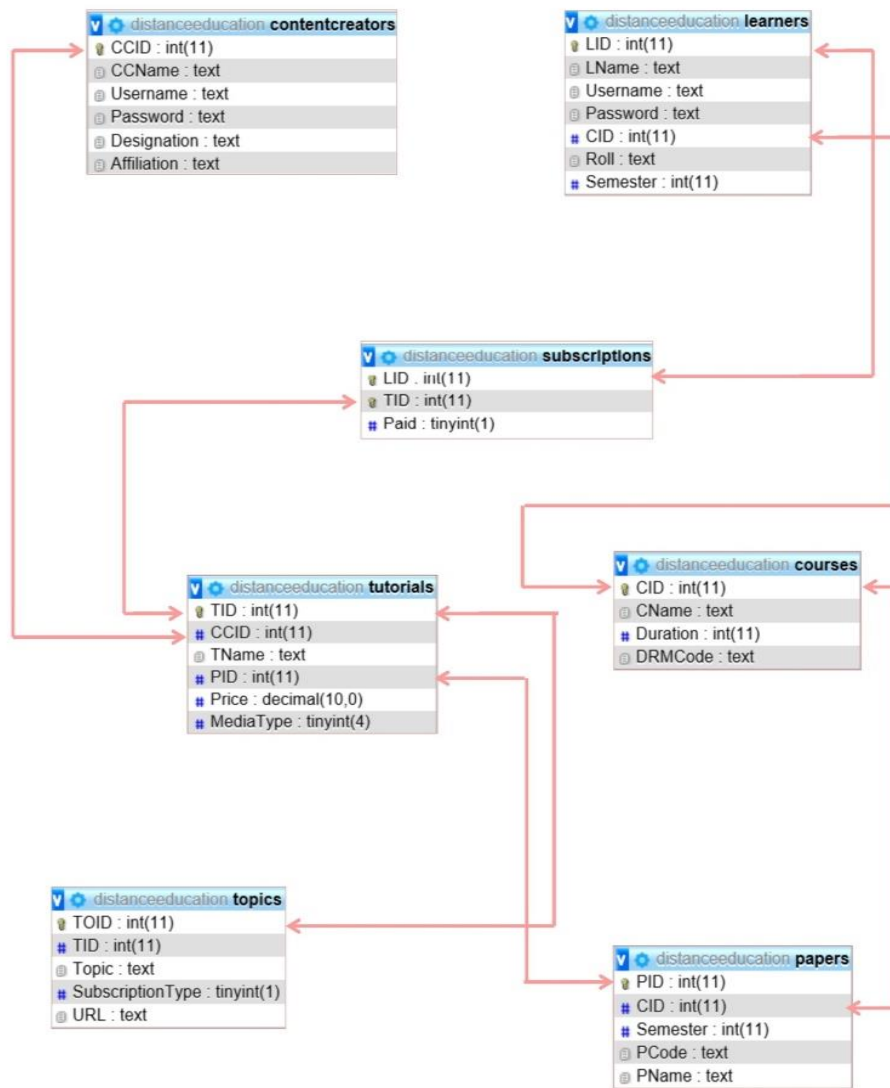


Fig. 12. DRMSDE Database.

VI. LIMITATIONS OF DRMSDE

Though our system is doing well with DE domain we have noted a few limitations of our study. In this section we are highlighting them:

- Our system allows only three types of users.
- If an unauthorized user tries to enter into the system then such entries are not noticed by the Administrative Manager.
- After the authentication and authorization process if a user download tutorial then our system has no control on that tutorial.

VII. SYSTEMS COMPARISONS

Now we compare DRMSDE with some of the existing MAS based education system and the results are represented by Table I.

From Table I, it is clear that except ABITS and BOKHARI-IMBLS other intelligent systems are not considered rights management into their systems. In ABITS, DRM is used partially were as in BOKHARI-IMBLS security agent is used for DRM. Our system has also authentication agent for DRM. Now we compare our system with BOKHARI-IMBLS, see Table II.

We think rights management is an important issue for the quality of DE and we focused fully on DRM in it that manages rights of the different user of the system.

Our goal is to protect DC from an unauthorized user and monitor the activity of authorized user so that learner cannot misuse the DC and use according to their rights. Whenever a learner is completed it course its accesses rights have become invalid.

TABLE I. SYSTEMS COMPARISONS

NAME OF SYSTEM	PURPOSE OF DEVELOPMENT	PROPOSED BY / DEVELOPED BY	TECHNOLOGICAL TOOLS	NAME OF AGENTS	DRM
ELECTROTUTOR [18]	MULTI-AGENT BASED E-LEARNING SYSTEM FOR DISTANCE LEARNING ENVIRONMENT	DISTRIBUTED INTELLIGENT LEARNING ENVIRONMENT	JADE, KQML	PEDAGOGICAL , COMMUNICATION , STUDENT MODEL , REMOTE	NO
AGENT BASED INTELLIGENT TUTORING SYSTEM(ABITS) [19]	ADOPTIVE WEB-BASED TUTORING SYSTEM	NICOLA CAPUANO, MARCO MARSELLA , SAVERIO SALERNO	HTML, VRML, CLASS, XML/RDF [10]	EVALUATION, AFFECTING AND PEDAGOGICAL	PARTIALLY NO AGENT FOR DRM
BAGHERA[20]	A WEB BASED ENVIRONMENT FOR TEACHING GEOMETRY PROOF	CARINE WEBBER , LORIS BERGIA, SYLVIE PESTY AND NICOLAS BALACHEFF	JATLITE, FIPA-ACL	STUDENT'S PERSONAL INTERFACE, TUTOR, MEDIATOR, TEACHER'S PERSONAL INTERFACE ,ASSISTANT	NO
MAS-PLANG[21]	TEACHING SUPPORT UNIT	CLARA-INÉS PEÑA, JOSE-L MARZO, JOSEP-LLUIS DE LA ROSA	JADE, JAVA SCRIPT, XML, RMI, CGI, FLASH	SONIA, SYNTHETIC, USER , DIDACTIC , SUPERVISOR , PEDAGOGIC, CONTROLLER, EXERCISE ADAPTER	NO
EMOTIONAL MULTI-AGENTS SYSTEM FOR PEER TO PEER E-LEARNING (EMASPEL) [22]	COLLECTIVE AND COLLABORATING E-LEARNING SYSTEM ON THE PEER TO PEER NETWORK	MOHAMED BEN AMMAR , MAHMOUD NEJI, ADEL.M ALIMI	MADKIT , JXTA	INTERFACE, EMOTIONAL, CURRICULUM , TUTOR , THE EMOTIONAL EMBODIED CONVERSATIONAL	NO
AGENT-BASED APPROACH TO DYNAMIC ADAPTIVE LEARNING (ABDAL)	WORKS FOR DISTANCE EDUCATION ENVIRONMENT	SHANGHUA SUN, MIKE JOY, AND NATHAN GRIFFITHS	APPLETS [23]	PREFERENCE , ACCOUNTING , EXERCISE, TEST	NO
ALLEGRO [24]	TO SUPPORT TEACHING LEARNING PROCESS	ROSA M. VICCARI, DEMETRIO A. OVALLE, JOVANI A. JIM'ENEZ	CASE BASED REASONING, LEARNING OBJECT, COLLABORATIVE FEATURE	TUTOR , STUDENT , INTERFACE, EXPERT, DIAGNOSIS, COLLABORATIVE	NO
BOKHARI INTELLIGENT MULTI-AGENT BASED E-LEARNING SYSTEM (BOKHARI-IMBLS) [9]	WEB-BASED INTERACTIVE E-LEARNING SYSTEM DESIGNED FOR THE DISTANCE LEARNING ENVIRONMENT	MOHAMMAD UBaidULLAH BOKHARI AND SADAF AHMAD	PROMETHEUS METHODOLOGY	STUDENT INTERFACE AGENT, TUTOR INTERFACE AGENT, COLLABORATION AGENT , INTELLIGENT DECISION SUPPORT AGENT , TEST/EVALUATION AGENT , LESSON PLANNING AGENT AND SECURITY AGENT	YES

TABLE II. BOKHARI-IMBLS vs. DRMSDE

	BOKHARI-IMBLS	DRMSDE
No of User	This System allow two users	DRMSDE allow three user
Right Management of Users	Not Consider	Rights Management is key to our system
Encryption of DC	Advanced Encryption Standard, or AES, is used to encrypt database	Development of encryption technique for DC is under process.
Security	Achieved by login id and password	DRMSDE has two level of security Authentication is done by user id and password Authorization is done by DRM code

VIII. CONCLUSION

DE and DRM are two popular domains of research. In this paper, we used both of them and implement a Multi-agent based model called DRMSDE using JADE. Our main objective is to protect DC from unauthorized users and also promote fair use of DC among authorized user. For DRM here we use Authentication and Authorization model that is widely accepted in the domain of education. Different users of the system are guided by intelligent Agents at each level so that we protect our system from unauthorized access efficiently. Agents interact with the database to verify the users' authenticity and authorization. After successful verification agents allow users to access the database. Though rights of the user may depend on institutional policy and our system is ready to easily accommodate those changes by modifying Agents or introducing new Agents if required. Our purpose is to increase security, quality, trust, and accessibility of DE with intelligent agents. The rights of users are solely maintained in our system. In future to enhance the quality of DRMSDE we will design some agents in our system that constantly monitors our system and inform the administrative manager if some unauthorized users are trying to access our DC, and for protection of DC we will develop a suitable encryption and decryption technique.

ACKNOWLEDGMENT

I acknowledge Prof Ahmet ŞANSLI for answering my questions related with his system EDU-DRM and allow me to access his paper "EDU-DRM: A digital rights management (DRM) system for K-12 education" which in press.

REFERENCES

- [1] A. Ozmen , A. Şansli , V. H.Şahin "EDU-DRM: A digital rights management (DRM) system for K-12 education" *ScientiaIranica* , in press.
- [2] N. Mclean, R. Iannella, "Digital rights management (DRM) in education – the need for standardization", Australian IMS Centre, 2002
- [3] A K Singh, S Karforma, S Mukhopadhyay, " Intelligent digital rights management system for distance education (DRMSDE) using multi-agent system", International Journal of Mechanical Engineering and Technology (IJMET) Vol. 9, Issue 10, pp. 429–437, October 2018.
- [4] J. Xie , C. C. Liu, "Multi-agent systems and their applications", Journal of International Council on Electrical Engineering. Vol. 7 , Issue 1, pp 188-197, 2017.
- [5] T. Manev , S. Filiposka, "Semantic aware multi-agent system advantages", International Journal of Informatics and Communication Technology (IJ-ICT), Vol. 3 , Issue 1, pp 1-12, 2014.
- [6] F Bellifemine, F. Bergenti, G. Caire, A. Poggi , "JADE- A JAVA agent development frame work", Springer , Multiagent Programming, Vol. 15, pp. 125-147, 2005.
- [7] A K Singh, S Karforma , S Mukhopadhyay, "A survey on digital rights management in distance education", 1st International Conference on Innovations in Computer Science (ICICS-2018), India, 21st and 22nd December 2018,
- [8] Collier , R Robson , "Digital Rights Management for Research and Education", Article , December 2, 2004.
- [9] M. U. Bokhari , S. Ahmad , " BOKHARI- Intelligent Multi-agent based e-Learning System (IMBLS) for Interactive Distance Learning" , Advances in Computer Science and Information Technology (ACSIT) , Vol 1, No 1, pp. 21-26 October, 2014
- [10] M. Martin , G. Agnew , D. L. Kuhlman , J. H. McNair , W. R. Rhodes , R. Tipton, "Federated Digital Rights Management" , D-Lib Magazine , Vol. 7 , Number 6, july/august 2002
- [11] R. McGreal, T. Anderson, G. Babin, S. Downes, N. Friesen, K. Harrigan, M. Hatala, D. MacLeod, M. Mattson , G. Paquette, G. Richards , T. Roberts , & S. Schafer, "EduSource: Canada's learning object repository network", International Journal of Instructional Technology and Distance Learning, Vol. 1, Issue 3, March 2004.
- [12] J. Dalziel, "Reflections on the COLIS (Collaborative Online Learning and Information Systems) demonstrator project and the "learning object lifecycle"", Winds of Change in the Sea of Learning: Proceedings of the 19th Annual Conference of the Australasian Society for Computers in Learning in Tertiary Education, Auckland, New Zealand , pp. 159-166, 2002.
- [13] F. Bellifemine, G. Caire, D. Greenwood, " Developing multi-agent systems with JADE", John Wiley & Sons Ltd, 2007.
- [14] V. Sandita, C. I. Popirlana , "Developing a multi – agent system in Jade for information management in educational competence domains", 2nd Global Conference on Business , Economics , Management and Tourism , Science Direct , pp. 478-486, Prague , 2014.
- [15] J. Su , C. Y. Wu, "JADE Implemented mobile multi-agent based , distributed information platform for pervasive health care monitoring", Elsevier Applied Soft Computing, Vol. 11, Issue 1, pp 315-325, 2011.
- [16] A. Gupta , D. K. Srivastava , S. Jain, "Auction System for automated E-commerce : Jade based multi-agent application", International Journal of Engineering and Computer Science, Vol. 5, Issue-09 , pp 18019-18024 , 2016.
- [17] Y. Etene , P. Owoche , R. Oboko " A multi-agent system to support ICT based distance learning through modeling of learner needs : the case of bahelar of education at the University of Nairobi", IOSR Journal of Computer Engineering , Vol. 18, Issue-5 , pp 26-31, 2016.
- [18] Ricardo Azambuja Silveira, Rosa Maria Vicari , Developing Distributed Intelligent Learning Environment with JADE – Java Agents for Distance Education Framework , Proceedings of the 6th International Conference on Intelligent Tutoring Systems, Biarritz, France and San Sebastian, Spain, 2002, 105-118
- [19] S. Ahmad , Literature Review , Designing Multiagent Intelligent System for Interactive e-Learning, PhD Thesis. Aligarh Muslim University, India , 2014.
- [20] C Webber, L Bergia, S Pesty and N Balacheff, Baghera project: a multi-agent architecture for human learning, Proceedings of the Workshop Multi-Agent Architectures for Distributed Learning Environments, AIED2001, San Antonio, TX, USA, pp-12-17, 2001
- [21] Clara-Inés Peña, Jose-L. Marzo, Josep-Lluis de la Rosa, Intelligent Agents in a Teaching and Learning Environment on the Web, Proceedings of the 2nd IEEE International Conference on Advanced Learning Technologies, ICALT2002, Kazan, Russia , pp- 21-27, 2002.
- [22] M. B. Ammar , M. Neji , A. M. Alimi , Emotional multi-agents system for peer to peer elearning (EMASPEL), DIWEB'06 Proceedings of the 5th WSEAS International Conference on Distance Learning and Web Engineering, Corfu Island, Greece, pp- 164-170 , 2005.
- [23] S. Sun, M. Joy, N. Griffiths, An agent-based approach to dynamic adaptive learning, in Agent Based Systems for Human Learning (ABSHL) Workshop, the 4th International Joint Conference on Autonomous Agents and Multi Agent Systems (AAMAS), Utrecht, Netherlands, pp-48-58, 2005.
- [24] R. M. Vicari, D. A. Ovalle, J. A. Jimenez, ALLEGRO: Teaching/Learning Multi-Agent Environment using Instructional Planning and Cases- Based Reasoning (CBR), in Centro Latinoamericano de Estudios en Informática (CLEI) Electronic Journal, vol 10 , issue 1, paper 4, 2007.

A Review on Security Issues and their Impact on Hybrid Cloud Computing Environment

Mohsin Raza^{*1}, Ayesha Imtiaz^{*2}, Umar Shoaib^{*3}
Faculty of Computer Science and Information Technology
University of Gujrat, Gujrat, Pakistan

Abstract—The evolution of cloud infrastructures toward hybrid cloud models enables innovative business outcomes, twin turbo drivers by the requirement of greater IT agility and overall cost-containment pressures. Hybrid cloud solutions combine the capabilities of both public clouds along with those of on-premises private cloud environments. In order to key benefit with hybrid cloud model, there are different security issues that have been shown to address. In this paper, we explain security issues in detail such as to maintain trust and authenticity of information, Identity management and compliance which is influencing in enterprises due to migration of IT cloud technologies are increasingly turning to hybrid clouds. Here, work outcomes with comparative study of different existing solution and target the common problems domains and security threads.

Keywords—Hybrid cloud; migration; security issues; security techniques

I. INTRODUCTION

Cloud computing topic has lot of rapid innovation on Internet from cloud service provider such as Amazon, Open Stacks EC2, through different types of virtual data centers operate across different types of IT environments. Gaining the several benefits, cloud computing provides a more elasticity enabling the on demand approach to an elastic pool of shared computing [1], [2]. In the past few years, several business enterprises are go mainstream that by rapid provisioning the cloud resources and to leverage the scale inherent in IT Infrastructure to cut costs and modernize IT operational for service delivery requirements rather than need of purchasing their own expensive IT infrastructure.

Today many enterprises for cost savings IT cloud technologies are increasingly turning to hybrid clouds, allowing them to combine the benefits of building private and public clouds as well as to leverage the scale inherent in their existing IT Infra-structure to cut costs and modernize IT operational agility for service delivery requirements.

Recently, survey covered that many enterprises are rapidly adopting a multi-cloud approach using different cloud service vendors to support their IT infrastructure [3]. According to survey respondents, Microsoft Azure use 58%, and Amazon Web Services use 52% as their cloud platforms providers. Additionally, Google Cloud use 19%, Oracle Cloud use 9%, and RackSpace use 7.3%.

Hybrid cloud computing is about aggregation and integration of computer, networking, applications, storage, security and management into unified, orchestrated management framework which enables enterprise IT and developers to leverage scale, flexibility and cost savings of existing in-house IT investment tools, systems and privacy policies scale to manage in the enterprise data center with their newly adopted cloud services[4], [5]. The IDC report predicts more than 80 per cent of IT enterprises will commit to hybrid architectures [6]. Hybrid models are shown in Fig. 1.

A Hybrid cloud includes a few addition features as discussed below.

A. Integration of Infrastructure and the Application Environment

Hybrid cloud platform is the capability spinning up workloads or virtual machines for infrastructure as a service same in both private and public clouds.

B. Interconnectivity

The parallel processes in which two coexisting environments communicate and interact facilitate the exchange of data, VMs and applications among individual clouds.

C. Portability of Applications

Using cloud aware development builds systems from reusable components that will work the same across cloud environments.

D. Monitoring and Management across Cloud Environments

In a Hybrid clouds, monitoring and management is essential for the health of the system, visibility into system health across clouds is crucial

In spite of such significant benefits, migration of IT cloud technologies from enterprises have important aspect over privacy, integrity, security concerns and compliance considerations due to reliability on multi cloud vendors such as Microsoft, Amazon and Google [7]. The descriptive study in this paper is summarised with a view to discuss and different security issues that have been shown to address. The approaches to counter security issues in Hybrid model are numerous with huge risks which have been kept out of scope [8].

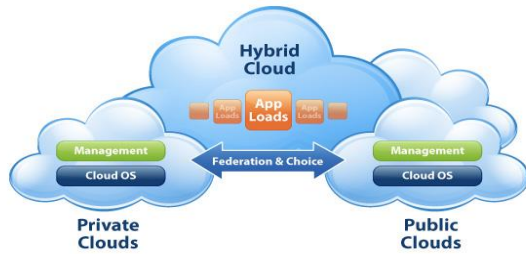


Fig. 1. Hybrid Cloud Model.

There are different security issues such as Data protection, migration issues, security management policy, to maintain trust and authenticity of information, Identity management and compliance and shared technology are the major security issues [9]. The rest of the paper is summarized as follows. In Section 2, we give an overview on work outcomes with comparative study of different existing solution and target the common problems domains and security threads from cloud, incompatible network policies. Section 3 presents hybrid cloud approach, there are different security issues that have been shown to address. Section 4 presents the conclusions of this research.

II. RELATED WORK

Security in the hybrid cloud is still a major concern for many IT organizations.

Undale et al. [10] describes comparison and performance review of AES, Blowfish and RC6 Symmetric cryptographic algorithm in hybrid cloud application with standard cryptographic techniques, such as Proxy encryption, ABE (Attribute based encryption) with its types. To make an efficient solution and to make an NP Complete solution of image encryption problem on hybrid cloud environment.

Gharat et al. [11] introduce several techniques have been developed for secure data and authentication and to maintain trustworthiness. For trust management system using feedback filtering approach will be explained. In this paper addresses different methods for data protection includes Single Encryption, Multitenancy and Multi level Virtualization, Authentication model including several scenarios.

Rao et al. [12] discusses big data Security using Hybrid Cloud are widely used, the traditional cryptographic methods are not suitable for big data. We are implementing the modified approach for the image and text encryption using method in which image is cut down into pieces and their pixel values get modified by using noise values. We proposed a approach for the efficient decryption technique by keeping the existing shuffling technique. With the encryption technique we have used steganography for text data storage. In this

paper, our aim is to achieve the image and text data privacy using hybrid cloud.

Sanjay et al. [13] focused on to identify the security threats in a hybrid cloud architectures for enterprises and suggested control method to access the data in Hybrid cloud approach using multi factor authentication from on-premises Active Directory. Federated Identities between on premises directory solution using Federated ID for the Identity infrastructure services is detailed. This paper suggests a security solution, which leveraging Active Directory Federation Services from the security of their user credential for organization, by creating Federated Trust Framework. To achieving federation trust is relying on various authentication servers such as Microsoft Active directory services.

Anukrati and Dubey et al. [14] address some challenges to consider when migrating to hybrid clouds and techniques can be addressed in hybrid infrastructure securities can be provide to protect encryption and decryption communication, key based security algorithms which are countered authentication and authorization techniques secured over the intra cloud communication in which an automatic, intelligent migration service in hybrid cloud relay on agent technology. In this research paper major areas of focus on a group of unified Identity & Access Management and privacy frameworks across cloud computing applications or services.

Hardayal and Shekhawat et al. [15] mainly concern the security risks and solutions in hybrid cloud computing for electronic governance. This study summarizes major security issues based on a precise literature review. Federated Identity in organizations for authentication of cloud service should address the challenges and solutions according to lifecycle of identity management, available authentication methods in trustworthy manner, integrity and confidentiality protection ensures. Data in transit is generally security risk lies, so encryption technique should be implies for data and finally suggests the feasible security solutions.

Patil et al. [16] introduce a secure Hybrid Cloud approach for encrypted deduplication of data using key generation. We propose secure hashing algorithm for avoiding deduplication, which generates a unique key for each file. The generated key is stored in private cloud and Key generation process involves inside the public cloud. For security consideration to encrypt the data before updating data into the cloud becomes necessary. For achieving authorized deduplication along with protect data security, hashing algorithm is used which makes technique very secure, to protect data from unauthorized access.

Following major problems are observed during the study. In the Table I below a comparative study about security issues in Hybrid cloud:

TABLE I. COMPARATIVE STUDY

S. No	Title	Author	Research	Year	Problem Domain
1.	Survey of Color Image Data Privacy in Hybrid Cloud	Bharati Kale, Onkar Undale,	How to improve performance and compare image data privacy with standard cryptographic algorithm and techniques in Hybrid cloud.	2015	To protect image data privacy
2.	Survey on Establishing Authentication Based Trust , Data Security in Hybrid Cloud	Dilip Motwani, Mithil Gharat,	Suggest different methods to protect data for Trust, Data Security, and Authentication including different scenarios.	2013	To maintain trust, protection of data security and authentication
3.	Big data Security using Hybrid Cloud	V.P Rao, Gaurav Khandar, Manas Kulkarni, Shubham Nayab	Big data Security by implementing the modified approach for the image and text encryption named as attributed based encryption for the protecting our data from the unauthorized access.	2015	A novel solution for securing the image and text data by using hybrid cloud
4	Discusses Security concerns for Enterprises Migrating to Hybrid Model	Sangwan, Sachin, Sanjay, Shabnam, Sunita Sangwan	In this research address the various security issues in Hybrid migration and Hybrid deployment proposed a solution for securing Authentication using federated ID for Federation identity in hybrid security.	2015	To identify the security issues for Enterprises in hybrid cloud.
5.	Addressing Security in Hybrid Cloud	Sandeep Sahu, Gunjita Shrivastava, Anukrati Dubey	Presents an automatic, intelligent migration service in hybrid cloud based on agent technology, Exploit migration service between our platform and ITRI public cloud on Hadoop.	2013	Proposes a secured intra cloud communication mechanism.
6.	Evaluation Hybrid Cloud in Electronic Government associated Security Risks Analysis and Solutions	D.P. Sharma and Hardayal Shekhawat	Various security issues identity, application, data, information, network and security issues and related solutions in current era that can decelerate its speed in government sector during adaptation.	2012	Security issues and solutions in Hybrid cloud especially for Electronic governance
7.	Survey on securely Hybrid Cloud Distributed Key Generation Authorization for Encrypted Data Deduplication	Navnath Kale, Akanksha Patil ,	Propose secure hashing algorithm for avoiding deduplication, which generates a unique key for each file and also use encryption techniques for security related to data from unauthorized access.	2015	To achieving authorized deduplication with protect data security

III. PROBLEM STATEMENT

The security issues in hybrid cloud include:

- Security controls and data protection
- Identity and access management
- Secure movement of data and workloads across data centers through transport security and network firewalls
- Securing data residing and processed in third-party environments through encryption and tokenization
- Compliance with regulatory and policy requirements
- Poorly constructed SLAs
- Reconfiguration issues
- Shared technology issues

Working with hybrid cloud still requires implementing proper data security and Integrity among these main security issues. In fact, Identity and Access Management involved in data security issues [17]. Data security refers to data confidentiality, integrity, authentication (CIA) in cloud [18].

A. Compliance with Regulatory and Policy Requirements

Not only you have to compensate public cloud and private cloud provider are in compliance audit practices, but you also must demonstrate coordination of other third parties or open-source tools between both clouds is compliant [19].

B. Poorly Constructed SLAs

Many cloud providers such as Amazon, Microsoft, Google and IBM support a large amount of customers by enhancing their web services. To make sure that public cloud provider can demonstrate the infrastructure meet those commitments, options and incentives detailed in the service level agreement (SLAs) [20]. To make trusted private cloud lives up to that similar to the SLA.

C. Reconfiguration Issues

Several issues are resulted due to migration of components from the private cloud to the public cloud due to reconfiguring components in hybrid cloud such as addressing, firewall and component placement [21].

D. Shared Technology Issues

Virtualization technologies are mostly approach in hybrid model [22]. VMWare, Microsoft Azure and Amazon EC2 Cloud Storage are few IT Infrastructure services. In virtualized environment, IaaS provider partitioned Virtual Machines (VMs) to multiple clients running on virtualization platform to access same physical server. There is a more prone for accessing data in one virtual machine from another virtual machine on same physical server [23].

Demonstrating threats in hybrid cloud security to introduce a secure authentication framework for hybrid cloud services is required [24]. So we will target numerous threats is shown in Table II and are as follows:

- Man in the Middle Attack (MITM) due to lack of encryption.
- Denial of Service Attacks (DoS) and Distributed Denial of Service Attacks (DDoS).
- Location certification attack.
- Cross Site scripting attack by inside attacker.
- Failure to identify and authenticate.
- Unprotected API exploits sensitive data to malicious attacks.

TABLE II. SECURITY THREATS IN HYBRID CLOUD ENVIRONMENTS

Attack	Description
Man in the Middle Attack	Attacker can modify and intercept communications and deploy third party involvement.
Smurf Attack	Attacker uses spoofed IP addresses for purpose of hiding the identity to generate flooded with traffic at the victim machine.
Denial of Service	DoS attacks try to render web service unavailable to users.
Side-Channel Attacks	Attacker gains information about the cryptographic technique.
Viruses and Worms	Attacker may use certain bad source code to compromise.
Tampering with data	An attacker may modify or fabricate information.
Cloud Malware Injection attack	Attacker inject implement of a maliciously service in cloud

IV. CONCLUSION

Hybrid cloud computing is inexorable paradigm where computing is on demand service of private and public both cloud. Emerging technologies related to any application should consider the several possible security threats. The various security issues presented would definitely useful the cloud users to suitable choice and hybrid cloud vendors to handle such kind of threats efficiently. Also, a study of hybrid model a framework of security and requirement of cloud security has been exploited and target with problem considerations. It continuously reduces burden of bulk of cost savings and complexity on users. Organization feels secure about their data against security considerations and fault interruptions. It suggests a robust way of serving user through modernize IT operational agility for service delivery requirements.

REFERENCES

- [1] Anupama Prasanth, "Cloud Computing Services: A Survey," International Journal of Computer Applications (0975 – 8887), Volume 46– No.3, May 2012.
- [2] Veerawali Behal and Rydhm Beri, "Cloud Computing: A Survey on Service Providers," International Journal for Innovative Research in Science & Technology| Volume 2 | Issue 10 | March 2016
- [3] Nitin Kumar, Shrawan Kumar Kushwaha and Asim Kumar, "Cloud Computing Services and its Application," Advance in Electronic and Electric Engineering, Volume 4, Number 1 (2014), pp. 107-112.
- [4] Caifeng Zou, Huifang Deng and Qunye Qiu, "Design and Implementation of Hybrid Cloud Computing Architecture Based on Cloud Bus," IEEE 9th International Conference on Mobile Ad-hoc and Sensor Networks, 2013.
- [5] M. Posey, "Journey to the Hybrid Cloud," White Paper Sponsored by: VMware, IDC #242798R2, September 2015.
- [6] "Hybrid Cloud 101: Hybrid Cloud Computing - Intel" Intel IT Center Solution Brief | The Path to Hybrid Cloud, September 2013.
- [7] K. Annappureddy, "Security Challenges in Hybrid Cloud Infrastructures," Aalto University, T-110.5290 Seminar on Network Security, 2010.
- [8] A. Dubey, G. Shrivastava and S. Sahu, "Security in Hybrid Cloud," Global Journal of Computer Science and Technology Cloud and Distributed, Volume 13 Issue 2 Version 1.0 Year 2013.
- [9] A. Kumar, "A Comparison of Security Challenges in Public and Private Clouds," International Journal of Latest Trends in Engineering and Technology (IJLTET), Vol. 3 Issue 3 January 2014.
- [10] O. S. Undale and B. Kale, "Achieving Big Data Privacy for Colour Images via Hybrid Cloud," International Journal of Innovative Research in Computer and Communication Engineering, Vol. 3, Issue 11, November 2015.
- [11] M. P. Gharat and D. Motwani, "Survey on Establishing Trust, Data Security and Authentication In Hybrid Cloud Computing," International Journal of Engineering Research & Technology (IJERT), Vol. 2 Issue 11, November 2013.
- [12] V. P. Rao, G. Khandar, M. Kulkarni and S. Nayab, "Big data Security using Hybrid Cloud," International Engineering Research Journal (IERJ), Volume 1 Issue 9 Page 957-659, 2015.
- [13] Sanjay, S. Sangwan, Sachin and S. Sangwan, "Addressing Security issues for Enterprises Migrating to Hybrid Cloud Computing Model," International Journal on Recent and Innovation Trends in Computing and Communication, Volume: 3 Issue: 6 Page 3618 – 3622, 2015.

- [14] A. Dubey, G. Shrivastava and S. Sahu, "Security in Hybrid Cloud," Global Journal of Computer Science and Technology Cloud and Distributed, Volume 13 Issue 2 version 1.0 Year 2013.
- [15] H. S. Shekhawat and D. P. Sharma, "Hybrid Cloud Computing in E-Governance: Related Security Risks and Solutions," Research Journal of Information Technology, 4(1): 1-6, 2012.
- [16] A. V. Patil and N. D. Kale, "A Secure Authorized Hybrid Cloud Distributed Key Generation for Encrypted Deduplication of Data," International Journal of Science and Research (IJSR), Volume 4 Issue 7, July 2015.
- [17] K. Subramanian, "Hybrid Clouds," A whitepaper sponsored by Trend Micro Inc, 2011.
- [18] S. Aldossary and W. Allen, "Data security, privacy, availability and integrity in cloud computing: issues and current solutions," Int. J. Adv. Comput. Sci. Appl., vol. 7, no. 4, pp. 485-498, 2016.
- [19] "Critical Security and Compliance Considerations for Hybrid Cloud Deployments," Advisory by 451 Research, Dec 2015.
- [20] J. Morin, J. Aubert and B. Gateau, "Towards Cloud Computing SLA Risk Management: Issues and Challenges," <https://www.researchgate.net/publication/232617525>, 19 May 2015.
- [21] M. Hajjat, X. Sun, Y. E. Sung, D. Maltz, S. Rao, K. Sripandikulchai and M. Tawarmalani, "Cloudward Bound: Planning for Beneficial Migration of Enterprise Applications to the Cloud," In SIGCOMM'10, August 30 - September 3 2010.
- [22] T. Pradhan, M. Patidar, K. Reddy and A. Asha, "Understanding Shared Technology in Cloud Computing and Data Recovery Vulnerability," International Journal of Computer SCiEnCe and technology, IJCST Vol. 3, ISSue 4, oCT - DeC 2012.
- [23] B. Singh, J. Singh and S. Kumar, "Virtualization Techniques and Virtualization Challenges in Cloud Computing: A Review," IJCAT - International Journal of Computing and Technology, Volume 2, Issue 6, June 2015.
- [24] A. Michael, A. Foladoyin and A. Oluyemi, "Threats to Hybrid Cloud Security," International Journal of Scientific & Engineering Research, Volume 9, Issue 2, February-2018.

Enhanced Random Early Detection using Responsive Congestion Indicators

Ahmad Adel Abu-Shareha¹

Information Technology and Computing Department
Arab Open University (AOU)
Riyadh, Saudi Arabia

Abstract—Random Early Detection (RED) is an Active Queue Management (AQM) method proposed in the early 1990s to reduce the effects of network congestion on the router buffer. Although various AQM methods have extended RED to enhance network performance, RED is still the most commonly utilized method; this is because RED provides stable performance under various network statuses. Indeed, RED maintains a manageable buffer queue length and avoids congestion resulting from an increase in traffic load; this is accomplished using an indicator that reflects the status of the buffer and a stochastic technique for packet dropping. Although RED predicts congestion, reduces packet loss and avoids unnecessary packet dropping, it reacts slowly to an increase in buffer queue length, making it inadequate to detect and react to sudden heavy congestion. Due to the aforementioned limitation, RED is found to be significantly influenced by the way in which the congestion indicator is calculated and used. In this paper, RED is modified to enhance its performance with various network statuses. RED technique is modified to overcome several disadvantages in the original method and enhance network performance. The results indicate that the proposed Enhanced Random Early Detection (EnRED) and Time-window Augmented RED (Windowed-RED) methods—compared to the original RED, ERED and BLUE methods—enhances network performance in terms of loss, dropping and packet delay.

Keywords—Congestion; random early detection; active queue management

I. INTRODUCTION

The evolution of the computer network and its broad usability for communication, remote controlling, organizational monitoring and information governing has resulted in the widespread utilization of its resources. Congestion is a phenomenon that occurs on a computer network when the traffic load exceeds the capabilities of these resources. The memory allocated by the network router is the most critical resource in the network that is susceptible to congestion, which can cause delays, packet loss and low network performance [1]. Congestion degrades the quality of services provided to the users and the applications. To predict congestion before it occurs, or before it starts to severely affect performance, various Active Queue Management (AQM) methods have been proposed. Although AQM methods were proposed to overcome the limitations of the first approach, i.e. Random Early Detection (RED)[2], RED is still the most commonly utilized method; this is because RED provides stable performance under various network statuses [3-6].

The AQM methods monitor the status of the router buffers, calculate the dropping probability (Dp) for each packet arrival, and implement packet dropping stochastically based on the calculated value. Accordingly, AQM methods take one of the two opposite decisions: packet accommodation and packet dropping. The role of the router is to accommodate the arrival packets to transfer them to the intended destination; However, to avoid congestion, packets are dropped when the buffer overflows and network performance degrading is expected [4]. Generally, the developed AQM methods consist of three main components: the congestion indicators used to monitor the buffer/network status, the function used to calculate Dp and the algorithm that determines when to use these equations and indicators [6]. For RED, Dp is calculated using a mathematical function with a reference to the average queue length (aql), a parameter that reflects the average length over time [7, 8].

The advantages of RED are summarized as follows: (1) RED predicts congestion before it affects network performance and reacts by dropping packets stochastically to avoid the effects of congestion; (2) RED, using random dropping, avoids global synchronization—a phenomenon that occurs when all senders reduce their transmission rates simultaneously for a period and then start increasing them again, also simultaneously; (3) RED uses aql to calculate the average queue length over time. Accordingly, when the arrival rate increases for a short while, aql does not increase rapidly. Thus, RED avoids dropping packets unnecessarily during short, heavy traffic [9]. Thus, the limitations can be summarized as follows: (1) RED exhibits low performance during sudden congestion, because it uses aql , which is insensitive to sudden changes in queue length; (2) RED causes packet delay in heavy traffic, because it does not monitor the router buffer delays [2, 9-11].

Using aql as a congestion indicator has its advantages and disadvantages. One advantage is that aql is able to avoid false, and thus deceptive, congestion indications. However, the disadvantages are the result of sudden high traffic and unexpected congestion. To overcome this disadvantage, it is recommended to use modified parameters that are equal to aql or to ease the dependency on aql to enhance network performance. However, RED is found to be badly influenced by the way in which the congestion indicator is calculated and used [4].

In this paper, RED is modified to enhance its performance with various network statuses. RED technique is modified to overcome several disadvantages in the original method and

enhance network performance. Enhanced Random Early Detection (EnRED) and Time-window Augmented RED (Windowed-RED) methods are proposed to address the problem of slow reaction time, and thus increase the number of queued packets in the buffer. The rest of the paper is organized as follows: Section II discusses the RED method in details and the disadvantages to be overcome are clarified. Section III presents the related work. The proposed Work is presented in Section IV; the simulation details are given in Section V and the related results is presented in Section VI. Finally, the conclusion is given in Section VII.

II. RED METHOD

RED is implemented, as given in Algorithm 1, in three stages; these are: (1) aql calculation, (2) Dp calculation and stochastic packet dropping, (3) buffer tracing.

Algorithm 1: RED

```

1  PARAMETER SETTING:  $w_q, Th_{min}, Th_{max}, D_{max}$ 
2  VARIABLE INITIALIZATION:  $aql:=0, count:=-1$ 
3  FOR-EACH A
4      1) CALCULATE  $aql$ :
5          IF ( $q$  equal to 0)  $\rightarrow aql:=(1-w)^{f(cTime-iTime)} * aql$ 
6          IF ( $q$  not equal to 0)  $\rightarrow aql:=(1-w)* aql + w_q * q$ 
7      2) CALCULATE  $Dp$  & IMPLEMENT packet dropping.
8          IF ( $min_{th} \leq aql < max_{th}$ )
9               $\rightarrow counter++$ 
10              $\rightarrow Dp'=D_{max} * (aql - Th_{min}) / (Th_{max} - Th_{min})$ 
11              $\rightarrow Dp = Dp' / (1 - counter * Dp')$ 
12             IF (Drop( $Dp$ ) is TRUE)
13                  $\rightarrow$  Drop-A,  $count := 0$ 
14         ELSE IF ( $aql > max_{th}$ )
15              $\rightarrow$  Drop-A
16              $\rightarrow counter:=0$ 
17         ELSE
18              $\rightarrow counter:=-1$ 
19     3) TRACE Buffer Idleness
20         IF ( $q$  equal to 0 &&  $Idle$  equal to False)
21              $\rightarrow iTime=cTime, Idle = TRUE$ 
22         ELSE  $Idle = False$ 

```

Parameters:

w_q : queue weight
 Th_{min} : minimum threshold
 Th_{max} : maximum threshold
 D_{max} : maximum probability value

Saved Variables:

A: current packet arrival
 Dp : packet-dropping probability
 Dp' : initial packet-dropping probability
 $cTime$: current time
 q : current queue size
 aql : average queue size
 $iTime$: idle time
 $Idle$: idle status true/false
 $count$: # of packets in medium buffer length that are not dropped. Count is a balanced parameter for Dp calculation

In the first stage, aql is calculated using two different equations. The first is used if the buffer is currently idle (see line #5). This equation is a function of the previous aql and the period of idleness. The second equation is used if the buffer is not idle, and it is a function of the previous aql and the current queue size q . In the second stage, Dp is calculated and the dropping is implemented or skipped according to the three scenarios.

In the first case, as given in line #8, Dp is calculated as a function of aql and another variable, $counter$, as well as a set of parameters. Subsequently, the packet is dropped or accommodated as a function of the calculated Dp , while the $counter$ variable is set to zero if the packet is dropped. The $counter$ parameter counts the number of packets in the critical case, which were not dropped according to the stochastic decision. The counter is simply increased with each accommodated packet, and is reset when a packet is dropped. As the value of the $counter$ increases, the Dp value increases significantly. This variable is required to avoid, as much as possible, dropping sequential packets to circumvent global synchronization. In the second case, the packet is dropped and the counter is set to zero [12]. In the third case, the packet is accommodated and the $counter$ is set to the value of negative one. A negative $counter$ value reduces the dropping probability when the status of the queue jumps from a low-queue state to a high-queue critical state. A Dp value that is calculated using a negative value for $counter$ will be of a low value. Accordingly, with sudden heavy traffic, the Dp value will increase slowly. Finally, in the third stage, the buffer tracing process saves the period of idleness [2, 12, 13].

RED calculates the value of aql with each packet arrival. The calculated value is then compared to two pre-determined threshold values (the minimum and maximum thresholds), which divide the buffer into three parts, as illustrated in Fig. 1. The value of aql based on the threshold comparison determines the action to be taken, which can be one of the following: (1) If the calculated aql value is less than the minimum threshold, then the arrival packet is accommodated with a Dp value equal to zero; no dropping occurs when aql is below the minimum threshold [14]. (2) If the aql value is greater than the maximum threshold, then the arrival packet is dropped with Dp equal to one; The arrival packet is firmly dropped when aql is greater than the maximum threshold. (3) A stochastic dropping process is implemented when aql is between the minimum and the maximum thresholds. In this case, Dp is calculated using a mathematical function $Dp(aql)$, which depends on the value of aql that affects Dp proportionally. As such, Dp increases as aql increases, and vice versa [14-17].

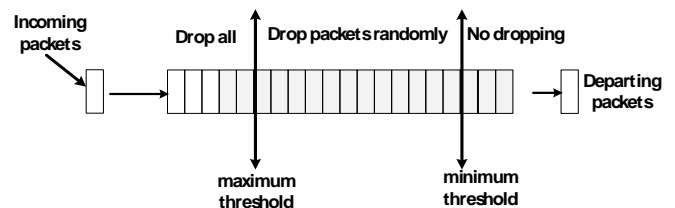


Fig. 1. Buffer Illustration and RED Actions and Parameters.

III. RELATED WORK

Various extensions to the **RED** method have been proposed in the literature to overcome the limitations discussed above. For example, **Gentle RED (GRED)** [12] was proposed to resolve the delay problem in **RED**. **GRED** uses a third threshold parameter, called the double maximum threshold, in addition to the other parameters (as illustrated in Fig. 2). The goal of the introduced threshold is to stabilize aql at a specific value. Accordingly, the computed aql value is compared to three thresholds: minimum, maximum and double maximum. This creates four cases for the calculated Dp rather than three. This extension, however, increases the dependency on parameter settings. Moreover, **GRED** is more sensitive to sudden congestion, because it reduces packet dropping compared to **RED**. Moreover, **GRED** exhibits poor performance when heavy congestion occurs while aql is below the maximum threshold. Thus, **Adaptive RED (ARED)** [13] was proposed to resolve the delay problem in **RED** while preserving the **RED** mechanism as much as possible. **ARED** used aql , *minimum* and *maximum* thresholds as the main parameters, in addition to a new parameter that represents the optimal target of the queue length, called target aql ($Taql$). Accordingly, aql is compared with three values in **ARED**, and Dp is calculated the same as in **RED**. However, the value of the initial dropping, D_{max} , which is fixed in **RED**, is calculated adaptively in **ARED**. The D_{max} value increases or decreased based on the value of aql compared to $Taql$.

Other methods extend **RED** by marginally modifying the original algorithm. For example, **PI** [18] uses traffic load value and aql value to calculate Dp . Accordingly, dropping increases when traffic load increases when aql is low to reduce delay. **Dynamic RED (DRED)** [19] extends **RED** by comparing instance queue length to a single threshold value. When queue length is below the threshold, no dropping is implemented. Moreover, when queue length is above the threshold, Dp increases or decreases based on queue length and the previous Dp value. **Random Exponential Marking (REM)** [20] extends **RED** using instance queue length, instead of aql , combined with the estimated load rate. However, instance queue length causes unnecessary packet dropping and false congestion. **BLUE** method [21] uses an adaptive value of Dp , which increases or decreases based on the estimated congestion status; This is similar to **ARED** and **DRED** in regard to packet loss and the threshold value. Various other AQM methods have been proposed in the literature, with different modifications made to the original **RED** mechanism for different purposes, as summarized in Table I.

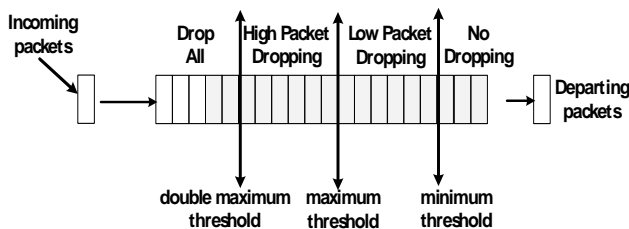


Fig. 2. Buffer Illustration and GRED Actions and Parameters.

TABLE I. SUMMARY OF RED'S EXTENSIONS

Method	Modification	Objectives
RED [2]	Original	Avoid global synchronization, reduce packet loss and dropping
GRED [12]	Use one more threshold to stabilize aql	Reduce delay
ARED [13]	Adaptively increase the initial dropping value based on aql	Reduce delay
PI [22]	Use load parameter (besides aql) to calculate Dp	Reduce delay
DRED [19]	Adaptively increase the initial dropping value based on ql	Reduce delay
REM [20]	Adaptively increase the initial dropping value based on ql and load rate	Reduce loss and maximize resource utilization
BLUE [21]	Adaptively increase the initial dropping value based on packet loss	Reduce packet loss
SRED [23]	Adaptively increase Dp value based on aql and number of active flows	Fair resource allocation
ERED [24]	Use q (besides aql) to calculate Dp .	Reduce packet loss
MRED [25]	Use the heuristic method to calculate Dp	Reduce packet loss
AVQ [26]	Use delay to calculate Dp	Reduce round-trip delay
RaQ [27]	Add more equations that calculate Dp based on aql	Maximize resource utilization
Yellow [28]	Use load to calculate Dp	Maximize resource utilization
CRED [3]	Use cloud membership degree calculation to calculate Dp	Reduce packet dropping
Adaptive Threshold RED [16]	Use rules set to calculate Dp based on aql and q	Reduce packet dropping
Adaptive- AQMRD [29]	Adaptive parameter tuning	Reduce packet dropping and solve parameterization problem
FLRED [8]	Use fuzzy logic to calculate Dp based on aql and delay	Solve parameterization problem

Overall, existing AQM methods can be broadly classified into two groups : The first involves methods that preserve the **RED** mechanism and parameters for monitoring and reacting, such as **GRED** [12] and **ARED** [13]; The other group contains methods that implemented major modifications while preserving the overall concepts of stochastic packet dropping.

Accordingly, the similarities among the existing AQM methods are: (1) AQM depends on stochastically packet dropping to avoid global synchronization; (2) AQM dropping probability is calculated with reference to the buffer or the network status; (3) AQM buffer monitoring is tracked and the decision-making is activated with each packet arrival.

The differences between the AQM methods can be summarized as follows: (1) Different congestion indicators and

parameters (such as aql , q , $load$, $delay$, $loss$) are utilized by different AQM methods. (2) Different decision-making scenarios are used for different AQM methods; RED used three scenarios (firmly dropping, stochastic dropping and no dropping), while other methods keep the stochastic dropping and add or remove other scenarios. (3) Different AQM methods use different heuristic equations and methods to calculate the dropping probability. These differences are motivated by different objectives, such as to reduce packet loss, reduce packet dropping, reduce round-trip delay, maximize resource utilization, and fair allocation. The first four objectives are conflicted, as reducing delay will minimize resource utilization and reducing dropping will increase delay.

RED is a well-known, stable AQM technique that was adapted by the Internet Engineering Task Force (IETF) in RFC 2309. For a long time, RED was utilized in distributed routers all over the world. Extended methods provide different capabilities and cause different QoS. Accordingly, replacing RED with different methods will harm the stability of the existing systems. Thus, it is necessary to enhance RED while maintaining its characteristics and configuration.

IV. PROPOSED WORK

As network technology evolves, the limitations of the RED have been discovered. RED can be viewed as a dual-mechanism method, in which the first mechanism is a multi-reaction process activated by the implemented algorithm and all the utilized parameters, except for aql . This mechanism reacts differently based on the status of the queue, as discussed above, and it is the reason behind the first and the second advantages of the RED method. The second mechanism is the RED congestion alert mechanism, which is implemented using aql . This mechanism is related to the third advantage and the first disadvantage. Accordingly, it is easier to point at the source of the limitation, which can be referred back to the utilization of aql . RED uses aql for two tasks: (1) As an indicator for monitoring to determine the reaction scenario; (2) As a parameter for dropping the probability calculation.

In fact, all of these tasks use aql in different ways. Since using aql has both positive and negative effects, replacing aql in all of these tasks is not a good approach; Instead, RED can use different bounds and parameters to gain an advantage and eliminate its disadvantages.

In the dropping calculation, using aql has proven to have the following advantages: (1) Avoid high dropping with limited increase in buffer length; (2) Avoid high delay with limited decrease in buffer length. These advantages refer to slow changes in aql value with the changes in the buffer length, which can be temporarily according to the busy nature of the traffic. To determine the reaction scenario, using three scenarios for packet dropping (based on a threshold comparison) is sufficient and has several advantages. However, using aql as a monitoring indicator has the disadvantage of providing an unreal indication of the queue status. This disadvantage refers to variations in aql as a result of sudden congestion. Because the slow variation has both advantages and disadvantages, the disadvantage of using aql is directly related to the monitoring of the queue rather than the dropping calculation. Accordingly, the decision between fully dropping,

no dropping, and stochastic dropping should be made based on the status of the buffer. Thus, instead of using aql to make a suitable decision, other indicators should be used to determine buffer status. Accordingly, an enhanced random early detection (EnRED) method and Windowed RED (WRED) method based on simple, yet efficient, monitoring parameters are presented.

A. Indicator Calculation

Two indicators are used to replace aql for congestion monitoring: instance queue length (q) and average queue length on a limited time window (aql_w). At any time, the number of packets queued in the router buffer is referred to as q . The advantages of using this indicator are: (1) No extra calculation is required, as q is used in RED to calculate aql ; (2) Overcome the disadvantages of using aql in the original RED. The indicator aql_w represents an equally averaged packet number on a limited time window. Unlike aql , which is calculated as a weighted average with low weights for current length, aql_w is calculated as the equal-weight average for a predetermined time window. Accordingly, aql_w intermediate q and aql in considering of past and recent queue length as illustrated in Fig. 3 [8]. The advantages of using this indicator are: (1) Can fully replace the existing aql for monitoring, decision making and probability calculation; (2) Overcome the disadvantages of using aql in the original RED, to some extent.

B. EnRED Mechanism

The proposed EnRED uses q to determine the reaction scenario for packet dropping as each packet arrives. This process requires a simple and direct modification to the original RED algorithm. As given in Algorithm 2, RED is modified at line #8 and line #14 by comparing q with the two thresholds, instead of using aql for comparison, as in the original RED. EnRED is implemented, as in Algorithm 2, in three stages. In the first stage, aql is calculated using two different equations. The first is used if the buffer is currently idle, as in line #5. The second is used if the buffer is not idle, and is a function of the previous aql and the current queue size q . In the second stage, Dp is calculated and the dropping is implemented or skipped according to three implemented scenarios. The first scenario, as given in line #8, is implemented when the queue length is between the minimum and maximum threshold. Queue length provides a true indication of buffer status, regardless of network status. Nevertheless, Dp is calculated as a function of the aql that reflects the status of the network. Subsequently, the packet is dropped or accommodated as a function of the calculated Dp , while the *counter* variable is set to zero if the packet is dropped. As the value of *counter* increases, the Dp value increases significantly, and vice versa. This variable is required to avoid, as much as possible, dropping sequential packets to circumvent global synchronization. The second case is implemented when the queue length exceeds the maximum threshold. In this case, the packet is dropped and the counter is set to zero. Finally, the third case is implemented when the queue length is below the minimum threshold, and results in packet accommodation and *counter* reset to the value of negative one. In the third stage, the buffer tracking process saves the period of idleness. Accordingly, packet monitoring in EnRED is the responsibility of the parameter q , while the dropping value is calculated based on aql .

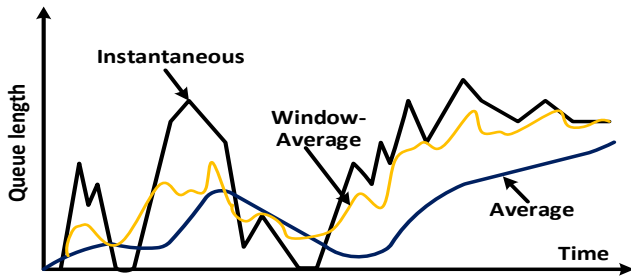


Fig. 3. The Shape of Different Indicators Overtime.

Algorithm 2: EnRED

```

1  PARAMETER SETTING:  $w_q, Th_{min}, Th_{max}, D_{max}$ 
2  VARIABLE INITIALIZATION:  $aql:=0, count:=-1$ 
3  FOR-EACH A
4      1) CALCULATE  $aql$ :
5          IF ( $q$  equal to 0)  $\rightarrow aql:=(1-w)^{f(cTime-iTime)} * aql$ 
6          IF ( $q$  not equal to 0)  $\rightarrow aql:=(1-w)* aql + w_q * q$ 
7      2) CALCULATE  $Dp$  & IMPLEMENT packet dropping.
8          IF ( $min_{th} \leq q < max_{th}$ )
9               $\rightarrow count++$ 
10              $\rightarrow Dp'=D_{max} * (aql - Th_{min}) / (Th_{max} - Th_{min})$ 
11              $\rightarrow Dp = Dp' / (1 - count * Dp')$ 
12             IF (Drop( $Dp$ ) is TRUE)
13                  $\rightarrow$  Drop-A,  $count := 0$ 
14         ELSE IF ( $q > max_{th}$ )
15              $\rightarrow$  Drop-A
16              $\rightarrow count:=0$ 
17         ELSE
18              $\rightarrow count:=-1$ 
19     3) TRACE Buffer Idleness
20     IF ( $q$  equal to 0 &&  $Idle$  equal to False)
21          $\rightarrow iTime=cTime, Idle = TRUE$ 
22     ELSE  $Idle = False$ 

```

C. Time-Window Augmented RED (Windowed-RED)

The proposed Windowed-RED (also WRED) is implemented using aql_w to determine the reaction scenario and to calculate dropping probability (Dp). This process required replacing all instances of aql with aql_w in the original RED algorithm; aql_w is implemented based on two scenarios, as given in lines #5 and #6. In the initial stage, aql_w is set to a value equal to q . Subsequently, aql_w is calculated on a window size that is equal to the buffer size; the window-tailed boundary is the current queue length. The dropping calculation and the dropping scenarios will be calculated based on aql_w , as given in lines #8–14. The tracing empty buffer is eliminated, as the utilized aql_w does not require empty buffer tracing. As in Algorithm 3, Windowed-RED is implemented in two stages: aql_w calculation and Dp calculation and stochastic packet dropping. In the first stage, aql_w is calculated in two ways. The first is used when Window-RED starts running (see line #5). In this case, aql_w is set to a value equal to q . While the second is used throughout the execution of the Window-RED, and is calculated as window-average of q . In the second stage, Dp is

calculated and the dropping is implemented or skipped according to three implemented scenarios. In the first case, as given in line #8, Dp is calculated as a function of aql_w and $count$. Then, the packet is dropped or accommodated as a function of the calculated Dp , while the $count$ variable is set to zero if the packet is dropped. As the value of $count$ increases, the Dp value increases as well, and vice versa. This variable is maintained to avoid global synchronization. In the second case, the packet is dropped and the counter is set to zero if aql_w is greater than the maximum threshold. In the third case, the packet is accommodated and the $count$ is set to the value of negative one if aql_w is less than the minimum threshold. Accordingly, packet monitoring in Windowed-RED and dropping calculation is the responsibility of the parameter aql_w , which is more sensitive to queue changes than aql .

Algorithm 3: WRED

```

1  PARAMETER SETTING:  $w_q, Th_{min}, Th_{max}, D_{max}$ 
2  VARIABLE INITIALIZATION:  $aql:=0, count:=-1$ 
3  FOR-EACH A
4      1) CALCULATE  $aql$ :
5          IF ( $\#ArrivedPackets < BufferSize$ )  $\rightarrow aql_w:=q$ 
6          Else  $\rightarrow aql_w:=A = \sum_{i=cTime}^{(cTime-BufferSize)+1} q_i / BufferSize$ 
7      2) CALCULATE  $Dp$  & IMPLEMENT packet dropping.
8          IF ( $min_{th} \leq aql_w < max_{th}$ )
9               $\rightarrow count++$ 
10              $\rightarrow Dp'=D_{max} * (aql_w - Th_{min}) / (Th_{max} - Th_{min})$ 
11              $\rightarrow Dp = Dp' / (1 - count * Dp')$ 
12             IF (Drop( $Dp$ ) is TRUE)
13                  $\rightarrow$  Drop-A,  $count := 0$ 
14         ELSE IF ( $aql_w > max_{th}$ )
15              $\rightarrow$  Drop-A
16              $\rightarrow count:=0$ 
17         ELSE
18              $\rightarrow count:=-1$ 

```

V. SIMULATION AND PARAMETER SETTINGS

In the simulation process, the router buffer is modelled as first-in-first-out (FIFO). The network as a whole is simulated using the discrete time queue model, which is commonly used in simulating and capturing the performance of AQM methods. Generally, the discrete time queue is represented by a sequence of time slots, each of which has a single departure process, a departure and arrival process, a single arrival or none of these. Accordingly, in each time slot, the arrival and departure process simulates the stochastic process based on a predefined arrival and departure rate. A discrete time queue implements the departure process, d_n , before arrival. Accordingly, d_n occurs at time slot $n-1$. Thus, the performance of the network can be captured accurately by counting and tracing the arrived, departure, lost, dropped, and other packets at each time slot [30, 31]. Eventually, these traced counters can be used to calculate the network performance accurately [4, 7, 32]. The simulation parameters are set to match the parameters recommended in the literature for RED; these parameters are listed in Table II. The arrival and departure rates are also set to create different traffic loads and congestion statuses.

TABLE II. SUMMARY OF RED'S EXTENSIONS

Parameter	Values
Probability of Packet Arrival	0.3–0.95
Probability of Packet Departure	0.3, 0.5
Total Number of Slots	2,000,000
Number of Slots for Warm-Up Period	800,000
Number of Slots for Results	1,200,000
Capacity of the Router Buffer	20
Queue Weight for <i>aql</i> Calculation	0.002
D_{max}	0.1
min_{th}	3
max_{th}	9

VI. RESULTS

The performance of the proposed EnRED and WRED is evaluated and compared to the original RED method, as well as to the BLUE and ERED methods. The performance is captured using the set of commonly utilized measures for network evaluation, which are delay, packet dropping, packet loss, and total packet missing at the router buffer. When the number of dropped packets using method *A* is more than the number of dropped packets using method *B*, and while loss is less in method *A*, then method *A* is considered to be more efficient than method *B*. Accordingly, to clearly illustrate this indistinct relationship between loss and drop using AQM methods, the total missing indicator is used in addition to the well-known measures.

The first experiment evaluates the proposed methods in comparison with the other methods under **extremely heavy traffic** load. Accordingly, the arrival probability, α , is set to a value of 0.9; the departure probability, β , is set to 0.3. According to the results depicted in Fig. 4, packet loss in EnRED and WRED is less than all other methods (Fig. 4(a)). Moreover, BLUE and RED lost less packets compared to ERED, which seems to perform badly under heavy traffic. In Fig. 4(b), the packet dropping rate of EnRED, WRED and RED is better than the rate of BLUE. ERED drops less packets compared to all other methods. Fig. 4(c) illustrates the total number of packets lost and dropped. All the methods are equal according to this measure, which means that the method with less packet loss is better. Accordingly, EnRED and WRED outperform all other methods; EnRED is slightly better than WRED, and RED is better than ERED and BLUE. Accordingly, the experiments showed that the proposed methods preserve the network performance and deal more efficiently with the queued packets compared to all other methods, as the utilized congestion indicators are more accurate than the indicators used in the other methods. Finally, in terms of packet delay, BLUE outperforms all other methods, while the proposed EnRED slightly outperforms RED and WRED, as illustrated in Fig. 4(d). According to the results presented in Fig. 4, packet dropping using the indicators selected in the proposed methods is much better than packet dropping in the original RED. This is because the utilized indicator is better at sensing congestion and avoiding packet

loss. Dropping and delay of the proposed methods are not the best this is because the proposed methods avoid loss. Nevertheless, delay and dropping for the proposed method are shown to be comparable with the best methods, except for ERED, for which the loss rate is huge.

The second experiment evaluates the compared methods under a **heavy traffic** load. Accordingly, the arrival probability is set to a value of 0.9, while the departure probability is set to 0.5. The results of this experiment, as illustrated in Fig. 5, are almost similar to the obtained results in the first experiment. Packet loss, using EnRED and WRED, is less than in all other methods (Fig. 5(a)). Moreover, BLUE and RED drop less packets compared to ERED. Fig. 5(b) reveals that the packet dropping of EnRED, WRED and RED is better than all other methods. Moreover, ERED drops less packets compared to all other methods. Fig. 5(c) illustrates the total packets lost and dropped. Accordingly, EnRED and WRED outperform the other methods, while EnRED is lightly better than WRED, and RED is better than ERED and BLUE. Finally, in terms of packet delay, BLUE outperforms all other methods, while the proposed EnRED slightly outperforms RED and WRED, as illustrated in Fig. 5(d).

The third experiment evaluates the methods based on **moderate traffic** load. Accordingly, both the arrival probability and departure probability are set to a value of 0.5. The results of this experiment are illustrated in Fig. 6. Loss is avoided by all methods (Fig. 6(a)). Similarly, dropping is not necessary when the traffic load is moderate, and thus the evaluated methods did not implement packet dropping except for the BLUE method, which scarified unnecessary packets (Fig. 6(b)). Fig. 6(c) reveals that BLUE is the worst in such a case, because it drops unnecessary packets. Finally, Fig. 6(d) illustrates that delay is almost equal in all evaluated methods except for the BLUE method, which exhibits an improved delay due to the implemented dropping. The fourth experiment evaluates and compares the proposed methods based on **light traffic** load, as illustrated in Fig. 7. Accordingly, the arrival probability is set to a value of 0.3 and the departure probability is set to 0.5. Moreover, no dropping or packet loss occurred, and the results are almost identical for all the compared methods.

Fig. 8 presents and compares the results of the various methods using the average of several arrival probabilities with a departure probability of 0.5. The results indicate that RED, EnRED and WRED are the best in terms of packet dropping, while BLUE outperforms ERED. For dropping, ERED is the best, while RED, EnRED and WRED outperform the BLUE method. In terms of delay, BLUE is the best, while EnRED outperform RED and WRED, which outperforms ERED. Accordingly, the proposed EnRED method and Windowed-RED method enhance network performance, avoid congestion and preserve delay in extremely heavy, heavy and moderate traffic. As noted, replacing the congestion indicator with a firm indicator or tightening the loose indicator with a more compact indicator in the windowed-RED significantly enhances RED performance.



Fig. 4. Performance Results under Extremely Heavy Traffic.

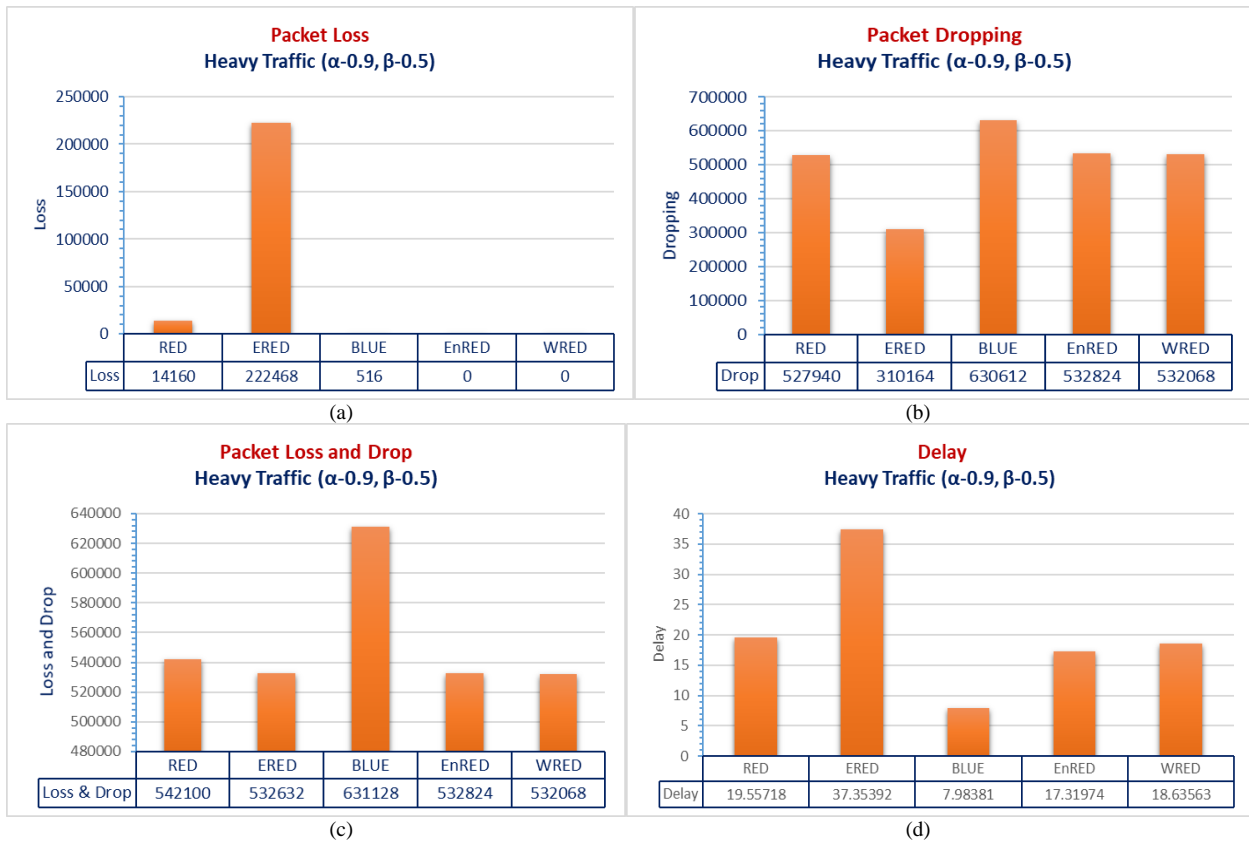


Fig. 5. Performance Results under Heavy Traffic.

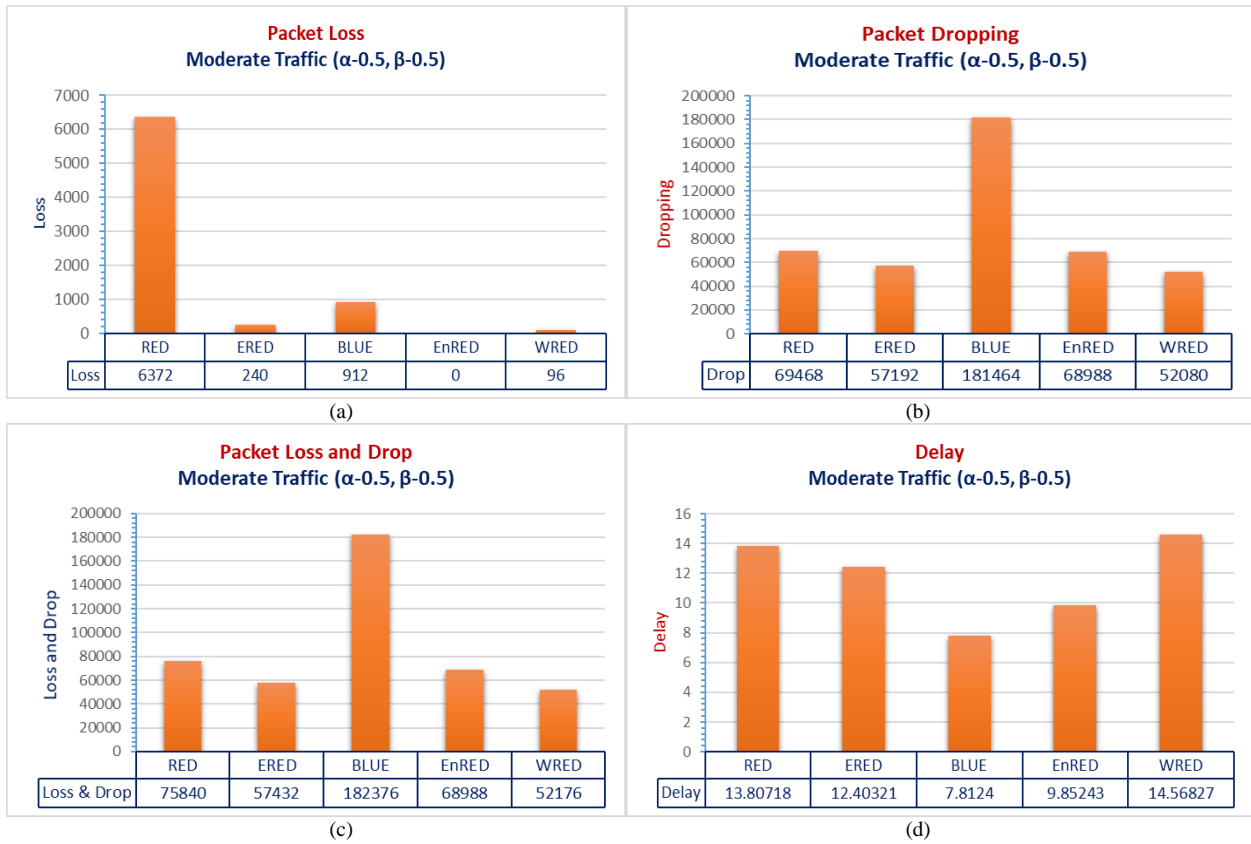


Fig. 6. Performance Results under Moderate Traffic.

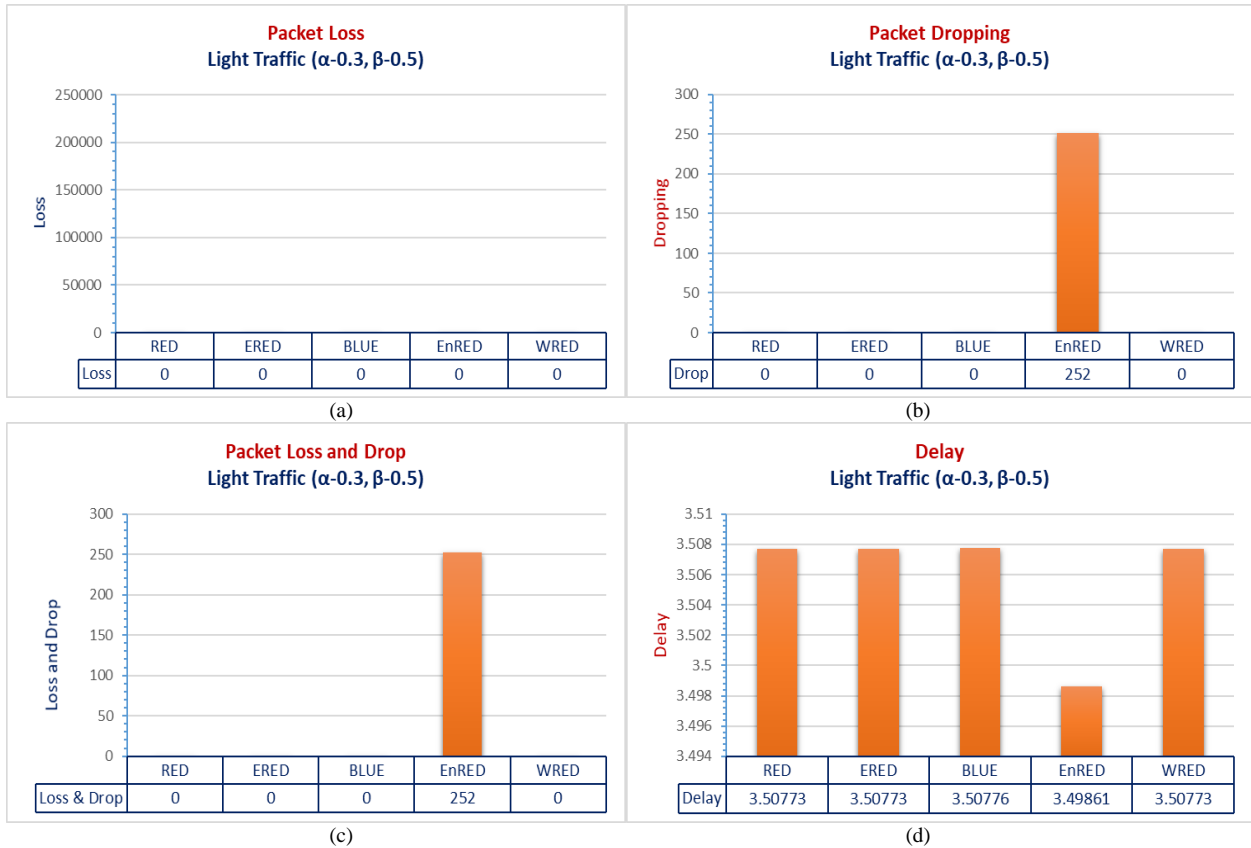


Fig. 7. Performance Results under Light Traffic.



Fig. 8. Performance Results for Various Arrival Rates.

VII. CONCLUSION

In this paper, the RED technique is analyzed, and the source of the shortcomings is identified. The loose congestion indicator in RED that leads to packet loss is fixed using two approaches: First, by preserving all the steps in the original RED and replacing the loose congestion indicator with a firmer one. Secondly, by replacing the loose congestion indicator and with a more confirmed one. Thus, both methods preserve the form of the original RED, and consequently, the stability of the existing systems that use RED. Although WRED is not as good as EnRED, it has the advantage of reducing the number of utilized parameters, and thus reducing the sensitivity of parameter initialization. The results also confirm that RED outperforms both ERED and BLUE. Future work should focus on using other indicators that enhance network performance and reduce overall delay.

REFERENCES

- [1] Sharma, N., et al., P-RED: Probability Based Random Early Detection Algorithm for Queue Management in MANET, in *Advances in Computer and Computational Sciences*, 2018, Springer. p. 637-643.
- [2] Floyd, S. and V. Jacobson, Random early detection gateways for congestion avoidance. *IEEE/ACM Trans. Netw.*, 1993. 1(4): p. 397-413.
- [3] Zhao, Y., et al., An Improved Algorithm of Nonlinear RED Based on Membership Cloud Theory. *Chinese Journal of Electronics*, 2017. 26(3): p. 537-543.
- [4] Yu-hong, Z., Z. Xue-feng, and T. Xu-yan, Research on the Improved Way of RED Algorithm S-RED. *International Journal of u-and e-Service, Science and Technology*, 2016. 9(2): p. 375-384.
- [5] Briscoe, B., *Insights from Curvy RED (Random Early Detection)*. 2015, Technical report TR-TUB8-2015-003, BT.
- [6] Jamali, S., N. Alipasandi, and B. Alipasandi, An Improvement over Random Early Detection Algorithm: A Self-Tuning Approach. *Journal of Electrical and Computer Engineering Innovations*, 2014. 2(2): p. 57-61.
- [7] Baklizi, M., et al., Fuzzy logic controller of gentle random early detection based on average queue length and delay rate. *International Journal of Fuzzy Systems*, 2014. 16(1): p. 9-19.
- [8] Abualhaj, M.M., A.A. Abu-Shareha, and M.M. Al-Tahrawi, FLRED: an efficient fuzzy logic based network congestion control method. *Neural Computing and Applications*, 2018. 30(3): p. 925-935.
- [9] Chen, W. and S.-H. Yang, The mechanism of adapting RED parameters to TCP traffic. *Computer Communications*, 2009. 32(13): p. 1525-1530.
- [10] Seifaddini, O., A. Abdullah, and a.H. Vosough, RED, GRED, AGRED CONGESTION CONTROL ALGORITHMS IN HETEROGENEOUS TRAFFIC TYPES, in *International Conference on Computing and Informatics*. 2013.
- [11] Alshimaa, I., et al., Enhanced Random Early Detection (ENRED). *International Journal of Computer Applications*, 2014. 92.
- [12] Floyd, S. Recommendations On Using the Gentle Variant of RED. <http://www.aciri.org/floyd/red/gentle.html> 2000.
- [13] Floyd, S., R. Gummadi, and S. Shenker, Adaptive RED: An Algorithm for Increasing the Robustness of RED's Active Queue Management. AT&T Center for Internet Research at ICSI, 2001.
- [14] Baklizi, M., et al., Performance assessment of AGRED, RED and GRED congestion control algorithms. *Information Technology Journal*, 2012. 11(2): p. 255.
- [15] Marin, A., et al. Performance evaluation of AQM techniques with heterogeneous traffic. in *2016 13th IEEE Annual Consumer Communications & Networking Conference (CCNC)*. 2016. IEEE.

- [16] Patel, Z.M. Queue occupancy estimation technique for adaptive threshold based RED. in Circuits and Systems (ICCS), 2017 IEEE International Conference on. 2017. IEEE.
- [17] Sun, J., M. Zukerman, and M. Palaniswami, Stabilizing RED using a fuzzy controller, in International Conference on Communications (ICC'07). 2007, IEEE. p. 266-271.
- [18] Silva, G.J., A. Datta, and S.P. Bhattacharyya, PI stabilization of first-order systems with time delay. Automatica, 2001. 37(12): p. 2025-2031.
- [19] Aweya, J., M. Ouellette, and D.Y. Montuno, A control theoretic approach to active queue management. Comput. Netw., 2001. 36(2-3): p. 203-235.
- [20] Lapsley, D. and S. Low. Random early marking: an optimisation approach to Internet congestion control. in Networks, 1999. (ICON '99) Proceedings. IEEE International Conference on. 1999.
- [21] Feng, W.-c., et al., BLUE: A New Class of Active Queue Management Algorithms. 1999, University of Michigan, Ann Arbor, MI, Technical Report.
- [22] Hollot, C.V., et al. On designing improved controllers for AQM routers supporting TCP flows. in INFOCOM 2001. Twentieth Annual Joint Conference of the IEEE Computer and Communications Societies. Proceedings. IEEE. 2001. IEEE.
- [23] Ott, T.J., T.V. Lakshman, and L. Wong. SRED: stabilized RED. in INFOCOM '99. Eighteenth Annual Joint Conference of the IEEE Computer and Communications Societies. Proceedings. IEEE. 1999.
- [24] Abbasov, B. and S. Korukoglu, Effective RED: An algorithm to improve RED's performance by reducing packet loss rate. Journal of Network and Computer Applications, 2009. 32(3): p. 703-709.
- [25] Koo, J., et al. MRED: a new approach to random early detection. in Information Networking, 2001. Proceedings. 15th International Conference on. 2001. IEEE.
- [26] Kunniyur, S. and R. Srikant, End-to-end congestion control schemes: Utility functions, random losses and ECN marks. Networking, IEEE/ACM Transactions on, 2003. 11(5): p. 689-702.
- [27] Sun, J. and M. Zukerman, RaQ: A robust active queue management scheme based on rate and queue length. Computer Communications, 2007. 30(8): p. 1731-1741.
- [28] Long, C., et al., The Yellow active queue management algorithm. Computer Networks, 2005. 47(4): p. 525-550.
- [29] Bhatnagar, S. and S. Patel, A stochastic approximation approach to active queue management. Telecommunication Systems, 2018. 68(1): p. 89-104.
- [30] Khatari, M. and G. Samara, Congestion control approach based on effective random early detection and fuzzy logic. arXiv preprint arXiv:1712.04247, 2017.
- [31] Guizani, M., et al., Network modeling and simulation: a practical perspective. 2010: John Wiley & Sons.
- [32] Tsavlidis, L., P. Efraimidis, and R.-A. Koutsiamanis, Prince: an effective router mechanism for networks with selfish flows. Journal of Internet Engineering, 2016. 6(1).

Recognition and Classification of Power Quality Disturbances by DWT-MRA and SVM Classifier

Fayyaz Jandan¹

Faculty of Electrical Engineering Department,
Quaid-e-Awam University of Engineering Science and
Technology Campus, Larkana, Pakistan

Syed Abid Ali Shaha³

PhD School of Engineering and Applied Sciences,
Aston University Birmingham UK

Suhail Khokhar²

Faculty of Electrical Engineering Department,
Quaid-e-Awam University of Engineering Science and
Technology, Nawabshah, Pakistan

Farhan Abbasi⁴

Faculty of Electrical Engineering Department,
Quaid-e-Awam University Campus of Engineering Science
and Technology, Larkana, Pakistan

Abstract—Electrical power system is a large and complex network, where power quality disturbances (PQDs) must be monitored, analyzed and mitigated continuously in order to preserve and to re-establish the normal power supply without even slight interruption. Practically huge disturbance data is difficult to manage and requires the higher level of accuracy and time for the analysis and monitoring. Thus automatic and intelligent algorithm based methodologies are in practice for the detection, recognition and classification of power quality events. This approach may help to take preventive measures against abnormal operations and moreover, sudden fluctuations in supply can be handled accordingly. Disturbance types, causes, proper and appropriate extraction of features in single and multiple disturbances, classification model type and classifier performance, are still the main concerns and challenges. In this paper, an attempt has been made to present a different approach for recognition of PQDs with the synthetic model based generated disturbances, which are frequent in power system operations, and the proposed unique feature vector. Disturbances are generated in Matlab workspace environment whereas distinctive features of events are extracted through discrete wavelet transform (DWT) technique. Machine learning based Support vector machine classifier tool is implemented for the classification and recognition of disturbances. In relation to the results, the proposed methodology recognizes the PQDs with high accuracy, sensitivity and specificity. This study illustrates that the proposed approach is valid, efficient and applicable.

Keywords—Power quality disturbances; discrete wavelet transform; multi resolution analysis; support vector machine

I. INTRODUCTION

Today, an industrial progress and trade perform a key role in the economic stability and growth of any country. Not only mechanical but electrical faults and disturbances are largely responsible for the consistent and quality supply of electricity. Rising use of electronic/ solid state converters and fast control equipment has become the requirement for industries as well as for utility companies to get uninterrupted production and supply facilities [1, 2]. Short circuit faults, lightning, switching of induction machines, motors, power transmission lines, capacitor banks, non-conventional power plant integrations etc.

are also the major causes of Power Quality Disturbances (PQD's). The term PQD is by and large outlined as the variation or distortion in normal voltage/ current amplitude, phase angle and frequency. These distortions/disturbances remarkably lessen the reliability, performance and life of electrical equipment. If such disturbances persist and not mitigated instantly, may cause failures of high voltage equipment (i.e. insulation degradation, failures in high-voltage and low-voltage protection systems, incorrect tripping by relaying systems etc.) leading to complete discontinuity of power transmission or distribution network supply systems [3]. PQDs are broadly categorized as, magnitude variation, transients and steady state variations or harmonics. Magnitude variations are classified as the voltage/current sag (0.1-0.9 P.U), swell (1.1-1.8 P.U), interruption (<0.1 P.U) [4], while transients can be further classified as impulsive and oscillatory transients. Consequently, steady-state PQDs are typically classed into harmonics, flicker and notch categories. Due to coinciding abnormal switching and other small operations in power system, variety of single and multiple PQDs (i.e. the combination of different disturbances) may rise [5].

Power quality is a growing concern since 1980s. Increasing researches in this area can be broadly categorized and congregated into six broad aspects. These aspects include PQ fundamental concepts, standards, effects, solutions, sources, instrumentation, mathematical modeling and analysis. For the research in automatic classification and recognition of power quality events, the power quality standards, time domain, transform domain wave analysis and machine learning algorithms are considered. PQDs can be mitigated to some extent by the application of several types and combinations of active/ passive filters and compensators. In order to avoid disturbances and their specific causes, continuous monitoring of voltage / current waveform patterns and instantaneous constraints must be analyzed. Although, the waveform event data collection and manual monitoring's by PQ analyzers are not much reliable and so also requires substantial computational time and resources. In consequence, automatic and intelligent algorithm based measures are adopted essentially for the detection, recognition and classification of

PQDs. This intelligent monitoring and analysis may also lead to help with the purpose of re-establishing and preserving the abnormal power supply in fraction of seconds without even slight interruption. Likewise, at troubleshooting from power generation to utilization systems, fault forecasting and moreover issues with integration of distributed generation (DG's) systems in power system can also be managed [6].

A lot of research work has been carried out in the area of recognition and classification of PQDs. Selection of PQD types, number and types of single and multiple disturbances under observation, choice of signal processing techniques according to their feature extraction capability, selection of features and choice of artificial intelligent technique conferring to classification performance characteristics are the main concerns and challenges. In literature, numerous signal processing techniques are used for waveform analysis. Some frequently used techniques can be classified as Fourier transforms (FT), Kalman filtering, wavelet transforms (WT), Stockwell-transform (S-Transform), Hilbert-Huang transform (HHT), Gabor transform (GT), etc. [3].

In power system PQDs inception is sometimes dynamically slow and sometimes abrupt; for that reason, PQD event detection in the time frame is important for analysis and monitoring. This brings to the application of Wavelet transform. However other transforms can also be implemented. But the limitations of erroneous detection in dynamic and sudden disturbances, complexity, non-localization in time or space and non-suitability with dynamic signal like PQDs, makes wavelet transform a robust and suitable tool for detection of the event in the time-frequency domain. For the classification, features are extracted, based on statistical parameters, from the decomposed and filtered levels of Discrete Wavelet Transform (DWT). These features are then used for the training and testing the artificial intelligence based classifiers [7, 8]. The classification can be applied by the number of techniques like Artificial Neural Network (ANN), Support Vector Machine (SVM), Fuzzy Expert System (FES), Neuro Fuzzy System (NFS) etc. [3, 9, 10]. Although support vector machine classifier has a lot of tuning parameters but it is suitable because of its high classification accuracy, robustness, and less computational time requirements [4, 11].

A brief literature review related to proposed algorithm is discussed as follows. Author in [26] proposed Gabor Transform (GT) and feed forward Neural Network to identify the arcing faults in power system. Author in [27] proposed HHT-PNN classification algorithm to detect and classify the single and multiple hybrid PQ disturbances. Author in [28] proposed S-Transform-Based ANN Classifier and Rule-Based Decision Tree. Author in [23] proposed a procedure to detect and classify PQ events having complex perturbations caught in a real time power distribution network using WT-SVM. Author in [4] proposed automatic pattern recognition of Single and Multiple Power Quality Disturbances based on wavelet norm entropy feature and PNN. Author in [25] proposed Variational Mode Decomposition (VMD) and S-transform for feature extraction along with SVM classifier. He selected features on filter and wrapper method. Author in [18] proposed WT-SVM for classification of single and hybrid PQDs and with PNN and feed forward neural network. Author in [9] proposed a

technique for optimal selections of features based in WT-PNN and artificial bee colony based algorithm. Author in [1] proposed tunable-Q wavelet transform and dual multi-class SVM for online detection of PQDs. In [29] a classification method for multiple power quality disturbances using empirical WT adaptive filtering and SVM classifier is proposed

In this study, a new power system disturbance waveform pattern recognition and classification algorithm is proposed with unique feature vector which identifies and classifies the single and hybrid power quality disturbances into classes. The selected PQDs for analysis are frequent in power system operations. These disturbances are generated through parametric model equations in MATLAB workspace/editor environment. Such mathematical model based generated disturbances are then passed through DWT filters, signal processing tool, where not only event detection in time frequency localization is achieved but also feature extraction is performed from approximation and detail levels. Extracted features are used for training and testing of artificial intelligence based support vector machine classifier for the automatic pattern recognition. Real time power system model in Matlab/Simulink environment can also be developed for the physical description of power system disturbances and can be implemented for validation of results [12].

This paper has been organized into six sections. Section I, discussed the detail background of the power quality, including general types of power quality disturbances, issues, causes and general aspects of power quality research and related work. Section II describes wavelet transform in detail. In Section III, support vector machine is discussed. Section IV deals with the methodology of proposed approach in detail. Section V presents results and discussions. Lastly conclusion is presented in Section VI.

II. WAVELET TRANSFORM

With wavelet transform (WT) a waveform is decomposed into the set of basis functions; such basis functions are termed as mother wavelets. A wavelet is fundamentally a wave alternation, having zero mean unlike sinusoid which extends to infinity; it extends and exists for a finite duration. Analysis with WT is well suited to non-periodic signals containing both stationary components and transients, such as the ones that can be found on PQDs. Some well-known mother wavelet types are shown in Fig. 1. The availability of wide range of wavelet derivatives is a key strength of WT analysis. Daubechies 4 (db4) wavelet class is mostly adopted in literature for the analysis of PQ disturbances because of its comparably similar characteristics with PQ events [13]. WT has baseband characteristics in frequency domain. The major advantage of analysis with wavelets is of varying window size, which is wide for slowly varying changes i.e. low frequencies, and narrow for abrupt changes. As a result, there is optimal time-frequency localization in all frequency ranges [14, 15].

WT technique has a significant role in discontinuity/event detection and it has also been found a powerful tool for the feature extraction from waveforms. WT can be achieved by two means i.e. by continuous wavelet transform (CWT) and discrete wavelet transform (DWT). With CWT, scaling and translation of mother wavelet $\phi(t)$ provide the information of

time frequency resolution of the original distorted waveform [16,17]. The mathematical equation of CWT for a given disturbance signal $x(t)$ with respect to $\varphi(t)$ is given as.

$$CWT(c, d) = \frac{1}{\sqrt{c}} \int_{-\infty}^{\infty} x(t) \varphi\left(\frac{t-d}{c}\right) dt \quad (1)$$

In equation (1) c and d are real positive numbers, where c is the scaling factor, inversely proportional to frequency, corresponding to signal dilation or shrinking in time domain. While d is the translation factor corresponds to wavelet shifting.

Although CWT is upright with time frequency analysis but it has some limitations. Computations with CWT by computer simulation is discretized CWT, which is not a true discrete transform. CWT require infinite inputs and the information provided is highly redundant therefore not convenient for computer analysis [18]. Waveform decomposition or reconstruction by CWT requires a significant amount of computational time. Furthermore, CWT is considered substantially sluggish to implement as compared to DWT. The general equation of DWT for signal $x(k)$ is given in equation (2).

$$DWT(m, n) = \frac{1}{\sqrt{c_0^m}} \sum_k x(k) \varphi\left(\frac{n - kd_0 c_0^m}{c_0^m}\right) \quad (2)$$

In the above equation, c_0 and d_0 are discrete scaling and discrete translation factors respectively. Having fixed constant values generally, $c_0 = 2$ and $d_0 = 1$, these parameters, c_0^m and $kd_0 c_0^m$, are taken as constants. Where m and n are the integers, representing frequency localization and time localization, correspondingly. The parameter c_0^m produces oscillatory frequency and length of the wavelet, whereas parameter $kd_0 c_0^m$, credits shifting (translation) position [5].

The idea for DWT computation is same as it is in CWT. In CWT, correlation among a wavelet at different scale and the given signal is calculated by varying the analysis window scale, shifting the window in time, multiplying by the given signal and then integrating over all times. Whereas in Discrete WT, signal x is passed through series of digital high pass (H.P) filters, to analyze high frequencies, and digital low pass (L.P) filters, to analyze low frequencies, where filters are at different cut-off frequencies to evaluate signals at different scales. In this whole process, the resolution of the signal is changed by filtering and the scale is changed by sampling operations [5, 19, 20].

1) *Multi-Resolution analysis:* Mallat and Meyer established the basic framework of Multi resolution analysis (MRA) algorithm. With MRA, decomposition of a waveform can be obtained at various resolution levels and scales of short waveforms i.e. mother wavelets. In literature, MRA is also termed as pyramidal coding which is similar to sub band coding method. Using MRA, multi-level resolution analysis can be performed, where decomposition is repeated up to more than a few levels for increasing frequency resolutions to get detail and approximation coefficient waveforms. MRA decomposition can be mathematically modeled as.

$$(x * g)(n) = \sum_{k=-\infty}^{\infty} x(k)g(n - k) \quad (3)$$

In MRA based wave decomposition, the sample waveform being investigated is passed through half band LP filter $g(k)$, having impulse response g (equation 3). This causes the convolution in discrete time. Similarly, the waveform is also passed concurrently through half band HP filter $h(k)$. For the first level decomposition i.e. down sampling by factor 2, the outputs of the HP and LP filters are referred to as detail level D1 and approximation level A1 respectively. In level 2 decomposition the obtained approximation A1 coefficients are passed through the same HP and LP filters to produce coefficients A2 and D2 respectively. Likewise, A2 coefficients are again passed through filters of the same cut off frequency limits and so on. In this way down sampling is applied for further levels of wave decomposition [19, 21]. This process is largely termed as multi-level decomposition [22]. The filter output relations are mathematically expressed in equation 4 and 5, where k represents number of samples.

$$\varphi(n) = \sqrt{2} \sum_k g(n) \varphi(2n - k) \quad (4)$$

$$\varphi(n) = \sqrt{2} \sum_k h(n) \varphi(2n - k) \quad (5)$$

DWT-MRA based decomposition is according to the Nyquist rule, where half the frequencies of the signal have now been removed and half the samples are discarded, schematically shown in Fig. 2. Similarly with this decomposition process the frequency band i.e. half of each filter output characterizes the signal. Therefore time resolution is reduced by factor 2. The frequency resolution is doubled for each next level of decomposition because of half the frequency band of the input of the previous level and so on [12, 14, 19, 23].

Expressions for the approximation A_j and detail level D_j coefficients are:

$$A_{j+1}(n) = \sum_k h(k - 2n)A_j(k) \quad (6)$$

$$D_{j+1}(n) = \sum_k g(k - 2n)A_j(k) \quad (7)$$

The relation for waveform $f(n)$ expanded related to its orthogonal basis of scaling and wavelet function is shown in equation 8. The equation is basically characterized by one set of scaling coefficient and one or several sets of wavelet coefficients

$$f(n) = \sum_k A_1(k)\varphi(n - k) + \sum_k \sum_{j=1} D_j(n)2^{-\frac{j}{2}}\varphi(2^j n - k) \quad (8)$$

In equation 6, 7 and 8, $j=1,2,3,\dots$, represents level of decompositions.

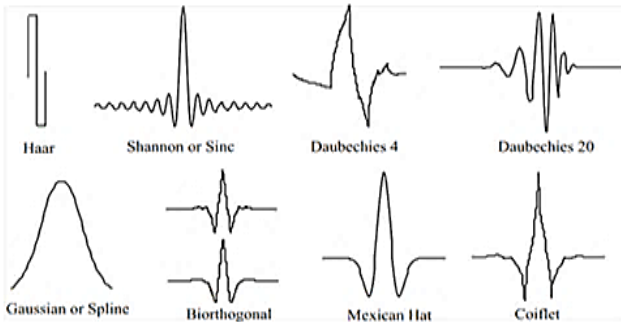


Fig 1. Some Common Types of Mother Wavelets.

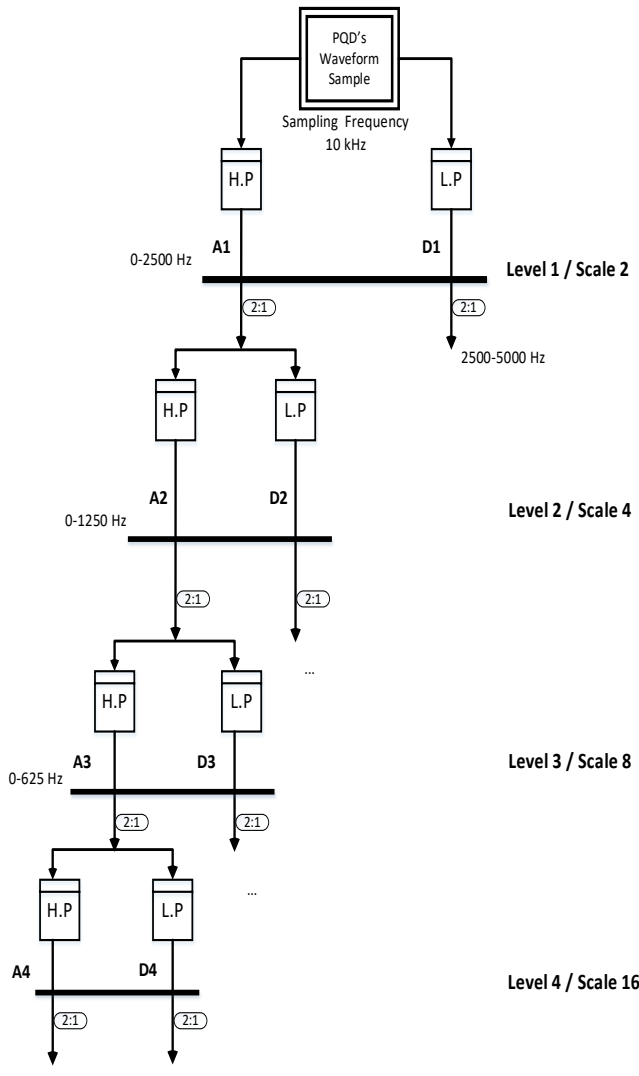


Fig 2. DWT-MRA Decomposition Process Schematic Diagram.

III. SUPPORT VECTOR MACHINE CLASSIFIER

The Support vector machine (SVM) tool, first presented by Vapnik (Vapnik, 1995), is a very powerful, high performance and computationally efficient family of supervised machine learning algorithm. It has wide application in classification and regression (time series prediction like estimation, forecasting, etc.) problems [8, 11]. For PQD waveform pattern recognition,

classification can be performed by utilizing various parameters. In literature, PQD classification is mostly based on statistical learning theory results [5, 8]. For two or more categorized classes of disturbance data, it acts as discriminative classifier typically defined by an optimal hyper plane, separates all the categorized classes by the decision boundary, as shown in Fig. 3. The hyper plane can be defined mathematically as:

$$g(x) = x'\theta + b = 0 \quad (9)$$

$\theta \in R$, for dimension d , comprises the coefficients expressing orthogonal vector to hyper plane.

Hyper plane is a linear decision boundary that splits the space for classification into two parts. Similarly, it can be a nonlinear decision surface boundary for classifying multiple classes data [24, 25]. For inseparable and complex data kernel functions are adopted. These functions transform data to large dimensional feature space where input data becomes more separable i.e. maximum margin hyper planes are established, related to original input feature space. Gaussian or radial basis function, sigmoid, polynomials, exponential radial basis functions, splines Etc. are the generally used types of Kernel functions in the literature [24]. In this work, Gaussian kernel is adopted for binary classification and feature mapping. The mathematical relation for Gaussian kernel is given as:

$$f(x_i, l_j) = \frac{\exp(-\|x_i - l_j\|^2)}{2\sigma^2} \quad (10)$$

In equation 10 x_i represents feature and l_j , land mark point whereas σ is a Gaussian kernel parameter, features $f(x_i, l_j)$ to vary more smoothly. For the classification let the training vector is $x_j \in R$, along with their categories $y_j = (-, +)$ where algorithm searches maximum margin length i.e. the region which contains no observations, for an optimal hyper plane and places the observations in the positive and negative class categories. From equation 9, for Separable classes classification, an objective is to minimize $\|\theta\|$ with respect to b and θ . So that for all feature vectors (x_j, y_j) , $y_j g(x_j) \geq 1$. When support vectors x_j are on the boundary, $y_j g(x_j) = 1$. To optimize and minimize the objective, SVM algorithm uses Lagrange multiplier, as shown in equation 11. To minimize the equation 11, subject to $\sum a_j y_j = 0$.

$$0.5 \sum_{j=1}^a \sum_{k=1}^n a_j a_k y_j y_k x_j x_k - \sum_{j=1}^n a_j \quad (11)$$

where $a_j \geq 0$ and $j=1,2,\dots,n$.

$$a_j [y_j g(x_j) - 1 + \delta_j] = 0 \quad (12)$$

$$\delta_j (C - a_j) = 0 \quad (13)$$

Whereas,

$$g(x_j) = \varphi(x_j)' \theta + b \quad (14)$$

In above equation φ is a kernel function. δ_j is entitled slack parameter and C is regularization parameter. For perfectly separable classes slack parameter, $\delta_j = 0$.

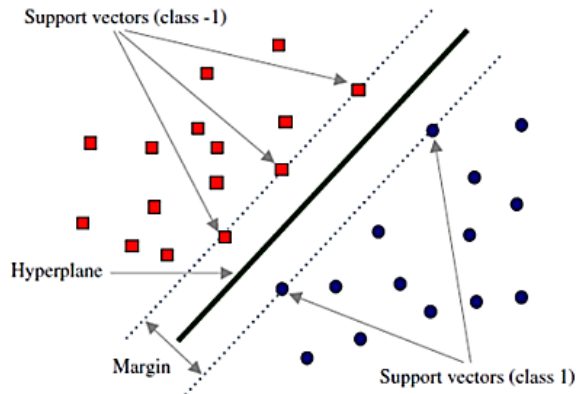


Fig 3. Support Vector Machine Classification Schematic.

In case of inseparable classes, minimizing equation 15 with respect to θ, b and δ_j , subject to equation 16.

$$0.5\|\theta\|^2 + C \sum \delta_j \quad (15)$$

$$y_j g(x_j) \geq 1 - \delta_j \quad (16)$$

Where $\delta_j \geq 0$, except $0 \leq a_j \leq C$, for all $j = 1, 2, 3, \dots, n$. SVM Score function is shown in equation 17 as:

$$\hat{g}(x) = \sum_{j=1}^n \hat{a}_j y_j x'_j + \hat{b} \quad (17)$$

Where \hat{b} is the bias estimate and \hat{a}_j is j th vector estimate. The SVM classifies new observation z using $\text{sign}(\hat{g}(z))$. Non-linear boundary in SVM works in transformed predictor space to get optimal hyper plane. The dual formalization for nonlinear SVM is represented in equation 18 with respect to a_1, a_2, \dots, a_n , subject to $\sum a_j y_j = 0$, where $0 \leq a_j \leq C$.

$$0.5 \sum_{j=1}^n \sum_{k=1}^n a_j a_k y_j y_k G(x_j, x_k) - \sum_{j=1}^n a_j \quad (18)$$

For all $j=1, 2, \dots, n$. and the KKT complementarity conditions. $G(x_j, x_k)$ are the elements of the Gram matrix. The resulting score function for SVM is given in equation 19.

$$\hat{g}(x) = \sum_{j=1}^n \hat{a}_j y_j G(x_j, x_k) + \hat{b} \quad (19)$$

SVM has better generalization ability (i.e. ability to learn a rule for classifying training data to ability of resulting rule to classify testing data.). It may handle large feature vector dimension space and also has no over fitting issue for large classification problems as compared to logistic regression and neural network or other conventional classifiers. SVM training is much easier than training artificial neural networks [1, 2].

IV. METHODOLOGY

The proposed algorithm for PQD recognition comprises of four stages, namely, PQ disturbances sample data generation, Feature extraction, classification and decision stage, as shown in flow chart, Fig. 4.

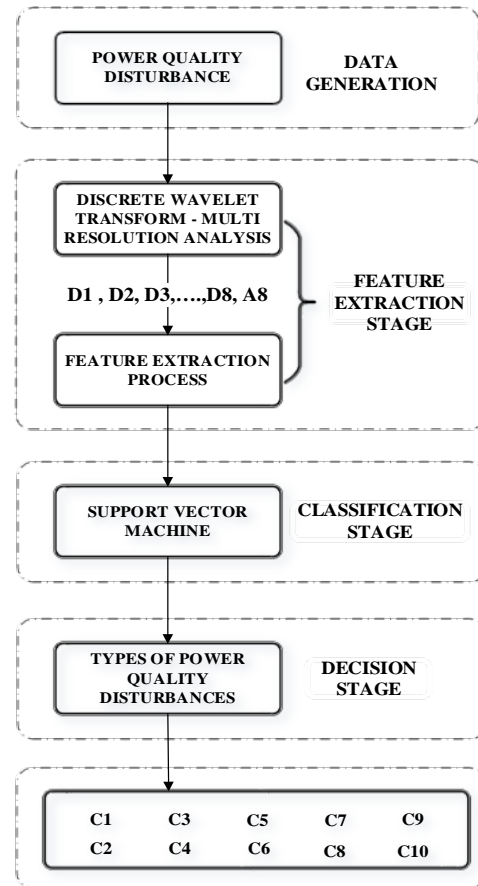


Fig 4. Flow Chart of Proposed Methodology.

A. PQ Disturbances Pattern Generation

Real Power quality waveforms may frequently exhibit slowly or abrupt changing trends, oscillations punctuated with harmonics, transients or other disturbances. In contrast, these changes are the important part of the data both perceptually and in terms of information of abnormality they provide. For the classification of disturbances, PQDs data can be obtained through real time PQ loggers or can be generated using parametric equations [25], where equation parameters are based on Categories & Characteristics of power system electromagnetic phenomenon, IEEE STD 1159-2009. PQD generation through parametric equations is expedient, variety of samples for any type of disturbance either single or multiple signals can be simulated. Disturbance magnitude and duration over cycles can be changed in a wide range and controlled manner according to disturbance type and IEEE standards. In this work events of pure voltage sine wave, sags, swells, interruptions, harmonics, impulsive transients, oscillatory transients, sag with harmonics and swell with harmonics are considered for generation. 100 random sample cases with 10 cycles at 50Hz (0.2 seconds) for each disturbance were produced. The sampling frequency was 10 kHz i.e. 200 points per cycle. Both magnitudes, as well as time of event occurrence, were diverse in accordance with the aforementioned standard. Fig. 5 shows only one random sample waveform of each category of generated disturbance.

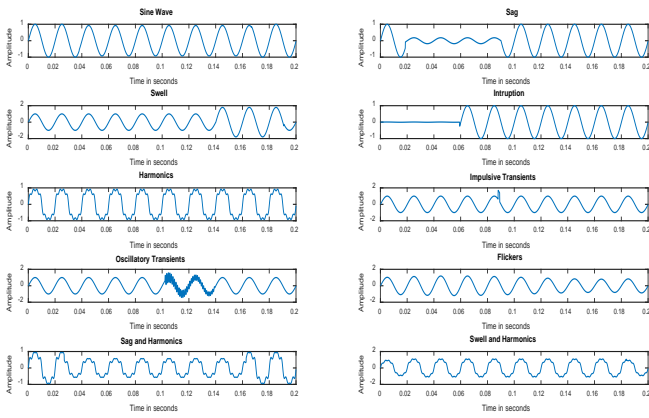


Fig 5. Generated Sample of Each Selected PQD Type through Parametric Equations.

B. Feature Extraction

Feature extraction stage is the most important step for the machine learning based pattern recognition and classification of PQD problems. Extracted features are the measured data, obtained from the waveform samples to develop a feature vector. This feature vector should be dimensionally concise so that learning and generalization process in classifier algorithms for classification can be implemented effectively. Feature extraction stage consists of two sub stages. In the first stage, all the generated samples for each disturbance class are decomposed up to 8 levels to get wavelet coefficients using DWT-MRA, where the wavelet coefficients are A_j approximation and D_j detail levels. Thus for each class of disturbance D_1 - D_8 and A_8 coefficients vectors are extracted. In order to reduce the obtained data and to enhance the classifiers performance effective and suitable statistical parameters are proposed for feature vector development in the second stage of feature extraction.

1) *Energy feature*: The energy feature mining is according to the property which states that energy of the signal in time domain and in the frequency domain are equal, as frequency domain signal $X[n]$, i.e. Fourier transformed signal contains all the information about $X[t]$. This property is termed as Parseval's Theorem.

$$E_{sig}(t) = \frac{1}{T} \int_0^T |x(t)|^2 dt \quad (20)$$

$$E_{sig}(n) = \frac{1}{N} \sum_{j=1}^N |X[n]|^2 \quad (21)$$

Where t denotes the time period and n is the sampling period of the signal waveform. The energy features of the PQDs are obtained from wavelet coefficients A_j and D_j , which are obtained at various frequency bands for each of the disturbance types. The energy feature vector consists of energy percentage corresponding to the respective wavelet coefficients, which are calculated by the relations shown in equation 22 and 23.

$$E_{D_i} = \sum_{j=1}^N |D_{i,j}|^2 \quad (22)$$

$$i = 1, 2, 3, \dots, l$$

$$E_{A_i} = \sum_{j=1}^N |A_{i,j}|^2 \quad (23)$$

$$E_i = [E_{A_1} E_{A_2} \dots E_{A_l} E_{A_l}, E_{D_1} E_{D_2} \dots E_{D_l} E_{D_l}] \quad (24)$$

E_{A_j} and E_{D_j} are the energies of wavelet-approximation and detail coefficients up to level j and E_i is the energy feature vector.

2) *Entropy feature*: Entropy parameter has been found suitable as a feature for PQD classification and recognition. In information theory entropy is generally regarded as the precise indicator of disorder ness, imbalance and uncertainties relating to random variables that may be gained by the observations (in this case D_i and A_8), whereas entropy is always greater than or equal to zero. Its outcomes can be generalized to provide information about specific events and outliers. Shannon entropy, a decreasing functions of a scattering of random variables and is maximum when all outcomes are equally to be expected. Following are the relations for Shannon entropy for detail and approximation level coefficients.

$$Ent_{D_i} = - \sum_{j=1}^N D_{i,j}^2 \log(D_{i,j}^2) \quad (25)$$

$$Ent_{A_i} = - \sum_{j=1}^N A_{i,j}^2 \log(A_{i,j}^2) \quad (26)$$

Where $A_{i,j}$ and $D_{i,j}$ is the probability of the occurrence of feature values $\{D_1, \dots, D_8, A_8\}$ and $i = 1, \dots, 10$. Over all entropy features obtained from the MRA based DWT for any PQ Signals are given by

$$Ent_i = [Ent_{D_1} Ent_{D_2} \dots Ent_{D_l} Ent_{D_l}, Ent_{A_8}] \quad (27)$$

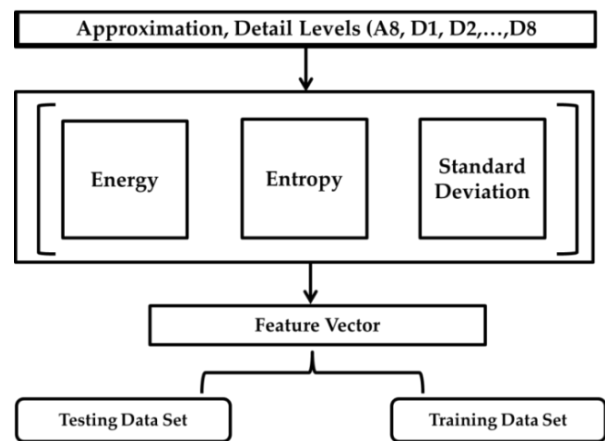


Fig 6. Feature Vector Development Flow Chart.

3) *Standard deviation*: Standard deviation feature measures the dispersion of an event frequency distribution or it can also be defined as a parameter that shows the way in which a probability function or probability density function is centered around its mean which is equal to the root of moment in which the deviation from mean is squared.

$$S.D_{D_j} = \sqrt{\frac{\sum_{j=1}^N (D_j - mean)^2}{N - 1}} \quad (28)$$

$$S.D_{A_j} = \sqrt{\frac{\sum_{j=1}^N (A_j - mean)^2}{N - 1}} \quad (29)$$

$$SD_i = E_i = [SD_{D_1} SD_{D_2} \dots SD_{D_i} SD_{D_i}] \quad (30)$$

$$Feature_i = [E_i Ent_i SD_i] \quad (31)$$

The feature vector obtained for i samples is used for the classification purpose in the classification stage for each of the PQDs type. Where half of the data is utilized for training the classifier and other half is used for testing the classifier performance. Schematic diagram for the feature vector development process is shown in Fig. 6.

C. Classification Stage

The $Feature_i$ feature vector, developed in equation 31, comprises of 27 dimensions of feature dataset for 100 samples of each of the PQ disturbance class i.e. 27×100 . From 100 samples of each disturbance class, half of the data set ($27 \times$

50) has been used for training the SVM classifier and rest of data is for testing purpose. For classification training with SVM one vs. one (1Vs.1) approach is adopted as shown in figure. Where in each SVM training node, $i=1$ class is trained against all classes. Similarly for next SVM training node that aforesaid $i=1$ class is replaced with $i=2$ class and training is done with all other classes. This process was iterated until all classes were passed through training. With this training process SVM develop algorithm functions i.e. $F(Cn)$, for binary data classification and outlier detection of n classes. Therefore 1 vs.1 approach may allow the SVM classifier to have a very upright training performance with this multi class classification problem. Testing of classifier, for each class, results the positive scores and negative scores for classified and misclassified class samples respectively. The label for classified disturbance sample was set to 1 and misclassified sample was set to 0. The input to the classifier is the time domain disturbance signal. Fig. 7 shows the one vs. one SVM binary classification schematic diagram. In this work, Lib-SVM Matlab Software toolbox library is used for classification. Lib-SVM consists of the default Sequential Minimal Optimization (SMO) solver; it reduces one-norm problem by a series of two point minimizations and contains bias terms and uses linear constraints in the model. RBF or Gaussian kernel was used for classifying non separable feature vectors i.e. nonlinear, where the kernel scale was set to 5.2 and box constraint to level 1 and extracted feature data was standardized for computational simplification.

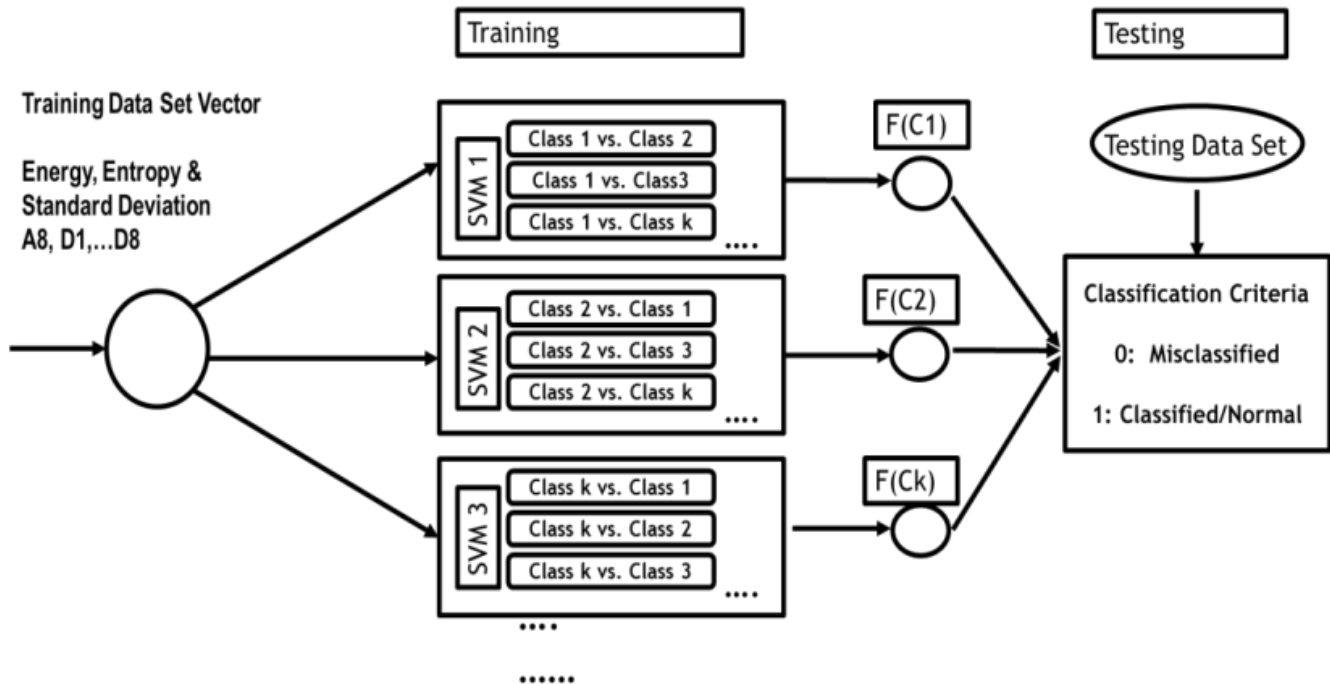


Fig. 7. One vs. One SVM Binary Classification Schematic.

VI. RESULTS AND DISCUSSION

For all that samples of ten generated disturbances, time frequency localization of each disturbance event is achieved and succeeded by the DWT-MRA technique. In order to show the DWT- MRA time frequency event localization characteristic, only one sample for sag with harmonics and its 1-5 detail, having high frequency, and 5th level discretized approximation coefficients, having the fundamental frequency components, are plotted in Fig. 8. These levels are obtained by decomposition of original generated sample via Daubechies fourth order (dB4) wavelet filter. For recognition and classification 1-8 details and 8th approximation coefficients are utilized for coefficients feature vector development. The first level signal has a frequency range of $f/2 - f/4$ i.e. 2500-5000Hz, where f is the sampling frequency. In the same way second level has frequency range of $f/4 - f/8$ i.e. 2500-1250 Hz. The third, fourth, fifth, sixth, seventh and eighth level decomposed disturbance signal have the frequency ranges of $f/8 - f/16, \dots, f/256 - f/512$ correspondingly.

To reduce the data set and to enhance the accuracy of classifier, statistical analysis is performed on coefficient vectors by pulling out energy, Shannon’s entropy and standard deviation information. Out of (27×100) of the samples of approximation and detail coefficient features half of samples i.e. (27×50) dimension of each disturbance are used for training SVM classifier. However, for testing the classifiers classification performance and evaluation of trained model, remaining extracted feature vectors are utilized in SVM predictor model for all the ten types of PQ disturbances. Such disturbance classes are presented in confusion matrix, shown in Table I, where the matrix is constructed with actual classes vs. classifiers predicted classes.

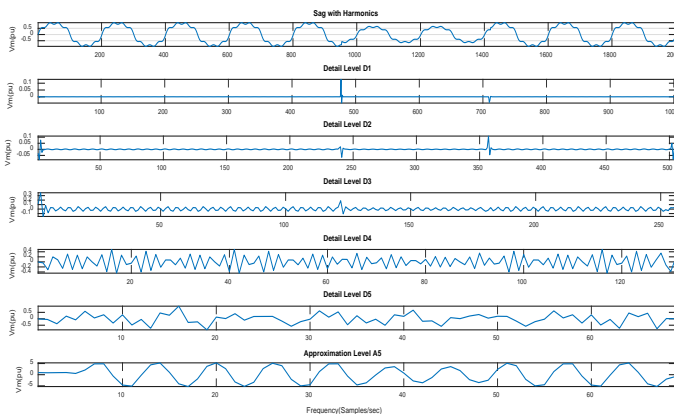


Fig 8. Generated Sag with Harmonics disturbance sample with its detail levels 1– 5 and 5th level Approximation coefficient waveforms.

TABLE I. CONFUSION MATRIX

		PREDICTED CLASSES									
		C1	C2	C3	C4	C5	C6	C7	C8	C9	C10
ACTUAL CLASSES	C1	50	0	0	0	0	0	0	0	0	0
	C2	0	44	0	6	0	0	0	0	0	0
	C3	0	0	49	0	0	0	0	1	0	0
	C4	0	4	0	46	0	0	1	0	0	0
	C5	0	0	0	0	50	0	0	0	0	0
	C6	6	0	0	0	0	43	1	0	0	0
	C7	9	0	0	0	0	0	41	0	0	0
	C8	2	0	0	0	0	0	0	48	0	0
	C9	0	0	0	0	0	0	0	0	50	0
	C10	0	0	0	0	0	0	0	0	1	49

In Tables I, II and III, C represents labels for disturbance types which are specified as follows:

- C1 Sine Wave
- C2 Sag
- C3 Swell
- C4 Interruption
- C5 Harmonics
- C6 Impulsive Transients
- C7 Oscillating Transients
- C8 Flickers
- C9 Sag and Harmonics
- C10 Swell and Harmonics

The diagonal elements in confusion matrix represent true positives (TP) i.e. correctly classified disturbances, whereas off diagonal elements shows misclassified disturbance samples. From matrix, all rows elements except diagonal element are false negatives (FN) i.e. sample is classified as predicted class but actually it is not. Similarly, all the column elements except diagonal elements are false positives (FP). Classifier performance summary is shown in Table II, where positive rate of disturbance class refers sensitivity of classifier or recall rate. The overall accuracy is found 94%.

TABLE II. CLASSIFIER PERFORMANCE SUMMARY

Classes	T.P Rates (%)	FN Rates (%)	Positive Predictive Rate (%)	False Discovery Rate(%)
C1	100%	--	75%	25%
C2	88%	12%	92%	8%
C3	98%	2%	100%	--
C4	92%	8%	88%	12%
C5	100%	--	100%	--
C6	86%	14%	100%	--
C7	82%	18%	98%	2%
C8	96%	4%	98%	2%
C9	100%	--	98%	2%
C10	98%	2%	100%	--
Overall Accuracy 94 %				

TABLE III. CORRECTLY CLASSIFIED VERSUS MISCLASSIFIED SAMPLE RESULTS

Types Of PQDs	Testing Patterns	Correct (Classified)	Misclassified
C1	50	50	00
C2	50	44	06
C3	50	49	01
C4	50	46	04
C5	50	50	00
C6	50	43	07
C7	50	41	09
C8	50	48	02
C9	50	50	00
C10	50	49	01
Average	50	47	3

Tables I, II and III clearly shows that proposed algorithms has effectively classified the eight distinct and two hybrid PQDs. Performance of classifier is found up to mark. As fifty disturbances sample patterns for all ten disturbance classes were employed for testing purpose in SVM classifier. In consequence, an average of 47 samples out of 50 is found correctly classified whereas 3 samples are found as misclassified. However class wise correctly classified and misclassified samples numbers are also tabulated in Table III. The classification results show that proposed algorithm is effective and due to its simplicity and less computational requirements it is suitable and nominally applicable.

VII. CONCLUSION

This paper has presented an automatic machine learning based PQDs pattern classification by adopting statistically unique extracted features of Energy, Entropy and Standard deviation. These features have been calculated from the range

of one to 8th level decomposed wavelet coefficients for each of the randomly generated disturbance samples. Such Disturbances were obtained from IEEE standard limits based parametric equations. With proposed feature combination and distinctive disturbance types, proposed approach of using multi-resolution analysis based discrete wavelet transform and support vector machine algorithm provides the better classification results with distinct and multiple power quality disturbance classes, in spite of small training data set. Classification using optimization algorithms for optimal feature selections are more effective due to non-selection redundant features, but it requires more computational resources, time and complex simulations. Therefore with small data set and limited resources, DWT-SVM with Gaussian kernel provides the best classification in this case. The proposed work exhibits a promising agreement with simulation results.

ACKNOWLEDGMENT

This work is supported by Quaid-e-Awam University Campus of Engineering Science and Technology, Larkana, Sindh Pakistan. And Quaid-e-Awam University of Engineering Science and Technology, Nawabshah, Pakistan

Conflicts of Interest: The authors declare no conflict of interest.

REFERENCES

- [1] K. Thirumala, M. S. Prasad, T. Jain, and A. C. Umarikar, "Tunable-Q wavelet transform and dual multiclass SVM for online automatic detection of power quality disturbances," IEEE Transactions on Smart Grid, vol. 9, pp. 3018-3028, 2018.
- [2] H. Liu, F. Hussain, Y. Shen, S. Arif, A. Nazir, and M. Abubakar, "Complex power quality disturbances classification via curvelet transform and deep learning," Electric Power Systems Research, vol. 163, pp. 1-9, 2018.
- [3] S. Khokhar, A. A. B. Mohd Zin, A. S. B. Mokhtar, and M. Pesaran, "A comprehensive overview on signal processing and artificial intelligence techniques applications in classification of power quality disturbances," Renewable and Sustainable Energy Reviews, vol. 51, pp. 1650-1663, 2015.
- [4] S. Khokhar, A. A. Mohd Zin, A. S. Mokhtar, and N. Zareen, "Automatic Pattern Recognition of Single and Multiple Power Quality Disturbances," Australian Journal of Electrical and Electronics Engineering, 2015.
- [5] M. ElNozahy, R. El-Shatshat, and M. Salama, "Single-phasing detection and classification in distribution systems with a high penetration of distributed generation," Electric Power Systems Research, vol. 131, pp. 41-48, 2016.
- [6] F. A. Borges, R. A. Fernandes, I. N. Silva, and C. B. Silva, "Feature extraction and power quality disturbances classification using smart meters signals," IEEE Transactions on Industrial Informatics, vol. 12, pp. 824-833, 2016.
- [7] Z. Liu, Q. Hu, Y. Cui, and Q. Zhang, "A new detection approach of transient disturbances combining wavelet packet and Tsallis entropy," Neurocomputing, vol. 142, pp. 393-407, Oct 22 2014.
- [8] M. Biswal and P. K. Dash, "Measurement and Classification of Simultaneous Power Signal Patterns With an S-Transform Variant and Fuzzy Decision Tree," IEEE Transactions on Industrial Informatics, vol. 9, pp. 1819-1827, 2013.
- [9] S. Khokhar, A. A. Mohd Zin, A. P. Memon, and A. S. Mokhtar, "A new optimal feature selection algorithm for classification of power quality disturbances using discrete wavelet transform and probabilistic neural network," Measurement, vol. 95, pp. 246-259, 2017.
- [10] S. Salcedo-Sanz, J. L. Rojo-Álvarez, M. Martínez-Ramón, and G. Camps-Valls, "Support vector machines in engineering: An overview,"

- Wiley Interdisciplinary Reviews: Data Mining and Knowledge Discovery, vol. 4, pp. 234-267, 2014.
- [11] S. Khokhar, A. A. M. Zin, A. P. Memon, and A. S. Mokhtar, "A new optimal feature selection algorithm for classification of power quality disturbances using discrete wavelet transform and probabilistic neural network," *Measurement*, vol. 95, pp. 246-259, 2017.
- [12] J. Barros, R. I. Diego, and M. de Apráziz, "Applications of wavelets in electric power quality: Voltage events," *Electric Power Systems Research*, vol. 88, pp. 130-136, 2012.
- [13] M. Tuljapurkar and A. A. Dharme, "Wavelet based signal processing technique for classification of power quality disturbances," in *Proceedings - 2014 5th International Conference on Signal and Image Processing, ICSIP 2014*, 2014, pp. 337-342.
- [14] A. A. Abdoos, Z. Moravej, and M. Pazoki, "A hybrid method based on time frequency analysis and artificial intelligence for classification of power quality events," *Journal of Intelligent & Fuzzy Systems*, vol. 28, pp. 1183-1193, 2015 2015.
- [15] M. B. Latran and A. Teke, "A novel wavelet transform based voltage sag/swell detection algorithm," *International Journal of Electrical Power & Energy Systems*, vol. 71, pp. 131-139, 10// 2015.
- [16] P. Kanirajan and V. S. Kumar, "Power Quality Disturbance Detection and Classification using Wavelet and RBFNN," *Applied Soft Computing*, vol. 35, pp. 470-481, 2015.
- [17] H. Erişti, Ö. Yıldırım, B. Erişti, and Y. Demir, "Optimal feature selection for classification of the power quality events using wavelet transform and least squares support vector machines," *International Journal of Electrical Power & Energy Systems*, vol. 49, pp. 95-103, 2013.
- [18] A. A. M. Z. Suhail Khokhar, M. A. Bhayo, A. S. Mokhtar, "Automated recognition of single & hybrid power quality disturbances using wavelet transform based support vector machine," *Jurnal Teknologi*, vol. 79, pp. 97-105, 2017.
- [19] S. Ekici, "Classification of power system disturbances using support vector machines," *Expert Systems with Applications*, vol. 36, pp. 9859-9868, 2009.
- [20] F. M. Arrabal-Campos, F. G. Montoya, R. Baños, J. Martínez-Lao, and A. Alcayde, "Simulation of power quality disturbances through the wavelet transform," in *Harmonics and Quality of Power (ICHQP)*, 2018 18th International Conference on, 2018, pp. 1-5.
- [21] N. Huang, S. Zhang, G. Cai, and D. Xu, "Power Quality Disturbances Recognition Based on a Multiresolution Generalized S-Transform and a PSO-Improved Decision Tree," *Energies*, vol. 8, pp. 549-572, Jan 2015.
- [22] S. Jeevitha and M. C. Mabel, "Analysis of Multi-Disturbance Power Signals on Compression: A Wavelet Based Approach," *Journal of Computational and Theoretical Nanoscience*, vol. 15, pp. 345-350, 2018.
- [23] D. De Yong, S. Bhowmik, and F. Magnago, "An effective Power Quality classifier using Wavelet Transform and Support Vector Machines," *Expert Systems with Applications*, vol. 42, 2015.
- [24] D. D. Ferreira, J. M. de Seixas, and A. S. Cerqueira, "A method based on independent component analysis for single and multiple power quality disturbance classification," *Electric Power Systems Research*, vol. 119, pp. 425-431, Feb 2015.
- [25] A. A. Abdoos, P. Khorshidian Mianaei, and M. Rayatpanah Ghadikolaei, "Combined VMD-SVM based feature selection method for classification of power quality events," *Applied Soft Computing*, vol. 38, pp. 637-646, 1// 2016G. Eason, B. Noble, and I. N. Sneddon, "On certain integrals of Lipschitz-Hankel type involving products of Bessel functions," *Phil. Trans. Roy. Soc. London*, vol. A247, pp. 529-551, April 1955. (*references*)
- [26] T. A. Kawady, N. I. Elkalashy, A. E. Ibrahim, and A.-M. I. Taalab, "Arcing fault identification using combined Gabor Transform-neural network for transmission lines," *International Journal of Electrical Power & Energy Systems*, vol. 61, pp. 248-258, 2014.
- [27] R. Kumar, B. Singh, and D. T. Shahani, "Recognition of Single-stage and Multiple Power Quality Events Using Hilbert-Huang Transform and Probabilistic Neural Network," *Electric Power Components and Systems*, vol. 43, pp. 607-619, 2015/04/03 2015.
- [28] R. Kumar, B. Singh, D. T. Shahani, A. Chandra, and K. Al-Haddad, "Recognition of Power-Quality Disturbances Using S-Transform-Based ANN Classifier and Rule-Based Decision Tree," *IEEE Transactions on Industry Applications*, vol. 51, pp. 1249-1258, Mar-Apr 2015.
- [29] K. Thirumala, S. Pal, T. Jain, and A. C. Umarikar, "A classification method for multiple power quality disturbances using EWT based adaptive filtering and multiclass SVM," *Neurocomputing*, 2019.

Smart Parking Architecture based on Multi Agent System

Sofia Belkhala¹, Siham Benhadou², Khalid Boukhdir³, Hicham Medromi⁴

Research Foundation for Development and Innovation in Science and Engineering
Engineering Research Laboratory (LRI), System Architecture Team (EAS), National and High School of Electricity and
Mechanic (ENSEM) Hassan II University
Casablanca, Morocco

Abstract—Finding a parking space in big cities is becoming more and more impossible. In addition, the emergence of car has created several problems relating to urban mobility for the city. But with the development of technology, these problems can be solved. In this paper, the problem of parking has been addressed by proposing an architecture to automate the parking process using the internet of things, artificial intelligence and multi agent systems.

Keywords—Smart parking; IoT; multi agent system; artificial intelligence; parking availability; IoT application

I. INTRODUCTION

In the past years, several urban traffic problems have emerged: increase in the car fleet, traffic jams, traditional infrastructure. Faced with these and other problems, cities must use technologies to remain competitive and provide a decent quality of life for their citizens by offering them several services, including the ability to travel efficiently. The concept of smart cities has emerged to achieve those goals, even if there is no exact definition of a smart city, [1] says that a city is smart if we use data, information and information technologies to improve urban performance by providing more effective services to citizens. The smart city encompasses several domains, governance, transportation, economy, etc. Our research work deals with the intelligent transport aspect and more specifically parking.

Indeed, large cities around the world suffer from traffic congestion problems; among its causes we find the parking. In fact, car parks are the point of departure and arrival of each driver, according to the British Parking Association [2] the search time of a place to park in London rises to about 8 minutes, this long search time may be also the case in most large cities around the world, it negatively affects urban mobility by causing traffic jams and accidents, as well as the environment by raising CO₂ emissions and fuel consumption. In addition, many cities have experienced an emergence of their housing stock, yet during planning we don't think about adding car parks, even in terms of road traffic, the usual thought is to widen the roads without thinking about adding parking spaces [3]. As a result, it has become necessary to have efficient car parks with a modern infrastructure and an intelligent management to replace the existing traditional car parks.

The rest of the paper is structured as follows. Starting with discussing the existing research in smart parking, the second section presents the notions of the agents, multi agent systems as well as distributed artificial intelligence, the fourth section focuses on the proposed architecture by defining the different agents and their mission. Finally, the conclusion highlights the horizons of this work.

II. STATE OF ART

The search for a parking space is done manually, the driver doesn't know where to go, his only desire is to find a place close to his destination, and this research can lead to a result by pure luck. Moreover, during this search, several phenomena can occur such as multiple cars chasing a single space, and blind search strategy. Automatizing parking process is the key to solve several urban mobility problems, and as a consequence improving life quality for the citizens. Thence, many researchers have been motivated to improve parking situation in cities. This research was mainly based on the use of the Internet of Things, because nowadays we use ubiquitous computing [4] rather than traditional one.

Authors in [5] worked on an automated parking system at low prices by using the Internet of Things (IoT), and more specifically the ultrasonic sensors to retrieve the state of the parking spaces, this information is shared with the drivers via a mobile application, which gives them also the opportunity to reserve parking places in advance. On the other hand, there are several solutions based on the sensors placed at the parking spaces, authors in [6] have used IR sensors as well as Radio-Frequency IDentification (RFID) technology to detect the license plate of the car, also the driver can book parking space if he pays online. For [7] they deployed optical sensors per parking space, so that the parking availability is communicated later to the drivers, [8] used a microcontroller to collect parking spaces information to communicate them after to the drivers.

Mobile and web applications based on sensors have emerged for parking management [9] [10] [11], ParkNet [9] is a solution based on ultrasonic sensors as well as the GPS module implemented in cars rather than the parking spaces, when the car is running, it is possible to collect information about the empty spaces and communicate it to the drivers looking for a parking space.

In addition to sensors, there are solutions that detect available parking spaces through image processing [12] [13] or crowdsourcing [14] [15]. Crowdsourcing is collecting data from user devices such as mobile phones, GPS devices, car sensors, etc. The value of information generated by these systems depends heavily on the number of participants. Each user contributes to the system by sharing information about empty or busy parking spaces. In return, they benefit from information such as the availability of parking in a given area.

In addition to the research cited above, some researchers have exploited artificial intelligence and specifically agents in their studies [16] [17] [18] [19]. Author in [16] developed a platform called Sencity based on the agents following the machine 2 machine architecture, the different services of the parking are presented through functions and agents who are in charge of choosing the best parking spaces according to the preferences of the drivers. Authors in [18] used the agents to negotiate the prices as well as find the most optimal place to park. Finally, [19] used the agents for two missions, (1) to automate the mission manager and to provide available parking spaces, (2) to handle requests from drivers seeking places in the city center.

According to the state of the art we find that the majority of architectures are mainly based on sensors communicating the parking status via a web or mobile application, but we don't have a general solution that integrates the cameras, RFID, payment terminals which will enrich and develop smart parking. In addition, the architectures proposed are generally based on the server client paradigm, it has a centralized database that doesn't manage the different parallel requests and if there is an internet problem the solution may not be operational. We also note the concern of the communication between the different connected objects and the data processing layer and the lack of control over the data collected.

To solve the parking problems, we don't need just to communicate the availability via Internet, but rather to automate the process from the beginning while including all services: booking, payment, identification guidance and security.

III. SMART PARKING SOLUTION BASED ON IOT, DAI AND MAS

A. Internet of things IoT

To improve the cities' infrastructure, and especially the urban mobility sector, researchers have used connected objects or so-called "Internet of Things". This term first used in 1999 by Kevin Ashton to describe the system that encompasses physical objects connected to the internet. With the development of technology, these connected objects have taken on a new dimension but with the same mission: the presence of a great variety of objects communicating with each other in order to achieve a mission [20]. For the parking presented in this paper, there are different connected objects such as: RFID, sensors, cell phones, exit terminals. The challenge for us was to be able to connect these objects, process the information collected and transmitted through the internet, after processing the information is used to meet the user's needs.

B. Multi Agent System MAS

According to [21] an agent is an entity that can be real or abstract, with a behavior aimed at satisfying a goal by considering the prerequisite skills (communicate, perceive, act), the environment where it is positioned as well as the commands it received. We distinguish different types of agents: active, adaptive cognitive, etc.

Furthermore, the force of the agents is their ability to integrate groups [21], integrating them in a system with other agents, they begin to acquire new capacities such as communication with other each other or play different roles in the system. Even so, MAS don't affect the internal structure of the agents nor the mission assigned to it as an individual. So, a MAS is a set of agents that communicate with each other and they can, in an environment, act on objects. The MAS have been exploited to enrich and enhance the concept of artificial intelligence by distributing knowledge on multiple agents before completing missions. Indeed, this approach allows to work with a distributed artificial intelligence which will improve the reliability of the systems as well as facilitate their extension.

C. Distributed Artificial Intelligence

Artificial intelligence is the ability of machines to simulate human intelligence. This simulation involves several steps: the acquisition and the rules for using the information known as learning, the reasoning to obtain results by exploiting the acquired data and finally the self-correction to improve the machine's performance [22].

One of the branches of artificial intelligence is Distributed Artificial Intelligence DAI. DAI is interested in setting up cooperative systems based on agents who have the capabilities, as mentioned before, of reasoning, planning and communication. In addition, for these systems to succeed it is necessary for it to have interpersonal planning to cooperate and reduce conflict, in addition to these systems have control, data (storage and processing) and decentralized knowledge.

Moreover, artificial intelligence, and more specifically, machine learning has known the emergence of reinforcement learning which is similar to the way humans learn. It is based on the idea that an agent learns to behave and interact with his environment by performing tasks and visualizing the results, (as a human being, agents continually explore and update their values) to maximize their rewards.

IV. PROPOSED ARCHITECTURE

The proposed solution will allow drivers to check in real time free parking spaces and be guided from their current location to the parking place assigned by the system. The objective is to simplify the parking process, while allowing all parties involved to communicate with each other and to seek help from the system operator.

The infrastructure of the smart parking is composed of several types of equipment, but the essentials ones are: Magnetic sensors, a fixed RFID reader, terminals (laptop, mobile phone, etc.), an OCR camera and display screens. All of these devices are connected to the system knowledge base.

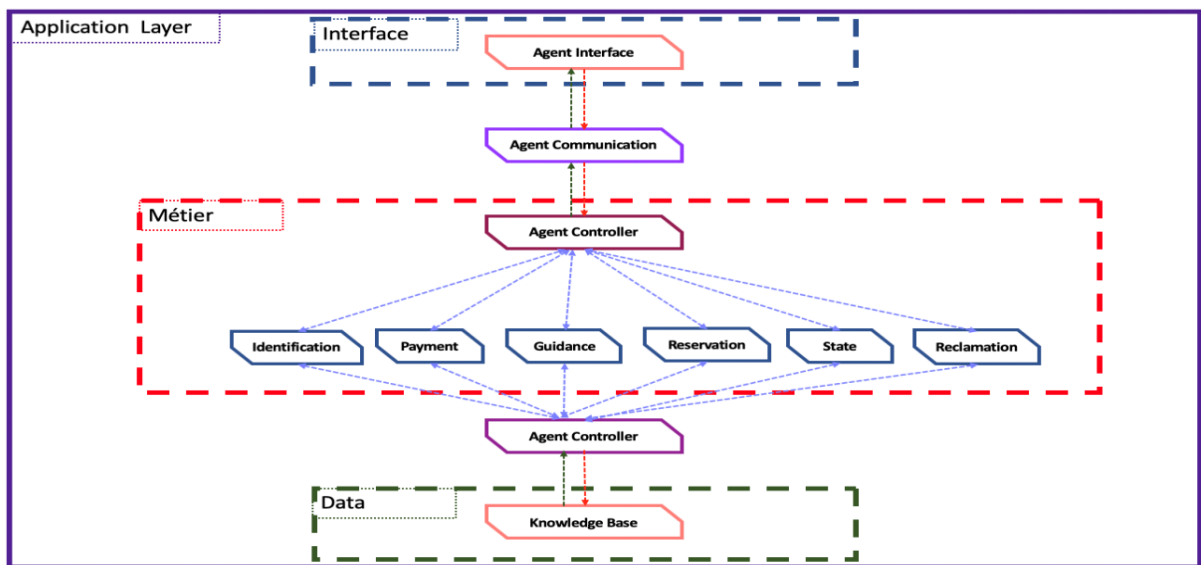


Fig. 1. Physical Layer Architecture.

Concerning the actors of the system there are two main actors: a user and administrator. A user is someone who benefits from the services. He can be either a subscriber or a visitor, both users can benefit from the features of the application with different privileges. The subscriber interacts with the web application, after authentication or registration, he can perform several operations such as checking the parking status, pay the subscription, reserve a place in advance, submit a claim, etc. on the other hand, the visitor can only check parking availability with a payment on the spot. Nevertheless, a traveler who doesn't have access to the application can also use the parking and he will be treated as a visitor upon payment.

Regard the Administrator, he has visibility of the entire system, manages users, and needs to make sure the application knowledge base is up-to-date.

A. Smart Parking Architecture

The proposed solution is a multi-agent system distributed over three main layers communicating with each other in real time to achieve the objectives assigned. In the following discuss the physical and the application layer will be discussed.

1) *The physical layer:* It consists mainly of connected objects such as: magnetic sensors, RFID terminals, cameras (as shown in Fig. 1). To guarantee the proper functioning, we chose to implement different agents to a well-defined role:

- **RFID Agent:** Agent who is responsible for identifying the driver and the car, checking the validity of its subscription, this agent must handle multiple entries at the same time.
- **Payment Agent:** Identify the payment method, the amount, if there is any discount, etc. after the payment is made, the agent must send a message to the exit agent to authorize the exit of the vehicle
- **Sensor Agent:** Is interested in sensor networks, their

operations, detects anomalies (if there are any), check the availability and the performance of each sensor.

- **Surveillance Agent:** Check and process the images/videos captured by the cameras to see if there are badly parked cars, or accidents. If an anomaly is detected, a message is sent to the control agent and in parallel the process of help or rescue is triggered (for example in the case of an accident a message is sent to the infirmary).
- **Control Agent:** Agent in communication with the different agents, he must make sure that everything works well. occupied spaces correspond to the number of occupied sensors and the vehicles authorized by the entry agent or the exit agent. If it does not, it uses the monitoring agent for verification. In addition, it is in communication with the input agent and the preference agents to choose the most suitable place and then communicate it to the display agent.
- **Display Agent:** Responsible for the display at the screens located at the entrance and the middle screens, this agent can display different message depending on what happens at the parking (guidance, user balance).
- **Entry Agent:** Agent responsible for identifying the person entered and his type, whether the terminal will deliver an entry ticket or not. This agent communicates with the control agent, to see if he should allow the entry.
- **Exit Agent:** Responsible for identifying the person at the exit, if the payment is made or no after it sends the information to the action agent to authorize (or not) the exit.
- **Preference Agent:** From user's behavior, this agent communicates with the control agent to specify if he must have a specific treatment (case of person with reduced mobility, electric car, etc.).

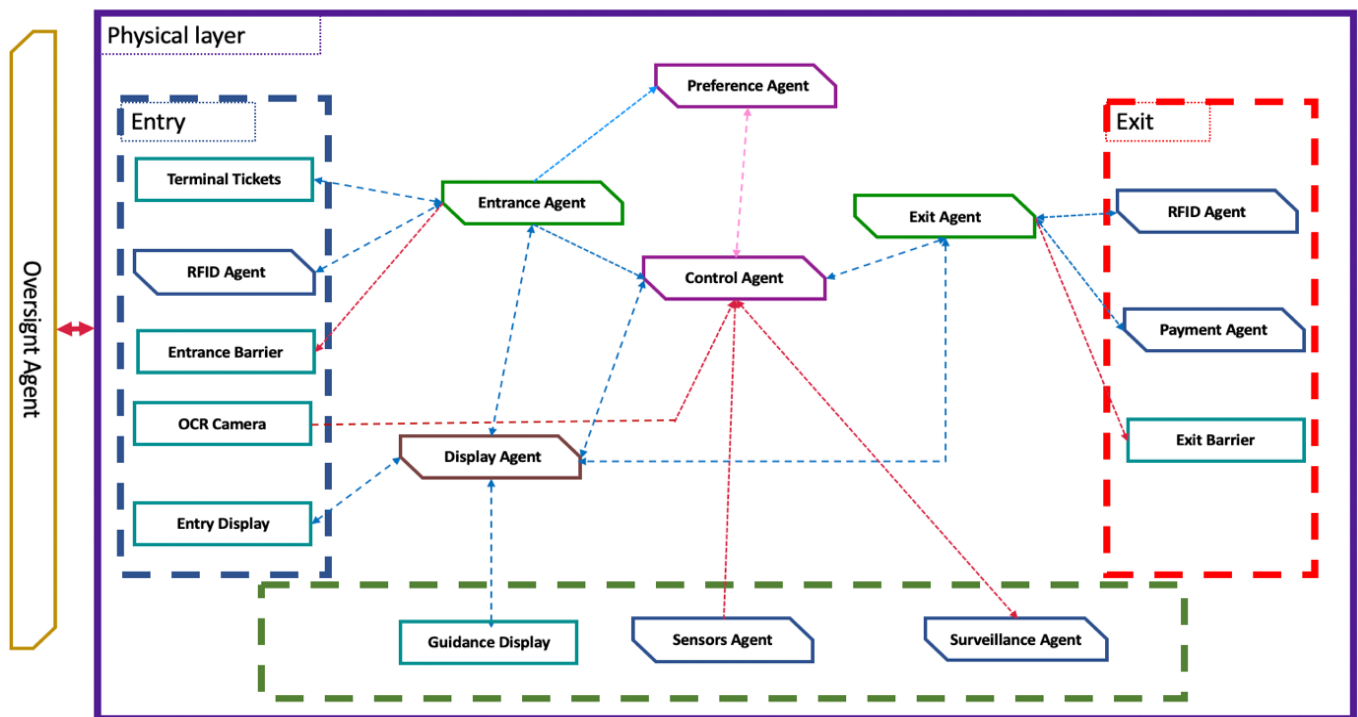


Fig. 2. Application Layer Architecture.

2) *The application layer*: It is the communication interface with the users, it also consists of different agents (as shown in Fig. 2):

- Agent interface: The intermediary between the system and the users, it receives the requests of the users and display the result after the treatment by the system.
- Communication Agent: Used to establish communication between the presentation layer and the business layer by forwarding requests and responses to the responsible agent.
- Controller Agent: Controller calls the business service that performs the processing associated with the action received by the communication agent. This service may call other services, as needed, at the same time.
- Identification Agent: Identifies the type of person connected to the application, and the privileges it has.
- Payment agent: For the case of a customer registered at the application level, this agent is in charge of all payment related services (updating drivers balance, informing reminds them to pay the subscription).
- Guidance Agent: Responsible for displaying to the user the most optimum path from its location to its parking spot
- Reservation Agent: Receives requests for bookings and processes them according to availability. In the case where the reservation request is confirmed, the information must be communicated to the communication agent of the physical layer.

- Agent State: Detect free / busy places by considering different requests from other actors in the system.
- Claims Agent: Responsible for handling customer complaints, by raising the key words of the complaint the agent will communicate in real time the complaint to the actors responsible of handling it.
- Knowledge Base: Gathers knowledge and rules specific to parking.

Agents communicate with each other to achieve the goal assigned by the system, they learn and improve their behavior by interacting with the environment. Also, they must cooperate, as they may not have sufficient information, or the most appropriate way to solve the problem. The integration of the learning system has made it possible to have a powerful and efficient system.

One of the strengths of the architecture is to be able to work even if one of the components breaks down because we have a distributed system that handles the different parallel requests.

V. CONCLUSION

Smart parking is considered the solution to the majority of traffic issues. Indeed, by setting up an intelligent and efficient system, the traffic will be better managed, the search time of a parking space will be reduced, the rates will be regulated which enables the parking to increase profits. by focusing on these and other objectives, we have put in place an intelligent parking system based on the Internet of Things and multi agent systems.

For our future work, we will detail the characteristics and the behaviors of each agent, how they communicate with each

other, the system hierarchy and how the different decisions are made.

REFERENCES

- [1] M. L. Marsal-Llacuna, J. Colomer-Llinàs, and J. Meléndez-Frigola, “Lessons in urban monitoring taken from sustainable and livable cities to better address the Smart Cities initiative,” *Technological Forecasting & Social Change* 2014.
- [2] <https://www.telegraph.co.uk/news/2017/02/01/motorists-spend-four-days-year-looking-parking-space/>
- [3] M. Manville, and D. Shoup, “Parking People, and Cities” *Journal of Urban Planning and Development*, Vol. 131, No. 4, December 1, 2005.
- [4] J. Gubbia, R. Buyyab, S. Marusic, M. Palaniswami, “Internet of Things (IoT): A vision, architectural elements, and future directions,” *Future Generation Computer Systems* 29 (2013) 1645–1660
- [5] R. Gupta, S. Pradhan, A. Haridas, and D.C. Karia, “Cloud Based Smart Parking System,” *Proceedings of the 2nd International Conference on Inventive Communication and Computational Technologies (ICICCT 2018) IEEE Xplore Compliant - Part Number: CFP18BAC-ART; ISBN:978-1-5386-1974-2*
- [6] B. M. Kumar Gandhi, and M. Kameswara Rao, “A Prototype for IoT based Car Parking Management System for Smart Cities,” *Indian Journal of Science and Technology*, Vol 9(17), DOI: 10.17485/ijst/2016/v9i17/92973, May 2016
- [7] (Automated Parking System using IOT)
- [8] Y. Raghavender Rao, “Automatic Smart Parking System using the Internet of Things (IOT),” *International Journal of Engineering Technology Science and Research* ISSN 2394 – 3386 Volume 4, Issue 5 May 2017
- [9] S. Mathur, S. Kaul, M. Gruteser, and W. Trappe, “ParkNet: A Mobile Sensor Network for Harvesting Real Time Vehicular Parking Information,” *MobiHoc S’09*, May 18, 2009, New Orleans, Louisiana, USA. ACM 978-1-60558-521-5/09/05.
- [10] R. Salpietro, L. Bedogni, M. Di Felice, and L. Bononi, “Park Here! A Smart Parking System based on Smartphones’ Embedded Sensors and Short Range Communication Technologies,” *2015 IEEE 2nd World Forum on Internet of Things (WF-IoT)* 14-16 Dec. 2015 Milan-Italy
- [11] N. Larisis, L. Perlepes, P. Kikiras, and G. Stamoulis, “U-Park : Parking Management System Based on Wireless Sensor Network Technology,” *SENSORCOMM 2012 : The Sixth International Conference on Sensor Technologies and Applications*
- [12] Z. Bin, J. Dalin, W. Fang, and W. Tingting, “A Design of Parking Space Detector Based on Video Image,” *The Ninth International Conference on Electronic Measurement & Instruments ICEMI’2009*
- [13] N. Thai-Nghe, and N. Chi-Ngon, “An Approach for Building an Intelligent Parking Support System,” *SoICT’14* December 04 - 05 2014, Hanoi, Viet Nam.
- [14] X. Chen, E. Santos-Neto, and M. Ripeanu, “Crowdsourcing for On-street Smart Parking,” *DIVANet’12*, October 21–22, 2012, Paphos, Cyprus
- [15] J. Villalobos, B. Kifle, D. Riley and J. U. Quevedo-Torrero, “Crowdsourcing Automobile Parking Availability Sensing Using Mobile Phones”.
- [16] M. Bilal, C. Persson, F. Ramparany, G. Picard and O. Boissier, “Multi-Agent based governance model for Machine-to-Machine networks in a smart parking management system,” *3rd IEEE International Workshop on SmART COmmunications in NETWORK Technologies*
- [17] I. Benenson, K. Martens, and S. Birfir, “PARKAGENT: An agent-based model of parking in the city,” *Computers, Environment and Urban Systems* 32 (2008) 431–439
- [18] C. Shu-Yan, L. Shih-Wei, and L. Chien-Chang, “Dynamic parking negotiation and guidance using an agent-based platform,” *Expert Systems with Applications* 35 (2008) 805–817
- [19] C. Di Napoli, D. Di Nocera, and S. Rossi, “Agent Negotiation for Different Needs in Smart Parking Allocation” *Springer International Publishing Switzerland* 2014
- [20] D. Giusto, A. Iera, G. Morabito, and L. Atzori, “The Internet of Things,” *Springer*, 2010. ISBN: 978-1-4419-1673-0.)
- [21] J. Ferber, *Coopération réactive et émergence*. Intellectica, 2(19), 19-52.
- [22] <https://searchenterpriseai.techtarget.com/definition/AI-Artificial-Intelligence>

Towards Implementing Framework to Generate Myopathic Signals

Amira Dridi^{1*}, Jassem Mtimet^{2*}, Slim Yacoub^{3*}

*Signal, Image and Technology of Information Laboratory, National Engineering School of Tunis
Tunis el Manar University, BP 37 Belvedere, 1002, Tunis, Tunisia

Abstract—In this paper, we describe a simulation system of myopathicsurface electromyography (sEMG) signals. The architecture of the proposed system consists of two cascading modules. SEMG signals of three pathological skeletal muscles (Biceps Brachii, InterosseusDorsalis, TibialisAnterior) were generated. Root Mean Square (RMS Envelope) and Power Spectral Density (PSD) were used to validate our system.

Keywords—Component; Surface Electromyography (sEMG); myopathy; root mean square; Power Spectral Density (PSD); skeletal muscles; biceps brachii; interosseous dorsalis; tibialis anterior

I. INTRODUCTION

Electromyography covers the study of muscle function through electrical signals. This medical examination collects measures and records the electrical signal that propagates in the nerves or in the muscle fibers (Action Potential). It consists of plotting the variations of the muscular membrane on the display screen; this diagnostic procedure is performed either in a non-invasive manner using skin contact electrodes (surface electromyography) or in an invasive manner using needle electrodes (invasive electromyography). These detection processes are often used in several fields such as: neuromuscular clinical diagnostics, rehabilitation, prosthesis control, muscle fatigue studies and gait analysis [1-4].

The mathematical modeling of surface electromyography (sEMG) is a method which allows to synchronize physiological parameters (e.g. recruitment frequency, conduction rate...) with simulated results in order to analyze their influences and to test the validity of the algorithms used to process this kind of signals [5-7]. Recently, research studies have focused on different approaches to modeling and to simulating sEMG signals, which are based on phenomenological as well as physiological aspect [8-10]. In [1] and [6], the authors propose an in-depth recapitulative study of these approaches.

Myopathic diseases are disorders in which skeletal muscle is mainly involved. Several factors can cause myopathies including inherited genetic defects (e. g. muscular dystrophies), endocrine, inflammatory or metabolic abnormalities. The different myopathies lead weakness and atrophy of skeletal muscles. Other symptoms of myopathy include fatigue, stiffness, and muscle cramps [11].

Some myopathies, such as muscular dystrophies, develop very early, while others develop later in patient life. Some of them gradually worsen over time and do not respond well to

treatment, while others appear treatable and often remain stable for long periods of time [1].

There are no several studies interested to model this kind of signals. However, their generation provides a significant contribution in several areas. For example, for classification purposes, a clinical study is required to build a classification model that is costly in terms of time and resources. In the interest of processing these signals, we propose a model that can be used to generate myopathic signals for different types of skeletal muscles.

The paper will be organized as follows: Section 2 presents the components of the myopathicsEMG signal generation system. Section 3 illustrates the experimental results of the proposed simulation model. Finally, in Section 4 we close with a brief conclusion.

II. MATERIALS AND METHODS

The physiological and anatomy studies of striated skeletal muscles reveal their composition in motor units (MU), which are composed of motoneurons and muscle fibers. In this section, we present a mathematical-based model which generates the electrical activity of myopathic muscular pathologies. The below diagrams (Fig. 1 and Fig. 2) represent the different components of our generation model.

A. Intracellular Action Potential Generation

The generation of the intracellular action potential (IAP) produces a transmembrane ionic current $I_m(t)$ that propagates along the outer membrane of muscle fiber (sarcolemma). Moreover, the fiber is considered as a propagation tube for axially circulating current [9]. We use the following formula to generate the aforementioned current [17]:

$$I_m(t) = C.A. (\lambda v)^2 . (\lambda . v . t) . (6 - 6 * \lambda . v . t + \lambda . v^2 . t^2) . e^{-\lambda vt} \quad (1)$$

With:

- A, C: constants affecting the amplitude of I_m
- λ : Scale factor for adapting the model to the real observations
- v: speed of current propagation along the fibers

Consequently, myopathic IAPs characterizing by a short duration and low amplitude are produced after a values modification in the responsible parameters of this phenomenon (A, λ).

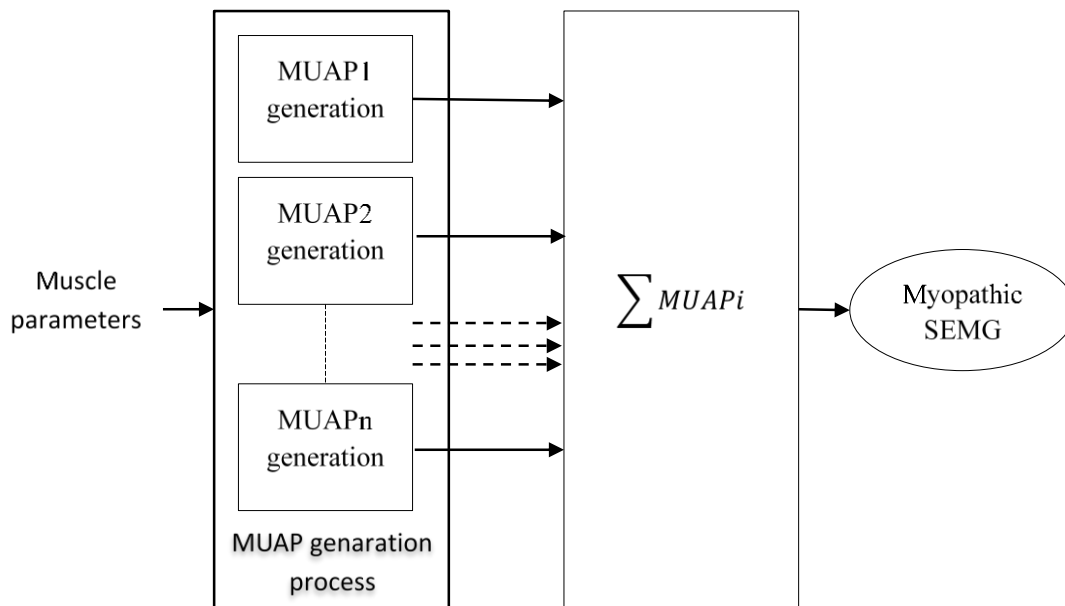


Fig. 1. Simulation Process of Myopathic SEMG.

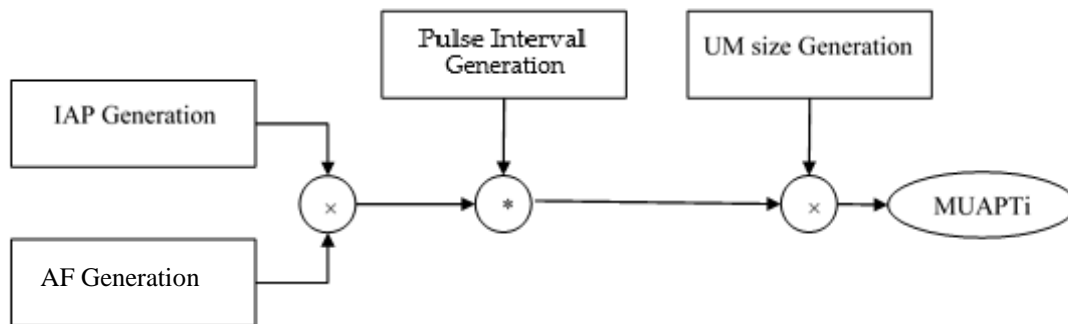


Fig. 2. Generation Process of MUAP_i.

B. Maintaining the Integrity of the Specifications

When the action potential (AP) propagates along the muscle fiber, it is automatically attenuated. In this subsection, we develop the process used to generate the appropriate attenuation function (AF) for myopathic signals. The mitigation equation is as follows [18]:

$$f = \frac{1}{4\pi\partial_e \sqrt{(z-z1)^2 + \partial_e((x-x1)^2 + (y-y1)^2)}} \quad (2)$$

Such as:

- (x,y,z) the origin coordinates
- (x1,y1,z1) electrode coordinates
- ∂_e : media conductivity

Y1 represents the distance between the muscle fiber and the detection electrode. Typically, it's a random value between 33.10^{-03} and 37.10^{-03} . ∂_e represents the conductivity value of

the medium. In the case of myopathic patient, the extracellular medium is characterized by a high conductivity compared to the normal one. For this purpose, we multiply the value of ∂_e by five.

C. Generation of Pulse Intervals

The MU discharge phenomenon is an essential process to generate SEMG signals. It depends on the inter-pulse interval (IPI) which represents the time interval between two successive pulses. Furthermore, this process is activated by exciting the motor unit MU_i at the randomly defined moment $t(i)$.

We suppose both the last excitation moment $t_{i(j-1)}$ and the firing rate (FR) of MU_i are known, we can then calculate the next excitation moment t_{ij} .

In order to simulate this process, we assume that firing rates follow a random truncated Poisson distribution between 8 and 42Hz.

Then, the excitation moment t_{ij} is determined using the following equation:

$$t_{ij} = t_{i(j-1)} + IPI_i \quad (3)$$

Where: $IPI_i = \frac{1}{FR_i}$

D. Structures Generation of Myopathic Motor units

Skeletal muscles, commonly composed of n motor units (MU) having different mechanical as well as electrical characteristics that vary according to their size. Whereas, the MU size is measured terms of the number of muscle fibers it contains.

In myopathic cases, the number of UMs composing the muscle remains unchanged; however, a reduction in their sizes is identified according to an affection percentage.

In order to generate the structure of Myopathic UM, we use the following random process:

$$MUsize_i = km_i - (km_i \times affect_{\%}) \quad (4)$$

Such as: km_i presents a random uniform distribution of number of fibers in normal UM_i and $I=[1...n]$.

E. Generation of SEMG

As we know, this step takes into consideration the muscle physiology, the conductor volume and the detection system. Whereas, SEMG signal recorded using a single monopolar electrode may be considered as a superposition of M motor unit action potentials located at different depths under the human skin and activated in semi-random manner.

$$SEMG(Z_A, t) = \sum_{m=1}^M MUAP_m(t) \quad (5)$$

When the detection system is bipolar, resulting signal is obtained using the difference between the SEMG recorded by two monopolar electrodes located in positions Z_A and Z_B .

$$SEMG(t) = SEMG(Z_A, t) - SEMG(Z_B, t) \quad (6)$$

III. RESULTS

Using the simulation model presented in the previous section, we simulate normal and myopathic signals. We assume that the used detection system is differential with two parallel placed electrodes. The following figure (Fig. 3) shows two illustration examples (normal and myopathic with a loss percentage equal to 50%). We can observe that signal relating to the muscle with anomaly presents a decrease in the amplitude and the duration of the MUAP.

Then, we focused on generating myopathic signals of three different skeletal muscles:

- Biceps brachii
- Interosseurs dorsalis
- Tibialis anterior

The composition of each muscle is described in Table I [12-14]. The obtained result is shown in Fig. 4.

For comparison purposes, we investigated the RMS factor (Fig. 5) as well as the PSD variation (Fig. 7-9) of the previously simulated signals [15, 16].

For each simulated signal, the RMS value where calculated. Given the SEMG signal $S(j)$, the RMS value is defined as:

$$RMS = \sqrt{\frac{1}{N} \sum_{j=1}^N S(j)^2} \quad (7)$$

With N represents the number of samples.

We performed a boxplot to analyze the RMS values obtained from the simulated signals of the different muscles. Fig. 6 shows the aforementioned boxplot; it represents six analyzed signals corresponding to three normal muscles and three myopathic muscles.

As we can see, there are significant differences between the mean values of RMS for the three simulated signals, corresponding to the normal muscles. Moreover, the RMS of myopathic muscles are substantially different from the normal one.

The result showed significant decrease in mean RMS from 146.10^{-4} to $3,6.10^{-4}$, from 5.10^{-5} to $112,5.10^{-5}$ and from $9,25.10^{-5}$ to 327.10^{-5} at the biceps brachii, the interosseous dorsalis and the tibialis anterior, respectively muscles.

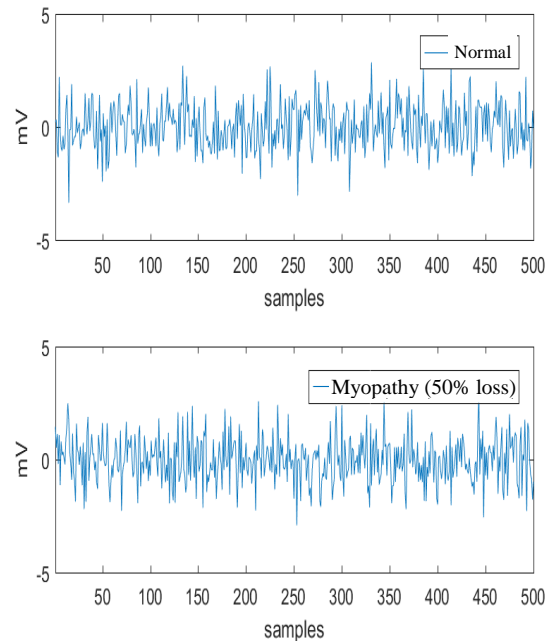


Fig. 3. Healthy and Myopathic SEMG Simulation Results.

TABLE I. SKELETAL MUSCLES COMPOSITION

Type of muscle	MU number	Number of fibers /UM
Biceps brachii (BB)	774	750 ±50
Interosseousdorsalis (IDA)	119	340 ±50
Tibialis anterior (TA)	445	270 ±50

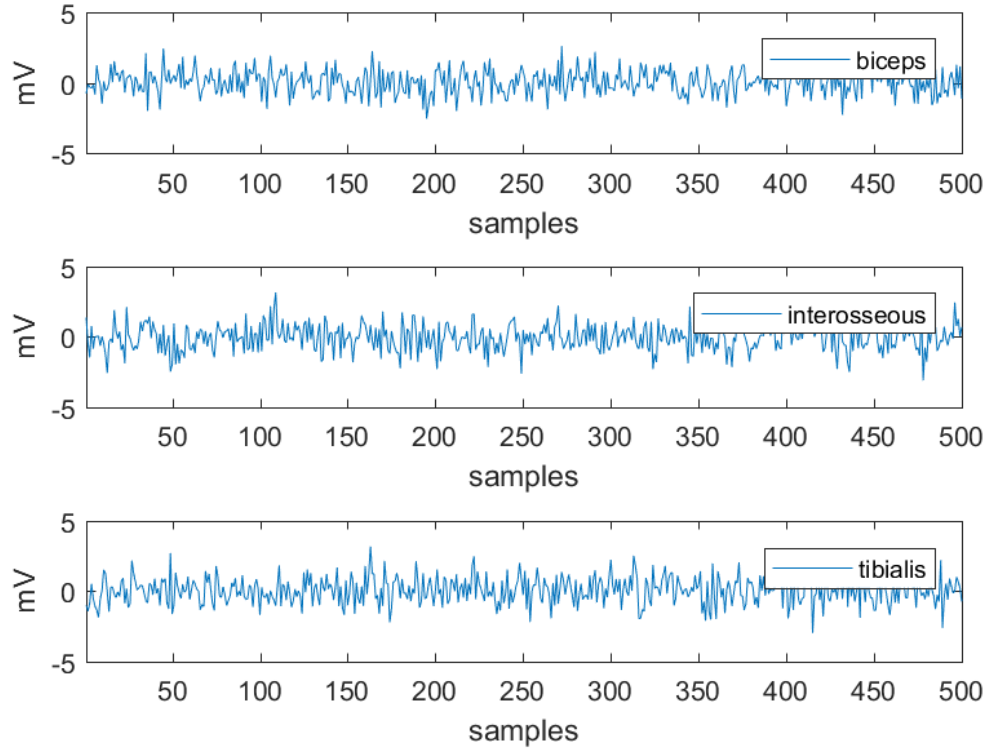


Fig. 4. Myopathic SEMG for different Muscles.

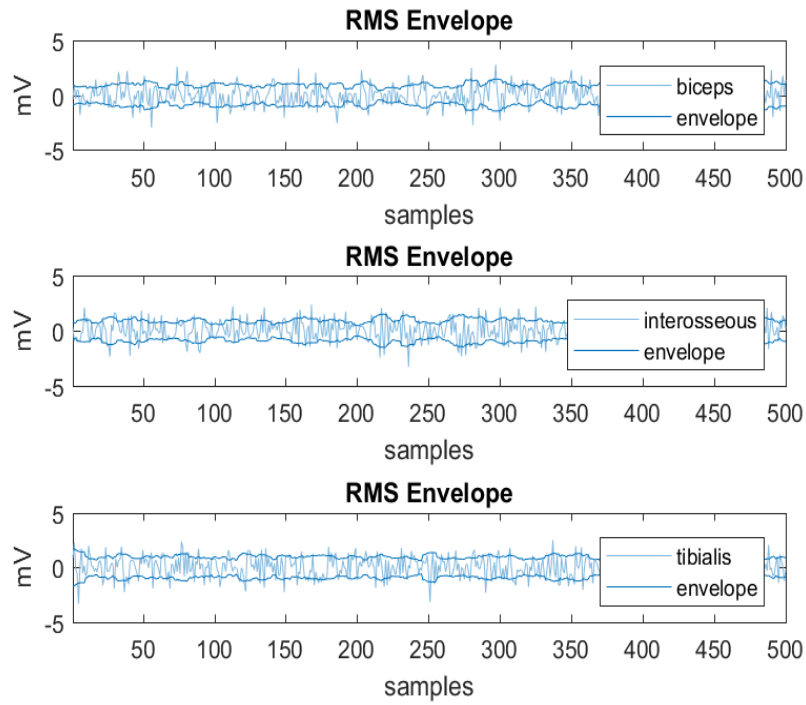


Fig. 5. RMS Envelope Results.

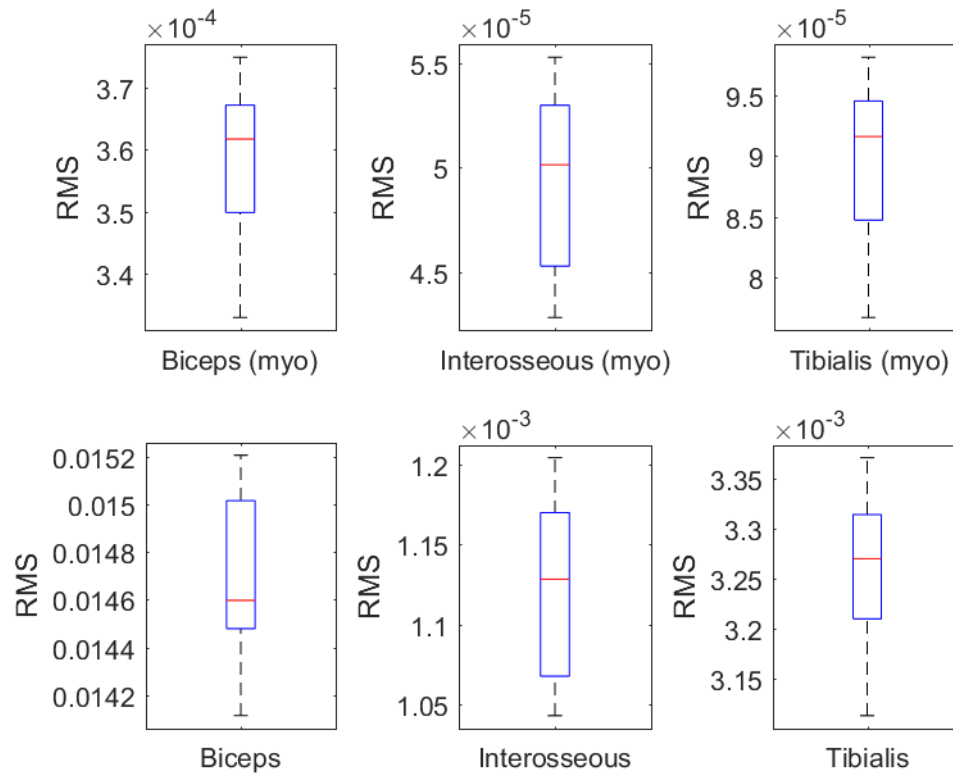


Fig. 6. Box Plot of RMS.

In order to evaluate the electrical activity of the obtained signal we calculate their peak frequency using the above equation:

$$PKF = \max(PSD_i) \quad (8)$$

Where PSD_i denote the SEMG power spectrum at frequency bin i and $i=1 \dots N$.

The boxplots in Fig. 10 illustrates the variation in the values of the PKF of different simulated signals. Based on the obtained results, we remark that all PKF of myopathic muscles is lower than those of normal muscles.

The peak frequency of myopathic patients' SEMG signals was significantly lower in tibialis than in other muscles ($9.9 \cdot 10^{-7}$ (TA) vs. $1.25 \cdot 10^{-7}$ (IDA) and $1.9 \cdot 10^{-5}$ (BB)).

As shown in Fig. 6-8, the simulated myopathic SEMG of biceps and interosseous muscles showed quite uniform frequencies, while tibialis's SEMG presented a more scattered frequency distribution. Therefore, the peak frequency was rather regular in biceps and interosseous myopathic SEMG signals, but variable in tibialis's SEMG, as exemplified in Fig. 9.

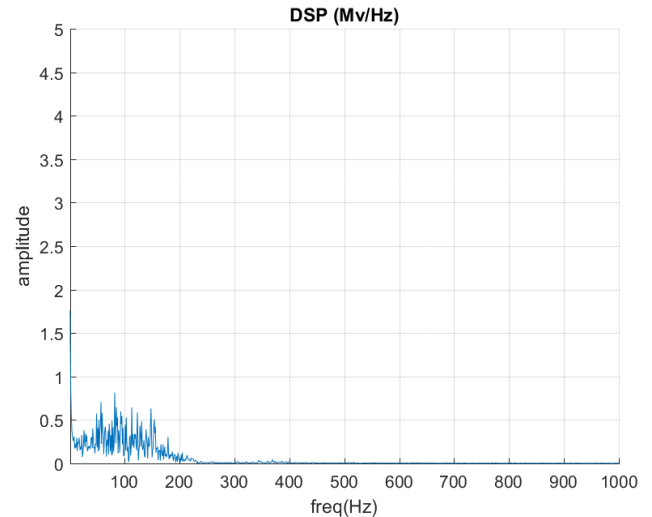


Fig. 7. PSD of Biceps SEMG Simulated Signal.

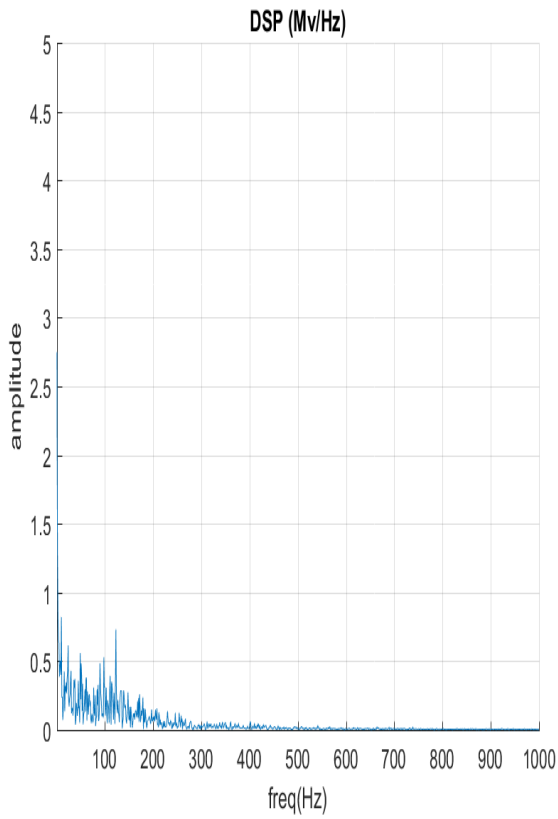


Fig. 8. PSD of Interosseus SEMG Simulated Signal.

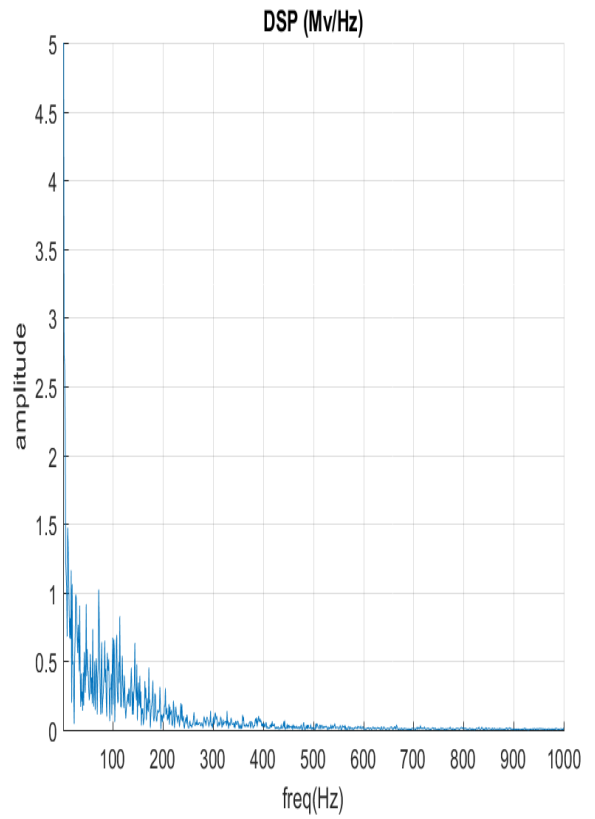


Fig. 9. PSD of Tibialis SEMG Simulated Signal.

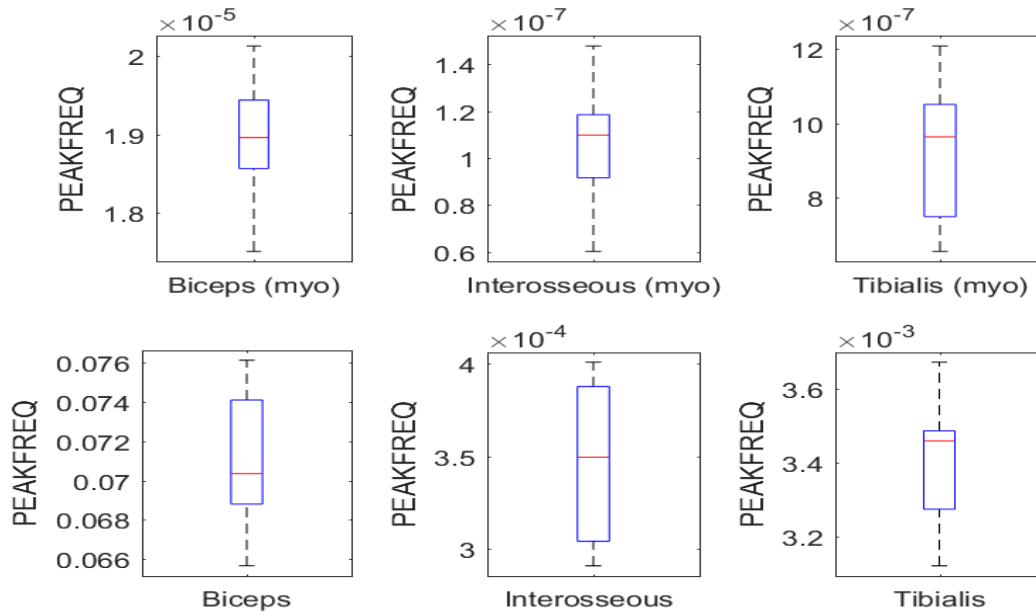


Fig. 10. Box plot of RMS.

IV. CONCLUSIONS

In this work, we presented a framework for simulating myopathic SEMG signals. It is composed of two main modules, the first one generates the MUAPs of each UM and the second one performs the spatiotemporally summing of the different MUAPs obtained from the first module. The obtained results allowed us to study the appearance and the characteristics of myopathic SEMG signals of different skeletal muscles such as: Biceps Brachii, Interosseus Dorsalis and Tibialis Anterior. After the simulation of this kind of pathological signals, we conducted a comparative study of the synthetically recorded myopathic dataset with those normal. RMS and peak frequency of PSD were used to compare the synthetic results generated by our framework.

In our future work, different validation algorithms can be used to improve the performance of our framework and other type of disorder (like neurological disorder) can be integrated.

REFERENCES

- [1] Robert Merletti and Dario Farina, editors. *Surface Electromyography: Physiology, Engineering and Applications*. John Wiley and Sons, Inc., Hoboken, New Jersey, USA., 2016.
- [2] Andrew Hamilton-Wright, and Daniel W. Stashuk, Physiologically Based Simulation of Clinical EMG Signals. *IEEE transactions on biomedical engineering*, vol. 52, no. 2, february 2005
- [3] K. C. McGill. *Surface electromyogram signal modelling*. Medical and Biological Engineering and Computing, 2004.
- [4] Neville Hogan and Robert W. Mann. Myoelectric signal processing: Optimal estimation applied to electromyography - part I: Derivation of the optimal myoprocessor. *IEEE Transactions on Biomedical Engineering*, 27(7):382–395, July 1980.
- [5] Eike Petersen and Philipp Rostalski. *A Comprehensive Mathematical Model of Surface Electromyography and Force Generation*. February 28, 2018
- [6] Javier Rodriguez-Falces, Javier Navallas, and Armando Malanda. EMG modeling. In Ganesh R. Naik, editor, *Computational Intelligence in Electromyography Analysis - A Perspective on Current Applications and Future Challenges*. InTech, October 2012.
- [7] Dario Farina, Luca Mesin, Simone Martina, and Roberto Merletti. A surface EMG generation model with multilayer cylindrical description of the volume conductor. *IEEE Transactions on Biomedical Engineering*, 2004.
- [8] Mylena Mordhorst, Thomas Heidlauf, and Oliver Röhrle. Predicting electromyographic signals under realistic conditions using a multiscale chemo-electro-mechanical finite element model. *Interface Focus*, 5, 2015. doi: 10.1098/rsfs.2014.0076.
- [9] D. Farina and R. Merletti. A novel approach for precise simulation of the EMG signal detected surface electrodes. *IEEE Transactions on Biomedical Engineering*, 2001.
- [10] Lora A Major and Kelvin E Jones. Simulations of motor unit number estimation techniques. *J. Neural Eng.* 2 (2005) 17–34
- [11] Jakob L. Dideriksen, Dario Farina, and Roger M. Enoka. Influence of fatigue on the simulated relation between the amplitude of the surface electromyogram and muscle force. *Philosophical Transactions of the Royal Society A: Mathematical, Physical and Engineering Sciences*, 2010.
- [12] Luca, Carlo J., Alexander Adam, Robert Wotiz, L. Donald Gilmore, and S. Hamid Nawab. Decomposition of surface EMG signals. *J Neurophysiol* 96: 1646–1657, 2006; doi:10.1152/jn.00009.2006.
- [13] George V. Dimitrov and Nonna A. Dimitrova. Precise and fast calculation of the motor unit potentials detected by a point and rectangular plate electrode. *Medical Engineering and Physics*, 1998.
- [14] A. J. Fuglevand, D. A. Winter, and A. E. Patla. Models of recruitment and rate coding organization in motor-unit pools. *Journal of Neurophysiology*, 1993.
- [15] Loredana R. Lo Conte, Roberto Merletti, and Guido V. Sandri. Hermite expansions of compact support waveforms: Applications to myoelectric signals. *IEEE Transactions on Biomedical Engineering*, 41(12):1147–1159, 1994.
- [16] C. Sinderby, L. Lindström, and A. E. Grassino. Automatic assessment of electromyogram quality. *Journal of Applied Physiology: Respiratory, Environmental and Exercise Physiology*, 79(5):1803–1815, 1995.
- [17] Van Veen, B. K., Wolters, H., Wallinga, W., Rutten, W. L., and Boom, H. B., The bioelectrical source in computing single muscle fiber action potentials. *Biophysical Journal*, 64(5):1492–1498, 1993.
- [18] Wheeler KA, Kumar DK, Shimada H. An accurate bicep muscle model with sEMG and muscle force outputs. *J Med Biol Eng.*; 30(6):393–8, 2010.

Towards the Performance Investigation of Automatic Melanoma Diagnosis Applications

Amna Asif¹

College of Computer Sciences and Information Technology
King Faisal University
Alahsa, Saudi Arabia

Iram Fatima²

College of Computer Sciences and Information Technology
King Faisal University
Alahsa, Saudi Arabia

Adeel Anjum³

Department of Computer Science
COMSATS Institute of Information Technology
Islamabad, Pakistan

Saif U. R. Malik⁴

Department of Computer Science
COMSATS Institute of Information Technology
Islamabad, Pakistan

Abstract—Melanoma is a type of skin cancer, one of the fatal diseases that appear as an abnormal growth of skin cells and the lesion part often looks like a mole on the skin. Early detection of melanoma from skin lesion by means of screening is an important step towards a reduction in mortality. For this purpose, numerous automatic melanoma diagnosis models based on image processing and machine learning techniques are available for computer-based applications (CBA) and smartphone-based applications (SBA). Since, the smartphones are available as most accessible and easiest methods with built-in camera option, SBA are preferred over CBA. In this paper, we explored the available literature and highlighted the challenges of SBA in terms of execution time due to the limited computing power of smartphones. To resolve this issue of storage of the smartphones, we proposed to develop an SBA that can seamlessly process the image data on the cloud instead of local hardware of the smartphone. Therefore, we designed a study to build a machine learning model of melanoma diagnosis to measure the time taken in preprocessing, segmentation, feature extraction, and classification on the cloud and compared the results with the processing time on the smartphone's local machine. The results showed there is a significant difference of p value <0.001 on the average processing time taken on both environments. As the processing on the cloud is more efficient. The findings of the proposed research will be helpful for the developers to decide the processing platform while developing smartphone applications for automatic melanoma diagnosis.

Keywords—Smartphones; computer based systems; melanoma diagnosis; cloud computing

I. INTRODUCTION

Skin cancer is the abnormal growth of tissues in the skin that often looks like a mole. When the cancerous tissues penetrate the inner layer of skin and spread in the whole body by blood and lymphatic vessels, the condition becomes life-threatening [1]. Melanoma is the most common type of skin cancer and the rate of malignant melanoma has been rising since last 30 years. According to the British Skin Foundation (BSF) [2], every year about 100,000 cases of skin cancer are diagnosed and approximately 2,500 people die due to this deadly disease. Therefore, a person requires self-awareness to

identify the early symptoms of the disease by using automatic screening of the skin from time to time. In this regard, the digital devices might help to detect this dangerous disease at the early stage [3]. Automation process of melanoma diagnosis started with the CBA (Computer Based Applications) and became part of the medical decision support system. Therefore, different computerized methods are used to prevail over varying problems, which help the users to identify the signs of the disease for seeking the medical help earliest. However, using such systems require the efforts of taking photos, uploading them and sending for the machine learning processing. In the current era, the smartphones are one of the growing industries in the world due to their utility and mobility. The current smartphones are available with the high-definition cameras that make it easy to take and upload a picture anytime. Furthermore, a big population of the world is the holder of the personal smartphones. It is predicted that there will be around 6.3 billion smartphone subscribers by the year 2021 [60]. It is very practical to provide the users with healthcare services through SBA (Smartphones Based Applications). However, we cannot deny the advantages of higher processing power and bigger storage in the CBA systems as compared to the SBA.

For both CBA and SBA, the automatic diagnosis of melanoma approaches consists of various similar steps of analysis like preprocessing, segmentation, features extraction, and classification. Many researchers contributed to improving each step by using different approaches such as ABCD-E rule [3-5], seven points checklist [6], three points checklist [7], and Menzies methods [8]. Even though numerous researchers explored different techniques for automatic diagnosis of the melanoma and making it available to a common user, many studies still indicate, that automatic detection of melanoma is yet an intricate problem [9]. Food and Drug Administration (FDA) [10] encourages smartphone based mHealth applications and they defined an appropriate procedure to regulate such applications. However, finding the suitable application in the app stores for smartphones with reliable results is still a challenging issue. Due to storage and processing limitations, SBA could not execute complex

algorithms that make it difficult for a common user to rely on them. Often, the users want such SBA systems that provide the efficient processing time. The app must be reachable, downloadable and executable on various types of smartphone's machines to support the users in the early diagnosis.

To identify the contributions and limitations of the proposed approaches of melanoma diagnosis, this paper explores the available literature on the CBA and SBA for automatic melanoma diagnosis techniques and algorithms. Therefore, our contributions in this paper are in three folds. First, we explored the existing systems for automatic detection of melanoma for CBA and SBA and identified that SBA are preferred over the CBA systems and owned by the wider population of users. Secondly, we discussed various approaches used in literature during the automatic detection of melanoma. As a result of this analysis, we identified the challenges and the limitations of availability of the smartphone apps to a common user. Thirdly, to overcome the limitations of storage and processing time of smartphones, we proposed the solution of offloading where smartphone application executed the detection process on the cloud instead of the local machine of the smartphone. Hence, we developed a melanoma detection model based on cloud and compared the performance of cloud computing with smartphone's hardware. The experimental result showed that the cloud takes significantly less time for processing the same data and algorithm in comparison to the smartphone's hardware.

The rest of this paper is structured as followed. In Section 2, we explore the available literature on skin cancer detection for CBA and SBA with the discussion on their pros and cons. Section 3 describes our proposed model to measure the processing time performance of machine learning based automatic melanoma detection model on the cloud in comparison to smartphone's local hardware. In Section 4, we analyze and evaluate the experimental results to validate the proposed approach. Finally, the conclusion and future work are presented in Section 5.

II. LITERATURE REVIEW

In this section, firstly, we explored the literature regarding the systematic review and the survey papers on the automatic melanoma detection systems. For discovering the contents, we searched on Google Scholar platform of the keywords of "smartphone", "melanoma", "systematic review", "skin cancer diagnosis", "machine learning", and "survey paper". Mainly, we have focused on the studies after the year 2007. Secondly, in the searched collection, we have selected more relevant studies concerning the review of studies related to the automatic diagnosis of melanoma. The remaining of this section is divided into three parts based on the findings from the previous literature: (1) Computer Based Applications (CBA), (2) Smartphone Based Applications (SBA), and (3) Overall system model of CBA and SBA for automatic diagnosis of melanoma.

A. Computer Based Applications (CBA)

Initially, the researchers have developed the melanoma detection algorithms for the computer-based solution to integrate them in the clinical decision support systems.

Hameed et al. [1] provided a comprehensive survey on image-based melanoma detection systems. The survey provides a comparison of melanoma detection preprocessing steps on the criteria of color space, hair detection, and hair repair techniques. Different types of segmentation have been explored in the survey such as color based, discontinuity-based, soft computing-based, region-based, and threshold-based segmentations. The authors deliberated various studies for appropriate feature extraction and found the color, ABCD rule, dermal, geometric, contour, histogram, and texture features. Different classification techniques were used, such as SVM, K-NN, Naïve Bayes Classifier, RBF, CART, and ANN, for the cancer detection. The maximum accuracy of cancer detection algorithms was up to 92.09 % with SVM. Therefore, it is required to explore further methods for improving the accuracy of the cancer detection system. Arasi et al., [2] reviewed various CBA systems for malignant melanoma detection. Their study investigated the best classification methods among the available techniques and results indicated the hybrid classifier, such as a combination of DWT (Discrete Wavelet Transforms) and k-nearest neighbor, was the winner because it resulted in high accuracy. Masood and Al-Jumaily [9], investigated various vivo imaging techniques for melanoma detection were photography, dermoscopy, multispectral imaging, and laser-based enhanced diagnosis, optical coherence tomography, ultrasound imaging, and magnetic resonance. The authors emphasized more on the importance of features extraction and selection as the correct features selection can lead to more accurate results. They recommended to use 5 to 10 features to get acceptable classification results. They discussed quality assessment criteria that included the limitations of previous research in image acquisition, extraction, and selection of features. Authors also discussed the risk of overfitting due to few events per variable and proposed a framework to highlight the importance of certain standard for validation as it was ignored in the previous research. They recommended providing quality data to get unbiased results.

B. Smartphone Based Applications (SBA)

Since the advent of smartphones, they became the main tool for accessing and manipulating the clinical information and adopted by many to provide the solution of automatic melanoma diagnostic. Rat et al. [11] performed a systematic review of 25 studies related to the melanoma diagnosis with the SBA. The purpose of the study was to provide an evidence on the diagnostic performance of automated smartphone apps and tele-dermatology. The study mainly focused on early detection of melanoma, the impact on patient medical learning, and feasibility criteria based on the efficiency of such apps in terms of time. The results showed the automated smartphone apps are missing of assessment in clinical practice conditions and resulted in low sensitivity measures with low photographic quality. Joel et al. [12] evaluated 188 images of skin lesions on four different mobile applications to measure the performance of the applications in detecting the melanoma and benign control lesions. The results showed that the sensitivity of four apps are ranged from 6.8% to 98.1%, specificity from 30.4% to 93.7%. Moreover, positive predictive values ranged from 33.3% to 42.1% and negative predictive values ranged from 65.4% to 97.0%. Wang et al. [13] made a review on the study

in [12] and classified it as an alarming situation as may be misinterpreted, which can place an unjust burden on users in two ways: first, if the lesion is high risk and classified as low risk then users may miss out the early timeframe to get treatment that can be more beneficial. Second, if the normal lesion is reported as high risk then it can cost the users in terms of their time and money to visit the physician and emotional stress because of this news. Nagoo et al. [14] conducted a perspective study of mobile application and evaluated 3 mobile apps of the data of 57 pigmented lesion images. The results showed that the sensitivity of apps ranged from 21% to 72% and specificity ranged 27% to 100.0% compared with the specialists' decisions. Two of the three apps were unable to analyze 14% and 18% of lesions. Interrater agreement results between the apps and dermatologists were also not so much satisfactory. Chadwick et al. [15] evaluated 15 images of previously excised skin lesions with 5 smartphone apps and found 80% sensitivity for melanoma identification with 3 apps and 20% to 100% specificities with the 5 apps. Therefore, the authors showed concerns about the usage of such mobile applications.

Chao et al. [16] divided the SBA of skin cancer detection and support into four different categories: (1) Educational, (2) Mole mapping, (3) Tele-dermatology, (4) Diagnostic, and (5) Research. The article discussed that although these applications are developed but needed to assess the safety and efficacy of smartphone skin diagnosis apps and should be evaluated for clinical efficacy. Kassianos et al., [17] provided a review of available 40 applications on mobile phones up to the year 2014 for the detection and management of melanoma. The evaluation has been done on the criteria of general information about the melanoma, sun exposure preventive advice, the assessment of present and future melanoma risks, applications providing an automatic classification of disease and mole monitoring over time. The results indicate, that the SBA skin cancer applications are providing general information about the melanoma and mole monitoring. Approximately, the same number of applications using lesions images to provide the dermatologist services and self-monitoring, and one-tenth applications are calculating the probability of the lesion being melanoma, and out of them, only one application is providing a validated risk model of future risk on melanoma. Similarly, none of the application was developed for cancer detection using established research methods. Furthermore, most of the applications are apple platform dependent. Some apps were not updated for more than 3 years and if updated there was not a discussion about whether the updates are based on new evidence or not. In the link to this study in the year 2018, Ngoo et al. [18] have made comparisons similar to methodology in [17] of smartphone applications for melanoma management. The app search and reviewing method were designed based on the quality and risk of bias checklist of studies. The apps were not considered for the reviewing purpose that was targeting the dermatologist and plastic surgeons, other than English, booking tools for cancer clinics or entertainment tools, and cosmetically focused. They have evaluated overall 43 smartphone applications based on their functionalities in terms of information of users regarding melanoma prevention and

assessment, analysis of the image using algorithm or forwarding to the dermatologist, tracing lesions overtime, and evidence of scientific research in the development. Mostly, applications were developed for the Apple devices 48.8% and only 23.3% were developed for the Android phones, furthermore, 27.9% were available on both platforms. Only 43.6% of applications were found in the year 2014 in Kassianos et al. study are still available in the year 2017 [18]. Moreover, the apps offering the algorithmic image analysis decreased to approximately half from 46.2% in the year 2014 to 23.35% in the year 2017. Out of 43, only 2 apps had peer reviewed research validating their model of care. However, no one referred that the scientific validation studies are performed internally during the development process but not published their work. If we compare the peer review evidence of apps development in the year 2017 and year 2014 then there is only a small increase in the number of apps from one to two.

III. OVERALL SYSTEM MODELS OF CBA AND SBA FOR AUTOMATIC DIAGNOSIS OF MELANOMA

Smart diagnoses play a vital role in diagnosing and taking the preventive action for the malignant melanoma. Previously, the research has been conducted in many application areas such as informative or educational, automatic melanoma diagnosis, tracking and monitoring of mole, and tele-dermatologist to provide a support for skin cancer care. This paper is mainly focused on the automatic diagnosis of melanoma conditions. The previous research investigated smart diagnostic methods are based on the traditional image processing and machine learning process in the CBA, whereas, in SBA, same steps are performed on the phone by using the limited computing power of the phone. The steps involved in the automatic diagnosis of melanoma are shown in Fig. 1. In this research, we will focus on the highlighted components of the model and the detail of each component is as follows.

A. Data Sources

The first step in the automatic diagnosis of melanoma is to get the accurate data. For this purpose, the captured images of the lesion are used to analyze for diagnosis purpose. The system works on the principals of automatic diagnosis of melanoma are trained on a dataset of similar images. In the published research of the last 10 years, it has been observed the dataset size varies from tens of images to thousands of images. The most prominent datasets used for the model training are Atlas of Dermoscopy [19], Interactive Atlas of Dermoscopy [20, 21], Healthcare centers in Kottayam [22], DermISand and DermQuest [23], Spectroscopic system [24], National Cancer Institute [25], Dermoscope [26], Dermquest, Dermnet [27], Dermnet Dermofit [2, 28], Allergologie [29], and PH2 database from Pedro Hispano hospital [30]. One of the limitations in training the melanoma diagnosis model is availability of open source melanoma images dataset. Mostly, the available resources are paid, however, there are few open source datasets are available from the International Skin Imaging Collaboration (ISIC) [31]. They have developed the dataset of 10015 dermatoscopic images and released for the purpose of the training set for academic machine learning and the users can access the dataset through ISIC archive [32].

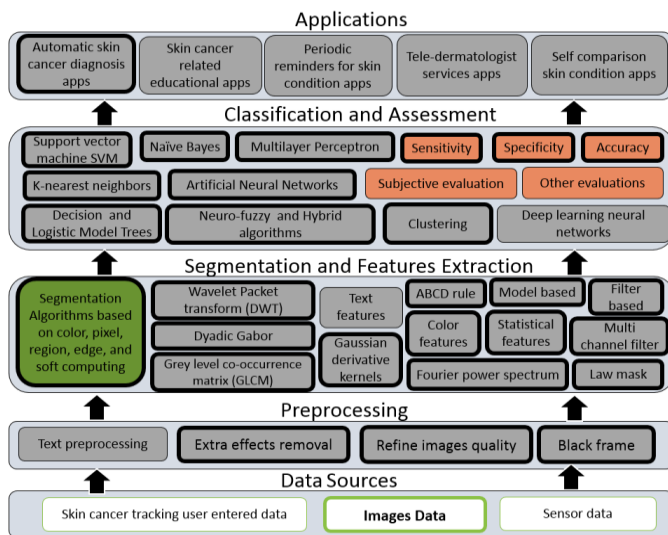


Fig. 1. Overall System Models of CBA and SBA for Automatic Diagnosis of Melanoma.

B. Preprocessing

The input of the automatic diagnosis system is the digital images on which the further steps can be applied. To the digital images, the preliminary processing is applied in which the extra effects of the image not required in further processing such as hair [33-36], irregular lighting, arteries, dermoscopic gel as noise. Due to these elements, the detection of lesion area with high accuracy is tough, so, it might result in a decrease of the exactness, and the processing time can be elevated. To refine the quality of the scan, cropping image [37], contrast intensification [26, 38], image resizing [29, 39], RGB to Greyscale imaging, morphological image processing, filters application [24], Gaussian filter [29] and color quantization, are applied to the scan which makes the image segmentation less challenging. Therefore, it is required to apply a few preliminary processing for the ejection of these elements. The RGB to grey scale conversion is done due to the thousands of colors in the RGB scale. Such a large amount of colors is strenuous to handle. For this purpose, the color quantization is used which reduces the colors in the lesion to approx. 20 for accurate quantization [40]. The inadequate image contrast makes the border detection in digital images another challenge. For this purpose, the image contrast is intensified to make the boundary of the lesion notable [41].

Other unwanted elements such as ink marks, bubbles, blood vessels, hairs, and skin lines exist in the dermoscopic image known as black frames. These black frames are introduced during the process of converting the details of the image into digital format. In digital format the details of the image are shown in bits, so, that bits can be addressed separately or in the form of sets i.e. byte. Multiple techniques have been introduced by the researchers for separating the black frames from the image. Celebi et al., [42] used a general-purpose filter such as the Gaussian (GF), median (MF), or anisotropic diffusion filters (ADF) techniques for separating the black frames. Korjakowska and Tadeusiewicz [36] made use of the identical color space in which the value of $L < 15$ was supposed to be black. Sultana et. al. [43] proposed technique for the

ejection of black frames and the hair from the scans. Shapes like ellipse and circle were applied to the scans to fix a limit for the black frames and skin areas.

C. Segmentation and Feature Extraction

After the preliminary processing, the healthy skin needs to be separated from the lesion by segmentation techniques such as color based, pixel based, region based, edge based and soft computing-based segmentation methods. The homogenous regions are separated based on shape, color, texture, and area [44]. Due to the smooth changeover of the lesion and the healthy skin, it is a difficult task to segment the regions accurately [45]. As per a few researchers, the identification of these two regions is more accurate if performed manually [29] but for automated diagnosis, the segmentation needs to be automated based on various segmentation algorithms. Silveira et al. [46] compared various segmentation techniques such as adaptive thresholding, adaptive snake, EM level set, and fuzzy-based split-and-merge algorithm. However, the best results are obtained using the adaptive snake and the EM level set. The techniques such as fuzzy logic are used in soft computing-based segmentation. Furthermore, one of the interactive segmentation techniques for images is Grab cut algorithm [47] that divides the image into four parts: (1) Exactly Background, (2) Probably Background, (3) Exactly Foreground, and (4) Probably Foreground.

After the segmentation, the next step is the feature extraction as this step plays an important role in skin lesion classification [1]. The purpose of features extraction is to select certain properties appropriate to the problem by reducing the amount of original data. As the computational efficiency of handheld devices is lower than the normal computers, therefore, proper features selection can increase the efficiency of classification, storage requirements, accuracy of results, ease training, and testing. Malignant melanoma is hard to distinguish from dysplastic nevi with the naked eye, but the situ neoplasm needs to be separated from dysplastic nevi for successful feature extraction. Spotting the most effective pattern classification and algorithm that segregates those lesions is vital. There are many features that can play an important role for skin lesion classification such as ABCD rule (including Asymmetry, Border irregularity, Color, and Diameter) [29], texture and shape features (including skin elasticity, epidermis volume, skin impedance and cellular, and collagen densities) [1, 48], and statistical features [49] (including mean values, standard deviations, entropy, skewness, and kurtosis). Various feature extraction techniques are found in the literature such as model based, statistical based and filtering based methods and among them, the multichannel filtering is very efficient and precise one [9]. To further reduce the unnecessary details researchers used wavelet packet transform [50], grey level co-occurrence matrix [51, 52], principal component analysis [53], decision boundary [44, 54], Fourier power spectrum [55] and Gaussian derivative kernels [56]. In general, dyadic Gabor [57], Law Mask and Wavelet Transform [58] are used for filters. It is observed that most of the time the features extraction process is subject to error [9]. The previous studies lack the discussion or have minor details regarding the meaning of the features and the criteria of their selection being used for classification purpose.

D. Classification

After the successful feature extraction there is a need to categorize these features for complete identification of the region. The focus of categorization is to differentiate the benign and malignant part based on the extracted features. Machine learning algorithms are used for categorization, which helps us to reach conclusion [59]. The classification can be divided into supervised, unsupervised and hybrid algorithms. In supervised classifications the dataset should be provided with appropriate labels of melanoma and non-melanoma. The previous literature showed the Support Vector Machine [29, 38], K-NN [37, 52], Naïve Bayes [24, 60], Artificial Neural Networks [24, 52, 61-63], Multilayer Perceptron [52, 62], Logistic Model Tree [20], Hidden Naive Bayes [44] Decision Trees [23, 64, 65], Proximal Support Vector Machine (PSVM) and Active Support Vector Machine (ASVM) [28] are the supervised machine learning algorithms used for automatic diagnosis of melanoma. Furthermore, the techniques like Clustering [63] and fuzzy C-means are unsupervised machine learning algorithms used for diagnosis purpose. Soft computing techniques like Neurofuzzy are used by Hybrid systems among emerging algorithms for diagnostic with higher accuracy rates [2]. Deep learning neural networks are found effective technique of the melanoma detection. In [66] Haenssle et al., compared the detection results of convolutional neural networks (CNN) with the group of 58 dermatologist diagnosis and CNN outperformed the team of dermatologists. CNN is applied for melanoma detection in [67] that resultant in 81% of accuracy.

E. Assessment

The usage of any application is dependent on its percentage of providing correct results. One of the approaches to identifying the correctness of the developed automatic melanoma diagnosis model is the validation of the trained model using the testing dataset. The assessment could be done by discrimination (how well melanoma and benign are differentiated) and calibration (resemblance between the prediction of modal to expert knowledge) [7]. The most common measures for performance evaluation in the previous literature is discrimination on the measurements of accuracy, sensitivity, and specificity. The previous research reported various level of accuracy on different automatic melanoma detection models such as DWT feature extraction with clustering and probabilistic neural network (PNN) resultant in 93% and 95 % accuracy [63], histogram analysis feature with fuzzy systems 90% accuracy [31], with feed forward back-propagation artificial neural network 95% and K-ANN 97.5% [61]. Similarly, ABCD rule and Histogram feature extraction with SVM reported accuracy of 80% [29], Morphological features, color features and GLCM features with combining Self Organizing Map (SOM) and Radial Basis Function (RBF) classification showed accuracy of 96.15 [27], differential evolution-based feature selection with SVM classification resultant in 89.1% accuracy [41]. 2-D Fast Fourier Transform, 2-D Discrete Cosine Transform, Complexity Feature Set, Color Feature Set, Lesion Orientation Feature, Lesion Margin Feature, and Lesion Intensity Pattern Feature with SVM classifier came up with 91.5% and 93.5% accuracy [62]. Histograms of edge intensity with SVM classifier reported with

accuracy 97.32% [21], Morphological and Watershed Algorithms feature extraction with a classifier of Naive Bayes reported the accuracy of 80%, J48, and MLP with the accuracy of 85% [62]. Segmentation using the Wavelet – Fuzzy C-Means algorithm then feature extraction using the ABCD rule and Grey Level Co-Occurrence Matrix (GLCM) with a reported accuracy of 88% [68].

F. Discussion

The previous studies have proved that it is possible to detect the melanoma problem with higher accuracy using the Computer Based Applications (CBA). This provides us the proof of concept that digital technology can facilitate a common user in detecting this deadly condition and to take preventive actions earliest by visiting the dermatologist. Although, the CBA are beneficial for their processing power, but, this technology has few limitations such as usability, size, convenience, and cost. In the traditional CBA, it is required to use a camera for capturing the image of lesion area and additional efforts to upload this image to the computing device for the future processing. Currently, the smartphones made this process more efficient.

There are many healthcare applications including melanoma care available on different mobile operating systems such as IOS and Android platforms. Most of the well-rated available applications are just for mole tracking and educating the users about the melanoma and a very few applications are available for the automatic detection of melanoma [18]. Though a huge amount of previous literature exists on developing the automatic melanoma diagnosis algorithms but the studies in [14, 17] discovered the limited availability of such SBA due to their support for the specific operating system. The reasons for lacking such SBA to the users should be investigated, even so, the availability of high-performance algorithms. Furthermore, the users who have access to such apps mentioned many limitations in their reviews, such as no device compatibility, the camera not taking photos, sign-in problems, technical problems, no support with updated versions of the operating system and the usability issues. The memory consumption and processing time issues should be considered to execute the melanoma detection algorithm using SBA. Since, the smartphones' hardware limitations make it difficult the processing of the proposed algorithms, furthermore, the melanoma diagnosis apps might take more hardware storage resources.

To increase the performance time without causing much battery consumption we proposed to offload the data on the cloud i.e. all the computations will be done at cloud and results will be sent back to the application from the cloud. In this way, the application will store data at the cloud rather than on the smartphone. Hence, the application would get more space for storage of data as compared to the smartphone's storage capacity, so time efficiency will be achieved. The focus of our study is the performance, not the accuracy, therefore, we did not consider the comparison of various machine learning classifiers. In our proposed model the same steps for automatic melanoma diagnosis have been tested in different processing environments of cloud and smartphone.

IV. PROPOSED METHOD TO ACHIEVE THE ADVANTAGES OF CBA AND SBA

The proposed method discusses the steps involved in the melanoma diagnosis on the cloud as compare the results with the processing time of same steps on a smartphone's hardware. The proposed methodology is divided into four main steps i.e. pre-processing, segmentation, feature extraction, and classification as shown in Fig. 2. The details of each module are described in the following sections.

A. Data

The dataset is taken from the Klinik und Poliklinik für Dermatologie und Allergologie, Technische Universität München, Germany [29] that consists of the dermoscopic images of skin lesion consists of 120 of melanoma and non-melanoma images and used for training and testing purpose. The dataset consists of images without any distracting elements like jewelry, clothes and any background. In the images' dataset, the region of interest was manually selected consisting of non-melanoma and melanoma skin pigments. We randomly split the dataset into two parts i.e. training and testing part with a ratio of 70% and 30%.

B. Pre-Processing

In the preprocessing stage, images are prepared by making them in same dimensions and noise-free to achieve better segmentation results. In this study, the images were available in the RGB format. Firstly, we have resized the images in 640 x 480 dimensions. Secondly, we have applied the Gaussian filter [29] with window size 3 to remove the noise.

C. Segmentation

The segmentation is done on the resultant images from preprocessing stage. Grab Cut [47] algorithm is used for the segmentation of the images to achieve good segmentation results in real time. We have provided the facility to the users to draw a rectangle around the lesion part. However, drawing the rectangle is users' dependent that may take long reliant on the ability of users, in many cases, it takes 4 to 5 seconds. To keep all the processes in the background thread and avoid the application crash, we have used AsyncTask [69].

D. Feature Extraction and Classification

It has already been discussed that successful classification is dependent on the appropriate set of the features. In this context, the main challenge is to select the features while considering the processing time out of many features of the segmented image. Using mobile-offloading strategy, storage and battery utilization limitations are almost eradicated but still to keep processing time as small as possible only limited features of the image are extracted so that processing speed will not be affected. In features extraction phase, we have mainly used the histogram and ABCD features [29]. The extracted features from the segmented image consist of the extracted area of the lesion, the perimeter of lesion, eccentricity, mean, standard deviation, L1 norm, L2 norm angle of lesion, major and minor axis of the lesion.

For the classification, the model is trained using the SVM [29] classifier. The main reason for selecting SVM is its simplicity and suitability for the classification of melanoma.

More sophisticated classifier such as deep neural network, convolutional neural networks, and ensemble models can also be applied but the discussion trade-off between the improved classification quality is beyond the scope of this work.

E. Implementation

We have used the Amazon S3 cloud services [70] for the implementation. As first step images were uploaded as an object to source bucket in Amazon S3. Amazon S3 detects this object created as an event and publishes the s3:ObjectCreated:* event to AWS Lambda by invoking the Lambda function and passing event data as the parameter. Further, AWS Lambda executes this Lambda function by assuming the executive role that is specified at the creation of the Lambda function. While calling the Lambda function, it receives the source bucket and objects key name from the event data as parameters. The Lambda function reads the object and creates a thumbnail using graphics libraries and saves it to the target bucket.

After the classification, the results are sent back to the application from the cloud in the form of a JSON object. The application then reads the JSON object and displays the result to the user in a form of a message stating if the lesion is cancerous or not. This allows to perform all the basic heavy computation at cloud that can preserve battery utilization of smartphone as well as reducing the performance time and saves the huge storage space of local machine by using the cloud storage.

F. Results and Discussion

This section reports the comparison of the processing time results of automatic melanoma detection model for the cloud and the smartphone's local machine. The processing time of automatic melanoma detection is recorded at each stage i.e. pre-processing, segmentation, feature extraction, and classification. The measurements are made to compare the melanoma detection image processing efficiency on both the smartphone's local machine and cloud processing. Furthermore, the accuracy of melanoma and non-melanoma images detection was measured. Table I presents the results of images processing and classification on the smartphone's local machine. The average time of the application for classifying of an image is 14938.00ms. Average time classifier used for training is 30405.00ms.

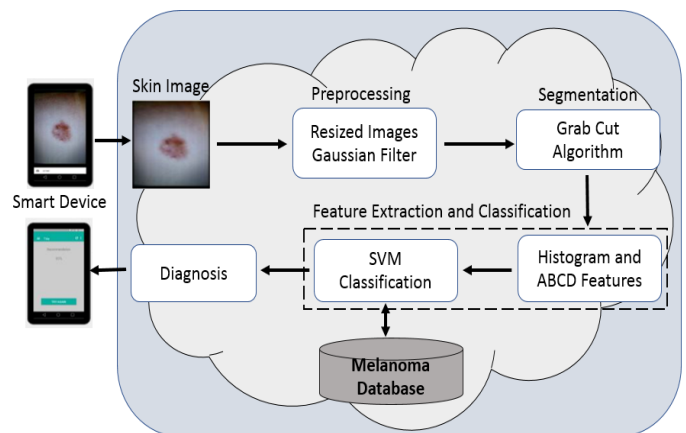


Fig. 2. Proposed Model of Automatic Melanoma Detection System.

Table II presents the results of images processing and classification on the cloud. The average time of the application for classifying the images is 1297.28ms. The results of our proposed model showed the difference between the average processing timings of melanoma images using cloud offloading and processing on smartphone's local machine 1.2 sec and 15 secs respectively. We applied Wilcoxon test [71] to find the difference between total image processing time in the cloud and smartphone local machine environment and found the p-value is $.0002 < 0.001$. Therefore, there is a significant difference in melanoma detection time in both environments. While processing the lesion image on smartphone's local machine the segmentation stage took significantly more time

and the average time exceeded to almost 14808.67 milliseconds as compared to average segmentation time on the cloud is 44.8 milliseconds. It means the most expensive stage in terms of processing time on the smartphone's local machine is segmentation. However, each stage of cloud processing is consuming on average less amount of time that can significantly contribute to make the melanoma detection process more efficient. Furthermore, we have found no difference in diagnostic accuracy in both conditions i.e. melanoma detection is 80% of the test images data and the accuracy of non-melanoma detection is 75% the test images data, as this is because the same algorithms are applied for each stage of classification in both environments.

TABLE I. PROPOSED MODEL PROCESSING TIMINGS IN (MS) ON SMARTPHONE LOCAL MACHINE FOR AUTOMATIC MELANOMA DETECTION

Image ID	Pre-Processing	Segmentation	Feature Extraction	Classification	Total Time on One Image (in ms)
1	151	18442	47	59	18607
2	182	18241	50	48	18387
3	202	15473	46	37	15593
4	152	12432	46	41	12560
5	153	11232	49	41	11363
6	158	23680	58	39	23816
7	160	12856	51	40	12987
8	133	14019	49	44	14156
9	157	16586	23	33	16675
10	137	13726	48	36	13846
11	152	13911	51	53	14068
12	149	12369	48	43	12503
13	166	12666	18	45	12774
14	164	13012	52	41	13146
15	132	13278	53	46	13423
16	161	11798	18	34	11884
17	165	21262	57	39	21397
18	133	11573	52	44	11713
Average	155.94	14808.67	45.33	42.39	14938.78
Average Time Consuming on the Classification Per Image = 14938 (15 Seconds Approx.)					

TABLE II. PROPOSED MODEL PROCESSING TIMINGS IN (MS) ON THE CLOUD FOR DIFFERENT PHASES OF AUTOMATIC MELANOMA DETECTION

Image ID	Pre-Processing	Segmentation	Feature Extraction and Classification	Total Time on One Image (in ms)
1	16	41	1323.85	1380.85
2	14	37	1443.45	1494.45
3	9	39	1245.47	1293.47
4	15	68	1134.08	1217.08
5	15	39	1056.01	1110.01
6	15	39	1110.45	1164.45
7	16	35	1251.36	1302.36
8	10	37	1219.36	1266.36
9	14	38	976.20	1028.20
10	15	35	1281.73	1331.73
11	16	43	1333.01	1392.01
12	38	106	1076.55	1220.55
13	18	45	1354.97	1417.97
14	16	38	1215.80	1269.80
15	9	31	1233.14	1273.14
16	15	46	978.09	1039.09
17	14	39	1826.99	1879.99
18	17	41	1211.42	1269.42
Average	15.67	44.28	1237.33	1297.28
Average Time Consuming on the Classification Per Image = 1297.28 (1.2 Seconds Approx.)				

Though, in both cases there are various challenges, in local hardware of smartphone, the bottleneck is the limited storage space and processing speed, while on the cloud it always required data streaming for uploading and downloading of images. A few limitations of our proposed study are that it is trained and on one type of dataset and accuracy of diagnosis is not measured on the various machine learning algorithms.

V. CONCLUSION AND FUTURE WORK

Early diagnosis of melanoma leads to its timely treatment, but if it is not, cancer can spread to other parts of the body and becomes hard to treat and can be fatal. The previous studies have discovered that technology may play an important role in the diagnosis of diseases like melanoma in its early stages. This can facilitate the patients to seek medical help earliest. The previous research showed that the diagnosis of melanoma is possible with the high accuracy by using machine learning algorithms in the CBA systems. However, the users preferred to use the SBA over the CBA system in their everyday life for healthcare monitoring and diagnosis. The limited availability and diagnostic inaccuracy of SBA can delay the timely diagnosis of melanoma and harm the users. One of the reasons for such limitations could be processing performance of image data and machine learning algorithms on the smartphone hardware. Therefore, we proposed to process the data and apply machine learning algorithms on the cloud instead of smartphone local hardware to increase the accuracy with time efficient solution. The results of our study showed that processing at the cloud takes significantly less time for all stages of diagnosis in comparison to smartphones local machines.

The lessons learned in this study can serve as the guidelines for the developers for developing systems for early cancer detection. In the future, we intend to train the model on the various dataset and report the accuracy by applying different machine learning algorithms including the deep neural networks. As, we are proposing to test the system by using deep learning neural networks as the skin can cancer detection algorithms. Since, it is an emerging example to enhance smartphones for cancer detection outside the dermatologists' clinics; it provides the capability of working on huge data-sets using tiny devices like smartphones.

ACKNOWLEDGMENT

This research was supported by the King Faisal University-Deanship of Scientific Research (DSR) with project ID: 160089.

REFERENCES

- [1] N. Hameed, A. Ruskin, K. A. Hassan, and M. Hossain, "A comprehensive survey on image-based computer aided diagnosis systems for skin cancer," in *Software, Knowledge, Information Management & Applications (SKIMA)*, 2016 10th International Conference on, 2016, pp. 205-214: IEEE.
- [2] M. A. Arasi, E.-S. A. El-Dahshan, E.-S. M. El-Horbaty, and A.-B. M. Salem, "Malignant Melanoma Detection Based on Machine Learning Techniques: A Survey," *Egyptian Computer Science Journal (ISSN: 1110-2586)*, vol. 40, no. 03, 2016.
- [3] H. Kaur and A. Singh, "A Review on Automatic Diagnosis of Skin Lesion Based on the ABCD Rule & Thresholding Method," *International Journal of Advanced Research in Computer Science and Software Engineering Research Paper*, vol. 5, no. 5, pp. 326-331.

- [4] F. Nachbar et al., "The ABCD rule of dermatoscopy: high prospective value in the diagnosis of doubtful melanocytic skin lesions," *Journal of the American Academy of Dermatology*, vol. 30, no. 4, pp. 551-559, 1994.
- [5] N. R. Abbasi et al., "Early diagnosis of cutaneous melanoma: revisiting the ABCD criteria," *Jama*, vol. 292, no. 22, pp. 2771-2776, 2004.
- [6] T. Wadhawan, N. Situ, H. Rui, K. Lancaster, X. Yuan, and G. Zouridakis, "Implementation of the 7-point checklist for melanoma detection on smart handheld devices," in *Engineering in Medicine and Biology Society, EMBC, 2011 Annual International Conference of the IEEE*, 2011, pp. 3180-3183: IEEE.
- [7] I. Zalaudek et al., "Three - point checklist of dermoscopy: an open internet study," *British journal of dermatology*, vol. 154, no. 3, pp. 431-437, 2006.
- [8] M. E. Vestergaard and S. W. Menzies, "Automated diagnostic instruments for cutaneous melanoma," in *Seminars in cutaneous medicine and surgery*, 2008, vol. 27, no. 1, pp. 32-36.
- [9] A. Masood and A. Ali Al-Jumaily, "Computer aided diagnostic support system for skin cancer: a review of techniques and algorithms," *International journal of biomedical imaging*, vol. 2013, 2013.
- [10] Food and D. Administration, "Mobile medical applications: guidance for industry and Food and Drug Administration staff," *Food and Drug Administration*, 2013.
- [11] C. Rat et al., "Use of Smartphones for Early Detection of Melanoma: Systematic Review," *Journal of medical Internet research*, vol. 20, no. 4, 2018.
- [12] J. A. Wolf et al., "Diagnostic inaccuracy of smartphone applications for melanoma detection," *JAMA dermatology*, vol. 149, no. 4, pp. 422-426, 2013.
- [13] J. V. Wang, L. W. Chapman, and M. S. Keller, "Challenges to smartphone applications for melanoma detection," 2017.
- [14] A. Ngoo, A. Finnane, E. McMeniman, J. M. Tan, M. Janda, and H. P. Soyer, "Efficacy of smartphone applications in high - risk pigmented lesions," *Australasian Journal of Dermatology*, vol. 59, no. 3, pp. e175-e182, 2018.
- [15] X. Chadwick, L. J. Loescher, M. Janda, and H. P. Soyer, "Mobile medical applications for melanoma risk assessment: False assurance or valuable tool?," in *System Sciences (HICSS)*, 2014 47th Hawaii International Conference on, 2014, pp. 2675-2684: IEEE.
- [16] E. Chao, C. K. Meenan, and L. K. Ferris, "Smartphone-based applications for skin monitoring and melanoma detection," *Dermatologic clinics*, vol. 35, no. 4, pp. 551-557, 2017.
- [17] A. Kassianos, J. Emery, P. Murchie, and F. M. Walter, "Smartphone applications for melanoma detection by community, patient and generalist clinician users: a review," *British Journal of Dermatology*, vol. 172, no. 6, pp. 1507-1518, 2015.
- [18] A. Ngoo, A. Finnane, E. McMeniman, H. P. Soyer, and M. Janda, "Fighting Melanoma with Smartphones: A Snapshot of Where We are a Decade after App Stores Opened Their Doors," *International journal of medical informatics*, vol. 118, pp. 99-112, 2018.
- [19] M. E. Celebi et al., "Automatic detection of blue-white veil and related structures in dermoscopy images," *Computerized Medical Imaging and Graphics*, vol. 32, no. 8, pp. 670-677, 2008.
- [20] R. Garnavi, M. Aldeen, and J. Bailey, "Classification of melanoma lesions using wavelet-based texture analysis," in *Digital Image Computing: Techniques and Applications (DICTA)*, 2010 International Conference on, 2010, pp. 75-81: IEEE.
- [21] S. Bakheet, "An svm framework for malignant melanoma detection based on optimized hog features," *Computation*, vol. 5, no. 1, p. 4, 2017.
- [22] K. Manjusha, K. Sankaranarayanan, and P. Seená, "Prediction of different dermatological conditions using naïve Bayesian classification," *International Journal of Advanced Research in Computer Science and Software Engineering*, vol. 4, no. 1, 2014.
- [23] J. Scharcanski and M. E. Celebi, *Computer vision techniques for the diagnosis of skin cancer*. Springer, 2013.
- [24] L. Li, Q. Zhang, Y. Ding, H. Jiang, B. H. Thiers, and J. Z. Wang, "Automatic diagnosis of melanoma using machine learning methods on

- a spectroscopic system," *BMC medical imaging*, vol. 14, no. 1, p. 36, 2014.
- [25] P. Wagholi, "Detection and Analysis of Skin Cancer in Skin Lesions by using Segmentation," *International Journal*, vol. 5, no. 4, 2015.
- [26] S. Jaiswar, M. Kadri, and V. Gatty, "Skin Cancer Detection Using Digital Image Processing," *International Journal of Scientific Engineering and Research*, vol. 3, no. 6, pp. 138-140, 2015.
- [27] A. D. Mengistu and D. M. Alemayehu, "Computer Vision for Skin Cancer Diagnosis and Recognition using RBF and SOM," *International Journal of Image Processing (IJIP)*, vol. 9, no. 6, pp. 311-319, 2015.
- [28] I. Immagulate and M. Vijaya, "Categorization of Non-Melanoma Skin Lesion Diseases Using Support Vector Machine and Its Variants," *International Journal of Medical Imaging*, vol. 3, no. 2, pp. 34-40, 2015.
- [29] M. A. Taufiq, N. Hameed, A. Anjum, and F. Hameed, "m-Skin Doctor: a mobile enabled system for early melanoma skin cancer detection using support vector machine," in *eHealth 360°*: Springer, 2017, pp. 468-475.
- [30] S. Joseph and J. R. Panicker, "Skin lesion analysis system for melanoma detection with an effective hair segmentation method," in *Information Science (ICIS)*, International Conference on, 2016, pp. 91-96: IEEE.
- [31] The International Skin Imaging Collaboration. Available: <https://www.isic-archive.com/#!/topWithHeader/wideContentTop/main>
- [32] P. Tschandl, C. Rosendahl, and H. Kittler, "The HAM10000 Dataset: A Large Collection of Multi-Source Dermatoscopic Images of Common Pigmented Skin Lesions," arXiv preprint arXiv:1803.10417, 2018.
- [33] Q. Abbas, M. E. Celebi, and I. F. García, "Hair removal methods: a comparative study for dermoscopy images," *Biomedical Signal Processing and Control*, vol. 6, no. 4, pp. 395-404, 2011.
- [34] Q. Abbas, I. F. Garcia, M. Emre Celebi, and W. Ahmad, "A feature - preserving hair removal algorithm for dermoscopy images," *Skin Research and Technology*, vol. 19, no. 1, pp. e27-e36, 2013.
- [35] Y. George, M. Aldeen, and R. Garnavi, "Skin hair removal for 2D psoriasis images," in *Digital Image Computing: Techniques and Applications (DICTA)*, 2015 International Conference on, 2015, pp. 1-8: IEEE.
- [36] J. Jaworek-Korjakowska and R. Tadeusiewicz, "Hair removal from dermoscopic color images," *Bio-Algorithms and Med-Systems*, vol. 9, no. 2, pp. 53-58, 2013.
- [37] S. Khakabi, P. Wighton, T. K. Lee, and M. S. Atkins, "Multi-level feature extraction for skin lesion segmentation in dermoscopic images," in *Medical Imaging 2012: Computer-Aided Diagnosis*, 2012, vol. 8315, p. 83150E: International Society for Optics and Photonics.
- [38] K. Kaur, "A Collaborative Biomedical Image-Mining Framework along with Image Annotation," *International Journal of Computer Applications*, vol. 116, no. 13, 2015.
- [39] S. Jain and N. Pise, "Computer aided melanoma skin cancer detection using image processing," *Procedia Computer Science*, vol. 48, pp. 735-740, 2015.
- [40] M. E. Celebi, Y. A. Aslandogan, and P. R. Bergstresser, "Unsupervised border detection of skin lesion images," in *Information Technology: Coding and Computing, 2005. ITCC 2005. International Conference on, 2005*, vol. 2, pp. 123-128: IEEE.
- [41] A. Masood and A. Al-Jumaily, "Differential evolution based advised SVM for histopathological image analysis for skin cancer detection," in *International Conference of the IEEE Engineering in Medicine and Biology Society*, 2015.
- [42] M. E. Celebi, H. Iyatomi, G. Schaefer, and W. V. Stoecker, "Lesion border detection in dermoscopy images," *Computerized medical imaging and graphics*, vol. 33, no. 2, pp. 148-153, 2009.
- [43] A. Sultana, I. Dumitrache, M. Vocurek, and M. Ciuc, "Removal of artifacts from dermatoscopic images," in *Communications (COMM)*, 2014 10th International Conference on, 2014, pp. 1-4: IEEE.
- [44] G. Schaefer, B. Krawczyk, M. E. Celebi, and H. Iyatomi, "An ensemble classification approach for melanoma diagnosis," *Memetic Computing*, vol. 6, no. 4, pp. 233-240, 2014.
- [45] I. Maglogiannis and C. N. Doukas, "Overview of advanced computer vision systems for skin lesions characterization," *IEEE transactions on information technology in biomedicine*, vol. 13, no. 5, pp. 721-733, 2009.
- [46] M. Silveira et al., "Comparison of segmentation methods for melanoma diagnosis in dermoscopy images," *IEEE Journal of Selected Topics in Signal Processing*, vol. 3, no. 1, pp. 35-45, 2009.
- [47] C. Rother, V. Kolmogorov, and A. Blake, "Grabcut: Interactive foreground extraction using iterated graph cuts," in *ACM transactions on graphics (TOG)*, 2004, vol. 23, no. 3, pp. 309-314: ACM.
- [48] M. Ritesh and S. Ashwani, "A Comparative Study of Various Color Texture Features for Skin Cancer Detection," in *Sensors and Image Processing*: Springer, 2018, pp. 1-14.
- [49] T. Wadhawan, N. Situ, K. Lancaster, X. Yuan, and G. Zouridakis, "SkinScan©: a portable library for melanoma detection on handheld devices," in *Biomedical Imaging: From Nano to Macro, 2011 IEEE International Symposium on*, 2011, pp. 133-136: IEEE.
- [50] M. K. A. Mahmoud, A. Al-Jumaily, and M. Takruri, "The automatic identification of melanoma by wavelet and curvelet analysis: study based on neural network classification," in *Hybrid Intelligent Systems (HIS)*, 2011 11th International Conference on, 2011, pp. 680-685: IEEE.
- [51] M. Beyer, "The GLCM Tutorial Home Page," ed, 2010.
- [52] M. A. Sheha, M. S. Mabrouk, and A. Sharawy, "Automatic detection of melanoma skin cancer using texture analysis," *International Journal of Computer Applications*, vol. 42, no. 20, pp. 22-26, 2012.
- [53] B. Bodanese, F. L. Silveira, R. A. Zangaro, M. T. T. Pacheco, C. A. Pasqualucci, and L. Silveira Jr, "Discrimination of basal cell carcinoma and melanoma from normal skin biopsies in vitro through Raman spectroscopy and principal component analysis," *Photomedicine and laser surgery*, vol. 30, no. 7, pp. 381-387, 2012.
- [54] F. E. Robles, J. W. Wilson, and W. S. Warren, "Quantifying melanin spatial distribution using pump-probe microscopy and a 2-D morphological autocorrelation transformation for melanoma diagnosis," *Journal of biomedical optics*, vol. 18, no. 12, p. 120502, 2013.
- [55] T. Tanaka, S. Torii, I. Kabuta, K. Shimizu, and M. Tanaka, "Pattern classification of nevus with texture analysis," *IEEE Transactions on Electrical and Electronic Engineering*, vol. 3, no. 1, pp. 143-150, 2008.
- [56] H. Zhou, M. Chen, and J. M. Rehg, "Dermoscopic interest point detector and descriptor," in *Biomedical Imaging: From Nano to Macro, 2009. ISBI'09. IEEE International Symposium on*, 2009, pp. 1318-1321: IEEE.
- [57] H. G. Stockmeier, H. Bäcker, W. Bäumler, and E. W. Lang, "BSS-Based Feature Extraction for Skin Lesion Image Classification," in *International Conference on Independent Component Analysis and Signal Separation*, 2009, pp. 467-474: Springer.
- [58] E. Guerra-Rosas, J. Álvarez-Borrego, and Á. Coronel-Beltrán, "Diagnosis of skin cancer using image processing," in *AIP Conference Proceedings*, 2014, vol. 1618, no. 1, pp. 155-158: AIP.
- [59] S. Deepa and B. A. Devi, "A survey on artificial intelligence approaches for medical image classification," *Indian Journal of Science and Technology*, vol. 4, no. 11, pp. 1583-1595, 2011.
- [60] B. Salah, M. Alshraideh, R. Beidas, and F. Hayajneh, "Skin cancer recognition by using a neuro-fuzzy system," *Cancer informatics*, vol. 10, p. CIN. S5950, 2011.
- [61] M. Elgamal, "Automatic skin cancer images classification," *IJACSA) International Journal of Advanced Computer Science and Applications*, vol. 4, no. 3, pp. 287-294, 2013.
- [62] A. Amarathunga, E. Ellawala, G. Abeyssekara, and C. Amalraj, "Expert system for diagnosis of skin diseases," *International Journal of Scientific & Technology Research*, vol. 4, no. 01, pp. 174-178, 2015.
- [63] Y. K. Jain and M. Jain, "Comparison between different classification methods with application to skin cancer," *International Journal of Computer Applications*, vol. 53, no. 11, 2012.
- [64] G. Capdehourat, A. Corez, A. Bazzano, R. Alonso, and P. Musé, "Toward a combined tool to assist dermatologists in melanoma detection from dermoscopic images of pigmented skin lesions," *Pattern Recognition Letters*, vol. 32, no. 16, pp. 2187-2196, 2011.
- [65] J. F. Alcón et al., "Automatic imaging system with decision support for inspection of pigmented skin lesions and melanoma diagnosis," *IEEE journal of selected topics in signal processing*, vol. 3, no. 1, pp. 14-25, 2009.
- [66] H. Haenssle et al., "Man against machine: diagnostic performance of a deep learning convolutional neural network for dermoscopic melanoma

- recognition in comparison to 58 dermatologists," *Annals of Oncology*, vol. 29, no. 8, pp. 1836-1842, 2018.
- [67] E. Nasr-Esfahani et al., "Melanoma detection by analysis of clinical images using convolutional neural network," in *Engineering in Medicine and Biology Society (EMBC), 2016 IEEE 38th Annual International Conference of the*, 2016, pp. 1373-1376: IEEE.
- [68] H. Castillejos-Fernández, O. López-Ortega, F. Castro-Espinoza, and V. Ponomaryov, "An Intelligent System for the Diagnosis of Skin Cancer on Digital Images taken with Dermoscopy," *Acta Polytechnica Hungarica*, vol. 14, no. 3, 2017.
- [69] D. MacLean, S. Komatineni, and G. Allen, "Advanced AsyncTask and Progress Dialogs," in *Pro Android 5*: Springer, 2015, pp. 317-341.
- [70] D. Poccia, *AWS Lambda in Action: Event-driven serverless applications*. Manning Publications Co., 2016, p. 384.
- [71] A. Field and G. Hole, *How to design and report experiments*. Sage, 2002.

Multi-Objective Ant Colony Optimization for Automatic Social Media Comments Summarization

Lucky¹, Abba Suganda Girsang²

Computer Science Department
BINUS Graduate Program - Master in Computer Science
Bina Nusantara University, Jakarta, Indonesia, 11480

Abstract—Summarizing social media comments automatically can help users to capture important information without reading the whole comments. On the other hand, automatic text summarization is considered as a Multi-Objective Optimization (MOO) problem for satisfying two conflicting objectives. Retaining the information from the source of text as much as possible and producing the summary length as short as possible. To solve that problem, an undirected graph is created to construct the relation between social media comments. Then, the Multi-Objective Ant Colony Optimization (MOACO) algorithm is applied to generate summaries by selecting concise and important comments from the graph based on the desired summary size. The quality of generated summaries is compared to other text summarization algorithms such as TextRank, LexRank, SumBasic, Latent Semantic Analysis, and KL-Sum. The result showed that MOACO can produce informative and concise summaries which have small cosine distance to the source text and fewer number of words compared to the other algorithms.

Keywords—Automatic text summarization; social media; ant colony optimization; multi-objective

I. INTRODUCTION

The massive usage of internet and social media has flooded users with a lot of information. Most of that information is in form of text such as news, blogs, reviews, comments, and social media status. Due to its large size, finding useful information by reading all that text can be very time consuming. For helping users to capture information quickly, several automatic text summarization algorithms such as TextRank [1], LexRank [2], Latent Semantic Analysis [3], SumBasic [4] and, KL-Sum [5] are created for extracting the important sentences from the large text.

Based on [6], the automatic text summarization methods can be categorized into two groups, extractive and abstractive. Extractive text summarization generates summary by selecting some representative sentences with high weight of importance. On the other hand, abstractive text summarization generates summary by combining information, compressing, and restructuring sentence. However, extractive text summarization is simpler and more lightweight in computation than abstractive text summarization. This is because abstractive text summarization needs deep understanding of language structure and context, which is a very difficult problem to be solved by machine. Until now, most of popular automatic text summarization algorithms such as TextRank, LexRank, Latent

Semantic Analysis, SumBasic, and KL-Sum are using extractive method.

Besides those popular automatic text summarization algorithms, some extractive text summarization techniques, especially for summarizing social media comments, have also been proposed. The studies by [7], [8] utilize term importance for selecting important comments. The other study by [9] implements sentence centrality method for selecting important sentences from a document. Some others such as [10]–[13] are using graph of comments and selecting some of important comments based on the given weight. Meanwhile, the studies by [14]–[17] tried to generate summary by constructing sentences from a graph of words or phrases. Although [14] said the method is abstractive, it can be classified as an extractive method because the new sentences are only generated from available words in the graph. The combination of graph and metaheuristic approach has also been applied by [18], [19]. They are utilizing graph of comments then use ACO algorithm for selecting some important comments from that graph.

According to [20], the purpose of summarization is creating the short version of certain text by reducing its size to half or less while still retaining its important information. However, creating too short summary potentially causes many information losses. On the other hand, too long summary is inefficient to be read. Therefore, automatic text summarization can be categorized as MOO problem where two conflicting objectives must be fulfilled. This paper proposes MOO approach for summarizing social media comments where two conflicting objectives such as retaining information from its source and producing concise output must be satisfied.

The remainder of this paper is organized as follows. Section II explains about the basic concept of Ant Colony Optimization and Multi-objective Ant Colony Optimization. Section III explains about related works. Section IV states about the research problem and objectives. Section V presents the detail of the proposed method. Section VI is about the evaluation results and discussion. Finally, the conclusions and future works are presented in Section VII.

II. BASIC CONCEPT

A. Ant Colony Optimization

ACO algorithm was proposed by Dorigo for choosing the shortest route in the Traveling Salesman Problem (TSP) [21]. It implements the usage of pheromone trails of ants when finding the shortest route from their nest to the source of food.

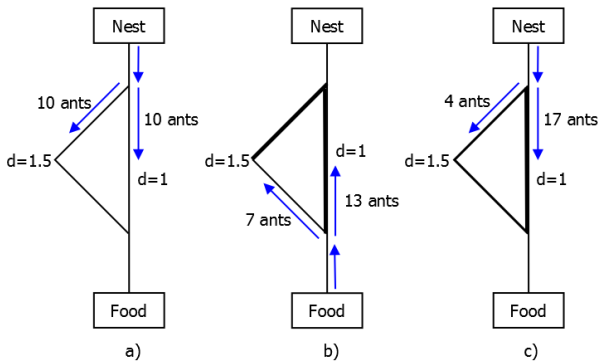


Fig. 1. The basic Concept of ACO.

In Fig. 1, there are two paths between nest and food source; one has a shorter distance ($d=1$) and the other one has a longer distance ($d=1.5$). At the first condition (a), there is no pheromone on both paths. Therefore, the probability that each ant chooses one of them is equal. In the second condition (b), since more ants can travel faster through the shorter path, the shorter path has stronger pheromone than the longer one. The pheromone level on the longer path also goes weaker because of the evaporation. So, the shortest path has a bigger chance to be chosen. The same thing happens in third condition (c) until all ants choose the shorter path.

In ACO, ants choose the path probabilistically using (1).

$$\rho_{ij}^k = \begin{cases} \frac{[\tau_{ij}]^\alpha \cdot [\eta_{ij}]^\beta}{\sum_{k \in allowed_k} [\tau_{ik}]^\alpha \cdot [\eta_{ik}]^\beta} & \text{if } j \in allowed_k \\ 0 & \text{otherwise} \end{cases} \quad (1)$$

Where, τ_{ij} is the pheromone level between node i and j . The η_{ij} is the heuristic information between node i and j . In the TSP case, η_{ij} is the inverse distance between node i and j . The α is the weight for the pheromone level and β is the weight heuristic information.

Pheromone level on each edge is updated on each iteration to improve the quality of the best solution found using (2) and (3).

$$\tau_{ij}(t) = (1 - \rho) \cdot \tau_{ij} + \sum_{k=1}^m \Delta\tau_{ij}^k \quad (2)$$

$$\Delta\tau_{ij}^k = \begin{cases} \frac{Q}{L_k} & \text{if } k\text{-th ant uses edge } (i, j) \text{ in its tour} \\ 0 & \text{otherwise} \end{cases} \quad (3)$$

In (2), ρ represents the pheromone evaporation coefficient and $\Delta\tau_{ij}^k$ represents the pheromone deposited by k -th ant when walking through the node i to j . In (3) Q is the pheromone deposition constant, and L_k is the total distance of k -th ant's tour.

B. Multi-Objective ACO

In single-objective optimization cases, the optimal solution is only one. For example, in single-objective TSP, the best solution is the route with the shortest distance. In MOO, where there are two or more objectives to be satisfied, there is no single best or optimal solution. Hence, some optimal solutions,

which are known as pareto-optimal or non-dominated solutions are presented [22].

Fig. 2 shows the example of pareto diagram in MOO for minimizing two objective functions. The orange dots are the optimal or non-dominated solutions found by MOO.

One of the MOACO algorithm is Bi-Criterion Ant [23], which is usually used to solve the optimization problems with two conflicting objectives. The equation for choosing the candidate node is shown in (4).

$$\rho_{ij}^k(t) = \begin{cases} \frac{[\tau_{ij}(t)]^{\lambda\alpha} \cdot [\tau_{ij}(t)']^{(1-\lambda)\alpha} \cdot [\eta_{ij}]^{\lambda\beta} \cdot [\eta_{ij}']^{(1-\lambda)\beta}}{\sum_{k \in allowed_k} [\tau_{ik}(t)]^{\lambda\alpha} \cdot [\tau_{ik}(t)']^{(1-\lambda)\alpha} \cdot [\eta_{ik}]^{\lambda\beta} \cdot [\eta_{ik}']^{(1-\lambda)\beta}} & \text{if } j \in allowed_k \\ 0 & \text{otherwise} \end{cases} \quad (4)$$

Where $\tau_{ij}(t)$ and $\tau_{ij}(t)'$ are the pheromone for the first and the second objective functions. The $\eta_{ij}(t)$ and $\eta_{ij}(t)'$ are the heuristic information for the first and the second objective functions. Meanwhile, λ can be described in (5).

$$\lambda = \frac{k-1}{m-1} \quad (5)$$

Where k is the k -th ant and m is the number of ants.

Because there are two variables for pheromone and heuristic information, the pheromone evaporation process is done using (6) and (7).

$$\tau_{ij} = (1 - \rho)\tau_{ij} \quad (6)$$

$$\tau'_{ij} = (1 - \rho)\tau'_{ij} \quad (7)$$

Where ρ is the pheromone evaporation constant.

Meanwhile, the pheromone deposition process is done using (8) and (9).

$$\tau_{ij} = \tau_{ij} + \frac{1}{F} \quad (8)$$

$$\tau'_{ij} = \tau'_{ij} + \frac{1}{F'} \quad (9)$$

Where F and F' are the result of the first and the second objective function.

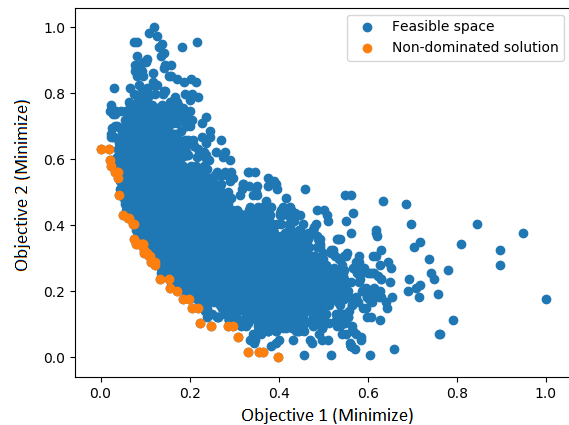


Fig. 2. Example of MOO Pareto Diagram.

III. RELATED WORKS

Some studies use statistics method for summarizing social media comments. For example, the study by [8] summarizes Twitter event by using Term Frequency – Inverse Document Frequency (TF-IDF) to score each comment then select some comments with the high score. The other study by [7] scores the importance of social media comments using statistical data such as user’s reputation, comment’s length, and also the informativeness score of each comment which is measured using TF-IDF and Mutual Information (MI) method.

Meanwhile, the graph method is commonly used in most of studies. In the studies by [14], [15] the graph is used to construct the connection between words in a group of comments. The edges between comments are calculated based on the words’ frequency and position. After that the sentence is constructed using the selected words based on the shortest edge. Similar study by [17] introduces the Phrase Reinforcement Graph for connecting words in Twitter comments. That graph use the longest sentences as the main path, then the words with high redundancy are selected to construct new sentence. The study by [16] is also using similar method as Phrase Reinforcement Graph, but phrases are used as node instead of words. The other studies by [10]–[13] are also using graph to construct the connection between comments. For choosing the important comments, PageRank algorithm is used by [10], [13] while [11], [12] use TextRank algorithm. Furthermore, [9] uses graph and sentence centrality concept for summarizing document. In that study, the centroid of document must be determined first. After that, the summary is produced by selecting some sentences with high cosine similarity score to the centroid.

The combination of graph and metaheuristic approach is implemented by [18], [19]. Those studies use graph to construct relation between social media comments then use ACO for selecting the important comments. The heuristic information for choosing comments is PageRank score, importance score based on TF-IDF, and social media statistics such as number of likes, reply, and share [18]. After that Jensen–Shannon Divergence (JSD) algorithm is used as the objective function to make sure that the produced summary can capture the important information from the source. On the other hand, [19] uses PageRank and MI score as the heuristic information then Trivergence of Probability Distribution (TPD) algorithm is used as the objective function to evaluate the produced summary.

IV. PROBLEM AND OBJECTIVE

Based on the previous studies, the statistics and graph methods are using step by step heuristic approach based on certain criteria. Both of them can’t consider other possible solution, therefore the produced solution potentially falls into local optimum. On the other hand, the metaheuristic approach such as ACO can explore more possible solutions to find a better result according to its objective function. But, as stated previously in Section I, automatic text summarization is an MOO problem because there are two conflicting objectives which must be fulfilled, such as producing concise output and retaining main idea from its original information as much as possible. However, until now, there are only few studies using

MOO approach for summarizing text. One of them is using Multi-Objective Artificial Bee Colony (ABC) algorithm [24]. But the main concern of that study is maximizing content coverage and minimizing redundancies in the summary.

Therefore, this paper tries to answer the main problem of text summarization which is how to produce concise and informative summary by selecting important sentences from a group of social media comments. Minimizing the length of summary and the difference between summary and the original text are two objectives which must be satisfied. Bi-Criterion Ant algorithm is chosen for constructing summary because it is specifically designed for solving two objectives optimization problem.

V. PROPOSED METHOD

The proposed system of MOACO for automatic social media comments summarization consists of some steps which are described in Fig. 3.

A. Data Collecting

The dataset of social media comments in this research is retrieved from Twitter by accessing the Twitter API using the API client script. Those comments are filtered using certain hashtag, range of dates, and language.

B. Data Pre-processing

In this step, the comments are cleaned from Re-tweet marks, HTML tags and special characters, repeating hashtags and mentions, and non-ASCII characters. The multiple spaces are also converted into single space. Repeating 3 characters or more in a word are converted into one character as well. However URL is not removed because it is usually used to refer to the source of information. The non-repeating hashtag or mention in the beginning or middle of sentences is also not removed because they can affect the meaning of overall sentence.

The detail of Regex pattern for the texts cleaning process can be seen in Table I.

TABLE I. REGEX PATTERN FOR CLEANING TEXTS

Regex Pattern	Target
^RT.+	Re-tweet mark
<[^>]+>	HTML tags
&[^\s];	HTML special characters
(?:\#[\w_]+[\w'_-]*[\w_]+)([\w_]+(?:\#[\w_]+[\w'_-]*[\w_]+)+)	Repeating hashtags
[]*(?:\#[\w_]+[\w'_-]*[\w_]+)\$	Hashtag at the end of sentence
(?:@[w_]+)([]+(?:@[w_]+)+)	Repeating mentions
[]*(?:@[w_]+)\$	Mention at the end of sentence
(?:[:;,:][oO\']?[D\]\(\ \ OpP])	Emoticons
[^\x00-\x7F]+	Non-ASCII characters
[]+	Duplicated spaces
([a-z])\1+	Repeating 3 or more characters in a word

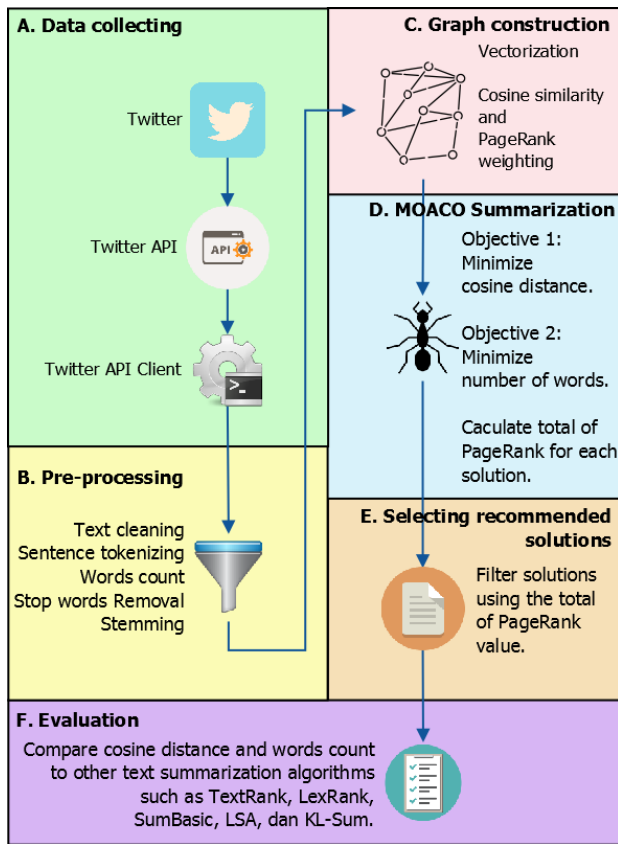


Fig. 3. The Steps in the Proposed System.

After all the comments are cleaned, each comment is tokenized into sentences. Then, the number of words for each sentence is counted. After that, the stop words in each sentence is removed using [25]. Then, the words in each sentence is stemmed into its basic form using [26]. Besides that, the sentences which are not normalized by stop words removal or stemming process are kept so they can be retrieved any time.

C. Graph Construction

At the beginning of graph construction, the sentences are vectorized using bag of words model. We argue that bag of words method is more suitable for social media comments. The reason is, the social media comments are usually short. They also have rare repeated words in one comment. Besides that, the repeated words across comments indicate that the topic is important.

After the sentences are vectorized, they are constructed into undirected graph and those sentences are treated as nodes. For reducing redundancies in summarization result, the edge between two nodes is only created if the cosine similarity between them below certain threshold. This method is inspired by [18].

The equation of cosine similarity is shown in (10).

$$\cos(X, Y) = \frac{\sum_i x_i y_i}{\sqrt{\sum_i (x_i)^2} \cdot \sqrt{\sum_i (y_i)^2}} \quad (10)$$

After that, each node in the graph is given the following weights.

- Cosine similarity with the centroid of source text. This method is based on sentence centrality concept in [9] which assumes that the sentence which is closer to the centroid is more important the others which are not. Based on that, the sentence with higher cosine similarity weight has a bigger probability to be chosen.
- Words count. This weight calculated in pre-processing step by counting the words on each sentence. The sentence with fewer number of words is more likely to be selected.

Besides those two weights, there is another weight used for sentences selection. It is the PageRank value which is used to rank a node in a graph according to its importance. The value of PageRank is calculated by walking the graph randomly and then calculates the rank of certain node by summing the PageRank value of nodes pointing to it, then divide it by the number of edges of its neighbors. That random walking process is repeated and the PageRank value for each node is recalculated until its value is converged or not changed anymore.

The formula for calculating PageRank is described in (11).

$$PR(C_i) = \alpha \sum_{C_j \in Neighbors} C_i \frac{PR(C_j)}{CountEdge(C_j)} + \frac{1-\alpha}{NodeCount} \quad (11)$$

$PR(C_i)$ is the PageRank value for comment C_i . It can be calculated by summing each of its neighbor's Page Rank value, $PR(C_j)$, which has been divided by its number of edges. The constant α is a damping factor which is usually set to 0.85. While $NodeCount$ is the number of nodes in a graph.

The main reason behind using PageRank value is for filtering the non-dominated solutions generated by MOACO. The detail explanation will be presented in the later section.

D. Text Summarization using MOACO

After the graph has been constructed and each of its node has been given some weights, the desired summary size should be defined. The summary size will determine how many sentences will be selected in a summary. If the source text has 100 sentences and summary size is 0.25, the summarization will generate 25 sentences.

In MOACO for text summarization there are two heuristic information for selecting sentences probabilistically. The first is the cosine similarity between the sentence and the centroid of its source text. The value can be calculated using (12).

$$\eta_{ij} = \cos(sentence\ j, centroid) \quad (12)$$

The second heuristic information is the number of words in the sentence and its value can be calculated using (13).

$$\eta_{ij}' = 1/WordCount(sentence\ j) \quad (13)$$

Based on those two heuristic information, ants tend to choose the sentence which has high cosine similarity to its centroid and fewer number of words. Furthermore, the solutions construction should satisfy two conflicting objectives which are minimizing the cosine distance between summary

and its source text and the words count in summary. Those two objective functions are shown in (14) and (15).

$$F = 1 - \cos(\text{summary}, \text{source text}) \quad (14)$$

$$F' = \text{WordCount}(\text{summary}) \quad (15)$$

It's important to note that when constructing the solutions, the cosine distance and the number of words should be normalized so they have the same scale between 0 and 1.

The pseudocode of MOACO for text summarization, which is adapted from [27], is shown in Fig. 4.

E. Selecting Recommended Solutions

Because there is no standard value of cosine distance and words count for a good summary, PageRank value is used to ensure that the summary captures the important information from its source. Because in this case, it is possible that the non-dominated solution has too small number of words with big cosine distance. That means the solution is bad because it contains less information although it is included in the non-dominated solutions. Thus, the recommended solutions are filtered using certain value of total PageRank based on the following assumptions.

- The total of PageRank value of all nodes in a graph is always 1. If there are 100 nodes or sentences in a graph with equal importance level, then the PageRank value of each sentence should be 0.01 (1/100). Therefore, if the defined summary size is 25% (25 sentences) from the source text, the total PageRank in that summary must be 0.25 (0.01 * 25).
- In the real case, the PageRank value of each node should be varied. And, a good summary should contain important sentences. So, the total PageRank in a good summary must be bigger than the percentage of the summary size. If the defined summary size is 25%, the recommended solutions must have the total of PageRank value above 0.25.

Based on the above assumptions, the PageRank value for filtering the recommended solutions should be above the percentage of desired summary size to ensure the summaries contain important sentences.

1. Initialize parameters
2. While termination condition is not met
3. Foreach ant in all ants
4. Select candidate sentence using (4) and (5)
5. Endforeach
6. Evaporate pheromone using (6) and (7)
7. Get ants which get the non-dominated solutions
8. Foreach ant in non-dominated ants
9. Deposit pheromone using (8) and (9)
10. Endforeach
11. Merge the list of non-dominated solutions
12. Calculate total PageRank of each solution
13. Endwhile

Fig. 4. Pseudocode of MOACO for Text Summarization.

F. Evaluation Method

Until now, there is no available gold standard or benchmark dataset for social media comments summarization. Besides that, the big effort is also needed for producing manual summarization by human. Therefore, some studies such as [28]–[31] proposed the automatic evaluation by calculating the cosine similarity or cosine distance between summary and the source text to measure how much information is covered in that summary.

This research also uses the same approach. For measuring how good a summary represents its source, cosine distance is used to compare the difference between them. Besides that, the length of summary is calculated using its number of words to measure its conciseness. To evaluate the performance of MOACO in summarizing social media comments, its result is compared to other text summarization algorithms such as TextRank, LexRank, Latent Semantic Analysis, SumBasic, and KL-Sum. Those benchmark algorithms are implemented using [32], the Python library for text summarization.

VI. EVALUATION AND DISCUSSION

A. Dataset Specification

The dataset of Twitter comments is about presidential election in Indonesia which is collected using #pilpres as a hashtag. Those comments are filtered using certain date range as well. The detail of the dataset specifications can be seen in Table II.

B. Evaluation Environment and Parameter Settings

The evaluation is done on a laptop with the specifications in Table III.

Furthermore, there are some parameters need to be initialized. Some of them are specific for MOACO which are shown in Table IV.

Some other parameters are required for graph construction and defining the expected summary size. They can be seen in Table V.

TABLE II. DATASET SPECIFICATIONS

Source	Twitter
Hashtag	#pilpres
Date range	Jan 17, 2019 – Jan 23, 2019
Language	Bahasa Indonesia
Total raw data	4856
Number of sentences after cleaning	241
Number of words after cleaning	2440
Vector Space Model dimension	241 rows, 941 columns

TABLE III. EVALUATION ENVIRONMENT

Processor	Intel i3
RAM	4 GB
Operating System	Arch Linux 64 bit
Programming Language	Python 3

TABLE IV. PARAMETERS FOR MOACO

Parameter	Value	Description
n	20	The number of ants
α	1	Weight for pheromone level
β	2	Weight for heuristics information
ρ	0.1	Pheromone evaporation constant
τ	0.01	Pheromone initialization constant
Q	1	Pheromone update constant
<i>iteration</i>	500	Number of iterations
<i>trial</i>	10	Number of trials for evaluation

TABLE V. ADDITIONAL PARAMETERS

Parameter	Value	Description
<i>summ_size</i>	0.25	The size of summary.
<i>graph_max_similarity</i>	0.8	Maximum limit of cosine similarity to create edge between two sentences.

C. Evaluation Framework

For a fair comparison between MOACO and the benchmark algorithms, the evaluation process is using the same dataset. Besides that, the stop words removal and stemming process are also using the same dataset [25] and library [26]. The detailed framework for the evaluation can be seen in Fig. 5.

Based on the evaluation framework in Fig. 5, the summaries produced by MOACO and benchmark algorithms are compared with the original text using cosine distance. Before the cosine distance comparison is done, both summaries are normalized using stop words removal and stemming process. The summary with smaller cosine distance value is

considered as better result. Besides cosine distance, the evaluation also compares the words count in both produced summaries. However the words count process is applied to the summaries directly without normalizing them using stop words removal or stemming process. Besides that, because MOACO generates more than one solution, its results should be averaged first. And, to ensure that the summary is still readable by human, the displayed result contains sentences which are not normalized by stop words removal or stemming.

D. Results

After run in 500 iterations and 10 trials, MOACO produces 51 non-dominated solutions. The chart in Fig. 6 shows that the cosine distance and words count are two conflicting objectives. When the cosine distance goes lower, the words count goes higher and vice versa.

From those 51 non-dominated solutions, the total of recommended solutions, which have the total of PageRank value above 0.25, are consisted of 48 solutions. The comparison between those recommended and un-recommended solutions are shown in Fig. 7.

Based on those recommended solutions, some statistics of them are calculated and presented in Table VI.

Meanwhile, the other text summarization algorithms yield the results which are shown in Table VII.

The results in Table VI and Table VII show that the average of cosine distance in MOACO summarization is the second best. It is only lose to LexRank. However, MOACO is able to produce the most concise summary. It was indicated by its average of words count which is smaller than other methods.

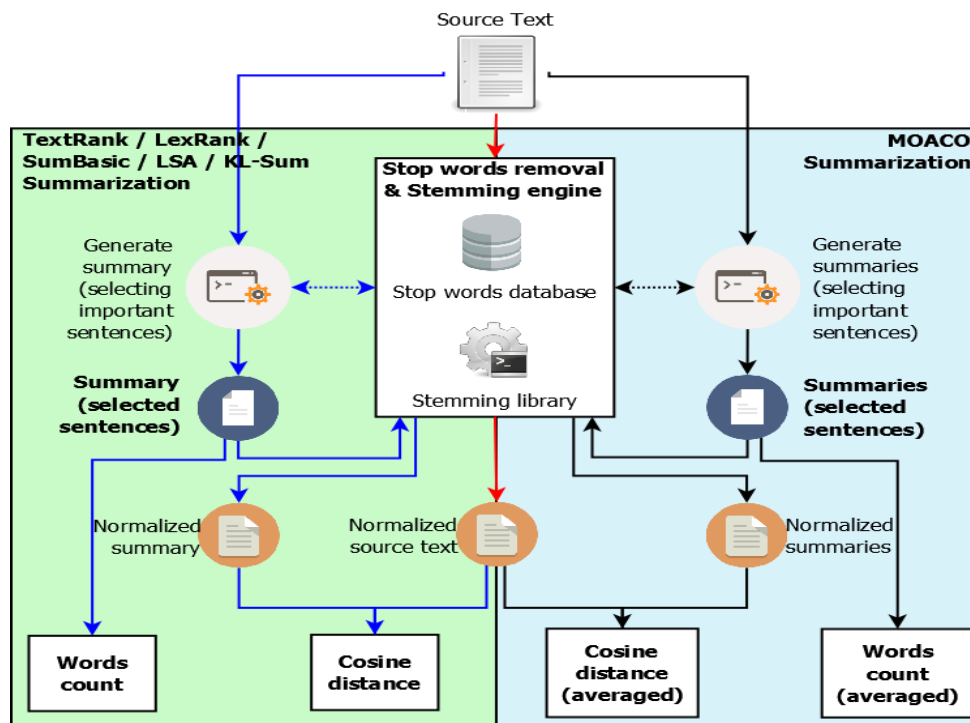


Fig. 5. The Evaluation Framework.

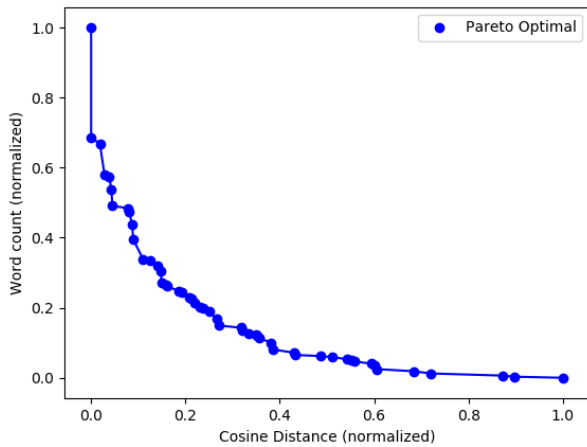


Fig. 6. The Pareto Optimal for MOACO Summarization Results.

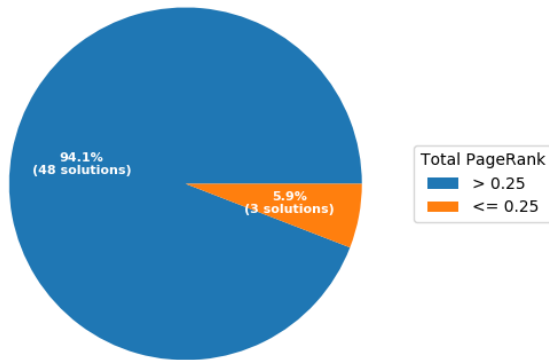


Fig. 7. The Comparison between Recommended and Un-Recommended Solutions.

TABLE VI. THE STATISTICS OF RECOMMENDED MOACO RESULTS

Statistics	Cosine Distance	Words Count
Minimum	0.092	311
Average	0.127	388
Maximum	0.182	629

TABLE VII. THE RESULTS OF OTHER TEXT SUMMARIZATION ALGORITHMS

Method	Cosine Distance	Words Count
TextRank	0.154	694
LexRank	0.117	650
SumBasic	0.245	549
Latent Semantic Analysis	0.151	831
KL-Sum	0.407	738

E. Discussions

In every text summarization, there must be information loss due to the size reduction of the original text. However, the most important thing is to ensure that the size reduction should only cause information loss as small as possible. We can assume the cosine distance is the same as the percentage of information loss or reduction. Not only because of its scale which is between 0 and 1, but also its usage for measuring the

difference between summary and its source. Meanwhile the percentage of size reduction can be calculated by subtracting the total words in the source text with the number of words in summary, then divide it with the total words in the source text.

In Fig. 8 and Table VIII we present the comparison between information loss and size reduction of summarization results produced by each method. As previously mentioned in Evaluation Framework section, MOACO produces more than one solution so its results must be averaged first.

According to Table VIII and Fig. 8, MOACO is better than TextRank, SumBasic, Latent Semantic Analysis, and KL-Sum in retaining main information in its summary. The cosine distance between its summary and the source text is smaller than those algorithms. MOACO is only losing to LexRank by 1%. However, that difference is not significant if compared to the size reduction produced by MOACO which reached 84.1% and much better than LexRank and the other algorithms as well.

In Fig. 7 we can also see that the number of recommended solutions produced by MOACO is quite high with 48 from total 51 solutions. So, 94.1% of the generated solutions by MOACO have the total of PageRank value above the summary size (0.25). That means most of the MOACO summaries are good because based on their total PageRank value they are assumed to contain important information from the original text.

The main strength of MOACO is it can probabilistically explore more possible solutions than other algorithms. By exploring more solutions, the possibility of finding the optimal solutions according to the objective functions is bigger than the other algorithms which just use the heuristic approach. However, one of the characteristic of every MOO, including MOACO, is the produced optimal solutions must be more than one. Because of no single best solution, users need to decide by themselves which one of those solutions will be used. In automatic text summarization case, this characteristic can be a weakness because users might only need one most optimal solution. Using the priority or weight for each objective in pareto optimal solutions and then sum them, as has been studied by [22], can be an option to obtain the most suitable solution from all available optimal solutions.

TABLE VIII. THE COMPARISON BETWEEN INFORMATION AND SIZE REDUCTION OF RESULTS PRODUCED BY EACH METHOD

Method	% Information reduction (smaller value is better)	% Size Reduction (bigger value is better)
MOACO (average)	12.7	84.1
TextRank	15.4	71.6
LexRank	11.7	73.4
SumBasic	24.5	77.5
Latent Semantic Analysis	15.1	65.9
KL-Sum	40.7	69.8

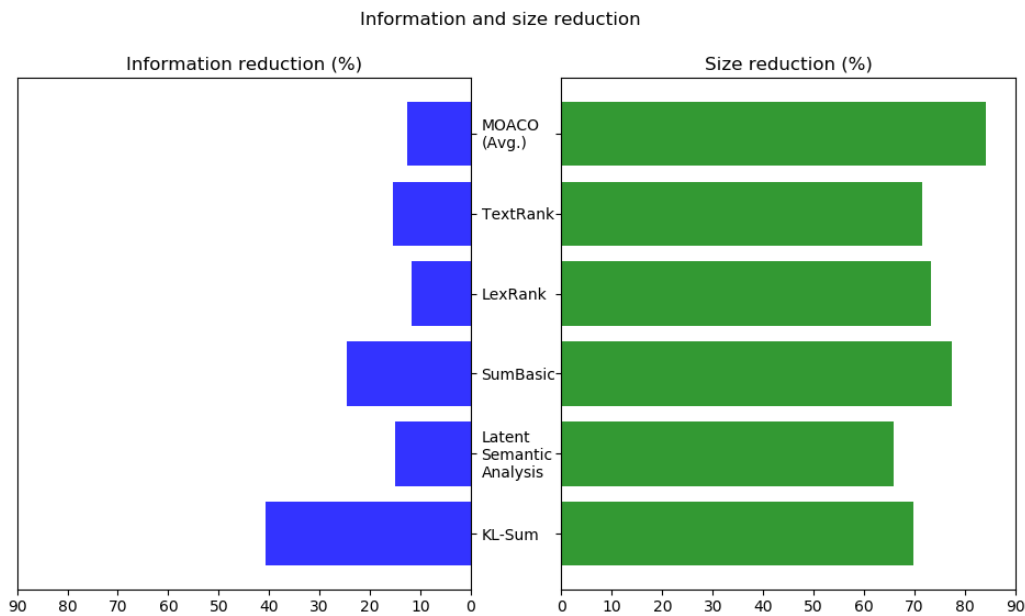


Fig. 8. Graph of Information and Size Reduction of Summaries Produced by Each Method.

VII. CONCLUSION AND FUTURE WORK

The evaluation results show that MOACO can generate summaries with competitive or even better cosine distance compared to other text summarization algorithms. Besides that the size of summaries produced by MOACO are also shorter in average. Moreover, most of those produced summaries have the total of PageRank value above the summary size. Therefore, we can conclude that MOACO algorithm is reliable for generating concise and informative summaries from the social media comments. However, more studies need to be done if we want to automatically retrieve only one most suitable summary using MOO approach. For the future work, we want to experiment with dataset other than social media comments, such as news, articles, or other text documents. Another next work could be comparing the MOACO automatic text summarization with other MOO algorithms such as Multi-Objective Particle Swarm Optimization, Multi-Objective Artificial Bee Colony, or Non-dominated Sorting Genetic Algorithm.

REFERENCES

- [1] R. Mihalcea and P. Tarau, "TextRank: Bringing Order into Texts," in Proceedings of EMNLP 2004, 2004, pp. 404–411.
- [2] G. ne, Erkan and D. R. Radev, "LexRank: Graph-based Lexical Centrality as Saliency in Text Summarization," Journal of Artificial Intelligence Research, vol. 22, 2004.
- [3] J. Steinberger and K. Ježek, "Using Latent Semantic Analysis in Text Summarization and Summary Evaluation," in Proceeding of ISIM '04, 2004, pp. 93–100.
- [4] L. Vanderwende, H. Suzuki, C. Brockett, and A. Nenkova, "Beyond SumBasic: Task-Focused Summarization with Sentence Simplification and Lexical Expansion," Information Processing & Management, vol. 43, no. 6, pp. 1606–1618, 2007.
- [5] A. Haghighi and L. Vanderwende, "Exploring Content Models for Multi-Document Summarization," in Proceedings of Human Language Technologies: NAACL 2009, 2009, pp. 362–370.
- [6] R. M. Aliguliyev, "A new sentence Similarity Measure and Sentence Based Extractive Technique for Automatic Text Summarization," Expert Systems with Applications, 2009.
- [7] C.-F. Hsu, E. Khabiri, and J. Caverlee, "Ranking Comments on the Social Web," Computational Science and Engineering, 2009.
- [8] D. Chakrabarti and K. Punera, "Event Summarization Using Tweets," in Proceedings of the Fifth International AAAI Conference on Weblogs and Social Media, 2011.
- [9] G. Algaphari, F. M. Ba-Alwi, and A. Moharram, "Text Summarization using Centrality Concept," International Journal of Computer Applications, vol. 79, no. 1, pp. 5–12, 2013.
- [10] E. Khabiri, J. Caverlee, and C.-F. Hsu, "Summarizing User-Contributed Comments," in Proceedings of the Fifth International AAAI Conference on Weblogs and Social Media, 2011.
- [11] R. Zhang, W. Li, D. Gao, and Y. Ouyang, "Automatic Twitter Topic Summarization With Speech Acts," IEEE Transactions on Audio, Speech, and Language Processing, vol. 21, no. 3, 2013.
- [12] R. Ferreira et al., "A Four Dimension Graph Model for Automatic Text Summarization," in 2013 IEEE/WIC/ACM International Conferences on Web Intelligence (WI) and Intelligent Agent Technology (IAT), 2013.
- [13] C. Llewellyn, C. Grover, and J. Oberlander, "Summarizing Newspaper Comments," in Proceedings of the Eighth International AAAI Conference on Weblogs and Social Media, 2014.
- [14] K. Ganesan, C. Zhai, and J. Han, "Opinosis: A Graph-Based Approach to Abstractive Summarization of Highly Redundant Opinions," in Proceedings of the 23rd International Conference on Computational Linguistics, 2010, pp. 340–348.
- [15] K. Filippova, "Multi-sentence compression: finding shortest paths in word graphs," in Proceedings of the 23rd International Conference on Computational Linguistics, 2010, pp. 322–330.
- [16] J. Nichols, J. Mahmud, and C. Drews, "Summarizing Sporting Events Using Twitter," in Proceedings of the 2012 ACM international conference on Intelligent User Interfaces, 2012, pp. 189–198.
- [17] B. Sharifi, M.-A. Hutton, and J. Kalita, "Summarizing Microblogs Automatically," in Human Language Technologies: The 2010 Annual Conference of the North American Chapter of the Association for Computational Linguistics, 2015, pp. 685–688.
- [18] M. A. Mosa, A. Hamouda, and M. Marei, "Ant Colony Heuristic for User-Contributed Comments Summarization," Knowledge-Based Systems, vol. 118, 2017.
- [19] M. A. Mosa, A. Hamouda, and M. Marei, "Graph coloring and ACO based summarization for social networks," Expert Systems with Applications, vol. 74, 2017.
- [20] D. Radev, E. Hovy, K. McKeown, "Introduction to the special issue on summarization," Computational Linguistics, vol. 28, pp. 399–408, 2002.

- [21] M. Dorigo, V. Maniezzo, and A. Colomi, "The Ant System: Optimization by a colony of cooperating agents," *IEEE Transactions on Systems, Man, and Cybernetics–Part B*, vol. 26, no. 1, pp. 1–13, 1996.
- [22] R. T. Marler and J. S. Arora, "The weighted sum method for multi-objective optimization: new insights," *Structural and Multidisciplinary Optimization*, vol. 41, no. 6, pp. 853–862, 2010.
- [23] S. Iredi, D. Merkle, and M. Middendorf, "Bi-Criterion Optimization with Multi Colony Ant Algorithms," in *International Conference on Evolutionary Multi-Criterion Optimization EMO 2001: Evolutionary Multi-Criterion Optimization, 2001*, pp. 359–372.
- [24] J. M. Sanchez-Gomez, M. A. Vega-Rodríguez, and C. J. Pérez, "Extractive multi-document text summarization using a multi-objective artificial bee colony optimization approach," *Knowledge-Based Systems*, vol. 159, pp. 1–8, 2018.
- [25] GitHub Inc., "GitHub - masdevid/ID-Stopwords: Stopwords collection of Bahasa Indonesia collected from many sources." [Online]. Available: <https://github.com/masdevid/ID-Stopwords>. [Accessed: 30-Sep-2018].
- [26] GitHub Inc., "GitHub - sastrawi/sastrawi: High quality stemmer library for Indonesian Language (Bahasa)." [Online]. Available: <https://github.com/sastrawi/sastrawi>. [Accessed: 30-Sep-2018].
- [27] A. S. Girsang, C.-W. Tsai, C.-S. Yang, "Rectifying the Inconsistent Fuzzy Preference Matrix in AHP Using a Multi-Objective BicriterionAnt," *Neural Processing Letters*, vol. 44, no. 2, pp. 519–538, 2016.
- [28] A. Louis and A. Nenkova, "Automatically evaluating content selection in summarization without human models," in *Proceedings of the 2009 Conference on Empirical Methods in Natural Language Processing, 2009*, pp. 306–314.
- [29] J. Steinberger and K. Ježek, "Evaluation Measures for Text Summarization," *Computing and Informatics*, vol. 28, no. 2, pp. 1001–1026, 2009.
- [30] E. ShafieiBavani, M. Ebrahimi, R. Wong, F. Chen, "Summarization Evaluation in the Absence of Human Model Summaries Using the Compositionality of Word Embeddings," in *Proceedings of the 27th International Conference on Computational Linguistics, 2018*, pp. 905–914.
- [31] X. Wan, F. Luo, X. Sun, S. Huan, and J. Yao, "Cross-language document summarization via extraction and ranking of multiple summaries," *Knowledge and Information Systems*, pp. 1–19, 2018.
- [32] GitHub Inc., "GitHub - miso-belica/sumy: Module for automatic summarization of text documents and HTML pages."

Classification of Melanoma Skin Cancer using Convolutional Neural Network

Rina Refianti¹, Achmad Benny Mutiara², Rachmadinna Poetri Priyandini³
Faculty of Computer Science and Information Technology, Gunadarma University
Jl. Margonda Raya No. 100, Depok 16424, Jawa Barat

Abstract—Melanoma cancer is a type of skin cancer and is the most dangerous one because it causes the most of skin cancer deaths. Melanoma comes from melanocyte cells, melanin-producing cells, so that melanomas are generally brown or black coloured. Melanomas are mostly caused by exposure to ultraviolet radiation that damages the DNA of skin cells. The diagnoses of melanoma cancer are often performed manually by using visuals of the skilled doctors, analyzing the result of dermoscopy examination and match it with medical sciences. Manual detection weakness is highly influenced by human subjectivity that makes it inconsistent in certain conditions. Therefore, a computer assisted technology is needed to help classifying the results of dermoscopy examination and to deduce the results more accurately with a relatively faster time. The making of this application starts with problem analysis, design, implementation, and testing. This application uses deep learning technology with Convolutional Neural Network method and LeNet-5 architecture for classifying image data. The experiment using 44 images data from the training results with a different number of training and epoch resulted the highest percentage of success at 93% in training and 100% in testing, which the number of training data used of 176 images and 100 epochs. This application was created using Python programming language and Keras library as Tensorflow back-end.

Keywords—Convolutional neural network; deep learning; image classification; LeNet-5; melanoma skin cancer; python

I. INTRODUCTION

The skin is a vital organ that covers the entire outside of the body, forming a protective barrier against pathogens and injuries from the environment. But because it is located on the outer part, the skin is prone to disease. One of these diseases is known as skin cancer. Skin cancer is an abnormality in skin cells caused by mutations in cell DNA. One of the most dangerous types of skin cancer is melanoma cancer. Melanoma is a skin malignancy derived from melanocyte cells, the skin pigment cells that produces melanin. Because these cells are still able to form melanin, melanoma is mostly brown or black colored [1].

Common symptoms of melanoma are the appearance of new moles or changes in existing moles. Changes to the mole can occur due to exposure to ultraviolet light that damages the DNA of skin cells and genes that control cell growth and division resulting in the formation of malignant cells.

One of the first steps to diagnosing melanoma is to do a physical examination using dermoscopy. With this dermoscopy examination, it can assess the size, color, and

texture of moles that being suspected as melanoma. To determine a person with melanoma, a dermatologist conducts research from the results of dermoscopy examinations obtained and matched them with medical science to produce conclusions, but the detection weaknesses are strongly influenced by human subjectivity that makes it inconsistent in certain conditions. Research with image-based can be maximized by utilizing information technology products, such as deep learning.

Deep learning has become a hot topic discussed in the machine learning world because of its significant capability in modeling various complex data such as images and sound. Convolutional Neural Network (CNN) is one of deep learning's methods that has the most significant result in image recognition because it tries to imitate the same way of recognizing images in visual cortex as humans so that they are able to process the same information [2,3].

The aim of this research is to build a system that can classify melanoma cancer through the images from the dermoscopy examination with Deep Learning training using the CNN method.

In the rest of paper, we show the theoretical background of CNN and the related work in Section II. In Section III the research methodology is presented. The experiments and results related to data of melanoma skin cancer are also shown in Section IV. The last section is conclusion and future work of our research.

II. THEORY AND RELATED WORK

A. Melanoma Cancer

Melanoma comes from melanocyte cells, melanin-producing cells that are usually present in the skin. Because most melanoma cells still produce melanin, melanoma is often brown or black. Fig. 1 shows the form of melanoma skin cancer.



Fig. 1. Dermoscopy Image of Melanoma Cancer.

Melanoma can appear on normal skin, or can appear as a mole or other area of the skin that undergoes changes. Some moles that arise at birth can develop into melanoma. In addition, melanoma can also occur in the eyes, ears, gingival of the upper jaw, tongue, and lips. Melanoma cancer is often characterized by the appearance of new moles or when there is a change in shape from an old mole. Normal moles usually have one color, round or oval, and are less than 6 millimeters in diameter [1], while melanoma has these characteristics:

- 1) Has more than one color
- 2) Has an irregular shape
- 3) Its diameter is greater than 6 mm
- 4) It feels itchy and can bleed

To distinguish normal moles from melanoma, it can be examined for its form with the ABCDE list, as follows:

- 1) Asymmetrical: melanoma has an irregular shape and cannot be divided in half.
- 2) Border: melanoma has an uneven and rough edge, unlike normal moles.
- 3) Color: melanoma is usually a mixture of two or three colors.
- 4) Diameter: melanoma is usually larger than 6 millimeters in diameter, and is different from ordinary moles.
- 5) Enlargement or evolution: moles that change shape and size after a while will usually become melanoma.

B. Deep Learning

Deep learning is a machine learning technique that utilizes many layers of nonlinear information processing to perform feature extraction, pattern recognition, and classification [2]. Deep Learning utilizes artificial neural networks to implement problems with large datasets. Deep Learning techniques provide a very strong architecture for Supervised Learning. By adding more layers, the learning model can better represent labelled image data. In deep learning, a computer learns to classify directly from images, text, or sound. Just as a computer is trained to use large numbers of data sets and then change the pixel value of an image to an internal representation or vector feature where classifiers can detect or classify patterns in the input [5].

C. CNN

Convolutional Neural Network (CNN) is one of deep learning's algorithms that is claimed to be the best model for solving problems in object recognition. CNN is the development of Multilayer Perceptron (MLP) which is designed to process two-dimensional data. CNN is included in the type of Deep Neural Network because of the high network depth and many applied to image data. In the case of image classification in research on virtual cortex on cat's visual sense, MLP is less suitable for use because it does not store spatial information from image data and considers each pixel to be an independent feature that results in unfavourable results.

CNN was first developed by Kunihiko Fukushima under the name NeoCognitron. This concept was later developed by Yann LeCun for numerical recognition and handwriting. In 2012, Alex Krizhevsky successfully won the 2012 ImageNet

Large Scale Visual Recognition Challenge competition with his CNN application. This is the moment of proof that the Deep Learning method with CNN method has proven to be successful in overcoming other Machine Learning methods such as SVM in the case of object classification in images [3].

In general, the layer type on CNN is divided into two, namely:

6) *Feature extraction layer*: Located at the beginning of the architecture is composed of several layers and each layer is composed of neurons connected to the local area (local region) of the previous layer. The first type layer is the convolutional layer and the second layer is the pooling layer. Each layer applies the activation function with its intermittent position between the first type and the second type. This layer accepts image input directly and processes it until it produces an output in the form of a vector to be processed in the next layer.

7) *The classification layer*: Composed of several layers and each layer is composed of fully connected neurons with other layers. This layer accepts input from the output feature image extraction layer in the form of a vector then transformed like Multi Neural Networks with the addition of several hidden layers. The output is class accuracy for classification.

CNN is thus a method for transforming the original image layer per layer from the image pixel value into the class scoring value for classification, where each layer has a hyper parameter and some do not have parameters (weight and bias on neurons).

On CNN there are four types of layers used, namely:

8) *Convolutional layer*: The Convolution Layer performs convolution operations at the output of the previous layer. Convolution operations are operations on two functions of real value arguments. This operation uses image input to produce the output function as a Feature Map. These inputs and outputs are two real-value arguments. Convolution operations in general can be written with the formula below:

$$s(t) = (x * \omega) \quad (1)$$

The equation $s(t)$ gives results in the form of a Feature Map as a single output with the first argument used is the input expressed as x and the second argument used is the kernel or filter which is stated as ω . Because the input used is an image that has two dimensions, it can be expressed as t as a pixel and replace it with the arguments i and j . Therefore, convolution operations with more than one dimension input can be written as follows:

$$s(i, j) = (K * I)(i, j) = \sum_m \sum_n I(i - m, j - n) K(m, n) \quad (2)$$

The above equation is the basic calculation for convolution operations where the pixels of the image are expressed as i and j . The calculation is commutative and appears when K as a kernel can be reversed relative to I as input. Convolution operation can be seen as matrix multiplication between image input and kernel where the results can be calculated with dot products. In addition, the output volume of each layer can be

adjusted using hyperparameters. Hyperparameter is used to calculate how many activation neurons in one output are stated in the equation below:

$$\frac{(W-F+2P)}{S+1} \quad (3)$$

From the equation above, the spatial size of the output volume can be calculated by the hyperparameter used is the volume size (W), filter (F), Stride applied (S), and the number of zero padding used (P). Stride is the value used to shift filters through image input and Zero Padding is the value to place zeros around the image border. In image processing, convolution means applying a kernel (yellow box) to the image in all possible offsets as shown in Fig. 3.

The green box as a whole is the image that will be convoluted. The kernel moves from the upper left corner to the lower right. So that the convolution of the image can be seen in the picture on the right. The purpose of convolution on image data is to extract features from the input image.

9) *Pooling layer*: Pooling Layer is a layer that uses functions with Feature Map as input and processes it with various statistical operations based on the nearest pixel value. Pooling layer on the CNN model is usually inserted regularly after several convolution layers. The Pooling layer in the CNN model architecture that is inserted between the convolution layers can progressively reduce the size of the output volume in the Feature Map, so as to reduce the number of parameters used and calculations on the network, and to control Overfitting. In most CNNs, the pooling method used is max pooling. Max pooling divides the output of the convolution layer into several small grids and then takes the maximum value from each grid to compile a reduced image matrix as shown in Fig. 4.

Grids that are red, green, yellow and blue are the grid groups whose maximum values will be selected. So that the results of the process can be seen in the grid collection on the right. The process ensures that the features obtained will be the same even though the image object experiences translation (shift). Using the CNN pooling layer aims to reduce the size of the image so that it can be easily replaced with a convolution layer with the same stride as the corresponding pooling layer. This form of pooling will reduce the Feature Map up to 75% of its original size.

10) *Fully connected layer*: Fully Connected Layer is a layer in which all activation neurons from the previous layer are connected all with neurons in the next layer and aim to transform data dimensions so that data can be classified linearly. Every neuron in the convolution layer needs to be transformed into one-dimensional data before it can be inserted into a fully connected layer. This causes data to lose spatial information and is not reversible so that the fully connected layer can only be implemented at the end of the network. The difference between the fully connected layer and the ordinary convolution layer is that in the convolution layer, the neurons are only connected to a certain area of the input, while the fully connected layer has neurons that are

completely connected. However, the two layers still operate dot products, so the function is not so different.

11) *Activation function*: In this paper the activation functions used are ReLu (Rectified Linear Units) and Softmax Classifier. ReLu activation increases the non-linear nature of decision making functions and all networks without affecting the receptive fields of Convolutional Layer. ReLu is also widely used because it can train neural networks faster. Softmax activation for this layer is another form of Logistic Regression algorithm that can be used to classify more than two classes. The usual classification used by the Logistic Regression algorithm is the classification of binary classes. Softmax provides more intuitive results and has a better probabilistic interpretation than other classification algorithms. Softmax makes it possible to calculate the probability for all labels. From the existing label, a real value vector is taken and converts it to a vector with a value between zero and one which, if all are added, will be worth one.

D. LeNet-5

LeNet-5 is a multi-layer network based on CNN, introduced by Yann LeCun. LeNet-5 is the development of the LeNet-1 and LeNet-4 where LeNet-5 has a greater number of free parameters or layers than its predecessor (Fig. 2).

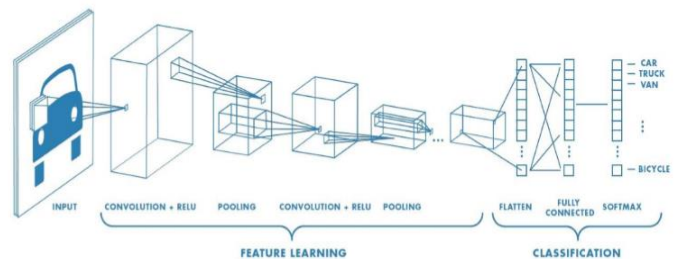


Fig. 2. Example of CNN with Multiple Layers [4].

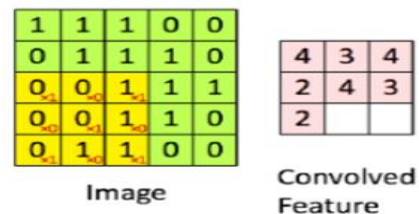


Fig. 3. Convolutional Operation.

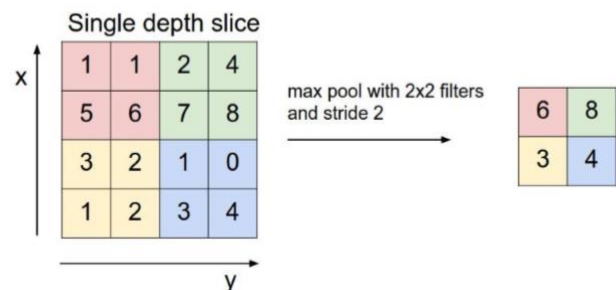


Fig. 4. Max Pooling Operation [3].

LeNet-5 consists of 7 layers where the input layer is not calculated. The LeNet-5 input layer is a 32x32 pixel image. The convolution layer in Fig. 5 is marked with the Cx symbol, the subsampling layer is marked with the Sx symbol, the fully connected layer is marked with the Fx symbol, and the last is the output layer which is the fully connected layer for class classification [6].

In the first layer there is a convolutional layer that studies 20 convolution filters with each 5x5 size and uses ReLu activation. Then the second layer is a pooling layer, using 2x2 size of MaxPooling. The third layer is a convolutional layer which studies 50 convolution filters with each 5x5 size and uses ReLu activation. The filter size is getting bigger in each layer, which is useful to deepen the architectural network studied by the system. Then the system proceed with the fourth layer, which is the pooling layer using 2x2 size of MaxPooling. In the fifth layer, the results of the previous layer process will be flattened into a vector. This layer is called a fully connected layer, where there are 120 nodes that are connected to each other. After that, the process continued with the sixth layer in the form of a fully connected layer with 84 connected nodes. Finally, at the seventh layer is a fully connected layer with softmax activation which connects 2 nodes as the end result of the class to be classified [6].

E. Keras

Keras is a high-level neural network library written in python and able to run on TensorFlow, CNTK, or Theano. This library provides features that are used with a focus on facilitating deeper development of deep learning.

F. Tensorflow

Tensorflow is an open-source software library, developed by the Google Brain team in order to support smart computing to support the search and learning of their products. Computing stated using Tensorflow can be executed with a variety of systems, ranging from mobile devices such as cellphones and tablets to hundreds of large-scale distributed systems of machines and thousands of computing devices such as GPU Cards. The system is flexible and can be used to express a variety of algorithms, including training and inference algorithms for deep neural network models, and has been used to conduct research and to spread machine learning systems to production in more than a dozen fields of computer science and other fields, including voice recognition, computer vision, robotics, information retrieval, natural language processing, geographical information extraction, and others [7].

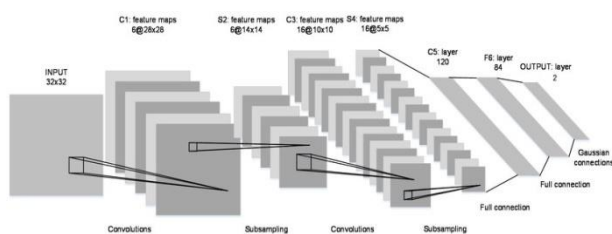


Fig. 5. LeNet-5 Architecture [6].

G. Related Work

The research has related with the works of: first, Andre Esteva et.al. 2017 [8], i.e. “level classification of skin cancer with deep neural networks; and second, T.J. Binker et al. 2018 [9], i.e. “Skin Cancer Classification Using Convolutional Neural Networks: Systematic Review”. Both researches are about general skin cancer, but our research is more specific for melanoma skin cancer.

III. RESEARCH METHODOLOGY

A. Data Collection

The dataset is obtained from ISIC (International Skin Imaging Collaboration) website, contains 220 images of dermoscopy examination. These 220 images consist of 110 melanoma cancer images and 110 non-melanoma cancer images.

B. Data Acquisition

The aim of data acquisition is to determine which objects will be used as research objects. The object of research is in the form of two-dimensional images in JPG format which contain images of melanoma cancer and non-melanoma, as in Fig. 6.

C. Pre-Processing

The dataset contains of different image resolution which require high cost of computation. It is necessary to rescale all the images to 32 x 32 pixels for this deep learning network.

D. Data Augmentation

Data augmentation is used to multiply the variation of images from the dataset by rotating the image, increasing or decreasing the image’s length and width, zooming in the image, and also flipping the image horizontally. The example of this data augmentation can be seen in Fig. 7.

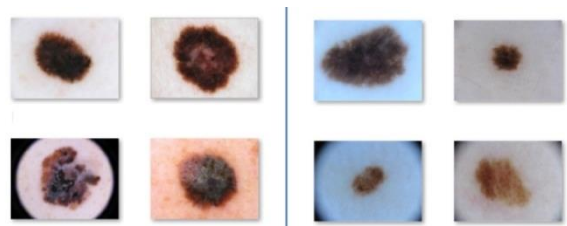


Fig. 6. Images of Melanoma and Non-Melanoma.

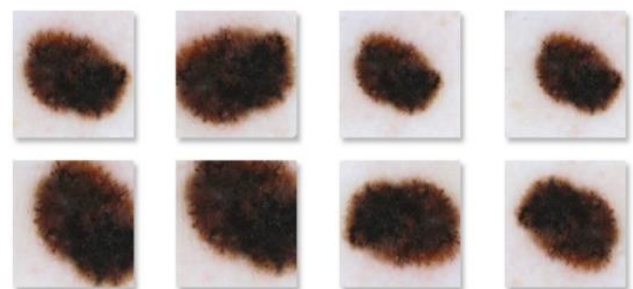


Fig. 7. Data Augmentation of Melanoma Cancer Image.

E. Training Data Process

Fig. 8 shows the process flow in conducting training on the dataset using CNN with LeNet-5 architecture.

The training process starts by reading the model name and number of epoch and batch size received from the user. Then the system reads the dataset with melanoma and non-melanoma categories. Then all the images from the dataset are resized into 32x32 pixel and the dataset augmentation will be generated. The system initializes LeNet-5 architecture and starts to train the network as much the number of epoch inputted by the user earlier. The training will produce a probability value for the two classification classes, where the class with the greatest probability value is the classification class predicted by the program. The training results are then stored in the form of a model file. After completing the training, the system will save the model and plot from the results of the training.

In this training there are parameters that are run constantly throughout the procedure, namely learning rate and batch size. The learning rate used is 0.001, where this parameter states the constants for learning speed from the network layer used. While the batch size parameter serves to determine the total amount of data used in one batch of training. In this paper, the batch size used is 32. Determination of batch size is considered from the memory capability of the device used to conduct the training process.

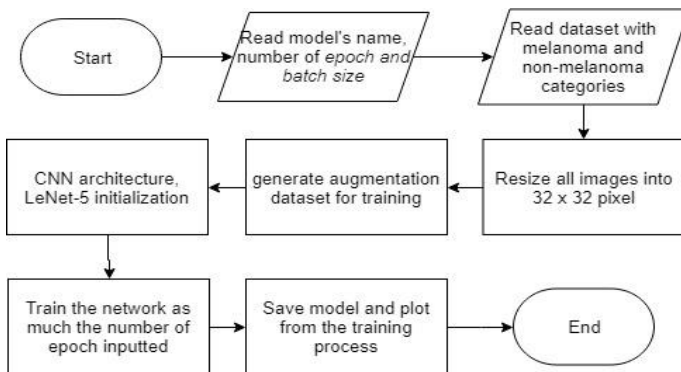


Fig. 8. Training Data Process Flow.

IV. EXPERIMENT AND RESULT

In this paper, the experiment was carried out by determining a different number of training data and epoch to get the best accuracy result. There were two section of training data, the first one used 154 images and the second one used 176 images. Each of the training data section was trained with 50 epochs and 100 epochs. Then, all the model resulted from the training were tested against 44 images of test data and calculated the percentage of precision, recall, and accuracy from the results of the testing using confusion matrix as in Table I.

$$\text{Precision} : \frac{TP}{TP+FP} \times 100\%$$

$$\text{Recall} : \frac{TP}{TP+FN} \times 100\%$$

$$\text{Accuracy} : \frac{TP+TN}{TP+TN+FP+FN} \times 100\%$$

TABLE I. CONFUSION MATRIX

Matrix		Actual Class	
		Melanoma	Non-Melanoma
Prediction Class	Melanoma	TP (True Positive)	FP (False Positive)
	Non-Melanoma	FN (False Negative)	TN (True Negative)

A. Experiment using 154 Train Data and 50 Epochs

The training process of this experiment was carried out using 50 epochs on 154 train data which consist of 77 images of melanoma and 77 images of non-melanoma. The plot result from this training can be seen in Fig. 9.

In Fig. 9 can be seen that from epoch 0 to 49 shows that training accuracy has increased with the final result of 0.92 while training loss has decreased with the final result of 0.28. The model from this training then was tested against 44 test data. This testing result can be seen in Table II.

Based on Table II with 44 images being tested, there are 40 correct images and 4 incorrect images in classification. From the table, the results in confusion matrix are shown in Table III.

$$\text{Precision} : \frac{TP}{TP+FP} \times 100\%$$

$$\frac{21}{21+3} \times 100\% = \frac{21}{24} \times 100\% = 88 \%$$

$$\text{Recall} : \frac{TP}{TP+FN} \times 100\%$$

$$\frac{21}{21+1} \times 100\% = \frac{21}{22} \times 100\% = 95 \%$$

$$\text{Accuracy} : \frac{TP+TN}{TP+TN+FP+FN} \times 100\%$$

$$\frac{21+19}{21+19+3+1} \times 100\% = \frac{40}{44} \times 100\% = 91 \%$$

The calculation of the confusion matrix above results 88 % of precision, 95 % of recall, and 91 % of accuracy.

A. Experiment using 154 Train Data and 100 Epochs

The training process of this experiment was carried out using 100 epochs on 154 train data which consist of 77 images of melanoma and 77 images of non-melanoma. The plot result from this training can be seen in Fig. 5.

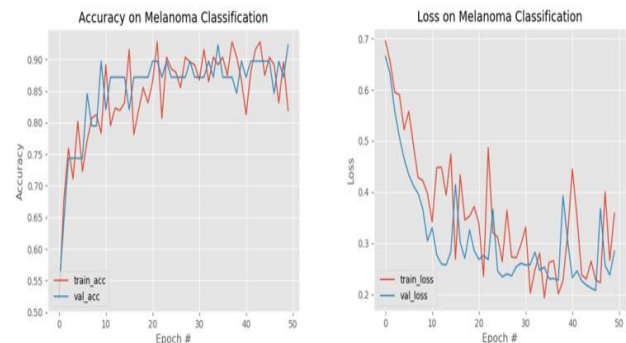


Fig. 9. Plot of Training Result with 154 Training Data and 50 Epochs.

TABLE II. TESTING RESULT USING 154 TRAIN DATA AND 50 EPOCHS

No	Filename	Category	Result	Answer
1	ISIC_0000030	Melanoma	Melanoma	True
2	ISIC_0000157	Melanoma	Melanoma	True
3	ISIC_0000288	Melanoma	Melanoma	True
4	ISIC_0000295	Melanoma	Melanoma	True
5	ISIC_0000301	Melanoma	Melanoma	True
6	ISIC_0000303	Melanoma	Melanoma	True
7	ISIC_0010036	Melanoma	Non Melanoma	*False
8	ISIC_0010217	Melanoma	Melanoma	True
9	ISIC_0010652	Melanoma	Melanoma	True
10	ISIC_0011112	Melanoma	Melanoma	True
11	ISIC_0011492	Melanoma	Melanoma	True
12	ISIC_0011508	Melanoma	Melanoma	True
13	ISIC_0011515	Melanoma	Melanoma	True
14	ISIC_0011517	Melanoma	Melanoma	True
15	ISIC_0011518	Melanoma	Melanoma	True
16	ISIC_0011693	Melanoma	Melanoma	True
17	ISIC_0011772	Melanoma	Melanoma	True
18	ISIC_0011774	Melanoma	Melanoma	True
19	ISIC_0011873	Melanoma	Melanoma	True
20	ISIC_0011878	Melanoma	Melanoma	True
21	ISIC_0011879	Melanoma	Melanoma	True
22	ISIC_0011944	Melanoma	Melanoma	True
23	ISIC_0000008	Non Melanoma	Non Melanoma	True
24	ISIC_0000012	Non Melanoma	Non Melanoma	True
25	ISIC_0000015	Non Melanoma	Non Melanoma	True
26	ISIC_0000018	Non Melanoma	Non Melanoma	True
27	ISIC_0000021	Non Melanoma	Non Melanoma	True
28	ISIC_0000058	Non Melanoma	Non Melanoma	True
29	ISIC_0000059	Non Melanoma	Non Melanoma	True
30	ISIC_0000064	Non Melanoma	Non Melanoma	True
31	ISIC_0000067	Non Melanoma	Non Melanoma	True
32	ISIC_0000086	Non Melanoma	Non Melanoma	True
33	ISIC_0000089	Non Melanoma	Non Melanoma	True
34	ISIC_0000093	Non Melanoma	Non Melanoma	True
35	ISIC_0000096	Non Melanoma	Melanoma	*False
36	ISIC_0000108	Non Melanoma	Non Melanoma	True
37	ISIC_0000109	Non Melanoma	Melanoma	*False
38	ISIC_0000113	Non Melanoma	Non Melanoma	True
39	ISIC_0000116	Non Melanoma	Non Melanoma	True
40	ISIC_0000121	Non Melanoma	Non Melanoma	True
41	ISIC_0000124	Non Melanoma	Non Melanoma	True
42	ISIC_0000125	Non Melanoma	Melanoma	*False
43	ISIC_0000128	Non Melanoma	Non Melanoma	True
44	ISIC_0000134	Non Melanoma	Non Melanoma	True

TABLE III. CONFUSION MATRIX FROM THE TESTING RESULT USING 154 TRAIN DATA AND 50 EPOCHS

Matrix		Actual Class	
		Melanoma	Non-Melanoma
Prediction Class	Melanoma	TP = 21	FP = 3
	Non- Melanoma	FN = 1	TN = 19

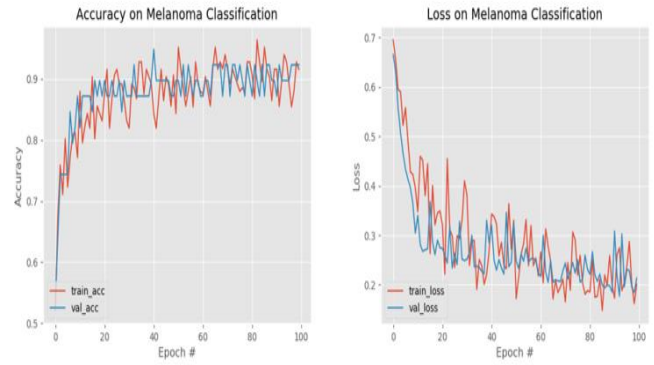


Fig. 10. Plot of Training Result with 154 Training Data and 100 Epochs.

In Fig. 10 can be seen that from epoch 0 to 99 shows that training accuracy has increased with the final result of 0.92 while training loss has decreased with the final result of 0.21. The model from this training then was tested against 44 test data. This testing result can be seen in Table IV.

Based on Table IV with 44 images being tested, there are 41 correct images and 3 incorrect images in classification. From the table, the results in confusion matrix are shown in Table V.

$$\text{Precision} = \frac{TP}{TP+FP} \times 100\%$$

$$\frac{21}{21+2} \times 100\% = \frac{21}{23} \times 100\% = 91\%$$

$$\text{Recall} = \frac{TP}{TP+FN} \times 100\%$$

$$\frac{21}{21+1} \times 100\% = \frac{21}{22} \times 100\% = 95\%$$

$$\text{Accuracy} = \frac{TP+TN}{TP+TN+FP+FN} \times 100\%$$

$$\frac{21+20}{21+20+2+1} \times 100\% = \frac{41}{44} \times 100\% = 93\%$$

The calculation of the confusion matrix above results 91 % of precision, 95% of recall, and 93% of accuracy.

B. Experiment using 176 Train Data and 50 Epochs

The training process of this experiment was carried out using 50 epochs on 176 train data which consist of 88 images of melanoma and 88 images of non-melanoma. The plot result from this training can be seen in Fig. 11.

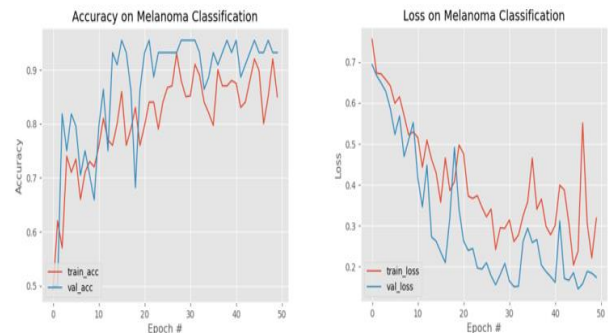


Fig. 11. Plot of Training Result with 176 Training Data and 50 Epochs.

In Fig. 6 can be seen that from epoch 0 to 49 shows that training accuracy has increased with the final result of 0.93 while training loss has decreased with the final result of 0.17. The model from this training then was tested against 44 test data. This testing result can be seen in Table IV.

Based on Table VI with 44 images being tested, there are 42 correct images and 2 incorrect images in classification. From the table, the results in confusion matrix are shown in Table VII.

TABLE IV. TESTING RESULT USING 154 TRAIN DATA AND 100 EPOCHS

No	Filename	Category	Result	Answer
1	ISIC_0000030	Melanoma	Melanoma	True
2	ISIC_0000157	Melanoma	Melanoma	True
3	ISIC_0000288	Melanoma	Melanoma	True
4	ISIC_0000295	Melanoma	Melanoma	True
5	ISIC_0000301	Melanoma	Melanoma	True
6	ISIC_0000303	Melanoma	Melanoma	True
7	ISIC_0010036	Melanoma	Non Melanoma	*False
8	ISIC_0010217	Melanoma	Melanoma	True
9	ISIC_0010652	Melanoma	Melanoma	True
10	ISIC_0011112	Melanoma	Melanoma	True
11	ISIC_0011492	Melanoma	Melanoma	True
12	ISIC_0011508	Melanoma	Melanoma	True
13	ISIC_0011515	Melanoma	Melanoma	True
14	ISIC_0011517	Melanoma	Melanoma	True
15	ISIC_0011518	Melanoma	Melanoma	True
16	ISIC_0011693	Melanoma	Melanoma	True
17	ISIC_0011772	Melanoma	Melanoma	True
18	ISIC_0011774	Melanoma	Melanoma	True
19	ISIC_0011873	Melanoma	Melanoma	True
20	ISIC_0011878	Melanoma	Melanoma	True
21	ISIC_0011879	Melanoma	Melanoma	True
22	ISIC_0011944	Melanoma	Melanoma	True
23	ISIC_0000008	Non Melanoma	Non Melanoma	True
24	ISIC_0000012	Non Melanoma	Non Melanoma	True
25	ISIC_0000015	Non Melanoma	Non Melanoma	True
26	ISIC_0000018	Non Melanoma	Non Melanoma	True
27	ISIC_0000021	Non Melanoma	Non Melanoma	True
28	ISIC_0000058	Non Melanoma	Non Melanoma	True
29	ISIC_0000059	Non Melanoma	Non Melanoma	True
30	ISIC_0000064	Non Melanoma	Non Melanoma	True
31	ISIC_0000067	Non Melanoma	Non Melanoma	True
32	ISIC_0000086	Non Melanoma	Non Melanoma	True
33	ISIC_0000089	Non Melanoma	Non Melanoma	True
34	ISIC_0000093	Non Melanoma	Non Melanoma	True
35	ISIC_0000096	Non Melanoma	Non Melanoma	True
36	ISIC_0000108	Non Melanoma	Melanoma	*False
37	ISIC_0000109	Non Melanoma	Non Melanoma	True
38	ISIC_0000113	Non Melanoma	Melanoma	*False
39	ISIC_0000116	Non Melanoma	Non Melanoma	True
40	ISIC_0000121	Non Melanoma	Non Melanoma	True
41	ISIC_0000124	Non Melanoma	Non Melanoma	True
42	ISIC_0000125	Non Melanoma	Non Melanoma	True
43	ISIC_0000128	Non Melanoma	Non Melanoma	True
44	ISIC_0000134	Non Melanoma	Non Melanoma	True

TABLE V. CONFUSION MATRIX FROM THE TESTING RESULT USING 154 TRAIN DATA AND 100 EPOCHS

Matrix		Actual Class	
		Melanoma	Non-Melanoma
Prediction Class	Melanoma	TP = 21	FP = 2
	Non- Melanoma	FN = 1	TN = 20

TABLE VI. TESTING RESULT USING 176 TRAIN DATA AND 50 EPOCHS

No	Filename	Category	Result	Answer
1	ISIC_0000030	Melanoma	Melanoma	True
2	ISIC_0000157	Melanoma	Melanoma	True
3	ISIC_0000288	Melanoma	Melanoma	True
4	ISIC_0000295	Melanoma	Melanoma	True
5	ISIC_0000301	Melanoma	Melanoma	True
6	ISIC_0000303	Melanoma	Melanoma	True
7	ISIC_0010036	Melanoma	Non Melanoma	*False
8	ISIC_0010217	Melanoma	Melanoma	True
9	ISIC_0010652	Melanoma	Melanoma	True
10	ISIC_0011112	Melanoma	Melanoma	True
11	ISIC_0011492	Melanoma	Melanoma	True
12	ISIC_0011508	Melanoma	Melanoma	True
13	ISIC_0011515	Melanoma	Melanoma	True
14	ISIC_0011517	Melanoma	Melanoma	True
15	ISIC_0011518	Melanoma	Melanoma	True
16	ISIC_0011693	Melanoma	Melanoma	True
17	ISIC_0011772	Melanoma	Non Melanoma	*False
18	ISIC_0011774	Melanoma	Melanoma	True
19	ISIC_0011873	Melanoma	Melanoma	True
20	ISIC_0011878	Melanoma	Melanoma	True
21	ISIC_0011879	Melanoma	Melanoma	True
22	ISIC_0011944	Melanoma	Melanoma	True
23	ISIC_0000008	Non Melanoma	Non Melanoma	True
24	ISIC_0000012	Non Melanoma	Non Melanoma	True
25	ISIC_0000015	Non Melanoma	Non Melanoma	True
26	ISIC_0000018	Non Melanoma	Non Melanoma	True
27	ISIC_0000021	Non Melanoma	Non Melanoma	True
28	ISIC_0000058	Non Melanoma	Non Melanoma	True
29	ISIC_0000059	Non Melanoma	Non Melanoma	True
30	ISIC_0000064	Non Melanoma	Non Melanoma	True
31	ISIC_0000067	Non Melanoma	Non Melanoma	True
32	ISIC_0000086	Non Melanoma	Non Melanoma	True
33	ISIC_0000089	Non Melanoma	Non Melanoma	True
34	ISIC_0000093	Non Melanoma	Non Melanoma	True
35	ISIC_0000096	Non Melanoma	Non Melanoma	True
36	ISIC_0000108	Non Melanoma	Non Melanoma	True
37	ISIC_0000109	Non Melanoma	Non Melanoma	True
38	ISIC_0000113	Non Melanoma	Non Melanoma	True
39	ISIC_0000116	Non Melanoma	Non Melanoma	True
40	ISIC_0000121	Non Melanoma	Non Melanoma	True
41	ISIC_0000124	Non Melanoma	Non Melanoma	True
42	ISIC_0000125	Non Melanoma	Non Melanoma	True
43	ISIC_0000128	Non Melanoma	Non Melanoma	True
44	ISIC_0000134	Non Melanoma	Non Melanoma	True

TABLE VII. CONFUSION MATRIX FROM THE RESULT OF EXPERIMENT USING 176 TRAIN DATA AND 50 EPOCHS

Matrix		Actual Class	
		Melanoma	Non-Melanoma
Prediction Class	Melanoma	TP = 20	FP = 0
	Non- Melanoma	FN = 2	TN = 22

$$\text{Precision: } \frac{TP}{TP+FP} \times 100\%$$

$$\frac{20}{20+0} \times 100\% = \frac{20}{20} \times 100\% = 100\%$$

$$\text{Recall : } \frac{TP}{TP+FN} \times 100\%$$

$$\frac{20}{20+2} \times 100\% = \frac{20}{22} \times 100\% = 91\%$$

$$\text{Accuracy : } \frac{TP+TN}{TP+TN+FP+FN} \times 100\%$$

$$\frac{20+22}{20+22+0+2} \times 100\% = \frac{42}{44} \times 100\% = 95\%$$

The calculation of the confusion matrix above results 100% of precision, 91% of recall, and 95% of accuracy.

B. Experiment Using 176 Train Data and 100 Epochs

The training process of this experiment was carried out using 50 epochs on 154 train data which consist of 77 images of melanoma and 77 images of non-melanoma. The plot result from this training can be seen in Fig. 12.

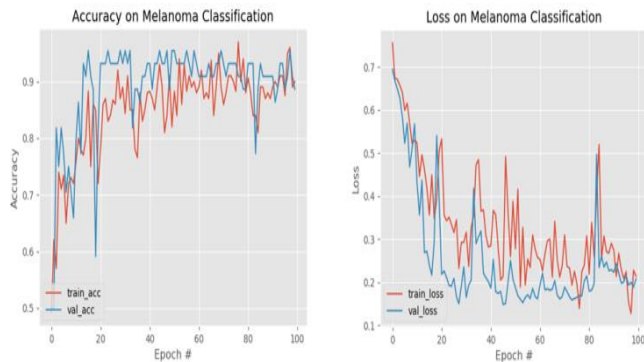


Fig. 12. Plot of Training Result with 176 Training Data and 100 Epochs.

In Fig. 12 can be seen that from epoch 0 to 99 shows that training accuracy has increased with the final result of 0.88 while training loss has decreased with the final result of 0.20. The model from this training then was tested against 44 test data. This testing result can be seen in Table VIII.

Based on Table VIII with 44 images being tested, there are 44 correct images and 0 incorrect images in classification. From the table, the results in confusion matrix are shown in Table IX.

$$\text{Precision: } \frac{TP}{TP+FP} \times 100\%$$

$$\frac{22}{22+0} \times 100\% = \frac{22}{22} \times 100\% = 100\%$$

$$\text{Recall : } \frac{TP}{TP+FN} \times 100\%$$

$$\frac{22}{22+0} \times 100\% = \frac{22}{22} \times 100\% = 100\%$$

$$\text{Accuracy : } \frac{TP+TN}{TP+TN+FP+FN} \times 100\%$$

$$\frac{22+22}{22+22+0+0} \times 100\% = \frac{44}{44} \times 100\% = 100\%$$

The calculation of the confusion matrix above results 100 % of precision, 100% of recall, and 100% of accuracy.

TABLE VIII. TESTING RESULT USING 176 TRAIN DATA AND 100 EPOCHS

No	Filename	Category	Result	Answer
1	ISIC_0000030	Melanoma	Melanoma	True
2	ISIC_0000157	Melanoma	Melanoma	True
3	ISIC_0000288	Melanoma	Melanoma	True
4	ISIC_0000295	Melanoma	Melanoma	True
5	ISIC_0000301	Melanoma	Melanoma	True
6	ISIC_0000303	Melanoma	Melanoma	True
7	ISIC_0010036	Melanoma	Melanoma	True
8	ISIC_0010217	Melanoma	Melanoma	True
9	ISIC_0010652	Melanoma	Melanoma	True
10	ISIC_0011112	Melanoma	Melanoma	True
11	ISIC_0011492	Melanoma	Melanoma	True
12	ISIC_0011508	Melanoma	Melanoma	True
13	ISIC_0011515	Melanoma	Melanoma	True
14	ISIC_0011517	Melanoma	Melanoma	True
15	ISIC_0011518	Melanoma	Melanoma	True
16	ISIC_0011693	Melanoma	Melanoma	True
17	ISIC_0011772	Melanoma	Melanoma	True
18	ISIC_0011774	Melanoma	Melanoma	True
19	ISIC_0011873	Melanoma	Melanoma	True
20	ISIC_0011878	Melanoma	Melanoma	True
21	ISIC_0011879	Melanoma	Melanoma	True
22	ISIC_0011944	Melanoma	Melanoma	True
23	ISIC_0000008	Non Melanoma	Non Melanoma	True
24	ISIC_0000012	Non Melanoma	Non Melanoma	True
25	ISIC_0000015	Non Melanoma	Non Melanoma	True
26	ISIC_0000018	Non Melanoma	Non Melanoma	True
27	ISIC_0000021	Non Melanoma	Non Melanoma	True
28	ISIC_0000058	Non Melanoma	Non Melanoma	True
29	ISIC_0000059	Non Melanoma	Non Melanoma	True
30	ISIC_0000064	Non Melanoma	Non Melanoma	True
31	ISIC_0000067	Non Melanoma	Non Melanoma	True
32	ISIC_0000086	Non Melanoma	Non Melanoma	True
33	ISIC_0000089	Non Melanoma	Non Melanoma	True
34	ISIC_0000093	Non Melanoma	Non Melanoma	True
35	ISIC_0000096	Non Melanoma	Non Melanoma	True
36	ISIC_0000108	Non Melanoma	Non Melanoma	True
37	ISIC_0000109	Non Melanoma	Non Melanoma	True
38	ISIC_0000113	Non Melanoma	Non Melanoma	True
39	ISIC_0000116	Non Melanoma	Non Melanoma	True
40	ISIC_0000121	Non Melanoma	Non Melanoma	True
41	ISIC_0000124	Non Melanoma	Non Melanoma	True
42	ISIC_0000125	Non Melanoma	Non Melanoma	True
43	ISIC_0000128	Non Melanoma	Non Melanoma	True
44	ISIC_0000134	Non Melanoma	Non Melanoma	True

TABLE IX. CONFUSION MATRIX FROM THE RESULT OF EXPERIMENT USING 176 TRAIN DATA AND 100 EPOCHS

Matrix		Actual Class	
		Melanoma	Non-Melanoma
Prediction Class	Melanoma	TP = 22	FP = 0
	Non- Melanoma	FN = 0	TN = 22

V. CONCLUSION AND FUTURE WORK

Classification of melanoma cancer images is carried out in 2 stages; the first stage is training the dataset to produce a model. The second stage is the process of classification which the system takes the image data, then initializes the model from the results of the training and makes predictions using the model, then the system takes the prediction results along with their probabilities and display the prediction results along with the image.

The experiment was conducted on 44 images of test data using a different number of training data (images) and epochs in the training process. The experiment obtained the highest accuracy of 93% in training result. Meanwhile, in testing result obtained 91% of accuracy for using 154 images and 50 epochs in training, then 93% accuracy for using 154 images and 100 epochs in training. The training conducted on 176 images and 50 epochs resulted in a 95% accuracy of testing result, while for the training using 176 images and 100 epochs resulted in 100% accuracy of testing result.

The experiment results prove that the amount of training data and epochs used for training affects the level of accuracy in classifying melanoma cancer images. The more data that is trained, the better the test results will be produced. Whereas 100 epochs is the optimal epoch to produce the best accuracy, this is supported by several other parameters of the LeNet-5 architecture, such as learning rate, number of layers, and the size of input pixels used during training.

Unfortunately, it is difficult to compare different classification methods because some approaches use non-public datasets for training and/or testing, thereby making

reproducibility difficult. Future publications should use publicly available benchmarks and fully disclose methods used for training to allow comparability.

REFERENCES

- [1] World Health Organization. 2018. *Skin Cancers*. Available: <http://www.who.int/uv/faq/skincancer/en/index1.html>.
- [2] L. Deng and Yu D., "Deep Learning: Methods and Applications", *Foundations and Trends in Signal Processing*, Vol. 7, No. 3 – 4, 2013
- [3] Y. LeCun, B. Boser, J.S. Denker, R.E. Howard, W. Hubbard, L.D. Jackel and D. Henderson, "Handwritten digit recognition with a back-propagation network", in *Advances in neural information processing systems* 2, pp. 396-404, Morgan Kaufmann Publishers Inc. San Francisco, CA, USA, 1990
- [4] I. Goodfellow, Y. Bengio, and A. Courville, *Deep Learning*, MIT Press, 2016
- [5] Y. LeCun, Y., Y. Bengio, dan G. Hinton, 2015. "Deep Learning", *Nature*, Vol 521, pp. 436-444, 2015, doi:10.1038/nature14539
- [6] Y. LeCun, L.D. Jackel, Leon Bottou, A. Brunot, C. Cortes, J. S. Denker, H. Drucker, J. Guyon, U. A. Muller, E. Sackinger, P. Simard and V. Vapnik, " Learning algorithms for classification: a comparison on Handwritten digit recognition", 1995, <http://yann.lecun.com/exdb/pubs/lecun-95b.djvu>
- [7] J. Wallen, [Online] Cheat sheet: TensorFlow, an open source software library for machine learning. Available: <https://www.techrepublic.com/article/tensorflow-googles-open-source-software-library-for-machine-learning-the-smart-persons-guide/>, 2017
- [8] A. Esteva, B. Kuprel, R.A. Novoa, J. Ko, S.M. Swetter, H.M. Blau and S. Thrun, "Dermatologist-level classification of skin cancer with deep neural networks", *Nature*, Vol. 542, pp 115-118, 2017
- [9] T.J. Brinker, A. Hekler, J.S. Utikal, N.Grabe, D. Schadendorf, J. Klode, C. Berking, T. Steeb, A.H. Enk, and C.von Kalle, "Skin Cancer Classification Using Convolutional Neural Networks: Systematic Review", *Journal of Medical Internet Research*, Vol. 20, No.10, pp. 11936- 11946, 2018

Leveraging a Multi-Objective Approach to Data Replication in Cloud Computing Environment to Support Big Data Applications

Mohammad Shorfuzzaman¹, Mehedi Masud²

Department of Computer Science, Taif University, Taif, Saudi Arabia

Abstract—Increased data availability and high data access performance are of utmost importance in a large-scale distributed system such as data cloud. To address these issues data can be replicated in various locations in the system where applications are executed. Replication not only improves data availability and access latency but also improves system load balancing. While data replication in distributed cloud storage is addressed in the literature, majority of the current techniques do not consider different costs and benefits of replication from a comprehensive perspective. In this paper, we investigate replica management problem (which is formulated using dynamic programming) in cloud computing environments to support big data applications. To this end, we propose a new highly distributed replica placement algorithm that provides cost-effective replication of huge amount of geographically distributed data into the cloud to meet the quality of service (QoS) requirements of data-intensive (big data) applications while ensuring that the workload among the replica data centers is balanced. In addition, the algorithm takes into account the consistency among replicas due to update propagation. Thus, we build up a multi-objective optimization approach for replica management in cloud that seeks near optimal solution by balancing the trade-offs among the stated issues. For verifying the effectiveness of the algorithm, we evaluated the performance of the algorithm and compared it with two baseline approaches from the literature. The evaluation results demonstrate the usefulness and superiority of the presented algorithm for conditions of interest.

Keywords—Big data applications; data cloud; replication; dynamic programming; QoS requirement; workload constraint

I. INTRODUCTION

Lately, cloud computing has become an attractive and mainstream solution for data storage, processing, and distribution [1]. It provides on-demand and elastic computing and data storage resources without the large initial investments usually required for the deployment of traditional data centers. Cloud computing facilitates the delivery of storage and computing resources as services without any restriction on the location [2]. It offers three types of architecture for service delivery such as SaaS (Software as a Service), PaaS (Platforms as a Service) and IaaS (Infrastructure as a Service) [3]. End users can use the software applications hosted by the cloud providers in a SaaS architecture. In case of IaaS architecture, virtualized storage and computing resources are provided by the cloud providers. Customers of IaaS can then access these resources and other services to complete the

application stack such as to create virtual machines and to deploy operating systems and middleware. As for PaaS architecture, the cloud providers allow users to develop, run and customize applications while the providers host them on their own hardware infrastructures.

Due to the benefits offered by cloud computing, organizations are now moving to the cloud. Some of the top cloud providers such as Amazon S3 [4], Google Cloud Platform [5], App iCloud¹, IBM Cloud², Microsoft Azure³, and DropBox⁴ provide cloud services to thousands of millions of users by means of geographically dispersed data centers across the globe. As such, end users are relieved of purchasing traditional expensive hardware (data centers) to process huge amount of data. Consequently, growing interests are shown in an effort to develop data-intensive applications that access massive amount data sets. To name a few, smart city applications and Healthcare Information Systems (HISs) are struggling with data bombardments that need immediate solutions to process these data for knowledge acquisition. These data-intensive applications demand for large-scale computing and storage resources and recent cloud computing advancement suits to meet these challenges. Lately, popular big data applications such as Facebook, Twitter, and Human Genome Project⁵, are making most use of computing framework such as MapReduce and Hadoop [6] for petabyte-scale data processing to extract insight.

The performance of these big data applications on cloud depends largely on the reliability, availability and efficient access to the data centers [7]. To address these issues data can be replicated in various locations in the system where applications are executed [8], [9], [10], [11]. This means that data partitions can be replicated across different data centers in the cloud. Replication not only improves data availability and access latency but also improves system load balancing. Many existing cloud systems adopt static replication strategies by replicating data in some physical locations without considering the issue of replication cost and terrestrial diversity. For instance, GFS (Google File System) [5], Amazon S3 [4], and HDFS (Hadoop Distributed File System) [9] implement a replication strategy where three copies of data

¹ App iCloud, <https://www.icloud.com/>

² IBM Cloud, <https://www.ibm.com/cloud/>

³ Azure: Microsoft's Cloud Platform, <https://azure.microsoft.com/>

⁴ Dropbox, <https://www.dropbox.com/>

⁵ Human Genome Project, <http://www.ornl.gov/hgmis/home.shtml>

are created at one time to increase reliability of target data. This replication strategy would result in increased (twice) replication cost which will adversely affect the effectiveness of the cloud system.

There are a number of critical issues that need to be addressed to achieve big data replication in cloud storage: *i)* Determining the degree of data replicas that should be created in the cloud to meet reasonable system and application requirements. This is an important issue for further research. Since excessive replication would increase the replica maintenance and storage cost creating too many or fixed replicas are not a good choice. *ii)* Distribution of these replicas to achieve higher efficiency and better system load balancing. *iii)* Maintaining consistency among replicas due to replica update or delete. These three correlated problems are jointly referred to as the replica management problem. In addition to that, some data replication strategies in the cloud consider energy efficiency issue to optimize the energy consumed by the data centers.

While data replication in distributed cloud storage is addressed in the literature, majority of the current techniques do not consider different costs and benefits of replication from a comprehensive perspective. Most of them provide emphasis on high availability, fast response and high efficiency. Even though critical, these average performance measures do not tackle the quality requirements demanded by various data-intensive applications. The performance of these algorithms gets better as the number of replicas increases. However, the increased number of replicas incurs higher degree of replication cost associated with storage and energy. Hence, the goal should be to minimize the required number of replicas to avoid high replica creation and maintenance cost. Accordingly, a good replica management strategy should be designed to balance a variety of tradeoffs. Moreover, as in the case of existing replication strategies, the increased number of replicas is cost prohibitive due to consistency management.

Given the issues and trends stated above, in this paper, we investigate replica management problem in cloud computing environments to support big data applications from a holistic view. To this end, we provide cost-effective replication of large amount of geographically distributed data into the cloud to meet the quality of service (QoS) requirements of data-intensive (big data) applications while ensuring that the workload among the replica data centers is balanced. Targeting a typical cloud platform that encompasses disparate data centers, we formulate cost-minimizing data replication problem, and present an effective distributed algorithm that optimizes the choice of energy efficient data centers into the cloud for allocating replicas taking into account the consistency among replicas due to update propagation. Thus, we build up a multi-objective optimization approach for replica management in cloud that seeks near optimal solution by balancing the trade-offs among the stated issues. Hence, we make the following contributions:

- Analyze the replica management problem to formulate mathematical models to describe the stated objectives such as application QoS requirements, system load

variance, and replica consistency and come up with a replication model considering overall replication cost.

- Propose a highly distributed offline replication scheme that computes data center locations in the cloud by minimizing overall replication cost to meet the above-mentioned stated objectives.
- Assess the benefit and applicability of our scheme using extensive simulation experiments over a wide range of parameters (e.g., no. of data centers, size and access rate of each data file, data center workload capacity constraint, traffic pattern, application QoS requirements, etc.).

The remainder of the paper is presented as follows. QoS-aware replica placement techniques are reviewed in Section 2. Section 3 presents the system design and architecture. The proposed replication algorithm is provided in Section 4. Sections 5 and 6 present simulation methods and obtained results, respectively. We conclude in Section 7 with directions of future work.

II. RELATED WORK

To date, a number of replication strategies have been adopted in many application areas such as cloud storage, large data storage, data grids, distributed systems and so on. These replication strategies are mainly divided into static and dynamic categories. The number of replicas created is fixed in static categories. As mentioned already, GFS [5] and HDFS [6] are adopting this strategy. However, this technique is lacking flexibility even though replica management is straightforward. Most of the current research work is focusing on dynamic replica placement strategies where the number and location of replicas created can vary depending on the application requirements.

Huang et al. [12] propose a reliability model for providing data service in cloud storage systems. The authors present the service model which sets off replica creation and selects storage site based on the relationships among the access reliability of the application nodes. The evaluation results show that the proposed method increase data service reliability with a significant decrease in the count of replicas created. The authors in [13] present a file replication mechanism in P2P file sharing systems which works based on swarm intelligence. The idea is to exploit the collective behavior of swarm nodes which share common interest and in close proximity. In contrast to other similar methods, this approach determines the replica locations according to the accrued query rates of nodes in the swarm instead of only one node. This results in fewer replicas and improved querying efficiency. The proposed technique also considers replica consistency using a message update mechanism in a top to bottom fashion.

Liu et al. [14] tackle the data replication problem in Online Social Network (OSN) by means of a careful data replication technique in dispersed datacenters (SD³). The goal is to lessen inter-datacenter communication while improving service latency. The replication technique takes into account update rates and visit rates to determine the user data for replication.

To ensure reduced inter-datacenter communication, the technique atomizes users' different type of data for replication. Experimental results demonstrate higher efficiency of SD³ compared to other replication methods. Yet, the authors in [15] come up with a data replication strategy called Cadros, for decentralized online social network (DOSN) to increase data availability. First, they have done a quantitative analysis of cloud storage to retrieve knowledge about storage capacity and then propose a model that predicts the level of data availability that Cadros can attain. The technique takes into account data partitioning in the cloud in such a way that minimizes the communication overhead and still aims at achieving desired level of data availability. At the same time, the paper also presents data placement strategies that aim to satisfy the stated objective in terms of other performance metrics.

Sun et al. [16] address the problem of an increase in overload nodes which causes poor service performance in cloud-P2P systems through a Dynamic Adaptive Replica Strategy (DARS). Special attention is given to reduce the number of overload nodes by determining appropriate time for replica creation. The replication strategy works based on the node's overheating similarity and exploits a fuzzy-logic based clustering algorithm to determine nodes for optimal replica placement. Experimental results reveal that DARS significantly reduces the number of overload nodes facilitating low replica access delay with high load balance.

A dynamic data replication for hierarchical cloud storage is proposed in [17]. The authors have used temporal locality of a data file to determine its popularity which means that recently used files are likely to be accessed again in near future. The replication of a certain data file is triggered when its popularity crosses a predefined threshold value. Moreover, the newly created replicas are stored in data centers that are directly connected. In a subsequent effort [18], this replication strategy is improved by the introduction of checkpoint mechanism to enhance data availability. Another cloud data replication strategy called CDRM (Cost-effective Dynamic Replication Management) [19] is proposed for heterogeneous environments. CDRM develops a system model to formulate the relationship between data availability and replication factor. It consistently maintains minimum number of replicas in the system and ensures proper balance of workload across the datacenter nodes and reduces access delay. The authors in [20] proposed a replication mechanism called RFH (Resilient, Fault-tolerant and High efficient) which is able to replicate data based on the varying query load. They have taken into account failure rate, size of the partitions, link capacity and the distance in replication cost calculation.

Gill and Singh [21] presented a dynamic replication algorithm for heterogeneous cloud data centers that ensures minimum number of replicas while maintaining desired level of data availability. Their algorithm works based on the concept of knapsack to minimize the replication cost while considering re-replication by moving replicas from high-cost data centers to low-cost ones. The algorithm is found to be effective in minimizing replication cost with satisfactory level of data availability. Boru et al. [22] propose a replication solution which optimizes energy efficiency of the system.

GreenCloud simulator is used for performance assessment for the replication technique. The simulation results show that the proposed replication strategy significantly improves data access time, network resource usage, and energy consumption. Long et al [23] propose a replica management strategy called MORM (Multi-objective Optimized Replication Management) to be used in cloud data storage. The idea is to make a trade-off among different important factors affecting replication decision. Another dynamic replication strategy called dynamic popularity aware replication strategy (DPRS) is proposed by Mansouri et al [24] which works based on the access popularity of data and considers parallel downloading of data segments from multiple data centers to improve access performance. Sun et al [25] addressed the replication problem from a different perspective where they handled the trade-off between access performance and consistency dynamically. The authors came up with a replication protocol called CC-Paxos to adaptively balance trade-off between latency and consistency which is independent of any underlying data stores. In addition to that, a number of other researchers [26-31] have proposed various dynamic replica creation and maintenance (e.g., consistency) techniques in distributed cloud storage systems.

At this point, it is evident that there has been reasonable effort in addressing data replication problem in cloud computing environment. Nevertheless, the current research has not adequately addressed the issue of QoS requirements. Few researchers in the literature have worked in this area. Among them, Lin et al. [32] proposed two algorithms that take into account QoS requirements while replicating data in cloud computing systems. The first algorithm is based on a greedy approach which adopts the concept of high-QoS first-replication (HQFR). In this case, the applications requiring QoS are ranked in the order of highest priority to lowest priority applications. However, this algorithm is not able to produce optimal solution. Hence, a second algorithm called minimum-cost maximum-flow (MCMF) is used to minimize replication cost and to maximize the number of replicas satisfying the specified QoS requirements. This algorithm produces near-optimal solution to the replication problem in polynomial time. Varma and Khatri [33] investigated the QoS-aware data replication problem in Hadoop Distributed File System (HDFS). In the original HDFS, a replication technique is used to copy data blocks without any quality restriction between client and the service provider. Hence, the authors consider replication time of an application as the QoS parameter and present an algorithm which can reduce replication cost compared to the existing algorithm. Yet another recent work [34] addresses the QoS aware replication problem for multimedia data in cloud. Naturally, multimedia data has stringent QoS requirement and hence replication of such data often requires fulfillment of QoS requirement from the users. Hence, the authors propose an algorithm to replicate multimedia data considering QoS requirement such as access delay, jitter, bandwidth usage, and loss or error rate implemented in an extended HDFS architecture. The simulation results demonstrate an important reduction in terms of number of replicas that violate the QoS requirement in contrast to the existing replication strategy adopted by Hadoop. In a recent effort, Shorfuzzaman [35] presents a

dynamic replica maintenance technique called DRMS in a multi-cloud environment taking into account various QoS requirements from users. Periodically replicas are relocated to new locations upon significant performance degradation. The simulation results show that the proposed technique improves response time for data access in contrast to its static counterpart where no maintenance takes place.

In addition to that, a number of QoS aware replication strategies are also available in data grid systems [36], [37], [38]. A least value replacement (LVR) strategy is proposed for data replication in data grids by the authors of [36] by taking into account user QoS and storage capacity constraint. The authors devised a replica replacement strategy that determines which replica should be replaced whenever the replica site is found to be full based on the access frequency and future value for a particular data file. Cheng et al. [37] address the replica placement problem in data grids based on general graphs by means of two heuristic algorithms namely, Greedy Remove and Greedy Add which take care of QoS requirements. The authors consider replica access cost and workload capacity of the replica servers in their cost model. Furthermore, the authors in [38] propose a dynamic QoS-aware replication scheme showing a complete lifecycle for determining positions for replica creation. The replication scheme also articulates how old replicas are relocated and replaced. The data is replicated based on its importance which is determined by its access popularity.

A number of replica placement algorithms are also available in other areas of interest such as distributed and mobile databases and P2P networks. As a whole, these replication strategies are not directly applicable to the target environment in our paper and thus we did not present them in the scope of this paper. In this paper, we present a fully distributed approach to data replication which aims at using a multi-objective model in cloud that seeks near optimal solution by minimizing total replication cost and by balancing the trade-offs among the stated objectives such as QoS requirements from applications, workload of replica data center nodes, consistency of created replicas.

III. SYSTEM DESIGN AND ARCHITECTURE

Our multi-objective data replication technique is designed based on the HDFS (Hadoop distributed file system) architecture and it is assumed that different cloud computing datacenters are placed in different geographical locations (Fig. 1). There is a three tier topology in HDFS architecture which consists of only one NameNode and a number of DataNodes arranged within multiple racks. The primary task of NameNode is to administer the file system namespace and to maintain a virtual map of how different data blocks are associated with different DataNodes. In Hadoop, DataNodes are meant for the execution of applications.

The request for data block (read and update) goes from an HDFS application to the NameNode which examines the pre-stored mapping for data blocks to DataNodes to find an appropriate DataNode to process the request. Each rack is equipped with an Ethernet switch for facilitating communication between the data nodes within the rack. For inter-rack communication, aggregated Ethernet switches are

used. Thus, a logical network topology based on tree structure is built with different switches which use the prevalent communication protocol called spanning tree protocol (STP). To this end, as shown in Fig. 1, core network, aggregation network and access network layers constitute the interconnect network in this scenario.

The three-tier cloud computing architecture as shown in Fig. 1 maintain a number of databases among which the central database (Central DB) is stationed in the highest layer. This database stores entire datasets that are accessed by the applications residing in the cloud. The other type of databases hosted by data centers is primarily used to improve data access efficiency and they are called datacenter database (Datacenter DB). These databases are intended for copying the most often accessed data items from Central DB. Furthermore, each rack is equipped with a rack-level database (Rack DB) which replicates data from datacenter databases.

A replica manager module in the NameNode performs analysis of data accesses periodically and determines which data items should be replicated and in which data nodes. The goal is to improve data access efficiency and balance workload of the data centers by spreading data replicas from central database to appropriate data centers down the hierarchy. Replica updates are only transferred from the central database to the databases in the data centers in the lower tiers. In addition to replica managers (as illustrated in Fig. 2), a scheduling broker and data centers constitute the system of cloud data service. The system is managed centrally by the scheduling broker whereas the locations of the replicas in different data centers are stored in replica managers.

A set of network links (E) interconnecting a set of data centers (V) forms the targeted cloud topology as an undirected tree $T = (V, E)$. The data transfer cost is calculated as the sum of the cost associated with each link along the path. Initially, all data are stored in the central DB and are disseminated down the cloud hierarchy in different data centers upon request from the users in the lowest tier. Over an interval of time, each user carries a count representing the access frequency of a specific data file which indicates the popularity of the file. Data consistency is maintained by propagating updates from the central DB to the replica server nodes. In this case, the associated cost is considered as maintenance cost for previously created replicas.

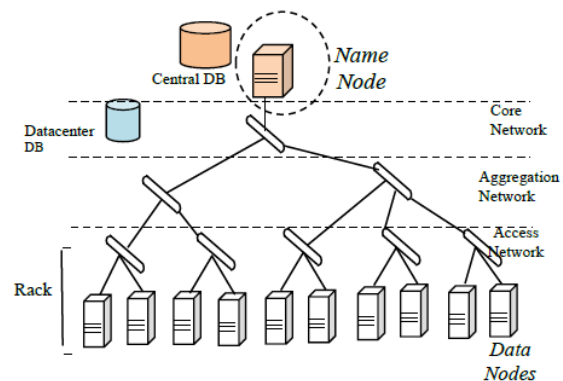


Fig. 1. Three-Tier Cloud Computing DataCenter Architecture based on HDFS [6].

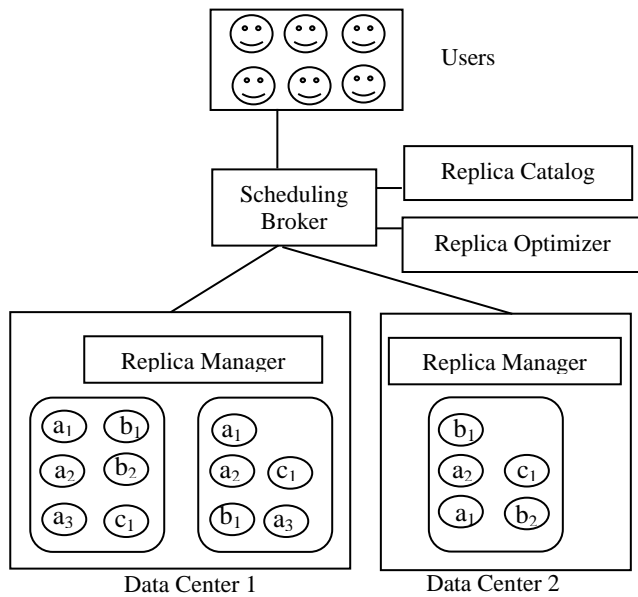


Fig. 2. Cloud Data Service Architecture.

Each data center node is associated with a workload constraint. The workload constraint refers to the maximum number of user requests that is served by a data center server for a certain period of time. It is expected that the incoming data requests from the users are satisfied while not exceeding the workload capacity of replica data centers each having a different workload constraint. If the aggregated workload of a data center server exceeds its capacity, the data center will be considered as overloaded.

Whenever a user needs to access data, it sends the request to the closest data center server along with the QoS constraints. A user (v) specifies his/her QoS requirement, $q(v)$, by means of an upper bound on some criteria. For example, a user may request for a data item within a specific time or from a specific distance in terms of network hops. The replication strategy then confirms that there is a data center server within this $q(v)$ to satisfy the request. If the request is not satisfied due to the absence of a data center server or any other reason the requirement is said to be violated.

A. Data Access Cost

As mentioned above, whenever a datacenter server receives a request for data it serves the request locally if data is present in the server. Alternatively, the request is served by any other closest replica server that holds the requested data. In our data cloud architecture, each user $v \in V$ carries an aggregated count, $count(v)$ which represents the total number of accesses for a particular data item over a time interval. This aggregated count determines the weighted communication cost for a user requesting the targeted data item. It is worthwhile to note that we have excluded the communication cost among the users and their directly associated datacenters as this does not affect the replica placement decision. The overall cost for data access is given as follows:

$$Total_{cost} = \sum_{f \in F} S_{cost} + C_{cost} + CMC_{cost} \quad (1)$$

where C_{cost} is the communication cost, CMC_{cost} is the data consistency maintenance cost and S_{cost} is the storage cost.

Given the set of replica data center servers R and the set of users requesting the data file (f) Q , the overall communication cost (C_{cost}) is computed as follows:

$$C_{cost} = \sum_{f \in F} \sum_{v \in R \cap u \in Q} count(u, f) \cdot d(u, v) \quad (2)$$

where F denotes different data file types and $count(u, f)$ represents the data access count of user u for file f .

The storage cost (S_{cost}) is determined as follows. Let $SC_{u,f}$ be the cost of storage associated with a file f stored at replica server (data center) u . Suppose f is replicated over R sites. The total cost for storage for f is

$$S = \sum_{u \in R} SC_{u,f} \quad (3)$$

where, $SC_{u,f}$ denotes the cost of storage of a file with type f in the data center u and the total cost for storage for different types (F) of files will be:

$$S_{cost} = \sum_{f \in F} \sum_{u \in R_f} SC_{u,f} \quad (4)$$

where, R_f denotes the set of replica servers that stores the file of type f .

The consistency maintenance cost for the replicas of a data file f with the update frequency $\mu(f)$, is formulated as follows:

$$CMC_{cost} = \sum_{f \in F} \sum_{T_v \cap R \neq \emptyset} \mu(f) \cdot d(v, p(v)) \quad (5)$$

where, $p(v)$ is the parent of node v and T_v is the sub-tree rooted at node v in the update distribution tree. The communication link $(v, p(v))$ participates in the update multicast process if $T_v \cap R \neq \emptyset$. Hence, the cost related to consistency maintenance is determined by aggregating the data transfer costs over the communication links $(v, p(v))$, when $v \neq r$.

B. Problem Definition

We now devise the replica placement problem in a large-scale cloud computing environment. In practice, the replica placement problem can be regarded as an optimization problem:

minimise $Total_{cost}$ and maximizing QoS

The goal is to select R data center locations from M probable data centers ($M > R$) by optimizing the cost (storage, communication, and consistency maintenance) of overall replication and satisfying specified QoS requirements of the users and the systems. More specifically, the goal is to identify a suitable replication strategy (i.e., the set of replica servers, R), with the minimal data access cost where the requests for data can be met by a datacenter server while meeting the user quality requirements and not exceeding the concerned data center's capacity limits.

IV. QoS-AWARE REPLICA PLACEMENT ALGORITHM

This section first presents our base distributed heuristic technique of multi-objective replica placement for cloud computing environment (RPCC). The proposed QoS-aware strategy will then be devised by extending the base algorithm

and incorporating both the users' and system's QoS requirements.

We demonstrate that our multi-objective RPCC can be designed as a dynamic programming problem and a distributed technique can be adopted to find its solution in a hierarchical cloud topology. In essence, the proposed technique breaks the overall reapplication problem into various sub-problems and advocates solving these sub-problems separately and combining the solutions to achieve the overall solution. Using the data access cost function, each data center node in the hierarchical cloud topology can determine the cost for creating a replica locally and transferring a replica from another data center up in the hierarchy as well. In RPCC, each data center needs to decide (based on the cost) whether it should create a replica locally or fetch the data from any replica server up in the hierarchy. A parent data center node accomplishes this by accumulating the results provided by its children. In reality, this is a bottom-up approach which begins from the lowest tier users and stops at tier-0. On the other hand, replica placement is done starting from the tier-0 and stopping at the lowest tier users (based on the previously calculated results). The details of the technique is discussed below.

We also define a cost vector to be used in calculating replication cost with respect to a particular data center node in the cloud hierarchy. Let v be a data center node and there is a sub-tree rooted at v . Now, let $Cost(v, rd)$ be the cost for replication contributed by the above sub-tree where rd denotes the replica distance from v towards the root data center. So, if this distance is zero (i.e., the replica is in v itself) the replication cost will include the communication cost for all descendants of v , the consistency maintenance cost and the storage cost at v . Moreover, if this distance is greater than zero (i.e., the replica is located at any data center sitting on the path from v towards the root), the replication cost will include the communication cost for all the descendants of v only.

A. Calculation of Replica Cost and Location

Now, each data center's replication cost is calculated by considering the location of a replica anywhere in the path from the node itself towards the origin server or root. The replication cost, $Cost(v, rd)$, for each data center node v is calculated based on the condition that the replica is located at some distance towards the root. As mentioned below, the optimum position of a replica is also calculated for each case. Once the cost vectors for all the children of a data center are calculated, the cost vector for the data center itself is calculated.

Given data center v , leaf (user), when $rd = 0$, the data center contains a replica in itself and thus QoS is satisfied. $Cost(v, 0)$ is calculated as the sum of the cost of storage at v and the cost of update to maintain replica consistency ($CMC_{cost}(v) + S_{cost}(v)$). Replica location is set to v . When $rd > 0$ we have two scenarios regarding the user QoS requirement, $q(v)$. First, if $rd \leq q(v)$ it means that the replica server (data center) is located at a distance which meets the user QoS requirement. The cost of replication of sub-tree T_v (i.e., v only for this case) contains the read cost for v only. Second, if $rd > q(v)$, the QoS requirement is not satisfied by the replica

and hence the communication cost is assigned to infinity. Now, the cost for $rd = 0$ is checked against the cost obtained with all possible distance, $rd \geq 1$, to identify the minimal cost for replication and location of replica. If for $rd = 0$ the cost ($Cost(v, 0)$) is smaller than the cost for greater values of rd , $Cost(v, rd)$ is assigned to $Cost(v, 0)$ and the location of the replica is set to the node itself. Otherwise, the replica will be created somewhere on the path towards the root and the location becomes rd -th ancestor of v . Replication cost will only be v 's communication cost (CC). Accordingly, the minimal replication cost $Cost(v, rd)$ and the respective replica server location (RSL) for v using each distance possibility ($rd \geq 0$) can be determined as follows:

$$Cost(v, rd) = \begin{cases} Cost(v, 0), & \text{if } Cost(v, 0) \leq CC(v, rd) \\ CC(v, rd), & \text{otherwise} \end{cases} \quad (6)$$

$$RSL(v, rd) = \begin{cases} v, & \text{if } Cost(v, 0) \leq CC(v, rd) \\ \text{node at distance of } rd & \text{otherwise} \end{cases} \quad (7)$$

Lemma 1. RPCC optimally places replicas in the sub-tree $T_v = T-r$ where r is the origin server or root and v is the leaf of the targeted cloud tree T .

Proof. To determine the replica placement for a sub-tree T_v where v is a leaf data center node in the tree T , we consider two possibilities. First, when d (i.e., distance between the user and the root) = 0, T consists of only one node which is the root. This results in no communication, storage, or consistency maintenance cost for replicas and hence the optimality of the algorithm trivially holds true. Second, when $d \geq 1$ (i.e., replica server is up on the way to the root) we need to compare the replication cost obtained for $d = 0$ (i.e., replica is in v itself) with the replication cost calculated for each value of d having $d \geq 1$ to decide on the optimal replication cost and locations of replicas. Now, if the cost for $d = 0$ (i.e., replica storage and update cost in v) is less than the cost for $d \geq 1$ (i.e., data access cost of v having a replica server up on the way to the root), placing a replica in v itself would be cheaper. On the contrary, the replica is placed at a higher data center node on the path to the root based on the value of d , which is optimal.

For a data center node v , non-leaf (i.e., non-user), when $rd = 0$, the node should contain a replica in itself. In this situation, the cost of replication, rep_cost will include the cost of all its children for $rd=1$, and the cost of storage and update for replica consistency at v (rep_cost)

$$= \sum_{j \in \text{child}(v)} Cost(j, 1) + CMC_{cost}(v) + S_{cost}(v)$$

However, we have to check whether it is less expensive to make a replica in each child of v by calculating the sum of costs of all its children, $Cost_{child}(v) = \sum_{j \in \text{child}(v)} Cost(j, 0)$ and comparing this with rep_cost . If $Cost_{child}(v)$ is less than rep_cost the replicas are placed in v 's children and the replica location is set to "children". Otherwise, the replica is created locally at v . Thus, for optimal replication cost and replica server locations, the dynamic programming equations are:

$$Cost(v, 0) = \begin{cases} Cost_{child}(v), & \text{if } Cost_{child} < rep_cost \\ rep_cost, & \text{otherwise} \end{cases} \quad (8)$$

$$RSL(v, rd) = \begin{cases} v, & \text{if } Cost_{child} < rep_cost \\ children, & \text{otherwise} \end{cases} \quad (9)$$

To find $Cost(v, rd)$ when $rd > 0$, we determine the sum of replication costs of all the v 's children considering replica at a location of $rd+1$ ($child_{cost} = \sum_{j \in child(v)} Cost(j, rd + 1)$). If $Cost(v, 0)$ is less than this sum, $Cost(v, rd)$ is assigned to $Cost(v, 0)$ and the location of replica is assigned to the site obtained from $RSL(v, 0)$. On the contrary, the replica is created somewhere on the path towards the root and the location is rd -th ancestor of v .

$$Cost(v, rd) = \begin{cases} Cost(v, 0), & \text{if } Cost(v, 0) < child_cost \\ child_cost, & \text{otherwise} \end{cases} \quad (10)$$

$$RSL(v, rd) = \begin{cases} RSL(v, 0), & \text{if } Cost(v, 0) < child_cost \\ \text{node at distance of } rd, & \text{otherwise} \end{cases} \quad (11)$$

Lemma 2. RPCC optimally places replicas in the sub-tree $T_v = T-r$ where r is the origin server or root and v is a non-leaf data center node of the targeted cloud tree T .

Proof. As stated earlier, when the children of a data center node complete the calculation of replication costs, the node itself starts to calculate the cost functions. In Lemma 1, we verified that replicas are allocated optimally in a leaf node for all replica distance values. Thus, we can infer that the non-leaf data center nodes one hop up from the bottom of T contain children (leaf nodes) whose calculated replication costs are optimal. Now, it remains to show that RPCC places replicas optimally in the sub-tree with a root being any internal data center, v , considering each possible value of d . First, when the value of d equals to 0, we observe by considering Equations (7) and (8) that the replication cost associated with sub-tree rooted at v is the least of the following two scenarios:

1) v itself contains a replica. The cost becomes the aggregate of the costs of the sub-trees having root as v 's children and the value of d equals to 1 and moreover storage and consistency maintenance cost at v .

2) v does not contain a replica. The replication cost can be obtained by aggregating the costs incurred from the sub-trees having v 's children as roots with $d = 0$.

Second, when $d \geq 1$ (i.e., replica server is up on the way to the root) we need to compare the replication cost obtained above for $d = 0$ (i.e., replica is in v itself) with the replication cost calculated for each value of d having $d \geq 1$ to decide on the optimal replication cost and locations of replicas. Now, if the cost for $d = 0$ is below the cost for $d \geq 1$ (i.e., communication cost of the sub-trees rooted at the children of v having a replica server up on the way to the root), placing a replica in v itself will be cheaper. Otherwise, it will be

preferable to create a replica at any upper node on the path to the root based on the value of d , which is optimal. The minimum cost thus calculated is optimal for any node v .

Theorem 1. RPCC optimally allocates replicas for the targeted cloud Tree, T for a given traffic pattern.

Proof. We provide the proof for our generalized replication problem with the targeted cloud tree topology. The proof is carried out based on induction where Lemma 1 is the induction base and Lemma 2 is the induction step.

B. Placing Replicas

Placement of replicas starts at the root of the targeted cloud tree and stops at the lowest-tier users. In this process, every data center finds whether or not a new replica will be created locally based on the calculated cost and location vector. Once the bottom-up calculation is done, the root or the origin server holds the optimum cost for data replication. $Cost(root, 0)$ of the whole cloud and the replica location $RSL(root, 0)$. The value of $RSL(root, 0)$ can be either r (the origin server itself) or "children" (the origin server's children nodes) which indicate that the replica is zero or one hop away (towards the users) from the origin server. So, the origin server sends a message $rd = 0$ or $rd = -1$. A data center node, v , which receives the message being one hop away increases the value of rd by one and investigates the value of $RSL(v, rd)$. If v becomes $RSL(v, rd)$'s value, a replica is created in v itself and the message $rd = 0$ is passed the children of v . If $RSL(v, rd)$ value is -1 it assigns $rd = -1$ and forwards it to the children. Finally, if the $RSL(v, rd)$ value is a data center node rd away up in the tree it sends rd message to its children without changing the value. When all the users at the leaves receive the message rd the replica placement process terminates.

C. Complexity Analysis

Analysis of the computational and message complexity of our algorithm is completed by performing the computation of cost and location vectors and the placement of replicas in the entire cloud. For every data center node v , we compute its $Cost(v, rd)$ for its sub-tree for each value of rd between 0 and distance to the origin server or root by merging the results of all its children. The computation of data center v is done by adding $|child(v)|$ rudiments of count $(x + 1)$, where x represents the distance between v and the origin data center and $|child(v)|$ represents the children count for data center v . Hence, the number of computations for data center v appears as $(x + 1) \cdot |child(v)|$. The total number of computations for all the data centers in the cloud is:

$$\sum_{v \in V} (x_v + 1) \cdot |child(v)|$$

where x_v represents the distance between v and the origin server.

Given, the number of data centers, $|V| = N$, we can observe that $x_v \leq N - 1$ for each value of v . Hence, the following can be deduced:

$$\sum_{v \in V} (x_v + 1) \cdot |child(v)| \leq N \cdot \sum_{v \in V} |child(v)| = N(N-1)$$

This equality holds since there are $N - 1$ children nodes in the cloud. This is because except the origin server, each datacenter node has a parent. Consequently, $O(N^2)$ is the overall computing cost of $Cost$ vectors for all the nodes. As for the message, the first is the cost vector that is sent by each node to its parents. The other message is rd sent by each node to its children. If $|V| = N$ is the total number of data center nodes and each node sends two messages, the message complexity is $O(N)$.

V. SIMULATION SETUP

For the performance evaluation of our proposed replication algorithm we have leveraged the use of a Java based simulator program. Our hierarchical cloud structure consists of four tiers having each tier with data centers. Each data center has five children and thus the total number of data centers becomes 155 including the users in the lowest tier. Requests for data come from the users only. Uniform distribution is used to model the available link bandwidth with the range [0.622, 2.5] (Gbps). According to the same distribution, data center storage capacities are also modeled. The simulation experiments use 2500 data files where the size of each data file is 10 GB. Hence, the total data size becomes nearly twenty-five tera byte (TB). To measure the efficacy of our system, we utilized five diverse storage settings of data centers which are created in accordance to the relative storage capacity of data centers. The relative storage capacity (RSC) is determined by a percentage of total storage size of all data centers compared to the overall data size in the system. For our experiments, we use RSCs ranging from 13% to 75%. The use of relative storage capacity is justified by the fact that it affects the decision to create replicas on data centers in contrast to their absolute storage capacities. Different storage settings as discussed above are shown in Fig. 3.

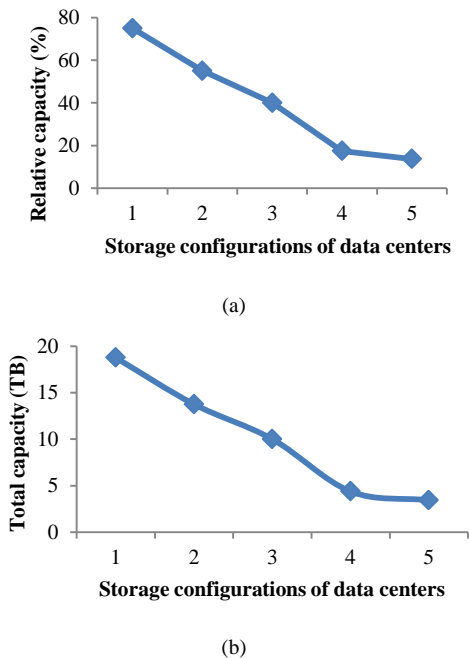


Fig. 3. Storage Configurations of Data Centers based on Relative (a) and Total (b) Capacity.

Upon requests for data from the users, each data center replica server tries to meet the request. However, the number of access requests served by each replica server is limited by its workload constraint. In our experiments, six different workload configurations according uniform distribution are used as shown in Fig. 4. Simulation experiments are done by submitting 50 different jobs each one having a fixed probability of being submitted.

The simulation experiment allows each job to access a sequence of data files. User requests for data files come according to Poisson distribution and each request is issued in an interval of 2500 milliseconds. Moreover, selected access patterns determine the sequence of files that will be accessed. In our experiment, two data access patterns namely Gaussian and Zipf distributions are used. The Zipf distribution is expressed as $P_i = K$, where P_i denotes the count for i th ranked file, K represents the most popular data file (by means of frequently accessed items) and s specifies the distribution shape. Also, the temporal locality present in the data access pattern is measured by this parameter s having values ranging from 0.65 to 1.24. The level of locality in the data is indicated by the value of s . We have experimented with a value of 0.85 for s and call it as Zipf-0.85 distribution. Besides, Gaussian distribution also known as normal distribution is used in our experiment. It is an important distribution in statistics and is frequently used in natural and social sciences to characterize real-valued random variables. Previously, other replication techniques [36], [37] in the literature have used similar data access patterns for their evaluation in data grids.

Our replication strategy was evaluated using the performance metrics which include job execution time, mean bandwidth use, storage utilization, number of replicas created, and rate of satisfaction for users. Job execution time refers to the overall time needed to execute the whole set of jobs and also takes into account the data access time. replica maintenance algorithm. The bandwidth usage for a data transfer is the data size times the aggregate costs of the data transfer route. The average cost for bandwidth usage is calculated by dividing the overall bandwidth usage by total data access counts. Storage consumption is the proportion of the data center storage occupied by the replicas in the system. Finally, user satisfaction rate represents number of users whose QoS constraints are met compared to the total number of users who requested for data access with some QoS constraints. The target is to reduce total job execution time and minimize average bandwidth and storage consumption while maximizing the user satisfaction rate.

Config.	Workload capacity constraint (GB)
1	[250-350]
2	[200-300]
3	[150-250]
4	[100-200]
5	[80-300]
6	[50-150]

Fig. 4. Workload Configuration of Data Centers.

VI. PERFORMANCE RESULTS

In this section, we discuss the experimental results of our proposed replication technique (RPCC) and compare it with Greedy Add and Greedy Remove [37] protocols from the literature. The QoS requirement of a user issuing a data access request is specified by a range in terms of distance from the user to the closest replica data center. This range is formulated using a uniform distribution. For instance, if a user specifies its QoS requirement of [1-2] it means that the replica data center containing the requested data is expected to be one or two hops away from the user.

A. Job Execution Time

Fig. 5 shows the job execution times based on different data center workload configurations for RPCC, Greedy Add, and Greedy Remove algorithms. In the experiment, the relative storage capacity is set to 75%, user QoS requirements of [1-3] and [0-1] are specified from a uniform distribution to permit both relaxed and relatively more constrained distance ranges respectively. For both the data access patterns (Zipf-0.85 and Gaussian), the total job execution times required by RPCC is shown to be lower than the other two algorithms. This is attributed to the fact that RPCC creates a moderate number of replicas in appropriate locations in the cloud hierarchy in contrast to Greedy Add and Greedy Remove techniques which in turn reduces access times for the data requests. Accordingly, this cuts down the overall job execution time. Fig. 6 shows the number of replicas created by all three algorithms during a sampling simulation period for the same workload and storage resource configurations. With the decrease in workload capacity of replica servers, an increased number of replicas are created (Fig. 6) and consequently job execution times drop in most cases but by varying amounts as shown in Fig. 6. Greedy Add mostly exhibits lower execution time than Greedy Remove. For relatively more constrained QoS requirement ([0-1]) and Gaussian access pattern, Greedy Remove unexpectedly shows lower job execution time compared to the other two algorithms.

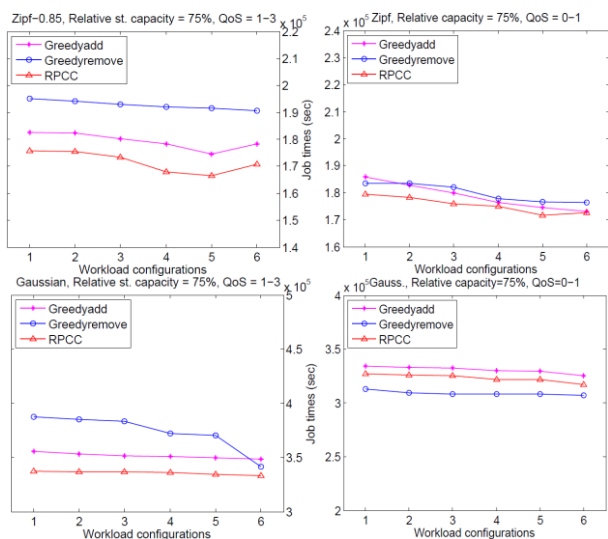


Fig. 5. Comparison of Job Times with 75% Relative Storage Capacity of Data Centers.

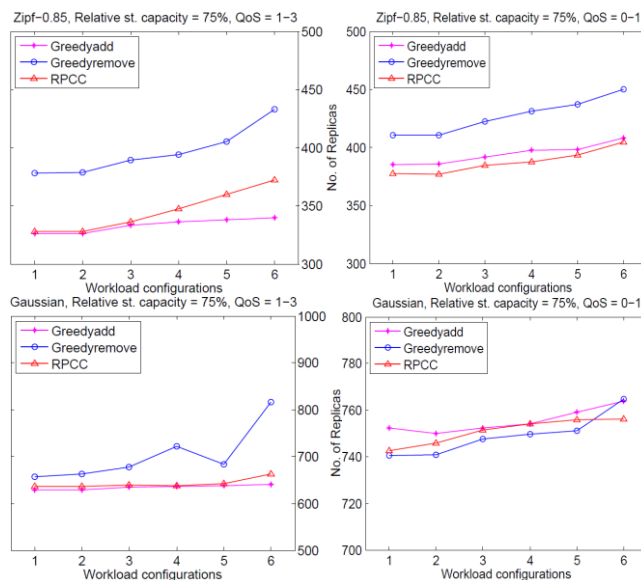


Fig. 6. Comparison of No. of Replicas for Varying user QoS Requirements.

Generally, the performance gain of RPCC over Greedy Add and Greedy Remove turns out to be more evident when user QoS constraints of broader ranges are used.

The job execution times using relative storage capacity of 17.5% are shown in Fig. 7 for the same data access patterns as before. Generally, RPCC exhibits shorter job times compared to Greedy Add and Greedy Remove. However, the use of more constrained storage size results in only a meager benefit for RPCC in terms of job times in most cases. Furthermore, job times for all three algorithms in this case got an increase by varying amount compared to the case when relative storage capacity of 75% is used.

Fig. 8 shows satisfaction rates of users for all methods using relative storage capacity of both 17.5% and 75%. Mostly, RPCC outperforms the other two algorithms. Particularly, the performance gain of RPCC over Greedy Add and Greedy Remove is more when the storage capacity of replica data centers (17.5% relative capacity) is restricted. Nevertheless, satisfaction rates of users decrease in case of constrained storage space of replica data centers regardless of quality requirements from users and the patterns used for data access as shown in Fig. 8.

B. Average Bandwidth Use

Both network providers and end-users deem bandwidth consumption as a key issue since undue bandwidth use can cause slowdowns due to network congestion. We include two different types of costs namely replication (create and update) cost and read cost to measure average bandwidth use.

Fig. 9 displays the average bandwidth cost in terms of varying workload for RPCC, Greedy Add, and Greedy Remove algorithms. As before, the relative storage capacity is set to 75% and 17.5%, user QoS constraints on replica server distances of [1-3] and [0-1] are specified from a uniform distribution to allow both relaxed and relatively more constrained ranges respectively. RPCC mostly shows moderate bandwidth consumption rate compared to Greedy

Add and Greedy Remove algorithms. The reason is that both data access (read) cost and replication cost are reduced on account of the placement of a modest number of well-placed replicas down the cloud hierarchy. On the other hand, Greedy Remove mostly exhibits the lowest bandwidth cost among the three algorithms. The reason is that more replicas are created in the upper part of the cloud hierarchy. The replication cost involved in this case is comparatively lower than the elevated data access (communication) cost. With the decrease in workload capacity of data center servers, a higher number of replicas are created and consequently the bandwidth cost increases for all three algorithms. For more constrained relative storage capacity (17.5%) of data centers, RPCC exhibits moderate bandwidth consumption compared to Greedy Add and Greedy Remove as before. Greedy Remove performs better than the other algorithms due to reduced replication cost with Gaussian access pattern irrespective of the user QoS ranges.

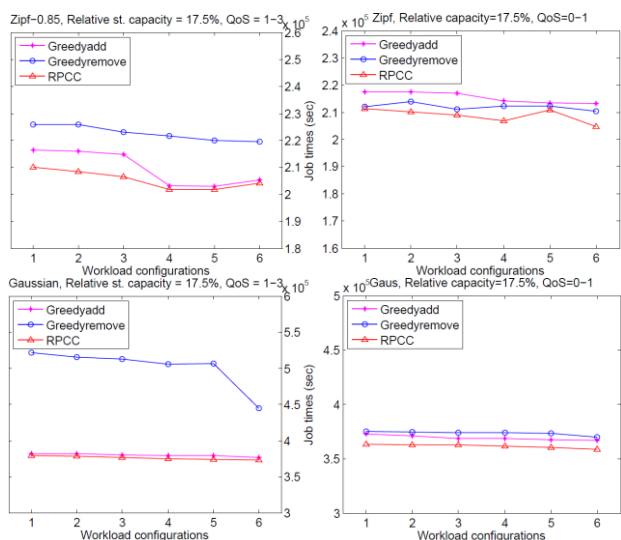


Fig. 7. Job Times with Relatively More Constrained Data Center Storage Capacity (17.5%).

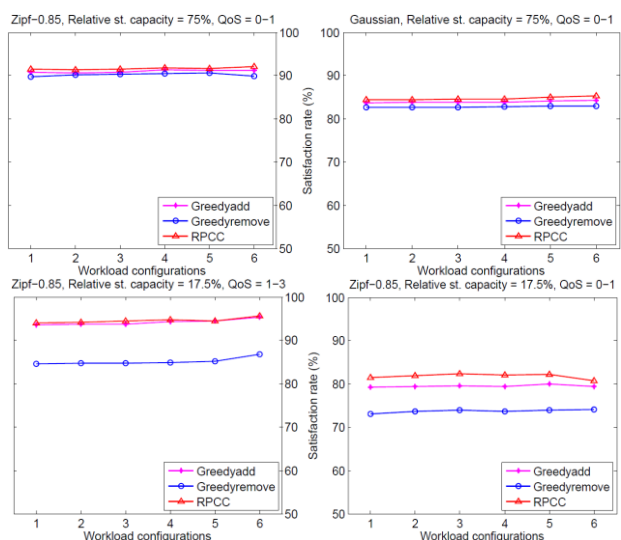


Fig. 8. Comparison of Satisfaction Rates for Varying Relative Storage Capacity of Data Centers.

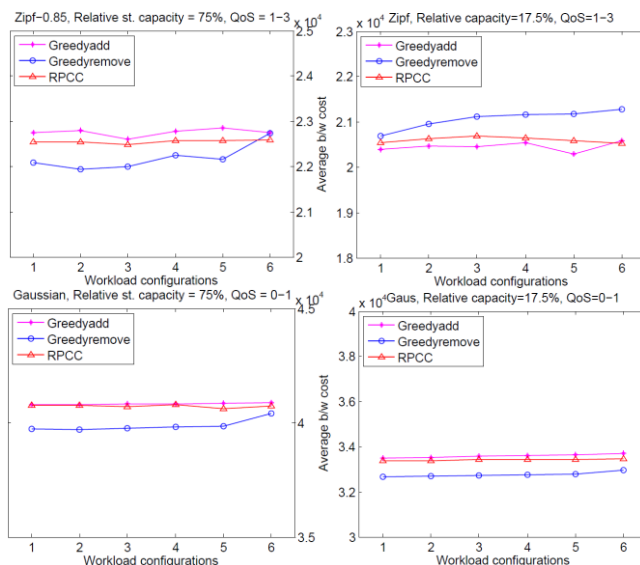


Fig. 9. Comparison of Average b/w Cost with Relative st. Capacity of 75% and 17.5%.

C. Storage Use

The storage resources used in the system is vital to grid providers. Since storages are relatively cheaper, we can come to a trade-off in case improvements in job execution times and network bandwidth consumption are achieved.

Fig. 10 shows the storage usage (y-axis) as a function of varying workload (x-axis) for all algorithms with a relative storage capacity of 75% and 17.5%. RPCC shows moderate storage usage compared to Greedy Add and Greedy Remove algorithms in all cases. When data centers' capacities in terms of workload decreases, the number of replicas created increases in most cases but by varying amounts.

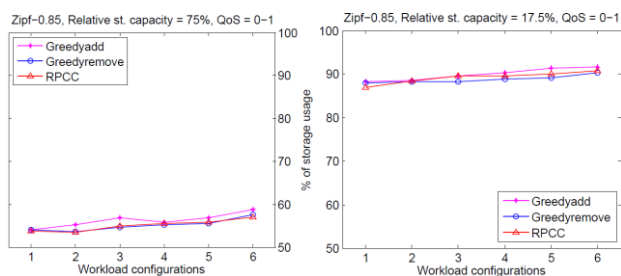


Fig. 10. Comparison of Storage Cost with More Constrained user QoS Range [0-1].

VII. CONCLUSIONS AND FUTURE WORK

In this paper, we studied the data replication problem in data cloud considering the QoS requirements from users to support big data applications. Aiming to put forward a multi-objective solution to the replication problem, user QoS constraints in terms of distance to replica data center servers and workload constraints of replica servers are considered. First, we formulate the replica placement problem as a dynamic programming problem. Second, we propose a novel distributed replica placement algorithm (RPCC) for a multi-tier cloud platform so as to avoid the limitations usually found

in centralized algorithms such as scalability, reliability, and performance bottlenecks. Performance analysis of the proposed algorithm was done in terms of job execution time, mean bandwidth usage, storage resource utilization, total number of replicas that are created during a simulation period, and satisfaction rates of users. The simulation results showed that RPCC can considerably reduce job execution times which include data access time while incurring modest bandwidth and storage costs compared to two other algorithms. These results are obtained by utilizing a variety of storage and workload setting of data center servers and data access patterns with a degree of temporal locality and randomness.

In the future, we envision to implement our proposed data replication technique in a physical cloud infrastructure. Besides, we plan to extend our replication technique to deal with the bandwidth constraints imposed on the network links.

REFERENCES

- [1] M. Armbrust, A. Fox, R. Griffith, A.D. Joseph, R.H. Katz, A. Konwinski, G. Lee, D.A. Patterson, A. Rabkin, I. Stoica, and M. Zaharia, "Above the Clouds: A Berkeley View of Cloud Computing," Technical Report UCB/EECS-2009-28, Dept. of EECS, California Univ., Berkeley, Feb. 2009.
- [2] J. M.D. Dikaiakos, D. Katsaros, P. Mehra, G. Pallis, and A. Vakali, "Cloud Computing: Distributed Internet Computing for IT and Scientific Research," IEEE Internet Computing, vol. 13, no. 5, pp. 10-13, Sept. 2009.
- [3] I.S. R. Buyya, C.S. Yeo, S. Venugopal, J. Broberg, and I. Brandic, "Cloud Computing and Emerging IT Platforms: Vision, Hype, and Reality for Delivering Computing as the fifth Utility," Future Generation Computer Systems, vol. 25, no. 6, pp. 599-616, June 2009.
- [4] Amazon. Amazon simple storage service (Amazon S3). Available: <http://aws.amazon.com/s3>
- [5] Ghemawat, S., H. Gobioff, and S.-T. Leung, The Google file system. SIGOPS Oper. Syst. Rev., 2003. 37(5): p. 29-43.
- [6] Hadoop at Twitter, <http://www.slideshare.net/kevinweil/hadoop-at-twitter-hadoop-summit-201>.
- [7] Bessani, A., Correia, M., Quaresma, B., Andr'e, F. and Sousa, P., DepSky: Dependable and Secure Storage in a Cloud-of-clouds, In Proc. of the 6th Conference on Computer Systems, pp. 31-46, 2011.
- [8] F. Wang, J. Qiu, J. Yang, B. Dong, X. Li, and Y. Li, "Hadoop High Availability through Metadata Replication," Proc. First Int'l Workshop Cloud Data Manage, pp. 37-44, 2009.
- [9] K. Shvachko, H. Kuang, S. Radia, and R. Chansler, "The Hadoop Distributed File System," Proc. IEEE 26th Symp. Mass Storage Systems and Technologies (MSST), pp. 1-10, June 2010.
- [10] A. Gao and L. Diao, "Lazy Update Propagation for Data Replication in Cloud Computing," Proc. Fifth Int'l Conf. Pervasive Computing and Applications (ICPCA), pp. 250-254, Dec. 2010.
- [11] W. Li, Y. Yang, J. Chen, and D. Yuan, "A Cost-Effective Mechanism for Cloud Data Reliability Management Based on Proactive Replica Checking," Proc. IEEE/ACM 12th Int'l Symp. Cluster, Cloud and Grid Computing (CCGrid), pp. 564-571, May 2012.
- [12] C.Q. Huang, Y. Li, H.Y. Wu, Y. Tang, X. Luo, Modeling and maintaining the reliability of data replica service in cloud storage system, Journal of Communication. 36 (3), 2014.
- [13] H. Shen, G.P. Liu, H. Chandler, Swarm intelligence based file replication and consistency maintenance in structured P2P file sharing systems, IEEE Trans.Computing, 64 (10), pp. 2953-2967, 2015.
- [14] G. Liu, H. Shen, H. Chandler, Selective data replication for online social networks with distributed datacenters, IEEE Trans. Parallel Distrib. Syst. 27 (8), pp. 2377-2393. 2016.
- [15] S. Fu, L. He, X. Liao and C. Huang, Developing the Cloud-integrated data replication framework indecentralized online social networks, Journal of Computer and System Sciences 82 (2016) 113-129, 2015.
- [16] S. Sun, W. Yao and X. Li, DARS: A dynamic adaptive replica strategy under high load Cloud-P2P, Future Generation Computer Systems, 78 (2018) 31-40, Aug 2017.
- [17] Sun D.W, Chang G.R. and Gao S., "Modeling a dynamic data replication strategy to increase system availability in cloud computing environments," Journal of Computer Science and Technology, vol. 27, no.2, pp. 256-272 Mar. 2012.
- [18] D.-W. Sun, G.-R. Chang, C. Miao, L.-Z. Jin, X.-W. Wang, Analyzing modeling and evaluating dynamic adaptive fault tolerance strategies n cloud computing environments, J. of Supercomputing, 66 (2013), 193-228, 2013.
- [19] Wei, Q., Veeravalli B., Bozhao G., Lingfang Z. and Dan F., CDRM: A cost-effective dynamic replication management scheme for cloud storage cluster., in 2010 IEEE International on Cluster Computing. 2010. p. 188 - 196
- [20] Y. Qu, N. Xiong, RFH: A resilient, fault-tolerant and high-efficient replication algorithm for distributed storage, in: 41st Int. Conf. Parallel Process., 2012, pp. 520-529.
- [21] N. Gill and S. Singh. A dynamic, cost-aware, optimized data replication strategy for heterogeneous cloud data centers. Future Generation Computer Systems, 65 (2016) 10-32, 2016.
- [22] D. Boru, D. Kliazovich, F. Granelli, P. Bouvry, and A. Y. Zomaya, Energy-Efficient Data Replication in Cloud Computing Datacenters, In Globecom 2013 Workshop- Cloud computing systems, networks, and applications, pp. 445-450, 2013.
- [23] Long Sai-Qin, Zhao Yue-Long, Chen Wei. MORM: A Multi-objective Optimized replication Management strategy for cloud storage cluster. Journal of Systems Architecture, 60 (2):234-44, 2014.
- [24] N. Mansouri, M. K. Rafsanjani, M.M. Javidi, DPRS: A dynamic popularity aware replication strategy with parallel download scheme in cloud environments, Simulation Modelling Practice and Theory 77 (2017) 177-196, 2017.
- [25] H. Sun, B. Xiao, X. Wang and X. Liu, Adaptive trade-off between consistency and performance in data replication, Softw. Pract. Exper. 47:891-906, 2017
- [26] L. Chen and D. B. Hoang, Adaptive data replicas management based on active data-centric framework in cloud environment, In Proceedings of IEEE International Conference on High Performance Computing and Communications, pp. 101-108, 2013.
- [27] Z. Ye, S. Li and J. Zhou, A Two-layer Geo-cloud based Dynamic Replica Creation Strategy, Applied Mathematics & Information Sciences, Vol. 8, No. 1, pp. 431-440, 2014.
- [28] J. Janpet and Y. Wen, Reliable and Available Data Replication Planning for Cloud Storage, In Proc. of the IEEE 27th International Conference on Advanced Information Networking and Applications, pp. 772-779, 2013.
- [29] S. Kirubakaran, S. Valarmathy and C. Kamalanathan, Data Replication Using Modified D2RS in Cloud Computing for Performance Improvement, Journal of Theoretical and Applied Information Technology, Vol. 58, No.2, pp. 460-470, 2013.
- [30] Li, L.L. , Wang, Q.C., Han, Y.J., Ma, X.H., Jiao, Y., A dynamic replication algorithm based on access popularity in cloud storage environment, In Proc. of International Conference on Materials Science and Computational Engineering, 2014.
- [31] N. Mansouri, Adaptive data replication strategy in cloud computing for performance improvement, Front. Comput. Sci., 10(5): 925-935, 2016.
- [32] J. Lin, C. Chen and J. M. Chang, QoS-Aware Data Replication for Data-Intensive Applications in Cloud Computing Systems, IEEE Transactions On Cloud Computing, Vol. 1, No. 1, pp. 101-115, 2013.
- [33] S. Varma and G. Khatri, QoS-Aware Data Replication in Hadoop Distributed File System, Int. J. Advanced Networking and Applications 7(3), pp. 2741-2751, 2015.
- [34] Kumar, P.J. and Ilango, P. MQRC: QoS aware multimedia data replication in cloud. International Journal of Biomedical Engineering and Technology, Vol 25, 2017.
- [35] M. Shorfuzzaman, "On the Dynamic Maintenance of Data Replicas based on Access Patterns in A Multi-Cloud Environment", International

- Journal of Advanced Computer Science & Applications (IJACSA), Vol.8. No. 3, pp. 207-215, 2017.
- [36] A.M. Soosai, A. Abdullah, M. Othman, R. Latip, M.N. Sulaiman, and H. Ibrahim, "Dynamic Replica Replacement Strategy in Data Grid," Proc. Eighth Int'l Conf. Computing Technology and Information Management (ICCM), pp. 578-584, Apr. 2012.
- [37] C. Cheng, J. Wu, and P. Liu, "Qos-aware, access-efficient, and storageefficient replica placement in grid environments," Journal of Supercomputing, vol. 49, no. 1, pp. 42-63, 2009.
- [38] V. Andronikou, K. Mamouras, K. Tserpes, D. Kyriazis, T. Varvarigou, Dynamic QoS-aware data replication in grid environments based on data "importance", Future Gener. Comput. Syst. 28 (2012) 544-553, 2012.

A Categorical Model of Process Co-Simulation

Daniel-Cristian Crăciunean¹, Dimitris Karagiannis²

Computer Science and Electrical Engineering Department, Lucian Blaga University of Sibiu, Sibiu, Romania¹
Faculty of Computer Science, University of Vienna, Vienna, Austria²

Abstract—A set of dynamic systems in which some entities undergo transformations, or receive certain services in successive phases, can be modeled by processes. The specification of a process consists of a description of the properties of this process as a mathematical object in a suitable modeling language. The language chosen for specifying a process should facilitate the writing of this specification in a very clear and simple form. This raises the need for the use of various types of formalisms that are faithful to the component subsystems of such a system and which are capable of mimicking their varied dynamics. Often in practice, the development of domain specific languages is used to provide building blocks adapted to the processes. Thus, the concept of multi-paradigm modeling arises which involves the combination of different types of models, the decomposition and composition of heterogeneous specified models as well as their simulation. Multi-paradigm modeling presents a variety of challenges such as coupling and transforming the models described in various formalisms, the relationship between models at different levels of abstraction, and the creation of metamodels to facilitate the rapid development of varied formalisms for model specification. The simulation can be seen as a set of state variables that evolve over time. Co-simulation is a synthesis of all simulations of the components of the system, coordinated and synchronized based on interactions between them. The theory of categories provides a framework for organizing and structuring formal systems in which heterogeneous information can be transferred, thus allowing for the building of rigorous cohesion bridges between heterogeneous components. This paper proposes a new model of co-simulation of processes based on the category theory.

Keywords—Process modeling; metamodel; modeling grammars; categorical grammars; category theory; categorical sketch; co-simulation, simulation

I. INTRODUCTION

Contemporary systems are, in most cases, integrated from subsystems with complex structures and behaviors from the real or virtual world with various behaviors. Given the diversity of the components and the resulting complexity of the systems, simulation plays an essential role in all phases of system development and optimization. Simulation models at the system level can be developed to help analyze requirements, evaluate potential architectural solutions, and develop detailed design, implementation, and simulation specifications. These models aim at meeting specific objectives of each phase [2,12,14].

The concept of process is one of the possible methods of mathematical modeling of dynamic systems behavior. A process is a mathematical model that represents the behavior of a dynamic system that performs actions. Many systems, especially technological systems, can be modeled as Discrete

Event System (DES) driven by discrete events evolving in relation to the occurrence of asynchronous events over time. These systems in which certain entities undergo transformations or receive certain services in successive phases can be modeled by processes.

The purpose of building a process that represents the behavior of a dynamic system is to facilitate the verification of system properties, simulation and system optimization. Therefore choosing the level of detail of the system's actions depends on the analyzed properties. Because a process does not take into account all the details, a behavior of an analyzed system can be represented by several processes that reflect either different degrees of detail of actions performed by a system or different points of view in relation to the intended purpose [12, 14].

Specifying a process consists of a description of the properties of this process in the form of a mathematical object. For this we need a proper modeling language. Therefore, the language chosen for specifying a process should facilitate the writing of this specification in a very clear and simple form. Thus, the need for the use of various types of formalisms that are faithful to the component subsystems of such a system and which are capable of mimicking their varied dynamics. Often in practice, the development of domain-specific languages, which provide building blocks adapted to DES models, is used in practice [4].

This heterogeneity of the systems inevitably implies the use of heterogeneous processes that provide through specific facilities a greater capacity to describe behaviors and interactions between subsystems than homogeneous processes. Thus, the concept of multi-paradigm modeling arises which involves the combination of different types of models, the decomposition and composition of heterogeneous specified models as well as their simulation.

Multi-paradigm modeling presents a variety of challenges such as coupling and transforming the models described in various formalisms, the relationship between models at different levels of abstraction, and the creation of metamodels to facilitate the rapid development of varied formalisms for model specification.

The simulation can be seen as a set of state variables that evolve over time. The variation space of the states of a simulation can be defined by two axes, a time axis, and a space axis. The objective of the simulation thus becomes, the calculation, ordered in time, of the state variable values. Co-simulation is a synthesis of all simulations of the components of the system, coordinated and synchronized based on interactions between them.

The theory of categories provides a framework for organizing and structuring formal systems in which heterogeneous information can be transferred, thus allowing for the building of rigorous cohesion bridges between heterogeneous components [8,15].

Multi-paradigm modeling involves, among other things, the transformation of structures from a given form into a form required to achieve this cohesion, which is often complicated. The category theory is based on the manipulation of structures consisting of objects and formal functions that coexist and work together as well as the preservation of these structures and their properties when they are transformed from one form into another through functors.

This paper proposes a new co-simulation model based on the category theory. In section 3 we present the construction of the simulation category, in section 4 we present the co-simulation model based on the categorical sketch and in section 4 we will see how the co-simulation category is built.

II. THEORETICAL FOUNDATIONS AND NOTES

A category \mathcal{C} is an algebra of formal functions in which the operation is the partial formal composition of functions [9,10]. The domains and codomains of functions form the set of objects of the category which we denote with $\text{ob}(\mathcal{C})$ and the formal functions are the arcs of the category. We will denote these objects in uppercase A, B, .. X, Y, Z, ... The set of arcs between two objects $f:X \rightarrow Y$ will be denoted with \mathcal{C} or $\text{Hom}(X,Y)$.

So, a category is a construct structured from two types of atomic elements, formal functions that we call arrows and objects that are the domains and codomains of formal functions. This structure, completed with the composition operation of arrows, forms an edifice with a remarkable expressivity called the category. Because the functions are formal and the objects of the category could be formal, which implies great flexibility that is essential for modeling.

A functor is an application between two categories: $\phi:\mathcal{C} \rightarrow \mathcal{D}$ which maps objects to objects, arrows to arrows, and preserves the structure, i.e. transfers certain properties from one category to another [9,10].

One very important thing for modeling is that a functor can also be viewed as the image of a category in another category, that is, it can be viewed as a substructure consisting of objects and arrows taken together as one entity in a larger structure. These substructures are models of a category in another category. The set of categories together with the functors between them and the composition operation of functors form a category that is called the functors category and is written with Cat .

Between two functors $\phi:\mathcal{C} \rightarrow \mathcal{D}$ and $\psi:\mathcal{C} \rightarrow \mathcal{D}$, which have common domains and codomains, we define applications that take the image of ϕ into the image of ψ , respecting some naturality conditions in relation to the arrows in the two categories, which are called natural transformations [9,10].

The structure formed from the set of functors that have common domains and codomains, as objects, along with the set

of natural transformations, as arrows, complemented by the composition of natural transformations is a category called the category of functors and natural transformations.

The essential difference between a graph and a category is the composition operation that exists in categories and does not exist in graphs [9,10]. But any graph \mathcal{G} can be extended to a category called the free category generated by \mathcal{G} which has as objects the nodes from \mathcal{G} , as arrows the arcs from \mathcal{G} plus the identity arrows added to each object, and the composition operation is the concatenation of the paths from \mathcal{G} . In this way, any graph homomorphism naturally extends to a unique functor between the free categories generated by the two graphs. Note that not every functor between two free categories can be restricted to a graph homomorphism. With this remark, we will use the notion of functor even when the domain and/or codomain are graphs.

The image of a graph \mathcal{P} in another graph \mathcal{G} through a functor $D:\rightarrow \mathcal{G}$ is called the diagram of \mathcal{P} in \mathcal{G} , and \mathcal{P} is called the graph shape of the diagram D . Similarly, the diagram can also be defined if \mathcal{G} is a category [9,10].

If we have a diagram $D:\rightarrow \mathcal{C}$ where \mathcal{G} is a graph and \mathcal{C} a category then a natural transformation from a constant diagram $\Delta_{\mathcal{C}}:\mathcal{G} \rightarrow \mathcal{C}$ to D is a commutative cone with the vertex C and the base D [3,4, 9,10].

Among the cones we can define morphisms compatible with the natural transformations from the cone definition and so the set of cones together with these morphisms form the cone category generated by diagram D . The limit of a diagram D in a category \mathcal{C} is a terminal element in the cone category generated by diagram D .

There are a series of particular limits, useful in modeling, such as the categorical product which is the limit of a discrete diagram or the limit of a cospan which is a pullback. The pullback for example is useful to characterize monomorphisms.

If we have a diagram $D:\rightarrow \mathcal{C}$ where \mathcal{G} is a graph and \mathcal{C} a category then a natural transformation from diagram D to a constant diagram $\Delta_{\mathcal{C}}:\mathcal{G} \rightarrow \mathcal{C}$ is a commutative cocone with the vertex C and the base D [3,4, 9,10].

Between cocones we can define morphisms compatible with the natural transformations from the definition of the cocones and so the set of cocones together with these morphisms form the category of cocones generated by the diagram D . The colimit of diagram D in a category \mathcal{C} is an initial element in the cocone category generated by diagram D .

There are a series of particular colimits, useful in modeling, such as the disjoint union which is the colimit of a discrete diagram or the colimit of a span which is a pushout. The pushout for example is useful to characterize epimorphisms.

The notion of model exists also in logic. Its definition is based on the mathematical logic language. In the category theory a model can be specified by sketches. The major advantage of the sketches in modeling is that they can be defined by graphical notation for specifying visual modeling grammars.

Thus a sketch $\mathcal{S}=(\mathcal{G}, \mathcal{D}, \mathcal{L}, \mathcal{K})$ consists of a graph \mathcal{G} and three collections of diagrams, namely \mathcal{D} which is a collection of commutative diagrams, \mathcal{L} which is a collection of cones and \mathcal{K} which is a collection of cocones [3,4,9,10].

The arrows of the graph \mathcal{G} are sketch operators that can be implemented at the meta-metamodel level, possibly with small adjustments at the metamodel level. The three collections \mathcal{D} , \mathcal{L} and \mathcal{K} can be fully implemented at the meta-metamodel level, thus ensuring the syntactic correctness of any metamodel specified by a sketch.

A model of a sketch $\mathcal{S}=(\mathcal{G}, \mathcal{D}, \mathcal{L}, \mathcal{K})$ is the image of the graph \mathcal{G} through a functor M in the Set category that complies with all the conditions imposed by the collections \mathcal{D} , \mathcal{L} and \mathcal{K} , i.e. it selects for each diagram in \mathcal{D} a commutative diagram in Set, for each cone from \mathcal{L} its limit and for each cocone from \mathcal{K} its colimit [3,4,9,10].

III. THE SIMULATION CATEGORY

The simulation consists in reproducing the dynamic behavior of a system in order to obtain conclusions about the behavior of the system. Simulation is very important for analyzing the behavior of complex systems. Simulation of a process in a certain formalism (such as PN, EPC, UML, BPMN) calculates the trace of the process execution in time represented by states, inputs and outputs. The simulation conclusions can be useful for determining the proper structure of the model, identifying the optimum values of the parameters, imitating system behavior, etc. [12,13,14]. In many cases, the model has predictive validity, i.e. it is able to predict the behavior of the system in the future [1,2].

Simulation of a system (behavior trace) can be described as a language on the set of states (inputs and outputs) in which each word represents a trajectory followed by states (inputs and outputs) of the system. Co-simulation composes the trajectories described by a set of components that interact. Interaction of components is made through incoming and outgoing ports that must be specified in the sketch that generates the model [2,11]. These will be associated to the nodes corresponding to the input and output constructs of the sketch.

Thus in [4], the sketch of the Medical Laser Manufacturing Systems (MLMS) metamodel specifies a model as a graph $\mathcal{G}=(X,\Gamma,\sigma,\theta)$ with imposed restrictions. The imposed restrictions lead to the sketch MLMS [4], $L^1(\text{MLMS})=(\mathcal{G},\mathcal{D},\mathcal{L},\mathcal{K})$ where: \mathcal{G} is the graph from Fig. 1, \mathcal{D} is the set of commutative diagrams $\mathcal{D}=\{D_1\}$, \mathcal{L} is the set of cones $\mathcal{L}=\{L_1,L_2,L_3,L_4\}$ and \mathcal{K} is the set of cocones $\mathcal{K}=\{K_1,K_2,K_3\}$.

The graph of the sketch contains the nodes corresponding to the atomic concepts of the modeling language such as: set of input buffers for the primary components (x_i), set of output buffers for finished products (x_o) stations (x_w), set of test stations (x_t) and nodes corresponding to the associations between them (Fig. 1).

The diagram D_1 defines the function $\mu:\Gamma \rightarrow X \times X$ which will become a monomorphism provided that the pullback of μ with μ defined by cone L_3 is equal to Γ . The Cartesian product is the limit of the discrete diagram L_2 . The function $\sigma_{wt}:\Gamma_{wt} \rightarrow X_w$

becomes a monomorphism provided that the pullback of σ_{wt} with σ_{wt} has to be Γ_{wt} , which is imposed by the cone L_4 . The Cocone L_1 will require ω to become a terminal object in Set. The condition that the graph is connected is imposed by the limit of the cocone K_1 which will become a terminal element in Set. The cocones K_2 and K_3 serve to partition the concepts of the model [4].

To these nodes we add the node ϕ_i in the graph of the sketch representing the input interface and the node ϕ_o which represents the output interface represented by the input and output ports of the model. These will be associated with the input and output concepts by the arrows π_i and π_o (Fig. 1), which will have to become bijective functions in each model.

For the arrow π_i to become a surjective function, the pushout of π_i with π_i should be equal to x_i , i.e. the diagram from Fig. 2 has to become a pushout diagram in the Set category. In order for the arrow π_i to become an injective function, the pullback of π_i with π_i will have to be equal to ϕ_i , i.e. the diagram from Fig. 3 has to become a pullback diagram in the Set category.

Analogously, the arrow π_o becomes a surjective function if the pushout of π_o with π_o is equal to ϕ_o , i.e. the diagram from Fig. 4 becomes a pushout diagram in the Set category. And the arrow π_o becomes an injective function if the pullback of π_o with π_o will be equal to x_o , i.e. the diagram from Fig. 5 will become a pullback diagram in the Set category.

Therefore, the introduction of interfaces in the metamodel sketch implies in this case the addition of two more cones to the set of cones \mathcal{L} according to Fig. 3 and Fig. 5 and adding two more cocones to the set \mathcal{K} according to Fig. 2 and Fig. 4. Finally, it follows that the set of cones is $\mathcal{L}=\{L_1,L_2,L_3,L_4,L_5,L_6\}$ and the set of cocones is $\mathcal{K}=\{K_1,K_2,K_3,K_4,K_5\}$.

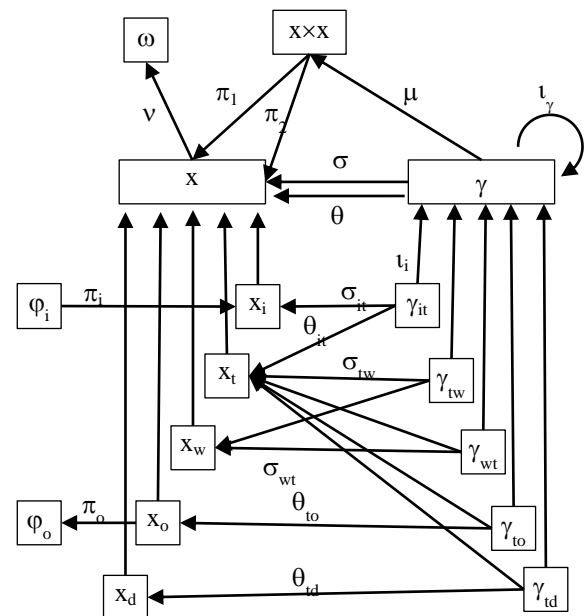


Fig. 1. The Graph of the MLMS Sketch.

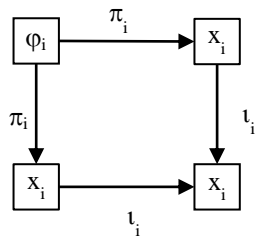


Fig. 2. Pushout Diagram.

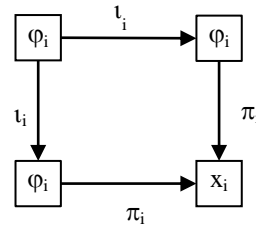


Fig. 3. Pullback Diagram.

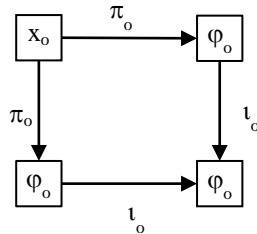


Fig. 4. Pushout Diagram.

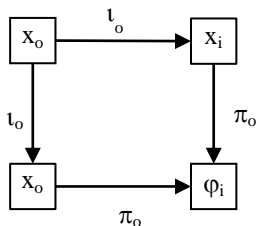


Fig. 5. Pullback Diagram.

A model of the sketch \mathcal{S} is a functor mapping the graph of the sketch in Set and all diagrams from \mathcal{D} in commutative diagrams, all cones from L in cone limits and all cocones from K in cocone colimits.

The sketch \mathcal{S} reflects the relation between the abstract definition of a class of models and the concrete models specified by the sketch. Therefore, the sketch is the formal object that specifies the metamodel that in turn represents a class of models and contains all the semantics necessary to express the syntactic constraints of the entities in this class of models.

Therefore, a concrete model of the sketch L^1 is a functor $H^2:L^1 \rightarrow \text{Set}$ that associates to the classes (nodes), in the sketch L^1 , set of extensions of these classes. The H^2 model associates

to the nodes (classes) from L^1 with sets of extensions of these classes representing all types of objects that make up the model, as well as all types of relations that can be defined between the entities of the model and the arcs are the sketch operators. We will denote with $L^2=H^2(L^1)$ a model of the sketch L^1 , i.e. a process constructed according to the grammatical rules imposed by the sketch L^1 .

The behavior of a process is based on the state idea determined by the values of the attributes. The simulation begins with an event initializing the process with the data describing its initial state. Values of attributes that constitute the state of the system at one time produce events that trigger the execution of some actions of the process. Execution of these actions changes the state of the process and as a result determine again the execution of some actions [3,4].

So if we know the state of a process at a certain moment we can simulate the evolution of the process without knowing the history of the previous states that determined the current state. This means that the current state of a process concentrates the entire previous evolution of the process.

In our case a state of the process is represented by an instance of the model [3,4]. An instance of the L^2 model is a functor $\phi:L^2 \rightarrow \text{Sets}$ with the property that $\phi \circ H^2$ is a model of the sketch L^1 , i.e. it complies with all the conditions imposed by the metamodel, and which associates to each set of classes from L^2 a set of instances, i.e. from each class one or more instances will be created.

If we have two instances $\phi, \psi:L^2 \rightarrow \text{Set}$ then we can define a natural transformation $\tau:\phi \rightarrow \psi$. The set of all instances together with all the natural transformations between them form a category that we call the process reaction category L^2 and we denote it with PRC. Thus, the evolution of the process from one state to another is represented by a natural transformation.

But the process has an initial state that in our case is an initial instance that we denote with \mathfrak{I}_0 . We consider a subcategory of the PRC category, which we call the process simulation category (PSC) that has the objects: $\text{Ob}(\text{PSC}) = \{\mathfrak{I}_k | \text{Hom}(\mathfrak{I}_0, \mathfrak{I}_k) \neq \emptyset\}$, and the arrows are all arrows from the RPC category that have domains and codomains in $\text{Ob}(\text{PSC})$. The paths from the PSC category that have as a starting point object the instance \mathfrak{I}_0 represent the traces of the model in the simulation or execution process.

In the context of our model, simulation traces are sequences of instances that can be obtained by natural successive transformations from the initial instant. Each trace represents an alternative to executing the process. Therefore, if $\mathfrak{I} = \text{ob}(\text{PSC})$ then the set of simulation traces form a language $L(\mathfrak{I}) \subseteq \mathfrak{I}^*$ defined as follows: $L(\mathfrak{I}) = \{ \mathfrak{I}_0 \mathfrak{I}_1 \dots \mathfrak{I}_n \in \mathfrak{I}^* \mid \mathfrak{I}_k = \tau(\mathfrak{I}_{k-1}) \text{ for } k \geq 1, \text{ and } \tau \text{ is a natural transformation and } \mathfrak{I}_0 \text{ is the initial instance} \}$

IV. CATEGORICAL MODEL OF CO-SIMULATION

The modeling of a large system involves the disassembly of the system into several real or virtual components from different domains integrated into a single model. Thus, the model is divided into several submodels, and each of these submodels requires the use of a certain formalism to specify

the process in optimal conditions of fidelity, robustness and simplicity.

A process describes the behavior of a natural or artificial entity, real or virtual, under conditions imposed by a particular context. The context can also be represented by other processes that interact with the considered process, which leads to processes composed of several subprocesses. Both the composed process and its individual components are characterized by inputs, outputs, and internal states between which transitions are made that define how inputs and states cause outputs. The overall behavior of a process is therefore a composition of the individual behavior of its subprocesses.

In this type of hierarchical modeling, in which each component is independently specified, a model is a collection of models that in the simulation process must work together to achieve the common goal. This results in a co-simulation process that integrates several independent simulation subprocesses that synchronize to interact with each other. The concept of co-simulation involves subprocess coupling techniques to build the behavior of the integrated process.

Each subprocess has to provide through its ports its functions for other subprocesses involved in co-simulation. Also, the outputs of a subprocess influence the evolution of other subprocesses, and therefore the evolution of each process, although it seems independent, also depends on the evolution of the other processes.

Combining dependent and independent behavior of subprocesses is essential to the optimum process evolution, but can cause major problems if it is not done correctly. Subprocesses must be coupled through their inputs and outputs to reproduce the behavior of the integrated process [8]. Thus co-simulation of a process is the sum of the correlated simulations of the coupled subprocesses.

To coordinate the co-simulation, an orchestrator is required to control how components of the model are synchronized, translates and transfers data from subprocess outputs to inputs of other subprocesses, according to an appropriate co-simulation scenario. In our approach, the orchestrator is represented by a categorical sketch whose graph has as nodes the sketches generating the submodels involved and a series of association relations that will implement the interactions between the models. The other components of the sketch will impose submodel coupling conditions. We will call this sketch: the sketch of the co-simulation model or co-simulation sketch.

We will consider a co-simulation sketch $\mathcal{S}=(\mathcal{G}, \mathcal{D}, \mathcal{L}, \mathcal{K})$, where the graph \mathcal{G} has as nodes objects representing sketches of models and as arcs sketch operators. For example, the graph of a sketch with three models could be the one in Fig. 6.

This graph already implies several conditions on the co-simulation model, namely:

- 1) The models of the sketches s_1 and s_3 do not interact directly with each other.
- 2) The models of the sketch s_1 interact directly only with the models from s_2 , and the models from the sketch s_2 interact with those from the sketches s_1 and s_3 .

- 3) The models from the sketch s_3 can interact with each other.

We can then introduce a set of other restrictions on the co-simulation model through the other components of the co-simulation sketch such as:

- 4) The models of the sketch s_3 should not contain loops, meaning there are no associations in which the source and target coincide.

This assumes that the coequalizer of the source and destination functions of the a_{33} association is the empty set, i.e. there is no arc in the model for which the destination and source coincide. In categorical terms, the coequalizer of σ_{33} and θ_{33} (Fig. 8) is the colimit of the diagram from Fig. 7, which we denote with K_1 . This colimit will have to become, in the Set category, the empty set, so as in Fig. 3, i.e. the colimit of the void diagram that we denote with K_2 and which becomes the initial object in the Set category.

- 1) The commutative diagram from Fig. 9, which we denote with D_1 , ensures the connection of model pairs two by two. Commutativity implies $\kappa_{12} \circ \kappa_{21} = id_{21}$, $\kappa_{21} \circ \kappa_{12} = id_{12}$, meaning that a_{12} and a_{21} are isomorphic. Similarly, a_{23} and a_{32} are also isomorphic.

- 2) Condition 5 does not assure us that there is only one pair of associations between two models. For this we have to put the condition that there is only one arc between any two models. Due to the isomorphism between a_{12} and a_{21} , it is sufficient to put the condition for one of them. We will put the condition for a_{12} .

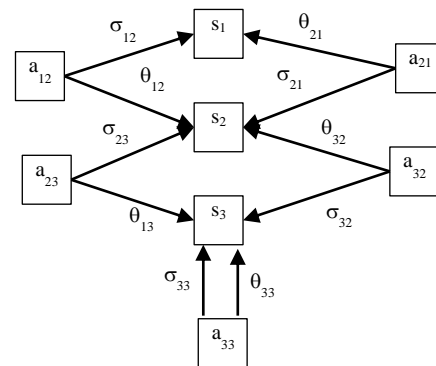


Fig. 6. The Graph of a Sketch with Three Models.

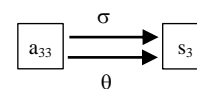


Fig. 7. Coequalizer Diagram.

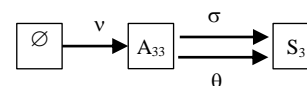


Fig. 8. Coequalizer of σ_{33} and θ_{33} .

In the metamodel sketch we will have to impose the condition that σ_{12} and θ_{12} be isomorphisms. But, σ_{12} and θ_{12} are epimorphisms if and only if the diagrams from Fig. 12 and Fig. 13 are pushout diagrams, i.e. σ_{12} and θ_{12} are epimorphisms. We denote these two diagrams with K_3 and K_4 . The functions σ_{12} and θ_{12} are monomorphisms if and only if the diagrams in Fig. 10 and Fig. 11 are pullback diagrams, i.e. σ_{12} and θ_{12} are monomorphisms. We denote with L_1 and L_2 these two limits.

For a_{23} and a_{32} the conditions are similar. So it also includes two more limits that we denote with L_3 and L_4 and two colimits that we denote with K_5 and K_6 .

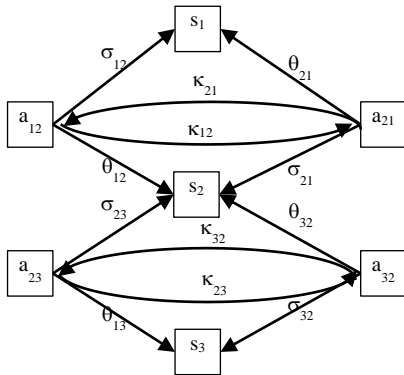


Fig. 9. Commutative Diagram.

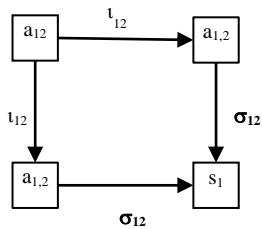


Fig. 10. Pullback Diagram.

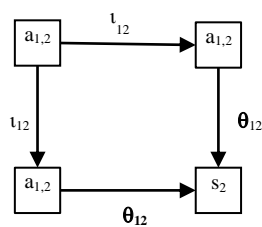


Fig. 11. Pullback Diagram.

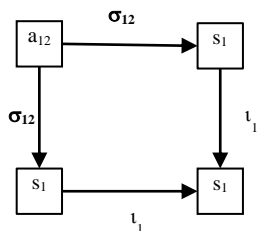


Fig. 12. Pushout Diagram.

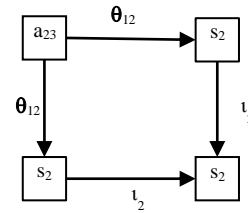


Fig. 13. Pushout Diagram.

1) The models of the sketch s_3 form a connected graph. This assumes that the equivalence relation induced by the functions σ_{33} and θ_{33} on the set of models generated by the sketch s_3 will determine a single equivalence class on the set of models generated by the sketch s_3 . For this, the diagram from Fig. 14 has to be a pushout diagram. That is, the span colimit determined by σ_{33} and θ_{33} is a terminal object in Set. We will denote with K_7 this diagram. We also need a terminal element from Set that is the limit of an empty diagram that we denote with L_5 .

The graph of the co-simulation sketch is shown in Fig. 15.

The final sketch of the co-simulation model is $\mathcal{S}=(\mathcal{G},\mathcal{D},\mathcal{L},\mathcal{K})$ where: \mathcal{G} is the graph from Fig. 4, $\mathcal{D}=\{D_1\}$, $\mathcal{L}=\{L_1,L_2,L_3,L_4,L_5\}$ and $\mathcal{K}=\{K_1,K_2,K_3,K_4,K_5,K_6,K_7\}$.

A model of a co-simulation sketch is a functor $M:\rightarrow\text{Set}$ that associates to each node of type sketch from the co-simulation sketch a set of models according to the model sketch corresponding to the node, to each node of type association a set of functions between models and the arcs that are the sketch operators will be interpreted accordingly. Mapping will be done with respect to the restrictions imposed by the components \mathcal{D} , \mathcal{L} and \mathcal{K} of the co-simulation sketch.

The functions corresponding to the association nodes will translate the source model outputs into inputs of the destination model, thus ensuring communication between the models involved in the co-simulation.

Each model will therefore respect the conditions imposed by the sketch that generated it and the set of all the models that interact in the co-simulation process will respect the conditions imposed by the co-simulation sketch.

A co-simulation model of the sketch \mathcal{S} from the example above could look like the one in Fig. 16 where we have denoted with hourglasses the models of the sketch s_1 , with rectangles the models of the sketch s_2 and with diamonds the models of the sketch s_3 . In this model we have 9 instances, 3 of each sketch. The arcs represented by lines in Fig. 16 are function types, images through the functor M of the association nodes in the co-simulation sketch. From them will create function instances that will do communication between the instances of the models. These functions, which we will call connection functions, map the outputs of a model to the inputs of another model. On the set of connection functions we can introduce the natural composing operation. The resulting construction generates a free category that has as objects the models and as arcs the connection functions. We will call this category: categorical model of co-simulation (CMCS).

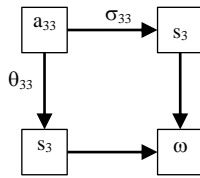


Fig. 14. Pushout Diagram.

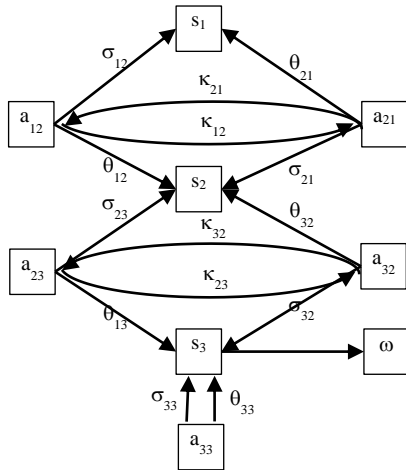


Fig. 15. The Graph of the Co-Simulation Sketch.

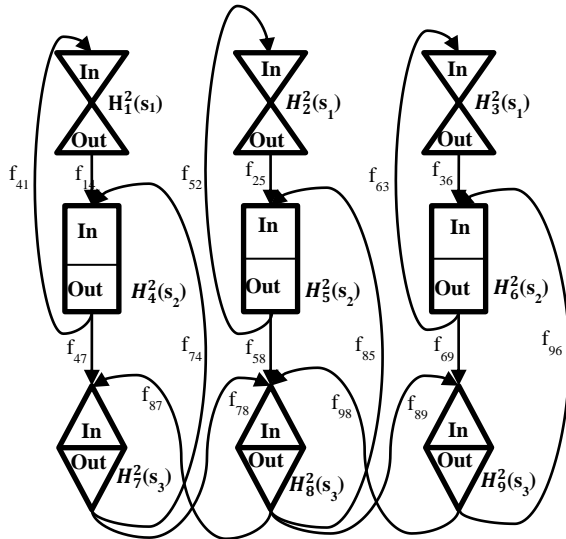


Fig. 16. Co-Simulation Model.

V. THE CO-SIMULATION CATEGORY

The categorical model of co-simulation was created. The instances of each co-simulation model have as an interaction support an orchestrator provided by the co-simulation sketch. This sketch is a graphical specification of a co-simulation model provided by the category theory.

Let's see how an instance of the categorical model of co-simulation looks like. In the categorical model of co-simulation, the interaction is achieved through the connection functions. But in the co-simulation process, interaction occurs between models in certain represented states, as described in

Section 3, through instance of component models. This means that interaction takes place between process simulation categories (PSC). It is natural that an instance of the categorical model of co-simulation will have to contain as objects process simulation categories (PSC) and as arrows connection functors between these categories that will be instances of the connection functions.

Therefore, an instance of the co-simulation model is a functor $\Phi:CMCS \rightarrow Set$ mapping each subprocess model M_i , $i=1,2,\dots,n$ to the process simulation category corresponding to PSC_i , $i=1,2,\dots,n$, as we saw in section 3, and each connection function $f_{i,j}$ for $i,j \in \{1,2, \dots, n\}$ to a connection functor $\phi_{i,j}$ for $i,j \in \{1,2, \dots, n\}$ between the appropriate categories. Obviously, the image of this functor in Set (Fig. 17) can also be structured as a category in which the objects are simulation categories, the arrows are the connection functors and the composition is the composition of the functors. We will name this category the Reactive Category of Co-Simulation (RCCS).

We denote the set of objects $ob(PSC_i)=\{\mathfrak{S}_i^1, \mathfrak{S}_i^2, \dots, \mathfrak{S}_i^k, \dots\}$ for all $i \in \{1,2,\dots,n\}$ and the arrows between two objects with \mathfrak{S}_i^k and \mathfrak{S}_i^l with τ_i^{kl} . A state \mathfrak{S}_k of the co-simulation model is a tuple of the form $\mathfrak{S}_k=(\mathfrak{S}_1^{k1}, \mathfrak{S}_2^{k2}, \dots, \mathfrak{S}_n^{kn})$ where $\mathfrak{S}_i^{ki} \in ob(PSC_i)$ for all $i \in \{1,2,\dots,n\}$.

We first consider that processes are parallel and independent. Then there is a macrotransition between two states $\mathfrak{S}_k=(\mathfrak{S}_1^{k1}, \mathfrak{S}_2^{k2}, \dots, \mathfrak{S}_n^{kn})$ and $\mathfrak{S}_l=(\mathfrak{S}_1^{l1}, \mathfrak{S}_2^{l2}, \dots, \mathfrak{S}_n^{ln})$ if for every pair of instances $\mathfrak{S}_j^{kj}, \mathfrak{S}_j^{lj}$ there is a transformation $\tau_j^{kl}:\mathfrak{S}_j^{kj} \rightarrow \mathfrak{S}_j^{lj}$. But the evolutions in the categories of co-simulation processes are not independent, some macrotransitions are independent and may evolve as above, other instances wait for rendezvous with instances of other subprocesses for information exchange that require synchronization [13,15].

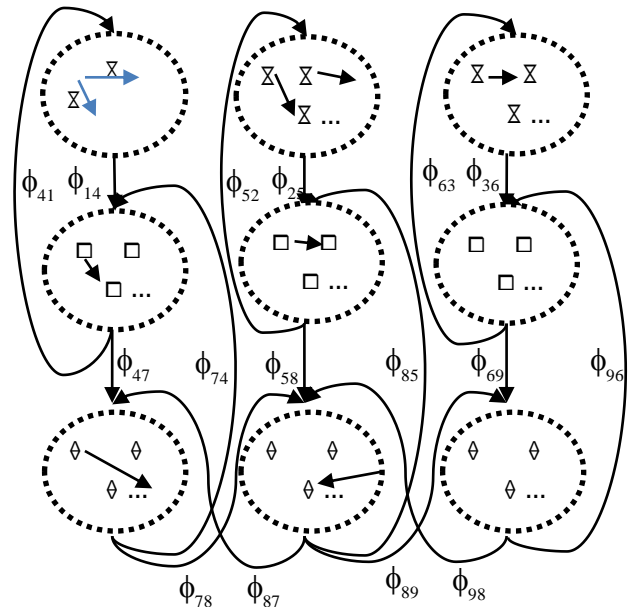


Fig. 17. Category of Co-Simulation.

For each process simulation category $PSC_i, i=1,2,..n$ we will construct a subcategory that we call the rendezvous category of the process $RCP_i, i=1,2,..n$ as follows: $ob(RCP_i)=\{\mathfrak{S}_i^k \in ob(PSC_i) \mid \exists j \text{ so that the execution of the transformation } \tau_i^{kj} \text{ depends on a rendezvous}\}$ and the arrows remain all from the PSC_i category which have the domains and codomains in $ob(RCP_i)$.

In this way, an instance of the co-simulation model becomes a functor $\Phi:CMCS \rightarrow Set$ that maps each subprocess model $M_i, i=1,2,..,n$ to the rendezvous category of the process $RCP_i, i=1,2,..,n$, and each connection function $f_{p,q}$ for $p,q \in \{1,2,..,n\}$ to a connection functor $\phi_{p,q}:RCP_p \rightarrow RCP_q$ for $p,q \in \{1,2,..,n\}$ between the rendezvous categories of process as follows: $\phi_{p,q}(\mathfrak{S}_p^k) = \mathfrak{S}_q^l$ if and only if the instance \mathfrak{S}_q^l needs as inputs the outputs of the instance \mathfrak{S}_p^k to be able to evolve. Defining $\phi_{p,q}$ on arrows is implicit. Obviously, each resulting structure $RCP_i, i=1,2,..,n$ is a category. We will call this category the category of co-simulation (CCS).

Then a macrotransition between two states $\mathfrak{S}_k = (\mathfrak{S}_1^{k_1}, \mathfrak{S}_2^{k_2}, \dots, \mathfrak{S}_n^{k_n})$ and $\mathfrak{S}_l = (\mathfrak{S}_1^{l_1}, \mathfrak{S}_2^{l_2}, \dots, \mathfrak{S}_n^{l_n})$ must meet the following conditions:

- For each pair of instances $\mathfrak{S}_i^{k_j}, \mathfrak{S}_j^{l_j}$ there is a transformation $\tau_j^{kj}: \mathfrak{S}_i^{k_j} \rightarrow \mathfrak{S}_j^{l_j}$. If $\mathfrak{S}_i^{k_j} = \mathfrak{S}_j^{l_j}$ then the transformation is the identity. In the simulation process this means that $\mathfrak{S}_i^{k_j}$ is waiting for a rendezvous.
- For each pair p and q there is a transformation from $\phi_{p,q}(\mathfrak{S}_p^{k_p})$ to $\mathfrak{S}_q^{m_q}$ in the RCP_q category if and only if there is a transformation from $\mathfrak{S}_p^{k_p}$ to $\phi_{q,p}(\mathfrak{S}_q^{m_q})$ in the RCP_p category.

Condition ii) is necessary to avoid the deadlock situation in the co-simulation flow, i.e. a state in which each member of the tuple waits for another member to send its outputs to an instance that is not in the tuple or to receive inputs from another instance that is not in the tuple. Of course, each instance can execute the identity transformation for a number of steps but not for infinite without the process evolving. The condition ii) ensures that all instances will have the rendezvous they are waiting for, and there will be no deadlock. But obeying this condition is related to the definition of functors $\phi_{p,q}$ for $p,q \in \{1,2,..,n\}$. For this, the functors $\phi_{p,q}$ and $\phi_{q,p}$ should be adjoint functors.

The functor $\phi_{p,q}:RCP_p \rightarrow RCP_q$ is the left adjoint of the functor $\phi_{q,p}: RCP_q \rightarrow RCP_p$ and $\phi_{q,p}$ is the right adjoint of $\phi_{p,p}$ and is denoted by $\phi_{p,q} \dashv \phi_{q,p}$ if and only if the set of arrows $Hom(\phi_{p,q} -, -)$ and $Hom(-, \phi_{q,p} -)$ are naturally isomorphic as functors of two variables with values in Set . We denoted with $-$ the place of a variable in the formula [9]. This means, in our case, that for each pair p and q there is a transformation from $\phi_{p,q}(\mathfrak{S}_p^{k_p})$ to $\mathfrak{S}_q^{m_q}$ in the RCP_q category if and only if there is a transformation from $\mathfrak{S}_p^{k_p}$ to $\phi_{q,p}(\mathfrak{S}_q^{m_q})$ in the RCP_p category, i.e. exactly the condition ii) from above.

But the two functors are adjoints [9,10] if there is a natural transformation $\eta_p: id_p \rightarrow \phi_{p,q} \circ \phi_{q,p}$, where id_p is the identity functor in the RCP_p category and η_p is the adjunct unit, so for any objects \mathfrak{S}_p^k from RCP_p and \mathfrak{S}_q^l from RCP_q and any arrow $\tau_p^{kt}: \mathfrak{S}_p^k \rightarrow \phi_{q,p}(\mathfrak{S}_q^l) = \mathfrak{S}_p^t$, there is a unique arrow $\tau_q^{tl}: \phi_{p,q}(\mathfrak{S}_p^k) = \mathfrak{S}_q^t \rightarrow \mathfrak{S}_q^l$ so that the diagram in Fig. 18 commutes.

We also have the dual characterization that if two functors $\phi_{p,q}$ and $\phi_{q,p}$ have the property $\phi_{p,q} \dashv \phi_{q,p}$ then there is a natural transformation $\varepsilon_q: \phi_{p,q} \circ \phi_{q,p} \rightarrow id_q$ called adjunct counity so that for any arrow $\tau_q^{tl}: \phi_{p,q}(\mathfrak{S}_p^k) = \mathfrak{S}_q^t \rightarrow \mathfrak{S}_q^l$, there is a unique arrow $\tau_p^{kt}: \mathfrak{S}_p^k \rightarrow \phi_{q,p}(\mathfrak{S}_q^l) = \mathfrak{S}_p^t$ so that the diagram in Fig. 19 commutes.

Therefore, if the natural transformations η_p or ε_q exists with the above properties, the two functors are adjoints. The natural transformation η_p provides a way to associate each arrow $\tau_p^{kt}: \mathfrak{S}_p^k \rightarrow \mathfrak{S}_p^t = \mathfrak{S}_p^t$ from the RCP_p category with an arrow $\tau_q^{tl}: \phi_{p,q}(\mathfrak{S}_p^k) = \mathfrak{S}_q^t \rightarrow \mathfrak{S}_q^l$ from the RCP_q category so that $\tau_p^{kt} = \phi_{q,p}(\tau_q^{tl}) \eta_p$.

In our case, the natural transformation $\eta_p: id_p \rightarrow \phi_{p,q} \circ \phi_{q,p}$ can be constructed taking into account the way the categories $RCP_i, i \in \{1,2,..,n\}$ have been defined as subcategories of the process simulation categories $PSC_i, i \in \{1,2,..,n\}$ in section 3. From this it follows that each $Hom(\mathfrak{S}_p^0, \mathfrak{S}_p^k)$ contains a natural transformation τ_p^{0k} for all $k \geq 0$. We will define every component $\eta_p^k: \mathfrak{S}_p^k \rightarrow \phi_{p,q} \circ \phi_{q,p}(\mathfrak{S}_q^l) = \mathfrak{S}_p^t$ as follows: for each $x \in \mathfrak{S}_p^k$ we define $\eta_p^k(x) = \tau_p^{0k}(\tau_p^{0k}(z)) = \tau_p^{0t}(z)$ where $z \in \mathfrak{S}_p^0$; $x = \tau_p^{0k}(z)$ and $\tau_p^{0k} \in Hom(\mathfrak{S}_p^0, \mathfrak{S}_p^k)$; $\tau_p^{0t} \in Hom(\mathfrak{S}_p^0, \mathfrak{S}_p^t)$. It is quite simple to prove that η_p defined as such respects the naturality property and thus is a natural transformation.

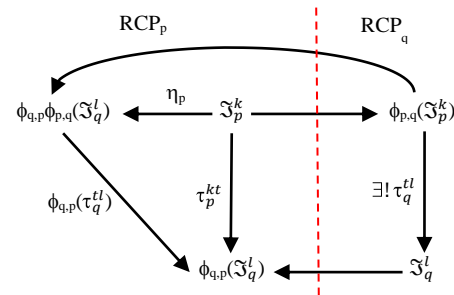


Fig. 18. Commutativ Diagram.

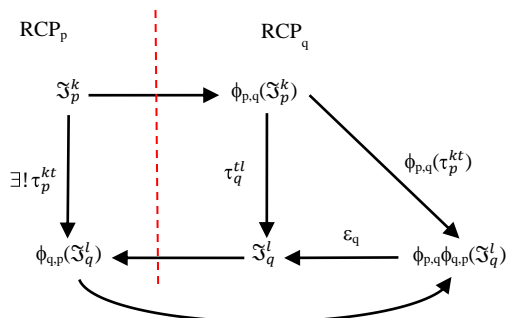


Fig. 19. Commutativ Diagram.

We observe that the component η_p^k of the natural transformation η_p exists if and only if the number of elements from \mathfrak{S}_p^k is greater or equal to the number of elements in \mathfrak{S}_p^t . Similarly, the natural transformation $\varepsilon_q: \phi_{p,q} \circ \phi_{q,p} \rightarrow \text{id}_q$ can be constructed in the RCP_q category. If the natural transformations η_p^k and η_q^k exist for all $k \geq 0$ then the two functors $\phi_{p,q}$ and $\phi_{q,p}$ are the adjuncts and the condition ii) is fulfilled. Otherwise we will have to try all the variants admitted by the model in question to define the functors $\phi_{p,q}$ and $\phi_{q,p}$ to obtain two adjunct functors. If there is no such option we will have to make changes at the model level. In principle, it should be observed that for each object \mathfrak{S}_p^k from the RCP_p category, the functor $\text{Hom}(\mathfrak{S}_p^k, \phi_{q,p}): \text{RCP}_q \rightarrow \text{Set}$ has a universal element [9]. But we will deal with this problem in a future paper.

VI. CONCLUSION

Multi-formalism modeling aims to facilitate the use of more modeling formalisms in certain situations where it is necessary to compose heterogeneous models, thus allowing experts from different disciplines to collaborate more effectively in the development of increasingly complex systems. This approach involves specifying processes through different modeling grammars.

Many times the solution to this challenge is the development of grammars specific to the component subprocesses starting from a common meta-metamodel that facilitates their coupling in a co-simulation process that allows the study of the overall system behavior. There is a gap of remarkable results in the field of modular coupling, of simulators in dynamic structure scenarios at the state level [2]. The concept of categorical modeling method along with the MM-DSL [3,4,5,6,7] language facilitates this approach. The present paper proposes a co-simulation category (CCS) as a model for the co-simulation state space. The categorical sketch for co-simulation can be specified in a graphical language provided by the category theory for specifying the syntax of the co-simulation model.

This facilitates the separation of the model specification from the execution algorithms. Universal constructs offered by the category theory can be implemented as universal algorithms and mechanisms [6,7] at the meta-metamodel level and used in each model for process coupling. This type of algorithms reduce the complexity of syntax specification for coupling and provides support for domain specific modeling and distributed execution. Thus, the universal constructs from the category theory can be seen as a collection of tools for specifying and structuring the dynamic coupling of processes.

Synchronization can be elegantly modeled by adjunct functors. Composition of adjuncts is also an adjunct [9]. We

have seen in section 5 the determination of the adjunct unit, if it exist it can be relatively simple. We will have to find general criteria for characterizing the situations in which these adjuncts exist. This problem as well as the problem of finding practical and efficient algorithms for determining synchronization adjuncts will be addressed in a future paper.

REFERENCES

- [1] Bernard P. Zeigler, Alexandre Muzy, Ernesto Kofman, Theory of Modeling and Simulation Discrete Event and Iterative System Computational Foundations - Academic Press 2019 , ISBN: 978-0-12-813370-5.
- [2] Claudio Gomes, Casper Thule, David Broman, Peter Gorm Larsen, Hans Vangheluwe - Co-simulation: State of the art, - ACM Computing Surveys, Vol. 1, No. 1, Article 1. Publication date: January 2016.
- [3] Daniel C. Crăciunean, Dimitris Karagiannis, 2018, Categorical Modeling Method of Intelligent WorkFlow. In: Groza A., Prasath R. (eds) Mining Intelligence and Knowledge Exploration. MIKE 2018. Lecture Notes in Computer Science, vol 11308. Springer, Cham.
- [4] Daniel C. Craciunean, Categorical Grammars for Processes Modeling” International Journal of Advanced Computer Science and Applications(IJACSA), 10(1), 2019. <http://dx.doi.org/10.14569/IJACSA.2019.0100105>
- [5] Dimitris Karagiannis, Robert Andrei Buchmann 2018, A Proposal for Deploying Hybrid Knowledge Bases: the ADOxx-to-GraphDB Interoperability Case, Published in HICSS, DOI:10.24251/hicss.2018.510.
- [6] Dimitris Karagiannis, N. Visic, 2011. Next Generation of Modelling Platforms. Perspectives in Business Informatics Research 10th International Conference, BIR 2011 Riga, Latvia, October 6-8, 2011 Proceedings
- [7] Dimitris Karagiannis, Heinrich C. Mayr, John Mylopoulos, 2016. Domain-Specific Conceptual Modeling Concepts, Methods and Tools. Springer International Publishing Switzerland 2016.
- [8] Vagner, D., Spivak, D. I., & Lerman, E. M., 2015. Algebras of open dynamical systems on the operad of wiring diagrams. *Theory and Applications of Categories*, 30, 1793-1822, Nov 30 2015.
- [9] Michael Barr, Charles Wells, 2012. Category Theory For Computing Science, Reprints in Theory and Applications of Categories, No. 22, 2012.
- [10] R. F. C. Walters, 2006. Categories and Computer Science, Cambridge Texts in Computer Science, Edited by D. J. Cooke, Loughborough University, 2006.
- [11] Robin Milner, 2009. The Space and Motion of Communicating Agents, Cambridge University Press, 2009. ISBN 978-0-521-73833-0
- [12] Weske, Mathias, 2012. Business Process Management - Concepts, Languages, Architectures, 2nd Edition. Springer 2012, ISBN 978-3-642-28615-5, pp. I-XV, 1-403.
- [13] Winskel Glynn, 2009. Topics in Concurrency, Lecture Notes, April 2009.
- [14] Wil M.P. van der Aalst, 2011. Process Mining Discovery, Conformance and Enhancement of Business Processes, Springer-Verlag Berlin Heidelberg 2011.
- [15] Diskin Z., König H., Lawford M., 2018. Multiple Model Synchronization with Multiary Delta Lenses. In: Russo A., Schürr A. (eds) Fundamental Approaches to Software Engineering. FASE 2018. Lecture Notes in Computer Science, vol 10802. Springer, Cham.

An Enhanced Concept based Approach for user Centered Health Information Retrieval to Address Readability Issues

Ibrahim Umar Kontagora¹, Isredza Rahmi A. Hamid², Nurul Aswa Omar³

Faculty of Computer Science and Information Technology, Universiti Tun Hussein Onn Malaysia (UTHM)^{1, 2, 3}
Batu Pahat, Johor Malaysia

Department of Computer Science, Niger State Polytechnic, Zungeru, Niger State, Nigeria¹

Abstract—Searching for relevant medical guidance has turn out to be a general and notable task executed by internet users. This diversity of quantifiable information explorers indicates the enormous range of information needs and consequently, a key prerequisite for the development of clinical retrieval systems that would satisfy the clinical information desires of non-clinical professionals and their care givers. This study focused on designing an enhanced model for clinical consumers balanced based medical information retrievals and also proposed an improved system model that would provide simpler medical meanings for every clinical grammer(s) established on a clinical released documents and clinical search results online. We evaluated and compared the enhanced model with the current models in the clinical domain, namely, QLM (“Query Likelihood Model”), LSI (“Latent Semantic Indexing”) and CBA (“Concept Based Approach”) using MeSH, Metamap and UMLS databases. The outcomes gotten from the investigational study confirmed that, the Enhanced model (ECBA) managed to achieve 0.9145, 0.9170 and 0.9156 on MAP (“Mean Average Precision”), P@10 (“Precision @ 10”) and NDCG@10 (“Normalized Discounted Cumulative Gains @ 10”) in that order. Hence, the superlative model to be deployed in addressing readability hitches is the Enhanced Concept Based method.

Keywords—*Concept-based approach; medical discharge reports; clinical reports; query expansion; latent semantic indexing; query likelihood model*

I. INTRODUCTION

Health information retrieval has become one of the most performed tasks on the internet today [10, 16]. Additionally, it has become extremely difficult to cope with the speed of release of new researches in the biomedical domain [23]. Searching online channels for medical guidance has turn out to be a common performed task by individuals on the web. [21, 23]. A fresh study piloted by United States shows that about 80 percent of online information seekers conduct internet search for their medical information [10, 30].

However, the incapability of the current approaches to address the diverse information desires for various classes of information seekers (clinical professional and nonprofessional), has made non-clinical professional and their care givers to further queries after reading through their displayed probe results online [32, 23]. The previous

researches targeted more on a specific group of information seekers with clinical acquaintance [26].

The Pursuit for medical guidance online has turn out to be a common and significant job executed by persons seeking for relevant health information on a specific disease [10, 23]. The increasing number of online health information probe has driven several number of assessment crusades concentrating on clinical information retrievals [16]. Some of these assessments campaigns aimed at identifying and addressing the medical information needs of non-clinical professional and their assistants through their medical documents as they enlist for clinical attention [31].

Patient portal is defined as an efficient and effective means of providing patients with a 24 hours free access to personal health information from any destination online [28,15]. Different from the traditional personal medical records, patient portals are financed and taken care of by the portal administrators [18, 26, 29]. One of the major merits of patient portal is that, it allows patients to take control of the management of their health [32, 17]. However, patients’ portals are predominantly available to outpatients [14]. Investigations have also revealed that, age is also one of the major contributory factor affecting the practice of patients portals, as there are more patronage on younger ages than the older ones [4, 5]. The work by [35] focused on evaluating the impacts and designing a patient portal for inpatient that would provide patients with a 24 hours free admittance to particular medical facts with internet connection from anywhere.

The work by [34] focused on the evaluation of user involvement as a key vital tool to the success of the design and implementation of a medical collaboration and communication platform aimed at improving medical care by medical team of clinicians. Even though medical information retrieval systems have the potential to enhance the safety and effectiveness of medical delivery, this potential is yet to be fully achieved [19, 31]. However, medical information retrieval systems require the full incorporation of friendly tools during their design that are context appropriate [7].

User centered design, user co-design and participatory design are the three main approaches adopted in involving users in user centered health information design [20, 24, 8]. Re-counted merits of users involvement in user centered

health information systems designs include the design of enhanced information retrieval systems that would better address the apprehension problem faced by laymen patients and their care givers in discovering information mined from their displayed search results online [31, 8]. Despite these merits, user centered health information systems design remains challenging to attain, as a result of technical, communal, structural and cultural influences [24, 8].

Preceding studies on medical information retrieval discloses that patients are continually inquisitive of knowing what exactly is written on their medical discharge documents and clinical reports [32, 16]. However, the unsatisfying concern is that, the medical tests are usually very proficient and tough to understand [20]. And for that, medical information retrieval becomes extremely admired as an efficient means of answering questions that might be asked by the patients [6]. Several assessment campaign communities have embarked on the conduction of domain-specific resources, organizing worldwide challenges / competitions / researches in the arena of biomedical information retrieval, in order to provide the needed information by medical experts and laymen patients [25, 31].

The core objective of this research study is to propose an improved system model and to design an enhanced approach using the concept based approach that would better address the apprehension problem faced by laymen patients and their care givers in discovering information mined from their displayed search results online. The proposed enhanced approach would provide simpler translations for all medical words found on the displayed search results online. The remaining sections of the paper are organized as follows. The reviewed related works is contained in Section 2, the proposed system model and improved approach are discussed in Section 3, the performance analysis is discussed in Section 4 and the conclusion of the work and recommendation for future work is contained in Section 5.

II. RELATED WORK

Previous related works have extracted and investigated data from the query logs of numerous commercial search engines [34]. However, the outcome of the investigation shows that, the concentration given to the creation of systems that meet up to the information desires of laymen patients is significantly low [10, 23]. Additionally, this has significantly contributed to the high rise of apprehension issues faced by the non-clinical professionals while reading through their retrieved search results displayed online [21]. Work by [35] proposed that sufficient consideration should be accorded to the information requests of various classes of information seekers.

The creation of consumer balanced information retrieval systems for laymen queries have proved difficult, as medical words apprehension still remained a major challenge from retrieved displayed search results by non-clinical professionals and their care givers [25, 16]. Several clinical retrieval systems are unable to integrate program modules that would provide simpler words/ translation for all medical grammars found in clinical release documents and clinical search results online [21, 37].

The wide acceptance of user centered clinical systems was as a result of excellent and proficient medical care delivery and life touching excellent impact it renders to end-users [1, 2, 10]. In an attempt to address the apprehension problem faced by the non-clinical professional patients and their assistants or care givers, the development of enhanced algorithms that would determine the successes and failures of a consumer balanced clinical systems in respect to addressing readability problems were projected by [34, 25]. How information retrieval systems could improve health delivery and accessibility to quality well-being systems was the focus of the work by [36, 37].

Previous researches on medical document retrieval also reveals that the curiosity of patients having a clear picture of the content was as a result of the professional nature of how clinical release documents and clinical search results are written online. However, the medical texts are usually very professional and difficult to follow and as such, they still need to consult other medical experts for the meanings of the terms contained in the search results [16, 22, 23]. In an attempt to effectively answer these questions raised by patients, highly robust algorithms were proposed by the researchers [6]. In addition, previous studies have also revealed that, queries that do not reflect users' specific information needs failed to address readability issues [21].

The complete implementation of electronic health information systems in different context has attracted advanced researches in health information retrievals [1, 32, 33]. Earlier studies had shown that, the timely availability of readable and accurate Information had improved health delivery and clinical decisions [22, 27]. Additionally, the acceptance and full implementation of electronic health information system by clinicians, has also contributed to the entire successes recorded in the recent time in tackling apprehension problems faced by non-clinical professionals patients in mining information explored from their clinical release documents and clinical search results online [10, 11, 36].

Despite the awareness of the existence of readability issues, previous researchers have continued to pay more attention in addressing medical practitioners' information needs [33, 20]. There was limited attention to addressing the information needs of non-clinical professional patients and their assistants by providing simpler interpretations for all medical grammars found on clinical release documents and clinical search results online [12]. The primary aim of a consumer balanced retrieval system is to provide medical information seekers with a patient centered information [13, 3, 37].

III. THE PROPOSED ENHANCED CONCEPT BASED APPROACH

The study proposed an enhanced method for consumer balanced health information retrieval systems that would address readability issues by providing simpler translations for all medical grammars seen on clinical release documents and clinical search results online. The enhanced method was improved by incorporating two special functions modules namely: the module for generating medical search queries in layman's forms and module for generating medical discharge

documents in layman's forms. The proposed approach provides layman's translation for every medical term(s) found on a medical discharge document or medical search queries results online. More so, it also fully incorporate and implement two additional special controlled vocabularies modules namely: medical terms controlled module and vocabulary controlled module. They restricts the search terms in a launched search query to most specific terms (MST), in order to prevent vocabulary mismatched issues.

A. A Model for the Proposed Enhanced Concept based Approach

From the Model of the proposed enhanced method in Fig. 1, the system first of all prompts the user to input the information to be searched for. Upon inputting the requested search information, it does two things, firstly, is to launch a search query and secondly, is to send a notification message to the Medical Concept Free Module that a search query has been launched. Upon receiving such notification, it refers to the search query, search and extract all the most specific medical terms (MST) in the search query. The extracted most specific medical terms (MST) are then moved to the vocabulary controlled module where the synonyms of all the extracted most specific terms (MST) are searched for and extracted from the dictionary of the selected online dataset. At this point, both the extracted most specific terms (MST) from the launched search query and their extracted synonyms terms from the selected dataset are then expanded into the new search query. Finally, it displays the search results with their layman's translations to the end-users as shown in Fig. 1.

In addition, the proposed approach was enhanced to limit its search terms to only most specific medical terms in the launched search queries, as well as the synonyms of these terms extracted from the dictionary of the selected dataset, in order to prevent vocabulary mismatched issues. However, these was achieved by the implementation of two additional program modules namely the Medical Concept Free Module and the Vocabulary Controlled Modules. The former ensures that only most specific medical terms in a launched search query are extracted, while the later ensures that only the synonyms of the extracted most specific terms from the dictionary of the selected database are searched for, extracted and expanded into the new search query.

1) The significance of our proposed enhanced method is that, it provides simpler translations for all medical grammars/words found on a retrieved clinical release documents and clinical search results online. Also, for the specific purpose of ensuring that, the medical grammars/words enclosed in the two text fragments (input and output) are related, the medical terms controlled module, as well as the vocabulary controlled modules were also created and integrated into the proposed enhanced method. By so doing, the improved method better addressed the enquiries that non clinical professional patients and their assistants do seek after perusing through their clinical release documents and clinical search results online. More so, the performance of the our improved method with the current approaches were evaluated using data were extracted from the dictionary of Medical

Subject Heading, Metamap, Unified Medical Language System and Khresmoi project 6 datasets.

B. The Enhanced Approach using Concept based Approach

The study proposed an improved approach using the concept based approach that addresses readability issues by providing simpler interpretations for all clinical words/grammars seen on patients' clinical release documents and clinical probe results online. The improved approach using the concept based approach was enhanced by incorporating two special functions modules namely: the module for generating clinical probe results in simpler forms and module for generating clinical released documents in simpler forms. The improved method which comprises of lines numbers 1 – 16 will also fully implement the two additional incorporated controlled vocabularies in order to avoid vocabulary mismatched issues.

The integrating strategy for the proposed approach is as shown in Fig. 2, where input N is the counts of words generated from the core search, C is concept terms and K is expansion terms. SQ represents search query and CC_n represents the n th concept, K signifies the counts of extension words, and ET_k symbolizes the k th extensions words. The k th is the tailed extensions words in an expansion query and the sign # signifies vacuum space. The dual quote symbols signify that the word contained will surface successively. The Medical Concept Free Module ensures that only most specific medical terms in a search query are searched for and extracted. Finally, inputted search information is end-users information request entered into the search query as shown in Fig. 2.

For the specific purpose of providing simpler translations for all the clinical grammars/words established on retrieved clinical released documents and clinical probe results online, the module for generating clinical probe results in simpler form provides the simpler interpretations for all the clinical grammars/words seen on the displayed clinical probe results online. While, the module for generating clinical released documents in simpler form provides the simpler interpretations for all the clinical grammars/words found on the displayed clinical released documents as shown in Fig. 3 and 5. The improved method was implemented in two levels for the purpose of medical document retrievals. (i) By searching and extracting only the labeled most specific concepts terms in a search query and their synonyms from the dictionary of the selected dataset and (ii) by providing layman's translations for all the medical grammars/words found on the retrieved clinical released documents and clinical search results online. Hence, it better address the information desires of non-clinical patients and their assistants.

C. Module for Generating Clinical Probe Results in Simpler form

Specifically, the creation and generation of clinical released documents and clinical search results in simpler form were achieved using Fig. 3 and 5 respectively. Fig. 3 is the module for generating Clinical Probe Results in Simpler form. It consists of lines numbers 17 to 29. It is designed in such a way that once a clinical probe query result is displayed, it

searches and provides the simpler interpretations for all the clinical grammars seen on the displayed clinical probe results online as contained in Fig. 4.

In Fig. 3, replace grammar refers to those found medical grammars in the clinical probe results whose simpler concepts are to be provided, @grammar refers to stored patients layman's terms in the dictionary of the selected dataset. Status gives the position of the search and excode tells the number of records found. However, this function provides the simpler interpretations for the entire clinical grammars/words seen on the clinical probe results.

Fig. 4 is the pictorial view of a generated output of a clinical query search result in Layman's/simpler Form generated by Fig. 3. The simpler grammar for such medical grammars can be gotten by clicking on the command button for layman's concept on the application web page for the proposed enhanced approach. Once a clinical probe result is displayed online, Fig. 3 searches and provides the simpler interpretations for the entire clinical grammars found on the displayed clinical probe result as could be seen in Fig. 4.

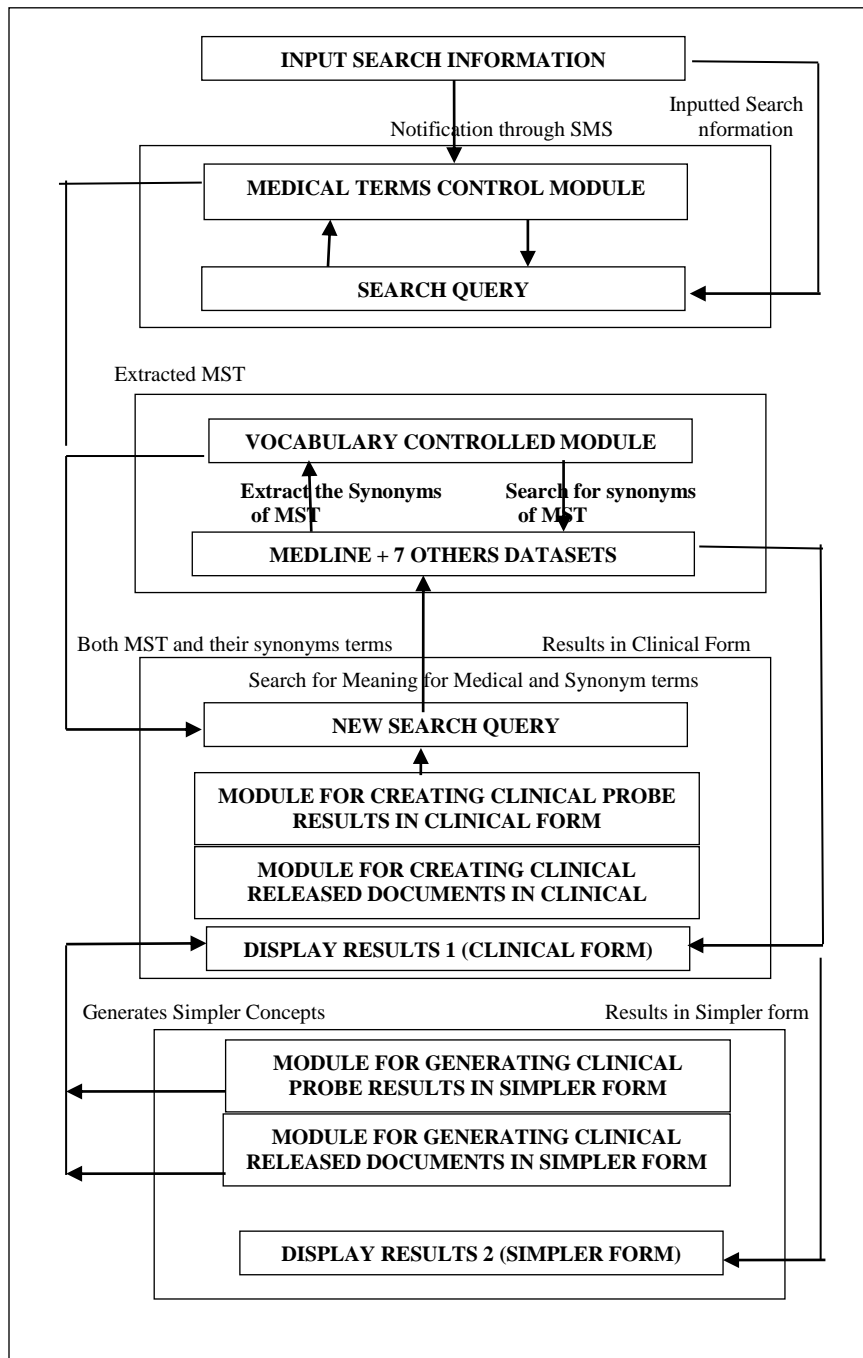


Fig. 1. A Model for the Proposed Enhanced Concept based Approach.

```
1  Input Search Information
2  [Medical Concept Free Control Module]
3  For all concepts  $n \in [1, N]$  do
4  Set  $SQ = \text{query}$ 
5   $SQ = "SQ" + "CC_n"$ 
6  [Vocabulary Controlled Module]
7  For all the extension words  $k \in [1, K]$ , do
8  New  $SQ = SQ \# "ET_k"$ 
9  End;
10 [Module for creating clinical probe results in clinical form]
11 [Module for creating clinical released documents in clinical form]
12 Display Results 1 (In clinical form)
13 [Module for generating clinical probe results in simpler form]
14 [Module for generating clinical released documents in simpler form]
15 Display Results 2 (In Simpler form)
16 End
```

Fig. 2. The Enhanced Concept based Information Retrieval Approach.

```
17 Declare: replacegrammar(grammar)
18 Fetch = Select " from patient-layman Terms"
19 Where grammar = @grammar
20 If grammar = @grammar then
21 Replacegrammar = Search "in kept Patient-Layman words"
22 Status = " 1 replacement establish"
23 Search code = 1
24 Generate Clinical Search Result in Layman's Forms
25 Else
26 Status = " No replacement establish for the identified grammar"
27 Search code = 0
28 Return grammar = (" + replacement + .....")
29 End.
```

Fig. 3. The Module for Generating Clinical Probe Results in Simpler Form.

D. Module for Generating Clinical Released Documents in Simpler Form

In order to generate the simpler interpretations for every medicinal terms seen on a retrieved clinical released documents online, Fig. 5 was created. Fig. 5 is the module for generating clinical released documents in simpler forms. It comprised of line numbers. 30 - 42. It is designed in such a way that, once a clinical released document is displayed online, it searches, locate and provide the simpler interpretations for the entire medical grammars/words found on the displayed clinical released document online. By so doing, it better address the information desires of non-clinical professionals and their assistants as they explore information contained in their clinical released documents online.

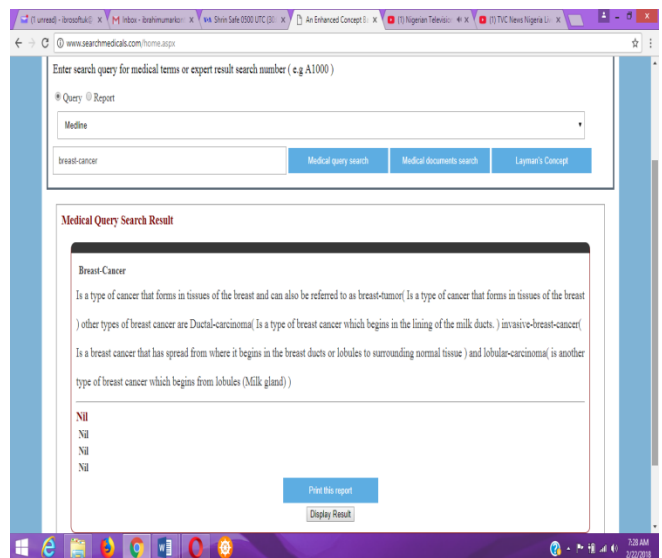


Fig. 4. The Pictorial View of Clinical Probe Result in Simpler Form.

```
30 Declare getlaymanRecord (grammar)
31 Scan = Highlight "among patient Data"
32 Place grammar = @grammar
33 If grammar = @grammar then
34 grammar = "Extract from Search - Query"
35 gmeaning = "Extract from the selected dataset"
36 Status = "1 document instituted"
37 Search code = 1
38 Generate clinical released documents in simpler form
39 Else
40 Status = "No document instituted for the established search"
41 Search code = 0
42 End.
```

Fig. 5. The Module for Generating Clinical Released Documents in Simpler Form.

In Fig. 5, getlaymanRecord refers to search for layman grammar, grammar means the medical terms found in a medical discharge document, @grammar refers to stored grammars in the selected dataset, while gmeaning stands for the meaning of grammars found in a search query. Status gives the position of the search and excode tells the number of records found.

Fig. 6 is the Pictorial View of a generated output of a clinical released document in simpler form generated by Fig. 5. Once a clinical released document is being displayed online, it searches and provides the simpler interpretations for all the clinical grammars found on the displayed clinical released document as displayed in Fig. 6:

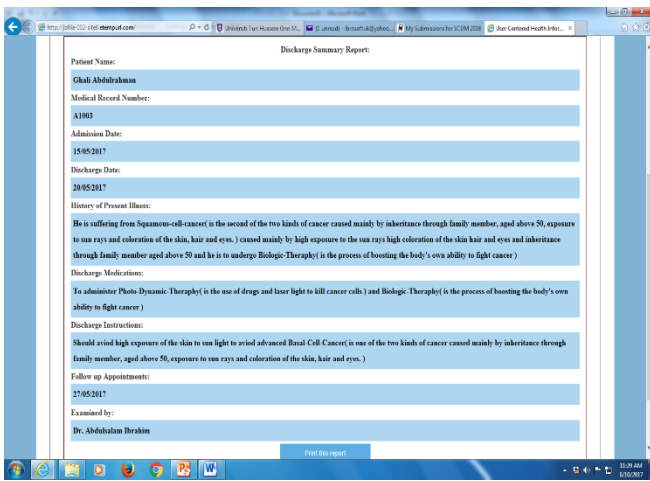


Fig. 6. The Pictorial View of Clinical Released Document in Simpler Form.

IV. PERFORMANCE ANALYSIS

This section presents the experimental setup, dataset and performance parameters used in evaluating the enhanced method using the concept based approach (ECBA) and the current methods namely the latent semantic indexing (LSI), the concept based approach (CBA) and the query likelihood model (QLM) and.

A. Experimental Setup

The experimental setup was carried out using HTML–Hyper-Text Mark-up Language, C#.net, JavaScript and CSSnc –Cascading Style Sheet using Windows 7 operating system with Intel (R) Core i7 processor, 3.40GHZ and 4Gigabytes Random Access Memory (RAM). HTML was used for designing the web application structure and C#.Net was used for creating and activating the application structure functionalities. JavaScript was used for making the web application dynamic and interactive and CSSnc was used for the beautification of the application looks.

B. Dataset

The study used Khresmoi Project 6, Metamap, MeSH and UMLS datasets in evaluating the systems performance. The datasets coverage is wide and comprehensive in the biomedical and health domain. All information in the pool were gotten from several online and free web databases among which are Diagnosia7 and Clinical.gov [23].

C. Performance Metrics

The performance of the current methods and the Enhanced Concept Based Approach were evaluated using 3 performance metrics namely:

a) P@10 (Precision at 10 documents)

P@10 computes the fraction of applicable documents at each ten (10) recalls. It can be computed as $P@10 = \frac{(A)_{10}}{(A+B)_{10}}$ with P being the Fraction of Applicable Documents Recovered at every ten (10) recalls, A is Recovered Applicable Documents and B is Recovered Non applicable Documents [9].

b) NDCG@10 (Normalized Discounted Cumulative Gain at 10 documents)

NDCG@10 calculates the collective achievement at separate point for a selected figure of p for all the significant document in the probe [9]. NDCG@10 is computed as $NCDG_p = \frac{DCG_p}{IDCG_p}$ where $IDCG_p =$

$(IDCG_p) = \sum_{i=1}^{REL} \frac{2^{rel_i-1}}{IDCG_p} \cdot REL$ signify the number of significant documents, DCG_p is used to highlight extremely significant documents seeming promptly in the outcome list [9]

c) MAP (Mean Average Precision)

MAP calculates the Mean Average Precision of applicable documents recovered from a probe. MAP is computed as $MAP = \frac{1}{N} \sum_{j=1}^N \frac{1}{Q_j} \sum_{i=1}^{Q_j} P(doc_i)$ where, Q_j is amount of applicable documents for probe j , N is amount of probes and $P(doc_i)$ is accuracy value at i th applicable document [9].

V. RESULT AND DISCUSSIONS

The performance of our enhanced method was evaluated using the performance parameters namely: MAP (“Mean Average Precision”), NDCG@10 (“Normalized Discounted Cumulative Gain at 10 documents”) and P@10 (“Precision at 10 documents”). We compared the enhanced method with the current methods namely: LSI (“Latent Semantic Indexing”), CBA (“Concept Based Approach”) and QLM (“Query likelihood Model”). The novelty of the enhanced method is that, it concentrates more in solving grammar apprehension issues faced by non-clinical patients and their assistants by providing simpler terms for every clinical grammars found on the displayed clinical released documents and clinical probe results online.

The results outcome contained in Table I and Fig. 7 revealed that, the enhanced method managed to achieve 91% accuracy in all the metrics, as compared to existing Concept Based Approached (CBA) which scored 80%, Query Likelihood Model (QLM) scored 77% and the Latent Semantic Indexing (LSI) scored 73% in all the four datasets. This clearly indicates that, the enhanced method, better addressed the clinical information desires of non-clinical professionals and their assistants as it provides simpler translations for the entire clinical grammars found on clinical released documents and clinical probe results online.

Sample data were extracted from the four datasets used namely: Medical Subject Heading (MeSH), Metamap, Khresmoi project6 and Unified Medical Language System (UMLS) for the precise task of evaluating the performance of the current methods and the enhanced method. The enhanced method was developed in a manner that, it provides simpler translations for the entire clinical grammars seen on displayed clinical released documents and clinical probe results online. The outcome of the simulation results obtained using the sample data extracted randomly from the four datasets used in the experiment is as shown in Fig. 7 and Table I:

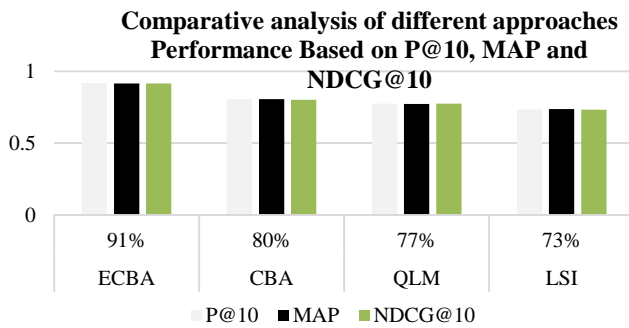


Fig. 7. Comparative Analysis of different Approaches Centered on MAP, NDCG@10 and P@10 Values.

TABLE I. A AMPLE SIMULATION RESULTS FOR ALL THE APPROACHES SHOWING THEIR ACCURACY PERCENTAGES USING THE MESH DATASET

APPROACH	ACCURACY (All Metrics) %	PERFORMANCE METRICS		
		P@10	MAP	NDCG@10
ECBA	91%	0.9170	0.9145	0.9156
CBA	80%	0.8058	0.8048	0.8020
QLM	77%	0.7746	0.7729	0.7743
LSI	73%	0.7336	0.7366	0.7313

Fig. 7 is the pictorial representation of the simulation results in Table I showing the performance of the current methods (QLM, CBA and LSI) and the enhanced method.

The experimental outcomes contained in Table I and Fig. 7 indicates that the enhanced method obtained a Precision@10 score of 0.9170, MAP score of 0.9145 and NDCG@10 score of 0.9156. Whereas, the three current approaches namely: Query Likelihood Model (QLM) obtained a Precision@10 score of 0.7746, MAP value of 0.7729 and NDCG@10 score of 0.7743, Latent Semantic Indexing (LSI) scored P@10 value of 0.7336, MAP score of 0.7366 and NDCG@10 value of 0.7313. And finally, the existing Concept Based Approach (CBA) scored a Precision@10 score of 0.8058, MAP value of 0.8048 and NCDG@10 value of 0.8020. The results indicates that the enhanced method better addressed the grammar apprehension problem faced by non-clinical professionals and their assistants while perusing through their clinical released documents and clinical search results online.

The enhanced method works statistically based on the integrating strategy: For all concepts $n \in [1, N]$ do, Set $SQ =$ query, that is, the entire medical grammars/words found in the search query would be searched for and extracted. $SQ = "SQ" + "CC_n"$, For the entire extension grammars $k \in [1, K]$, select all most specific concept terms. New $SQ = SQ \# "ET_k"$. N is the amount of grammars gotten from the core query, SQ signifies search query and CC_n represents the n th concept. K Signifies the amount of growth words while ET_k signifies the k th extension terms. The k th is the last extension concept in an extended query and the sign $\#$ signifies universal words. And the duo quote marks specifies that the thread contained must appear successively. The

statistical analysis also revealed that, in every 10 retrieved medical documents, the Enhanced Concept Based Approach (ECBA) precisely scored 0.9170 (91%) as retrieved appropriate and comprehensible documents in relation to P@10, as against the existing Concept Based Approach (CBA) which scored 0.8058 (80%), Query Likelihood Model (QLM) scored 0.7746 (77%) and finally the Latent Semantic Indexing (LSI) which scored 0.7336 (73%). In relation to NDCG@10, ECBA attained 0.9156 (91%), QLM scored 0.7743 (77%), LSI 0.7313 (73%) and CBA 0.8020 (80%) as appropriate and understandable retrieved documents and lastly in reference to MAP, ECBA Scored 0.9145 (91%), QLM scored 0.7729 (77%), LSI scored 0.7366 (73%) and CBA scored 0.8048 (80%).

VI. CONCLUSION

The investigational results attained in Fig. 7 and Table I obviously revealed that, in every 10 (100%) retrieved documents from a search query, the Enhanced Concept Based approach (ECBA) presents 91% as relevant and readable documents. While Latent Semantic Indexing (LSI), Query Likelihood Model (QLM) and the Concept Based Approach presents 73%, 77% and 80% as relevant and readable documents respectively. The logical reasons behind these outcomes gotten by ECBA, CBA, QLM and LSI can be elucidated by the results in Fig. 7 and Table I, where the proposed enhanced approach incorporated program modules that provides simpler interpretation for every clinical grammar found on the displayed clinical released documents and clinical probe results online.

The Enhanced method proved to better address the clinical grammar apprehension issues stumble upon by non-clinical professional patients and their assistants while reading through their clinical released documents and clinical search results online, as 91% of every retrieved information by the Enhanced method are relevant and readable, as against the Latent Semantic Indexing (LSI) 73%, Query Likelihood Model (QLM) 77% and Concept Based Approach (CBA) 80%. The Enhanced method outweighs the Latent Semantic Indexing, the Query Likelihood Model and the Concept Based Approach by 11% to 18% in respect to Precision@10 NDCG@10 and MAP values. These improved outcomes was realized due to the ability of the Enhanced method to provide simpler interpretation for every clinical grammar found on the clinical released documents and clinical search results online. The study recommends that advance work on this research work should comprise of designing models and algorithms that would address clinical grammar apprehension issues faced by non-clinical professionals and their assistants on retrieved videos, images and audios.

ACKNOWLEDGMENT

The authors wish to express their profound appreciation and gratitude to the management of Universiti Tun Hussein Onn Malaysia (UTHM) for funding the research. The research was funded under UTHM TIER-1 Grant with vot number H107 and Ministry of Education Malaysia under FRGS Grant with vot number K047.

REFERENCES

- [1] H. Ayatollahi et al., "Factors influencing the use of IT in the emergency department". A qualitative study, *Health Inf. J.* 16 (3) (2010) 189–200.
- [2] I. R. Bardhan and M. F. Thouin, "Health information technology and its impact on the quality and cost of healthcare delivery, *Decis*". *Support Syst.* 55 (2) (2013) 438–449.
- [3] J. Bassi and F. Lau, "Measuring value for money". A scoping review on economic evaluation of health information systems, *J. Am. Med. Inform. Assoc.* 20 (4) (2013) 792–801.
- [4] J. Barron et al., "Exploring three perspectives on feasibility of a patient portal for older adults, *Stud*". *Health Technol. Inf.* 202 (2014) 181–184.
- [5] S. Brahmandam et al., "Willingness and ability of older adults in the emergency department to provide clinical information using a tablet computer, *J*". *Am. Geriatr. Soc.* 64 (11) (2016) 2362–2367.
- [6] C. Bellegarda et al., "Concept-based medical document retrieval: THCIB at CLEF eHealth lab 2013 task 3". In: *Proceedings of the ShARe/CLEF eHealth Evaluation Lab.* (2013).
- [7] M. C. Beuscart-Zépher et al., "The human factors engineering approach to biomedical informatics projects". *State of the art, results, benefits and challenges, Yearb. Med. Inf.* 10 (2007) 9–27.
- [8] K. Cresswell et al., "Anything but engaged". User involvement in the context of a national electronic health record implementation, *Inform. Prim. Care* 19 (4) (2011) 191–206.
- [9] L. Dybkjaer et al., "An Overview of evaluation methods". *Evaluation of Text and Speech Systems in TREC Ad-hoc Information Retrieval and TREC Question Answering.* 2007, Springer, Dordrecht, the Nethe
- [10] Kontagora, I.U., Hamid, I.R.A. and Omar, N.A., "An Enhanced Concept based Approach for User Centered Health Information Retrieval to Address Presentation Issues". In *International Journal of Advanced Computer Science and Applications (IJACSA)*, 10(2), pp 232 – 242, 2019. <http://dx.doi.org/10.14569/IJACSA.2019.0100131>.
- [11] E. W. Ford et al., "Resistance is futile: but it is slowing the pace of EHR adoption nonetheless, *J. Am*". *Med. Inform. Assoc.* 16 (3) (2009) 274–281.
- [12] D. T. Ford, "Are electronic health records the future of dental practice?". *J. Calif. Dent. Assoc.* 43 (5) (2015) 238.
- [13] A. Fuad and C. Y. Hsu, "High rate EHR adoption in Korea and health IT rise in Asia, *Int*". *J. Med. Inf.* 81 (9) (2012) 649–650.
- [14] S. R. Greysen et al., "Tablet computers for hospitalized patients". A pilot study to improve inpatient engagement, *J. Hosp. Med.* 9 (6) (2014) 396–399.
- [15] T. Irizarry et al., "Curran, Patient portals and patient engagement". A state of the science review, *J. Med. Internet Res.* 17 (6) (2015) e148.
- [16] N. Ksentini et al., "Miracl at CLEF 2014: eHealth information retrieval task". In: *Proceedings of the ShARe/CLEF eHealth Evaluation Lab.*
- [17] C. S. Kruse et al., "The effect of patient portals on quality outcomes and its implications to meaningful use: asystematic review, *J.Med*". *Internet Res.* 17 (2) (2015) e44.
- [18] C. S. Kruse et al., "Patient and provider attitudes toward the use of patient portals for the management of chronic disease: a systematic review, *J. Med*". *Internet Res.* 17 (2) (2015) e40.
- [19] A. L. Kellermann and S. S. Jones, "What it will take to achieve the asyet-unfulfilled promises of health information technology, *Health Aff*". (Millwood) 32 (1) (2013) 63–68.
- [20] A. Kushniruk and C. Nøhr, "Participatory design, user involvement and health IT evaluation, *Stud*". *Health Technol. Inform.* 222 (2016) 139–151.
- [21] K. Dramé et al., "Query Expansion using External Resources for Improving Information Retrieval in the Biomedical Domain". In *CLEF (Working Notes)*, 2014, (pp. 189-194).
- [22] J. King et al., "Clinical benefits of electronic health record use". National findings, *HealthServ.Res.*49 (1pt.2), (2014) 392–404.
- [23] I. U. Kontagora and I. R. A. Hamid, "Comparative Studies of Information Retrieval Approaches in User-Centered Health Information System". In: Ghazali R., Deris M., Nawi N., Abawajy J. (eds) *Recent Advances on Soft Computing and Data Mining. SCDM 2018. Advances in Intelligent Systems and Computing*, vol 700. Pp 171 – 180. Springer, Cham.
- [24] A. Lee et al., "Root cause analysis of serious adverse events among older patients in the Veterans Health Administration, *Joint Comm*". *Res.* 40 (6) (2014) 253–262.
- [25] L. Goeuriot1 et al., "ShARe/CLEF eHealth Evaluation Lab 2015, Task 3". *Information Retrieval to Address Patients' Questions when Reading Clinical Reports.*
- [26] M. Maher et al., "A novel health information technology communication system to increase caregiver activation in the context of hospital-based pediatric hematopoietic cell transplantation". A pilot study, *JMIR Res. Protoc.* 4 (4) (2015) e119.
- [27] L. Nguyen et al., "Electronic health records implementation". An evaluation of information system impact and contingency factors, *Int. J. Med. Inf.* 83 (11) (2014) 779–796.
- [28] Office of the National Coordinator, What is a Patient Portal?, "Available from: (2017),<https://www.healthit.gov/providers-professionals/faqs/what-patient-portal>"
- [29] F. Pinciroli and C. Pagliari, "Understanding the evolving role of the Personal Health Record, *Compute*". *Biol. Med.* 59 (2015) 160–163.
- [30] E. Papoutsis et al., "Patient and public views about the security and privacy of electronic health records (EHRs) in the UK". Results from a mixed methods study, *BMC Med. Inform. Decis. Mak.* 15 (1) (2015) 1.
- [31] A. H. Pollack et al., "Leveraging physicians and participatory design to develop novel clinical information tools". *AMIA Annual Symposium Proceedings/AMIA Symposium AMIA Symposium.* 2016 (2016) 1030–1039.
- [32] M. Rigby et al., "Patient portals as a means of information and communication technology support to patient-centric care coordination—the missing evidence and the challenges of evaluation". A joint contribution of IMIA WG EVAL and EFMI WG EVAL, *Yearb. Med Inf.* 10 (1) (2015) 148–159.
- [33] W. J. Rudman et al., "Integrating medical and dental records". A new frontier in health information management, *J. AHIMA* 81 (10) (2010) 36–39.
- [34] J. J. Rodrigues et al., "Analysis of the security and privacy requirements of cloud-based electronic health records systems, *J. Med*". *Internet Res.* 15 (8) (2013) e186.
- [35] H. Suominen et al., "The Proceedings of the CLEFeHealth2012 – the CLEF 2012 Workshop on Cross-Language Evaluation of Methods, Applications, and Resources for eHealth Document Analysis". (2015), NICTA.
- [36] T. Schleyer et al., "Advancing oral medicine through informatics and information technology". A proposed framework and strategy, *Oral Dis.* 17 (s1) (2011) 85–94.
- [37] W. Shen et al., "An investigation of the effectiveness of concept-based approach in medical information retrieval GRIUM @ CLEF2014eHealthTask 3". In *Proceedings of the ShARe/CLEF eHealth Evaluation Lab,* (2014).

Microcontroller-based RFID, GSM and GPS for Motorcycle Security System

Kunnu Purwanto¹, Iswanto², Tony Khristanto Hariadi³, Muhammad Yusvin Muhtar⁴

Department of Electrical Engineering,
Universitas Muhammadiyah Yogyakarta,
Yogyakarta, Indonesia

Abstract—The crime level including motorcycle theft has been increasing. It occurs regardless the time and place. The owner of the motorcycle needs to ensure the security of his motorcycle by adding either manual or electronic lock. However, both the manual and electronic locks are still incapable to protect the motorcycle from the theft. Based on the problem, this research created an automatic motorcycle safety system, namely, germs narcissistic. Germs narcissist is the key innovation of automatic vehicle security using, GPS (global positioning system), and GSM (global system for mobile communication), and RFID (Radio Frequency Identification). This system was created by using short message service (SMS) to provide vehicle information such as time, position, and alarm informed to the owner of the motorcycle. The arrangement of the technologies can be used as a practical and effective safety key of motorcycle.

Keywords—Microcontroller; GPS; GSM; RFID; motorcycle

I. INTRODUCTION

A rampant motorcycle theft proves that the hospital's motorcycle security system is poor. The need for an additional security system is considered very necessary to avoid the theft. Such conditions require vehicle owners to pay more attention to the vehicle safety so that a good security system is needed.

Supporting the description of the case, many simple or advanced security tools for motorcycle have been developed. Several manufacturers have already provided such security systems such as keys to the motorcycle handle bar and alarm systems for four-wheel vehicles. However, the security systems provided by the manufacturers are less assuring in the recent modern era. There should be an additional security. Nasir & Mansor [1] developed security systems of two-wheeled vehicles with the use of technology. They created an automatic key for a two-wheeled vehicle by using a microcontroller. A security system for four-wheeled vehicles using wireless sensor network technology has been developed by Tang et al. [2] and Sehgal et al. [3] succeeded in developing a security system using SMS to track missing motor vehicles.

In this study, a Very Important Person (VIP) [4] model of security system is implemented. To outline, a VIP security model consists of several layers namely the first, the second, the third secure points and so forth. Two layers of security were applied. The first is Authentication method and the second is Point Positioning.

The authentication method is widely applied to many computer security systems whereas the Point Positioning

method is used in global positioning system. Rui Chen [5] applied authentication method for wireless network security system. Hameed et al. [6] used Point Positioning method to compare the accuracy of the data processing of global positioning system -online from some global positioning system data Processing services.

Basically, the principle of Authentication method is a method to access certain systems such as password [7], fingerprint, eye retina [8], face recognition [9], ID number (unique number) [10] and others. The study used the introduction of the ID number. By using RFID technology, there will be no duplication or same ID numbers.

A Point Positioning [11]–[13] method or also called an absolute method is the basic method in global positioning system which aims to obtain a position in real-time with good accuracy [14]–[16]. In the security system, a standard security system by applying the Authentication method is used as the first secure point. The motorcycle rider should first introduce his ID number to turn on the motor vehicle. The Global Positioning System (GPS) for tracking systems position by applying Point Positioning method [17]–[19] was used as the second secure point.

All systems are regulated by a single component, namely Microcontroller [12], [20], [21]. The controller of the systems is Radio Frequency Identification (RFID). By implementing the Authentication method, the security of the motorcycle is significantly improved because the rider must enter his ID number to unlock the handle bar and turn the engine on. By using Point Positioning method, the position can be identified in real-time with good accuracy. In addition, by applying the methods, the motorcycle owner can track the motorcycle position and turn the engine off when it is stolen.

The design of the security system places Arduino as the main controller in which there is a short message alert feature that provides information about the location of the motorcycle. The system is expected to be an innovative motorcycles security system.

II. RESEARCH METHOD

The design of double security system based on RFID would be applied to the motorcycle model that has a large trunk. The double security system is based on RFID as shown in Fig. 1. The system consists of two inputs, namely RFID and global positioning system sensors. The inputs are processed using a

microcontroller. The outputs are LED and LCD indicators. In addition, the system is also connected with a relay to turn off and turn on the engine. The Global System Mobile communication system is used by the system to contact vehicle owners. It is an open-loop control system. The control system refers to the detection output results provided by the Radio-frequency identification detection system. No feedback is provided for the correction process.

The interactive double security system for motorcycle based on RFID consists of several subsystems namely identification, detection, controllers, and output subsystems.

1) *Identification subsystem:* The identification subsystem conducts input identification. The RFID detection subsystem consists of RFID tag, RFID Reader and Microcontroller Arduino nodemcu as the main controller as shown in Fig. 2. The RFID tag issues data by using the Wi-Fi signal, and then the data are read by a Wi-Fi receiver using an RFID reader. The output of RFID reader data is read by the microcontroller using serial communication.

The figure shows that the RFID Reader reads the RFID identification data, and then send the RFID information to the Arduino nodemcu microcontroller.

2) *Detection subsystem:* Global positioning system detection subsystem consists of satellites, global positioning system Receiver and the Microcontroller Arduino nodemcu as the main controller [22]. It can be seen in Fig. 3 that the data from the satellite are received by the global positioning system receiver, then the global positioning system data are sent to the Arduino microcontroller to be processed into a longitude and latitude positions.

The satellite detects the presence of the global positioning system receiver and transmits the data in NMEA and GGA formats as information. The data are then sent to Microcontroller Arduino Nodemcu.

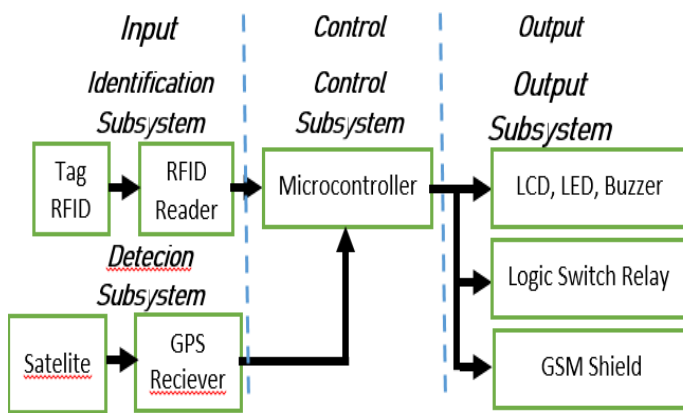


Fig. 1. Block Diagram of the Overall System.

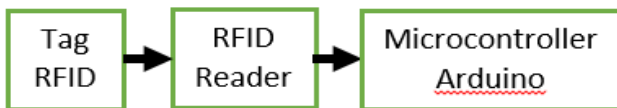


Fig. 2. Block Diagram of RFID Identification Subsystem.



Fig. 3. The Block Diagram of GPS Detection Subsystem.

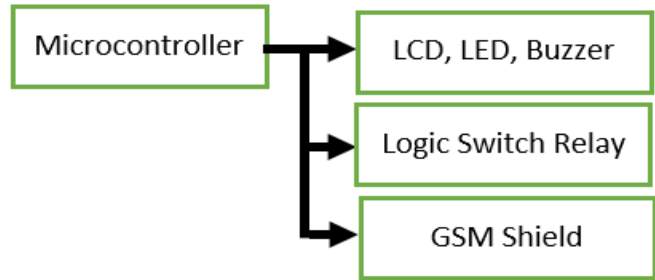


Fig. 4. The Block Diagram of GPS Detection Subsystem.

3) *Output subsystem:* Fig. 4 shows an output microcontroller consisting of Minimum Output [20], Relay Action [21] and Global System Mobile Communication subsystem. Lamp and alarm are mounted in the microcontroller output subsystem as indicators which indicate the input and a 16x2 LCD which indicates the data viewer output [22]. An action subsystem is a subsystem that serves as an ignition circuit connecting the two-wheel motor vehicles. It can be realized by using a Relay as the automatic switch.

Arduino Nodemcu microcontroller is capable of providing a high condition voltage of 5 volts initial output as a trigger to activate the relay so that the motor circuit ignition systems is possible to be connected to the vehicle key switch so that the ignition system will only be activated when the ignition relay and the circumstances are connected. A Global System Mobile communication subsystem serves as a tool that supports communication between the microcontroller and the vehicle owner's mobile phone. The LinkSprite ATWIN GSM Shield module compatible for Arduino Nodemcu microcontroller is used to realize the Communication subsystem. The GSM module requires ATcommand protocol to perform so that it should be described in the Arduino microcontroller program code.

III. RESULTS AND ANALYSIS

Tool and system tests were conducted in stages that examine each component/tool, the subsystems, and the overall system.

1) *Test on each component / tool function:* The test was conducted to avoid errors resulted from one of the components/tools which is not functioning by using digital multi-meter measurement tool and software for each device.

a) *Test on voltage source:* To determine the voltage capacity from the voltage source whether it could provide the voltage needed by the system, the voltage source test was conducted. The voltage source was connected to the voltage regulator circuit consisting of several components of the regulators such as IC 7805, IC 7809, and IC 7812 to adjust the requirements of the voltage on the system.

The test generated the error values calculated by the following formula:

$$\text{Error} = |\text{Ideal Voltage Value} - \text{Average Measured Voltage Value}|$$

b) *Test on tags and RFID reader:* Three units of Radio-frequency identification tags were carried out by using Radio-frequency identification Tester software. The Radio-frequency identification minimum circuit was connected to one unit of portable computer ACER 4752G. It would transmit the data contained in the Radio-frequency identification tag serially to the computer unit via a USB. In the first tag test, the data were obtained in tag1 number 8802570. In the second tag test, the data were obtained in tag2 number 8806445. In the third tag test, the data were obtained in tag3 number 7706262.

c) *Microcontroller nodemcu test:* The test aimed to determine the conditions of Microcontroller nodemcu whether it was in a good condition or not. Test main controller Microcontroller nodemcu was conducted by using software IDE (Integrated Development Environment) 1.0.5 Arduino. The microcontroller fitness could be determined by connecting it to the computer then upload the sample program to the Nodemcu by using the Arduino IDE software.

2) *Subsystem test:* The test was conducted to ensure that the subsystem was able to perform its function according to the needs of the system. The test was carried out on the detection subsystem, control subsystem and output subsystem, and then whether the output results were in accordance to the system or not was observed.

a) *Radio-frequency identification subsystem test:* In the subsystems test, an Radio-frequency identification Reader ID-12 LA, an Arduino nodemcu microcontroller unit, a series of minimum output systems, and an Arduino IDE 1.0.5 software were used. This test was conducted to identify the ability of Radio-frequency identification subsystem in reading RFID tags, transmitting the ASCII data information to the microcontroller Arduino nodemcu and displaying a series of Arduino IDE 1.0.5 software on the monitor. The Radio-frequency identification test using three card tags is shown in Table I. It can be seen that the Radio-frequency identification tag card has a universal number in the form of a Hexsa number.

3) *Test on global positioning system detection subsystem:* A CN-06 U-blox global positioning system Receiver, an Arduino Nodemcu microcontroller unit, a U-Center global positioning system Evaluation Software, computers, and an Arduino IDE 1.0.5 software were used in the test. Retrieval global positioning system data namely latitude and longitude data were taken at several points in inside and outside Muhammadiyah University area in Yogyakarta randomly. Global positioning system Detection Subsystem Test Results are presented in Table II. There are three global positioning system testing locations and each location has latitude and longitude data.

4) *Action relay subsystem test:* The test used a relay activator circuit, a 12 Volt voltage source, a Microcontroller Nodemcu, computers, and an Arduino IDE 1.0.5 software to determine the circuit performance as the switch connects and breaks the relay based on the instructions given by the main control of the Microcontroller. The command was affected by the input received from the computer via serial communication by using a USB. The relay subsystem test result is presented in table 3. The table shows the relay experimental data using the characters 0 and 1. Character "1" places the relay in connecting position to turn LED lights on, whereas the character "0" places the relay in disconnecting position so that the LED light off. When the character 0 was tested, the microcontroller logic was low so that the relay was off, but when the character 1 was tested, the microcontroller logic was high so that the relay was on.

5) *Test on GSM communications subsystem:* A microcontroller Arduino Nodemcu, SSCOM32E software, Arduino IDE 1.0.5 software, sim900 GPRS/GSM Shield module, a mobile phone, and a computer were used in the test. The test was conducted to ensure that the sim900 GPRS/GSM Shield module was able to realize the communication between the microcontroller Arduino with the mobile phone.

Linksprite sim900 GPRS/GSM Shield is a communication module compatible for microcontroller Arduino nodemcu. The module supports GSM service. sim900 GPRS/GSM Shield supports SMS (Short Message Service) in Text format and PDU (binary). The 900 MHz frequency of Sim900 GPRS/GSM Shield is very supportive to be used in Indonesia. Testing the characters in GPRS/GSM is shown in table 4. It can be seen that the characters AT+CMGS = "\+6285267897892\" is used for SMS and ATD characters +6285267897892 is used for a call.

6) *System test:* The test was performed on the operating system and the entire system by combining subsystems into a single integrated system. It was also performed to test the functionality of the system as shown in Fig. 5 and to observe the outputs or results of system operations. The system test is the test conducted after integrating the existing subsystems.

TABLE I. RESULTS OF IDENTIFICATION RFID SUBSYSTEM TEST

No	Tag	Data
1	Tag 1	2C006DF56CD8
2	Tag 2	6F008654833E
3	Tag 3	6F0086548439

TABLE II. TEST RESULTS OF GPS DETECTION SUBSYSTEM

No	Location	Data LATITUDE	Data LATITUDE
1	Location 1	-7.809535	110.320494
2	Location 2	-7.808446	110.321219
3	Location 3	-7.811648	110.321586

TABLE III. RESULT OF RELAY ACTION SUBSYSTEM TEST

No	Character	Microcontroller	condition Relay
1	0	Low	Off
2	1	High	On
3	0	Low	Off

TABLE IV. GSM COMMUNICATION TEST RESULTS

No	Character	Microcontroller
1	0	AT + CMGS = \"+6285267897892\"
2	1	ATD+6285267897892;

Table V shows a time delay for some of the actions given as a response to some of the condition listed in the table. The table shows that the system performs time delay to turn the relay and LCD on and to send SMS.

Preparation Time delay is a time delay that occurs when a new system is turned on. Delay time relay On is a time delay needed after the input conditions of RFID tag is correct and the key which was switched on to activate the relay. The delay time relay Off 1 was the delay needed after that was switched off to inactivate the relay. The delay time relay Off 2 was the delay needed after the input conditions of GSM character input are fulfilled to activate the relay. The system encountered a delay time of preparation by an average of 5.6 seconds after getting power from the voltage source. The system was able to response to the input conditions with the average time delay of 1.6 seconds.

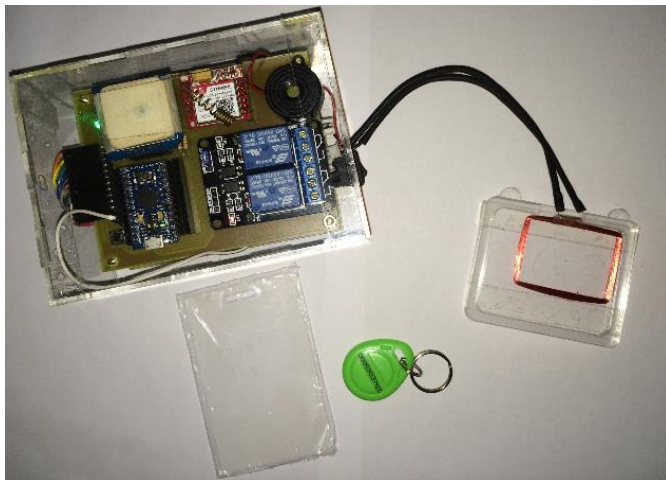


Fig. 5. System Realization.

TABLE V. SYSTEM TEST RESULTS

No	Input Media	Output Media	Output	Time delay
1	Subsystem RFID	Subsystem Relay	Relay On	1,2 ms
2	Subsystem GPS	Subsystem Microcontroller	LCD	1.6 ms
3	Subsystem GSM	Subsystem Microcontroller	SMS	2.1 ms

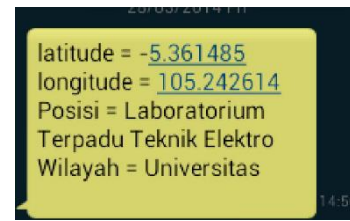


Fig. 6. SMS System Display on Mobile Phones of Vehicle users.

Table V shows the various input conditions and forms of action provided by the system. Microcontroller Arduino nodemcu provides the actions by connecting the Relay when the data of RFID tag are appropriate and making a phone call to the phone number registered. When the RFID tag data are corresponding, the vehicle is on. the microcontroller also sends information about the location of the vehicle in the form of a short message to the phone number listed as shown in Fig. 6.

IV. DISCUSSION

Based on the results of the tests that have been carried out on the systems for identification, detection, actions and communication, the results obtained is in accordance with the provisions of the system functionality. The system is able to distinguish RFID tags objects as the access key to the engine from ASCII data stored in the tag and then takes action by connecting a series of vehicle engines. The system is able to distinguish the incoming SMS characters through LinkSprite GSM Shield module and then takes action by replying to SMS providing vehicle position information so that the system is able to communicate with the mobile devices of the owner.

The identification, detection, and communication on the systems needs a series of communication process using the main data processor Microcontroller Arduino Nodemcu. The main data processor Microcontroller Arduino Nodemcu has a pair of pins of serial communication of data transmitter (Tx), and data receiver (Rx) in which it is capable only of communicating with the process of receiving data at one time. The system which has three serial communication process, namely, (RFID identification, detection of global positioning system and GSM communications) is needed. The need is fulfilled by using two pairs of fake pin serial addition utilizing the program code libraries "SoftwareSerial" and "AltSoftSerial". The Baud Rate of 9600 is used for the pin. Basically, fake pin serials have the same principle as the original serial pins discovered in the Arduino Nodemcu, but they work interchangeably in a very short time having the risk of accumulated delay time.

The results of the tests showed a time delay experienced by the system work is caused by several factors; one of those is the influence of environmental conditions such as building construction and weather capable of disrupting the state of signals for data communications and the effect of time delay program. The performance of the global positioning system receiver to receive data from satellites and transmit it to the microcontroller Arduino Nodemcu is deeply affected by the buildings construction that block the radio waves transmission between the global positioning system receiver and the satellites. The weather affects the performance of GSM Shield

in receiving the data in the form of a short message or a call during a loss of signal. The time delay in the program uploaded to the microcontroller is the major delay of the time delay value of the system.

V. CONCLUSION

Double security systems have been realized interactively on two-wheel motor vehicles and it is capable of distinguishing the RFID tag based on the ASCII data saved to turn on the vehicle and providing information about the vehicle location. The system is equipped with an emergency safety feature by utilizing GSM communication to turn off the machine when it is stolen. The accuracy of the information is affected by the time delay of the system and environmental conditions. To make the system effective, the time delay of the entire system can be tolerated with the average value of the preparation delay time of 5.6 seconds and average delay time of 1.6 s. That the voltage source system is in a good condition is shown by the error acquisition of 4,067% on the source system voltage.

REFERENCES

- [1] M. A. M. Nasir and W. Mansor, "GSM based motorcycle security system," in 2011 IEEE Control and System Graduate Research Colloquium, 2011, pp. 129–134.
- [2] V. Tang, Y. Zheng, and J. Cao, "An Intelligent Car Park Management System based on Wireless Sensor Networks," in 2006 First International Symposium on Pervasive Computing and Applications, 2006, pp. 65–70.
- [3] V. K. Sehgal, M. Singhal, B. Mangla, S. Singh, and S. Kulshrestha, "An embedded interface for GSM based car security system," Proc. - 2012 4th Int. Conf. Comput. Intell. Commun. Syst. Networks, CICSyN 2012, pp. 9–13, 2012.
- [4] Z. Yihua, "VIP customer segmentation based on data mining in mobile-communications industry," in 2010 5th International Conference on Computer Science & Education, 2010, pp. 156–159.
- [5] Rui Chen, "Research on security authentication of hierarchy distributed Wireless Sensor Network," in 2010 The 2nd International Conference on Computer and Automation Engineering (ICCAE), 2010, vol. 3, pp. 275–278.
- [6] S. A. Hameed, S. Abdulla, M. Ershad, F. Zahudi, and A. Hassan, "New automobile monitoring and tracking model: Facilitate model with handhelds," in 2011 4th International Conference on Mechatronics (ICOM), 2011, no. May, pp. 1–5.
- [7] B. Gurung, P. W. C. Prasad, A. Alsadoon, and A. Elchouemi, "Enhanced Virtual Password Authentication Scheme Resistant to Shoulder Surfing," in 2015 Second International Conference on Soft Computing and Machine Intelligence (ISCMCI), 2015, pp. 134–139.
- [8] T. R. Borah, K. K. Sarma, and P. H. Talukdar, "Retina recognition system using adaptive neuro fuzzy inference system," in 2015 International Conference on Computer, Communication and Control (IC4), 2015, pp. 1–6.
- [9] Bhagwat Keshav S. and Patil Pradeep M., "Face authentication using fusion of 3D Shape and Texture," in 2014 International Conference on Advances in Engineering & Technology Research (ICAETR - 2014), 2014, pp. 1–6.
- [10] Yi-Qi Gui and Jie Zhang, "A new authentication RFID protocol with ownership transfer," in 2013 International Conference on ICT Convergence (ICTC), 2013, pp. 359–364.
- [11] I. Iswanto, A. Ataka, R. Inovan, O. Wahyunggoro, and A. Imam Cahyadi, "Disturbance Rejection for Quadrotor Attitude Control Based on PD and Fuzzy Logic Algorithm," Int. Rev. Autom. Control, vol. 9, no. 6, p. 405, 2016.
- [12] R. Mubarak, D. V. Firmansyah, D. Haryanto, N. P. Apriyanto, U. Mahmudah, and I. Iswanto, "Motorcycle-Security using Position Searching Algorithm Based on Hybrid Fuzzy-Dijkstra," Indones. J. Electr. Eng. Comput. Sci., vol. 3, no. 2, pp. 468–474, 2016.
- [13] I. Iswanto, O. Wahyunggoro, and A. I. Cahyadi, "Hover Position of Quadrotor Based on PD-like Fuzzy Linear Programming," Int. J. Electr. Comput. Eng., vol. 6, no. 5, pp. 2251–2261, 2016.
- [14] Iswanto, O. Wahyunggoro, and A. I. Cahyadi, "Trajectory and altitude controls for autonomous hover of a quadrotor based on fuzzy algorithm," in 2016 8th International Conference on Information Technology and Electrical Engineering (ICITEE), 2016, pp. 1–6.
- [15] N. M. Raharja, E. Firmansyah, and A. I. Cahyadi, "Hovering Control of Quadrotor Based on Fuzzy Logic," Int. J. Power Electron. Drive Syst., vol. 8, no. 1, pp. 492–504, 2017.
- [16] T. P. Tunggul, A. Supriyanto, N. M. Z. R, I. Faishal, I. Pambudi, and Iswanto, "Pursuit Algorithm for Robot Trash Can Based on Fuzzy-Cell Decomposition," Int. J. Electr. Comput. Eng., vol. 6, no. 6, pp. 2863–2869, 2016.
- [17] Iswanto, O. Wahyunggoro, and A. I. Cahyadi, "Path planning of decentralized multi-quadrotor based on fuzzy-cell decomposition algorithm," in 7TH INTERNATIONAL CONFERENCE ON MECHANICAL AND MANUFACTURING ENGINEERING: Proceedings of the 7th International Conference on Mechanical and Manufacturing Engineering, Sustainable Energy Towards Global Synergy, 2017, pp. 0200601–02006010.
- [18] Iswanto, O. Wahyunggoro, and A. I. Cahyadi, "Trajectory and Altitude Controls For Autonomous Hover of a Quadrotor Based on Fuzzy Algorithm," in 2016 8th International Conference on Information Technology and Electrical Engineering (ICITEE), 2016, pp. 4–9.
- [19] I. Iswanto, O. Wahyunggoro, and A. I. Cahyadi, "3D Object Modeling Using Data Fusion from Laser Sensor on Quadrotor," in ADVANCES OF SCIENCE AND TECHNOLOGY FOR SOCIETY: Proceedings of the 1st International Conference on Science and Technology 2015 (ICST-2015), 2016, pp. 170001–1 – 170001–7.
- [20] A. N. N. Chamim, D. Ahmadi, and Iswanto, "Atmega16 Implementation As Indicators Of Maximum Speed," Int. J. Appl. Eng. Res., vol. 11, no. 15, pp. 8432–8435, 2016.
- [21] A. N. N. Chamim, M. H. Gustaman, N. M. Raharja, and Iswanto, "Uninterruptable Power Supply based on Switching Regulator and Modified Sine Wave," Int. J. Electr. Comput. Eng., vol. 7, no. 3, pp. 1161–1170, 2017.
- [22] T. P. Tunggul, A. Latif, and Iswanto, "Low-cost portable heart rate monitoring based on photoplethysmography and decision tree," in ADVANCES OF SCIENCE AND TECHNOLOGY FOR SOCIETY: Proceedings of the 1st International Conference on Science and Technology 2015 (ICST-2015), 2016, p. 090004.

Efficient Arnold and Singular Value Decomposition based Chaotic Image Encryption

Ashraf Afifi

Department of Computer Engineering
Computers and Information Technology college
Taif University, Al-Hawiya 21974, Kingdom of Saudi Arabia

Abstract—This paper proposes an efficient image encryption that is based on Arnold transform (AT) and the Singular value decomposition (SVD). The proposed method employs AT on a plain image to transpose all image pixels in the positions, then a diffusion process is applied to the resulted encrypted image via SVD decomposing into three segments. The decryption process aims to derive the plain image from the cipher image. Matlab simulation experiments are done to examine the suggested method. The achieved results show the superiority of the suggested approach with respect to encryption quality.

Keywords—Encryption arnold transform; singular value decomposition; chaotic image encryption

I. INTRODUCTION

Nowadays, the internet and multimedia networks have captured attention in information security researches. Encryption is employed to achieve security. Image encryption is used increasingly in military, communication networks, medical image applications [1-6].

The security of multimedia data which have a high relationship among neighboring pixels has drawn a great attention, recently. The conventional data encryption techniques like AES, IDEA, Triple-DES, and other symmetric ciphering techniques are well known but they may be unsuitable for efficient image ciphering [7].

The main characteristics of chaotic techniques are their high sensibility to control parameters and initial conditions, thus their features can be exploited for achieving the required cryptographic characteristics. In 1998, Fridrich suggested the primary public framework for chaos-based image ciphering. This framework is made up of diffusion and confusion mechanisms [8]. Firstly, the pixels of image are shuffled by employing a 2D chaotic map such as cat, baker, and standard maps. After that, the values of pixels are sequentially altered utilizing a specific discretized 1D chaotic map through the diffusion mechanism. The Fridrich's framework has been considered the most common architectures in different proposed chaos-based image ciphering techniques [9-11].

This paper is mainly focusing on the communications applications with high security levels using AT based SVD security schemes. This scheme is worked by transposing the plain image. Then, the original image will be independently AT then decomposed into three matrices via SVD.

The remainder of the paper has been organized as follows: Section 2 covers the methodology and the main tools employed

in the proposed method, namely the AT and SVD. Section 3 is devoted to detail the enciphering and deciphering phases of the suggested AT SVD image cipher. Section 4 explores the AT SVD of the image cipher detailed security study. Finally, Section 5 presents the conclusions.

II. METHODOLOGY

This section presents a literature survey on the AT and SVD which were used for image encryption method.

A. The AT

The AT is defined as the Cat's mapping [19]. It aims to shift the pixels' positions instead of changing their estimates. Recently, it was employed for image ciphering and watermarking [12-15]. The AT of a pixel (a, b) of an image $f(a, b)$ of size $N \times N$ pixels is defined by $f(a', b')$ and can be expressed mathematically:

$$\begin{bmatrix} a' \\ b' \end{bmatrix} = AT((a, b), N) = \begin{bmatrix} 1 & 1 \\ 1 & 2 \end{bmatrix} \begin{bmatrix} a \\ b \end{bmatrix} \pmod{N} \quad (1)$$

Where $\begin{bmatrix} a \\ b \end{bmatrix}$ and $\begin{bmatrix} a' \\ b' \end{bmatrix}$ represent the initial and the position of pixel of shifted image, respectively. 'Mod' defines the modular arithmetic operation. The parameter N is the target image size, which is used to determine the period of AT. The AT period is determined by [16]:

$$Period = \min\{p : [AT(f(a, b), N)]^p = f(a, b)\} \quad (2)$$

Where "min" defines the minimum value and p defines the number of iterations. The number of times AT is represented fixed at different values along with different N for improving the image ciphering security [20].

B. The SVD

The SVD is one of the best fit and reliable techniques for matrix decomposition employed in linear algebra. This analogous to the Hermite matrix or symmetry matrix employing a background of eigenvectors. Such method is not only efficient but also stable in decomposing the image into a collection of linearly independent segments, each of which has its energy contribution [17]. Regarding $m \times n$ matrix, orthogonal matrices U and V exist, each with $m \times n$ elements, respectively.

The SVD of X is defined as:

$$X = U * S * V^T \quad (3)$$

Where $S = \text{diag}(\sigma_1, \sigma_2, \dots, \sigma_\Gamma)$, where $\sigma_i, (i = 1, \dots, \Gamma)$ are the singular values of the matrix X with $\Gamma = \min(m, n)$ and satisfying $\sigma_1 \geq \sigma_2 \geq \dots \geq \sigma_\Gamma$.

The right singular vectors are the first columns of V and the left singular vectors are the first columns of U . The SVD technique can be applied in digital image cipher and watermarking. The image can be split into three segments then secure them in a variety of ways so that only at the time all the three image segments come together and are multiplied with the right order the information could be retrieved [18-20]

III. THE SUGGESTED AT-SVD CIPHERING METHOD

In this section, the suggested AT- SVD image cryptosystem will be defined in terms of two basic processes namely the encryption and decryption.

A. Encryption Process

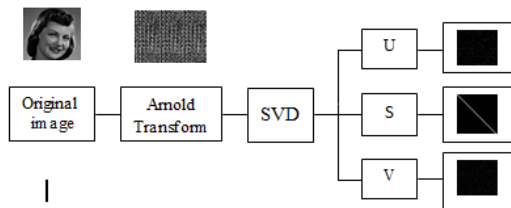
This process can be listed in the following steps:

- The clear image is independently shuffled employing the AT.
- The scrambled plain image is decomposed into three encrypted segments with SVD into USV as illustrated in Fig. 1(a).

B. Decryption Process

This process can be listed in the following steps:

- The three encrypted images are firstly multiplied by applying the SVD.
- The inverse AT is implemented to the resulted ciphered image to retrieve the decrypted image as illustrated in Fig. 1(b).



(a). AT-SVD Encryption Block Diagram.

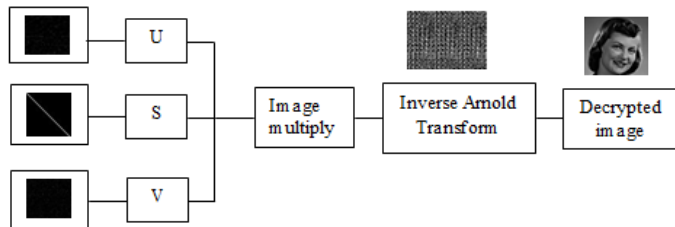


Fig. 1. AT-SVD Decryption Block Diagram.

IV. SIMULATION RESULTS AND PERFORMANCE ANALYSIS

Several measuring tests are carried out to examine the proposed AT- SVD image cryptosystem. Also, its performance is compared with the AT. Tests are performed using 512x512-sized Girl, Peppers and Baboon images as illustrated in Fig. 2.

The ciphering outcomes after employing the proposed AT-SVD image cryptosystem and conventional AT are shown in Fig. 3 Girl, Peppers and Baboon images respectively. It is shown that encrypting with the suggested AT- SVD image cipher succeeded in all images concealment in details.

A. Information Entropy

The information entropy determines the expected entropy value included for the ciphered image. The information entropy is defined as [21-23]:

$$H(K) = - \sum_{i=1}^{2^N-1} P(K_i) \log P(K_i) \quad (4)$$

where $P(K_i)$ represents the probability of symbol. It is shown that the image is good if it has a high estimation of entropy. The entropy information estimations for the cipher images uses the suggested AT- SVD image cipher and AT as depicted in Table I. The information entropy results, illustrate the efficiency of the suggested AT- SVD image cipher when compared to AT cipher. Finally, the entropy outcomes of ciphered image channels resulted by the proposed AT-SVD image cipher is the same with their comparing values in AT plain images.

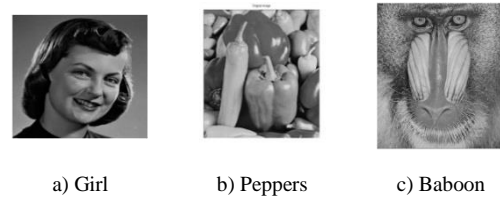


Fig. 2. Test Images - Girl, Peppers and Baboon.

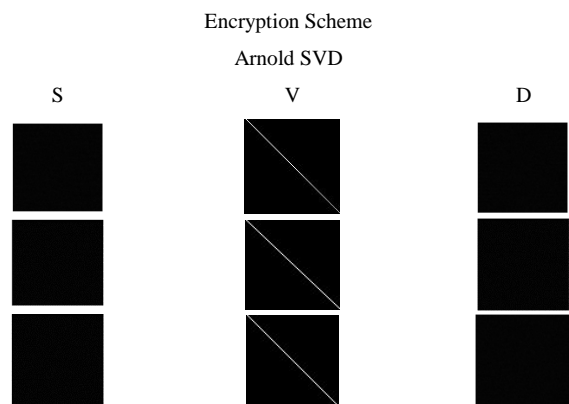


Fig. 3. Ciphered Results of Girl, Peppers and Baboon Images Employing Arnold and the Proposed Arnold SVD Image Cryptosystem.

TABLE I. ENTROPY OUTCOMES OF CIPHERED GIRL, PEPPERS AND BABOON IMAGES EMPLOYING ARNOLD AND THE PROPOSED ARNOLD SVD IMAGE CRYPTOSYSTEM

Image	Encrypted image with Arnold and Arnold SVD			
	Arnold	Arnold SVD		
		S	V	D
Girl	7.0818	4.5749	0.0329	3.1633
Peppers	7.5937	4.5775	0.0332	3.1732
Baboon	7.3583	4.5758	0.0296	3.1706

B. Histogram Test

The histogram test is performed to ensure that the suggested AT- SVD image cipher. For better encryption, the ciphered image’s histograms should be completely different from the plain image’s histograms. Fig. 4 illustrates the histograms of Girl, Peppers and Baboon images and the histogram of their ciphered versions. The histograms of ciphered Girl, Peppers and Baboon plain images are completely distinguishable from the Girl, Peppers and Baboon plain images histograms.

C. Encryption Quality Results

The correlation coefficient (Cc), the histogram deviation (D_H) and irregular deviation (D_I) and, are calculated for comparing the quality of different ciphered images. The correlation coefficient $r(I_{mg}, E_{nt})$ is estimated between the original and ciphered image that arranged like 1-D sequences as [21-23]:

$$r(I_{mg}, E_{nt}) = \frac{\text{cov}(I_{mg}, E_{nt})}{\sqrt{D(I_{mg})} \sqrt{D(E_{nt})}}, \tag{5}$$

$$\text{cov}(I_{mg}, E_{nt}) = \frac{1}{L} \sum_{l=1}^L (I_{mg}(l) - \text{Mean}(I)) (E_{nt}(l) - \text{Mean}(E_{nt})), \tag{6}$$

$$D(I_{mg}) = \frac{1}{L} \sum_{l=1}^L (I_{mg}(l) - \text{Mean}(I_{mg}))^2, \tag{7}$$

$$D(E_{nt}) = \frac{1}{L} \sum_{l=1}^L (E_{nt}(l) - \text{Mean}(E_{nt}))^2, \tag{8}$$

where L is the pixel numbers within the source image. The aim is to get small Cc estimations between the original image $I_{mg}(x_i, y_j)$ and cipher $E_{nt}(x_i, y_j)$ image. Table II shows the Cc estimates among the source image and encrypted image for AT and the suggested AT- SVD image cipher. The outcomes proof that the suggested AT-SVD image cipher achieve Cc values that are close to ones achieved by AT in Girl, Peppers and Baboon image. This archives the success of the proposed AT- SVD image cipher with respect to Cc experiment.

The D_H calculates the encryption quality between the source and the cipher images. The D_H can be computed as [21-23]:

$$D_H(I, E) = \frac{\left| \sum_{i=0}^{255} d(i) \right|}{M \times N}, \tag{9}$$

where $d(i)$ is the absolute difference amplitude value among the enciphered and the source image histograms of at level i . The estimates M and N resemble the plain image dimensions. The main object is to verify higher D_H value confirming the encrypted images are deviated from their corresponding image. Table III illustrates the D_H experiment calculations for the original and ciphered image using AT and the proposed AT- SVD image cipher. The results of the proposed AT- SVD image cipher give larger D_H values compared with Arnold.

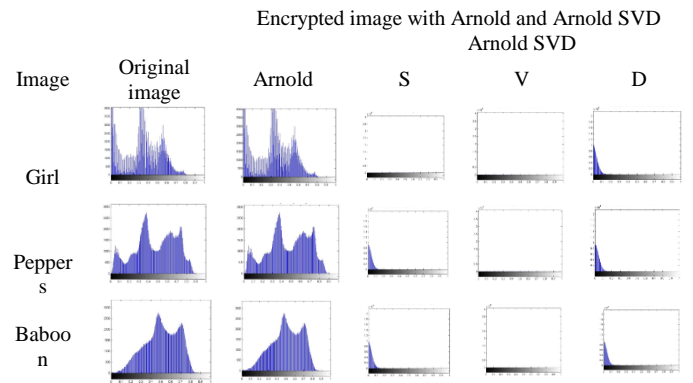


Fig. 4. Histogram Results of the Original Images and Encrypted using Proposed Arnold and Arnold SVD.

TABLE II. CC BETWEEN PLAIN AND ENCRYPTED IMAGES EMPLOYING SUGGESTED ARNOLD AND ARNOLD SVD

Image	Encrypted image with Arnold and Arnold SVD			
	Arnold	Arnold SVD		
		S	V	D
Girl	-0.0022	0.003167	-0.0015	-0.0013
Peppers	-0.0031	0.0015	-0.0025	0.0056
Baboon	-0.0093	0.0018	0.000829	-0.00538

TABLE III. HISTOGRAM DEVIATION BETWEEN SOURCE AND CIPHER IMAGES USING IMAGES USING PROPOSED ARNOLD AND ARNOLD SVD

Image	Encrypted image with Arnold and Arnold SVD			
	Arnold	Arnold SVD		
		S	V	D
Girl	0	1.5209	1.4610	1.3033
Peppers	0	1.8117	1.4978	1.5864
Baboon	0	1.9499	1.4985	1.7166

The D_I characterizes the encryption quality in terms of deviation outcomes [22-24]. The irregular deviation can be estimated as [22-24]:

$$D_I = \frac{\left| \sum_{l=0}^{255} h_d(l) \right|}{M \times N}, \quad (10)$$

$$h_d(i) = \left| h(i) - M \right|, \quad (11)$$

where the histogram of ciphered image at level i is $h(i)$, and M is the calculated average value for ciphered image an ideal consistent histogram. The main aim is to achieve lower D_I values that show a good quality of ciphered. Table IV show D_I estimates for AT and the suggested AT- SVD image cipher. The suggested AT- SVD image cipher has tiny Im_d values against AT which conforms their achieved encrypted quality.

D. Differential Result

The differential test measures how the cipher images with AT and our AT- SVD image cipher are affected by one-pixel modification. Two common measurements are used; unified average changing Intensity (UACI) and number-of pixels changing rate (NPCR). Assume two cipher images E_1 and E_2 having their source images with only one-pixel difference. In E_1 and E_2 , the pixel estimates at index (a_i, b_j) are $E_1(a_i, b_j)$ and $E_2(a_i, b_j)$, respectively. In bipolar array $D(a_i, b_j)$ with equal ciphered image sizes, the coefficients $D(a_i, b_j)$ are calculated with $E_1(a_i, b_j)$ and $E_2(a_i, b_j)$ values. If $E_1(a_i, b_j) = E_2(a_i, b_j)$, then $D(a_i, b_j) = 1$; otherwise $D(a_i, b_j) = 0$. The NPCR can be calculated as [24-25]:

$$NPCR(E_1, E_2) = \frac{\sum_{i,j} D(a_i, b_j)}{W \times H} \times 100\%, \quad (12)$$

Where, W and H correspond to the width and the height of the ciphered image. The UACI can be calculated as [22-24]:

$$UACI(E_1, E_2) = \frac{1}{M \times N} \left[\sum_{x_i y_j} \frac{E_1(a_i, b_j) - E_2(a_i, b_j)}{255} \right] \times 100\%, \quad (13)$$

TABLE IV. IRREGULAR DEVIATION BETWEEN SOURCE AND ENCRYPTED IMAGES USING IMAGES USING PROPOSED ARNOLD AND ARNOLD SVD

Image	Encrypted image with Arnold and Arnold SVD			
	Arnold	Arnold SVD		
		S	V	D
Girl	1.9844	1.9844	1.9839	1.9844
Peppers	1.9844	1.9844	1.9839	1.9844
Baboon	1.9844	1.9844	1.9833	1.9844

The UACI computes the mean intensity of difference among the two ciphered images. The outcomes of the NCPR and the UACI values are shown in Table V. The outcomes ensure that the proposed AT-SVD image cipher is too sensitive to little modifications, but the AT ciphering is less sensitive to small modifications in image.

E. Noise Immunity Measure

The robustness of the proposed AT-SVD image cipher in the AWGN existence is measured in the process of deciphering.

- The PSNR

The PSNR estimates the encryption image components. The PSNR is expressed as [24-25]:

$$PSNR(I, D) = 10 \log_{10} \frac{(255)^2}{\sum_{i=0}^W \sum_{j=0}^H [I(x_i, y_j) - D(x_i, y_j)]^2} \quad (14)$$

where, $I(x_i, y_j)$ and $D(x_i, y_j)$ are the gray level of the intensity value at location (x_i, y_j) of the original and decipher image, respectively. High PSNR estimates show good resistance to noise. The noise resistance values are given in Tables VI and VII. The outcomes prove that the suggested AT-SVD image cipher has good resistance to noise thus it can be a best choice for ideal telecommunication applications.

- The SSIM

The SSIM can be computed as [25]:

$$SSIM(x, y|w) = \frac{(2\bar{w}_x \bar{w}_y + V_1)(2\sigma_{w_x w_y} + V_2)}{(\bar{w}_x^2 + \bar{w}_y^2 + V_1)(\sigma_{w_x}^2 + \sigma_{w_y}^2 + V_2)} \quad (15)$$

TABLE V. ESTIMATIONS OF NPCR AND UACI FOR TWO ENCRYPTION IMAGES FOR TESTED IMAGES USING SUGGESTED ARNOLD AND ARNOLD SVD

Image		Encrypted image with Arnold and Arnold SVD			
		Arnold	Arnold SVD		
			S	V	D
Girl	NCPR	98.1594	100	24.5590	100
	UACI	0	0	0	0
Peppers	NCPR	99.9992	100	47.5876	100
	UACI	0	0	0	0
Baboon	NCPR	99.9935	100	52.7199	100
	UACI	0	0	0	0

TABLE VI. PSNR ESTIMATES OF IMAGES IN THE EXISTENCE OF AWGN WITH DIFFERENT SNR (SNR IN DB) USING ARNOLD SVD

Image	PSNR			
	AWGN			
	10 dB	20 dB	30 dB	40 dB
Girl	-11.3978	3.3322	7.6368	8.3292
Peppers	-18.9071	-1.8042	4.6188	5.6515
Baboon	-19.4560	-2.2318	4.3681	5.4727

TABLE VII. PSNR IMAGES ESTIMATES IN THE EXISTENCE OF AWGN WITH DIFFERENT SNR (SNR IN DB) USING ARNOLD SVD

Image	PSNR			
	AWGN			
	10 dB	20 dB	30 dB	40 dB
Girl				
Peppers				
Baboon				

where, V_1, V_2 are minor constants, \bar{w}_x and \bar{w}_y are the mean of w_x and w_y regions, respectively. $\Sigma_{w_x}^2$ is the variance of w_x region and $\sigma_{w_x w_y}$ is covariance among two regions w_x and w_y . The SSIM outcomes are given in Table VIII. The values prove that the suggested AT- SVD image cryptosystem has better resistance to noise.

• The FSIM

The FSIM permits to evaluate the deciphered image and can be defined as [25]:

$$FSIM = \frac{\sum_{x \in \Omega} B_L(x) \cdot PV_m(x)}{\sum_{x \in \Omega} PC_m(x)} \quad (16)$$

where Ω is the special domain of image, $B_L(x)$ corresponds the overall equivalance between $PV_m(x)$ and two images is phase congruency value. Large FSIM values make the noise immunity better. The FSIM measures outcomes are given in Table IX. The results prove that the AT- SVD image cryptosystem is noise resistant.

TABLE VIII. SSIM ESTIMATES IN THE EXISTENCE OF AWGN WITH DIFFERENT SNR (SNR IN DB) USING ARNOLD SVD

Image	Structure Similarity Index (SSIM)			
	AWGN			
	10 dB	20 dB	30 dB	40 dB
Girl	$9.085 \cdot 10^{-6}$	$3.662 \cdot 10^{-4}$	0.0048	0.0337
Peppers	$1.058 \cdot 10^{-6}$	$9.065 \cdot 10^{-5}$	$4.74 \cdot 10^{-4}$	0.0022
Baboon	$9.77 \cdot 10^{-7}$	$9.659 \cdot 10^{-5}$	$2.769 \cdot 10^{-4}$	0.0010

TABLE IX. FSIM ESTIMATES IN THE EXISTENCE OF AWGN WITH DIFFERENT SNR (SNR IN DB) USING ARNOLD SVD

Image	Structure Similarity Index (FSIM)			
	AWGN			
	10 dB	20 dB	30 dB	40 dB
Girl	0.0029	$3.66 \cdot 10^{-4}$	0.1645	0.5218
Peppers	$8.76 \cdot 10^{-4}$	0.0167	0.0845	0.2653
Baboon	$8.858 \cdot 10^{-4}$	0.0183	0.0783	0.1992

V. CONCLUSION

An efficient chaotic encryption of images based on AT and SVD is the main finding of this paper. In the proposed technique, the plain image is submitted to AT confusion and SVD diffusion. For the decryption phase, the cipher image segments are composed by the SVD diffuser and then inversely transformed by AT in order to derive the original image. A set of experiments have been performed in order to test the AT-SVD image cryptosystem. The obtained outcomes prove the efficiency of the suggested AT- SVD image cipher.

REFERENCES

- [1] R. Tao, J. Lang, Y. Wang, "Optical image encryption based on the multiple parameter fractional Fourier transform," *Opt. Lett.* 33, pp. 581–583, 2008.
- [2] H.M. Ozaktas, A. Koc, I. Sari, M.A. Kutay, "Efficient computation of quadratic phase integrals in optics," *Opt. Lett.* 31, pp. 35–37, 2006.
- [3] Z. Liu, S. Liu, "Randomization of the Fourier transform," *Opt. Lett.* 32, pp. 478–480, 2007.
- [4] Z. Liu, S. Liu, "Double image encryption based on iterative fractional Fourier transform," *Opt. Commun.* vol. 275, pp. 324–329, 2007.
- [5] Chengqing L, Shujun L, Asim M, Nunez J, Alvarez G, "On the security defects of an image encryption scheme", *Image Vis comp.*; 2781371-81, 2009.
- [6] Chengqing L, Lo K., "Optimal quantitative cryptanalysis of permutation-only multimedia ciphers against plaintext attacks", *Signal Process*, 91:949-54, 2011.
- [7] Li, S., Chen, G., Zheng, X.: Chaos-based encryption for digital images and videos. In: Furht, B., Kirovski, D. (eds.) *Multimedia Security Handbook*. CRC Press, Florida (2004).
- [8] J. Fridrich, "Symmetric ciphers based on two-dimensional chaotic maps," *International Journal of Bifurcation and Chaos in Applied Sciences and Engineering*, vol. 8, no. 6, pp. 1259–1284, 1998.
- [9] R. Ye, H. Huang, Application of the Chaotic Ergodicity of Standard Map in Image Encryption and Watermarking, *I. J. Image, Graphics and Signal Processing*, 19–29, 2010.
- [10] H. Liu, X. Wang, Color image encryption using spatial bit-level permutation and high-dimension chaotic system, *Optics Communications*, 284, 3895–3903, 2011.
- [11] R. Ye, A novel chaos-based image encryption scheme with an efficient permutation-diffusion mechanism, *Optics Communications*, 284, 5290–5298, 2011.
- [12] ZJ, Liu, I, Xu, T, Liu, H, Chen, P.F, Li, C, Lin, S.T., Liu. *Optics Communications* 284,123, 2011.
- [13] W. Chen, C, Quan, C.J, Tay, *Optics Communications* , pp. 282-3680, 2009.
- [14] X.P,Deng, D.M, Zhao, *Optics Communications*, pp. 284-5623, 2011.
- [15] Z.J, Liu,M, Gong Y.K, Dou, F, Liu , S, Lin, M.A, Ahmed, J.M, Dai, S.T. S.T. Liu, *Optics and Lasers in Engineering*, pp. 50-248, 2012.
- [16] Vilardy JM, Torres CO, Jumenez, C "Double image encryption method using the Arnold transform in the fractional Hartley domain" *Proc SIE* 8785, [87851R-87851/SR], 2013.
- [17] Bhatnagar G, Wu QMJ, Raman B., "SVD –based robust watermarking using fractional cosine transform, *DPIE*, 7708, 1-11, 2010.
- [18] Gaurav B, Bhatnagar, Q.M, Jonathan WU, "Selective image encryption based on pixels of interest and singular value decomposition" *DSP journal*, vol. 22,648-663, 2012.
- [19] Linfei Chen, Daomu Zhao, Fan Ge, "Image encryption based on singular value decomposition and Arnold transform in fraction domain" *Optics communication journal*, vol. 291, 98-103, 2013.
- [20] Phool Singh, A.K.. Yadav, Kehar Singh, "Phase image encryption in the fractional Hartley domain using Arnold transform and singular value decomposition" *Optics and Laser in Engineering journal*, vol. 91, 187-195, 2017.

- [21] Andrew B. Watson, "Image Compression Using the Discrete Cosine Transform", Technical Report, NASA Ames Research Center, *Mathematica Journal*, 4(1), 1994, p. 81-88, 1994.
- [22] J. Fridrich, "Symmetric Ciphers Based on Two-dimensional Chaotic Maps," *International Journal of Bifurcation and Chaos*, vol. 8(6), pp. 1259-1284, 1998.
- [23] Osama S. Faragallah, "Digital Image Encryption Based on the RC5 Block Cipher Algorithm," *Sensing and Imaging: An International Journal*, vol. 12(3), pp. 73-94, Springer, 2011.
- [24] Osama S. Faragallah, "An Enhanced Chaotic Key-Based RC5 Block Cipher Adapted to Image Encryption," *International Journal of Electronics*, vol. 99(7), pp. 925-943, Taylor & Francis, 2012.
- [25] Ensherah A. Naeem, Mustafa M. Abd Elnaby, Hala S. El-sayed, Fathi E. Abd El-Samie, and Osama S. Faragallah, "Wavelet Fusion for Encrypting Images with Few Details", *Computers and Electrical Engineering*, vol. 60, pp. 450-470, 2016

AUTHOR'S PROFILE



Ashraf Afifi received the B.Sc.(Hons.), M.Sc., and Ph.D. degrees in Electronic and Communication Engineering from Zagazig University, Egypt, in 1987, 1995, and 2002, respectively. He is currently Associate Professor with the Department of Computer Engineering, Faculty of Computers and Information Technology, Taif University, Saudi Arabia.

He is a coauthor of about 35 papers in international journals and conference proceedings. His research interests cover communication security, image processing, and image encryption.

Finding Attractive Research Areas for Young Scientists

Nouman Malik¹, Hikmat Ullah Khan², Muhammad Ramzan³, Muhammad Shahzad Faisal⁴, Ahsan Mahmood⁵

Department of Computer Science, COMSATS University Islamabad, Attock, Pakistan^{1, 5, 4}

Department of Computer Science, COMSATS University Islamabad, Wah Cantt, Pakistan²

School of Systems & Technology, University of Management and Technology, Lahore³

Department of Computer Science and IT, University of Sargodha, Sargodha, Pakistan³

Abstract—The selection of the research area is very vital for new researchers. One of the major issues for researchers is the selection of the domain of research on which he/she can carry out research. This case is very vital on the grounds that it decides the future of the researchers in that research area. Finding hot and attractive research areas is not considered in the relevant literature of Scientometrics. In this regard, the correct decision of the selection of the research domain helps the researchers to show better performance as well gain a good academic career. The main aim of this research study is to figure out the attractive research areas for the researchers, especially who are at the starting stage of their research life. To the best of our knowledge, this research area is still very limited due to limited work done in this area. So in order to distinguish the attractive research field for the new researchers, new rising fields are identified by applying the well-known g-index, which is widely used for finding the top authors in academic networks. In addition, we compute diverse, relevant features of the research fields which help us to identify top research area. The results demonstrate that the proposed methodology is capable to recommend the attractive research fields for potential future research work. An extensive empirical analysis has been carried out using the widely used academic database of DBLP.

Keywords—Research field; scientometrics; attractive areas; g-index

I. INTRODUCTION

In the field of Research one of the basic thing is to choose a field of interest for research purpose that also determine the future of a scientist. In the initial stages of the research, the research finds a particular research field that is among particular other research field, but sometimes, researchers find it pretty hard to find a research area that is related to their interest and that is overall an attractive research field for the research community. Some topics are popular, but not attractive, some topics are very attractive, but doesn't guarantee more citations. While there is a race for better research topics by the research community, one of the most important issues of the emerging researchers is to choose a topic that is an attractive topic in the domain in which they are working.

While the research searches for a research topic, they want their research area to be attractive. Attractiveness is an important word and most of the research wants their area to be attractive. In this regard, researchers try to find attractive research areas. Usually papers with shorter titles are more

attractive than the paper with the longer titles [1]. Similarly, there are other ways that make a paper attractive. In this regard, researchers proposed many techniques to identify the attractiveness of the research papers [2]. In this regard, authors collaboration with the other authors also plays an important role in the attractiveness of the [3]. While author collaboration, paper titles, readability and other factors play an important role in the attractiveness of the paper our task in this paper is to identify yet another method that find attractive research areas. For this purpose, G-index is used. As G-index is an improved method and it computes the productivity of the science, it performs better and gives better results.

The ultimate objective of this paper is to provide the new researchers with some ideas of new attractive research fields. This way they will have a list of some attractive fields that relate to their interests so they can work in the field of their interest that is an attractive research area for the research community. Sometimes, if the chosen research area is not an attractive research idea it may result in a low number of citations and difficult publication by the quality journals because these days' journals also try to publish papers that are attractive for the research community. So we propose a method on the basis of G-index that finds the attractive research areas for the users. The findings will help the new scientists finding new attractive fields for their research. This in return sometimes provides more citations and easy publication in the quality journals.

The rest of the paper is divided as follows: Section II discusses the related work in the field of Scientometrics; Section III discusses the proposed Research Methodology; Section IV discusses the findings of the research paper while the paper is concluded in the next section.

II. RELATED WORK

In this section, we discuss the important research work done in the field of Scientometrics to rank the journals, rank the important research areas and conferences.

Although in the recent research, researchers didn't highly focus on finding attractive research fields, there are some research works that are based on similar works. Lee proposed a method on the basis of co-word analysis to find out the trends in publications [4]. However, the research in this field is halted due to the non-availability of the keyword analysis approach available for this domain [5]. Therefore, having a proper

dataset available for this task is as important as the field itself because it's really hard to find relevant workable dataset for this research area.

In this regard, different focuses have been made by the researchers including co-citation approaches to find the trending research areas [6] and different sort of ranking algorithms to rank the important research areas [7]. Similarly, researchers also ranked Conferences on the basis of index and other properties [8] and also used other kind of indexes to rank the authors and journals like Ds index [9]. The researchers also proposed solutions for emerging researchers to help them find the useful topics that produce impactful research papers [2]. Researchers also used social network ranking measures to rank the authors [10].

In this field, many researchers focused on only journals and authors. However, there are some scientists who focused on the characteristics of the research its self like they ranked the journals, conferences, authors stats, publishers, etc. According to Bogdan et.al, Importance of different conferences also play an important role in the ranking of the research [11]. Similarly, the researchers also proposed the problems and discontent in the journal ranking system [12].

In this field as our focus is to extract the attractive research areas one of the main tasks is also to rank the journals and conferences. Different approaches have been used in this field. one of the recent approach is to rank journals on the basis of clustering and scaling techniques [13]. Other than that many researchers have worked to compare the difference between very known terms in the field of research. And how it impacts the actual outcome of the research and attractiveness of the topic [14]. With the help of these calculations it will become easy to predict the hot and attractive research areas and how research fields correlate well with actual scientific research trends[15].

In order to find the attractive research areas, we focus on using G-index for finding the attractive research fields among the papers. As G-index solves most of the problems in the H-index, G-index works better and usually results in better results.

III. RESEARCH METHODOLOGY

The proposed research methodology is divided into four steps. Each step contains a number of sub-steps. In the first step, the data is extracted and processed. For this purpose, the dataset is prepared, the dataset is classified and data is preprocessed. In the second step, Taxonomy of the dataset is calculated using the IEEE and ACM taxonomy by extracting the computer science domain words and then extraction of all the papers related to the computer Science. For this purpose, 3 level hierarchical taxonomy is extracted. In the third step, attractive research areas are computed by using G-index and other features this step consist of four parts including recent article extraction, article impact extraction, journals reputation computation and author's influence computation. In the fourth step the research output is evaluated by finding the topic sensitive extensions and journals output is evaluated. The proposed framework for this research is given in Fig. 1.

A. Problem Statement

The problem statement consists of multiple steps, in the first steps research work is evaluated, then the journal's reputation is evaluated, then the articles are classified, then attractive research areas are identified, these steps are given in the form of a statement below:

On the basis of this analysis a subset $A^{pi} \subseteq A$ and the researchers who have articles p^i where the research fields belonging to $F^{pi} \subseteq F$, and each author a^j has a number of papers $P^{aj} \subseteq P$ while each of the research fields F^n contains a subset of papers $P^{fn} \subseteq P$. So the above scenario can be given in the form of a graph as shown in the Fig. 2.

So this shows that our ultimate goal is to identify research areas F that are actually attractive research areas for author's a^j for whom the metrics G_v^{aj} receive low values for this purpose, for this purpose, a special score is introduced S^{fn} for each field. Therefore, the problem consists of two sub-problems, first calculation of G_v^{aj} to evaluate the value of a^j and G_u^{bi} to evaluate the value of b^i .

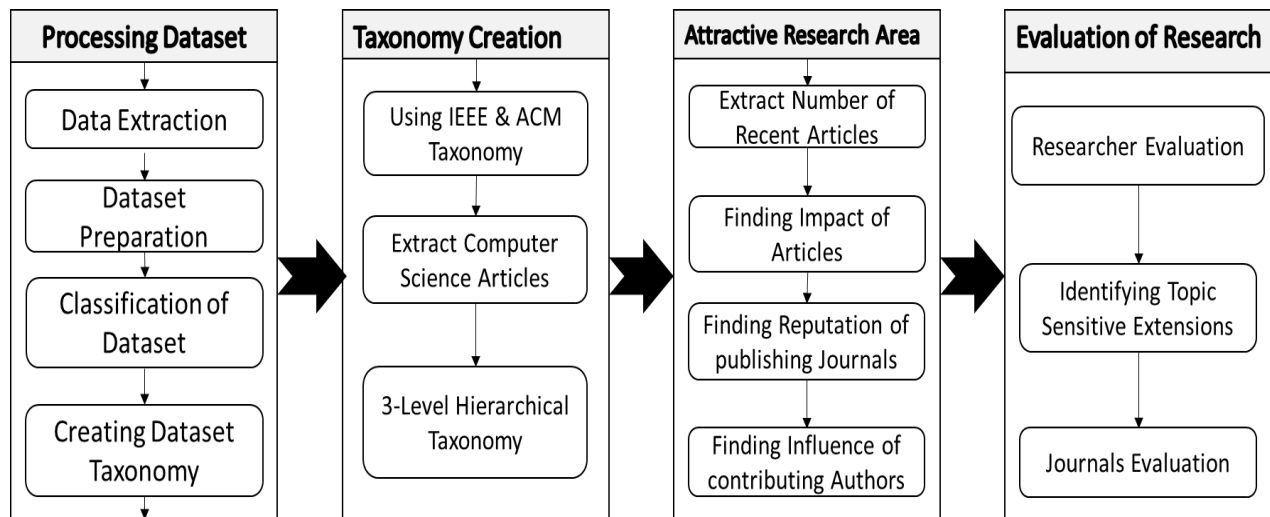


Fig. 1. Proposed Framework of Research.

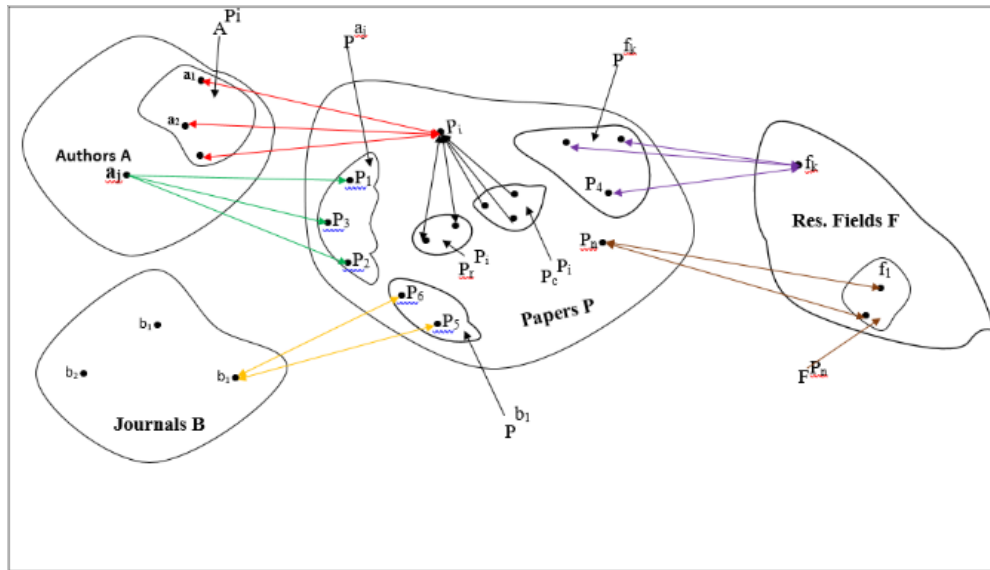


Fig. 2. Graph Representation of Connected Universe.

B. Dataset and Taxonomy

In the first step data set is collected, extracted, preprocessed and taxonomies are computed on the basis of IEEE and ACM taxonomy.

C. Research Evaluation

After classifying the dataset, reputed scientists are computed. For this purpose, G-index is used. In Table 1 contains the summarized information of G-index.

D. Identify Prestigious Journals

The next important step is to find the prestigious journal. This will help in finding the particular topics published in their journals and their importance. The main reason behind finding, identifying Prestigious Journal's so that if we are able to calculate that and if the number of articles on a particular topic is published in those journals. We noted that using h-index metrics for journal is not a good way due to its limitations. Therefore, G-index is used to evaluate the importance of a journal. This also computes if the impact of the journal is increasing with time or not.

E. Popular Research Areas

After computing the prestige journals, the popular research areas are computed using the popularity measures. For this purpose, well known journals and their articles are used. Equation 1 shows the method of computing the popular research areas. In this equation S^{fn} is special score, F^n is an arbitrary research area, P^{fn} are the papers belong to f^n , P^i is an arbitrary paper, P^{pi} are papers referred by P^i authors who created P^i .

TABLE I. SUMMARY OF THE METRICS FOR EVALUATING THE WORK OF A SCIENTIST

V	Symbol	Meaning
1	G_v^{aj}	G-index for authors
2	G_μ^{bi}	G-index for journals

$$S_{1,y}^{fn} = |P_Y^{Fn}| + \sum_{i=1}^{|P^{Fn}|} |P_{C,Y}^{Pi}| + \sum_{i=1}^{|P^{Fn}|} |A^{Pi}| \tag{1}$$

F. Attractive Research Areas for New Scientists

Finally, the attractive research areas are calculated from the data. In this regard one important thing to note is that not all attractive fields are popular and not all the popular fields are attractive. In other words, popularity and attractiveness are two different things.

The attractiveness of a research is computed by using the equation as shown in Equation 2. According to the equation 2, S^{fn} is special score, F^n is an arbitrary research area, P^{fn} are the papers belong to f^n , P^i is an arbitrary paper, P^{pi} is the set of the papers referred by P^i authors who created P^i , B^i is an arbitrary Journal, h^{bi} is the metrics evaluating the prestige of b^i , Y^i is the year of publication, A^j is an arbitrary Author, D_s^{aj} is a metric evaluating work of an author then the attractiveness of a research area can be given as shown in the Equation 2.

$$S_{2,v,\mu}^{fn} = \sum_{i=1}^{|P^{fn}|} \frac{|P_c^{Pi}| G_\mu^{bi}}{(\Delta Y_i)^\delta} \left(\sum_{j=1}^{|A^{Pi}|} \frac{\lambda}{G_v^{aj}} \right) \tag{2}$$

From Equation 1 and Equation 2 a scoring formula to evaluate the criteria can be given as shown in the Equation 3.

$$S_{3,v,\mu}^{fn} = \sum_{i=1}^{|P^{fn}|} \frac{G_\mu^{bi}}{(\Delta Y_i)^\delta} \left(\sum_{x=1}^{|P_c^{Pi}|} \frac{1}{(\Delta Y_x)^\delta} \sum_{j=1}^{|A^{Pi}|} \frac{\lambda}{G_v^{aj}} \right) \tag{3}$$

IV. RESULTS AND DISCUSSIONS

This section discusses the results and findings of the research. According to our findings we computed the top journals, authors, etc. We discuss the details of each field.

To the best of our knowledge, there is no publically available dataset for the taxonomy. Therefore, in order to manage the records, after extraction and preprocessing of the dataset it was required to manage the dataset in terms of domains and sub-domains. Therefore, we used IEEE taxonomy for this purpose. This helps us identifying the papers according to their titles and relevant matches in the IEEE taxonomy. We

have expelled repeated articles and those which were surrendered by the ideal meta-data, e.g. authors, journal or date of publication). At the end, 429,398 Articles were filtered out to form one data set. For the classification of data set, we will use the taxonomy of IEEE and will segregate articles in 1168 research fields.

Table II shows Top 30 authors using G-index. According to the results, Xiaoou Tang is the top author according to the G-index while the results clearly shows that g-index is a more productive way to find the top authors because of its structure of computing the productivity. Similarly, Jian Sun, Athanasios V. Vasilakos and other are among the top authors according to the G-index results.

Similarly, Table III shows the Top 15 journals according to the G-index. The results show that “Computer Vision and Pattern Recognition” is the top journal according to its G-index while some more popular journals are not among the top journals. The results show that in some cases, more citations doesn’t guarantee the quality of a journal.

TABLE II. TOP 30 AUTHORS USING G INDEX

Authors Name	g-index	Citations
Xiaoou Tang	19	321
Jian Sun	18	301
Athanasios V. Vasilakos	16	202
Pushmeet Kohli	16	137
Rob Fergus	15	116
Yoshua Bengio	15	163
Yi Ma	15	149
Jeffrey G. Andrews	15	137
Jitendra Malik	15	136
Andrea Vedaldi	15	118
Xuelong Li	14	178
Fabrizio Benevenuto	14	119
Florent Perronnin	14	121
Patrick Pérez	14	135
Shuicheng Yan	13	105
Axel Legay	13	103
Xiaogang Wang	13	101
Ajith Abraham	13	114
Hervé Jégou	13	107
Thomas Pock	13	97
Ruslan Salakhutdinov	13	110
Shahram Izadi	13	108
Jiawei Han	12	111
Guiwu Wei	12	99
Guanrong Chen	12	103
Min Chen	12	106
Constantine Caramanis	12	102
Nanning Zheng	12	119
David Parker	12	100
Carsten Rother	12	106

TABLE III. TOP 15 JOURNALS USING G-INDEX

Venue	Citations	G index
computer vision and pattern recognition	3862	40
European conference on computer vision	3237	38
Expert Systems With Applications	2136	36
Information Sciences	1536	39
IEEE Transactions on Information Theory	1350	35
Neuroimaging	1324	33
international conference on machine learning	1159	35
soft computing	1125	34
national conference on artificial intelligence	1080	33
Pattern Recognition	1063	31
Neurocomputing	1056	28
IEEE Transactions on Signal Processing	1048	27
IEEE Transactions on Image Processing	1037	25
human factors in computing systems	1024	22
international conference on robotics and automation	1018	21

After finding the top authors and journals, the most attractive fields are calculated according to the $S_{2,u,v}^{fn}$. According to the results, Information systems are the most attractive research area. When we take a look at the current research trends we find a number of the top papers and a huge number of authors work on these top attractive fields. Similarly, topics like Cloud computing, Computer vision, clustering, etc. are also among the top attractive fields according to the computed results. The results are given in Table IV.

TABLE IV. RANKING OF THE MOST ATTRACTIVE FIELDS OF RESEARCH ACCORDING TO THE S SCORE

FIELDS	$S_{2,u,v}^{fn}$
Information systems	3876.67
Design	3757.71
Clustering	3502.77
Metrics	2994.54
Cloud computing	2898.46
Architectures	2495.53
Reliability	1695.12
Modes of Computation	1529.73
Computer vision	755.45
Ontologies	726.69
Process management	444.84
Use cases	407.24
Principal component analysis	349.26
E-learning	314.84
Optimization algorithms	288.79
Visual analytics	286.93
Virtual reality	238.05
Object detection	236.50
Network structure	182.36
Semi-supervised learning	140.32

TABLE V. RANKING OF THE MOST ATTRACTIVE FIELDS OF RESEARCH ACCORDING TO THE S^{fn} SCORE

FIELDS	$S_{3,u,v}^{fn}$
Design	317140175.4
Information systems	221320024.1
Clustering	149408805.1
Scheduling	147660053.1
Machine learning	136784635
Cloud computing	117475456.7
Metrics	76569737.89
Reliability	70164301.07
Cryptography	62359568.67
Smartphones	40330966.19
Virtual reality	38987674.02
Computer vision	36799319.45
E-learning	33101525.04
Computational geometry	31443517.04
Architectures	26015802.42
Ontologies	21223968.58
Network security	20525337.71
Multimedia information systems	13862564.98
Reconfigurable computing	12633623.18
Real-time systems	10901137.37

Table V shows results according to $S_{3,u,v}^{fn}$. According to these results, Design is the top research field. Similarly, the fields like Information system, clustering, scheduling is also among the top fields computed by the system. All these fields are attractive research fields according to the modern research areas.

V. CONCLUSION

In this paper, we examined the issue of identifying attractive research areas for new scientists. Since in the modern scientific age, with the presence of a huge number of research topics, this is an issue, we first identified each of the fields one by one. We recognize the top authors by G-index and then find the top journals according to G-index. Similarly, by using these results, the Top most popular research areas are computed. Similarly, the attractive research areas are computed by further processing of the previous results. For this purpose, we introduced two scoring patterns and combined multiple different factors into these patterns. In this work, the strategy for evaluating the work of the scientists, we presented the usage of G-index. This index is performing better than the H-index that only check the number of citations and number of

papers. This G-index computes the productivity of the papers and journals by using a much better procedure.

Our strategies have been confirmed tentatively by utilizing a vast set of self-crawled research articles. The examinations gave some significant findings: The first is that there are exist some research areas which in spite of their popularity, they are not attractive for researchers who are presently beginning of their research career. Then again, some research fields are unpopular be that as it may; they give fantastic open doors at these researchers.

REFERENCES

- [1] F. Habibzadeh and M. Yadollahie, "Are Shorter Article Titles More Attractive for Citations? Cross-sectional Study of 22 Scientific Journals," *Croat. Med. J.*, vol. 51, no. 2, pp. 165–170, Apr. 2010.
- [2] L. Akritidis, D. Katsaros, and P. Bozanis, "Identifying attractive research fields for new scientists," *Scientometrics*, vol. 91, no. 3, pp. 869–894, Jun. 2012.
- [3] H. Hou, H. Kretschmer, and Z. Liu, "The structure of scientific collaboration networks in Scientometrics," *Scientometrics*, vol. 75, no. 2, pp. 189–202, Dec. 2007.
- [4] W. H. Lee, "How to identify emerging research fields using scientometrics: An example in the field of Information Security," *Scientometrics*, vol. 76, no. 3, pp. 503–525, Sep. 2008.
- [5] R. L. Ohniwa, A. Hibino, and K. Takeyasu, "Trends in research foci in life science fields over the last 30 years monitored by emerging topics," *Scientometrics*, vol. 85, no. 1, pp. 111–127, Oct. 2010.
- [6] S. P. Upham and H. Small, "Emerging research fronts in science and technology: patterns of new knowledge development," *Scientometrics*, vol. 83, no. 1, pp. 15–38, Apr. 2010.
- [7] A. Sidiropoulos and Y. Manolopoulos, "Generalized comparison of graph-based ranking algorithms for publications and authors," *J. Syst. Softw.*, vol. 79, no. 12, pp. 1679–1700, Dec. 2006.
- [8] M. Farooq, H. U. Khan, T. Iqbal, and S. Iqbal, "An index-based ranking of conferences in a distinctive manner," *Electron. Libr.*, Feb. 2019.
- [9] M. Farooq, H. U. Khan, S. Iqbal, E. U. Munir, and A. Shahzad, "DS-Index: Ranking Authors Distinctively in an Academic Network," *IEEE Access*, vol. 5, pp. 19588–19596, 2017.
- [10] F. Bibi, H. U. Khan, T. Iqbal, M. Farooq, I. Mehmood, and Y. Nam, "Ranking Authors in an Academic Network Using Social Network Measures," *Appl. Sci.*, vol. 8, no. 10, p. 1824, Oct. 2018.
- [11] B. Vasilescu, A. Serebrenik, T. Mens, M. G. J. van den Brand, and E. Pek, "How healthy are software engineering conferences?," *Sci. Comput. Program.*, vol. 89, Part C, pp. 251–272, Sep. 2014.
- [12] J. R. F. Arruda et al., "The Journal Impact Factor and its discontents: steps toward responsible metrics and better research assessment," *Open Scholarsh. Initiat. Proc.*, vol. 1, no. 0, Apr. 2016.
- [13] C. J. A. Bradshaw and B. W. Brook, "How to Rank Journals," *PLOS ONE*, vol. 11, no. 3, p. e0149852, Mar. 2016.
- [14] H. Kianifar, R. Sadeghi, and L. Zarifmahnoudi, "Comparison between impact factor, Eigenfactor metrics, and SCImago journal rank indicator of pediatric neurology journals," *Acta Informática Médica*, vol. 22, no. 2, p. 103, 2014.
- [15] N. Yamashita, M. Numao, and R. Ichise, "Predicting Research Trends Identified by Research Histories via Breakthrough Researches," *IEICE Trans. Inf. Syst.*, vol. E98.D, no. 2, pp. 355–362, 2015.

Improvement in Classification Algorithms through Model Stacking with the Consideration of their Correlation

Muhammad Azam¹, Dr. Tanvir Ahmed², Dr. M. Usman Hashmi³, Rehan Ahmad⁴, Abdul Manan⁵, Muhammad Adrees⁶, Fahad Sabah⁷

Department of CS&IT, The Superior College, Lahore, Pakistan^{1, 2, 3, 5, 6, 7}
Department of Computer Science, The University of Lahore, Lahore, Pakistan⁴

Abstract—In this research we analyzed the performance of some well-known classification algorithms in terms of their accuracy and proposed a methodology for model stacking on the basis of their correlation which improves the accuracy of these algorithms. We selected; Support Vector Machines (svm), Naïve Bayes (nb), k-Nearest Neighbors (knn), Generalized Linear Model (glm), Latent Discriminant Analysis (lda), gbm, Recursive Partitioning and Regression Trees (rpart), rda, Neural Networks (nnet) and Conditional Inference Trees (ctree) in our research and performed analyses on three textual datasets of different sizes; Scopus 50,000 instances, IMDB Movie Reviews having 10,000 instances, Amazon Products Reviews having 1000 instances and Yelp dataset having 1000 instances. We used R-Studio for performing experiments. Results show that the performance of all algorithms increased at Meta level. Neural Networks achieved the best results with more than 25% improvement at Meta-Level and outperformed the other evaluated methods with an accuracy of 95.66%, and altogether our model gives far better results than individual algorithms' performance.

Keywords—Classification algorithms; model stacking; correlation; k-nearest neighbor; pre-processing; meta classifiers

I. INTRODUCTION

Text classification is a method of allocating certain categories to text documents based on certain criterion. Number of classification algorithms in data mining is used to classify the appropriate class or category for text document on the basis of input algorithm used for classification. Many text classification methods are developed for efficiently solving the problem of identifying and classifying data.

The massive increase in the data being collected by information devices, needs for doing data mining and analyses on this big data, there is a need for scaling up and improving the performance of traditional data mining and learning algorithms. There exist some learning techniques with a purpose to construct a meta-classifier by joining some classifiers, usually by ensembles, voting or stacking, generated on the same data and increase the performance of algorithms [1] [2]. Grouping of the predictions of base-level classifiers with the consideration of their correlation, together with the correct class values constitute a meta-level dataset. This is the type of meta-learning which is an advanced form of stacking is addressed in this paper.

The exertion presented in this research is set in the stacking structure. Note that combining classifiers with stacking is be considered as meta-learning whereas Meta-learning means learning about learning, in practice, meta-learning takes as input results formed by learning and generalizes on them. The proposed technique can be done with tasks; (1) selection and learning of an appropriate classifier; (2) combination of predictions of base-level classifiers on the basis of correlation; (3) learning of Meta Classifiers

We proposed an extension of stacking, using an extended set of meta-level features. We show that the extension performs better than existing stacking approaches and selecting the best classifier by cross validation. The best among state-of-the-art methods is stacking with Neural Networks (nnet).

The remainder of this paper is organized as follows. Section 2 consists of literature review and surveys some other recent classification and stacking approaches and their results. Section 3 introduces our extension to stacking with correlation: the use of an extended set of meta-level features and classification via different models at the meta-level. The setup for the experiments and results of best classifiers is described in Section 4. Section 5 discusses the conclusions and future work.

II. LITERATURE REVIEW

Text widely held in a short form, which is generally used in real-time systems like news, short comment, micro-blog and numerous other fields. With the advancements in the uses of text messages, emails, online information, product reviews and movie reviews etc., data is increasing more and more. Most of the data is unusable for us while other data is important for us. So, it is required to extract the useful data from the big data. But there are number of complications with the classification of short text, for example it has irregularity, fewer features and so on.

Classification is one of the tasks most frequently carried out by so-called Intelligent Systems. Thus, a large number of techniques have been developed based on Artificial Intelligence (Logic-based techniques, Perceptron-based techniques) and Statistics (Bayesian Networks, Instance-based techniques). The goal of supervised learning is to build a concise model of the distribution of class labels in terms of predictor features. The resulting classifier is then used to assign

class labels to the testing instances where the values of the predictor features are known, but the value of the class label is unknown. This paper describes various classification algorithms and the recent attempt for improving classification accuracy-ensembles of classifiers [3].

Ensemble method is an approach to generate classifiers by applying dissimilar learning algorithms to a single dataset [4] complicated methods for combining classifiers are typically used in this setting. Model stacking is often used to learn a combining method in addition to the ensemble of classifiers [5]. To encounter the issues in classification, Jun Xiang et al. proposed a method in which they pretreated the dataset first, and then selected the important features. They used semi-supervised learning technique and Support Vector Machines (SVM) to improve the previous methods with a large number of short text datasets. They also showed a good improvement in their experimental results [6].

Prof. Purvi Rekh and Hiral Padhiyar have been attentive to the problem of short words that are used in SMS as “hpy” for “happy”, “bday” for “birthday” which decreases classification accuracy; they showed that replacement of such words with full forms, better accuracy can be achieved. They used Decision tree Algorithm for classification of SMS data as it gives better accuracy than other classifiers. But still replacing all probable short words for the given word dynamically by the full form is an issue [7].

Naïve-Bayes and k-NN classifiers are two machine learning approaches for text classification. Rocchio is the classic technique for text classification in information retrieval. Based on these three methods and using classifier combination methods, Behzad Moshiri et al. proposed a new method in text classification. This is a supervised technique in which documents are characterized as vectors and each component of the vector is connected with a particular word. They proposed voting techniques, Decision Template and OWA operator process to combine the classifiers. Their experimental results showed that the approaches decreased the error in classification to 15% whereas they used training data from 20 newsgroups dataset [8].

C.Karthika et al. proposed another text document classifier by combining the nearest neighbor classification (knn) approach with the Support Vector Machines (SVM). The objective of this study suggested SVM-NN method is to decrease the effect of parameters in classification accuracy. At training level, the SVM is applied to decrease the training samples for each of the class to their support vectors (SVs). The SVs from different classes are then used as the training data of nearest neighbor in which the distance function or similarity measures is used to calculate the which category does the testing data fits. This method also reduced time consumption [9] [24]. Another research presents a technique for enhancement explicitly intended to work with Twitter data with consideration of their structure, length and specific language; a kind of sentiment analysis. The approach used is simply extendible to other languages and capable enough to process the tweets in real time. They showed that using the training models produced with the technique described can

increase the performance of sentiment classification, regardless of the domain and distribution of the test sets [10].

Another technique for improvement in accuracy of classification algorithms is ensemble method. Ensemble of classifiers, or a logical grouping of different classifiers, frequently results in improved classifications as compare to a single classifier. Though, the question about what classifiers should be selected for a given condition to create an ideal ensemble has been debated time and again. Furthermore, this technique is often computationally expensive since it requires the implementation of multiple classifiers for a single task. To provide solution of these problems, Dan Zhu et al. proposed a hybrid method for choosing and merging the models to build ensembles by incorporating Data Envelopment Analysis and stacking. Their results show the effectiveness of the proposed approach [11].

R. Mousavia et al. proposed improved Static Ensemble Selection (SES) using NSGA-II multi-objective genetic algorithm called; SES-NSGAI. The first technique in its first phase selects the best classifiers with their combiner, by immediate optimization of error and diversity objectives. In the second phase, the Dynamic Ensemble Selection-Performance (DES-P) is upgraded by using the suggested technique of first phase. The other proposed method in this research is a hybrid methodology that uses the abilities of both SES and DES methodologies and is called Improved DES-P (IDES-P). So, combining static and dynamic ensemble approaches with using NSGA-II. Results of this research approve that the proposed techniques outperform the other ensemble methods in terms of classification accuracy over 14 datasets [12].

Georgios Paliouras et al. examined the efficiency of voting and stacking. A new framework is suggested that put up famous methodologies for information extraction (IE) using stacking. To generate a meta-level data set that consists of feature vectors they performed cross-validation on the base-level data set, which contains text documents marked with related information. A classifier is then learned using the new vectors. Hence, base-level IE methods are combined with a common classifier at the meta-level. Findings of this research show that both voting and stacking are improved while using probabilistic estimates by the base-level methods. Stacking, showed consistently effective over all domains with comparably or better than voting and at all times improved than the best base-level methods [13].

Combined classification methods mutually infer all classes of a relational data set, by means of the inferences about any class label to affect inferences about related class. Kou and Cohen introduced an effective relational model on the basis of stacking that has comparable accuracy to more refined and combined inference approaches. While using experiments on both real and synthetic data, they showed that the main reason for the performance of the stacked model is the reduction in favoritism from learning the stacked model on inferred classes rather than true classes. Moreover, they revealed that the performance of the combined inference and stacked models can be recognized to an implied weighting of local and relational features at learning stage [14].

Fatemeh Nemati Koutanaeia et al. have established a three stage hybrid data mining model of feature selection and ensemble learning classification algorithms. The first stage, deals with the data collection and pre-processing. In the second stage, four Feature Selection (FS) algorithms are employed which include principal component analysis (PCA), genetic algorithm (GA), information gain ratio, and relief attribute evaluation function. Parameters setting of FS techniques is based on the accuracy resulted from the execution of the support vector machine (SVM) algorithm. Then after choosing the suitable model for every selected feature, they are applied to the base and ensemble algorithms. At this stage, the best FS algorithm with its parameters setting is specified for the next stage which is; modeling of the proposed model. At third stage, the algorithms are employed for the dataset prepared from each FS algorithm. The findings of this research showed that in the second stage, PCA is the best FS algorithm. In the third stage, the classification results indicated that the artificial neural network (ANN) adaptive boosting (AdaBoost) method has higher accuracy [15]. Some other researchers who worked for the improvement of classification algorithms used Genetic Algorithms (GAs) [16] which combine survival of the fittest among string structures with a structured yet randomized information exchange to form a search algorithm. These algorithms have been used in machine learning and data mining applications [17], [18]. GAs has also been used in optimizing other learning techniques, such as neural networks [19].

Riyaz Sikora et al. proposed a “modified stacking ensemble machine learning algorithm using genetic algorithms”. They used data sets for their study taken from the UCI Data Repository. Five learning algorithms were used in the stacking algorithm: J48, Naïve Bayes, Neural Networks, IBk, and OneR. The best enhancement in performance was on the Chess set, where the modified stacking algorithm was able to increase the prediction accuracy by more than 10% compared to the standard stacking algorithm. The training time is also considered for both versions of the stacking algorithm. On average the modified stacking algorithm takes more time than standard stacking algorithm as it encompasses running the GA. They also proposed that training time can be significantly reduced by running the individual learning algorithms in parallel [20].

KaiquanXu et al. proposed a novel graphical model to extract and visualize comparative relations between products from customer reviews, with the interdependencies among relations taken into consideration, to help enterprises discover potential risks and further design new products and marketing strategies [22].

III. DATASETS

As stated earlier we tested our proposed methodology to three pre-available datasets, IMDB Movie Reviews, Amazon Products Reviews, Yelp dataset. This section discusses these datasets in detail.

A. Scopus

The bibliographic data retrieved from the Scopus for the purpose of analysis. The data contains all types of documents

published by institutes of Pakistan during 1996 to 2010. The data of each document includes author names, title, abstract, date, document type, addresses, and cited references etc. Since this study is focused on improvement in accuracy of classification algorithms and the subjected dataset is very big, we precisely extracted and analyzed the data of abstracts of publications from Scopus for some selected categories like; Computer Science, Medicine, Engineering, Agricultural & Biological Sciences and Mathematics.

B. IMDB Movie Reviews

This is a dataset for binary sentiment classification containing substantially more data than some other benchmark datasets. The core dataset contains 50,000 reviews divided evenly into 25000 train and 25000 test sets. The overall distribution of labels is balanced (25000 positive and 25000 negative). It also includes an extra 50,000 unlabeled reviews for unsupervised learning. The whole collection, does not allow more than 30 reviews for any given movie because reviews for the same movie to have associated ratings. Additionally, the training and testing sets are comprised of non-overlapping set of movies. Whole dataset has been labeled with “neg” or “pos” labels for negative and positive reviews respectively, a negative review has a score ≤ 4 out of 10, and a positive review has a score ≥ 7 out of 10. Reviews with neutral category are not included in the train/test sets. We selected 10,000 reviews (5,000 positive and 5,000 negative) in our analysis as per machine constraints.

C. Amazon Products Reviews

It comprises of sentences labeled with positive or negative sentiment, extracted from products reviews. Format: sentence \t score \n whereas the score is either 1 (for positive) or 0 (for negative). The sentences come from website: amazon.com there exist 500 positive and 500 negative sentences. Once again for this dataset, sentences that have a clearly positive or negative connotation have been selected; the goal was for no neutral sentences to be selected.

D. Yelp Dataset

This dataset contains sentences labelled with positive or negative sentiment, extracted from reviews of different restaurants Format: sentence \t score \n whereas the score is either 1 (for positive) or 0 (for negative). The sentences come from website: yelp.com there exist 500 positive and 500 negative sentences. As in earlier datasets the goal was for no neutral sentences to be selected this dataset also contains sentences that have a clearly positive or negative connotation.

IV. TOOLS

Getting data in structured form, preparation of data for analysis and performing analysis on data we used different tools. Tools allow various definitions, ranging from an extension of classical data mining to texts to more sophisticated formulations like “the use of large online text collections to discover new facts and trends about the world itself” [21]. Following sections discuss the tools we used during our research:

A. Text Collector

Text collector is a tool which integrates number of text files into single file of any format; .txt, .csv etc. By using this tool we converted the IMDB movie reviews dataset from .txt files into single .csv file.

B. RStudio

RStudio is an integrated development environment (IDE) for R. It includes a console, syntax-highlighting editor that supports direct code execution, as well as tools for plotting, history, debugging and workspace management. RStudio is available in open source and commercial editions and runs on the various operating systems or in a browser connected to RStudio Server or RStudio Server Pro RStudio is a tool which includes other open source software components. RStudio provides the facility to execute R code directly from the source editor. It easily manages multiple working directories using projects. RStudio has an integrated R help and documentation and interactive debugger to diagnose and fix errors quickly.

RStudio is the tool that we used for the preprocessing of data and classification of publications using different algorithms and improvement in efficiency of algorithms. RStudio includes other open source software components and libraries which includes number of predefined functions and algorithms. We used some of these functions and algorithms in our research.

V. METHODOLOGY

The following sections, discuss data set creation, feature creation from text, feature selection, base classifiers, and learning methods along with the experimental design we proposed and used for our analysis.

A. Proposed Model

This paper proposed a hybrid approach based on supervised learning techniques to improve the accuracy of some predictive models pre-available for text classification. Basically it is a

kind of model ensembling with combining different models using stacking with consideration of separate model's correlation and base classifier's accuracy to allow combined predictor to get best from each model. On the basis of existing algorithms in R and correlation between these algorithms we propose the hybridization of algorithms. The algorithms were chosen on the basis of diversity of their correlation and accuracy.

As shown in Fig. 1 the subjected method is concerned with combining multiple classifiers generated by using different classification algorithms on the basis of their correlation on a single dataset S at a time. Initially a set of base-level classifiers C1, C2, . . . , CN is generated. Then, a meta-level classifier is learned using combined outputs of the base-level classifiers with actual classes and the testing dataset without class attribute.

In our proposed Hybrid Classification Algorithm; first three steps of this algorithm refers to the arrangement and pre-processing of data. The running time for these three steps depends upon the algorithm & tool used to get data structured & split data to train & test form. But on the whole, it does not affect the overall running time of this algorithm as the dominating steps for complexity of this algorithm are from 7 to 10. As far as steps 5 & 6 are concerned the running time is $\Theta(n(g_i(n)))$ where $g_i(n)$ refer to running time of classifier i. It can be different for deferent classification techniques e.g. running time for knn, is $O(n)$ which is also discussed later in this section. Step 7 runs $((n - 1) - 1 + 2)$ times i.e n times while step 8 runs $n(n - (i + 1) + 2)$ times i.e. $n(n - i + 1)$ time & step 9 runs $n(n - i + 1)(n - 1 + 2)$ times i.e. $n(n - i + 1)(n + 1)$ times while step 10 runs $n(n - i + 1)(n + 1)g_i(n)$. So total running time after execution of first three times.

$$T(n) = n(g_i(n)) + n + n(n - i + 1) + n(n - i + 1)(n + 1) + n(n - i + 1)(n + 1)g_i(n) \tag{1}$$

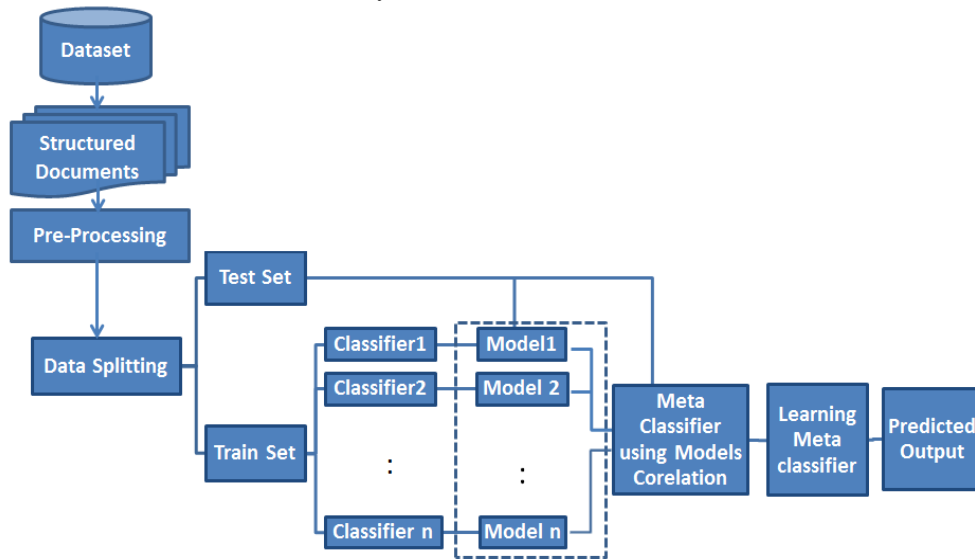


Fig. 1. Proposed Model for Text Classification.

Algorithm

Hybrid Classification (DataSet, v(m)[], fr [] [] [])

1. Begin
2. Structure Documents
3. Pre-processing Steps
4. Data Splitting to train & Test Sets
5. For i=1 to n
6. v [i] = cl [i] (Train set, test set)
7. For i=1 to n-1
8. For j = i+1 to n
9. For k=1 to n
10. Fr [i] [j] [k] = cl [k] (v [i], v [j], test set, actual class)
11. End

The simplified mathematical form of running time for steps 5 to 10 can be expressed as;

$$T(n) = O(n^3 gi(n)) \tag{2}$$

Where gi (n) refers to the running time if kth classifier i.e. cl [k] this is a general form as gi(n) refers to the running time of individual classifier at that particular execution time. We can be specific by taking an example of knn Classifier

KNN Algorithm

1. Begin
2. Input x of unknown classification
3. Set k, i < n
4. Iniznlize i = 1
5. Do Until (k = nearest neighbours to x found)
6. Compute distance for x to x,
7. if (i < k) then
8. include x_i in set of k- nearest neighbour
9. else if (x_i classes to x than any previous nearest neighbour) then
10. Delete the further nearest neighbours
11. include xi in the set of K- nearest neighbour
12. End if
13. End Do
14. initialize i = 1
15. Do until (x assigned membership in all classes)
16. Compute Ui (x)
17. increment i
18. End Do
19. End

This algorithm shows Pseudo code of knn Algorithm from step 2 to 4, The time complexity is O (1) step 5 until step 13 has time complexity O(n) time 14- has O(1). Step 15 until step 18 has O (n). So that running time is

$$T(n) = O(1) + O(n) + O(1) + O(n) = O(n) \tag{3}$$

So time complexity for knn Algorithm is O (n). When we use knn ask meta classifier the time complexity for hybrid classification algorithm become i.e.

$$T (n) = O (n^3 gi(n)) \tag{4}$$

$$O (n^3 (O (n)) = O (n^4) \tag{5}$$

As gi(n) = O(n) Specifically for knn Classifier.

Working of hybrid classification algorithm first three time of algorithm refers to prepare the data as input to the classifiers used in this study i.e. get data in structured form , pre-processing steps like; cleaning, removing stop word etc. and splitting data into train and test set identifying classes. Since we are using different data set (Yelp, Amazon Reviews etc.), so these steps will be performed in all these datasets.

In step 5 and 6 different classifiers cl [i] are applied on these data sets and results is stored in vectors v [i]: as shown in Fig. 2.

These resulted vectors are then provided as input to meta classifiers along with test set and actual class in time 10. Steps 7 to 9 gives variations to classifier and to resulted vectors formed in steps 5 to 6 (Fig. 3).

On the basis of the results, calculated we can predict class for the new data more accurately as discussed in the following section.

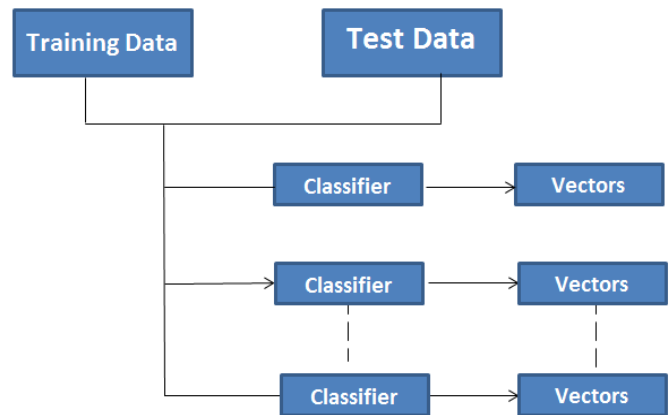


Fig. 2. Vectors Source Generation.

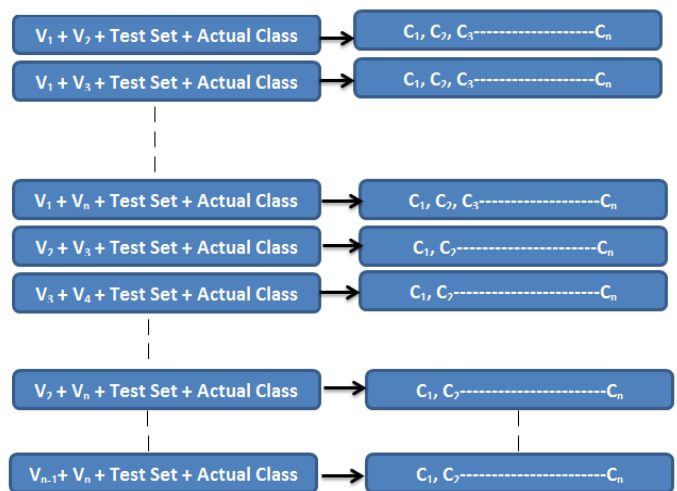


Fig. 3. Dataset Generation for Meta Classifier.

VI. RESULTS AND DISCUSSION

A major goal of our research was the development of an automated and effective algorithm for category detection framework that researchers, business analysts and practitioners could use to assess and infer more objective information from data obtained in large databases. In this research, we examined the classification effectiveness of both base classifiers and hybrid classifiers with in a text mining context.

The results obtained by all base-level systems in the domains of interest are initially presented in this section, Table I shows the base level classifier's accuracies for different datasets with Training and Testing 70% to 30% ratio respectively, instead of discussing in detail the individual classifiers' performance we would be investigating whether any improvement in the best results for each domain is possible at meta-level. Then, the meta-level data is analyzed, in order to determine whether and how the predictions of the base-level systems are correlated. This study is intended to serve as a basis for a comparative evaluation of voting against stacking. Then all combination methods are comparatively evaluated, while also comparing against the best base-level results. More detailed analysis of the experimental results is provided in later sections.

Table I shows that gbm, glm and lda perform better than other classifiers in case of Scopus dataset with accuracies of 67.00%, 66.33% and 63.33% respectively, in case of IMDB Movie Reviews dataset gbm, svm and glm perform better than other classifiers with accuracies of 72.92%, 72.58% and 72.33% respectively, whereas nnet, rda and svm perform better than others whereas in case of Amazon Products Reviews dataset with accuracies of 76.33%, 75.33% and 72.67% respectively and in case of Yelp dataset lda, nnet and rda give better results than other classifiers with accuracies of 69%, 68.67% and 68.33%, respectively.

We evaluated the selected methods for constructing stack of heterogeneous classifiers with stacking and shown that they perform (at best) comparably to selecting the best classifier from the stack by using their correlation values.

Table II shows the correlation between subjected algorithms for the Scopus Dataset. It can be seen that the table is symmetrical about diagonal and algorithms with negative correlations are highlighted and will be considered while stacking the algorithms. Support Vector Machines has negative correlations with k-Nearest Neighbour, Generalized Linear Model, Recursive Partitioning and Regression Trees, rda and Neural Networks, out of which Generalized Linear Model has the lowest correlation value whereas we discussed the results of stacked algorithms in next section. Naïve Bayes has negative correlations with k-Nearest Neighbour.

Table IV shows the correlation between subjected algorithms for the IMDB Movie Reviews Dataset. It can be seen that the table is symmetrical about diagonal and algorithms with negative correlations are highlighted and will be considered while stacking the algorithms. Support Vector Machines has negative correlations with k-Nearest Neighbour, Recursive Partitioning and Regression Trees, rda, Neural Networks and Conditional Inference Trees, out of which

Neural Networks has the lowest correlation value whereas we discussed the results of stacked algorithms in next section. Naïve Bayes has negative correlations with k-Nearest Neighbour, gbm, rda, and Conditional Inference Trees, out of which gbm has the lowest correlation. k-Nearest Neighbour has negative correlations with Support Vector Machines, nb, Linear Discriminant Analysis and rda, out of which Linear Discriminant Analysis has the lowest correlation with k-Nearest Neighbour. Generalized Linear Model has negative correlations with rda and Neural Networks, out of which rda has the lowest correlation. Linear Discriminant Analysis has negative correlation with k-Nearest Neighbour and Conditional Inference Trees. gbm has negative correlations with nb, Recursive Partitioning and Regression Trees, rda, and Neural Networks, out of which nb has the lowest correlation. Recursive Partitioning and Regression Trees has negative correlation with Support Vector Machines, gbm and rda. rda has negative correlation with Support Vector Machines, nb, k-Nearest Neighbour, Generalized Linear Model, gbm, Recursive Partitioning and Regression Trees and Conditional Inference Trees with lowest correlation of -0.2190 with Naïve Bayes. Neural Networks has negative correlation with Support Vector Machines, Generalized Linear Model and gbm. Conditional Inference Trees has negative correlation with Support Vector Machines, nb, Linear Discriminant Analysis and rda out which Linear Discriminant Analysis has a lowest correlation.

Table V shows the results obtained from Meta Level classifiers for IMDB movie reviews dataset. In Table V each cell represents the accuracies of Meta level classifiers can be read as base classifier1 from top most row, classifier from left most column and meta classier from the lowest row. It can be seen that every algorithm at Meta level performs better than its individual performance some algorithms remarkably produces improved results as Neural Networks algorithm. Talking about the performances of these algorithms one by one; Support Vector Machines has an accuracy of 72.58% as a base classifier but when it has been stacked with different classifiers it performs better it can be seen that Support Vector Machines when stacked with Conditional Inference Trees gives 78.67% accuracy, when stacked with Neural Networks its accuracy raises to 78.75% and when stacked with Generalized Linear Model and nb it gives almost same and better results with accuracy of 78.42%. nb has an accuracy of 66.42% as a base classifier but when it has been stacked with different classifiers it performs better it can be seen that nb when stacked with Support Vector Machines gives 73.75% accuracy which is far more better than its individual accuracy, when it has been stacked with Generalized Linear Model its accuracy raises to 73.58% and when stacked with Linear Discriminant Analysis it gives results with accuracy of 73.17%. k-Nearest Neighbour has an accuracy of 61.67% as a base classifier it can be seen that when it has been stacked with different classifiers it performs better as it performs best when stacked with Conditional Inference Trees gives 73.50% accuracy, when stacked with Generalized Linear Model and Linear Discriminant Analysis its accuracy raises to 73.08% and when it has been stacked with gbm and Recursive Partitioning and Regression Trees it gives results with accuracy of 72.92%. Generalized Linear Model has an accuracy of 72.33% as a base classifier but when it has been stacked with rda gives 77.92%

accuracy, when stacked with gbm, Recursive Partitioning and Regression Trees and Neural Networks its accuracy raises to 77.83% and when it has been stacked with nb, k-Nearest Neighbour and Linear Discriminant Analysis it gives results with accuracy of 77.75%.

Linear Discriminant Analysis has an accuracy of 71.58% as a base classifier it can be seen that when it has been stacked with different classifiers it performs better as it performs best when stacked with Neural Networks gives 77.17% accuracy, when stacked with Support Vector Machines its accuracy raises to 77.08% and when it has been stacked with Generalized Linear Model it gives results with accuracy of 76.83%. gbm has an accuracy of 72.92% as a base classifier it performs best when stacked with Support Vector Machines gives 75.83% accuracy, when stacked with Linear Discriminant Analysis its accuracy raises to 75.58% and when it has been stacked with Generalized Linear Model it gives results with accuracy of 75.50%. Recursive Partitioning and Regression Trees has an accuracy of 66.25% as a base classifier it can be seen that when it has been stacked with gbm it gives 72.92% accuracy, when stacked with Support Vector Machines its accuracy raises to 72.58% and when it has been stacked with Generalized Linear Model it gives results with accuracy of 72.33%. rda has an accuracy of 70.75% as a base classifier it can be seen that when it has been stacked with Support Vector Machines it gives 76.17% accuracy, when stacked with gbm or Neural Networks its accuracy raises to 75.92% and when it has been stacked with k-Nearest Neighbour it gives results with accuracy of 75.33%. Neural Networks produces remarkably improved results with at meta level although its accuracy at base level is; 71.25 but when it has been stacked with Support Vector Machines it gives 96.58% accuracy, and when it is stacked with Generalized Linear Model it gives accuracy of 93.92% and it gives 92.33% accuracy when stacked with k-Nearest Neighbour. ctree performs best when stacked with Support Vector Machines it gives 73.08% accuracy, when it is stacked with gbm it gives

72.92% accuracy and when ctree is stacked with Generalized Linear Model or Linear Discriminant Analysis ctree gives 72.42% accuracy.

It is notable that although gbm, Generalized Linear Model, Linear Discriminant Analysis and Support Vector Machines performs better than Neural Networks at base level for the IMDB Movie Reviews dataset but the Neural Networks achieved the best results and outperformed the other evaluated methods at meta level. It achieved 96.58% accuracy when stacked with the Support Vector Machines. It is a remarkable performance considering their individual performance. From Table V, it can be seen that there is a 25.33% rise in accuracy of nnet when stacked with the svm, it also got the second highest raise of 22.67% when stacked with glm. knn stands second in rising accuracy for IMDB Movie Reviews dataset.

TABLE I. ACCURACIES OF BASE-LEVEL CLASSIFIERS FOR DIFFERENT DATASETS

	Algorithm	Scopus Dataset	IMDB Movie Reviews	Amazon Products Reviews	Yelp Dataset
1	svm	62.67%	72.58%	72.67%	67.33%
2	nb	60.67%	66.42%	50.33%	58.33%
3	knn	48.00%	61.67%	65.00%	60.00%
4	glm	66.33%	72.33%	71.00%	72.33%
5	lda	63.33%	71.58%	71.67%	69.00%
6	gbm	67.00%	72.92%	68.67%	63.67%
7	rpart	44.67%	66.25%	66.33%	55.00%
8	rda	62.67%	70.75%	75.33%	68.33%
9	nnet	60.83%	71.25%	76.33%	68.67%
10	ctree	55.00%	64.58%	67.67%	62.00%

TABLE II. CORRELATION BETWEEN SUBJECTED ALGORITHMS FOR SCOPUS DATASET

		Classifier 1									
		svm	nb	knn	glm	lda	gbm	rpart	rda	nnet	ctree
Classifier 2	svm	X	0.0841	-0.1126	-0.3058	0.3996	0.0677	-0.2069	-0.1742	-0.0936	0.0705
	nb	0.0841	X	-0.4455	0.1130	0.0414	0.1783	0.1491	0.0176	0.2825	0.1447
	knn	-0.1126	-0.4455	X	0.0903	0.0933	-0.1845	0.0035	0.2476	-0.1955	0.0535
	glm	-0.3058	0.1130	0.0903	X	0.1479	0.1217	0.0990	0.1402	0.1048	-0.1632
	lda	0.3996	0.0414	0.0933	0.1479	X	0.0608	0.0035	0.2479	-0.0395	-0.1722
	gbm	0.0677	0.1783	-0.1845	0.1217	0.0608	X	0.1032	0.4150	-0.0100	0.0371
	rpart	-0.2069	0.1491	0.0035	0.0990	0.0035	0.1032	X	-0.0977	0.2052	0.1959
	rda	-0.1742	0.0176	0.2476	0.1402	0.2479	0.4150	-0.0977	X	-0.0585	-0.3308
	nnet	-0.0936	0.2825	-0.1955	0.1048	-0.0395	-0.0100	0.2052	-0.0585	X	0.1487
	ctree	0.0705	0.1447	0.0535	-0.1632	-0.1722	0.0371	0.1959	-0.3308	0.1487	X

TABLE III. ACCURACIES OF META-LEVEL SYSTEMS FOR SCOPUS DATASET

		Base Level Classifier 1									
		svm	nb	knn	glm	lda	gbm	rpart	rda	nnet	ctree
Base Level Classifier 2	svm	X	67.83%	57.17%	89.67%	72.67%	77.33%	55.00%	69.83%	94.00%	63.83%
	Nb	89.33%	X	59.17%	68.17%	73.00%	71.50%	55.17%	70.00%	96.17%	64.33%
	knn	89.67%	68.17%	X	73.67%	72.50%	70.50%	44.67%	68.83%	96.17%	67.50%
	glm	89.67%	68.00%	59.67%	X	74.00%	70.67%	57.83%	70.17%	96.33%	64.83%
	Lda	89.50%	67.33%	53.67%	72.50%	X	70.50%	55.67%	69.00%	96.83%	67.00%
	gbm	90.83%	68.33%	60.00%	70.50%	73.67%	X	59.00%	71.67%	85.67%	59.83%
	rpart	87.50%	41.00%	54.00%	44.67%		70.00%	X	68.83%	95.67%	66.17%
	rda	90.17%	67.33%	55.33%	68.83%	72.83%	70.83%	54.50%	X	90.33%	61.00%
	nnet	89.33%	68.00%	55.17%	96.17%	73.83%	71.00%	55.17%	70.17%	X	61.00%
ctree	90.67%	42.17%	54.83%	67.50%	75.33%	70.50%	52.17%	70.33%	96.83%	X	
		svm	nb	knn	glm	lda	gbm	rpart	rda	nnet	ctree
		Meta Level Classifier									

TABLE IV. CORRELATION BETWEEN SUBJECTED ALGORITHMS FOR IMDB MOVIE REVIEWS

		Classifier 1									
		svm	nb	knn	glm	lda	gbm	rpart	rda	nnet	ctree
Classifier 2	svm	X	0.2346	-0.0592	0.1892	0.2502	0.0289	-0.0551	-0.0998	-0.1703	-0.1053
	nb	0.2346	X	-0.1788	0.0153	0.6190	-0.3584	0.2927	-0.2190	0.1139	-0.2964
	knn	-0.0592	-0.1788	X	0.1399	-0.3326	0.2301	0.0083	-0.2133	0.0213	0.4319
	glm	0.1892	0.0153	0.1399	X	0.2797	0.2554	0.0557	-0.1660	-0.0159	0.0868
	lda	0.2502	0.6190	-0.3326	0.2797	X	0.0024	0.1538	0.0535	0.1733	-0.4086
	gbm	0.0289	-0.3584	0.2301	0.2554	0.0024	X	-0.0890	-0.0970	-0.2891	0.3520
	rpart	-0.0551	0.2927	0.0083	0.0557	0.1538	-0.0890	X	-0.2048	0.1413	0.1564
	rda	-0.0998	-0.2190	-0.2133	-0.1660	0.0535	-0.0970	-0.2048	X	0.2474	-0.1535
	nnet	-0.1703	0.1139	0.0213	-0.0159	0.1733	-0.2891	0.1413	0.2474	X	0.2069
	ctree	-0.1053	-0.2964	0.4319	0.0868	-0.4086	0.3520	0.1564	-0.1535	0.2069	X

TABLE V. ACCURACIES OF META-LEVEL SYSTEMS FOR IMDB MOVIE REVIEWS DATASETS

		Base Level Classifier 1									
		svm	nb	knn	glm	lda	gbm	rpart	rda	nnet	ctree
Base Level Classifier 2	svm	X	73.75%	72.50%	77.17%	77.08%	75.83%	72.58%	76.17%	96.58%	73.08%
	Nb	78.42%	X	72.67%	77.75%	76.42%	73.17%	66.42%	75.42%	85.83%	67.00%
	knn	78.17%	72.25%	X	77.75%	76.25%	73.17%	66.25%	75.33%	92.33%	64.92%
	glm	78.42%	73.58%	73.08%	X	76.83%	75.50%	72.33%	75.75%	93.92%	72.42%
	Lda	78.17%	73.17%	73.08%	77.75%	X	75.58%	71.58%	75.08%	80.75%	72.42%
	gbm	78.33%	72.92%	72.92%	77.83%	76.50%	X	72.92%	75.92%	89.92%	72.92%
	rpart	77.75%	72.25%	72.92%	77.83%	76.33%	73.08%	X	75.67%	90.92%	66.25%
	rda	77.83%	72.25%	72.67%	77.92%	76.42%	73.42%	70.75%	X	84.33%	71.67%
	nnet	78.75%	73.00%	72.58%	77.83%	77.17%	75.08%	71.25%	75.92%	X	72.17%
ctree	78.67%	72.67%	73.50%	77.67%	76.00%	73.33%	66.25%	75.50%	84.92%	X	
		svm	nb	knn	glm	lda	gbm	rpart	rda	nnet	ctree
		Meta Level Classifier									

Table VI shows the correlation between subjected algorithms for the Amazon Products Reviews Dataset. It can be seen that the table is symmetrical about diagonal and algorithms with negative correlations are highlighted and will be considered while stacking the algorithms. Support Vector Machines has negative correlations with k-Nearest Neighbour, Generalized Linear Model, gbm, rda and Conditional Inference Trees, out of which rda has the lowest correlation value whereas we discussed the results of stacked algorithms in next section. Naïve Bayes has negative correlations with Generalized Linear Model, gbm, rda and Conditional Inference Trees, out of which Generalized Linear Model has the lowest correlation. k-Nearest Neighbour has negative correlations with Support Vector Machines, Generalized Linear Model, Linear Discriminant Analysis, rda and Neural Networks, out of which Neural Networks has the lowest correlation with k-Nearest Neighbour. Generalized Linear Model has negative correlations with Support Vector Machines, nb, k-Nearest Neighbour, linear Discriminant Analysis, Recursive Partitioning and Regression Trees and rda, out of which linear Discriminant Analysis has the lowest correlation. Linear Discriminant Analysis has negative correlation with k-Nearest Neighbour, Generalized Linear Model, gbm Recursive Partitioning and Regression Trees, rda and Conditional Inference Trees. gbm has negative correlations with Support Vector Machines, nb, Linear Discriminant Analysis and Neural Networks out of which nb has the lowest correlation. Recursive Partitioning and Regression Trees has negative correlation with Generalized Linear Model, Linear Discriminant Analysis, rda and Neural Networks. rda has negative correlation with Support Vector Machines, nb, k-Nearest Neighbour, Generalized Linear Model, Recursive Partitioning and Regression Trees and Neural Networks with lowest correlation of -0.2678. Neural Networks has negative correlation with k-Nearest Neighbour, gbm, Recursive Partitioning and Regression Trees, rda and Conditional Inference Trees. Conditional Inference Trees has negative correlation with Support Vector Machines, nb, Linear Discriminant Analysis and Neural Networks out which nb has a lowest correlation.

Table VII shows the results obtained from Meta Level classifiers for Amazon Products reviews dataset. Exactly same as Table III in Table VII each cell represents the accuracies of Meta level classifiers can be read as base classifier1 from top most row, classifier from left most column and meta classifier from the lowest row. It can be seen that every algorithm at Meta level performs better than its individual performance some algorithms remarkably produces improved results as Support Vector Machines, Generalized Linear Model and Neural Networks algorithm.

Talking about the performances of these algorithms one by one; Support Vector Machines has an accuracy of more than 90% for all stacked models whereas it has 72.67% accuracy as a base classifier for Amazon Reviews dataset. It can be seen that Support Vector Machines when stacked with Neural Networks it gives 91.67% accuracy which is the highest one, when stacked with Conditional Inference Trees or k-Nearest Neighbour or gbm or Recursive Partitioning and Regression Trees its accuracy raises to 91.33% and when stacked with Linear Discriminant Analysis or nb it gives almost same and

better results with accuracy of 91.00%. Naïve Bayes has an accuracy of 50.33% as a base classifier but when it has been stacked with different classifiers it performs better it can be seen that Naïve Bayes when stacked with Support Vector Machines or rda it gives 71.00% accuracy which is far more better than its individual accuracy, when it has been stacked with Conditional Inference Trees its accuracy raises to 70.33% and when stacked with Neural Networks it gives results with accuracy of 69.67%. k-Nearest Neighbour has an accuracy of 65.00% as a base classifier it can be seen that when it has been stacked with different classifiers it performs better as it performs best when stacked with Neural Networks gives 76.33% accuracy, when stacked with Generalized Linear Model or rda its accuracy raises to 75.33% and when it has been stacked with Support Vector Machines it gives results with accuracy of 75.00%. Generalized Linear Model has an accuracy of 71.00% as a base classifier but when it has been stacked with any of; Naïve Bayes, k-Nearest Neighbour, gbm, Recursive Partitioning and Regression Trees, Neural Networks or Conditional Inference Trees it gives 91.67% accuracy, when stacked with Linear Discriminant Analysis its accuracy raises to 91.00% and when it has been stacked with Support Vector Machines it gives results with accuracy of 90.00%.

Linear Discriminant Analysis has an accuracy of 71.67% as a base classifier it can be seen that when it has been stacked with different classifiers it performs better as it performs best when stacked with Neural Networks gives 88.00% accuracy, when stacked with rda its accuracy raises to 87.67% and when it has been stacked with gbm it gives results with accuracy of 87.00%. gbm has an accuracy of 68.67% as a base classifier it performs best when stacked with Neural Networks gives 78.00% accuracy, when stacked with rda its accuracy raises to 76.67% and when it has been stacked with Linear Discriminant Analysis or Support Vector Machines it gives same results with accuracy of 75.67%. Recursive Partitioning and Regression Trees has an accuracy of 66.33% as a base classifier it can be seen that when it has been stacked with Neural Networks it gives 76.33% accuracy, when stacked with rda its accuracy raises to 75.33% and when it has been stacked with Support Vector Machines it gives results with accuracy of 72.67%. rda has an accuracy of 75.33% as a base classifier it can be seen that when it has been stacked with Neural Networks it gives 83.00% accuracy, when stacked with Support Vector Machines or Linear Discriminant Analysis or gbm its accuracy raises to 76.67% and when it has been stacked with Generalized Linear Model or Recursive Partitioning and Regression Trees or Conditional Inference Trees it gives results with accuracy of 76.33%.

Neural Networks produces remarkably improved results with at meta level although its accuracy at base level is; 76.33 but when it has been stacked with all classifiers except; Linear Discriminant Analysis and gbm it gives 92.33% accuracy, and when it is stacked with Linear Discriminant Analysis or gbm it gives accuracy of 92.00%. Conditional Inference Trees performs best when stacked with rda or Neural Networks it gives 76.33% accuracy, when it is stacked with Recursive Partitioning and Regression Trees it gives 75.33% accuracy and when ctree is stacked with Support Vector Machines it

gives 72.67% accuracy. Although its accuracy as individual classifier is 67.67%.

Neural Networks at base level for the Amazon Products Reviews dataset has the highest accuracy and it has achieved the best results and outperformed the other evaluated methods at meta level. But other base classifiers like; Support Vector Machines, Generalized Linear Model and Linear Discriminant Analysis also gives remarkable results as compared to their individual performances.

From Table VII it can be seen that there is a glm and Naïve Bayes got highest raise in accuracy which is 20.67%. svm also improved a lot and got raise of 19% as its highest improvement. Although nnet at Meta level for Amazon Products Reviews once again outperforms all other classifiers but it had not got such improvement as glm, Naïve Bayes and svm acquired.

Table VIII shows the correlation between subjected algorithms for the Yelp Dataset. It can be seen that the table is symmetrical about diagonal and algorithms with negative correlations are highlighted and will be considered while stacking the algorithms. Support Vector Machines has negative correlations with Generalized Linear Model, Linear Discriminant Analysis, gbm, Recursive Partitioning and Regression Trees, rda, Neural Networks and Conditional Inference Trees, out of which gbm has the lowest correlation value whereas we discussed the results of stacked algorithms in next section. Naïve Bayes has negative correlations with gbm, rda, Neural Networks and Conditional Inference Trees, out of which rda has the lowest correlation. k-Nearest Neighbour has negative correlations with gbm, Recursive Partitioning and Regression Trees, and Conditional Inference Trees, out of which Conditional Inference Trees has the lowest correlation with k-Nearest Neighbour. Generalized Linear Model has negative correlations with Support Vector Machines, gbm, Recursive Partitioning and Regression Trees, rda, Neural Networks and Conditional Inference Trees, out of which Support Vector Machines has the lowest correlation. Linear Discriminant Analysis has negative correlation with Support Vector Machines, Neural Networks and Conditional Inference Trees. gbm has negative correlations with Support Vector Machines, nb, k-Nearest Neighbour, Generalized Linear Model, and rda, out of which Support Vector Machines has the lowest correlation. Recursive Partitioning and Regression Trees have negative correlation with Support Vector Machines, k-Nearest Neighbour, Generalized Linear Model, rda, Neural Networks and Conditional Inference Trees. rda has negative correlation with Support Vector Machines, nb, Generalized Linear Model, gbm, and Recursive Partitioning and Regression Trees with lowest correlation of -0.2253 with Naïve Bayes. Neural Networks has negative correlation with Support Vector Machines, nb, Linear Discriminant Analysis and Recursive Partitioning and Regression Trees. Conditional Inference Trees has negative correlation with Support Vector Machines, nb, k-Nearest Neighbour, Generalized Linear Model, Linear Discriminant Analysis and Recursive Partitioning and Regression Trees out of which Linear Discriminant Analysis has a lowest correlation.

Table IX shows the results obtained from Meta Level classifiers for Yelp dataset. Similarly as Table III, Table V and Table VII in Table IX each cell represents the accuracies of Meta level classifiers can be read as base classifier1 from top most row, classifier from left most column and meta classifier from the lowest row. It can be seen that every algorithm at Meta level performs better than its individual performance some algorithms remarkably produces improved results as Neural Networks algorithm.

Talking about the performances of these algorithms one by one; Support Vector Machines has an accuracy of 67.33% as a base classifier but when it has been stacked with different classifiers it performs better it can be seen that Support Vector Machines when stacked with Generalized Linear Model gives 88.67% accuracy, when stacked with Naïve Bayes or gbm or Neural Networks its accuracy raises to 88.33% and when stacked with Recursive Partitioning and Regression Trees and Conditional Inference Trees it gives almost same and better results with accuracy of 88.00%. Naïve Bayes has an accuracy of 58.33% as a base classifier but when it has been stacked with different classifiers it performs better it can be seen that nb when stacked with Generalized Linear Model gives 62.33% accuracy which is far more better than its individual accuracy, when it has been stacked with Support Vector Machines or rda its accuracy raises to 62.00% and when stacked with Linear Discriminant Analysis or Neural Networks it gives results with accuracy of 61.33%.

k-Nearest Neighbour has an accuracy of 60% as a base classifier it can be seen that when it has been stacked with different classifiers it performs better as it performs best when stacked with Generalized Linear Model gives 75.33% accuracy, when stacked with Linear Discriminant Analysis its accuracy raises to 71.67% and when it has been stacked with Support Vector Machines or Neural Networks it gives results with accuracy of 71.00%. Generalized Linear Model has an accuracy of 72.33% as a base classifier but when it has been stacked with Naïve Bayes gives 89.33% accuracy, when stacked with gbm, k-Nearest Neighbour or Neural Networks its accuracy raises to 88.67% and when it has been stacked with Support Vector Machines, Recursive Partitioning and Regression Trees, rda or Conditional Inference Trees it gives results with accuracy of 88.33%.

Linear Discriminant Analysis has an accuracy of 69.00% as a base classifier it can be seen that when it has been stacked with different classifiers it performs better as it performs best when stacked with Support Vector Machines or Naïve Bayes or ctree gives 85.33% accuracy, when stacked with k-Nearest Neighbour or Generalized Linear Model or Recursive Partitioning or Regression Trees or rda its accuracy raises to 85.00% and when it has been stacked with gbm it gives results with accuracy of 83.67%. gbm has an accuracy of 63.67% as a base classifier it performs best when stacked with Generalized Linear Model gives 74.67% accuracy, when stacked with Neural Networks its accuracy raises to 72.00% and when it has been stacked with Linear Discriminant Analysis it gives results with accuracy of 69.33%. Recursive Partitioning and Regression Trees has an accuracy of 55.00% as a base classifier it can be seen that when it has been stacked with Linear Discriminant Analysis it gives 69.00% accuracy, when

stacked with Neural Networks its accuracy raises to 68.67% and when it has been stacked with rda it gives results with accuracy of 68.33%. rda has an accuracy of 68.33% as a base classifier it can be seen that when it has been stacked with Generalized Linear Model or Neural Networks it gives 73.67%

accuracy, when stacked with Linear Discriminant Analysis its accuracy raises to 72.33% and when it has been stacked with Support Vector Machines or Recursive Partitioning and Regression Trees or ctree it gives results with accuracy of 69.00%.

TABLE VI. CORRELATION BETWEEN SUBJECTED ALGORITHMS FOR AMAZON PRODUCT REVIEWS

		Classifier 1									
		svm	nb	knn	glm	lda	gbm	rpart	rda	nnet	ctree
Classifier 2	svm	1.0000	0.2497	-0.1361	-0.0737	0.1340	-0.0168	0.0430	-0.2395	0.2976	-0.2189
	nb	0.2497	1.0000	0.1007	-0.5704	0.0471	-0.2166	0.0795	-0.2977	0.1876	-0.3439
	knn	-0.1361	0.1007	1.0000	-0.0160	-0.1508	0.0680	0.2929	-0.1714	-0.4354	0.1879
	glm	-0.0737	-0.5704	-0.0160	1.0000	-0.3277	0.1365	-0.0824	-0.0158	0.0186	0.1538
	lda	0.1340	0.0471	-0.1508	-0.3277	1.0000	-0.0018	-0.1847	-0.0317	0.3914	-0.2228
	gbm	-0.0168	-0.2166	0.0680	0.1365	-0.0018	1.0000	0.1992	0.0684	-0.1427	0.5784
	rpart	0.0430	0.0795	0.2929	-0.0824	-0.1847	0.1992	1.0000	-0.0177	-0.1555	0.2982
	rda	-0.2395	-0.2977	-0.1714	-0.0158	-0.0317	0.0684	-0.0177	1.0000	-0.2678	0.0376
	nnet	0.2976	0.1876	-0.4354	0.0186	0.3914	-0.1427	-0.1555	-0.2678	1.0000	-0.1654
	ctree	-0.2189	-0.3439	0.1879	0.1538	-0.2228	0.5784	0.2982	0.0376	-0.1654	1.0000

TABLE VII. ACCURACIES OF META-LEVEL SYSTEMS FOR AMAZON PRODUCT REVIEWS DATASETS

		Base Level Classifier 1									
		svm	nb	knn	glm	lda	gbm	rpart	rda	nnet	ctree
Base Level Classifier 2	svm	X	71.00%	75.00%	90.00%	86.67%	75.67%	72.67%	76.67%	92.33%	72.67%
	nb	91.00%	X	72.00%	91.67%	85.67%	72.33%	66.33%	75.33%	92.33%	67.67%
	knn	91.33%	64.67%	X	91.67%	85.67%	73.67%	67.00%	75.33%	92.33%	72.33%
	glm	91.00%	68.67%	75.33%	X	85.33%	73.67%	71.00%	76.33%	92.33%	71.67%
	lda	91.00%	69.00%	72.00%	91.00%	X	75.67%	71.67%	79.67%	92.00%	68.67%
	gbm	91.33%	67.67%	72.00%	91.67%	87.00%	X	68.67%	76.67%	92.00%	67.67%
	rpart	91.33%	68.33%	73.00%	91.67%	85.67%	71.00%	X	76.33%	92.33%	75.33%
	rda	90.33%	71.00%	75.33%	86.33%	87.67%	76.67%	75.33%	X	92.33%	76.33%
	nnet	91.67%	69.67%	76.33%	91.67%	88.00%	78.00%	76.33%	83.00%	X	76.33%
	ctree	91.33%	70.33%	72.67%	91.67%	85.67%	69.67%	69.67%	76.33%	92.33%	X
		svm	nb	knn	glm	lda	gbm	rpart	rda	nnet	ctree
		Meta Level Classifier									

TABLE VIII. CORRELATION BETWEEN SUBJECTED ALGORITHMS FOR YELP DATASET

	svm	nb	Knn	glm	lda	gbm	rpart	rda	nnet	ctree
svm	1.0000	0.2683	0.2940	-0.2098	-0.0528	-0.4631	-0.2577	-0.0581	-0.0776	-0.0312
nb	0.2683	1.0000	0.1602	0.1623	0.1807	-0.0290	0.0897	-0.2253	-0.1466	-0.0169
knn	0.2940	0.1602	1.0000	0.3066	0.0170	-0.1122	-0.1745	0.2178	0.0227	-0.1786
glm	-0.2098	0.1623	0.3066	1.0000	0.1036	-0.1541	-0.0655	-0.0227	0.0757	-0.1758
lda	-0.0528	0.1807	0.0170	0.1036	1.0000	0.0478	0.3140	0.0922	-0.2034	-0.3327
gbm	-0.4631	-0.0290	-0.1122	-0.1541	0.0478	1.0000	0.3848	-0.0032	0.0539	0.2208
rpart	-0.2577	0.0897	-0.1745	-0.0655	0.3140	0.3848	1.0000	-0.1085	-0.1425	-0.0548
rda	-0.0581	-0.2253	0.2178	-0.0227	0.0922	-0.0032	-0.1085	1.0000	0.0848	0.0722
nnet	-0.0776	-0.1466	0.0227	0.0757	-0.2034	0.0539	-0.1425	0.0848	1.0000	0.1223
ctree	-0.0312	-0.0169	-0.1786	-0.1758	-0.3327	0.2208	-0.0548	0.0722	0.1223	1.0000

TABLE IX. ACCURACIES OF META-LEVEL SYSTEMS FOR YELP DATASETS

		Base Level Classifier 1									
		svm	nb	knn	glm	lda	gbm	rpart	rda	nnet	ctree
Base Level Classifier 2	svm	X	62.00%	71.00%	88.33%	85.33%	67.67%	67.33%	69.00%	94.33%	67.33%
	nb	88.33%	X	60.33%	89.33%	85.33%	64.00%	62.67%	68.67%	94.33%	62.00%
	knn	87.33%	60.67%	X	88.67%	85.00%	64.67%	60.00%	68.67%	91.00%	72.33%
	glm	88.67%	62.33%	75.33%	X	85.00%	74.67%	72.33%	73.67%	94.33%	69.00%
	lda	87.67%	61.33%	71.67%	88.00%	X	69.33%	69.00%	72.33%	94.33%	65.00%
	gbm	88.33%	60.33%	61.67%	88.67%	83.67%	X	63.67%	68.33%	94.33%	62.00%
	rpart	88.00%	58.33%	60.67%	88.33%	85.00%	63.67%	X	69.00%	93.33%	68.33%
	rda	87.00%	62.00%	62.67%	88.33%	85.00%	68.33%	68.33%	X	94.33%	68.67%
	nnet	88.33%	61.33%	71.00%	88.67%	83.33%	72.00%	68.67%	73.67%	X	70.67%
	ctree	88.00%	59.33%	61.33%	88.33%	85.33%	65.00%	62.00%	69.00%	94.00%	X
		svm	nb	knn	glm	lda	gbm	rpart	rda	nnet	ctree
		Meta Level Classifier									

Neural Networks produces remarkably improved results with at meta level although its accuracy at base level is; 71.25 but when it has been stacked with all except k-Nearest Neighbour and ctree it gives 94.33% accuracy, and when it is stacked with ctree it gives accuracy of 94.00% and it gives 91.00% accuracy when stacked with k-Nearest Neighbour. ctree performs best when stacked with Neural Networks it gives 70.67% accuracy, when it is stacked with Generalized Linear Model it gives 69.00% accuracy and when ctree is stacked with rda the ctree gives 68.67% accuracy. Once again Neural Networks achieved the best results and outperformed the other evaluated methods at meta level. It achieved 94.33% accuracy when stacked which is a remarkable performance considering its individual performance.

From Table IX, it can be seen that there is a 25.66% rise in accuracy of nnet when stacked with the svm, nb, glm, lda, gbm and rda it also got the second highest raise of 25.33% when stacked with ctree. svm stands second in rising accuracy for Yelp dataset.

VII. CONCLUSIONS

In this research we presented a modified version of the standard stacking algorithm that uses a correlation between algorithms to create a Meta classifier. We tested the individual learning algorithms and Meta classifiers over different textual datasets; IMDB Movie Reviews, Amazon Product Reviews and Yelp Dataset and showed the improvement in performance over the individual learning algorithms as well as over the standard stacking algorithm. We have concluded that our approach performs better than other mentioned document classification approaches with a highest improvement of 25.66% in Yelp Dataset and 96.58% accuracy for IMDB Movie Reviews. The proposed solution can be of good use in many intelligence applications.

REFERENCES

- [1] Opitz, D., & Maclin, R. (1999). Popular ensemble methods: An empirical study. "Journal of artificial intelligence research", 11, 169-198.
- [2] Džeroski, S., & Ženko, B. (2004). Is combining classifiers with stacking better than selecting the best one?. "Machine learning", 54(3), 255-273.
- [3] Kotsiantis, S. B., Zaharakis, I. D., & Pintelas, P. E. (2006). Machine learning: a review of classification and combining techniques. "Artificial Intelligence Review", 26(3), 159-190.
- [4] Merz, C. J. (1999). Using correspondence analysis to combine classifiers. "Machine Learning", 36(1-2), 33-58.
- [5] Wolpert, D. H. (1992). Stacked generalization. "Neural networks", 5(2), 241-259.
- [6] Yin, C., Xiang, J., Zhang, H., Yin, Z., & Wang, J. (2015). Short text classification algorithm based on semi-supervised learning and SVM. "International Journal of Multimedia and Ubiquitous Engineering", 10(12), 195-206.
- [7] Padhiyar, H., & Padhiar, D. N. (2013). Improving Accuracy of Text Classification for SMS Data. International Journal for Scientific Research & Development, 1(10), 181-189.
- [8] Danesh, A., Moshiri, B., & Fatemi, O. (2007, July). Improve text classification accuracy based on classifier fusion methods. Information Fusion, 2007 10th International Conference on (pp. 1-6). IEEE.
- [9] Sivakumar, M., Karthika, C., & Renuga, P. (2014). A Hybrid Text Classification Approach using KNN and SVM. Int. J. Innov. Res. Sci. Eng. Technol, 3(3), 1987-1991.
- [10] Balahur, A. (2013). Sentiment analysis in social media texts. In Proceedings of the 4th workshop on computational approaches to subjectivity, sentiment and social media analysis (pp. 120-128).
- [11] Mousavi, R., & Eftekhari, M. (2015). A new ensemble learning methodology based on hybridization of classifier ensemble selection approaches. Applied Soft Computing, 37, 652-666.
- [12] Sigletos, G., Paliouras, G., Spyropoulos, C. D., & Hatzopoulos, M. (2005). Combining information extraction systems using voting and stacked generalization. Journal of Machine Learning Research, 6(Nov), 1751-1782.
- [13] Fast, A., & Jensen, D. (2008, December). Why stacked models perform effective collective classification. In Data Mining, 2008. ICDM'08. Eighth IEEE International Conference on (pp. 785-790). IEEE.

- [14] Koutanaei, F. N., Sajedi, H., & Khanbabaei, M. (2015). A hybrid data mining model of feature selection algorithms and ensemble learning classifiers for credit scoring. *Journal of Retailing and Consumer Services*, 27, 11-23.
- [15] Goldberg, D. E. (1989). *Genetic Algorithms in Search, Optimization & Machine Learning*.
- [16] Agusti, L. E., Salcedo-Sanz, S., Jiménez-Fernández, S., Carro-Calvo, L., Del Ser, J., & Portilla-Figueras, J. A. (2012). A new grouping genetic algorithm for clustering problems. *Expert Systems with Applications*, 39(10), 9695-9703.
- [17] Sikora, R., & Pirmuthu, S. (2005). Efficient genetic algorithm based data mining using feature selection with Hausdorff distance. *Information Technology and Management*, 6(4), 315-331.
- [18] Sexton, R. S., Sriram, R. S., & Etheridge, H. (2003). Improving decision effectiveness of artificial neural networks: a modified genetic algorithm approach. *Decision Sciences*, 34(3), 421-442.
- [19] Sikora, R. (2015). A modified stacking ensemble machine learning algorithm using genetic algorithms. In *Handbook of Research on Organizational Transformations through Big Data Analytics* (pp. 43-53). IGI Global.
- [20] Hearst, M. A. (1999, June). Untangling text data mining. In *Proceedings of the 37th annual meeting of the Association for Computational Linguistics on Computational Linguistics* (pp. 3-10). "Association for Computational Linguistics".
- [21] Xu, K., Liao, S. S., Li, J., & Song, Y. (2011). Mining comparative opinions from customer reviews for Competitive Intelligence. "Decision support systems", 50(4), 743-754.
- [22] Ting, K. M., & Witten, I. H. (1999). Issues in stacked generalization. *Journal of artificial intelligence research*, 10, 271-289.
- [23] Karman, S. S., & Ramaraj, N. (2008). Similarity-Based Techniques for Text Document Classification. *Int. J. SoftComput*, 3(1), 58-62.

Image Retrieval using Visual Phrases

Benish Anwar¹, Junaid Baber², Atiq Ahmed³, Maheen Bakhtyar⁴,
Sher Muhammad Daudpota⁵, Anwar Ali Sanjrani⁶, Ihsan Ullah⁷
Department of Computer Science and Information Technology^{1,2,3,4,6,7}
University of Balochistan, Pakistan
Department of Computer Science⁵
Sukkar IBA University, Pakistan

empty

Abstract—Keypoint based descriptors are widely used for various computer vision applications. During this process, keypoints are initially detected from the given images which are later represented by some robust and distinctive descriptors like scale-invariant feature transform (SIFT). Keypoint based image-to-image matching has gained significant accuracy for image retrieval type of applications like image copy detection, similar image retrieval and near duplicate detection. Local keypoint descriptors are quantized into visual words to reduce the feature space which makes image-to-image matching possible for large scale applications. Bag of visual word quantization makes it efficient at the cost of accuracy. In this paper, the bag of visual word model is extended to detect frequent pair of visual words which is known as frequent item-set in text processing, also called visual phrases. Visual phrases increase the accuracy of image retrieval without increasing the vocabulary size. Experiments are carried out on benchmark datasets that depict the effectiveness of proposed scheme.

Keywords—Image processing; image retrieval; visual phrases; apriori algorithm; SIFT

I. INTRODUCTION

Information extraction from the images is a very important process in image processing and computer vision. It is used to extract information from images to interpret and understand their contents for image processing applications. Image-feature extraction is one of the driving factors in interpreting and processing images for the development of various computer vision areas.

Content Based Image Retrieval (CBIR)¹ [1] is an image processing technique to retrieve an image and its contents with a given object query from the large database efficiently. One of the key issues is to search the visual information and phrases with computer vision techniques for image retrieval data from a huge database. The objective and goal of searching a query is one of the applications of image processing in computer vision. Applications include medical image databases like Computerized Tomography (CT), Magnetic Resonance Imaging (MRI), and ultrasound, World Wide Web (WWW), scientific databases and consumer electronics that include digital camera and games, etc.

Visual information and media are common applications in the media channels and social media. These applications and image retrieval contents have gained enough attention for the researchers to develop an efficient and robust application inside

the image retrieval databases. One of the most fundamental issue in image retrieval is the space or memory amongst the feature descriptors of the images and low level features are required to save feature descriptor memory [2].

One of the most commonly used feature technique in image processing is Scale Invariant Feature Transform (SIFT) for the image databases [3]. SIFT performs better in various computer vision tasks and it is robust to geometric transformations intrinsically [4]. Conventionally, distance is computed to match one object to another object in image retrieval tasks for any given point in all images. In SIFT, all keypoints are identified and represented in a given image first of all. The nearest point in an image is the keypoint for matching one image to another one. Local keypoint descriptors mainly face two computational issues (1) space feature and (2) to find two similar images from the databases.

In order to overcome above mentioned issues in SIFT descriptor local keypoint features, local key descriptors are quantized using Bag of Visual Words (BoVW) technique. Various quantization techniques are used for image processing and retrieval databases like, Fisher Vector [6], VLAD [7–9], binary quantizer and BoVW model [10].

BoVW model is commonly employed in literature for image processing and computer vision oriented applications which include image retrieval [10, 11] and image classification [8]. BoVW model concept has originated from the documents retrieval, text retrieval, and image retrieval for representing most occurring words or number of frequency words in the document files. For normalizing the vocabulary size in any document, stop words and most occurring words are deleted and later, stemmed or lemmatization techniques are applied for the remaining words. Same idea is applicable on clustered descriptors and visual domain. Clustered center of descriptors is considered as a visual word. Learning process is performed by clustering from the large database which is an off-line procedure. Representation of visual words can be shown with histograms obtained from any image. Quantization process and description representation is explained in section III-A. BoVW model considers each visual word a single entity which is one of its limitations [12]. Words are grouped based on their frequency in the documents for training purpose in text processing applications. Training set is frequent item set in text processing words.

This work is structured as follows. Next section briefly presents some of the existing approaches and discusses their limitations. Next, the proposed model is devised for coping up

¹CBIR is also known as Query by Image Content (QIBC)

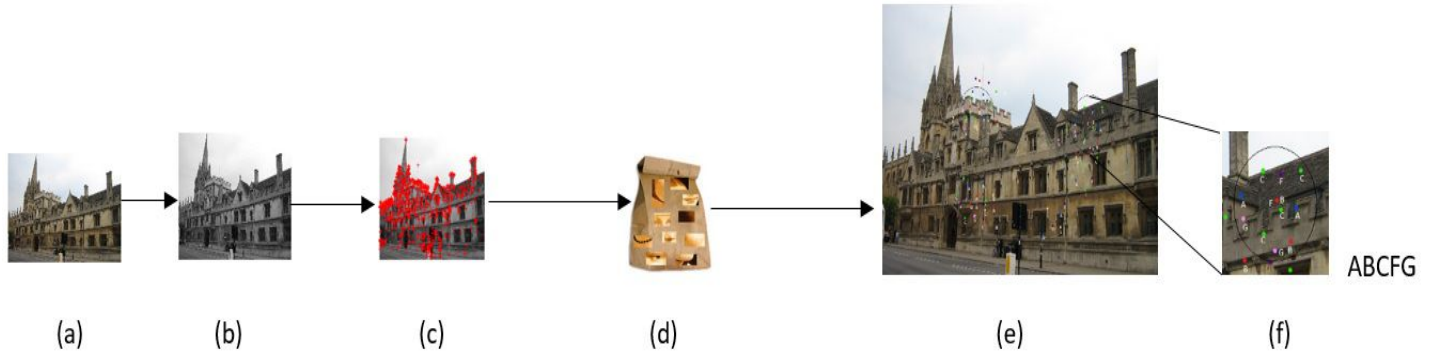


Fig. 1. Abstract flow diagram of the proposed approach to model the Apriori algorithm [5] to find the frequent visual words. Figures (a-c) show the original image which is converted into gray scale and later represented by the SIFT keypoint descriptors, (d) maps each keypoint to its nearest visual word, (e) shows few keypoints with radius r , and (f) shows one keypoint which is converted into a transaction.

with those limitations and finally, evaluations of the proposed model are presented with a short conclusion in the last section.

II. LITERATURE REVIEW

There are two main categories of image retrieval techniques; (1) text based search, where, images are annotated manually to perform retrieval tasks in the text based managed system database and (2) content based search, where, annotation automatically retrieves images using visual content words including colors, shapes, textures or any other information that can be extracted from images [13, 14]. They are indexed by using indexing techniques for large scale retrieval.

Recently, convolution neural network (CNN) has come up as one of the state-of-the-art classifiers by obtaining better performance on various computer vision applications. CNN is used both; as a feature vector and as a classifier for the image classification in most of the frameworks reported [15]. Object search, scene retrieval, video retrieval, and video Google are some of the active research areas based on this technique which is also known as text based search.

In SIFT, first keypoints are located at a length of 128 of vector for each keypoint [3]. Using SIFT, keypoints range from 2.5 K to 3.0 K for an individual image. Visual words are then quantized against each local keypoint descriptor to single image feature. BoVW model gives successful and promising results for image retrieval in large databases where performance accuracy and a low recall rate is obtained using a standard query expansion method in text retrieval documents.

SIFT descriptors are used with variety of techniques for the same type of problems to improve the performance in order to generate robust and distinctive results. To search object computational efficiency, the feature descriptors are clustered or quantized to hamming space [16] or to a single image feature [17] from a large corpora of image databases.

In image retrieval, all leading methods from a large corpora image database rely on same technique with variants [11]. Each image is processed to extract features in high dimensional feature space from a large corpora of image databases. Feature

descriptors are quantized to represent features to the visual word in smaller discrete size corpus vocabulary.

Another approach for searching is the use of phrases which are obtained by visual words. This technique has two major drawbacks. Phrases which are defined only show us the co-occurrence of visual text in the whole image and its neighbor[18]. They do not give us the spatial information between the words instead, they only provide the neighbor information and never give long-range interaction. It never defines the spatial layout of visual words and there is a weak spatial verification. Secondly, the total number of phrases increases exponentially in the number of words. A subset from the phrase set can be selected for this purpose by using some algorithm, however, this might remove a large portion of phrases. In these phrases, some words are removed which might prove to be important for image representation in future.

Geometry-preserving Visual Phrases (GVP) [19] takes spatial information in the examining step and is deployed in a specific spatial arrangement. This algorithm is inspired by [20] which is used for object categorization. It defines the co-occurrences of GVP within the whole image by building the kernel of support vector machine for object categorization and it is not used for the large databases. Authors extend their algorithm for a large image database. For this purpose, they increase little memory usage in the searching method with BOV model that provides with more spatial information. For improving the searching efficiency, they use their approach with GVP into the min-hash function [21]. This approach increases the searching and retrieval accuracy by adding some spatial information in addition to the computational cost.

In the modern era, mobile phone demand is increasing and people frequently ask for added features on their devices and many companies also fulfill their demands and add more and more features in their products. Identification of landmarks is one of the most prominent applications, with the help of which people take the information about different places by taking the pictures of those locations which is very useful for visitors [22]. In the next section, we present the proposed model which is based on BoVW.

III. PROPOSED APPROACH

In this section, BoVW based model is proposed. The discriminative power of visual words can be increased by using visual phrases [22]. It is inspired from text-based searching where two words are concatenated to make one phrase based on the frequencies of occurring together in a large corpus.

To model the same idea in visual search, it is needed to define words and transactions in visual space. Images are represented by a set of local keypoint descriptors such as SIFT [3]. Searching the images which are based on raw SIFT descriptors is computationally expensive [10]. BoVW is widely used to make image search feasible for large databases. BoVW are treated as words in the proposed framework analogous to text based searching [10, 23–25]. Later in this section, BoVW is explained which is followed by frequent item-set algorithm (Apriori) and finally, BoVW based proposed framework is explained.

A. Bag of Visual Words

Bag of visual word model is widely used for feature quantization. Every key point descriptor, $x_j \in \mathbb{R}^d$, is quantized into a finite number of centroids from 1 to k , where k denotes the total number of centroids also known as visual words which are denoted by $\mathcal{V} = \{v_1, v_2, \dots, v_k\}$ and each $v_i \in \mathbb{R}^d$. Let us consider a frame f which is represented by some local key point descriptors $f^X = \{x_1, x_2, \dots, x_m\}$, where $x_i \in \mathbb{R}^d$. In BoVW model, a function \mathcal{G} is defined as:

$$\mathcal{G} : \mathbb{R}^d \mapsto [1, k] \quad (1)$$

$$x_i \mapsto \mathcal{G}(x_i)$$

where, \mathcal{G} maps descriptor $x_i \in \mathbb{R}^d$ to an integer index. Mostly, Euclidean distance is used to decide the index for the function \mathcal{G} . For given point x_i , Euclidean distance is computed with all the centroids, which are named as visual words, and the index of centroid is selected whose distance is the minimum with the x_i . For a given frame f and bag of visual word \mathcal{V} , $\mathcal{I}_f = \{\mu_1, \mu_2, \dots, \mu_k\}$ is computed. μ_i indicates the number of times v_i has appeared in frame f , and \mathcal{I} is the unit normalized at the end. Mostly, k -mean or hierarchical k -mean clustering is applied and centroids (visual words) \mathcal{V} are obtained. The value of k is kept very large for image matching or retrieval applications, the suggested value of k in this proposed approach is 1 million. Accuracy of quantization mainly depends on the value of k , if the value is small then two different keypoint descriptors will be quantized to same visual words which will decrease the distinctiveness, or if the value is very large then two similar keypoint descriptors, which are slightly distorted, can be assigned different visual words which decreases the robustness [10] [26].

B. Frequent Item-set Detection

Apriori is well-known data mining algorithm which is used for finding frequent item-sets from transactions [27]. Let the items be denoted by $\mathcal{I} = \{i_1, i_2, \dots, i_{k'}\}$, and the transactions by $\mathcal{T} = \{t_1, t_2, \dots, t_m\}$, where each t_i contains combination of more than 1 items, i.e., $t_i = \{i_1, i_4, i_7\}$ contains three items, $i_{1,4,7} \in \mathcal{I}$. As stated above, the experiments in this paper covers only 3 frequent item-sets by following:



Fig. 2. PCA-SIFT dataset used for image retrieval

- 1) Minimum support, decision threshold to decide whether given item-set is frequent or not, is decided experimentally or statistically.
- 2) Generate the 1-item-sets after comparing all items \mathcal{I} with minimum support. The one frequent item sets are denoted by L_1 .
- 3) The L_1 is joined along each other and create candidates for 2-item-sets, taking 2-combination of L_1 item-sets, denoted by C_2 , candidate for 2-frequent item-sets.
- 4) Each pair in C_2 is compared with minimum support. The value of minimum support is set 0.75, which implies that any item-set is considered frequent if it appears in at least 75% of the transactions. All those items in C_2 are treated as frequent if those item sets were present in at least 75% of the transactions and denoted by L_2 .
- 5) Similarly, L_3 is calculated.

C. Frequent Visual Word Detection

Now, Apriori approach is extended to the visual phrases. To detect frequent item-set, called as visual phrases in this paper, each keypoint descriptor is mapped to a visual word which is treated as an item. Every image is represented by set of visual words, as shown in Fig. 1 (a-e).

To create the transactions out of visual words, radius r around each keypoint is drawn and all the visual words within that radius are treated as one transactions, as shown in Fig. 1 (e-f). The value of r if increased to large number of pixels, then the length of the transaction is very high. In this paper, we experimented by keeping $r = 100$.

Oxford 5K [28] dataset is used for the training of visual words and detection of frequent visual words. Oxford 5K dataset contains 5065 images of 11 different landmarks. There are 3.5K keypoints, on average, using Hessian Affine detector.

D. Dataset

To evaluate the proposed framework, PCA-SIFT dataset is used which is one of the challenging datasets used in several works and can be downloaded online ². The dataset is shown in Fig. 2. There are 10 different scenes with each having three severe transformations. Transformations include change in scale, rotation, zooming, viewpoint change, and different intensities of illumination.

²<http://www.cs.cmu.edu/~yke/pcasift/>

E. Experimental Setup

During the experiments, 10000 visual words are learned which are treated as items. To obtain 10000 visual words, which are basically centroids, obtained by k-mean clustering. In training phase, Oxford 5K dataset is used for feature extraction and clustering, SIFT is extracted from all the images and pooled into one feature set. Later, k-mean clustering is applied by keeping the value $k = 10000$. VLFEAT³ library is used for k-mean clustering.

Once the visual words are learned and images are represented by visual words, transactions are generated, as explained in previous section and Figure 1 as well. Frequent visual words are identified using Apriori algorithm using R-package.

The baseline is same as explained in Equation 1, the image f is represented by $\mathcal{I}_f = \{\mu_1, \mu_2, \dots, \mu_k\}$. Let the visual phrases be denoted by $\mathcal{F} = \{\phi_1, \phi_2, \dots, \phi_{k'}\}$ where ϕ_i is the unordered pair of three frequent visual words identified by Apriori algorithm. For every ϕ_i the frequency is also stored in separate file, the frequency is taken into account if there are more than one frequent items under the radius of given keypoint x_i . The given image is quantized same as Equation 1, the only difference is that \mathcal{V} is replaced with \mathcal{F} , the function \mathcal{G} is redefined as $\mathcal{G}^{\mathcal{F}}$ below

$$\mathcal{G}^{\mathcal{F}} : \mathbb{R}^d \mapsto [1, k'] \\ x_i \mapsto \mathcal{G}^{\mathcal{F}}(x_i) \quad (2)$$

where $\mathcal{G}^{\mathcal{F}}$ maps the given keypoint descriptor x_i to an index from frequent visual words \mathcal{F} . The $\mathcal{G}^{\mathcal{F}}$ is computed as follow

- For given image, repeat the steps explained in Figure 1 (a-e).
- Draw the circle of radius r for every keypoint, record the other keypoints within that circle, denoted by t , as illustrated in Figure 1 (f).
- Find the 3-combination of all the elements in t_i for the given keypoint x_i , and check all those combinations in \mathcal{F} .
- The index from \mathcal{F} is assigned to the keypoint x_i if any of the 3-combination of the transaction t is present in \mathcal{F} . Most of the times, there are more than one combinations of t present in \mathcal{F} , so the index of most frequent ϕ is assigned to x_i .

Finally, Video Google [29] approach is used for matching the visual words between pair of the images.

The mean average precision (mAP) is used to evaluate the proposed framework. Precision \mathcal{P} is obtained as follow

$$\mathcal{P} = \frac{\mathcal{E}}{\mathcal{O}} \quad (3)$$

where, \mathcal{E} denoted correctly retrieved, and \mathcal{O} denotes total retrieved. Precision is calculated at different values of recall \mathcal{R} which can be computed as follow

$$\mathcal{R} = \frac{\mathcal{E}}{\mathcal{W}} \quad (4)$$

³<http://www.vlfeat.org/>

TABLE I. RETRIEVAL ACCURACY OF PROPOSED FRAMEWORK COMPARED WITH BOVW MODEL.

Scene	BoVW	Visual Phrases
S_1	0.6806	0.6806
S_2	0.5667	1.0000
S_3	1.0000	1.0000
S_4	0.7292	0.5255
S_5	0.7255	0.9167
S_6	0.5143	0.6000
S_7	0.6556	0.8667
S_8	0.7255	1.0000
S_9	1.0000	0.8667
S_{10}	0.7667	0.8333
mAP	0.7364	0.8289

where, \mathcal{W} denotes the total number of images to be retrieved and total true positives for a given query. For each query, an average precision is computed, and finally, mean of all average precisions (mAP) is computed as illustrated in Table I.

Table I shows the average precision for each scene and finally mAP, for proposed framework and BoVW model. It can be seen that the proposed framework achieves perfect precision for some of the scenes.

IV. CONCLUSION

This paper presents the extension of BoVW model. Images are represented by local keypoint descriptors which are later quantized into visual words (BoVW). Instead of representing every keypoint with single visual word, the model is extended to pair the visual words which are known as visual phrases. This idea is inspired from text based search engines where text document is represented by set of frequent item-sets. In this paper, up to three frequent item-sets are discovered and image is represented by L_3 frequent item-sets. Experiments on benchmark dataset show the increase in mean average precision (mAP) which is increased from 0.7364 to 0.8289. The same framework can be extended to L_n -frequent item sets for very large databases which is also the future work of proposed framework.

REFERENCES

- [1] A. Araujo and B. Girod, "Large-scale video retrieval using image queries," *IEEE Transactions on Circuits and Systems for Video Technology*, vol. 28, no. 6, pp. 1406–1420, June 2018.
- [2] K. Yan, Y. Wang, D. Liang, T. Huang, and Y. Tian, "Cnn vs. sift for image retrieval: Alternative or complementary?" in *Proceedings of the 2016 ACM on Multimedia Conference*. ACM, 2016, pp. 407–411.
- [3] J. Zhao, N. Zhang, J. Jia, and H. Wang, "Digital watermarking algorithm based on scale-invariant feature regions in non-subsampled contourlet transform domain," *Journal of Systems Engineering and Electronics*, vol. 26, no. 6, pp. 1309–1314, Dec 2015.
- [4] J. J. Foo and R. Sinha, "Pruning sift for scalable near-duplicate image matching," in *Proceedings of the eighteenth conference on Australasian database-Volume 63*. Australian Computer Society, Inc., 2007, pp. 63–71.
- [5] A. Bhandari, A. Gupta, and D. Das, "Improvised apriori algorithm using frequent pattern tree for real time applications in data mining," *Procedia Computer Science*, vol. 46, pp. 644–651, 2015.
- [6] F. Perronnin and C. Dance, "Fisher kernels on visual vocabularies for image categorization," in *Computer Vision and Pattern Recognition, 2007. CVPR'07. IEEE Conference on*. IEEE, 2007, pp. 1–8.
- [7] H. Jégou and A. Zisserman, "Triangulation embedding and democratic aggregation for image search," in *Proceedings of the IEEE conference on computer vision and pattern recognition*, 2014, pp. 3310–3317.
- [8] A. Bergamo, S. N. Sinha, and L. Torresani, "Leveraging structure from motion to learn discriminative codebooks for scalable landmark

- classification,” in *Proceedings of the IEEE Conference on Computer Vision and Pattern Recognition*, 2013, pp. 763–770.
- [9] Z. Wang, W. Di, A. Bhardwaj, V. Jagadeesh, and R. Piramuthu, “Geometric vlad for large scale image search,” *arXiv preprint arXiv:1403.3829*, 2014.
- [10] J. Baber, M. N. Dailey, S. Satoh, N. Afzulpurkar, and M. Bakhtyar, “Bigoh: Binarization of gradient orientation histograms,” *Image and Vision Computing*, vol. 32, no. 11, pp. 940–953, 2014.
- [11] Q. Zhu, Y. Zhong, B. Zhao, G. Xia, and L. Zhang, “Bag-of-visual-words scene classifier with local and global features for high spatial resolution remote sensing imagery,” *IEEE Geoscience and Remote Sensing Letters*, vol. 13, no. 6, pp. 747–751, June 2016.
- [12] Y. S. Koh and S. D. Ravana, “Unsupervised rare pattern mining: A survey,” *ACM Trans. Knowl. Discov. Data*, vol. 10, no. 4, pp. 45:1–45:29, May 2016.
- [13] J. Ragan-Kelley, A. Adams, D. Sharlet, C. Barnes, S. Paris, M. Levoy, S. Amarasinghe, and F. Durand, “Halide: Decoupling algorithms from schedules for high-performance image processing,” *Commun. ACM*, vol. 61, no. 1, pp. 106–115, Dec. 2017.
- [14] J. Thies, M. Zollhofer, M. Stamminger, C. Theobalt, and M. Niessner, “Face2face: Real-time face capture and reenactment of rgb videos,” *Commun. ACM*, vol. 62, no. 1, pp. 96–104, Dec. 2018.
- [15] R. Tao, E. Gavves, C. G. Snoek, and A. W. Smeulders, “Locality in generic instance search from one example,” in *Proceedings of the IEEE Conference on Computer Vision and Pattern Recognition*, 2014, pp. 2091–2098.
- [16] J. Baber, M. Bakhtyar, W. Noor, A. Basit, and I. Ullah, “Performance enhancement of patch-based descriptors for image copy detection,” *International Journal of Advanced Computer Science and Applications*, vol. 7, no. 3, pp. 449–456, 2016.
- [17] W. Zhou, Y. Lu, H. Li, Y. Song, and Q. Tian, “Spatial coding for large scale partial-duplicate web image search,” in *Proceedings of the 18th ACM international conference on Multimedia*. ACM, 2010, pp. 511–520.
- [18] L. Torresani, M. Szummer, and A. Fitzgibbon, “Learning query-dependent prefilters for scalable image retrieval,” in *Computer Vision and Pattern Recognition, 2009. CVPR 2009. IEEE Conference on*. IEEE, 2009, pp. 2615–2622.
- [19] W. Wei, C. Tian, and Y. Zhang, “Robust face pose classification method based on geometry-preserving visual phrase,” in *2014 IEEE International Conference on Image Processing (ICIP)*, Oct 2014, pp. 3342–3346.
- [20] Y. Zhang and T. Chen, “Efficient kernels for identifying unbounded-order spatial features,” in *Computer Vision and Pattern Recognition, 2009. CVPR 2009. IEEE Conference on*. IEEE, 2009, pp. 1762–1769.
- [21] O. Chum, J. Philbin, A. Zisserman *et al.*, “Near duplicate image detection: min-hash and tf-idf weighting,” in *BMVC*, vol. 810, 2008, pp. 812–815.
- [22] T. Chen, K.-H. Yap, and D. Zhang, “Discriminative soft bag-of-visual phrase for mobile landmark recognition,” *IEEE Transactions on Multimedia*, vol. 16, no. 3, pp. 612–622, 2014.
- [23] J. Delhumeau, P.-H. Gosselin, H. Jégou, and P. Pérez, “Revisiting the vlad image representation,” in *Proceedings of the 21st ACM international conference on Multimedia*. ACM, 2013, pp. 653–656.
- [24] J. Baber, S. Satoh, N. Afzulpurkar, and C. Keatmanee, “Bag of visual words model for videos segmentation into scenes,” in *Proceedings of the Fifth International Conference on Internet Multimedia Computing and Service*. ACM, 2013, pp. 191–194.
- [25] H. Kato and T. Harada, “Image reconstruction from bag-of-visual-words,” in *Proceedings of the IEEE conference on computer vision and pattern recognition*, 2014, pp. 955–962.
- [26] M. Haroon, J. Baber, I. Ullah, S. M. Daudpota, M. Bakhtyar, and V. Devi, “Video scene detection using compact bag-of-visual word models,” *Advances in Multimedia*, 2018.
- [27] S. Fong, R. P. Biuk-Aghai, and S. Tin, “Visual clustering-based apriori arm methodology for obtaining quality association rules,” in *Proceedings of the 10th Intl. Symposium on Visual Information Communication & Interaction*. New York, NY, USA: ACM, 2017, pp. 69–70.
- [28] J. Philbin, O. Chum, M. Isard, J. Sivic, and A. Zisserman, “Object retrieval with large vocabularies and fast spatial matching,” in *Computer Vision and Pattern Recognition, 2007. CVPR’07. IEEE Conference on*. IEEE, 2007, pp. 1–8.
- [29] J. Sivic and A. Zisserman, “Video google: A text retrieval approach to object matching in videos,” in *null*. IEEE, 2003, p. 1470.

An Improved Particle Swarm Optimization Algorithm with Chi-Square Mutation Strategy

Waqas Haider Bangyal¹

Department of Computer Science
University of Gujrat, Pakistan

Hafsa Batool³

Department of Computing and Technology
Iqra University, Islamabad, Pakistan

Jamil Ahmed⁵

Kohat University of Science and Technology
(KUST), Pakistan

Hafiz Tayyab Rauf²

Department of Computer Science
University of Gujrat, Pakistan

Saad Abdullah Bangyal⁴

Department of Computer Science
Abasyn University, Islamabad, Pakistan

Sobia Pervaiz⁶

Department of Software Engineering
University of Gujrat, Gujrat, Pakistan

Abstract—Particle Swarm Optimization (PSO) algorithm is a population-based strong stochastic search strategy empowered from the inherent way of the bee swarm or animal herds for seeking their foods. Consequently, flexibility for the numerical experimentation, PSO has been used to resolve diverse kind of optimization problems. PSO is much of the time caught in local optima in the meantime taking care of the complex real-world problems. Considering this, a novel modified PSO is introduced by proposing a chi square mutation method. The main functionality of mutation operator in PSO is quick convergence and escapes from the local minima. Population initialization plays a critical role in meta-heuristic algorithm. Moreover, in this work, to improve the convergence, rather applying random distribution for initialization, two quasi random sequences Halton and Sobol have been applied and properly joined with chi-square mutated PSO (Chi-Square PSO) algorithm. The promising experimental result suggests the superiority of the proposed technique. The results present foresight that how the proposed mutation operator influences on the value of cost function and divergence. The proposed mutated strategy is applied for eight (8) benchmark functions extensively used in the literature. The simulation results verify that Chi-Square PSO provide efficient results over other tested algorithms implemented for the function optimization.

Keywords—Particle Swarm Optimization; Chi-Square Mutation; Population Initialization.

I. INTRODUCTION

The term “swarm intelligence” is practiced as to explain the algorithm and distributed problem solvers, motivated by the common actions of colonies of insects and other animal groups. Swarm Intelligence (SI) based systems are normally buildup of simple agents of population that are communicating internally with each other and with their environment [1].

Likewise, other evolutionary algorithms (EAs), the particle swarm optimization (PSO) technique is a population based meta-heuristic search approach that devised from nature aspect. Such type of approaches commonly needs extra objective function evaluations that compared with gradient search techniques. These techniques offer stunning features like easiness in the numerical implementation for both discrete and continuous optimization problems and more powerful solution creations for seeking the global solutions. PSO algorithm seeks the optimum solution inside the population called as flock or swarm. PSO avails the advantage from two type of training: cognitive

training focused on particle’s own history while social training concentrated on swarm history of information sharing collected from all the individuals of the swarm.

Kennedy and Eberhart formally introduced PSO, it got enticed notable attraction in last decade. Vast majority of research on this subject is concerned either with the mathematical analysis or to enhance the algorithm for attaining the quicker, robust, and scalable candidate solutions. Main motivation of the posterior, stuck in local optima by the solution or premature convergence. An EA is trapped to the local optima, if it is not capable to investigate all the search space except the explored region, and another area persists that hold a best solution better than to the currently find solution. One of the major causes for the deficiency of diversity is premature convergence.

Diversity is vital important for vigorous searching in the given search space while the mutations are fundamental operators to give the dynamic diversity inside the swarm [2]. Besides the designing of new mutation operator, researchers have placed fewer efforts to explore that how to use the mutation operator [3] and to find what type of diversity supposed to be available in the swarm. Hence, after the detail exploration of diversity concept focused on qualification and quantification studies, this paper presents new mutation strategy and operator to give useful diversity in the swarm. The new proposed technique has been used on the selected benchmark functions. From these test cases, it is shown that proposed technique has given the better results than other variants of PSO. The core objective of this strategy was to find which particle should be mutated and when; it should be mutated. The proposed technique also gives controlled diversity in the swarm.

The rest of the paper is structured like this: Section 2 reviews the technical background of PSO algorithm where Standard PSO is discussed in Section 3. Section 4 carries the proposed algorithm. In Section 5, the computational simulation results and comparison are carried out. Conclusion and future work are presented in Section 6.

II. LITERATURE REVIEW

PSO might have some problems associated to rate of convergence, premature converged solution, poor accuracy and failure of diversity. Several modifications have been introduced till now to overcome these issues [4]. Improved approaches can split

into two types concentrating on improvements of hardware and software. The hardware is concerned with parallel computing. While the software improvements can be more categorized like integrating with other heuristic techniques, motivation from other stochastic methods, manipulating and restructuring of velocity update equation, managing the neighborhood topology, tuning the parameters during the update phase and swarm size.

PSO has been incorporated with other metaheuristic algorithm named as hybridization. The standard hybrid application is to employ PSO with other stochastic based technique like GA or other evolutionary computing algorithms. Furthermore, other approach is to utilize the gradient-based approach as incorporated segment. Restructuring the equations (2.2) and (2.3) has the significant importance in the improvements of the algorithm. In such rearranging or manipulations and updation of the equation of velocity is expanded [5] with an additional factor or reducing it rely on the technique.

Standard PSO parameters ω , c_1 and c_2 can be used as constant, periodically, chaotic, random, adaptive, linear changeable or nonlinear relying on time or other concerns like cost function and velocity measures. Neighborhood topologies created by choosing the position vector of particle from P_i to P_g . In standard algorithm of PSO, individual particle is pulled towards the particle's personal best and global best.

Consequently, none else personal particle's best position vector will take the appealing impact on a single particle itself and also best position vector also will not be modified at each epoch. At present, various neighborhood topologies are presented [6], population of swarm is also explored in many different dimensions.

By selecting swarm size dynamically might be encouraging to find out the solution few optimization real world problems [7]. Motivation from other population based search algorithm like GA, opposition based learning techniques, simulating annealing are the famous approaches used for the fundamental working enhancement of the standard PSO. In addition, GA common operator's selection, crossover, elitism and mutation can be incorporated in PSO architecture [8].

Mutation is mainly used in GA operators due to shortcomings of PSO [9], because of deficient diversity that drives the swarm particles to approach the position discovered yet in the swarm cause local minima. Lack of diversity improving techniques, majority of optimization approaches cannot be effectively explore or exploit the given search space. Mutation operator set up the new particles by altering the current particle in the swarm [10], so incorporating diversity in the swarm and probably stopping stagnation of exploration for local minima.

Consequently, the mutation application technique draws some new modification to the algorithm like condition for mutation application, the placement of mutation is to apply and choose the different distribution sequences. In order to find the criterion for mutation applications, description of diversity threshold [11], similarity and mutation probability ration may be used. Similarly, for viable random distribution, sequences are Cauchy distribution, Chaotic distribution, Beta distribution and Gaussian distribution.

Higashi and Iba [12] implemented initial practice of mutated operator by introducing the random number based on Gaussian

distribution for changing the particle dimension. Likewise Higashi, a new mutation operator is proposed by Stacey et al [13] by mutilating the particle using a number drawn from cauchy distribution to keep the diversity.

Pant et al. [14] gave a new mutation operator named as Sobol mutation operator that utilizes the quasi-random sequences to explore the search space better than random distribution. To keep the diversity in the swarm Zavala et al. [15] gave two separate perturbation operators known as C-perturbation operator and M-perturbation operator and implemented to personal best position in lieu of perturbing the position vector of particle in the swarm.

Jia et al. [16] used two mutation operator called as Chaotic mutation operator and Gaussian mutation operator. By using chaotic mutation operator, global searching was performed while to solve the issue of local exploitation, Gaussian mutation was integrated into PSO. To avoid from local minima, Wu et al. [17] proposed a novel mutation named as cloud mutation having the features of randomness; and keeping the capability of standard cloud model.

Chen et al. [18] defined a novel mutation operator named as adaptive mutation. In this variant, they contain the potential particle for mutation around the global best discovered by either particle in given search space during preliminary epochs.

Liu et al. [19] defined new mutation operator with names Chaotic PSO by integrating chaos in PSO having adaptive inertia weight. To avoid from premature convergence and keeping the diversity in swarm, Yang et al. [20] proposed a new mutation operator that uses the chaotic probability into the algorithm having inertia weight linear decreasing.

Liu et al. [21] defined an improved version of PSO focused on the concept of collectivity in which resemblance focus on current global best position vector and a particle in the swarm. Biao et al. [22] proposed PSO based on fast position convergence, in order to prevent from unwanted epochs in each local optima, and it is used only when required.

According to [23], by proposing the intelligent PSO called (PSO-IM) based on intelligent mutation. PSO-IM includes two types of mutation, uniform mutation and non uniform mutation. Tournament selection strategy is adopted to select particles randomly in each tournament for mutation operation while mutation probability (p_m) is controlled dynamically with fuzzy controllers. The process of tournament selection continues until a predetermined number of individuals selected.

Uniform mutation replaced selected particles by a random number while non uniform mutation applied on rest of particles to overcome local minima. The performance of PSO-IM was tested on six popular nonlinear global optimization problems and four nonlinear reliability problems .

PSO-IM outperforms the original PSO in all test cases. K. Wang and F. Li [24] brought dynamic chaotic behavior in PSO called (dcmPSO) to gain global exploration at the start of iteration and local exploitation at the end of the iteration. The logistic map turns the mutation process into chaotic state. At the end of iteration a temporary leader is found. If the temporary leader does not improved for a predefined constant number. Then chaotic state turns on to update temporary leader. The

proposed technique proved its effectiveness on Park-Ramirez bioreactor dynamic problem.

The mutation operator gives the diversity ability in the swarm. Thus, for mutation application, mutation operator types and their application technique is the major decision portion. Besides the proposing of new mutation operator to avoid from local minima, the researchers put very limited attempts to examine how to use these new deigned mutated operators through the PSO procedure and find which kind of diversity in the swarm should be available.

III. PARTICLE SWARM OPTIMIZATION

PSO is a relatively new metaheuristic optimization search algorithm that uses the pool of best solutions to find the optimum solution. The search of optimum solution is managed by adopting the social behavior of bees, herds of animal and bird flock [25]. Considering the ants' colonies, bee swarm, flock of birds, animal herds and school of fish revealed that collective venture of a bunch is normally more productive than single effort. Each single entity inside a group has a specific ability to achieve the goal. During working in a group, action of a candidate led not only by the candidate's understanding to accomplish the goal but also through the social action. The entire candidates inside a group share the experience by following the common goal, and each individual discover not only from its own experience as well as from experience of its neighbors. This accelerates the searching process considerably fast. This kind of social interaction was the origination of the PSO algorithm, elaborated in the paper.

PSO works on bunch of candidates. Each candidate termed as a particle which depicts a solution for the optimization problem. For n dimensional problem, a particle depicted by n-dimensional vector, x represents a particle position. Each particle has a fitness value that shows the worth of individual's solution representation. Swarm's particle moves in n dimension given search space. Beside the position vector in search space, each particle has velocity vector that finds the step size and direction of particle motion. Social communication emulated by making neighbors inside the swarm. Each particle saves its own personal best position discovered until now and can inquire neighbor particles for the best position as found by the neighboring particles so far. PSO neighboring swarm information sharing techniques have been discussed in the literature [26].

The architecture and size of neighbor finds the method where information shared between the particles. PSO seeks for an optimum solution by moving the particles over the n dimensional search space. For each step k, position vector of particle X_{id}^k updated by adding the velocity vector V_{id}^{k+1} of the particle to the prior position vector.

$$X_{id}^{k+1} = X_{id}^k + V_{id}^{k+1} \quad (1)$$

The velocity vector of the particle finds out the step size and direction. The velocity equation is given below:

$$V_{id}^{k+1} = V_{id}^k + c_1 r_1 (p_{id} - x_{id}) + c_2 r_2 (p_{gd} - x_{id}) \quad (2)$$

Where acceleration coefficients c_1 and c_2 applied to measure the effect of cognitive part (second term of equation 2.2) and

social component (third term of equation 2.2); r_1 and r_2 are random numbers vectors, where each part taken from uniform distribution in the range between zero and one. In each iteration value of r_1 and r_2 changed. p_{id} is particle personal best position acquired by the particle 'y' yet; where as p_{gd} is the best global position discovered by any particle in the neighbor of particles.

Although in the original form of PSO, none method exists to restrain the velocity. It causes the feeble nature of algorithm, particularly in the area of local minima. In the back adaptations of PSO, this insufficiency was handled by incorporating two new parameters, named as inertia weight proposed by Shi and Eberhart [27] and constriction factor (ω) presented by Clerc [28]. Therefore, each particle is approaching to the best position confronted by itself until now, along with entire best position found by the neighborhood particles, so far. A maximum velocity $V_{(max)}$ occasionally adjusted to restrict particle velocity in each dimension of the search space. Velocity clamping performed to stop the particles from traveling the search space quickly, since extremely big steps stop particles from exploiting good areas of the search space. $V_{(max)}$ is implemented by stopping V_{id}^k in each dimension space [29]. Major advancement in PSO is the addition of inertia weight term to restrain the influence of value of older velocity on new velocity is given below:

$$V_{id}^{k+1} = \omega V_{id}^k + c_1 r_1 (p_{id} - x_{id}) + c_2 r_2 (p_{gd} - x_{id}) \quad (3)$$

Where the term ω is named as inertia weight; two positive constants c_1 and c_2 are cognitive and social parameter, respectively.

Currently, Clerc [5] inducted one more parameter named as constriction factor, which may help to anchor the convergence. The constriction factor model clarifies the system by choosing ω , c_1 and c_2 for the guaranteed convergence. By selecting these parameters values accurately, the velocities of all particles are selected in the range $[-V_{(max)}, V_{(max)}]$. Eberhart and Shi investigate the performance of PSO using velocity clamping $V_{(max)}$ with constriction factor. The experimental outcomes showed that incorporation of constriction factor [30] boosts the convergence of algorithm. When constriction factor is examined on test benchmark problems, it remained unsuccessful to attain the certain threshold error for the given problem within allotted stipulated number of epochs. Subsequently it was established that as the particles remained away from the given search space, the constriction factor unsuccessful to attain the given number of epochs. After setting the velocity clamping to constriction factor, the performance was enhanced for all benchmark problems.

After adjusting the values of c_1 and c_2 in the equation, it might provide for accelerating the convergence of the algorithm. Choosing the default values $c_1 = c_2 = 2$ was suggested but the simulation results shows that different combination according to the problem nature may give better performance. Latest work [10] reveals that it could be still best to select a smaller social parameter than cognitive parameter. r_1 and r_2 are random numbers vectors where each part taken from uniform distribution in the range $U(0,1)$, has been utilized to keep the diversity. Magnitude of the velocities managed by the constriction parameter factor ω like $V_{(max)}$ parameter practiced in the initial version of PSO. The algorithm gives the quicker convergence speed, when ω and $V_{(max)}$ are collectively used.

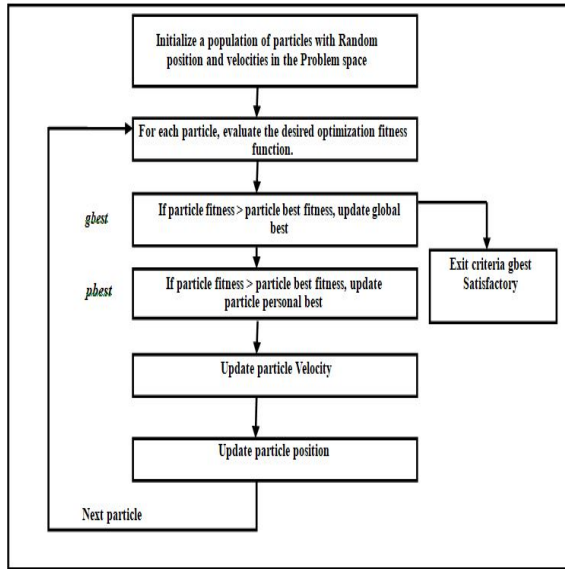


Fig. 1. Standard PSO.

Three primarily operators are normally used in EA approaches: the selection, the recombination and the mutation operator. PSO does not have a recombination operator. Stochastic improvement of a particle towards its past best position, notwithstanding the best particle of the swarm [31], mimics the recombination method in EA. In PSO, transfer of information occur only among the particles of the swarm by their own experience and the experience of best particle in the population, rather choosing the fitness from elite “parent” to the off spring in GA’s. Furthermore, in PSO position updating vector matches the mutation operator in GA. PSO relate to the kind of EAs that does not practice the concept of “survival of fittest”. It does not use the selection procedure directly. Hence, particle with less fitness can exist during optimization process and possible visit any point of the search space in the swarm. Pseudo code of standard PSO is presented in the Fig. 1:

IV. PROPOSED METHODOLOGY SCHEME

PSO is an evolutionary intelligent searching approach relies on the population. It is used to find the optimum solution in the search space based on collective cooperation and contest between the groups. Like other swarm intelligence techniques, PSO algorithm faces the problem of premature convergence. In PSO algorithm, nature of particle is determined by its global best location and previous best location of the particle discovered yet [32]. When these best particles trapped in local minima, the current particle could be fallen in local minima. To recover from this phenomenon, chi-square mutation operator is introduced. If particle is fallen in local minima, proposed mutation operator will support it, recover it from local minima and move this particle to another location far from the local minima. In this proposed technique, global best particle is mutated by Chi -Square. By using chi-square in PSO, PSO takes a long jump to escape from local minima. The chi square distribution is one of the mathematical distributions which have large usage in statistical work. The term *chisquare* (pronounced as *ch*). The Greek letter X is used to represent this distribution. The probability density function (pdf) of the

chi-squared distribution is given in Equation 4.

$$mut(x) = Zx(1 + Chi - square(\partial)) \quad (4)$$

in the Eq 4 (∂) is fixed as 0.1 and Zx refereed as numerical object . Normally in population, based meta heuristic search algorithm like PSO, working performance relies on population initialization, which finds the succeeding methodology evaluations. Standard PSO uses the random uniform distribution numbers for initialization of population [33].

Because of this and the issues of large dimensions, search space exploration is ineffective and non-distribution of swarm particles may take place. It causes the slow convergence and creates the process to escape from local minima. Recently, to avoid these shortcomings, different population initialization methodologies have been developed and utilized in various research fields to prevent from premature convergence in metaheuristic algorithms and enhance the efficient exploration in search space.

Quasi random sequences are not as much random than the pseudo random sequences, however these are more strong for computational techniques who rely on creation of the random numbers. A few famous quasi random numbers are Sobol, Halton, Torus, Faure and Vander Corput.

Such sequences have been employed for initialization. A simulation outcome depicts a remarkable progress over standard PSO that employed uniform distribution. The experimental results revealed that using QRS for initiation of population enhance the performance of meta heuristic algorithms. The flow chart of the proposed technique is presented in Fig. 2. The prime phases of proposed technique are given in Algorithm 1.

V. EXPERIMENTAL RESULTS

The proposed chi-square mutated PSO (Chi-Square PSO) is simulated in C++ and applied on computer with 2.3 GHz Core (M) 2 Duo CPU processor . In order to measure the execution of the proposed chi-square PSO algorithm, a group of benchmark functions has been utilized to do the comparison with many other improved PSO techniques with traditional PSO, Adaptive PSO and different initialization techniques. Eight non-linear test functions are chosen here to examine the optimization outcomes of proposed Chi-Square PSO that are normally applied to investigate the performance of any technique.

A. Experimental Setup

The parameters for simulation used as $c1=c2=1.45$, inertia weight w is used in the interval $[0.9,0.4]$ and swarm size is 20. For all the simulation, the function dimensions are $D=10, 20$ and 30 and maximum number of epochs is 3000. For fair comparison, all techniques apply similar parameters. In order to check the performance of each technique, all algorithms tested for 30 runs.

B. Benchmark Functions

This segment contains the eight benchmark functions applied to test the performance evaluation of the proposed algorithm. List of these functions is available in the Table I, D shows the dimensionality of the problem, S represents the interval of the variables and $fmin$ denotes the common global optimum minimum value.

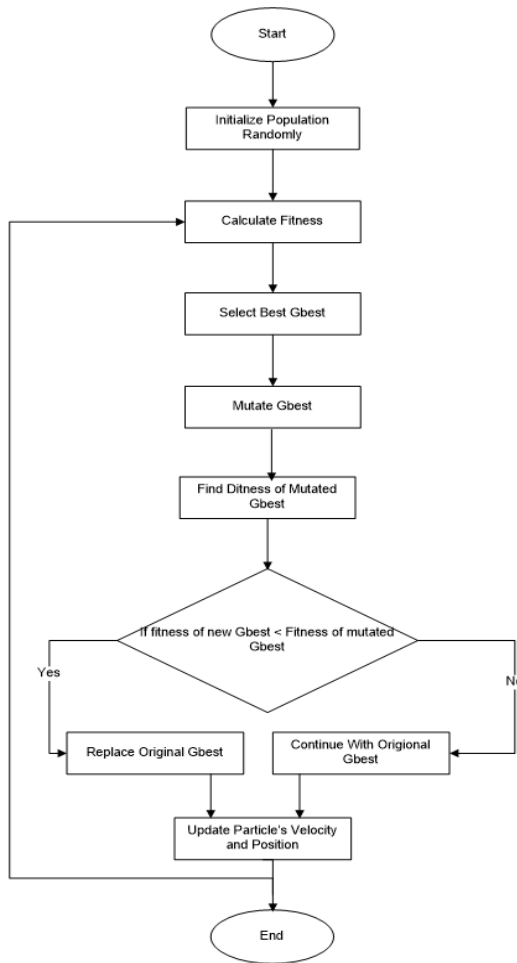


Fig. 2. Flow Chart for proposed PSO

C. Discussion

The main objective is to examine the progress produced by the proposed technique. For a fair comparison, the performance of following PSO variants is tested: Standard PSO, PSO with adaption mutation (AMPSO), Chi-Square PSO and also compared the results Chi-Square PSO with Sobol initialization and Chi-Square PSO with Halton initialization using mutation operator and without using the mutation operator. From Fig. 3 to 8, it is shown that not only the Chi-Square PSO provide fast convergence speed over AMPSO and from standard PSO. Simulation Results depicts that proposed technique improve the exploration capability but also provide fast convergence and achieve the global diversities and global optima. Table II shows the comparative results.

VI. CONCLUSION

This paper introduces a new approach of PSO algorithm by proposing a Chi-Square mutation operator and using two different quasi random initialization techniques have been joined with proposed PSO and employed on function optimization problems. The proposed mutation strategy maintains the diversity of the swarm and improves the global searching capability. The simulation results show that the proposed mutated PSO has better convergence accuracy and can escape

Algorithm 1 Proposed PSO

- 1: Step 1: Initialization
- 2: Set epoch number $I=0$, swarm population size NP, the particles dimensions D in the swarm, w_{max} , w_{min} , C1, C2, For each particle P_i in the swarm
- 3: Step 1.1: Initialize the Particle position X_i
- 4: Step 1.2: Initialize the Particle velocity V_i
- 5: Step 1.3: Calculate the fitness value f_i
- 6: Step 1.4: Set global best position g_{best} with the particle with best-evaluated fitness function computed value in the swarm.
- 7: Step 1.5: Set the personal best location p_{best} of each particle in the swarm as $P_i = X_i$.
- 8: Step 2: Compare the value of current particle's fitness in the swarm and its previous best location p_{best} . If the particle fitness is better than p_{best} , then substitute the p_{best} with its current fitness; else retain the particle P_i unchanged
- 9: Step 3: Compare the value of current particle's fitness in the swarm and its global best location g_{best} . If the particle fitness is better than g_{best} , then substitute the global best position g_{best} with its current fitness; else retain the particle P_i unchanged
- 10: Step 4: Execute chi square mutation to each particle
- 11: Step 5: Updating the each particle velocity using the equation
- 12: Step 6: Updating the each particle position using the equation
- 13: Step 7: Apply chi square mutation on the global best particle by using Eq (4).
- 14: If mutated particle is better than current P_i , substitute the current particle P_i with mutated particle; else retain the particle P_i unchanged
- 15: Step 8: If the stopping criteria met, stop the epoch process; else go to step 2

from premature convergence successfully and compared with other recognized variants of PSO. The future work is to theoretically examine its effects and employ it some real world complex optimization problems. For future research work, it will be exciting to focus on the proposed approach to many real-world engineering applications. Furthermore, it is interestingly important to implement the proposed technique for engineering optimization problem to enhance its practicability and rightness.

TABLE I. EIGHT STANDARD BENCHMARK FUNCTIONS

Function Name	Objective Function	Search space
Sphere	$Min f(x) = \sum_{i=1}^n x_i^2$	$-5.12 \leq x_i \leq 5.12$
Grienwank	$Min f(x) = \frac{1}{4000} \sum_{i=1}^n x_i^2 - \prod_{i=1}^n \cos(\frac{x_i}{\sqrt{i}}) + 1$	$-600 \leq x_i \leq 600$
Rosenbrock	$Min f(x) = \sum_{i=1}^{n-1} [1000(x_{i+1} - x_i^2)^2 + (x_i - 1)^2]$	$-5 \leq x_i \leq 5$
Rastrigin	$Min f(x) = 10n + \sum_{i=1}^n [x_i^2 - 10\cos(2\pi x)]_i$	$-5.12 \leq x_i \leq 5.12$
Ackley	$Min f(x) = -20\exp(-0.2\sqrt{\frac{1}{n} \sum_{i=1}^n [x_i^2 - \exp(\frac{1}{n} \sum_{i=1}^n \cos(2\pi x_i)) + 20 + e}$	$-30 \leq x_i \leq 30$
Schwefel	$Min f(x) = \sum_{i=1}^n -x_i \sin(-1\sqrt{ x_i })$	$-500 \leq x_i \leq 500$
De Jong's	$Min f(x) = \sum_{i=1}^n (x_i^2)$	$-5.12 \leq x_i \leq 5.12$
Axis parallel hyper-ellipsoid	$Min f(x) = \sum_{i=1}^n (i \cdot x_i^2)$	$-5.12 \leq x_i \leq 5.12$

TABLE II. COMPREHENSIVE RESULTS

Sr	Name	DIM	Iter	Results						
				PSO	AMPSO	CPSO	HD-CPSO without CPSO	HD-CPSO with CPSO	SD-CPSO without CPSO	SD-CPSO with CPSO
F1	Sphere	10	1000	3.03E-02	9.87E-02	2.40E-03	3.01E-02	5.60E-03	5.65E-02	2.20E-03
		20	2000	5.72E+00	5.25E+00	5.99E-01	2.47E+00	5.89E-01	3.34E+00	4.03E-01
		30	3000	1.98E+01	1.84E+01	2.29E+00	9.17E+00	1.70E+00	9.51E+00	4.56E+00
F2	Grienwank	10	1000	5.71E-01	5.18E-01	3.81E-01	8.84E-01	6.60E-01	6.91E-01	4.35E-01
		20	2000	1.39E+01	1.38E+01	2.70E+00	8.14E+00	2.33E+00	9.78E+00	2.03E+00
		30	3000	5.37E+01	4.49E+01	8.86E+00	3.56E+01	6.49E+00	2.77E+01	9.59E+00
F3	Rosenbrock	10	1000	2.69E+01	4.30E+00	2.98E+00	7.11E+00	4.24E+00	6.87E+00	2.92E+00
		20	2000	5.85E+01	3.37E+01	2.76E+01	3.69E+01	1.90E+01	2.66E+01	1.95E+01
		30	3000	1.82E+02	1.20E+02	5.20E+01	1.01E+02	5.09E+01	7.27E+01	3.70E+01
F4	Rastrigin	10	1000	3.21E+02	3.22E+02	3.27E+02	3.08E+02	3.21E+02	3.21E+02	3.29E+02
		20	2000	3.95E+02	3.94E+02	3.78E+02	3.82E+02	3.51E+02	3.85E+02	3.44E+02
		30	3000	4.75E+02	4.73E+02	4.23E+02	4.24E+02	3.87E+02	4.51E+02	3.82E+02
F5	Ackley	10	1000	1.51E+01	1.51E+01	1.51E+01	1.51E+01	1.50E+01	1.51E+01	1.51E+01
		20	2000	1.53E+01	1.53E+01	1.53E+01	1.54E+01	1.54E+01	1.53E+01	1.53E+01
		30	3000	1.53E+01	1.53E+01	1.53E+01	1.54E+01	1.53E+01	1.53E+01	1.53E+01
F6	Schwefel	10	1000	8.88E-17	0.00E+00	0.00E+00	0.00E+00	0.00E+00	0.00E+00	1.78E-16
		20	2000	0.00E+00	0.00E+00	0.00E+00	0.00E+00	0.00E+00	0.00E+00	0.00E+00
		30	3000	0.00E+00	0.00E+00	0.00E+00	0.00E+00	0.00E+00	0.00E+00	0.00E+00
F7	De Jong's	10	1000	1.08E-02	1.68E-02	3.14E-04	5.06E-02	1.70E-03	5.65E-02	7.00E-04
		20	2000	4.48E+00	3.17E+00	9.17E-01	1.94E+00	2.50E-01	3.34E+00	5.29E-01
		30	3000	1.45E+01	1.52E+01	4.18E+00	6.81E+00	1.50E+00	9.51E+00	2.29E+00
F8	Axis parallel hyper-ellipsoid	10	1000	5.27E-01	4.51E-01	5.20E-02	1.52E+00	1.87E-02	6.49E-01	1.89E-01
		20	2000	2.92E+01	3.69E+01	1.20E+01	3.57E+01	4.22E+00	2.08E+01	4.95E+00
		30	3000	1.95E+02	3.69E+01	4.61E+01	1.18E+02	3.30E+01	8.11E+01	3.20E+01

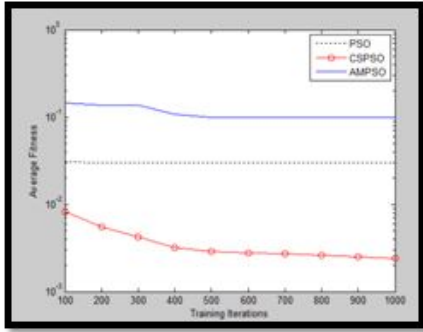


Figure (3.a)

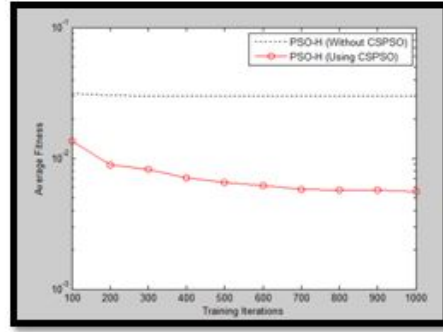


Figure (3.b)

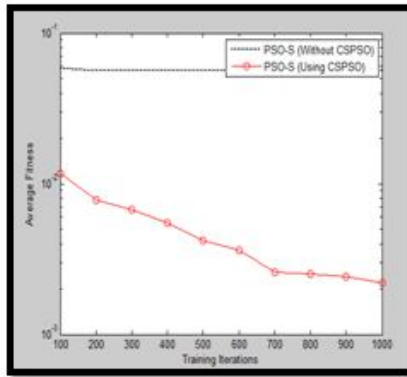


Fig. 3. Function F1 (3.a) using Chi-Square PSO (3.b) PSO-Halton(Using Chi-Square PSO) (3.c) PSO-Sobol(Using Chi-Square PSO)

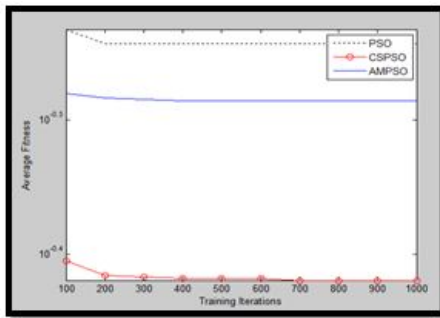


Figure (4.a)

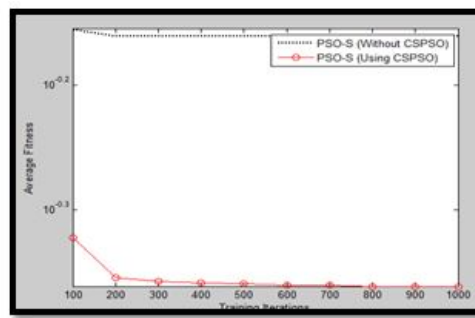


Figure (4.b)

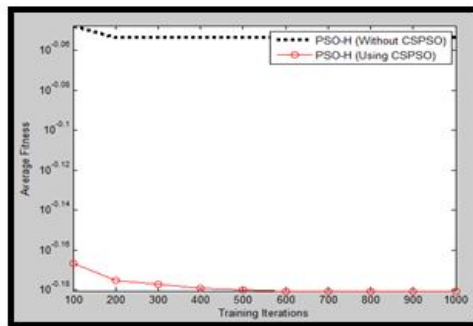


Fig. 4. Function F2 (4.a) using Chi-Square PSO (4.b) PSO-Halton(Using Chi-Square PSO) (4.c) PSO-Sobol(Using Chi-Square PSO)

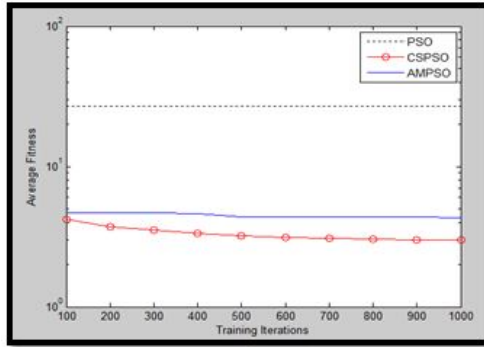


Figure (5.a)

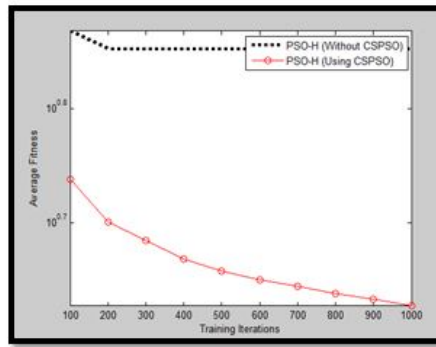


Figure (5.b)

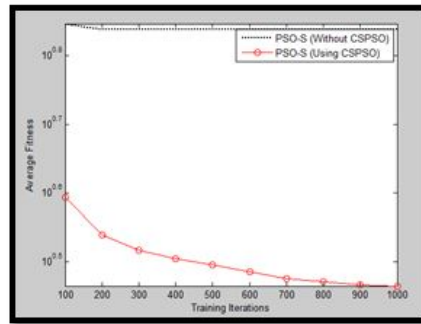


Fig. 5. Function F3 (5.a) using Chi-Square PSO (5.b) PSO-Halton(Using Chi-Square PSO) (5.c) PSO-Sobol(Using Chi-Square PSO)

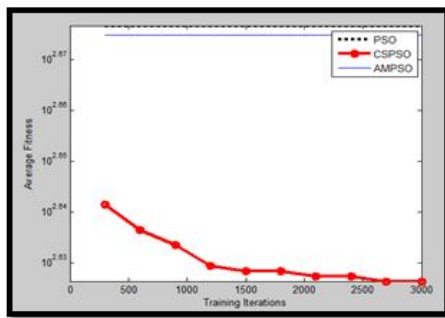


Figure (6.a)

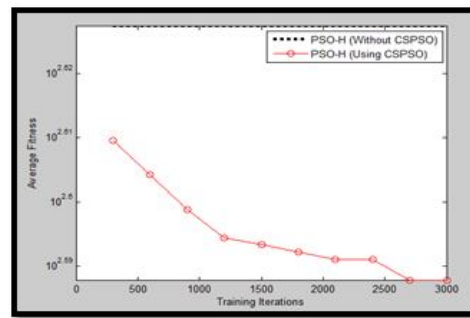


Figure (6.b)

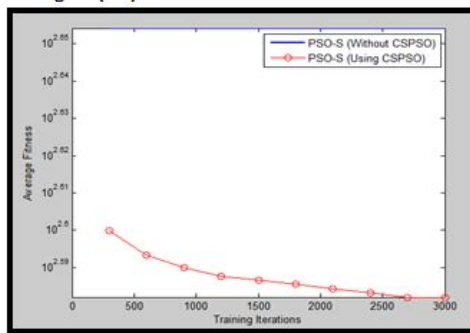


Figure (6.c)

Fig. 6. Function F4 (6.a) using Chi-Square PSO (6.b) PSO-Halton(Using Chi-Square PSO) (6.c) PSO-Sobol(Using Chi-Square PSO)

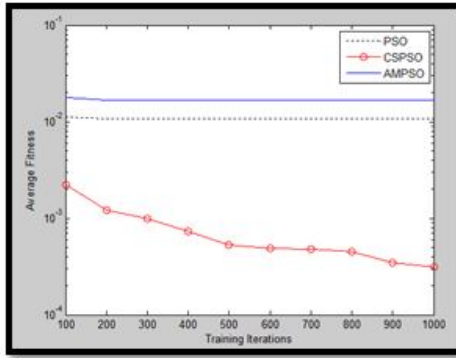


Figure (7.a)

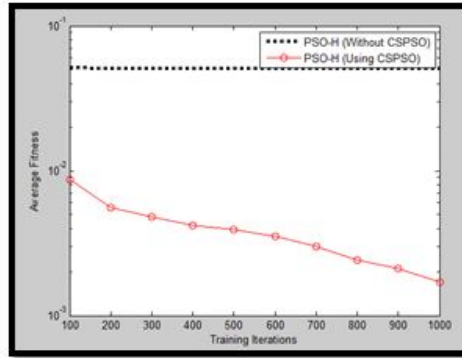


Figure (7.b)

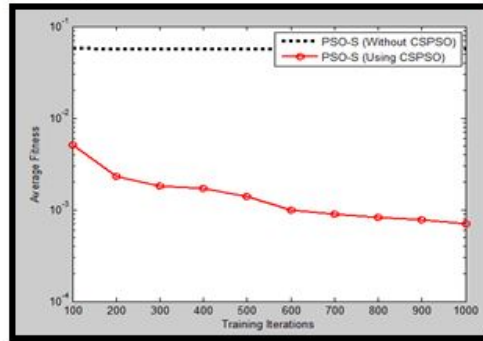


Figure (7.c)

Fig. 7. Function F7 (7.a) using Chi-Square PSO (7.b) PSO-Halton(Using Chi-Square PSO) (7.c) PSO-Sobol(Using Chi-Square PSO)

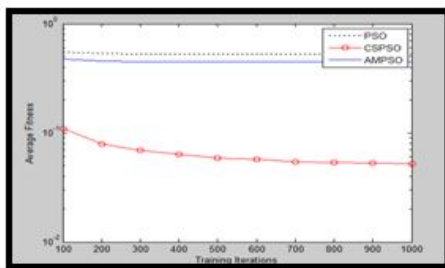


Figure (8.a)

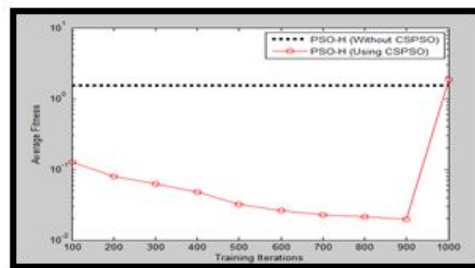


Figure (8.b)

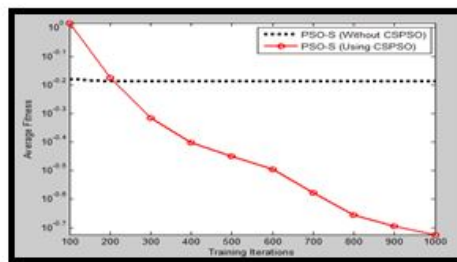


Figure (8.c)

Fig. 8. Function F8 (8.a) using Chi-Square PSO (8.b) PSO-Halton(Using Chi-Square PSO) (8.c) PSO-Sobol(Using Chi-Square PSO)

REFERENCES

- [1] W. H. Bangyal, J. Ahmad, H. T. Rauf, and S. Pervaiz, "An improved bat algorithm based on novel initialization technique for global optimization problem," *International journal of advanced computer science and applications*, vol. 9, no. 7, pp. 158–166, 2018.
- [2] —, "An overview of mutation strategies in bat algorithm," *international journal of advanced computer science and applications*, vol. 9, no. 8, pp. 523–534, 2018.
- [3] N. D. Jana, J. Sil, and S. Das, "Particle swarm optimization with population adaptation," in *Evolutionary Computation (CEC), 2014 IEEE Congress on*. IEEE, 2014, pp. 573–578.
- [4] Y. Shi *et al.*, "Particle swarm optimization: developments, applications and resources," in *evolutionary computation, 2001. Proceedings of the 2001 Congress on*, vol. 1. IEEE, 2001, pp. 81–86.
- [5] M. Clerc and J. Kennedy, "The particle swarm-explosion, stability, and convergence in a multidimensional complex space," *IEEE transactions on Evolutionary Computation*, vol. 6, no. 1, pp. 58–73, 2002.
- [6] J. Kennedy and R. Mendes, "Neighborhood topologies in fully informed and best-of-neighborhood particle swarms," *IEEE Transactions on Systems, Man, and Cybernetics, Part C (Applications and Reviews)*, vol. 36, no. 4, pp. 515–519, 2006.
- [7] R. Mendes, "Population topologies and their influence in particle swarm performance," *PhD Final Dissertation, Departamento de Informática Escola de Engenharia Universidade do Minho*, 2004.
- [8] Y.-T. Kao and E. Zahara, "A hybrid genetic algorithm and particle swarm optimization for multimodal functions," *Applied Soft Computing*, vol. 8, no. 2, pp. 849–857, 2008.
- [9] A. Alfi and H. Modares, "System identification and control using adaptive particle swarm optimization," *Applied Mathematical Modelling*, vol. 35, no. 3, pp. 1210–1221, 2011.
- [10] A. Ratnaweera, S. K. Halgamuge, and H. C. Watson, "Self-organizing hierarchical particle swarm optimizer with time-varying acceleration coefficients," *IEEE Transactions on evolutionary computation*, vol. 8, no. 3, pp. 240–255, 2004.
- [11] E. S. Peer, F. van den Bergh, and A. P. Engelbrecht, "Using neighbourhoods with the guaranteed convergence pso," in *Swarm Intelligence Symposium, 2003. SIS'03. Proceedings of the 2003 IEEE*. IEEE, 2003, pp. 235–242.
- [12] N. Higashi and H. Iba, "Particle swarm optimization with gaussian mutation," in *Swarm Intelligence Symposium, 2003. SIS'03. Proceedings of the 2003 IEEE*. IEEE, 2003, pp. 72–79.
- [13] A. Stacey, M. Jancic, and I. Grundy, "Particle swarm optimization with mutation," in *Evolutionary Computation, 2003. CEC'03. The 2003 Congress on*, vol. 2. IEEE, 2003, pp. 1425–1430.
- [14] M. Pant, R. Thangaraj, V. P. Singh, and A. Abraham, "Particle swarm optimization using sobol mutation," in *Emerging Trends in Engineering and Technology, 2008. ICETET'08. First International Conference on*. IEEE, 2008, pp. 367–372.
- [15] A. E. Muñoz Zavala, A. Hernández Aguirre, E. R. Villa Diharce, and S. Botello Rionda, "Constrained optimization with an improved particle swarm optimization algorithm," *International Journal of Intelligent Computing and Cybernetics*, vol. 1, no. 3, pp. 425–453, 2008.
- [16] D. Jia, L. Li, Y. Zhang, and X. Chen, "Particle swarm optimization combined with chaotic and gaussian mutation," in *Intelligent Control and Automation, 2006. WCICA 2006. The Sixth World Congress on*, vol. 1. IEEE, 2006, pp. 3281–3285.
- [17] X. Wu, B. Cheng, J. Cao, and B. Cao, "Particle swarm optimization with normal cloud mutation," in *Intelligent Control and Automation, 2008. WCICA 2008. 7th World Congress on*. IEEE, 2008, pp. 2828–2832.
- [18] J. Chen, Z. Ren, and X. Fan, "Particle swarm optimization with adaptive mutation and its application research in tuning of pid parameters," in *Systems and Control in Aerospace and Astronautics, 2006. ISSCAA 2006. 1st International Symposium on*. IEEE, 2006, pp. 5–pp.
- [19] B. Liu, L. Wang, Y.-H. Jin, F. Tang, and D.-X. Huang, "Improved particle swarm optimization combined with chaos," *Chaos, Solitons & Fractals*, vol. 25, no. 5, pp. 1261–1271, 2005.
- [20] M. Yang, H. Huang, and G. Xiao, "A novel dynamic particle swarm optimization algorithm based on chaotic mutation," in *Knowledge Discovery and Data Mining, 2009. WKDD 2009. Second International Workshop on*. IEEE, 2009, pp. 656–659.
- [21] J. Liu, X. Fan, and Z. Qu, "An improved particle swarm optimization with mutation based on similarity," in *Natural Computation, 2007. ICNC 2007. Third International Conference on*, vol. 4. IEEE, 2007, pp. 824–828.
- [22] B. Cai, Z. Li, D. Fu, J. Hu, P. Ou, and Q. Li, "Mutated fast convergent particle swarm optimization and convergence analysis," in *First International Conference on Intelligent Networks and Intelligent Systems*. IEEE, 2008, pp. 5–8.
- [23] S. Sheikhpour and A. Mahani, "Particle swarm optimization with intelligent mutation for nonlinear mixed-integer reliability-redundancy allocation," *International Journal of Computational Intelligence and Applications*, vol. 16, no. 01, p. 1750003, 2017.
- [24] K. Wang and F. Li, "A dynamic chaotic mutation based particle swarm optimization for dynamic optimization of biochemical process," in *Information Science and Control Engineering (ICISCE), 2017 4th International Conference on*. IEEE, 2017, pp. 788–791.
- [25] R. Eberhart and J. Kennedy, "A new optimizer using particle swarm theory," in *Micro Machine and Human Science, 1995. MHS'95., Proceedings of the Sixth International Symposium on*. IEEE, 1995, pp. 39–43.
- [26] Y. Shi and R. C. Eberhart, "Empirical study of particle swarm optimization," in *Evolutionary computation, 1999. CEC 99. Proceedings of the 1999 congress on*, vol. 3. IEEE, 1999, pp. 1945–1950.
- [27] Y. Shi and R. Eberhart, "A modified particle swarm optimizer," in *Evolutionary Computation Proceedings, 1998. IEEE World Congress on Computational Intelligence., The 1998 IEEE International Conference on*. IEEE, 1998, pp. 69–73.
- [28] M. Clerc, "The swarm and the queen: towards a deterministic and adaptive particle swarm optimization," in *Evolutionary Computation, 1999. CEC 99. Proceedings*

- of the 1999 Congress on, vol. 3. IEEE, 1999, pp. 1951–1957.
- [29] H. Fan, “Study on v_{max} of particle swarm optimization,” in *Proc. of the Workshop on Particle Swarm Optimization, 2001*, 2001.
- [30] R. C. Eberhart and Y. Shi, “Comparing inertia weights and constriction factors in particle swarm optimization,” in *Evolutionary Computation, 2000. Proceedings of the 2000 Congress on*, vol. 1. IEEE, 2000, pp. 84–88.
- [31] —, “Comparison between genetic algorithms and particle swarm optimization,” in *International conference on evolutionary programming*. Springer, 1998, pp. 611–616.
- [32] M. R. Bonyadi and Z. Michalewicz, “Analysis of stability, local convergence, and transformation sensitivity of a variant of the particle swarm optimization algorithm,” *IEEE Transactions on Evolutionary Computation*, vol. 20, no. 3, pp. 370–385, 2016.
- [33] J. Kennedy and R. C. Eberhart, “A discrete binary version of the particle swarm algorithm,” in *Systems, Man, and Cybernetics, 1997. Computational Cybernetics and Simulation., 1997 IEEE International Conference on*, vol. 5. IEEE, 1997, pp. 4104–4108.

Real Time Analysis of Crowd Behaviour for Automatic and Accurate Surveillance

E Padmalatha¹, Karedla Anantha Sashi Sekhar², Dasarada Ram Reddy Mudiam³
Dept of Computer Science and Engineering
Chaitanya Bharathi Institute of Technology
Gandipet, Hyderabad 500075

Abstract—Surveillance in this modern era is a necessity. Creating an alert in case of emergencies and disturbances is of very much importance. As the number of simultaneous camera feeds increase, burden on human supervisor also increases. The proposed system is a way to aid human supervisor in the surveillance job. Creating alerts in real time will help responding quickly to crucial situations. With this in mind, we propose the following things: (1) Generation of ViF (Violent Flow Descriptors) as high-level features in real time. (2) Using generated ViF's of a Video Dataset for training a neural net and testing its accuracy. (3) Developing a system that can detect the signs of disturbance among the crowd in real time and can learn from the decisions it makes.

Keywords—Real time surveillance; violent flow descriptors; neural network

I. INTRODUCTION

Cost of surveillance equipment in this digital era is minimal. In the view of public safety, CCTV cameras are installed in crowded and densely populated areas. The footage from CCTV cameras are continuously monitored by humans in order to respond in case of emergencies. This is a routine and tedious job for a human to continuously pay attention to multiple screens. Surveillance by humans is inefficient as it is limited to human capacity and may not be error free. If computers are replaced by humans to perform surveillance and generate alerts, it may aid the humans to respond quickly to the alerts. If we consider the amount of video footage generated simultaneously, we need a solution which can handle input at this scale.

The research done until now focuses on increasing the accuracy but makes a significant trade off with speed. We here focus on a scalable and efficient algorithm which focuses on both accuracy and generating alerts in real-time.

Generation of ViF [1] is already been experimented previously. So as to generate ViF, there is a detailed process that has to be followed. Starting with the videos, they have standard aspect ratio of 3:4 and are of very low quality. As the crowd behavior is completely random, detecting breakouts in the crowd becomes a real challenge. Also the content of the video is considered to be originated from a CCTV camera hence any other source of information such as subtitles and audio cannot be used. Continuous surveillance system is of much importance and very less attention is given to it.

In this proposed system, we try to implement an algorithm which accurately detects violence in real-time. Through this

algorithm we try to obtain safer surroundings and have a quick response time to violent incidents.

II. PREVIOUS WORK

A. Optical Flow

Optical Flow is the core part of Violence Detection. Optical Flow is the relative motion between two image frames which are taken at times t and $t+\Delta t$ at every pixel position. Methods for determination of Optical Flow can be listed as Phase correlation [8], Block-based method [9], Differential methods and Discrete Optimization methods. The most commonly used methods are Lucas Kanade and Horn-schunck optical flow methods [6], which come under Differential methods based on solving first order derivative. We used C Liu's [2] optical flow algorithm for our task which will be used to further obtain Flow Vector Magnitude. Suppose V_x and V_y are the velocities of a pixel along x and y axis obtained through optical flow algorithm, then the flow vector magnitude can be obtained as, $m_t = \sqrt{V_{x,t}^2 + V_{y,t}^2}$. C Liu's Optical flow algorithm was originally written in C language and mex files were written for compatibility with MATLAB. We used bob package [3] for using that particular algorithm in Python.

B. Violent Flow Descriptors

ViF (Violent Flow Descriptors) [1] have been used previously to obtain global level features of a video. After obtaining the flow vector magnitude (m), we calculate the binary vector. This binary vector is calculated for each pixel which reflects the change in magnitude.

$$b_{x,y,t} = \begin{cases} 1, & \text{if } |m_{x,y,t+1} - m_{x,y,t}| \geq \theta \\ 0 & \text{otherwise} \end{cases} \quad (1)$$

After obtaining the binary vector for each frame, we add binary vectors which are obtained for all the frames and normalize the value with the number of frames taken under consideration.

$$\bar{b}_{x,y} = \frac{1}{T} \sum_t b_{x,y,t} \quad (2)$$

This \bar{b} generated is divided into $M*N$ non-overlapping cells and collecting magnitude changes of each cell separately. These magnitude changes are then represented by a fixed size histogram. These $M*N$ histograms are further concatenated to obtain a single descriptor vector which is known as the ViF.

III. METHODOLOGY

Doing real time automatic surveillance on CCTV footage has many challenges and limitations. There are two assumptions which we make, the first assumption is to keep the camera away from the area under surveillance, there has to be standard distance between the CCTV camera and the area to be monitored. The main challenge we face is to keep the processing in terms of real-time, which means all the processing has to be done in less than 1/25th of a second. Our system should have the ability to handle multiple video sources at a time. This has been achieved by continuously accepting frames through multiprocessing using threads. First part is we calculate the Optical flow which is the most time consuming of all the processes. Then we use the calculated optical flow to obtain flow vector magnitude. Next we generate ViF which are further used for training and classification.

A. Algorithm

The main part of building the system is to have a well built algorithm. First the video is preprocessed, then we calculate the optical flow which is most time consuming. Feature Extraction is done next which is used for training a multilayer perceptron [5]. So as to make the system scalable for multiple video sources, we have embedded threading and multi-processing. The built algorithm is robust and can handle faulty video sources.

B. Global Feature Extraction

1) *Video Preprocessing*: Video coming from source is preprocessed. Considering the video aspect ratio as 3:4. The surveillance footage is consider to be standard definition (scale = 240:320). The input frames coming in are resized to 75:100 size and then converted to gray-scale. The length and breadth of the videos are almost reduced by one-third. For video processing OpenCV [7] package has been used.

2) *Optical Flow*: Ce. Liu [2] optical flow algorithm has been used to calculate the optical flow. This algorithm has been used particularly since it is highly efficient and robust. It returns three values, v_x (velocity vector along x-axis), v_y (velocity vector along y-axis) and w (wrap). The vectors are in the same shape of the resized frame width and height.

3) *Violent Flow Descriptors*: Violent Flow Descriptor [1] (Global Features) Algorithm is being used which has been already been implemented previously in MATLAB. So as to increase the scalability of the algorithm, system has been implemented using basic multiprocessing and threads. Violent Flow Descriptors use flow vector magnitude's output. Histogram equalization on normalized binary vector for the whole set of frames under consideration is performed to obtain a single feature vector. The ViF's obtained are then used for training and classification purposes. If the number of bins are fixed as 21 (0.0 to 1.0, interval of 0.05) and consider both M, N as 4, then for a standard definition video of scale 240:320, 336 features are obtained exactly ($21 * 4 * 4$). Values of these 336 features range from 0.0 to 1.0.

C. Neural Network

1) *Structure*: For the given dataset once violent flow descriptors are generated, neural net training using these features

is done. Built four layered neural net, one input layer, two dense layers and one output layer. Input layer accepts 350 inputs and gives 336 outputs. Middle dense layers accept 336 inputs and give 336 outputs. Output layer accepts 336 inputs and gives 1 output. For input a nd dense layers ReLU (Rectifier Linear Unit) activation function is used and for the output layer Sigmoid function is being used.

2) *Training*: For building neural net Keras [10] and Tensorflow are being used. Initially the data needs to be formatted so that it fits into input layer of Neural Net. The Violent Flow Features generated for each video will be in the format of numpy array of dimensions 336*1. Array is reshaped into 1*336 dimensions, so that the features of single video fit into the input layer of neural net as one data tuple. Further, concatenation of reshaped feature array of each video into a single array is done so that the final input to the neural net will be an array of dimensions 246*336 as there are 246 videos (violent and non-violent) in the dataset. On the other hand, pre known outputs (0(non-violent) or 1(violent)) of each video are stored in an array of dimensions 246*1 to train neural net and to calculate accuracy. After data is ready we can proceed to build the neural net into the structure mentioned above. Using Keras Sequential neural net with dense layers can be built.

A model is compiled for which we must specify a logarithmic loss function which evaluates a set of weights and also an optimizer to set learning rate. Keras has a logarithmic loss function for binary classification problem defined as binary-crossentropy and Adam Optimizer which is an efficient optimizer of choice. Number of epochs for which the training must be carried out, batch size (number of instances evaluated to perform weight changes) and the input data for training the model are provided as parameters. Trained model is stored into a file of hd5 format using hdpv python package.

3) *Violence Detection*: This phase involves detection of disturbance or violence in live crowd surveillance videos in real time. The input surveillance video is preprocessed and Violent Flow Descriptors are generated dynamically in Real Time. For each second of video, features are extracted and are given as input to the trained model for classification and violence detection. If some disturbance or violence is detected, it will be reported as an alert stating that it is violence along with the time it has occurred within a second of occurrence.

4) *Feedback*: In the Violence Detection phase, as the real time surveillance takes place, the features generated for every second are tested against trained model for classification and violence detection. Those features, along with their actual output (provided by human) generated by the trained model are given as feedback to the model. This allows continuous training of neural net model which helps to increase the accuracy of classification and also faster detection of violence.

D. Extraction of Interesting Features

AdaBoost is an ensemble of weak classifiers. AdaBoost is an algorithm which could tell us the important set of features that help us classify our features. For this the Feature Selection Algorithm through AdaBoost [4] is used. Once the features are arranged in increasing order of the error rates, we can obtain the features among total 336 features which are highly

efficient in classifying videos. The weak classifiers used here are decision stumps (decision tree of height 1).

IV. IMPLEMENTATION

In the below subsections we provide the implementation details and the outputs analysis. Clear analysis of the system will be done in the next section.

A. Continuous Surveillance

We used two sets of configurations for calculating processing speeds of the system. First Configuration consists of 4GB RAM, Intel Centrino Processor with Ubuntu OS. Second Configuration consists of 8GB RAM, Intel i5 Processor with Debian OS.

For a video which is not initially violent but later on becomes violent, the proposed system is able to detect the exact instance where the video frames go from violent to non-violent. Considering Real-Time CCTV feed, within a second of occurrence of violence our system is able to detect the violence and raise an alert.

```
loaded model from disk
FPS is : 30.0
violent --- 5 seconds , processing time : 5.74629306793
violent --- 9 seconds , processing time : 9.68529391289
violent --- 11 seconds , processing time : 11.6434879303
violent --- 29 seconds , processing time : 28.7351050377
violent --- 33 seconds , processing time : 32.4793879986
violent --- 39 seconds , processing time : 38.1013178825
violent --- 41 seconds , processing time : 40.0718650818
violent --- 45 seconds , processing time : 43.8183250427
violent --- 76 seconds , processing time : 70.0854079723
violent --- 80 seconds , processing time : 73.7055718899
violent --- 104 seconds , processing time : 94.7628529072
violent --- 110 seconds , processing time : 100.153498888
violent --- 124 seconds , processing time : 112.719841957
violent --- 130 seconds , processing time : 118.084775925
violent --- 132 seconds , processing time : 119.904102087
violent --- 134 seconds , processing time : 121.691713095
violent --- 136 seconds , processing time : 123.467772007
violent --- 138 seconds , processing time : 125.274302006
violent --- 140 seconds , processing time : 127.064712048
violent --- 162 seconds , processing time : 146.576081991
violent --- 172 seconds , processing time : 155.607837915
violent --- 174 seconds , processing time : 157.406991005
violent --- 182 seconds , processing time : 164.669116974
violent --- 184 seconds , processing time : 166.488634109
violent --- 186 seconds , processing time : 168.348366022
violent --- 188 seconds , processing time : 170.149859905
Done
```

Fig. 1. Processing Speeds with Intel Centrino Processor

```
Loaded model from disk
FPS is : 30.0
violent --- 5 seconds , processing time : 4.34860682487
violent --- 9 seconds , processing time : 7.25317382812
violent --- 11 seconds , processing time : 8.71798682213
violent --- 29 seconds , processing time : 21.9189689159
violent --- 33 seconds , processing time : 24.8225078583
violent --- 39 seconds , processing time : 29.1507589817
violent --- 41 seconds , processing time : 30.5916497707
violent --- 45 seconds , processing time : 33.4507169724
violent --- 76 seconds , processing time : 55.4075779915
violent --- 80 seconds , processing time : 58.2983269691
violent --- 104 seconds , processing time : 75.7260508537
violent --- 110 seconds , processing time : 80.1277518272
violent --- 124 seconds , processing time : 90.3564748764
violent --- 130 seconds , processing time : 94.698748827
violent --- 132 seconds , processing time : 96.1417148113
violent --- 134 seconds , processing time : 97.5626308918
violent --- 136 seconds , processing time : 98.9930028915
violent --- 138 seconds , processing time : 100.432123899
violent --- 140 seconds , processing time : 101.866064787
violent --- 162 seconds , processing time : 117.839699984
violent --- 172 seconds , processing time : 125.074666977
violent --- 174 seconds , processing time : 126.504262924
violent --- 182 seconds , processing time : 132.335903883
violent --- 184 seconds , processing time : 133.779084921
violent --- 186 seconds , processing time : 135.228977919
violent --- 188 seconds , processing time : 136.651611805
Done
```

Fig. 2. Processing Speeds with Intel i5 Processor

Above are two figures showing running time of the system. The total length of video taken under consideration is nearly 200 seconds. Proposed system is able to detect the exact second of violence occurrence i.e where the frames go from non-violent to violent. With Intel centrino processor Fig. 1, the processing is being completed nearly in 180 seconds (20 seconds faster than run time of video). With Intel i5 processor Fig. 2, the processing of entire video is being done nearly in 140 seconds (1 minute faster than run time of video). With each detection of violence outbreak, the corresponding time taken by the system to detect that is being shown.

B. Accuracy

The accuracy obtained by ViF's [1] as global features using a linear SVM is 81.30% for existing system. Proposed system has an accuracy of nearly 85%.

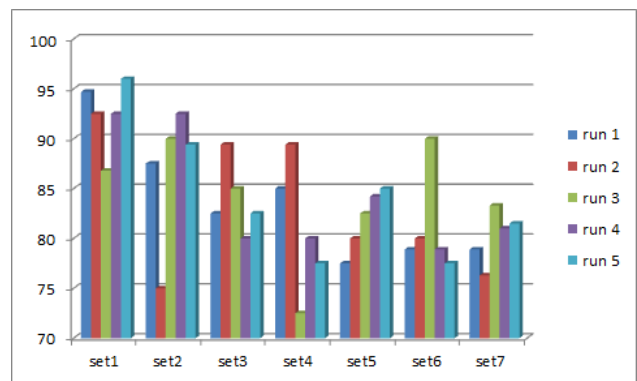


Fig. 3. Bar Plot of Obtained Accuracy Values in N Folds

The bar graph in Fig. 3 shows the result of N-folds cross verification with N=7. There are total 5 runs(execution of n-folds once in a run). In each run we consider 7 heaps in total.

Each heap containing equal number of videos. Among these videos violent and non-violent videos are distributed evenly. Violent and Non Violent videos are placed randomly in heaps. This gives us an idea how robust the proposed system is. The minimum accuracy we obtain for a heap in any run is greater than 70%.

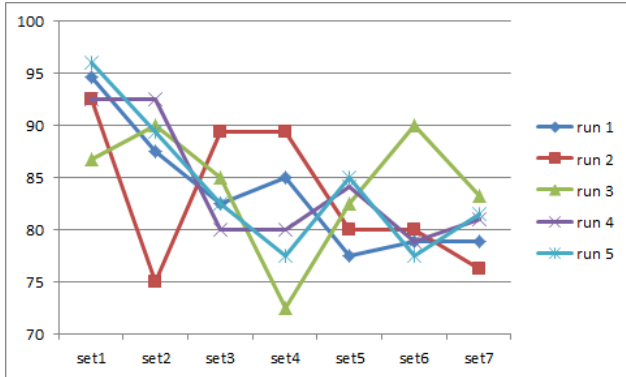


Fig. 4. Line Plot of Obtained Accuracy Values in N Folds

Fig. 4 shows the line graph, it is same as Fig. 4, but gives us the clear picture of accuracies of each set in its corresponding run. Each run has been assigned a different color. From this we can clearly identify minimum and maximum accuracy. The maximum obtained accuracy is nearly 96% and minimum accuracy is of 73%.

```
(bob_py2) dasarada@dasarada:~/Desktop/ASAGS/keras (copy)$ python keras_neural_ne
tworks_training_70_30_random.py
Using TensorFlow backend.
2018-04-13 13:23:35.658603: I tensorflow/core/platform/cpu_feature_guard.cc:137]
Your CPU supports instructions that this TensorFlow binary was not compiled to
use: SSE4.1 SSE4.2 AVX AVX2 FMA
accuracy is : 0.9027777777777778
--- 58.6380441189 seconds ---
[[33  2]
 [ 5 32]]
0.9027777777777778
[76, 8, 111, 75, 50, 74, 25, 56, 55, 83, 102, 129, 9, 17, 85, 101, 35, 117, 107,
64, 104, 97, 95, 38, 14, 96, 81, 93, 67, 48, 112, 62, 87, 115, 61, 109, 11, 119
, 36, 4, 22, 30, 89, 66, 71, 33, 114, 60, 21, 37, 24, 100, 34, 121, 16, 10, 51,
5, 18, 6, 128, 77, 110, 125, 53, 43, 68, 103, 108, 65, 58, 19, 39, 2, 3, 28, 122
, 127, 84, 59, 13, 90, 105, 54, 98, 29, 94, 124, 26, 1, 46, 42, 76, 8, 111, 75,
50, 74, 25, 56, 55, 83, 102, 129, 9, 17, 85, 101, 35, 117, 107, 64, 104, 97, 95,
38, 14, 96, 81, 93, 67, 48, 112, 62, 123, 87, 115, 61, 109, 11, 119, 36, 4, 22,
30, 89, 66, 71, 33, 114, 60, 21, 37, 24, 100, 34, 121, 16, 10, 51, 5, 18, 6, 12
8, 77, 110, 125, 53, 43, 68, 103, 108, 65, 58, 19, 39, 2, 3, 28, 122, 127, 84, 5
9, 13, 90, 105, 54, 98, 29, 94, 124, 26, 1, 46]
[70, 113, 12, 82, 78, 92, 23, 45, 80, 73, 120, 40, 27, 118, 69, 52, 88, 86, 32,
7, 126, 47, 41, 15, 57, 31, 63, 91, 49, 116, 72, 106, 20, 44, 99, 42, 70, 113, 1
2, 82, 78, 92, 23, 45, 80, 73, 120, 79, 40, 27, 118, 69, 52, 88, 86, 32, 7, 126,
47, 41, 15, 57, 31, 63, 91, 49, 116, 72, 106, 20, 44, 99]
```

Fig. 5. Accuracy Obtained by training with 70% of data and testing with 30% of data

TABLE I. CONFUSION MATRIX FOR 70:30 DATASET

	p	n
P	33	2
N	5	32

The dataset which contains 246 videos is divided in the ratio of 70:30. 70% of the data is used to train the neural net, 30% of the data is used to test the accuracy of generated model. Output in Fig. 5 shows that the accuracy obtained is 90.27% .

As we can see the confusion matrix in Table I, the number of False Negatives are just 2, that means there are only 2 cases in the test set which are actually violent but our system was not able to detect it. Whereas there were 5 cases in which videos were not violent but our system detected some violence. Following are the results obtained:

- Accuracy = TP/(total) = 0.9027
- True Positive Rate = TP/(Positives)= 0.9428
- Precision = TP/(Predicted yes) = 0.8684
- Specificity = TN/(Actual no) = 0.8648
- Misclassification Rate = (FP + FN)/(total) = 0.097

The above accuracy tests were done on a dataset [1] containing 246 videos. Shortest Video is of 1 second and Longest Video is of 6 seconds. These collections of videos have equal number of violent and non-violent videos. This kind of dataset is known as “in the wild” dataset. Videos present in the dataset are of standard CCTV resolution (scale = 240:320) and of similar aspect ratio (3:4).

V. RESULTS AND DISCUSSION

Consider the following scenes obtained through surveillance footage:



Fig. 6. Violence Not started



Fig. 7. Violence about to start



Fig. 8. Violence slightly started



Fig. 9. Violence furiously started

Above are four figures which show four different phases of surveillance video. Initially in Fig. 6, Violence has not yet started. In Fig. 7 Violence is about to start, people are slightly pushing each other. Fig. 8 shows the start of violence and in Fig. 9 Violence has started furiously.

```
(bob_py2) sekhar@ubuntu:~/Desktop/ASAGS/continuous_system$ python test_violence_video.py
Using TensorFlow backend.
2018-03-19 01:19:11.227351: I tensorflow/core/platform/cpu_feature_guard.cc:140]
Your CPU supports instructions that this TensorFlow binary was not compiled to
use: AVX2 FMA
[[ 2.56899511e-07]]
[[ 0.14527404]]
[[ 0.2733964]]
[[ 0.99957734]]
[[ 0.99810362]]
[[ 0.66406441]]
[[ 0.06192874]]
```

Fig. 10. System's output for the above video

In Fig. 10, it shows the output of the system for the particular video shown in previous figures. As we can see for the initial frame, output value is very less, as the scene gets tense in Fig. 7, the system output value increases. When the violence starts in Fig. 9, output value increases to 0.999 indicating violence. Later on in the video violence decreases gradually and hence the output value falls down to 0.06.

VI. CONCLUSION AND FURTHER WORK

Timely detection of violence in real time is of much importance. System is able to accurately detect violent scenarios in real time. It is scalable enough to process three to four parallel video streams at a time with a household PC setup. Whatever work has been done is to give attention and importance to accurate real time surveillance.

Further the accuracy can be greatly improved by using results of Feature Selection algorithm of AdaBoost. As explained above, once we arrange the features in increasing order of their error rate, we get order of importance of 336 features. In that particular order, we can associate the weights of input layer in neural net. The features which are highly important can have a higher weight at their input node and as the importance decreases, weights can also be decreased. This may make a difference in increasing the accuracy of neural net.

ACKNOWLEDGMENT

We would like to thank Dr. T Hassner [1] for his contributions towards real time surveillance, this project would not have been possible without the generation of Violent Flow Descriptors (VIFs).

REFERENCES

- [1] T. Hassner, Y. Itcher, O. Kliper Gross. *Violent Flows: Real-Time Detection of Violent Crowd Behavior*, 3rd IEEE International Workshop on Socially Intelligent Surveillance and Monitoring (SISM) at the IEEE Conf. on Computer Vision and Pattern Recognition (CVPR), June 2012
- [2] Ce. Liu. *Beyond Pixels: Exploring New Representations and Applications for Motion Analysis*, Massachusetts Institute of Technology, Ph.D. Thesis, 2009
- [3] Anjos, André AND El Shafey, Laurent AND Wallace, Roy AND Günther, Manuel AND McCool, Christopher AND Marcel, Sébastien. *Bob: a free signal processing and machine learning toolbox for researchers*, 20th ACM Conference on Multimedia Systems (ACMMM), Nara Japan, 2012
- [4] Ruihu Wang. *AdaBoost for Feature Selection, Classification and Its Relation with SVM, A Review*. Department of Science and Technology Chongqing University of Arts and Sciences Yongchuan, Chongqing 402160, CHINA
- [5] Zhen Zhang, Weimin Shao and Hong Zhang. *A learning algorithm for multilayer perceptron as classifier*. IJCNN'99. International Joint Conference on Neural Networks. Proceedings.
- [6] Ibrahim Kajo, Aamir Saeed Malik and Nidal Kamel. *An evaluation of optical flow algorithms for crowd analytics in surveillance system*. 2016 6th International Conference on Intelligent and Advanced Systems (ICIAS)
- [7] Ivan Culjak, David Abram, Tomislav Pribanic, Hrvoje Dzapo and Mario Cifrek. *A brief introduction to OpenCV*. 2012 Proceedings of the 35th International Convention MIPRO.
- [8] Marius Drulea and Sergiu Nedevschi. *Motion Estimation Using the Correlation Transform*. IEEE Transactions on Image Processing, 2013.
- [9] Jobin T Philip, Binoshi Samuvel, K. Pradeesh and N. K. Nimmi. *A comparative study of block matching and optical flow motion estimation algorithms*. 2014 Annual International Conference on Emerging Research Areas: Magnetism, Machines and Drives.
- [10] Petra Vidnerova and Roman Neruda. *Evolving keras architectures for sensor data analysis*. 2017 Federated Conference on Computer Science and Information Systems.

Impacts of Unbalanced Test Data on the Evaluation of Classification Methods

Manh Hung Nguyen^{1,2}

¹Posts and Telecommunications Institute of Technology (PTIT)

²UMI UMMISCO 209 (IRD/UPMC), Hanoi, Vietnam

Abstract—The performance of a classifier in a supervised machine learning problem is popularly evaluated by using the *accuracy, precision, recall, and F1-score*. These parameters could evaluate very well classifiers in the case that the number of positive label sample and the number of negative label sample in the testing set are balanced or nearly balanced. However, these parameters may miss-evaluate the classifiers in some case where the positive and negative samples in the testing set is unbalanced. This paper proposes some update in these parameters by taking into account the *unbalanced factor* which represents the unbalance ratio of positive and negative samples in the testing set. The new updated parameters are then experimentally evaluated to compare to the traditional parameters.

Keywords—*Supervised machine learning evaluation; accuracy; f1 score; unbalanced factor*

I. INTRODUCTION

The problem of classification (texts, images, voice...) is already popular in the machine learning community. One of popular methods is supervised machine learning. In which, there are two main phases. First, *training phase*, a set of samples which are already classified with a label, called *training set*, will be used to extract some common features of samples of the same label. This work is done by a classifier. Second, at the *testing phase*, if there is a new sample s , the assignment of a label to the sample s is decided by the classifier trained in the *training phase*.

The performance of the classifier is popularly evaluated by using the *accuracy, precision, recall, and F1-score* parameter which are calculated based on the definition of Salton et al. [7]:

$$Accuracy = \frac{TP + TN}{TP + FP + FN + TN} * 100\% \quad (1)$$

$$Precision = \frac{TP}{TP + FP} * 100\% \quad (2)$$

$$Recall = \frac{TP}{TP + FN} * 100\% \quad (3)$$

$$F_1 - score = 2 * \frac{Precision * Recall}{Precision + Recall} \quad (4)$$

where: TP is the number of true positive; FP is the number of false positive; FN is the number of false negative; TN is the number of true negative.

These parameters could evaluate very well classifiers in the case that the number of positive label sample and the number of negative label sample in the testing set are balanced or nearly balanced.

However, these parameters may miss-evaluate the classifiers in some case where the positive and negative samples in the testing set is unbalanced. For instance, let's consider in a case of positive major of testing set in which, there are 90% of samples are positive label and 10% are negative label. There is a very simple classifier which always returns TRUE for any testing sample. In that case, we have:

- $TP = 0.9x$
- $TN = 0$
- $FP = 0.1x$
- $FN = 0$
- $Accuracy = \frac{0.9x + 0}{0.9x + 0.1x + 0 + 0} * 100\% = 90.00\%$
- $Precision = \frac{0.9x}{0.9x + 0.1x} * 100\% = 90.00\%$
- $Recall = \frac{0.9x}{0.9x + 0.1x} * 100\% = 100\%$
- $F_1 - score = 2 * \frac{90 * 100}{90 + 100} = 94.73\%$

where x is the number of sample in the testing set.

With the value of accuracy and F1-score is about 90.00% and 94.75%, respectively, any evaluator could conclude that this is a good classifier. Meanwhile the classifier is very simple and idiot one: it always returns true for any sample. Intuitively, these parameters are lost its objective in this case.

In order to avoid the miss-evaluated in the case of unbalanced testing data, this paper proposes some update in these parameters by taking into account the *unbalanced factor* which represents the unbalance ratio of positive and negative samples in the testing set. The new updated parameters are then experimentally evaluated to compare to the traditional parameters. The paper is organised as follows: Section II presents our proposal of unbalanced factor in the output parameters. Section III presents our experiments to evaluate the proposed update in output parameters. Finally, Section IV is a conclusion.

II. PROPOSAL

We make used the basic concepts based on the definition of Salton et al. [7]:

- *Number of true positive (TP)*: This is the number of samples which are assigned to the considered label.

And in the results, it is also assigned to the same label.

- *Number of false positive (FP)*: This is the number of samples which are NOT assigned to the considered label. But in the results, it is assigned to the label.
- *Number of false negative (FN)*: This is the number of samples which are assigned to the considered label. But in the results, it is NOT assigned to the label.
- *Number of true negative (TN)*: This is the number of samples which are NOT assigned to the considered label. And in the results, it is NOT assigned to the label.

We take into account the *unbalanced factor* which is defined as the ratio between the number of positive sample and that of negative sample in the testing set:

$$\alpha = \frac{\text{number of positive sample in the testing set}}{\text{number of negative sample in the testing set}} \quad (5)$$

This *unbalanced factor* of testing set is then applied in the output parameters by updating the concept of *accuracy*, *precision*, *recall*, and *F-score* as follows:

$$\text{Accuracy} = \frac{TP + \alpha * TN}{TP + \alpha * FP + FN + \alpha * TN} * 100\% \quad (6)$$

$$\text{Precision} = \frac{TP}{TP + \alpha * FP} * 100\% \quad (7)$$

$$\text{Recall} = \frac{TP}{TP + FN} * 100\% \quad (8)$$

$$F_1 - \text{score} = 2 * \frac{\text{Precision} * \text{Recall}}{\text{Precision} + \text{Recall}} \quad (9)$$

Intuitively, these updates could replace the *traditional output parameters* in the case the *unbalanced factor* equals to 1. It means that the testing set is balanced or nearly balanced.

Let's return to the paradox example in Section I with a very simple classifier which always returns TRUE for any testing sample, in the case of positive major of testing set in which, there are 90% of samples are positive label and 10% are negative label. If the *unbalanced factor* is taken into account, we will have:

- $TP = 0.9x$
- $TN = 0$
- $FP = 0.1x$
- $FN = 0$
- The unbalanced factor $\alpha = \frac{0.9x}{0.1x} = 9$
- $\text{Accuracy} = \frac{0.9x + 9 * 0}{0.9x + 9 * 0.1x + 0 + 9 * 0} * 100\% = 50.00\%$
- $\text{Precision} = \frac{0.9x}{0.9x + 9 * 0.1x} * 100\% = 50.00\%$
- $\text{Recall} = \frac{0.9x}{0.9x + 0.1x} * 100\% = 100\%$
- $F_1 - \text{score} = 2 * \frac{50 * 100}{50 + 100} = 66.67\%$

where x is the number of sample in the testing set.

With the value of accuracy and F1-score is about 50.00% and 66.67%, respectively, any evaluator could conclude that this is a below-average classifier. This is suitable to the classifier which is very simple and idiot one: it always returns true for any sample. Intuitively, these new updated parameters could help us to avoid the case of miss-evaluate the simple classifier in an unbalanced testing set.

III. EVALUATION

This section presents an experiment to evaluate the proposed output parameters in the balance and unbalanced testing set.

A. Dataset

This experiment evaluates the proposed model on the dataset of 20 Newsgroups [4]. This dataset contains about 20000 texts, divided into 20 subjects. The longest text has more than 20000 words. The shortest text has about 75 words. The average length of text in this dataset is about 370 words. This dataset is widely used in machine learning and information retrieval domain, in the problem of text classification. The distribution of texts by 20 class labels is presented in Table I.

TABLE I. DISTRIBUTION OF LABELED DATA IN THE 20 NEWSGROUPS DATA SET

Topics	Number of text
alt.atheism	779
comp.graphics	973
comp.os.ms-windows.misc	985
comp.sys.ibm.pc.hardware	982
comp.sys.mac.hardware	961
comp.windows.x	980
misc.forsale	972
rec.autos	990
rec.motorcycles	994
rec.sport.baseball	994
rec.sport.hockey	999
sci.crypt	991
sci.electronics	981
sci.med	990
sci.space	987
soc.religion.christian	997
talk.politics.guns	910
talk.politics.mideast	940
talk.politics.misc	775
talk.religion.misc	628

B. Scenario

The main scenario of this experiment is defined as follows:

- Using the same training set.
- Using the same classifier. In this experiment, we use the classifier of Multinomial Naive Bayes (MNB) [3]. This algorithm improves the Naive Bayes model with the Multinomial Naive Bayes (MNB) algorithm. It had already proved its good performance in texts

classification as presented in several recent works [5], [6].

- Testing with different sets: balanced testing set, and unbalanced testing set (YES major, and NO major).
- This scenario is repeated in ten times, and then comparing the output parameters in the case with/without unbalanced factor.

1) *Building of training set*: The training set is built for each label, based on the one-vs-all method [1], as following scenario:

- For each label, select randomly 500 texts whose label is the considered label, and 500 other texts whose label is different from that label.
- Divide this set into ten subsets (for running of ten times): each subset has about 100 texts, in which, 50 texts have the considered label, 50 remain texts have other label.
- For each text in each training subset, remove all stop-words.
- Split the remain character sequence into 1-gram, 2-grams, and 3-grams. The combination of three grams from 1-gram to 3-grams is proved that is the best case for the dataset of 20Newsgroups in the work of Nguyen [5]. That is the reason we use this combination in the experiment.
- Transform it into a vector of TF-IDF [7] value.
- Training with Multinomial Naive Bayes (MNB) [3] classifier¹

2) *Building of testing set*: The three testing sets are also built for each label as following scenario:

- Unbalanced testing set with ratio of 20:80 (NO major - called 20:80 testing set):
 - Select randomly 200 texts whose label is that label, and 800 other texts whose label is different from that label.
 - Divide this set into ten subsets (for running of ten times): each subset has about 100 texts, in which, 20 texts have the considered label, 80 remain texts have other label.
- Balanced testing set with ratio of 50:50 (YES/NO balance - called 50:50 testing set):
 - Select randomly 500 texts whose label is that label, and 500 other texts whose label is different from that label.
 - Divide this set into ten subsets (for running of ten times): each subset has about 100 texts, in which, 50 texts have the considered label, 50 remain texts have other label.
- Unbalanced testing set with ratio of 80:20 (YES major - called 80:20 testing set):

- Select randomly 800 texts whose label is that label, and 200 other texts whose label is different from that label.
- Divide this set into ten subsets (for running of ten times): each subset has about 100 texts, in which, 80 texts have the considered label, 20 remain texts have other label.

- For each text in each testing subset, remove all stop-words.
- Split the remain character sequence into 1-gram, 2-grams, and 3-grams.
- Transform it into a vector of TF-IDF value.
- Testing with Multinomial Naive Bayes (MNB) classifier.

C. Output Parameters

We consider the output parameters in two cases: without *unbalanced factor* (classical), and with *unbalanced factor* (new proposed).

1) *Output parameters without unbalanced factor*: In this case, we use the *traditional output parameters* of *Accuracy*, and *F1-score* as the definition of Salton et al. [7] (formula 1 and 4).

2) *Output parameters with unbalanced factor*: In this case, we take into account the *balance factor* - α of the *testing set*. Therefore, we use the output parameters defined in Section II: *accuracy* (formula 6), and *F1-score* (formula 9).

D. Results

The results from the case using output parameters without/with *unbalanced factor* are presented in the Tables II, and III, respectively. These results indicate that the variation of *accuracy* and *F1-score* in the case without *unbalanced factor* is much higher than that in the case with unbalanced factor. For instance, in the case of label *comp.graphics* (the 2nd row in the Tables II and III): The *accuracy* varies from 83.83% to 89.58% and 95.35% in the testing set of 20:80, 50:50, and 80:20 respectively if the *unbalanced factor* is not taken into account. Meanwhile, if the *unbalanced factor* is taken into account, the *accuracy* becomes more stable with value of 90.01%, 89.58%, and 90.30% in the testing set of 20:80, 50:50, and 80:20 respectively.

The same to the value of *F1-score*: It varies from 68.26% to 90.33% and 97.16% in the testing set of 20:80, 50:50, and 80:20 respectively if the *unbalanced factor* is not taken into account. Meanwhile, if the *unbalanced factor* is taken into account, the *F1-score* becomes more stable with value of 90.88%, 90.33%, and 91.08% in the testing set of 20:80, 50:50, and 80:20 respectively.

This principle is appear in almost topics of the considered dataset. Consequently, the average value of *accuracy* and *F1-score* overall 20 topics in the case with *unbalanced factor* are more stable than that in the case without *unbalanced factor* (the last row in the Tables II and III): At the level of *accuracy*, its value varies from 88.35% to 93.07% and 96.08% in the case without *unbalanced factor*. Meanwhile, in

¹These classifiers are called from API of Weka open source library [2] for Java.

TABLE II. COMPARISON OF ACCURACY AND F1-SCORE (%) WITHOUT THE *unbalanced* factor ON THREE TESTING SETS

Topics	Accuracy			F1-score		
	20:80 ($\alpha=0.25$)	50:50 ($\alpha=1$)	80:20 ($\alpha=4$)	20:80 ($\alpha=0.25$)	50:50 ($\alpha=1$)	80:20 ($\alpha=4$)
alt.atheism	91.83	95.38	98.08	81.15	95.53	98.82
comp.graphics	83.83	89.58	95.35	68.26	90.33	97.16
comp.os.ms-windows.misc	94.17	90.03	86.87	84.95	89.24	91.12
comp.sys.ibm.pc.hardware	76.78	87.06	94.24	59.88	88.47	96.53
comp.sys.mac.hardware	82.87	90.22	95.35	67.02	90.94	97.13
comp.windows.x	89.04	92.74	95.76	75.96	92.97	97.35
misc.forsale	85.30	90.81	95.35	70.46	91.39	97.13
rec.autos	90.26	93.27	96.57	78.34	93.60	97.88
rec.motorcycles	90.78	94.96	97.17	79.07	95.18	98.25
rec.sport.baseball	92.35	96.41	97.47	82.15	96.54	98.44
rec.sport.hockey	94.96	97.66	98.08	87.42	97.72	98.80
sci.crypt	87.30	94.50	97.37	73.60	94.77	98.39
sci.electronics	85.91	91.16	95.15	71.47	91.65	97.02
sci.med	88.43	94.07	97.27	75.81	94.31	98.19
sci.space	93.57	95.61	97.07	84.65	95.73	98.67
soc.religion.christian	96.00	97.79	98.28	89.81	97.85	98.94
talk.politics.guns	88.17	93.84	96.87	74.86	94.09	98.07
talk.politics.mideast	94.43	96.97	98.69	86.26	97.04	99.19
talk.politics.misc	73.48	87.00	94.75	57.38	88.47	96.84
talk.religion.misc	87.57	92.32	95.76	73.73	92.76	97.38
Average	88.35	93.07	96.08	76.11	93.43	97.55

TABLE III. COMPARISON OF ACCURACY AND F1-SCORE (%) WITH THE *unbalanced* factor ON THREE TESTING SETS

Topics	Accuracy			F1-score		
	20:80 ($\alpha=0.25$)	50:50 ($\alpha=1$)	80:20 ($\alpha=4$)	20:80 ($\alpha=0.25$)	50:50 ($\alpha=1$)	80:20 ($\alpha=4$)
alt.atheism	94.66	95.38	96.40	94.89	95.53	96.52
comp.graphics	90.01	89.58	90.30	90.88	90.33	91.08
comp.os.ms-windows.misc	93.12	90.03	90.27	93.00	89.24	89.60
comp.sys.ibm.pc.hardware	85.55	87.06	87.01	87.28	88.47	88.54
comp.sys.mac.hardware	89.43	90.22	91.71	90.41	90.94	92.20
comp.windows.x	92.78	92.74	94.16	93.17	92.97	94.35
misc.forsale	90.91	90.81	92.31	91.65	91.39	92.76
rec.autos	94.11	93.27	94.06	94.45	93.60	94.39
rec.motorcycles	94.22	94.96	94.84	94.52	95.18	95.08
rec.sport.baseball	95.17	96.41	95.63	95.38	96.54	95.82
rec.sport.hockey	96.75	97.66	97.81	96.84	97.72	97.86
sci.crypt	92.12	94.50	94.36	92.69	94.77	94.73
sci.electronics	91.28	91.16	91.18	91.97	91.65	91.79
sci.med	93.00	94.07	94.70	93.52	94.31	94.96
sci.space	95.71	95.61	95.58	95.86	95.73	95.81
soc.religion.christian	97.58	97.79	97.33	97.64	97.85	97.43
talk.politics.guns	92.84	93.84	94.25	93.34	94.09	94.56
talk.politics.mideast	96.43	96.97	97.58	96.54	97.04	97.70
talk.politics.misc	83.95	87.00	87.32	86.26	88.47	88.78
talk.religion.misc	92.47	92.32	92.56	93.01	92.76	92.99
Average	92.60	93.07	93.47	93.17	93.43	93.85

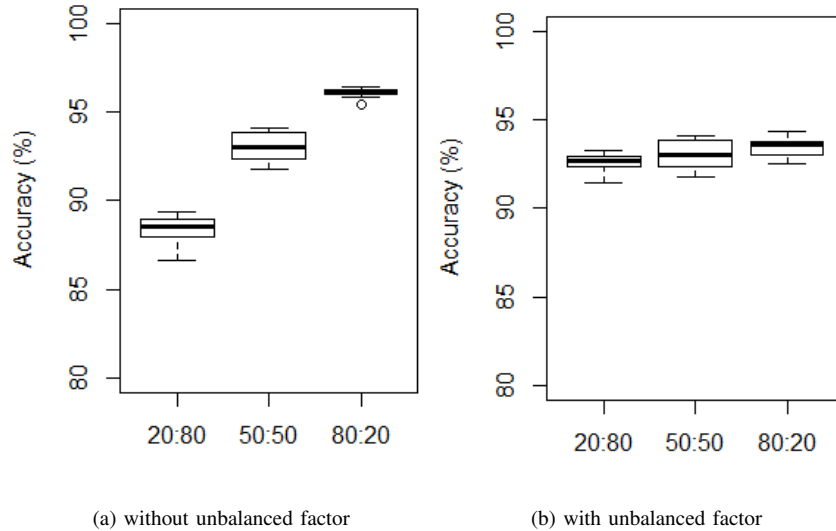


Fig. 1. Variation of Accuracy in three testing sets in the case without and with *unbalanced factor*.

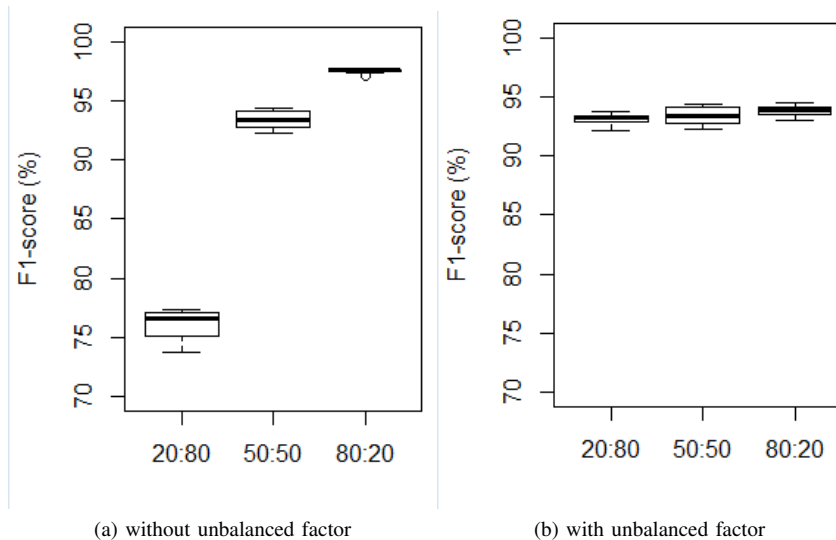


Fig. 2. Variation of F1-score in three testing sets in the case without and with *unbalanced factor*.

the case with *unbalanced factor*, its value has a small change from the 92.60% to 93.07% and 93.47% in the testing set of 20:80, 50:50, and 80:20 respectively. At the level of *F1-score*, its value varies from 76.11% to 93.43% and 97.55% in the case without *unbalanced factor*. Meanwhile, in the case with *unbalanced factor*, its value has a small change from the 93.17% to 93.43% and 93.85% in the testing set of 20:80, 50:50, and 80:20 respectively.

In order to see the difference in detail from the two considered cases, we compared the results from ten times of testing on each output parameters. At the level of *accuracy* (Fig. 1), its value in the case without *unbalanced factor* is significantly different from the testing set of 20:80, 50:50, and 80:20 (Fig. 1(a)). Meanwhile, there is no significant difference from its value in the case with *unbalanced factor* (Fig. 1(b)): this value is stably about 93%. The same results at the level of *F1-score* (Fig. 2), its value in the case without *unbalanced*

factor is significantly different from the testing set of 20:80, 50:50, and 80:20 (Fig. 2(a)). Meanwhile, there is no significant difference from its value in the case with *unbalanced factor* (Fig. 2(b)): this value is stably within 93-94%.

In summary, the experiment results indicate that the *unbalanced factor* could bring the value of *accuracy* and *F-score* of a classification method more stable. In other words, it could make the value of *accuracy* and *F-score* of a classification method more independent from the unbalanced ratio of label in the testing set.

IV. CONCLUSION

This paper proposed some update in the output parameters in evaluation of supervised machine learning methods (*accuracy*, *precision*, *recall*, *F1-score*) by taking into account the *unbalanced factor* which represents the unbalance ratio of

positive and negative samples in the testing set. The new updated parameters are then experimentally evaluated to compare to the traditional parameters. The experiment results indicate that the new updated parameters could evaluate the classifier with a stable value in spite of the change of unbalanced ratio between the positive and negative samples in the testing set.

REFERENCES

- [1] Christopher M. Bishop. *Pattern Recognition and Machine Learning (Information Science and Statistics)*. Springer-Verlag, Berlin, Heidelberg, 2006.
- [2] Mark Hall, Eibe Frank, Geoffrey Holmes, Bernhard Pfahringer, Peter Reutemann, and Ian H. Witten. The weka data mining software: An update. *SIGKDD Explorations Newsletter*, 11(1):10–18, November 2009.
- [3] Ashraf M. Kibriya, Eibe Frank, Bernhard Pfahringer, and Geoffrey Holmes. Multinomial naive bayes for text categorization revisited. In *Proceedings of the 17th Australian Joint Conference on Advances in Artificial Intelligence, AI'04*, pages 488–499, Berlin, Heidelberg, 2004. Springer-Verlag.
- [4] Ken Lang. Newsweeder: Learning to filter netnews. In *Proceedings of the Twelfth International Conference on Machine Learning*, pages 331–339, 1995.
- [5] Manh Hung Nguyen. On the distinction of subjectivity and objectivity of emotions in texts. *International Journal of Advanced Computer Science and Applications (IJACSA)*, 9(9):584–589, 2018.
- [6] R.G. Rossi, R. M. Marcacini, and S. O. Rezende. Benchmarking text collections for classification and clustering tasks. Technical Report 395, Institute of Mathematics and Computer Sciences - University of Sao Paulo, 2013.
- [7] Gerard Salton and Michael J. McGill. *Introduction to Modern Information Retrieval*. McGraw-Hill, Inc., New York, NY, USA, 1986.

A Hybrid Exam Scheduling Technique based on Graph Coloring and Genetic Algorithms Targeted Towards Student Comfort

Osama Al-Haj Hassan^{*,1}, Osama Qtaish^{†,2}, Maher Abuhamdeh^{‡,3}, Mohammad Al-Haj Hassan^{§,4}

^{*}Computer Networks Department, Isra University, Amman, Jordan

[†]Software Engineering Department, Isra University, Amman, Jordan

[‡]Computer Information Systems Department, Isra University, Amman, Jordan

[§]Computer Science Researcher, Amman, Jordan

Abstract—Scheduling is one of the vital activities needed in various aspects of life. It is also a key factor in generating exam schedules for academic institutions. In this paper we propose an exam scheduling technique that combines graph coloring and genetic algorithms. On one hand, graph coloring is used to order sections such that sections that are difficult to schedule comes first and accordingly scheduled first which helps in increasing the probability of generating valid schedules. On the other hand, we use genetic algorithms to search more effectively for more optimized schedules within the large search space. We propose a two-stage fitness function that is targeted toward increasing student comfort. We also investigate the effect and potency of the crossover operator and the mutation operator. Our experiments are conducted on a realistic dataset and the results show that a mutation only hybrid approach has a low cost and converges faster toward more optimized schedules.

Keywords—Exam scheduling; optimization; graph coloring; genetic algorithms; time tabling; fitness value

I. INTRODUCTION

Several life activities exploit scheduling to ensure efficient and proper operation including exam scheduling that is used in academic institutions for producing high quality exam schedules [1], [2], [3].

Exam scheduling is an optimization problem that aims to produce valid and optimized exam schedules. Several criteria govern the concept of ‘Optimized Exam Schedule’. For example, a schedule might be optimized based on finishing the whole examination period in a minimum number of days. It can also be optimized based on having the minimum number of exams for a given student per day. Another way of optimizing an exam schedule is maximizing the time period between exams for a given student which gives the student more time to prepare for his exams. In other words, the criterion upon which an exam schedule is optimized largely depends on the administration and their notion of a good schedule.

Exam scheduling problem is a case of graph coloring problem which is known to be NP-Complete [4]. Therefore, in real-world scenarios where exists a large number of faculties, courses, sections and students; finding the optimum exam schedule is a time consuming and cumbersome process. Accordingly, the aim of exam scheduling algorithms is generating exam schedules that are closer to the optimum schedule. Since it is very difficult to know the optimum schedule in the first place, then any improvement on the fitness of schedules would

be considered as one step closer to the optimum schedule.

We consider exam scheduling in an academic institution setting where academic faculties consist of departments. Those departments offer courses that have sections. Therefore, the aim of the exam scheduling process is to schedule sections in a way that generates optimized schedules.

Graph coloring is one of the techniques used for exam scheduling. It depends on a greedy approach that schedules sections in the current best possible slot such that no hard scheduling constraint is violated. It generates high quality exam schedules in an efficient way. However, due to its greedy nature and huge search space, it fails to find more optimized exam schedules.

Exam scheduling problem can be tackled using genetic algorithms which are approaches that depend on randomization to explore the large search space of possible solutions. The search space is explored in a time and resource intensive manner. Due to their randomized nature, they are able to find more optimized exam schedules. However, they are time intensive techniques. We explain our methodology as follows. The techniques that rely on randomization are the most effective for exam scheduling problem. Some of those approaches are genetic algorithms, ant colony, bee colony, particle swarm, and memetic algorithms. The reason behind that success is because it is nearly impossible to find the most optimized solution in problems with large search space using exhaustive search. Therefore, the randomized nature of the previously mentioned algorithms helps in scanning many areas of the large search space to find better solution. However, those randomized approaches tend to be blind in the way they cover the search space and accordingly might miss several good solutions. Consequently, it is strongly advised to support those techniques with other more focused approaches that help in guiding the randomized algorithms to cover the areas of the search space that are more likely to have higher quality solutions. This is why we choose a hybrid approach that utilizes the randomized nature of genetic algorithms and the guided search of graph coloring.

A. Contribution

In this paper, we develop a technique in which we combine graph coloring and genetic algorithms to design a hybrid approach that generates exam schedules that come closer to finding optimum schedules. Our paper contribution is laid out

in the following points:

- Exploiting graph coloring and genetic algorithms in a realistic scenario comprising realistic exam scheduling constraints.
- Proposing a new course registration dataset as a contribution to the research community.
- Designing a unique two-stage fitness function that focuses on increasing student's comfort during the examination period.
- Investigating the necessity of existence of crossover and mutation operators via inspecting their cost and effectiveness.

This paper is organized as follows. In Section II we present literature conducted in the areas of graph coloring and genetic algorithms and both of them combined. Then, in Section III we define the exam scheduling problem in the context of graph coloring and genetic algorithms. After that, we propose our hybrid exam scheduling approach in Section IV. Following that, we evaluate our approach in Section V. Finally, we conclude our work in Section VI.

II. RELATED WORK

In this section, we investigate different research work related to graph coloring, genetic algorithms and combining both of them.

A. Graph Coloring

Graph coloring has been used in several works for scheduling purposes. In [1] authors employ graph coloring to generate course timetabling and exam timetabling and they take into consideration several hard and soft constraints in the process. Their work focuses on measuring the degree of satisfaction of constraints and they try to achieve even distribution of courses. Authors in [2] exploit graph coloring to generate exam schedules by following a two phase scheme such that in phase one they schedule exams regardless of number of available seats in halls. Then, in phase two, they check if the number of needed seats in the generated schedule exceeds the number of available seats. If that happens, then they remove the scheduling of some exams and reschedule them again. In [5], authors provide a performance study for various graph coloring algorithms including First Fit, Welsh and Powell, Largest Degree Ordering, Degree of Saturation, Incidence Degree Ordering and Recursive Largest First. Graph coloring is used in [6] to enhance communication with users in massive multiple input multiple output wireless networks. The idea is to use graph coloring for pilot assignment instead of assigning pilot randomly on users which leads to reduced inter-cell interference between users. Most research focus on using graph coloring in situations where the graph does not change (static). However, the research in [7] investigates using graph coloring in problems where the graph is dynamic. They take into consideration random and heuristic changes on the graph. Graph coloring for dynamic graphs is also investigated in [8] where authors focus on a technique to ensure high effectiveness and high efficiency. They achieve that by performing incremental color propagation as the graph changes. An attempt to reduce

the time needed to color a graph is conducted in [9] where authors identify edge cover graphs and independent graphs within the graph to be colored. The graph coloring attempts for solving the scheduling problem only generate good enough solutions but they fail in finding near optimal solutions.

B. Genetic Algorithms

Genetic algorithms are key optimization techniques which have been used in various problems. In [10], a genetic algorithm is developed to help robots choose the most optimal path to their goal. It is also used in real time task scheduling [11] where the goal is to minimize the number of processors needed to accomplish all the given tasks. Authors in [12] focus on solving the exam timetabling problem using a genetic algorithm that maximizes time between student classes. This ensures that students have enough time and comfort to succeed in their exams. Scheduling tasks that include batch delivery on machines is investigated in [13]. It is achieved by using a genetic algorithm that minimizes job completion time while at the same time minimizes machine deterioration. A genetic algorithm for project scheduling is proposed in [14] where it is assumed that project tasks cannot be preempted and they use finite resources. Their goal is to minimize project completion time. Authors in [15] present a genetic algorithm for task scheduling in cloud computing. They analyze user characteristics and type of requests in order to classify jobs and their requirements. A genetic algorithm is utilized in [16] to find optimal buses routes that pick up and drop students at different locations. The employed genetic algorithm is able to find the shortest path for university buses. In [17] the graph coloring problem is solved using a Michigan genetic algorithm where each chromosome of the population represents one vertex and therefore the population represents one solution. Each chromosome evolves to find a better coloring decision and this evolution is also supported with local search to find better coloring decisions. The genetic algorithms that we mentioned in this section have a main shortcoming which is starting with bad solutions and that results in increasing the convergence time for the genetic algorithm.

C. Hybrid Graph Coloring and Genetic Algorithms

Several attempts have been performed to combine graph coloring and genetic algorithms. In [18], authors employ graph coloring to build their initial population and then they utilize genetic algorithms to evolve to better solutions using a fitness function that calculates the number of conflicts for each solution. Authors in [19] propose a technique that depends on varying weights for measuring conflicts and their fitness function relies on minimizing the number of colors used in finding solutions. The research conducted in [20] experiments with an algorithm that uses Tabu search and authors claim that eliminating the Tabu search component from the algorithm does not degrade the algorithm effectiveness. The work proposed in [21] adds parallelism to genetic algorithms and graph coloring combination, authors use sub populations (islands) that evolve to find solutions. Authors in [22] propose using adaptive parent selection and mutation techniques that work with genetic algorithms and graph coloring. Authors in [23] propose a hybrid approach that is targeted to exam scheduling problem and their fitness value depends on number of conflicts

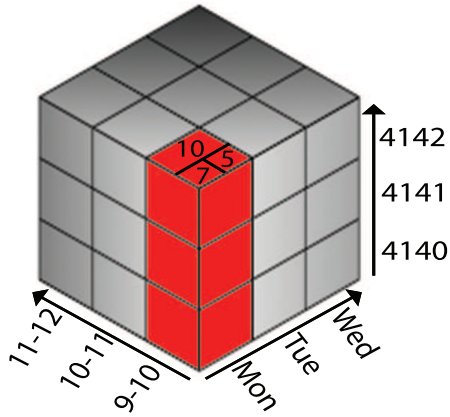


Fig. 1. Representation of ‘Slot’ and ‘Color’.

in exam schedules. Our work is different in two points; first, none of the previous hybrid approaches investigates the use of graph coloring combined with genetic algorithms specifically designed for exam scheduling settings except the work in [23]. However, the work in [23] does not discuss the possibility of omitting the crossover or the mutation operator. Second, none of the previous hybrid techniques investigates the necessity of existence of crossover or mutation operators except the work in [19]. However, the work in [19] does not target the exam scheduling problem, and therefore their choice of fitness function is too general. Also, the work in [19] does not clarify in details how crossover operator is performed while maintaining valid solutions. Moreover, our two-stage fitness function is different than what is used in the previous works.

III. PROBLEM DEFINITION

To make a concrete definition of exam scheduling problem, it is important to clarify the definition of a ‘slot’ in which an exam can be scheduled and the definition of a ‘color’ that a section can be assigned. We will also explain the scheduling problem in the context of graph coloring and genetic algorithms.

A. Slot and Color Definition

Suppose that $DayList = \{D_1, D_2, \dots, D_d\}$ is a set of days during which an exam can be scheduled. Also, suppose that $TimeList = \{T_1, T_2, \dots, T_t\}$ is a set of existing time periods in each day. Suppose also that $HallList = \{H_1, H_2, \dots, H_h\}$ is a set of halls available in each time period. Each intersection of a day D_i and time period T_j is considered a color such that $ColorList$ is a list of length $d * t$ that contains all colors. For example, the q^{th} color in colors list corresponds to day D_i and time period T_j and is denoted as $C_q^{i,j}$. For presentation purposes, we only use the subscript of colors in the manuscript unless we needed to mention the day and time period to which a color belongs. A slot represents preserving number of seats in a given hall in a specific day and time for a single exam. Based on that, $SlotList$ is a set of slots to which exams are assigned such that a single ‘slot’ is denoted as $S_{k,w}^{i,j}$ which represents holding an exam in day D_i and time period T_j where the exam takes place in hall H_k wherein w seats are

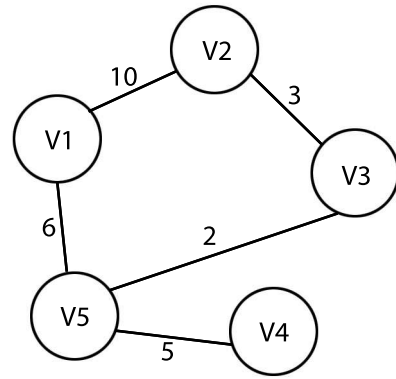


Fig. 2. Graph representation of exam scheduling problem.

reserved for the exam out of the total capacity of hall H_k . This representation of a color and a slot is illustrated in Fig. 1. For example, in Fig. 1 the slot marked with number ‘5’ is a slot in which an exam is scheduled such that it is held on ‘Monday’ at ‘9-10’ in hall ‘4142’ where ‘5’ seats are reserved for the exam out of 22 seats that represents the total hall capacity. Based on our previous definition, a single slot can be occupied by only one exam. Most related works represent a slot as a (Day,Time) pair. In our opinion, our definition is more precise and closely reflects reality and it eases the stage of implementing the algorithm. Since a color is represented by a day and time pair, then all slots that belong to the same day and time are said to have the same color. For example, in Fig. 1, all slots of day ‘Monday’ and time ‘9-10’ belong to the same color which we mark in red.

B. Graph Coloring for Exam Scheduling

In graph coloring, the exam scheduling problem can be thought of as follows. Suppose $VertexList = \{V_1, V_2, \dots, V_v\}$ is a set of vertices in an undirected graph such that each vertex represents a section of a course. $EdgeList = \{E_1, E_2, \dots, E_e\}$ is a set of edges such that an edge between two vertices (sections) represents the number of common students who are currently registered in the two sections. An example is illustrated in Fig. 2. This graph is represented as an adjacency matrix where the value at the intersection of two sections represents the number of common students between them (Table I). Recall that any two slots that share the same day and time are given the same color. Therefore, the exam scheduling problem can be solved by applying graph coloring where the exam of each section is scheduled in a slot such that no two adjacent vertices (sections with common students) are assigned slots of the same color. Graph coloring depends on a greedy approach that schedules sections in the current best possible slot.

C. Genetic Algorithms for Exam Scheduling

Genetic algorithms use the concept of evolution to find high quality schedules. In the context of exam scheduling, a chromosome represents a solution for the exam scheduling problem where each section is scheduled in a slot of a

TABLE I. ADJACENCY MATRIX OF THE GRAPH IN FIGURE 2.

	V ₁	V ₂	V ₃	V ₄	V ₅
V ₁	0	10	0	0	6
V ₂	10	0	3	0	0
V ₃	0	3	0	0	2
V ₄	0	0	0	0	5
V ₅	6	0	2	5	0

TABLE II. CHROMOSOME REPRESENTATION EXAMPLE.

0	1	2	3	4	5	6	7
C ₁	C ₂	C ₃	C ₄	C ₅	C ₆	C ₇	C ₈
V ₁ ,V ₉	V ₂	V ₄	V ₅ ,V ₇	V ₃ ,V ₉	V ₈	V ₁₁	V ₁₀

Algorithm 1 Initialization Code

Input: VertexList,dayIndex,TimePeriodIndex

Output: None

- 1: createDayIndex();
 - 2: createTimePeriodIndex();
 - 3: sectionListDegreeOrdering();
 - 4: sectionListWeightOrdering();
-

given color. In other words, a chromosome represents a ready exam schedule. For example, Table II shows an example of a chromosome representing 11 sections and the colors that are used for each section’s exam. A population of chromosomes is created where each chromosome has a specific fitness value that determines how good the exam schedule is. Several chromosomes are chosen from this population for mating and mutation. The mating process generates offspring consisting of new chromosomes. The offspring chromosomes replace chromosomes in the population that have fitness value worse than the fitness value of offspring chromosomes. This round of evolution is repeated for several generations hoping that the evolution process will eventually generate more optimized chromosomes (schedules).

IV. THE HYBRID APPROACH

In this section we describe the design and algorithms of the hybrid approach.

A. Day Index and Time Period Index

The forthcoming algorithm normally needs to traverse day list and time period list. For convenience purposes, we create an index for day list and an index for time period list. The indexes are simply arrays that control the order in which we traverse the elements in the day list and time period list. Initially, the day index and the time period index are set to the normal array indexes that start from zero and end with the array size minus 1. However, the hybrid approach relies on randomization, and therefore, these two indexes will be manipulated in a random fashion and utilized in the hybrid approach which helps in generating diverse exam schedules. Consequently, lines 1 and 2 of the code in Algorithm 1 are executed as part of the initial steps of the hybrid approach. Due to presentation purposes, we do not provide pseudocode for most of the functions in the forthcoming algorithms.

B. Section List Ordering

Recall that a section is a vertex in the exam scheduling undirected graph. Therefore, the degree of a section is the number of adjacent nodes. In other words, the degree of a section is the number of sections with which it has common students. The weight of a section is the largest weight among weights of the edges connecting the section with its adjacent sections. For example, in Fig. 2, the degree of section 5 is 2 and its weight is 6. In our algorithm we order sections list in descending order based on their degree. After that, sections of the same degree are ordered in descending order based on their weight. Sections in the start of the list will be scheduled first. The rationale behind this is that sections with high degree and weight have higher number of students in common with other sections, and therefore, scheduling this type of sections is difficult. Consequently, it is better to start scheduling these sections early while we still have many available slots. This is why lines 3 and 4 of the code in Algorithm 1 are executed as part of the initial steps of the hybrid approach.

C. The Graph Coloring Part

The graph coloring algorithm is shown in Algorithm 2. For each section, we first test if the section has already been colored (assigned a slot). If this is true, then we move on to the next section (Lines 2-5). All colors will be searched for an available slot (lines 6-12) such that exam scheduling constraints are not violated. Among the available slots, the chosen one for the section’s exam is the one that keeps the number of students having two exams in the same day as minimum as possible. This is why we need variables ‘minTwoExamsCount’ (line 6) and ‘selectedSlot’ (line 7) to keep track of the slot that would currently generate the minimum number of students with two exams in the same day if the slot is chosen for the exam assignment. Notice that lines 9 and 11 make use of the previously mentioned indexes to access the days and time periods. This gives us the flexibility of accessing the days and time periods in the order we desire. Line 12 represents the color in which the algorithm tries to find a slot available for the section’s exam. After that (Line 14), we call Algorithm 3 which goes through a set of scheduling constraints and returns a slot for the exam if possible. If the output of the aforementioned algorithm is ‘null’, then it means that no available slot was found in that color and hence we move on to the next color (Lines 15-18). Otherwise, we find how many students would have two exams in the same day if the exam is scheduled in the returned slot. We keep track of the slot that minimizes this number as much as possible(Lines 19-23). Eventually, a slot may be found such that it does not violate any constraint while at the same time it generates the greedy minimal number of students with two exams in the same day. This slot is used for the section’s exam (line 26). If no slot is found, then the section stays uncolored. Now, we briefly explain each one of the constraints in the order they appear in line 2 of Algorithm 3.

- Constraint 1: We make sure the maximum number of exams for instructor per day is not reached.
- Constraint 2: Sometimes, there would be certain days and time periods during which the instructor is not available. For example, the instructor is leaving for a

Algorithm 2 Graph Coloring

Input: Previously mentioned lists

Output: A slot for each section if possible

```
1: for (each section  $V_i$  in VertexList) do
2:   Section sec= $V_i$ ;
3:   if (sec.color  $\neq$  null) then
4:     continue;
5:   end if
6:   int minTwoExamsCount=Integer.MAXVALUE;
7:   Slot selectedSlot=null;
8:   for (each day  $D_j$  in DaysList) do
9:     int dayPosition=dayIndex[j];
10:    for (each TimePeriod  $T_k$  in TimePeriodList) do
11:      int periodPosition=timePeriodIndex[k];
12:      Color col=colorList[dayPosition,periodPosition];
13:      boolean validColor=true;
14:      Slot slot=ExamSchedulingConstraints(col,sec);
15:      if (slot == null) then
16:        validColor=false;
17:        continue;
18:      end if
19:      int examCount=twoExamsCount(col,sec);
20:      if (examCount<minTwoExamsCount) then
21:        minTwoExamsCount=examCount;
22:        selectedSlot=slot;
23:      end if
24:    end for
25:  end for
26:  sec.examTimeSlot=slot;
27: end for
```

conference trip. If this is one of those days and time periods, then this assignment is considered invalid.

- Constraint 3: Some academic institutions operate in a morning and evening system. In this case, a class held in the morning session cannot have its exam scheduled in the evening session.
- Constraint 4: We make sure the maximum number of exams per color is not reached; this is usually used to balance distribution of exams between colors.
- Constraint 5: An exam cannot be held in the same day, time, and hall in which a class is being held.
- Constraint 6: An exam cannot be held in the same day, time, and hall in which another exam is being held.
- Constraint 7: An exam cannot be held in a given day, time if there exists common students with another class held in the same day and time as those students can either attend the class or the exam.
- Constraint 8: An exam cannot be held in a given day, time if there exists common students with another exam held in the same day and time as those students cannot attend both exams simultaneously.
- Constraint 9: An exam cannot be held in a given day, time if there exists another class for the same instructor in the same day and time.
- Constraint 10: An exam cannot be held in a given

Algorithm 3 Exam Scheduling Constraints

Input: Color col, Vertex sec

Output: Slot

```
1: Slot slot=null;
2: if (isDailyMaxExamsForInstructor(col,sec) or
3: Not(canColorBeUsedForInstructor(col)) or
4: Not(colorWithinLimit(col,sec)) or
5: isMaxExamsPerColorReached(col) or
6: isClashWithAnotherSectionClass(col,sec) or
7: isClashWithAnotherSectionExam(col,sec) or
8: studentsOfSectionHaveClassInColor(col,sec) or
9: studentsOfSectionHaveExamsInColor(col,sec) or
10: instructorOfSectionHaveClassInColor(col,sec) or
11: instructorOfSectionHaveExamsInColor(col,sec) or
12: (slot=findAvailableHallForExam(col,sec))==null or
13: studentsCountWithThreeExamsViolated(col,sec) then
14:   return null;
15: else
16:   return slot;
17: end if
```

day, time if there exists another exam for the same instructor in the same day and time.

- Constraint 11: We try to find an available hall for the exam in the given color.
- Constraint 12: We check sure that placing an exam here does not cause a student to undertake 3 exams in the same day.

D. The Hybrid Part

In the hybrid approach, we utilize graph coloring in a genetic algorithm for the purpose of generating high quality schedules.

1) *Fitness Value:* Fitness value is the criterion used for deciding which chromosome (solution) is better than the other. Basically, the answer to the question ‘What is a good schedule?’ governs the decision of defining and computing the fitness value. As we mentioned in Section I, a good exam schedule is something debatable. In this work, we compare two schedules based on two stages such that if the first stage failed to determine the best schedule among the two schedules, then we use the second stage for that purpose. In stage 1, we define a ‘good schedule’ as a schedule that has the minimum total number of students having ‘two exams in the same day’ throughout all exam schedule days. For example, if a given schedule has 30 students having 2 exams in the same day over the exam schedule period and another schedule has 20 students having the same issue, then the later schedule is better. This choice of fitness function ensures a more comfortable exam schedule for students because we minimize the chance for a student to undertake two exams in the same day. Suppose that $StudentList = \{U_1, U_2, \dots, U_u\}$ represents a set of students. Based on that, the fitness function can be formulated as in Equation 1. The fitness function is the summation of the value TE for all students $\{U_1, \dots, U_u\}$ in all days $\{D_1, \dots, D_d\}$ such that TE equals 1 if the summation of exams for a given student U_g in all time periods $\{T_1, \dots, T_t\}$ of a given day D_i equals two, otherwise TE equals zero. Here, EC_{ijg} represents the

exams count for student U_g in day D_i in time period T_j . We can see that our optimization problem is a minimization one where the goal is reaching a schedule with minimum fitness value.

$$F = \sum_{g=1}^u \sum_{i=1}^d TE : TE = \begin{cases} 1, & \text{if } \sum_{j=1}^t EC_{ijg} = 2 \\ 0, & \text{otherwise} \end{cases} \quad (1)$$

In addition, we aim to maximize the time between consecutive student exams. So, if two schedules are considered equal based on stage 1, then in stage 2 we find the average number of gaps between consecutive exams for all students. Consequently, the schedule with more gaps between consecutive exams is considered better. This value can be found by computing Equation 2. $S_{h1,w1}^{i1,j1}$ represents the slot assigned for the first exam and $S_{h2,w2}^{i2,j2}$ constitutes the slot assigned for the next consecutive exam for a given student. So, if $i_2 = i_1$, then the two exams are held in the same day and therefore the gap between the two exams is actually the gap between the time periods to which the two slots belong ($j_2 - j_1 - 1$). However, if $i_2 \neq i_1$, this means that the two exams are held in different days. Accordingly, we calculate the gap between that two exams as follows. First, we compute the day difference ($i_2 - i_1$) and then we add 1 to the result for the purpose of giving this case a higher weight than the case in which the two exams belong to the same day. Second, we multiply the result with the total number of time periods in a given day (t). The final value CE is divided by number of students (u) to find the average number of gaps between two consecutive student exams. The combination of stage 1 and stage 2 leads the algorithm to generate schedules that are more comfortable to students.

$$F = \frac{\sum_{g=1}^u \sum_{i=1}^d CE(S_{h1,w1}^{i1,j1}, S_{h2,w2}^{i2,j2})}{u} \quad (2)$$

$$: CE = \begin{cases} j_2 - j_1 - 1, & \text{if } i_2 = i_1 \\ (i_2 - i_1 + 1) \times t, & \text{if } i_2 \neq i_1 \\ 0, & \text{otherwise} \end{cases}$$

2) *Population Generation:* We start by creating a population (pool) of chromosomes (solutions). The population size is a parameter we control in the system. Instead of randomly choosing section/slot assignment, we use graph coloring to build each chromosome. The rationale behind this decision is as follows. The sections ordering step in the graph coloring algorithm increases the probability of generating good quality exam schedules because the sections with high degree and high weight are the toughest to schedule. Therefore it is important to schedule them first. This leaves various scheduling options for the rest of sections and consequently we end up with good quality exam schedules. Moreover, random Section/Slot assignment will generate invalid exam schedules because there are many constraints that need to be met before a given section's exam can be assigned to a specific slot. Random Section/Slot assignment is blind of these constraints and generates invalid schedules. Fixing invalid schedules is a time consuming inefficient process that we try to avoid as much as possible. In addition, even if random section/slot assignment happened to produce valid schedules, the fitness value of the schedules is going to be high (poor schedules) and that would increase the time needed for the evolution part of the hybrid approach to

converge to an optimized solution. The population generation part of the algorithm is represented by lines 1-6 in Algorithm 4 .

Algorithm 4 Hybrid Approach

Input: Previously mentioned lists

Output: A slot for each section if possible

```

1: for (i = 0 to populationSize-1) do
2:   randomizeDaysListIndex();
3:   randomizeTimePeriodsListIndex();
4:   chromosome[i]=graphColoringPart();
5:   computeFitnessValue(chromosome[i]);
6: end for
7: for (i = 1 to numberOfGenerations) do
8:   Schedule[] parents=getTwoSchedulesForMating();
9:   Schedule[] offspring=performCrossover(parents);
10:  Schedule offspring0=performMutation(offspring[0]);
11:  Schedule offspring1=performMutation(offspring[1]);
12:  survivalSelection(offspring0);
13:  survivalSelection(offspring1);
14: end for

```

3) *Parent Selection:* The evolution process is performed through several generations. The number of generations is a parameter that we control in the system. The type of genetic algorithm we use is incremental in which two chromosomes are selected for mating (Crossover) in each generation. We use roulette wheel selection for choosing the two chromosomes. In roulette wheel selection, a slice in a pie (wheel) represents the probability that a chromosome will be selected for mating. Since our optimization problem is a minimization problem, then the slice area is inversely proportional to the fitness value of the chromosome. In other words, a chromosome with lower fitness value (Better Schedule) occupies a larger slice in the pie. Parent selection step is represented in line 8 of the code in Algorithm 4 .

4) *Crossover Operator:* The two chosen chromosomes (Table III and Table IV) will undergo a crossover (mating) process. The type of crossover we use is a multi point crossover where two points a_1 and b_1 are chosen randomly from the range $[0,z]$ where z is the length of chromosome (number of colors) and $b_1 > a_1$. Next, the section assignments in the middle section of the two parents are swapped (Table V and Table VI). Here we make sure that $\{b_1 - a_1 \leq z\}$ so that the swapping process is not performed over more than half of the chromosome length. Otherwise, the crossover process will turn into producing totally different chromosomes than its parents. Also, emphasizing this restriction decreases the cost of the crossover process which in turn increases the efficiency of the system. The swapping process generates cases where a section is assigned to two different slots (Conflict). For example, Table IX shows two conflicts in offspring 1 and two conflicts in offspring 2. In the case of a conflict, we use two ways of conflict resolution. We try the first one

TABLE III. PARENT I

C_1	C_2	C_3		C_4	C_5	C_6		C_7	C_8
V_1, V_2	V_7	V_5, V_8		V_3	V_4, V_6	V_9		V_{11}	V_{10}

TABLE IV. PARENT 2

C_1	C_2	C_3		C_4	C_5	C_6		C_7	C_8
V_7, V_{10}	V_1	V_3		V_2, V_4	V_9	V_5		V_6, V_{11}	V_8

TABLE V. OFFSPRING 1 BEFORE CONFLICT RESOLUTION

C_1	C_2	C_3		C_4	C_5	C_6		C_7	C_8
V_1, V_2	V_7	V_5, V_8		V_2, V_4	V_9	V_5		V_{11}	V_{10}

TABLE VI. OFFSPRING 2 BEFORE CONFLICT RESOLUTION

C_1	C_2	C_3		C_4	C_5	C_6		C_7	C_8
V_7, V_{10}	V_1	V_3		V_3	V_4, V_6	V_9		V_6, V_{11}	V_8

TABLE VII. OFFSPRING 1 AFTER CONFLICT RESOLUTION

C_1	C_2	C_3		C_4	C_5	C_6		C_7	C_8
V_1	V_2, V_7	V_8		V_3, V_4	V_9	V_5		V_6, V_{11}	V_{10}

TABLE VIII. OFFSPRING 2 AFTER CONFLICT RESOLUTION

C_1	C_2	C_3		C_4	C_5	C_6		C_7	C_8
V_7, V_{10}	V_1	V_6		V_3	V_4	V_2, V_9		V_{11}	V_5, V_8

and if it does not work then we go for the second one. The first conflict resolution way is that we cancel the Section/Slot assignment that came from the same parent and we allow the new Section/Slot assignment coming from the other parent via the swapping process. This type of conflict resolution might fail because forcing a section’s exam to be scheduled in a specific slot may violate exam scheduling constraints such as a student having two exams in the same day and time or exceeding the number of exams allowed for a student in a given day. In this case, we follow the second conflict resolution way in which we cancel the Section/Slot assignment that came from the same parent and use the graph coloring algorithm to schedule the section’s exam in an acceptable slot that does not violate exam scheduling constraints. Notice that a new problem results after crossover and before conflict resolution. The problem is that few sections are missing from the offspring chromosomes. V_3 and V_6 are missing from offspring 1 and V_2 and V_5 are missing from offspring 2. We resolve this issue by calling the graph coloring routine after crossover is concluded which assigns appropriate slots for the missing sections. The new places for the missing sections are marked in blue color. The crossover step is performed at line 9 of the code in Algorithm 4. Tables VII and VIII show the final chromosomes (schedules) after executing the conflict resolution process.

5) *Mutation Operator*: In the mutation step, we use a mutation rate such that for each section we generate a random number between 0 and 1 and if the number is less than or equal to the mutation rate, then we cancel Section/Slot assignment. After performing this step for all sections, we run the graph coloring Algorithm 2 to find a slot for each section affected by the previous step which results in creating new Section/Slot assignments. Lines 10 and 11 carry out the mutation step.

6) *Survival Selection*: After crossover and mutation steps are concluded, we have two offspring chromosomes that represent valid exam schedules. So, we calculate the fitness

TABLE IX. CONFLICT RESOLUTION OF THE CONFLICTS AT TABLES V, VI

Num	Conflict	Conflict Resolution 1	Conflict Resolution 2
Offspring 1	V_2 in C_4 and C_1	-unassign(V_2, C_1) -assign(V_2, C_4) -Result: Fail	-unassign(V_2, C_1) -graphcoloring() -Result: (V_2, C_2)
Offspring 1	V_5 in C_6 and C_3	-unassign(V_5, C_3) -assign(V_5, C_6) -Result: Success	Not Needed
Offspring 2	V_3 in C_4 and C_3	-unassign(V_3, C_3) -assign(V_3, C_4) -Result: Success	Not Needed
Offspring 2	V_6 in C_5 and C_7	-unassign(V_6, C_7) -assign(V_6, C_5) -Result: Fail	-unassign(V_6, C_7) -graphcoloring() -Result: (V_6, C_3)

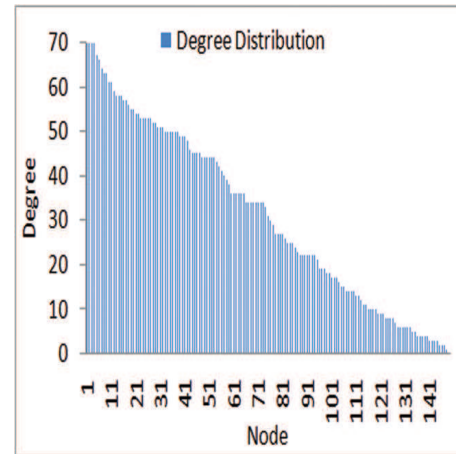


Fig. 3. Degree distribution of nodes.

value for each of them. If the fitness value for a given offspring chromosome happened to be less than the least fitness value among population chromosomes, then the offspring chromosome replaces that chromosome with the least fitness value. In the cases where fitness value of the offspring does not outperform any chromosome in the population, then the offspring is discarded. Survival selection is realized at lines 12 and 13 of the code in Algorithm 4 .

V. EXPERIMENTS AND RESULTS

The algorithms we test in this section are as follows. The first one is the original hybrid approach we explained earlier (Original). The second one is a variation of the original algorithm in which we remove the crossover step and rely only on mutation (MutationOnly). The third one is the graph coloring algorithm (Graph). We implemented the aforementioned algorithms in an exam scheduling software developed using java language and MySQL database management system. The fitness value measured in the experiments refers to the number of students who have two exams in the same day throughout the examination period. For more accurate results, we perform 50 runs and take the average of the output numbers.

The dataset we employ in our experiments [24] is a new dataset that we propose for the research community. The dataset contains complete registration information that

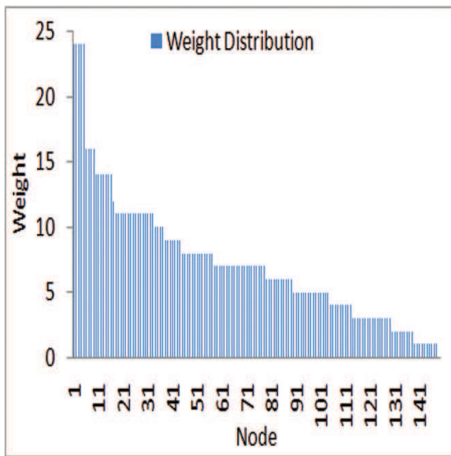


Fig. 4. Weight distribution for nodes.

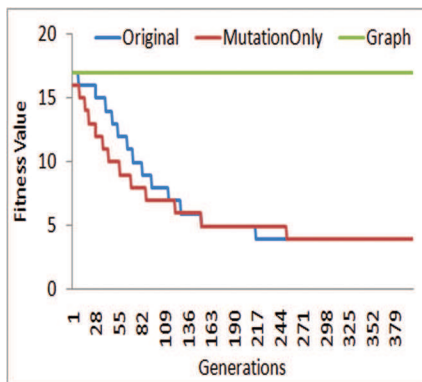


Fig. 5. Convergence of techniques.

reflects the real scenario during the 2017/2018 second semester in faculty of information technology at Isra University. Our dataset contains 89 courses, 143 sections, 24 instructors, 686 students, and 25 halls. Our experiments assume that exams take place during a span of 10 days such that each day contains 13 overlapping morning time periods and 3 evening time periods. In order to increase the degree of difficulty of finding valid exam schedules, we take into consideration the first and second exams and we exclude the final exams. This is because there are classes held during the first and the second exams, and therefore, the number of available halls in each time period is considerably less than the number of available halls during final exams which in turn makes scheduling harder. The process of finding valid exam schedules becomes more challenging when each section has common students with many other sections (Degree Increase). The challenge even escalates when the number of common students between each two sections is higher (Weight Increase). Therefore, in Fig. 3 and Fig. 4 we plot the degree distribution and weight distribution for sections. This helps in giving the reader a sense of the dataset under consideration. In Fig. 5, we aim to find which technique generates better schedules (lower fitness value). Here, we fix the number of generations at 500 and mutation rate at 0.5 and population size at 200. We found that the graph coloring technique is the worst because it depends on a greedy approach and hence it cannot explore the whole search space. On the other hand, both original and mutation

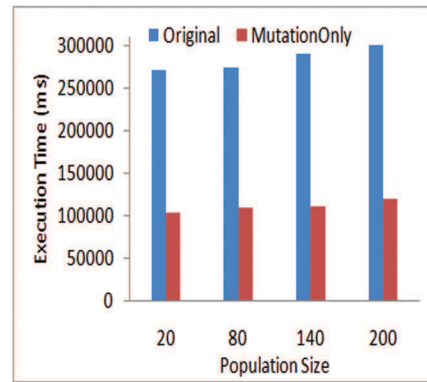


Fig. 6. Execution Time of techniques.

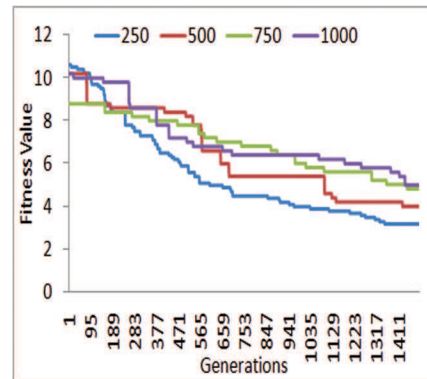


Fig. 7. Convergence speed for 'mutationOnly' when population size increases

only techniques are able to find more optimized schedules than graph coloring approach because of their genetic nature that helps to cover more area of the search space. However, looking back at the same Fig. 5, we notice that the mutation only solution converges faster than the original approach. In other words, the mutation only solution improves faster toward finding more optimized schedules. Consequently, we conclude that the mutation operator is more effective than the crossover operator in progressing toward more optimized schedules. In the second experiment illustrated in Fig. 6, we measure the execution time (milliseconds) of the original and mutation only techniques such that mutation rate is fixed at 0.5 and number of generations is fixed at 1500. We noticed that original approach is slower than the mutation only approach. This is due to the fact that crossover might generate conflicts and consequently time is spent to resolve those conflicts. This is why the crossover operator takes more time than the mutation operator that does not cause conflicts. Moreover, in the same figure we vary population size between 20 and 200 and the result shows that the execution time for both techniques increases when population size increases because more time is needed to generate the initial population. Also, both techniques require iterating through solutions of the population which takes more time as the population size increases. In the next experiment in Fig. 7 we investigate the effect of increasing population size (from 250 to 1000) on the speed of convergence for the mutation only algorithm such that we fix the mutation rate at 0.5 and number of generations at 1500. The figure shows that when population size decreases the algorithm converges

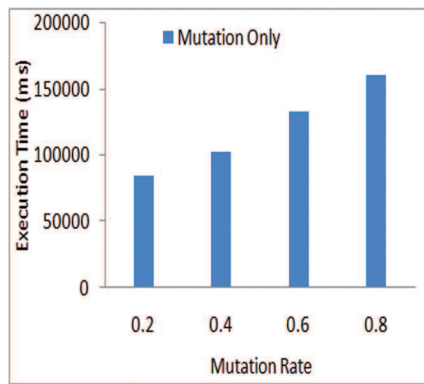


Fig. 8. Execution time for 'mutationOnly' when mutation rate increases.

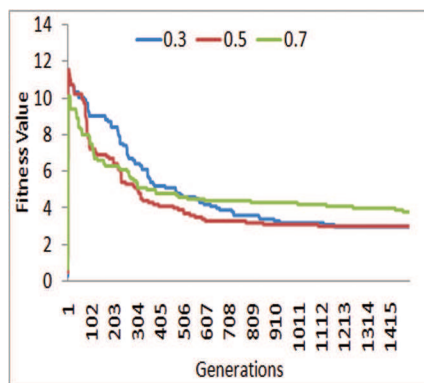


Fig. 9. Convergence speed for 'mutationOnly' when mutation rate increases.

faster. We noticed that when population size increases, the algorithm still manages to find the best possible exam schedule. However, it is interesting to point out that our experiments show that the fastest convergence occurred when population size equals to 1 which conforms with the result found in [19]. Next, we evaluate the effect of changing mutation rate on convergence and execution time. Fig. 8 shows that execution time increases when mutation rate increases which is the result of increasing number of operations that cancels the assignment of sections and makes scheduling decision for them again. In the previous experiment, population size is fixed at 200 and number of generations is fixed at 1500. We use the same fixed values in Fig. 9 in which we notice that increasing the mutation rate leads to faster convergence up to a point where increasing mutation rate generates reversible result (slower convergence). This actually makes sense because when the mutation rate increases the difference between the chromosomes before and after mutation becomes bigger. As a consequence, the chromosome after mutation becomes a totally new chromosome which would not preserve the quality genes in the parents which defies the concept of evolution. In our experiments, we obtained best results when mutation rate is 0.4. The previous set of experiments shows that combining graph coloring and genetic algorithms is effective in finding more optimized schedules. Also, the experiments indicate that the crossover operator is a costly operator and it is not as effective as the mutation operator.

VI. CONCLUSION AND FUTURE WORK

In this paper, we proposed a hybrid approach that combines graph coloring and genetic algorithms for finding more optimized exam schedules. Our focus was to generate exam schedules in which we minimize the total number of students who have two exams in the same day. At the same time, we increased the gap between consecutive student exams. This helped in generating more comfortable exam schedule for students. Also, several types of realistic exam scheduling constraints were taken into consideration. Moreover, we evaluated our technique using realistic registration dataset. Our evaluation showed that relying on mutation instead of crossover leads to increased effectiveness and is not as computationally expensive. The hybrid approach generates promising results in terms of finding more optimized schedules that increase student comfort throughout the examination period. We relied on student comfort to measure the quality of schedules by minimizing the number of students who have two exams in the same day. So, as a future work, we aim to expand student comfort by adding more details such as increasing the gap between exams for a given student. Moreover, we are planning to investigate more measures for deciding the quality of schedules and incorporate those measures in a realistic exam scheduling tool such that the user can pick the measure he needs.

REFERENCES

- [1] R. Ganguli and S. Roy, "A study on course timetable scheduling using graph coloring approach," *international journal of computational and applied mathematics*, vol. 12, no. 2, pp. 469–485, 2017.
- [2] S. Saharan and R. Kumar, "Graph coloring based optimized algorithm for resource utilization in examination scheduling," *Applied Mathematics and Information Sciences*, vol. 10, no. 3, pp. 1193–1201, May 2016.
- [3] N. G. N. Anand Nayyar, Dac-Nhuong Le, *Advances in Swarm Intelligence for Optimizing Problems in Computer Science*. Chapman and Hall/CRC, 2018.
- [4] M. R. Garey and D. S. Johnson, *Computers and Intractability: A Guide to the Theory of NP-Completeness*. New York, NY, USA: W. H. Freeman & Co., 1990.
- [5] N. M. Gandhi and R. Misra, "Performance comparison of parallel graph coloring algorithms on bsp model using hadoop," in *2015 International Conference on Computing, Networking and Communications (ICNC)*, Feb 2015, pp. 110–116.
- [6] H. T. Dao and S. Kim, "Vertex graph-coloring-based pilot assignment with location-based channel estimation for massive mimo systems," *IEEE Access*, vol. 6, pp. 4599–4607, 2018.
- [7] B. Hardy, R. Lewis, and J. Thompson, "Tackling the edge dynamic graph colouring problem with and without future adjacency information," *Journal of Heuristics*, vol. 24, no. 3, pp. 321–343, Jun 2018.
- [8] L. Yuan, L. Qin, X. Lin, L. Chang, and W. Zhang, "Effective and efficient dynamic graph coloring," *Proceedings of the VLDB Endowment*, vol. 11, no. 3, pp. 338–351, Nov. 2017.
- [9] H. Patidar and D. P. Chakrabarti, "A novel edge cover based graph coloring algorithm," *International Journal of Advanced Computer Science and Applications*, vol. 8, no. 5, 2017.
- [10] I. Ashiru, C. Czarnecki, and T. Routen, "Characteristics of a genetic based approach to path planning for mobile robots," *Journal of Network and Computer Applications*, vol. 19, no. 2, pp. 149–169, 1996.
- [11] J. Oh and C. Wu, "Genetic-algorithm-based real-time task scheduling with multiple goals," *Journal of Systems and Software*, vol. 71, no. 3, pp. 245–258, 2004, computer Systems.
- [12] C. Kalayci and A. Gungor, "A genetic algorithm based examination timetabling model focusing on student success for the case of the college of engineering at pamukkale university, turkey," *Gazi University Journal of Science*, vol. 25, pp. 137 – 153, 2011.

- [13] M. Saidi-Mehrabad and S. Bairamzadeh, "Design of a hybrid genetic algorithm for parallel machines scheduling to minimize job tardiness and machine deteriorating costs with deteriorating jobs in a batched delivery system," *Journal of Optimization in Industrial Engineering*, vol. 11, no. 1, pp. 35–50, 2018.
- [14] R. L. Kadri and F. F. Boctor, "An efficient genetic algorithm to solve the resource-constrained project scheduling problem with transfer times: The single mode case," *European Journal of Operational Research*, vol. 265, no. 2, pp. 454 – 462, 2018.
- [15] K. Kaur, N. Kaur, and K. Kaur, "A novel context and load-aware family genetic algorithm based task scheduling in cloud computing," in *Data Engineering and Intelligent Computing*. Singapore: Springer Singapore, 2018, pp. 521–531.
- [16] M. A. Mohammed, M. K. A. Ghani, R. I. Hamed, S. A. Mostafa, M. S. Ahmad, and D. A. Ibrahim, "Solving vehicle routing problem by using improved genetic algorithm for optimal solution," *Journal of Computational Science*, vol. 21, pp. 255 – 262, 2017.
- [17] M. R. Mirsaleh and M. R. Meybodi, "A michigan memetic algorithm for solving the vertex coloring problem," *Journal of Computational Science*, vol. 24, pp. 389 – 401, 2018.
- [18] S. M. Douiri and S. Elbernoussi, "Solving the graph coloring problem via hybrid genetic algorithms," *Journal of King Saud University - Engineering Sciences*, vol. 27, no. 1, pp. 114 – 118, 2015.
- [19] A. Eiben, J. van der Hauw, and J. van Hemert, "Graph coloring with adaptive evolutionary algorithms," *Journal of Heuristics*, vol. 4, no. 1, pp. 25–46, Jun 1998.
- [20] C. A. Glass and A. Prügel-Bennett, "Genetic algorithm for graph coloring: Exploration of galinier and hao's algorithm," *Journal of Combinatorial Optimization*, vol. 7, no. 3, pp. 229–236, Sep 2003.
- [21] Z. Kokosiński, M. Kołodziej, and K. Kwarciany, "Parallel genetic algorithm for graph coloring problem," in *Computational Science - ICCS 2004*. Berlin, Heidelberg: Springer Berlin Heidelberg, 2004, pp. 215–222.
- [22] M. Hindi and R. V. Yampolskiy, "Genetic algorithm applied to the graph coloring problem," in *Proceedings of the 23rd Midwest Artificial Intelligence and Cognitive Science Conference*, 2012, pp. 60–66.
- [23] W. Erben, "A grouping genetic algorithm for graph colouring and exam timetabling," in *Practice and Theory of Automated Timetabling III*. Berlin, Heidelberg: Springer Berlin Heidelberg, 2001, pp. 132–156.
- [24] [dataset] Osama Al-Haj Hassan, "Student registration dataset of faculty of information technology at isra university, amman, jordan, mendeley data, v1," 2018.

Developing a Framework for Analyzing Heterogeneous Data from Social Networks

Aritra Paul¹, Mohammad Shamsul Arefin², Rezaul Karim³
Department of Computer Science & Engineering
Chittagong University of Engineering & Technology
Chittagong 4349, Bangladesh

Abstract—Due to the rapid growth of internet technologies, at present online social networks have become a part of people's everyday life. People shares their thoughts, feelings, likings, disliking and many other issues at social networks by posting messages, videos, images and commenting on these. It is a great source of heterogeneous data. Heterogeneous data is a kind of unstructured data which comes in a variety of forms with an uncertain speed. In this paper, we develop a framework to collect and analyze a significant amount of heterogeneous data obtained from the social network to understand the behavioural patterns of the people at the social networks. In our framework, at first we crawl data from a well-known social network through Graph API that contains post, comments, images and videos. We compute keywords from the users' comments and posts and separate keywords as noun, verb, and adjective with the help of an XML based parts of speech tagger. We analyze images related to each user to find out how a user like to move. For this purpose, we count the number of users in an image using frontal face detection classifier. We also analyze video files of the users to find the categories of videos. For this purpose, we divide each video into frames and measure the RGB properties, speed, duration, frame's height and width. Finally, for each user we combine information from text, images and videos and based on the combined information we develop the profile of the user. Then, we generate recommendations for each user based on activities of the user and cosine similarity between users. We perform several experiments to show the effectiveness of our developed system. From the experimental evaluation, we can say that our framework can generate results up to a satisfactory level.

Keywords—Heterogeneous data; recommendation systems; cosine similarity; video categorization

I. INTRODUCTION

The term heterogeneous data comes from the concept of 'Big Data', is a term for data-set that are so large and complex that traditional data processing applications are inadequate to deal with them. It often refers simply in user's behavior analytics, predictive analytics or certain another data analytics method that extracts value from data. The concept of big data stands on 4V theory. This 4V are actually Value, Velocity, Variety, and Variability. Among 4V, heterogeneous data is directly related to Variety. It means a huge amount of data in different nature or formats. Most of the cases the data-set is unstructured including text, images, videos, audio files, web-links etc. And in this era of data science, one of the biggest sources of this heterogeneous data is Social Networks.

Nowadays online social networks are part of people's everyday life. It is a theoretical construct useful in social science to study relationships between individuals, groups,

organization or even entire societies. The term is used to describe a social structure determined by such interaction. It is a medium where individuals interact with several groups of individuals by posting status, uploading images, videos, sharing feelings and so on. Interaction pattern varies from individuals to individuals. We can observe different interaction pattern for different groups of users. That means social networks are a great source of heterogeneous data. The importance of developing framework let us know the real interest of the users. Categorization of the user is very important for knowing the type of users, determine the type of multimedia they are most interested, how they interact with other users and by the place they visited we can get an idea of their interests. The methodology we use for the analysis can be applied not only to online social networking systems but also to any social multimedia sites like content sharing sites.

The analysis is done after crawling a huge set of data from a social network. The structure of the social networks emerged from their interactions shows how this knowledge can help to design new systems or improve the existing systems. However, we analyze user who interacts with each other through social networks. We study well to discover the user's behavior in online social networks.

Heterogeneous data never come in a structured way actually it's an unstructured data type. So handling this unstructured data is tough in a normal relational database. That's why we prefer Bigdata and NoSQL platform like Hadoop. Hadoop allows handling unstructured data with billions of rows and millions of columns. The motivation of our work is to understand user's behavior in online social networks and how it is changing over time. The research is carried out to achieve following goals:

- To develop a framework for analyzing heterogeneous data from social networks.
- To categorize the users based on their activities.
- To develop a short profile of the user.
- To develop a recommendation system for users.

In this paper in Section 2, we present related works in data analysis from social network, their advantages, and limitations. In Section 3, we enumerate our methodology concisely. Section 4 shows the experimental result of our efforts. In Section 5 we conclude the paper.

II. RELATED WORK

There are some categorizations and measurement analysis systems that are operating in a single language only. A. Mislove et al. [1] developed a system for the measurement and analysis of online Social Networks where they examine data gathered from four popular online social networks: Flickr, YouTube, LiveJournal, and Orkut. They tried to crawl the publicly accessible user links on each site and obtained a large portion of each social network's graph. They presented a large-scale measurement study including analysis of the structure of multiple online social networks. M. Maia et al. [2] studied well to discover user behavior in online social networks but the correlation of user's behavior within these networks is not considered widely. However, it has some limitation, 1st one is, it can crawl less amount of data and the 2nd one is, the analysis is based on only on the measure of friendship relation. Here authors developed a system to analyze the behavior of the YouTube user grouping them through K-based clustering algorithm. The advantage of this system is it can group user with similar behavior.

Benevenuto et al. [3] designed a system which identifies influential users and their network impact. An interesting fact is knowing the influence of users and being able to predict it can be a strategic advantage for many applications. The most famous application to researchers and marketers is viral marketing. There is one main limitation of current research efforts on identifying influential users in social network analysis: lacking of an effective approach for modeling, predicting, and measuring the influence. Utilizing the session information, the author first examined the number of concurrent users, concurrent sessions, that accessed social networks. The beginning of each day is marked on the horizontal axis. They see a diurnal pattern with strong peaks around 3 PM, at all-times, there are at least 50 people who are using the social network aggregator service. At peak times, the number of concurrent users surpasses 700 which is more than a 10-fold increase over the minimum. Drops in usage on certain days indicate clear patterns like weekly patterns, where weekends showed a much lower usage than weekdays. The strong diurnal pattern in social network workloads has also been observed in accessing message and applications on the Social network and in the content generation of blog posts and answers in user-generated content websites. The system is designed with a probability of activity over time and it has little access to social network API. They worked on the passing time of the users. J. Thomas et al. [4] focus on the integrative analysis method for heterogeneous data. They explained two different methods one is for Bayesian network method and another one is multiple kernel-based method. The limitation is the author has not indicated any better methods but simply telling which one is harder to prove.

Author [5] developed a system to identify malicious posts from Facebook in real time. They have done this using Facebook graph API. It gives quite a good result but it has some limitation too. Their framework deals only with text posts considering there are no spam posts.

In [6] author offered a parallel computing based method to extract a social network individuals from fused data, by using cumulative association Data Graph. They implemented a supervised learning framework to parameterize the extraction

algorithms. The advantage is data access methods are compared broadly.

In [7] author showed the limitations of finding patterns and comprehend the structure with many nodes and links. To overcome the limitations they identified, they offered a structured technique for structural analysis of social networks. The advantage is, the network layout is kept stable for each action so that, users can perceive patterns with a flexible interface.

S. A. Catanese et al. [8] author narrated the collection and analysis of huge data describing the connections between participants in online social networks. They approached two alternative methods which are well defined and also evaluated practically against the popular social network Facebook. For data crawling, they introduced two approaches one is BFS crawler and another one is Uniform crawler. However, it has some limitation and that is, they approached two methods for data crawling but they did not try parallel crawling which would make the output more relevant. Wilson et al.

[9] used the adoption behaviors referring to some activities or topics (tweets, products, Hash-tags, URLs, etc.) shared among users implicitly and explicitly such as users forwarding a message to their friends, sometimes recommending a product to others, joining some groups having similar interests, and posting messages about the same topics or issues, etc.

There are some drawbacks of existing social network influence models based on either static networks or the influence maximization diffusion process are most existing models are descriptive models rather than predictive models. There are very few models that are able to predict user's future influence. Using a discrete-time model to model diffusion process in continuous time is very computationally expensive. There are some system proposed and classified by the researchers. They classified system as:

- Crawling Social Network for Social Network Analysis Purposes
- Measurement and analysis of Social Network
- Characterizing User Behavior in online Social Networks
- Development of a social Network Crawler for Opinion Trend Monitoring and Analysis Purposes

A. Crawling from Social Networks

This crawling framework is proposed by A. Mislove et al. [1]. They introduced automated scripts and by using it on a cluster of 58 machines, they crawled the social graphs of some social network. They selected Flickr, LiveJournal, Orkut, YouTube for crawling data. They described their work through the collection and analysis of massive amount data, describing the connections between participants in online social networks. Alternative approaches to a social network data collection are defined and evaluated in practice against the popular Social network websites. They describe a set of tools that they developed to analyze specific properties of such social-network graphs, i.e. degree of distribution, centrally measures, scaling laws and distribution of friendship.

B. Social Network Analysis

Breadth-first-search (BFS) is a well-known graph traversal algorithm which is optimal and easy to be implemented, in particular for visiting unweight, undirected graphs. For these reasons, it has been adopted in several Online social networks (OSN) crawling tasks. Starting from a seed node, the algorithm discovers rest neighbors of the seed, putting them in a FIFO queue. Nodes in the queue are visited in order of appearance, so the coverage of the graph could be represented as an expanding wave front. This algorithm, concludes its execution when all the discovered nodes have been visited. For large graphs, like OSNs, this stopping condition would imply huge computational resources and time. In practice, we have established termination criteria which is a coverage of at least three sub-levels of friendships and a running time of 240 hours, so as resulting in an incomplete visit of the graph. Chau et al. [10] assert that an incomplete BFS sampling leads to a biased results, particularly towards high degree nodes. Even, our experimentation data acquired through BFS sampling does not show a statistically significant bias. We investigate this aspect in comparison with others and that is obtained using a sampling technique which is proved to be unbiased.

The Uniform sampling of a social network has been introduced by Gjoka [11], he provided proof of correctness of this approach but implementation details omitted here. Social network relies on a well-designed system of user-IDs assignment, spreading in the space of 32-bit range. So as the rejection sampling methodology is viable, this approach requires the generation of a queue of random user-IDs to be requested to a social network, querying for their existence. If so, the user and his/her friend list are extracted, otherwise, the user-ID is discarded and the polling proceeds to the next. The advantage of this approach relies on the independence of the distribution of user-IDs with respect to the distribution of friendship in the graph.

C. Characterizing user Behaviour in Online Social Networks

Here, we briefly provide a comprehensive view of users behavior in OSNs by characterizing the type, frequency, and sequence of activities users are engaged in. They [3] developed a new analysis strategy, which they call the clickstream model. This model is used to identify and describe representative user behaviors in Online Social Networks(OSN) based on clickstream data. The modeling of the system implies two steps. The first step is to identify dominant user activities in clickstreams. This step involves enumerating all features users engaged in on OSNs at the level of the basic unit, which they call user activity. They manually annotated each log entry of the clickstream data with the appropriate activity class (e.g, friend invitation, browsing photos), based on the information available in the HTTP header. Because a user can conduct a wide range of activities in a typical OSN site, they further tried to group semantically similar activities into a category by utilizing the web page structure of OSN sites (i.e, which set of activities can be conducted on a single page) and manually grouping related activities into categories. The next step of modeling is to compute the transition rates between the user activities. To represent the sequence in which activities are conducted, they built a first-order Markov chain of user activities and compute the probability transition between every

pair of activity states. To gain a holistic view, they built a Markov chain which describes how users transition occurs from one category to another.

D. Social Network Crawler for Option Trend Monitoring and Analysis Purpose

This is a system prototype to analysis trend in a social network. The proposed system crawl data from Social network, indexes the data and provides a user interface where end users can search and see the trend of the topics of their choice. The main objective of this system is to propose a framework that can contribute to the improvement of the way government official and communicate in regard to service delivery in rural areas. The premise of this system is that if the government can keep track of the citizen's opinions and thoughts about service delivery, it can help improve the delivery of such services. This research and the implementation of the trend analysis tool is undertaken in the context of the Siyakhula Living Lab which is an Information and Communication Technologies for development intervention for Dwesa marginalized community located in the Eastern Cape province of South Africa.

III. METHODOLOGY

We have followed a modular approach for the development of this framework. The system architecture of this framework comprises 7 basic modules; Social Network Access Module, Data Crawling Module, Data Separation Module, Data Storing Module, Data Categorization Module, Developing profile Module and Recommending Module. The whole structure is shown in Fig. 1. We have used Hadoop HBase as the storage system and applied NoSQL which gives our system a dynamic property. We have initialized our storage system according to row key value and column according to our categorized data.

A. Social Networking Access Module

First of all, it is not trivial to tackle large-scale mining issues: for example, measure the crawling overhead in order to collect the whole Social network graph which is to be exact 44 Terabytes of data to be downloaded and handled. However, even when such data can be acquired and stored locally, it is non-trivial to devise and implement functions that traverse and visit the graph or evaluate simple metrics. For all these reasons, it is common to work with a small but representative sample of the graph. Extensive research has been conducted on sampling techniques for large graphs but, only in the last few years, some studies have a light on the partial bias that introduced standard methodologies.

First of all, we have to establish a network connection to get access from the social networks. The network connection will allow us to get access from the Graph API. Then from the Graph API, we need to download the RestFB package in order to get access from the Graph API. The Graph API gave the pathway to get access tokens for collecting data from the social network.

Then with the Java crawler, we have crawled data simultaneously from social network more than 15 days. The data then categorized into status, links, images, videos, and audios. We have used Hadoop database to store this data. Before storing this data in Hadoop we have organized reliable data into a

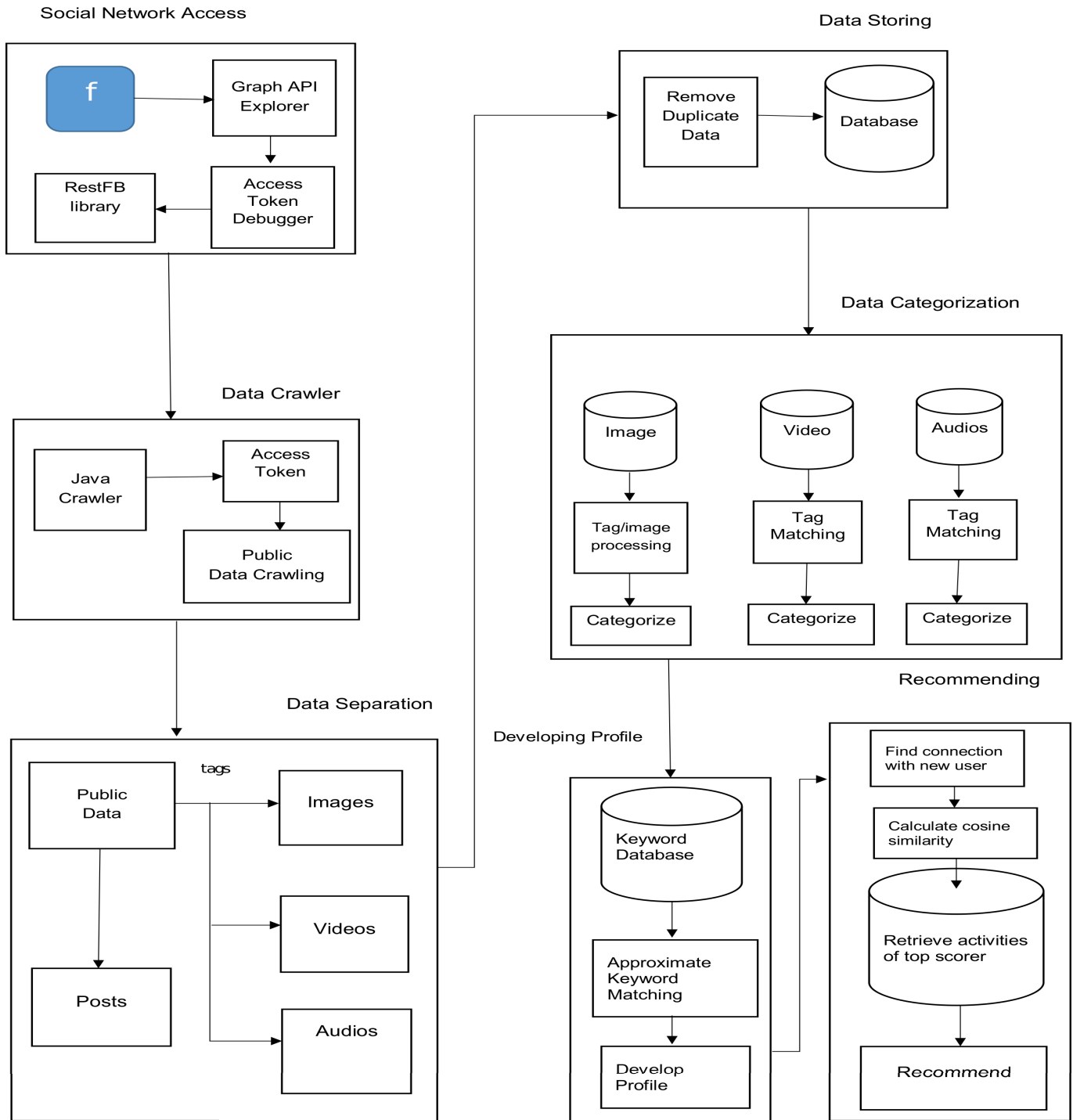


Fig. 1. System architecture

CSV file. Then load the CSV file into HBase by map reducing through bulk load method.

1) *Data Crawling Module:* Users can modify their privacy setting and Social network ensures several levels of information hiding; by default, users can only access private information of other users belonging to their friendship network, while friend list pages are publicly accessible. To maintain this status, Social network implements several rules, some behavioral

terms which prohibits data mining, but the friend list can be dispatched through a script which asynchronously fills the Web page, preventing naive techniques of data extraction.

Companies providing social network services like Social network, build their fortune on behavioral and targeted advertising, exploiting the huge amount of information they own about users and their activity to show them normalized ads, to increase visibility and earnings of advertised

companies. This is why they are loath to share information about users and the usage of their network. Moreover, several questions related to user's privacy are abducted. The working algorithm is given below.

Algorithm 1 : Crawl Data

Input : User's access token

Require : Write data into a CSV file

Begin

call Graph API

call RestFB API

accesstoken = "put token here";

client ← *accesstoken*

user = "me";

endpoint = "feed";

u.csv ← write(*user.get(data), endpoint*);

End

Here we first collect user's access token through Graph API and store it in a variable. And after that we pull user's data through Rest API. Here we need an end point to crawl data and we use "feed". As we are crawling data through access token we keep user type as "me". We write this data in a CSV file simultaneously.

B. Data Storing Module

In Data storing module, there are two parts. One is keyword extraction another is storing. We extracted keyword from status by an XML based POS(parts of speech) tagger. We identified noun, verb, and adjective through this tagger. The keyword extraction algorithm is given below.

Algorithm 2 : Keyword Extraction

Input : Sentences and list of word

Require : Find the keyword

Begin

Load xml file;

Call SAX parser & parse the loaded xml file;

for each independent word **do**

SAXparser.parse (file, "word");

if true **then**

return(token);

else

continue;

end if

end for

remove("\\s", token);

write(token);

End

Here we extract keyword based on noun, verb, and adjective from a sentence. To extract this we use an XML based POS tagger named Word.xml. We parse a list of the word through SAX XML parser and if we found match we return the token from the XML file. Then we remove the symbols(<>) from the token and store it. Keywords are also stored in the database for future communication. We analyze video by converting video files into frames. Then we calculate each pixel to measure amount of red, green and blue color. In the second part we stored our data separately in HBase after removing duplicate data if there exists any. It makes

our data more reliable. Along with crawl data, this module also handles storage of important information for retrieval purpose. The data storage algorithm in HBase is given below.

Algorithm 3 : Store Data

Input : Crawled data (CSV file)

Require : Store the data

Begin

Create table through HBase shell name as Data, having field Name, Story type, Story, Status, ID, Time, Keyword, URL. Exit from shell.

Copy CSV file from local to HBase.

Copy CSV file from HBase to Hadoop.

Call Bulk-Load method of Hadoop.

End

Here we first store our data in a CSV file to make our data more reliable. Then we store the file in Hadoop HBase by Bulk-load method. The bulk-load method uses the map-reduce algorithm which makes our data more reliable. There are columns like 'name', 'story type', 'story', 'status', 'id', 'time', 'keyword', 'url', etc. Under 'keyword' column there is 3 sub column: 'noun', 'verb', 'adjective'. So we first create our table with desired column family and column qualifier. Then we move our CSV file into Hadoop and call bulk load method to put all data into the table from the CSV file.

C. Data Separation Module

The data what we have crawled includes all type of data like images, videos, audios, posts, links both in English and Bangla; in a word everything. So before we store this data we have to separate this data and this separation is done based on tags. We also store this tags for the final data processing. The Data Separation algorithm is given below.

Algorithm 4 : Data Separation

Input : Crawled data

Require : Separation

Begin

Column family: status;

Column family: video;

Column family: image;

Column family: audio;

i = 0;

while *tag*[*i*] ≠ null **do**

if *tag*[*i*] == \status" **then**

status ← *content*[*i*];

else

if *tag*[*i*] == \video" **then**

video ← *content*[*i*];

else

if *tag*[*i*] == \image" **then**

image ← *content*[*i*];

else

if *tag*[*i*] == \audio" **then**

audio ← *content*[*i*];

end if

end if

end if

end if

i ← *i* + 1;

end while
End

Here we first create 4 column families: status,image, video, audio. Then we check tag type of a user's status and contents and according to the tags we keep keep status or contents in our desired column family.

D. Data Analysis Module

In Data Analysis module, we analyze categorized images, videos, based on tags and running further processing. There is two section. Image analysis and video analysis.

For image files We apply image processing to find out the number of people in images. We use OpenCV library and apply frontal face detection XML file(haarcascade) to count the number of people. We also apply OpenCV library to find out the length, duration, speed, total frame number, average height and width of frames etc. This process is beneficiary for recommendation module and to develop a specific short profile for the users. The algorithm is given below.

Algorithm 5 : Count People from Image

Input :User's image

Require : Number of people present in the images

Begin

facecascade ← CascadeClassifier ('haarcascade.xml');

imgcount = 0, *total* = 0;

while *name* == *user* and *url*[*i*] ≠ null **do**

imgcount ← *imgcount* + 1;

img ← *url*[*i*];

Mat src ← (*file*)*img*;

facetedetection ← face cascade.detect(*src*);

face ← *facetedetection.length*();

total ← *total* + *length*;

i ← *i* + 1;

end while

avg ← *total*/*imgcount*;

End

Fig. 2 shows an example of frontal face detection which helps us to determine the number of people present in the image uploaded by user. And based on its result we consider how a user likes to move. Does he likes to move with his friends most or not. and make an average for whole file. We also calculate frame speed, duration, height and width of the videos and for this we use some built in method of OpenCV(*Cap_Prop_**). The algorithm is given below.

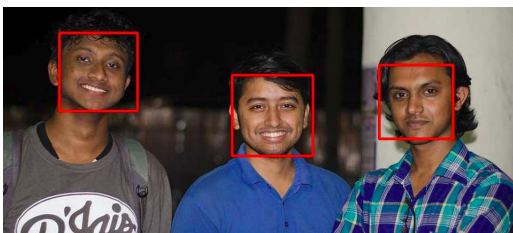


Fig. 2. An example of frontal face detection

TABLE I. AN EXAMPLE OF MEASURED VIDEO PROPERTIES

User	FPS	Frame no	H	W	R(%)	G(%)	B(%)
Rajib	17.9	677	420	420	38.2	32.5	29.3
Niloy	30	909	240	240	36.2	33.3	30.4
Fahim	30	909	240	240	36.2	33.3	30.4
Abir	25.05	474	352	352	36.2	32.4	31.4
Jawad	14.22	574	400	400	35.6	34.2	30.2

Algorithm 6 : Video Analysis

Input :User's video

Require : Properties

Begin

while *name* == *user* and *video*[*i*] ≠ null **do**

VideoCapturecapture ← *path*;

while *capture* is open **do**

fps ← *capture.videoio*, *Cap_Prop_FPS*;

number ← *capture.videoio*, *Cap_Prop_Frame_Count*;

duration ← *number*/*fps*;

height ← *capture.videoio*, *Cap_Prop_Frame_Height*;

width ← *capture.videoio*, *Cap_Prop_Frame_width*;

end while

initialize a 2D matrix;

counter = 0, *red* = 0, *green* = 0, *blue* = 0;

for *ilwidth* **do**

for *jlheight* **do**

rgb[] ← *getPixel*(*capture*, *i*, *j*)

red ← *red* + *rgb*[0];

green ← *green* + *rgb*[1];

blue ← *blue* + *rgb*[2];

end for

end for

total ← *red* + *green* + *blue*;

avgred ← *red*/*total*;

avggreen ← *green*/*total*;

avgblue ← *blue*/*total*;

end while

End

Table I shows an example of measured video properties from user video files. We consider the average value here. Here 'H' means frame height, 'W' means frame width, 'R' means red color, 'G' means green color, 'B' means blue color.

E. Profile Module

We have stored a keyword data-set and that data-set is used for matching. The keywords will be matched with the categorized data-set. When we will found more than one keyword in one user's data-set we will assume that user into a predefined category and that will help to develop a profile for the user and this task will be done under Develop Profile module. The working algorithm is given below.

Algorithm 7 : Profile Development

Input :User name and keyword list

Require : Select the desired data table

Begin

apply single column value filter for the user;

while *keywordlist* ≠ null **do**

apply single column value filter for the proper keyword;

initialize filter list;

filterlistproperty ← MUST PASS ALL;

```

filterlist ← single column value filter;
scan (filterlist) ← table
if result ≠ null then
    write(category);
else
    go back to the beginning of while ;
end if
end while
End

```

Here we filter out the user and keyword through single column value filter which is a special filter in HBase. Then we add this filters into a filter list which must have to pass both filters and then scan it against our table. The profile of a user depends on the return value of the scanned result.

F. Recommendation Module

If a new user joins in a social network we want to recommend movies, travel places, music, or story books for him/her. In the recommend module, we do this two different way. Considering (i) status and comments (ii) image and videos. Here we first normalize user profile and convert that into vector plane. Then we calculate the score based on the cosine similarity between selected user and rest of the user simultaneously.

We first analyze user's profile based on status and posts and run Cosine Similarity to find out best match among other users. To find cosine similarity we first normalize users profile and convert it into vector plane. Then we check cosine similarity between user and other user and generate a score between 0 and 1. And based on this score we tried to show top five matched user in a table.

Secondly we consider Images and video uploaded in user's profile. We categorize videos into three types based on the tags: funny, musical and sporty. Then we process videos and find out its total frame number, length, height, width, speed and RGB properties and make average of them. Then we check cosine similarity again and based on top score we generate a second table and this time instead of status and image we consider only image and video. If we find same user in this two table then we recommend user the activities of those users. If no match is found then we suggest top users activity only. The algorithm is given below.

Algorithm 8 : Recommend User

Input :User name and keyword list

Require : Select the desired data table

```

Begin
if selecteduser ≠ null then
    scan ← user;
    vector ← (Vector)userprofile;
    filterlist ← (table.user ≠ selecteduser);
    i ← 0;
    while filterlist(i) ≠ null do
        listA ← CosineSimilarity (user, filterlist(i));
        listB ← Cosinesimilarity(file(user),
file(filterlist(i)));
        sort(listA);
        sort(listB);
        listC ←duplicate of listAandlistB;

```

TABLE II. MEASURING COSINE SIMILARITY BASED ON STATUS AND COMMENT

N	H	S	E	T	M	M	F	S	S
a	a	a	m	o	u	o	o	p	c
m	p	d	o	u	s	v	o	o	o
e	p	t	r	i	i	d	r	r	r
	y		i	i	c	e	i	t	e
			o	s			e	y	
			n	t					

Ratul	0	1	0	1	1	1	0	1	-
Fahim	1	1	0	1	1	1	0	0	0.79
Rajib	1	1	1	1	1	0	1	1	0.67
Kibria	0	0	0	0	1	1	1	1	0.67
Abrar	0	0	0	1	0	0	0	1	0.63
Riad	0	0	0	0	1	0	0	1	0.63

TABLE III. MEASURING COSINE SIMILARITY BASED ON IMAGE AND VIDEO

N	F	M	S	U	U	U	U	S
a	u	u	p	s	s	s		s
m	n	s	o	e	e	e	e
e	n	i	r	r	r	r		r
	y	c	t	l	2	3		N
								e

Ratul	1	1	0	1	0	1	0	0	-
Fahim	1	1	0	1	0	1	0	0	0.99
Shajal	1	0	0	1	0	0	0	0	0.82
Abir	1	1	1	1	0	0	0	0	0.82
Dip	0	1	0	1	0	0	0	0	0.71
Tarek	0	0	1	1	0	0	0	0	0.63

```

i ← i + 1;
end while
if listC ≠ empty then
    showactivities(listC);
else
    showactivities(listA(0));
    showactivities(listB(0));
end if
end if
End
function COSINESIMILARITY((A[], B[]))
for i < A.length do
    dotproduct ← dotproduct + (A[i] * B[i]);
    normA ← normA + (A[i] * A[i]);
    normB ← normB + (B[i] * B[i]);
end for
result ← sqrt(normA) * sqrt(normB);
return (dotproduct/result)
end function

```

Here we first scan user profile and convert into vector plane. Then we filter out all users except recommending user. Then we run cosine similarity based on status comments and image, videos and keep the result in two different list. Based on score we find out same users from two list and keep them another list and suggest activities of this users to the recommending user.

Table II shows an example of cosine similarity measure procedure. Here we calculate cosine similarity of a user (Ratul) with respect to five other users. Here We consider only user's status and comments. And Table III shows cosine similarity based on user's images and videos.

G. Crawling and Information Retrieval in Bangla

Finding the relevant keywords from the Bangla text database has significantly different characteristics than the

same for English text database. In Bangla, there are so many variations of words. By just adding some postfixes, many different words can be formed. But these varied words have a similar meaning. So unless any mechanism is adopted, the varied words will be considered as distinct words. But as all the words have similar meaning, so all these words are relevant to a query with any of the words. Otherwise, queries with these different words will give different relevance value, which will degrade the retrieval efficiency. For this reason, it is very much important to find the root of the varied words having a similar meaning. These root words are used everywhere instead of all the varied words to keep necessary information for calculating relevance with the query. So it is absolutely necessary to find the roots of the words from the variations of the words by doing the morphological analysis for efficient information retrieval. But in English, there is a little variation of words. So it is not necessary to find the root of the words by doing the similar analysis.

On the other hand, there are many synonyms of words exists in Bangla. That means there are different words having different roots and the same meaning. So an efficient technique is required to manage the synonyms for efficient information retrieval. But if they are not managed in an efficient way then the system will treat all the synonyms of the same meaning as distinct words. This will degrade the efficiency of the information retrieval system.

Existing Bangla text database contains both Unicode and non-Unicode texts. It is difficult to search uniformly the database with both the type of text. But the required information may be found in any type of text. So it is very necessary to make a mechanism to handle both of the types of text uniformly.

H. Storage of Keyword Information into HBase

Keywords are used for different purposes. They are used to determine the data-set which are related to the analysis purposes. Keywords are also used to string matching. They are stored into the HBase by a column keyword. And this keyword column is sub divided into three sub-column: keyword: noun, keyword: verb, keyword: adjective. This three sub-columns are under keyword column family. Counting the frequency of the keyword in the data-set we find the strength of the keyword. The UserID, Public Post and No of String matched fields of the Data table represent UserID of public Post, Title, and number of String present in that data-set. In occurrence table, the field Keyword and No of the string matched is used to represent in how many posts a keyword occurs.

IV. EXPERIMENTAL RESULT

We crawled data directly from the social network with the help of access token provided by the user. We wrote it in a CSV (comma separated value) file first. Due to unstructured type of posts we found some bad lines. We also found some uncategorized character emerged from emoticon most probably. So we have to remove to run reliable analysis on the stored data. In this way we managed about 65 CSV files and after that, we merged all to a single CSV file by running command in the Linux terminal. It is also noticed that due to merging we lost some data. We tried several time but the

TABLE IV. CORRECTNESS (%) OF DATA CRAWLING

No of posts crawled	Bad Lines	Line removed for uncategorized character	Data lost for merging CSV files	Processed data found	Correctness (%)
10373	831	373	127	9042	87.17

TABLE V. CORRECTNESS OF DATA ANALYSIS BASED ON POSTS AND COMMENTS

No	Language	No.of post crawled	No.of comments crawled	No. of posts and comments	Match found	Correct (%)
1	English	3645	448	39	3412	83.36
2	Bangla	4390	559	183	3121	63.06

result is same and the reason behind it is unknown. In Table IV, we have tried to show the correctness of data crawling of our system.

We have considered posts and comments both in Bangla and English for the analysis. In this sense it is also a bilingual analysis framework. We used a bilingual dictionary for this task which has helped us to find out keywords. The more the words in dictionary the more it shows the accuracy. We used an XML file as dictionary. We stored about one lakh word with its property whether it is noun, verb, adjective, or adverb. However, we did not consider the all type of structure of sentences. In Table V, we showed the correctness of our data analysis based on posts and comments.

We have analyzed images and videos through OpenCV Java library. We tried to count the number of people presents in the images and videos and for that we have used Haar Classifier of OpenCV. It is a classifier which helps to detect frontal face of a person. We have counted the number of exists people through frontal face detection process. The result is not always accurate but reliable on average. Table VI shows the amount of experimental data as well as images and videos we have considered in this process and it's accuracy.

A. Performance of the Whole Framework

To calculate the performance of the whole system we have first calculated the performance of each module separately. Then combined all the result systematically. We have considered total 9042 posts and comments. The overall performance is showed in Fig. 3 and 4.

Where Fig. 3 shows the performance based on posts and comments, Fig. 4 shows based on person detected in images and videos.

V. CONCLUSION

The number of users in social networks has increased rapidly in last few years that makes social networks a great source of information. The data of these social networks are heterogeneous in nature as data in these social networks are

TABLE VI. CORRECTNESS OF DATA ANALYSIS BASED ON IMAGES AND VIDEOS

No.	Data type	No. of file	Total person present	Detected person	Correctness (%)
1	Image	325	912	698	76.54
2	Video	33	27	21	77.78

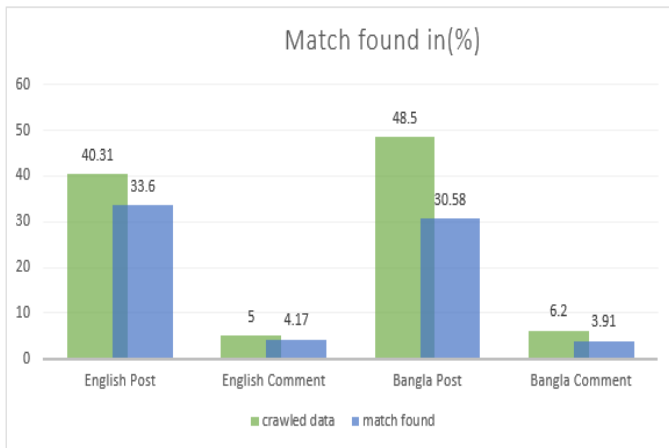


Fig. 3. Performance Measurement (Status & Comments)

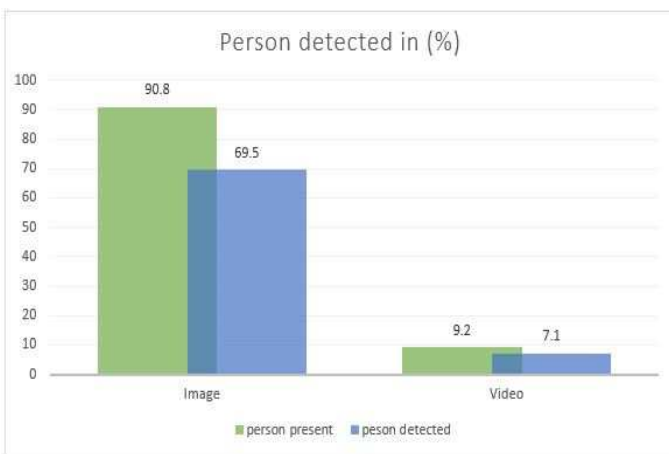


Fig. 4. Performance measurement (person detection)

of different forms such as text, videos, images etc. Proper analysis of these data can make the decision making tasks of the people and the organizations easier. Considering this fact, in this paper, we developed a heterogeneous data analysis framework to understand the users of social media, their

interests, activities etc and based on these information of the users we generate recommendation for them. Our developed system can categorize the users based on their activities and can develop a concise profile of the users effectively. In future, we plan to analyze the performance of our system under large volume of heterogeneous data. In addition, we want to develop methods so that the system can work in multilingual domain.

REFERENCES

- [1] A. Mislove, M. Marcon, K. Gummadi, P. Druschel and B. B. Bhattacharjee, Measurement and Analysis of Online Social Networks, IMC '07 Proceedings of the 7th ACM SIGCOMM Conference on Internet Measurement, ACM, 2007, pp 29-42.
- [2] M. Maia, J. Almeida and V. Almeida: Identifying User Behavior in Online Social Networks, SocialNets '08 1st Workshop on Social Network Systems, 2008, pp: 1-6.
- [3] F. Benevenuto, T. Rodrigues, M. Cha and V. Almeida: Characterizing User Behavior in Online Social Networks, IMC '09 9th ACM SIGCOMM conference on Internet measurement, ACM 2009, pp 49-62.
- [4] J. Thomas, L. Sael: Overview of Integrative Analysis Methods for Heterogeneous Data, 2015 International Conference on Big Data and Smart Computing (BIGCOMP), 2015, pp: 266-270.
- [5] P. Dewan, P. Kumaraguru, Towards Automatic Real Time Identification of Malicious Posts on Facebook, 2015 13th Annual Conference on Privacy, Security and Trust (PST), 2015, pp: 85-92.
- [6] A. Farasat, G. Gross and R. Nagi, Alexander G. Nikolaev: Social Network Analysis with Data Fusion, IEEE Transactions on Computational Social Systems, 2016, Vol 3(2), pp 88-99.
- [7] A. Perer, B. Shneiderman: Balancing Systematic and Flexible Exploration of Social Networks, IEEE Transactions on Visualization and Computer Graphics, 2006, Vol 12(5), pp: 693-700.
- [8] S. Catanese, P. De Meo, E. Ferrara, G. Fiumara, A. Provetti: Crawling Facebook for Social Network Analysis Purposes, WIMS '11 Proceedings of the International Conference on Web Intelligence, Mining and Semantics, 2011, Article no: 52.
- [9] C. Wilson, B. Boe, A. Sala, K.P.N. Puttaswamy, B.Y. Zaho: User Interactions in Social Networks and their Implications, EuroSys '09 Proceedings of the 4th ACM European conference on Computer systems, ACM, 2009, Vol 2 pp: 205-218.
- [10] D. Chau, S. Pandit, S. Wang and C. Faloutsos: Parallel Crawling for Online Social Networks, WWW '07 Proceedings of the 16th international conference on World Wide Web, 2007, pp: 1283-1284.
- [11] M. Gjoka, M. Kurant, C. Butts, A. Markopoulou: Walking in Facebook: A Case Study of Unbiased Sampling of OSNs, 2010 Proceedings IEEE INFOCOM, 2010, pp: 2498-2506.

Energy Efficient Camera Solution for Video Surveillance

Misbah Ahmad¹, Imran Ahmed², Kaleem Ullah³, Iqbal Khan⁴, Ayesha Khattak⁵, Awais Adnan⁶
Center of Excellence in Information Technology
Institute of Management Sciences (IMSciences) Hayatabad, Peshawar (Pakistan)

Abstract—Video surveillance is growing rapidly, new problems and issues are also coming into view which needs serious and urgent attention. Video surveillance system requires a beneficial energy efficient camera solution. In this paper, a single overhead camera solution is introduced which overcomes the problems existing in various frontal and overhead based surveillance systems. This will increase the efficiency and accuracy of surveillance system i.e. frontal and overhead. In this paper, two energy efficient overhead camera models are presented. The first model consists of a single overhead camera with a wide angle lens which covers a wide field of view addresses problems present in the traditional surveillance system. The second model, presents a single smart centralized overhead camera which controls various frontal based cameras. Several factors associated with camera models such as field of view, focal length and distortion are also discussed. Impact of the surveillance cameras are finally discussed which shows that a single energy efficient overhead camera surveillance system can solves many problems present in traditional surveillance system like power consumption, storage, time, human resource and installation cost and small coverage area.

Keywords—Energy efficient; video surveillance; overhead camera

I. INTRODUCTION

Nowadays in computer vision, one of the active, attractive and most important research area in video surveillance. The estimated urban population in 2030 will be round about 5 billion which is 60% of the total world population [1]. With this significant increase in the population, people might suffer from a series of security and privacy threats. Various government organizations are spending billions of dollars every year on domestic security around the globe. The sole purpose of spending this huge amounts of the money is to enhance the surveillance systems. Further more, with increasing trend of camera installation at both public and private places, a huge amount of data and storage are also required.

The process of monitoring certain objects/scene called surveillance. There are basically three types of video surveillance i.e manual, semi-autonomous and fully-autonomous. One of the widely used video surveillance type is manual, where a video content is analyzed by a human operator. While Semi-autonomous video surveillance required significant human intervention along with video processing (e.g simple motion detection). In contrast the fully-autonomous video surveillance system, has no human intervention at all. The input video sequence is taken and high-level decision-making tasks are performed including abnormal event detection and gesture recognition [2]. With an increase in urbanization, a rising economy and social transformation people have started moving

from rural areas to cities, which results in further increase of cities population.

Information technology has a significant impact on human life. Information and communication are highly deployed resource in our daily lives. For security purposes, various surveillance cameras (including sensors, smart cameras) are installed all over the place in the cities (e.g banks, shopping malls, airports and streets etc). These installed cameras capture a large number of videos and images which are used for various surveillance purposes. Some of these videos may also pose a threat to the privacy of people. These surveillance systems require human operators for constant monitoring which means that the effectiveness and response of these surveillance systems are highly dependent on fully vigilant human monitoring capabilities. Furthermore, the area under surveillance and the total number of cameras installed at a particular location is also limited by the human resource availability. The long duration of video monitoring by the human operator is also impractical and unfeasible. Some of under develop countries also suffering from energy crises (electricity), therefore in such circumstances continuous supply of electricity to surveillance system is difficult. So, in this paper, we present an energy efficient single camera solution that can be operated on less amount of power requirement by a small number of human operators.

Single Overhead Camera plays a vital role in overcoming the problems present in both traditional frontal and overhead based surveillance system. In this paper, an energy efficient camera solution is presented which helps to overcome certain issues like camera installation cost, power consumption, human resource, occlusion handling and privacy. Energy Efficient camera solution has gained a lot of attention in the recent years in many applications, not limited to traditional surveillance system, but includes developing fields such as elderly care, entertainment or home automation. The developed idea is energy efficient and affordable solution which improves, security and video surveillance. The single overhead based camera solution can benefit people and the city in a variety of aspects: energy, environment, industry, living, and services.

The main contribution of this work is to propose an energy efficient camera model, which can be further expended to control other surveillance cameras. Furthermore it is discussed, how this model can improve the existing surveillance system and how it can be applied in the privacy protection system. Lastly, the impact and factors of the developed energy efficient overhead based camera model on the surveillance system is also discussed. The remainder of the paper is organized as follows: In Section II we summarize the related work, in

Section III we presented the developed camera models while in Section IV we discuss different factors and impacts of presented models while Section V concludes the paper.

II. RELATED WORK

In video surveillance a variety of work has been done in last few decades based on frontal based camera system. Mikolajczyk et al. [3] described the method for detecting human in a single image which can detect full body as well as close up views in presence of clutter and occlusion. MIT pedestrian data set is used for training and testing. Yeh et al. [4] proposed a dual cooperative camera system for frontal surveillance (Fig. 1). Two cameras have been used correctly tracking the target object. The two cooperative cameras were able to correctly analyze the human body shape while the other predict the motion, position and height of human body. The experimental results shows that proposed algorithm performed well considering clear close up views for both multiple and single object.

Natarajan et al. [5] highlighted several issues in existing frontal based surveillance systems. In this survey they focused on Multi-Camera Coordination and Control (MC3) architectures and the functionalities for both centralized and distributed camera architecture. Bialkowski et al. [6] developed a person re-identification method based on color and texture models. A new challenging multicamera surveillance database was developed. They captured indoor video sequence with people in different poses. Chua et al. [7] studied out the unusual behaviour of a person in surveillance video sequence. They presented vision-based fall detection technique for human. Due to the property of human shape that varies from different camera angles instead of conventional ellipse or bounding box techniques. They focused on three points to represent a person shape. The technique is based on human shape. Cohen et al. [8] proposed an overhead based person recognition system. They considered top view images of the persons. Therefore Dataset of 12 individuals (Low quality images) each having 60 frames of multiple poses like sitting, standing, different rotations and translations were used. A Smart conference room (constrained environment) was considered for this purpose where cameras were mounted on the ceiling so that it cover the entire room. Ahmed et al. [9] proposed a new feature based algorithm for detecting person from extreme position by using an overhead camera in industrial environment. Three type of appearance viewed were observed i.e. direct under the camera, the diagonal view and when person moves away from camera. SCOVIS, a real-world industrial dataset was used. Another overhead based person detection work has also been done by [10].

Nakatani et al. [12] proposed an image based person identification method from top-View. The person's area in a captured image was identified first by using background subtraction. The proposed method was valid only in the situation where people stop in front of a door. Pizzo et al. [13] presented a method for counting people using zenithal mounted cameras which were able to provide accurate counting under different realistic conditions. Real world environments were adopted where people counting was characterized by natural illumination (OUT-DOOR) or where the source of illumination was very artificial (INDOOR). Garca et al. [14] used a single fixed camera for detecting people from overhead view and tried

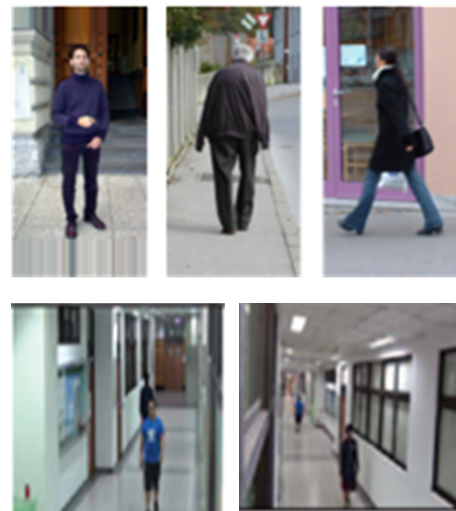


Fig. 1. Some of the images captured from frontal surveillance cameras. [4], [11]

to solve the problem of occlusion. An efficient and reliable feature descriptor for human detection in a top-view depth image was presented by [15] (see Fig. 2).

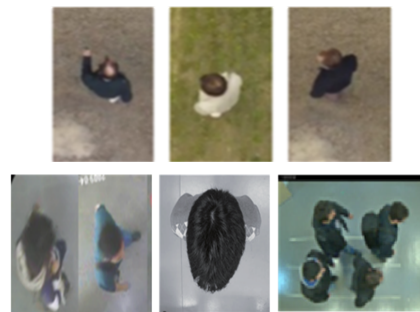


Fig. 2. Some of the images captured from Overhead surveillance cameras [16] [17] [18]

Carletti et al. [19], presented a top view method based on depth map images for person detection. The depth images were captured using single sensor mounted in zenithal position in both indoor and outdoor environments. SIFT-FAST algorithm for counting people in a crowded environment was proposed by [20]. They used traditional CCTV video sequences for detection purposes. To address the variation in human visual appearance Paul Blondel et al. [16] considered a multi-view camera images. The Multiview images were captured from both frontal, azimuthal and overhead view. Liu et al. [21] proposed a new hybrid-overlapping alliance of cameras for the purpose of tracking both overlapping and non-overlapping. They focused on depth images instead of RGB. Burbano et al. [22] focused on embedded smart camera network to detect and track people from overhead view. Tseng [23] proposed a real-time surveillance system comprised of multiple depth cameras located indoor for person detection and tracking.

III. CONCEPTUAL CAMERA MODELS

In this section, we presented an overhead based single energy efficient camera models. These models are able to

perform well in several real-life scenarios as discussed in the introduction. It also helps to overcome the occlusion problems, in traditional frontal surveillance system, as can be shown in Fig. 3. In the first row of Fig. 3 it can be clearly seen that in different real-life environments the camera recording contained different occlusion problems either by some other object (heavy machinery, walls, or other person) or sometimes due to self-occlusion. The overhead camera can overcome the occlusion problem as seen in the second row of Fig. 3 in much better way. It can be seen that single overhead camera easily overcome the problem of occlusion in such scenarios e.g person occluded by each other or by some heavy machinery. In this section different camera parameters including field of View (*FOV*), focal length of lens and distortion effect are also discussed briefly. Fig. 3 shows that in most of the cases the traditional frontal based camera surveillance system suffers from occlusion problem.

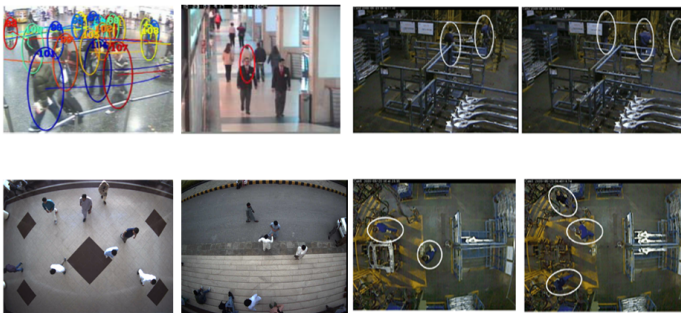


Fig. 3. In first Row images were captured by frontal camera that shows the issue of occlusion while in second row some of the images are shown that were captured by single overhead camera that solves the issue of occlusion. [10] [24]

A. Single Overhead Energy Efficient Camera Model

This paper introduce energy efficient single overhead camera solution that saves the power consumption issues of the surveillance system. The Single Overhead Based Energy Efficient Camera Model covers wide scene as shown in Fig.4 and solves the problem of occlusion. The Field of view (*FOV*) for the overhead camera has also been calculated as shown in Fig.4. Different Camera parameters including Focal Length and distortion caused by camera are also discussed in this section.

1) *Field of View vs. Height*: The field of view of overhead camera has been shown in below Fig. 4. It can be clearly seen in the image that *FOV* depends on camera installation height *h*, width *w* and length *l* of the scene. To calculate the field of view from the Fig. 4 the below equation can be considered.

$$FOV = 2 \tan^{-1} \frac{w}{h} \quad (1)$$

In equation 1 *h* is the height of camera from floor and *w* is the width of scene. The *FOV* is represented as θ . So that equation 1 can also be written as:

$$\theta = 2 \tan^{-1} \frac{w}{h} \quad (2)$$

From Fig. 4 θ can be calculated as:

$$\theta = 2\alpha \quad (3)$$

The equation 3 can be also be written as follows:

$$\alpha = \frac{\theta}{2} \quad (4)$$

By putting the value of θ in equation 4 we get;

$$\alpha = \tan^{-1} \frac{w}{h} \quad (5)$$

In case where θ or α and width *w* is given and camera height *h* is unknown, using equation 5 camera height can be calculated as:

$$h = \frac{w}{\tan \alpha} \quad (6)$$

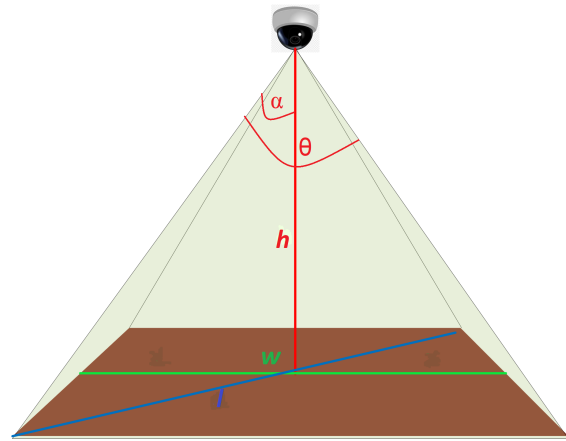


Fig. 4. The *FOV* of the overhead camera: *h* represents height, *w* represents width, *l* is the diagonal length of scene. While θ is the field of view *FOV*

2) *Using Focal Length to calculate FOV*: The coverage area or *FOV* of overhead camera can also be calculated using focal length of the lens. Basically focal length is the distance between the lens and the image sensor when the subject is in focus, usually camera comes with focal length (e.g. 28 mm, 50 mm, or 100 mm). In Fig. 5 the focal length of the sensor has been shown Fig. 5.

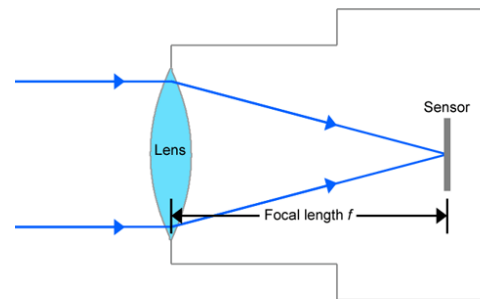


Fig. 5. Focal length of camera sensor.

To calculate the focal length of the installed camera Fig. 6 has been considered. In Fig. 6 h_s is the horizontal sensor dimension (number of horizontal pixels multiplied by the pixel

size) h is the height between installed camera position and floor while w is the width of the scene.

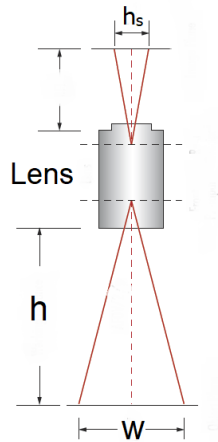


Fig. 6. The focal length of camera lens: h_s is the horizontal sensor dimension, h is the height between installed camera position and floor while w is the width of the scene.

The below equation 7 is calculated using above Fig. 6. In equation 7 h_s is the horizontal sensor dimension (number of horizontal pixels multiplied by the pixel size) and f is the focal length of the lens, both in millimeters; the w and h must be measured in the same unit system.

$$f = \frac{h_s \times h}{w} \quad (7)$$

By using the focal length information FOV' can also been calculated as shown in equation:

$$FOV' = 2 \tan^{-1} \frac{h}{2f} \quad (8)$$

where h is camera height and f is the focal length of camera.

In Fig. 4 it can be clearly seen that installed overhead camera provides larger FOV as compared to the traditional frontal based camera. The camera installation height can be adjusted according to the application requirement. In Fig. 7 the wide FOV of overhead images can be clearly seen. The overhead camera also helps to minimize the number of installed cameras at any location which needs wider view by adjusting camera installation height. As because the wide FOV , it covers the entire scene as shown in below Fig. 7. In Fig. 7 it can be clearly seen that how single overhead camera is used to cover the wide scene, which is covered by multiple frontal cameras as shown in Fig. 7.

B. Hybrid Camera Model Surveillance

This work is not limited up to just single camera model, but extends the conceptual solution to control multiple surveillance cameras. The one energy efficient overhead camera can be used as a centralized camera to handle surveillance in complex environments where we need frontal images i.e facial detection and recognition. As shown in Fig. 3, using overhead significantly solves the problem of occlusion, but at cost of two limitations i.e self occlusion (e.g. at middle of the image person torso

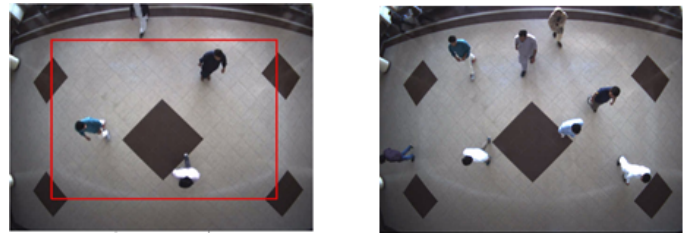


Fig. 7. Field of View of Single Overhead Camera. It can be seen that using single overhead camera at certain height provide better coverage of the wide scene.

is occluded with upper body part), another limitation of the single overhead camera model could be the clear visibility of facial images. While viewing a person from overhead view it could be difficult to capture frontal images.

To overcome these types of problems in a typical surveillance system a method is presented using a centralized camera which is further connected to others frontal cameras. So in that way where facial images or full person body is required the overhead camera enables the frontal camera to captures the video or images of the person.

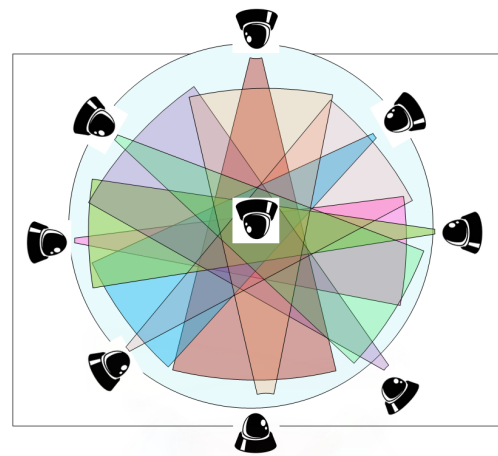


Fig. 8. Single Centralized Overhead conceptual camera Solution.

In Fig. 8 the conceptual solution of the Single Overhead Energy Efficient Camera Model is shown. It can be seen from the Fig. 8 that to cover the wide scene, eight different frontal based cameras are used while that scene can be easily cover by the one overhead camera. But in such a scenario, where the frontal images is necessary the extended conceptual model can be used to control other surveillance cameras. Like in Fig. 9 it can be seen that from F1 to F8 the frontal based cameras are installed while one overhead camera O is installed at center on the top of floor to control other cameras. When there is no human traffic all eight cameras will be at stand-by (not recording) mode. The particular camera will be activated by the overhead camera in case of motion at the particular location. In case if the person is coming towards F1 the overhead camera sends signal to F1 to switch on recording mode from the reset mode and start recording image or video at particular time.

Similarly if the person is moving towards F8 the overhead camera send back signal to F8 to captured the video at

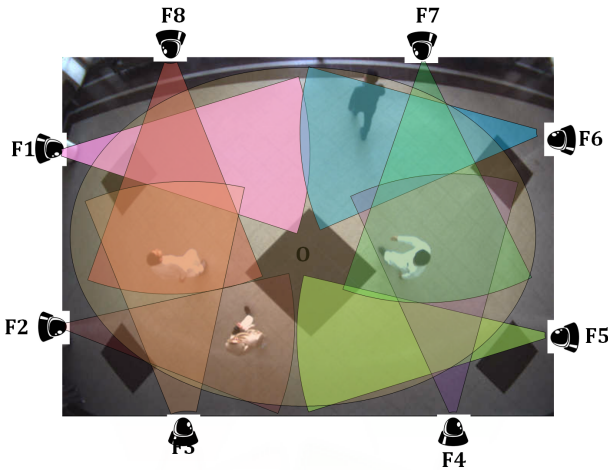


Fig. 9. Conceptual model of Single topview camera to control other frontal based. This Figure shows the conceptual model with other frontal based cameras. The *FOV* of eight different frontal cameras has been shown by shaded area which is small as compared to Overhead Camera *O*. It can be seen that how single overhead camera covers the wide scene which is covered by multiple frontal cameras. The topview camera can also be used with multiple frontal cameras.

that movement. In such a way without effecting the power, storage and time the overhead camera enables the frontal based cameras to captured the videos when needed. In Fig. 9, one centralized camera is use as a central camera so the other cameras will be at rest or stand by the state when not needed. Now this overhead camera model helps in facial expression recognition and suspicious activity controlling scenarios etc. To control other frontal based cameras we can enhance the model using sensors that detect motion or spatial information. This also helps to save power or energy during timings where person facial recognition is not necessary.

IV. FACTORS EFFECTING CONCEPTUAL CAMERA MODELS

To analyze the efficiency and effectiveness of the single overhead camera. The proposed solution provides an energy efficient camera solution for surveillance system, that can be operated on low power. So instead of reducing the resolution power of surveillance cameras, we can use single camera and record some good videos. In this section different factors have been analyzed e.g distortion, power consumption, storage, privacy issues, Human resource requirement and installation costs.

A. Distortion in Overhead Images

Overhead images provide a larger field of view *FOV* and solves the occlusion problems but it may suffer from image distortion. Moreover it might create problems for researchers to detect, count and track the person in overhead images accurately due to distortion. There are two types of distortions: optical and perspective. Both types result in some kind of deformation in images. Optical distortion is usually caused by the design of optical lens. Perspective distortion is due to the position of the camera relative to the subject. The overhead camera usually suffers from radial distortion as shown in Fig.

10. It can be seen, that straight lines in the left image and straight footpath edges in right image of Fig. 10 becomes radial due to the distortion.

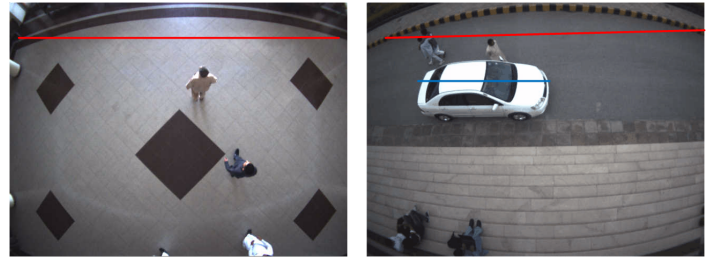


Fig. 10. Effect of distortion caused by wide angle overhead camera: The curve line at the top of both images can be seen due to radial distortion, which need to be straight.

To calculate the radial distortion for the above images. The parameters including x_d , y_d and r_d have been considered as shown in Fig. 11 r_d . In Fig. 11 r_d is the radial distance, x_d is horizontal distance and y_d is the vertical distance of the scene. It can be seen that the distortion effect in the image increases with increase in radial distance r_d . Due to the distortion effect square boxes in Fig. 11 looks like affine rectangles.

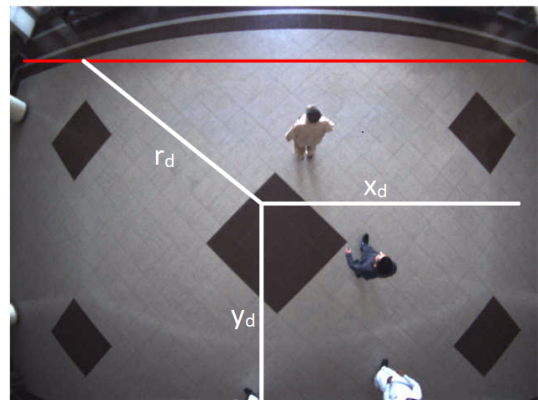


Fig. 11. Effect Radial distortion caused by overhead camera. The effect of distortion increases with increase in radial distance r_d .

The general formulae for calculating radial distortion using Fig. 11 is as follows. In equation 9 r_d is radial distance of distorted image from central points x_d and y_d . k is the distortion factor. By using the below equation the distorted image can be converted in to undistorted image.

$$r_u = r_d(1 + k_d^2) \quad (9)$$

B. Privacy Issues

With increasing use of surveillance technology, it somewhere reducing the privacy of human. The concept of surveillance privacy varies with cultures. In most of scenarios there is no need to monitor the person from their facial images or videos so in such cases, the overhead would be the better choice to monitor the public places just from an overhead view without violating the privacy of the people.

C. Power Consumption's

With the increasing rate demand and supply of video surveillance more cameras and sensors are required. These

installed surveillance cameras and sensors use a noticeable amount of power over a years' time i.e. energy for power, transmission and distribution of video or images data. According to [25] a single surveillance camera used up to 40 Watt of power per year. As a surveillance system is made up of multiple cameras or sensors, a recording device monitors and wires, etc. These energy consumption lead us to provide an energy efficient camera solution that overcomes these energy consumption's issues and provide some smart energy surveillance solution that can save energy consumption in many aspects and also prevent a blackout of power and failure of cameras and sensors. In Fig. 12 we have shown increase in the number of cameras increases the energy consumption rate in the surveillance system. As from the above discussion we have seen that using one overhead camera saves cost and energy consumptions.

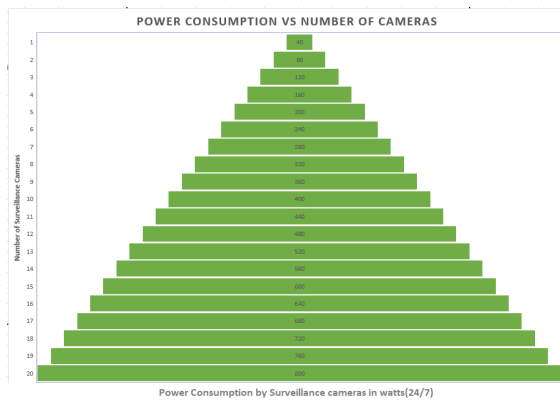


Fig. 12. The General Overview of Power Consumption per day increases with increase with the number of installed camera.

D. Data Storage

As discussed earlier in surveillance system with multiple cameras requires a large amount of storage space for recording videos and images. A single camera recording can occupy 25 to 50 GB of storage space per day. This storage space increases with increasing rate of video quality, camera stream, camera resolution, average frame rate, number of camera, per camera frame rate, per day recordings, number of desired days for storage and bandwidth etc. Similarly, the compression rate required to support the centralized storage, analysis and retrieval of an organization's growing mountain of video footage as shown in Fig. 13. After the power consumption, the second challenge is the storage, the latest HD model cameras occupied the space 25 Gb per day while the latest IP based camera used to HD cameras 10- 12 GB day (for the 2-megapixel camera). The storage capacity occupied by the surveillance cameras depends on the quality of the video. The storage capacity depends on video frame rate, resolution and compression rate. It also depends on the recorded video colour model which may be RGB, grey and Infrared. In Fig. 13 it can be clearly seen that how the storage increase with number of installing cameras.

E. Human Monitoring

Installing cameras and sensors are not enough for the video surveillance system. After installation, the videos are also

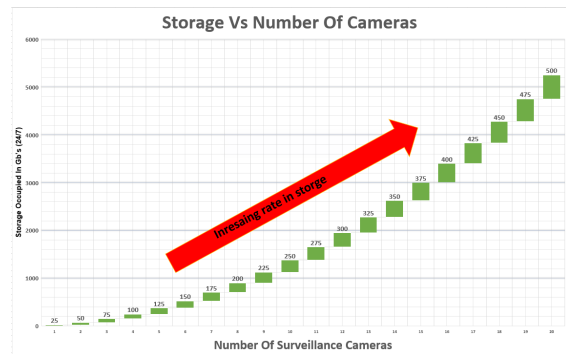


Fig. 13. Storage capacity in Gb's per day occupied by Surveillance cameras.

required to be monitored by human operators in vigilant way. Fig. 14 shows that the multiple camera footage which need proper and accurate monitoring. And as there is not a single camera in traditional surveillance system so that to properly monitor the number of cameras is also a hectic task.



Fig. 14. Footage of multiple surveillance cameras shows the difficulty of surveillance monitoring [6].

Also, this kind of monitoring is sometime restricted to a small area because of complex environments. Some times because there is a only single human operator who is responsible for monitoring of multiple cameras. The careless of the human operator may lead to security threats. Also instead of hiring multiple human operators for the surveillance system to monitor multiple cameras by installing one overhead camera, we can saves the human resource cost too.

F. Installation of Multiple Cameras

As with increasing rate of video surveillance instead of hiring multiple security officers for monitoring. Many organization prefer to install security cameras and sensors. Installation of multiple cameras and sensor is not easy, therefore instead of installing multiple cameras in this paper, we have presented a one camera solution that can saves the installation hectic and cost of multiple cameras by covering the wide scenes using overhead camera.

G. Overall Installation Cost

Now a days, technology able to capture of sharper and crisper IP video surveillance footages. But, such advanced technology comes at a cost particularly in terms of the investment in video surveillance storage. Apart from monitoring and power consumption, installation of multiple cameras is

also expensive. Sometimes it is very expensive for small organization to purchase cameras and other equipment needed for the surveillance system. It is not just a one-time expense but with the advancement in technology, it is the necessary need to keep upgrading it with time. In such scenarios installing a single overhead camera is affordable and effective solution. Camera installation also depends on coverage area, larger the coverage area more number of cameras are needed, security Needs (in high security or sensitive areas), External or Internal (for outdoor you need expensive water and weather proff cameras) Wired or Wireless and Monitored (including IP based cameras) Monitored or Monitored (is the human operator required for proper monitoring or not). As shown in Fig. 15 that how the installation cost of camera installation increases with number of installed cameras.

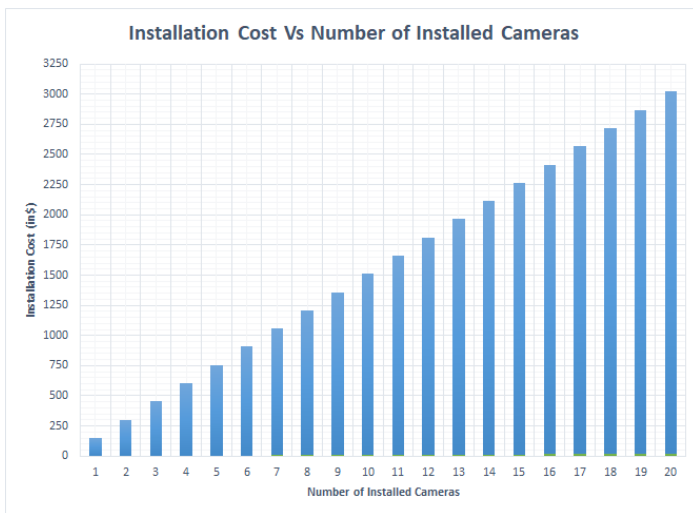


Fig. 15. The installation cost increases exponentially with increasing number of cameras.

V. CONCLUSION

In this paper, we discussed the different issues present in traditional surveillance systems. We presented a smart energy efficient single overhead based wide angle lens camera models. The presented models are smart in term of surveillance by covering the large field of view and solving the problem of occlusion. Furthermore, the single overhead based camera model is also used as a centralized camera to make a hybrid surveillance system by controlling frontal based cameras. It also solves the privacy issues in the different real-life environment. We have analyzed the installation cost and energy usage of multiple camera solutions and come up with the solution that installing an overhead camera will able to solve the above-discussed issues. In this paper we opened a new direction in which activity, suspicious motion, unusual activities, behaviours gait analysis etc can be done using overhead view in contrast to the frontal view. All type of techniques or methods that are developed in the frontal view can also be considered in overhead view. As all the time we don't need facial images, in such scenario we can also use the hybrid view model. Instead of camera calibration, we can use a hybrid model consisting of one overhead camera and required number of frontal cameras. We can also use the overhead camera as a motion detection. It can also be used as

an alerting signal for other frontal cameras. In short, we can use the overhead camera system as a facilitating system for a frontal view.

This paper sheds more light on the smart surveillance system solutions. In future, we will extend this work with smart sensor based surveillance system. We will also intend to implement the discussed models in future surveillance systems. We also use the discussed models for 3D modelling, image stitching, camera calibration and more ground-breaking research ideas.

VI. ACKNOWLEDGMENT

We are thankful to the Institute of Management Sciences and Higher Education Commission (HEC) Pakistan, funding for this research work via NRPU project under project number 5840/KPK/NRPU/RND/HEC/2016.

REFERENCES

- [1] UN, 2019 (accessed March 3, 2019), <https://www.un.org/development/desa/en/news/population/2018-revision-of-world-urbanization-prospects.html/>.
- [2] M. S. K. Mishra, F. JTMCOE, and K. Bhagat, "A survey on human motion detection and surveillance," *International Journal of Advanced Research in Electronics and Communication Engineering (IJARECE) Volume*, vol. 4, 2015.
- [3] K. Mikolajczyk, C. Schmid, and A. Zisserman, "Human detection based on a probabilistic assembly of robust part detectors," in *European Conference on Computer Vision*. Springer, 2004, pp. 69–82.
- [4] J.-S. Yeh, C.-C. Chang, T.-L. Chia, S.-Y. Chiang, and P.-S. Huang, "Cooperative dual camera surveillance system for real-time object searching and close-up viewing," in *Intelligent Green Building and Smart Grid (IGBSG), 2016 2nd International Conference on*. IEEE, 2016, pp. 1–5.
- [5] P. Natarajan, P. K. Atrey, and M. Kankanhalli, "Multi-camera coordination and control in surveillance systems: A survey," *ACM Transactions on Multimedia Computing, Communications, and Applications (TOMM)*, vol. 11, no. 4, p. 57, 2015.
- [6] A. Bialkowski, S. Denman, S. Sridharan, C. Fookes, and P. Lucey, "A database for person re-identification in multi-camera surveillance networks," in *Digital Image Computing Techniques and Applications (DICTA), 2012 International Conference on*. IEEE, 2012, pp. 1–8.
- [7] J.-L. Chua, Y. C. Chang, and W. K. Lim, "A simple vision-based fall detection technique for indoor video surveillance," *Signal, Image and Video Processing*, vol. 9, no. 3, pp. 623–633, 2015.
- [8] I. Cohen, A. Garg, and T. S. Huang, "Vision-based overhead view person recognition," in *Pattern Recognition, 2000. Proceedings. 15th International Conference on*, vol. 1. IEEE, 2000, pp. 1119–1124.
- [9] I. Ahmed and J. N. Carter, "A robust person detector for overhead views," in *Pattern Recognition (ICPR), 2012 21st International Conference on*. IEEE, 2012, pp. 1483–1486.
- [10] I. Ahmed and A. Adnan, "A robust algorithm for detecting people in overhead views," *Cluster Computing*, pp. 1–22, 2017.
- [11] N. Dalal and B. Triggs, "Histograms of oriented gradients for human detection," in *Computer Vision and Pattern Recognition, 2005. CVPR 2005. IEEE Computer Society Conference on*, vol. 1. IEEE, 2005, pp. 886–893.
- [12] R. Nakatani, D. Kouno, K. Shimada, and T. Endo, "A person identification method using a top-view head image from an overhead camera," *JACIII*, vol. 16, no. 6, pp. 696–703, 2012.
- [13] L. Del Pizzo, P. Foggia, A. Greco, G. Percannella, and M. Vento, "A versatile and effective method for counting people on either rgb or depth overhead cameras," in *Multimedia & Expo Workshops (ICMEW), 2015 IEEE International Conference on*. IEEE, 2015, pp. 1–6.

- [14] J. García, A. Gardel, I. Bravo, J. L. Lázaro, M. Martínez, and D. Rodríguez, "Directional people counter based on head tracking," *IEEE Transactions on Industrial Electronics*, vol. 60, no. 9, pp. 3991–4000, 2013.
- [15] T.-W. Choi, D.-H. Kim, and K.-H. Kim, "Human detection in top-view depth image," *Contemporary Engineering Sciences*, vol. 9, no. 11, pp. 547–552, 2016.
- [16] P. Blondel, A. Potelle, C. Pégard, and R. Lozano, "Human detection in uncluttered environments: From ground to uav view," in *Control Automation Robotics & Vision (ICARCV), 2014 13th International Conference on*. IEEE, 2014, pp. 76–81.
- [17] D. de Oliveira and M. Wehrmeister, "Using deep learning and low-cost rgb and thermal cameras to detect pedestrians in aerial images captured by multicopter uav," *Sensors*, vol. 18, no. 7, p. 2244, 2018.
- [18] Y. Jiang and J. Ma, "Combination features and models for human detection," in *Proceedings of the IEEE Conference on Computer Vision and Pattern Recognition*, 2015, pp. 240–248.
- [19] V. Carletti, L. Del Pizzo, G. Percannella, and M. Vento, "An efficient and effective method for people detection from top-view depth cameras," in *Advanced Video and Signal Based Surveillance (AVSS), 2017 14th IEEE International Conference on*. IEEE, 2017, pp. 1–6.
- [20] Z. Q. Al-Zaydi, D. L. Ndzi, M. L. Kamarudin, A. Zakaria, and A. Y. Shakaff, "A robust multimedia surveillance system for people counting," *Multimedia Tools and Applications*, vol. 76, no. 22, pp. 23 777–23 804, 2017.
- [21] A.-S. Liu, T.-W. Hsu, P.-H. Hsiao, Y.-C. Liu, and L.-C. Fu, "The manhunt network: People tracking in hybrid-overlapping under the vertical top-view depth camera networks," in *Advanced Robotics and Intelligent Systems (ARIS), 2016 International Conference on*. IEEE, 2016, pp. 1–6.
- [22] A. Burbano, S. Bouaziz, and M. Vasiliu, "3d-sensing distributed embedded system for people tracking and counting," in *2015 International Conference on Computational Science and Computational Intelligence (CSCI)*. IEEE, 2015, pp. 470–475.
- [23] T.-E. Tseng, A.-S. Liu, P.-H. Hsiao, C.-M. Huang, and L.-C. Fu, "Real-time people detection and tracking for indoor surveillance using multiple top-view depth cameras," in *2014 IEEE/RSJ International Conference on Intelligent Robots and Systems*. IEEE, 2014, pp. 4077–4082.
- [24] S. Tang, B. Andres, M. Andriluka, and B. Schiele, "Multi-person tracking by multicut and deep matching," in *European Conference on Computer Vision*. Springer, 2016, pp. 100–111.
- [25] Reolink, 2019 (accessed February 3, 2019), <https://reolink.com/cctv-ip-security-camera-power-consumption/>.

A Gender-neutral Approach to Detect Early Alzheimer's Disease Applying a Three-layer NN

Shithi Maitra¹, Tonmoy Hossain², Abdullah Al-Sakin³,
Sheikh Inzamamuzzaman⁴, Md. Mamun Or Rashid⁵, Syeda Shabnam Hasan⁶
Department of Computer Science and Engineering
Ahsanullah University of Science and Technology
Dhaka, Bangladesh

Abstract—Early diagnosis of the neurodegenerative, irreversible disease Alzheimer's is crucial for effective disease management. Dementia from Alzheimer's is an agglomerated result of complex criteria taking roots at both medical, social, educational backgrounds. There being multiple predictive features for the mental state of a subject, machine learning methodologies are ideal for classification due to their extremely powerful feature-learning capabilities. This study primarily attempts to classify subjects as having or not having the early symptoms of the disease and on the sidelines, endeavors to detect if a subject has already transformed towards Alzheimer's. The research utilizes the OASIS (Open Access Series of Imaging Studies) longitudinal dataset which has a uniform distribution of demented, non-demented subjects and establishes the use of novel features such as socio-economic status and educational background for early detection of dementia, proven by performing exploratory data analysis. This research exploits three data-engineered versions of the OASIS dataset with one eliminating the incomplete cases, another one with synthetically imputed data and lastly, one that eliminates gender as a feature—eventually producing the best results and making the model a gender-neutral unique piece. The neural network applied is of three layers with two ReLU hidden layers and a third softmax classification layer. The best accuracy of 86.49% obtained on cross-validation set upon trained parameters is greater than traditional learning algorithms applied previously on the same data. Drilling down to two classes namely demented and non-demented, 100% accuracy has been remarkably achieved. Additionally, perfect recall and a precision of 0.8696 for the 'demented' class have been achieved. The significance of this work consists in endorsing educational, socio-economic factors as useful features and eliminating the gender-bias using a simple neural network model without the need for complete MRI tuples that can be compensated for using specialized imputation methods.

Keywords—Alzheimer's disease; dementia; exploratory data analysis; synthetically imputed data; socio-economic factors; specialized imputation

I. INTRODUCTION

Alzheimer's disease is a growing concern among the world's retired population. It is an irreversible, progressive, neurodegenerative brain disorder that gradually dismantles memory and reasoning skills and eventually, the ability to carry out the simplest of tasks. In 2015, there were approximately 29.8 million [1] people worldwide who had been diagnosed with Alzheimer's disease and the number is increasing day by day. This number is expected to be over 100 million by 2050 [2]. It most often affects about 6% of people 65 years' or older [3]. Furthermore, Alzheimer's disease, historically not

thought to be a normal part of aging, is now considered the most common form of dementia among elderly people which resulted in about 1.9 million deaths in 2015 [4]. Therefore, its socio-economic implications are enormous, carrying a major negative influence upon society and caregivers.

The National Institute of Neurological and Communicative Disorders and Stroke (NINCDS) and the Alzheimer's Disease and Related Disorders Association (ADRDA), now known as the Alzheimer's Association, have defined the most commonly used NINCDS-ADRDA Alzheimer's Criteria as definite, probable, possible and unlikely for diagnosis in 1984 [5]. Clinicians have long advocated early diagnosis i.e., at the possible and probable stages provided medications are frequently more effectual at the onset of the disease and drug-free interventions are also available to decelerate the atrophy of cerebral tissue. Furthermore, a demented state may well represent treatable and reversible medical conditions, other than early Alzheimer's in which case the earlier the actions, the better the results. Moreover, an early diagnosis allows the patient to carve out practicable medical and financial decisions while also potentially allowing caregivers to develop better support system for the affected [6]. More justifications endorsing the early detection include amplified opportunities to participate in clinical trials, additional time to record memories, improved safety etc.

Prognostically, Alzheimer's disease is diagnosed based on a person's medical history, narratives by relatives and behavioral observations. Neuropsychologically, tests such as the Mini-Mental State Examination (MMSE) are recognized to evaluate cognitive impairments indicative of a positive diagnosis of the disease [7]. Radiographically, Alzheimer's disease is characterized by the loss of neurons and synapses in the cerebral cortex and in certain subcortical regions [8]. The hippocampal atrophy, ventricle enlargement and cortex shrinkage are sensitive features of Alzheimer's disease. Therefore, doctors perform scans like Computed Tomography (CT), Magnetic Resonance Imaging (MRI), or Positron Emission Tomography (PET), to rule out other possible causes for the symptom. Analytically, this study shows years of education (EDUC) and Socio-Economic Status (SES) measured on a scale ranging from 1 to 5 as significant features in early detection of the disease. These perspectives justify MMSE, Clinical Dementia Rating (CDR), Estimated Total Intracranial Volume (eITV), Normalized Whole Brain Volume (nWBV), EDUC, SES as distinctive features characterizing Alzheimer's.

Due to the availability of OASIS longitudinal MRI data and machine-learning methodologies, one can measure the similarity of an individual's cortical atrophy with that of a representative Alzheimer's disease patient cohort. The recent bio-medical researches are gaining momentum using Neural Networks (NN). Neural Network models, consisting of multiple hidden layers having different activation units, are transcending traditional learning algorithms like Logistic Regression, Support Vector Machine etc in performance. Neural Networks are able to fit very complex functions with numerous independent variables as features. Such models can discover patterns spread across multiple dimensions upon refinement of its initial parameters through many epochs using the back-propagation algorithm. The derivatives calculated at each step of backpropagation indicates in which direction the parameters should be refined and a learning rate defines its magnitude. The weights represent the mapping from one layer to the other creating a layered, hierarchical architecture. The early hidden layers learn comparatively simpler features while the latter ones learn sophisticated features upon the previously learned simpler features.

In this paper, a simple three-layer Neural Network architecture has been trained using the OASIS longitudinal MRI dataset to classify among patients as having early Alzheimer's disease. Imputing data precluded the need for complete tuples making the best use of available data. The study introduces years of education and socio-economic status as two novel features while further nullifying gender as a feature in order to gain better performance measures.

The organization of this paper dictates the second section as presentations of related work, the third section as a narration of methodology, the fourth section as a tabulation of results and the final section as concluding remarks.

II. RELATED WORK

Artificially intelligent former and recent researches undertaken on detection of early or matured stage Alzheimer's can be categorized along three paradigms: detection applying machine learning on structured data, detection using convolutional neural networks on radiographs and detection using hybrid methods combining the former two. Detection of Early Alzheimer's poses a supervised classification problem, some literature on which are reviewed below.

A. Traditional Machine Learning Algorithms

Datta et al. [9] explored ML for classifying dementia using the University of California, Irvine's Alzheimer's Research Center's data. Six ML methods were applied to a database of 578 patients and controls. The neuropsychologists applied the Diagnostic and Statistical Manual of Mental Disorders-04 criteria to classify dementia status. The researchers extracted age, sex, job, education and responses of patients to questions from the Alzheimer's database as features. Using the Frequently Asked Questions (FAQ > 8) and Blessed Orientation-Memory-Concentration (BOMC > 10) tests recommended by Agency for Health Care Policy and Research, accuracies were 69% and 63% respectively, which were 14% to 20% worse than results obtained by ML methods. Combining the two tests (FAQ & BOMC) resulted

in a 60% accuracy. Experiments showed that ML methods can detect dementia 15% to 20% more accurately than applying either the FAQ, BOMC or their combined cut-off criteria.

In another endeavor [10], the researchers utilized MRI related data generated by the Open Access Series of Imaging Studies (OASIS) project. There was an emphasis on exploring the relationship between each feature of MRI tests and dementia of the patient. They conducted exploratory data analysis to state the relationship among data explicitly through visualizations so as to discover the correlations before feature extraction or prediction. Missing values were handled in two ways: dropping of tuples having missing values and replacing corresponding values exploiting off-the-shelf inference libraries. Subjects were classified applying traditional Logistic Regression, SVM, Decision Tree, Random Forest Classifier and AdaBoost the results of which are depicted in Fig. 1.

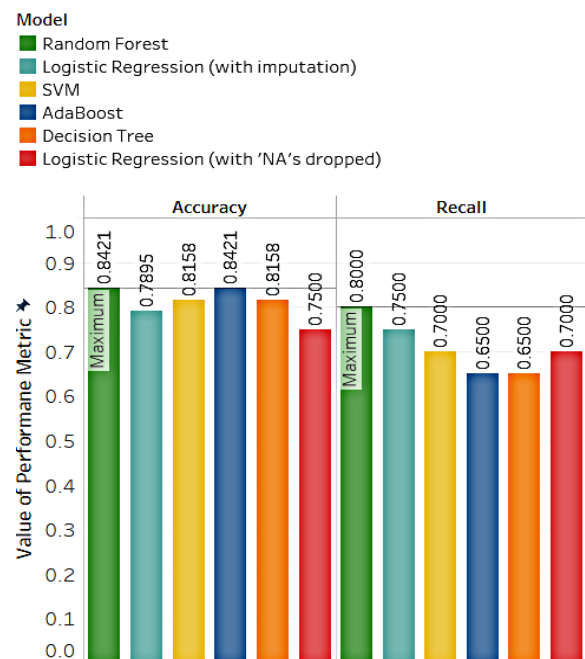


Fig. 1. Results obtained upon applying traditional ML algorithms

Alvarez et al. [11] presented a computer-assisted diagnostic tool based on Principal Component Analysis and Support Vector Machine (SVM) for improving the Alzheimer's diagnosis accuracy by means of SPECT (Single Photon Emission Computed Tomography) images. This process reduced the dimensionality of the feature space from ~500000 to ~100, thus facing the small sample size problem. The application of SVM to high dimensional and small sample size problems still remained a challenge and improving the accuracy SVM-based approaches is a field in development.

B. Convolutional Neural Networks (CNN) on Radiographs

Sarraf et al. [12] classified Alzheimer's data by using CNN deep learning LeNet architecture. For this study, Alzheimer's inflicted patients (24 female and 19 male) and 15 elderly normal control subjects with a mean age of 74.95 years were selected from Alzheimer's Disease Neuroimaging Initiative

dataset. The pre-processing steps for the anatomical data involved the removal of non-brain tissue from T1 anatomical images using Brain Extraction Tool. The product of preprocessing was 45x54x45x300 images in which the first 10 slices of each image were removed for containing no functional information. The researchers adjusted LeNet-5 for functional Magnetic Resonance Imaging (fMRI) data. LeNet differentiated Alzheimer’s from normal control and the average accuracy reached 96.8588%.

C. Hybridized Approach using Neural Networks

Gulhare et al. [13] proposed a Deep Neural Network (DNN) classification method to diagnose Alzheimer’s from MRI. The resulting attributes were respectively the area of the extracted region, the perimeter, mean, standard deviation, 28 horizontal distances (D_1, D_2, \dots, D_{28}), the height and the coordinates of the center of gravity of the region (G_x, G_y). The database included a longitudinal collection of 150 (88 female and 62 male) subjects aged 60 to 96. 72 of the subjects were characterized as non-demented while 78 as demented. The DNN consisted of multiple hidden layers and a softmax layer. The classifier rendered a maximum accuracy of 96.6% with different pairs of attributes. It classified with an accuracy of 90.3% retaining all attributes. The DNN approach showed better performance compared to SVM.

III. PROPOSED METHODOLOGY

The OASIS longitudinal MRI dataset went through intensive preprocessing and exploratory analysis which resulted in three reproductions of the dataset with significant features that were eventually modeled to produce phenomenal results (Fig. 2).

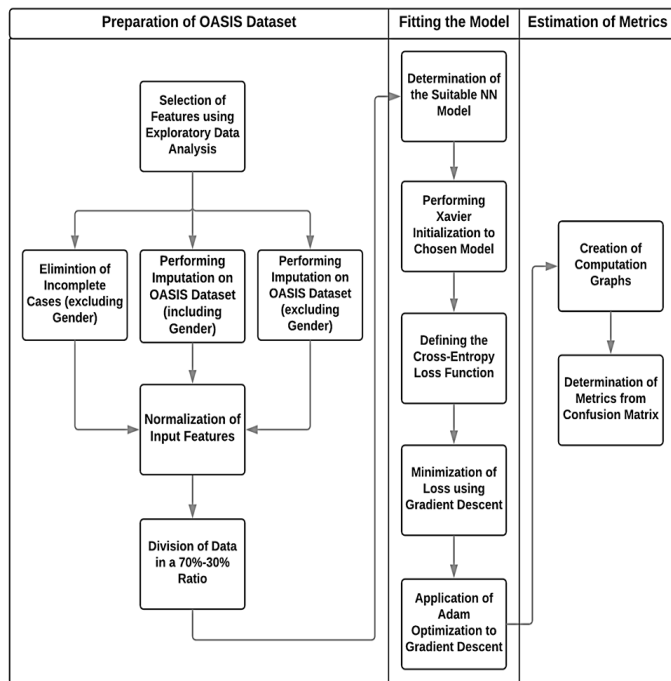


Fig. 2. Workflow for the proposed detection of early Alzheimer’s disease.

A. Preparation of OASIS Dataset

1) Selection of Features using Exploratory Data Analysis (EDA): Exploratory data analysis is a statistical process to summarize tendencies within data, aided by visualizations. EDA was primarily applied on OASIS dataset for extracting insights beyond formal modeling to hypothesize features reinforced by data.

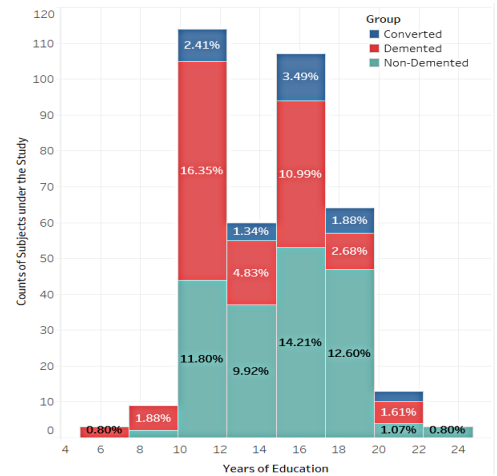


Fig. 3. Percentage of total subjects having respective years of education

An exploratory visualization shows that demented (and converted) subjects have experienced comparatively fewer years of education. Concretely, the subjects who received 10 to 12 years’ schooling, are mostly demented while we see an opposite scenario as learning prolongs—qualifying years of education as a feature to detect early Alzheimer’s (Fig. 3).

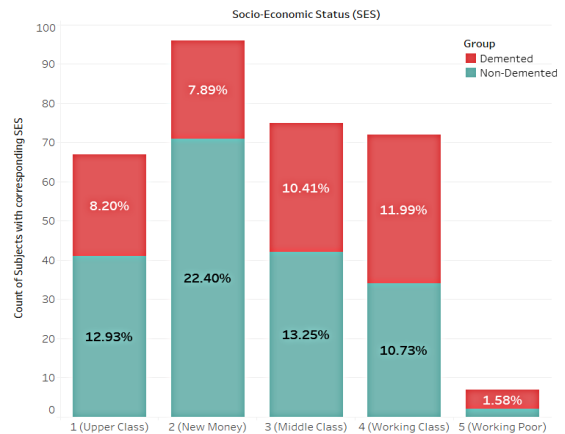


Fig. 4. Percentage of subjects belonging to respective socio-economic status.

Another summarization shows that as a transition is made towards working class from the upper class, the rate of dementia increases as a general trend justifying socio-economic status as another feature characterizing early Alzheimer’s (Fig. 4).

In another discovery, it is explored as a trend that demented patients tend to have fewer years of education with a hum-

ble socio-economic background, the opposite being true for healthy subjects (Fig. 5).

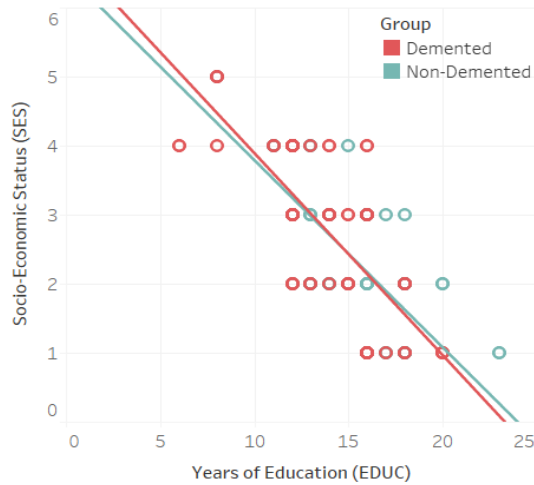


Fig. 5. Trend lines distinguishing subjects with respect to education and socio-economic rank

Subjects found negatively affected often provided reversed result in subsequent visits where CDR raised from ‘questionable’ to ‘mild’. Delay in MRI is expounded by degeneration in tissue. Medically indicative features e.g., MMSE, age, eITV, nWBV, ASF have also been selected, thus assembling ten significant features for early Alzheimer’s diagnosis (Fig. 7).

2) *Elimination of Incomplete Cases (excluding Gender):* Missing values in tuples are treated differently in various linguistic frameworks. Representations such as NaN, garbage values are problematic as they hail from a different distribution causing their derivatives to lead to useless parameters. Thus incomplete tuples have been subsetted out using R, bringing down the number of training examples from 373 to 354.

3) *Performing Data Imputation (including/excluding Gender):* Imputation is a statistical process of assigning a value by inference to a missing field taking into consideration other existing fields and summary of the dataset. In the OASIS dataset, socio-economic status (SES) and Mini-Mental State Examination (MMSE) were missing for some demented patients which were imputed using a tailored version of mean imputation according to the algorithm below (Fig. 6).

This retained all 373 tuples making the best use of available data. However, excluding gender as a feature provided a gender-neutral version of the dataset.

4) *Division of Data into a 70%-30% Ratio:* According to standard machine learning practices, OASIS dataset has been split into a larger training set and a comparatively smaller cross-validation set. 70% of the data have been used for training, assigning 248 tuples for the training purpose while setting aside the rest 30% comprising 106 records for cross-validation. Imputation raised these numbers to 262 and 111, respectively.

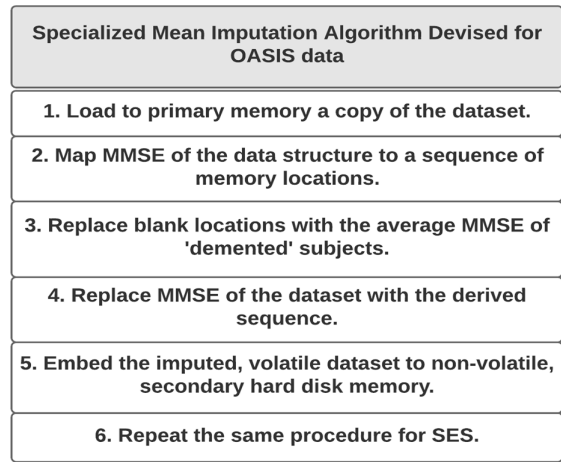


Fig. 6. Specialized Mean Imputation Algorithm.

5) *Normalization of Input Features:* While pre-processing data, it is crucial that parameters belong to the same scale for a fair comparison between them and for the gradient descent to converge following an oriented trajectory. Normalization rescales all numerics in the range [0, 1] using the formula below:

$$x_{new} = \frac{x - x_{min}}{x_{max} - x_{min}} \quad (1)$$

The OASIS dataset is replete with data hailing from different units and scales. The range of scales for Cognitive Dementia Rating and years of education are not identical, so is the case for any other collection of features—thus justifying normalization.

B. Fitting the Model

1) *Determination of the Suitable Neural Network Model:* Numeric representations of the features constitute the input layer of the model. The weighted inputs propagate through two ReLU-activated hidden layers each containing ten neurons. Finally, a SoftMax layer computes the probabilities for the classes, labeling as the highest (Fig. 7).

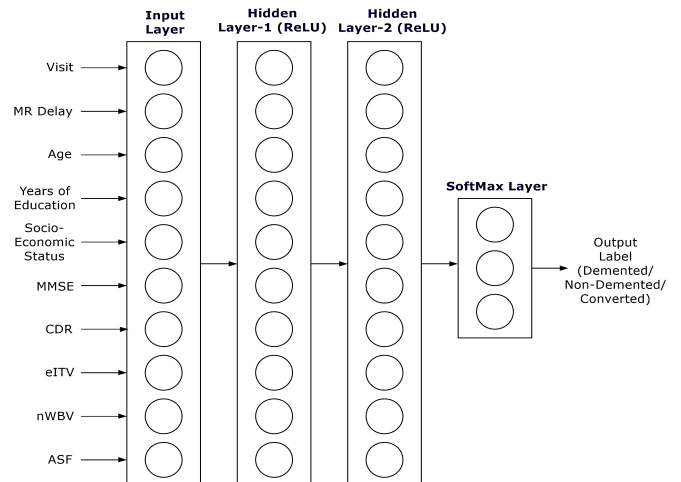


Fig. 7. The proposed three-layer neural network.

The hyper-parameters have been elected for the following rationale:

- **Number of layers, neurons:** Two hidden layers are chosen to prevent overfitting with ten hidden units, to preclude underfitting.
- **Learning rate:** A small learning rate of 0.0001 has been chosen to prevent overshooting across the minima.
- **Number of epochs:** The model was trained for a large 1500 epochs to quantify an optimum set of parameters.
- **Size of minibatch:** Complementing primary storage, 32 tuples were assigned per minibatch.
- **Adam Optimization parameters:** β_1 : 0.9, β_2 : 0.999, ϵ : 1e-08

2) *Performing Xavier Initialization to Chosen Model:* Xavier initialization ensures delicate initialization of weights in order to keep the signal in a reasonable range of values through multiple layers. This initialized the weights in the network by drawing them from a distribution with zero mean and a specific variance as,

$$Var(W) = \frac{1}{n_{in}} \quad (2)$$

Where W is the initialization distribution for the neuron in question and n_{in} is the number of neurons feeding into it. The distribution used is typically Gaussian or uniform.

3) *Defining the Cross-Entropy Loss Function:* The cross-entropy loss function has been optimized for the three-class classification problem with a view to obtaining the greatest refinement of the parameters. Represented here is precisely the cross-entropy, summed over all training examples [14]:

$$\begin{aligned} & -\log L(\{y^{(n)}\}, \{\hat{y}^{(n)}\}) \\ &= \sum_n [-\sum_i y_i \log \hat{y}_i^{(n)}] = \sum_n H(y^{(n)}, \hat{y}^{(n)}) \end{aligned} \quad (3)$$

where n indicates the number of training examples, y_n denotes the ground-truth value for an individual example, $\hat{y}^{(n)}$ is the prediction of the model and i represents the sequence of activation within a layer.

4) *Minimization of Loss using Gradient Descent:* A set of parameters θ is to be chosen so as to minimize error $J(\theta)$. The gradient descent algorithm starts with some initial θ , then repeatedly performs the update [14]:

$$\theta_j := \theta_j - \alpha \frac{\partial}{\partial \theta_j} J(\theta) \quad (4)$$

This update is simultaneously performed for all features, i.e., $j = 0, 1, \dots, n$ where α is the learning rate. This is a very natural algorithm that repeatedly takes a step in the direction of the steepest decrease of $J(\theta)$. To implement the algorithm, the partial derivative term has to be computed. If there is only one training example (x, y) , we have [14],

$$\begin{aligned} \frac{\partial}{\partial \theta_j} J(\theta) &= \frac{\partial}{\partial \theta_j} \frac{1}{2} (h_\theta(x) - y)^2 \\ &= 2 \cdot \frac{1}{2} (h_\theta(x) - y) \cdot \frac{\partial}{\partial \theta_j} (h_\theta(x) - y) \\ &= (h_\theta(x) - y) \cdot \frac{\partial}{\partial \theta_j} (\sum_{i=0}^n \theta_i x_i - y) \\ &= (h_\theta(x) - y) \cdot x_j \end{aligned}$$

$$\text{Therefore, } \frac{\partial}{\partial \theta_j} J(\theta) = (h_\theta(x) - y) \cdot x_j \quad (5)$$

To modify this method for a training set of more than one examples, it is to be replaced with the following algorithm [14]:

Repeat until convergence {

$$\theta_j := \theta_j + \alpha \sum_{i=1}^m (y^{(i)} - h_\theta(x^{(i)})) x_j^{(i)} \quad (\text{for every } j)$$

}

5) *Application of Adam Optimization to Gradient Descent:* Adam is an algorithm for first-order gradient-based optimization of stochastic objective functions, based on adaptive estimates of lower-order moments. The parameters for Adam Optimization are as follows:

- α : The learning rate or step size. Learning rate decay, permissible in Adam, has not been used for Alzheimer's classification.
- β_1 : The exponential decay rate for the first moment estimates (e.g. 0.9).
- β_2 : The exponential decay rate for the second-moment estimates (e.g. 0.999). This value is set close to 1.0 on problems with a sparse gradient.
- ϵ : A very small number to prevent any division by zero in the implementation (e.g. 10E-8).

C. Estimation of Metrics

Single-figure performance measures are customary to measure the proficiency of a learning model. Evaluation metrics such as accuracy, precision, recall are significant within the medical research arena and are computed using confusion matrices created via computation graphs.

1) *Creation of Computation Graphs:* A computational graph is the representation of a collective mathematical function using the frameworks of graph theory. Complying with the ethos of graph theory, a computation graph consists of nodes and edges. The nodes are indicative of either operations (denoted by round shapes) or operands (denoted by rectangular shapes) while the directed edges delineate the sequence of mathematical operations to be performed.

The NN framework of TensorFlow demands a computation graph to be devised before running it as a session to calculate

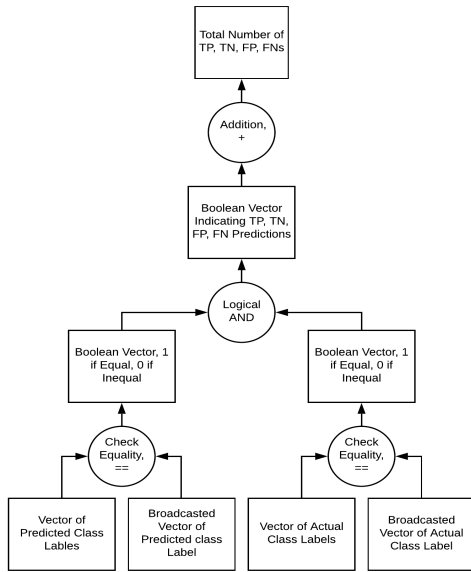


Fig. 8. Generalized computation graph for determining entries of the confusion matrix

the numerics. For this purpose, we manually concoct a computation graph (Fig. 8) in a bottom-up manner to determine the entries associated with the confusion matrix i.e.,

- predicted demented and actually demented, true positives (TPs)
- predicted demented while actually non-demented, false positives (FPs)
- predicted non-demented and actually non-demented, true negatives (TNs)
- predicted non-demented while actually demented, false negatives (FNs)

The popular one-hot boolean representation of class labels has been used for the purpose. We define another computation graph for calculating the accuracy of the implemented model on the cross-validation set (Fig. 9).

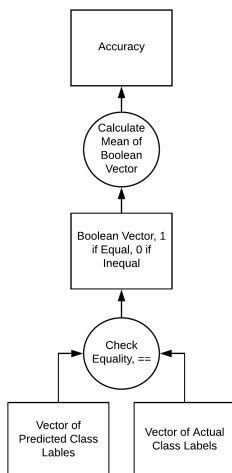


Fig. 9. Computation graph depicting computation of accuracy.

Upon checking for equality, the output boolean vector indicates positively the training examples identified correctly as possessing early Alzheimer's. Thus, the statistical mean of this data structure provides the fraction of correctly identified patients for the classifier.

2) *Determination of Metrics from Confusion Matrix:* In the jargon of machine learning, concretely in the problem of statistical classification, a confusion matrix is a specific tabular layout used to explain the performance of a classification model on a set of cross-validation data for which the true labels are available. Rows of the matrix represent the instances in a predicted class while columns represent the instances in an actual class (or vice versa). The name originates from that it makes viable to see if the system is confusing the classes (i.e. commonly mislabeling one as another).

		predicted class		
		demented	non-demented	converted
actual class	demented	predicted demented and actually demented, TPs	predicted non-demented while actually demented, FNs	predicted converted while actually demented
	non-demented	predicted demented while actually non-demented, FPs	predicted non-demented and actually non-demented, TNs	predicted converted while actually non-demented
	converted	predicted demented while actually converted	predicted non-demented while actually converted	predicted converted and actually converted

Fig. 10. Confusion matrix for early Alzheimer's classification problem with a focus on categories 'demented' and 'non-demented'.

The matrix (Fig. 10) is a special kind of contingency table, with two dimensions and identical sets of classes in both dimensions. For our medical diagnosis problem, we select accuracy, precision and recall as evaluation metrics using the terms calculated in the confusion matrix.

i) Accuracy

- Accuracy attempts to answer the following question: What proportion of predictions (both demented and non-demented) was actually correct?
- Accuracy is mathematically defined as follows:
 $accuracy = (TP+TN)/(P+N)$
- A model that produces no false predictions provides an accuracy of 1.0.

ii) Precision

- Precision attempts to answer the following question: What proportion of 'demented' identifications was actually correct?

- Precision has been calculated as follows:
 $precision = TP/(TP+FP)$
- A model that produces no false positives renders a precision of 1.0.

iii) Recall

- Recall attempts to answer the following question: What proportion of actual ‘demented’ was identified correctly?
- Mathematically, recall has been defined as follows:
 $recall = TP/(TP+FN)$
- A model that produces no false negatives delivers a recall of 1.0.

IV. EXPERIMENTAL RESULTS AND DISCUSSION

The experimental results (Fig. 13) of this study encompass three iterations on the three-layer model, each using a different data-engineered revision of the OASIS longitudinal MRI data. Even the lowest accuracy achieved among these three iterations in the research surpasses the accuracies achieved using orthodox machine learning methods [10].

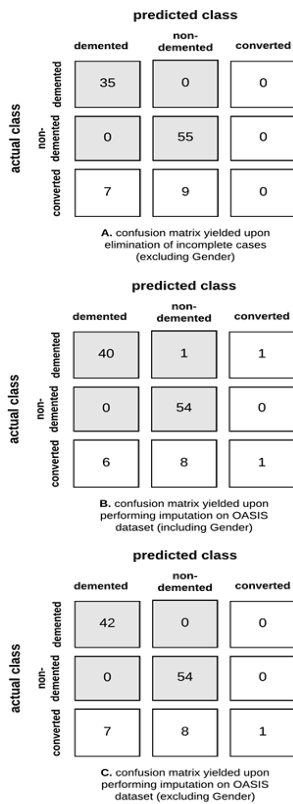


Fig. 11. Confusion matrices resulting from the application of three reproductions of the OASIS data to the proposed model with a focus on categories ‘demented’ and ‘non-demented’.

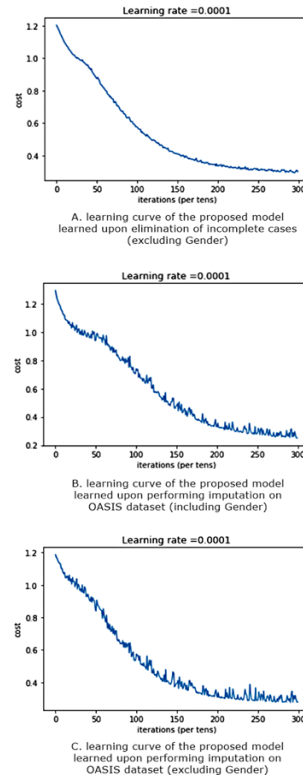


Fig. 12. Learning curves of the proposed neural network learned over three adaptations of the OASIS dataset.

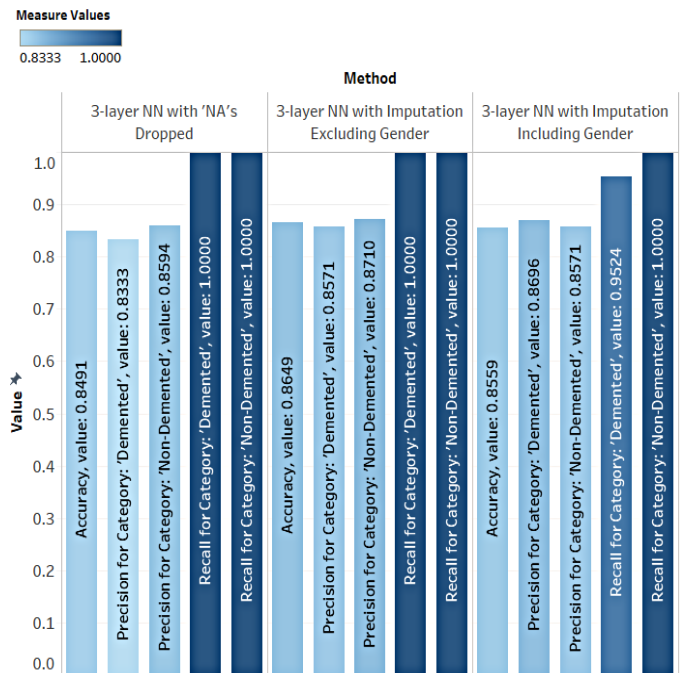


Fig. 13. Metrics yielded by the proposed neural network in general.

A. Metrics Yielded upon Elimination of Incomplete Cases (excluding Gender)

The variation of the dataset which dropped training examples containing at least one absent attribute value, in fact, made a waste of the available entries within the incomplete tuple and came up with the performance measures shown in Fig. 13 in general.

Although this is the variation in the study to yield the least accuracy, yet it outsmarted all typical machine learning techniques on the OASIS data. Drilled down to just two classes (Fig. 11.A) as having (demented) or not having (non-demented) early Alzheimer’s, the classifier produces impressive results as given in Table I according to the formulae given in Section III.C.2.

TABLE I. METRICS EVALUATED AS PER APPROACH A

performance measure	calculated value
accuracy	$(35+55)/(35+0+0+55)=1.0000$
precision	$35/(35+0)=1.0000$
recall	$35/(35+0)=1.0000$

B. Metrics Yielded upon Performing Imputation on OASIS Dataset (including Gender)

The variation of the dataset using customized, statistical mean imputation method made the best use of available data and synthesized artificially inferred data to replace the missing attributes. This statistically analytical approach created realistic data and also included gender as a feature rendering the general metrics as summarized in Fig. 13.

This variation of the dataset outperformed the previous metrics in approach A. Focusing on just two classes (Fig. 11.B) as having (demented) or not having (non-demented) early Alzheimer’s, the model produces successful results as the following (Table II).

TABLE II. METRICS EVALUATED AS PER APPROACH B

performance measure	calculated value
accuracy	$(40+54)/(40+1+0+54)=0.9894$
precision	$40/(40+0)=1.0000$
recall	$40/(40+1)=0.9756$

C. Metrics Yielded upon Performing Imputation on OASIS Dataset (excluding Gender)

This variation of the dataset is statistically imputed with customization as per labels, similar to the approach followed in B except for that gender has been eliminated as an input feature. The adaptation is an imputed version of the dataset described in A. This delivered the metrics as tabulated in Fig. 13 in general. This edition of the dataset outshined approach B and all other learning models (Fig. 1), making the model unbiased towards gender. Concentrating on just two classes (Fig. 11.C) as having (demented) or not having (non-demented) early Alzheimer’s, the model produces remarkable results like

the following (Table III):

TABLE III. METRICS EVALUATED AS PER APPROACH C

performance measure	calculated value
accuracy	$(42+54)/(42+0+0+54)=1.0000$
precision	$42/(42+0)=1.0000$
recall	$42/(42+0)=1.0000$

The research primarily being an attempt to classify the subjects as having or not having early Alzheimer’s, tends to center its attention on just two categories namely, demented and non-demented. Due to an uneven share of the ‘converted’ category in the dataset, the model performed incompetently on this category which is venial given the purpose of the research.

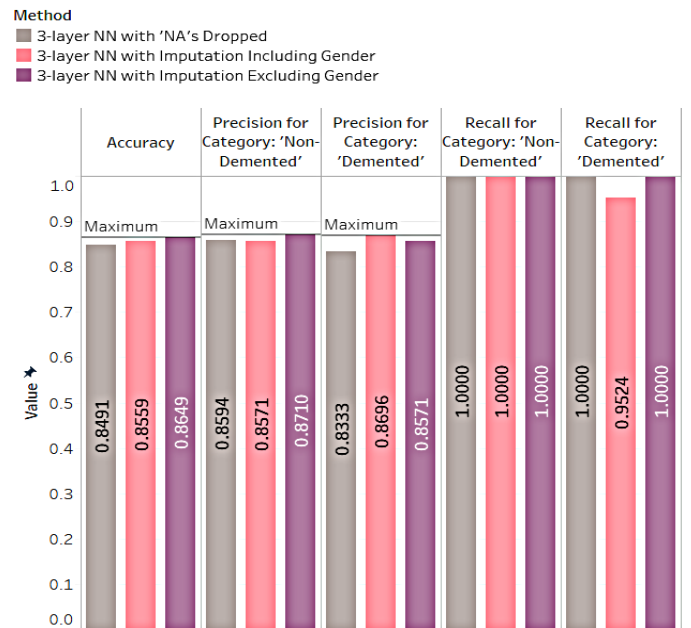


Fig. 14. Comparison of differently learned weights (Fig. 12) on the basis of performance measures.

While deployment of the model, the dataset can be engineered depending on utility as they each excelled in different metrics. Should accuracy be the foremost priority, parameters learned using the gender-exclusive imputed dataset will be an ideal pick. Likewise, parameters derived by training on any imputed dataset should suffice for perfect precision or recall (Fig. 14).

The simplistic, gender-neutral, three-layer neural network proposed superseded other hyper-parametrically tuned machine learning approaches (Fig. 15) through all three iterations using different variations of the OASIS dataset, performing greatly in terms of medically significant metrics (accuracy, precision, recall). Furthermore, the model has been trained (Fig. 12) on structured data, the business value of which is generally greater while the cost of acquisition is relatively lower than medical imagery.

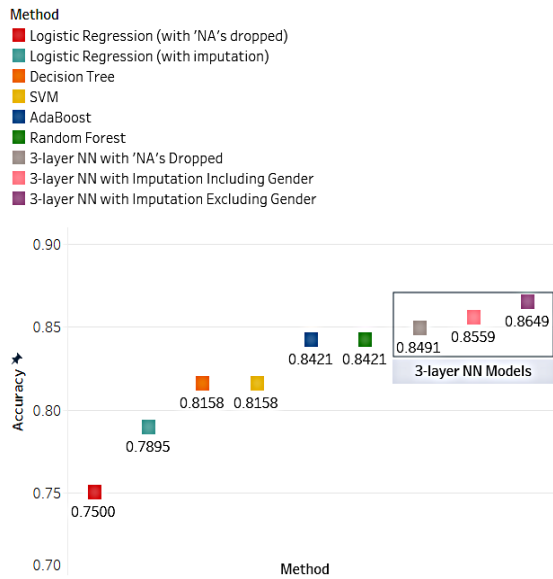


Fig. 15. Comparison among traditional learning models and proposed model.

V. FUTURE WORKS AND CONCLUDING REMARKS

Traditional machine learning methods, being efficient in predicting results upon carefully selected features, have thus far been a convenient approach towards early Alzheimer's detection. This study proves a simplistic neural network approach to be an even better methodology for its remarkable feature-extraction properties leading to best performance metrics (e.g., accuracy, precision and recall) obtained so far on the OASIS dataset.

However, the scope of this study can be broadened to classify among more stages of dementia upon data augmentation. Due to scarcity of data, this experiment performed dismally on the 'converted' category, causing a dent to the overall metrics—although providing tremendous results in the 'demented' and 'non-demented' categories which surpassed all conventional results.

This unique study introduces two novel features namely a person's socio-economic standing and educational background—bringing into question the role of gender in the prediction. This research also precludes the need for complete MRI data for a patient as the missing attributes can be inferred using customized imputation methods. This makes the model feasible, cost-effective. This study has unleashed new dimensions to current researchers intriguing them to look for features in a broader scope.

REFERENCES

- [1] GBD 2015 Disease Injury Incidence Prevalence Collaborators (October 2016). "Global, regional, and national incidence, prevalence, and years lived with disability for 310 diseases and injuries, 1990–2015: a systematic analysis for the Global Burden of Disease Study 2015". *Lancet*. 388 (10053):1545602. doi:10.1016/S01406736(16)316786. PMC 5055577. PMID 27733282.
- [2] Forecasting the global burden of Alzheimer's disease. *Alzheimer's & Dementia*. 2007;3(3):186–91. doi:10.1016/j.jalz.2007.04.381. PMID 19595937. World population prospects: the 2006 revision, highlights [PDF]. 2007.
- [3] Mendez MF (November 2012). "Early-onset Alzheimer's disease: non-amnesic subtypes and type 2 AD". *Archives of Medical Research*. 43 (8): 677–85. doi:10.1016/j.arcmed.2012.11.009. PMC 3532551. PMID 23178565.
- [4] GBD 2015 Mortality Causes of Death Collaborators (October 2016). "Global, regional, and national life expectancy, all-cause mortality, and cause-specific mortality for 249 causes of death, 1980–2015: a systematic analysis for the Global Burden of Disease Study 2015". *Lancet*. 388 (10053): 1459–544. doi:10.1016/S0140-6736(16)31012-1. PMC 5388903. PMID 27733281
- [5] Clinical Diagnosis of Alzheimer's Disease: Report of the NINCDS-ADRDA Work Group under the Auspices of Department of Health and Human Services Task Force on Alzheimer's Disease. *Neurology*. 1984;34(7):939–44. doi:10.1212/wnl.34.7.939. PMID 6610841.
- [6] Verywell Health. (2019). 12 Benefits of Early Detection in Alzheimer's Disease. [online] Available at: <https://www.verywellhealth.com/12-benefits-of-early-detection-in-alzheimers-disease-98046> [Accessed 15 Jan. 2019]
- [7] The mini-mental state examination: a comprehensive review. *Journal of the American Geriatrics Society*. 1992;40(9):92235. doi:10.1111/j.15325415.1992.tb01992.x. PMID 1512391
- [8] Neuropathologic Changes in Alzheimer's Disease. *The Journal of Clinical Psychiatry*. 2003;64 Suppl 9:7–10. PMID 12934968.
- [9] Datta, Piew, W. R. Shankle, and Michael Pazzani. "Applying machine learning to an Alzheimer's database." *Proceedings of the AAAI-96 Spring Symposium AI in Medicine: Applications of Current Technologies*, Stanford, CA, USA. 1996.
- [10] Kaggle.com. (2019). DETECTING EARLY ALZHEIMER'S — Kaggle. [online] Available at: <https://www.kaggle.com/hyunseokc/detecting-early-alzheimer-s> [Accessed 10 Jan. 2019].
- [11] Alvarez, Ignacio, et al. "Alzheimer's diagnosis using eigenbrains and support vector machines." *International Work-Conference on Artificial Neural Networks*. Springer, Berlin, Heidelberg, 2009.
- [12] Sarraf, Saman, and Ghassem Tofghi. "Classification of alzheimer's disease using fmri data and deep learning convolutional neural networks." *arXiv preprint arXiv:1603.08631* (2016).
- [13] Gulhare, Kajal Kiran, S. P. Shukla, and L. K. Sharma. "Deep Neural Network Classification method to Alzheimer's Disease Detection." *International Journals of Advanced Research in Computer Science and Software Engineering*, ISSN: 2277-128X (Volume-7, Issue-6), June 2017
- [14] Ng, Andrew. "CS229 Lecture notes." *CS229 Lecture notes 1* (2000) [Accessed 29 Nov. 2018].

Optimal Pragmatic Clustering for Wireless Networks

Suzan Basloom¹, Nadine Akkari², Ghadah Aldabbagh³
Faculty of Computing and Information Technology
Department of Computer Science
King Abdulaziz University, Jeddah, Saudi Arabia

Abstract—Nodes' clustering in wireless networks is one of the solutions that used to improve network performance. This paper discusses the clustering in wireless networks. Then it presents a novel clustering algorithm named Pragmatic Genetic Algorithm (PGA). It combines two of the well known artificial intelligence techniques: K-means and Genetic algorithm. The proposed algorithm aims at minimizing the execution time of the clustering, especially in time-sensitive wireless networks applications. The performance of PGA has been compared with the classical clustering algorithms, namely, K-means and KGA. The experiments have been conducted using synthetic and real data from public repositories. PGA obtained excellent results in execution and stable accuracy even when the number of nodes was increased.

Keywords—Clustering; genetic algorithm; K-means; wireless networks

I. INTRODUCTION

Machine-based decisions making is an important aspect that attracted the scientific research community. Artificial intelligence (AI) has proposed a plethora of machine learning algorithms to improve the decision-making process. These algorithms have been embedded in many modern devices such as cars, cameras, sensors, and networks, to make the proper decision and improve overall performance. Some of these decisions must be made in a real-time manner to maintain system stability. For example, in mobile networks, the decision of moving the current connection from one access point to another for the handover [1] must be done in a time faster than the node speed. The delay in such a process can break the connection which will affect the user satisfaction level (USL).

However, finding the optimum decision (solution) using machine learning algorithms needs long execution time to converge. This long execution makes any system manager choose the approaches that make the decision in a shorter time even if its accuracy was not the best. Clustering is one of the unsupervised machine learning algorithms. It classifies data elements into groups based on the similarity between them. There are many clustering algorithms such as K-means, DBSCAN, Mean-Shift, etc. K-means is the most common algorithm because of its short execution time and acceptable results, but it faces the problem of local minima [2].

Clustering has been used in wireless networks to improve network performance. It divides nodes into small groups based on specific criteria such as distance, energy, or route as shown in Fig. 1. Clustering has proved its ability to simplify the networks' task management. Its applications can be found in sensor networks [3] where the nodes are clustered to send their data to the sink node which is responsible for forwarding them to the server.

Also, it is used in dense networks to increase the networks' capacity and coverage area through tethering or relaying [4], [5]. Edge-nodes in such networks are tethered to the closer nodes to the access point, cluster-head, to forward their data. The cluster-head needs to have a certain amount of energy to forward the received packets or it must be replaced. To change the cluster-head, a real-time clustering must be conducted. This re-clustering process is critical and needs to be executed in a short time to maintain stable performance.

Moreover, the clustering is applied in proactive mobility management approaches [6]. In such approaches, the next attaching point of a mobile node is pre-predicted on the go, based on its mobility behavior. This type of clustering is time sensitive and need to be updated frequently.

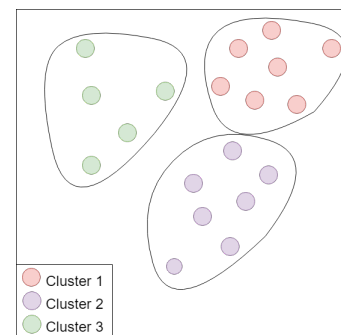


Fig. 1. Nodes Clustering

This paper's contribution is to propose an algorithm called Pragmatic Genetic Algorithm (PGA) to enhance the clustering execution time in wireless networks.

The rest of the paper is organized as follows. Section II a brief background is presented including the wireless network characteristics, definitions of K-means and genetic algorithm, and reasons for using them in this paper. Section III shows the related works that combine K-means and genetic algorithm for the clustering process. Section IV presents the proposed algorithm PGA. The simulation environment and results are discussed in Section V. The conclusion is in Section VI.

II. BACKGROUND

This section overviews wireless networks challenges and how the clustering is used to overcome their effects. After that, it justifies the reasons behind choosing to combine K-means and Genetic Algorithm (GA). Followed by a brief explanation of both approaches.

A. Wireless Networks Characteristics

Wireless networks provide a location independent connection, where a node can be connected anywhere at anytime. The media in such networks is the air, which propagates a variety of electromagnetic waves in different frequencies and powers. These waves [7], in addition to the weather effects, can attenuate by distance, interfere and congest with each other. To control such effects many solutions have been proposed such as specifying the coverage area of the access points, determining the transmission power, and selecting frequencies for each type of wireless technology. Wireless networks have characteristics that challenge the network management processes which must be considered while clustering the network. Some of these characteristics summarized below.

1) *Architecture*: Wireless networks are classified into two architectures: infrastructure and infrastructure-less [8]. Infrastructure scheme has pre-constructed access points, that control the connection between the network's nodes. On the other hand, nodes in the infrastructure-less scheme can be connected directly as in the Ad hoc networks. Based on the network architecture the clustering algorithm could be done central-based or distributed-based.

2) *Coverage area*: Wireless signals [9] can propagate for a specific distance based on its band, which includes different frequency, phase, and amplitude. Hence, each wireless technology has a specific coverage area based on the used wireless band. For instance, *IEEE802.11g* works on 2.5 GHz band [10] with a coverage area up to 60 m_2 . On the other hand, LTE tower works on 698–787 MHz band and could cover an area up to 1 Km_2 .

3) *Energy*: Mobile nodes have limited power and in many cases cannot be recharged immediately which represent a challenge in network design. Nodes' clustering can minimize the power limitation and increase the network lifetime using cooperative communication.

4) *Mobility*: The most convenient feature in wireless networks is mobility. The mobility represents a hot topic in network management which plays a major role in providing seamless movement between a network access points. Clustering the network nodes or the access points can provide better mobility management in the network.

B. Why K-means with GA

This paper studies the combination of Genetic Algorithm (GA) and K-means for the following reasons:

- K-means is a simple fast-executing clustering technique.
- GA is the most popular heuristic approach used based on Jones et al. [11] overview.
- GA can optimize multiple objectives which go along with wireless networks which have multi-conflicting parameters needed to be optimized.
- K-mean and GA are computationally simpler compared to other AI techniques such as neural networks. This is because they require only swapping and shifting of genes in chromosomes.

C. K-means

K-means clustering algorithm [12] starts by generating random k centroids. The first clusters are created based on the Euclidian distance between the centroids and the nodes. After that the centroids are updated based on the calculated mean of each cluster. This process is repeated until the new centroids remain the same as the previous ones.

D. Genetic Algorithm

Conventional Genetic Algorithm (GA) is inspired by the theory of evolution. In nature, weak organisms are faced with extinction. The stronger ones have the opportunity to pass their genes to next generations via reproduction. In GA, a

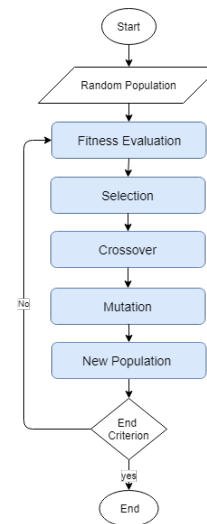


Fig. 2. Genetic Algorithm

chromosome represents a unique solution in the population. The population is usually randomly initialized. The GA uses two operators to create a new generation of chromosomes from previously existing chromosomes. These two operators are selection and reproduction. In the selection step, two chromosomes are selected that have the highest fitness value to be the parents for the next generation. After that, reproduction will start with two sub-steps: crossover and mutation. In the crossover, an offspring is generated by combining the two parent's chromosomes. This gives the offspring the opportunity to inherit good genes. Usually, the crossover rate is very high, typically 0.9 percent. In mutation, a random change is introduced into characteristics of chromosomes. The mutation rate is very small, typically less than 0.1 percent. After that the next generation is reproduced as depicted in the flowchart in Fig. 2.

The procedure of the basic genetic algorithm is given as follows [13]:

- 1) Set $t=1$. Randomly generate N solutions to form the first population P_1 .
- 2) Fitness Assignment: Evaluate and assign a fitness value to each solution $x \in P_1$ based on the objective function.
- 3) Selection: Select two solutions x and y from P_1 which have the best fitness values to be used in the creation of the new population P_t .

- 4) Crossover: Using a crossover operator (one point or more) to generate the new offspring and add them to Q_t .
- 5) Mutation: based on predefined mutation rate (always a low rate) mutate some of the new offspring $x \in Q_t$.
- 6) If the stopping criterion is satisfied, terminate the search and return the current population, else, set $t = t + 1$ go to Step 2.

III. RELATED WORKS

This section presents the previous works that combine GA with K-means to enhance the clustering process. These works can be classified into three categories: improving the centroid location, reducing the local minima, and generating a unique solution at each run. A brief description of these categories presented below.

In [14], author added the GA algorithm to K-means to find the optimal clustered data. The clusters went through GA operations (selection and reproduction) to create generations. These generations recreated many times based on the distance fitness-function. The results show a better clusters formation compared to clustering by K-means. The main drawback of this solution is the high number of iterations needed to find the optimal solution.

On the other hand, a combination of K-means and the genetic algorithm has been used in [13], [15] to search for the optimal centroids. The clusters are initially created around random centroids of n dimensions. The new centroids are calculated based on the mean of the nodes that belongs to that cluster (the fitness function). When the newly calculated centroid has the same value as the previous centroid the process will be terminated. To evaluate the performance of GA-clustering, artificial and real-life data sets are used. GA-clustering outperformed K-means clustering results. The n -dimensional centroids could add complexity to the calculations.

Moreover, [16] also uses a K-means and GA as a solution to the multi-objective resource allocation problem. The K-means clustering algorithm used to divide the population into different-sized populations. The crossover and mutation are alternately applied to create the next generation. The aim of the work is to preserve diversity into the solutions, instead of having a similar solution each time.

IV. PROPOSED ALGORITHM

This paper proposes a pragmatic clustering algorithm combines K-means and GA, because of the need for a fast executing clustering algorithm for the wireless networks.

The proposed PGA is different from the previous works by adding two fitness values to the clustering process. PGA flowchart is depicted in Fig. 3. The first fitness value is calculated between the centroids and the population, while the second fitness value is calculated between the centroids themselves. This fitness could eliminate unwanted crossovers. Hence reduces the execution time that is needed to define the clusters. The PGA algorithm steps are as follows:

- 1) Generated a number of k chromosomes based on K-mean algorithm.
- 2) Calculate the fitness value of each node to the chromosomes using distance Eq. 1.
- 3) Specify node's cluster such that the node belongs to the shortest distance centroid.
- 4) Calculate the fitness value between the chromosomes using distance value (proposed step) Eq. 1.
- 5) Starts the GA operations between chromosomes such that crossover will start if the crossover-centroids are apart away. This step could eliminate the creation of very close centroids which will result in unfitted individual. This will reduce the execution time needed if this crossover included.

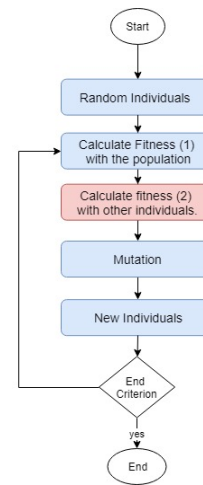


Fig. 3. Proposed Pragmatic GA Clustering PGA.

The details of PGA steps follow the main five steps of the GA as follows:

A. Representation and Initial Population

The initial individuals P_1 is randomly chosen and stored in a list of decimal numbers. Each individual (chromosome) in the population represent k centroids.

B. First Fitness Value Calculation

The mean of the distances between the each individual and nodes is calculated based on equation 1. The result is saved in the last digit of each chromosome, which represents the first fitness value.

$$d = \sqrt{\frac{x_2 - x_1}{y_2 - y_1}} \quad (1)$$

C. Selection

There are many selection strategies used for the GA. PGA uses the Roulette wheel selection strategy [17] which selects two individuals (parents), that have the highest first-fitness values to create the new individuals (children), for the next generation P_t .

D. Second Fitness Value Calculation

The second fitness value is calculated based on the distance between the individuals themselves based on the equation 1. This step is added in order to eliminate the crossover between adjacent-centroids. The crossover between adjacent centroids will create non-uniformed clusters. Also, it will add unwanted calculations to the first-fitness step, where the newly created clusters will have low fitness values. The second fitness step will calculate the fitness of all combinations between the selected individuals (centroids). Then the highest fitness combination will be used in the crossover process.

E. Crossover

Crossover exchanges the genes of the individuals (parents) to generate the offspring. The crossover in GA could be done on a single point or more. In this paper, a One-point crossover strategy is used as appeared in Fig. 4. The probability of crossover is usually high, but for this paper, it depends on the second fitness value. If the fitness value is high, the crossover will be conducted otherwise it will not.

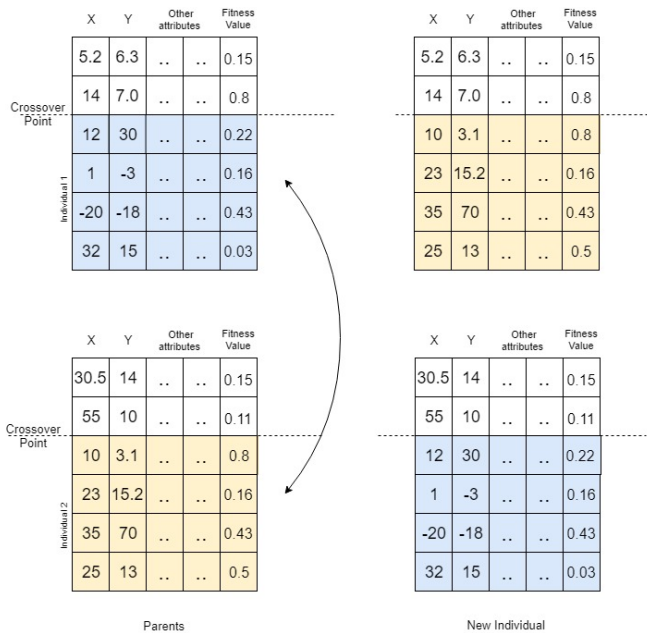


Fig. 4. Crossover in PGA

F. Mutation

Mutation is an occasional alternative of a character in a chromosome. In mutation, a character will be changed if a randomly generated number is equal or less than the probability of the mutation. The probability of mutation in GA is usually very small.

G. Elitism

The purpose of the elitism strategy is to move the good genes from the previous iteration to the next. So the centroids that has the best fitness values can be used in the creation of the new population.

H. Stopping Criterion

The algorithm will stop when it reaches to the predefined number of generations.

V. EXPERIMENTS AND ANALYSIS

To validate the proposed PGA algorithm, we use synthetic and real data sets. The experiments and their results are described below. The initial values of the GA algorithm, for all experiments are shown in Table I. Two metrics are used to evaluate the performance of the proposed algorithm as follows:

- **Execution time:** It is the time the program takes to reach to the final clusters.
- **Accuracy:** The percentage of the right created clusters by the algorithm, compared to pre-known results of the used data set.

TABLE I. THE USED GA PARAMETERS

Parameter	Value
Crossover Probability	0.8
Mutation Probability	0.01
Number of Individuals	20
Generations	100

A. Experiment 1

In this experiment, “Iris” data set [18] is used, which is commonly used for testing machine learning algorithms performance [19], [20]. This data set represents different categories of irises with four feature values: the sepal length, sepal width, petal length and the petal width in centimeters. It has 150 records which are categorized into three classes with 50 samples each. Therefore the chosen number of clusters (k) is three. The aim of this experiment is to compare the performance of the proposed PGA algorithm with the K-means and KGA. KGA [16] is an algorithm that uses the GA algorithm to improve the K-means centroid. The accuracy is calculated by comparing the clustering results with the pre-known correct answers of the Iris data set.

It can be seen in Table II that PGA has the best accuracy compared to K-means and KGA. On the other hand, K-means has the best execution time but with the lowest accuracy. PGA is better than KGA by 5% in execution time and accuracy in this experiment. Fig. 5 shows the result of clustering the “Iris” data set by PGA.

TABLE II. EXPERIMENT 1 RESULTS

Algorithm	Iteration	accuracy
K-means	0.03	49%
KGA	28	79%
PGA	21	81%

B. Experiment 2

In this experiment 200-400 points in R^2 are randomly generated to from four classes. The classes are taken in such a way that the distance from a point to its class-centroid is less than the distance of that point to other classes centroids as appeared in Fig. 6.

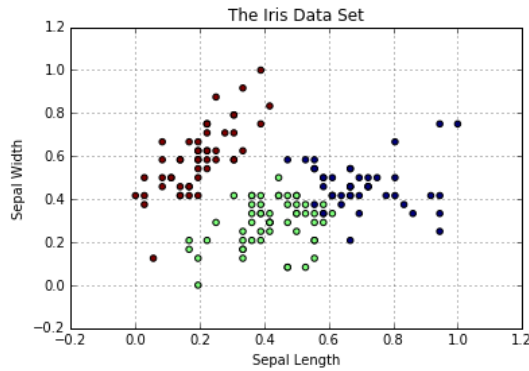


Fig. 5. Iris Clustering by PGA

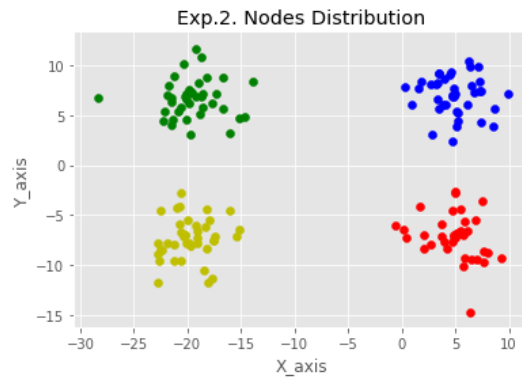


Fig. 6. Exp.2 Nodes Distribution.

TABLE III. EXPERIMENT 2 RESULTS

Number of Nodes	200		300		400	
	Algorithm	Time	Accuracy	Time	Accuracy	Time
K-means	0.1	50%	0.3	25%	0.5	24%
KGA	78	65%	81	68%	108	75%
PGA	51	75%	56	71%	76	75%

The results of experiment 2 are depicted in Tables III. PGA-clustering attains the best value of accuracy compared to K – means and KGA . PGA has stable accuracy even when the number of nodes increased. K -means, on the other hand, attains the best execution time but with the lowest accuracy especially when the number of nodes is increased.

The addition of the second fitness value to the PGA eliminate the unwanted calculations. These calculations could be added if the incorrect clusters (clusters with close centroids) are generated by the crossover process. This is can be seen in the result of PGA in the former experiments.

VI. CONCLUSION

In this paper, we have presented a new clustering technique called PGA . It aims at improving the execution time that is needed to cluster group of nodes. Clustering is an important class of unsupervised learning techniques that have attracted the attention of the research community over the last few years.

The proposed approach is a novel contribution, which adds a second fitness value to the clustering process. PGA

combines the benefits of Genetic algorithm and K -means. This combination can omit some of the drawbacks of each algorithm such as the local minima of the K -means and the long execution time of GA .

We have tested the proposed algorithm in different synthetic and real clustering problems. The results of our testing of execution times clearly show that PGA outperformed K -means and KGA algorithms while maintaining good accuracy results.

REFERENCES

- [1] R. Ahmad, E. A. Sundararajan, N. E. Othman, and M. Ismail, "Handover in lte-advanced wireless networks: state of art and survey of decision algorithm," *Telecommunication Systems*, pp. 1–26, 2017.
- [2] J. Qin, W. Fu, H. Gao, and W. X. Zheng, "Distributed k -means algorithm and fuzzy c -means algorithm for sensor networks based on multiagent consensus theory," *IEEE transactions on cybernetics*, vol. 47, no. 3, pp. 772–783, 2017.
- [3] S. Basloom, N. Akkari, and G. Aldabbagh, "Wireless sensor networks: Cross-layer optimization performance," in *Computer Communications Workshops (INFOCOM WKSHPS), 2016 IEEE Conference on*. IEEE, 2016, pp. 950–955.
- [4] S. Basloom, A. Nazar, G. Aldabbagh, M. Abdullah, and N. Dimitriou, "Resource allocation using graph coloring for dense cellular networks," in *2016 International Conference on Computing, Networking and Communications (ICNC)*. IEEE, 2016, pp. 1–5.
- [5] M. Hajjar, G. Aldabbagh, and N. Dimitriou, "Using clustering techniques to improve capacity of lte networks," in *Communications (APCC), 2015 21st Asia-Pacific Conference on*. IEEE, 2015, pp. 68–73.
- [6] P. Kuila and P. K. Jana, "Energy efficient clustering and routing algorithms for wireless sensor networks: Particle swarm optimization approach," *Engineering Applications of Artificial Intelligence*, vol. 33, pp. 127–140, 2014.
- [7] A. F. Molisch, *Wireless communications*. John Wiley & Sons, 2012, vol. 34.
- [8] A. Gupta and R. K. Jha, "A survey of 5g network: Architecture and emerging technologies," *IEEE access*, vol. 3, pp. 1206–1232, 2015.
- [9] S. S. Rakib and R. Hadani, "Signal modulation method resistant to echo reflections and frequency offsets," Jul. 14 2015, uS Patent 9,083,595.
- [10] V. Ssorin, A. Artemenko, A. Sevastyanov, and R. Maslennikov, "Compact bandwidth-optimized two element mimo antenna system for 2.5–2.7 ghz band," in *Proceedings of the 5th European Conference on Antennas and Propagation (EUCAP)*. IEEE, 2011, pp. 319–323.
- [11] D. F. Jones, S. K. Mirrazavi, and M. Tamiz, "Multi-objective meta-heuristics: An overview of the current state-of-the-art," *European journal of operational research*, vol. 137, no. 1, pp. 1–9, 2002.
- [12] A. K. Jain, "Data clustering: 50 years beyond k-means," *Pattern recognition letters*, vol. 31, no. 8, pp. 651–666, 2010.
- [13] U. Maulik and S. Bandyopadhyay, "Genetic algorithm-based clustering technique," *Pattern recognition*, vol. 33, no. 9, pp. 1455–1465, 2000.
- [14] C. A. Murthy and N. Chowdhury, "In search of optimal clusters using genetic algorithms," 1996.
- [15] S. Bandyopadhyay and U. Maulik, "An evolutionary technique based on k-means algorithm for optimal clustering in rn," *Information Sciences*, vol. 146, no. 1-4, pp. 221–237, 2002.
- [16] A. Mousa, M. El-Shorbagy, and M. Farag, "K-means-clustering based evolutionary algorithm for multi-objective resource allocation problems," *Appl. Math*, vol. 11, no. 6, pp. 1681–1692, 2017.
- [17] A. Shukla, H. M. Pandey, and D. Mehrotra, "Comparative review of selection techniques in genetic algorithm," in *2015 International Conference on Futuristic Trends on Computational Analysis and Knowledge Management (ABLAZE)*. IEEE, 2015, pp. 515–519.
- [18] R. A. Fisher, "The use of multiple measurements in taxonomic problems," *Annals of eugenics*, vol. 7, no. 2, pp. 179–188, 1936.

- [19] M. De Marsico, M. Nappi, D. Riccio, and H. Wechsler, "Mobile iris challenge evaluation (miche)-i, biometric iris dataset and protocols," *Pattern Recognition Letters*, vol. 57, pp. 17–23, 2015.
- [20] T. Gupta and S. P. Panda, "A comparison of k-means clustering algorithm and clara clustering algorithm on iris dataset," *International Journal of Engineering & Technology*, vol. 7, no. 4, pp. 4766–4768, 2018.

Analysis of ECG Signal Processing and Filtering Algorithms

Zia-ul-Haque^{*1}, Rizwan Qureshi^{†2}, Mehmood Nawaz^{‡3}, Faheem Yar Khuhawar^{*4}, Nazish Tunio^{‡5}, Muhammad Uzair^{§6}

^{*}Dept. of Telecommunication Engineering, Mehran University of Engineering & Technology, Jamshoro, PK

[†]Department of Electronic Engineering, City University of Hong Kong

[‡]COMSATS University, Islamabad, Wah Campus Pakistan

[§]Department of Information Technology, Shaheed Benazir Bhutto University, Naushahro Feroze Campus, Pakistan

Abstract—Electrocardiography (ECG) is a common technique for recording the electrical activity of human heart. Accurate computer analysis of ECG signal is challenging as it is exceedingly prone to high frequency noise and various other artifacts due to its low amplitude. In remote health care systems, computer based high level understanding of ECG signals is performed using advanced machine learning algorithms. The accuracy of these algorithms relies on the Signal-to-Noise-Ratio (SNR) of the input ECG signal. In this paper, we analyse various methods for removing the high frequency noise components from the ECG signal and evaluate the performance of several adaptive filtering algorithms. The result suggest that the Normalized Least Mean Square (NLMS) algorithm achieves high SNR and Sign LMS is computationally efficient.

Keywords—Electrocardiogram; power line interference; electromyography; adaptive filter; Least Mean Square

I. INTRODUCTION

The rapid advancement in the fields of electronic and communication technologies and new developments in computational algorithms such as deep learning and big data analysis have resulted in new ways of providing health care [1]. The bulky medical apparatus have been replaced by smaller electronic gadgets connected with personal computers, laptops and smart phones (Fig. 1). For example, the company Bio Telemetry, Inc., [2] offers remote healthcare services to over one million patients over the internet [3]. One of the key components of the computerized remote health care systems is the automatic analysis and understanding of ECG signal by advanced computer algorithms.

The accuracy of the analysis usually depends on the quality of the input ECG signal. The recorded ECG signal has low amplitude and is often contaminated with multiple types of noises such as power line interference (PLI), electro surgical noise, lead wire problems, base-line drift and high frequency noise components [4]. Several signal filtering methods exists in the literature to remove specific types of noise component from the ECG signal to improve its SNR. In this paper, we perform a comparative evaluation of four basic types of filtering methods including Least Mean Square (LMS), Normalized LMS (NLMS), Log LMS, and Sign LMS for ECG signal enhancement and remove the high frequency noise from the ECG signal. The high frequency is generated due to electromyography (EMG) and instrumentation noise. We perform detailed experiments on the ECG signals provided by the MITDB [5] database and compare the performance in terms

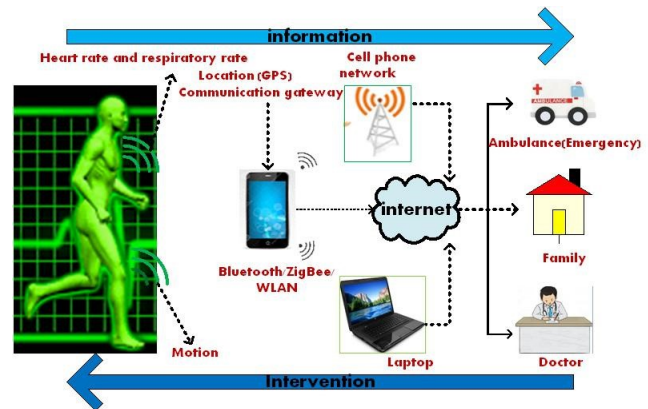


Fig. 1. An illustration of a simple remote health care system.

of the SNR, convergence rate and computational complexity of these algorithms. Our analysis shows that the performance of NLMS is superior than the other adaptive methods in terms of SNR and Sign LMS is computationally efficient. These results can help us in choosing the appropriate filter for ECG signal enhancement and automatic ECG analysis.

The paper is organized as follows. Section II and III discusses related work and digital filters. In Section IV, adaptive filtering algorithms are described, where as Section V presents simulation and results. Finally, conclusion are drawn along with future prospects.

II. RELATED WORK

Luo and Johnston [6] presented a comprehensive review for ECG signal processing. Qureshi *et al.* [7] evaluated the performance of multistage adaptive filter for ECG signal enhancement. Liu *et al.* [8] proposed a method composed of genetic algorithm and empirical mode decomposition for feature selection. Shadarmand *et al.* [9] proposed a method for the classification of patient heartbeat types based on block based neural network and particle swarm optimization.

A typical ECG signal waveform consists of the six parameters shown in Fig. 2. In the acquisition and transmission process, ECG wave is corrupted with different types of noises including biological noises and environmental noise or instrument noise (Fig. 3).

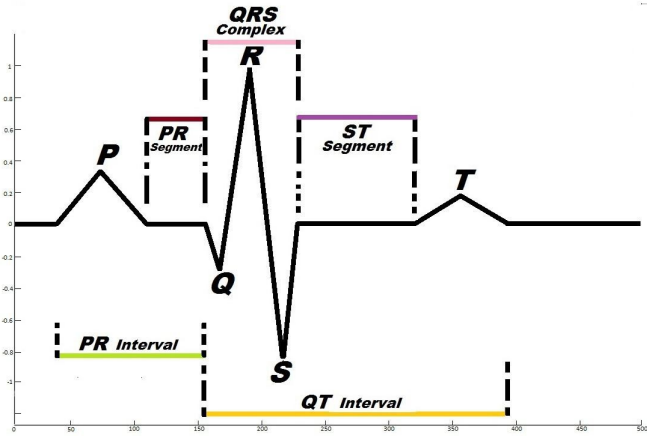


Fig. 2. Six features of a typical ECG signal.

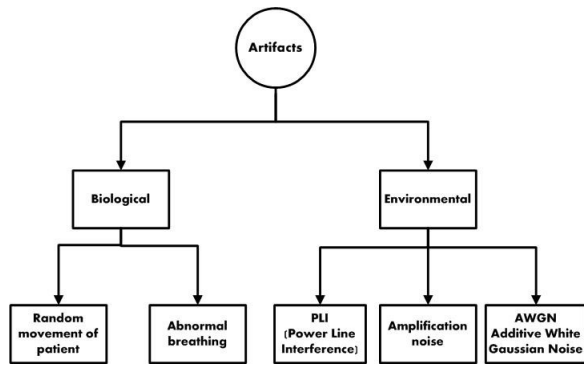


Fig. 3. Common artifacts that corrupts the ECG Signal.

Biological artifact is due to the movement of the subject itself, i.e. random movement of patient. Environmental artifacts are caused by power line interference, instrumentation error and additive white Gaussian noise. The low amplitude features are especially affected by high frequency noise.

III. DIGITAL FILTERS

The aim of the pre-processing is to achieve a noise free signal and enhance its features accurately. Digital filters can be categorized into two major types as shown in Fig. 4, i.e. fixed type of filters where the coefficients of the filters are fixed and adaptive filter where the coefficients change adaptively.

Fixed filters are well suited for stationary environment and can be used for eliminating the powerline interference 60/50 Hz noise. When we know which frequency is to be eliminated, fixed filters are the best choice. In case of non-stationary signals such as ECG, filters designed using advanced learning algorithms are the optimum choice. After reviewing the literature carefully, we have chosen adaptive filters as a potential candidate for the processing of ECG signal because of its flexibility to adapt to the changes in the signal. As ECG is a non-linear signal, adaptive filters are well suited for its processing.

Adaptive filters have many sub types based on their objective function. LMS, Normalized LMS and Recursive Least Squares (RLS) are some common types of adaptive filters [10].

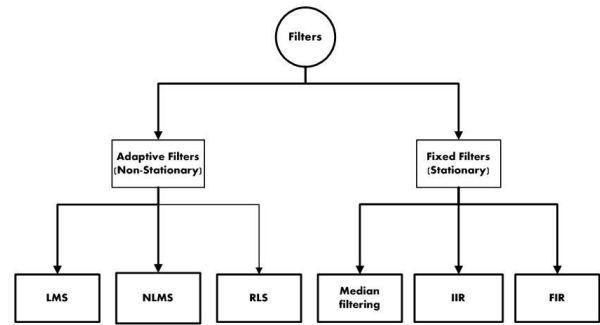


Fig. 4. Two categories of filters used for ECG signal pre-processing.

On the other hand, random noise or high frequency noise requires a more intelligent and adaptive processing mechanism. Some common filter design methods include Finite Impulse Response (FIR), Infinite Impulse Response (IIR) and Median/Average filtering.

In FIR design, the output of the filter is the weighted sum of past input values which is finite [11] and can be represented by the equation:

$$Y[n] = \sum_{k=0}^M b_k x[n-k] \quad (1)$$

where $x[n]$ denotes the input signal and b_k are the filter coefficients and $Y[n]$ is the output response.

IIR filter has infinite impulse response and acts like a feedback loop which never terminates when a single impulse is applied to it. It has both zeros and poles in the system [12]. IIR filters may not be stable because of the infinite response. IIR filter can be mathematically expressed as:

$$Y[n] = \sum_{i=0}^N a_i x[n-i] + \sum_{j=1}^N b_j Y[n-j] \quad (2)$$

where N is the filter's order, a_i and b_j are the filter coefficients and the output depends on past inputs and past outputs. IIR filters can be graphically expressed as shown in Fig. 5.

Median/Average filtering is used to suppress artifacts and to preserve edge features [13]. It is computed using a running average like operations on the signal with different coefficients. In the absence of low frequency noise, signal is not distorted and as such this type of filtering is computationally efficient [2].

An adaptive filter has the ability to adapt to the change in the signal over time. Therefore, adaptive filtering is very well suited for non-linear problem [14] such as ECG noise removal. An adaptive filter has two input signals (Fig. 6): one is the base input signal and other one is the reference signal. The filter compares them and calculates the error. The error is then minimized iteratively based on some objective function [15]. We have chosen adaptive filters for the pre-processing of ECG signal because of its intelligent performance under unknown conditions. Some popular algorithms for adaptive filters are

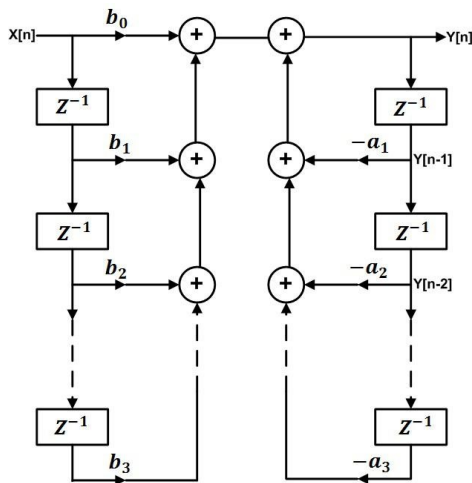


Fig. 5. Direct form 2 IIR filter graphical representation.

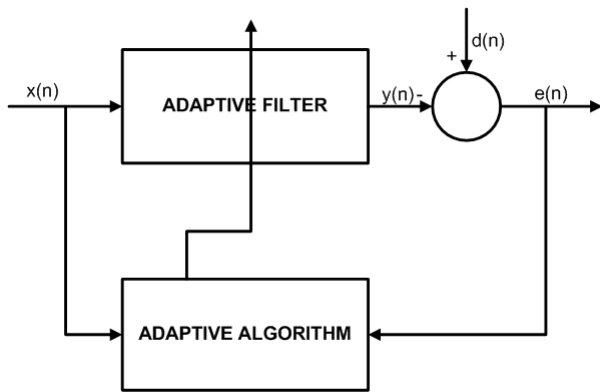


Fig. 6. A graphical representation of adaptive filter.

LMS, NLMS and RLS. Once the signal is filtered and artifacts are removed machine learning algorithms can be used to perform high level tasks such as identification of healthy and non healthy ECG signals or improved visualization of the ECG features (Fig. 7).

IV. ADAPTIVE FILTERING ALGORITHMS

We have implemented and tested four popular adaptive algorithms [16]. These include the Least Mean Square (LMS), Normalized LMS (NLMS), Log LMS and Sign LMS.

A. Least Mean Square (LMS)

LMS minimizes the square of the error and is the most simple and popular adaptive algorithm. LMS algorithm is easy and computationally efficient [17]. The weights are updated using the following operation.

$$W(n+1) = W(n) + 2\mu(x(n))e(n) \quad (3)$$

Where μ is the step size. The step size determines the step of the error to be adjusted [8]. The error signal is expressed as $e(n) = d(n) - y(n)$. The convergence of LMS is slow and the other issue is the selection of step size.

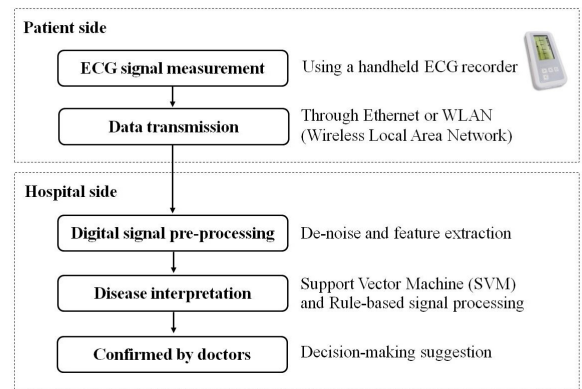


Fig. 7. Typical high level tasks performed by a remote health care system.

B. Normalized Least Mean Square (NLMS)

NLMS algorithm is designed to address the issue of step size selection. In NLMS method, the step size is designed to be adaptive. If the error signal is large then the step size is computed to be large and if the error is small, the step size remains smaller. Initially the step size is chosen to be 0.01 and normalized using the equation (4). NLMS uses variable step size $\mu(n)$ [8].

$$\mu(n) = \frac{a}{(c + \|x(n)\|^2)} \quad (4)$$

$$W(n+1) = W(n) + \mu(n)e(n)x(n) \quad (5)$$

The only difference between NLMS and LMS is the step size. The convergence speed increases in NLMS at a cost of increased computational complexity.

C. Log LMS

Log LMS algorithm is designed for applications where high speed adaptive filters are required such as echo cancellation or ECG de-noising. It is highly desirable to reduce the complexity of the hardware [18]. Log LMS is mathematically expressed as:

$$W(n+1) = W(n) + \mu * Q[e(n)]x(n) \quad (6)$$

where $Q(\cdot)$ denotes the quantization function, which is defined as $Q(\cdot) = 2^{\log(n)} * e(n)$. This filter converts the input signal to a power of two which reduces its complexity.

D. Sign LMS

Instead of quantizing the error, Sign LMS algorithm quantizes the input signal by a simple sign function for faster adaptation. Thus, the Sign LMS filter can be expressed mathematically as:

$$\text{sgn}(x) = \begin{cases} 1 & x < 0 \\ -1 & x > 0 \\ 0 & x = 0 \end{cases} \quad (7)$$

$$W(n + 1) = W(n) + \mu * sgn[x(n)]e(n) \quad (8)$$

In this filter function, the multiplication operation is replaced with shifting operation which makes the algorithm computationally efficient.

In addition to the above algorithms, kernel algorithms based on the reproducing kernel hilbert spaces (RKHS) are popular for non-linear problems. As ECG is a non-linear signal, kernel algorithms are also well suited. LMS algorithms coupled with the Gaussian kernel or polynomial kernel is also applied for ECG signal pre-processing.

E. Feature Extraction

After de-noising, the features can be extracted using discrete wavelet transform [19], principal component analysis [20] (PCA) or independent component analysis [21] (ICA) or any other pattern recognition technique. Some of the common features include R-peak, R-R interval and QRS amplitude. These feature can be fed into any classifier, such as support vector machine [22] or neural networks [23] to classify the ECG signal. In this work, our focus is on the preprocessing of ECG signal based on the fact that if a signal is noise free, it can be more accurately classified.

V. RESULTS AND DISCUSSION

We performed experiments on the ECG signals downloaded from MITDB [5] database. The database is widely used for research on ECG signal processing and analysis for the study of cardiac diseases. Various types of high frequency noises are generated using MATLAB based on the prior knowledge (Fig. 9). Similarly, a reference signal is also generated using MATLAB (Fig. 8). SNR, convergence rate and computation time is used as a performance metric. SNR is calculated using the equation (9).

$$SNR = \frac{P_{signal}}{P_{noise}} \quad (9)$$

Where P_{signal} and P_{noise} represents the average signal power and average noise power respectively. The SNR is converted into decibel using following formula:

$$SNR_{db} = 10 * \log(SNR) \quad (10)$$

The Mean square error (MSE) is used to measure the quality of the estimate of adaptive algorithms. MSE measures the average of the square of the errors.

Table I shows the SNR and time complexity of the four algorithms. These results are the average of five ECG signal. Note that the value of SNR is in decibel and time is in seconds.

Fig. 10, 11, 12 and 13 show the de-noising results of the LMS, NLMS, Log LMS and Sign LMS algorithms, respectively, on a representative ECG signal. These algorithms have eliminated the high frequency noise successfully. Fig. 14, 15 and 16 show the MSE of the LMS, NLMS and Log-LMS algorithm respectively. It can be seen from these figures that NLMS converges more faster than LMS.

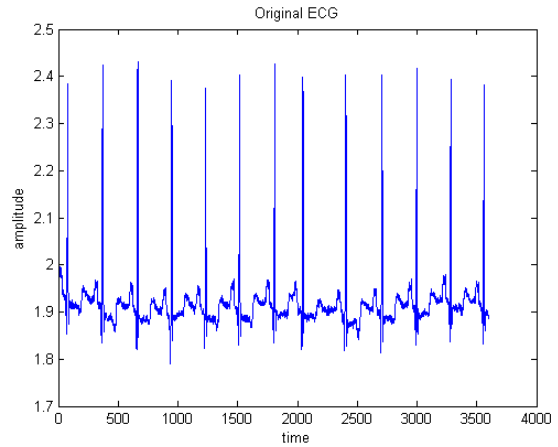


Fig. 8. Reference signal.

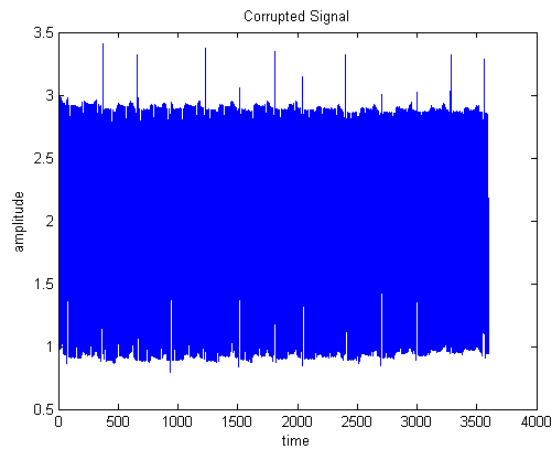


Fig. 9. Corrupted signal.

The time complexity of adaptive algorithms are calculated using MATLAB 2017a. All simulations are performed at Intel (R) Core i5- CPU 4590 @ 3.3GHZ with 8 GB RAM. These results combined with the simulation results of Table I show that the Sign LMS has lower computational complexity and the NLMS has higher SNR.

It can be concluded that different adaptive algorithm have their pros and cons, but based on observations we recommend NLMS for removing the high frequency, because of the highest SNR it has achieved in our experiments.

TABLE I. SNR AND COMPUTATION COMPLEXITY OF DIFFERENT ALGORITHMS.

LMS		NLMS		Log LMS		Sign LMS	
Time	SNR	Time	SNR	Time	SNR	Time	SNR
2.95	11.86	3.05	22.17	2.85	14.5	1.15	16.5

VI. CONCLUSION

Remote health-care systems are becoming increasingly popular that provide time efficient treatment and advanced medical services to remote areas using Internet. ECG signal processing is a key module of these systems. We have evaluated four pre-processing algorithms for ECG noise removal.

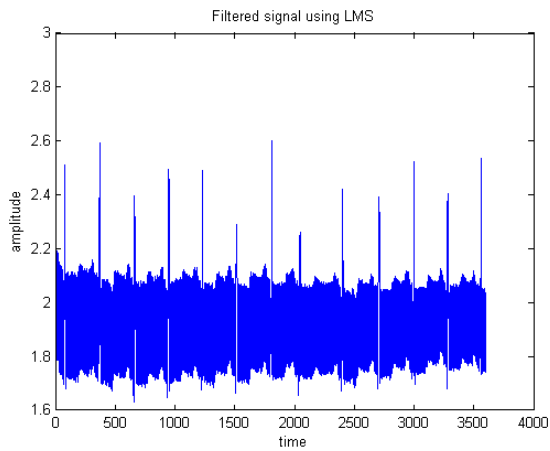


Fig. 10. LMS output.

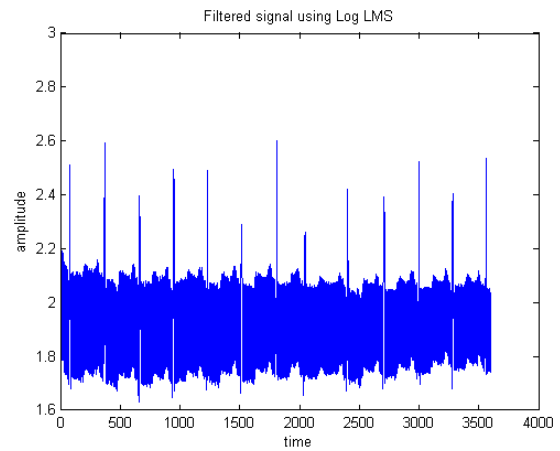


Fig. 12. LOG LMS output.

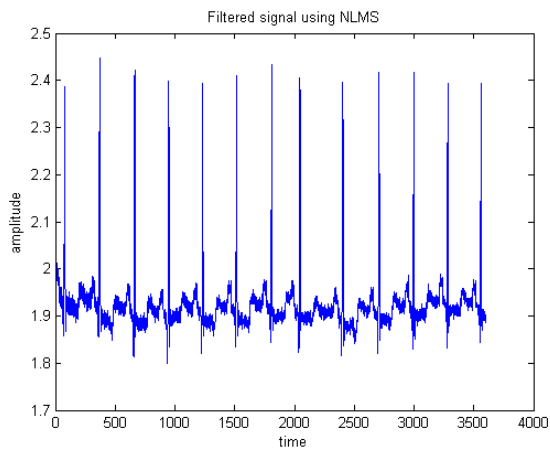


Fig. 11. NLMS Output.

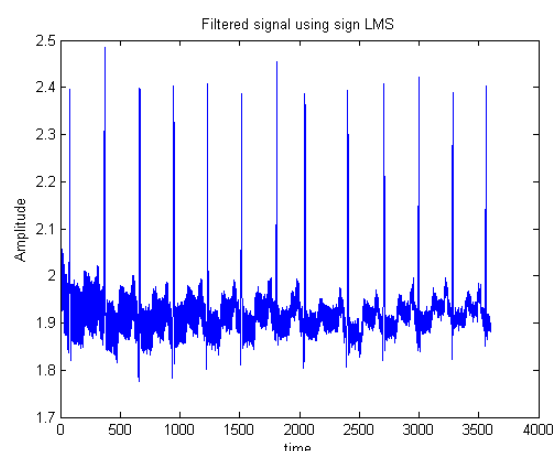


Fig. 13. Sign LMS output.

These techniques can be efficiently utilized to provide a deeper insight of ECG signal processing and can be useful for ECG based remote health systems. Our experiments show that the NLMS algorithm can achieve better SNR compared to other algorithm at a cost of greater computational complexity.

These adaptive algorithms can also be used on other physiological signal such as EEG or EMG. Once the signal is de-noised, we can extract the features and train a classifier for automated ECG analysis. Recently now, deep learning has performed remarkably well on many applications. In the future it will be interesting to see how deep learning methods can be applied to achieve more significant information from the ECG signal and a complete automated ECG analysis system can be realized.

REFERENCES

- [1] Gunther. Eysenbach. What is e-health? *Journal of medical Internet research*, 3(2):e20, 2001.
- [2] VS Chouhan and Sarabjeet Singh Mehta. Total removal of baseline drift from ecg signal. In *Computing: Theory and Applications, 2007. ICCTA'07. International Conference on*, pages 512–515. IEEE, 2007.
- [3] Sapal Tachakra, XH Wang, Robert SH Istepanian, and YH Song. Mobile e-health: the unwired evolution of telemedicine. *Telemedicine Journal and E-health*, 9(3):247–257, 2003.
- [4] Seema Nayak, Dr MK Soni, and Dr Dipali. Bansal. Filtering techniques for ecg signal processing. *International Journal of Research in Engineering & Applied Sciences*, 2(2):671–679, 2012.
- [5] Anton Amann, Robert Tratnig, and Karl Unterkofler. Detecting ventricular fibrillation by time-delay methods. *IEEE Transactions on Biomedical Engineering*, 54(1):174–177, 2007.
- [6] Shen Luo and Paul Johnston. A review of electrocardiogram filtering. *Journal of Electrocardiology*, 43(6):486–496, 2010.
- [7] Rizwan Qureshi, Muhammad Uzair, and Khurram Khurshid. Multistage adaptive filter for ecg signal processing. In *Communication, Computing and Digital Systems (C-CODE), International Conference on*, pages 363–368. IEEE, 2017.
- [8] Hyun-Chool Shin, Ali H Sayed, and Woo-Jin Song. Variable step-size nlms and affine projection algorithms. *IEEE signal processing letters*, 11(2):132–135, 2004.
- [9] Yong Lim and Sydney Parker. Fir filter design over a discrete powers-of-two coefficient space. *IEEE Transactions on Acoustics, Speech, and Signal Processing*, 31(3):583–591, 1983.
- [10] Sadaf Khan, Syed Muhammad Anwar, Waseem Abbas, and Rizwan Qureshi. A novel adaptive algorithm for removal of power line interference from ecg signal. *Science International*, 28(1), 2016.
- [11] JG Proakis. Mdg. *Digital Signal Processing: Principles, Algorithms, and Applications: Prentice-Hall*, 1999.
- [12] Rainer Storn. Differential evolution design of an iir-filter. In *Evolutionary Computation, 1996., Proceedings of IEEE International Conference on*, pages 268–273. IEEE, 1996.

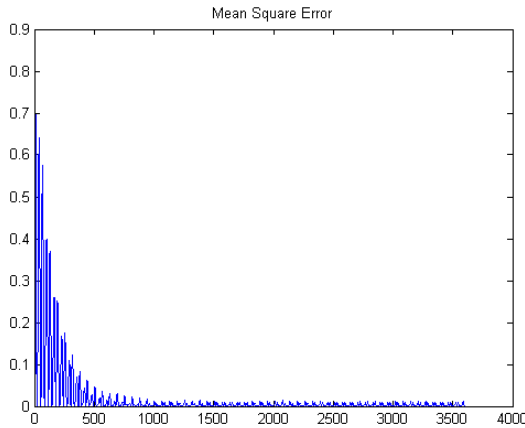


Fig. 14. MSE of NLMS algorithm.

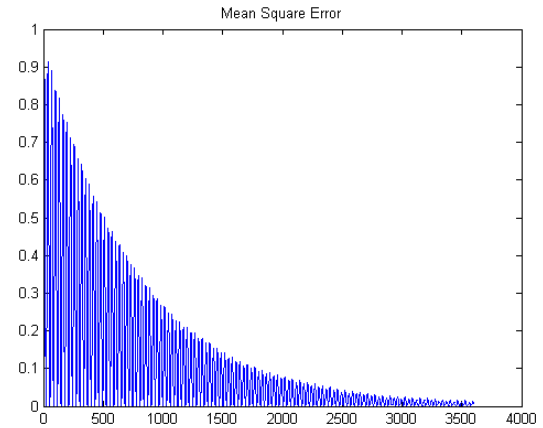


Fig. 16. MSE of Log LMS

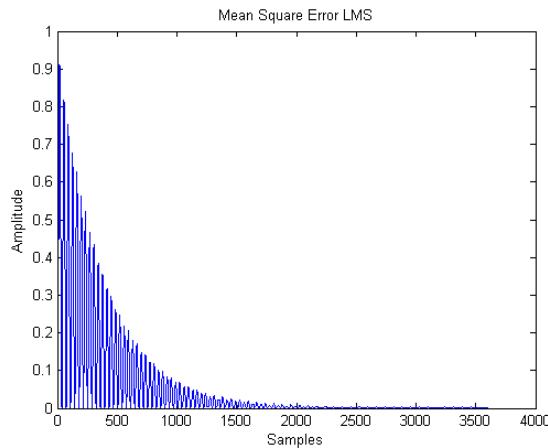


Fig. 15. MSE of LMS algorithm.

independent component analysis in removing artefacts from the electrocardiogram. *Neural Computing & Applications* (105 - 116), 2006.

- [22] Abdelhamid Daamouche. A wavelet optimization approach for ecg signal classification. *Biomedical Signal Processing and Control*, 2012).
- [23] G. Krishna Prasad and J. S. Sahambi. Classification of ecg arrhythmias using multi-resolution analysis and neural networks. In *Conference on convergent technologies for Asia-Pacific region. Vol. 1. IEEE*, TENCON, 2003.

- [13] Jacek M Lkeski and Norbert Henzel. Ecg baseline wander and powerline interference reduction using nonlinear filter bank. *Signal processing*, 85(4):781–793, 2005.
- [14] Syed Zahurul Islam, Syed Zahidul Islam, Razali Jidin, and Mohd Alauddin Mohd Ali. Performance study of adaptive filtering algorithms for noise cancellation of ecg signal. In *Information, Communications and Signal Processing, 2009. ICICS 2009. 7th International Conference on*, pages 1–5. IEEE, 2009.
- [15] Nitish V Thakor and Y-S Zhu. Applications of adaptive filtering to ecg analysis: noise cancellation and arrhythmia detection. *IEEE transactions on biomedical engineering*, 38(8):785–794, 1991.
- [16] Alireza K Ziarani and Adalbert Konrad. A nonlinear adaptive method of elimination of power line interference in ecg signals. *IEEE Transactions on Biomedical Engineering*, 49(6):540–547, 2002.
- [17] Bernard Widrow, John M McCool, Michael G Larimore, and C Richard Johnson. Stationary and nonstationary learning characteristics of the lms adaptive filter. *Proceedings of the IEEE*, 64(8):1151–1162, 1976.
- [18] Evangelos Eleftheriou and D Falconer. Tracking properties and steady-state performance of rls adaptive filter algorithms. *IEEE transactions on acoustics, speech, and signal processing*, 34(5):1097–1110, 1986.
- [19] V. K. Srivastava and Devendra Prasad. Dwt-based feature extraction from ecg signal. *American J. of Eng. Research (AJER)* 2.3 44-50., (2013).
- [20] et al. Castells, Francisco. Principal component analysis in ecg signal processing. *EURASIP Journal on Advances in Signal Processing*, 2007.
- [21] Gari Clifford He, Taigang and Lionel Tarassenko. Application of

Non-Linear EH Relaying in Delay-Transmission Mode over $\eta - \mu$ Fading Channels

Ayaz Hussain^{†1}, Inayat Ali^{†2}, Ramesh Kumar^{††3}, Zahoor Ahmed^{†4}

[†]Department of Electrical Engineering, Balochistan University of Engineering & Technology, Khuzdar, Pakistan

^{††}Department of Electronic Engineering, Dawood University of Engineering & Technology, Karachi, Pakistan

Abstract—Energy harvesting is a technique to harvest energy from RF (radio frequency) waves. The RF signals have the ability to convey energy and information concurrently. The EH in cooperative relaying systems may increase the capacity and coverage of wireless networks. In this work, we study a dual-hop (two-hop) relaying. This system has three nodes: a source, a relay, and a destination. The source and destination have multiple antennas. We account a non-linear EH model and TSR (time-switching-based relaying) protocol at the single-antenna relay node. We evaluate the system performance over $\eta - \mu$ fading channels. With a saturation threshold, a non-linear EH receiver restrains the harvested power. In the TSR protocol, the relay changes mode between the EH and information processing, by which a fraction of time is used with each process. The fading model $\eta - \mu$ incorporates some fading models as notable cases, viz., Nakagami- m , One-sided Gaussian, Nakagami- q (Hoyt), and Rayleigh. The system performance is analyzed in terms of the average capacity and throughput for different saturation threshold power levels, divers antennas arrangements, and different parameter values of η and μ .

Keywords—EH relay; non-linear EH model; $\eta - \mu$ fading; TSR protocol; throughput

I. INTRODUCTION

Energy harvesting (EH) is a technology to gather energy from the surrounding radio frequency (RF) waves and got outstanding recognition to sustain a network lifetime [1]–[14]. The RF signals have an ability to convey energy and information concurrently, therefore, it is possible to collect or harvest the energy from the RF waves and that harvested energy can easily be reserved or used for electronic equipment to work [6].

RF-based EH technology is studied in cooperative relaying networks [2]–[14] (and references therein), where from the received RF signals, a relay node collects energy. Dual-hop (or Two-hop) relaying is a popular technique to obtain greater capacity and larger coverage of wireless networks [14]. There are two well-known methods for relaying data: AF (amplify-and-forward) method and DF (decode-and forward) method. In an AF relay method, a relay of a dual-hop system amplifies the received message of the source node and forwards it to the next receiver or destination. In a DF relay method, the received message at the relay node is decoded first then forwarded to the next receiver or destination. Recently, a lot of research papers are written on energy harvesting in a two-hop DF relaying system in the literature [2]–[14].

There are two main EH protocols for two-hop relaying systems: PSR (power-splitting-based relaying) protocol and

TSR (time switching-based relaying) protocol. The relay alternatively splits the received signal power from the source node and time into two parts in the PSR and TSR protocols, respectively [6]. A non-linearity of an EH relay/receiver restrict the level of the harvested energy because it is not a practical node. The performance of a two-hop DF EH relaying network based on a non-linear mode of EH receiver was investigated for classical fading channels in [6]–[12] and for general $\kappa - \mu$ shadowed and $\eta - \mu$ fading channels, respectively, in [6] and [13]. In [6], a DF EH relaying system was studied based on non-linear EH receiver with hardware impairments and performance was analyzed under $\kappa - \mu$ shadowed fading channels. In [7], the performance of an AF EH relaying system with a non-linear energy harvester for Nakagami- m fading channels was analyzed. A partial DF relay selection scheme with a non-linear energy harvester was investigated in [8]. In [9], using a non-linear EH receiver model, a two-hop relaying system was investigated where multiple-antennas were installed at the destination and source only and performance was analyzed for a different number of antennas. In interference-limited environments of Nakagami- m , the DF relaying system performance with a non-linear energy harvester is analyzed in [10]. In [11], the authors investigated the secrecy performance for a two-hop DF relaying with a non-linear energy harvester. In this system, the best relay is selected using CSI (channel state information) which assists the source to send its message signal to the destination. In [12], an AF non-linear EH relaying system was studied with perfect and imperfect CSI. Recently, a non-linear EH relay receiver in conjunction with the energy harvesting PSR protocol in a two-hop EH relaying for $\eta - \mu$ fading channels was examined in a delay-limited transmission mode [13].

Despite the importance of a delay-tolerant transmission mode and a non-linear EH relay receiver in a two-hop EH cooperative relaying network, the impact on the system performance owing to a non-linear model of EH receiver node (i.e., EH relay receiver) with a TSR protocol in a delay-tolerant transmission mode under $\eta - \mu$ fading channels is not studied yet.

In this paper, in a delay-tolerant transmission mode, the impact on the system performance due to a non-linearity of EH receiver in a two-hop EH relaying is investigated under $\eta - \mu$ fading environments. We consider a TSR method [4] to analyze the system performance in $\eta - \mu$ fading environments. The fading model $\eta - \mu$ is a general model, therefore, from this fading model, some special cases can be obtained with special parameters, viz. Rayleigh, One-sided Gaussian, Hoyt, and Nakagami- m [15]. Therefore, from our results which are

obtained using the general $\eta - \mu$ fading channels, we can figure out some identical and non-identical cases, such as, the Rayleigh/Rayleigh, One-sided Gaussian/One-sided Gaussian, Nakagami- m /Nakagami- m , Hoyt/Hoyt, and combinations of such fading links.

The remaining sections of our paper are sectioned as follows: In Section II, firstly, we give a brief introduction of the considered system model and then we describe the $\eta - \mu$ channel model and its particular cases; in Section III, performance analysis of the assumed system is provided; the identical and non-identical fading cases which are obtained from the $\eta - \mu$ fading scenario are discussed in Section IV; in Section V, based on the obtained expressions, the numerical as well simulated results are given; in the last section, the conclusion of our paper is concluded.

II. SYSTEM AND CHANNEL MODELS

A. System Model

We account a two-hop relaying system which is exhibited in Fig. 1. This system has three nodes, namely a source node S which transmit signals to a relay, a relay node R that transmits received signal to a destination, and a destination node D which receives signals of the source node via the relay node. The multiple-antennas, N_1 and N_2 , respectively, are installed at S and D. A single-antenna relay node has no external source of energy, hence, it harvests or generates energy from the obtained RF waves from the source node and utilizes that generated power to send the information of S to D. A TSR protocol is considered at the relay node [4]. Let \mathbf{h}_1 and \mathbf{h}_2 are the $N_1 \times 1$ and $1 \times N_2$ channel vectors, respectively, of S to R and R to D. For the TSR protocol, the transmission block structure

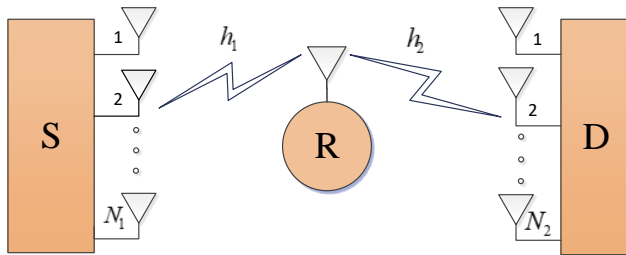


Fig. 1. System model

for information processing and EH is shown in Fig. 2 [4], where block time is designated by T . In the block time T , S transfers the message to D and α shows the fragment of the block time. In a TSR method, R node alternatively switches the received signal in $\alpha : (1-\alpha)T$ proportion. The node R harvests energy in the fragment of α and the rest fragment $(1-\alpha)T$ is separated into two sub-portions; $(1-\alpha)T/2$ is employed for S to R communication and $(1-\alpha)T/2$ is employed for R to D communication. In line with the TSR protocol, the received signals are sent to the information processor and energy harvester for time $(1-\alpha)T/2$ and αT , respectively. The harvested energy for αT is obtained as [8]

$$E_h = \zeta P_s \|\mathbf{h}_1\|^2 \alpha T, \quad (1)$$

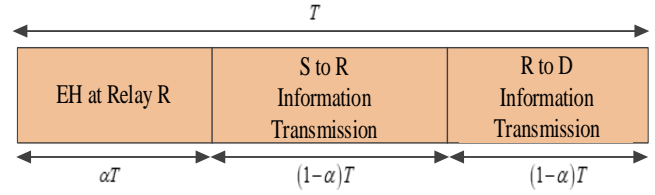


Fig. 2. In the TSR scheme, transmission block structure for EH and information processing [4].

where ζ designates the efficiency of energy conversion and P_s is the power which is transmitted by the source.

We consider a non-linear EH receiver. When the input power of a non-linear EH receiver is above the saturation level of the threshold power P_{th} , it produces a sustained transmit power ζP_{th} [6]. Thus, the relay transmit power, P_r , can be written as [6]

$$P_r = \frac{2\zeta\alpha}{(1-\alpha)} \min\left(P_s \|\mathbf{h}_1\|^2, P_{th}\right). \quad (2)$$

The SNR (signal-to-noise ratio) at the relay node and destination node, are respectively, given by [4] [8]

$$\gamma_R = \frac{P_s \|\mathbf{h}_1\|^2}{\sigma_{a,r}^2 + \sigma_{c,r}^2} \quad (3)$$

and

$$\gamma_D = \begin{cases} \frac{2\alpha\zeta P_s \|\mathbf{h}_1\|^2 \|\mathbf{h}_2\|^2}{(1-\alpha)(\sigma_{a,d}^2 + \sigma_{c,d}^2)}, & P_s \|\mathbf{h}_1\|^2 \leq P_{th}, \\ \frac{2\alpha\zeta P_{th} \|\mathbf{h}_1\|^2}{(1-\alpha)(\sigma_{a,d}^2 + \sigma_{c,d}^2)}, & P_s \|\mathbf{h}_1\|^2 > P_{th}, \end{cases} \quad (4)$$

where $\sigma_{a,r}^2$ and $\sigma_{c,r}^2$ are the noise and convergence variances at the relay node, respectively. Additionally, $\sigma_{a,d}^2$ and $\sigma_{c,d}^2$ are the noise and convergence variances at the destination node, respectively.

TABLE I. THE $\eta - \mu$ DISTRIBUTION AND ITS SPECIAL CASES [13]

Distribution	η	μ
Rayleigh	$\eta \rightarrow 0$	$\mu = 0.5$
Nakagami- m	$\eta \rightarrow 1$	$\mu = m/2$
Hoyt	$\eta \rightarrow q^2$	$\mu = 0.25$

B. The $\eta - \mu$ Channel Model

The $\eta - \mu$ is a general fading model. This fading model incorporates few fading models as notable cases, viz., Nakagami- m , Onw sided Gaussian, Nakagami- q (Hoyt), and Rayleigh [15]. Let γ_ℓ ($\ell = 1, 2$) is the instantaneous SNR of the ℓ th link. The PDF (probability density function) of γ_ℓ ($\ell = 1, 2$) cab be written as [15, eq. (3)]

$$f_{\gamma_\ell}(\gamma) = \frac{2\sqrt{\pi} h_\ell^{N_\ell \mu_\ell}}{\Gamma(N_\ell \mu_\ell) H_\ell^{N_\ell \mu_\ell - 0.5}} \left(\frac{\mu_\ell}{\bar{\gamma}_\ell}\right)^{N_\ell \mu_\ell + 0.5} \gamma^{N_\ell \mu_\ell - 0.5} \times \exp\left(\frac{2\mu_\ell h_\ell}{\bar{\gamma}_\ell} \gamma\right) I_{N_\ell \mu_\ell - 0.5}\left(2\frac{\mu_\ell H_\ell}{\bar{\gamma}_\ell} \gamma\right), \quad (5)$$

herein, η_ℓ and μ_ℓ are the fading parameters, $I_\nu(\cdot)$ denotes the ν -th order of the modified Bessel function of the 1st kind, $h_\ell = (2 + \eta_\ell^{-1} + \eta_\ell)/4$, $H_\ell = (\eta_\ell^{-1} - \eta_\ell)/4$ [15], $I_\nu(\cdot)$ denotes the average SNR of the ℓ -the link, and $\Gamma(\cdot)$ shows the Gamma function.

In Table I, we summarized the special or particular cases of the η - μ fading model where q and m shows the fading parameters of the distributions, respectively, Hoyt and Nakagami- m .

III. PERFORMANCE ANALYSIS

In this section, firstly, the average capacity is described, then based on the average capacity expression, the achievable throughput is eventually obtained.

A. Average Capacity Analysis

The statistical mean of the mutual information between the transmitter (i.e., source) and receiver (i.e., destination) is the average capacity. For a DF EH relaying system, the average capacity can be obtained as [6]

$$\bar{C} = \min(\bar{C}_R, \bar{C}_D) \quad (6)$$

where $\bar{C}_R = \frac{1}{2}E[\log_2(1 + \gamma_R)]$, $\bar{C}_D = \frac{1}{2}E[\log_2(1 + \gamma_D)]$, $E[\cdot]$ denotes the expectation operator, and γ_R and γ_D are given by (3) and (4), respectively.

B. Throughput Analysis

The throughput of a dual EH relaying system with beamforming based on non-linear EH receiver in a mode of a delay-tolerant transmission is provided as [6]

$$\tau = \frac{(1 - \alpha)\bar{C}}{2} \quad (7)$$

Utilizing (7) and with the aid of Matlab, we can acquire the optimal time-switching ratio α^* and the optimal throughput τ^* numerically.

IV. SPECIAL CASES

Some particular cases are included in the η - μ fading model, namely Nakagami- m , Rayleigh, and Hoyt. Hence, the average capacity and throughput expressions for the different fading cases can be obtained from (6) and (7) with special parameters as given in Table I. Subsequently, the possible fading conditions are Rayleigh/Rayleigh, Rayleigh/Nakagami- m , Rayleigh/Hoyt, Nakagami- m /Nakagami- m , Nakagami- m /Rayleigh, Hoyt/Hoyt, Nakagami- m /Hoyt, Hoyt/Rayleigh, and Hoyt/Nakagami- m . These special cases are also discussed in [13, Table II] for delay-limited transmission mode.

V. NUMERICAL RESULTS

TABLE II. THE VALUES OF PARAMETERS USED IN SIMULATION

Parameter	Value	Parameter	Value
1	ζ	5	$\sigma_{c,r}^2$
2	P_s	6	$\sigma_{c,r}^2$
3	λ_1	7	$\sigma_{s,d}^2$
4	λ_2	8	$\sigma_{c,d}^2$

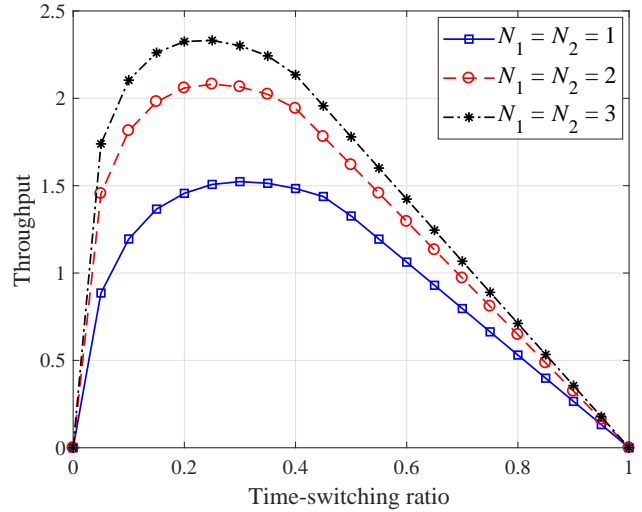


Fig. 3. Throughput against time-switching ratio for different arrangement of antennas when $P_{th} = 3$, $\mu_1 = \mu_2 = 1$, and $\eta_1 = \eta_2 = 0.9$.

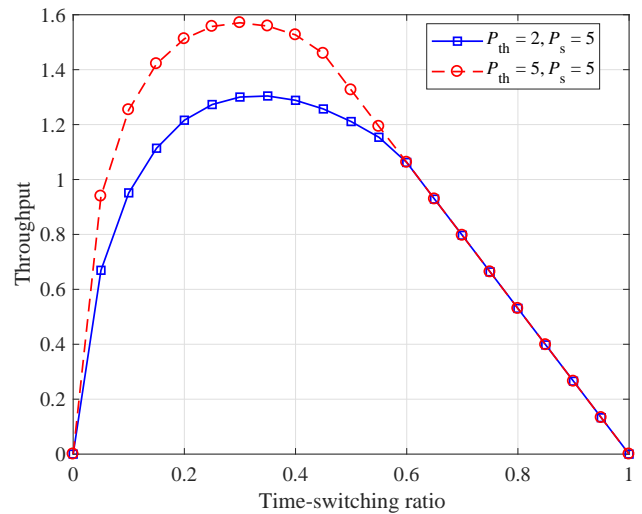


Fig. 4. Throughput against time-switching ratio for saturation threshold power levels, P_{th} , when $\mu_1 = \mu_2 = 1$, $\eta_1 = \eta_2 = 0.9$, and $N_1 = N_2 = 2$.

Here, in Section V, the performance is evaluated of the two-hop EH relaying system that has a non-linear model of EH relay receiver in η - μ fading environment. We set some basic parameters throughout simulations as presented in Table II, unless otherwise stated.

Fig. 3 shows the throughput, τ , against time-switching ratio, α , for divers antennas organizations. As expected, the throughput is increased with increasing the number of antennas. The throughput increases as time-switching ratio, α , grows from 0 to α^* (i.e., a point of optimal-value of the time-switching ratio where the system achieves the maximum throughput), and the value of the throughput lowers as α grows from the optimal-value α^* to 1.

Fig. 4 reveals the average capacity in η - μ fading environment by considering the linear and non-linear energy harvesting receiver when we set $N_1 = N_2 = 2$, $\eta_1 = \eta_2 = 1$,

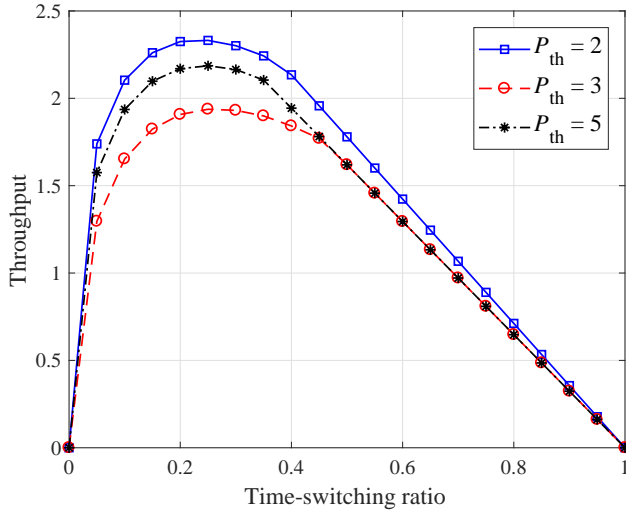


Fig. 5. Throughput against time-switching ratio for saturation threshold power levels, P_{th} , when $\mu_1 = \mu_2 = 1$, $\eta_1 = \eta_2 = 0.9$, and $N_1 = N_2 = 2$.

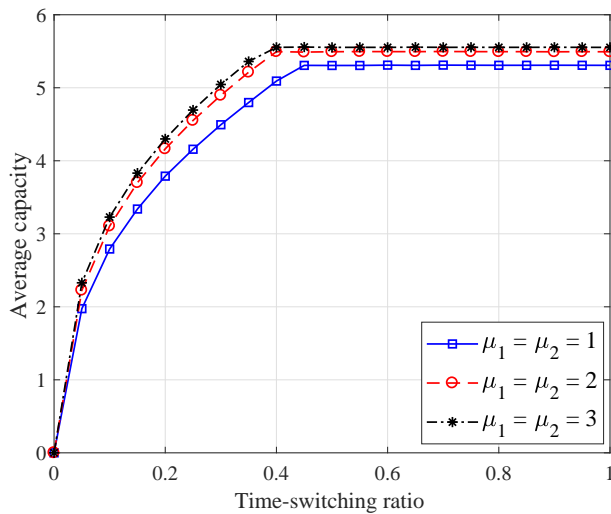


Fig. 6. Average capacity against time-switching ratio for different μ (i.e., μ_1 or μ_2) when $P_{th} = 3$, $N_1 = 2$, $N_2 = 2$, $\eta_1 = 1$ and $\eta_2 = 1$.

and $\mu_1 = \mu_2 = 2$. From Fig. 4. one can notice that the system performance is better with a linear EH relay receiver as compared to a non-linear EH relay receiver. The receiver for energy harvesting is a non-linear node and yields a sustained transmit power ζP_{th} if the given power to the receiver for energy harvesting is at a higher level than a saturation power P_{th} .

In Fig. 5, the performance based on throughput with respect to time-switching ratio is shown for different saturation threshold power levels. From Fig. 5, it is seen that the performance in terms of throughput improves with the saturation level of threshold power P_{th} . The enhancement in the amount of saturation threshold power decreases the probability of saturation of the EH receiver; in fact, the EH receiver of relay need more power to harvest energy.

Fig. 6 exhibits the average capacity performance versus

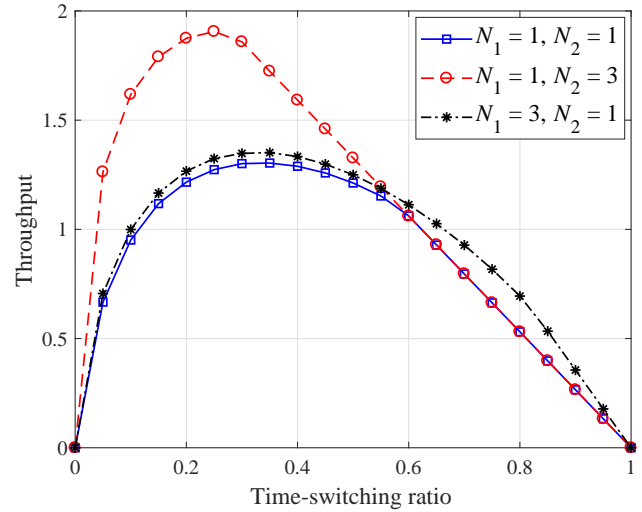


Fig. 7. Throughput performance for various antenna arrangements when $\mu_1 = \mu_2 = 1$, $\eta_1 = \eta_2 = 0.5$, and $P_{th} = 3$.

time-switching ratio for distinct values of μ (μ_1 , μ_2). From this, we perceive that the increment in parameter μ , subsequently, raises the overall performance.

Fig. 7 shows the throughput performance when we set different number of antennas. In a non-linear EH mode, it is seen that the throughput performance is better when we set $N_1 < N_2$ as compared to $N_1 < N_2$.

VI. CONCLUSION

A DF EH cooperative relaying with beamforming that has a non-linear EH relay receiver is studied in $\eta - \mu$ fading environments. We assumed a non-linear EH relay receiver and time switching TSR protocol at the relay node. With respect to the number of antennas, parameter μ , amount of saturation threshold power, we evaluated our system in different environments of $\eta - \mu$ fading. From our obtained results, we concluded that the effect of the saturation level of threshold power can be reduced with beamforming techniques. The special cases of fading channels can be deduced from the general model of $\eta - \mu$ fading, therefore, we can obtain new analytical results for various classical (Rayleigh, Hoyt, and Nakagami- m) and general fading conditions.

ACKNOWLEDGMENT

Our research work is supported and funded by ORIC, Balochistan UET, Khuzdar, Balochistan, Pakistan.

REFERENCES

- [1] X. Lu, P. Wang, D. Niyato, and *et al.*, "Wireless networks with RF energy harvesting: A contemporary survey", *IEEE Commun. Surv. Tutorials*, vol. 17, no. 2, pp. 757–789, 2015.
- [2] A. Hussain, Z. Ahemd, I. Ali, and S.H., Kim, "Energy harvesting relaying network in a delay-tolerant transmission mode over $\kappa - \mu$ shadowed fading channels", *International Journal of Computer Science and Network Security*, vol. 18, no. 3, pp. 119–125, 2018.
- [3] A. Hussain, Z. Ahmed, U. Rajpoot, and *et al.*, "Energy harvesting relaying network with hardware impairments in $\eta - \mu$ fading environment", *International Journal of Computer Science and Network Security*, vol. 18, no. 4, 2018.

- [4] A.A. Nasir, X. Zhou, S. Durrani, and R.A. Kennedy, "Throughput and ergodic capacity of wireless energy harvesting based DF relaying network", proc. IEEE ICC 2014, Sydney, Australia, June 10–14, 2014.
- [5] O.S. Badarneh, F.S. Almeahmadi, I.S. Ansari, and X. Yang, "Wireless energy harvesting in cooperative decode-and-forward relaying networks over mixed generalized $\eta - \mu$ and $\kappa - \mu$ fading channels", Transaction on Emerging Telecommunication Technology, DOI: 10.1002/ett.3262, pp.1–18, 2017.
- [6] A. Hussain, S.-H. Kim, and S.-H. Chang, "Non-linear energy harvesting relaying with beamforming and hardware impairments in $\kappa - \mu$ shadowed fading environment", Transactions on Emerging Telecommunication Technology, <https://doi.org/10.1002/ett.3303>, 2018.
- [7] Y. Dong, M.J. Hossain, and J. Cheng, "Performance of wireless powered amplify and forward relaying over Nakagami- m fading channels with nonlinear energy harvester", IEEE Commun Lett., vol.20, no.4, pp.672–675, 2016.
- [8] T.M. Hoang, T.T. Duy, and V.N.Q. Bao, "On the performance of non-linear wirelessly powered partial relay selection networks over Rayleigh fading channels", proc. 3rd NICS 2016, Danang, Vietnam, September 14–16, 2016.
- [9] J. Zhang, and G. Pan "Outage analysis of wireless-powered relaying MIMO systems with non-linear energy harvesters and imperfect CSI", IEEE ACCESS, vol.4, no., pp.7046–7053, 2016.
- [10] A. Cvetkovic, V. Blagojevic, and P. Ivaniš, "Performance analysis of nonlinear energy-harvesting DF relay system in interference-limited Nakagami- m fading environment", ETRI Journal, vol.39, no., pp.803–812, 2017.
- [11] J. Zhang, G. Pan and Y. Xie "Secrecy outage performance for wireless-powered relaying systems with nonlinear energy harvesters", Front. Inform. Technol. Electron. Engg., vol.18, no.2, pp.246–252, 2017.
- [12] K. Wang, Y. Li, Y. Ye, and H. Zhang "Dynamic power splitting schemes for non-Linear EH relaying networks: perfect and imperfect CSI", Proc. VTC2017-Fall, Toronto, Canada September 24–27, 2017,
- [13] A. Hussain, N.H. Phulpoto U. Rajput, F. Abbas, and Z. A. Baloch, "Non-Linear energy harvesting Dual-hop DF relaying system over $\eta - \mu$ fading channels", International Journal of Advanced Computer Science and Applications (IJACSA), vol.9, no.6, pp.423–426, 2018.
- [14] A. Hussain, S.-H. Kim, and S.-H. Chang, "Dual-hop variable-gain AF relaying with beamforming over $\kappa - \mu$ shadowed fading channels", proc. IEEE GLOBECOM 2016, Washington DC, USA, December 6–8, 2016.
- [15] A. Hussain, S.-H. Kim, and S.-H. Chang, "On the performance of dual-hop variable-gain AF relaying with beamforming over $\eta - \mu$ fading channels", IEICE Transactions on Communications, vol.E100.B, no.4, pp.619–626, 2017.

Exploring Mechanisms for Pattern Formation through Coupled Bulk-Surface PDEs in Case of Non-linear Reactions

Muflih Alhazmi

School of Mathematical and Physical Sciences, University of Sussex,
Pevensey 2 Building, Falmer Campus, Brighton BN1 9QH, UK
Mathematics Department, Faculty of Science, Northern Border University, Arar, KSA

Abstract—This work explores mechanisms for pattern formation through coupled bulk-surface partial differential equations of reaction-diffusion type. Reaction-diffusion systems posed both in the bulk and on the surface on stationary volumes are coupled through linear Robin-type boundary conditions. The presented work in this paper studies the case of non-linear reactions in the bulk and surface, respectively. For the investigated system is non-dimensionalised and rigorous linear stability analysis is carried out to determine the necessary and sufficient conditions for pattern formation. Appropriate parameter spaces are generated from which model parameters are selected. To exhibit pattern formation, a coupled bulk-surface finite element method is developed and implemented. The numerical algorithm is implemented using an open source software package known as deal.II and show computational results on spherical and cuboid domains. Also, theoretical predictions of the linear stability analysis are verified and supported by numerical simulations. The results show that non-linear reactions in the bulk and surface generate patterns everywhere.

Keywords—Bulk-surface; Reaction-diffusion; Finite-Element-Method (FEM); Partial Differential Equations (PDEs)

I. INTRODUCTION

Most biological and chemical processes that can be explored through reaction and diffusion of chemical species are often modelled by systems of partial differential equations (PDEs) [1]–[3]. A special class of these are reaction-diffusion equations, which are used to analyse and quantify various biological processes such as the natural evolution of pattern formation on animal coats, developmental embryology, immunology, ecological dynamics [4]–[7]. The study of reaction-diffusion systems in general has been and continues to be an interesting topic for research in various branches of scientific studies. In order to quantify the evolution of chemical reaction kinetics associated to biological processes, it is a usual approach to employ a system of partial differential equations describing the chemical reactions, which is investigated through mathematical techniques to reveal the long-term behaviour of the evolving kinetics [8], [9].

Alan Turing was one of the first scientists to suggest in 1952 the use of a system of reaction-diffusion equations to model how two or more chemical substances evolve when they are simultaneously subject to a specific reaction rate and each one of them diffuses independently of the other. Alan Turing suggested that the theory of biological pattern formation can be mathematically formulated by a system of partial

differential equations [10]. The study in [11] is a theoretical set-up through coupling reaction-diffusion system to provide insight on trajectory of a particle during the process of bulk excursion, when it unbinds from the surface without a regular occurrence.

Turing's theory suggests that pattern formation occurs, when a system experiences diffusion-driven instability [10], [12], which is a concept that is hypothetically responsible for the emergence of spatial variation in the concentration density of a chemical species. Diffusion-driven instability takes place in the evolution of a system, when a uniform stable steady state is destabilised by including the effects of the diffusion process in the system. It is a non-trivial property of the diffusion operator that it can be responsible to destabilise a stable steady state of a system of partial differential equations, because a diffusion operator by itself has the property to homogenise small spatial perturbations, therefore, intuitively if diffusion is added to a system of reaction kinetics that is stable in the absence of diffusion, then small perturbations near a uniform steady state are expected to ensure that the evolution of the reaction-kinetics converges to the uniform steady state.

Researchers in applied mathematics and computational science also explore bulk-surface reaction-diffusion systems (BSRDSs), which are employed in special kinds of models for biological processes, where species react and diffuse in the bulk of a domain and these are coupled with other species that react and diffuse on the surface of the domain. Bulk-surface reaction-diffusion systems are employed as a framework to model the chemical interaction of bulk-surface problems arising in cell biology [13]. In particular the framework proposed by [13] aims to provide improved computational and algorithmic efficiency, which is mainly achieved, through employing the usual diffusion on local tangential planes as an approximation of Laplace-Beltrami operator. The framework proposed by [13] is applied to a realistic cell-like geometry, which produces results that are in agreement with quantitative experimental analysis on fluorescence-loss in photo-bleaching. Another example of a computational approach to solving coupled systems of BSRDEs is the work presented in [14], where they proposed a computational approach to bulk-surface reaction-diffusion systems on time-dependent domains.

In general there are two main aspects to the study of bulk-surface reaction-diffusion equations. The first approach is to solve systems of bulk-surface numerically. Finite element

method is the usual choice of the numerical method in the literature, for example there is a detailed study in [15], suggesting some results on the numerical analysis, existence and convergence of finite element approximation when bulk-surface reaction-diffusion equations (BSRDEs) are posed with Robin-type boundary conditions. A priori error bounds on the finite element approximate numerical solution are also both derived in certain norms and verified numerically. The work in [15] is concentrated mainly on the numerical analysis side of the particular scheme they present, which lacks to provide any insight on the stability analysis of the proposed system. Though, it is a reasonable decision to exclude stability analysis due to consistency and relevance of contents, however with improvements in computational efficiency of BSRDEs, it is crucial that attention is given to stability analysis of such systems.

Bulk-surface systems with a single PDE posed in the bulk and coupled with another PDE on the surface also play a vital role in the understanding the interaction of receptor-ligand in the process of a signalling cascade [16]. In [16] the existence of solutions is proven with some computational results associated to the theoretical problem, again lacking to provide insight on the stability behaviour of the dynamics modelled by the coupled system. Even though the results achieved in [16] are mathematically sound from a numerical analysis and computational viewpoint, it would provide a complementary back-up to the work if it is equipped with detailed results of stability analysis.

Stability and bifurcation analysis are two other usual analytical approaches to understanding the dynamical properties of reaction-diffusion system near a uniform steady state [17]–[21]. It is evident from the literature on the subject of stability analysis that a very limited amount of work is done on stability analysis in a coupled bulk-surface set-up. This is mainly due to the extensive complexity associated in deriving the relevant conditions for diffusion-driven instability when equations from the bulk are coupled with equations on the surface. One of the first detailed studies on stability analysis of BSRDEs is conducted in [20], where it is analytically proven that a certain suitable parameter range exists for equations in the bulk that can induce spatial pattern on the surface.

Coupled systems of bulk-surface reaction-diffusion equations (BSRDEs) are one of the several generalisations of reaction-diffusion theory to explore numerous applications in mathematical biology. Processes that involve bulk-surface reaction and/or diffusion are found in various research disciplines such as experimental research in organic chemistry, where a bulk-surface photografting process is used as an efficient tool to create thick grafted layers of hydrophobic polymers in a very short span of time [22], [23].

Bulk-surface reaction kinetics are also used to investigate the behaviour of chemical reactions in the interior of a cell, and to explore how a set of specific reaction kinetics in the interior of a cell evolve to influence the surface of the cell [24]. We also find bulk-surface reaction-diffusion equations that model a particular aspect of cellular functions with relevance to chemical signalling. In [25] a detailed mathematical model is developed for this particular investigation, to explore the dynamics of pattern formation in the consequences of bulk-surface coupling reaction kinetics. Moreover, bulk-surface

reaction-diffusion equations help to reveal the mechanism of symmetry breaking which is one of the essential steps before the emergence of polarisation of biological cells or buds in yeast cells, the direction of cell motility [25].

Bulk-surface reaction-diffusion system are also used to model how surface active agents (surfactants) evolve on the surface of a system, in which the chemical concentration is coupled through a given reaction with the substance in the bulk [26]. BSRDSs also arise in mathematical models for the dynamics of lipid raft formation on biological membranes [27], where the formation of the layer on a biological membrane is modelled as the consequence of coupling conditions with species that react and diffuse in the bulk. A further example of biological application employing bulk-surface reaction-diffusion systems is presented in [28], where they model the mediation of cellular metabolism and signalling in part by trans-membrane receptors that undergo the process of diffusion in cell membrane. From the variety of applications that employ BSRDSs, one realises that a robust study of such systems can provide solutions to a great number of important questions in mathematical biology. This in turn requires in-depth and rigorous study of BSRDSs in an attempt to achieve extensive insight on the evolving properties of these models. Most of the published work presented in the current section on the study of BSRDSs either investigate an over-simplified case scenario with the aim of mathematical tractability or a complex model with limitations on the robustness of analytical and numerical findings.

In this paper, the presented study is motivated to explore BSRDSs with a realistic degree of complexity through a four-component reaction-diffusion system, two of which are posed on the surface and the other two are posed the bulk. The equations in the bulk and on the surface also satisfy coupling conditions through the evolution dynamics on the surface is influenced by the reaction-diffusion process inside the bulk. It can prove of great importance to obtain insight on the pattern formation properties of such systems. The tools to achieve this in the current thesis are the combined application of linear stability theory, mode isolation and the finite element method.

The remaining part of the paper is organised as follows. Section 2 a study is conducted through the application of rigorous linear stability theory which is applied to analytically explore and predict the pattern formation properties associated to the adopted bulk-surface reaction-diffusion system. This is done through investigating the necessary conditions for diffusion-driven instability for the system. Section 3 presents deriving a set of sufficient conditions for diffusion-driven instability, which complements the necessary conditions of the previous section in order to insure that spatial pattern is obtained. In Section 4 the theoretical formulation for the finite element method is presented for the investigated system. Section 5 contains the numerical simulations obtained using Deal.II library to verify the analytical predictions associated to the pattern formation properties for the three systems. Finally, Section 6 concludes the presented work in this paper.

II. ANALYSIS OF COUPLED SYSTEM OF BULK-SURFACE REACTION-DIFFUSION EQUATIONS

In this section, we formulate and present the coupled systems of bulk-surface reaction-diffusion equations on stationary

volumes, in which two of the equations are posed in the bulk and coupled with two other equations that are posed on the surface bounding the corresponding stationary volume. Reaction-diffusion systems posed both in the bulk and on the surface are coupled through linear Robin-type boundary conditions.

For the investigated system we analyse non-linear reaction kinetics both in the bulk and on the surface. The details of the scaling process that makes the system studied in this paper dimensionless is presented. Also, linear stability analysis is carried out both in the absence and presence of diffusion, the necessary and sufficient conditions for steady state to be stable are derived in the absence of diffusion. In the presence of diffusion, the necessary conditions for diffusion-driven instability are derived. The theoretical results for this system show that the bulk dynamics and the surface dynamics drive pattern formation.

Let $\Omega \subset \mathbb{R}^3$ be a stationary domain with boundary that is a compact hyper-surface denoted by $\Gamma \subset \mathbb{R}^2$. Let $u : \Omega \times (0, T] \rightarrow \mathbb{R}$ and $v : \Omega \times (0, T] \rightarrow \mathbb{R}$ denote the concentration of two chemical species which react and diffuse in Ω . Let $r : \Gamma \times (0, T] \rightarrow \mathbb{R}$ and $s : \Gamma \times (0, T] \rightarrow \mathbb{R}$ denote two chemical species residing on the surface.

When the species from the bulk and surface are coupled only through the reaction kinetics and there is no cross-diffusion, it means that all four species diffuse independently of each other, which can be written in dimensional form with independent diffusion rates as follows:

$$\begin{cases} \begin{cases} u_t = D_u \Delta u + f(u, v), \\ v_t = D_v \Delta v + g(u, v), \\ r_t = D_r \Delta_\Gamma r + f(r, s) - h_1(u, v, r, s), \\ s_t = D_s \Delta_\Gamma s + g(r, s) - h_2(u, v, r, s), \end{cases} & \text{in } \Omega \times (0, T] \\ \begin{cases} r_t = D_r \Delta_\Gamma r + f(r, s) - h_1(u, v, r, s), \\ s_t = D_s \Delta_\Gamma s + g(r, s) - h_2(u, v, r, s), \end{cases} & \text{on } \Gamma \times (0, T] \end{cases} \quad (1)$$

with coupling boundary conditions

$$\begin{cases} \frac{\partial u}{\partial \nu} = h_1(u, v, r, s), \\ d_\Omega \frac{\partial v}{\partial \nu} = h_2(u, v, r, s), \end{cases} \quad \text{on } \Gamma \times (0, T]. \quad (2)$$

where, Ω is a three dimensional fixed domain bounded by a compact surface denoted by Γ , which means that it is a boundary-free connected and closed surface. The strictly positive constants $D_u > 0$, $D_v > 0$, $D_r > 0$ and $D_s > 0$ the independent diffusion rates corresponding to the variables indicated in the respective subscripts of each D .

We assume $f(.,.)$ and $g(.,.)$ to be non-linear functions. The coupling conditions of the system is represented by h_1 and h_2 which are functions of u, v, r and s . h_1 and h_2 denote reactions of substances through boundary interface, therefore they depend on all four species namely u, v, r and s .

We explicitly define $h_1(u, v, r, s)$ and $h_2(u, v, r, s)$ to be

$$h_1(u, v, r, s) = \alpha_1 r - \beta_1 u - \kappa_1 v \quad (3)$$

$$h_2(u, v, r, s) = \alpha_2 s - \beta_2 u - \kappa_2 v. \quad (4)$$

The constants $\alpha_1, \alpha_2, \beta_1, \beta_2, \kappa_1$ and κ_2 are positive parameters of system (1). We also assume that from all the species we initially have some positive quantity present, which we denote

by u^0, v^0, r^0 and s^0 , which provides the initial conditions for system (1) written as

$$\begin{aligned} u(\mathbf{x}, 0) &= u^0(\mathbf{x}), & v(\mathbf{x}, 0) &= v^0(\mathbf{x}), \\ r(\mathbf{x}, 0) &= r^0(\mathbf{x}), & \text{and } s(\mathbf{x}, 0) &= s^0(\mathbf{x}). \end{aligned}$$

In this system, we focus on the widely known *activator-depleted* model also known as the Brusselator model where the reaction kinetics are non-linear, given by

$$\begin{aligned} f(u, v) &= k_1 - k_2 u + k_3 u^2 v, & \text{and} & \\ g(u, v) &= k_4 - k_3 u^2 v, \end{aligned} \quad (5)$$

with positive parameters k_1, k_2, k_3 and k_4 .

A. Non-Dimensionalisation

The system of equations is non-dimensionalised using a specific scale, in space or time, for observing the prospective solution within the specified scale range. In the new system after non-dimensionalisation, the variables and parameters are all unitless and the parameters will be fewer than in system (1). The non-dimensional variables is introduced with a hat and these are written as $\hat{u}, \hat{v}, \hat{r}$ and \hat{s} with the corresponding scaling factors u^*, v^*, r^* and s^* , respectively. The process of non-dimensionalisation is only represented for the bulk-equations in three spatial dimensions, and the process is identical to non-dimensionalise the surface equations where a two-dimensional surface is embedded in three dimensional space. We choose L to denote the scaling factor for length (L_b for the bulk and L_s for the surface) and t^* to denote the scaling factor for time (t_b^* for the bulk and t_s^* for the surface), The dimensional and the non-dimensional variables are related through

$$u = u^* \hat{u}, \quad v = v^* \hat{v}, \quad r = r^* \hat{r}, \quad s = s^* \hat{s},$$

where for the bulk we use the scaling given by

$$x = L_b \hat{x}, \quad y = L_b \hat{y}, \quad z = L_b \hat{z}, \quad t = t_b^* \tau$$

and for the surface equations we use

$$x = L_s \hat{x}, \quad y = L_s \hat{y}, \quad z = L_s \hat{z}, \quad t = t_s^* \tau.$$

We substitute for each dimensional variable its corresponding product of non-dimensional variable and the scaling factor leading to

$$\frac{u^*}{t_b^*} \frac{\partial \hat{u}}{\partial \tau} = D_u \frac{u^*}{L_b^2} \Delta \hat{u} + k_1 - k_2 u^* \hat{u} + k_3 u^{*2} v^* \hat{u}^2 \hat{v}, \quad (6)$$

$$\frac{v^*}{t_b^*} \frac{\partial \hat{v}}{\partial \tau} = D_v \frac{v^*}{L_b^2} \Delta \hat{v} + k_4 - k_3 u^{*2} v^* \hat{u}^2 \hat{v}, \quad \text{in } \hat{\Omega} \times (0, \hat{T}] \quad (7)$$

$$\begin{aligned} \frac{r^*}{t_s^*} \frac{\partial \hat{r}}{\partial \tau} &= D_r \frac{r^*}{L_s^2} \Delta_\Gamma \hat{r} + k_1 - k_2 r^* \hat{r} + k_3 r^{*2} \hat{r}^2 s^* \hat{s} - \\ &\alpha_1 r^* \hat{r} + \beta_1 u^* \hat{u} + \kappa_1 v^* \hat{v}, \end{aligned} \quad (8)$$

$$\begin{aligned} \frac{s^*}{t_s^*} \frac{\partial \hat{s}}{\partial \tau} &= D_s \frac{s^*}{L_s^2} \Delta_\Gamma \hat{s} + k_4 - k_3 r^{*2} \hat{r}^2 s^* \hat{s} - \alpha_2 s^* \hat{s} + \\ &\beta_2 u^* \hat{u} + \kappa_2 v^* \hat{v}, \quad \text{on } \hat{\Gamma} \times (0, \hat{T}] \end{aligned} \quad (9)$$

where $\hat{\Omega}$ and $\hat{\Gamma}$, respectively denote unit cube and its six sided surface. The scaling \hat{T} denotes the final time for the non-dimensional system.

Multiplying (6), (7), (8) and (9) by $\frac{t_b^*}{u^*}$, $\frac{t_b^*}{v^*}$, $\frac{t_s^*}{r^*}$ and $\frac{t_s^*}{s^*}$, respectively provided that u^* , v^* , r^* and s^* are non-zero. We may choose to define $t_b^* = \frac{L_b^2}{D_u}$ and $t_s^* = \frac{L_s^2}{D_r}$ and factoring out some parameters will result in writing the system as:

$$\left\{ \begin{array}{l} \left\{ \begin{array}{l} \frac{\partial \hat{u}}{\partial \hat{\tau}} = \Delta \hat{u} + \frac{L_b^2 k_2}{D_u} \left[\frac{k_1}{k_2 u^*} - \hat{u} + \frac{k_3}{k_2} u^{*2} v^* \hat{u}^2 \hat{v} \right], \\ \frac{\partial \hat{v}}{\partial \hat{\tau}} = d_\Omega \Delta \hat{v} + \frac{L_b^2 k_2}{D_u} \left[\frac{k_4}{k_2 v^*} - \frac{k_3}{k_2} u^{*2} \hat{u}^2 \hat{v} \right], \\ \text{in } \hat{\Omega} \times (0, \hat{T}] \end{array} \right. \\ \left\{ \begin{array}{l} \frac{\partial \hat{r}}{\partial \hat{\tau}} = \Delta_\Gamma \hat{r} + \frac{L_s^2 k_2}{D_r} \left[\frac{k_1}{r^* k_2} - \hat{r} + \frac{k_3}{k_2} r^{*2} s^* \hat{r}^2 \hat{s} - \frac{\alpha_1}{k_2} \hat{r} + \frac{u^*}{r^* k_2} \beta_1 \hat{u} + \frac{v^*}{r^* k_2} \kappa_1 \hat{v} \right], \\ \frac{\partial \hat{s}}{\partial \hat{\tau}} = d_\Gamma \Delta_\Gamma \hat{s} + \frac{L_s^2 k_2}{D_r} \left[\frac{k_4}{s^* k_2} - \frac{k_3}{k_2} r^{*2} \hat{r}^2 \hat{s} - \frac{\alpha_2}{k_2} \hat{s} + \frac{u^*}{s^* k_2} \beta_2 \hat{u} + \frac{v^*}{s^* k_2} \kappa_2 \hat{v} \right], \\ \text{on } \hat{\Gamma} \times (0, \hat{T}] \end{array} \right. \end{array} \right. \quad (10)$$

where $d_\Omega = \frac{D_v}{D_u}$ and $d_\Gamma = \frac{D_s}{D_r}$ express the non-dimensional positive ratios of diffusion parameters. Requiring the terms $\frac{k_3}{k_2} u^{*2} = 1$ and $\frac{k_3}{k_2} r^{*2} = 1$ to be non-dimensional respectively imply defining $u^* = \sqrt{\frac{k_2}{k_3}}$ and $r^* = \sqrt{\frac{k_2}{k_3}}$. The scaling factors v^* and s^* through a similar process may be derived as

$$\begin{aligned} \frac{k_3}{k_2} \sqrt{\frac{k_2}{k_3}} v^* = 1 &\Rightarrow v^* = \sqrt{\frac{k_2}{k_3}} \quad \text{and} \\ \frac{k_3}{k_2} \sqrt{\frac{k_2}{k_3}} s^* = 1 &\Rightarrow s^* = \sqrt{\frac{k_2}{k_3}}. \end{aligned} \quad (11)$$

Substituting (12) in system (10) results in

$$\left\{ \begin{array}{l} \left\{ \begin{array}{l} \frac{\partial \hat{u}}{\partial \hat{\tau}} = \Delta \hat{u} + \gamma_\Omega [a_2 - \hat{u} + \hat{u}^2 \hat{v}], \\ \frac{\partial \hat{v}}{\partial \hat{\tau}} = d_\Omega \Delta \hat{v} + \gamma_\Omega [b_2 - \hat{u}^2 \hat{v}], \\ \frac{\partial \hat{r}}{\partial \hat{\tau}} = \Delta_\Gamma \hat{r} + \gamma_\Gamma [a_2 - \hat{r} + \hat{r}^2 \hat{s} - \rho_3 \hat{r} + \mu \hat{u} + \delta_2 \hat{v}], \\ \frac{\partial \hat{s}}{\partial \hat{\tau}} = d_\Gamma \Delta_\Gamma \hat{s} + \gamma_\Gamma [b_2 - \hat{r}^2 \hat{s} - \rho_4 \hat{s} + \mu_1 \hat{u} + \delta_3 \hat{v}], \\ \text{on } \hat{\Gamma} \times (0, \hat{T}] \end{array} \right. \end{array} \right. \quad (12)$$

where the new dimensionless parameters $\gamma_\Omega = \frac{L_b^2 k_2}{D_u}$, $\gamma_\Gamma = \frac{L_s^2 k_2}{D_r}$, $a_2 = \frac{k_1 \sqrt{\frac{k_3}{k_2}}}{k_2}$, $b_2 = \frac{k_4 \sqrt{\frac{k_3}{k_2}}}{k_2}$, $\rho_3 = \frac{\alpha_1}{k_2}$, $\rho_4 = \frac{\alpha_2}{k_2}$, $\mu = \frac{\beta_1}{k_2}$, $\mu_1 = \frac{\beta_2}{k_2}$, $\delta_2 = \frac{\kappa_1}{k_2}$ and $\delta_3 = \frac{\kappa_2}{k_2}$ are defined as a consequence of the scaling choice used for u^* , v^* , r^* and s^* .

The boundary and initial conditions are non-dimensionalised through the same choice of scaling factors for all variables. For notational convenience we drop all the hats from the non-dimensional variables to obtain the full system of BSRDEs given by (1) in its non-dimensional form as

$$\left\{ \begin{array}{l} \left\{ \begin{array}{l} \frac{\partial u}{\partial t} = \Delta u + \gamma_\Omega [a_2 - u + u^2 v], \\ \frac{\partial v}{\partial t} = d_\Omega \Delta v + \gamma_\Omega [b_2 - u^2 v], \\ \frac{\partial r}{\partial t} = \Delta_\Gamma r + \gamma_\Gamma [a_2 - r + r^2 s - \rho_3 r + \mu u + \delta_2 v], \\ \frac{\partial s}{\partial t} = d_\Gamma \Delta_\Gamma s + \gamma_\Gamma [b_2 - r^2 s - \rho_4 s + \mu_1 u + \delta_3 v], \\ \text{on } \Gamma \times (0, T] \end{array} \right. \end{array} \right. \quad (13)$$

with linear boundary conditions

$$\left\{ \begin{array}{l} \nabla u \cdot \nu = \gamma_\Gamma [\rho_3 r - \mu u - \delta_2 v], \\ d_\Omega \nabla v \cdot \nu = \gamma_\Gamma [\rho_4 s - \mu_1 u - \delta_3 v]. \end{array} \right. \quad \text{on } \Gamma \times (0, T], \quad (14)$$

The non-dimensional initial conditions for all equations are given by

$$\begin{aligned} u(\mathbf{x}, 0) &= u^0(\mathbf{x}), \quad v(\mathbf{x}, 0) = v^0(\mathbf{x}), \\ r(\mathbf{x}, 0) &= r^0(\mathbf{x}) \quad \text{and} \quad s(\mathbf{x}, 0) = s^0(\mathbf{x}). \end{aligned}$$

The parameter γ_Ω is known as the reaction scaling parameter in the bulk and γ_Γ is the reaction scaling parameter on the surface and both are non-dimensional.

B. Linear Stability Analysis in the Absence of Diffusion

Definition 2.1: (Uniform steady state): [10], [29] A point (u_0, v_0, r_0, s_0) is a uniform steady state of the coupled system of bulk-surface reaction-diffusion equations (13) if it solves the nonlinear algebraic system given by

$f_i(u_0, v_0, r_0, s_0) = 0$, for all $i = 1, 2, 3, 4$ and satisfies the boundary conditions given by (14).

We derive the uniform steady state by solving the algebraic system

$$f_1(u, v, r, s) = \gamma_\Omega (a_2 - u + u^2 v) = 0, \quad (15)$$

$$f_2(u, v, r, s) = \gamma_\Omega (b_2 - u^2 v) = 0, \quad (16)$$

$$f_3(u, v, r, s) = \gamma_\Gamma (a_2 - r + r^2 s - \rho_3 r + \mu u + \delta_2 v) = 0, \quad (17)$$

$$f_4(u, v, r, s) = \gamma_\Gamma (b_2 - r^2 s - \rho_4 s + \mu_1 u + \delta_3 v) = 0, \quad (18)$$

such that the boundary conditions given by (14) are also satisfied

$$\gamma_\Gamma [\rho_3 r - \mu u - \delta_2 v] = 0, \quad (19)$$

$$\gamma_\Gamma [\rho_4 s - \mu_1 u - \delta_3 v] = 0. \quad (20)$$

We add (15) and (16) to obtain

$$a_2 - u_0 - u_0^2 v_0 + b_2 - u_0^2 v_0 = 0 \Rightarrow u_0 = a_2 + b_2. \quad (21)$$

Upon substituting u_0 into (16), we find

$$v_0 = \frac{b_2}{(a_2 + b_2)^2}.$$

Through a similar straightforward algebraic manipulations we also find the steady state expressions for r_0 and s_0 in the form

$$r_0 = a_2 + b_2, \quad \text{and} \quad s_0 = \frac{b_2}{(a_2 + b_2)^2}. \quad (22)$$

Therefore, the uniform steady state solution satisfying system (13) is of the form

$$(u_0, v_0, r_0, s_0) = \left(a_2 + b_2, \frac{b_2}{(a_2 + b_2)^2}, a_2 + b_2, \frac{b_2}{(a_2 + b_2)^2} \right). \quad (23)$$

Substituting the uniform steady state (23) in (17) and (18), leads to state condition on the parameters. The condition on the parameters is derived by direct substitution of 23 and algebraic manipulations through the following steps result in

$$\begin{aligned} -\rho_3 (a_2 + b_2) + \mu (a_2 + b_2) + \delta_2 \frac{b_2}{(a_2 + b_2)^2} &= 0, \\ \Rightarrow (a_2 + b_2)^3 &= -\frac{b_2 \delta_2}{\mu - \rho_3}. \end{aligned} \quad (24)$$

$$-\rho_4 \frac{b_2}{(a_2 + b_2)^2} + \mu_1(a_2 + b_2) + \delta_3 \frac{b_2}{(a_2 + b_2)^2} = 0,$$

$$\Rightarrow (a_2 + b_2)^3 = -\frac{b_2(\delta_3 - \rho_4)}{\mu_1}. \quad (25)$$

Combining (24) and (25) we obtain the required condition on the parameters in the form

$$\frac{b_2\delta_2}{\mu - \rho_3} = \frac{b_2(\delta_3 - \rho_4)}{\mu_1},$$

$$(\mu - \rho_3)(\delta_3 - \rho_4) = \delta_2\mu_1. \quad (26)$$

Therefore, in order for (23) to be a steady state of system (13), a condition on the parameters is required to hold, which is

$$(\mu - \rho_3)(\delta_3 - \rho_4) - \delta_2\mu_1 = 0. \quad (27)$$

These findings are summarised in the following theorem.

Theorem 2.1: (Existence and uniqueness of the uniform steady state) [20] The coupled system of BSRDEs (13) with conditions (14) admits a unique non-zero steady state given by

$$(u_0, v_0, r_0, s_0) = \left(a_2 + b_2, \frac{b_2}{(a_2 + b_2)^2}, a_2 + b_2, \frac{b_2}{(a_2 + b_2)^2} \right), \quad (28)$$

provided the following compatibility condition on the coefficients of the coupling terms is satisfied

$$(\mu - \rho_3)(\delta_3 - \rho_4) - \delta_2\mu_1 = 0. \quad (29)$$

Finally, we set out the summary of the necessary and sufficient conditions for $\text{Re}(\lambda) < 0$ in Theorem 2.2.

Theorem 2.2: (Necessary and sufficient conditions for $\text{Re}(\lambda) < 0$) [10], [29] The necessary and sufficient conditions such that the zeros of the polynomial $p_4(\lambda)$ have $\text{Re}(\lambda) < 0$ are given by the following conditions:

$$f_{1u} + f_{2v} < 0, \quad (30)$$

$$f_{1u}f_{2v} - f_{1v}f_{2u} > 0, \quad (31)$$

$$f_{3r} + f_{4s} < 0, \quad (32)$$

$$f_{3r}f_{4s} - f_{3s}f_{4r} > 0. \quad (33)$$

C. Linear Stability Analysis in the Presence of Diffusion

We start by analysing the system by taking the diffusion terms into account and performing the linear stability analysis. We introduce a small perturbation in the neighbourhood of the steady state, namely, (u_0, v_0, r_0, s_0) . We introduce the small perturbations up to the linear term in the form of

$$u(\mathbf{x}, t) = u_0 + \varepsilon w_1(\mathbf{x}, t),$$

$$v(\mathbf{x}, t) = v_0 + \varepsilon w_2(\mathbf{x}, t),$$

$$r(y, t) = r_0 + \varepsilon w_3(y, t),$$

$$s(y, t) = s_0 + \varepsilon w_4(y, t),$$

where $0 < \varepsilon \ll 1$.

If we substitute these small perturbations into the system we obtain

$$\frac{\partial u(\mathbf{x}, t)}{\partial t} = \frac{\partial(u_0 + \varepsilon w_1(\mathbf{x}, t))}{\partial t} = \varepsilon \frac{\partial w_1(\mathbf{x}, t)}{\partial t},$$

$$\frac{\partial v(\mathbf{x}, t)}{\partial t} = \frac{\partial(v_0 + \varepsilon w_2(\mathbf{x}, t))}{\partial t} = \varepsilon \frac{\partial w_2(\mathbf{x}, t)}{\partial t},$$

$$\frac{\partial r(y, t)}{\partial t} = \frac{\partial(r_0 + \varepsilon w_3(y, t))}{\partial t} = \varepsilon \frac{\partial w_3(y, t)}{\partial t},$$

$$\frac{\partial s(y, t)}{\partial t} = \frac{\partial(s_0 + \varepsilon w_4(y, t))}{\partial t} = \varepsilon \frac{\partial w_4(y, t)}{\partial t}$$

and also

$$\Delta u(\mathbf{x}, t) = \Delta(u_0 + \varepsilon w_1(\mathbf{x}, t)) = \varepsilon \Delta w_1(\mathbf{x}, t),$$

$$d_\Omega \Delta v(\mathbf{x}, t) = d_\Omega \Delta(v_0 + \varepsilon w_2(\mathbf{x}, t)) = d_\Omega \varepsilon \Delta w_2(\mathbf{x}, t),$$

$$\Delta_\Gamma r(y, t) = \Delta_\Gamma(r_0 + \varepsilon w_3(y, t)) = \varepsilon \Delta_\Gamma w_3(y, t),$$

$$d_\Gamma \Delta_\Gamma s(y, t) = d_\Gamma \Delta_\Gamma(s_0 + \varepsilon w_4(y, t)) = d_\Gamma \varepsilon \Delta_\Gamma w_4(y, t).$$

Similarly we substitute such perturbations in the reaction terms. Since we know that at the steady state $f(u_0, v_0, r_0, s_0)$, $g(u_0, v_0, r_0, s_0)$, $h_1(u_0, v_0, r_0, s_0)$ and $h_2(u_0, v_0, r_0, s_0)$ all equal zero, therefore we aim to collect terms in such a way to determine the relative expressions for the steady state in each equation. Furthermore, we aim to perform linear stability analysis. Performing the algebra and cancelling the expressions for steady state and ignoring higher order terms will transform the equations into linearised system of equations.

For the remaining of this work, the analysis is restricted to circular and spherical domains, where the Cartesian coordinates are transformed to polar coordinates. The coordinate transformation is done mainly for the convenience of applying the separation variables. A close form solution can be written in the form:

$$w_1(\mathbf{x}, t) = \psi_{k_l, m}(\mathbf{x}) u_{l, m}(t),$$

$$w_2(\mathbf{x}, t) = \psi_{k_l, m}(\mathbf{x}) v_{l, m}(t),$$

$$w_3(y, t) = \phi(y) r_{l, m}(t),$$

$$w_4(y, t) = \phi(y) s_{l, m}(t),$$

which are substituted in the linearised system of equations, to obtain

$$\psi_{k_l, m}(\mathbf{x}) u'_{l, m}(t) = \Delta \psi_{k_l, m}(\mathbf{x}) u_{l, m}(t),$$

$$\psi_{k_l, m}(\mathbf{x}) v'_{l, m}(t) = \Delta \psi_{k_l, m}(\mathbf{x}) v_{l, m}(t),$$

$$\phi(y) r'_{l, m}(t) = \Delta_\Gamma \phi(y) r_{l, m}(t),$$

$$\phi(y) s'_{l, m}(t) = \Delta_\Gamma \phi(y) s_{l, m}(t),$$

For equations on the surface the relations may be written as

$$\frac{r'_{l, m}(t)}{r_{l, m}(t)} = \frac{\Delta_\Gamma \phi(y)}{\phi(y)} = -l(l+1),$$

$$\frac{s'_{l, m}(t)}{s_{l, m}(t)} = \frac{\Delta_\Gamma \phi(y)}{\phi(y)} = -l(l+1),$$

whereas for the bulk the relations take the form

$$\begin{aligned} \frac{u'_{l,m}(t)}{u_{l,m}(t)} &= \frac{\Delta\psi_{k_{l,m}}(\mathbf{x})}{\psi_{k_{l,m}}(\mathbf{x})} = -k_{l,m}^2, \\ \frac{v'_{l,m}(t)}{v_{l,m}(t)} &= \frac{\Delta\psi_{k_{l,m}}(\mathbf{x})}{\psi_{k_{l,m}}(\mathbf{x})} = -k_{l,m}^2, \end{aligned}$$

We consider a coordinate transformation in which a vector \mathbf{x} may define every point in the bulk by the variables r (radial distance from the origin) and \mathbf{y} (a point on the surface), with the relationship $\mathbf{x} = r\mathbf{y}$ where $r \in (0, 1)$, $\mathbf{y} \in \Gamma$.

Since the eigenvalue of the problem on the surface depends on l itself, therefore we may consider positive integers only, and m can be any integer with the restriction $|m| \leq l$. This is because the eigenvalues of both problems are equal at $r = 1$. Note that if $r = 1$ for the eigenvalue problem in the bulk, then the eigenvalues associated to the usual diffusion operator must coincide with those associated to Laplace-Beltrami operator on the surface, which means the following relation must hold.

$$-k_{l,m}^2 = -l(l+1)$$

Now we summarise the results in the following theorem:

Theorem 2.3: [10], [29] *The necessary conditions for diffusion-driven instability for the coupled system of BSRDEs (13) and (14) are given by*

$$f_{1u} + f_{2v} < 0, \quad (34)$$

$$f_{1u}f_{2v} - f_{1v}f_{2u} > 0, \quad (35)$$

$$f_{3r} + f_{4s} < 0, \quad (36)$$

$$f_{3r}f_{4s} - f_{3s}f_{4r} > 0, \quad (37)$$

and

$$\begin{aligned} d_{\Omega}f_{1u} + f_{2v} > 0 \quad \text{and} \\ [d_{\Omega}f_{1u} + f_{2v}]^2 - 4d_{\Omega}(f_{1u}f_{2v} - f_{1v}f_{2u}) > 0. \end{aligned} \quad (38)$$

and/or

$$\begin{aligned} d_{\Gamma}f_{3r} + f_{4s} > 0 \quad \text{and} \\ [d_{\Gamma}f_{3r} + f_{4s}]^2 - 4d_{\Gamma}(f_{3r}f_{4s} - f_{3s}f_{4r}) > 0. \end{aligned} \quad (39)$$

III. MODE ISOLATION AND PARAMETER SPACE GENERATION

In this section we proceed with the process of deriving sufficient conditions for diffusion-driven instability that shall complement the necessary conditions found in section II to ensure the emergence of spatial patterns. As the standard requirement of this process, we start by extracting excitable wavenumber through the analysis of critical diffusion ratio. Eigenvalues and eigenfunctions of the laplace operator are briefly discussed on the surface. The results for mode isolation for the excitable wavenumber are employed to computationally find Turing parameter spaces on the real positive parameter plane. We also present the process of coordinate transformation from Cartesian to spherical of the usual laplace operator. Finally, we analyse and compare the shift and dependence of Turing spaces for equations in the bulk with those Turing spaces that are derived for equations on the surface.

A. Critical Diffusion Ratio and Excitable Wavenumber

For the bulk, the conditions (34), (35) and (38) are necessary but not sufficient for the emergence of an inhomogeneous spatial structure. The sufficient condition requires the existence of some finite wavenumbers $k^2 \in (k_{-}^2, k_{+}^2)$, where k_{\pm}^2 are the roots of the equation $H_2(k^2) = 0$. Also, for the surface the conditions (36), (37) and (39) are necessary but not sufficient for diffusion-driven instability and the sufficient condition requires the existence of some finite wavenumbers $l(l+1) \in (l(l+1)_{-}, l(l+1)_{+})$ where $l(l+1)_{\pm}$ are the roots of the equation $H_1(l(l+1)) = 0$.

When the minimum $H_2(k^2) = 0$, we require that

$$f_{1u}f_{2v} - f_{1v}f_{2u} = \frac{(d_c f_{1u} + f_{2v})^2}{4d_c} \quad (40)$$

For fixed parameters on the kinetics in the bulk, the critical diffusion d_c is obtained using the following form:

$$d_c^2 f_{1u}^2 - (2f_{1u}f_{2v} - 4f_{1v}f_{2u})d_c + f_{2v}^2 = 0. \quad (41)$$

Corresponding to the critical diffusion coefficient d_c , there exists a critical wavenumber k_c^2 that obtained by:

$$k_c^2 = \pm\gamma_{\Omega}\sqrt{\frac{(f_{1u}f_{2v} - f_{1v}f_{2u})}{d_c}}. \quad (42)$$

This is the critical wavenumber, the sufficient condition for Turing instability with the necessary conditions (34), (35) and (38) satisfied, which leads the system to evolve into spatial pattern.

Similarly, the critical diffusion coefficient d_c on the surface can be obtained from the following equation:

$$d_c^2 f_{3r}^2 - (2f_{3r}f_{4s} - 4f_{3s}f_{4r})d_c + f_{4s}^2 = 0. \quad (43)$$

The critical wavenumber on the surface is given by

$$l(l+1)_c = \pm\gamma_{\Gamma}\sqrt{\frac{(f_{3r}f_{4s} - f_{3s}f_{4r})}{d_c}}, \quad (44)$$

which provides the sufficient condition for diffusion-driven instability on the surface.

For fixed kinetics parameter values $a_2 = 0.1$, $b_2 = 0.9$, we use the first derivatives of f_1, f_2, f_3 and f_4 and the values $u_0 = a_2 + b_2 = 0.1 + 0.9 = 1$, $v_0 = \frac{b_2}{(a_2+b_2)^2} = 0.9$. Substituting these values into (41), one obtains

$$d_c^2(0.64) - (5.6)d_c + 1 = 0,$$

for which the two roots are given by

$$d_c = 8.56762745781 > 1, \quad \text{and} \quad (45)$$

$$d_c = 0.18237254218 < 1. \quad (46)$$

Since the diffusion coefficient must be greater than 1, then we only take the critical diffusion coefficient ratio as $d_c = 8.56762745781$.

Fig. 1 shows the plot of $H_2(k^2)$ as a function of k^2 . All three possibilities for diffusion coefficient d with respect to the critical diffusion d_c are plotted.

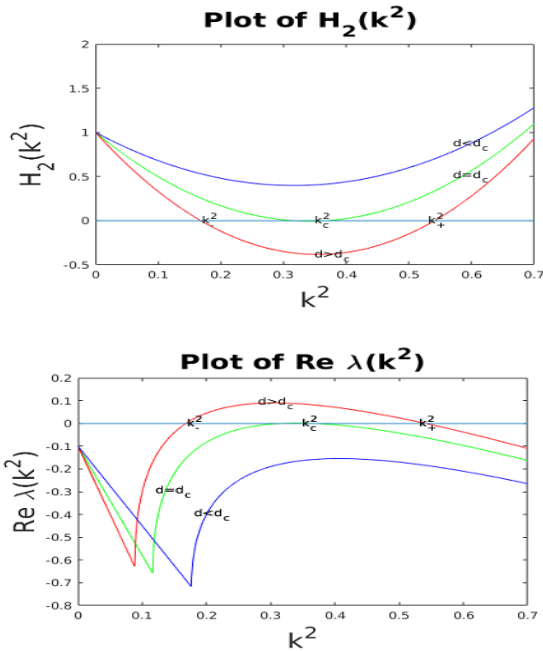


Fig. 1. Plot of $H_2(k^2)$ is shown in (a) When $d > d_c$, then $H_2(k^2) < 0$ for a finite range of $k^2 > 0$ Plot of the largest of the eigenvalue $\lambda(k^2)$ as a function of k^2 is shown in (b) When $d > d_c$, there is a range of wavenumbers $k_-^2 < k^2 < k_+^2$ which are linearly unstable

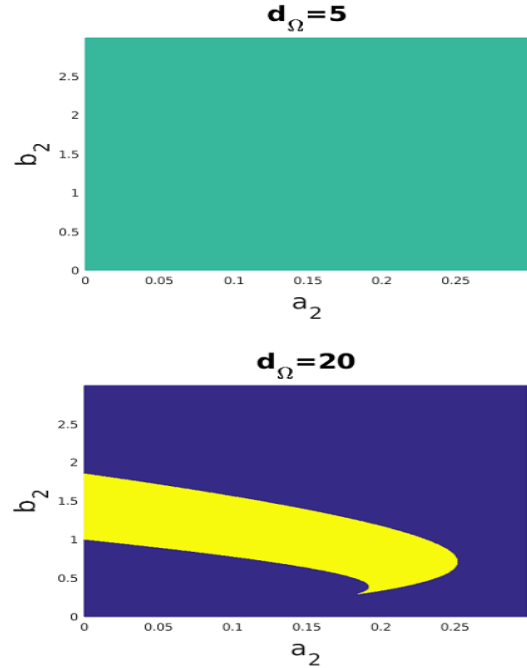


Fig. 2. When $d < d_c$, then there is no region in parameter space that corresponds to Turing instability, which is shown in (a). When $d > d_c$, then the diffusion-driven instability region in parameter space exists that corresponds to Turing instability and is shown in (b).

B. Mode Isolation in the Bulk

With the help of linear stability analysis, certain modes can be isolated to help find the admissible set of parameter values d_Ω and γ_Ω for diffusion-driven instability. The necessary conditions for diffusion-driven instability are

$$f_{1u} + f_{2v} < 0, \quad (47)$$

$$f_{1u}f_{2v} - f_{1v}f_{2u} > 0, \quad (48)$$

$$d_\Omega f_{1u} + f_{2v} > 0 \text{ and} \quad (49)$$

$$[d_\Omega f_{1u} + f_{2v}]^2 - 4d_\Omega(f_{1u}f_{2v} - f_{1v}f_{2u}) > 0. \quad (50)$$

One of the sufficient conditions however, for diffusion-driven instability is that the eigenvalues of the laplace operator should fall in the real interval between the small and the large eigenvalues of the system. It means that:

$$\gamma L = k_-^2 < k^2 < k_+^2 = \gamma R \quad (51)$$

must hold with L and R expressed by

$$L = \frac{(d_\Omega f_{1u} + f_{2v}) - \sqrt{(d_\Omega f_{1u} + f_{2v})^2 - 4d_\Omega(f_{1u}f_{2v} - f_{1v}f_{2u})}}{2d_\Omega}, \quad (52)$$

and

$$R = \frac{(d_\Omega f_{1u} + f_{2v}) + \sqrt{(d_\Omega f_{1u} + f_{2v})^2 - 4d_\Omega(f_{1u}f_{2v} - f_{1v}f_{2u})}}{2d_\Omega}, \quad (53)$$

respectively. Therefore, for sufficient condition to exists for diffusion-driven instability, the excitable modes must exist and belong to the interval (51).

Consider the one-dimensional case, the eigenvalues are $k_l^2 = l^2\pi^2$. In order to find the excitable wavenumbers, in

To verify that $d < d_c$ does not allow Turing pattern to evolve, the necessary conditions are tested on the parameter space (a_2, b_2) where a_2 and b_2 are the positive constants of the Schnakenberg reaction kinetics. It is found that when $d < d_c$, there is no region in the parameter space that would become unstable due to diffusion in the system. This is shown in Fig. 2(a). Similarly when $d > d_c$, then we see that the unstable region is formed in the parameter space (yellow region in Fig. 2(b), which corresponds to the parameter values that would result in the system to evolve into a Turing pattern.

addition to the necessary conditions (47) - (50) and (51), one requires the sufficient condition of the form

$$k_{l-1}^2 < k_-^2 < k_l^2 < k_+^2 < k_{l+1}^2. \quad (54)$$

Fig. 3 represents the real part of the larger eigenvalue as a function of k^2 . In Figure 3 the parameter $d_\Omega = 10$ was fixed and the value of γ_Ω was varied, which suggested that when $\gamma_\Omega = 15$ and $\gamma_\Omega = 60$ then no wavenumber excited, however if $\gamma_\Omega = 30$ and $\gamma_\Omega = 90$ then only one wavenumber is excited for each value which are k_1^2 and k_2^2 respectively, with $k_1 = \pi$ and $k_2 = 2\pi$. For $\gamma_\Omega = 187$, there are two excitable wavenumbers which are of the form $k_2^2 = (2\pi)^2$ and $k_3^2 = (3\pi)^2$.

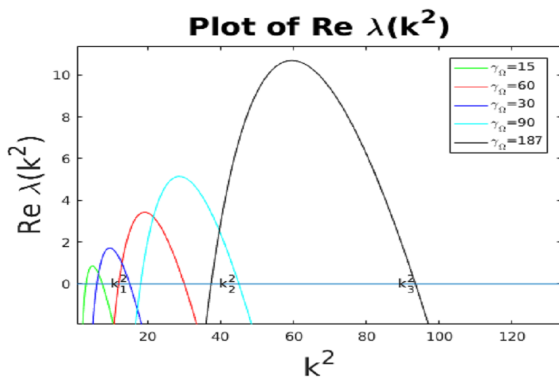


Fig. 3. Plot of the real part of eigenvalue $\lambda(k^2)$ as a function of k^2 . For fixed $d_\Omega = 10$ and increasing γ_Ω , we see that when $\gamma_\Omega = 30$ there is only one wavenumber excited ($k_1^2 = \pi^2$), when $\gamma_\Omega = 90$ there is only one wavenumber excited ($k_2^2 = (2\pi)^2$). There are two excitable wavenumbers namely ($k_2^2 = (2\pi)^2$ and $k_3^2 = (3\pi)^2$) when $\gamma_\Omega = 187$.

A similar approach is applied to the case in two dimensions. The values of d_Ω and γ_Ω are computed. We are interested in finding combination of d_Ω and γ_Ω , such that the curve $Re(\lambda(k^2))$ encapsulates only one excitable wavenumber. The algorithm is outlined through the following steps;

- Define $d_\Omega = d_c + \epsilon$ where $0 < \epsilon \ll 1$ and $d_c = 8.5676$.
- Compute k_-^2 and k_+^2 .
- If $k_{l,m}^2 > k_+^2$ as shown in Figure 4 then increase the value of γ_Ω by 1, till the curve includes the wavenumber by shifting to the right.
- If $k_{l,m}^2 < k_-^2$ then decrease the value of γ_Ω by 1, till the curve includes the wavenumber by shifting to the left.
- If there exist two excitable wavenumbers as shown in Figure 5(a) then we decrease ϵ till we obtain a unique excitable wavenumber as shown in Fig. 5(b).

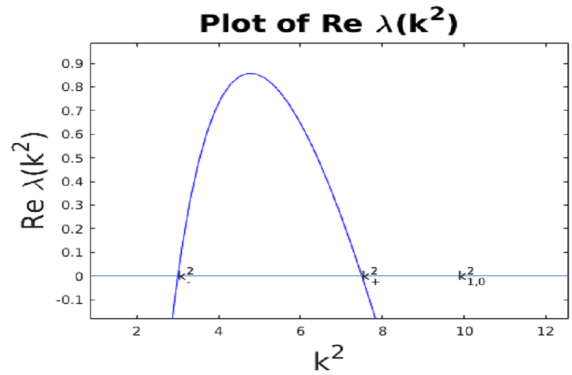


Fig. 4. Plot of the real part of eigenvalue $\lambda(k^2)$ as a function of k^2 . For all parameter values suitable for diffusion-driven instability, d_Ω and γ_Ω are varied to capture the excitable wavenumber.

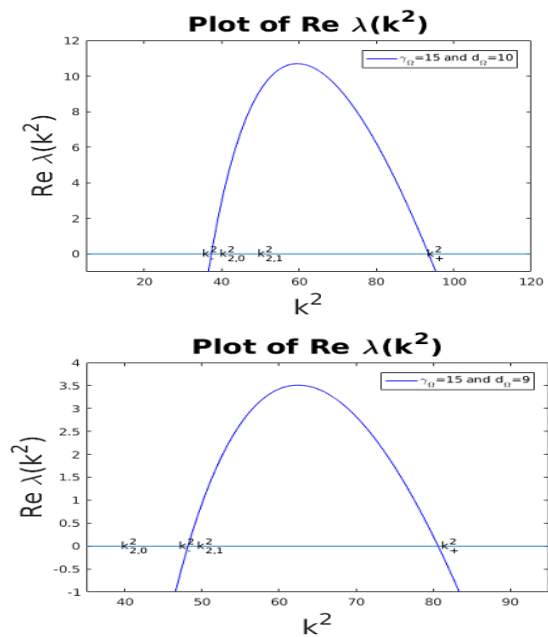


Fig. 5. Plot of the real part of eigenvalue $\lambda(k^2)$ as a function of k^2 , where we see that in Figure (a) there exist two excitable wavenumbers. By decreasing ϵ we extract a unique excitable wavenumber shown in Fig. (b)

A similar procedure may be employed to extract excitable wavenumbers from the spectrum of Laplace-Beltrami operator as a sufficient condition for Turing pattern to be formed on the surface.

C. Turing (Parameters) Space on the Surface

The Turing (parameters) spaces for equations posed on the surface and the conditions for these are obtained and outlined as

$$f_{3r} + f_{4s} < 0, \quad (55)$$

$$f_{3r}f_{4s} - f_{3s}f_{4r} > 0, \quad (56)$$

$$d_\Gamma f_{3r} + f_{4s} > 0 \text{ and} \quad (57)$$

$$[d_\Gamma f_{3r} + f_{4s}]^2 - 4d_\Gamma(f_{3r}f_{4s} - f_{3s}f_{4r}) > 0. \quad (58)$$

The parameter spaces are derived on the actual positive real parameter plane (a_2, b_2) , for two choices of diffusion ratios, namely, $d_\Gamma = 20$ and $d_\Gamma = 30$ as shown in Fig. 6.

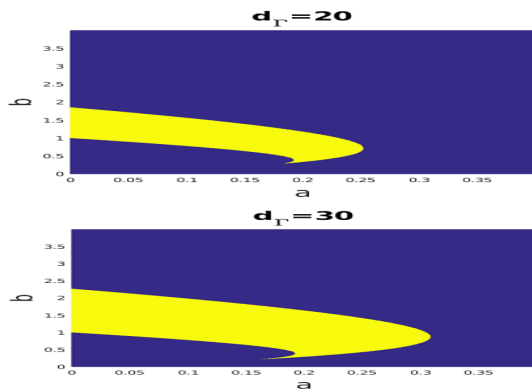


Fig. 6. Turing space for Schnakenberg model for different values of d_Γ . Unstable region is shown in the parameter space (yellow region).

D. Turing Spaces in the Bulk and on the Surface

The following sub-figures 7, 8 show diffusion-driven instability spaces for the conditions on diffusion-driven instability given by (34)-(39) in the bulk and on the surface. We combine the Turing spaces (more than one space) in the bulk and on the surface together. We note that if d_Ω is chosen the same as d_Γ , there is no difference in the region corresponding to Turing space as shown in Sub-figure 9(c). In Sub-figures 9(a) and (b), it can be seen that for larger value of the diffusion coefficient the Turing space is significantly larger than that for the smaller value of the diffusion coefficient. In the context of pattern formation it means that regions corresponding to diffusion driven instability enlarge with an increase in the diffusion coefficient.

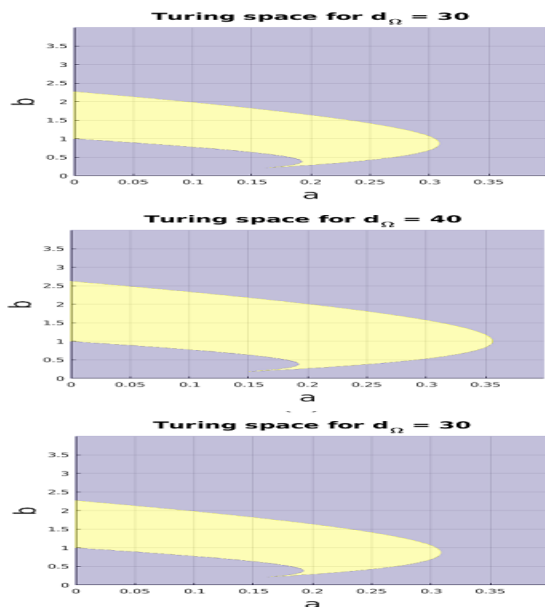


Fig. 7. First row shows that the Turing space for the bulk for parameter choices $d_\Gamma = 30$. Second and third rows show that the Turing space in the bulk with different parameter choices (second row $d_\Gamma = 30$ and (third row $d_\Gamma = 30$).

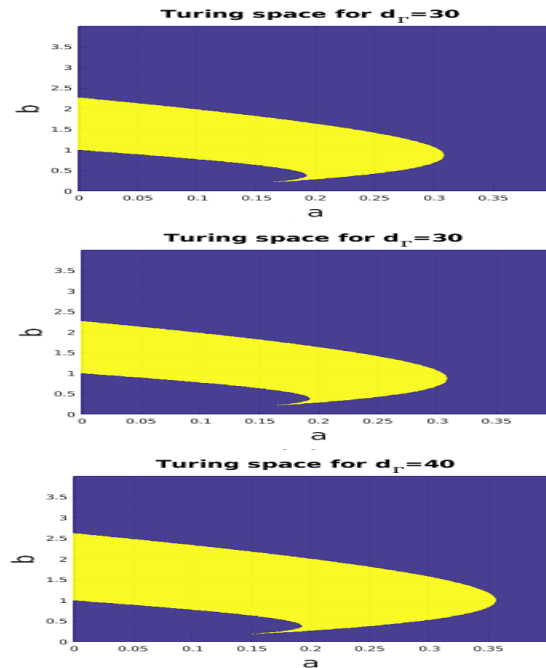


Fig. 8. First row shows that the Turing space for the surface for parameter choices $d_\Omega = 30$. Second and third rows show that the Turing space on the surface separately with different parameter choices (second row $d_\Omega = 40$ and (third row $d_\Omega = 40$).

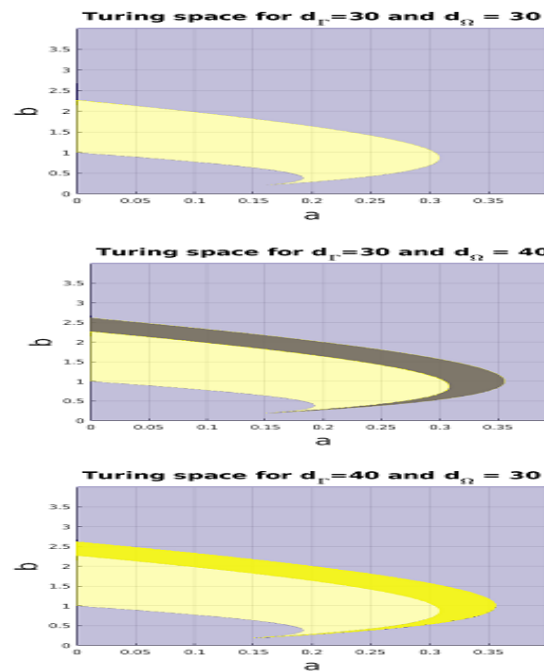


Fig. 9. Sub-figure (a) shows that the Turing space for both the bulk and the surface (cream colour) is shown to exactly coincide for parameter choices $d_\Gamma = 30$ and $d_\Omega = 30$. Sub-figure (b) shows that the Turing space on the surface (cream colour) forms a proper subset of those derived for the bulk equations (union of cream and grey regions) when $d_\Gamma = 30$ and $d_\Omega = 40$. Sub-figure (c) shows that the Turing space for equations on the surface (union of yellow and cream colour regions) with $d_\Gamma = 40$ produces larger region, which contains the spaces for the bulk equation with $d_\Omega = 30$ as proper subset, upon submerging.

IV. FEM FOR REACTION-DIFFUSION EQUATIONS ON STATIONARY VOLUMES

This section serves to provide the theoretical formulation required to obtain numerical solutions through the finite element method for the system that were explored in Section II. The Sobolev and Hilbert function spaces are the basis used to obtain the weak formulation. The methods of space and time discretisations were investigated and also the time-stepping schemes. We present the weak formulation with the corresponding finite element formulation through a fully implicit treatment by employing the extended form of Newton's method for vector valued functions.

A. Weak Formulation

In order to derive the weak formulation, we multiply (13) by a test function say $\varphi \in H^1(\Omega)$ for the bulk and $\psi \in H^1(\Gamma)$ for the surface and integrated over Ω for the bulk and over Γ for the surface written as

$$\begin{aligned} & \int_{\Omega} \frac{\partial u}{\partial t} \varphi \, d\Omega - \int_{\Omega} \Delta u \varphi \, d\Omega = \gamma_{\Omega} \int_{\Omega} [a_2 - u + u^2 v] \varphi \, d\Omega, \\ & \int_{\Omega} \frac{\partial v}{\partial t} \varphi \, d\Omega - \int_{\Omega} d_{\Omega} \Delta v \varphi \, d\Omega = \gamma_{\Omega} \int_{\Omega} [b_2 - u^2 v] \varphi \, d\Omega, \\ & \quad \text{in } \Omega \times (0, T] \\ & \int_{\Gamma} \frac{\partial r}{\partial t} \psi \, d\Gamma - \int_{\Gamma} \Delta_{\Gamma} r \psi \, d\Gamma \\ & = \gamma_{\Gamma} \int_{\Gamma} [a_2 - r + r^2 s - \rho_3 r + \mu u + \delta_2 v] \psi \, d\Gamma, \\ & \int_{\Gamma} \frac{\partial s}{\partial t} \psi \, d\Gamma - \int_{\Gamma} d_{\Gamma} \Delta_{\Gamma} s \psi \, d\Gamma \\ & = \gamma_{\Gamma} \int_{\Gamma} [b_2 - r^2 s - \rho_4 s + \mu_1 u + \delta_3 v] \psi \, d\Gamma, \quad \text{on } \Gamma \times (0, T]. \end{aligned}$$

Using the Green's formula for the second terms in the above with the boundary conditions (14), we obtain

$$\begin{aligned} & \int_{\Omega} \frac{\partial u}{\partial t} \varphi \, d\Omega + \int_{\Omega} \nabla u \cdot \nabla \varphi \, d\Omega = \gamma_{\Omega} \int_{\Omega} [a_2 - u + u^2 v] \varphi \, d\Omega \\ & + \gamma_{\Gamma} \int_{\Gamma} (\rho_3 r - \mu u - \delta_2 v) \varphi \, d\Gamma, \\ & \int_{\Omega} \frac{\partial v}{\partial t} \varphi \, d\Omega + d_{\Omega} \int_{\Omega} \nabla v \cdot \nabla \varphi \, d\Omega = \gamma_{\Omega} \int_{\Omega} [b_2 - u^2 v] \varphi \, d\Omega \\ & + \gamma_{\Gamma} \int_{\Gamma} (\rho_4 s - \mu_1 u - \delta_3 v) \varphi \, d\Gamma, \quad \text{in } \Omega \times (0, T] \\ & \int_{\Gamma} \frac{\partial r}{\partial t} \psi \, d\Gamma + \int_{\Gamma} \nabla_{\Gamma} r \cdot \nabla_{\Gamma} \psi \, d\Gamma \\ & = \gamma_{\Gamma} \int_{\Gamma} [a_2 - r + r^2 s - \rho_3 r + \mu u + \delta_2 v] \psi \, d\Gamma, \\ & \int_{\Gamma} \frac{\partial s}{\partial t} \psi \, d\Gamma + d_{\Gamma} \int_{\Gamma} \nabla_{\Gamma} s \cdot \nabla_{\Gamma} \psi \, d\Gamma \\ & = \gamma_{\Gamma} \int_{\Gamma} [b_2 - r^2 s - \rho_4 s + \mu_1 u + \delta_3 v] \psi \, d\Gamma, \quad \text{on } \Gamma \times (0, T]. \end{aligned}$$

B. Spatial Discretisation of the Weak Formulation

We discretise the original domain Ω and its boundary Γ to obtain Ω_h and Γ_h where $\Omega_h \subset \Omega$ and $\Gamma_h \subset \Gamma$ with

N_{Ω} and N_{Γ} to be the number of vertices on associated to their respective discretisation. Let V_{Ω_h} and V_{Γ_h} denote the finite element function spaces associated to the discretised domains Ω_h and Γ_h respectively.

The finite element formulation is then to seek u_h, v_h, r_h and s_h in $V_{\Omega_h} \cup V_{\Gamma_h}$ such that on each \mathbf{x} in $\Omega_h \cup \Gamma_h$ and $t > 0$ the equations

$$\begin{aligned} & \int_{\Omega_h} \frac{\partial u_h}{\partial t} \varphi_h \, d\Omega_h + \int_{\Omega_h} \nabla u_h \cdot \nabla \varphi_h \, d\Omega_h = \\ & \gamma_{\Omega} \int_{\Omega_h} [a_2 - u_h + u_h^2 v_h] \varphi_h \, d\Omega_h \\ & + \gamma_{\Gamma} \int_{\Gamma_h} (\rho_3 r_h - \mu u_h - \delta_2 v_h) \varphi_h \, d\Gamma_h, \\ & \int_{\Omega_h} \frac{\partial v_h}{\partial t} \varphi_h \, d\Omega_h + d_{\Omega} \int_{\Omega_h} \nabla v_h \cdot \nabla \varphi_h \, d\Omega_h = \\ & \gamma_{\Omega} \int_{\Omega_h} [b_2 - u_h^2 v_h] \varphi_h \, d\Omega_h \\ & + \gamma_{\Gamma} \int_{\Gamma_h} (\rho_4 s_h - \mu_1 u_h - \delta_3 v_h) \varphi_h \, d\Gamma_h, \\ & \int_{\Gamma_h} \frac{\partial r_h}{\partial t} \psi_h \, d\Gamma_h + \int_{\Gamma_h} \nabla_{\Gamma} r_h \cdot \nabla_{\Gamma} \psi_h \, d\Gamma_h = \\ & \gamma_{\Gamma} \int_{\Gamma_h} [a_2 - r_h + r_h^2 s_h - \rho_3 r_h + \mu u_h + \delta_2 v_h] \psi_h \, d\Gamma_h, \\ & \int_{\Gamma_h} \frac{\partial s_h}{\partial t} \psi_h \, d\Gamma_h + d_{\Gamma} \int_{\Gamma_h} \nabla_{\Gamma} s_h \cdot \nabla_{\Gamma} \psi_h \, d\Gamma_h = \\ & \gamma_{\Gamma} \int_{\Gamma_h} [b_2 - r_h^2 s_h - \rho_4 s_h + \mu_1 u_h + \delta_3 v_h] \psi_h \, d\Gamma_h, \end{aligned}$$

are true for all test functions $\varphi_h \in V_{\Omega_h}$ and $\psi_h \in V_{\Gamma_h}$, respectively.

Let $\{\varphi_i\}_{i=1}^{N_{\Omega}}$ and $\{\psi_i\}_{i=1}^{N_{\Gamma}}$ be the set of piecewise bilinear basis functions. It is known that the spaces V_{Ω_h} and V_{Γ_h} are spanned by the basis functions $\{\varphi_i\}_{i=1}^{N_{\Omega}}$ and $\{\psi_i\}_{i=1}^{N_{\Gamma}}$ respectively. Thus, u_h, v_h, r_h and s_h may be expanded in terms of linear combinations of its corresponding basis functions namely $\{\varphi_i\}_{i=1}^{N_{\Omega}}$ and $\{\psi_i\}_{i=1}^{N_{\Gamma}}$. Substituting the expressions $u_h = \sum_{i=1}^{N_{\Omega}} U_i \varphi_i$, $v_h = \sum_{i=1}^{N_{\Omega}} V_i \varphi_i$, $r_h = \sum_{i=1}^{N_{\Gamma}} R_i \psi_i$, and $s_h = \sum_{i=1}^{N_{\Gamma}} S_i \psi_i$ in the finite element formulations leads to a system of differential equations written in matrix notation as

$$\begin{aligned} & M_0 \mathbf{U}_t + \gamma_{\Omega} M_0 \mathbf{U} + A_0 \mathbf{U} - \gamma_{\Omega} B_0(\mathbf{U}, \mathbf{V}) \mathbf{U} \\ & - \gamma_{\Gamma} (\rho_3 M_{10} \mathbf{R} - \mu M_{00} \mathbf{U} - \delta_2 M_{00} \mathbf{V}) = \gamma_{\Omega} a_2 \mathbf{C}_0, \\ & M_0 \mathbf{V}_t + d_{\Omega} A_0 \mathbf{V} + \gamma_{\Omega} B_0(\mathbf{U}, \mathbf{U}) \mathbf{V} \\ & - \gamma_{\Gamma} (\rho_4 M_{10} \mathbf{S} - \mu_1 M_{00} \mathbf{U} - \delta_3 M_{00} \mathbf{V}) = \gamma_{\Omega} b_2 \mathbf{C}_0, \\ & M_1 \mathbf{R}_t + \gamma_{\Gamma} M_1 \mathbf{R} + A_1 \mathbf{R} - \gamma_{\Gamma} B_1(\mathbf{R}, \mathbf{S}) \mathbf{R} \\ & + \gamma_{\Gamma} (\rho_3 M_{11} \mathbf{R} - \mu M_{01} \mathbf{U} - \delta_2 M_{01} \mathbf{V}) = \gamma_{\Gamma} a_2 \mathbf{C}_1, \\ & M_1 \mathbf{S}_t + d_{\Gamma} A_1 \mathbf{S} + \gamma_{\Gamma} B_1(\mathbf{R}, \mathbf{R}) \mathbf{S} \\ & + \gamma_{\Gamma} (\rho_4 M_{11} \mathbf{S} - \mu_1 M_{01} \mathbf{U} - \delta_3 M_{01} \mathbf{V}) = \gamma_{\Gamma} a_2 \mathbf{C}_1, \end{aligned}$$

where the matrices with their corresponding entries are given

by

$$(M_0)_{ij} = \int_{\Omega_h} \varphi_i \varphi_j d\Omega_h, \quad (A_0)_{ij} = \int_{\Omega_h} \nabla \varphi_i \cdot \nabla \varphi_j d\Omega_h,$$

$$\mathbf{C}_0 = \int_{\Omega_h} \varphi_j d\Omega_h, \quad (B_0(\mathbf{U}, \mathbf{V}))_{ij} = \int_{\Omega_h} (U_i \varphi_i)(V_i \varphi_i) \varphi_i \varphi_j d\Omega_h,$$

$$(B_0(\mathbf{U}, \mathbf{U}))_{ij} = \int_{\Omega_h} (U_i \varphi_i)(U_i \varphi_i) \varphi_i \varphi_j d\Omega_h,$$

and the entries for $M_1, A_1, B_1(\mathbf{R}, \mathbf{S})$ and \mathbf{C}_1 , are expressed in similar way to those expressed for matrices with subscript 0. The entries of the matrices that are constructed from the combination of function spaces defined in the bulk and on the surface are defined by

$$(M_{10})_{ij} = \int_{\Gamma_h} \psi_i \varphi_j d\Gamma_h, \quad (M_{01})_{ij} = \int_{\Gamma_h} \varphi_i \psi_j d\Gamma_h,$$

$$(M_{00})_{ij} = \int_{\Gamma_h} \varphi_i \varphi_j d\Gamma_h, \quad \text{and} \quad (M_{11})_{ij} = \int_{\Gamma_h} \psi_i \psi_j d\Gamma_h,$$

where M is the mass matrix and A is the stiffness matrix, B is the matrix corresponding to the non-linear terms and \mathbf{C} is the column vector.

C. Mesh Generation (using Deal. II)

The usual approach to discretising Ω and Γ is such that, Ω is first discretised and denoted by Ω_h . The union of those elements from Ω_h whose vertices lie on $\partial\Omega$ is considered as the discretisation of Γ , which is denoted by Γ_h . Bulk is discretised by quadrilateral elements each with uniform structure throughout Ω_h . Triangulation Γ_h is also a uniform set of 2 dimensional quadrilaterals consisting of the external faces of all the bulk elements that have at least one vertex on Γ_h .

D. Time Discretisation

We discretise the time interval $[0, T]$ into a finite number of uniform subintervals such that $0 = t_0 < t_1 \dots < t_J = T$. Let τ be the time steps and J be a fixed positive integer, then $T = J\tau$. We denote the approximate solution at time $t_n = n\tau$ by $u_h^n = u_h(\cdot, t_n)$ where $n = 0, 1, \dots, J$ and similar for the other variables. A fully implicit Euler scheme is used to solve the system in time. The fully implicit scheme applied to the uniform time discretisation. We can obtain the fully discretised system as

$$M_0 \frac{\mathbf{U}^n - \mathbf{U}^{n-1}}{\tau} + \gamma_\Omega M_0 \mathbf{U}^n + A_0 \mathbf{U}^n - \gamma_\Omega B_0(\mathbf{U}^n, \mathbf{V}^n) \mathbf{U}^n - \gamma_\Gamma (\rho_3 M_{10} \mathbf{R}^n - \mu M_{00} \mathbf{U}^n - \delta_2 M_{00} \mathbf{V}^n) = \gamma_\Omega a_2 \mathbf{C}_0,$$

$$M_0 \frac{\mathbf{V}^n - \mathbf{V}^{n-1}}{\tau} + d_\Omega A_0 \mathbf{V}^n + \gamma_\Omega B_0(\mathbf{U}^n, \mathbf{U}^n) \mathbf{V}^n - \gamma_\Gamma (\rho_4 M_{10} \mathbf{S}^n - \mu_1 M_{00} \mathbf{U}^n - \delta_3 M_{00} \mathbf{V}^n) = \gamma_\Omega b_2 \mathbf{C}_0,$$

$$M_1 \frac{\mathbf{R}^n - \mathbf{R}^{n-1}}{\tau} + \gamma_\Gamma M_1 \mathbf{R}^n + A_1 \mathbf{R}^n - \gamma_\Gamma B_1(\mathbf{R}^n, \mathbf{S}^n) \mathbf{R}^n + \gamma_\Gamma (\rho_3 M_{11} \mathbf{R}^n - \mu M_{01} \mathbf{U}^n - \delta_2 M_{01} \mathbf{V}^n) = \gamma_\Gamma a_2 \mathbf{C}_1,$$

$$M_1 \frac{\mathbf{S}^n - \mathbf{S}^{n-1}}{\tau} + d_\Gamma A_1 \mathbf{S}^n + \gamma_\Gamma B_1(\mathbf{R}^n, \mathbf{R}^n) \mathbf{S}^n + \gamma_\Gamma (\rho_4 M_{11} \mathbf{S}^n - \mu_1 M_{01} \mathbf{U}^n - \delta_3 M_{01} \mathbf{V}^n) = \gamma_\Gamma b_2 \mathbf{C}_1.$$

Algebraic manipulation and rearrangement of each equation, leads to write the system a different form which is

$$\mathbf{F}_1(\mathbf{U}^n, \mathbf{V}^n, \mathbf{R}^n, \mathbf{S}^n) = 0,$$

$$\mathbf{F}_2(\mathbf{U}^n, \mathbf{V}^n, \mathbf{R}^n, \mathbf{S}^n) = 0,$$

$$\mathbf{F}_3(\mathbf{U}^n, \mathbf{V}^n, \mathbf{R}^n, \mathbf{S}^n) = 0,$$

$$\mathbf{F}_4(\mathbf{U}^n, \mathbf{V}^n, \mathbf{R}^n, \mathbf{S}^n) = 0,$$

where

$$\mathbf{F}_1(\mathbf{U}^n, \mathbf{V}^n, \mathbf{R}^n, \mathbf{S}^n) = \left(\left(\frac{1}{\tau} + \gamma_\Omega \right) M_0 + A_0 \right) \mathbf{U}^n - \gamma_\Omega B_0(\mathbf{U}^n, \mathbf{V}^n) \mathbf{U}^n - \gamma_\Omega a_2 \mathbf{C}_0 - \frac{1}{\tau} M_0 \mathbf{U}^{n-1} - \gamma_\Gamma (\rho_3 M_{10} \mathbf{R}^n - \mu M_{00} \mathbf{U}^n - \delta_2 M_{00} \mathbf{V}^n),$$

$$\mathbf{F}_2(\mathbf{U}^n, \mathbf{V}^n, \mathbf{R}^n, \mathbf{S}^n) = \left(\frac{1}{\tau} M_0 + d_\Omega A_0 \right) \mathbf{V}^n - \frac{1}{\tau} M_0 \mathbf{V}^{n-1} - \gamma_\Gamma (\rho_4 M_{10} \mathbf{S}^n - \mu_1 M_{00} \mathbf{U}^n - \delta_3 M_{00} \mathbf{V}^n) - \gamma_\Omega b_2 \mathbf{C}_0 + \gamma_\Omega B_0(\mathbf{U}^n, \mathbf{U}^n) \mathbf{V}^n,$$

$$\mathbf{F}_3(\mathbf{U}^n, \mathbf{V}^n, \mathbf{R}^n, \mathbf{S}^n) = \left(\left(\frac{1}{\tau} + \gamma_\Gamma \right) M_1 + A_1 \right) \mathbf{R}^n - \gamma_\Gamma B_1(\mathbf{R}^n, \mathbf{S}^n) \mathbf{R}^n - \gamma_\Gamma a_2 \mathbf{C}_1 - \frac{1}{\tau} M_1 \mathbf{R}^{n-1} + \gamma_\Gamma (\rho_3 M_{11} \mathbf{R}^n - \mu M_{01} \mathbf{U}^n - \delta_2 M_{01} \mathbf{V}^n),$$

$$\mathbf{F}_4(\mathbf{U}^n, \mathbf{V}^n, \mathbf{R}^n, \mathbf{S}^n) = \left(\frac{1}{\tau} M_1 + d_\Gamma A_1 \right) \mathbf{S}^n + \gamma_\Gamma B_1(\mathbf{R}^n, \mathbf{R}^n) \mathbf{S}^n - \gamma_\Gamma b_2 \mathbf{C}_1 - \frac{1}{\tau} M_1 \mathbf{S}^{n-1} + \gamma_\Gamma (\rho_4 M_{11} \mathbf{S}^n - \mu_1 M_{01} \mathbf{U}^n - \delta_3 M_{01} \mathbf{V}^n).$$

In order to solve the system of non-linear equation, the employing the extended form of Newton's method for vector valued functions lead to write

$$\mathbf{J}_{\mathbf{F}_i} |_A (\mathbf{u}_{k+1}^n - \mathbf{u}_k^n, \mathbf{v}_{k+1}^n - \mathbf{v}_k^n, \mathbf{r}_{k+1}^n - \mathbf{r}_k^n, \mathbf{s}_{k+1}^n - \mathbf{s}_k^n) = -\mathbf{F}_i(A), \quad (59)$$

where, $A = (\mathbf{u}_k^n, \mathbf{v}_k^n, \mathbf{r}_k^n, \mathbf{s}_k^n)$ the index $i = 1, 2, 3, 4$ and

$$\mathbf{J}_{\mathbf{F}} |_A = \begin{pmatrix} \frac{\partial \mathbf{F}_1 A}{\partial \mathbf{u}_k^n} & \frac{\partial \mathbf{F}_1 A}{\partial \mathbf{v}_k^n} & \frac{\partial \mathbf{F}_1 A}{\partial \mathbf{r}_k^n} & \frac{\partial \mathbf{F}_1 A}{\partial \mathbf{s}_k^n} \\ \frac{\partial \mathbf{F}_2 A}{\partial \mathbf{u}_k^n} & \frac{\partial \mathbf{F}_2 A}{\partial \mathbf{v}_k^n} & \frac{\partial \mathbf{F}_2 A}{\partial \mathbf{r}_k^n} & \frac{\partial \mathbf{F}_2 A}{\partial \mathbf{s}_k^n} \\ \frac{\partial \mathbf{F}_3 A}{\partial \mathbf{u}_k^n} & \frac{\partial \mathbf{F}_3 A}{\partial \mathbf{v}_k^n} & \frac{\partial \mathbf{F}_3 A}{\partial \mathbf{r}_k^n} & \frac{\partial \mathbf{F}_3 A}{\partial \mathbf{s}_k^n} \\ \frac{\partial \mathbf{F}_4 A}{\partial \mathbf{u}_k^n} & \frac{\partial \mathbf{F}_4 A}{\partial \mathbf{v}_k^n} & \frac{\partial \mathbf{F}_4 A}{\partial \mathbf{r}_k^n} & \frac{\partial \mathbf{F}_4 A}{\partial \mathbf{s}_k^n} \end{pmatrix}, \quad (60)$$

and the entries of \mathbf{J}_F are expressed by

$$\begin{aligned}\frac{\partial \mathbf{F}_1 A}{\partial \mathbf{u}_k^n} &= \left(\frac{1}{\tau} + \gamma_\Omega\right) M_0 + A_0 - 2\gamma_\Omega B_0(\mathbf{u}_k^n, \mathbf{v}_k^n) + \gamma_\Gamma \mu M_{00}, \\ \frac{\partial \mathbf{F}_1 A}{\partial \mathbf{v}_k^n} &= -\gamma_\Omega B_0(\mathbf{u}_k^n, \mathbf{u}_k^n) + \gamma_\Gamma \delta_2 M_{00}, \\ \frac{\partial \mathbf{F}_1 A}{\partial \mathbf{r}_k^n} &= -\gamma_\Gamma \rho_3 M_{10}, \\ \frac{\partial \mathbf{F}_1 A}{\partial \mathbf{s}_k^n} &= 0, \\ \frac{\partial \mathbf{F}_2(A)}{\partial \mathbf{u}_k^n} &= 2\gamma_\Omega B_0(\mathbf{u}_k^n, \mathbf{v}_k^n) + \gamma_\Gamma \mu_1 M_{00}, \\ \frac{\partial \mathbf{F}_2 A}{\partial \mathbf{v}_k^n} &= \frac{1}{\tau} M_0 + d_\Omega A_0 + \gamma_\Omega B_0(\mathbf{u}_k^n, \mathbf{u}_k^n) + \gamma_\Gamma \delta_3 M_{00}, \\ \frac{\partial \mathbf{F}_2 A}{\partial \mathbf{r}_k^n} &= 0, \\ \frac{\partial \mathbf{F}_2 A}{\partial \mathbf{s}_k^n} &= -\gamma_\Gamma \rho_4 M_{10}, \\ \frac{\partial \mathbf{F}_3 A}{\partial \mathbf{u}_k^n} &= -\gamma_\Gamma \mu M_{01}, \\ \frac{\partial \mathbf{F}_3 A}{\partial \mathbf{v}_k^n} &= -\gamma_\Gamma \delta_2 M_{01}, \\ \frac{\partial \mathbf{F}_3 A}{\partial \mathbf{r}_k^n} &= \left(\frac{1}{\tau} + \gamma_\Gamma\right) M_1 + A_1 - 2\gamma_\Gamma B_1(\mathbf{r}_k^n, \mathbf{s}_k^n) + \gamma_\Gamma \rho_3 M_{11}, \\ \frac{\partial \mathbf{F}_3 A}{\partial \mathbf{s}_k^n} &= -\gamma_\Gamma B_1(\mathbf{r}_k^n, \mathbf{r}_k^n), \\ \frac{\partial \mathbf{F}_4 A}{\partial \mathbf{u}_k^n} &= -\gamma_\Gamma \mu_1 M_{01}, \\ \frac{\partial \mathbf{F}_4 A}{\partial \mathbf{v}_k^n} &= -\gamma_\Gamma \delta_3 M_{01}, \\ \frac{\partial \mathbf{F}_4 A}{\partial \mathbf{r}_k^n} &= 2\gamma_\Gamma B_1(\mathbf{r}_k^n, \mathbf{s}_k^n), \\ \frac{\partial \mathbf{F}_4 A}{\partial \mathbf{s}_k^n} &= \frac{1}{\tau} M_1 + d_\Gamma A_1 + \gamma_\Gamma B_1(\mathbf{r}_k^n, \mathbf{r}_k^n) + \gamma_\Gamma \rho_4 M_{11}.\end{aligned}$$

Substituting (60) in (59) and simplifying, we obtain

$$\begin{aligned}& \left[\left(\frac{1}{\tau} + \gamma_\Omega \right) M_0 + A_0 - 2\gamma_\Omega B_0(\mathbf{u}_k^n, \mathbf{v}_k^n) \right] (\mathbf{u}_{k+1}^n) \\ & + [-\gamma_\Omega B_0(\mathbf{u}_k^n, \mathbf{u}_k^n)] (\mathbf{v}_{k+1}^n) \\ & - \gamma_\Gamma [(\rho_3 M_{10}) \mathbf{r}_{k+1}^n - (\mu M_{00}) \mathbf{u}_{k+1}^n - (\delta_2 M_{00}) \mathbf{v}_{k+1}^n] \\ & = -2\gamma_\Omega B_0(\mathbf{u}_k^n, \mathbf{v}_k^n) \mathbf{u}_k^n + \gamma_\Omega a_2 \mathbf{C}_0 + \frac{1}{\tau} M_0 \mathbf{u}^{n-1}, \\ & [2\gamma_\Omega B_0(\mathbf{u}_k^n, \mathbf{v}_k^n)] (\mathbf{u}_{k+1}^n) \\ & + \left[\frac{1}{\tau} M_0 + d_\Omega A_0 + \gamma_\Omega B_0(\mathbf{u}_k^n, \mathbf{u}_k^n) \right] (\mathbf{v}_{k+1}^n) \\ & - \gamma_\Gamma [(\rho_4 M_{10}) \mathbf{s}_{k+1}^n - (\mu_1 M_{00}) \mathbf{u}_{k+1}^n - (\delta_3 M_{00}) \mathbf{u}_{k+1}^n] \\ & = 2\gamma_\Omega B_0(\mathbf{u}_k^n, \mathbf{u}_k^n) \mathbf{v}_k^n + \gamma_\Omega b_2 \mathbf{C}_0 + \frac{1}{\tau} M_0 \mathbf{v}^{n-1},\end{aligned}$$

$$\begin{aligned}& \left[\left(\frac{1}{\tau} + \gamma_\Gamma \right) M_1 + A_1 - 2\gamma_\Gamma B_1(\mathbf{r}_k^n, \mathbf{s}_k^n) \right] (\mathbf{r}_{k+1}^n) \\ & + [-\gamma_\Gamma B_1(\mathbf{r}_k^n, \mathbf{r}_k^n)] (\mathbf{s}_{k+1}^n) \\ & + \gamma_\Gamma [(\rho_3 M_{11}) \mathbf{r}_{k+1}^n - (\mu M_{01}) \mathbf{u}_{k+1}^n - (\delta_2 M_{01}) \mathbf{v}_{k+1}^n] \\ & = -2\gamma_\Gamma B_1(\mathbf{r}_k^n, \mathbf{s}_k^n) \mathbf{r}_k^n + \gamma_\Gamma a_2 \mathbf{C}_1 + \frac{1}{\tau} M_1 \mathbf{r}^{n-1},\end{aligned}$$

$$\begin{aligned}& [2\gamma_\Gamma B_1(\mathbf{r}_k^n, \mathbf{s}_k^n)] (\mathbf{r}_{k+1}^n) + \left[\frac{1}{\tau} M_1 + d_\Gamma A_1 + \gamma_\Gamma B_1(\mathbf{r}_k^n, \mathbf{r}_k^n) \right] (\mathbf{s}_{k+1}^n) \\ & + \gamma_\Gamma [(\rho_4 M_{11}) \mathbf{s}_{k+1}^n - (\mu_1 M_{01}) \mathbf{u}_{k+1}^n - (\delta_3 M_{01}) \mathbf{v}_{k+1}^n] \\ & = 2\gamma_\Gamma B_1(\mathbf{r}_k^n, \mathbf{r}_k^n) \mathbf{s}_k^n + \gamma_\Gamma b_2 \mathbf{C}_1 + \frac{1}{\tau} M_1 \mathbf{s}^{n-1},\end{aligned}$$

which can be written in a matrix form as

$$\begin{pmatrix} \frac{\partial \mathbf{F}_1 A}{\partial \mathbf{u}_k^n} & \frac{\partial \mathbf{F}_1 A}{\partial \mathbf{v}_k^n} & \frac{\partial \mathbf{F}_1 A}{\partial \mathbf{r}_k^n} & \frac{\partial \mathbf{F}_1 A}{\partial \mathbf{s}_k^n} \\ \frac{\partial \mathbf{F}_2 A}{\partial \mathbf{u}_k^n} & \frac{\partial \mathbf{F}_2 A}{\partial \mathbf{v}_k^n} & \frac{\partial \mathbf{F}_2 A}{\partial \mathbf{r}_k^n} & \frac{\partial \mathbf{F}_2 A}{\partial \mathbf{s}_k^n} \\ \frac{\partial \mathbf{F}_3 A}{\partial \mathbf{u}_k^n} & \frac{\partial \mathbf{F}_3 A}{\partial \mathbf{v}_k^n} & \frac{\partial \mathbf{F}_3 A}{\partial \mathbf{r}_k^n} & \frac{\partial \mathbf{F}_3 A}{\partial \mathbf{s}_k^n} \\ \frac{\partial \mathbf{F}_4 A}{\partial \mathbf{u}_k^n} & \frac{\partial \mathbf{F}_4 A}{\partial \mathbf{v}_k^n} & \frac{\partial \mathbf{F}_4 A}{\partial \mathbf{r}_k^n} & \frac{\partial \mathbf{F}_4 A}{\partial \mathbf{s}_k^n} \end{pmatrix} \begin{pmatrix} \mathbf{u}_{k+1}^n \\ \mathbf{v}_{k+1}^n \\ \mathbf{r}_{k+1}^n \\ \mathbf{s}_{k+1}^n \end{pmatrix} = \begin{pmatrix} -2\gamma_\Omega B_0(\mathbf{u}_k^n, \mathbf{v}_k^n) \mathbf{u}_k^n + \gamma_\Omega a_2 \mathbf{C}_0 + \frac{1}{\tau} M_0 \mathbf{u}^{n-1} \\ 2\gamma_\Omega B_0(\mathbf{u}_k^n, \mathbf{u}_k^n) \mathbf{v}_k^n + \gamma_\Omega b_2 \mathbf{C}_0 + \frac{1}{\tau} M_0 \mathbf{v}^{n-1} \\ -2\gamma_\Gamma B_1(\mathbf{r}_k^n, \mathbf{s}_k^n) \mathbf{r}_k^n + \gamma_\Gamma a_2 \mathbf{C}_1 + \frac{1}{\tau} M_1 \mathbf{r}^{n-1} \\ 2\gamma_\Gamma B_1(\mathbf{r}_k^n, \mathbf{r}_k^n) \mathbf{s}_k^n + \gamma_\Gamma b_2 \mathbf{C}_1 + \frac{1}{\tau} M_1 \mathbf{s}^{n-1} \end{pmatrix}.$$

V. CONCLUSION

Bulk-surface reaction-diffusion system is explored through studying non-linear reaction kinetics with linear Robin-type boundary conditions. For non-linear reaction kinetics are posed both in the bulk and on the surface, then with appropriate parameter choices, such system is able to give rise to pattern formation everywhere. Parameters can also be chosen for this system such that pattern emerges in the bulk and extends to the surface, however it forms no pattern on the internal boundary layer. It is worth noting that the emergence of no pattern in the internal boundary layer is a consequence of parameter choice in the system and not the exhaustive results associated to it.

The weak formulation of coupled bulk-surface reaction-diffusion system was obtained to set-up the premises for discretisation in space through employing the standard finite element method. The full coupled system of BSRDEs was simulated using a fully implicit time-stepping scheme through the application of extended form of Newton's method for vector valued functions. Using fully implicit time-stepping scheme, we numerically demonstrate that this system allows patterns to emerge everywhere.

The generality, robustness and applicability of the presented theoretical computational framework for coupled system of bulk-surface reaction-diffusion equations set premises to study experimentally driven models where coupling of bulk and surface chemical species is prevalent. Examples of such applications include cell motility, pattern formation in developmental biology, material science and cancer biology.

REFERENCES

- [1] N. F. Britton and et al., "Reaction-diffusion equations and their applications to biology," *Academic Press*, 1, 1986.

- [2] S. Kondo and R. Asai, "A reaction-diffusion wave on the skin of the marine angelfish pomacanthus," *Nature*, vol. 6543, pp. 376–765, 1995.
- [3] H.-K. Janssen, "On the nonequilibrium phase transition in reaction-diffusion systems with an absorbing stationary state," *Zeitschrift fuer Physik B Condensed Matter*, vol. 42, no. 2, pp. 151–154, 1981.
- [4] J. D. Murray, "A pre-pattern formation mechanism for animal coat markings," *Journal of Theoretical Biology*, vol. 88, no. 1, pp. 161–199, 1981.
- [5] M. C. Mullins, M. Hammerschmidt, D. A. Kane, J. Odenthal, M. Brand, F. V. Eeden, M. Furutani-Seiki, M. Granato, P. Haffter, and C.-P. Heisenberg, "Genes establishing dorsoventral pattern formation in the zebrafish embryo: the ventral specifying genes," *Development*, vol. 123, no. 1, pp. 81–93, 1996.
- [6] R. J. D. Boer, L. A. Segel, and A. S. Perelson, "Pattern formation in one-and two-dimensional shape-space models of the immune system," *Journal of theoretical biology*, vol. 155, no. 3, pp. 295–333, 1992.
- [7] L. A. Segel and J. L. Jackson, "Dissipative structure: an explanation and an ecological example," *Journal of theoretical biology*, vol. 37, no. 3, pp. 545–559, 1972.
- [8] J. P. Keener and J. Sneyd, "Mathematical physiology," *Springer*, vol. 1, 1998.
- [9] J. D. Logan, "An introduction to nonlinear partial differential equations," *John Wiley & Sons*, vol. 89, 2008.
- [10] A. M. Turing, "The chemical basis of morphogenesis," *Philosophical Transactions of the Royal Society of London. Series B, Biological Sciences*, vol. 237, no. 641, pp. 37–72, 1952.
- [11] A. V. Chechkin, I. M. Zaid, M. A. Lomholt, I. M. Sokolov, and R. Metzler, "Bulk-mediated diffusion on a planar surface: full solution," *Physical Review E*, vol. 86, no. 4, 2012.
- [12] J. D. Murray, "Mathematical biology. ii spatial models and biomedical applications," *Interdisciplinary Applied Mathematics*, vol. 18, 2001.
- [13] I. L. Novak, F. Gao, Y.-S. Choi, D. Resasco, J. C. Schaff, and B. M. Slepchenko, "Diffusion on a curved surface coupled to diffusion in the volume: Application to cell biology," *Journal of computational physics*, vol. 226, no. 2, pp. 1271–1290, 2007.
- [14] P. Hansbo, M. G. Larson, and S. Zahedi, "A cut finite element method for coupled bulk-surface problems on time-dependent domains," *Computer Methods in Applied Mechanics and Engineering*, pp. 96–116, 2016.
- [15] C. M. Elliott and T. Ranner, "Finite element analysis for a coupled bulk-surface partial differential equation," *IMA Journal of Numerical Analysis*, vol. 33, no. 2, pp. 377–402, 2013.
- [16] C. M. Elliott, T. Ranner, and C. Venkataraman, "Coupled bulk-surface free boundary problems arising from a mathematical model of receptor-ligand dynamics," *SIAM Journal on Mathematical Analysis*, vol. 49, no. 1, pp. 360–397, 2017.
- [17] K. Krischer and A. Mikhailov, "Bifurcation to traveling spots in reaction-diffusion systems," *Physical review letters*, vol. 73, no. 23, 1994.
- [18] A. Hagberg and E. Meron, "Pattern formation in non-gradient reaction-diffusion systems: the effects of front bifurcations," *Nonlinearity*, vol. 7, no. 3, 1994.
- [19] D. Iron, J. Wei, and M. Winter, "Stability analysis of turing patterns generated by the schnakenberg model," *Journal of mathematical biology*, vol. 49, no. 4, pp. 358–390, 2004.
- [20] A. Madzvamuse, A. H. Chung, and C. Venkataraman, "Stability analysis and simulations of coupled bulk-surface reaction-diffusion systems," *In Proc. Royal Society A*, vol. 471, 2015.
- [21] J. Wei and M. Winter, "Existence and stability of a spike in the central component for a consumer chain model," *Journal of Dynamics and Differential Equations*, vol. 27, no. 3-4, pp. 1141–1171, 2015.
- [22] W. Yang and B. Ranby, "Bulk surface photografting process and its applications. i. reactions and kinetics," *Journal of Applied Polymer Science*, vol. 62, no. 3, pp. 533–543, 1996a.
- [23] W. Yang and B. Ranby, "Bulk surface photografting process and its applications. ii. principal factors affecting surface photografting," *Journal of Applied Polymer Science*, vol. 62, no. 3, pp. 545–555, 1996b.
- [24] H. Levine and W.-J. Rappel, "Membrane-bound turing patterns," *Physical Review E*, vol. 72, no. 6, 2005.
- [25] A. Ratz and M. Roger, "Symmetry breaking in a bulk-surface reaction-diffusion model for signalling networks," *Nonlinearity*, vol. 27, no. 8, 2014.
- [26] A. Hahn, K. Held, and L. Tobiska, "Modelling of surfactant concentration in a coupled bulk surface problem," *PAMM*, vol. 14, no. 1, pp. 525–526, 2014.
- [27] H. Garcke, J. Kampmann, A. Ratz, and M. Roger, "A coupled surface-cahn-hilliard bulk-diffusion system modeling lipid raft formation in cell membranes," *Mathematical Models and Methods in Applied Sciences*, vol. 26, no. 6, pp. 1149–1189, 2016.
- [28] A. Bruce, A. Johnson, J. Lewis, M. Raff, K. Roberts, and P. Walter, "Molecular biology of the cell 5th edn," *new york: Garland science*, 2007.
- [29] J. D. Murray, "Mathematical biology," *ii: spatial models and biochemical applications*, vol. 2, 2003.

Efficient Load Balancing in Cloud Computing using Multi-Layered Mamdani Fuzzy Inference Expert System

Naila Samar Naz¹, Sagheer Abbas², Muhammad Adnan Khan², Benish Abid³, Nadeem Tariq³, Muhammad Farrukh Khan⁴

Department of Computer Science, University of Lahore, Pakistan^{1,3}

School of Computer Science, National College of Business Administration & Economics, Lahore, Pakistan²

National College of Business Administration & Economics, Lahore, Pakistan⁴

Abstract—In this article, a new Multi-Layered mamdani fuzzy inference system (ML-MFIS) is propound for the Assessment of Efficient Load Balancing (ELB). The proposed ELB-ML-MFIS expert System can categorise the level of ELB in Cloud computing into Excellent, Normal or Low. ELB-ML-MFIS Expert System for ELB in cloud computing is developed under the guidelines from the Microsoft Organization and Pakistan's Punjab Information Technology Board (PITB) Standard. ELB-ML-MFIS Expert System uses input Cloud Computing parameters such as Data-Center, Virtual-Machine, and Inter -of-Things (IOT) for different layers. This article also analyses the intensities of the Parametres and the results achieved by using the Proposed ELB-ML-MFIS Expert System. All these parameters and results are discussed with the experts of Pakistan's Punjab Information Technology Board (PITB), Lahore. The accuracy of the proposed ELB-ML-MFIS Expert System is more accurate as compared to other approaches used for it.

Keywords—PITB; IOT; Virtual-Machine; Data-center; ML, ELB; MFIS

I. INTRODUCTION

Cloud computing [1] [2] is an emerging business framework and an Internet-based model where clients' information can be accessed by Internet browsers. This is a calculation mode that is determined by the availability of potent and extensible resources that services is used to represent platforms, software platforms, or storage. Cloud computing has been defined more broadly for everything related to offering web hosting services. This concept is based on computer sharing, Web Storage, and software resources provided by third parties.

Many types of clouds can be developed as a public, private cloud and hybrid [2]. The Framework of cloud computing is used only for a consortium and that is managed by a consortium or third party and may be on or off campus. On the other hand, public clouds sell resources to everyone on the Internet, and their infrastructure is provided to the public and belongs to an organization that sells cloud resources. Private cloud is a proprietary site or database that provides limited-edition hosting services or groups of people. Hybrid Clouds are a cloudy climate that includes the benefits of various cloud types. This organization provides and controls some of the resources inside and gives outsiders in the cloud. Ideally, hybrid cloud technology allows businesses to benefit from scalability, efficiency, flexibility and cost effectiveness.

II. LITERATURE REVIEW

In [3] research article an Algorithm designed by using the approach of centralized inherent efficiency, which was energy efficient and error-tolerant for the distributed environment like cloud computing. This was also give the best solution for the problem of Load Balancing in Cloud Computing by using the resource of interactive power aware line up.

This article [4] the researchers searched for the word "cloud computing", its pros, cons and many repairs for existing platforms. Also discuss the quantitative results conducted by Planet Lab, a computer cloud platform. This two-step process Algorithm also used the three level network of cloud computing for the combining of LBO (load balanced Opportunities) and LBOM (load balancing of mines). That can use better performance and maintain a balanced system load. [6].

PALB [7] keeps the status of all the tablet tabs and depending on the usage rate, the number of computer nodes to work. It shows a load balancing method based on cloud computing and provide access to local compute node resources while minimizing the total energy used by the local cloud.

Companies and institutions are focusing on computer use and large-scale archives and scanners, which are implemented through the use of various agents and collaborations with cloud computing. The different purpose of this task is that data operations are adapted to work in distribution mode, using additional images that can be saved and handled separately by different agents in a system that facilitates parallel large image processing [8].

Balance in the cloud storage as a way to be implemented in different data centers to ensure the possibility of using the network by reducing the computer hardware to reject austerity programs and reducing recurrence presence of clouds is a major problem in the cloud computing [9].

The Researchers analyzes the performance of computer services for the use of scientific data and measures the amount of presence in the Many-Task-Computing (MTC) users who freely use the program for scientific purposes. They have also

made a real assessment of four type of commercial cloud computing services [10].

III. LOAD BALANCING

A. Load Balancing in Virtual Data Centers

Virtual Data Centers that have unforeseeable user traffic need a good balance strategy. The response time automatically increase to process a request when the data center load focused on multiple servers, while the other freeware. Distributing storage between all fake printers can provide better response time. Previous work gives many techniques for balancing of burdens. These approaches are defined as follows:

B. First Come First Serve (FC-FS)

This is the first balanced load model with the simplest working principle [10]. Without the prior knowledge, it usually sends the request to the next virtual machine. It starts from the Virtual-Machine first after you have assigned the last Virtual-Machine task to the list.

C. Min-Min Load Balancer (MM-LB)

In the Minimum Minute Balance storage [11], the best response time is used to schedule tasks to match the Virtual-Machine. The lowest time the Virtual-Machine has done to complete the request is the best response time [12]. It also calculates the current response time of all Virtual-Machines. Response Time is the time it takes to show the last user request. VM's current response time is lower than the best response time, with this Method. MM-LB Instant updates, best response times with current response time, and timing of the work of the VM, or scheduling the VM with the best response time [13].

D. Active Monitoring Load Balancer (AM-LB)

Active load balances are more stable for checking than RR balance loads [14-15]. It checks the current load status of each VM and defines the loaded VM tasks very little. This LB immediately enact for the Balance Surveillance Balance Load to obtain the appropriate Virtual-Machine [16]. An Overview of this Algorithm given in paragraph 1.1 in the Active LB sweeps the recent work of each Virtual-Machine and returns the Virtual-Machine with the minimal task level [17]. Then it expands the number of its tasks by 1. [18] When the process is completed in the Virtual-Machine, the AM-LB Data Center is divided to reduce the current distribution of the Virtual-Machine.

IV. PROPOSED EFFICIENT LOAD BALANCING IN CLOUD COMPUTING MULTI-LAYERED MFIS BASED EXPERT SYSTEM (ELB-ML-MFIS ES)

In this article, a novel multi-layered HMFIS based Expert System is proposed for the ELB in cloud computing as shown in Fig. 1. In propound ELB in cloud computing Multi-Layered MFIS based Expert System (ELB-ML-MFIS-ES) use all possible suitable parameters about Cloud Computing. Some other Cloud Computing elements are not used which are not applicable in Cloud Computing. By Cloud Computing

elements characteristics, the expert system is divided into multiple layers which present the complete structure of the proposed method shown in Fig. 2. Level-1 layers exams the existence of Data Center elements, Virtual Machine, and IoT parameters. Final layer calculates the ELB in Cloud Computing on the bases of level-1 layers output as shown in Fig. 2 and 3.

The values of Data -Centre, Virtual- Machine and IOT parameter are also used to build up a lookup table of proposed ELB-ML-HMFIS-ES as shown in Table I. In propound system thirteen, input parameters are used to Assessment the ELB in Cloud Computing. Propound ELB-Multilayer fuzzy inference expert system mathematically can be written as

$$\mu_{D \cap V \cap I}(d, v, i) = \min[\mu_D(d), \mu_V(v), \mu_E(e), \mu_I(i)] \quad (1)$$

1) *Input fuzzy sets:* To Assessment the ELB the statistical values of fuzzy input variables are used. The numerical values are divided into three categories which are Excellent, Medium and Low (Low and balancing in cloud computing) after the discussion with IT- expert. The portrayal of all information factors with their numerical qualities are appeared Table I.

2) *Fuzzy output variable:* In this research, multi-layered architecture is propounded to Assessment the ELB in Cloud Computing. The output variables of all level-1 layers & final layer are shown in Table II.

3) *Membership functions:* The participation capacity of this framework gives bend an incentive between 0, 1 and furthermore gives a scientific capacity which offers measurable estimations of information and yield variable [5]. Member ship functions of Input and output variables are used in Propound ELB- Multilayer-mamdani fuzzy inference Expert System which are given in Table III.

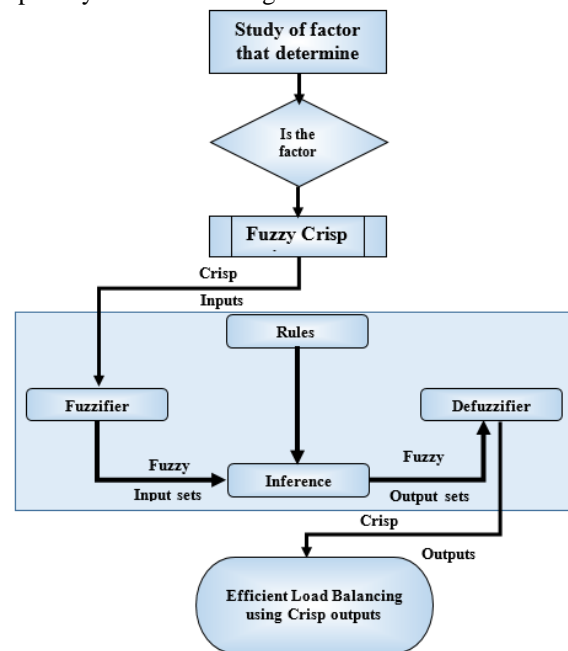


Fig. 1. Propound ELB-Multilayer-Mamdani Fuzzy Inference Expert System Methodology.

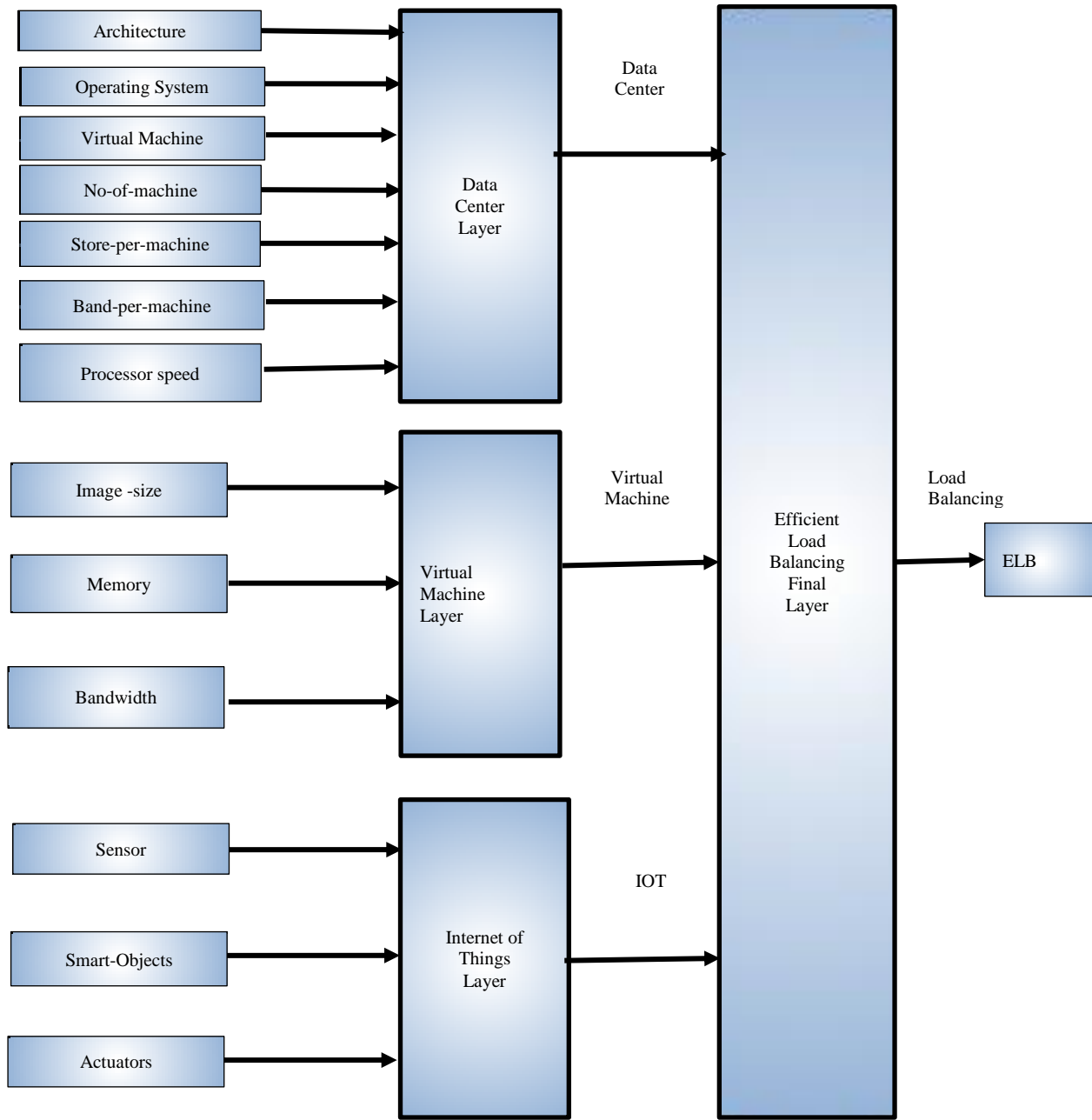


Fig. 2. Propound ELB-Multilayer-Mamdani Fuzzy Inference Expert System.

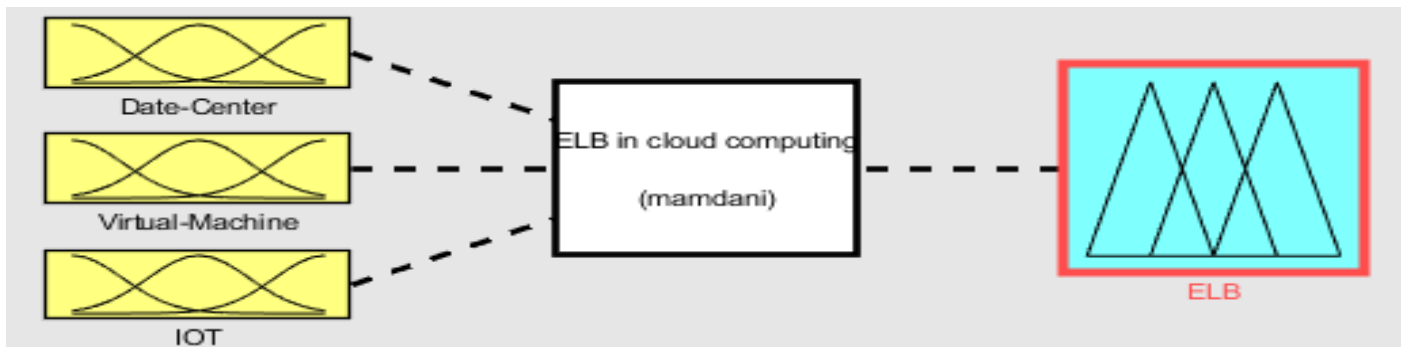


Fig. 3. Final Layer of Propound ELB-Multilayer-Mamdani Fuzzy Inference Expert System.

TABLE I. INPUT VARIABLE OF PROPOUND ELB- MULTILAYER- MAMDANI FUZZY INFERENCE EXPERT SYSTEM [11, 13]

Data-Center			
Properties/Parameter	Excellent	Medium	Low
Architecture(A)	$\leq 30 X$	$30 X \leq N \leq 60 X$	$60 X \geq$
Operating-System(OS)	No	No	Yes
VMM	No	No	Yes
Processor Speed	$\leq 20 MIPS$	$20 MIPS \leq T \leq 50 Mips$	$50 MIPS \geq$
No-of-Machine	≤ 200	$170 \leq T \leq 530$	$500 \geq$
Memory-per-Machine	≤ 600	$550 \leq T \leq 1050$	$1000 \geq$
Virtual-Machine			
Properties/Parameter	Excellent	Medium	Low
Image-size(IS)	0.14 – 0.22	≤ 0.16	≥ 0.2
Memory (M)	0.0038 – 0.0052	≤ 0.004	≥ 0.005
Bandwidth (B)	0.038 – 0.052	≤ 0.04	≥ 0.05
IOT			
Properties/Parameter	Excellent	Medium	Low
Sensors (S)	≤ 0.01	0.008 – 0.052	≥ 0.05
Smart-Objects(SO)	≤ 0.6	0.5 – 1.6	≥ 1.5
Actuators(A)	≤ 0.012	0.01 – 0.052	≥ 0.05

4) *Fuzzy prepositions*: A fuzzy compound suggestion is a structure of nuclear fuzzy recommendations utilizing the connectives "or," "and," and "not" which speak to the fuzzy association, crossing points and supplement, separately [12-14]. Here, d, v, & i variables represent Data-center, virtual machine, and IOT. Then the following fuzzy propositions hold:

$$t: d \times v \times i \rightarrow L_b \quad (2)$$

fuzzy master framework chips away at likelihood so all info and yield variable qualities are mapped from genuine range to likelihood ranges (range 0-1).[19] Here the function t-norm for final layer in equation (2) is defined as:

$$t: [0, 1] \times [0, 1] \times [0, 1] \times \rightarrow [0, 1] \quad (3)$$

Equation (3) changes the participation elements of fuzzy arrangements of Data-centre, Virtual-Machine, and IOT for a Final layer of propound fuzzy derivation framework among enrolment capacity of the crossing point of Data-centre, Virtual-Machine and IOT that is:

$$t[\mu_D(d), \mu_V(v), \mu_I(i)] = \min[\mu_D(d), \mu_V(v), \mu_I(i)] \quad (4)$$

In Equation (3), for the capacity t; getting qualified as a crossing point, following sayings must be fulfilled and will be called as t-standard:

Axiom t1: Bounded Condition

$$t(0, 0) = 0; t(\gamma, 1) = t(1, \gamma) = \gamma$$

Axiom t2: Commutativity

$$t(\alpha, \beta) = t(\beta, \alpha)$$

Axiom t3: Non-decreasing

If $\alpha \leq \alpha'$ and $\beta \leq \beta'$, then $t(\alpha, \beta) \leq t(\alpha', \beta')$

Axiom t4: Associativity

$$t[t(\alpha, \beta), \gamma] = t[\alpha, t(\beta, \gamma)]$$

Eq. (4) can be written regarding t-norm as:

$$\mu_{D \cap V \cap I \cap T}(d, v, i) = t[\mu_D(d), \mu_V(v), \mu_I(i)] \quad (5)$$

From Eq. (4) & (5)

$$\mu_{D \cap V \cap I \cap T}(d, v, i) = \min[\mu_D(d), \mu_V(v), \mu_I(i)] \quad (6)$$

5) *Lookup table*: Table for propound ELB- Multilayer-mamdani fuzzy inference Expert System contains 20 input, output rules from 30 as shown in table 4. In this table, we have 3 inputs and one output that represents multiple rules base on the inputs and respected outputs are obtained. With the help of IT-Expert and The Punjab Information Technology Board Department, Pakistan, this lookup table is developed.

TABLE II. OUTPUT VARIABLE OF PROPOUND ELB- MULTILAYER- MAMDANI FUZZY INFERENCE EXPERT SYSTEM

Sr #	Layers	Output Variables	Semantic Sign
1	Level-1 Layers	Data-Center, Virtual- machine, Internet-of-Things(IOT)	Excellent
			Medium
			Low
2	Final Layer	Efficient Load Balancing	Excellent
			Medium
			Low

TABLE III. MEMBERSHIP FUNCTIONS OF INPUT AND OUTPUT VARIABLES USED IN PROFOUND ELB-MULTILAYER-MAMDANI FUZZY INFERENCE EXPERT SYSTEM

Variables	membership function(MF)	graphical representation of membership functions
Data center=D $\mu_D(d)$	$\mu_{D,Excellent}(d) = \begin{cases} 1, & 0 \leq d \leq 0.3 \\ \frac{0.3-d}{1.0}, & 0.3 \leq d \leq 0.35 \\ 0, & d \geq 0.35 \end{cases}$ $\mu_{D,Medium}(d) = \begin{cases} \frac{d-0.3}{1.0}, & 0.3 \leq d \leq 0.35 \\ 1, & 0.35 \leq d \leq 0.4 \\ \frac{0.7-d}{1.0}, & 0.4 \leq d \leq 0.6 \\ 0, & d \geq 0.6 \end{cases}$ $\mu_{D,low}(d) = \begin{cases} 0, & 0.6 \leq d \leq 0.65 \\ \frac{0.7-d}{2}, & 0.65 \leq d \leq 0.7 \\ 1, & d \geq 0.7 \end{cases}$	
Virtual-Machine=V $\mu_V(v)$	$\mu_{V,Excellent}(v) = \begin{cases} 1, & 0 \leq v \leq 0.3 \\ \frac{0.3-v}{1.0}, & 0.3 \leq v \leq 0.35 \\ 0, & v \geq 0.35 \end{cases}$ $\mu_{V,Medium}(v) = \begin{cases} \frac{v-0.3}{1.0}, & 0.3 \leq v \leq 0.35 \\ 1, & 0.35 \leq v \leq 0.4 \\ \frac{0.7-v}{1.0}, & 0.4 \leq v \leq 0.6 \\ 0, & v \geq 0.6 \end{cases}$ $\mu_{V,low}(v) = \begin{cases} 0, & 0.6 \leq v \leq 0.65 \\ \frac{0.7-v}{2}, & 0.65 \leq v \leq 0.7 \\ 1, & v \geq 0.7 \end{cases}$	
IOT=I $\mu_I(i)$	$\mu_{I,Excellent}(i) = \begin{cases} 1, & 0 \leq i \leq 0.3 \\ \frac{0.3-i}{1.0}, & 0.3 \leq i \leq 0.35 \\ 0, & i \geq 0.35 \end{cases}$ $\mu_{I,Medium}(i) = \begin{cases} \frac{i-0.3}{1.0}, & 0.3 \leq i \leq 0.35 \\ 1, & 0.35 \leq i \leq 0.4 \\ \frac{0.7-i}{1.0}, & 0.4 \leq i \leq 0.6 \\ 0, & i \geq 0.6 \end{cases}$ $\mu_{I,low}(i) = \begin{cases} 0, & 0.6 \leq i \leq 0.65 \\ \frac{0.7-i}{2}, & 0.65 \leq i \leq 0.7 \\ 1, & i \geq 0.7 \end{cases}$	
Output $(\mu_{ELB}(L_b))$	$\mu_{ELB,excellent}(L_B) = \begin{cases} 1, & 0 \leq lb \leq 0.3 \\ \frac{0.3-lb}{1.0}, & 0.3 \leq lb \leq 0.35 \\ 0, & lb \geq 0.35 \end{cases}$ $\mu_{ELB,Medium}(L_B) = \begin{cases} \frac{lb-0.3}{1.0}, & 0.3 \leq lb \leq 0.35 \\ 1, & 0.35 \leq lb \leq 0.4 \\ \frac{0.7-lb}{1.0}, & 0.4 \leq lb \leq 0.6 \\ 0, & lb \geq 0.6 \end{cases}$ $\mu_{ELB,Low}(L_B) = \begin{cases} 0, & 0.6 \leq lb \leq 0.65 \\ \frac{0.7-lb}{2}, & 0.65 \leq lb \leq 0.7 \\ 1, & lb \geq 0.7 \end{cases}$	

TABLE IV. LOOKUP TABLE OF PROPOUND ELB-MULTILAYER-MAMDANI FUZZY INFERENCE EXPERT SYSTEM

Rules	Data-Center	Virtual-Machine	IOT	ELB
1	E	E	E	E
2	E	E	M	E
3	E	E	L	M
4	E	M	E	E
5	E	M	M	M
6	E	M	L	M
7	E	L	E	E
8	E	L	M	M
9	E	L	L	L
10	M	E	E	E
11	M	E	M	M
12	M	E	L	M
13	M	M	E	M
14	M	M	M	M
15	M	M	L	M
16	L	E	E	E
17	L	M	E/M/L	L
18	L	L	E	L
19	L	E	E	E
20	E/M/L	E/M/L	E/M/L	L

Fuzzy IF-THEN standards are the contingent explanation connected to the participation capacities. These principles are components of the fuzzy standard base. Others parts like tenets surface, rules watcher, and so on are rely on fuzzy guideline base so fuzzy principles base is a noteworthy component of FIS. Fuzzy rule base of our expert system has 30 rules at the final layer. Rules are denoted by RL^n , where $1 \leq n \leq 30$.

$RL^1 = \mathbf{IF}$ Data-center is Excellent AND Virtual-Machine elements are excellent AND IOT are excellent **THEN** Load Balancing is Excellent

$RL^2 = \mathbf{IF}$ Data-center is Excellent AND Virtual-Machine elements are excellent AND IOT are medium **THEN** Load Balancing is Excellent

$RL^3 = \mathbf{IF}$ Data-center is Excellent AND Virtual-Machine elements are excellent AND IOT are low **THEN** Load Balancing is low

$RL^{30} = \mathbf{IF}$ Data-center is low AND Virtual-Machine elements are low AND IOT are low **THEN** Load Balancing is low

6) *Inference engine*: Fuzzy surmising is the path toward mapping from an offered commitment to a yield using fuzzy rationale. Its fundamental segment of Fuzzy surmising is enrollment capacities, fuzzy rationale administrators, and on the off chance that rules. A single fluffy association is made

by all precepts in the fluffy rule base. It lies under the interior thing on the information which can be seen as a simply fuzzy IFTHEN rule.[19-20] All guidelines in the fluffy principle base are joined into a solitary fluffy connection that lies under inward item on info universes of talk, which is then seen as a just fuzzy IFTHEN rule. A sensible administrator for joining the principles is association. Let RL^n be a fuzzy relation that represents fuzzy IF-THEN rule of the Final Layer of the propound ELB-ML-MFIS Expert System; which is,

$$RL^n = D^n \times V^n \times I^n \rightarrow L_b^n \tag{7}$$

The Equation (7) can be written as

$$\mu_{D \cap V \cap I}(d, v, i,) = \mu_D(d) \cap \mu_V(v) \cap \mu_I(i) \tag{8}$$

The rules of the final layer are interpreted as a single fuzzy relation defined by

$$R_{30} = \bigcup_{n=1}^{30} RL^n \tag{9}$$

This blend of principles is called Mamdani mix. Expect I and Ψ be any two fuzzy sets and furthermore info and yield of fuzzy surmising motor individually. To see R_{30} as a solitary fuzzy IF-THEN principle by utilizing the summed up modus ponens, we get the output of the fuzzy inference engine as

$$\mu_{Excellent \cap Medium \cap Low}(\Psi) = \sup_{i \in (D, V, I)} t[\mu_i(d, v, i), \mu_{R_{30}}(d, v, i, L_b)] \tag{10}$$

The Product Inference Engine (PIE) of proposed ELB-ML-MFIS Expert System can be written as

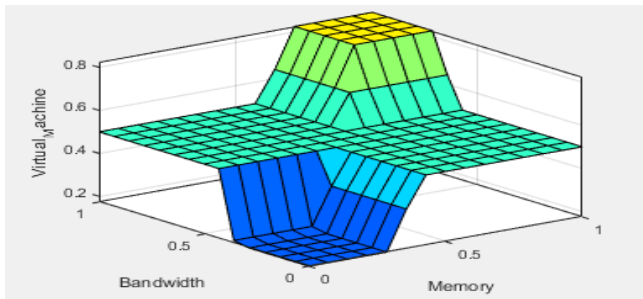
$$\mu_{\Psi}(\text{LoadBalancing}) = \max_{1 \leq n \leq 30} \left[\sup_{i \in (d, v, i)} \left(\prod_{j=1}^{90} \left(\begin{matrix} \mu_{D_j, V_j, I_j}(d, v, i,) \\ (d_1, v_2, i_3) \end{matrix} \right) \right) \right] \tag{11}$$

7) *De-Fuzzifier*: A standout amongst the most basic segments of an Expert framework is Defuzzifier. It the way toward mapping the fuzzy sent to the fresh yield. There are Three types of the defuzzifier COG Defuzzifier, the center of Average Defuzzifier and Maximum defuzzifier. From these, the best Defuzzifier is “center of gravity Defuzzifier”. [21-22]In our propound ELB-ML-MFIS expert system the COG Defuzzifier is used. The COG Defuzzifier indicates the λ^* as the focal point of the region secured by the participation capacity of Ψ , that is,

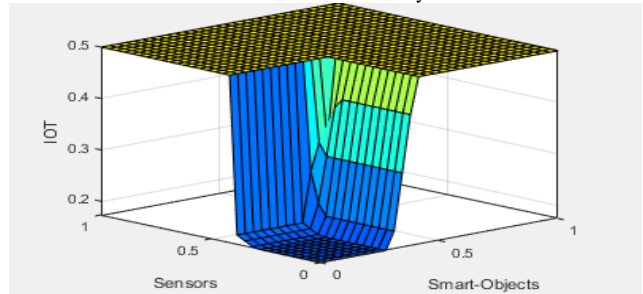
$$\lambda^* = \frac{\int \Psi \mu_{\Psi}(\Psi) d\Psi}{\int \mu_{\Psi}(\Psi) d\Psi} \tag{12}$$

The Graphical Representation of Defuzzifier of all layers of propound ELB-ML-MFIS Expert System is shown in Fig. 4(a)-4(d).

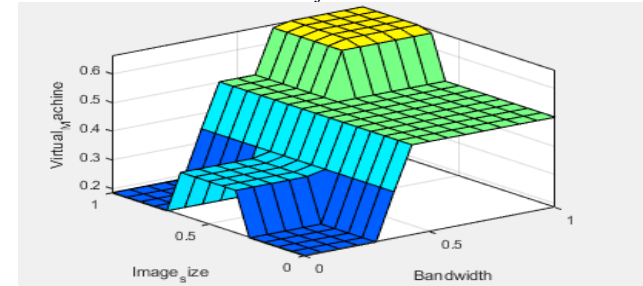
Fig. 4(a) shows load balancing of cloud concerning virtual machine components (bandwidth and Memory). It observed that in Fig. 4(a) load balancing of cloud is Excellent (Yellow shade) when Memory is ≤ 13 and Bandwidth is ≤ 3 . And load balancing of cloud is Medium (Greenish Shade) when Memory lies between 12 to 16 Bandwidth & Bandwidth is occupied between 2.5 to 5.5. Another wise load balancing of cloud is slow.



(a) Rules Surface of Load Balancing based Upon Virtual Machine Values: Bandwidth and Memory.



(b) Rules Surface of Load Balancing based Upon IOT: Sensors and Smart Objects.



(c) Rules Surface of Load Balancing based Upon Virtual Machine: Image Size and Bandwidth.

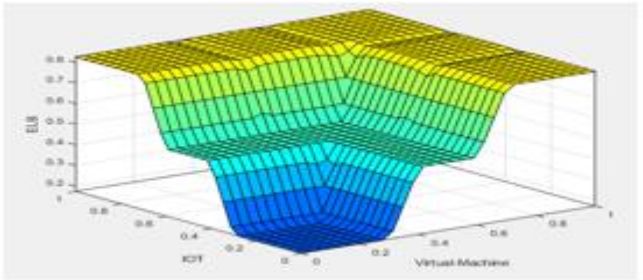


Fig. 4. (d) Rules Surface of Load Balancing Final Layer based upon IOT and Virtual Machine.

Fig. 4(d) shows load balancing of cloud concerning IOT & Virtual Machine components. It observed that in Fig. 4(d) load balancing of cloud is Excellent (Yellow shade) when Probability of both components intensity is ≥ 0.65 . And load balancing of cloud is Normal (Greenish Shade) when

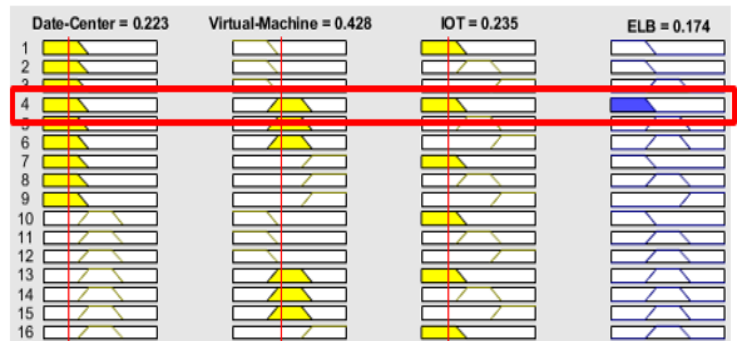
Probability of both components intensity is lies between 0.35 to 0.65. Otherwise, load balancing of cloud is low.

Similarly, remaining Fig. 4(b)-4(c) are also representing the water quality by prevailing different input parameter values. Yellow, Greenish & Bluish shade represents water quality is Excellent, Normal & low (polluted) respectively.

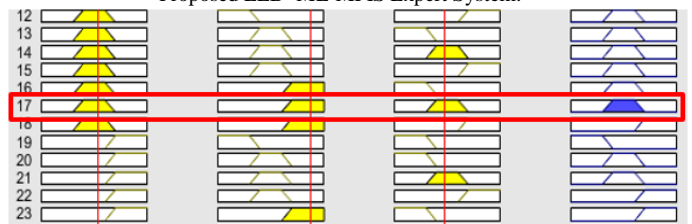
8) *Simulation results:* Fig. 5(a) shows that if Data-Center detection value is low, Virtual-Machine value is medium and IOT is low then the load balancing in cloud computing is low (Not good).

Fig. 5(b) shows that if Data-Center detection value is medium, Virtual-Machine is excellent and IOT is Normal, the load balancing in cloud computing is medium. (Good)

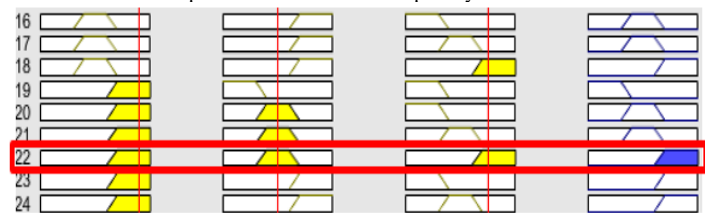
Fig. 5(c) shows that if Data-Center detection value is excellent, Virtual-Machine is and IOT is Excellent then load balancing in cloud computing is Excellent. (Good)



(a) Final Layer, Lookup Diagram of Low Load Balancing in Cloud for Proposed ELB -ML-MFIS Expert System.



(b) Final Layer, Lookup Diagram of Normal Load Balancing in Cloud for Proposed ELB -ML-MFIS Expert System.



(c) Final Layer, Lookup Diagram of Excellent Load Balancing in Cloud for Proposed ELB-ML-MFIS Expert System.

TABLE V. ACCURACY OF THE PROPOSED ELB-ML-MFIS EXPERT SYSTEM

Rules	Data-center	Virtual-Machine	IOT	Human Expert Decision	Proposed ELB-ML-MFIS-ES Decision	Probability of Correctness(P_c)	The probability of Error's ($P_e=1-P_c$)
1	E(0.87)	E(0.79)	M(0.51)	E (Good)	E (Good)	1	0
2	M(0.61)	E(0.91)	E(0.86)	E (Good)	E (Good)		
3	E(0.92)	E(0.76)	E(0.83)	E (Good)	E (Good)		
4	E(0.88)	M(0.56)	E(0.89)	E (Good)	E (Good)		
5	M(0.61)	M(0.36)	E(0.71)	E (Good)	M(Good)		
6	M(0.48)	E(0.87)	E(0.87)	E (Good)	E (Good)		
7	M(0.64)	E(0.86)	M(0.47)	E (Good)	E (Good)		
8	M(0.56)	E(0.93)	E(0.75)	E (Good)	E (Good)		
9	M(0.55)	E(0.79)	M(0.54)	M(Good)	M(Good)		
10	E(0.69)	M(0.48)	M(0.53)	M(Good)	M(Good)		
11	E(0.95)	M(0.59)	M(0.59)	M(Good)	M(Good)		
12	E(0.85)	M(0.68)	E(0.93)	M(Good)	E(Good)		
13	M(0.53)	E(0.80)	M(0.46)	M(Good)	M(Good)		
14	M(0.55)	M(0.61)	M(0.55)	M(Good)	M(Good)		
15	M(0.47)	M(0.51)	E(0.75)	L (Not-good)	L (Not-good)	1	0
16	M(0.49)	B(0.19)	L(0.21)	L (Not-good)	L (Not-good)		
17	M(0.61)	M(0.44)	L(0.11)	L (Not-good)	L (Not-good)		
18	E(0.89)	M(0.42)	E(0.79)	L (Not-good)	L (Not-good)		
19	M(0.54)	E(0.78)	L(0.01)	L (Not-good)	L (Not-good)		
20	E(0.71)	E(0.81)	L(0.21)	L (Not-good)	L (Not-good)		

V. CONCLUSION

The main impartial of this research is to design an expert system to the assessment of ELB in Cloud Computing developed under the guidelines from the Microsoft Cloud Computing Organization and Punjab Information Technology Board, Pakistan. The propound Expert System is straightforward to use for professional and non-professionals. The proposed ELB-multilayer-mamdani fuzzy inference Expert System can categorise the level of Load Balancing in cloud computing into Excellent, Normal or Low. ELB-multilayer-mamdani fuzzy inference Expert System uses input Cloud Computing parameters such as bacterial, physical, chemical and radioactive for different layers. It's also observed that Propound ELB- multilayer-mamdani fuzzy inference Expert System gives more accurate results. The coherence of the proposed system can be ameliorate using other soft computing approaches like Neural network, Neuro-Fuzzy, etc.

REFERENCES

[1] Rajkumar Buyya, Chee Shin Yeo, Srikumar Venugopal, James Broberg, and Ivona Brandic, Cloud Computing and Emerging IT Platforms: Vision, Hype, and Reality for Delivering Computing as the 5th Utility, Future Generation Computer Systems, Volume 25, Number 6, Pages: 599-616, ISSN: 0167-739X, Elsevier Science, Amsterdam, The Netherlands, June 2009.

[2] Rodrigo N. Calheiros, Rajiv Ranjan, Anton Beloglazov, César A. F. De Rose, and Rajkumar Buyya, "CloudSim: A Toolkit for Modeling and Simulation of Cloud Computing Environments and Evaluation of

Resource Provisioning Algorithms", Software: Practice and Experience, Volume 41, Issue 1, pages 23–50, January 2011.

[3] T V R Anandarajan, M A Bhagyabini, "Co-operative scheduled Energy aware load-balancing technique for an efficient computational cloud", IJCSI, volume 8, issue 2, March 2011.

[4] D A Mansai, P NGO, "Understanding Cloud Computing: Experimentation and Capacity Planning", Proc. Computer Measurement Group Conf, Dallas, TX, Dec. 7-11, 2009.

[5] Menno Dobber, Rob van der Mei, and Ger Koole "Dynamic Load Balancing and Job Replication in a Global -Scale Grid Environment: A Comparison" IEEE TRANSACTIONS ON PARALLEL AND DISTRIBUTED SYSTEMS, vol. 20, no.2, pp 207, Feb 2009.

[6] Kuo-Qin Yan; Wen-Pin Liao; Shun-Sheng Wang, "Towards a Load Balancing in a three-level cloud computing network", 3rd IEEE International Conference on Computer Science and Information Technology (ICCSIT), 2010, Vol -1, pp.-108-113, 2010.

[7] Jeffrey M. Galloway, Karl L. Smith, Susan S. Vrbsky, "Power Aware Load Balancing for Cloud Computing", Proceedings of the World Congress on Engineering and Computer Science 2011 Vol I WCECS 2011, October 19-21, 2011.

[8] Raul' Alonso-Calvo, Jose Crespo, Miguel Garcia'ia- Remesal, Alberto Anguita, and Victor Maojo "On distributing load in cloud computing: A real application for very-large image datasets", International Conference on Computational Science, ICCS 2010, pp. - 2669-2677, 2010.

[9] Zenon Chaczko Venkatesh Mahadevan, Shahrzad Aslanzadeh and Christopher Mcdermid, "Availability and Load Balancing in Cloud Computing", 2011 International Conference on Computer and Software Modeling IPCSIT vol.14, IACSIT Press, Singapore, 2011.

[10] B. Wickremasinghe, R. Calheiros, and R. Buyya, "CloudAnalyst: A CloudSim-Based Visual Modeller for Analysing Cloud Computing Environments and Applications," in 24th IEEE Int. Conf. on Advanced Information Networking and Applications, Perth, Australia, 2010, pp.446-452.

- [11] X. Kon, C. Lin, Y. Jiang, W. Yan, and X. Chu, "Efficient Dynamic Task Scheduling in Virtualized Data Centers with Fuzzy Prediction," *J. of Network and Computer Applications*, vol. 34, issue. 4, pp.1068-1077, July 2011.
- [12] Alexandru Iosup, Member, IEEE, Simon Ostermann, Nezhir Yigitbasi, Member, IEEE, Radu Prodan, Member, IEEE, Thomas Fahringer, Member, IEEE, and Dick Epema, Member, IEEE, "Performance Analysis of Cloud Computing Services for Many -Tasks Scientific Computing", *IEEE TPDS, MANY-TASK COMPUTING, NOVEMBER 2010*.
- [13] Martin Randles, David Lamb, A. Taleb-Bendiab, "A Comparative Study into Distributed Load Balancing Algorithms for Cloud Computing", *IEEE 24th International Conference on Advanced Information Networking and Applications Workshops*, 20-23, pp. 551-556, April 2010.
- [14] Meenakshi Sharma, Pankaj Sharma, Sandeep Sharma, "Efficient Load Balancing Algorithm in VM Cloud Environment", *IJCST Vol. 3, Issue 1*, pp.- 439-441, Jan. - March 2012
- [15] R. Shimonski. "Windows 2000 & Windows Server 2003 Clustering and Load Balancing", Emeryville. McGraw-Hill Professional Publishing, CA, USA (2003), p 2, 2003.
- [16] Ali M. Alakeel, "A Guide to Dynamic Load Balancing in Distributed Computer Systems", *IJCSNS International Journal of Computer Science and Network Security*, VOL.10 No.6, June 2010.
- [17] R. X. T. and X. F. Z, "A Load Balancing Strategy Based on the Combination of Static and Dynamic, in *Database Technology and Applications (DBTA), 2010 2nd International Workshop 2010*, pp. 1-4, 2010.
- [18] IETF, 2010, Extensible Messaging and Presence Protocol (XMPP): CoreRFC3920, <http://datatracker.ietf.org/doc/rfc3920/>, viewed on 25th of Nov 2010.
- [19] Y. F. Wong and W. C. Wong. "A fuzzy-decision-based routing protocol for mobile ad hoc networks" *10th IEEE International Conference on Network*, pp. 317-322, 2002.
- [20] G. V. S. Raju, G. Hernandez, and Q. Zou, "Quality of service routing in ad hoc networks", *IEEE Wireless Communications and Networking Conference*, Vol. 1, pp. 263 -265, 2000.
- [21] W. Pedrycz and F. Gomide, "An introduction to fuzzy sets: analysis and design", complex adaptive systems. MIT Press, 1998.
- [22] J. J. Buckley, E. Eslami, and E. Esfandiari. "An introduction to fuzzy logic and fuzzy sets" *advances in soft computing*, Physica Verlag, 2002.

Performance Analysis of Multilayer Perceptron Neural Network Models in Week-Ahead Rainfall Forecasting

Lemuel Clark P. Velasco¹, Ruth P. Serquiña², Mohammad Shahin A. Abdul Zamad³, Bryan F. Juanico⁴,
Junneil C. Lomocso⁵

Mindanao State University-Iligan Institute of Technology
Premier Research Institute of Science and Mathematics
Iligan City, The Philippines

Abstract—Multilayer perceptron neural network (MLPNN) is considered as one of the most efficient forecasting techniques which can be implemented for the prediction of weather occurrence. As with any machine learning implementation, the challenge on the utilization of MLPNN in rainfall forecasting lies in the development and evaluation of MLPNN models which delivers optimal forecasting performance. This research conducted performance analysis of MLPNN models through data preparation, model designing, and model evaluation in order to determine which parameters are the best-fit configurations for MLPNN model implementation in rainfall forecasting. During rainfall data preparation, imputation process and spatial correlation evaluation of weather variables from various weather stations showed that the geographical location of the chosen weather stations did not have a direct correlation between stations with respect to rainfall behavior leading to the decision of utilizing the weather station having the most complete weather data to be fed in the MLPNN. By conducting performance analysis of MLPNN models with different combinations of training algorithms, activation functions, learning rate, and momentum, it was found out that MLPNN model having 100 hidden neurons with Scaled Conjugate Gradient training algorithm and Sigmoid activation function delivered the lowest RMSE of 0.031537 while another MLPNN model having the same number of hidden neurons, the same activation function but Resilient Propagation as training algorithm had the lowest MAE of 0.0209. The results of this research showed that performance analysis of MLPNN models is a crucial process in model implementation of MLPNN for week-ahead rainfall forecasting.

Keywords—Multilayer perceptron neural network; performance analysis; rainfall forecasting

I. INTRODUCTION

Multilayer perceptron neural network (MLPNN) is considered as a widely used artificial neural networks architecture in predictive analytics functions. The architecture of an artificial neural network, that is, its structure and type of network is one of the most important choices concerning the implementation of neural networks as forecasting tools. The design of MLPNN is motivated by the structure of a biological neuron system capable of parallel processing like a human brain, but the processing elements of this machine learning tool has gone far from their biological inspiration [1, 2, 3]. For this

reason, MLPNN have been successfully used by most of the researchers in the field of forecasting, science and engineering to predict the behavior of both linear and nonlinear systems without the need to make assumptions that are implicit in most traditional statistical approaches [2, 4, 5, 6]. With all its promising results, the biggest challenge with MLPNN is the selection of an appropriate model since there are different MLPNN model structures, training algorithms, activation functions, learning rate, momentum and number of epochs to choose from [1, 7]. This makes it hard to find the proper model for a particular problem [4]. Modelers and researchers who use MLPNN in forecasting still rely on performance analysis of MLPNN models in order to implement domain-specific applications that generate close to accurate predictions.

The field of rainfall forecasting is one of the domains that utilize MLPNN in generating predictions of various granularities [1, 3, 5]. Rainfall is the metric used to measure the amount of rain that accumulates at any given point in the earth's surface. This measurement is usually reported in millimeters and is most often associated with its more violent counterpart which is flooding. Out of the historical data collected from various rain gauges, MLPNN models show great potential in discovering patterns from preprocessed data which in turn forecast rainfall used for life-saving applications such as flood management and airport administration. The nature of the combination of meteorological parameters such as relative humidity, air pressure, wet bulb temperature, cloudiness, and rainfall at the point of measurement as well as from surrounding stations poses challenges in data preparation as well as in the input and hidden layers of MLPNN models [7, 8]. Furthermore, in the output layers of MLPNN applications for rainfall forecasting, modelers usually generate week-ahead forecast to give ample time for decision makers in the dissemination of disaster preparedness measures to the affected stakeholders [3]. With the consideration of the continuous data gathered from rainy and non-rainy periods, data representation, data cleaning, correlation evaluation and data transformation are also modeling challenges that need to be considered before using any MLPNN model as a supervised learning framework in the forecast of life-saving predictions [1, 5, 8]. With this, performance analysis of MLPNN models that takes into consideration appropriate data preparation which optimizes

various neural networks parameters is an important function in week-ahead rainfall predictions.

The choice of a dataset and the quality of its data is a defining factor in the accuracy of the MLPNN model's output. Data quality for the dataset has to be maintained else the prediction process of the MPNN and its testing will potentially suffer from anomalies and inconsistencies [9, 10]. In addition, the selection of the study area, time span of the data, and important variables in the dataset must be conducted in order to produce the best possible case scenario for the research problem. Furthermore, without the proper representation of MLPNN model results, discussions, and error assessment, rainfall forecasting will fail to capture the validity of its output and leave these implementation efforts vulnerable to misinterpretation [2, 8]. Thus, the choice of the MLPNN model, multiple runs of data pre-processing, model construction, and the analysis and presentation of MLPNN model performance are all required to present a working solution to the prediction of rainfall and other weather phenomena. This research aims to focus on evaluating the performance of MLPNN models in choosing a suitable candidate for implementation in week-ahead rainfall forecasting. Specifically, this study exhibits foundational methodologies in MLPNN model design creation which involves data preparation procedures and decisions on the parameter values to be implemented. The results of this study can provide methods on testing the validity and accuracy of MLPNN models as well as comparing and measuring the performance of its various forecasting parameters. This study hopes to contribute to the recent technology of rainfall forecasting by evaluating MLPNN models which can be used to optimally implement close to accurate predictions that provide accurate rainfall forecast to specific localities.

II. METHODOLOGY

A. Rainfall Data Preparation

Data preparation involves the exploration, analysis, and other general pre-processing methods and techniques that must be performed before data is fed to the MLPNN model. Initially, data selection and data representation which are the processes of choosing the appropriate dataset and the representation of

key variables to be considered as well as the transformation of non-numeric variables into numerical representations need to be followed by testing these variables for correlation with rainfall and spatial autocorrelation along with other geographic locations [9, 11, 12]. Weather data gathered from Tutiempo Network S.L. of seven weather stations in Mindanao, the Philippines was considered due to the geographical surface area and proximity within the path of a number of storms and typhoons. Moreover, the weather dataset shown in Table I was segregated into multiple years for each of the seven stations segregated by their month with each month constituting of daily recorded observations. The 12-year weather data from 2006-2017 from the seven weather stations totaling to 398,853 units of data underwent data preparation. Additionally, ISO 8601 standard for dates, yyyy/mm/dd was also used to represent the dates corresponding the weather data.

Missing data is a type of data anomaly in weather and climate data that occurs when measuring instruments fail, leaving behind gaps in the dataset. The percentage of missing data in the dataset was computed in order to determine how much data was missing. It is important to determine the percentage of missing data in a dataset because it can cause significant prediction error when data is not uniform [11]. It is an important calculation to make because without understanding the scale of missing data, it would be difficult to gauge how much the imputation process will affect overall accuracy. The larger the amount of missing data, the larger amount of values that have to be filled in by the imputation process, thus lesser missing data implies better overall accuracy. Aside from determining the total of missing data per set, the missing data per climate variable is also an important metric to determine. It needs to be accounted for due to later steps involving individual variables being used for correlation measurements. A variable that has a large number of missing data will also affect the computation of the Pearson's correlation coefficient to be conducted in the study. Random Forests Imputation method was then used to fill in the identified missing data. The Random Forests Imputation method is an ensemble learning method for classification and regression which uses multiple decision trees and outputs either the mode for classification problems or the mean prediction for regression problems of the individual trees.

TABLE I. WEATHER DATA VARIABLES

SYMBOL	CLIMATE FEATURE	UNIT	SYMBOL	CLIMATE FEATURE	UNIT
T	Average Temperature	°C	V	Average Wind Speed	km/h
TM	Maximum Temperature	°C	VM	Maximum Sustained Wind Speed	km/h
Tm	Minimum Temperature	°C	VG	Maximum speed of wind	km/h
SLP	Atmospheric Pressure at Sea Level	hPa	RA	Indicate whether there was rain or drizzle	0 or null
H	Average Relative Humidity	%	SN	Indicate if it snowed	0 or null
PP	Total Rainfall/ Snowmelt	mm	TS	Indicate whether there was a storm	0 or null
VV	Average Visibility	km	FG	Indicate whether there was fog	0 or null

Variable correlation evaluation was then conducted to determine which variables in the weather dataset are correlated against the target variable which is rainfall. As suggested by researches, to confirm which of the variables in the dataset fit the criteria, the Pearson's Correlation Formula was used to determine the correlation strength of each climatological variable with regards to rainfall [13]. Results range between $[-1, +1]$, indicating weak to strong correlation with values close to 0 indicating no correlation. For this study, a 95% confidence interval was used with a considered p -value of less than or equal to 0.005. As shown in Equation 1, the Pearson's Correlation Formula was run multiple times for each rainfall combination per weather station. The Pearson's Correlation Coefficient r provided values of two different variables x_i and y_i of equal cardinality n where \bar{x} and \bar{y} are the means of the two variables respectively.

$$r = \frac{\sum_{i=1}^n (x_i - \bar{x})(y_i - \bar{y})}{\sqrt{\sum_{i=1}^n (x_i - \bar{x})^2} \sqrt{\sum_{i=1}^n (y_i - \bar{y})^2}} \quad (1)$$

As applied in this study, x_i was used to denote rainfall values and y_i was used to denote values for one other climate variable aside from rainfall like average temperature and humidity.

In order to increase the predictive power and include more data for training the MLPNN, the identification of clusters was conducted in the entire geographic area using Spatial Autocorrelation. This will result in the identification of a base weather station along with other stations in the initial study area that has rainfall values spatially correlated with one another. The data present in the base station and the identified stations that exhibit correlation was included as inputs for the MLPNN to predict the rainfall values of the base station. To test for particular locations that exhibit local spatial autocorrelation of their values, Local Moran's I , an extension of the Pearson's Correlation formula with the addition of a spatial weights matrix which represents the weight given to the distance between points in space was used. A 95% confidence interval was used, meaning that a p -value of less than or equal to 0.005 was considered. The Local Moran's I for location i provided two locations in space i and j as shown in Equation 2, where z_i and z_j are the deviations from the mean at both locations, S_i^2 being the standard deviation at location i and ω_{ij} being a spatial weights matrix.

$$I_i = \frac{z_i}{S_i^2} \sum_j w_{i,j} z_j \quad (2)$$

As applied in this study, z_i and z_j are deviations from the mean at weather stations i and j . To acquire a spatial weights matrix, a list of neighbors was needed. The k -nearest neighbor algorithm was used to generate a list of neighbors. The algorithm returns a list of neighbors that correspond to the number k attached to each weather station. The local Moran formula was applied in different stages, at each stage increasing the number of neighbors for each weather station. After the list of neighbors was acquired, a row standardized weight matrix was calculated from it. Since the list of neighbors differs at every iteration k , a different weight matrix was generated at every step. Once a spatial weight matrix has been generated, the local Moran formula was then calculated.

Since the spatial weights matrix differs at every iteration of k , a different set of Moran indices were calculated. After transforming the dataset using Min-Max Normalization, the dataset was then partitioned into different sets namely the Training Set and the Testing Set. The dataset was partitioned according to the number of years instead of percentages as suggested by researches on rainfall forecasting conducted in tropical counties [11, 12].

B. MLPNN Model Evaluation

The MLPNN architecture and model define the structure of the neural network which includes the number of layers, the direction of data flow in each layer, number of neurons per layer, and how these neurons are arranged. The neurons comprising the input layer is completely and uniquely determined once the specifications of the training data have been identified with the number of neurons comprising the input layer to be equal to the number of features in the data set. According to researches, the three most significant data inputs in rainfall prediction aside from the actual daily rainfall or precipitation values are relative humidity, air pressure and average temperature as these core elements constitutes the formation of rain or storm [4, 14]. Temperature affects the evaporation process causing increase in humidity while pressure affects the flow of air carrying these two. In order to predict rainfall with a high level of accuracy, these three parameters should be used. But since this research also considers the correlation between stations and its variables, other input data such as wind speed and visibility will also be tested with the aim to find out if the results yields an acceptable correlation evaluation, then the variable will be included as an input. The next matter to be resolved following the identification of the input layer is the number of hidden layers to be used along with its hidden neuron. According to the studies, a single hidden layer of a MLPNN is sufficient enough to approximate any complex nonlinear function with any desired accuracy [2, 4, 10]. As for the number of neurons in the hidden layer, the formula shown in Equation 3 as suggested by a study would give an upper bound limit of values that will not result in over fitting [15]. Stathakis' formula uses an arbitrary scaling factor from 2-10 that is multiplied by the sum of the total input plus total output in order to gradually decrease the value of the number of neurons as the arbitrary factor reaches to 10.

$$Nh = \frac{Ns}{(\alpha * (Ni + No))} \quad (3)$$

In this formula, Nh is the total number of hidden neurons to be calculated. This is done by dividing the total number of samples in the training data set Ns with the product of the arbitrary scaling factor α multiplied to the sum of the total input Ni with the addition of the total number of output No . The result will be tested individually as the number of input neurons in the hidden layer decreases. Along with other MLPNN parameters, models that reach the local minima with the lowest MAE and RMSE will be selected as the optimal number of hidden neurons. Since this study aims to predict rainfall data on a weekly basis, the number of output neurons will correspond to the requirement which is to produce 7 prediction outputs corresponding to 7 days as represented by the 7 output neurons.

This work is supported by the Mindanao State University-Iligan Institute of Technology (MSU-IIT) as an internally funded research under the Premier Research Institute of Science and Mathematics (PRISM) Applied Mathematics and Statistics Group.

Training algorithms, activation functions, learning rates and the momentum are important MLPNN model parameters that should be identified. The MLPNN training algorithm is the parameter that tunes the network so that its outputs are close to the desired values [16]. In choosing the training algorithm, several factors have to be considered including the complexity of the problem, the number of data points in the training set, the number of weights and biases in the network, the error goal and whether the network is being used for pattern recognition or function approximation [5, 16]. Since this study is dealing with rainfall forecasting which relies heavily on statistical calculations given historical data in order to get future values, the researchers focused on the function approximation algorithms. Function approximation algorithm shown in Equation 4 allowed researchers to find ways of separating objects into different classification given an input vector x , a weight vector w , and a threshold value T , an output of 1 indicating membership of a classification, consequently an output of 0 indicating exclusion from the class [17]. With this, a select function approximation algorithm will be used for the training algorithms.

$$\sum_i w_i (x_i) > T \quad (4)$$

The activation function indicates the output of a neuron in terms of its input. Activation functions are important in order for the MLPNN to learn and make sense of complicated and non-linear complex functional mappings between inputs and response variable [6, 12]. Its main purpose is to convert the input signal of a node to an output signal which will be used as input in the next layer. There are a number of activation functions that can be used such as Sigmoid, Threshold and Linear activation functions. Among MLPNN implementations, the activation functions often chosen for rainfall forecasting are the logistic sigmoid and hyperbolic tangent [2, 3, 8, 16]. These functions are used because they are mathematically convenient and are close to linear near origin while saturating rather quickly when getting away from the origin allowing MLPNN to model strongly and mildly nonlinear mappings.

As for the learning rate η , which determines how fast weights changes in order to reach local minimum, the goal is to find a value low enough that the network converges to an acceptable result but high enough that the network do not have to spend years just training. Some studies in rainfall prediction use 0.8 as the default value for learning rate [6, 18, 19]. There can be a situation in the MLPNN model where the algorithm converges to a local minimum or saddle point and may think it reached the global minima leading to a sub-optimal result. Momentum is used to avoid this situation though a value between 0 and 1 that increases the size of the steps taken towards the minimum by trying to jump from local minima. If the momentum is large, then the learning rate should be kept small. A large value of momentum also means that the convergence will happen fast. But if both the momentum and learning rate are kept at large values, it might skip the minimum with a huge step, or else momentum cannot reliably avoid local minima and slows down training of the system.

Momentum also helps in smoothing out the variations, if the gradient keeps changing direction. A right value of momentum can be either learned by trial and error within 0.1 and 0.9 as suggested in a research or through cross-validation [5]. Thus, this study simulated different combinations of training algorithms and activation functions along with a range of values for momentum and learning rate in formulating the MLPNN models.

After identifying the model architecture and formulating different models, the researchers conducted a supervised training process of each model by feeding the training data set into the MLPNN. Training is an essential step in order for the MLPNN models to do forecasting [10]. It is during this process that the MLPNN adapts itself to a stimulus and eventually produces a desired response. In conducting the supervised training, the training data set already underwent data preparation in which it was imputed to fill the missing values, correlation evaluated to remove variables that have no significant influence in rainfall, normalization to normalize dataset into (0, 1). When feeding the training data set into the MLPNN model, an ideal or desired output was introduced along with the input stimulus. Then the response is compared with the desired output and if response differs from the desired value, the network generates an error signal, which was used to calculate the adjustment that should be made to the network's synaptic weights so that the actual output matches the target output possibly getting an error close to zero. In order to test the accuracy of the trained models, testing was conducted. Testing results was used to compute the MAE and RMSE for the error measurement in order to identify the optimal model. To properly compute the MAE and RMSE, the researchers group the data by week from Day 1-7 i.e. January 1 to January 7 as first week then increment the starting day of the next week by 1 each time. So that the second week starts at Day 2-8 i.e. January 2 to January 8, so on and so forth. This process continues until the whole result has been grouped by week. MAE and RMSE were then calculated per week. Once it was done, the average of all values obtained was calculated and recorded. These steps were repeated for all formulated models. The model that produced the smallest MAE and RMSE error will be chosen as the optimal MLPNN model of the performance analysis.

III. RESULTS AND DISCUSSION

A. Rainfall Data Preparation Results

There were variables in the dataset that were found to be variables that have no bearing in the prediction of rainfall, as they merely indicate the occurrence of different weather phenomena. These variables were RA, SN, TG, and FG; these variables along with the columns they represent were removed from the dataset. The percentage of missing data in the dataset was then calculated in order to better understand the amount of information lost during the recording of the data. Table II shows the amount of missing data present per weather station and its percentage when compared to the total amount of data units.

TABLE II. MISSING DATA PER WEATHER STATION

Station	Missing data	Total data	%of missing data	Station	Missing data	Total data	%of missing data
Butuan	442	39789	1.11%	Malaybalay	2741	39789	6.89%
Davao	216	39789	0.54%	Surigao	974	39789	2.45%
Dipolog	359	39789	0.90%	Zamboanga	252	39789	0.63%
Hinatuan	601	39789	1.51%				

The three stations that exhibit the least amount of missing data are Davao Airport, Zamboanga, and Dipolog with 0.54%, 0.63%, and 0.90% respectively. These stations are the prime candidates to use as the base station due to the missing values being brought down to the minimum, ensuring that the accuracy of the dataset is true to the real world and not artificially filled in through imputation. Stations with the most missing data are Malaybalay with 6.89%, Surigao with 2.45%, and Hinatuan with 1.51%. Tables III and IV shows the state of the dataset during pre-imputation and post-imputation for a chosen weather station for the first 3 days of January 2006, respectively. This research requires the usage of an imputation technique due to succeeding methodologies requiring a complete set of data. Correlation formulas need as many existing data as possible in order to determine an accurate correlation measure. Removing the missing data while possible results in information loss; in some stations the information loss will be severe like Malaybalay. Furthermore, by not imputing the missing data the research loses out on predictive power when developing the MLPNN. This is an important factor to consider since without much data, the forecasting accuracy will be severely affected.

For each dataset, the rainfall variable and another variable in the same set were tested using Pearson’s Product-Moment Correlation Test. After the Pearson’s Correlation test was performed on the dataset, the results were given in pairs of two, the first element being the value of the coefficient, and the second being the *p*-value of the coefficient. This is an important step because more data was needed to include in the MLPNN and other climate variables are the best indicator for correlation with rainfall. Furthermore, since rainfall is the target climate variable to be forecasted, other climate variables are bound to influence the amount of, frequency, and severity of rainfall. Thus, correlation between variables and rainfall was calculated. It is important to recall that the study will be using a 95% confidence interval, so *p*-values less than or equal to 0.005 will be considered. Among the seven sets of data, Zamboanga station has the most variables correlated with rainfall being 8 and the least amount of variables being correlated is Hinatuan with 5. Dipolog and Malaybalay stations have 6 correlated variables, while Davao Airport and Surigao has 7 correlated variables. Fig. 1 and 2 graphically shows the Pearson’s *r* and their *p*-values, respectively.

Once the variables correlated with rainfall were determined, spatial autocorrelation was measured between stations in close proximity with each other using Local Moran’s *I*. The list of neighbors was acquired by using the *k*-

nearest neighbor algorithm. Each *k* indicates the number of neighbors attached to a weather station, so for example *k*=2 means that there are two weather stations attached to every station in the study area and *k*=5 means that there are five weather stations attached to every station. This step was conducted to determine potential clusters in the study area for initial consideration. Without determining potential clusters, the autocorrelation measurement can no longer be called a Local Indicator of Spatial Autocorrelation which cannot be used for the scope of this study. The results of the process are shown in Table V where each column marked by *k* represents the number of neighbors attached to a particular station. Davao’s closest neighbor would be Malaybalay at *k*=1, at *k*=2 there will be two stations attached as neighbors: Hinatuan and Malaybalay. This process repeats for all seven weather stations.

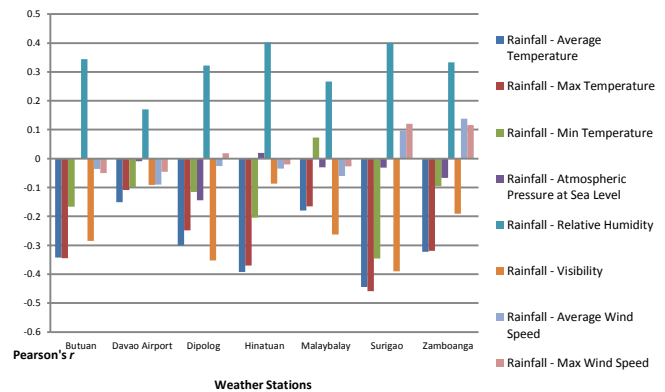


Fig. 1. Graph of All Collected Pearson’s *r*.

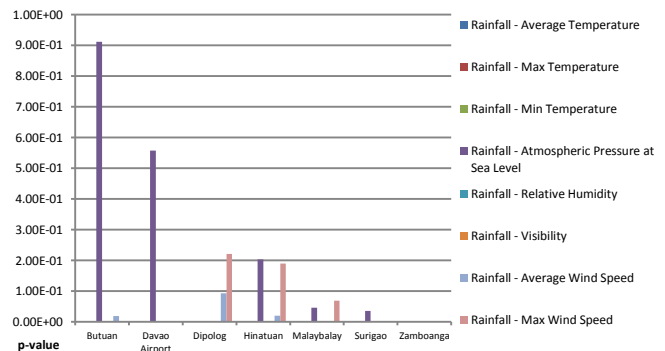


Fig. 2. Graph of All Collected *p*-Values.

After the list of neighbors was acquired, a row standardized weight matrix was calculated from it. A row standardized weight matrix is a matrix whose values represent the numerical weight the algorithm gives to emphasize the importance of the distance between two neighboring points in space. The higher the number, the more weight is given to the distance between locations. This weight matrix was needed to calculate the local Moran index for every identified potential cluster under consideration. Table VI shows the results of that process at $k=1$, where k is the number of neighbors attached to a weather station.

After the weights matrix was calculated, the required parameters of the local Moran formula were now met. The

process was iterated for every value of k , increasing the number of neighbors. A different set of Moran indices and p -values were calculated at every iteration. It was observed that due to extreme values of rainfall, there were cases when the Moran index returns a Not a Number (NaN). These situations were encountered when there exists a day where the rainfall values across all considered weather stations were 0. In this situation, the value was converted to a 0. Tables VII and VIII details a sample table of the local Moran indexes per day at $k=1$ as well as the p -values associated with them, respectively. These results are important because they determine whether or not the Moran indices throughout time are uniform and consistent, as well as determine if these Moran indices are significant at the accepted 95% confidence interval.

TABLE III. PRE-IMPUTATION DATASET OF THE WEATHER STATION

Y	M	D	T	TM	Tm	SLP	H	PP	VV	V	VM
2006	1	1	28.1	32.3	23.5	1008.8	87	0	15.9	3.5	10.7
2006	1	2	27.6	28.8	25.7	1009.2	86	9.91	12.6	4.4	7.2
2006	1	3									

TABLE IV. POST-IMPUTATION DATASET OF THE WEATHER STATION

Y	M	D	T	TM	Tm	SLP	H	PP	VV	V	VM
2006	1	1	28	32	24	1009	87	0	16	3.5	11
2006	1	2	28	29	26	1009	86	9.9	13	4.4	7.2
2006	1	3	27	30	24	1010	87	11	14	3	9.9

TABLE V. RESULT OF THE K-NEAREST NEIGHBOR ALGORITHM

Station	$k=1$	$k=2$	$k=3$	$k=4$	$k=5$	$k=6$
Butuan	Surigao	Malaybalay	Hinatuan	Davao	Dipolog	Zamboanga
Davao	Malaybalay	Hinatuan	Butuan	Surigao	Dipolog	Zamboanga
Dipolog	Malaybalay	Zamboanga	Butuan	Surigao	Davao	Hinatuan
Hinatuan	Butuan	Malaybalay	Davao	Surigao	Dipolog	Zamboanga
Malaybalay	Butuan	Davao	Hinatuan	Surigao	Dipolog	Zamboanga
Surigao	Butuan	Hinatuan	Malaybalay	Dipolog	Davao	Zamboanga
Zamboanga	Dipolog	Malaybalay	Davao	Butuan	Surigao	Hinatuan

TABLE VI. RESULT OF THE SPATIAL WEIGHTS MATRIX AT $K=1$

	Butuan	Davao	Dipolog	Hinatuan	Malaybalay	Surigao	Zamboanga
Butuan	0.000000	0.000000	0.000000	0.3333333	0.3333333	0.3333333	0.000000
Davao	0.000000	0.000000	0.000000	0.000000	1.000000	0.000000	0.000000
Dipolog	0.000000	0.000000	0.000000	0.000000	0.500000	0.000000	0.500000
Hinatuan	1.000000	0.000000	0.000000	0.000000	0.000000	0.000000	0.000000
Malaybalay	0.3333333	0.3333333	0.3333333	0.000000	0.000000	0.000000	0.000000
Surigao	1.000000	0.000000	0.000000	0.000000	0.000000	0.000000	0.000000
Zamboanga	0.000000	0.000000	1.000000	0.000000	0.000000	0.000000	0.000000

TABLE VII. SAMPLE TABLE OF COLLECTED LOCAL MORAN INDEXES AT $K=1$ OF A CHOSEN WEATHER STATION

Station	Day1	Day2	Day3	Day4	Day5	Day6	Day7
Butuan	-0.23741	0.11511024	-0.5840033	-0.4812947	0.34175831	-0.10306089	-0.0260774
Davao	0.1613777	0.41525523	0.381054	0.5636944	-0.03057254	-0.41368012	0.59088377
Dipolog	0.1359339	0.06561247	0.3668329	0.3555742	0.38138875	0.42227707	0.51195061
Hinatuan	-1.1727723	0.78774914	-0.9067904	-1.0368087	1.13056531	0.08142846	-0.04060727
Malaybalay	0.1839798	0.08734511	0.3770831	0.4908609	-0.01572634	0.09587238	0.37478806
Surigao	0.2302712	-0.22120921	-1.2262734	-0.8615195	-0.12905408	-0.63906866	-0.06406317
Zamboanga	0.1115774	0.06323564	0.3645246	0.2567042	0.80314769	0.39171443	0.51685907

TABLE VIII. SAMPLE TABLE OF COLLECTED P VALUES AT K=1 OF A CHOSEN WEATHER STATION

Station	Day1	Day2	Day3	Day4	Day5	Day6	Day7
Malaybalay	0.1815233	0.26302077	0.1015762	0.06259734	0.35697344	0.2583876	0.1023129
Surigao	0.2284913	0.53194755	0.8828206	0.77941166	0.48061866	0.7447528	0.4540085
Dipolog	0.2394622	0.31630871	0.1784729	0.18571222	0.14882041	0.1202729	0.1200828
Davao	0.2693683	0.19619077	0.2693726	0.20909464	0.43020454	0.634613	0.1968113
Zamboanga	0.3010429	0.3677157	0.275534	0.31943323	0.10507711	0.2183319	0.2207365
Butuan	0.5728002	0.24091351	0.8356553	0.76843441	0.10846802	0.4375946	0.3709408
Hinatuan	0.9703086	0.08033877	0.7969135	0.83260397	0.04684826	0.3648206	0.4435583

Each of the rows in the table correspond to each weather station, each of the columns represent the days in the time frame, and each data cell the Moran index associated with the day and station. As can be observed, some values do not conform to the typical range for the Local Moran's Index formula, which is -1 to $+1$. A researcher has already established that the Local Moran Index formula does not actually have a set range of $(-1, +1)$ [20]. Moreover, the exact range of indices actually conforms to the smallest and largest eigenvalue of among $n-1$ eigenvalues of the weights matrix W . So this means that depending on the spatial weights matrix generated, the values for the indices will differ and might not conform to the usual standard range. The spatial weights matrix is more effective when the locations in question are close to each other, and thus have more weight established between them. Furthermore, the results differ at every day with values indicating a positive relationship other a negative relationship indicating a sporadic pattern.

As shown, the collected p -values for each Local Moran index of each weather station across all the days of the time frame, 2006-2017. Each of the rows in the table correspond to each weather station, each of the columns represent the days in the time frame and each data cell the p -value of the Moran index that correspond to the day and weather station. The p -values are all above 0.005, the maximum requirement for a value to be considered significant at a 95% confidence interval. This indicates that the calculated Moran indices are not considered to be significant for study which creates a problem. From the generated values, a line graph was drawn up to show the variation of each Moran Index value per day. The same process can also be generated for the p -values per day. The line graphs are for the Moran Indexes and p -values taken at $k=1$ for a chosen weather station across the entire time span ranging from 2006 – 2017, respectively. Fig. 3 shows that for all the days in the duration 2006 – 2017, the calculated Moran indices for each day come out to an interval between 1 and -1.5 . Although it does not conform to the range, it still indicates whether or not particular locations have correspondence. However, Fig. 4 further shows that the Moran indices do not exhibit uniform and consistent values through time. This means that these Moran indices are highly variable and differ at points in time, making these values sporadic and difficult to predict. As shown, none of the Moran indices calculated are within a 95% confidence interval. This means that none of these indices are significant and cannot be used as indicators for spatial autocorrelation.

Upon further calculation of Local Moran indexes and their p -values with increasing k , the number of neighbors attached, it was found out that any and all settings result to the same pattern. The pattern being indices not conforming to the standard range, and the p -values being greater than the 95% confidence interval will allow. This means that according to the formula, none of the locations in the geographic space have correlation with regards to their rainfall values, regardless of the number of neighbors attached. This may be due to factors that cannot be controlled, such as the topography between each station or the distance between locations. The shorter the distance the greater would be the correspondence, however as shown, it will seem that the distance between stations are too much to determine an accurate measure of relationship. Furthermore, the topography of Mindanao, the Philippines consists of flat plains and mountain ranges, and other types of topography which directly influences the behavior of rain clouds or storms as they approach each station.

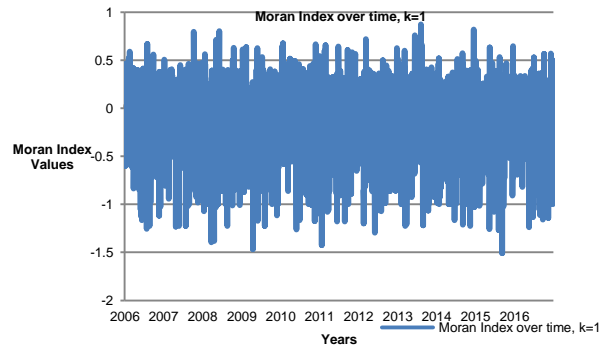


Fig. 3. Local Moran Indexes at $k=1$ for a Chosen Weather Station.

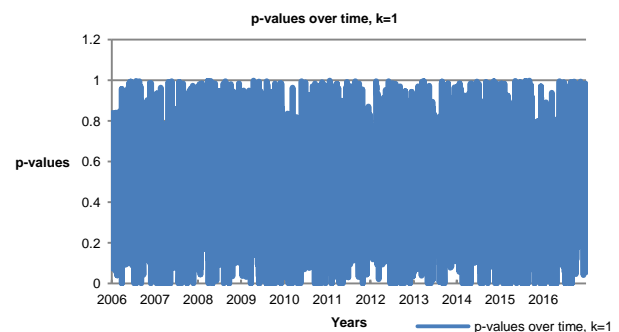


Fig. 4. Collected P-Values at $K=1$ for a Chosen Weather Stations

With this, since none of the stations exhibit rainfall correlation, an alternate course of action was taken. Instead of using correlation and neighboring stations' rainfall values as an addition for feeding data into the MLPNN, a single station's data was used to feed data to the MLPNN. The selection of this single station depended primarily on the percentage of missing data on its dataset reducing the need to impute the remaining missing data and the number of local variables correlated with the location's rainfall attribute. Ultimately, data set from the Davao station with its 0.54% missing data percentage and having 7 climate variables correlated with rainfall was used in the alternate action. In total, the Davao dataset will bring with it 11 variables to be used as data for the MLPNN: 8 climate variables including the rainfall variable and 3 numerical variables, corresponding to the day of the month, month, and year, respectively. As shown in Table IX, the Training Set starts at the beginning of the time series which is the 1st of January 2006 and ends on the 31st of December 2016. The Testing Set starts right after the end of the Training Set which is the 1st of January 2017 and ends in the 31st of December 2017.

B. MLPNN Model Evaluation Results

The architecture defines the structure of the MLPNN which includes the number of inputs in the input layer, number of neurons in the hidden layer and the number of outputs in the output layer. Shown in Fig. 5 are the input layer, hidden layer and output layer of the MLPNN. With respect to the number of input neurons, results of the data preparation process led the researchers in identifying the final eleven variables to be used as inputs in the input layer namely (1) average temperature, (2) minimum temperature, (3) maximum temperature, (4) average wind speed, (5) maximum wind speed, (6) relative humidity, (7) total rainfall, (8) visibility, (9) day, (10) month, and (11) year. These parameters resulted in a high *p*-value indicating its correlation with respect to rainfall. This implies that these parameters influence the formation of rain at some point, thus its inclusion as inputs. A study found out that the three most significant data inputs in rainfall prediction aside from daily rainfall or precipitation are relative humidity, air pressure, and average temperature [14]. Air pressure on the other hand was not included as the final input after getting a *p*-value greater than 0.005 or not within a 95% confidence interval on the correlation evaluation of each variable with respect to rainfall as shown in Table X. This implies that for the Davao dataset, air pressure does not hold weight in rainfall forecasting. The logical explanation would be due to Davao's topography and geography that has been captured by the MLPNN during the training phase using years of data about Davao's air pressure readings.

TABLE IX. DATA PARTITIONING

Study Set	Month/s or Year/s Used	Number of months/years used	Amount of data records
Training Set	2006-2016	12 years	4019 records
Testing Set	2017	1 year	365 records

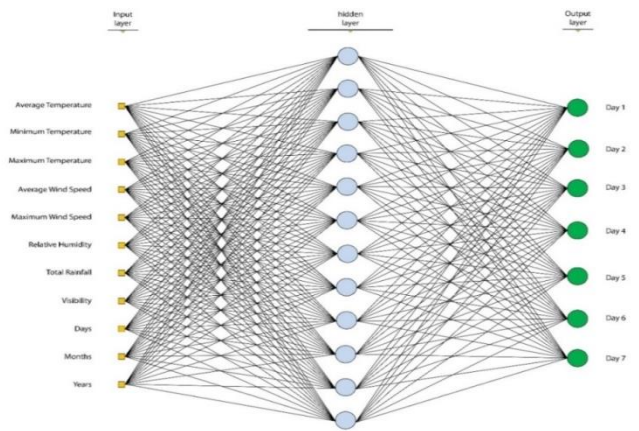


Fig. 5. The Architecture of the Multi-Layer Perceptron Neural Network.

In a study which used present hourly rainfall data and meteorological parameters of relative humidity, air pressure, temperature, visibility, and rainfall from surrounding rain gauge stations as input variables, the MLPNN was able to promisingly predict rainfall 1 to 6 hours ahead at 75 rain gauge stations as forecast point [4]. For the number of neurons in the hidden layer, the result of the Stathakis formula are shown in Table XI and was used as the values to be tested as the number of neurons in the hidden layer [15]. The number of hidden neurons is the maximum number of neurons that can be used with respect to the arbitrary scaling factor. Thus, if the scaling factor is 10, the number of hidden neurons the researchers can use are between 1-22 starting with the maximum value gradually decreasing as the researcher tests each value.

Another important observation the researchers had was the behavior of the models with respect to the number of hidden neurons. It was observed that Hyperbolic Tangent activation function does not converge to the maximum error unless the number of hidden neuron is less than 50. Anything above that number simply does not converge. However, Sigmoid exhibits the opposite since it converges to maximum error when the number of hidden neurons is greater than 50. Considering all these observations and running the MLPNN model multiple times with those range of values, 50 neurons for the Hyperbolic Tangent activation function and 100 neurons for the Sigmoid function were identified as the optimum number of hidden neurons to use for the respective activation functions. According to a study on hidden neurons in MLPNN, as the number of hidden nodes increases, the local minima point's also increases [21]. Increasing the number of hidden neurons enables the MLPNN to reach deeper local minima but also increases the possibility of getting stuck as the increase in the number of local minima is directly proportional with the increase in hidden nodes. Another study also found out that the Sigmoid's function values lies in the range from 0 to 1 which means that at some point in the graph, the gradient is approaching to zero and the network tends to stop learning on that point [22]. This can be addressed by increasing the number of neurons in the hidden layer in order to scale the Sigmoid Activation function. Thus, those behaviors observed might be due to these restrictions and limitations. As for the number of neurons in the output layer, the main objective of the study is to forecast week-ahead rainfall. This means that the MLPNN

model will be running on machine mode giving the neural network multiple output nodes, 7 output nodes to be exact, which represents the 7 days of the week from Monday to Sunday in no particular sequence to be predicted. The training algorithm is the parameter that tunes the network so that its outputs are close to the desired values [4, 10, 19]. Among the function approximation algorithms, most of the studies in rainfall forecasting use Backpropagation, Resilient Propagation and Quick Propagation as their training algorithms [1, 4, 7, 8, 18]. After evaluating more researches and looking at related studies, the researchers were able to identify two additional function approximation algorithms aside from the three mentioned that were suited for rainfall forecasting namely: Scaled Conjugate Gradient and Levenberg-Marquardt [7, 12, 19]. A total of five training algorithms, namely, Backpropagation, Resilient Propagation, Quick propagation, Scaled Conjugate Gradient, and Levenberg-Marquardt were used.

As for the learning rate, the researcher used the default standard value of 0.001-0.8 suggested by studies [5, 6, 18, 19].

With the 0.8 values, researchers were able to reach acceptable percent errors on their respective models which gives reasonable bases for using the same standard learning rate value. Moreover, higher learning rates speed the convergence process, but can result in overshooting or non-convergence. Consequently, lower learning rates product more reliable results at the expense of increased training time. For the momentum parameter, it is important to take note not to set the parameter too high as it can create a risk of overshooting the minimum values that can cause the system to become unstable but not too low as well as it cannot reliably avoid local minima and slow the training of the system. The optimal value of momentum can be achieved through trial and error between 0.1 and 0.9 as these values had been tested to work best with Backpropagation, Resilient Propagation, and Quick propagation approximation functions [1, 8, 18]. After these parameters had been identified, different models were formulated and used the same learning rate of 0.001 and momentum of 0.8 with training and testing results shown in Table XII.

TABLE X. EVALUATION RESULT FOR DAVAO VARIABLES

Davao Variables	Correlation Evaluation	p-Value	Davao Variables	Correlation Evaluation	p-Value
Ave Temp	-0.1512712	2.20E-16	Rel. Humidity	0.1703603	2.20E-16
Max Temp	-0.1082898	5.22E-13	Visibility	-0.09161644	1.04E-09
Min Temp	-0.09997687	2.70E-11	Ave. Wind Speed	-0.08984917	2.17E-09
Air Pressure	-0.00881795	0.5578	Max. Wind Speed	-0.0460988	0.00217

TABLE XI. RESULT OF STATHAKIS'S FORMULA

Arbitrary Scaling Factor	Hidden Neurons	Arbitrary Scaling Factor	Hidden Neurons	Arbitrary Scaling Factor	Hidden Neurons
2	112	5	45	8	28
3	74	6	37	9	25
4	56	7	32	10	22

TABLE XII. MLPNN MODEL EVALUATION TRAINING RESULTS

Models	Training Algorithm	Activation Function	Max Error Reached
Model 1	Back Propagation	Sigmoid	0.0011
Model 2	Resilient Propagation		0.00129
Model 3	Quick Propagation		0.00143
Model 4	Scaled Conjugate Gradient		0.00157
Model 5	Levenberg-Marquardt		Did not reach max error
Model 6	Back Propagation	Hyperbolic Tangent	0.00145
Model 7	Resilient Propagation		0.00136
Model 8	Quick Propagation		0.00141
Model 9	Scaled Conjugate Gradient		0.00138
Model 10	Levenberg-Marquardt		Did not reach max error
Model 11	Back Propagation	Gaussian	Did not reach max error
Model 12	Resilient Propagation		Did not reach max error
Model 13	Quick Propagation		Did not reach max error
Model 14	Scaled Conjugate Gradient		Did not reach max error
Model 15	Levenberg-Marquardt		Did not reach max error
Model 16	Back Propagation	Sin	Did not reach max error
Model 17	Resilient Propagation		Did not reach max error
Model 18	Quick Propagation		Did not reach max error
Model 19	Scaled Conjugate Gradient		Did not reach max error
Model 20	Levenberg-Marquardt		Did not reach max error

All MLPNN models were run using the same identified parameters. With respect to the number of neurons in the hidden layer, since the researcher found an important observation about the behavior of some activation function with respect to the number of neurons, models were categorized into two: (1) Models running with 100 hidden neurons (2) Models running with 50 hidden neurons. That means each model was run twice for 50 and 100 hidden neurons then identified which models do converge and reach max error. Results showed that most of Gaussian and Sin models did not reach the maximum error so these models will not be included in the testing phase while most of Sigmoid and Hyperbolic Tangent models except Models 5 & 10 with Levenberg-Marquardt training algorithm reached a maximum error. A study which had almost similar setup trained an MLPNN with Sigmoid activation function using 50 hidden neurons and found out that although 50 hidden neurons was faster to learn, the model produces a smooth curve with more error, thus increasing the number of hidden neurons to 300 solved that problem [7]. During the testing phase, models that reached maximum error were used. These trained MLPNN models were loaded back and the testing dataset were fed. As shown in Table XIII, MAE and RMSE were then calculated in order to assess the performance of the MLPNN models.

For models running in 100 hidden neurons, Model 2 with Sigmoid activation function and Resilient Propagation training algorithm got the lowest MAE while Model 4 with Sigmoid activation function and Scaled Conjugate Gradient training algorithm got the lowest RMSE. For those running in 50 hidden neurons, Model 9 with Hyperbolic Tangent activation function and SCG training algorithm has the lowest MAE and RMSE. A graphical representation of MAE and RMSE is shown in the Fig. 6.

In order to determine the optimum performing model for the 100 hidden neurons, the researchers decided to use RMSE as the deciding factor in determining the optimal MLPNN model since there is only a 0.000664 difference between model 2 and 4. Thus, the best optimal MLPNN model for the 100 hidden neurons was Model 4 and for the 50 hidden neurons was Model 9. It can be noticed that both of these models used SCG as their training algorithm.

TABLE XIII. MAE AND RMSE DURING TESTING PHASE

Models	MAE	RMSE	Remarks
Model 1	0.025051015	0.041653867	100 hidden neurons
Model 2	0.020899512	0.034208070	
Model 3	0.023180201	0.037797543	
Model 4	0.021564216	0.031537630	
Model 6	0.022685495	0.031717446	50 hidden neurons
Model 7	0.022258201	0.031266462	
Model 8	0.028053257	0.039392566	
Model 9	0.021483081	0.030660975	

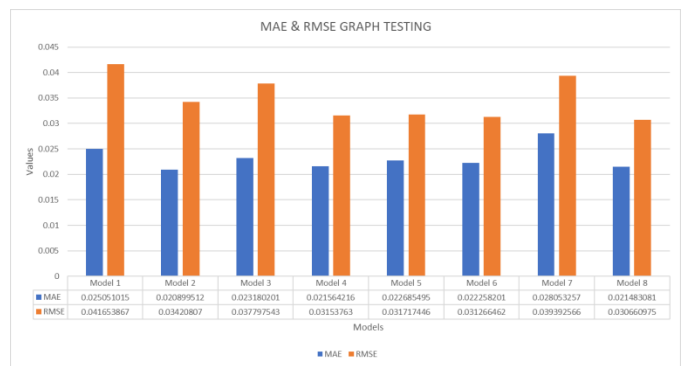


Fig. 6. MAE and RMSE During the Testing Phase.

IV. CONCLUSION AND RECOMMENDATIONS

Performance analysis of MLPNN models was conducted in this study among the weather station datasets in order to identify which MLPNN models can be optimally implemented in week-ahead rainfall forecasting. Techniques on weather data preparation, MLPNN model design along with its training and testing was conducted in this study. During rainfall data preparation, imputation process was a crucial part in addressing incorrect and inaccurate values in the datasets as it can greatly affect the outcome of the data being predicted. Random Forest Imputation technique was able to fill in the missing 5% rainfall values on the dataset. Pearson’s Correlation was also able to correlate 95% of the total inputs identified except for air pressure. However, the Moran’s Spatial Autocorrelation showed that geographical location of the stations did not have a direct correlation between stations with respect to rainfall prediction. During MLPNN model design creation, it was found out that the number of neurons for the hidden layer plays an important role in the prediction outcome as some models behaved differently with respect to the number of neurons. Other parameters such as activation function, training algorithm, learning rate and momentum was substantial to minimal effects on the outcome of the prediction. With this, an MLPNN model with Sigmoid activation function used 100 neurons in the hidden layer while an MLPNN model with Hyperbolic Tangent activation function used 50 hidden neurons. The MLPNN models that had the lowest MAE and RMSE were the ones who used Sigmoid and Hyperbolic Tangent as the activation function and Scaled Conjugate Gradient as the training algorithm with MAE of 0.021564 and 0.021483, RMSE of 0.031537 and 0.030660, respectively.

The researchers would like to recommend further studies on the aspect of hidden neuron selection and the behaviors of activation functions and training algorithm with respect to these hidden neurons. The need to explore different methods in selecting MLPNN parameters is also highly recommended as this will help establish a reliable MLPNN model performance analysis on rainfall forecasting. The researchers also suggest that further studies would be conducted on proper ways of performing training and testing that are suited and optimized for MLPNN architecture in weather forecasting as this will also help in improving the accuracy of the models which are subject to performance analysis. Overall, the results of this study showed that MLPNN models have the potential to be a viable week-ahead rainfall forecasting technique given that proper

data preparation, model architecture selection, model formulation and model validation are performed.

ACKNOWLEDGMENT

The authors would like to thank the support of the MSU-IIT Office of the Vice Chancellor for Research and Extension through PRISM-Premiere Research Institute in Science and Mathematics for their assistance in this study.

REFERENCES

- [1] Khalili, N., Khodashenas, S.R., Davary, K., Karimaldini, F. (2011). Daily Rainfall Forecasting for Mashhad Synoptic Station using Artificial Neural Networks. IPCBEE vol. 19, IACSIT Press, Singapore, 2011
- [2] L. C. Velasco, D. L. Polestico, G. P. Macasieb, M. B. Reyes and F. Vasquez, "Load Forecasting using Autoregressive Integrated Moving Average and Artificial Neural Network" International Journal of Advanced Computer Science and Applications(IJACSA), 9(7), 2018. <http://dx.doi.org/10.14569/IJACSA.2018.090704>
- [3] S. K. Nanda, D. P. Tripathy, S. K. Nayak, S. Mohapatra, "Prediction of Rainfall in India using Artificial Neural Network Models" IJISA International Journal of Intelligent Systems and Applications, Vol. 5(12), pp 1-22, 2013, doi:10.5815/ijisa.2013.12.01
- [4] N. Q. Hung, S. Babel, S. Weesakul, N. K. Tripathi, "An Artificial Neural Network Model for Rainfall Forecasting in Bangkok Thailand" Hydrology and Earth System Sciences, 13(1), pp 1413-1425, doi: 10.5194/hess-13-1413-2009, 2009
- [5] K. K. Kuok, S. Haron, C.P. Chan, "Hourly Runoff Forecast at Different Leadtime for a Small Watershed using Artificial Neural Networks" International Journal of Advances in Soft Computing and its Applications, 3(1), 2011.
- [6] R. Bustami, C. Hong, D. Lim, "River Bedup Catchment Water Level Prediction Using Pre-developed ANN Model of Siniawan Catchment" UNIMAS e-Journal of Civil Engineering, Volume 2(1), 2011
- [7] S. Mahajan, H. Mazumdar, H., "Rainfall Prediction using Neural Net based Frequency Analysis Approach," International Journal of Computer Applications, Volume 84 (9), pp 0975 – 8887, 2013
- [8] K. Abhishek, A. Kumar, R. Ranjan, S. Kumar, "A Rainfall Prediction Model using Artificial Neural Network" IEEE Control and System Graduate Research Colloquium, 2013, doi: 10.1109/ICSGRC.2012.6287140
- [9] J. V. Broeck, S. A. Cunningham, R. Eeckels, K. Herbst, "Data cleaning: Detecting, diagnosing, and editing data abnormalities" PLoS Medicine, Volume 2(10), 2005, doi:10.1371/journal.pmed.0020267
- [10] L. C. Velasco, C. Villezas, P. N. Palahang, and J. A. Dagaang, "Next day electric load forecasting using Artificial Neural Networks". In Proceedings of the IEEE International Conference on Humanoid, Nanotechnology, Information Technology, Communication and Control, Environment and Management (HNICEM), Cebu, 2015
- [11] V. K. Dabhi, S. Chaudhary, "Hybrid Wavelet-Postfix-GP Model for Rainfall Prediction of Anand Region of India," Advances in Artificial Intelligence, 2014(717803), pp 1-11, 2014, doi:10.1155/2014/717803
- [12] P. Singh, B. Borah B. "Indian summer monsoon rainfall prediction using artificial neural network," Stochastic Environmental Research and Risk Assessment, Volume 27(7), pp. 1585-1599, 2013, doi:10.1007/s00477-013-0695-0
- [13] C. J. Matyas, J. A. Silva, "Extreme Weather and Economic Well-being in Rural Mozambique. Natural Hazards, 66(1), 31-49. doi:10.1007/s11069-011-0064-6, 2013
- [14] J. B. Omotosho, A. A. Balogun, K. Ogunjobi, "Predicting Monthly and Seasonal Rainfall, Onset and Cessation of The Rainy Season in West Africa Using Only Surface Data". International Journal of Climatology, 20(1), pp 865–880. doi : 10.1002/1097-0088(20000630)20:8 2000
- [15] D. Stathakis, "How many hidden layers and nodes?", International Journal of Remote Sensing, 30(8), pp 2133-2147, 2009
- [16] N. K. Goyal, "Software development efforts prediction using artificial neural network", The Institution of Engineering and Technology, ISSN 1751-8806 doi:10.1049/iet-sen.2015.0061, 2015
- [17] W. H. Wilson, Function approximation, Artificial Intelligence Group, School of Computer Science and Engineering, University of NSW, 2019
- [18] V. K. Somvanshi, O. P. Pandey, P. K. Agrawal, N. V. Kalanker, M. R. Prakash, R. Chand, "Modelling and prediction of rainfall using artificial neural network and ARIMA techniques", The Journal of Indian Geophysical Union, 10(2), pp 141-151. doi=10.1.1.575.614, 2006
- [19] A. Mislan, S. Hardwinarto, D. Sumaryono, M. Aipassa, "Rainfall Monthly Prediction Based on Artificial Neural Network: A Case Study in Tenggara Station, East Kalimantan – Indonesia," Procedia Computer Science, Volume 59(1), pp 142-151, 2015, doi: 10.1016/j.procs.2015.07.528
- [20] Y. Maruyama, "An alternative to Morans I for spatial autocorrelation" Statistics Theory, Cornell University, arXiv:1501.06260 (Math, Stat), 2015.
- [21] K. Vora, S. Yagnik, "A New Technique to solve local Minima problem with large number of hidden nodes on Feed Forward Neural Network", International Journal of Engineering Development and Research, 2(2), pp 1978-1981, ISSN: 2321-9939, 2014
- [22] D. Gupta, "Fundamentals of Deep Learning – Activation Functions and When to Use Them?", Deep Learning, Analytics Vidhya, 2017

Android based Receptive Language Tracking Tool for Toddlers

Sadia Firdous¹, Madhia Wahid², Amad Ud Din³, Khush Bakht⁴, Muhammad Yousuf Ali Khan⁵, Rehna Batool⁶,
Misbah Noreen⁷

Department of Computer Science, Fatima Jinnah Women University (FJWU), Rawalpindi, Pakistan^{1, 2, 6, 7}

Department of Physics, Fatima Jinnah Women University, Rawalpindi, Pakistan³

Department of Electronic Engineering, Fatima Jinnah Women University, Rawalpindi, Pakistan⁴

Department of Electrical Engineering, Gomal University, D I Khan, Pakistan⁵

Abstract—Today's Android-based applications are gaining more popularity among users, especially among kids. Many Android-based applications are available related to speech therapy of a child but these have left some loopholes. Talking kids is the solution to those applications. It is an Android-based receptive language tracking tool for toddlers that emphasis to improve child's hearing capability and helps to learn, understand and develop receptive language vocabulary. It includes the colourful images of the daily routine things with their sound in a native accent so that child can learn the daily routine items. Child assessment is also included in this application for monitoring child performance. On the basis of child assessment, the activity log is maintained for keeping track of the child performance. The collected results are showing the successful development of receptive language vocabulary in toddlers with the help of 'Talking kids'.

Keywords—Receptive language; mobile application; hearing impairment

I. INTRODUCTION

As the Android operating system is getting more popular the application based on Android interests more attention [1]. Today's many Android-based applications are available related to speech therapy of a kid but all these have some limitations. In this paper, we will look at Android-based mobile application development that is Talking Kids. It is an Android-based receptive language tracking tool for toddlers that focuses to enhance child's hearing ability and helps him to learn and understand language. It does not require an internet connection but only for installation. It is a comprehensive application which consists of different scenarios and categories in which children practice different words and daily life things. Colourful pictures of daily life items along with their pre-recorded sounds in a native accent are presented to the child to increase his hearing ability and to help him in learning communication skills. This application has one relationship category in which parents can add their own pictures and record their own sound. The application has a 'Monitoring' scenario to check a receptive vocabulary of the kid. The application has an 'Activity Log' feature to maintain a record of the child according to his performance in Monitoring.

A. Background Study

Receptive language is the ability of an individual to understand information. It includes getting the words,

sentences, and meaning of what others are talking about [2]. It has great importance for better understanding and effective communication. Children who find difficulty in understanding things are to follow guidelines at school or at home. Difficulties in understanding language may lead to listening problems and behavioural issues [3].

B. Receptive Language Disorder

Receptive language disorder includes difficulty in understanding what others are talking. An individual shows receptive language disorder due to any neurological illness or injury. In some cases, it is developmental which is common in kids. Kids start speaking with the delay in developmental disorder. According to research, about 5% of school-age children have a language disorder. About more than 1.1 million children of 6.1 million got a special education under IDEA (Individuals with Disabilities Education Act) in public schools. In the 2005–2006 school years, these children were aided under the class of language impairment [4].

1) *Speech and language development track*: Speech and language development indicators for normal children are given in Table I. These tables show the normal speech development track of a kid. This table is showing that normal speech development chart usually starts with birth and at the age of 3-4 year toddler has a significant vocabulary to recognize things as well as to understand instructions. If a kid is not following this normal speech development track, management is required.

C. Causes of Delayed Speech and Language Development

There are different causes that make kids incapable to understand speech and language clearly. Some possible causes are:

1) *Hearing impairment*: Hearing impairment is the inability to hear. It can either be total or partial. Speech development delays due to condensed revelation to language in hearing-impaired children [5].

2) *Learning disability*: Learning disability is a neurological disorder. Children with learning disabilities may have difficulty in reading, writing, spelling, reasoning, and recalling and/or recognizing information [5].

3) *Autism*: Autism is a disorder that affects communication skills of a kid. It includes a range of conditions categorized by challenges with repetitive behaviours, social skills, speech and nonverbal communication. Speech Communication problems are an early sign of autism [5].

4) *Neurological problems*: Neurological problems are disorders of the nervous system that affect the muscles required for speaking. It includes cerebral palsy, muscular dystrophy and traumatic brain injury c.

5) *Other conditions*: Down syndrome, intellectual disabilities and premature birth of a child are some other reasons for speech delay [4]. Moreover extreme environmental dispossession can also cause speech delay. If a child is neglected and involved in other activities like using mobiles and other electronic gadgets unreasonably than he/she will not learn how to speak. These neglected children have less interaction with their parents. They do not hear their parents and in the result, they are unable to develop language and speaking skills [5].

TABLE I. NORMAL SPEECH DEVELOPMENT [5]

Age	Language level
Birth	Cries
2-3 months	Cries differently in different circumstances
3-4 months	Babbles randomly
5-6 months	Babbles rhythmically
6-11 months	Babbles in imitation of real speech, with expression
12 months	Says 1-2 words; recognizes the name; imitates familiar sounds; understands simple instructions
18 months	Uses 5-20 words, including names
1 & 2 years	Says 2-word sentences; vocabulary is growing; waves goodbye; makes "sounds" of familiar animals; uses words (like "more") to make wants to be known; understands "no"
2 & 3 years	Identifies body parts; calls self "me" instead of a name; combines nouns and verbs; has a 450-word vocabulary; uses short sentences; matches 3-4 colours, knows big and little; likes to hear the same story repeated; forms some plurals.
3 & 4 years	Can tell a story; sentence length of 4-5 words; the vocabulary of about 1000 words; knows last name, the name of the street.
4 & 5 years	Sentence length of 4-5 words; uses past tense; the vocabulary of about 1500 words; identifies colours, shapes; asks many questions like "why?" and "who?"
5 & 6 years	Sentence length of 5-6 words; the vocabulary of about 2000 words; can tell you what objects are made of; knows spatial relations (like "on top" and "far"); knows address; understands same and different; counts ten things; knows right and left hand; uses all types of sentences

D. Management

By using the following areas of cure effected individuals can get the benefit.

1) *Augmentative and alternative communication (AAC)*: This is a helping method involves gestures, storyboards, or computers that say words out loud. These things act as a therapy material in order to make the person familiar with specific or general things [6].

2) *Speech therapy*: To improve speech and language skills, a rehabilitation platform called speech therapy is used. With the help of speech therapy children who cannot speak clearly can improve their speaking skills. Speech therapy builds language skills of kids by making them aware of new words, sentences, and instructions. It also improves their listening and communication skills [7, 25].

3) *Other treatments*: amilies can be trained so that they become able to provide language development to their child. Special education classes can be provided at school. In case of severe impairment, preschool education can be provided [8].

II. RECENT TRENDS IN RESEARCH WITH RESPECT TO INFORMATION TECHNOLOGY (IT)

IT researchers have proposed different speech therapy tools and system for hearing impaired children. Pentiu et al. proposed a system known as Computer-Based Speech Training (CBTS). This system helps children with hearing deficits and pronunciation complications. CBTS is basically a medical tool that helps in the diagnosis of the problem and used to perform the repetitive task automatically. This system also manages important records and provides a timely response. CBTS system was designed in Logomon, Romanian language. Fuzzy expert system and semantic rules were used to design the basic architecture of CBTS. 1000 plus exercises were added in its database that is regularly updated on the basis of child performance. According to testing criteria, CBTS is an assisted therapy scheme with good system validation [8].

Hearing impairment is the major hurdle in developing communication language. It can be treated by using a different type of hearing assistance like a Cochlear implant. But these treatments can only improve hearing abilities, not speaking abilities. Brennan-Jones et al. conversed an application approach Auditory-verbal therapy (AVT). The main objective of AVT is to provide basic communication skills for a specific age group (birth to 18 years). It is an advanced application methodology including different sessions that involve a child's family. With the proper use of technology, improvements can be made in speaking abilities [9].

Children with a speech disorder and hearing impairment face difficulties in understanding their native language. Lee and Gibbon discussed an application approach known as Non-Speech Oral Motor Treatment (NSOMT). It is used by pathologists to enhance child's learning capabilities. The main objective of this application methodology is to deal with specific errors of speech and to improve the speaking abilities of hearing-impaired children. NSOMT is the non-speech action involves some exercises such as chewing, smiling, lips movement, swallowing and many others that are a helpful

parameter to generate sound. But the effectiveness of this application approach is dubious and requires more studies [10].

Hearing loss is one of the major health problems that affect the quality of life severely. Kids with hearing impairment have poor communication skills and social interaction. Rabelo and Melo examined treatment procedures achieved in public rehabilitation centre. The key factor in counselling activities is that the family is involved in the whole process. Electronic devices, used in counselling comprise of a broad range of information about daily life activities. Rehabilitation centres provide appropriate assistance to children, to make them able to persist in society successfully [11].

The act of communication is the basic feature of mental and behavioural development, learning and gaining knowledge. Rabelo et al studied the orofacial and cervical regions that include drinking, swallowing, eating, inhalation and speech processes. There can be learning delays during childhood that leads to unwanted results. Four speech therapists are involved in this research. They considered noise factor and different morphological features like lips, face, cheeks, tongue and smile movements. This study concludes that the occurrence of speech disorder is high and needs more research to tackle this problem [12].

Cognitive abilities of hearing-impaired children may lose due to auditory faults. Hearing impairment is a key reason for language disorder. Shojaei et al. evaluate language development in Persian children with auditory failings. According to their study early identification effect syntax and semantic skills of hearing-impaired children. Moreover, in different age groups, these skills vary [13].

In addition to traditional education system learning applications are helpful to educate children. These practice applications are based on the lesson, demonstration, gaming and presentation, finding, problem solving and recreation. Some practical applications are used to structure the mind maps by using images, audio, and video. These practice applications almost replace old digital learning processes. Now learning material is available in the form of more handy digital tools which are friendlier and provide good interaction to children to understand and learn digital educational material [14].

A. Mobile Application

1) *Speech therapy*: Speech therapy is a wonderful application that helps children with hearing defects to learn different words with proper phonation. It contains images for better learning of impaired children. They hear words and speak them accordingly. An interesting feature of the application is that it writes the spoken word and praises children if it is right [15, 25].

2) *Constant therapy*: Constant Therapy is an application that aids people and children having speech disorders. It gives prizes to winners. This application contains different levels with different tasks that aid the impaired child to develop his learning and speaking skills. Children have to speak words which they hear and awards are given to them on the basis of spoken words [16].

3) *Articulation speech therapy*: It is used to condense speech and language disorders in children with auditory defects. It contains images for a better understanding of kids. This application is used by parents for management of their impaired children [17,18].

4) *Talking mats*: Talking mats is an advanced communication tool. It helps children with communication problems to understand and direct their thoughts. The application is developed in Java using Android studio plugin version 3.1.2 with gradle version 4.4. Android built-in database 'SQLite' is created. This application is only for a single user so there is no need to use the server database. Also, the data of two users is confidential from one another so the local database is enough for this application. The main flow of Talking Kids is given in the below figure. It is a multi-module application; the modules of this application are given in Fig. 1.

B. User Registration

For using this application first the user must be registered and the registration is done by the parents.

C. User Login

If the user is already registered the user has a login for this application. It requires a username and password to continue.

D. Scenario Selection

This application comprises two different scenarios learning and monitoring. When the learning scenario is selected the child will learn images related to different categories. In the monitoring scenario, different questions were asked to check developed receptive vocabulary of the child. The activity log is maintained for keeping track of user performance. It gives choice to the user to exit from application. This application uses distinguishing, specially designed symbols that are smart to all ages and skills [18-24].

There are many research and mobile applications in this field but each of them has some flaws. Mobile applications with good sound quality are not free at play store. 'Talking Kids' would be free of cost at play store, as it includes images with good quality sounds. The most important audio stimulus is pre-recorded in a native accent.

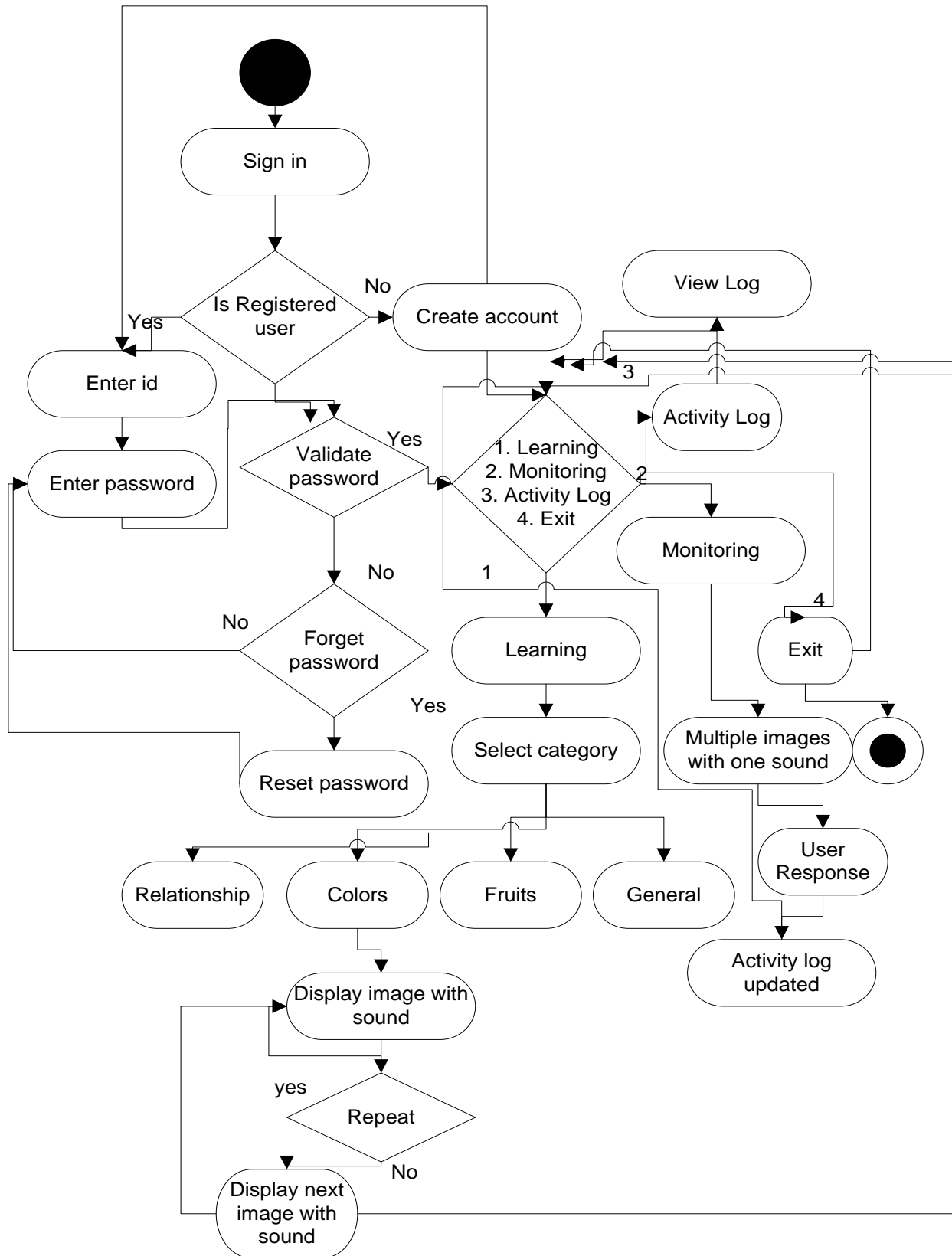


Fig. 1. Flow Diagram of 'Talking Kid's'.

III. DESIGN METHODOLOGY

Waterfall model is used for software development in the proposed application. This model is used because the requirements of this application are very well known as clear and fixed. Also, the technology used for implementing this application is understood, there is no ambiguity.

A. Category Selection

This module consists of different categories of animals/birds, vegetables/fruits, colours, relationship and the general. The choice is given to the user for selecting the category of his own choice.

B. Animals/Birds

This category includes images of animals and birds. The image displays corresponding to sound.

C. Vegetables/Fruits

It includes images of vegetables and fruits and corresponding pre-recorded audios.

D. Colour

It includes images of colours and corresponding pre-recorded audios.

E. Relationship

This category allows parents to add images of their own choice like child's immediate relations. The audio can also be recorded corresponding to the image.

F. General

This category includes the images of daily routine items with their pre-recorded audio, so that child is able to recognize these things. Screenshots of "Talking kids" are given in Fig. 2.



Fig. 2. Screenshots of 'Talking Kid's'.

IV. RESULTS AND DISCUSSION

‘Talking Kids’ helps kids to develop receptive language vocabulary and distinguish things. It assists them to cognize what is said to them, that is the main aim to make them able to cognize and react to given instructions.

It eases the burden of parents and gives compensation for expensive sessions of a speech-language pathologist. It does not require parents to remain stuck with a child, as they just start the application and choose the required scenario after this the kid can learn easily. Different classifications are added in this application in order to build the language of the child. Performance record helps parents to check the improvement of their kid. “Talking Kids” provides better outcomes as kids like to intermingle portable electronic gadgets.

Comparison of “Talking Kids” with other mobile applications is given in Table II. As compared to previously developed software/web and android based application “Talking Kids” is a multi-module application that permits parents to add images and record corresponding sounds. It includes colourful graphics, images, background music and audios in native accent to make a kid learn easily.

Five kids, of 2-6 year age who were suffering from hearing impairment, were taken to test the ‘Talking kids’. This testing is done by a speech therapist. As shown in Fig. 3 “Talking kids” help these kids to learn, understand and develop receptive language vocabulary in a number of speech therapy sessions in the time period of seven weeks. Each sample (kid) has a different improvement speed. After doing sessions by the speech therapist with the help of “Talking kids” kids showed improved receptive vocabulary.

TABLE II. COMPARISON WITH THE PREVIOUS APPLICATIONS

Application Name	Modules in Applications		
	Learning	Child Assessment	Record Keeping
Speech Therapy [15]	***	-	-
Articulation Speech Therapy [17]	*****	***	***
Memory Game [19]	***	-	-
Speech Essentials Therapy app [20]	*****	*	*
This Work ‘Talking Kids’	*****	***	*****
Perfect: *****		Average: ***	
Below Average: *		Not included: -	

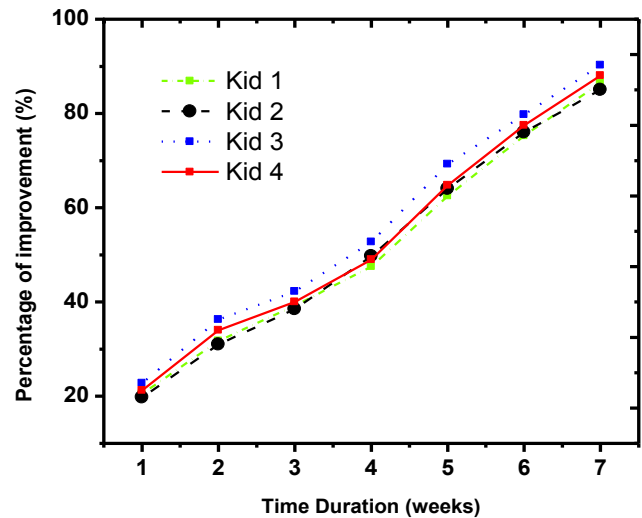


Fig. 3. Receptive Language Vocabulary Developing Pattern.

V. CONCLUSION

The main objective behind developing Talking Kids was to provide a rehabilitation platform to hearing-impaired children to develop receptive language vocabulary. The proposed application includes the different images and their pre-recorded audios in native accent. It also includes one category which allows parents to add the pictures of their own choice so that the child can learn his/her immediate relations. This application is beneficial to the child as they feel happy to interact with mobile gadgets, also it will save the expensive session of a speech-language pathologist.

ACKNOWLEDGEMENT

I am deeply thankful to my supervisor and Fatima Jinnah Women University (FJWU) for providing a research environment.

REFERENCES

- [1] K. M. Fletcher, G. R. Lyon, L. S. Fuchs, and M. A. BarnesYoung, Learning disabilities: From identification to intervention. Guilford Publications, 2018.
- [2] M. E. Dunn, T. Burbine, C. A. Bowers, and S. Tantleff-Dunn, “Moderators of stress in parents of children with autism”, Community Mental Health Journal, vol. 37, pp. 5-39, 2001.
- [3] L. Ma, L. Gu, and J. Wang, “Research and development of mobile application for Android platform,” Int. J. Multimed. Ubiquitous Eng., vol. 9, no. 4, pp. 187–198, 2014.
- [4] P. Yoder, L. R. Watson, and W. Lambert, “Value-added predictors of expressive and receptive language growth in initially nonverbal preschoolers with autism spectrum disorders”, Journal of Autism and Developmental Disorders, vo. 45(5), pp. 1254–1270, 2015.
- [5] M. A. Nippold, “Later language development: School-age children, adolescents, and young adults”, ERIC, 2016.
- [6] C. F. Norbury and E. S. Barke, Editorial: new frontiers in the scientific study of developmental language disorders. J. Child Psychol. Psychiatry vol. 58, pp. 1065–1067, 2017.

- [7] S. K. Pillai, V. Anand, and S. Babu, "Assessment of Speech and Language Delay among 0 - 3-Year-old Children using Language Evaluation Scale, Indian Journal of Child Health," vol. 6, no. 87, pp. 2–6, 2017.
- [8] C. J. Plack, *The sense of hearing*, Third Edition, Routledge, 2018.
- [9] W. A. Broman, Sarah H and Nichols, Paul L and Kennedy, *Preschool IQ: Prenatal and early developmental correlates*, Routledge, 2017.
- [10] V. A. Sigafoos, Jeff and van der Meer, Larah and Schlosser, Ralf W and Lancioni, Giulio E and O'Reilly, Mark F and Green, "Augmentative and Alternative Communication (AAC) in intellectual and developmental disabilities," in *Computer-Assisted and Web-Based Innovations in Psychology, Special Education, and Health*, Elsevier, pp. 255–285, 2016.
- [11] C. Adams et al., "The Social Communication Intervention Project : a randomized controlled trial of the effectiveness of speech and language therapy for school-age children who have pragmatic and social communication problems with or without autism spectrum disorder," pp. 233–244, 2012.
- [12] M. A. Fletcher, M. Jack, and G. R. Lyon, and L. S. Fuchs, and Barnes, "Learning disabilities: From identification to intervention", Second Edition, Guilford Publications, 2018.
- [13] S. G. Pentiu, O. A. Schipor, M. Danubianu, M. D. Schipor, and I. Tobolcea, "Speech therapy programs for a computer aided therapy system," *Elektron. ir Elektrotehnika*, vol. 7, no. 7, pp. 87–90, 2010.
- [14] C. G. Brennan-Jones, J. White, R. W. Rush, and J. Law, "Auditory-verbal therapy for promoting spoken language development in children with permanent hearing impairments," *Cochrane Database Syst. Rev.*, vol. 2014, no. 3, 2014.
- [15] S. Y. A. Lee and F. E. Gibbon, "Non-speech oral motor treatment for children with developmental speech sound disorders," *Cochrane Database Syst. Rev.*, no. 3, 2015.
- [16] G. R. G. Rabelo and L. P. F. de Melo, "Counselling in the rehabilitating process for hearing impaired children by parents' perspective," *Rev. CEFAC*, vol. 18, no. 2, pp. 362–368, 2016.
- [17] A. T. V. Rabelo et al., "Speech and language disorders in children from public schools in Belo Horizonte," *Rev. Paul. Pediatr.*, vol. 33, no. 4, pp. 453–459, 2015.
- [18] E. Shojaei, Z. Jafari, and M. Gholami, "Effect of early intervention on language development in hearing-impaired children," *Iran. J. Otorhinolaryngol.*, vol. 28, no. 1, pp. 13–21, 2016.
- [19] L. Kolås, H. Nordseth, and R. Munkvold, "Learning with educational apps," no. January 2015, 2016.
- [20] "speech therapy exercise." [Online]. Available: https://play.google.com/store/apps/details?id=appinventor.ai_davidlobomartinez.SpeechTherapyExercises. [Accessed: 20-May-2018].
- [21] "Constant Therapy." [Online]. Available: <https://play.google.com/store/applications/details?id=com.constanttherapy.android.main&hl=en>. [Accessed: 20-May-2018].
- [22] "Articulation speech therapy." [Online]. Available: https://play.google.com/store/applications/details?id=applicationinventor.ai_coolbhavana1.articulation_worksheets&hl=en. [Accessed: 20-May-2018].
- [23] "Talking Mats." [Online]. Available: <https://play.google.com/store/applications/details?id=air.com.talkingmats.talkingmats&hl=en>. [Accessed: 20-May-2018].
- [24] "Memory game." [Online]. Available: https://play.google.com/store/apps/details?id=appinventor.ai_coolbhavana1.MemoryGame_kids. [Accessed: 02-May-2018].
- [25] "Speech Essentials Therapy app." [Online]. Available: <https://play.google.com/store/apps/details?id=com.speechessentials.speechessentials&hl=en>. [Accessed: 02-May-2018].

An Agent-based Simulation for Studying Air Pollution from Traffic in Urban Areas: The Case of Hanoi City

KAFANDO Rodrigue¹, HO Tuong Vinh², NGUYEN Manh Hung³

^{1,2}IFI, Vietnam National University in Hanoi, Vietnam

^{2,3}UMI UMMISCO 209 (IRD/UPMC), Hanoi, Vietnam

³Posts and Telecommunications Institute of Technology (PTIT), Vietnam

Abstract—In urban areas, traffic is one of the main causes of air pollution. Establishing an effective solution to raise public awareness of this phenomenon could help to significantly reduce the level of pollution in urban areas. In this study, we design and implement an agent-based simulation allowing to study the principles of production and dispersion of pollutants from road traffic in urban areas. The simulation takes into account different factors that can produce pollutants from the urban zone (the case of Hanoi city in Vietnam): roads and streets, vehicles (types, quantity), traffic, wind direction, etc. With this simulation, one can observe and study the emission and dispersion of pollutants from traffic by conducting experiments with various scenarios and parameters. This work is an interesting solution to sensitize the public's awareness on the air pollution from traffic in urban areas, so that people can change their behaviors to reduce the air pollution.

Keywords—Air pollution; agent-based simulation; traffic

I. INTRODUCTION

Nowadays, air pollution is one of the topics of reflection that affects policy-makers around the world. It is a phenomenon that continues to grow overnight because all the human activities contributing to the evolution of new technologies which contribute enormously on this way. In urban areas, like Hanoi City, the main source of pollution is road traffic. Indeed, the means of displacements of the population are among others vehicles that produce particles or pollutants dispersing in the air and strongly denature it chemical composition. Unfortunately, this transformation has a negative effect on the climate and the health of the population. According to [1], air pollution is the alteration of air quality that can be characterized by measurements of chemical, biological or physical gas pollutants, particles, radio logical and sometimes liquid in the air, with consequences detrimental to human health, living beings, climate, or materials.

The main objective of this research work is to propose a decision-making approach on urban air pollution by exploring multi-agent systems under the GAMA platform [2]. This approach will show not only the importance of multi-agent systems, but also allow the population, through awareness sessions, how their daily activities contribute to increasing the pollutants but especially how they could avoid or reduce it considerably. Why the multi-agent systems? Simulation based on multi-agent systems is an approach that is used to reproduce a physical phenomenon from the series of calculations. It leads to the description of the result of this phenomenon, as if it

had really taken place because all the actors are represented by agents which embody the capacities of the real actors. This advantage of multi-agents systems will contribute to set up all things understandable. It is an advantage that mathematical models cannot deal with.

Some existing methods are used to model air pollution from road traffic. However, the results produced by these studies are difficult to be interpreted by the general public. The results of these studies are not self-explanatory and require some advanced skills for being interpreted. Among these studies, we noticed the one most related which was set up by Emery et al. [3]. In their study, multi-agents approach has been used to observe the air pollution by taking into account the nature of the automobile park such as gasoline and diesel.

Our approach goes beyond of this study by putting out the principle of the pollutant emission and the mains factors which favor their dispersion by implementing an existing parametric model. The results of this study will be a powerful sensitization tools by the way that everyone will be able to understand and interpret without having a particular advanced skills.

After a detailed study of air pollution modeling methods in urban areas, we chose to build our multi-agent system based on the Operational Street Pollution Model (OSPM) [4]. The OSPM model is one of the standard models used for air pollution modeling in urban areas.

This paper is organized as follows: Section II presents some related works in the field of urban pollution modelling and simulation. Section III presents the proposed model that allows modeling and visualizing the pollution in urban, taking into account traffic factors. Section IV presents the implementation of the model and detail discussion of the simulation results applied to Hanoi city. Finally Section V presents provides some conclusions as well as a discussion about future research.

II. STATE OF ART

Several topics were discussed on the modeling of urban air pollution produced by road traffic. Among these subjects, we can note the work of Berkowiz et al. [5] which aimed model air pollution from road traffic at street level using the Operational Street Pollution Model (OSPM). Indeed, the OSPM model, as its name suggests, is a model used in urban areas to model air pollution along streets. In the city of Dijon, Emery et al. [6], [7] have carried out a simulation of

road traffic based on multi-agent system in order to evaluate automobile air pollution (AAP) from traffic data based on 210 sensors, hence the name of the SCAUP model (Multi-Agent Simulation from Urban Counters for Automobile Air Pollution). To realize it, two categories of models have been used, namely the macroscopic model and the microscopic model under the GAMA platform. In the article of Khalesian et al. [8] a micro-simulation approach of multi-agent traffic based on GIS (geographic information system) information was set up to determine atmospheric pollution, in particular the CO particles generated in a case of traffic congestion. The pollutants taken into account were PM10, SOx and NOx particles. In order to be able to assess and predict the dispersion of air pollution in Delhi city (India), a study was conducted by Kumar et al. [9] using geographic information system (GIS), which is a powerful tool for making more efficient and flexible methods, and a geographic interface simulation system. The study showed that in this city, a large part of the pollution was due to road traffic, either 72% versus 20% for industrial sector.

In the sanitary field, pollution scrupulously affects local population health and surrounding areas. Thus, to evaluate this impact in the Baie Area in San Francisco, a team of researchers [10] have implemented a new method that allows to estimating air pollution by modeling the traffic state, traffic induced pollution and dispersion of pollutants along a highway in real time. They used the Gaussian dispersion model, which is a that allows to calculate the concentrations in small spaces. Masoud Fallah Shorshani [11], during his doctoral dissertation developed during his study an evaluation on the feasibility and relevance of a model chain in order to simulate the impact of the traffic on air pollution and runoff, considering traffic account, vehicle emissions, atmospheric transport and processing processes, the watersheds and the processes of leaching and transport by runoff. During his study, he made two models, one static or the boxed model with hourly time steps and the other dynamics or Gaussian plume model, for the traffic and associated pollutants.

In Table I, we highlight the models studied while presenting the strengths and weaknesses of each of these studies.

We note that there are several models and that each of these models is adapted to particular conditions while presenting its advantages and disadvantages. The most criteria discriminant rely on the geographic space to be modeled and also the available data. For our study, from the different analyzes that we carried out, several simulation tools are at our disposal. We have for example MATSim, NETlogo, or GAMA platforms, which offers us great advantages when it comes to integrating data with the Geographic Information System (GIS). As for the pollution dispersion model atmospheric, we will use models that integrate geographical areas information. We have among others the models of the street shaped Canyon, the parallel model CALINE3 developed by Samaranayake et al. [10], the Gaussian plume model already mentioned. The rest of our work will be based on the OSPM model proposed by Berkowiz et al. [5] whose choice was motivated by its characteristics and parameters that cover better our case of study which is the Hanoi city. OSPM model will be presented in the next part.

TABLE I. SUMMARY OF SOME EXISTING WORKS

Models	Data	Remarks
Operational Street Pollution Model (OSPM) [5]	-Meteorological data - Traffic data	- Usage of weather conditions - Usage of wind influence - Becomes ineffective with a large variation of the wind flow - Limited to restricted geographical areas.
- Macroscopic and microscopic models [6] [7] - GAMA Platform	- Data collected from 210 sensors - Number of vehicles - Average speed	- Consideration of the spatio-temporal dimension of traffic by using sensors - Large scale coverage - Requires a lot of data (displacement, localization) - Not taking into account temporal variations (static) - High calculation time - Mandatory data pre-processing
Gaussian plume Model and Neural Network (GPM and NN) [12]	Meteorological data from two years (train & test)	- Consideration of uncontrolled sources - Consideration of climatic parameters (wind speed, weather, Humidity) - Good prediction: supervised learning with neural networks - Large scale area - Limited number of pollutants taken into account during the study (PM10, SOx, NOx)
- Model of Gualtieri and Tartaglia - Platform : ArcGIS (8)	- Number of vehicles - Vehicles speed	- Wind direction and speed - solar radiation - Air temperature - Building height - Used only for CO (not applicable for pollutants involving chemicals process during the dispersion)
- Gaussian plume dispersion pattern (Gaussian plume dispersion model) through the emission factors, and the traffic volume traffic [9]; - Platform: Geomatica10	- Road counting data - Meteorological data - GIS data	- Flexible - Large scale application - Requires a lot of data - Complex interpretation of data from satellite observations
- Gaussian dispersion model [10]	- Number of vehicles and their average speed - Meteorological data	- Good performance for measurements on intersections - Real-time modeling - Integration of the traffic model, weather conditions, and emission models - System usable for other sources of pollution information - Less effective for strong variations in weather conditions - Favorable for non-reactive pollutants
- Box model [11] - Gaussian plume model	- Traffic data - Fleet data (gasoline, fuel) - 26 pollutants - Using Origin-Destination Matrix (O / D) - Types of vehicles	- Real time vehicles tracking in the network - Taking into account numerous pollutants - High error rate in case of strong variations of weather conditions - Underestimation of some pollutants like NO2 over short distances - No consideration of infrastructures in the dispersion of pollutants (Gaussian plume model)

III. PROPOSED SOLUTION

A. Overall Model

Fig. 1 describes a functional model that we designed to describe the air pollution simulation coming from road traffic. In this model, we have essentially three parts. The traffic network which is defined with the vehicles as input data, and the road traffic calculation as output data. In order to calculate the pollutant emission, we take into account the traffic data and the meteorological data in input to observe the pollutants. The last part is the modulation of pollutants dispersion that allows us to observe pollutants dispersion by visualization on traffic area and graphs.

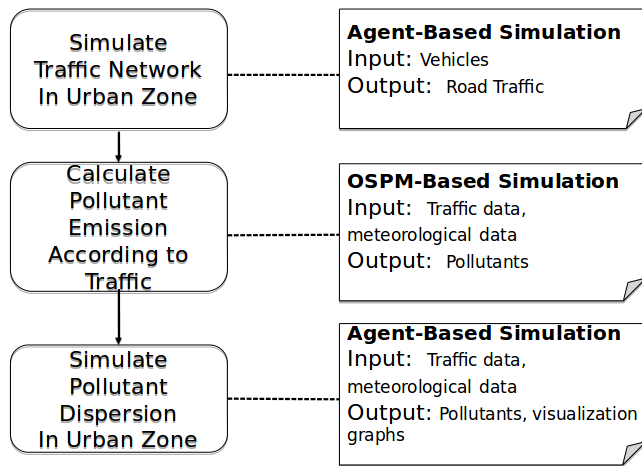


Fig. 1. Functional Model of Proposed Air Pollution Simulation

B. OSPM Model

1) *OSPM model description:* The choice of this model is guided by a set of parameters. Each of the existing models has been developed for some specific conditions.

As a reminder, the main goal of our work is to implement a model that will allow us to simulate air pollution based on multi-agents systems to point out how it grows.

The model to be considered should take into account the geographical dimension to be assessed, the environmental constraints (buildings, trees, etc.), the meteorological constraints (wind, humidity, etc.), the types of pollutants emitted by the traffic and all other phenomena that can influence the dispersion of pollutants in the air. Given the different factors above, and taking into account the existing models, we have chosen to set up a model similar to those used to simulate pollutant levels along urban streets. It's about Operational Street Pollution Model (OSPM) [13].

The Operational Street Pollution Model (OSPM) is a practical model of pollution used in urban areas, particularly at the level of streets in the form of canyon [4]. Developed by the Department of Environmental Sciences of the University of Aarhus in 1989, it has undergone enormous changes over the years [14]. The pollutants concentrations are calculated using a combination of two models [13] that are the plume model and the boxed model.

The plume model calculates the direct contribution of wind to the expansion of pollutants. At this level, with this model, it is assumed that traffic and emissions are uniformly distributed on the entire street. The transmission field is treated as infinitesimal aligned sources line perpendicular to the direction of the wind at the street level. OSPM model does not consider the wind in cross diffusion. Wind direction at street level is supposed to be reflected in relation to the wind at roof level. The box model is used to estimate the contribution of recycled or swirled wind. The implementation of the OSPM model consists of a set of calculations to consider the different conditions and parameters which contribute into the modeling of pollutants dispersion [5].

Referring to the article of Raducan [15], the main assumptions of the model can be summarized as follows:

- All emissions are assumed to be homogeneous along the street.
- When the wind blows perpendicular to the axis of the street, a vortex is form.
- The upwind or upstream side receives a direct contribution from the traffic and some of the pollutants recirculating inside the street.
- The downstream side receives mainly the contribution of recirculating components.
- The concentration of pollutants on both sides of the street is assumed equivalent when the wind blows is zero or blows parallel to the street.
- The direct contribution is calculated using a Gaussian plume model assuming that the pollutants disperse linearly with the distance of the plume.
- The recirculating wind is described using a boxed model.
- The OSPM model can model turbulence in the street assuming it consists of two parts: ambient turbulence (depends on wind speed) and traffic-induced turbulence (which is important when wind speed is weak). In addition, OSPM is a model that integrates a simple photo-chemistry involving nitrogen monoxide (NO), dioxide nitrogen (NO₂) and O₃ (NO + O₃ <=> NO₂ + O₂).

The principle of a pollutant emission by moving vehicles is obtained by summing the particles generated by each type of vehicle while taking into account their emission factor.

$$Q(p) = \sum_{i=1}^n (TypeVehi * FacCoeff_p * P) \text{ where:}$$

- Q(p): The total quantity of the pollutant p generated by all the vehicles during the simulation.
- TypeVehi: The type of vehicle considered.
- FactCoeff(p): The emission factor. Indeed, each vehicle has an emission factor characterizing its contribution level of pollution by type of pollutant.
- P: This is a uniform emission probability that we have defined for each vehicle regardless of the type of pollutant.

So, we can illustrate the model as shown in Fig. 2.

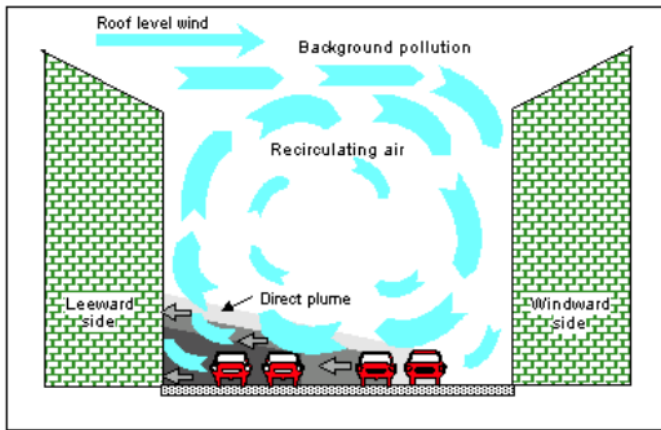


Fig. 2. OSPM figure illustration [4]

2) *OSPM model input data:* The OSPM model operates primarily based on two categories of input data. These are meteorological data and traffic data.

a) *Meteorological data:* As shown in the illustrative Fig. 2, meteorological data is strongly involved in the construction of the model. Among these elements, we have the wind which is characterized by its speed and direction, and the temperature of the air. However, this model requires that the wind speed and direction correspond to the flow conditions over the canyon of the street, while the temperature and solar radiation should match the average in all conditions in the canyon of the street.

b) *Traffic data:* Traffic data is very important for the implementation of the OSPM model. Among these elements, we distinguish vehicles that are categorized by their number, their average speed, and the type of fleet to which it belongs (gasoline or diesel). In addition, we have the heights of the buildings and the width of the concerned street.

C. MAS (Multi-Agent System) model

The multi-agent simulation is done through the implementation of a multi-agent system. It is a system composed of several agents performing each activity individually or in interaction with other agents for the purpose of performing or performing an action. This system will simulate behaviors of the real phenomena of everyday life in order to be able to see their impacts or their modes of operation. In our case, the interaction medium is the street on which the vehicles are moving and the desired behavior is how vehicles emit pollutants and how they disperse in the air. As for agents, they represent everything that goes into the constitution of our entire model. Each agent has its own characteristics.

1) *Agents extraction:* In this part, we define the different agents that enter into the construction of our system. Based on the proposed model (simplified OSPM), we distinguish between two main types of agents: fixed agents and mobile agents.

- 1) Fixed agents: we distinguish by fixed agent, the set of agents that don't affect movements during the simulation. These agents are, buildings, traffic lights,

and trees. Most of these agents are obtained from the corresponding GIS simulation environment.

- 2) Mobile Agents: So-called mobile agents are the agents that undergo movements during the simulation. According to our system, we can name the wind, the vehicles, and the pollutants that we want to simulate. Thus, we define the characteristics (behaviors and attributes of each agent) as follows:

- Vehicle agent (Fig. 3)
Vehicles are moving agents that move along the street. There are several kinds of vehicles in the city of Hanoi. We distinguish cars, motorbikes, bus, and trucks. Vehicles move with their speed while respecting a certain distance between them. They generate pollutants as they move. However, the type and amount of gas generated depends on the emission factor of the latter. We consider the times at which the inhabitants move less and the hours at which the traffic is denser. Congestion cases will be taken into account during peak hours.
- Pollutant agent (Fig. 3)
Pollutants are the gases generated by vehicles. They are of various natures, for example: CO₂, NO₂, PM2.5, PM10, etc. More the number of vehicles as the number of pollutants increases, so does the amount of pollutants. In addition to the number of vehicles we also have their average speed. Indeed, when we observe a state of congestion, the average speed of the vehicles decreases considerably thus provoking a high concentration in this area.
- Wind agent (Fig. 3)
Wind is an agent that directly acts on the dispersion of pollutants according to its speed of movement and direction. Higher is its intensity, more rapid is the dispersion.
- Tree agent (Fig. 3)
The trees are placed along the street. They intervene in the limitation or the mitigation of the pollutants dispersion and also in the chemical transformations which certain pollutants undergo ($\text{NO} + \text{O}_3 \rightleftharpoons \text{NO}_2 + \text{O}_2$). The reduction of pollution in the canyon streets is much less important than their contributions in its elevation.

The UML diagram 3 below shows the different interaction between agents draw above.

At the end of this study, we present in Fig. 4 the conceptual model that we draw for the multi-agents system simulation.

Our model consists mainly of tree parts. The first outline the input data, the second shows how the OSPM model's designed on GAMA, and the last part sorts the output data.

In the first part, we first build the simplified OSPM model from meteorological data, here only the wind is taken into account, the data of the street, and the data from the road traffic namely the vehicles while taking into account of their category and property as the emission factor. The simplified OSPM

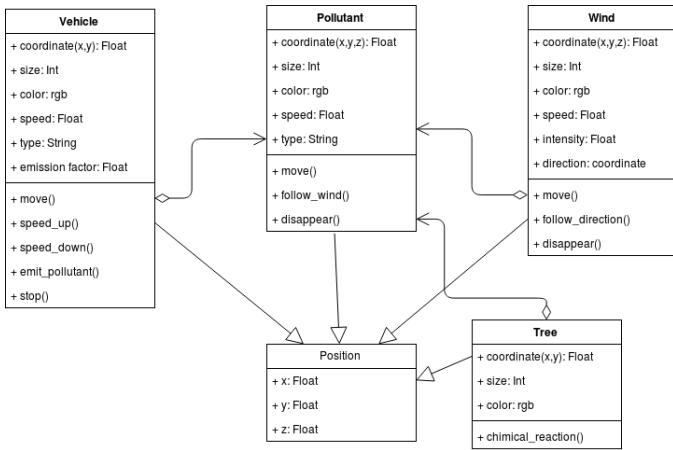


Fig. 3. Agents interaction

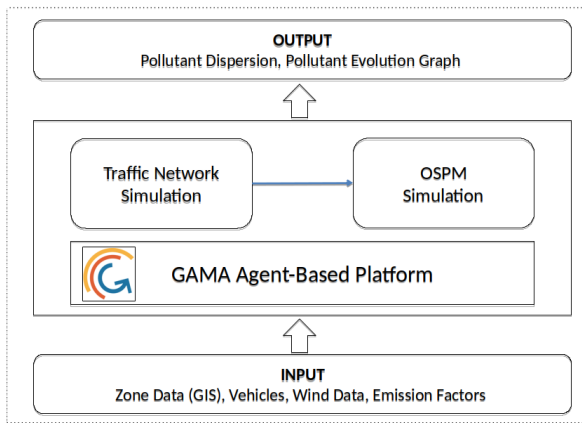


Fig. 4. Design Model of Proposed Air Pollution Simulation

model obtained is implemented under the GAMA platform whose simulation environment is the set of GIS data recovered on OpenStreetMap in the second.

In the last one, we visualize the results produced by the system. The output consists of three types. Firstly it is the evolution and the dispersion of pollutants on the map. Secondly, it is a quantification of the number of particles of each pollutant produced during the simulation, a statistical representation to illustrate the evolution of each pollutant as a function of time and the number of vehicles on the road is presented lastly.

2) *Simulation*: Simulation is the phase during which we put our system into execution. At the end of it, we get the results produced by our model. These results will allow us to evaluate the performance of the system. Thus, we present the simulation scenarios, the stopping conditions and finally the evaluation parameters.

a) *Scenarios of the simulation*: The scenarios of the simulation can be summed up in two main parts, namely, the initial phase and the actions repeated during the simulation.

1) Initialization

TABLE II. MODEL EVALUATION CRITERIA

Input data	Output data
<ul style="list-style-type: none"> The number of vehicles by type The simulation time The speed and direction of the wind 	<ul style="list-style-type: none"> Quantity of pollutants by type Evolution graphs Illustration of polluted areas

- Import the map (GIS contained in the shape file);
 - Initialize the number of vehicles to 0
 - Generate the wind;
 - Create vehicles with different destinations;
 - Assign an energy to each vehicle;
 - Create the trees.
- 2) Repeat
- Vehicles travel on different roads;
 - Each vehicle emits pollutants
 - The energy of each vehicle decreases when its moving. When its energy ends, its traffic stops;
 - The traffic lights change color;
 - The wind moves in one direction to regularize the traffic;
 - Pollutants move in the direction of the wind.

b) *Simulation stop conditions*: Stopping the simulation is conditioned by the observed results

c) *Evaluation parameters*: Rating parameters are the parameters on which we will base ourselves to know if the model is good or not. They are located on both sides namely at the input of the model and at the output of the model. When we submit input data to the model, results are expected at the output. However, the results can corroborate with those expected or not. So we define our parameters as shown in the Table II.

IV. IMPLEMENTATION AND EXPERIMENTAL ON ROAD TRAFFIC SIMULATION

A. Input Data Description

As with any parametric model, we still need input data for validation. The data used are:

- The vehicles: In our model, we mainly design four types of vehicles that are: trucks, personal cars, bus and motorbikes. The choice of these data is guided by the reality of Hanoi. Indeed, the city of Hanoi is mainly driven by these four types of vehicles. Each type of vehicle is affected by an emission factor ([16], p.193) which able to determine the participation of each one in the emission of the pollutants. We considered four types of pollutants which are the most caused by road traffic. Table III presents the contribution of each of the vehicles cited in the emission of pollutants.
- The wind: The wind is one of the main elements that enters into the dispersion of pollutants. When we applied wind, pollutants are systematically redirected towards the direction of the latter and are dispersed

TABLE III. EMISSION FACTOR

Type of vehicle	Emission Factor(%)	Pollutant
Truck	0.80	PM
	2.75	CO
	11.00	NO _x
	0.40	SO ₂
Bus	1.50	PM
	3.10	CO
	7.60	NO _x
	0.64	SO ₂
Car	0.10	PM
	3.62	CO
	1.50	NO _x
	0.17	SO ₂
Motorbike	0.10	PM
	3.62	CO
	0.30	NO _x
	0.03	SO ₂

along environment. Thus, even places where there is no consequent traffic, are polluted due to transport by the wind. The main features that distinguish are its intensity and direction.

- The trees: Like the wind, the trees intervene in the dispersion of the pollutants firstly and also favor the generation of certain pollutants like the CO₂ by the principle of the photosynthesis.
- The map: It is our simulation environment. We extracted part of the city of Hanoi from OpenStreetMap that we imported into QGIS to get the shape file, the shape file we used under the GAMA platform. Fig. 5 saw us the selection on OpenStreetMap.



Fig. 5. Simulation environment

In addition to these data, taking into account the complete model proposed in the second part, there are other parameters that may be use but that we haven't used in the simplified model. It is:

- the size of the buildings that are located along each street;
- the width of the street: it allows to estimate the number of vehicles that it can contain and to deduce also the cases of congestion.

B. Discussion

Initially, i.e. before starting the simulation, our environment is as shown in Fig. 6. In order, we show in Fig. 7, the different vehicles on the road during the traffic.

Fig. 8 presents all the agents present in our environment once the simulation is launched. As mentioned above, we have

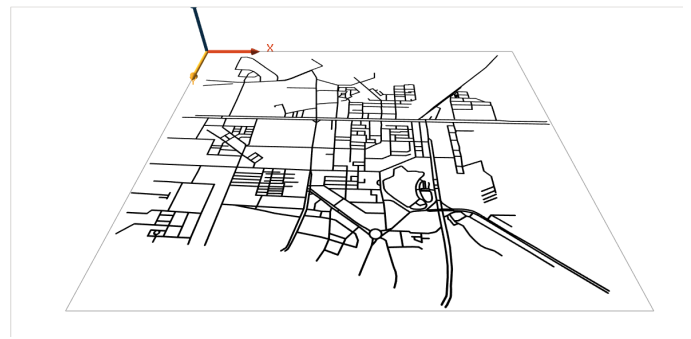


Fig. 6. Initial environment



Fig. 7. Traffic network

considered four types of vehicles that are personal cars, bus, trucks and motorcycles. As for pollutants, we also note the four types of pollutants that are NO_x, CO, PM and SO₂ that we have chosen to take into account in our system. As indicated

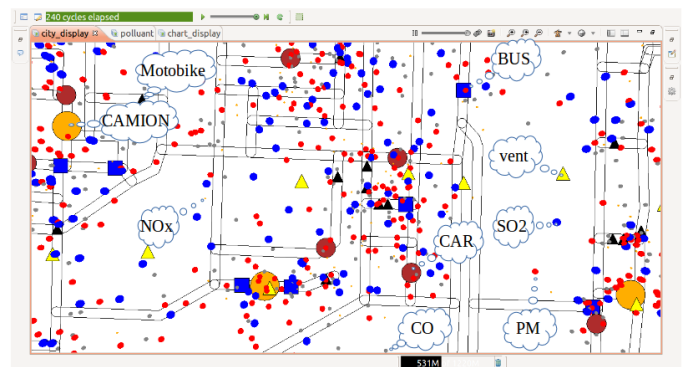


Fig. 8. Agent list

in scenarios section, we simulate the dispersion of pollutants mainly taking into account three cases.

- 1) The first case is one in which we consume a fairly stable wind. These are the periods during which the wind direction remains unstable. We find that pollutants are dispersed around the environment, but without forming an agglutination at a given place, for example. In addition, areas where there are no vehicles are also affected because pollutants are dispersed little everywhere: this is explained by the instability of the wind direction.

- The second case is when we consider that sometime, the wind has a direction and moves with a speed that can also be varied. We took two different directions in this parity. The results obtained are shown in Fig. 9 where we present how pollutants evolve in the direction of the wind.

We notice that when the wind moves with a precise direction, one of the very important points is that even the places where there is no heavy traffic for example the residential areas are flooded with large quantities of pollutants. The wind therefore favors not only the dispersion, but also pollution transport from places with heavy traffic to places almost 'safely'.

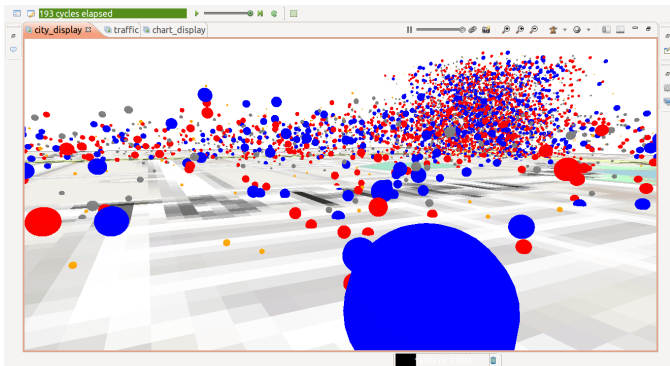


Fig. 9. Pollution map when applying a directional wind

- The third case we have illustrated is traffic congestion. Indeed, congestion related to road traffic is one of the recurrent phenomena that we see everyday, especially in peak hours. Several situations can explain congestion. It may be due either to the hours of descents or days start times during which the number of vehicle becomes very important on the road.

We have seen with the results obtained an increase in the level of pollutants at intersections. Indeed, the number of vehicles is considerable in these places and the flow of traffic becomes very slow. Each vehicle moves at a very low speed and releases a lot of particles causing a lot of pollution in these places. We present a simulation case in Fig. 10.

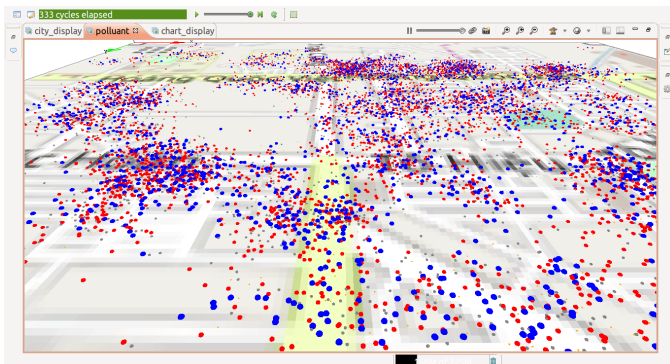


Fig. 10. Pollution map in a case of congestion.

To better track the impact of traffic on the level of pollution, we proceeded to establish a follow-up in statistical form. During the simulation phase,

TABLE IV. EXPERIMENTAL RESULTS

Freq(veh/s)	Nb_Vehi	Quantity of pollutant (count)			
		PM	CO	NO _x	SO ₂
5	360	1413	2353	3254	1807
10	720	2657	4843	6512	3642
15	1008	3859	7104	9611	5313

we progressively assessed the number of particles released for all vehicles indiscriminately over time. We illustrated our experiment in two cases. Firstly, we considered the situation where the traffic is high, during the open days in the week. The second case was highlighted in the case of the week-end. Indeed, the traffic during the week-end is more important than the others days of the week.

Fig. 11 presents the evolution of each type of pollutant during the simulation.

Table IV sums the different cases of simulations that we made. This process allows us to even quantitatively the evolution of pollutants and their dispersion as a function of time and the number of vehicles in motion.

To better situate our experimentation, we played mainly on two characteristics parameters: the speed of creation of the vehicles, and the simulation time. For this, we set a uniform simulation time of 250 cycles while playing on the frequency of the vehicles generation. The creation frequencies of the vehicles used are 5, 10 and 15 vehicles/s.

The quantity of pollutants increases over time with the number of vehicles. Moreover, while maintaining respectively the same simulation time, in the three cases of different frequencies, the increase in the pollution level goes hand in hand with the latter. This clearly explains that the number of vehicles in circulation induces directly on the quantity of pollutants produced. Moreover, with generating the vehicles in a fixed time, that shows us how the quantity of pollutants stay stable at the end of this time. During the experimentation, we set the time at 500 seconds, 334 vehicles has been generated and were running at this time. The stability of the pollution at $t=700s$ is due by the fact that all vehicle are stopped running because of the lack of energy. That allows to show the impact of traffic in the increase of pollution.

In this part we can notice from the results obtained that the wind is a very important factor that enters into the principle of the dispersion of pollutants. When it moves with a precise direction, it leads to a transportation of pollutants in the residential areas as well as in places not involving high traffic. In addition to that, we were able to show that more the number of vehicles is high in a place, the traffic become slower and contribute to increase the level of pollution.

As a reminder, the main objective of our work is the establishment of a decision support system on urban air pollution through the exploration of multi-agent systems. The results obtained from this study can be used in four (04) major points such are:

- A practical demonstration tool for a public awareness.



Fig. 11. Evolution of pollutants during the time

During an awareness session, it is more effective to present the public with simulation cases close to the reality. Indeed, the majority of the population are not able to interpret mathematical results, hence the ineffectiveness of modeling methods based on complex results. People need more or less real illustrations to understand the impact or the spread of their practices on air pollution.

- Better control over the parameters favoring the dispersion of pollutants. In our study, we were able to highlight the impact of the wind on the dispersion mainly in two cases namely in the presence of a stable wind and wind which have a high speed with a given direction. This point is very important because it allows to have an idea in advance of the risk areas during the different seasons of the year thus allowing to take adequate preventive measures for the concerned population protection.
- Explicitly exposing the most polluted places. During our study, we highlighted the most exposed areas to air pollution. This is the case of traffic congestion. As indicated above, in case of congestion, the flow of traffic increases, thus inducing a strong release of pollutants at these locations. In the case of non-dispersion or slow dispersion, the concern environments become more and more unbearable due to the pollutants in these places. This is the perfect case when we are expecting a stable wind without direction.
- An highlight of the impact of the car fleet on air pollution. As stated by Justin Emery [6], the nature of the car fleet has an important impact on air pollution. An awareness of the types of vehicles based on their fleet will allow population to have what kind of vehicle is needed to help fight against air pollution.

V. CONCLUSION

During this work, we are able to study the principles of emission and dispersion of pollutants released by vehicles in urban area (the case of Hanoi City). In the section devoted to the theoretical studies, we have evaluated different techniques and models already existing for urban air pollution modeling.

After this exploration, we proposed to simulate with the OSPM model which is one of the most explicit pollution model for urban case studies.

Among the emission factor's (Table III), the number of vehicles is one the important factors which affects directly the quantity of pollutants. About the principle of dispersion, our work are focused on the impact of the wind, to show how the wind intervenes or contributes on the pollutants dispersion. We designed three mains cases where we saw the results when applying a wind with a specific direction (Fig. 9), and a stable wind by taking into account a case of traffic jam (Fig. 10). The results obtained allow us to highlight the impact of road traffic on air pollution and also phenomena that favor their dispersion. These illustrations will undoubtedly show the target audience in an understandable way the impact of the different vehicles on the air pollution as well as the contribution of the wind in its evolution.

However, much remains to be done because the model we have achieved during the simulation is only a simplified version of the original OSPM model.

As a perspective, for an improvement of the work carried out, we recommend the application or the implementation of the following points:

- A representation of pollutants in the form of cloud. Indeed, in the work already done, the pollutants that we simulated, each has been represented as an agent, which weighs down the system. In order to make it optimal, it would therefore be necessary to represent the whole in the form of a cloud while varying the color of the latter according to the amount of each of the pollutants in order to be able to highlight them. This approach will make it possible to summarize all the pollutants in a single agent, which will contribute to greatly reduce the calculation time. For its implementation, one of the possible options would be to cover the entire area with a grid. Then, you will have to map between each cell of the grid with the vehicles that are located. As each vehicle produces several categories of pollutants, we can color each cell according to the types of vehicles that are there from the color assigned to each of the pollutants. From there, we could have a multi-colors grid whose color varies with the passage of time according to the flow that knows the traffic and even to locate the most polluted places.
- Increase the number of vehicles during the simulation. When the number of vehicles is important, the results will be even more convincing and can help us draw more reliable conclusions.
- Consider the car park. It is undoubtedly the type of fuel (petrol, diesel) that the vehicle uses greatly induces the types and amount of pollutants released by the vehicle. It would therefore be necessary to distinguish them in order to obtain finer and more plausible results.
- Provide field data for model feeding and validation. Indeed, the results that we obtain at the output of our model are related to the data used for the simulation

of the model. Field data will be an additional factor a model close to reality. For example, vehicle types count, measurements on meteorological data (wind, humidity, etc.), and all the other parameters of the original model (OSPM). As for the validation of the model, measurements of funds taken in the field will make it possible to make comparisons with the results obtained at the exit of the model.

REFERENCES

- [1] D. Duong/CVN, "Hanoi : vers la modernisation du parc de véhicules en 2018 - le courrier du VietNam."
- [2] A. Grignard, P. Taillandier, B. Gaudou, D. A. Vo, N. Q. Huynh, and A. Drogoul, "Gama 1.6: Advancing the art of complex agent-based modeling and simulation," in *PRIMA 2013: Principles and Practice of Multi-Agent Systems* (G. Boella, E. Elkind, B. T. R. Savarimuthu, F. Dignum, and M. K. Purvis, eds.), (Berlin, Heidelberg), pp. 117–131, Springer Berlin Heidelberg, 2013.
- [3] J. Emery, N. Marilleau, N. Martiny, T. Thévenin, T. Nguyen-Huu, M. A. Badram, A. Grignard, H. Hbdid, A.-M. Laatabi, and S. Toubhi, "Marrakair: une simulation participative pour observer les émissions atmosphériques du trafic routier en milieu urbain," in *Treizèmes Rencontres de Théo Quant*, (Besançon, France), May 2017.
- [4] O. Hertel, *Operational Street Pollution Model (OSPM). Evaluation of the model on data from St. Olavs street in Oslo*. Danmarks Miljøundersøgelser, 1989.
- [5] R. Berkowicz, O. Hertel, S. Larsen, N. Sørensen, and M. Nielsen, "Modelling traffic pollution in streets," *National Environmental Research Institute, Roskilde, Denmark*, vol. 10129, no. 10136, p. 20, 1997.
- [6] J. Emery, *La ville sous électrodes: de la mesure à l'évaluation de la pollution atmosphérique automobile.: vers une simulation multi-agents du trafic routier en milieu urbain*. PhD thesis, Dijon, 2016.
- [7] J. Emery, N. Marilleau, N. Martiny, T. Thévenin, and J. Villery, "L'apport de la simulation multi-agent du trafic routier pour l'estimation des pollutions atmosphériques automobiles," in *Douzièmes Rencontres de Théo Quant*, 2015.
- [8] M. Khalesian, P. Pahlavani, and M. Delavar, "Gis-based multi-agent traffic micro simulation for modelling the local air pollution," 2008.
- [9] A. Kumar, R. K. Mishra, and S. Singh, "Gis application in urban traffic air pollution exposure study: a research review," *Suan Sumandha J Sci Technol*, vol. 2, no. 1, pp. 1–13, 2014.
- [10] S. Samaranyake, S. Glaser, D. Holstius, J. Monteil, K. Tracton, E. Seto, and A. Bayen, "Real-time estimation of pollution emissions and dispersion from highway traffic," *Computer-Aided Civil and Infrastructure Engineering*, vol. 29, no. 7, pp. 546–558, 2014.
- [11] M. Fallah Shorshani, *Modélisation de l'impact du trafic routier sur la pollution de l'air et des eaux de ruissellement*. PhD thesis, Paris Est, 2014.
- [12] S. Ghazi, J. Dugdale, and T. Khadir, "Modelling air pollution crises using multi-agent simulation," in *System Sciences (HICSS), 2016 49th Hawaii International Conference on*, pp. 172–177, IEEE, 2016.
- [13] P. Kastner-Klein, R. Berkowicz, and E. Plate, "Modelling of vehicle-induced turbulence in air pollution studies for streets," *International Journal of Environment and Pollution*, vol. 14, no. 1-6, pp. 496–507, 2000.
- [14] K. E. Kakosimos, O. Hertel, M. Ketzler, and R. Berkowicz, "Operational street pollution model (ospm)—a review of performed application and validation studies, and future prospects," *Environmental Chemistry*, vol. 7, no. 6, pp. 485–503, 2010.
- [15] G. Raducan, "Pollutant dispersion modelling with ospm in a street canyon from bucharest," *Romanian Report in Physics*, vol. 60, pp. 1099–1114, 2008.
- [16] N. T. Hung, *Urban air quality modelling and management in Hanoi, Vietnam*. National Environmental Research Institute, Aarhus University, 2010.

Spin-Then-Sleep: A Machine Learning Alternative to Queue-based Spin-then-Block Strategy

Fadai Ganjaliyev

School of IT and Engineering,
ADA University, Baku, Azerbaijan

Abstract—One of the issues with spinlock protocols is excessive spinning which results in a waste of CPU cycles. Some protocols use the hybrid, spin-then-block approach to avoid this problem. In this case, the contending thread may prefer relinquishing the CPU instead of spinning, and resumes execution once notified. This paper presents a machine learning framework for intelligent sleeping and spinning as an alternative to the spin-then-block strategy. This framework can be used to address one of the challenges faced by this strategy: the delay in the critical path. The work suggests a reinforcement learning based approach for queue-based locks that aims at having threads learn to spin or sleep. The challenges of the suggested technique and future work are also discussed.

Keywords—Spinlock; spin-then-block; reinforcement learning; queue-based lock; intelligent sleeping

I. INTRODUCTION

Spinlocks have been widely used in multicore systems as a mechanism to guarantee concurrent access of threads to a critical section of code. A thread will poll (spin on) a variable in a loop to grab the lock, to enter such a shared piece of code. Once the lock is free, the thread will flip it and can enter the critical section. After it has finished executing the critical region, it flips the flag back to its original value so that other threads can acquire the lock as well.

Researchers have developed different types of spinlock protocols. Test-and-test-and-set with exponential backoff (TTSE) is the simplest among them [1]. Here, all threads spin on a globally shared lock flag by issuing a read operation on it until the lock is found free. At this point, a thread issues the test-and-set atomic instruction to acquire the lock. A random delay is inserted between consecutive spins, to reduce the simultaneous thread attack upon lock release. TTSE protocol is recommended for low and medium contention levels, as it scales poorly when contention for the lock is high.

Ticket locks [2] maintain global counters to provide concurrent access of threads to a critical section. The lock is composed of two variables: a ticket and a grant variable. Whenever a thread wants to acquire the lock, it atomically increments grant variable value and spins unless the two are equal. Once these variables are equal, the thread can enter the critical section. When the thread exits the critical section, it advances the value of the grant variable. Ticket locks

guarantee First-In-First-Out (FIFO) order but suffer from the same issue of “thundering herd” that TTSE protocol does.

Queue-based locks [3, 4, 5] spread contention on the lock by maintaining a list of linked nodes created by contending threads. Threads do not spin on a single lock variable, but each thread spins on a flag of its successor [3] or the flag of its own [4], thereby spreading contention among different memory locations in the system. Once the lock holder exits critical section, it updates either its flag (when predecessor spins on it) or the predecessor’s flag (when the predecessor spins on its flag). Though vulnerable to preemption [6], queue-based locks are an elegant solution for high contention, and they guarantee FIFO order.

Spinlocks are an attractive synchronization solution when the critical section is short. However, when contention for the lock is high, spinning can be inefficient either, since concurrent threads may cause unnecessary CPU utilization. To avoid burning CPU cycles, the spin-then-block approach is used: a thread does not spin but relinquishes the CPU, and upon lock release, the holder wakes up the waiting thread which in turn grabs the lock. From the other hand, this adds up to the critical path of the application because every unlock phase requires waking up the waiting thread. A better option would be not to block and sleep until notified but to go into a timed sleep so that to wake up just in time – right before the lock release. Thus, this would achieve two important goals at the same time: first, avoid unnecessary CPU burn and second, remove lock handoff delay. We call it *spin-then-sleep* strategy.

The questions this work addresses are the following: Once a node created by a contending thread joins a queue, should the thread spin or should it sleep? Also, if it decides to take a sleep, then how much it should sleep? For the first question, the thread has to estimate which either of the two ways will utilize fewer CPU cycles. As to the second question, the thread has to be able to predict when the lock will be released.

Key idea: The suggestion is to treat the thread as an agent whose goal is to automatically learn the cheapest and fastest way to acquire lock via interaction with the system.

The rest of this paper is structured as follows: Section 2 reviews related work. A short background is provided in Section 3. The suggested approach is presented in Section 4. Finally, the challenges, limitations and future work are discussed in Section 5.

II. RELATED WORK

This paper presents an approach that can serve as an alternative to the spin-then-block strategy. The key feature is to feed adaptivity into spinning and sleeping. So, the closest works to the one presented here are adaptive spinlocks [7, 8, 9], that have been of particular interest to researchers as well. These works aim at making spinlocks self-aware. That is the algorithm monitors and tunes itself accordingly. Thus, in [7] a reactive algorithm is developed which utilizes three protocols: TTSE, combining tree [10] and MCS lock [4] which is a queue-based lock. The algorithm switches between protocols depending on the contention level on the lock. For example, when the TTSE protocol fails to get the lock after some number of times, it switches to the MCS lock. In the opposite direction, the algorithm makes a switch when the queue is found to be empty for a number of successful fetch-and-op requests.

Another work [8] develops a backoff protocol that does not require experimentally tuned parameters. Here, the finding is that backoff delay depends strongly on the delay outside of critical section (DoCS) which is defined as the time between when the lock holder releases the lock and the first attempt to reacquire the lock. A heuristic, $base_l$, is found that depends on DoCS and which has the following form:

$$base_l = \frac{a \cdot DoCS + b}{DoCS^2} \# \quad (1)$$

The DoCS variable is computed via overhead that is defined as follows:

$$overhead = \frac{\text{latency of remote memory reference}}{\text{latency of L1 cache reference}} \# \quad (2)$$

The algorithm needs only this variable. Function $base_l$ is computed once for each lock, and the algorithm adjusts backoff delay from this value depending on the load level that is divided into two phases: load rising phase and load dropping. Whenever a spinning thread observes a rise or drop in the load, it adjusts its delay derived from the variable $base_l$.

Authors of [9] have developed a spinlock library Smartlocks that uses reinforcement learning method of machine learning to achieve a user-defined goal which can be related to performance, power, problem-specific criteria or some combination of these. The application must be connected to a specific framework that measures the performance characteristics of it. Performance related data that arrive from this interface serve as a reward signal to the machine learning engine of the Smartlocks that run in separate helper threads. The library currently supports TTSE, Ticket Locks, MCS and a few other and maintains three main components: The Protocol Selector, the Wait Strategy Selector, and the Lock Acquisition Scheduler. Protocol Selector is responsible for switching between protocols when a predefined threshold of contention level is reached. The Wait Strategy Selector defines what action threads must take when they fail to get the lock and is not implemented since each protocol has a fixed waiting strategy. The function of the Lock Acquisition Scheduler component is to generate policies for lock acquisition and to switch between them. The policy is

not updated at every lock acquisition request but every few attempts which are not related to application lock acquisitions.

III. BACKGROUND

This section gives brief information on the spin-then-block strategy. We also motivate the need for intelligent learning of sleep duration, as well as when to spin and when to sleep and provide a short background on reinforcement learning too.

A. Anatomy of Spin-Then-Block Strategy

Once a thread links its node to a queue of nodes created by contending threads for acquiring the lock, it has two options: spin or release CPU and resume when notified. If the contention for the lock is low, the thread would prefer spinning, since it will provide faster lock acquisition and avoid scheduler interaction. In case the contention for the lock is high, the thread may prefer giving up the CPU by suspending itself which involves a context switch. The thread, then, will wait until the lock holder explicitly wakes it up upon lock release. The notification will be followed by another context switch, to restore the state of the thread to what it was before the suspension. This behavior is known as a spin-then-block method. Solaris mutex [11] is an example of it. This mutex spins at low and medium contention and switches to blocking when contention rises. Spin-then-block strategy suffers from one major drawback: notification and subsequent wakeup of the waiting thread lengthen the critical path. If the thread could approximate timestamp of lock release, then it could have gone into timed sleep so that to wake up right before the lock is freed which would eliminate lock handoff delay, thereby reducing the length of the critical path. The third option is to spin for a while and then park itself out which is known as spin-then-park strategy. In this work, we don't consider this.

B. Motivation

An important factor here is duration of the sleep. Assume, a thread T_1 which holds the lock is executing the critical section. Suppose, it has acquired the lock at time t'_1 and will release it at time t_1 . A thread T_2 adds a node to the queue and sleeps such that it wakes up at $t_2 < t_1$. Another thread T_3 , then, enters the system, links its node to the queue and sleeps as well such that it will wake up at $t_3 > t_1$. Once thread T_2 wakes up at time t_2 , it will spin from t_2 to t_1 . If, in comparison to $t_1 - t'_1$ the difference $t_1 - t_2$ is huge, then the sleep duration was too small which will cause unnecessary spinning. Thread T_2 could have slept instead, should it predict lock release time more accurately.

Additionally, thread T_3 will not be able to grab the lock once it is free, since by the time lock is released it will not have its sleep finished (if a thread that has gone into a timed sleep, there is no way to wake it up). Thread T_3 should have slept for shorter amount of time. In other cases, a thread should not sleep at all if sleeping for the smallest amount of time always yields sleeping more than necessary, no matter how many threads contend for the lock and how loaded the system is. In this case pure spinning should be the preferred choice. Fig. 1 illustrates these scenarios. Hence, it is crucial to be able to decide whether sleeping at all is a good choice or not and if it is then to sleep for such a period of time that will

minimize spinning by maximizing sleep duration without sleeping unnecessarily (still sleeping even though the lock is free).

C. Reinforcement Learning Paradigm

Reinforcement Learning (RL) is a class of supervised learning algorithms in machine learning [12]. The goal of RL is to have an agent learn how to behave in an uncertain environment by interacting with it. A scalar reward signal guides the learning process and the agent has to learn to maximize it.

RL is formalized using the Markov Decision Process (MDP). MDP is defined as a tuple $\langle S, A, T, R \rangle$, where S is a set of states, A is a set of actions, T is a transition probability function, and R is a scalar reward. A state is collection of characteristics that represent every state that the agent can be in. The transition function a is probability distribution over the state space for each state $s \in S$ and action $a \in A$. Reward function is an expected reward for performing an action in a state. Transition function together with reward function defines the model of the environment.

RL is a *model-free* technique, i.e. it assumes that the agent does not possess any information about the environment. Thus, the agent must interact with the environment to collect the reward. At each step, the agent senses the current state, chooses an action and transitions to the next state followed by receiving a reward for choosing this action at this state. The goal of the agent is to learn an optimal policy that maps states to actions and maximizes its cumulative reward over the long-term. The agent tries to learn the optimal policy without learning transition and reward functions. Fig. 2(a) depicts agent-environment interaction.

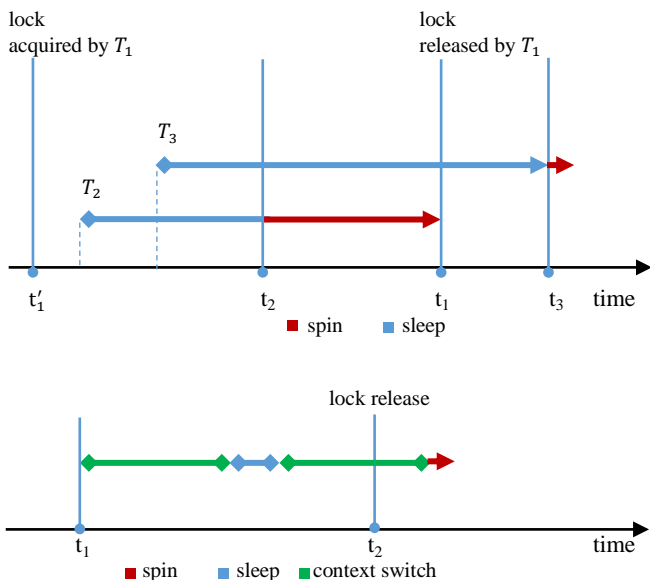


Fig. 1. (a). Sleeping and Spinning Redundantly; Thread T_2 could have Continued Sleeping from t_2 to t_1 Rather than Spin; Thread T_3 should not have Slept from t_1 to t_3 ; (b). Sleeping for the Shortest Amount of Time Always Yields Unnecessary Sleeping Since the Lock is Passed by.

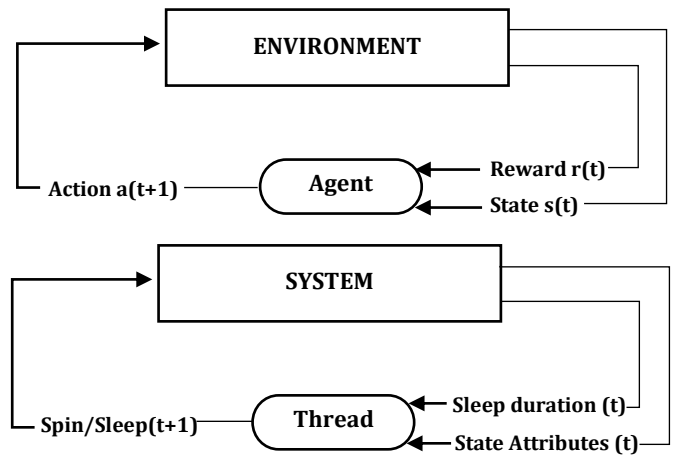


Fig. 2. A Reinforcement Learning Agent Interacting with the Environment; (b) Thread as an RL-Agent.

Fig. 2(b) shows how spin-then-sleep strategy maps to the RL framework. The thread, which represents the agent, takes actions, such as spin or sleep. As a result, the thread receives a reward signal. The reward can be designed in different ways. For example, if any sleep that does not yield unnecessary waiting is enough, then the reward can take only three values: 0 for pure spinning, 1 for a sleep that does not result in unnecessary sleeping and -1, otherwise. The thread then transitions to a different state where it takes the same or different actions. In this way, thread learns the best action at each state. The next section discusses the state, and the reward structure is in more detail.

IV. RL-BASED SPIN-THEN-SLEEP STRATEGY

This section explains how the spin-then-sleep strategy can be formulated as an RL problem. It describes what serves as a reward, action, and state.

Reward. The reward has to lead to the goal. A thread that linked its node to a queue has two choices to proceed: spin only or sleep followed by spinning. The latter should be preferred if it does not yield redundant sleeping because it will be cheaper. Otherwise, pure spinning is preferred. From the other hand, to eliminate spinning completely, the thread may sleep for a sufficiently large period of time. In such a case, upon wakeup, the thread will grab the lock right away because it is free. However, the lock could have been freed long ago. The length of the critical path will be delayed dramatically then. Thus, upon acquiring the lock, the thread must know whether its sleep resulted in unnecessary sleeping or not. The thread can find it out by requiring *at least one spin to fail and the subsequent spin to succeed*. At least one failed spin will guarantee that by the time the thread requests the lock, the holder has not yet released it yet. So, the reward is defined as follows: given that a sleep followed by spinning does not result in redundant sleeping, the more a thread sleeps, the more reward it receives. On the contrary, if a sleep for some duration followed by spinning does result in redundant sleeping, then it receives a negative reward. Pure spinning gets a reward of 0. Fig. 3 depicts these cases.

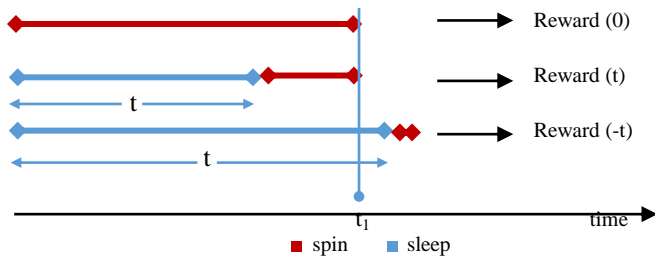


Fig. 3. Rewards for Sleeping and Spinning. Lock is Released at Time t_1 .

```
acquire_lock (duration, ...) {  
  if (duration = 0) then spin;  
  else {sleep(duration); spin;}  
}
```

Fig. 4. Pseudo Code for Action Acquire_Lock.

Action. Spinlock protocols usually maintain three methods: a method for lock acquisition, lock release, and execution of critical section. Typically, it is the method for lock acquisition, say `spin()`, where thread continuously spins until it gets the lock. This method of the protocol and routine for sleeping (which includes sleep and wakeup), say `sleep()`, can be united into a single action of the thread as an agent, say `acquire_lock()`. That is, the action `acquire_lock` acts as a function of a single parameter – sleep duration. If this duration is zero, then no sleeping is involved, and the thread only spins. Otherwise, it sleeps for the specified duration and spins the rest of the time. Fig. 4 shows a pseudo code for this. Additionally, the thread-agent will have other two actions (for execution of critical section and lock release) that are no different from the two methods of the thread. Action `acquire_lock` will always be followed by the action for executing critical section which in turn is followed by the action for releasing the lock.

State. It is assumed that the system is running on Linux. In order to derive state attributes, one needs to determine what affects the time it takes the thread to resume when it intends to take a sleep. Whenever a thread is about to do so, the scheduler is invoked. Scheduler activity results in scheduling latency and dispatch latency. The former is the time it takes to make scheduling decisions, i.e. time to insert a thread into scheduler runqueue (queue of threads that are ready to run on CPU but cannot because CPU is busy) or pick up one from the runqueue to run on CPU. Starting from the 2.6.23 kernel, Linux implements the Completely Fair Scheduler (CFS) [13]. CFS spends $O(\log N)$ time for insert and delete operations, where N is the number of threads in the runqueue, and constant time for a search operation. It achieves that by making use of the red-black tree to hold tasks sorted by their weights and always picking up the leftmost node of the tree to run on the CPU. Thus, scheduler latency which is essentially a function of number threads in the runqueue (perhaps of priority classes as well), contributes to time it takes the thread to be rescheduled on CPU.

Dispatch latency is the time it takes to complete a context switch which is the time to store the state of the thread going into sleep and restore the state of another thread to run. After the first context switch is completed, the current thread now

sleeps. Sleep duration should take into consideration the number of contending threads for the lock. The more threads contend for the lock, the more a thread should sleep to eliminate spinning as much as possible. Once sleep duration is over, there is no guarantee that it will get access to the CPU immediately (in an overloaded system). It depends on how loaded (busy) the system is. The load of the system can be expressed as a function of scheduler runqueue and number of threads executing on CPU, for example, as a ratio of average number of threads running on CPU to the average number of threads in the scheduler runqueue per unit of time.

Therefore, the number of threads in the scheduler runqueue, number of threads currently running on CPU and number of threads contending for the lock can serve as candidates for state attributes. At this point, the spin-then-sleep strategy can be regarded as an RL problem.

V. DISCUSSIONS AND CONCLUSION

Modeling of the spin-then-sleep strategy as a reinforcement learning problem promises competitive results. However, certain challenges and limitations are encountered as well.

State space, as well as action space, is continuous. Therefore, the learning process may be inefficient both from performance and storage point of view. Besides, since the state space is large, the thread may never have a chance to visit the same state more than once. Hence, the thread will not be able to try actions at that particular state. In such a case, a generalization technique such as CMAC [14] can be utilized. One can use it to generalize the learned experience from previous states to new states.

Another challenge is related to the exploration-exploitation tradeoff. From one side, threads need to try different actions to see their results (rewards), and from the other hand, threads are not willing to spend much time on learning, since they have to progress the application for which performance is crucial. To balance the exploration-exploitation tradeoff, one can use soft-max policy. To improve it further, one can trigger computations (reward calculation, policy update) not after every action of every thread but every few actions, like in [9] or every few time units.

Reward evaluation is easy to do, and policy update can be embedded into threads lock release phase which, intuitively, should require much fewer CPU cycles than lock handoff. Another option is to have additional threads to maintain it. However, if each lock would maintain a separate policy, then space requirements can be dramatic. Locks can be clustered on some property. An appropriate candidate for it can be the length of critical section protected by the lock. Locks clustered to a particular group will maintain a separate policy. It, thus, will reduce the number of total policies, even though additional contention points may arise as multiple threads may attempt to update the same policy at the same time. Future experiments will reveal more details on this.

Though the presented approach is generally quite promising, there exist situations in which case it cannot be applicable. First, it assumes that context switch time is constant which is not always the case. The direct cost of

context switch that includes pipeline flush and Translation Lookaside Buffer (TLB) reload will be different for different threads. Moreover, context switch also has associated indirect cost. When a thread wakes up and resumes execution, it may not find the data it needs in the CPU cache, and thus a cache miss will occur. This will affect the time it takes the thread to resume. For different memory access models, this cost will vary. Also, the reward structure is entirely agnostic of the load of the scheduler. It targets at minimizing the cost associated with lock acquisition and may do so even at the expense of deteriorating scheduler performance. In an extremely overloaded system, mostly sleeping will be preferred but too many context switches can make the scheduler very busy.

This work has explored one of the challenges faced by the spin-then-block method related to critical path delay at the lock handoff phase. As a solution, a more generic, a machine learning based approach is suggested to have threads learn when to sleep or spin. The technique models lock acquisition and release as a reinforcement learning problem. It can also be used to release the software designer from hardcoding cases that decide sleeping or spinning. As of now, no experimental setup has been done to test this design. Future studies will concentrate on running experiments to improve it, for example, by refining the reward structure. Certain developments can be made to reduce the action space as well. All this is a part of future work.

ACKNOWLEDGMENT

This work has been carried out in Center for Data Analytics Research at ADA University.

REFERENCES

- [1] T. E. Anderson, "The Performance of spin lock alternatives for shared-memory multiprocessors," *IEEE Transactions on Parallel and Distributed Systems*, vol. 1, pp. 6-16, 1990.
- [2] D. P. Reed, R. K. Kanodia, "Synchronization with event counts and sequencers," *Communications of the ACM*, vol. 22, pp. 115-123, 1979.
- [3] J. M. Mellor-Crummey, M.L. Scott, "Algorithms for scalable synchronization on shared-memory multiprocessors," *ACM Transactions on Computer Systems*, vol. 9, pp. 21-65, 1991.
- [4] P. S. Magnusson, A. Landin, E. Hagersten, "Quelocks on cache coherent multiprocessors," *Proceedings of Eighth International Parallel Processing Symposium*, pp. 165-171, 1994.
- [5] A. Kägi, D. Burger, J. R. Goodman, "Efficient synchronization: let them all eat QOLB," *Proceedings of the Twenty-Fourth Annual International Symposium on Computer Architecture*, pp. 170-180, 1997.
- [6] B. He, W. N. Scherer, M. L. Scott, "Preemption adaptivity in time-published queue-based spin locks," *Proceedings of the Twelfth International Conference on High Performance Computing*, pp. 7-8, 2005.
- [7] B. H. Lim, A. Agarwal, "Reactive synchronization algorithms for multiprocessors," *ACM SIGOPS Operating System Review*, vol. 28, pp. 25-35, 1994.
- [8] P. H. Ha, M. Papatrifiantofilou, P. Tsigas, "Reactive spin-locks: a self-tuning approach," *Proceedings of the Eighth International Symposium on Parallel Architectures, Algorithms and Networks*, pp. 33-39, 2005.
- [9] J. Eastep, D. Wingate, M. D. Santambrogio, A. Agarwal, "Smartlocks: self-aware synchronization through lock acquisition scheduling," *Proceedings of the Seventh International Conference on Autonomic Computing*, pp. 215-224, 2010.
- [10] J. R. Goodman, M. K. Vernon, P. J. Woest, "Efficient synchronization primitives for large-scale cache-coherent multiprocessors," *Proceedings of the third international conference on Architectural support for programming languages and operating systems*, pp. 64-75, 1989.
- [11] J. Mauro, R. McDougall, "Solaris internals: core kernel components," Sun Microsystems Press, 2001.
- [12] R. Sutton, "Reinforcement Learning: An Introduction," MIT Press, 2017.
- [13] C. S. Wong, I. Tan, and R. D. Kumari, F. Wey, "Towards achieving fairness in the linux scheduler," *ACM SIGOPS Operating Systems Review*, vol. 42, pp. 34-43, 2008.
- [14] R. Sutton, "Generalization in Reinforcement Learning: Successful Examples Using Sparse Coarse Coding," MIT Press, 1996.

Triangle Hyper Hexa-cell Interconnection Network A Novel Interconnection Network

Asmaa Aljawawdeh¹, Esraa Emriziq², Saher Manaseer³

¹Computer Science Department
The University of Jordan

²Business Information Technology Department
The University of Jordan

³Computer Science Department
The University of Jordan

Abstract—The interconnection networks play the main role in many applications, because it has a direct influence on it. Nowadays; the challenge is to find suitable topology that can deal with fewer requirements and min-cost. One of the most famous interconnection structures is the cube; it is used to build many interconnection networks such as the cube Hyper hexa cell topology. This work proposes a new topology; a hybrid topology between hyper hexa cell topology and triangle topology. In the propose interconnection network, the focus on the diameter which is less than the cube hyper hexa cell within one in any dimension and this effect on many parameters such as execution time. In the simulation environment, the radix sort being applied on the suggested Interconnection network using dimension number two on both; Triangle Hyper Hexa-cell and Cube Hyper Hexa-cell. Depending on the comparison between both topologies; in Theoretical and practical. The result shows the best performance for Triangle Hyper Hexa-cell. Practically; the measured parameter was the execution time in the simulation environment. Theoretically, the topological properties for both have been measured and got the equations for both, such as: number of nodes in every dimension, the number of edges, the network degree, and the diameter. This architecture will promise to be useful, more powerful for new-generation parallel architectures, and more effective for many applications and can be applied in different fields.

Keywords—Interconnection network; hyper hexa-cell; parallel system; radix sort; triangle hyper hexa-cell; triangle topology

I. INTRODUCTION

Parallel computing is one of the most trending area in computer architecture nowadays. The parallel computing means to compute simultaneously the jobs, tasks or instructions which reflects on performance criteria. The principle of parallel is to divide job into small jobs and start sub-jobs simultaneously[1]. Interconnection network provide ways to send and receive data between nodes processing. The parallel structures interconnections are divided into two well-known classifications which are [2][3]: 1- Static (direct connection). 2- Dynamic (intermediate stages). One of the most significant application that depends on the topology design is the Processors. The Processors are designed as groups, wherein each group contains processors connected along short distance networks such as the hypercube, Bus and Ring [4][5]. The main key in any interconnection network performance is the topology that used to build it [4][2][6]. One of the most famous interconnection networks is the cube-based architectures, that

being widely used according to its benefits in structure, such as low diameter, low cost and less complexity [6]. Some other familiar and well-known interconnection networks are: Mesh, Torus and hyper cube that used specially in digital communications systems[5][7]. Parallel systems are being used widely nowadays, this led to introduce new interconnection networks to support parallel processing. In this research paper we will introduce anew interconnection network by using a combination between two interconnection network.

II. RELATED WORKS

In [4] the authors used all-reduce communication operations to evaluated and analyzed on three interconnection network (the single port OTIS-Mesh, all port OTIS-Mesh and all-port-EDN-OTIS-Mesh) on different number of EDN (Extended Dominating Node), all OTIS-Mesh achieve better results for max and min number of communication than both single-port and all-port-OTIS-Mesh, the worst results in their proposed technique show performs about 146 and 142 better than other techniques. One of the disadvantage in this research appears on poor latency and the authors didn't include various collective communication operations such as scatter, reduction or another type of OTIS approaches like Hyper Hexa-cell and OTIS-Hyper cube.

In [2], the authors designed and implemented new topology OTIS Hyper Hexa Cell (OHHC) over OTIS-Mesh to integrate strength point for both HHC and OTIS characteristic, then evaluated for various terms such as diameter, minimum and maximum node degree, optical cost and bisection width. Their proposed topology showed improvement in terms and effectiveness for large parallel systems. One of the weakness in their approach that was no clear problem to solving such as load balancing, TSP and sorting algorithms.

In [1], the authors designed embedded hex-cell algorithm for n number of nodes in a tree-hyper cube network, which includes multiprocessor system. The proposed algorithm on tree-hyper cube can perform for irregular shape, but this study didn't perform for regular shape and show some weakness such as increase cost, dilation one, and congestion one and expansion. The authors suggested that their proposed algorithm on various topologies will reducing weakness for future works.

III. TOPOLOGICAL PROPERTIES OF TRIANGLE HYPER HEXA-CELL

This section first presents the important topological properties theoretical for both Triangle hyper Hexa Cell Topology and default Triangle Topology. Then a simulation was performed in order to measure the performance for both Triangle hyper Hexa Cell Topology and Cube Hyper Hexa Cell through applying the radix sort algorithm.

A. Topological Properties

The fundamental properties of Triangle Hyper Hexa-cell including the total number of nodes and edges, diameter, and cost factor.

- 1) Nodes:
Nodes defined as processing elements .The number of nodes in a Triangle Hyper Hexa-cell is given in Table I comparing with default Triangle topology.
- 2) Edges:
The edge is defined as the connection between two nodes.The number of edges for every node in a Triangle Hyper Hexa-cell is given in Table I comparing with triangle topology.
- 3) Degree of Network:
The degree of a node is defined as the total number of edges connected to that node. The degree of a network is defined as the largest degree of all the vertices that being used in the graph representation.
- 4) Diameter:
The diameter of a topology is defined as the shortest distance between the farthest two nodes in the topology.

Table I shows eight equations which measure and calculate the metric values for both topologies. The letter “d” in the below equations is representing the number of dimensions.

TABLE I. METRICS (RULES) FOR BOTH TOPOLGIES

Metrics	Triangle
No. of edges in every node	= d
No. of nodes	= (3 * (2d-1))/2
Degree of network	= (No. of edges * No. of nodes)/2 = d*((3*(2d-1))/2) /2 = d*((3*(2d-1)) /4
Diameter	= d-1
Metrics	Tria-HHC
No. of edges in every node	= d+3
No. of nodes	= ((3 * (2d-1) /2) *6 = 9 * (2d-1)
Degree of network	= (No. of edges * No. of nodes)/2 = ((d+3)* 9* ((2d-1)) /2
Diameter	= d+1

B. Topology Structure and Design

After defined the equations in the previous table, now we will determine the main properties for the proposed topology.

By using previous figures for the structure and rules in order to create and build the dimension number two structure for the Triangle Hyper Hexa cell (Tria-HHC). In this paper research, we use “Tria-HHC” name as an abbreviation for Triangle Hyper Hexa cell which is the proposed interconnection . For Triangle topology, Fig. 1(a), (b), (c) shows the structure and number of nodes in each dimension (two, three and four), respectively.

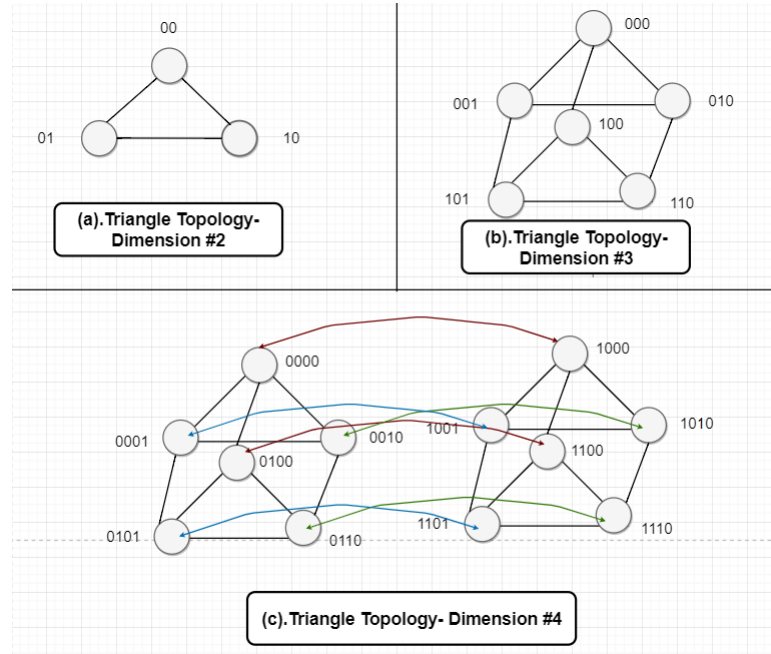


Fig. 1. Triangle topology.

The Triangle Hyper Hexa cell consists of two parts (Hyper Hexa cell and Triangle) as shown in Fig. 2 , which are being combined for building the new structure.

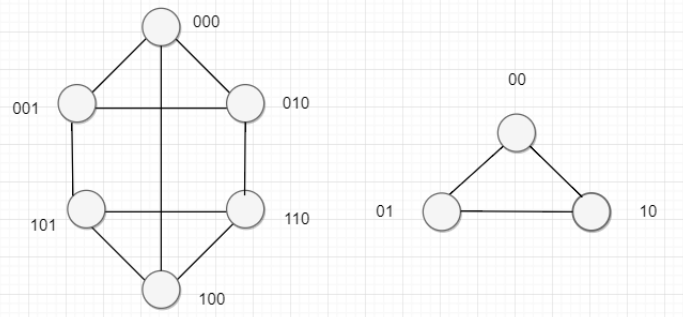


Fig. 2. Tria-HHC Parts

The Connection between nodes can be noticed in Fig. 3. Also, the metrics equations for dimension two achieved the real numbers by comparing the equations output with Fig. 3.

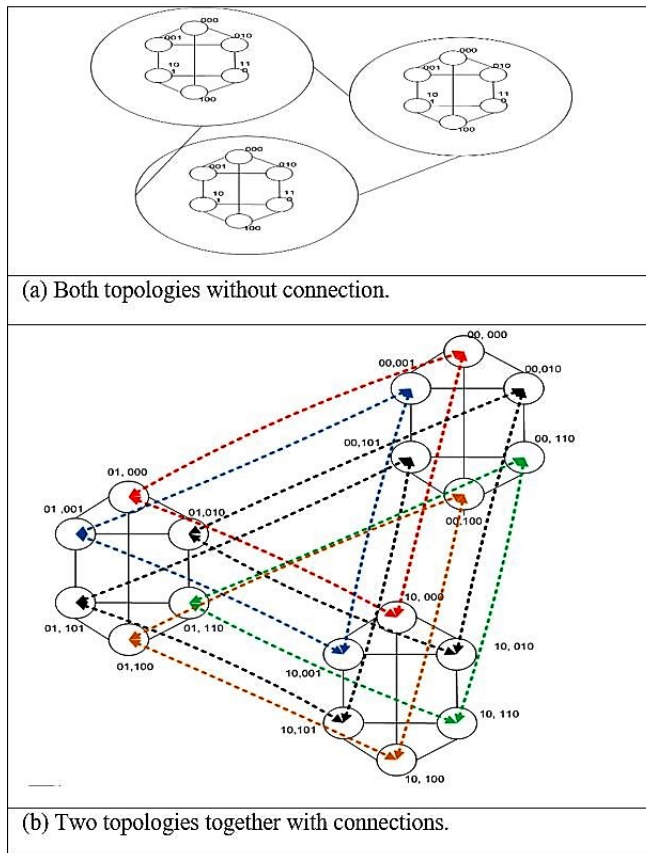


Fig. 3. Triangle Hyper Hexa cell (Tria-HHC)

The connection between nodes inside the hyper Hexa cell will be as it is, and between every two hyper hexa cell will be a connection for same nodes position(opposite) which basically depends on Triangle node's connections. Even though we must be careful about the number labeling.

C. Labeling and Naming

The naming rule for every node in the new hybrid interconnection is to make two parts of labeling separated by a comma. The first part of the name label to determine the External connection node name which is on the left side of a comma and it's defined as the group name. The other one to determine the internal connection, which is the same like default Hyper Hexa Cell and its existence on the right side. The two parts separated by a comma. The left part will change in every dimension. The number of bits will be the same number for dimension number, for example, if we have dimension two, in order to label the external part for the nodes we will add two bits (which will be the value of the Triangle label in fact) to the left plus a comma with its internal label as shown in Fig. 3 and so on for other dimensions.

D. Radix Sort

Sorting is one of the basic algorithms of computer science field and it is the most important part in many computation problems. Sorting plays a great role in many large-scale applications. Among successful sorting algorithms proposed

in the last few decades, the radix sort is best suitable for many applications and highly effective for parallel topologies [8]. A Sorting algorithm takes input a sequence of elements, and it outputs a permutation of the sequence in order. Radix sort is an integer sort, which is a sorting algorithm that sorts all elements numbers based on a single digit at a time[9]. There are two types of radix sorting: Most significant digit (MSD) radix sort starts sorting from the beginning of strings (most significant digit). LSD radix sort starts sorting from the end of strings (least significant digit) [10]. The Radix sort type which used in this simulation is the Most significant digit (MSD) version.

E. Simulation Environment

1) Materials used :

The materials that being used as mentioned in Table II.

TABLE II. SIMULATION MATERIALS

	Properties	Other Properties
Laptop used	Lenovo ThinkPad L50	OS: Win 7 Ultimate - 32bit service pack 1, Memory: 2G CPU: Intel Core I5 Model: 2520M – 2.5GHz.
Programming Language	Asp.net - C # (Console)	Microsoft Visual Studio Professional 2010 /Version : 10.0.40219.
Dimension Used	Two	used for both topologies (HHC and Tria-HHC)
Algorithm	Radix Sort algorithm	

2) The dataset used:

Random numbers were being used and created by a Method that creates a range between 1 to 999. Every integer number in the array equals 4 bytes (at least using 600,000 in the array). For example: 600,000 = 2,400,000 bytes = 2.28882 MB.

Table III shows the size of the dataset that has been used in the simulation. The data size that has been used in the experiment were converted using a website online converter.

TABLE III. DATA SIZE

Data size for Integer array	Data size in Bytes	Data size in MB
600,100	2,400,400	2.2892
1,000,000	4,000,000	3.8147
1,500,000	6,000,000	5.72205
2,000,000	8,000,000	7.62939
2,500,000	10,000,000	9.53674

3) Data Distribution and Collected Data between Nodes:

The same concept rule for data distribution and data gathering being applied in both topologies (Cube hyper hexa cell and Triangle Hyper Hexa Cell). In every hyper hexa cell (Internal) we used a two nodes for distributing data, then the same two nodes (in reverse) gathering the result from nodes in reverse method of the data distribution method. The remaining four nodes are used for applying the radix sort algorithm on its partitioned data. In every

Hyper Hexa Cell, there will be two nodes for data distribution and the same for data gathering, those two nodes work between inside nodes and outside nodes. The remaining four nodes will be used for Sorting. Fig. 4 and Fig. 5 illustrated this process in both Internal and External Cube Hyper Hexa cell nodes. The same methods applied for Triangle Hyper Hexa-cell.

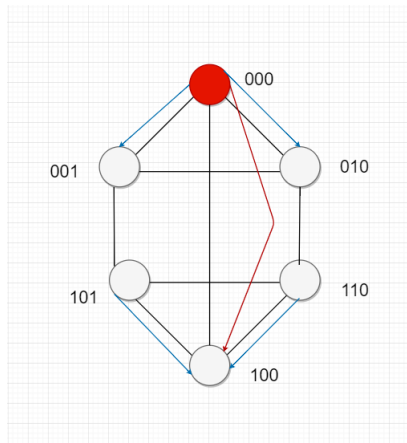


Fig. 4. Hyper Hexa cell -Distribution Data Internal

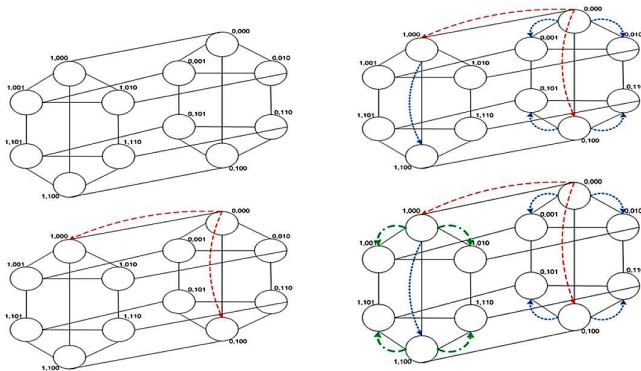


Fig. 5. Cube Hyper Hexa cell -Distribution Data External.

IV. RESULTS AND DISCUSSIONS

The collected results from the simulation after applying the radix sort on different structures are shown in Table IV which followed by a chart. The results show the time measurements (execution time) for the three structures: Triangle HHC, Cube HHC, and series (not parallel). The time execution is the computation time added to communication time. The time unit that is used in this simulation is Milliseconds. For validation, every experiment is repeated for 5 times and then calculated the average for those five experiments. It is clear that the series without parallel takes a lot of time, but by comparing the other topologies (Tria-HHC and Cube HHC), we can notice from Fig. 6 there is a difference in the Execution time. The performance for Tria-HHC is better than the Cube HHC depends on time measurements. Although there are some cases for time convergence, which could be explained through the increasing communication time between

nodes. Theoretically, depending on equations the Diameter for Tria-HHC is always less than one in every dimension comparing to Cube HHC. The best performance depending on equations, theoretical and simulation is the Triangle Hyper Hexa Cell (Tria-HHC).

TABLE IV. THE COLLECT RESULTS

DATA	600,100	1,000,000	1,500,000	2,000,000	2,500,000
Series	188.264	318.369	477.205	643.911	785.356
Tria-HHC	112.582	140.574	185.741	281.455	305.163
Cube-HHC	131.565	184.494	222.635	286.829	318.518

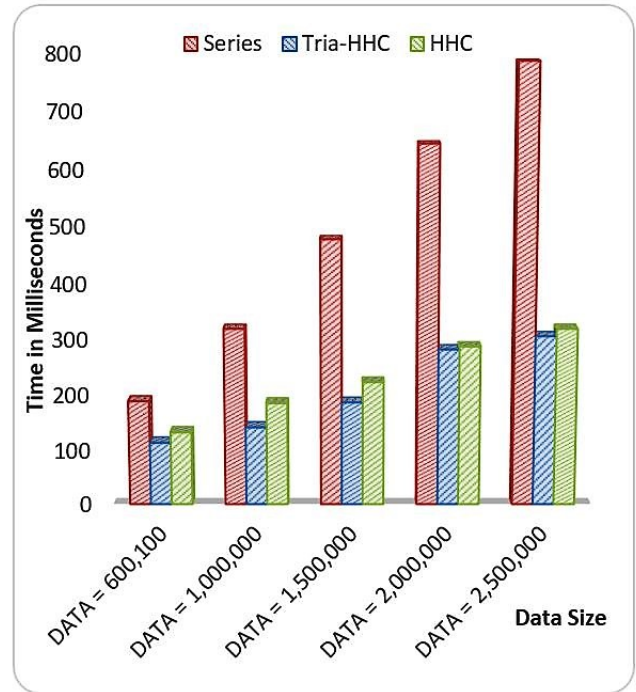


Fig. 6. Time measurement for Series, Cube HHC and Triangle HHC (Tria-HHC)

V. CONCLUSION AND FUTURE WORK

This paper presents a new interconnection topology called Triangle Hyper HexaCell. It consists of two topologies: Triangle and HyperHexaCell. The proposed topology is being useful in performance, according to its unique structure with a less diameter than the default Cube Hyper Hexa Cell. This will decrease the cost and the collected results show less time for Tria-HHC when applying the radix sort algorithm on the dimension number two into both cube HHC and Tria-HHC. There are routing algorithms which could be applied to this structure and other applications that depend on large-scale parallel computing systems will be efficient more using this topology. Future work, this topology can be applied in different fields and could be more useful. It is possible to combine three topologies together not only two.

REFERENCES

[1] Qatawneh, A. (2013). Embedding Hex-Cells into Tree-Hypercube Networks. International Journal of Computer Science Issues (IJCSI), 10(3), 136-143.

- [2] Mahafzah, B. A., Sleit, A., Hamad, N. A., Ahmad, E. F., & Abu-Kabeer, T. M. (2012). The OTIS hyper hexa-cell optoelectronic architecture. *Computing*, 94(5), 411-432.
- [3] Akhtar, A. H. & Lucas, K. T. (2014). Comparison of Communication Algorithms on OTIS-HHC and OTIS-Ring Parallel Architectures.
- [4] MAHAFAZH, B. A. and SERHAN, S. I. & TAHBOUB, R. Y. All-Reduce Communication Operation in OTIS-Mesh Interconnection Network.
- [5] Mohammad, Q. and Alamoush, A. and Basem, S. and Al Assaf, M. M. & Daoud, M. S. (2015). Embedding bus and ring into hex-cell interconnection network. *International Journal of Computer Networks & Communications (IJCNC)*, 7(3).
- [6] Alam, M. & Varshney, A. K. (2015). A Comparative Study of Interconnection Network. *International Journal of Computers and Applications*, 127(4), 37-43.
- [7] Yadav, S. & Krishna, C. R. (2014, August). CCTorus: A New Torus Topology for Interconnection Networks. In *Int'l Conference on Advanced Computational Technologies & Creative Media (ICACTCM'2014)* (pp. 8-14).
- [8] Liu, X. & Deng, Y. (2014, December). Fast radix: A scalable hardware accelerator for parallel radix sort. In *Frontiers of Information Technology (FIT), 2014 12th International Conference on* (pp. 214-219). IEEE.
- [9] Horsmalahi, P. (2012). Comparison of bucket sort and radix sort. arXiv preprint arXiv:1206.3511.
- [10] Polychroniou, O. & Ross, K. A. (2014, June). A comprehensive study of main-memory partitioning and its application to large-scale comparison and radix-sort. In *Proceedings of the 2014 ACM SIGMOD international conference on Management of data* (pp. 755-766). ACM.

Growth Characteristics of Age-based Anthropometric Data from Human Assisted Remote Healthcare Systems

Mehdi Hasan¹

Department of Advanced
Information Technology,
Kyushu University, Fukuoka, Japan

Fumuhiko Yokota³

Institute of Decision Science
for a Sustainable Society
Kyushu University, Fukuoka, Japan

Rafiqul Islam⁵

Medical Information Center
Kyushu University Hospital
Fukuoka, Japan

Mariko Nishikitani²

Institute of Decision Science
for a Sustainable Society
Kyushu University, Fukuoka, Japan

Akira Fukuda⁴

Department of Advanced
Information Technology
Kyushu University, Fukuoka, Japan

Ashir Ahmed⁶

Department of Advanced
Information Technology
Kyushu University, Fukuoka, Japan

Abstract—This paper reports growth characteristics (height, weight, BMI, waist and hip) of Bangladeshi males at the age of 20 to 100, analyzed from 13,069 samples randomly collected from 54 locations in Bangladesh since the year 2010. The US CDC (Center for Disease Control and Prevention) demonstrates growth pattern charts for boys and girls from 2 to 20 years of age. Very few literatures report growth characteristics after the age of 20. This is due to the fact that there is no significant growth after the age of 20 for height. However, weight, BMI, waist, hip size do change over time. Our Portable Health Clinic system has for many years been archiving remote health care data records from different ages and socioeconomic levels in many locations throughout Bangladesh. This research aims to explore whether there are any significant clinical growth patterns over age. We analyzed our data and demonstrated the growth patterns. For height, there is no sharp change until the age of 49, but after the age of 50, we observe a slight decline of height and a sharp decline after the age of 80. Weight grows until the age of 49 and decline after that. Waist and Hip show similar growth characteristics with weight. The plots are demonstrated in 7 different percentiles (5th, 10th, 25th, 50th, 75th, 90th and 95th) to get an idea of the range of respective growth of males in Bangladesh.

Keywords—Age and gender-based growth characteristics; portable health clinic; human assisted remote healthcare system

I. INTRODUCTION

Growth monitoring is the single most useful tool for defining health and nutritional status in children at both the individual and population[1]. This growth charts are widely used as a clinical and research tool to assess nutritional status and the general health and well-being of infants, children, and adolescents [2]. Optimal growth depends on genetic constitution, normal endocrine function, adequate nutrition, a nurturing environment, and an absence of chronic disease. Fetal, infant, maternal, and environmental factors can interact to impair intrauterine and postnatal growth [3]. Genetic differences in birth-weight among various populations are small and, although there are some racial/ethnic differences in growth [4], these differences are now known to be relatively minor

compared to worldwide variations in growth which are due to health and environmental influences (e.g. poor nutrition, infectious disease, socio-economic status) [6]. The most popular approach of growth pattern metrics developed and widely used by the CDC comprise a series of percentile curves that illustrate the distribution of selected body measurements related to the age of boys and girls. The CDC curves are based on compiled anthropometric measurements that were performed only once on the infants and toddlers who were sampled [7]. However, these CDC growth charts and their many derivatives only address the ages 2-20 years. As far as we know, there are currently no corresponding charts reflecting the same set of characteristics of human development for ages greater than 20. We aim to see if there are any significant clinical growth patterns, specifically regarding height, weight, BMI, waist, and hip for humans over the age of 20 years. We have been collecting and archiving 10 anthropometric data items from 54 different areas of Bangladesh since 2010 [5], [8], [9]. We are working on error detection, consumer behavior [10], [11], [12], [13] and healthcare well-being [14] areas. However, in this study we became interested in looking at this data to determine whether there are any significant growth patterns for individuals more than 20 years old, and therefore, the possibility of extending the very useful CDC charts. Due to the nature of Bangladesh, the uniform collection of health data can be challenging, and therefore, this long-term project was managed by our Portable Health Clinic (PHC) system, which is jointly administered by the Faculty of Information Engineering of Kyushu University, Japan, and Grameen Communications of Bangladesh [11], [15], [16]. In this effort, we focused 5 anthropometrics data: height, weight, BMI, waist, and hip. Because the underlying data was collected in often remote areas and digitized by health care workers in the field. The PHC is an e-Health system specifically designed to help provide medical advice and care in remote environments, both urban and rural. In both settings, the approach to the measurement, examination, and monitoring of health status, as well as facilitating consults by physicians, is the same. This service offers two types of packages that can be selected

based on the needs of a given patient. The system comprises three main components: a set of back-end data servers, a medical call center, and numerous inexpensive front-end portable medical briefcase with monitor, roughly 20cm X 12cm in size, consisting of medical sensors and measuring equipment, which are used to identify non-communicable diseases. The briefcase system also includes a tablet computer loaded with the Android application GramHealth [17], and it can store and share a wide range of remotely gathered health care data with physicians at major health care centers [18]. The PHC service utilizes two different actors, a health care worker and an ICT assistant, having independent roles and responsibilities, and each receiving a short but intensive training program. In the first step, a patient is registered at a service location by the health care worker [19], who then conducts a health checkup using the various capabilities of the PHC monitoring briefcase, and issues the patient a registration card with a unique ID [20]. The values of the patients 10 different anthropometric data are written on the back of the registration card. To store the data properly in the PHC software, the ICT assistant double checks the data and inputs it according to the patient registration card [21].

The rest of the paper is structured as follows: Section II describes the motivation and objective of this research, Section III explains the data preprocessing and analysis methodology of our approach, Section IV describes the obtained results from our analysis followed by a discussion of the findings and finally we conclude our research at Section V.

II. MOTIVATION AND OBJECTIVES

Extensive research has documented the pattern of human growth, with regard to height, weight, and BMI, up to the age of 20. As rigorously developed and promoted by the CDC, this information has been utilized worldwide as a series of percentile curves that illustrate the distribution of selected body measurements. However, very few studies have reported this class of growth patterns using health checkup data that has been collected from Bangladesh, particularly after the age of 20. Our previous study has been reported that within the various percentile categories, we found different growth patterns; however, we could not determine a clear indication in terms of a specific age where the significant change from growth to decline occurs. Therefore, in this study our objective is to use a unique dataset to explore whether there may be identifiable growth characteristics of human growth after age of 20 by 5 interval age groups and consider the possible implications of our findings.

III. METHODOLOGY

Anthropometric data has been collected from 54 locations from 2010 to 2018. We found 40,391 records in the database. We took the following steps to analyze the data.

- Step-1: Remove the incomplete, unusual and uninterested data: After removing incomplete, unusual data and uninterested (age ≥ 20) data, we selected $N=25,447$ records for our experiment. Number of male was $N_m=13,069$ and number of female was $N_f=12,378$.

- Step-2: Group the data into 5 years intervals: We classified the data into 15 groups, each group contains 5 years age intervals i.e. 20-24, 25-29, ..., 95-99.
- Step-3: Plot the growth charts: We plotted five anthropometric factors e.g. Height, Weight, BMI, Waist, HIP vs. each age group. Each anthropometric item in correspondence with age by seven difference percentiles (5th, 10th, 25th, 50th, 75th, 90th, and 95th) to view the distribution patterns. The curve was smoothened by using Local Polynomial Regression (LPR).

In our study, we considered anthropometric items (height, weight, BMI, waist, and hip) to explore whether clear patterns are evident.

IV. DATA ANALYSIS: RESULTS AND DISCUSSIONS

This section explains the results obtained from the data analysis mentioned in Section III. The growth patterns of each anthropometric parameters are plotted and the patterns are explained.

A. Male Height

Fig. 1 shows the growth characteristics of male height based on age where x-axis represents age groups (year) and y-axis represents height(cm) for male. We find three clusters of age with similar characteristics.

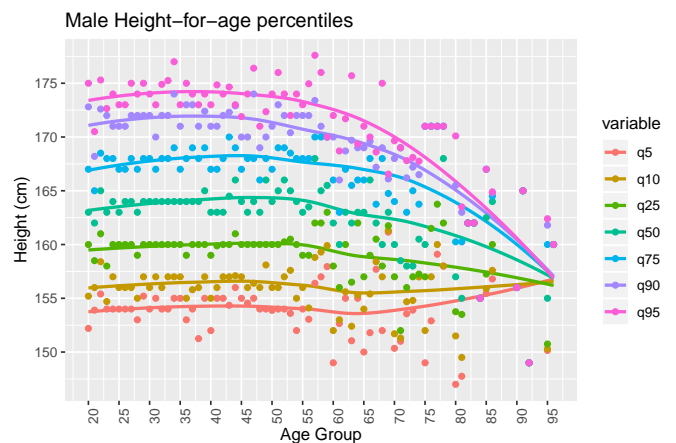


Fig. 1. Male Height for Age 20-100: 5th to 95th Percentile

- 1) Age level 20-49: There is no significant change in the growth at this age level. The reason could be the following: there is no significance change because generally male stop growing at the age of 18-20. Therefore, our findings comply with the natural growth of human being.
- 2) Age level 50-79: A decremented pattern is observed at this age zone. There could be two reasons for the height decreases with age: (a) biologically, our bone starts shrinking after this age level (b) a person of 79 years old now, was at 20 years of old in 1960s. At that period, the average height of male was 162-164cm, reported by [26], [27]. Their growth height stopped at the age of 20. That is why the growth pattern shows a decremental characteristics.

- 3) Age level 80-100: There is a drastic height loss in this age zone. Height of people may not decrease so drastically. This is quite surprising. We assume that this pattern is not representative. In fact, there are only 37 data samples (as in Fig. 2). Also, it can be assumed that the people were short at when their growth level stopped at their age of twenty which happened sixty to eighty years ago. People at that time, were generally short.

According to MedlinePlus [28], the tendency to become shorter occurs among all races and both sexes. Height loss is related to aging changes in the bones, muscles, and joints. People typically lose almost one-half inch (about 1 centimeter) every 10 years after age 40. Height loss is even more rapid after age 70. You may lose a total of 1 to 3 inches (2.5 to 7.5 centimeters) in height as you age. One can help prevent height loss by following a healthy diet, staying physically active, and preventing and treating bone loss.

Frequency distribution of surveyed male data (N=13,069)

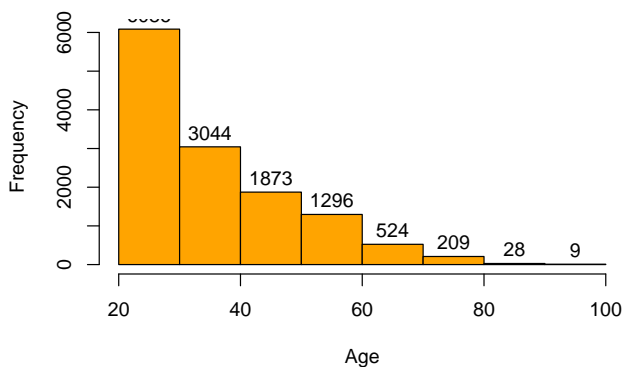


Fig. 2. Frequency of Male Data Samples

B. Male Weight

Fig. 3 shows the growth characteristics of male weight vs. age groups. The graphs are also plotted in seven difference percentiles. Our observations from this graph are the following:

- 1) Age level 20-49: An incremental pattern is observed at this age zone. Males gradually gain weight until the age of 50. This pattern is quite natural.
- 2) Age level 50-79: A decremental pattern is observed. Males lose weight at this age level. This pattern is also quite natural.
- 3) Age level 80-100: Very interesting pattern is observed at this age level. According to the graph, the weight is increasing at this age level which is not natural. It is assumed that the number of sample data is not representative at this age level. As described earlier, there are only 24 samples at age group 80-84, only 9 samples at 85-89 age group, 8 samples at 90-94 age group and only 2 samples at 95-99 age group. Therefore, we need more samples to draw a conclusion.

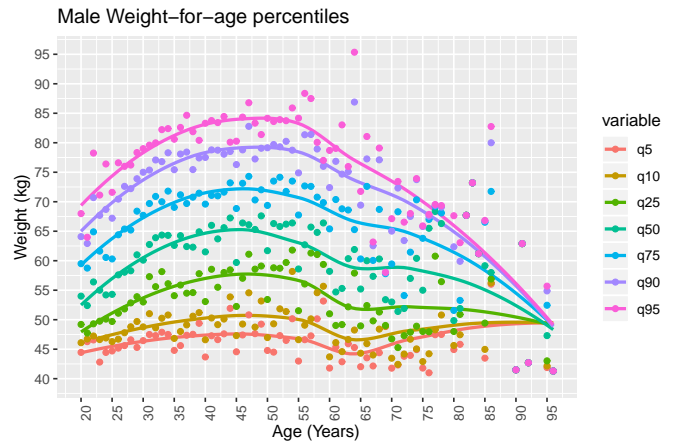


Fig. 3. Male Weight for Age 20-100: 5th to 95th Percentile

C. Male BMI

Fig. 4 shows the male BMI vs. age groups. Body mass index (BMI) is calculated using the formula (kg/m²) and defined as weight (kg) divided by height (m) squared.

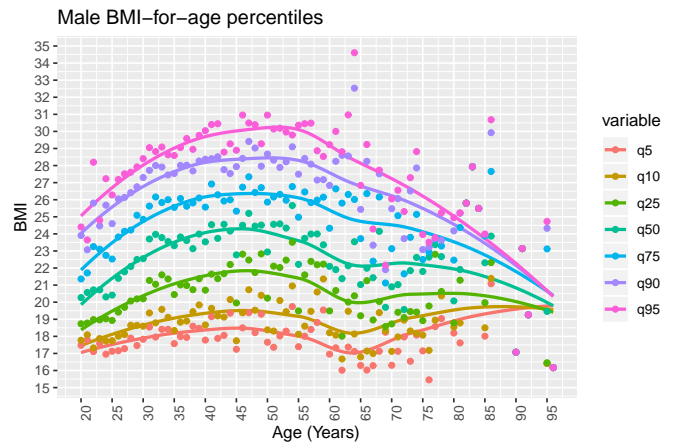


Fig. 4. Male BMI for Age 20-100: 5th to 95th Percentile

From the graph, we can observe the followings:

- 1) Age level 20-44: An incremental pattern is observed at this age zone. BMI is weight (in kilograms) height squared (in centimeters). We observed similar pattern at the age group in height. This pattern is quite natural.
- 2) Age level 45-64: A decremental pattern of BMI is observed. As people gain weight, without changing the height, this pattern is natural.
- 3) Age level: Age level 65-80: There is a drastic drop after the age of 60. in this age zone. This is surprising. There is a smooth decline of BMI after the age of 60. These are our eyeball measurements. More accurate mathematics are required to detect the cutoff point.

D. Male Waist

Fig. 5 shows the growth of male waist size over age.

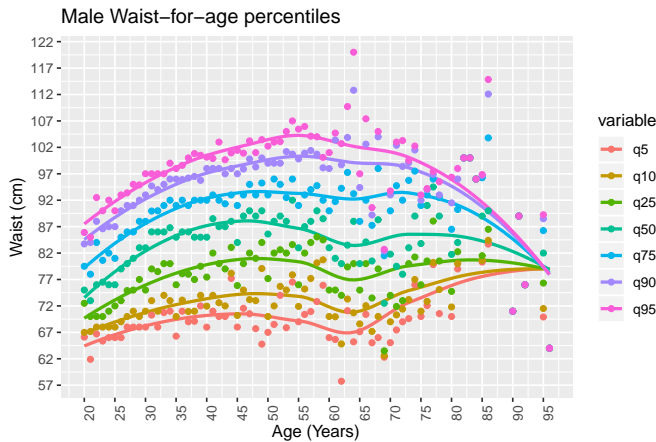


Fig. 5. Male Waist for Age 20-100: 5th to 95th Percentile

- 1) Age level 20-44: An incremental pattern is observed at this age zone. Males gradually change waist until the age of 44. This pattern is quite natural.
- 2) Age level 45-64: A slight decremental pattern is observed. It is assumed the bone starts shrinking at this age level.
- 3) Age level 65-100: This is quite surprising. We assume that this pattern is not representative.

E. Male Hip

Fig. 5 shows the growth of male hip size over age.

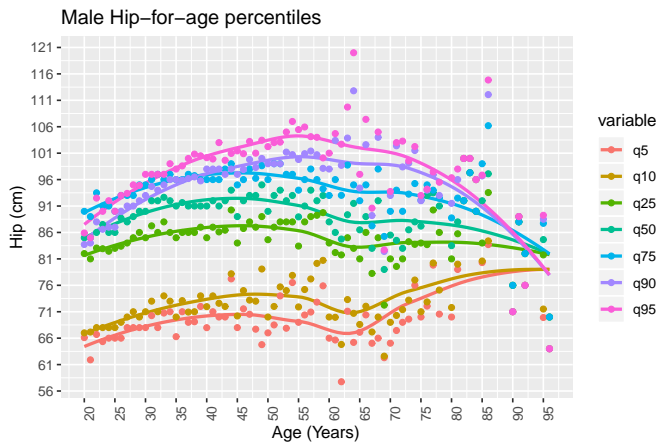


Fig. 6. Male Hip for Age 20-100: 5th to 95th Percentile

- 1) Age level 20-44: An incremental pattern is observed at this age zone. Males gradually gain weight and become fatty who do not do regular exercise.
- 2) Age level 45-79: A decremental pattern is observed. This pattern is also quite natural.
- 3) Age level 80-100: There is a drastic hip change in this age zone. Hip of people may not decrease so drastically. This is quite surprising. We assume that this pattern is not representative. In fact, there are only 37 data samples (as in Fig. 2).

Our present analysis described the relationship of age and male hip comprise a series of percentile curves. Most people

stop growing in height by the time they hit age 20 though the hip bones can keep growing even as people enter their 70s. In order to explain more rigorously this growth pattern for the male hip, we would in principle need a continuous record of the anthropometric items of each specific person in the sample.

V. CONCLUSION

This study investigated anthropometric growth patterns, specifically regarding height, for males over the age of 20 years. Over forty thousands health records were randomly collected by using our portable health clinic system from 54 locations in Bangladesh since the year 2010. Incomplete records, uninterested records (young patients, age ≤ 20 years) were removed. Finally $N=25,447$ (male: $N=13,069$ and female: $N=12,378$) records were considered. We plotted the mean of anthropometric item in correspondence with age by 7 different percentiles (5th, 10th, 25th, 50th, 75th, 90th and 95th) to represent the growth patterns of different age groups. The obtained curves were smoothened by Local Polynomial Regression (LPR). The resulting plots comprise a series of percentile (5th, 10th, 25th, 50th, 75th, 90th, and 95th) curves that illustrate the distribution by height, weight, BMI, waist, and hip. For height, there is no sharp change until the age of 49, but after the age of 50, we observe a slight decline of height and a sharp decline after the age of 80. Weight grows until the age of 49 and decline after that. Waist and Hip show similar growth characteristics with weight. A very small samples were available from old people (≥ 80 years old). The obtained growth patterns at this age level are not representative. The study will continue to collect more samples, find growth pattern for females and compare with those of males. Once the range for age based anthropometric data is known, it will be much easier to predict measurement errors of the patients for remote healthcare systems.

ACKNOWLEDGMENT

This research work has been supported by multiple organizations. JSPS KAKENHI, Grant Number 18K11529 and the Future Earth Research Fund, Grant number 18-161009264 jointly financed the core research. Institute of Decision Science for a Sustainable Society (IDS3) Kyushu University, provided travel expenses for data collection, and Grameen Communications, Bangladesh provided technical assistance.

REFERENCES

- [1] D. Onis, J. Habicht, "Anthropometric reference data for international use: recommendations from a World Health Organization Expert Committee", *The American Journal of Clinical Nutrition*, vol. 64, Issue 4, pp. 650-658, October 1996.
- [2] R.J. Kuczmarski, G.L. Ogden, S.S. Guo, L.M. Grummer-Strawn, K.M. Flegal, Z. Mei, R. Wei, L.R. Curtin, A.F. Roche, C.L. Johnson, "2000 CDC Growth Charts for the United States: Methods and Developments", *Vital and Health Statistics*, vol. 246, pp. 1-190, 2002.
- [3] B.J. Pinyerd, "Assessment of infant growth", *Journal of Pediatric Health Care*, vol. 6, Issue 5, pp. 302-308, October 1992.
- [4] J.P. Habicht, R. Martorell, C. Yarbrough, R.M. Malina, R.E. Klein, "Height and weight standards for preschool children: how relevant are ethnic differences in growth potential?", *The Lancet*, vol. 303, Issue 7858, pp. 611-615, April 1974.
- [5] Z. Mei, R. Yip, F. Trowbridge, "Improving trend of growth of Asian refugee children in the USA: Evidence to support the importance of environmental factors on growth", *Asia Pacific Journal of Clinical Nutrition*, vol. 7, Issue 2, pp. 111-116, 1998.

- [6] E. Kai, A. Ahmed, "Technical Challenges in Providing Remote Health Consultancy Services for the Unreached Community", In Proceedings 27th International Conference on Advanced Information Networking and Applications Workshops, 2013, pp. 1016-1020.
- [7] RJ. Kuczmariski, CL. Ogden, LM. Grummer, KM. Flegal, SS. Guo, R. Wei, Z. Mei, LR. Curtin, AF. Roche, CL. Johnson. "CDC growth charts: United States", *Adv data*, vol. 8, Issue 314, pp. 1-27, 2000.
- [8] A. Ahmed, AR. Hargrave, Y. Nohara, RI. Maruf, PP. Ghosh, N. Nakashima, H. Yasuura, "Portable Health Clinic: A Telemedicine System for UnReached Communities", *Smart Sensors and Systems*, Springer International Publishing, 2015. pp.449-467.
- [9] TR. Khan, J. Kamau, I. Hossain, KM. Hossein, A. Ahmed, "Visualization of Personalized Healthcare Data", in Proceedings of the 1st International Conference on Healthcare, SDGs and Social Business, 2017, pp. 32-33.
- [10] MN. Hossain, KM. Hossein, R. Chakrabarty, H. Okajima, H. Kitaoka, A. Ahmed, "Social Adoption of ICT Based Healthcare Delivery Systems in Rural Bangladesh", In Proceedings of the International Conference on Advanced Information & Communication Technology, Chittagong, Bangladesh, 2016.
- [11] MN. Hossain, F. Yokota, N. Sultana, A. Ahmed, "Factors Influencing Rural End-Users? Acceptance of e-Health in Developing Countries: A study on Portable Health Clinic in Bangladesh", *Telemedicine and e-Health*, 2018.
- [12] MN. Hossain, H. Okajima, H. Kitaoka, A. Ahmed, "Consumer Acceptance of eHealth among Rural Inhabitants in Developing Countries (A Study on Portable Health Clinic in Bangladesh)", *Procedia Computer Science*, vol. 111, pp. 471-478, 2017.
- [13] MN. Hossain, F. Yokota, A. Fukuda, A. Ahmed, "Factors affecting rural patients? primary compliance with e-prescription: a developing country perspective", *Telemedicine and e-Health*, doi.org/10.1089/tmj.2018.0081, 2018.
- [14] TR. Khan, KM. Hossein, RI. Maruf, A. Fukuda, and A. Ahmed, "Measurement of Illness and Wellness Score of Non-Communicable Disease Patients", In Proceedings of IEEE TENCON, 2017.
- [15] T. Osugi, J. Kamau, AR. Hargrave, E. Abdullah, A. Ahmed, "Healthcare Services on Wheels for Unreached Communities", *International Journal of Social Science and Humanity*, vol. 6, Issue 8, pp. 594-599, 2016.
- [16] Y. Nohara, E. Kai, P. Ghosh, R. I. Matuf, A. Ahmed, M. Kuroda, S. Inoue, T. Hiramatsu, M. Kimura, S. Shimizu, K. Kobayashi, Y. Baba, H. Kashima, K. Tsuda, M. Sugiyama, M. Blondel, N. Ueda, M. Kitsuregawa, N. Nakashima, "Health Checkup and Telemedical Intervention Program for Preventive Medicine in Developing Countries: Verification Study", *Journal of Medical Internet Research*, vol.17, Issue 1, 2015. e2. doi: 10.2196/jmir.3705
- [17] A. Ahmed, S. Inoue, E. Kai, N. Nakashima, Y. Nohara, "Portable Health Clinic: A Pervasive Way to Serve the Unreached Community for Preventive Healthcare", In Proceedings HCI, 2013.
- [18] K. Masahiro, Y. Akaoka, Y. Koga, Y. Nohara, N. Nakashima, P. P. Ghosh, R. I. Maruf, A. Ahmed, "Reverse standardization from public e-health service", In Proceedings of the 2014 ITU kaleidoscope academic conference, 2014, pp. 135-142.
- [19] A. Ahmed, A. R. Hargrave, Y. Nohara, E. Kai, Z. H. Ripon, N. Nakashima, "Targeting Morbidity in Unreached Communities Using Portable Health Clinic System", in Proceedings IEICE Transactions, 2014, pp. 540-545.
- [20] A. Ahmed, L. Kabir, E. Kai, S. Inoue, "GramHealth: A bottom-up approach to provide preventive healthcare services for unreached community", In Proceedings 35th Annual International Conference of the IEEE Engineering in Medicine and Biology Society (EMBC), 2013, pp. 1668-1671.
- [21] Y. Ling, Y. An, X. Hu, "An error detecting and tagging framework for reducing data entry errors in electronic medical records (EMR) system", In Bioinformatics and Biomedicine (BIBM), In Proceedings IEEE International Conference, 2013, pp. 249-254.
- [22] S. William, J. Susan, "Locally Weighted Regression: An Approach to Regression Analysis by Local Fitting", *Journal of the American Statistical Association*, 1988, pp. 596-610.
- [23] World Health Organization. "Physical Status: The Use and Interpretation of Anthropometry", Report of a WHO Expert Committee. WHO Technical Report Series 854, Geneva, 1995.
- [24] JJ. Henry, "Routine growth monitoring and assessment of growth disorders", *J Pediatr Health Care*, vol. 6, Issue 5, pp. 6:291- 301, 1992.
- [25] J. Krick, P. Murphy-Miller, S. Zeger, E. Wright. "Pattern of growth in children with cerebral palsy", *Journal of the American Dietetic association*, vol. 96, Issue 7, pp. 680-685, 1996.
- [26] https://en.wikipedia.org/wiki/List_of_average_human_height_worldwide, accessed on January 2019.
- [27] Subramanian SV, Ozaltin E, Finlay JE (2011) "Height of Nations: A Socioeconomic Analysis of Cohort Differences and Patterns among Women in 54 Low- to Middle-Income Countries". *PLoS ONE* 6(4): e18962. <https://doi.org/10.1371/journal.pone.0018962>
- [28] <https://medlineplus.gov/ency/article/003998.htm>, accessed on January, 2019

Density based Clustering Algorithm for Distributed Datasets using Mutual K-Nearest Neighbors

Ahmed Salim

Dept. of Math., Faculty of Sci., Zagazig University, Zagazig, P. O. Box 44519, Egypt

Dept. of Math., Faculty of Sci. and Arts, Al-mithnab, Qassim University, P. O. Box 931, Buridah 51931, Al-mithnab, KSA

Abstract—Privacy and security have always been a concern that prevents the sharing of data and impedes the success of many projects. Distributed knowledge computing, if done correctly, plays a key role in solving such a problem. The main goal is to obtain valid results while ensuring the non-disclosure of data. Density-based clustering is a powerful algorithm in analyzing uncertain data that naturally occur and affect the performance of many applications like location-based services. Nowadays, a huge number of datasets have been introduced for researchers which involve high-dimensional data points with varying densities. Such datasets contain data points with high-density regions surrounded by data points with sparse density. The existing clustering approaches handle these situations inefficiently, especially in the context of distributed data. In this paper, we design a new decomposable density-based clustering algorithm for distributed datasets (DDBC). DDBC utilizes the concept of mutual k-nearest neighbor relationship to cluster distributed datasets with different density. The proposed DDBC algorithm is capable of preserving the privacy and security of data on each site by requiring a minimal number of transmissions to other sites.

Keywords—Privacy; mutual k-nearest neighbor; Density-based; clustering; security; DDBC

I. INTRODUCTION

Distributed Databases is a database that may be stored in different computers in the same physical location, or may be distributed over a network of interconnected computers. Unlike parallel systems, in which the processors are tightly coupled and constitute a single database system, a distributed database system consists of loosely coupled sites that share no physical components.

In a distributed setting, a database D is implicitly defined in n explicit databases D_i s located at n different sites. We model a database D_i (that consists of a set of attributes) at the i^{th} site by a relation include several tuples.

Local databases may be conferred to computation, but data normalization can't be assumed to be performed for their schemas.

The implicit database D with which the computation is to be performed is a subset of the set of tuples generated by a Join operation performed on all D_i s. However, the tuples of D can't be made explicit at any one site due to entire local databases, D_i 's, can't be moved to a single site.

Therefore, the tuples of D must remain implicitly specified; which leads to the problem addressed by the proposed privacy preserving mining algorithm.

No doubt, that clustering of data points in a data space has regions with different density requires an effective algorithm to identify how many clusters should be used to classify the data points, especially data that is located at different geographic sites. Most of the algorithms are designed and developed to work on data that is available in one site. These algorithms cannot deal with distributed databases, and moving databases located in various sites is not an easy task. This is because of the huge size of these databases, ownership, and the most critical issues are privacy and security.

In a training data space, data points that belong to one class can have data density different from that for data points that belong to another class. In such a situation classifying entire data space to a correct class can become a difficult task due to the varying density of each existing class. To classify such datasets, we need a classifier that is sensitive to this property of the dataset.

The existing classifiers designed so far have problems. They have too many parameters to adjust before optimal results are obtained. The data space in Fig. 1 has two classes. The first class is a dense cluster containing point $R1$ and the other class comprise of only one data point, Q , which is far away from the dense class.

Using traditional k-nearest neighbor (kNN) classifier, with $k = 1$, if we want to classify P than P will be classified as a member of the dense cluster as point $R1$ is closer to P than any other point in the data space. We can clearly see that it does not belong to dense class but to the class same as point Q . kNN will classify points P and Q in same class.

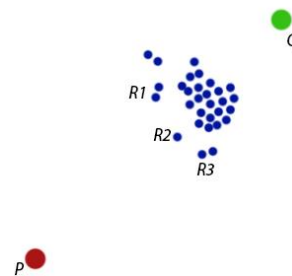


Fig. 1. Blue Points are Class 1, Green Point is Class 2 and P is Query Point.

Designing an algorithm that can handle the density-based clustering with distributed databases presents a whole new set of difficulties. This is especially true when we want to consider more than 2-dimensional points, which is often the case.

One easy way for this to occur is to send all of the data points to one central site and then perform the exact same algorithm. This is certainly a correct and viable method, but the problems with this method are that communication is more expensive than their computations. Moreover, the network sites may reject to move their data due to privacy, security, and size considerations; so what is needed is an algorithm that can have more computations occur at the individual database sites, and then transmit a minimal amount of information to a central site so as to reduce communication costs. This paper utilizes the concept of mutual k-nearest neighbor relationship to cluster points with different density exist at different sites. The new algorithm preserves the privacy and security of the data at each site by asking transmission of only minimal information to other sites. With this new method, there is less work done by the central node and more work is done at each database sites. This will be referred to as the decentralized method henceforth.

There has never been an algorithm designed that can cluster distributed databases based on density. There are some algorithms for clustering partitioned database but with some constraints on the partitioned data such as [22-24] presenting a method for k-means clustering when various sites contain various attributes for a combined set of entities, and the work in [26,27] discussing a privacy-preserving k-means algorithm for distributed databases. However, the presented algorithm only works for a horizontally distributed database split into two parts. Our proposed algorithm works for vertically and horizontally partitioned databases in d-dimensional space and does not put any limitation on the number of partitions.

The remaining of the paper is organized as follows: Section 2 describes related research. In Section 3, we describe our methodology for handling the proposed problem. In Section 4, we describe our proposed algorithm. The example scenario of our algorithm is given in Section 5. The analysis and complexity computing of the proposed algorithm is given in Section 6. In Section 7, we study the properties of our algorithm via simulation. We conclude our paper in Section 8.

II. RELATED RESEARCH

In order to benefit from the high performance of multiprocessor computer systems, many efforts have been made to develop and implement parallel pattern analysis algorithms [1-11]. Improvement for the k-means algorithm (IMR-KCA) proposed in [1]. IMR-KCA provides a selection model to simplify the calculations with multiple clustering centers by analyzing the flaws of vast redundancy in traditional k - means algorithms.

The work in [2] proposed a parallel graph-based data clustering algorithm using CUDA GPU, based on exact clustering of the minimum spanning tree in terms of minimum isoperimetric criteria, general superiority of this parallel

algorithm over other competing algorithms in terms of accuracy and speed.

In [3], the authors proposed Spark's GraphX based algorithm for density peaks clustering. Comparing to MapReduce implementation the system in [3] improves the performance significantly.

To speed up clustering for a large-scale dataset, parallel k-means clustering algorithm proposed in [4]. The proposed algorithm based on mahout API. Experimental results have shown a marked improvement in the speed of clustering for large datasets.

The performance of Modified Parallel K-Means algorithm and Parallel Genetic K-Means algorithm analyzed in [5] using Java Join and Fork Method.

Various distributed algorithms have been proposed to improve the computational performance of data clustering and its applications [12-20].

In [12], the authors proposed a distributed k-means clustering algorithm based on the attribute-weight-entropy regularization technique. Partial clustering problems in the distributed model presented in [13] and algorithms with communication sublinear of the input size were proposed.

Design and implementation of a distributed k-means clustering algorithm for text documents analysis proposed in [14]. The study of the k-means problem in the distributed dimension setting discussed in [15].

In [16], the authors proposed to construct two models: the first model that captures the system level characteristics of how computation, communication change as the cluster size increases and the second model, which captures how convergence rates change with cluster sizes.

The two main differences between our proposed algorithm and the above algorithms are as follows:

First, the above algorithms minimize the number of processors, however, in our work, the number of processors is fixed and we seek to minimize the number of exchanged messages among the sites; second, the above algorithms only read data at other sites, however, our algorithm performs computations at local sites and returns local results.

There are some works in the area of privacy preserving clustering algorithms of horizontally and vertically partitioned data [22-25] where these algorithms assumed that the data for one entity is split across multiple sites, and every site has information for all the entities for a particular set of the attributes.

However, our formulation models are more general situation than the case of a single key and non-overlapping attribute sets for single records distributed at different sites [22].

Our goal is to enable the collaboration and participation between different databases that designed independently and may have a random intersection of attribute sets with the other databases at different sites.

In [26, 27], the authors presented a multi-round algorithm for mining horizontally partitioned databases using a privacy-preserving kNN classifier. The motivation for their work is the fact that data from various private databases are needed for research that benefits many organizations but the privacy of such data should not be breached. Therefore, the goal of the research was to develop a classifier that provides stringent privacy required classified information while maintaining efficiency at the cost of little less accuracy. The problem of classification is divided into two parts.

The first part consists of selecting the nearest neighbor preserving the privacy of the database it searches. The second part includes the classification of the global database on the basis of the nearest neighbor selection of the previous part. The authors claim that their approach offers a trade-off between accuracy, efficiency, and privacy.

In this paper, we propose a decomposable version of the mutual k-Nearest neighbor-clustering algorithm that works in this desired manner with a set of networked databases.

A point in the d-dimensional space considered as a representation for each tuple in the implicit join D and the distance between two points corresponds to the distance between two tuples.

An initiator site communicates to the entire sites that involved in the task and asking them for results of some computations that executed at each site. Maybe followed by some new requests of results until the global results are obtained at the initiator site.

At first sight, the process seems simple, where every site can run the mutual-KNN clustering algorithm locally and could preserve complete privacy. However, this could not work as shown in Fig. 2.

From Fig. 2 consider that it is required to perform clustering on the data in the figure. From the vertical axis's point of view, we can see that there are two clusters centered at about 2 and 5.5. However, from the 2d point of view, we can see the difference in the horizontal axis dominates. By the higher dimensionality, the problem becomes exacerbated [22].

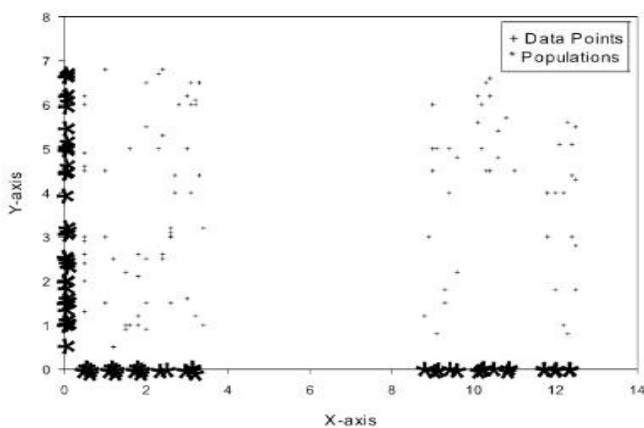


Fig. 2. 2D-Problem that Cannot Converted to Two 1D- Problems (Adapted from [22]).

III. DISTRIBUTED DATABASE AND COMPUTATION SCENARIO

A. Vertically and Horizontally Data Distribution

1) *Vertically distributed databases:* In this model, each database D_i contains tuples that created by a set of different attributes with some attributes that may share with D_j , $j \neq i$, and some attributes unique to D_i that are not shared with any other databases.

Vertically distributed databases require to perform computations in the implicit Join, D , considering that the tuples of D are not allowed to be explicit.

The decomposed algorithm must be able to calculate common attributes among D that it is would have helped in enumerating the tuples of the Joined D , as if D were explicit. The case of a single key and not shared attribute sets for single records distributed at different sites is considered as a special case in this formulation model.

2) *Horizontally distributed databases:* a set of components D_1, D_2, \dots, D_n such that each D_i contains tuples consisting of the same set of attributes A ; but a distinct set of data tuples resides at each D_i . Every D_i resides on various site and all tuples in each D_i , taken together, form the global database D .

B. Problem Statement

A number of vertically or horizontally databases that distributed at different sites jointly compose an implicitly joined global database that has all the data relevant to clustering or any other computational tasks. Algorithms that work with an imagined implicit join of the local databases are more desirable than that work with an individual local database; and this is due to constraints of the security, privacy, and size of the local databases.

Assume that D is the global database that formed by merging or joining n local databases (D_1, D_2, \dots, D_n) and each D_i consists of a set of set of attributes A_i . Therefore,

$$A = \bigcup_{i=1}^n A_i \quad (1)$$

Where A is the set of attributes of D .

Shared attributes form a subset s_{ij} , partitions D_i and D_j .

$$s_{ij} = \bigcup_{x=i,j} A_x \quad (2)$$

The set of all shared attributes S of D formed by the union of all s_{ij} , $i \neq j$. I.e. S has all shared attributes between all sites.

Our target to perform clustering of D , at the initiator site D_{init} (one of the sites) without moving D_1, D_2, \dots, D_n to D_{init} because of the security, privacy, and size of the local databases reasons.

As a result, local computations should be converted to global computations. The local computations at every site should be performed considering the shared attributes constants, besides, the local results should participate in the global solution at D_{init} .

IV. DECOMPOSABLE DENSITY-BASED CLUSTERING USING MUTUAL K-NEAREST NEIGHBORS (DDBC)

In this section, we describe the **DDBC** algorithm. The **DDBC** is based on the concept of mutual k -NN relationship between data points in the implicit database \mathbf{D} . The initiator sends requests (queries or agents) to the sites in order to figure out the two-way nearest neighboring relationship among the implicit data points. A and B can only become a mutual nearest neighbor pair if both A has B and B has A as their nearest neighbor.

- Definition

Two points A and B with distance $D_{A,B}$ are mutual k -nearest neighbors if: (1) there are less than k points between A and B and (2) there are m ($m > k$) points, but at least $(m - k)$ of these points have already found their mutual k -nearest neighbor, thus they refuse any new mutual nearest neighbor relationship with other points.

A. Decomposition of Global Computation

In order to find the cluster centers in \mathbf{D} , each site represented by an agent. Each agent has the capability to perform computation locally, or able to move from one location to another to perform computations or collect statistics. Without moving local databases to one site, these agents collaborate with each other to cluster the implicit database \mathbf{D} , while, these agents may exchange messages and summaries of their local results. D_{init}

Computing Shared Relation and Decomposition of d^D (Procedure 1)

1. First, the initiator finds the shared attributes and the shared values among sites by exchanging a number of messages.
2. Then the initiator creates the shared relation by executing the following steps:
 - a. Using the shared attributes and values, the initiator creates the **PreShared** relation as the cross product of the different values of the attributes in the set S .
 - b. Then, the initiator generates the Shared relation by removing from **PreShared** any tuple that does not exist at any of participating site.
 - c. Set index for the **Shared** relation starting with zero.

An agent at D_{init} sends a request to the agents of the collaborated sites to start the computations. The presented algorithm is designed to minimize communication between across sites and to handle various sets of collaborated sites and various sets of shared attributes between sites. Furthermore, the proposed algorithm preserves the privacy of the communicated data.

To clarify the decomposition process, assume that the required global computation is to find the distance $d^D(p_1, p_2)$ between 2 tuples $p_1 = (x_1, x_2, \dots, x_d)$ and $p_2 = (y_1, y_2, \dots, y_d)$ in the global database \mathbf{D} (\mathbf{D} located at one site).

$$d^D(p_1, p_2) = \sqrt{\sum_{i=1}^d (x_i - y_i)^2}, \quad (3)$$

Where, $\mathbf{D} = \{x_t | x_t \in R^d\}$.

However, in a distributed environment, \mathbf{D} exists as a set of partitions at various sites and $\mathbf{D}_1, \mathbf{D}_2, \dots, \mathbf{D}_n$ cannot be moved. The operation d^D can be decomposed to produce equivalent results by executing the following procedure.

From the definition of **Shared** relation, we can note that each tuple in **Shared** relation with index j represents a class (we will call it class j) of implicit tuples in \mathbf{D} .

Now we can decompose the operation d^D to produce the same results as in case of explicit databases. We divide the distance into two parts shared distance and unshared distance. First the shared distance $d^D(p_1, p_2, \text{Shared})$ is the distance between the values of shared attributes that computed at the initiator as follows:

$$d^D(p_1, p_2, \text{Shared}) = \sum_{\text{shared}} (x_i - y_i)^2 \quad (4)$$

where x_i and y_i are the values of shared attributes in p_1 and p_2 .

The unshared distance $d^{Di}(p_1, p_2, \text{Shared})$ can be computed by an agent at D_i (partition D_i at site i) and the shared values of the attributes at D_i .

$$d^{Di}(p_1, p_2, \text{Shared}) = \sum_{\text{unshared}} (x'_i - y'_i)^2 \quad (5)$$

Where x'_i and y'_i are the values of unshared attributes in p_1 and p_2 which correspond to x_i and y_i .

$d^{Di}(p_1, p_2, \text{Shared})$ can be computed by finding the unshared distances at the same class and between the tuples at different classes. Then, the results are aggregated at the initiator to get the global unshared distance.

Using equation (4) and (5) the decomposition of operation d^D will be.

$$d^D(p_1, p_2) = \sqrt{d^D(p_1, p_2, \text{Shared}) + d^{Di}(p_1, p_2, \text{Shared})} \quad (6)$$

As described above, each shared tuple with index j corresponding to a class of implicit tuples at least one tuple, the next procedure is to find the distances between each pair of implicit tuples inside each class j (if j has more than one tuple) and the third procedure is to find the distances between each pair of implicit tuples from different classes.

B. Computing Distances between Implicit Points inside each Class (Procedure 2)

This procedure aims to find the distance between every pair of implicit points inside each class.

1) *Data structures*: Distance table exists at the initiator site. The table contains five columns:

- a) Index column stores the index of the Shared tuples,
- b) Pair column stores the identification of the points of each pair,
- c) *SharedDistance* column stores the distance between the *Shared* attributes in the implicit tuples which can be computed using equation (4),
- d) *UnsharedDistance* column stores the distance between the *Unshared* attributes in the implicit tuples which can be computed using equation (5),
- e) *TotalDistance* column stores the total distance and can be computed using equation (6).

For each shared tuple, the initiator requests from each site the unshared distance between the unshared attributes that match with the shared tuple and sends the results back to the initiator. Finally, the initiator finds the total distance using equation (6).

2) *Local computation*: For all *Shared* tuple k , all site computes the unshared distances using Equation (5).

- a) **for each** *Shared* tuple k **do**
- b) At each D_i do
- c) Select all tuples that belong to the shared k ,
- d) Compute the unshared distances between every two tuples inside class k ,
- e) Return the values of the unshared distances to the initiator site.

3) *Global computation*: For every *Unshared* distance from D_i , the initiator finds the sum of all combinations C_i (one from each D_i).

- a) $Distance[k][SharedDistance] = 0$ // The distances between the shared attributes inside class k .
- b) for every C_i do
- c) $Distance[k][UnsharedDistance_i] = \sum_{between\ all\ sites} C_i$
- d) $Distance[k][TotalDistance_i] = \sqrt{Distance[k][UnsharedDistance_i]}$

C. Computing Distances between implicit Points in Different Classes (Procedure 3)

This procedure aims to find the distance between every pair of implicit points between classes.

1) *Local computation*: For every u and v (two classes or shared tuples), the initiator request from every site to compute the unshared distances between the implicit tuples (one in class u and one in class v) using equation (5).

- a) **for each** combination (j, k) of indices **do**
- b) At each D_i do
- c) Select all tuples that belong to classes j , and k ,
- d) Compute the unshared distances between every two implicit tuples that belong to different classes j and k ,
- e) Return the values of the unshared distances to the initiator site.

2) *Global computation*: For every *Unshared* distance from D_i , the initiator finds the sum of all combinations C_i (one from each D_i). The initiator computes the summation of this combination.

- a) $Distance [(u,v)][SharedDistance] =$ the distance between the shared attributes in classes j and k .
 - b) for every C_i do
 - c) $Distance[(j,k)][UnsharedDistance_i]=$
 - d) $Distance[(j,k)][TotalDistance_i]=$
- $$\sqrt{\frac{Distance[k][UnsharedDistance_i] + Distance[(j,k)][SharedDistance]}{\sum_{between\ all\ sites} C_i}}$$

D. Computing Distances between every pair of implicit tuples (Procedure 4)

The main goal of this procedure is to find the distance between every pair of implicit tuples using the computed distances (shared and unshared). This will be executed at the initiator site.

1) for each *site* i , construct the set $CountTup_i = \{N_j^i : j = 1, 2, \dots, l\}$, where N_j^i is the number of tuples that belong to class j at site i and l is the number of Shared tuples.

2) Construct the global matrix $CountMatrix [l][n]$ by considering each $CountTup_i$ as a column, where $i = 1, 2, \dots, n$, where n is the number of participating sites.

3) For every value $CountMatrix[j][i]$, define the sequence $Count_j = \{1, 2, \dots, CountMatrix[j][i]\}$.

4) For every class j , construct the matrix $MapMatrixl[c][n]$ as the Cartesian product of all sequences $Count_j^i$ s, where c is the number of tuples in class j in the implicit data.

5) For every $UnSharedDist_j^i$ set, construct the square matrix $UnSharedDist-Matrix_j^i [p][p]$, where p is the number of tuples in class j at site i ($p = CountMatrix [j][i]$). This matrix represents the unshared distances between each pair of tuples that belongs to class j at site i .

6) For every $UnSharedDist_{j,k}^i$ set, construct the matrix $UnSharedDist-Matrix_{j,k}^i [p][q]$, where p is the number of tuples in class j and q is the number of tuples in class k at site i ($q = CountMatrix [k][i]$). This matrix represents the unshared distances between any pair of tuples; one in class j and the other in class k at site i .

7) Using the above-constructed matrices, compute the global matrix $Distance_Matrix [w][w]$, where w is the number of tuples in the explicit database. The elements of this matrix will be computed by taking the square root to the sum of the Shared and Unshared distances as in Equation (6).

E. Finding Mutual k -Nearest Neighbors (M - k NN) (Procedure 5)

In this procedure, the initiator finds the two-way (i.e. mutual) nearest k neighbors of each point. The k value of a point will keep increasing until that point finds its mutual nearest neighbors.

- 1) *Data structure*: The mutual table exists at the initiator site. It has four columns:
 - 2) *Point_ID* column to identify each point,
 - 3) k_p column to specify the maximum number of nearest neighbors that each point can have,
 - 4) *k-NN* column stores the k-NNs of each point,
 - 5) *M-kNN* column specifies the mutual k-NNs of each point.
- a) $k_p = k_g$ // where k_g (global) is the initial k for all points
- b) Repeat
- c) for every $P_i \in P$ do
- d) $Mutual[P_i][kNN] = \text{Find NearestNeighbors}(P_i, k_{pi})$ // find the k-nearest neighbors
- e) **for every** $P_j \in kNN(P_i)$
- f) **if** $P_i \in kNN(P_j)$
- g) $Mutual[P_i][M-kNN] = P_j$
- h) **end for**
- i) **if** $Mutual[P_i][M-kNN] = \emptyset$
- j) $k_{pi} = k_{pi} + 1$
- k) **end for**
- l) Until N iterations or all points found their M-kNN

F. Generating Initial Set of Clusters (Procedure 6)

In this procedure, the points in *Mutual* table constructed in the Finding Mutual k-Nearest Neighbors Procedure will be used to create initial clusters that will be stored in table *InitialClusters* through the following steps. First, the radius of each point is found using Equation (7) and stored in *InitialClusters*. Second, the points are sorted based on their radius.

$$R_p = \frac{\sum_{i=1}^k d_i}{k} \quad (7)$$

Finally, the points are read sequentially in order to label them as follows: For each point P_i , we check if it's not given a label, we set it as class initiator and assign a new label for it (i.e. the point that begins creating a cluster including its M-kNN). Then we check its M-kNN and assign them labels according to the following two scenarios:

- 1) If a mutual k-nearest neighbor (P_j) has not been assigned an initiator, point P_i becomes its initiator.
- 2) If (P_j) is already assigned to an initiator we have two cases:
 - a. If the distance of (P_j) with its previous initiator $>$ distance of (P_j) with (P_i) Assign (P_i) as the initiator of the point.
 - b. If the distance of the point with its previous initiator $<$ distance of (P_j) with (P_i): Make no changes.

Find initial clusters

1. $cluster = 1$
2. **for every** $P_i \in P$ **do**

3. **if** cluster label C_i is not set **then**
4. $C_i = cluster$
5. **for every** $P_j \in P$ **do**
6. **if** cluster label C_j is not set **then**
7. $C_j = cluster$
8. **else**
9. get P_k cluster exemplar of P_j
10. **if** $distance(P_i, P_j) < distance(P_j, P_k)$ **then**
11. $C_j = cluster$
12. **end if**
13. $cluster = cluster + 1$
14. **end for**
15. **end for**

G. Merging clusters (Procedure 7)

This procedure is based on the inter-cluster distance which is measured based on some metrics as follows:

- **Linkage**: A point has a linkage to a cluster N if there is at least 1 point in N that is M-kNN of point p
- **Closeness**: Closeness of cluster $Cluster_i$ to $Cluster_j$ is number of points in $Cluster_i$ that has a Linkage to $Cluster_j$
- **Sharing**: Sharing S of cluster $Cluster_i$ into $Cluster_j$ is number of Mutual k-Nearest Neighbor pairs that have one in $Cluster_i$ and other in $Cluster_j$
- **Connectivity**: If $Cluster_i$ has k_i points and $Cluster_j$ has k_j points. Connectivity of $Cluster_i$ to $Cluster_j$ is defined as:

$$Connectivity_{ij} = \left(\frac{Sharing}{k_i * k_j} \right) * \left(\frac{Closeness}{k_i} \right) \quad (8)$$

The merging process starts with finding the connectivity between every two clusters and select the clusters that have the highest connectivity value to each other in order to merge them. Thus the new cluster is a combination of the points of the two clusters. The calculations of the connectivity will be repeated between the new cluster and the other clusters. This process is repeated until no clusters can be merged.

Construct Final Clusters

1. Calculate initial *ConnectMatrix CM*
2. Repeat
3. **for every** $C_i \in C$ **do**
4. $NeighboringClusters = \text{Find NeighboringClusters}(C_i, k)$
// the neighbors are selected based on the highest connectivity value
5. **for every** $C_j \in NeighboringClusters(C_i)$
6. **if** $C_i \in NeighboringClusters(C_j, \text{HIGHEST})$
7. $C_{new} = \text{Merge}(C_i, C_j)$
8. Update(CM)
9. **endif**
10. **end for**
11. **end for**

12. Until no more merging can be done or required clusters have been achieved

V. EXAMPLE SCENARIO

In this section, we present an example scenario to clarify our proposed algorithm and prove the cases described in Definition 1. The objective here is to determine the distance between every possible pair of points in order to cluster the points based on the density.

Assume that the local databases D_1 and D_2 from site 1 and site 2, respectively are shown in Table I. We consider D_1 and D_2 consisting of points in a 3-d space. As a result, the implicit database will contain the points $A=(0, 0, 1)$, $B=(2, 3, 1)$, $C=(2, 2, 1)$, $D=(3, 3, 1)$, $E=(3, 2, 1)$, and $F=(5, 5, 1)$.

From Table I, the Shared attribute is y, and the Shared values are {0, 3, 2, 5}. The indexed Shared relation showed in Table II:

- Local Computations

For each Shared k, each site will compute the unshared distance. The execution of proposed algorithm for Shared index 1 and the combination (0, 1) as follows:

- For Index 1

- At Site1: the unshared distance will be $d_1 = (2-3)^2 = 1$.
- At Site2: The unshared distance will be $d_1 = 0$.
- At the coordinator site: we have the following update:

$Distance[1][SharedDistance]=0$,
 $Distance[1][UnsharedDistance]=1$, and

$Distance[1][TotalDistance] = 1$

- For combination (0, 1)

- At Site1: the unshared distance between classes 0, and 1 will be $d_1 = (0-2)^2 = 4$, and $d_2 = (0-3)^2 = 9$.
- At Site2: the unshared distance between classes 0, and 1 will be $d_1 = (1-1)^2 = 0$.
- At coordinator site: the Shared distance between the shared attributes of the two classes (0, 1), will be $Distance[(0,1)][SharedDistance] = (0-3)^2 = 9$, $Distance[(0,1)][UnsharedDistance]_1 = 4 + 0 = 4$, $Distance[(0,1)][UnsharedDistance]_2 = 9 + 0 = 9$. As a result, the total distance table will be updated using equation (6) as follows: $Distance[(0,1)][TotalDistance]_1 = 3.61$, $Distance[(0,1)][TotalDistance]_2 = 4.24$.

Table III contains the calculated distances. From Table III, we can find the points that correspond to the calculated values. By transmitting message to every site to find tuples that correspond index 1, and then join the founded tuples, we get the following pair: $p1=(2, 2, 1)$, $p2=(2, 3, 1)$; $p1$ and $p2$ represent point C and B, respectively.

As shown in Table IV, A and F did not find any M-kNN at the first iteration thus we keep increasing their k_p until they find their M-kNN. Point A and F have met each other at the third iteration (Table V).

At this stage, we compute the radius of each point using Eq. (7) and then we sort them according to their radius. After that, we label the points as described above. The results are shown in Table VI. Table VII shows the two initial constructed clusters from the labeled points.

TABLE I. D1 AND D2 AT SITE 1 AND SITE 2

Site1		Site2	
X	y	Y	Z
0	0	0	1
2	3	3	1
2	2	2	1
3	3	3	1
3	2	2	1
5	5	5	1

TABLE II. SHARED RELATION

Index	Y
0	0
1	3
2	2
3	5

TABLE III. DISTANCE TABLE

Index	Shared Distance	Unshared Distance	Total Distance	Pair
0	0	0	0	-
1	0	1	1	(B,D)
2	0	1	1	(C,E)
3	0	0	0	-
0,1	9	4	3.61	(A,B)
0,1	9	9	4.24	(A,D)
0,2	4	4	2.83	(A,C)
0,2	4	9	3.61	(A,E)
0,3	25	25	7.07	(A,F)
1,2	1	0	1	(B,C)
1,2	1	1	1.41	(B,E)
1,2	1	1	1.41	(D,C)
1,2	1	0	1	(D,E)
1,3	4	9	3.61	(B,F)
1,3	4	4	2.83	(D,F)
2,3	9	9	4.24	(E,F)
2,3	9	4	3.61	(C,F)

TABLE IV. M-KNN AT FIRST ITERATION ($k_p=2$ FOR ALL POINTS)

Points	k_p	k-NN	M-kNN
A	2	D, C	
B	2	C,D	C, D
C	2	B, E	B, E
D	2	B, E	B, E
E	2	C, D	C, D
F	2	D, B	

TABLE V. M-KNN AT THIRD ITERATION ($k_p=5$ FOR A AND F)

Points	k_p	k-NN	M-kNN
A	5	D, C, B, E, F	F
B	2	C,D	C, D
C	2	B, E	B, E
D	2	B, E	B, E
E	2	C, D	C, D
F	5	D, B, C, E, A	A

TABLE VI. GENERATING PRELIMINARY CLUSTERS

Points	M-kNN	Radius	Cluster No.
B	C, D	1	B=1, C=1, D=1
C	B, E	1	C=1, E=1
D	B, E	1	D=1, E=1
E	C, D	1	E=1, C=1, D=1
A	F	7.07	A=2
F	A	7.07	F=2

TABLE VII. INITIAL CLUSTERS

Cluster	Members
C_1	B, C, D, E
C_2	A, F

Now, we check if we can merge any of the constructed clusters using Eq. (8) to compute the connectivity between the initial clusters. As shown in Table VIII, all the obtained connectivity values are zero, therefore, no clusters will be merged. The clusters in Table VII will be considered our final clusters.

TABLE VIII. COMPUTATION OF CONNECTIVITY

Clusters	Connectivity
$C_{1,2}$	0
$C_{2,1}$	0

VI. COMPLEXITY ANALYSIS

The density-based clustering of points that are distributed vertically among different sites requires part of the computations to be done locally at each site and the other part is done globally at the initiator site. The cost of the local computations is based on the number of messages exchanged between the various sites [21]. The way that the messages are exchanged is based on the agent scenario. Both cases for the agent will be analyzed: stationary agent and mobile agent.

Assume that there are n relations, D_1, D_2, \dots, D_n , lie in n various network sites, l number of tuples in Shared relation and r number of tuples in PreShared relation.

A. Communication Analysis

- Stationary Agent
- Centralized method

The number of messages is the total of the number of the messages required to retrieve the Shared values, check the existence of each Pre-shared tuple, computing the distance between every pair of points inside each class and between classes. Thus the sum of exchanged messages will be:

1. n messages to find Pre-shared from the local sites,
 2. $n*r$ exchanged message to compute shared from pre-shared,
 3. $(l * n)$ exchanged messages to compute the unshared distances inside classes ($UnSharedDist_1^j$),
 4. $\binom{l}{2} * n$ exchanged messages to compute the unshared distances between tuples in different classes $UnSharedDist_{j,k}^i$, where $\binom{l}{2}$ is the number of all possible combinations of two tuples in class j and class k .
 5. $l*n$ exchanged messages to compute the "CounTup _{i} " sets.
- Total number of messages = $n(1 + r + l(l + 3)/2)$

- DDBC method:

Unlike a centralized method, in DDBC the Shared tuple is going to be sent to all or any sites at the same time then the summaries are received in parallel.

In this case the cost is decreased to:

$$\text{Total Exchanged Messages} = (1 + r + l(l + 3)/2).$$

All of the above analysis considers only the total number of messages and do not include the complexity of the computations done at each local site. The local computations are typically searched operations with complexity $O(m)$, where m is the number of tuples in each site. Thus, the total cost of the local computation will be:

$$\text{Total Local Cost}_{\text{centralized}} = nm(1 + r + l(l + 3)/2)$$

$$\text{Total Local Cost}_{\text{DDBC}} = m(1 + r + l(l + 3)/2)$$

B. Mobile Agent

In this scenario, the mobile agent visits each site and does the local computation for each site. In our algorithm, three visits to each site will be enough to compute: The Pre-shared tuples, Shared tuples and the unshared distance in each class,

unshared distance between classes. Thus the total number of messages will be $3*n$.

As shown in the analysis, the total number of messages does not depend on the size of the local databases. This is beneficial, as the communication complexity remains the same despite the growing size of the local databases. Although it might affect the cost of the local computations on each site, our decomposable version still better when compared to a database joined explicitly from the local sites.

The joined database (i.e. implicit database) would generate (m^n) tuples in the worst case in addition to the cost of joining which is $(n*m)$. The complexity is even worse running procedures 2 and 3 to compute the distance between each pair of points in the implicit database as the cost will be $O(m^{2n})$, but in our decomposable version, the cost is $O(m)$ for each of the n sites. In addition, the number of messages to generate the implicit database is much more than the number of messages required in our algorithm.

Another advantage of the decomposable approach is preserving the privacy of the local databases since the computation is done locally and not all tuples are retrieved by the initiator. In addition, this approach doesn't affect the integrity of the local databases as all of the operations on the database are just queries (i.e. reading queries).

C. Computation Analysis

The rest of the algorithm steps are done globally at the initiator site using the table generated by procedure 1 and no more communication is needed with the local sites. In procedure 5, we sort the pairs according to the distances using quick sort which takes $O(P^2 \log P)$ as we have P points and P^2 pairs. To find the M -kNN, we scan the sorted table for the k -nearest neighbors which takes $O(P^2)$ and then scan the neighbors of each point to check for mutuality, however, as the number of neighbors is constant we can ignore it. Since procedure 5 is repeated for i iterations which is also constant then the total complexity for this procedure is $O(P^2 \log P)$.

In procedure 6, the creation of the initial clusters is done by scanning the list of the points and neighbors of points when needed, which results in complexity of $O(j*P)$ where j is number of neighbors for each point and since it's constant we can remove it, thus procedure 6 complexity is $O(P)$.

Finally, in procedure 6 the connectivity matrix is computed initially for every pair of clusters which is $O(C^2)$ where C is a number of clusters. For a constant number of iterations, the merging is done according to the highest connectivity and connectivity matrix is updated.

However, since the number of clusters is strictly smaller than the number of points the complexity of procedure 6 is intuitively less than $O(P^2 \log P)$. The total complexity of the Algorithm at the initiator site starting from procedure 5 will be $(P^2 \log P)$.

VII. EXPERIMENTAL RESULTS

In order to show the advantages of our algorithm, we have conducted a number of experiments to show that the DDBC algorithm designed for a distributed environment, without

transferring all the databases to a single site, can provide the same results as the algorithm in a centralized environment.

The experiments have been performed to find the impact of the number of tuples per database (NTuples), the number of sites (NSites), and the average number of shared tuples between local databases (AvgShared) on the results.

In the first test, we show the effect of NSites on the time and the number of exchanged messages, by increasing NSites by one starting from 2 to 6.

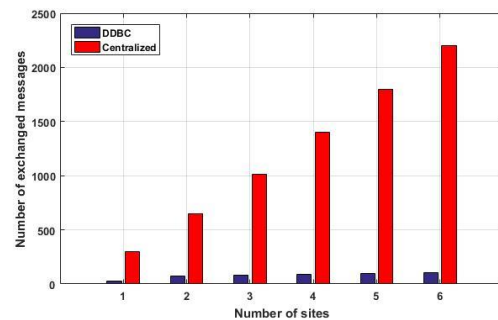
Fig. 3 shows the effect of NSites in the **DDBC** algorithm (in an implicit database **D**) on both of exchanged messages (ExMsg) and elapsed time (ET). We can see that there is direct relation between NSites and number of exchanged messages. Moreover, as NSites increased more time elapsed.

In the second test, we show the relation between NTuples and ExMsg and ET by varying AvgShared from 5 to 25 with an increment of 5.

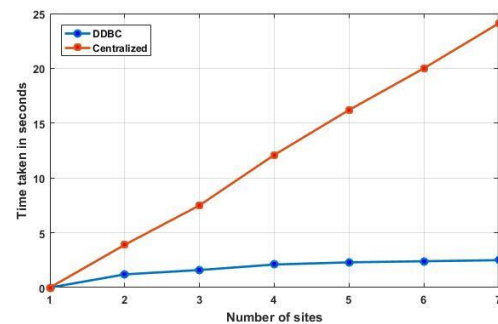
Fig. 4 shows that ExMsg and ET increased as AvgShared increased that is to run the **DDBC** algorithm in an implicit database **D**.

Finally, we show how the ET and ExMsg vary with NSites. Fig. 5 shows the relation between NTuples and ExMsg and ET in the **DDBC** algorithm.

Notice that the elapsed time to run **DDBC** increases as NTuples increased for one summary per message exchange in a centralized method. On the other hand, the elapsed time to run **DDBC** significantly reduced in the optimized method as NTuples increased.



(a) Exchanged Message.



(b) Elapsed Time.

Fig. 3. Analysis of DDBC on Vertically Partitioned Data (Distributed) and Centralized Method by Varying Number of Sites.

VIII. CONCLUSION

In this paper, we proposed a decomposable version of Density-based clustering for vertically distributed datasets located at different geographical sites. The algorithm composed of four procedures. Overall, the algorithm gives identical results to those would have been achieved by creating an implicit database at the initiator site and applying the algorithm on this database. However, our decomposable version minimizes the total communication cost between the initiator site and the local sites as well as the number of operations done in each site compared to those done on the implicit database.

Moreover, our algorithm preserves the privacy and integrity of these sites. In the current version we decompose the first part of the algorithm which finds the M-kNN into two parts, the first part finds the distance between every pair which is done in a decomposable way and the second part finds M-kNN based on the obtained results and it's executed at the initiator site. We are planning to improve the algorithm by doing the density-based clustering on each local site and create initial clusters, and then we combine these initial clusters at the initiator site in order to find the final clusters. As future work, multithreaded programming to parallelize message passing operations between points and clusters can be adapted this will make the M-kNN algorithm more efficient to cluster data on a big scale.

ACKNOWLEDGMENT

The authors gratefully acknowledge Qassim University, represented by the Deanship of Scientific Research, on the material support for this research under the number (3515-mcs-2018-1-14-S) during the academic year 1440 AH /2019 AD.

REFERENCES

- [1] Zhuo Tang, Kunkun Liu, Jinbo Xiao, Li Yang, Zheng Xiao, A parallel k-means clustering algorithm based on redundancy elimination and extreme points optimization employing MapReduce, *Concurrency Computat.: Pract. Exper.* e4109 Published online in Wiley Online Library (wileyonlinelibrary.com). DOI: 10.1002/cpe.4109, 2017.
- [2] Ramin Javadian, Saleh Ashkboosb, An Efficient Parallel Data Clustering Algorithm Using Isoperimetric Number of Trees, arXiv:1702.04739 [cs.DC], 2017.
- [3] Rui Liua, Xiaoge Lia, Liping Dua, Shuting Zhia, Mian Wei, Parallel Implementation of Density Peaks Clustering Algorithm Based on Spark, *International Congress of Information and Communication Technology (ICICT 2017)*, *Procedia Computer Science* 107, pp. 442 – 447, 2017.
- [4] X. Daoping, Z. Alin and L. Yubo, A Parallel Clustering Algorithm Implementation Based on Apache Mahout, 2016 Sixth International Conference on Instrumentation & Measurement, Computer, Communication and Control (IMCCC), Harbin, pp. 790-795. doi: 10.1109/IMCCC.2016.9, 2016.
- [5] N. Francis and J. Mathew, Implementation of parallel clustering algorithms using Join and Fork model, 2016 Online International Conference on Green Engineering and Technologies (IC-GET), Coimbatore, pp. 1-5. doi: 10.1109/GET.2016.7916820, 2016.
- [6] I. S. Dhillon, D. S. Modha, A data-clustering algorithm on distributed memory multiprocessors, in: *Large-Scale Parallel Data Mining*, Springer, pp. 245–260, 2000.
- [7] C. F. Olson, Parallel algorithms for hierarchical clustering, *Parallel computing* 21 (8), pp. 1313–1325, 1995.

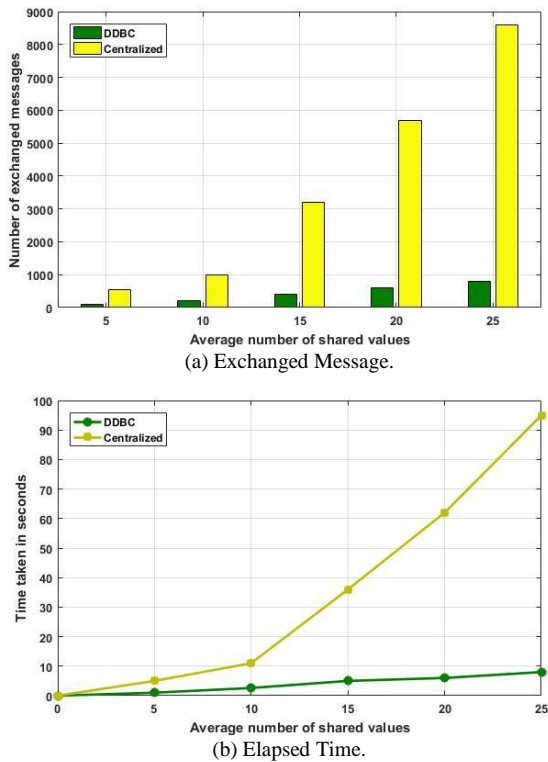


Fig. 4. Analysis of DDBC Algorithm and Centralized Method with a different Number of Shared Tuples.

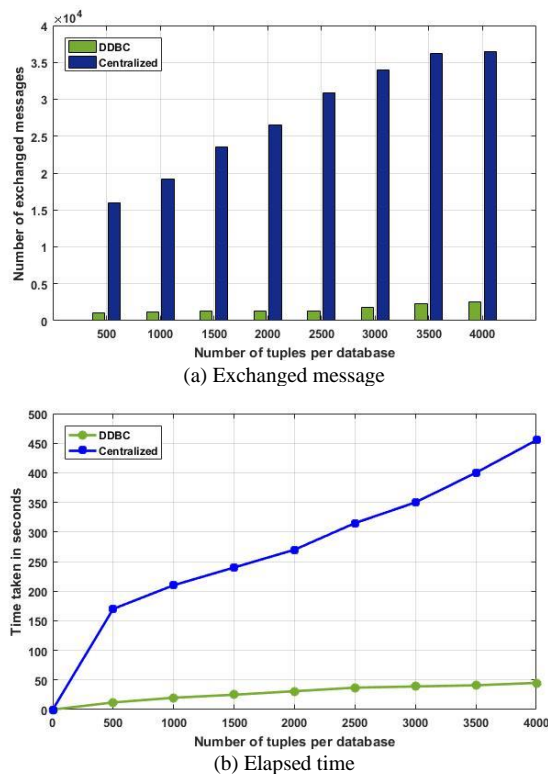


Fig. 5. Analysis of DDBC Algorithm and Centralized Method using a different Number of Tuples.

- [8] E. Dahlhaus, Parallel algorithms for hierarchical clustering and applications to split decomposition and parity graph recognition, *Journal of Algorithms* 36 (2), pp. 205–240, 2000.
- [9] A. E. Aboutabl, M. N. Elsayed, A novel parallel algorithm for clustering documents based on the hierarchical agglomerative approach, *Int. J. Comput. Sci. Inf. Technol.(IJCSIT)* 3 (2), pp.152–163, 2011.
- [10] W. Zhao, H. Ma, Q. He, Parallel k-means clustering based on mapreduce, in: *Cloud Computing*, Springer, pp. 674–679, 2009.
- [11] J. Wassenberg, W. Middelman, P. Sanders, An efficient parallel algorithm for graphbased image segmentation, in: *Computer Analysis of Images and Patterns*, Springer, pp. 1003–1010, 2009.
- [12] J. Zhou, Y. Zhang, Y. Jiang, C. L. P. Chen and L. Chen, A distributed K-means clustering algorithm in wireless sensor networks, *International Conference on Informative and Cybernetics for Computational Social Systems (ICSS)*, Chengdu, pp. 26-30. doi: 10.1109/ICSS.2015.7281143, 2015.
- [13] Sudipto Guha, Yi Li, Qin Zhang, Distributed Partial Clustering, *SPAA '17 Proceedings of the 29th ACM Symposium on Parallelism in Algorithms and Architectures*, pp. 143-152, 2017.
- [14] Martin Sarnovsky, Noema Carnoka, Distributed Algorithm for Text Documents Clustering Based on k-Means Approach, *Information Systems Architecture and Technology: Proceedings of 36th International Conference on Information Systems Architecture and Technology – ISAT 2015 – Part II*, pp. 165-174, 2015.
- [15] Hu Ding, Yu Liu, Lingxiao Huang, Jian Li , K-means clustering with distributed dimensions, *Proceedings of the 33rd International Conference on Machine Learning*, New York, NY, USA 16. *JMLR: W&CP* volume 48, 2016.
- [16] Xinghao Pan, Shivaram Venkataraman, Zizheng Tai, Joseph Gonzalez, Hemingway: Modeling Distributed Optimization Algorithms, arXiv:1702.05865 [cs.DC], 2017.
- [17] E.Januzaj, H.-P.Kriegel, M.Pfeifle. Scalable Density-Based Distributed Clustering[C]//Proceedings of PKDD04:231-244, 2004.
- [18] W.Ni,G.Chen,Y.J.Wu,etc.Local Density Based Distributed Clustering Algorithm. *Journal of Software*, 19(9):2339-2348, 2008.
- [19] M.M.Zhen,G.L.Ji.DK-Means-An Improved Distributed Clustering Algorithm[J].*Journal of Computer Research and Development*,44(2):84-88, 2007.
- [20] L.Li,J.Y.Tang,B.Ge,etc. k-DmeansWM: An Effective Distributed Clustering Algorithm Based on P2P[J]. *Computer Science*,37(1): 39-41, 2010.
- [21] Wang, C.—Chen, M.: On the Complexity of Distributed Query Optimization: *IEEE Transactions on Knowledge and Data Engineering*, Vol. 8, No. 4, pp. 650–662, 1996.
- [22] J.Vaidya, C.Clifton. Privacy-Preserving K-Means Clustering Over Vertically Partitioned Data[C] *Proceedings of ACM SIGKDD03*: pp. 206-215, 2003.
- [23] Shrikant, J. Privacy Preserving Data Mining Over Vertically Partitioned Data. PhD Dissertation, Purdue University 2004.
- [24] X. Lin, C. Clifton, M.Zhu. Privacy Preserving Clustering with Distributed EM Mixture Modeling[J]. *Knowledge and Information Systems*, 8(1): 68-81, 2005.
- [25] Y. Yao, G. L. Ji.: Distributed Clustering Algorithm Based on Privacy Protection [J]. *Computer Science*,36(3): pp. 100-105, 2009.
- [26] L. Xiong, S. Chitti and L. Liu, Mining Multiple Private Databases Using a kNN Classifier, *AMC SAC*, pp 435-440, 2007.
- [27] Inan, A. Kaya, S. V. Saygin, Y. Savas, E. Hintoglu, A. A. Levi, A.: Privacy Preserving Clustering on Horizontally Partitioned Data. *Data & Knowledge Engineering (DKE)*, Vol. 63, No. 3, pp. 646–666, 2007.

Development of Talent Model based on Publication Performance using Apriori Technique

Zulaiha Ali Othman¹, Noraini Ismail², Mohd Zakree Ahmad Nazri³, Hamidah Jantan⁴

Center for Artificial Intelligence Technology, Faculty of Information Science and Technology^{1,2,3}

Universiti Kebangsaan Malaysia, Bangi, Selangor, Malaysia

Faculty of Computer and Mathematical Sciences, Universiti Teknologi MARA (UiTM), Dungun, Terengganu, Malaysia⁴

Abstract—The main problem or challenge faced by Human Resource Management (HRM) is to recognize, develop and manage talent efficiently and effectively. This is because HRM is responsible for selecting the correct talent for suitable positions at the right time, aligned with their existing qualifications, talents and achievements. Furthermore, the decision in identifying talent for a position must be fair, truthful and appropriate. In the academic field, publication is a core component in the evaluation of academic talent that is affected by research, supervision and conference. Therefore, this study proposed an academic talent model based on publication factor using the Apriori technique for the purpose of promotion. This study applies the Apriori based Association Rules algorithm to identify a set of meaningful rules for the assessment of significant relevant talents for the promotion of academic staff in local universities. The findings have successfully developed a model based on talent acquisition of knowledge related to the issuance and have been evaluated by comparing the guidelines for the promotion of academic experts. This knowledge helps to improve the quality of the evaluation process of academic talent management and future planning in HRM.

Keywords—Human resource management; apriori based association rules; promotion's guideline

I. INTRODUCTION

The presence of 21st century has demanded the need for creation of new knowledge through a solid synergy among intellectuals. Hence, the strategy to mobilize all potential intellectuals, especially among academicians in local universities, is crucial. In addition, strengthening the field of education and driving excellence at local and global levels are in line with Malaysia's aspiration to achieve a fully developed nation. Therefore, HRM in any organization including higher educational institutions plays an important role too.

According to [1], human resources are the essential drivers that will determine the success of an organization. Besides that, having a talented and competitive workforce is very important in an organization to address any challenges [2]. Thus, HRM should set a goal in selecting the right and suitable academicians for proper positions. This is to ensure that the positions given are aligned with their existing qualifications, talents and achievements. However, the main problem or challenge faced by HRM in local universities is in recognizing, developing and managing talent efficiently and effectively. This is because human judgment and decision making have limits and can affect their fairness, truthfulness and appropriateness in identifying talent for a position [3].

Therefore, the use of data mining approach should be applied in the field of HRM through the diversification of techniques. Data Mining is a popular method that is able to explain the acquisition of useful knowledge and patterns from the data. Then, the knowledge can be used to help in decision-making processes [4]. According to [5], the researchers point out that rule mining has proven to be an effective technique to extract useful information from a large database. Also, reasoning with logical rules is more acceptable and understandable to users than a black box system.

The knowledge acquisition through data exploration is very useful for a variety of purposes. Based on the study in [6], the knowledge gained from the data collections using association rules helps in improving the professionalism level of academicians in the studied departments. In that regard, this data analysis gives many advantages to the organization and helps them in decision making to formulate more accurate planning [7]. The studies in [6] and [7] discussed the development of an overall academic model, but this study will focus on specific knowledge for the academician publication model which is a key element in the promotion process in local universities.

The main objective of this study is to determine meaningful rules that can be used as a guidance in the promotion of academicians using a data set from HRM in a local university. This study includes four main sections: Section II describes the proposed framework and technique used. Then, the results are presented and analyzed in Section III. Finally, Section IV concludes the major finding of this study.

II. DATA PREPARATION AND METHOD

In data mining, the preparation of data plays an important role, especially in choosing meaningful and relevant attributes. This process greatly can influence the finding results obtained at the end of the study in which the knowledge produced has precise, understandable, reliable and interesting features [7]. In this study, the data preparation process involves five steps; i) data collection, ii) data cleansing, iii) data integration, iv) data reduction, and v) data transformation. The method or technique used in extracting a meaningful pattern in the data set is the Apriori based Association Rules Technique. All the steps taken in data preparation and the technique used in this study are explained as follows:

A. Data Collection

This research is a continuation of the study in [8] that has succeeded in producing an academic talent prediction model for selected Higher Education Institutions involving experiments on raw data from HRM academic section databases from 1994 to 2010. The study in [8] was carried out using 15 raw data sets comprising 3220 data records, with a total number of attributes at 1140. The raw data sets include Demographics, Publications, Supervision, Conference, Research, Personnel History, Awards, Administrative and Performance Tasks.

However, this study does not take all the talent attributes from the study in [8], but focuses only on the publishing talent attributes. This is because the publishing attribute is a key component of academic achievement measurement for the process of knowledge development in Higher Education Institutions that leads to increased supervisory, research and conferencing. Therefore, this study only selected 1938 data records and 35 attributes which involved the collection of all academic staff data including Lecturer, Senior Lecturer, Associate Professor and Professor.

B. Data Cleansing

Data cleansing is the first step in the pre-processing phase that involves the task of filling in the missing values, controlling noise data, identifying outliers and correcting inconsistent data which can help in improving the quality of the data [9], [10].

In the data cleansing phase of this study, HRM data patterns from past researches have to be identified by reviewing the entire contents of items or values by columns (attributes of academicians such as Gender, Race, Job Status, Current Status, Education, Length of Service, Year Promoted to Lecturer, Year Promoted to Senior Lecturer, Year Promoted to Associate Prof., Year Promoted to Prof., Actual Position, Number of Publications, Number of Supervision, Number of Research and Number of Conferences) and rows (Records of Academic ID starting from K01 up to K3220). Based on the detailed review, there were some error problems. Among the forms of error in the survey data are non-uniform distributions of data, data containing unrelated or irrelevant attributes, repeating attributes, and data values in inconsistent attributes. Therefore, it is important to undergo data cleaning steps first to address the problem.

This research was funded by Ministry of Higher Education using grant KRA-2018-001 and KRA-2018-015.

This study focuses on publishing factors that have these five main criteria which are Demography, Publication, Supervision, Research and Conference, as shown in Table I. Therefore, attributes that are irrelevant such as Total Performance Scores, Number of Awards and Number of Holding Administrative Positions are removed from the data set. In addition, the data set is also inconsistent because it contains too many values of 0. The attributes containing the value of 0 for a record of 80 percent and above is also eliminated from the data set.

C. Data Integration

Integration data involves the process of merging data to obtain a balanced set of data. The process of merging data in this study is carried out through the decision or assessment by the expert and the relevant analysis which involves the merger of the attributes and the merging of items within the attributes. According to [11], the merger phase or data integration will contribute to the three aspects of data quality that is complete (completeness), sufficient (minimality) and understandability.

A total of 6 attributes are selected for the data integration process involving the attributes of Races, Job Status, Current Status, Education, Publication and Role of Research. In past research, the Races attribute consisted of 27 types of races but this study combines the attribute into 2 categories only, which are Malay and non-Malay. For the attribute of Job Status, this study combines 8 categories into 2 categories that are permanent and non-permanent. Next, the Current Status attribute that contains up to 8 current status types is combined into 2 active and inactive categories. The attribute for qualification in education is consolidated into three categories, namely doctors, masters and others, which previously had 31 categories altogether. The publication attribute comprising 20 different types of publications were divided into four major publications, namely book publications, proceedings, journals, and other publications. For the research related attribute, the role of academics in research with 9 types of roles in previous research were combined into 2 main roles, namely the role of research head and researcher. Table II shows the summarization of the selected attributes that underwent the integration process.

TABLE I. MAIN CRITERIA OF ACADEMIC TALENT

No.	Criteria	Attributes
1.	Demographic	Gender, Race, Job Status, Current Status, Education, Length of service, Year promoted to Lecturer, Year promoted to Senior Lecturer, Year promoted to Associate Prof., Year promoted to Prof. and Actual Post.
2.	Publication	Book publication, Proceeding publication, Journal publication, Other publication, and Total publications.
3.	Supervision	Total supervision
4.	Research	Research grant 2006, Research grant 2007, Research grant 2008, Research grant 2009, Research grant 2010, and Total of research grants.
5.	Conferences	Presenters, Chairman, Evaluator, Participant, Others, Department Conference, University Conference, National Conference, International Conference, and Total of Conference.

TABLE II. MERGING ATTRIBUTES

No.	Attributes	No. Attributes Merger	
		Before	After
1.	Races	27	2
2.	Job Status	8	2
3.	Current Status	8	2
4.	Education	31	3
5.	Publication	20	4
6.	Role in Research	9	2

D. Data Reduction

Data reduction is defined as a process of data compression to reduce the effort in analysis [10]. Prior to the data reduction process, the statistical analysis of each academic record item (row) and attribute item (column) is executed in advance to see the percentage number of item content or values in each HRM data record and attribute. The data records and attributes that have 80 per cent and above of 0 values will affect the quality of the data and consequently will affect the quality of the rules generation. Furthermore, low data quality will result in weak modeling [12]. Hence, the irrelevant task of reducing data records is important in this study to provide meaningful data for further analysis and to improve the quality of rules set production. At the same time, it can overcome constraints in data complexity and reduce data size.

Following the data reduction process, only 1938 records were selected for the experimental process. This process involves reducing the number of data records by 1282 compared to the total number of data records which was 3220. The computations for data reduction of the actual sample HRM datasets are shown in Formula 1 below:

$$\text{Percent of reduction Academician record} = \frac{\text{Number of 0 value data}}{\text{Academician record}} \times 100 \tag{1}$$

As a result, K01 id record is not removed from the data set because the value of 0 for the data record is 33.33% which fulfills the requirement that only 80 percent or above will be removed from the data record.

E. Data Transformation

Transformation data is the final process in the data pre-processing phase after data cleansing, data integration and data reduction. In data transformation, the data format were converted in order to make the mining process more efficient and the pattern of knowledge gained is easier to understand [13]. Through this study, each numerical data set was discretized using the WEKA (Waikato Environment for Knowledge Analysis) software. The data set was transformed according to its representation or value of a specified range based on an interval distribution using a binning method. The execution of discretization tasks is intended to reduce the continuous attributes by dividing the values of attribute into intervals [5]. Therefore, the data set is discriminated in the appropriate form to facilitate analysis as well as to minimize the space of the data.

In this study, the transformation technique used is the Equal Frequency Binning. This technique is applied to 29 attributes of HRM data set that has a numerical attribute value. It involves the following attributes; Length of Service, Year Promoted to Lecturer, Year Promoted to Senior Lecturer, Year Promoted to Associate Prof., Year Promoted to Prof., Actual Position, Published Books, Published Proceedings, Published Journals, Other Publications, Number of Publications, The Head of Research, The Researcher, Research Grant 2006, Research Grant 2007, Research Grant 2008, Research Grant 2009, Research Grant 2010, Total of Research Grants, Presenter, Chairman, Assessors, Participants, Others, Department Level Conferences, University Level Conferences, National Level Conferences, International Conferences and Total of Conferences. For attribute actual position, Position A represents Lecturer; Position B represent Senior Lecturer; Position C represent Associate Profesor; and Position D represent Professor. Table III above shows the sample of discretization on HRM data set.

The next process is the development of an academic publication model using the association rules technique. The description of association rules mining is discussed in detail in the next sub-section. The development of the academic publication model will be explained more clearly in Section III.

TABLE III. ATTRIBUTE TRANSFORMATION

No.	Attribute	Discrete	Symbol
1	Published books	0	A1
		1-2	A2
		≥3	A3
2	Published proceedings	0-1	B1
		2-6	B2
		≥7	B3
3	Published journals	0-1	C1
		2-6	C2
		≥7	C3
4	Other publications	0	D1
		1-3	D2
		≥4	D3
5	Number of publications	0-3	E1
		4-10	E2
		11-26	E3
		≥27	E4
6	Student supervision	0	F1
		1-34	F2
		≥35	F3
7	Actual position	A	G1
		B	G2
		C	G3
		D	G4

F. Apriori based Association Rules Technique

The Association Rules technique was introduced by Agrawal and Srikant in 1994 by seeking relevant rules that exist in a database [14]. Association Rules mining refer to the findings of items which are frequently associated together in a given data set. The actual task of the Association Rules is to find a pattern or relationship between the attributes that often appear together in a database and generate a set of rules. According to [15], the goal of Association Rule is to detect the relationship or correlation between absolute variable values (attributes) in a data set. This technique also allows analysts and researchers to uncover hidden patterns in large data sets.

An important measure of mining in Association Rules is the setting of the threshold value, the minimum support level and the minimum confidence level. In order to generate meaningful rules, the experiments need to be carried out by setting a high support value as well as high confidence value. However, if the outcome of the rules is not satisfactory due to the small number of rules generated or no meaningful rules are found, then the next experiment will be performed by setting a lower threshold value [10].

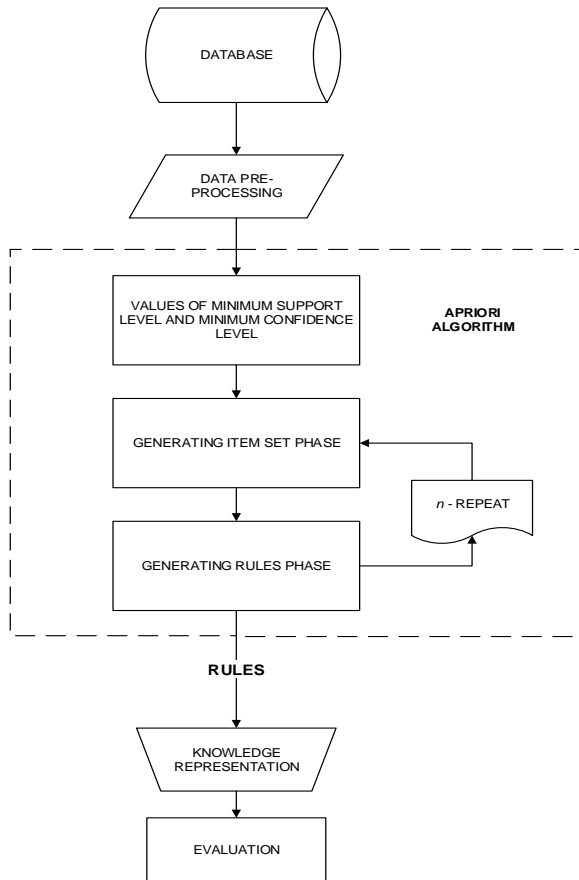


Fig. 1. Apriori based Association Rules Generation Steps.

Determining the value of minimum support and minimum confidence level is an important task as it affects the quality of the rules generated in terms of strength, legality, reliability and usability. The minimum support value measures and determines the frequency of items that often indicate the occurrence of rules in the database. Therefore, the minimum

support value is an important parameter in the Association Rule because that value will control the number and form of rules generated. On the other hand, the minimum confidence value measures the strength of rules obtained from the database [16]. The minimum confidence value is calculated on the generating phase of the rules to test the strength of a formed rule. According to [17], the best rules are the rules that have a high level of confidence. Conversely, if the confidence value is low, the resulting rules are not strong and will be removed.

Apriori is the most popular algorithm in Association Rules mining. In this study, the Apriori algorithm will be used in performing experiments to produce a set of rules. The Apriori algorithm works by generating frequent items set and subsequently generating Association Rules from the regular set of items. There are two main phases in the process of implementing the Apriori algorithm which are generating frequent item sets and selection of rules from regular item sets. Fig. 1 shows the steps of generating Association Rules using the Apriori algorithm.

III. EXPERIMENT AND RESULTS

This experiment was conducted using WEKA software to find the Association Rules in HRM data sets and the Apriori algorithm was used to find data-based rules. Only 1938 data sets and 35 attributes were selected for this experiment. In this study, rule generation is governed by parameter tuning, such as minimum support and minimum confidence level. This experiment used four different minimum support values which are 0.05, 0.1, 0.15 and 0.2, and the minimum confidence level of the threshold was set from 10% to 90%. Next, each generated rules is selected based on the pre-determined selection criteria. Step selection of the rules in this study is shown in Fig. 2. The example of the generated rules is shown in Tables IV-VII.

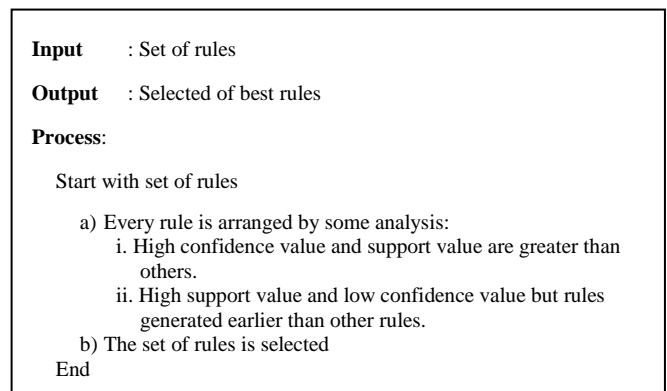


Fig. 2. Rules Selection Criteria.

A high level of minimum confidence generates good rules from a data set. However, if the experiment is set to a level of confidence that is too high, the rules generated will be less even if the resulting rules are stronger. For the purpose of meeting the needs of the study, minimum confidence is reduced to see the relevance results of the low confidence level. The experiments conducted involved the relationship between the five main criteria for publication talent factors: Demographics, Publications, Supervision, Research and

Conferences through four most important relationships in the association, namely "Publications and Demographics", "Publications and Research", "Publications and Supervision" and "Publishing and Conference". A strong relationship between the selected attributes serves as a set of rules for an experiment-based knowledge representation. The following sections illustrate the rules of the association extracted for

each relationship that is arranged according to the highest minimum confidence. Section A shows the rules for "Publications and Demographics", section B indicating "Publishing and Supervision" rules, section C shows rules for "Publications and Conferences" and section D shows rules for "Publications and Research".

TABLE IV. SAMPLE RULES FOR PUBLICATION AND DEMOGRAPHIC

No.	Rules	Min Support	Frequency	Min Confidence
1	IF otherpublication=0 ACTUALPOST=A THEN yearpromotedtobeB=0 AND yearpromotedtobeC=0 AND yearpromotedtobeD=0.	1	97	0.2
2	IF otherpublication=0 OR publishedjournal=0-1 ACTUALPOST=A THEN races=M AND yearpromotedtobeB=0 AND yearpromotedtobeC=0 AND yearpromotedtobeD=0.	0.89	163	0.15
3	IF education=Master OR otherpublication=0 OR publishedjournal=0-1 races=M ACTUALPOST=A THEN yearpromotedtobeB=0 AND yearpromotedtobeC=0 AND yearpromotedtobeD=0.	1	318	0.15
4	IF yearpromotedtobeC=0 AND otherpublication=0 ACTUALPOST=B THEN yearpromotedtobeD=0.	0.88	148	0.15
5	IF ACTUALPOST=A THEN races=M AND education=Master AND yearpromotedtobeB=0 AND yearpromotedtobeC=0 AND yearpromotedtobeD=0 AND publishedjournal=0-1 AND otherpublication=0.	0.42	1563	0.1

TABLE V. SAMPLE RULES FOR PUBLICATION AND SUPERVISION

No.	Rules	Min Support	Frequency	Min Confidence
1	IF totalpublication=0-3 AND totalsupervision=0 ACTUALPOST=A THEN publishedjournal=0-1 OR otherpublication=0 OR publishedproceeding=0-1.	0.9	76	0.1
2	IF otherpublication=0 AND totalpublication=0-3 AND totalsupervision=0 ACTUALPOST=A THEN publishedjournal=0-1.	0.9	76	0.1
3	IF publishedbook=0 OR totalpublication=0-3 OR publishedproceeding=0-1 ACTUALPOST=A THEN totalsupervision=0.	0.8	155	0.1
4	IF publishedproceeding=0-1 OR publishedjournal=0-1 OR otherpublication=0 AND publishedbook=0 ACTUALPOST=A THEN totalsupervision=0.	0.8	155	0.1
5	IF publishedproceeding=0-1 AND totalpublication=0-3 ACTUALPOST=A THEN totalsupervision=0.	0.8	155	0.1

TABLE VI. SAMPLE RULES FOR PUBLICATION AND CONFERENCE

No.	Rules	Min Support	Frequency	Min Confidence
1	IF publishedjournal=0-1 OR otherpublication=0 OR publishedbook=0 ACTUALPOST=A THEN conference5=0.	0.9	28	0.15
2	IF otherpublication=0 ACTUALPOST=A THEN conference2=0.	0.78	22	0.15
3	IF internationalconference=0-2 OR universityconference=0 ACTUALPOST=A THEN otherpublication=0.	0.79	302	0.1
4	IF conference1=0-3 ACTUALPOST=A THEN publishedjournal=0-1.	0.79	302	0.1
5	IF publishedproceeding=0-1 AND totalpublication=0-3 ACTUALPOST=A THEN conference5=0.	0.9	257	0.1

TABLE VII. SAMPLE RULES FOR PUBLICATION AND RESEARCH

No.	Rules	Min Support	Frequency	Min Confidence
1	IF publishedbook=0 OR publishedjournal=0-1 OR otherpublication=0 ACTUALPOST=A THEN G2006=0-74.	0.91	154	0.15
2	IF totalpublication=0-3 AND headofresearch=0 ACTUALPOST=A THEN publishedjournal=0-1 OR otherpublication=0.	0.9	148	0.1
3	IF totalpublication=0-3 AND headofresearch=0 ACTUALPOST=A THEN publishedjournal=0-1 OR otherpublication=0 OR G2006=0-74.	0.96	803	0.1
4	IF publishedprosiding=0-1 AND headofresearch=0 ACTUALPOST=A THEN publishedjournal=0-1.	0.9	148	0.1
5	IF publishedprosiding=0-1 AND headofresearch=0 ACTUALPOST=A THEN publishedjournal=0-1 OR G2006=0-74 OR G2007=0-107.	0.9	1517	0.1

A. Experimental Study of Association between Official Position, Demographic and Publication

In producing the set of Association Rules for the acquisition of knowledge on the HRM regarding the selection of criteria in the promotion process, the study selected data at 80 percent and below for the number of items in the data record containing blank values (0). The five main criteria are Demography, Publication, Supervision, Research and Conference. This experiment is intended to see the relevance attribute of Actual Position (ACTUALPOST = n), Publication attributes (totalpublication = n, publishedjournal = n, publishedbook = n, publishedproceeding = n and otherpublications = n), and Demographics attributes (gender = n, Races = n, education = n, jobstatus = n, grade = n, performance = n and lengthofservice = n) use support weights between 0.2 to 0.05 while confidence value is set between 0.3 to 0.9.

The results of this experiment show the relevant rules for Publication and Demographics were found at the support value of 0.2 and at the confidence value of 1.0. The actual position of academic practitioners A are found to have never been in B, C and D positions. Actual position A also has a number of working years exceeding 9 years and non-permanent positions. In terms of the academic level of education, all relevant results show the level of education at Master's level. As for involvement in publications, the academic staff in position A published journals and proceedings of 0 to 1 publication and never published for other publications.

On the other hand, the resulting rules for the actual position of academic practitioners B show that academicians have never been in positions C and D. The academic level is post-Doctoral Philosophy, current status is active and the race is Malay. For engagement in publications, academic practitioners B essentially published journals of 2 to 6 and the publication of proceedings was more than 7 while never published books and other publications.

Meanwhile, actual position C has been in C position for 1 to 4 years and never been in position D. The academicians are also Malay, still in regular position, current status is active and

education level is Doctor of Philosophy. For the involvement in publications, academic practitioners C have been published in proceedings and journals of more than 7 publications and have published 3 books.

The actual position D has also never been in D position for more than 1 year and has never been in position B. The academicians are also Malay, the current status is active and education level is Doctor of Philosophy. For the involvement in publications, academic practitioners D have been published in proceedings and journals of more than 7 publications.

B. Experimental Study of Association between Publication and Supervision

The second experiment is to see the relevance of the Actual Position attributes (ACTUALPOST = n), Student Supervision (totalsupervision = n), and Number of Publications (totalpublication = n, publishedjournal = n, publishedbook = n, publishedproceeding = n dan otherpublication = n) where minimum support level is set between 0.2 to 0.05 and the minimum confidence level is set between 0.3 to 0.9.

The result shows that the rules for attributes Student Supervision and Total Publications of academicians began to be generated at the minimum support value of 0.1 and the minimum confidence value from 0.9 to 0.7 which is for the academicians at position A only. For actual position A, the relevance of the relationship is never supervised students and the derivatives produced by academicians for the publication of proceedings are 0 to 1, journal publication is 0 to 1, book publication is 0, other publications is 0, and number of total publications is 0 to 3 and 4 to 10. The publication of 4 to 10 has a low frequency value; therefore the relevance of the actual position A is appealing based on all the above relevance besides having a publication of 4 to 10.

The result for the support value of 0.05 and the confidence value of 0.7 and 0.3 has found relevance to the academic practitioners of actual position A. The rules show that position A never supervised students and has a publication number from 4 to 10. The actual position B association is found at the support value of 0.05 and the confidence value of 0.7, 0.5 and 0.4. The rules show position B never supervised students and

has no book publications at support value of 0.05 and confidence of 0.7. Subsequently, the relevance of the actual position B generated at the support value of 0.05 and the confidence value of 0.5 indicates the relevance of the actual position B, and the supervision of students is 1 to 34 and has published 2 to 6 journals or published 2 to 6 proceedings. The same minimum support value of 0.05 and the minimum confidence value of 0.4 result in association between the actual position B and supervision of students is supervised from 1 to 34 students, but never published books or other publications. This suggests that the relationship between actual position B with the supervision of students is 1 to 34, and the publication of journals is 2 to 6 or the publication of proceedings is 2 to 6.

Lastly, the association of actual position C was found at the minimum support value of 0.05 and minimum confidence values of 0.9 to 0.4. The generated rules found that position C has an association between the publication of books in excess of 3 or published proceedings in excess of 7 or the total publication is over 27 and supervision of students is in excess of 35 persons. The findings for the associations of actual position D begin with minimum support of 0.05 and minimum confidence 0.9 to 0.7. The findings indicate that job position D has an association between the publication of proceedings in excess of 7 or a total publication number exceeding 27 or journal publications exceeding 7 and supervision of students exceeding 35 persons.

C. *Experimental Study of Association between Publication and Proceedings*

This experiment is intended to see the relevance of the attributes Actual Position (ACTUALPOST = n), Publication (publishedjournal = n, publishedbook = n, and other publications = n), and Proceedings (conference = n) use minimum support values of 0.2 to 0.05 while minimum confidence values are set between 0.3 to 0.9.

These experimental results show the relevance rules for the Actual Position, Publication and Conference found at the support value of 0.15 and at the confidence value of 0.9. An academic practitioner of position A was never a Chairman, Registrar or Assessor and other duties during a conference. However, they have been the Presenter for 0 to 3 times and Participants for 0 to 2 times. At the conference level participated, academic practitioners of position A had never attended University or Department level conferences, but had participated in an international conference of 0 to 2 times and at a national level of 1 to 2 times. For engagement in publications, position A has never published books and other publications, while publishing journals and proceedings for 0 to 1 time. The total number of publications is 1 to 3 times.

On the other hand, academician practitioners in position B are found to be participating in conferences, whereby they have never been the Chairman, Registrar or Assessor and others. However, the academicians have been presenters for 0 to 3 times. At the conference level participated, the academic practitioner B had never attended the University or

Department conferences, but had participated in an international conference of 0 to 2 times. For the involvement in publications, the findings show that academicians in position B has never published books and other publications, but published journals and proceedings 0 to 1 time.

Furthermore, the academic practitioners in position C are also found to have been the Chairman more than 47 times, the Registrar or the Assessor more than 3 times, and the Participant more than 28 times. At the conference level participated, academic practitioners C had attended the Department level conference more than 3 times, the International level more than 13 times, the national level more than 8 times, and the University level more than 3 times. The total attendance of the conference is over 29 times. For engagement in publications, academicians in position C have published journals and proceedings more than 7 times, while the total of publications is over 27 times.

For academicians who have the actual position D, it was found that the academicians have been Spokesman more than 47 times, Chairman more than 3 times and Participants more than 28 times, and Registrars or Valuers more than 3 times. At the conference level participated, the C academic staff member had participated in the International level conference more than 13 times. The total attendance of the conference is over 29 times. For involvement in publications, academicians in position D had published journals and proceedings more than 7 times.

D. *Experimental Study of Association between Publication and Research*

This research is aimed to look at the relevance of the Actual Position attributes (ACTUALPOST = n), Research attributes (headofresearch = n, researcher = n, G2006 = n, G2007 = n, G2008 = n, G2009 = n, G2010 = n, and totalG = n), and Publication attributes (totalpublication = n, publishedjournal = n, publishedbook = n, publishedproceeding = n and otherpublication = n) that use minimum support of 0.2 to 0.05 while minimum confidence values are set between 0.3 to 0.9.

These experimental results show the relevance association of the Actual Position, Publication and Research was found at minimum support value of 0.15 and minimum confidence value of 0.91. Academic practitioners A are found to have never been a research head and are only a member of the researcher between 0 and 1 times. For the grants received, a researcher of position A received a research grant in 2006 from RM0.00 to RM74,000.00, in 2007 from RM0.00 to RM107,000.00, in 2008 from RM0.00 to RM830,000.00, in 2009 from RM0.00 to RM490,000.00 and in 2010 from RM0.00 to RM240,000.00. The number of research grants received from 2006 to 2010 is RM0.00 to RM13,800.00. For engagement in publications, academic practitioners of A position did not publish books and other publications, while publication of journals and proceedings were 0 to 1 time. The total number of publications for academic practitioners of A position is 0 to 3 times.

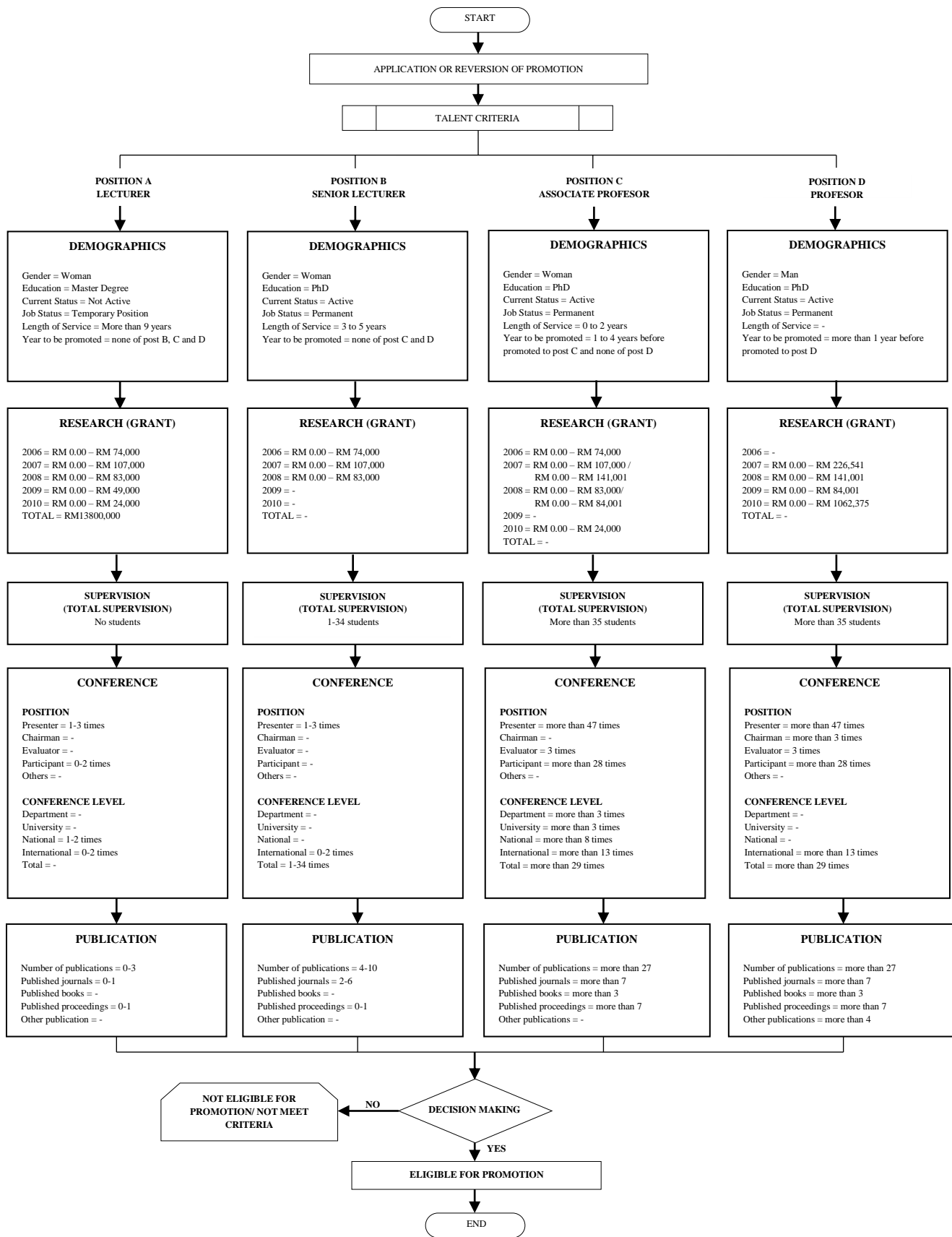


Fig. 3. The Talent Model based on Publication Performance.

Through these experiments, the resulting rules for academic practitioners in B position show that academicians have become researchers of 1 to 2 grants and received a research grant in 2006 from RM0.00 to RM74,000.00, in 2007 from RM0.00 to RM107,000.00, and in 2008 from RM0.00 to RM83,000.00. For engagement in publications, academic practitioners in B position did not publish books and other publications, while publishing proceedings and journals were 0 to 1 time. There are also rules found that academic members of B position published journals 2 to 6 times and the total number of publications are 4 to 10 times.

This experiment also shows that academic practitioners in C position have been a research head for more than 3 times and a researcher for more than 10 times. For the grants received, they received a research grant in 2006 from RM0.00 to RM74,000.00, in 2008 more than RM141,001.00, and in 2009 more than RM 84,001.00. As for the involvement in the publication, academic practitioners of C position did not publish any books, while the publication of journals and proceedings were more than 7 times, and the total number of publications was more than 27. Other than that, there are also academic members of the C positions who obtained a research grant in 2007 from RM0.00 to RM107,000.00, in 2008 from RM0.00 to RM83,000.00 and in 2010 from RM0.00 to RM24,000.00, and did not publish any books and other publications but published proceedings and journals 0 to 1 times.

Academic practitioners of position D have also been a research head for more than 3 times and a researcher for over 10 times. For the grants, the academicians in position D received more than RM226,541.00 in 2007, in 2008 more than RM141,001.00, and in 2009 more than RM84,001.00. The number of research grants received from 2006 to 2010 is over RM106,2375.00. For the involvement in publications, academic practitioners in position D published journal and proceedings more than 7 times, other publications more than 4 times, and the total number of publication is more than 27 times.

Fig. 3 shows the academic publication model based on the decision of association rules extracted using the Apriori algorithm that will be used for promotion. The main factors that are interpreted through five main criteria are Demographics, Publications, Supervision, Research and Conferences, which have helped create interesting rules for forming links that ultimately serve as a source of reference in appraising decision-making. The development of the model is based on the results of experimental relationships between "publication with research", "publication with supervision", "publication with conference" and "publication with demographics" talent attributes. The relevance association generated through this experiment is the basis of academic rank promotion selection criteria by generating the relevancy relationship frequency between the selected attributes.

IV. CONCLUSION

This study is the continuation of [8] that uses HRM data from an IPT in talent management through Apriori based Association algorithm methods. The result of this study shows the decision of talent model based on publication

performance. The difficulty in determining suitable talent for promotion is one of the major problems faced by any department or division that manages human resource-based operations. Furthermore, research in related areas are also less practiced locally or internationally, especially involving academics. Therefore, the Apriori based Association Rules technique has been applied in this study to further elaborate on other production functions in data mining, but focuses more on academic talent publication modeling. The advantage of applying the Apriori technique in the development of the talent model is that Apriori is able to generate the frequent item sets with candidate item set generation which discovers the relevant patterns in the data set. Moreover, Apriori also performs multiple scans for generating candidate sets. However, although this study has achieved its stated objectives, there are several suggestions that can be considered. One of them is the findings of relevance rules can be extended to non-academic staff for promotion. Non-academic staff also contributes in the support segment in driving excellence of academic institutions. Then the interesting attributes of the promotion have to be adjusted for the purpose of appraisal of higher rules of effectiveness. It is recommended that the assessment attributes are based on course days, number of successful and failed interviews, annual leave taken and assessment of other attributes that can be used as plus measures in HRM management and preparation of database records. Last but not least is extending the scope of the study in terms of selecting attributes from the HRM dataset.

ACKNOWLEDGMENT

This research was funded by Ministry of Higher Education using grant KRA-2018-001 and KRA-2018-015.

REFERENCES

- [1] M. M. Tafti, M. Mahmoudsalehi, and M. Amiri, "Critical success factors, challenges and obstacles in talent management," *Ind. Commer. Train.*, 2017.
- [2] P. F. Buller and G. M. McEvoy, "A Model for Implementing a Sustainability Strategy through HRM Practices," *Bus. Soc. Rev.*, 2016.
- [3] H. Jantan, A. Razak Hamdan, and Z. Ali Othman, "Human Talent Prediction in HRM using C4 . 5 Classification Algorithm," *Int. J. Comput. Sci. Eng.*, 2010.
- [4] M. Saron and Z. A. Othman, "Model Base On Human Resource System Using Classification Technique," *IJCEM Int. J. Comput. Eng. Manag.*, vol. 15, pp. 1-8, 2012.
- [5] S. H. Liao, P. H. Chu, and P. Y. Hsiao, "Data mining techniques and applications - A decade review from 2000 to 2011," *Expert Systems with Applications*. 2012.
- [6] G. Shmueli, P. C. Bruce, I. Yahav, N. R. Patel, and K. C. Lichtendahl Jr, *Data mining for business analytics: concepts, techniques, and applications* in R. John Wiley & Sons, 2017.
- [7] J.Han, J.Pei, M.Kamber, *Data Mining: Concepts and Techniques*. 2012.
- [8] H. R. Jantan, A. A. Hamdan, and Z. Othman, "Human Talent Forecasting using Data Mining Classification Techniques," *Int. J. Technol. Diffus.*, 2010.
- [9] S. Ramírez-Gallego, B. Krawczyk, S. García, M. Woźniak, and F. Herrera, "A survey on data preprocessing for data stream mining: Current status and future directions," *Neurocomputing*, vol. 239, pp. 39-57, 2017.
- [10] W. A. Wan Abu Bakar, M. Y. Md. Saman, Z. Abdullah, M. M. Abd Jalil, and T. Herawan, "Mining dense data: Association rule discovery on benchmark case study," *J. Teknol.*, 2016.

- [11] S. Sarawagi and V. T. Raisinghani, "Cleaning Methods In Data Warehousing," 1999.
- [12] Z. A. Othman, N. Ismail, and M. T. Latif, "Association pattern of NO₂ and NMHC towards high ozone concentration in Klang," in *Electrical Engineering and Informatics (ICEEI), 2017 6th International Conference on*, 2017, pp. 1–6.
- [13] M. A. Hall, E. Frank, G. Holmes, B. Pfahringer, P. Reutemann, and I. H. Witten, "The WEKA data mining software: an update," *SIGKDD Explor.*, 2009.
- [14] R. Agrawal and R. Srikant, "Fast algorithms for mining association rules," in *94 Proceedings of the 20th International Conference on Very Large Data Bases*, 1994.
- [15] P. Sagar Bhise and S. Kale, "Efficient Algorithms to find Frequent Itemset Using Data Mining," 2017.
- [16] S. K. Solanki and J. T. Patel, "A Survey on Association Rule Mining," in *2015 Fifth International Conference on Advanced Computing & Communication Technologies*, 2015.
- [17] A. A. Aziz, N. U. R. H. Ismail, and F. Ahmad, "Mining Students' Academic Performance," *Jatit Ls*, 2013.